

DEVELOPMENT OF A NOVEL RING CONTRACTION STRATEGY
AND APPLICATION TO THE TOTAL SYNTHESIS OF
PRESILPHIPERFOLANOL NATURAL PRODUCTS

Thesis by

Allen Yu Hong

In Partial Fulfillment of the Requirements for the Degree of

Doctor of Philosophy

California Institute of Technology

Pasadena, California

2013

(Defended December 7, 2012)

© 2013

Allen Yu Hong

All Rights Reserved

To my family

for their constant support and dedication

ACKNOWLEDGEMENTS

Even before I began writing, I knew it would be impossible to adequately thank all of the people who have helped me over the last few years.

The person I need to thank most for helping me during my graduate work is none other than Prof. Brian Stoltz. He has been a generous, supportive, and thoughtful advisor who has helped me make it through the most difficult moments of graduate school and catalyzed my transformation toward scientific independence. It is truly rare to find a professor who is not only knowledgeable and devoted to the science, but also cares deeply about his students and their personal development. He expects us to be rigorous, thoughtful, and inquisitive in everything that we do. He even encourages us to come up with our own ideas (“submarine projects”) as a way of furthering our scientific curiosity. Brian goes to great lengths to equip the lab with the best instruments and resources we need to succeed in our research. It is evident that he sacrifices a lot for the lab, so I am grateful to be able to learn so much from him over the last few years.

My committee members Prof. Sarah Reisman, Prof. John Bercaw, Prof. Dave Tirrell, and Dr. Scott Virgil have provided their unique scientific perspectives during my time here and have greatly influenced my approach to tackling chemistry problems. Sarah is a kind and thoughtful committee member who has always asked engaging questions and provided useful advice. She is almost like a second advisor to us. Our group and her group share so many things: joint group meetings, the third floor of Schlenger, synthetic compounds and chiral ligands, as well as a sense of camaraderie. It has been great to work alongside Sarah’s first few classes while watching the lab take off and become

successful. I am also quite fortunate to have John Bercaw on my committee. He provides a unique and seasoned organometallic perspective on the problems I am facing in my research and encourages me to think more deeply about transition metal-catalyzed reactions. The knowledge I have gained from in his classes and in informal discussions proved valuable as the application of key organometallic transformations enabled me to overcome major obstacles in my research. Dave Tirrell, who is the most recent member to join my thesis committee, has encouraged me to think about the broader implications about my proposals and my chemistry. He is always willing to make time in his busy schedule to meet with me and talk about my work. Scott has also been a friendly and knowledgeable person to have around. He is a source of broad chemical knowledge and always seems know have an answer for whatever has me stumped. His door is always open and he is always interested in whatever questions I might have. I am thankful for all of the patience and guidance from my thesis committee.

I would also like to thank my past advisors and mentors for motivating me to pursue graduate work in chemistry: Prof. Richmond Sarpong, Dr. Ahamindra Jain, Dr. Hongtao Liu, Dr. Zheng-Yu Yang, Dr. Lianhong Xu, and Richard Gibson. I especially enjoyed doing research in the Sarpong group and working with my fellow undergraduates. I learned a great deal during undergraduate subgroups (back when Richmond had more time for that sort of thing), and developed a stronger synthetic chemistry foundation as a result. Dr. Ahamindra Jain demonstrated a similar level of attention and enthusiasm for young scientists, always cheerful and in the mood to talk about chemistry. I extend my gratitude to my supervisors at Gilead Sciences, who always looked out for me and took it upon themselves to help me succeed in medicinal chemistry and beyond. Richard Gibson

at the Student Learning Center at UC-Berkeley not only motivated me to get involved in organic chemistry tutoring, but also helped me develop presentation and teaching skills. I would also like to thank Ally Finkel for being an inspiring and cheerful person to talk to during my summer internship with QB3.

The Stoltz group has certainly grown and changed over the years, but the things that have always stayed the same are the sense of community and collaboration in the group. I would like to express my gratitude to everyone who has helped me learn the ropes when it came to doing new and unfamiliar reactions, putting together formal seminars, and writing research proposals while keeping the lab environment upbeat and pleasant. Thank you to everyone who helped read over my work, especially in these particularly hectic last few months. I can only hope that I have been able to help out in the same way as a labmate and provide useful advice and knowledge in return.

I have been lucky to learn from some of the most hard-working and intelligent individuals in the Stoltz group. One of my first projects involved Pd-catalyzed oxidative cyclization reactions (no catchy team name as far as I can tell). Dave Ebner took it upon himself to teach me the best tricks that he had learned in graduate school. Additionally, Narae Park was another person I could go to when I need help with difficult transformations. I have since joined Team Tsuji to explore Pd-catalyzed asymmetric allylic alkylation reactions. I had the chance to learn about Pd-catalyzed decarboxylative protonations (and review writing!) from J. T. Mohr. When it came to allylic alkylation reactions, I was pretty spoiled. I learned much from Doug Behenna, J. T. Mohr, Nat Sherden, and Mike Krout, who each brought their different areas of expertise to the table. More recently, it has been exciting to work with Dr. Kristy Tran and Dr. Scott Virgil to

get some hands-on experience with the Symyx high-throughput screening instrumentation. It has also been a pleasure to work with Doug Duquette, Corey Reeves, and Nathan Bennett, who have developed their own unique insight into the transformations we do. Since I was interested in pursuing natural product synthesis, it was not long before I joined forces with the Ring Contraction Faction, which featured the likes of Mike Krout, Thomas Jensen, Chris Henry, Phil Kun-Liang Wu, Takeharu Toyoshima, Doug Duquette, and Nathan Bennett. Thanks to the Caltech SURF program, I had the opportunity to pursue an exploratory project for the synthesis and application of novel chiral olefin-oxazoline based ligands with a freshman undergraduate student, Annie Chin. She brought a cheerful attitude to the lab and demonstrated poise beyond her years. I am thankful for her hard work on the project. I would also like to thank Maria Cano for her effort in the preparation of related chiral olefin-imine ligands.

I have had the extraordinary fortune of being able to work with some people outside of my group to tackle some interesting problems that extend beyond our group's immediate expertise. Rob Ely at Boston College and Jessica Wu at Harvard University provided me with valuable tips on regioselective 1,4-hydroboration reactions, while Fang Gao at Boston College gave me similar pointers on copper-catalyzed allylic substitution reactions. Dr. Yu Lan and Prof. Ken Houk at UCLA and Dr. Young Hong and Prof. Dean Tantillo at UC Davis have provided valuable computational insight for several of the research projects described in this thesis. Prof. Suzana Leitão and Prof. Pedro Joseph-Nathan have provided crucial spectral data for our work with the presilphiperfolanol natural products. Although I won't have a chance to work with Dr. Ryan Lauchli and Prof. Frances Arnold on engineered terpene cyclases, it has been an

enlightening experience to be able to learn more about how our chemical engineering colleagues are tackling interesting problems. I wish them the best of luck as they begin collaborations with Dr. Alex Marziale from our lab.

My hoodmates and labmates have provided indispensable company in the Stoltz group during my graduate career. Back in 264 Crellin, I had the chance to work beside Dave Ebner. He and Dr. Scott Virgil helped me clean out and set up my previously unoccupied and dust-ridden hood. Jenn Stockdill and Thomas Jensen were also pleasant and accommodating labmates. Shortly after I started working in lab, Nathan joined the group at an absurdly early time in April or May, making me a second year graduate student after only two or three months in the group. Although Dave Ebner graduated several months later after receiving his Ph.D., I was incredibly fortunate to be able to work with Dr. Chris Henry, who would invite me to join him on some of his legendary death hikes through the local San Gabriel or the southern Sierra mountains.

During our move to Schlenger, things got shuffled around a bit. I've enjoyed setting up home base in the relatively quiet and small office, where I've worked alongside not only Dr. Chris Henry and Nathan Bennett, but also Nat Sherden, Dr. Michele Gatti, Kelly Kim, Doug Duquette, Nick O'Connor, Dr. Guillaume Lapointe, Dr. Alex Marziale, Dr. Fabian Piller, Maria Cano, Dr. Yoshitaka Numajiri, Taiga Yurino, Chris Gilmore, Pam Tadross, and Dr. Amanda Jones. One of the highlights of small office banter was the basketball-related smack talk between Chris Henry and Jonny Gordon... I had grand visions of their future as a superstar assistant professor and postdoc tandem, but unfortunately that never became a reality. Nat and Michele were both delightful people in the small office who were not only hilariously funny, but also good sources of

chemistry knowledge as well. Doug has also been a pleasant person to talk to in the office. More recently, Kelly and Nick, as well as Seojung Han and Katerina Korch, have joined me during weekly trips to Ernie's taco truck and it has been nice to get to know the youngest members of the group.

With the offices in Schlinger separated from the lab spaces, I have had the chance to work with other folks in the Stoltz group as well. Nathan Bennett has been a great person to share a fume hood with, and Dr. Chris Henry, Nat Sherden, and Max Loewinger have provided plenty of entertaining conversations as our next-door neighbors over the years. At the end of the bay, it was not an uncommon sight to see Dr. Florian Vogt and Chris Gilmore making fun of each other all day long. More recently, Boger Liu and Seojung Han have joined the bay and been great coworkers during my last year here.

I am indebted to the numerous people who have helped look over my research proposals, manuscripts, presentations, posters, and thesis chapters over the years and offered valuable input. Thanks go to Doug Behenna, Dr. Grant Shibuya, Dr. Phil Wu, Dr. Jimin Kim, J. T. Mohr, Mike Krout, Dr. Chris Henry, Dr. Thomas Jensen, Doug Duquette, Corey Reeves, Floh Vogt, Kristy Tran, Guillaume Lapointe, Nick O'Connor, Kelly Kim, Nathan Bennett, Christopher Haley, Dr. Alex Marziale, Jeff Holder, Gloria Sheng, Dr. Jake Cha, Chris Gilmore, Pam Tadross, and perhaps many more. Thanks also go to Rob Craig for helping me obtain crucial data from the X-ray facility. Additionally, I would also like to thank Dr. Andy McClory, Dr. Charles Liu, and Dr. Ryan McFadden for providing valuable career insight when I was a younger student. Dr. Grant Shibuya continues to provide me with helpful advice, particularly when it comes to making the most of my time as a postdoctoral scholar in the Vanderwal laboratory at UC Irvine.

The Caltech staff has been instrumental to my success during graduate school. Dr. Dave VanderVelde and Dr. Scott Ross have provided valuable assistance in the NMR laboratory and never turned down my usual requests for help with setting up unfamiliar experiments or troubleshooting the Linux workstations. I also must thank Larry Henling for providing crucial X-ray crystal structures that provided the much-needed evidence for the structural reassignment of naturally isolated presilphiperfolan-1-ol. Lynne Martinez does a great deal of behind-the-scenes work as the administrative assistant for our group and the Reisman group, so we can credit her for keeping things running smoothly on a daily basis. Rick Gerhart is a master of glassblowing because he has been able to construct or repair any piece of glassware. It has only been a few months since Tom Dunn left, but we already miss his expertise and service to our group. We are thankful that Jeff Groseth has joined the Caltech staff and filled an important and central role in the division. While I haven't had a chance to work with him, I am sure that he will be as indispensable as Tom was to the different chemistry groups on campus. Joe Drew and Ron Koen are vital to the department as they are the ones who make sure we have the shipments we need to continue our research. When I was a first and second year graduate student, they helped me out a great deal during my occasional bouts with scientific supply ordering. Art Seiden, Larry Martinez, and Caz Scislowicz help keep the campus safe and informed and it's been a great working with them as the group safety officer. I would like to thank Chung-Whan Lee for taking up the mantle of Stoltz group safety officer. The "careful cap" is now in your hands. Additionally, I would like to extend my gratitude to Agnes Tong, Laura Howe, Anne Penney for getting me started at Caltech and helping me make sense of the different requirements and deadlines while also being

cheerful people to talk to during my occasional trips back to Crellin. Thanks also go to Natalie Gilmore and Felicia Hunt at the Graduate Studies Office who have not only helped me navigate the thesis preparation and submission process but also provided me with a travel grant that enabled me to attend my first chemistry conference.

I would also like to thank the Caltech for providing me with an institute fellowship during my first year of graduate school. I am indebted to the Caltech Summer Undergraduate Research Fellowship Program, particularly the William N. Lacey Fund, for sponsoring Annie Chin's research project. Roche and Abbott Laboratories provided generous awards for my graduate research and I am grateful for the opportunities to learn more about pharmaceutical research at their research sites. Additionally, I would like to acknowledge the National Institutes of Health for supporting the Pd-catalyzed asymmetric alkylation chemistry in the Stoltz group and thank them in advance for providing me with a postdoctoral fellowship for future work with Prof. Chris Vanderwal.

My personal thanks go to many of my friends and family who have supported me during these often challenging times in graduate school. Dad, Mom, and Jason have been the most warm and supporting family I could ever ask for and I hope I can make you proud with the work I have done. I would also like to thank my extended family, too. My grandparents, aunts, uncles, and cousins made many sacrifices so our generation could come to this country and succeed, so in many ways we are truly fortunate.

My Caltech friends and classmates have provided the necessary emotional anchoring to help me stay sane through during the more difficult parts of graduate school. Matt Winston and Gloria Sheng have been there since the beginning, even after several memorable kayaking mishaps. Perhaps most importantly, they have accompanied me

during my weekly trips to Alhambra, San Gabriel, or Arcadia to satisfy my Asian food cravings. My friends in the Stoltz group have not only helped me make it through graduate school, but also helped me avert dinner party disasters, survive grueling mountain hikes, and treated me to outdoor summer concerts. Dr. Chris Henry, Dr. Kristy Tran, Dr. Kathrin Höferl-Prantz, Dr. Phil Wu, Dr. Grant Shibuya, Kelly Kim, and Nick O'Connor have been great labmates and friends. Next door in the Reisman lab, I have often spent time pestering Kangway Chuang, Maddi Kieffer, Dr. Jake Cha, and Raul Navarro, who are all kind souls and joined me on my occasional food adventures. Young In Oh, Nicole Bouley, Eric Lee, and Clara Cho have also been great people to hang out with in my spare time. Of course, we will always remember Long Phan.

I need to thank my LA friends who have made Southern California feel like a second home. Thanks go to Matt Hui, Jason Coe, Jeremy Chen, Owen Leong, Wendy Gu, Jerry Cheung, Julie Tieu, Brandy Au, Bertha Haslim, and Hannah Lam for making this place special. I'm also fortunate to be able to hang out with my old roommates down here. It's been fun to catch up with Albert Lew and Luis Reyes over the weekends. I'd also like to thank the friends back home: Amy Lee, Sharon Lee, Cheryl Leung, Tammy Chu, Pauline Sze, Ashik Manandhar, Lina Peng, Mandy Li, Katy Yu, Kathy Zhang, Anthony Suen, Christina Wang, Julian Shun, Frank He, Susan Fang, and Stephan Woo. Of course, I can't forget the Treehouse crew and all the times we had as housemates in college.

Without the continued support of all of these people, this work certainly would not have been possible.

ABSTRACT

Biologically active and structurally complex natural products provide a powerful driving force for the development of novel reaction methodology. Major advances can reshape the way chemists approach the construction of challenging chemical bonds.

In this work, we begin by describing the development of a catalytic asymmetric synthesis of five and seven-membered rings containing all-carbon quaternary stereocenters. Enantioselective Pd-catalyzed decarboxylative allylic alkylation reactions of β -ketoester substrates afforded a variety of chiral seven-membered α -quaternary vinylogous esters. Initial attempts to convert these compounds to γ -quaternary cycloheptenones led to the discovery of a two-carbon ring contraction reaction, which provided isomeric γ -quaternary acylcyclopentenones. Subsequent adjustment of reaction parameters provided divergent access to the originally targeted cycloheptenones. Numerous synthetic applications of the two versatile product types are demonstrated. The methodology expands on our previous investigations of six-membered ring scaffolds and provides additional chiral building blocks for asymmetric total synthesis.

The ring contraction approach to acylcyclopentenones was further developed in the total synthesis of the presilphiperfolanols, which are important intermediates in sesquiterpene biosynthesis. Key to our synthetic route to the tricyclic core was the application of intramolecular Diels–Alder and Ni-catalyzed 1,4-hydroboration reactions. From these efforts, the enantioselective total synthesis of presilphiperfolan-1 β -ol was achieved. Future research efforts seek to extend the synthetic route to presilphiperfolan-9 α -ol and study the synthetic compounds in biomimetic carbocation rearrangement processes.

TABLE OF CONTENTS

Acknowledgements	iv
Abstract.....	xiii
Table of Contents	xiv
List of Figures.....	xxiii
List of Schemes.....	xl
List of Tables.....	xlvii
List of Abbreviations.....	li

CHAPTER 1

1

The Construction of All-Carbon Quaternary Stereocenters Using Pd-Catalyzed Asymmetric Allylic Alkylation Reactions in Total Synthesis

1.1	Introduction and Background	1
1.2	Reaction Design and Mechanistic Considerations	3
1.2.1	General Aspects of Pd-Catalyzed Allylic Alkylation	3
1.2.2	Development of Methods for Enolate Generation.....	4
1.2.3	Development of Asymmetric Allylation Reactions	6
1.3	Catalytic Asymmetric Synthesis of Natural Products.....	10
1.3.1	Total Syntheses of Hamigeran B and Allocyathin B ₂	10
1.3.2	Total Syntheses of Dichroanone and Liphagal	16
1.3.3	Total Syntheses of Elatol, α -Chamigrene, Laurencenone C	20
1.3.4	Formal Synthesis of Platencin	24
1.3.5	Formal Synthesis of Hamigeran B	27
1.3.6	Total Syntheses of Carissone and Cassiol	28
1.3.7	Total Syntheses of Flustramides A and B, Flustramines A and B	32
1.3.8	Total Syntheses of Cyanthiwiggins B, F, and G.....	35
1.4	Conclusion and Outlook.....	38
1.5	Notes and References.....	39

CHAPTER 2**46***Catalytic Asymmetric Synthesis of Cyclopentanoid and Cycloheptanoid Core Structures Using Pd-Catalyzed Asymmetric Alkylation*

2.1	Introduction and Background.....	46
2.2	β -Ketoester Synthesis and Pd-Catalyzed Asymmetric Alkylation Reactions..	48
2.3	Observation of the Unusual Reactivity of β -Hydroxycycloheptanones	53
2.4	Ring Contraction Strategy for Preparing γ -Quaternary Acylcyclopentenones ...	57
2.5	Synthesis of Acylcyclopentene Derivatives Using Site-Selective Transformations.....	66
2.6	Carbonyl Transposition Approach to γ -Quaternary Cycloheptenones	71
2.7	Synthesis of Cycloheptenone Derivatives Using Transition-Metal Catalyzed Cyclizations.....	76
2.8	Unified Strategy for the Synthesis of Complex Polycyclic Natural Products	79
2.9	Conclusion	81
2.10	Experimental Section	83
2.10.1	Materials and Methods	83
2.10.2	Preparative Procedures	86
2.10.2.1	Preparation Parent Vinylogous Ester 147	86
2.10.2.2	Preparation of β -Ketoesters 148	88
2.10.2.3	Synthesis of PHOX Ligands	115
2.10.2.4	Enantioselective Pd-Catalyzed Decarboxylative Alkylation Screening Protocol	121
2.10.2.5	Preparation of Chiral Vinylogous Esters 149	122
2.10.2.6	Synthetic Studies on the Reduction/Rearrangement of Six- and Seven-Membered Vinylogous Esters.....	140
2.10.2.7	Ring Contraction Screening Protocol	147
2.10.2.8	Preparation of β -Hydroxyketones and Acylcyclopentenones.....	149
2.10.2.9	Large Scale Synthesis of Acylcyclopentene 135a	174
2.10.2.10	Initial Synthetic Studies on the Organometallic Addition/Rearrangement of 149a	176
2.10.2.11	Preparation of Acylcyclopentene Derivatives	181
2.10.2.12	Revised Approach to the Reduction/Rearrangement and Organometallic Addition/Rearrangement of 149a	207
2.10.2.13	Grignard and Organolithium Reagents	213

		xvi
2.10.2.14	Carbonyl Transposition to γ -Quaternary Cycloheptenones	217
2.10.2.15	Preparation of Polycyclic Cycloheptenone Derivatives by Ring-Closing Metathesis	241
2.10.2.16	Preparation of Polycyclic Cycloheptenone Derivatives by Other Methods	254
2.10.2.17	Determination of Enantiomeric Excess	259
2.11	Notes and References	262

APPENDIX 1 **273**

Spectra Relevant to Chapter 2

APPENDIX 2 **523**

X-Ray Crystallography Reports Relevant to Chapter 2

A2.1	Crystal Structure Analysis of 164	524
------	--	-----

APPENDIX 3 **534**

Theoretical Investigation of the Unusual Stability of β -Hydroxycycloheptanones

A3.1	Introduction and Background	534
A3.2	Quantum Calculations	535
A3.3	Future Directions	537
A3.4	Notes and References	538

CHAPTER 3 **539**

The Catalytic Asymmetric Total Synthesis of Presilphiperfolanol Natural Products

3.1	Introduction and Background	539
3.1.1	Isolation and Structural Elucidation	539
3.1.2	Biosynthesis of the Presilphiperfolanols	543
3.1.3	Broader Relevance of the Presilphiperfolanols	546
3.1.4	Biological Activity	549
3.2	Previous Synthetic Studies Toward Presilphiperfolanol Natural Products ..	551
3.2.1	Biomimetic Cation-Polyene Cyclizations of Caryophyllene and Isocaryophyllene	552
3.2.2	Weyerstahl Synthesis of (\pm)-Presilphiperfolan-9 α -ol	555

3.2.3	Piers' Radical Cyclization Strategy and Synthesis of (±)-Epi-9-Norpresilphiperfolan-9-one.....	559
3.2.4	Summary of Previous Synthetic Studies	562
3.3	Asymmetric Alkylation/Ring Contraction Approach to the Presilphiperfolanol Natural Products	562
3.3.1	Retrosynthetic Analysis	563
3.3.2	Conjugate Addition/Robinson Annulation Strategy	565
3.3.3	Intramolecular Diels–Alder Strategy	567
3.3.4	Summary and Outlook.....	574
3.4	Total Synthesis of (–)-Presilphiperfolan-1β-ol and Related Analogs	575
3.4.1	Revised Retrosynthetic Analysis	575
3.4.2	Asymmetric Alkylation and Ring Contraction.....	576
3.4.3	Intramolecular Diels–Alder Studies	578
3.4.4	Elaboration of Methyl/Isoprenyl Acylcyclopentene	579
3.4.5	Further Intramolecular Diels–Alder Studies	583
3.4.6	Completion of (–)-Presilphiperfolan-1β-ol and Unnatural Analogs.....	585
3.4.7	Structural Revision and Proposed Biosynthesis of (–)-Presilphiperfolan-1β-ol.....	588
3.4.8	Summary and Outlook.....	591
3.5	Planned Synthesis of (–)-Presilphiperfolan-9α-ol	592
3.5.1	Protonation Approach.....	592
3.5.2	Modified IMDA Approach	594
3.6	Planned Rearrangement of Presilphiperfolanols to Other Sesquiterpene Natural Products	596
3.7	Conclusion	597
3.8	Experimental Section	599
3.8.1	Materials and Methods	599
3.8.2	Preparative Procedures	603
3.8.2.1	Methallyl/Methyl Acylcyclopentene Route	603
3.8.2.2	Synthesis of (–)-Presilphiperfolan-1β-ol and Analogs	618
3.8.2.3	Progress Toward the Asymmetric Synthesis of (–)-Presilphiperfolan-9α-ol	665
3.8.3	Methods for Determination of Enantiomeric Excess	670
3.8.4	Comparison of Spectral Data for Synthetic and Reported Presilphiperfolanols 224 and 223	671

3.9	Notes and References	677
APPENDIX 4		698
<i>Synthetic Summary for Presilphiperfolanol Natural Products</i>		
APPENDIX 5		703
<i>Spectra Relevant to Chapter 3</i>		
APPENDIX 6		797
<i>X-Ray Crystallography Reports Relevant to Chapter 3</i>		
A6.1	Crystal Structure Analysis of 353	798
A6.2	Crystal Structure Analysis of 224	808
A6.3	Crystal Structure Analysis of 356	823
APPENDIX 7		837
<i>Theoretical Investigation of the Relative Free Energies of Presilphiperfolanol Natural Products and Synthetic Intermediates</i>		
A7.1	Introduction and Background	837
A7.2	Quantum Calculations	837
APPENDIX 8		842
<i>Theoretical Investigation of the Terpene Cyclization Pathways Relevant to Presilphiperfolanol Natural Products</i>		
A8.1	Introduction and Background	842
A8.2	Quantum Calculations	842
APPENDIX 9		853
<i>Enantioselective Protonations</i>		
A9.1	Introduction and Background	853
A9.2	Important Factors in Achieving Enantioselective Protonation	854
A9.3	Enantioselective Protonation in Enzymatic Systems	856
A9.3.1	Decarboxylase Enzymes	856

A9.3.2	Esterase Enzymes	860
A9.4	Strategic Approaches to Nonenzymatic Enantioselective Protonation	862
A9.4.1	General Considerations	862
A9.4.2	Enantioselective Protonation by Means of Chiral Proton Donor	863
A9.4.3	Enantioselective Protonation by Means of Chiral Brønsted Base	875
A9.4.4	Enantioselective Hydrogen Atom Transfer	888
A9.5	Conclusion	889
A9.6	Notes and References	890

APPENDIX 10**896***Pd-Catalyzed Asymmetric Allylic Alkylation of α -Oxygenated Enolates: Synthetic Studies and Mechanistic Hypotheses*

A10.1	Introduction and Background.....	896
A10.2	Pd-Catalyzed Asymmetric Alkylation of Cyclic α -Oxygenated Substrates	902
A10.2.1	Previous Evaluation Silyl Enol Ether and Enol Carbonate Substrates.....	903
A10.2.2	Evaluation of α -Oxygenated β -Ketoester Substrates	905
A10.2.3	Recent Investigation of <i>N</i> -Acyl Lactam Substrates.....	909
A10.2.4	Possible Mechanistic Implications of α - and α' -Interacting Asymmetric Alkylation Substrates	911
A10.3	Conclusion	913
A10.4	Experimental Section	914
A10.4.1	Materials and Methods	914
A10.4.2	Preparative Procedures	916
A10.4.2.1	α -Benzoyloxy β -Ketoester Substrate Synthesis.....	916
A10.4.2.2	Pd-Catalyzed Decarboxylative Alkylation Reactions.....	920
A10.5	Notes and References	923

APPENDIX 11**927***Pd-Catalyzed Asymmetric Allylic Alkylation of Dienolates: The Synthesis of α - and γ -Quaternary Cyclohexenones*

A11.1	Introduction and Background.....	927
A11.2	Asymmetric Pd-Catalyzed Decarboxylative Alkylation of Cyclic α,β -Unsaturated δ -Ketoester Substrates	932

		xx
A11.2.1	Reaction Design	932
A11.2.2	Synthesis of α,β -Unsaturated δ -Ketoester Substrates	933
A11.2.3	Preliminary Studies and Proof of Concept	935
A11.2.4	Concurrent Investigation of Substrates Inspired by Synthetic Efforts Toward Przewalskin B	939
A11.3	Symyx High-Throughput Reaction Screening	944
A11.4	Future Directions	945
A11.5	Conclusion	947
A11.6	Experimental Section	949
A11.6.1	Materials and Methods	949
A11.6.2	Preparative Procedures	951
A11.6.2.1	δ -Ketoester Substrate Synthesis	951
A11.6.2.2	Pd-Catalyzed Decarboxylative Alkylation Reactions.....	956
A11.6.2.3	High-Throughput Reaction Screening	962
A11.7	Notes and References	966

APPENDIX 12 **970**

Progress Toward the Total Synthesis of Crinine and Related Amaryllidaceae Alkaloids

A12.1	Introduction and Background.....	970
A12.2	Synthetic Strategies Toward Crinine-Type Alkaloids	972
A12.2.1	α -Arylation/ α -Alkylation Cascade Strategy	974
A12.2.2	Allylative Dearomatization Strategy	978
A12.2.3	Oxidative Cyclization Approach	981
A12.2.4	C–H Activation/Intramolecular Amination Strategy.....	985
A12.3	Progress Toward the Synthesis of (\pm)-Oxocrinine	987
A12.3.1	Stork Enamine Alkylation Route	988
A12.3.2	Metalloenamine-Mediated Aziridine Opening Route.....	991
A12.4	Recent Developments in the Total Synthesis of Crinine-Type and Related <i>Amaryllidaceae</i> Alkaloids	996
A12.4.1	Zhang's Pd-Catalyzed α -Alkylation/ α -Arylation Strategy in the Total Synthesis of (\pm)-Mesembrine	996
A12.4.2	Dixon's Syntheses of (\pm)-Buphanidrine and (\pm)-Powelline by β -Ketoester α -Arylation.....	998
A12.4.3	Enantioselective Allylative Dearomatization Reactions Catalyzed by	

	Palladium(0) and Iridium (I)	999
A12.4.4	You's Enantioselective Dienone Desymmetrization	1000
A12.5	Conclusion	1001
A12.6	Experimental Section	1002
A12.6.1	Materials and Methods	1002
A12.6.2	Preparative Procedures	1004
A12.6.2.1	Synthesis of γ -Aryl γ -Allyl Cyclohexenone 731	1004
A12.6.2.2	Synthesis of γ -Aryl γ -Ethylamino Cyclohexenone 750	1010
A12.7	Notes and References	1020

APPENDIX 13 **1026**

Modular Synthesis of Olefin-Oxazoline (OlefOX) Ligands and Applications in Transition Metal-Catalyzed Reactions

A13.1	Introduction and Background	1026
A13.2	Synthesis of Olefin-Oxazoline (OlefOX) Ligands	1030
A13.2.1	Development of an Improved OlefOX Ligand Synthesis	1030
A13.2.2	Steric/Electronic Modification of OlefOX Ligands	1033
A13.2.3	Application of OlefOX Ligands to Asymmetric Transition Metal Catalyzed Reactions	1038
A13.3	Synthesis of Related <i>Spiro</i> -Ketimine-Olefin Ligands	1039
A13.4	Future Directions	1041
A13.5	Recent Developments in C ₁ -Symmetric Ligand Design	1042
A13.6	Conclusion	1044
A13.7	Experimental Section	1045
A13.7.1	Materials and Methods	1045
A13.7.2	Preparative Procedures	1047
A13.7.2.1	Synthesis of Achiral OlefOX Ligand 801b	1047
A13.7.2.2	General OlefOX Ligand Synthesis Procedures	1050
A13.7.2.3	Characterization Data for OlefOX Ligands 801	1051
A13.8	Notes and References	1059

APPENDIX 14 **1064**

Notebook Cross-Reference

Comprehensive Bibliography	1084
Index	1123
About the Author	1130

LIST OF FIGURES

CHAPTER 1

The Construction of All-Carbon Quaternary Stereocenters Using Pd-Catalyzed Asymmetric Allylic Alkylation Reactions in Total Synthesis

Figure 1.1. Natural Products as an Inspiration for the Development of Asymmetric Catalysis	2
Figure 1.2. Selected Chiral Ligands for Pd-Catalyzed Asymmetric Allylic Alkylation Reactions	8
Figure 1.3. Ruthenium Olefin Metathesis Catalysts.....	23

CHAPTER 2

Catalytic Asymmetric Synthesis of Cyclopentanoid and Cycloheptanoid Core Structures Using Pd-Catalyzed Asymmetric Alkylation

Figure 2.1. Application of Cyclopentanoid, Cyclohexanoid, and Cycloheptanoid Cores Toward Stereoselective Natural Product Synthesis.....	47
Figure 2.2. General Access to Enantioenriched Cyclopentanoid and Cyclohexanoid Cores.....	48
Figure 2.3. Selective Functionalizations on Sites A–E of Acylcyclopentenones 135	68
Figure 2.4. Chiral Fused and Spirocyclic Structures Prepared by Asymmetric Allylic Alkylation	80
Figure 2.5. Pd-Catalyzed Asymmetric Allylic Alkylation in the Total Synthesis of Natural Products....	81

APPENDIX 1

Spectra Relevant to Chapter 2

Figure A1.1. ¹ H NMR (500 MHz, CDCl ₃) of compound 147	275
Figure A1.2. Infrared spectrum (thin film/NaCl) of compound 147	276
Figure A1.3. ¹³ C NMR (125 MHz, CDCl ₃) of compound 147	276
Figure A1.4. ¹ H NMR (500 MHz, CDCl ₃) of compound 148a	277
Figure A1.5. Infrared spectrum (thin film/NaCl) of compound 148a	278
Figure A1.6. ¹³ C NMR (125 MHz, CDCl ₃) of compound 148a	278
Figure A1.7. ¹ H NMR (300 MHz, CDCl ₃) of compound 148b	279
Figure A1.8. Infrared spectrum (thin film/NaCl) of compound 148b	280
Figure A1.9. ¹³ C NMR (75 MHz, CDCl ₃) of compound 148b	280
Figure A1.10. ¹ H NMR (300 MHz, CDCl ₃) of compound 148c	281
Figure A1.11. Infrared spectrum (thin film/NaCl) of compound 148c	282
Figure A1.12. ¹³ C NMR (75 MHz, CDCl ₃) of compound 148c	282

Figure A1.13. ^1H NMR (300 MHz, CDCl_3) of compound 148d	283
Figure A1.14. Infrared spectrum (thin film/ NaCl) of compound 148d	284
Figure A1.15. ^{13}C NMR (75 MHz, CDCl_3) of compound 148d	284
Figure A1.16. ^1H NMR (300 MHz, CDCl_3) of compound 148e	285
Figure A1.17. Infrared spectrum (thin film/ NaCl) of compound 148e	286
Figure A1.18. ^{13}C NMR (75 MHz, CDCl_3) of compound 148e	286
Figure A1.19. ^1H NMR (300 MHz, CDCl_3) of compound 148f	287
Figure A1.20. Infrared spectrum (thin film/ NaCl) of compound 148f	288
Figure A1.21. ^{13}C NMR (75 MHz, CDCl_3) of compound 148f	288
Figure A1.22. ^1H NMR (300 MHz, CDCl_3) of compound 148g	289
Figure A1.23. Infrared spectrum (thin film/ NaCl) of compound 148g	290
Figure A1.24. ^{13}C NMR (75 MHz, CDCl_3) of compound 148g	290
Figure A1.25. ^1H NMR (300 MHz, CDCl_3) of compound 148h	291
Figure A1.26. Infrared spectrum (thin film/ NaCl) of compound 148h	292
Figure A1.27. ^{13}C NMR (75 MHz, CDCl_3) of compound 148h	292
Figure A1.28. ^1H NMR (300 MHz, CDCl_3) of compound 148i	293
Figure A1.29. Infrared spectrum (thin film/ NaCl) of compound 148i	294
Figure A1.30. ^{13}C NMR (75 MHz, CDCl_3) of compound 148i	294
Figure A1.31. ^1H NMR (300 MHz, CDCl_3) of compound 148ac	295
Figure A1.32. ^{13}C NMR (75 MHz, CDCl_3) of compound 148ac	296
Figure A1.33. Infrared spectrum (thin film/ NaCl) of compound 148ac	296
Figure A1.34. ^1H NMR (300 MHz, CDCl_3) of compound 148j	297
Figure A1.35. Infrared spectrum (thin film/ NaCl) of compound 148j	298
Figure A1.36. ^{13}C NMR (75 MHz, CDCl_3) of compound 148j	298
Figure A1.37. ^1H NMR (300 MHz, CDCl_3) of compound 148k	299
Figure A1.38. Infrared spectrum (thin film/ NaCl) of compound 148k	300
Figure A1.39. ^{13}C NMR (75 MHz, CDCl_3) of compound 148k	300
Figure A1.40. ^1H NMR (300 MHz, CDCl_3) of compound 148l	301
Figure A1.41. Infrared spectrum (thin film/ NaCl) of compound 148l	302
Figure A1.42. ^{13}C NMR (75 MHz, CDCl_3) of compound 148l	302
Figure A1.43. ^1H NMR (300 MHz, CDCl_3) of compound 148ad	303
Figure A1.44. Infrared spectrum (thin film/ NaCl) of compound 148ad	304
Figure A1.45. ^{13}C NMR (75 MHz, CDCl_3) of compound 148ad	304
Figure A1.46. ^1H NMR (300 MHz, CDCl_3) of compound 148m	305
Figure A1.47. Infrared spectrum (thin film/ NaCl) of compound 148m	306

Figure A1.48. ^{13}C NMR (75 MHz, CDCl_3) of compound 148m	306
Figure A1.49. ^1H NMR (300 MHz, CDCl_3) of compound 148n	307
Figure A1.50. Infrared spectrum (thin film/ NaCl) of compound 148n	308
Figure A1.51. ^{13}C NMR (75 MHz, CDCl_3) of compound 148n	308
Figure A1.52. ^1H NMR (500 MHz, CDCl_3) of compound 191	309
Figure A1.53. Infrared spectrum (thin film/ NaCl) of compound 191	310
Figure A1.54. ^{13}C NMR (125 MHz, CDCl_3) of compound 191	310
Figure A1.55. ^1H NMR (500 MHz, CDCl_3) of compound 192	311
Figure A1.56. Infrared spectrum (thin film/ NaCl) of compound 192	312
Figure A1.57. ^{13}C NMR (125 MHz, CDCl_3) of compound 192	312
Figure A1.58. ^1H NMR (300 MHz, CDCl_3) of compound 193	313
Figure A1.59. Infrared spectrum (thin film/ NaCl) of compound 193	314
Figure A1.60. ^{13}C NMR (75 MHz, CDCl_3) of compound 193	314
Figure A1.61. ^1H NMR (500 MHz, CDCl_3) of compound 150	315
Figure A1.62. Infrared spectrum (thin film/ NaCl) of compound 150	316
Figure A1.63. ^{13}C NMR (125 MHz, CDCl_3) of compound 150	316
Figure A1.64. ^1H NMR (500 MHz, CDCl_3) of compound 149a	317
Figure A1.65. Infrared spectrum (thin film/ NaCl) of compound 149a	318
Figure A1.66. ^{13}C NMR (125 MHz, CDCl_3) of compound 149a	318
Figure A1.67. ^1H NMR (300 MHz, CDCl_3) of compound 149b	319
Figure A1.68. Infrared spectrum (thin film/ NaCl) of compound 149b	320
Figure A1.69. ^{13}C NMR (75 MHz, CDCl_3) of compound 149b	320
Figure A1.70. ^1H NMR (300 MHz, CDCl_3) of compound 149c	321
Figure A1.71. Infrared spectrum (thin film/ NaCl) of compound 149c	322
Figure A1.72. ^{13}C NMR (75 MHz, CDCl_3) of compound 149c	322
Figure A1.73. ^1H NMR (300 MHz, CDCl_3) of compound 149d	323
Figure A1.74. Infrared spectrum (thin film/ NaCl) of compound 149d	324
Figure A1.75. ^{13}C NMR (75 MHz, CDCl_3) of compound 149d	324
Figure A1.76. ^1H NMR (300 MHz, CDCl_3) of compound 149e	325
Figure A1.77. Infrared spectrum (thin film/ NaCl) of compound 149e	326
Figure A1.78. ^{13}C NMR (75 MHz, CDCl_3) of compound 149e	326
Figure A1.79. ^1H NMR (300 MHz, CDCl_3) of compound 149f	327
Figure A1.80. ^{13}C NMR (75 MHz, CDCl_3) of compound 149f	328
Figure A1.81. Infrared spectrum (thin film/ NaCl) of compound 149f	328
Figure A1.82. ^1H NMR (300 MHz, CDCl_3) of compound 149g	329

Figure A1.83. Infrared spectrum (thin film/NaCl) of compound 149g	330
Figure A1.84. ^{13}C NMR (75 MHz, CDCl_3) of compound 149g	330
Figure A1.85. ^1H NMR (300 MHz, CDCl_3) of compound 149h	331
Figure A1.86. ^{13}C NMR (75 MHz, CDCl_3) of compound 149h	332
Figure A1.87. Infrared spectrum (thin film/NaCl) of compound 149h	332
Figure A1.88. ^1H NMR (300 MHz, CDCl_3) of compound 149i	333
Figure A1.89. Infrared spectrum (thin film/NaCl) of compound 149i	334
Figure A1.90. ^{13}C NMR (75 MHz, CDCl_3) of compound 149i	334
Figure A1.91. ^1H NMR (300 MHz, CDCl_3) of compound 149j	335
Figure A1.92. ^{13}C NMR (75 MHz, CDCl_3) of compound 149j	336
Figure A1.93. Infrared spectrum (thin film/NaCl) of compound 149j	336
Figure A1.94. ^1H NMR (300 MHz, CDCl_3) of compound 149k	337
Figure A1.95. Infrared spectrum (thin film/NaCl) of compound 149k	338
Figure A1.96. ^{13}C NMR (75 MHz, CDCl_3) of compound 149k	338
Figure A1.97. ^1H NMR (300 MHz, CDCl_3) of compound 149l	339
Figure A1.98. ^{13}C NMR (75 MHz, CDCl_3) of compound 149l	340
Figure A1.99. Infrared spectrum (thin film/NaCl) of compound 149l	340
Figure A1.100. ^1H NMR (300 MHz, CDCl_3) of compound 149m	341
Figure A1.101. Infrared spectrum (thin film/NaCl) of compound 149m	342
Figure A1.102. ^{13}C NMR (75 MHz, CDCl_3) of compound 149m	342
Figure A1.103. ^1H NMR (300 MHz, CDCl_3) of compound 149n	343
Figure A1.104. Infrared spectrum (thin film/NaCl) of compound 149n	344
Figure A1.105. ^{13}C NMR (75 MHz, CDCl_3) of compound 149n	344
Figure A1.106. ^1H NMR (300 MHz, CDCl_3) of compound 149o	345
Figure A1.107. Infrared spectrum (thin film/NaCl) of compound 149o	346
Figure A1.108. ^{13}C NMR (75 MHz, CDCl_3) of compound 149o	346
Figure A1.109. ^1H NMR (300 MHz, CDCl_3) of compound 149p	347
Figure A1.110. Infrared spectrum (thin film/NaCl) of compound 149p	348
Figure A1.111. ^{13}C NMR (75 MHz, CDCl_3) of compound 149p	348
Figure A1.112. ^1H NMR (300 MHz, CDCl_3) of compound 149q	349
Figure A1.113. Infrared spectrum (thin film/NaCl) of compound 149q	350
Figure A1.114. ^{13}C NMR (75 MHz, CDCl_3) of compound 149q	350
Figure A1.115. ^1H NMR (300 MHz, CDCl_3) of compound 194	351
Figure A1.116. Infrared spectrum (thin film/NaCl) of compound 194	352
Figure A1.117. ^{13}C NMR (75 MHz, CDCl_3) of compound 194	352

Figure A1.118. ^1H NMR (300 MHz, CDCl_3) of compound 151	353
Figure A1.119. Infrared spectrum (thin film/ NaCl) of compound 151	354
Figure A1.120. ^{13}C NMR (75 MHz, CDCl_3) of compound 151	354
Figure A1.121. ^1H NMR (300 MHz, CDCl_3) of compound 152	355
Figure A1.122. Infrared spectrum (thin film/ NaCl) of compound 152	356
Figure A1.123. ^{13}C NMR (75 MHz, CDCl_3) of compound 152	356
Figure A1.124. ^1H NMR (500 MHz, CDCl_3) of compound 160	357
Figure A1.125. Infrared spectrum (thin film/ NaCl) of compound 160	358
Figure A1.126. ^{13}C NMR (125 MHz, CDCl_3) of compound 160	358
Figure A1.127. ^1H NMR (500 MHz, CDCl_3) of compound 137a	359
Figure A1.128. Infrared spectrum (thin film/ NaCl) of compound 137a	360
Figure A1.129. ^{13}C NMR (125 MHz, CDCl_3) of compound 137a	360
Figure A1.130. ^1H NMR (500 MHz, CDCl_3) of compound 154a	361
Figure A1.131. Infrared spectrum (thin film/ NaCl) of compound 154a	362
Figure A1.132. ^{13}C NMR (125 MHz, CDCl_3) of compound 154a	362
Figure A1.133. ^1H NMR (300 MHz, CDCl_3) of compound 154b	363
Figure A1.134. Infrared spectrum (thin film/ NaCl) of compound 154b	364
Figure A1.135. ^1H NMR (300 MHz, CDCl_3) of compound 154c	365
Figure A1.136. Infrared spectrum (thin film/ NaCl) of compound 154c	366
Figure A1.137. ^1H NMR (300 MHz, CDCl_3) of compound 154d	367
Figure A1.138. Infrared spectrum (thin film/ NaCl) of compound 154d	368
Figure A1.139. ^1H NMR (300 MHz, CDCl_3) of compound 154e	369
Figure A1.140. Infrared spectrum (thin film/ NaCl) of compound 154e	370
Figure A1.141. ^1H NMR (300 MHz, CDCl_3) of compound 154f	371
Figure A1.142. Infrared spectrum (thin film/ NaCl) of compound 154f	372
Figure A1.143. ^1H NMR (300 MHz, CDCl_3) of compound 154g	373
Figure A1.144. Infrared spectrum (thin film/ NaCl) of compound 154g	374
Figure A1.145. ^1H NMR (300 MHz, CDCl_3) of compound 154h	375
Figure A1.146. Infrared spectrum (thin film/ NaCl) of compound 154h	376
Figure A1.147. ^1H NMR (300 MHz, CDCl_3) of compound 154i	377
Figure A1.148. Infrared spectrum (thin film/ NaCl) of compound 154i	378
Figure A1.149. ^1H NMR (300 MHz, CDCl_3) of compound 154j	379
Figure A1.150. Infrared spectrum (thin film/ NaCl) of compound 154j	380
Figure A1.151. ^1H NMR (300 MHz, CDCl_3) of compound 154m	381
Figure A1.152. Infrared spectrum (thin film/ NaCl) of compound 154m	382

Figure A1.153. ^1H NMR (300 MHz, CDCl_3) of compound 154o	383
Figure A1.154. Infrared spectrum (thin film/ NaCl) of compound 154o	384
Figure A1.155. ^1H NMR (400 MHz, CDCl_3) of compound 154p	385
Figure A1.156. Infrared spectrum (thin film/ NaCl) of compound 154p	386
Figure A1.157. ^1H NMR (300 MHz, CDCl_3) of compound 154q	387
Figure A1.158. Infrared spectrum (thin film/ NaCl) of compound 154q	388
Figure A1.159. ^1H NMR (300 MHz, CDCl_3) of compound 154n	389
Figure A1.160. Infrared spectrum (thin film/ NaCl) of compound 154n	390
Figure A1.161. ^1H NMR (500 MHz, CDCl_3) of compound 135a	391
Figure A1.162. Infrared spectrum (thin film/ NaCl) of compound 135a	392
Figure A1.163. ^{13}C NMR (125 MHz, CDCl_3) of compound 135a	392
Figure A1.164. ^1H NMR (300 MHz, CDCl_3) of compound 135b	393
Figure A1.165. Infrared spectrum (thin film/ NaCl) of compound 135b	394
Figure A1.166. ^{13}C NMR (75 MHz, CDCl_3) of compound 135b	394
Figure A1.167. ^1H NMR (300 MHz, CDCl_3) of compound 135c	395
Figure A1.168. Infrared spectrum (thin film/ NaCl) of compound 135c	396
Figure A1.169. ^{13}C NMR (75 MHz, CDCl_3) of compound 135c	396
Figure A1.170. ^1H NMR (300 MHz, CDCl_3) of compound 135d	397
Figure A1.171. Infrared spectrum (thin film/ NaCl) of compound 135d	398
Figure A1.172. ^{13}C NMR (75 MHz, CDCl_3) of compound 135d	398
Figure A1.173. ^1H NMR (300 MHz, CDCl_3) of compound 135e	399
Figure A1.174. Infrared spectrum (thin film/ NaCl) of compound 135e	400
Figure A1.175. ^{13}C NMR (75 MHz, CDCl_3) of compound 135e	400
Figure A1.176. ^1H NMR (300 MHz, CDCl_3) of compound 135f	401
Figure A1.177. Infrared spectrum (thin film/ NaCl) of compound 135f	402
Figure A1.178. ^{13}C NMR (75 MHz, CDCl_3) of compound 135f	402
Figure A1.179. ^1H NMR (300 MHz, CDCl_3) of compound 135g	403
Figure A1.180. Infrared spectrum (thin film/ NaCl) of compound 135g	404
Figure A1.181. ^{13}C NMR (75 MHz, CDCl_3) of compound 135g	404
Figure A1.182. ^1H NMR (300 MHz, CDCl_3) of compound 135h	405
Figure A1.183. Infrared spectrum (thin film/ NaCl) of compound 135h	406
Figure A1.184. ^{13}C NMR (75 MHz, CDCl_3) of compound 135h	406
Figure A1.185. ^1H NMR (300 MHz, CDCl_3) of compound 135i	407
Figure A1.186. Infrared spectrum (thin film/ NaCl) of compound 135i	408
Figure A1.187. ^{13}C NMR (75 MHz, CDCl_3) of compound 135i	408

Figure A1.188. ^1H NMR (300 MHz, CDCl_3) of compound 135j	409
Figure A1.189. Infrared spectrum (thin film/ NaCl) of compound 135j	410
Figure A1.190. ^{13}C NMR (75 MHz, CDCl_3) of compound 135j	410
Figure A1.191. ^1H NMR (300 MHz, CDCl_3) of compound 135m	411
Figure A1.192. Infrared spectrum (thin film/ NaCl) of compound 135m	412
Figure A1.193. ^{13}C NMR (75 MHz, CDCl_3) of compound 135m	412
Figure A1.194. ^1H NMR (300 MHz, CDCl_3) of compound 135n	413
Figure A1.195. Infrared spectrum (thin film/ NaCl) of compound 135n	414
Figure A1.196. ^{13}C NMR (75 MHz, CDCl_3) of compound 135n	414
Figure A1.197. ^1H NMR (400 MHz, CDCl_3) of compound 135p	415
Figure A1.198. Infrared spectrum (thin film/ NaCl) of compound 135p	416
Figure A1.199. ^{13}C NMR (100 MHz, CDCl_3) of compound 135p	416
Figure A1.200. ^1H NMR (300 MHz, CDCl_3) of compound 135q	417
Figure A1.201. Infrared spectrum (thin film/ NaCl) of compound 135q	418
Figure A1.202. ^{13}C NMR (75 MHz, CDCl_3) of compound 135q	418
Figure A1.203. ^1H NMR (500 MHz, CDCl_3) of compound 135n	419
Figure A1.204. Infrared spectrum (thin film/ NaCl) of compound 135n	420
Figure A1.205. ^{13}C NMR (125 MHz, CDCl_3) of compound 135n	420
Figure A1.206. ^1H NMR (500 MHz, CDCl_3) of compound 146	421
Figure A1.207. Infrared spectrum (thin film/ NaCl) of compound 146	422
Figure A1.208. ^{13}C NMR (125 MHz, CDCl_3) of compound 146	422
Figure A1.209. ^1H NMR (500 MHz, CDCl_3) of compound 137r	423
Figure A1.210. Infrared spectrum (thin film/ NaCl) of compound 137r	424
Figure A1.211. ^{13}C NMR (125 MHz, CDCl_3) of compound 137r	424
Figure A1.212. ^1H NMR (500 MHz, CDCl_3) of compound 154r	425
Figure A1.213. Infrared spectrum (thin film/ NaCl) of compound 154r	426
Figure A1.214. ^1H NMR (500 MHz, CDCl_3) of compound 156r	427
Figure A1.215. Infrared spectrum (thin film/ NaCl) of compound 156r	428
Figure A1.216. ^{13}C NMR (125 MHz, CDCl_3) of compound 156r	428
Figure A1.217. ^1H NMR (500 MHz, CDCl_3) of compound 135r	429
Figure A1.218. Infrared spectrum (thin film/ NaCl) of compound 135r	430
Figure A1.219. ^{13}C NMR (125 MHz, CDCl_3) of compound 135r	430
Figure A1.220. ^1H NMR (300 MHz, CDCl_3) of compound 163	431
Figure A1.221. Infrared spectrum (thin film/ NaCl) of compound 163	432
Figure A1.222. ^{13}C NMR (75 MHz, CDCl_3) of compound 163	432

Figure A1.223. ^1H NMR (500 MHz, CDCl_3) of compound 164	433
Figure A1.224. Infrared spectrum (thin film/ NaCl) of compound 164	434
Figure A1.225. ^{13}C NMR (125 MHz, CDCl_3) of compound 164	434
Figure A1.226. ^1H NMR (400 MHz, CDCl_3) of compound 165	435
Figure A1.227. Infrared spectrum (thin film/ NaCl) of compound 165	436
Figure A1.228. ^{13}C NMR (100 MHz, CDCl_3) of compound 165	436
Figure A1.229. ^1H NMR (300 MHz, CDCl_3) of compound 166	437
Figure A1.230. Infrared spectrum (thin film/ NaCl) of compound 166	438
Figure A1.231. ^{13}C NMR (75 MHz, CDCl_3) of compound 166	438
Figure A1.232. ^1H NMR (300 MHz, CDCl_3) of compound 167	439
Figure A1.233. Infrared spectrum (thin film/ NaCl) of compound 167	440
Figure A1.234. ^{13}C NMR (75 MHz, CDCl_3) of compound 167	440
Figure A1.235. ^1H NMR (300 MHz, CDCl_3) of compound 195	441
Figure A1.236. Infrared spectrum (thin film/ NaCl) of compound 195	442
Figure A1.237. ^{13}C NMR (75 MHz, CDCl_3) of compound 195	442
Figure A1.238. ^1H NMR (300 MHz, CDCl_3) of compound 168	443
Figure A1.239. Infrared spectrum (thin film/ NaCl) of compound 168	444
Figure A1.240. ^{13}C NMR (75 MHz, CDCl_3) of compound 168	444
Figure A1.241. ^1H NMR (300 MHz, CDCl_3) of compound 196	445
Figure A1.242. ^{13}C NMR (75 MHz, CDCl_3) of compound 196	446
Figure A1.243. Infrared spectrum (thin film/ NaCl) of compound 196	446
Figure A1.244. ^1H NMR (300 MHz, CDCl_3) of compound 169	447
Figure A1.245. Infrared spectrum (thin film/ NaCl) of compound 169	448
Figure A1.246. ^{13}C NMR (75 MHz, CDCl_3) of compound 169	448
Figure A1.247. ^1H NMR (300 MHz, CDCl_3) of compound 197	449
Figure A1.248. Infrared spectrum (thin film/ NaCl) of compound 197	450
Figure A1.249. ^{13}C NMR (75 MHz, CDCl_3) of compound 197	450
Figure A1.250. ^1H NMR (300 MHz, CDCl_3) of compound 171	451
Figure A1.251. Infrared spectrum (thin film/ NaCl) of compound 171	452
Figure A1.252. ^{13}C NMR (75 MHz, CDCl_3) of compound 171	452
Figure A1.253. ^1H NMR (300 MHz, CDCl_3) of compound 172	453
Figure A1.254. ^{13}C NMR (75 MHz, CDCl_3) of compound 172	454
Figure A1.255. Infrared spectrum (thin film/ NaCl) of compound 172	454
Figure A1.256. ^1H NMR (400 MHz, CDCl_3) of compound 173	455
Figure A1.257. Infrared spectrum (thin film/ NaCl) of compound 173	456

Figure A1.258. ^{13}C NMR (100 MHz, CDCl_3) of compound 173	456
Figure A1.259. ^1H NMR (500 MHz, CDCl_3) of compound 174	457
Figure A1.260. ^{13}C NMR (125 MHz, CDCl_3) of compound 174	458
Figure A1.261. Infrared spectrum (thin film/ NaCl) of compound 174	458
Figure A1.262. ^1H NMR (500 MHz, CDCl_3) of compound 175	459
Figure A1.263. Infrared spectrum (thin film/ NaCl) of compound 175	460
Figure A1.264. ^{13}C NMR (125 MHz, CDCl_3) of compound 175	460
Figure A1.265. ^1H NMR (500 MHz, CDCl_3) of compound 176	461
Figure A1.266. Infrared spectrum (thin film/ NaCl) of compound 176	462
Figure A1.267. ^{13}C NMR (125 MHz, CDCl_3) of compound 176	462
Figure A1.268. ^1H NMR (500 MHz, CDCl_3) of compound 177	463
Figure A1.269. Infrared spectrum (thin film/ NaCl) of compound 177	464
Figure A1.270. ^{13}C NMR (125 MHz, CDCl_3) of compound 177	464
Figure A1.271. ^1H NMR (300 MHz, CDCl_3) of compound 179	465
Figure A1.272. Infrared spectrum (thin film/ NaCl) of compound 179	466
Figure A1.273. ^{13}C NMR (75 MHz, CDCl_3) of compound 179	466
Figure A1.274. ^1H NMR (300 MHz, CDCl_3) of compound 170	467
Figure A1.275. Infrared spectrum (thin film/ NaCl) of compound 170	468
Figure A1.276. ^{13}C NMR (125 MHz, CDCl_3) of compound 170	468
Figure A1.277. ^1H NMR (500 MHz, CDCl_3) of compound 181	469
Figure A1.278. ^{13}C NMR (125 MHz, CDCl_3) of compound 181	470
Figure A1.279. Infrared spectrum (thin film/ NaCl) of compound 181	470
Figure A1.280. ^1H NMR (500 MHz, CDCl_3) of compound 183	471
Figure A1.281. Infrared spectrum (thin film/ NaCl) of compound 183	472
Figure A1.282. ^{13}C NMR (125 MHz, CDCl_3) of compound 183	472
Figure A1.283. ^1H NMR (500 MHz, CDCl_3) of compound 184	473
Figure A1.284. Infrared spectrum (thin film/ NaCl) of compound 184	474
Figure A1.285. ^{13}C NMR (125 MHz, CDCl_3) of compound 184	474
Figure A1.286. ^1H NMR (500 MHz, CDCl_3) of compound 137s	475
Figure A1.287. Infrared spectrum (thin film/ NaCl) of compound 137s	476
Figure A1.288. ^{13}C NMR (125 MHz, CDCl_3) of compound 137s	476
Figure A1.289. ^1H NMR (500 MHz, CDCl_3) of compound 137t	477
Figure A1.290. Infrared spectrum (thin film/ NaCl) of compound 137t	478
Figure A1.291. ^{13}C NMR (125 MHz, CDCl_3) of compound 137t	478
Figure A1.292. ^1H NMR (500 MHz, CDCl_3) of compound 137u	479

Figure A1.293. Infrared spectrum (thin film/NaCl) of compound 137u	480
Figure A1.294. ¹³ C NMR (125 MHz, CDCl ₃) of compound 137u	480
Figure A1.295. ¹ H NMR (500 MHz, CDCl ₃) of compound 137v	481
Figure A1.296. Infrared spectrum (thin film/NaCl) of compound 137v	482
Figure A1.297. ¹³ C NMR (125 MHz, CDCl ₃) of compound 137v	482
Figure A1.298. ¹ H NMR (500 MHz, CDCl ₃) of compound 137w	483
Figure A1.299. Infrared spectrum (thin film/NaCl) of compound 137w	484
Figure A1.300. ¹³ C NMR (125 MHz, CDCl ₃) of compound 137w	484
Figure A1.301. ¹ H NMR (500 MHz, CDCl ₃) of compound 137x	485
Figure A1.302. Infrared spectrum (thin film/NaCl) of compound 137x	486
Figure A1.303. ¹³ C NMR (125 MHz, CDCl ₃) of compound 137x	486
Figure A1.304. ¹ H NMR (500 MHz, CDCl ₃) of compound 137y	487
Figure A1.305. Infrared spectrum (thin film/NaCl) of compound 137y	488
Figure A1.306. ¹³ C NMR (125 MHz, CDCl ₃) of compound 137y	488
Figure A1.307. ¹ H NMR (500 MHz, CDCl ₃) of compound 137z	489
Figure A1.308. Variable Temperature ¹ H NMR (500 MHz, DMSO-d ₆) of compound 137z	490
Figure A1.309. Infrared spectrum (thin film/NaCl) of compound 137z	491
Figure A1.310. ¹³ C NMR (125 MHz, CDCl ₃) of compound 137z	491
Figure A1.311. ¹ H NMR (500 MHz, CDCl ₃) of compound 137aa	492
Figure A1.312. Infrared spectrum (thin film/NaCl) of compound 137aa	493
Figure A1.313. ¹³ C NMR (125 MHz, CDCl ₃) of compound 137aa	493
Figure A1.314. ¹ H NMR (500 MHz, CDCl ₃) of compound 137ab	494
Figure A1.315. Infrared spectrum (thin film/NaCl) of compound 137ab	495
Figure A1.316. ¹³ C NMR (125 MHz, CDCl ₃) of compound 137ab	495
Figure A1.317. ¹ H NMR (500 MHz, CDCl ₃) of compound 198	496
Figure A1.318. Infrared spectrum (thin film/NaCl) of compound 198	497
Figure A1.319. ¹³ C NMR (125 MHz, CDCl ₃) of compound 198	497
Figure A1.320. ¹ H NMR (500 MHz, CDCl ₃) of compound 185x	498
Figure A1.321. Infrared spectrum (thin film/NaCl) of compound 185x	499
Figure A1.322. ¹³ C NMR (125 MHz, CDCl ₃) of compound 185x	499
Figure A1.323. ¹ H NMR (500 MHz, CDCl ₃) of compound 185y	500
Figure A1.324. Infrared spectrum (thin film/NaCl) of compound 185y	501
Figure A1.325. ¹³ C NMR (125 MHz, CDCl ₃) of compound 185y	501
Figure A1.326. ¹ H NMR (500 MHz, C ₆ D ₆) of compound 185s	502
Figure A1.327. Infrared spectrum (thin film/NaCl) of compound 185s	503

Figure A1.328. ^{13}C NMR (125 MHz, C_6D_6) of compound 185s	503
Figure A1.329. ^1H NMR (500 MHz, CDCl_3) of compound 185t	504
Figure A1.330. Infrared spectrum (thin film/ NaCl) of compound 185t	505
Figure A1.331. ^{13}C NMR (125 MHz, CDCl_3) of compound 185t	505
Figure A1.332. ^1H NMR (500 MHz, CDCl_3) of compound 185u	506
Figure A1.333. Infrared spectrum (thin film/ NaCl) of compound 185u	507
Figure A1.334. ^{13}C NMR (125 MHz, CDCl_3) of compound 185u	507
Figure A1.335. ^1H NMR (500 MHz, CDCl_3) of compound 185v	508
Figure A1.336. Infrared spectrum (thin film/ NaCl) of compound 185v	509
Figure A1.337. ^{13}C NMR (125 MHz, CDCl_3) of compound 185v	509
Figure A1.338. ^1H NMR (500 MHz, CDCl_3) of compound 185z	510
Figure A1.339. Infrared spectrum (thin film/ NaCl) of compound 185z	511
Figure A1.340. ^{13}C NMR (125 MHz, CDCl_3) of compound 185z	511
Figure A1.341. ^1H NMR (500 MHz, CDCl_3) of compound 185w	512
Figure A1.342. Infrared spectrum (thin film/ NaCl) of compound 185w	513
Figure A1.343. ^{13}C NMR (125 MHz, CDCl_3) of compound 185w	513
Figure A1.344. ^1H NMR (500 MHz, CDCl_3) of compound 187	514
Figure A1.345. Infrared spectrum (thin film/ NaCl) of compound 187	515
Figure A1.346. ^{13}C NMR (125 MHz, CDCl_3) of compound 187	515
Figure A1.347. ^1H NMR (500 MHz, CDCl_3) of compound 188	516
Figure A1.348. Infrared spectrum (thin film/ NaCl) of compound 188	517
Figure A1.349. ^{13}C NMR (125 MHz, CDCl_3) of compound 188	517
Figure A1.350. ^1H NMR (500 MHz, CDCl_3) of compound 189a	518
Figure A1.351. NOESY (500 MHz, CDCl_3) of compound 189a	519
Figure A1.352. Infrared spectrum (thin film/ NaCl) of compound 189a	520
Figure A1.353. ^{13}C NMR (125 MHz, CDCl_3) of compound 189a	520
Figure A1.354. ^1H NMR (500 MHz, CDCl_3) of compound 189b	521
Figure A1.355. NOESY (500 MHz, CDCl_3) of compound 189b	522
Figure A1.356. Infrared spectrum (thin film/ NaCl) of compound 189b	523
Figure A1.357. ^{13}C NMR (125 MHz, CDCl_3) of compound 189b	523

APPENDIX 2

X-Ray Crystallography Reports Relevant to Chapter 2

Figure A2.1. Semicarbazone 164 is shown with 50% probability ellipsoids.....	524
Figure A2.2. Semicarbazone 164 (CCDC 686849).....	528

APPENDIX 3*Theoretical Investigation of the Unusual Stability of β -Hydroxycycloheptanones*

Figure A3.1. The Mechanisms and the Calculated Free Energies of the Dehydration Reaction.	536
--	-----

CHAPTER 3*The Catalytic Asymmetric Total Synthesis of Presilphiperfolanol Natural Products*

Figure 3.1. Presilphiperfolanol (Prebotrydial) Natural Products.....	540
Figure 3.2. Structural Reassignments of Presilphiperfolan-1 β -ol (223).....	542
Figure 3.3. Natural Products with Dehydrated or Oxidized Presilphiperfolanol Skeletons	543
Figure 3.4. Selected Co-isolated Sesquiterpenes from Rhizome <i>Echinops giganteus</i> var. <i>lelyi</i>	547
Figure 3.5. Natural and Unnatural Presilphiperfolanol Analogs Investigated for Antifungal Activity.....	551
Figure 3.6. Summary of Attempted Cross-Metathesis Reactions	571
Figure 3.7. X-ray Crystal Structures of Compounds 353 , 356 , and 224	587
Figure 3.8. Comparison of ^1H NMR Spectra of Reported and Synthetic 223 and 224	589
Figure 3.9. Summary of Spectral Comparisons (^1H and ^{13}C NMR).....	589

APPENDIX 5*Spectra Relevant to Chapter 3*

Figure A5.1. ^1H NMR (500 MHz, CDCl_3) of compound 313	705
Figure A5.2. Infrared spectrum (thin film/ NaCl) of compound 313	706
Figure A5.3. ^{13}C NMR (125 MHz, CDCl_3) of compound 313	706
Figure A5.4. ^1H NMR (500 MHz, CDCl_3) of compound 314	707
Figure A5.5. Infrared spectrum (thin film/ NaCl) of compound 314	708
Figure A5.6. ^{13}C NMR (125 MHz, CDCl_3) of compound 314	708
Figure A5.7. ^1H NMR (500 MHz, CDCl_3) of compound 315	709
Figure A5.8. Infrared spectrum (thin film/ NaCl) of compound 315	710
Figure A5.9. ^{13}C NMR (125 MHz, CDCl_3) of compound 315	710
Figure A5.10. ^1H NMR (500 MHz, CDCl_3) of compound 364	711
Figure A5.11. Infrared spectrum (thin film/ NaCl) of compound 364	712
Figure A5.12. ^{13}C NMR (125 MHz, CDCl_3) of compound 364	712
Figure A5.13. ^1H NMR (500 MHz, CDCl_3) of compound 308	713
Figure A5.14. Infrared spectrum (thin film/ NaCl) of compound 308	714

Figure A5.15. ^{13}C NMR (125 MHz, CDCl_3) of compound 308	714
Figure A5.16. ^1H NMR (500 MHz, CDCl_3) of compound 304	715
Figure A5.17. Infrared spectrum (thin film/ NaCl) of compound 304	716
Figure A5.18. ^{13}C NMR (125 MHz, CDCl_3) of compound 304	716
Figure A5.19. ^1H NMR (500 MHz, CDCl_3) of compound 319	717
Figure A5.20. Infrared spectrum (thin film/ NaCl) of compound 319	718
Figure A5.21. ^{13}C NMR (125 MHz, CDCl_3) of compound 319	718
Figure A5.22. ^1H NMR (500 MHz, CDCl_3) of compound 320	719
Figure A5.23. Infrared spectrum (thin film/ NaCl) of compound 320	720
Figure A5.24. ^{13}C NMR (125 MHz, CDCl_3) of compound 320	720
Figure A5.25. ^1H NMR (500 MHz, CDCl_3) of compound 324	721
Figure A5.26. Infrared spectrum (thin film/ NaCl) of compound 324	722
Figure A5.27. ^{13}C NMR (125 MHz, CDCl_3) of compound 324	722
Figure A5.28. ^1H NMR (500 MHz, CDCl_3) of compound 327	723
Figure A5.29. Infrared spectrum (thin film/ NaCl) of compound 327	724
Figure A5.30. ^{13}C NMR (125 MHz, CDCl_3) of compound 327	724
Figure A5.31. ^1H NMR (500 MHz, CDCl_3) of compound 339	725
Figure A5.32. Infrared spectrum (thin film/ NaCl) of compound 339	726
Figure A5.33. ^{13}C NMR (125 MHz, CDCl_3) of compound 339	726
Figure A5.34. ^1H NMR (500 MHz, CDCl_3) of compound 338	727
Figure A5.35. Infrared spectrum (thin film/ NaCl) of compound 338	728
Figure A5.36. ^{13}C NMR (125 MHz, CDCl_3) of compound 338	728
Figure A5.37. ^1H NMR (500 MHz, CDCl_3) of compound 337	729
Figure A5.38. Infrared spectrum (thin film/ NaCl) of compound 337	730
Figure A5.39. ^{13}C NMR (125 MHz, CDCl_3) of compound 337	730
Figure A5.40. ^1H NMR (500 MHz, CDCl_3) of compound 340	731
Figure A5.41. ^{13}C NMR (125 MHz, CDCl_3) of compound 340	732
Figure A5.42. Infrared spectrum (thin film/ NaCl) of compound 340	732
Figure A5.43. ^1H NMR (500 MHz, CDCl_3) of compound 365	733
Figure A5.44. Infrared spectrum (thin film/ NaCl) of compound 365	734
Figure A5.45. ^{13}C NMR (125 MHz, CDCl_3) of compound 365	734
Figure A5.46. ^1H NMR (500 MHz, CDCl_3) of compound 336	735
Figure A5.47. Infrared spectrum (thin film/ NaCl) of compound 336	736
Figure A5.48. ^{13}C NMR (125 MHz, CDCl_3) of compound 336	736
Figure A5.49. ^1H NMR (500 MHz, C_6D_6) of compound 336	737

Figure A5.50. ^{13}C NMR (125 MHz, C_6D_6) of compound 336	738
Figure A5.51. ^1H NMR (500 MHz, C_6D_6) of compound 335	739
Figure A5.52. Infrared spectrum (thin film/ NaCl) of compound 335	740
Figure A5.53. ^{13}C NMR (125 MHz, C_6D_6) of compound 335	740
Figure A5.54. ^1H NMR (500 MHz, C_6D_6) of compound 341	741
Figure A5.55. Infrared spectrum (thin film/ NaCl) of compound 341	742
Figure A5.56. ^{13}C NMR (125 MHz, C_6D_6) of compound 341	742
Figure A5.57. ^1H NMR (500 MHz, CDCl_3) of compound 342	743
Figure A5.58. Infrared spectrum (thin film/ NaCl) of compound 342	744
Figure A5.59. ^{13}C NMR (125 MHz, CDCl_3) of compound 342	744
Figure A5.60. ^1H NMR (500 MHz, CDCl_3) of compound 345	745
Figure A5.61. Infrared spectrum (thin film/ NaCl) of compound 345	746
Figure A5.62. ^{13}C NMR (125 MHz, CDCl_3) of compound 345	746
Figure A5.63. ^1H NMR (500 MHz, C_6D_6) of compound 346	747
Figure A5.64. Infrared spectrum (thin film/ NaCl) of compound 346	748
Figure A5.65. ^{13}C NMR (125 MHz, C_6D_6) of compound 346	748
Figure A5.66. ^1H NMR (500 MHz, C_6D_6) of compound 347	749
Figure A5.67. Infrared spectrum (thin film/ NaCl) of compound 347	750
Figure A5.68. ^{13}C NMR (125 MHz, C_6D_6) of compound 347	750
Figure A5.69. ^1H NMR (500 MHz, CDCl_3) of compound 351	751
Figure A5.70. Infrared spectrum (thin film/ NaCl) of compound 351	752
Figure A5.71. ^{13}C NMR (125 MHz, CDCl_3) of compound 351	752
Figure A5.72. ^1H NMR (500 MHz, CDCl_3) of compound 306	753
Figure A5.73. Infrared spectrum (thin film/ NaCl) of compound 306	754
Figure A5.74. ^{13}C NMR (125 MHz, CDCl_3) of compound 306	754
Figure A5.75. ^1H NMR (500 MHz, C_6D_6) of compound 306	755
Figure A5.76. ^{13}C NMR (125 MHz, C_6D_6) of compound 306	756
Figure A5.77. ^1H NMR (500 MHz, C_6D_6) of compound 343	757
Figure A5.78. Infrared spectrum (thin film/ NaCl) of compound 343	758
Figure A5.79. ^{13}C NMR (125 MHz, C_6D_6) of compound 343	758
Figure A5.80. ^1H NMR (500 MHz, C_6D_6) of compound 366	759
Figure A5.81. Infrared spectrum (thin film/ NaCl) of compound 366	760
Figure A5.82. ^{13}C NMR (125 MHz, C_6D_6) of compound 366	760
Figure A5.83. ^1H NMR (500 MHz, CDCl_3) of compound 352	761
Figure A5.84. Infrared spectrum (thin film/ NaCl) of compound 352	762

Figure A5.85. ^{13}C NMR (125 MHz, CDCl_3) of compound 352	762
Figure A5.86. ^1H NMR (500 MHz, C_6D_6) of compound 352	763
Figure A5.87. ^{13}C NMR (125 MHz, C_6D_6) of compound 352	764
Figure A5.88. ^1H NMR (500 MHz, CDCl_3) of compound 353	765
Figure A5.89. Infrared spectrum (thin film/ NaCl) of compound 353	766
Figure A5.90. ^{13}C NMR (125 MHz, CDCl_3) of compound 353	766
Figure A5.91. ^1H NMR (500 MHz, C_6D_6) of compound 353	767
Figure A5.92. ^{13}C NMR (125 MHz, C_6D_6) of compound 353	768
Figure A5.93. ^1H NMR (500 MHz, C_6D_6) of compound 354	769
Figure A5.94. Infrared spectrum (thin film/ NaCl) of compound 354	770
Figure A5.95. ^{13}C NMR (125 MHz, C_6D_6) of compound 354	770
Figure A5.96. ^1H NMR (500 MHz, C_6D_6) of compound 367	771
Figure A5.97. Infrared spectrum (thin film/ NaCl) of compound 367	772
Figure A5.98. ^{13}C NMR (125 MHz, C_6D_6) of compound 367	772
Figure A5.99. ^1H NMR (500 MHz, C_6D_6) of compound 355	773
Figure A5.100. Infrared spectrum (thin film/ NaCl) of compound 355	774
Figure A5.101. ^{13}C NMR (125 MHz, C_6D_6) of compound 355	774
Figure A5.102. ^1H NMR (500 MHz, C_6D_6) of compound 356	775
Figure A5.103. Infrared spectrum (thin film/ NaCl) of compound 356	776
Figure A5.104. ^{13}C NMR (125 MHz, C_6D_6) of compound 356	776
Figure A5.105. ^1H NMR (500 MHz, C_6D_6) of compound 357	777
Figure A5.106. Infrared spectrum (thin film/ NaCl) of compound 357	778
Figure A5.107. ^{13}C NMR (125 MHz, C_6D_6) of compound 357	778
Figure A5.108. ^1H NMR (500 MHz, C_6D_6) of compound 368	779
Figure A5.109. Infrared spectrum (thin film/ NaCl) of compound 368	780
Figure A5.110. ^{13}C NMR (125 MHz, C_6D_6) of compound 368	780
Figure A5.111. ^1H NMR (500 MHz, C_6D_6) of compound 223	781
Figure A5.112. Infrared spectrum (thin film/ NaCl) of compound 223	782
Figure A5.113. ^{13}C NMR (125 MHz, C_6D_6) of compound 223	782
Figure A5.114. ^1H NMR (500 MHz, C_6D_6) of compound 224	783
Figure A5.115. Infrared spectrum (thin film/ NaCl) of compound 224	784
Figure A5.116. ^{13}C NMR (125 MHz, C_6D_6) of compound 224	784
Figure A5.117. ^1H NMR (500 MHz, CD_2Cl_2) of compound 224	785
Figure A5.118. ^1H NMR comparison of reported natural compound 224 (500 MHz, C_6D_6) and synthetic compound 224 (500 MHz, C_6D_6).	786

Figure A5.119. ^1H NMR comparison of reported natural compound 224 (500 MHz, C_6D_6) and synthetic compound 223 (500 MHz, C_6D_6).	787
Figure A5.120. ^1H NMR comparison of reported natural compound 223 (400 MHz, C_6D_6) and synthetic compound 223 (500 MHz, C_6D_6).	788
Figure A5.121. ^{13}C NMR comparison of reported natural compound 223 (100 MHz, C_6D_6) and synthetic compound 223 (125 MHz, C_6D_6).	789
Figure A5.122. ^1H NMR (500 MHz, CDCl_3) of compound 286	790
Figure A5.123. Infrared spectrum (thin film/ NaCl) of compound 286	791
Figure A5.124. ^{13}C NMR (125 MHz, CDCl_3) of compound 286	791
Figure A5.125. ^1H NMR (500 MHz, CDCl_3) of compound 359	792
Figure A5.126. Infrared spectrum (thin film/ NaCl) of compound 359	793
Figure A5.127. ^{13}C NMR (125 MHz, CDCl_3) of compound 359	793
Figure A5.128. ^1H NMR (500 MHz, CDCl_3) of compound 360	794
Figure A5.129. Infrared spectrum (thin film/ NaCl) of compound 360	795
Figure A5.130. ^{13}C NMR (125 MHz, CDCl_3) of compound 360	795
Figure A5.131. ^1H NMR (500 MHz, CDCl_3) of compound 361	796
Figure A5.132. Infrared spectrum (thin film/ NaCl) of compound 361	797
Figure A5.133. ^{13}C NMR (125 MHz, CDCl_3) of compound 361	797

APPENDIX 6

X-Ray Crystallography Reports Relevant to Chapter 3

Figure A6.1. α -Hydroxyketone 353 (CCDC 889570).	798
Figure A6.2. α -Hydroxyketone 353 (CCDC 889570).	801
Figure A6.3. Tertiary alcohol 224 (CCDC 889569).	808
Figure A6.4. Tertiary alcohol 224 , crystal form A (CCDC 889569).	811
Figure A6.5. Tertiary alcohol 224 , crystal form B (CCDC 889569).	812
Figure A6.6. Tertiary Alcohol 356 (CCDC 911859).	823
Figure A6.7. Tertiary alcohol 356 , crystal form A (CCDC 889569).	826

APPENDIX 8

Theoretical Investigation of the Terpene Cyclization Pathways Relevant to Presilphiperfolanol Natural Products

Figure A8.1. Structures of terpenes and terpene alcohols of interest.	844
Figure A8.2. Possible reaction pathway to the cations that proceed to alcohols 2 , 5	

and closely related terpenes and terpene alcohol(s).....	847
Figure A8.3. Possible reaction pathway to the cation that proceeds to the epimer 224	848
Figure A8.4. Possible reaction pathway to the cation that proceeds to the epimer 224	849
Figure A8.5. Possible reaction pathway to the cations that proceed to 240, 245, 246	850
Figure A8.6. Reaction energy profiles (kcal/mol) for formation of 221–223, 240–247 computed with <i>mPW1PW91/6-31+G(d,p)//B3LYP/6-31+G(d,p)</i>	851
Figure A8.7. Reaction energy profile (kcal/mol) for formation of 224 and 398 computed with <i>mPW1PW91/6-31+G(d,p)//B3LYP/6-31+G(d,p)</i>	852

APPENDIX 11

Pd-Catalyzed Asymmetric Allylic Alkylation of Dienolates: The Synthesis of α - and γ -Quaternary Cyclohexenones

Figure A11.1. Symyx Reaction Screening of an Asymmetric Dienolate Alkylation Reaction	945
Figure A11.2. Symyx Workflow for Asymmetric Alkylation Reactions with Substrate 619	962

APPENDIX 13

Modular Synthesis of Olefin-Oxazoline (OlefOX) Ligands and Applications in Transition Metal-Catalyzed Reactions

Figure A13.1. Chiral C ₂ -Symmetric and C ₁ -Symmetric Bidentate Ligand Scaffolds	1027
Figure A13.2. Steric and Electronic Modification of the OlefOX Ligand Scaffold.....	1034

LIST OF SCHEMES

CHAPTER 1

The Construction of All-Carbon Quaternary Stereocenters Using Pd-Catalyzed Asymmetric Allylic Alkylation Reactions in Total Synthesis

Scheme 1.1. General Mechanism for Pd-Catalyzed Allylic Alkylation Reactions	4
Scheme 1.2. The Enolate Alkylation Problem and Approaches to Selective Enolate Formation.....	5
Scheme 1.3. Tsuji Reactions for the Allylation of Non-Shielded, Non-Stabilized Enolates	6
Scheme 1.4. Pd-Catalyzed Asymmetric Allylic Alkylation Reactions with Allyl Enol Carbonate, Silyl Enol Ether, and β -Ketoester Substrate Classes	8
Scheme 1.5. Total Synthesis of Hamigeran B.....	13
Scheme 1.6. Total Synthesis of Allocyathin B ₂ and Formal Synthesis of Erinacine A.....	15
Scheme 1.7. Total Synthesis of Dichroanone.....	17
Scheme 1.8. Total Synthesis of Liphagal.....	19
Scheme 1.9. Total Syntheses of Laurencenone C, α -Chamigrene, the Proposed Structure of Laurencenone B, and Elatol.....	22
Scheme 1.10. Formal Synthesis of Platencin.....	26
Scheme 1.11. Formal Synthesis of Hamigeran B	28
Scheme 1.12. Extension of β -Ketoester Substrate Scope to Vinylogous Thioester Scaffolds.....	29
Scheme 1.13. Total Synthesis of Carissone and Formal Synthesis of α -Eudesmol	30
Scheme 1.14. Total Synthesis of Cassiol	31
Scheme 1.15. Total Syntheses of Flustramides A and B, Flustramines A and B	34
Scheme 1.16. Double Enantioselective Decarboxylative Allylic Alkylation Reactions	36
Scheme 1.17. Total Syntheses of Cyanthiwiggins B, F, and G.....	37

CHAPTER 2

Catalytic Asymmetric Synthesis of Cyclopentanoid and Cycloheptanoid Core Structures Using Pd-Catalyzed Asymmetric Alkylation

Scheme 2.1. Synthesis of Parent Vinylogous Ester 147 and β -Ketoester Substrates 148	50
Scheme 2.2. Observation of the Unusual Reactivity of β -Hydroxycycloheptanone 154a	54
Scheme 2.3. Proposed Ring Contraction Mechanism.....	55
Scheme 2.4. Attempted Stork–Danheiser Manipulations on Unsubstituted Rings.....	56
Scheme 2.5. Organometallic Addition to Vinylogous Ester 149a	63

Scheme 2.6. Ring Contraction Screen on β -Hydroxyketone 154r	64
Scheme 2.7. Confirmation of Absolute Stereochemistry and Multi-Gram Scale Reactions	66
Scheme 2.8. Functionalization of Multiple Acylcyclopentene Reactive Sites.....	70
Scheme 2.9. Stepwise and One-Pot Formation of Cycloheptenone 137a	72
Scheme 2.10. Synthesis of β -Substituted Cycloheptenones	73
Scheme 2.11. General Reaction Mechanism for Carbonyl Transposition	73
Scheme 2.12. Different Work-Up Conditions for Carbonyl Transposition Reactions	
Employing sp^3 versus sp^2 Carbon Nucleophiles.....	76
Scheme 2.13. Synthesis of Additional [7–6] Bicycles and [7–5–5] Tricycles.....	78

APPENDIX 3

Theoretical Investigation of the Unusual Stability of β -Hydroxycycloheptanones

Scheme A3.1. Experimental Observations of the Unusual Stability of β -Hydroxycycloheptanone ...	535
---	-----

CHAPTER 3

The Catalytic Asymmetric Total Synthesis of Presilphiperfolanol Natural Products

Scheme 3.1. Modified Bohlmann–Hanson Mechanism for Presilphiperfolane Biosynthesis.....	545
Scheme 3.2. Rearrangement of Presilphiperfolan-8 α -ol to Other Sesquiterpene Skeletons	548
Scheme 3.3. Rearrangement of Presilphiperfolanols to Other Sesquiterpene Natural Products	549
Scheme 3.4. Strategy for the Rearrangement of Caryophyllenyl and Isocaryophyllenyl Skeletons....	552
Scheme 3.5. Reported Rearrangements of Caryophyllene Skeletons.....	554
Scheme 3.6. Reported Rearrangements of Isocaryophyllene (262).....	555
Scheme 3.7. Synthesis of Key Tricyclic Olefin Intermediate 283	557
Scheme 3.8. Weyerstahl's Completion of (\pm)-Presilphiperfolan-9 α -ol (222)	559
Scheme 3.9. Synthesis of Radical Cyclization Precursor 297	560
Scheme 3.10. Radical Cyclization Cascades with Precursors 297 and 298	561
Scheme 3.11. Attempted Epimerization of the C(1)-Methine Hydrogen of Ketone 285	562
Scheme 3.12. Retrosynthetic Analysis of Presilphiperfolanol Natural Products.....	564
Scheme 3.13. Conjugate Addition Cascade and Robinson Annulation Strategy	565
Scheme 3.14. Evaluation of a Simple Model System Based on Acylcyclopentene 135a	567
Scheme 3.15. Improved Acylation and Alkylation of Vinylogous Ester 147	568
Scheme 3.16. Asymmetric Alkylation and Ring Contraction Sequence with β -Ketoester 313	569
Scheme 3.17. Examples of Attempted Cross-Metathesis Reactions with Acylcyclopentene 308	570
Scheme 3.18. Synthesis of Methyl Ketone 324	572

Scheme 3.19. Various Attempts to Prepare Acylcyclopentene 306	573
Scheme 3.20. Retrosynthetic Analysis of Presilphiperfolanol Natural Products.....	576
Scheme 3.21. Synthesis of Isoprenol-Derived Acylimidazole 339	577
Scheme 3.22. Asymmetric Alkylation and Ring Contraction Sequence with β -Ketoester 338	578
Scheme 3.23. IMDA Reaction on Substrate 335	579
Scheme 3.24. Planned IMDA Reaction on Substrate 343	580
Scheme 3.25. Modification of Acylcyclopentene 336 and Synthesis of Silyl Dienol Ether 343	583
Scheme 3.26. IMDA/Rubottom Oxidation with Silyl Dienol Ether 343	584
Scheme 3.27. Wittig Methylenation and Hydrogenation of α -Hydroxyketone 353	585
Scheme 3.28. Wittig Methylenation and Hydrogenation of α -Hydroxyketone 352	587
Scheme 3.29. Proposed Biosynthesis of Presilphiperfolan-1 β -ol (223) and Structural Revision of Reported "Presilphiperfolan-1-ol" (223)	590
Scheme 3.30. Divergent Strategy for the Preparation of Presilphiperfolan-9 α -ol (222)	592
Scheme 3.31. Planned Formal Synthesis of Presilphiperfolan-9 α -ol via IMDA Substrate 343	594
Scheme 3.32. Planned Formal Synthesis of Presilphiperfolan-9 α -ol via IMDA Substrate 361	595
Scheme 3.33. Planned Biomimetic Rearrangements of Synthetic Presilphiperfolanols 223 and 222	597

APPENDIX 4

Synthetic Summary for Presilphiperfolanol Natural Products

Scheme A4.1. Retrosynthetic Analysis of Presilphiperfolanol Natural Products	699
Scheme A4.2. Synthesis of Isoprenyl Carbamate 339	699
Scheme A4.3. Synthesis of Vinylogous Ester 147	699
Scheme A4.4. Asymmetric Alkylation/Ring Contraction Sequence to Methyl/Isoprenyl Acylcyclopentene 336	700
Scheme A4.5. Synthesis of gem-Dimethyl Acylcyclopentene 306	700
Scheme A4.6. IMDA/Rubottom Sequence and Completion of Presilphiperfolan-1 β -ol (223)	701
Scheme A4.7. Synthesis of Alcohols 355 and 356	701
Scheme A4.8. Synthesis of Presilphiperfolan-1 β -ol (223) and Alcohol 224	701
Scheme A4.9. Planned Formal Synthesis of Presilphiperfolan-9 α -ol (222) via IMDA Substrate 343	702
Scheme A4.10. Planned Formal Synthesis of Presilphiperfolan-9 α -ol (222) via IMDA Substrate 361	702

APPENDIX 8*Theoretical Investigation of the Terpene Cyclization Pathways
Relevant to Presilphiperfolanol Natural Products*

Scheme A8.1. Carbocation rearrangements leading to terpenes 240 and 399 and terpene alcohols, 222–224 , 240 , 243 , and 245–246	845
Scheme A8.2. Carbocation rearrangements leading to the epimer presilphiperfolanol 398 and terpene 224	846

APPENDIX 9*Enantioselective Protonations*

Scheme A9.1. Enantioselective Tautomerization of an Isolated Enol.....	856
Scheme A9.2. Enzymatic Decarboxylative Protonation with Wild-Type and Mutant Decarboxylases.....	858
Scheme A9.3. Enzymatic Oxidation/Decarboxylation/Protonation/Oxidation Cascade.....	860
Scheme A9.4. Enzymatic Hydrolysis of Enol Acetates.....	860
Scheme A9.5. Kim's Enolate Protonation.....	864
Scheme A9.6. Eames's Enolate Protonation.....	864
Scheme A9.7. Rouden's Decarboxylative Protonation	865
Scheme A9.8. Donohoe's Partial Pyrrole Reduction.....	866
Scheme A9.9. Rueping's Quinoline Reduction/Protonation	867
Scheme A9.10. Yamamoto's Enol Silane Protonation.....	868
Scheme A9.11. Yanagisawa's Lithium Enolate Protonation	869
Scheme A9.12. Yanagisawa's Enol Silane Protonation	870
Scheme A9.13. Levacher's Enol Silane Protonation.....	871
Scheme A9.14. Deng's Conjugate Addition/Protonation	872
Scheme A9.15. Tan's Conjugate Addition/Protonation.....	873
Scheme A9.16. Hénin/Muzart Norrish Type II Fragmentation/Protonation	873
Scheme A9.17. Fu's Addition of Hydrazoic Acid to Ketenes Followed by Curtius Rearrangement.....	874
Scheme A9.18. Fu's Addition of Alcohols to Ketenes	876
Scheme A9.19. Rovis' Protonation of Chloroenolates	877
Scheme A9.20. Scheidt's Protonation of Homoenolate Equivalents.....	878
Scheme A9.21. Frost's Rh-Catalyzed Conjugate Addition/Protonation.....	879
Scheme A9.22. Sibi's Rh-Catalyzed Conjugate Addition/Protonation	880
Scheme A9.23. Hayashi's Rh-Catalyzed Conjugate Addition/Protonation	880

Scheme A9.24. Conjugate Addition/Protonation with a Nitrogen Nucleophile Catalyzed by Palladium.....	881
Scheme A9.25. Divergent Pathway Consisting of β -Hydride Elimination, Hydride Transfer, and Protonation	882
Scheme A9.26. Friedel–Crafts-Type Conjugate Addition Followed by Enantioselective Protonation	883
Scheme A9.27. Trauner's Nazarov Cyclization/Enantioselective Protonation	884
Scheme A9.28. Stoltz' Palladium-Catalyzed Decarboxylative Protonation Reactions.....	885
Scheme A9.29. Kanai and Shibasaki's Gadolinium-Catalyzed Protonation Reactions.....	887
Scheme A9.30. Radical Conjugate Addition Followed by Enantioselective H-Atom Transfer.....	888

APPENDIX 10

Pd-Catalyzed Asymmetric Allylic Alkylation of α -Oxygenated Enolates: Synthetic Studies and Mechanistic Hypotheses

Scheme A10.1. Strategies for the Formation of Tertiary α -Oxygenated Ketone Motifs	897
Scheme A10.2. Asymmetric Alkylation of Linear α -Oxygenated Substrates by Trost.....	898
Scheme A10.3. Mechanistic Pathways for the Asymmetric Alkylation of α -Oxygenated Substrates.....	899
Scheme A10.4. Asymmetric Alkylation of Cyclic α -Oxygenated Substrates by Trost.....	900
Scheme A10.5. Asymmetric Alkylation of Additional Cyclic α -Oxygenated Substrates by Trost.....	901
Scheme A10.6. Asymmetric Alkylation of Dioxanone Derivatives and Further Manipulations.....	902
Scheme A10.7. Asymmetric Alkylation of α -Oxygenated Silyl Enol Ether Substrates.....	903
Scheme A10.8. Asymmetric Alkylation of α -Oxygenated Enol Carbonate Substrates	904
Scheme A10.9. Asymmetric Alkylation of a β -Ester Enol Carbonate Substrate	904
Scheme A10.10. Synthesis of α -Acyloxy β -Ketoester Substrates.....	905
Scheme A10.11. Asymmetric Alkylation of a Vinylogous Ester-Derived β -Ketoester Substrate	906
Scheme A10.12. Asymmetric Alkylation of a Tetralone-Derived β -Ketoester Substrate	909
Scheme A10.13. Asymmetric Alkylation of <i>N</i> -Acyl Lactams	911
Scheme A10.14. Interacting Substrate Types and Possible Transition States	912

APPENDIX 11

Pd-Catalyzed Asymmetric Allylic Alkylation of Dienolates: The Synthesis of α - and γ -Quaternary Cyclohexenones

Scheme A11.1. Pd-Catalyzed α -Selective and γ -Selective Alkylation of Dienolates	928
---	-----

Scheme A11.2. Pd-Catalyzed γ -Selective Alkylation of Dienolates in Total Synthesis	930
Scheme A11.3. Pd-Catalyzed γ -Alkylation Reactions	931
Scheme A11.4. Asymmetric Alkylation of Dienolates	933
Scheme A11.5. Unoptimized Synthetic Route Toward Monocyclic Substrates.....	934
Scheme A11.6. Unoptimized Synthetic Route Toward Bicyclic Substrates.....	935
Scheme A11.7. Early Investigation of δ -Ketoester Substrates	936
Scheme A11.8. Possible Inner-Sphere Transition States for Asymmetric Dienolate Alkylation	937
Scheme A11.9. δ -Ketoester Substrates Inspired by Przewalskin B and Nootkastatin 1	940
Scheme A11.10. Synthesis of Monocyclic Substrates	941
Scheme A11.11. Synthesis of Bicyclic Substrates.....	942
Scheme A11.12. Asymmetric Alkylation of Additional δ -Ketoester Substrates	943
Scheme A11.13. Comparison of Asymmetric Alkylation Substrates	946

APPENDIX 12

Progress Toward the Total Synthesis of Crinine and Related Amaryllidaceae Alkaloids

Scheme A12.1. Representative <i>Amaryllidaceae</i> Alkaloids	971
Scheme A12.2. Pd-Catalysis Strategies Toward Crinine and Related <i>Amaryllidaceae</i> Alkaloids	973
Scheme A12.3. Development of Novel Asymmetric Reactions by Interception of Pd Enolates	974
Scheme A12.4. α -Arylation/ α -Allylation Approach to Crinine	976
Scheme A12.5. A Possible Mechanistic Pathway for α -Arylation/ α -Allylation Reaction.....	977
Scheme A12.6. Allylative Dearomatization Approach to Crinine	979
Scheme A12.7. Summary of Allylative Dearomatization Screening Efforts	980
Scheme A12.8. Asymmetric Aerobic Pd(II)-Catalyzed Wacker-Type Heterocyclizations.....	982
Scheme A12.9. Oxidative Cyclization Approach to Crinine.....	983
Scheme A12.10. Stereochemical Outcomes of <i>Anti</i> -Aminopalladation with Substrates 717 and 718	984
Scheme A12.11. Stereochemical Outcomes of <i>Syn</i> -Aminopalladation with Substrates 717 and 718	984
Scheme A12.12. Stereochemical Outcomes of <i>Syn</i> and <i>Anti</i> -Aminopalladation with Substrate 723	985
Scheme A12.13. C–H Activation/Intramolecular Cyclization Approach to Crinine	986
Scheme A12.14. Retrosynthetic Analysis of Oxocrinine.....	988
Scheme A12.15. Stork Enamine Alkylation and Robinson Annulation.....	989
Scheme A12.16. Attempted Allyl Functionalization	990

Scheme A12.17. Proposed Completion of (±)-Oxocrinine by Allyl Functionalization	991
Scheme A12.18. Metalloenamine Alkylation Using Aziridines and Amine Carbamoylation.....	992
Scheme A12.19. Planned Completion of (±)-Oxocrinine by Pyrrolidine Formation	994
Scheme A12.20. Synthesis of Oxidative Cyclization and C-H Activation Substrates	995
Scheme A12.21. Reported Pd-Catalyzed α -Arylation/ α -Allylation of Vinylogous Esters	997
Scheme A12.22. Reported Pd-Catalyzed α -Arylation of β -Ester Lactams	998
Scheme A12.23. Reported Pd(0) and Ir(I)-Catalyzed Allylative Dearomatization Reactions	999
Scheme A12.24. Reported Cyclohexadienone Desymmetrization with Sulfonamide Nucleophiles	1000

APPENDIX 13

Modular Synthesis of Olefin-Oxazoline (OlefOX) Ligands and Applications in Transition Metal-Catalyzed Reactions

Scheme A13.1. Glorius' Application of OlefOX Ligands (801) to Rh-Catalyzed Conjugate Additions.....	1028
Scheme A13.2. Glorius' Synthesis of OlefOX Ligands 801	1029
Scheme A13.3. Retrosynthetic Analysis of OlefOX Ligands	1030
Scheme A13.4. Divergent Synthesis of PHOX and OlefOX Ligands from Bromoaryl Oxazolines.....	1031
Scheme A13.5. A General Synthesis of OlefOX Ligands by Pd Catalyzed Cross-Coupling.....	1032
Scheme A13.6. Attempted Transition-Metal Catalyzed Reactions with Achiral OlefOX Ligand 801b	1039
Scheme A13.7. Synthesis of Spiro-Ketimine-Olefin Ligands.....	1040
Scheme A13.8. Synthesis of Novel η^2 - η^6 Chiral C ₁ N-Ligands from a Common Precursor	1042
Scheme A13.9. Recent Developments in OlefOX Ligand Synthesis.....	1043
Scheme A13.10. Recent Developments in the Design of Novel Chiral C ₁ -Symmetric Ligands.....	1044

LIST OF TABLES

CHAPTER 2

Catalytic Asymmetric Synthesis of Cyclopentanoid and Cycloheptanoid Core Structures Using Pd-Catalyzed Asymmetric Alkylation

Table 2.1. Solvent and Ligand Effects on Enantioselective Decarboxylative Allylation	51
Table 2.2. Scope of the Pd-Catalyzed Enantioselective Alkylation of Cyclic Vinylogous Esters	53
Table 2.3. Ring Contraction Reaction Optimization	59
Table 2.4. Ring Contraction Reaction Substrate Scope	61
Table 2.5. Scope of Organometallic Addition/Elimination	74
Table 2.6. Formation of Bi- and Tricyclic Systems Through Ring-Closing Metathesis	77
Table 2.7. Sources of Grignard and Organolithium Reagents	213
Table 2.8. Methods for the Determination of Enantiomeric Excess (Chiral HPLC and SFC)	259
Table 2.9. Methods for the Determination of Enantiomeric Excess (Chiral GC)	261

APPENDIX 2

X-Ray Crystallography Reports Relevant to Chapter 2

Table A2.1. Crystal data and structure refinement for semicarbazone 164 (CCDC 686849)	525
Table A2.2. Atomic coordinates ($\times 10^4$) and equivalent isotropic displacement parameters ($\text{\AA}^2 \times 10^3$) for semicarbazone 164 (CCDC 686849)	528
Table A2.3. Bond lengths [\AA] and angles [$^\circ$] for semicarbazone 164 (CCDC 686849)	530
Table A2.4. Anisotropic displacement parameters ($\text{\AA}^2 \times 10^4$) for semicarbazone 164 (CCDC 686849)	532
Table A2.5. Hydrogen bonds for semicarbazone 164 (CCDC 686849) [\AA and $^\circ$]	533

APPENDIX 3

Theoretical Investigation of the Unusual Stability of β -Hydroxycycloheptanones

Table A3.1. The Ring Strain Enthalpies of Six- and Seven-Membered Rings.	537
---	-----

CHAPTER 3

The Catalytic Asymmetric Total Synthesis of Presilphiperfolanol Natural Products

Table 3.1. Metal-Catalyzed 1,4-Hydroboration/Oxidation Screen	582
---	-----

Table 3.2. Intramolecular Diels–Alder/Rubottom Oxidation Screening.....	646
Table 3.3. Methods for the Determination of Enantiomeric Excess (Chiral HPLC)	670
Table 3.4. Comparison of Optical Rotation Data for Synthetic and Reported Natural ³ “Presilphiperfolan-1-ol” (224) and Reported Natural “9-epi-Presilphiperfolan-1-ol” (223).....	672
Table 3.5. Comparison of ¹ H NMR Data for Synthetic and Reported Natural “Presilphiperfolan-1-ol” (224)	673
Table 3.6. Comparison of ¹ H NMR Data for Synthetic and Reported Natural “9-epi-Presilphiperfolan-1-ol” (223).....	674
Table 3.7. Comparison of ¹³ C NMR Data for Synthetic and Reported Natural “Presilphiperfolan-1-ol” (224), Synthetic and Reported Natural “9-epi-Presilphiperfolan-1-ol” (223).....	675
Table 3.8. Comparison of ¹ H NMR Data for Synthetic and Reported Synthetic 224	676
Table 3.9. Comparison of ¹³ C NMR Data for Synthetic and Reported Synthetic 224	676

APPENDIX 6

X-Ray Crystallography Reports Relevant to Chapter 3

Table A6.1. Crystal data and structure refinement for α -hydroxyketone 353 (CCDC 889570).....	799
Table A6.2. Atomic coordinates ($\times 10^4$) and equivalent isotropic displacement parameters ($\text{\AA}^2 \times 10^3$) for α -hydroxyketone 353 (CCDC 889570).....	802
Table A6.3. Bond lengths [\AA] and angles [$^\circ$] for 353 (CCDC 889570)	803
Table A6.4. Anisotropic displacement parameters ($\text{\AA}^2 \times 10^4$) for α -hydroxyketone 353 (CCDC 889570).	806
Table A6.5. Hydrogen coordinates ($\times 10^3$) and isotropic displacement parameters ($\text{\AA}^2 \times 10^3$) for α -hydroxyketone 353 (CCDC 889570).....	807
Table A6.6. Hydrogen bonds for α -hydroxyketone 353 (CCDC 889570) [\AA and $^\circ$].....	807
Table A6.7. Crystal data and structure refinement for tertiary alcohol 224 (CCDC 889569).....	809
Table A6.8. Atomic coordinates ($\times 10^4$) and equivalent isotropic displacement parameters ($\text{\AA}^2 \times 10^3$) for tertiary alcohol 224 (CCDC 889569).....	813
Table A6.9. Bond lengths [\AA] and angles [$^\circ$] for tertiary alcohol 224 (CCDC 889569)	814
Table A6.10. Anisotropic displacement parameters ($\text{\AA}^2 \times 10^4$) for tertiary alcohol 224 (CCDC 889569).....	820
Table A6.11. Hydrogen coordinates ($\times 10^3$) and isotropic displacement parameters	

($\text{\AA}^2 \times 10^3$) for tertiary alcohol 224 (CCDC 889569)	821
Table A6.12. Hydrogen bonds for tertiary alcohol 224 (CCDC 889569) [\AA and $^\circ$]	822
Table A6.13. Crystal data and structure refinement for tertiary alcohol 356 (CCDC 911859).....	824
Table A6.14. Atomic coordinates ($\times 10^4$) and equivalent isotropic displacement parameters ($\text{\AA}^2 \times 10^3$) for tertiary alcohol 356 (CCDC 911859).....	827
Table A6.15. Bond lengths [\AA] and angles [$^\circ$] for tertiary alcohol 356 (CCDC 911859)	828
Table A6.16. Anisotropic displacement parameters ($\text{\AA}^2 \times 10^4$) for tertiary alcohol 356 (CCDC 911859).....	834
Table A6.17. Hydrogen coordinates ($\times 10^3$) and isotropic displacement parameters ($\text{\AA}^2 \times 10^3$) for tertiary alcohol 356 (CCDC 911859)	835
Table A6.18. Hydrogen bonds for tertiary alcohol 356 (CCDC 911859) [\AA and $^\circ$]	836

APPENDIX 7

Theoretical Investigation of the Relative Free Energies of Presilphiperfolanol Natural Products and Synthetic Intermediates

Table A7.1. Relative Free Energies of Various Presilphiperfolane Structures	838
---	-----

APPENDIX 10

Pd-Catalyzed Asymmetric Allylic Alkylation of α -Oxygenated Enolates: Synthetic Studies and Mechanistic Hypotheses

Table A10.1. Solvent and Ligand Effects on the Asymmetric Alkylation of a Vinylogous Ester-Derived β -Ketoester Substrate.....	907
---	-----

APPENDIX 11

Pd-Catalyzed Asymmetric Allylic Alkylation of Dienolates: The Synthesis of α - and γ -Quaternary Cyclohexenones

Table A11.1. Further Optimization of Pd-Catalyzed Asymmetric Dienolate Alkylation.....	939
--	-----

APPENDIX 12

Progress Toward the Total Synthesis of Crinine and Related Amaryllidaceae Alkaloids

Table A12.1. Summary of α -Arylation/ α -Allylation Screening Efforts.....	978
--	-----

APPENDIX 13*Modular Synthesis of Olefin-Oxazoline (OlefOX) Ligands and Applications in Transition Metal-Catalyzed Reactions*

Table A13.1. Region C Modification of OlefOX Ligands.....	1036
Table A13.2. Region A Modification of OlefOX Ligands.....	1037

APPENDIX 14**1064***Notebook Cross-Reference*

Table A14.1. Notebook Cross-Reference for Compounds in Chapter 2	1065
Table A14.2. Notebook Cross-Reference for Compounds in Chapter 3	1074
Table A14.3. Notebook Cross-Reference for Compounds in Appendix 10	1078
Table A14.4. Notebook Cross-Reference for Additional Compounds in Appendix 10.....	1079
Table A14.5. Notebook Cross-Reference for Compounds in Appendix 11	1079
Table A14.6. Notebook Cross-Reference for Compounds in Appendix 12	1080
Table A14.7. Notebook Cross-Reference for Compounds in Appendix 13	1082

LIST OF ABBREVIATIONS

Å	Ångstrom
λ	wavelength
μ	micro
μ waves	microwave irradiation
$[\alpha]_D$	specific rotation at wavelength of sodium D line
[H]	reduction
[O]	oxidation
°C	degrees Celsius
Ac	acetyl
acac	acetylacetonate
AcOH	acetic acid
AIBN	2,2'-azobisisobutyronitrile
Anal.	combustion elemental analysis
APCI	atmospheric pressure chemical ionization
app	apparent
aq	aqueous
Ar	aryl
atm	atmosphere
B3LYP	3-parameter hybrid Becke exchange/ Lee–Yang–Parr correlation functional
BAr _F	tetrakis(3,5-bis(trifluoromethyl)phenyl)borate
Bn	benzyl
Boc	<i>tert</i> -butyloxycarbonyl
BOM	benzyloxymethyl

BOX	bis-oxazoline ligand
bp	boiling point
br	broad
Bu	butyl
Bz	benzoyl
<i>c</i>	concentration for specific rotation measurements
ca.	about (Latin circa)
calc'd	calculated
CAN	ceric ammonium nitrate
cat	catalytic
Cbz	carbobenzyloxy
CCDC	Cambridge Crystallographic Data Centre
CDI	1,1'-carbonyldiimidazole
cf.	compare (Latin confer)
CI	chemical ionization
cm ⁻¹	wavenumber(s)
cod	1,5-cyclooctadiene
comp	complex
Cp	cyclopentadienyl
Cy	cyclohexyl
CyCH ₃	methylcyclohexane
Cy-JohnPhos	(2-biphenyl)dicyclohexylphosphine
d	doublet
D	deuterium
DABCO	1,4-diazabicyclo[2.2.2]octane
dba	dibenzylideneacetone
DBU	1,8-diazabicyclo[5.4.0]undec-7-ene

DCE	1,2-dichloroethane
DDQ	2,3-dichloro-5,6-dicyano- <i>p</i> -benzoquinone
dec	decomposition
DFT	density functional theory
DIBAL	diisobutylaluminum hydride
DMA	<i>N,N</i> -dimethylacetamide
DMAD	dimethyl acetylenedicarboxylate
DMAP	4-dimethylaminopyridine
dmdba	bis(3,5-dimethoxybenzylidene)acetone
DMDO	dimethyldioxirane
DME	1,2-dimethoxyethane
DMF	<i>N,N</i> -dimethylformamide
DMSO	dimethyl sulfoxide
dppb	1,4-bis(diphenylphosphino)butane
dppf	1,1'-bis(diphenylphosphino)ferrocene
dr	diastereomeric ratio
e.g.	for example (Latin <i>exempli gratia</i>)
E_A	activation energy
EC ₅₀	median effective concentration (50%)
EDC	<i>N</i> -(3-dimethylaminopropyl)- <i>N'</i> -ethylcarbodiimide
ee	enantiomeric excess
EI	electron impact
equiv	equivalent
ESI	electrospray ionization
Et	ethyl
EtOAc	ethyl acetate
FAB	fast atom bombardment

FID	flame ionization detector
g	gram(s)
GC	gas chromatography
gCOSY	gradient-selected correlation spectroscopy
h	hour(s)
$h\nu$	light
HBPin	4,4,5,5-tetramethyl-1,3,2-dioxaborolane; pinacolborane
HFIP	1,1,1,3,3,3-hexafluoro-2-propanol
HMDS	1,1,1,3,3,3-hexamethyldisilazane
HMPA	hexamethylphosphoramide
HPLC	high-performance liquid chromatography
HRMS	high-resolution mass spectroscopy
Hz	hertz
i.e.	that is (Latin id est)
<i>i</i> -Bu	<i>iso</i> -butyl
IBX	2-iodoxybenzoic acid
IC ₅₀	median inhibition concentration (50%)
IMDA	Intramolecular Diels–Alder reaction
IPA	isopropanol, 2-propanol
<i>i</i> -Pr	isopropyl
IR	infrared (spectroscopy)
IRC	intrinsic reaction coordinate
J	coupling constant
K	Kelvin(s) (absolute temperature)
kcal	kilocalorie
KHMDS	potassium hexamethyldisilazide
L	liter; ligand

LDA	lithium diisopropylamide
lit.	literature value
m	multiplet; milli
<i>m</i>	meta
M	metal; molar; molecular ion
<i>m/z</i>	mass to charge ratio
<i>m</i> -CPBA	<i>meta</i> -chloroperoxybenzoic acid
Me	methyl
MHz	megahertz
min	minute(s)
MM	mixed method
MMPP	magnesium monoperoxyphthalate
mol	mole(s)
MOM	methoxymethyl
mp	melting point
Ms	methanesulfonyl (mesyl)
MS	molecular sieves
MVK	methyl vinyl ketone
n	nano
N	normal
nbd	norbornadiene
NBS	<i>N</i> -bromosuccinimide
<i>n</i> -Bu	butyl
Ni(cod) ₂	bis(1,5-cyclooctadiene)nickel(0)
NMO	<i>N</i> -methylmorpholine <i>N</i> -oxide
NMR	nuclear magnetic resonance
NOE	nuclear Overhauser effect

NOESY	nuclear Overhauser enhancement spectroscopy
Nu	nucleophile
<i>o</i>	ortho
OlefOX	olefin-oxazoline ligand
<i>p</i>	para
PCC	pyridinium chlorochromate
Pd/C	palladium on carbon
PDC	pyridinium dichromate
Ph	phenyl
pH	hydrogen ion concentration in aqueous solution
PhCH ₃	toluene
PhH	benzene
PhMe	toluene
PHOX	phosphinooxazoline ligand
Piv	pivaloyl
<i>pK_a</i>	<i>pK</i> for association of an acid
PMB	<i>p</i> -methoxybenzyl
pmdba	bis(4-methoxybenzylidene)acetone
ppm	parts per million
PPTS	pyridinium <i>p</i> -toluenesulfonate
Pr	propyl
Py	pyridine
PyOX	pyridyl oxazoline ligand
q	quartet
R	generic for any atom or functional group
Ref.	reference
<i>R_f</i>	retention factor

rt	room temperature
s	singlet or strong or selectivity factor
sat.	saturated
Selectfluor	1-chloromethyl-4-fluoro-1,4-diazoniabicyclo[2.2.2]octane bis(tetrafluoroborate)
SFC	supercritical fluid chromatography
S _N 2	second-order nucleophilic substitution
S _N 2'	nucleophilic substitution with allylic rearrangement
sp	sparteine
sp.	species
t	triplet
TBAA	tetrabutylammonium acetate
TBAF	tetrabutylammonium fluoride
TBAI	tetrabutylammonium iodide
TBAT	tetrabutylammonium difluorotriphenylsilicate
TBDPS	<i>tert</i> -butyldiphenylsilyl
TBHP	<i>tert</i> -butyl hydroperoxide
TBME	<i>tert</i> -butyl methyl ether
TBS	<i>tert</i> -butyldimethylsilyl
<i>t</i> -Bu	<i>tert</i> -butyl
TES	triethylsilyl
Tf	trifluoromethanesulfonyl (triflyl)
TFA	trifluoroacetic acid
TFAA	trifluoroacetic anhydride
TFE	2,2,2-trifluoroethanol
THF	tetrahydrofuran

TIPS	triisopropylsilyl
TLC	thin-layer chromatography
TMEDA	<i>N,N,N',N'</i> -tetramethylethylenediamine
TMG	1,1,3,3-tetramethylguanidine
TMS	trimethylsilyl
TOF	time-of-flight
Tol	tolyl
TON	turnover number
t_R	retention time
Ts	<i>p</i> -toluenesulfonyl (tosyl)
UV	ultraviolet
<i>v/v</i>	volume to volume
w	weak
<i>w/v</i>	weight to volume
X	anionic ligand or halide
Xantphos	4,5-bis(diphenylphosphino)-9,9-dimethylxanthene

CHAPTER 1

The Construction of All-Carbon Quaternary Stereocenters Using Pd-Catalyzed Asymmetric Allylic Alkylation Reactions in Total Synthesis[†]

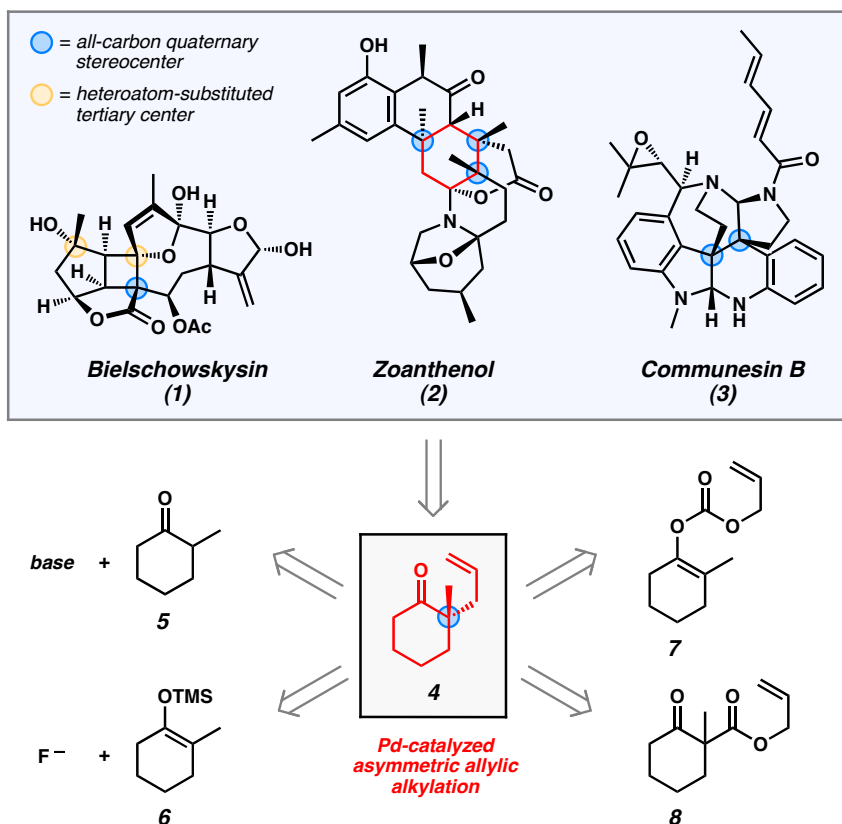
1.1 INTRODUCTION AND BACKGROUND

Complex natural products serve a vital role in chemistry as a driving force for the invention of novel chemical transformations.¹ The fundamental synthetic challenges posed by all-carbon quaternary stereocenters² contained in many natural products have inspired the development of novel synthetic methods for the enantioselective construction these important motifs. In particular, the research area of Pd-catalyzed asymmetric allylic alkylation^{3,4} has significantly advanced in response to synthetic limitations identified during efforts toward complex molecules (Figure 1.1). Modern catalytic enantioselective methods of this type have led to the development of novel strategies for the efficient and direct assembly of challenging cyclic core structures in many natural products and additionally provided powerful, broadly applicable tools for the

[†] A similar version has been published. See: Hong, A. Y.; Stoltz, B. M. *Eur. J. Org. Chem.* **2013**, Early View, DOI: 10.1002/ejoc.201201761.

functionalization of highly substituted ketone-derived enolates. In this short review, the direct construction of all-carbon quaternary stereocenters at nucleophilic enolates via Pd-catalyzed allylic alkylation reactions will be discussed within the broader context of challenges derived from total synthesis. An all-carbon quaternary stereocenter, which is composed of a central carbon atom bound to four carbon substituents, should be distinguished from a heteroatom-substituted tertiary center, which bears one heteroatom and three carbon substituents (Figure 1.1). In the following discussions, particular attention will be given to reported syntheses that have appeared since the most recent reviews.⁵ Total syntheses featuring enantioselective tertiary stereocenter formation⁶ or catalyst-controlled diastereoselective transformations⁷ will not be discussed in detail.

Figure 1.1. Natural Products as an Inspiration for The Development of Asymmetric Catalysis



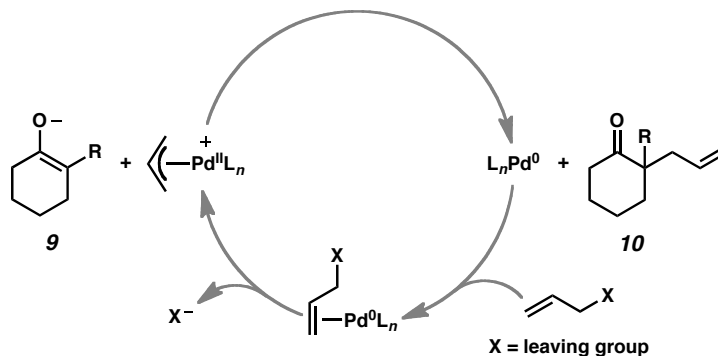
1.2 REACTION DESIGN AND MECHANISTIC CONSIDERATIONS

Pd-catalyzed allylic alkylation reactions have found increasingly wide synthetic applications due to the continued evolution of the methodology. The invention of highly enantioselective transformations for the assembly of all-carbon quaternary stereocenters has facilitated the efficient asymmetric synthesis of numerous complex natural products. While a number of factors have been instrumental to the success of these Pd-catalyzed reactions in complex settings, advances in substrate scope and identification of suitable chiral ligands for these substrate types have had a direct impact on the general utility of these reactions.

1.2.1 GENERAL ASPECTS OF Pd-CATALYZED ALLYLIC ALKYLATION

In a typical allylic alkylation reaction, a Pd(0) complex undergoes initial olefin coordination and subsequent oxidative addition to an allyl electrophile (Scheme 1.1). Expulsion of the leaving group leads to a cationic Pd(II) π -allyl complex. Upon combination with an enolate in the reaction mixture, subsequent C–C bond formation can lead to the α -quaternary ketone product and regenerate the initial Pd(0) complex. The precise reaction mechanism can vary based on the choice of ligand, palladium precursor, substrate, allyl source, additive, and solvent.

Scheme 1.1. General Mechanism for Pd-Catalyzed Allylic Alkylation Reactions



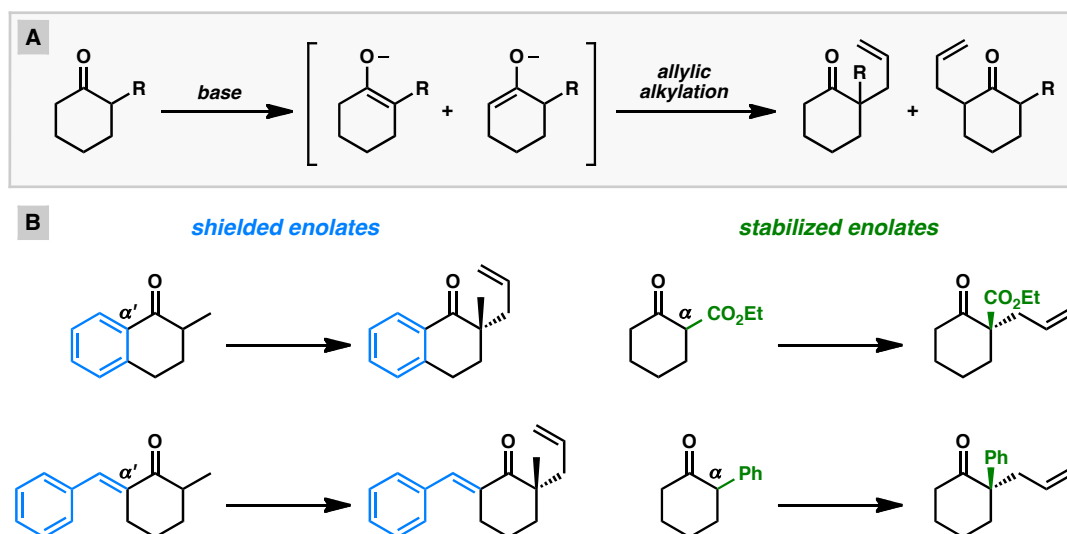
1.2.2 DEVELOPMENT OF METHODS FOR ENOLATE GENERATION

Various methods have been employed for the generation of ketone enolates for Pd-catalyzed asymmetric allylic alkylation reactions, but important advances in the past decade have rendered these transformations more practical and useful for the preparation of complex molecules. An unavoidable and general problem in the allylation of differentially substituted ketones with multiple acidic sites is the formation of isomeric enolates, which can proceed to different products in the presence of a palladium π -allyl complex (Scheme 1.2A).

In order to circumvent this problem, many groups have employed substrates that contain either α' -blocking groups to shield undesired sites of deprotonation or α -electron withdrawing groups to greatly reduce the pK_a of the desired site of deprotonation (Scheme 1.2B). While both of these strategies have afforded control of regioselective deprotonations in asymmetric alkylation reactions and enantioselective transformations on these types of substrates have been documented,^{8,9,10,11} this approach can introduce unwanted functional groups into cyclic ketone scaffolds. The modification or removal of

this vestigial functionality from the α -quaternary ketone products can greatly diminish the general application of these compounds in total synthesis.

Scheme 1.2. The Enolate Alkylation Problem and Approaches to Selective Enolate Formation

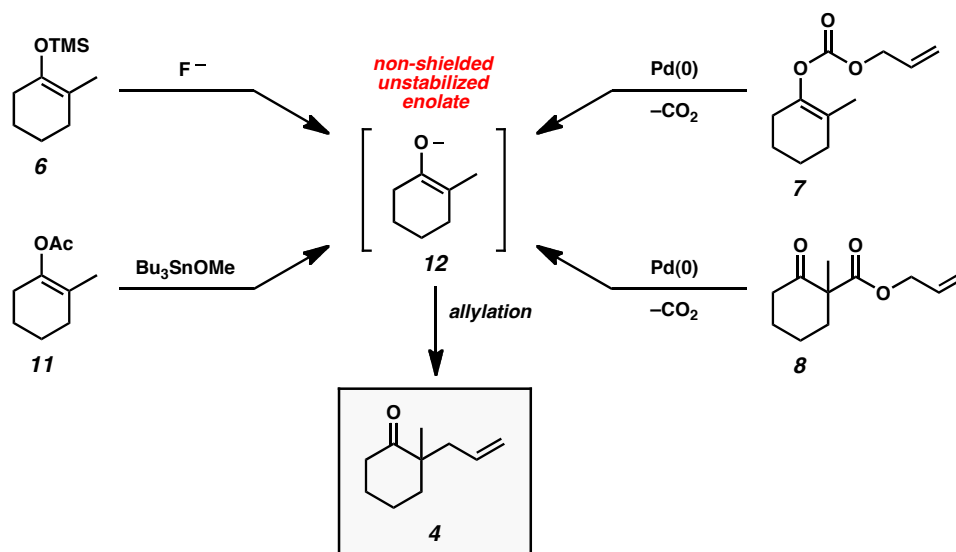


The general synthesis of chiral α -quaternary ketone building blocks using Pd-catalyzed asymmetric allylic alkylation reactions of non-biased unstabilized enolates constituted a major synthetic challenge until the past decade. The lack of established methods for the preparation of relatively simple compounds such as ketone **4** (Figure 1.1) in high ee presented a significant obstacle to the synthesis of complex natural products with all-carbon quaternary stereocenters.

Alternative methods for selective enolate generation could be found in the work of Tsuji and co-workers from the 1980s (Scheme 1.3). Using either enol acetate¹² or silyl enol ether¹³ substrates in the presence of appropriate additives, it was possible to unmask the latent enolates as a single isomer. Subsequent allylic alkylation provided α -

quaternary ketone product without ancillary group incorporation. Additionally, Tsuji's work showed that it was possible to incorporate allyl fragments into the substrate by using allyl enol carbonates¹⁴ or allyl β -ketoesters.^{15,16} The in situ formation of both an allyl electrophile and an enolate nucleophile could be conveniently initiated by a Pd(0) catalyst with both of these substrate types. With all of these methods explored by Tsuji, the enolates formed under the reaction conditions maintain high regiochemical fidelity and smoothly proceed to the corresponding allylation products. While these methods provided promising strategies for generating enolates in a widely applicable manner, asymmetric variants of these transformations did not surface until over 20 years later.

Scheme 1.3. Tsuji Reactions for the Allylation of Non-Shielded, Non-Stabilized Enolates



1.2.3 DEVELOPMENT OF ASYMMETRIC ALLYLATION REACTIONS

In the past decade, contributions from predominantly the Stoltz and Trost groups have helped address the difficulty of performing Pd-catalyzed asymmetric allylic alkylations

on non-stabilized unbiased enolates to give α -quaternary ketones. In the earliest report by Stoltz in 2004, numerous chiral bidentate ligands were screened for their ability to promote high asymmetric induction in reactions with allyl enol carbonate and silyl enol ether substrates (Scheme 1.4).^{17a} Ultimately, it was found that treatment of these substrates with the combination of (*S*)-*t*-Bu-PHOX (**13**) and Pd₂(dba)₃ provided the highest degree of enantioenrichment in the α -quaternary ketone products. Other *P,N*- and *P,P*-chelating ligands were investigated, but they proved to be less effective under the optimized conditions. Carbocyclic substrates with various ring sizes could undergo the transformation to give products in high ee. Examples of benzannulated and non-benzannulated substrates were reported.

Shortly afterward, a study from the Trost group in 2005 described the development of a different catalyst system for the decarboxylative allylic alkylation of allyl enol carbonates (Scheme 1.4).¹⁸ A screen of various Trost bis-phosphine ligands with modified diamine backbones and arylphosphines revealed that ligand (*R,R*)-**17** was most effective for this transformation. Complexation of this ligand with Pd₂(dba)₃·CHCl₃ provided an effective catalyst for the synthesis of chiral α -quaternary ketone products with various ring sizes. While most of the examples consist of benzannulated substrates, two examples of non-benzannulated ketones were presented. Notably, several cyclic ketones with incorporated heterocycles could also be prepared. The catalyst system was additionally shown to be applicable for the formation of α -tertiary ketones.

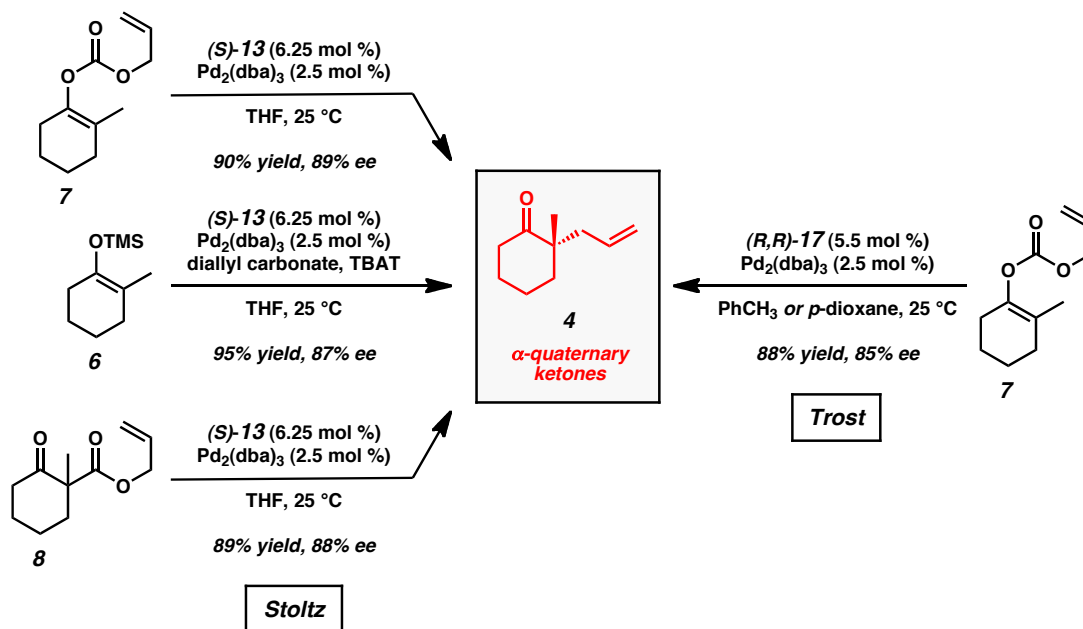
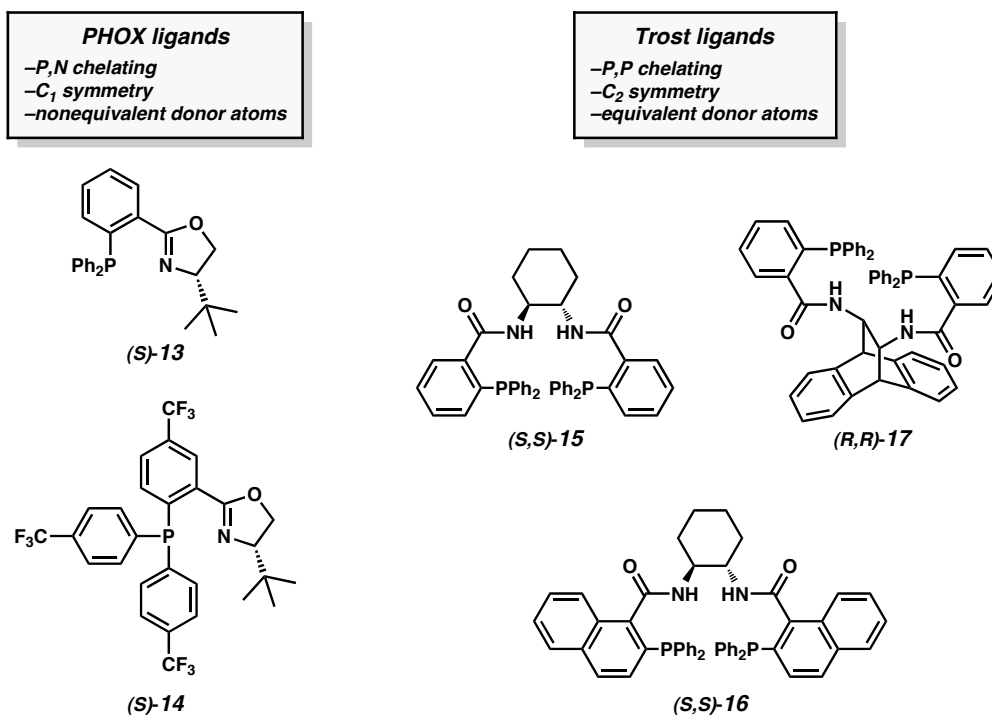
Scheme 1.4. Pd-Catalyzed Asymmetric Allylic Alkylation Reactions with Allyl Enol Carbonate, Silyl Enol Ether, and β -Ketoester Substrate Classes

Figure 1.2. Selected Chiral Ligands for Pd-Catalyzed Asymmetric Allylic Alkylation Reactions



Subsequent work by the Stoltz group extended the asymmetric alkylation methodology with the PHOX ligand system to β -ketoester substrates (Scheme 1.4).^{17b,c} Since the starting materials are racemates, the destruction and reconstruction of stereochemical information through the intermediacy of a prochiral enolate must take place in order for these compounds to form asymmetric alkylation products in what has been termed a stereoablative process.¹⁹ Despite this key mechanistic difference, these substrates demonstrated similar yields and levels of asymmetric induction compared to the silyl enol ethers and enol carbonates. The development of reactions for this class of substrates had practical advantages since various α -substituents could be introduced under relatively mild conditions, and β -ketoester substrates typically have higher thermal and chemical stability than silyl enol ether and enol carbonate substrates.

The bis-phosphine and phosphinooxazoline-type ligands described in the examples above have enjoyed notable success in the construction of challenging all-carbon quaternary stereocenters to prepare key intermediates for natural product synthesis (Figure 1.2). Trost ligands²⁰ possess C_2 symmetry and equivalent donor atoms as well as amide functionality capable of hydrogen bonding. To date, numerous ligands with modified backbone scaffolds and arylphosphine substitution have been reported. Structural modification of these ligands has led to changes in reactivity in cases with multiple possible asymmetric alkylation pathways. PHOX ligands,²¹ which were pioneered by Pfaltz, Helmchen, and Williams, have also proven to be useful ligands for asymmetric allylic alkylation reactions. These ligands possess C_1 symmetry and non-equivalent donor atoms. This lack of symmetry has important ligand design implications

since the oxazoline and arylphosphine regions of the ligand can be tuned somewhat independently. Overall, the ligand classes have unique and complementary steric and electronic features that make them particularly useful and adaptable for Pd-catalyzed asymmetric allylic alkylation reactions in total synthesis.

1.3 CATALYTIC ASYMMETRIC SYNTHESIS OF NATURAL PRODUCTS

The development of Pd-catalyzed asymmetric allylic alkylation reactions of non-biased unstabilized enolates for the synthesis of α -quaternary ketone products has provided a powerful tool for total synthesis. The following case studies not only illustrate important advances in synthetic chemistry, but also provide examples of how broader, long-standing problems in the field have been identified and overcome in the process of constructing complex molecules.

1.3.1 TOTAL SYNTHESSES OF HAMIGERAN B AND ALLOCYATHIN B₂

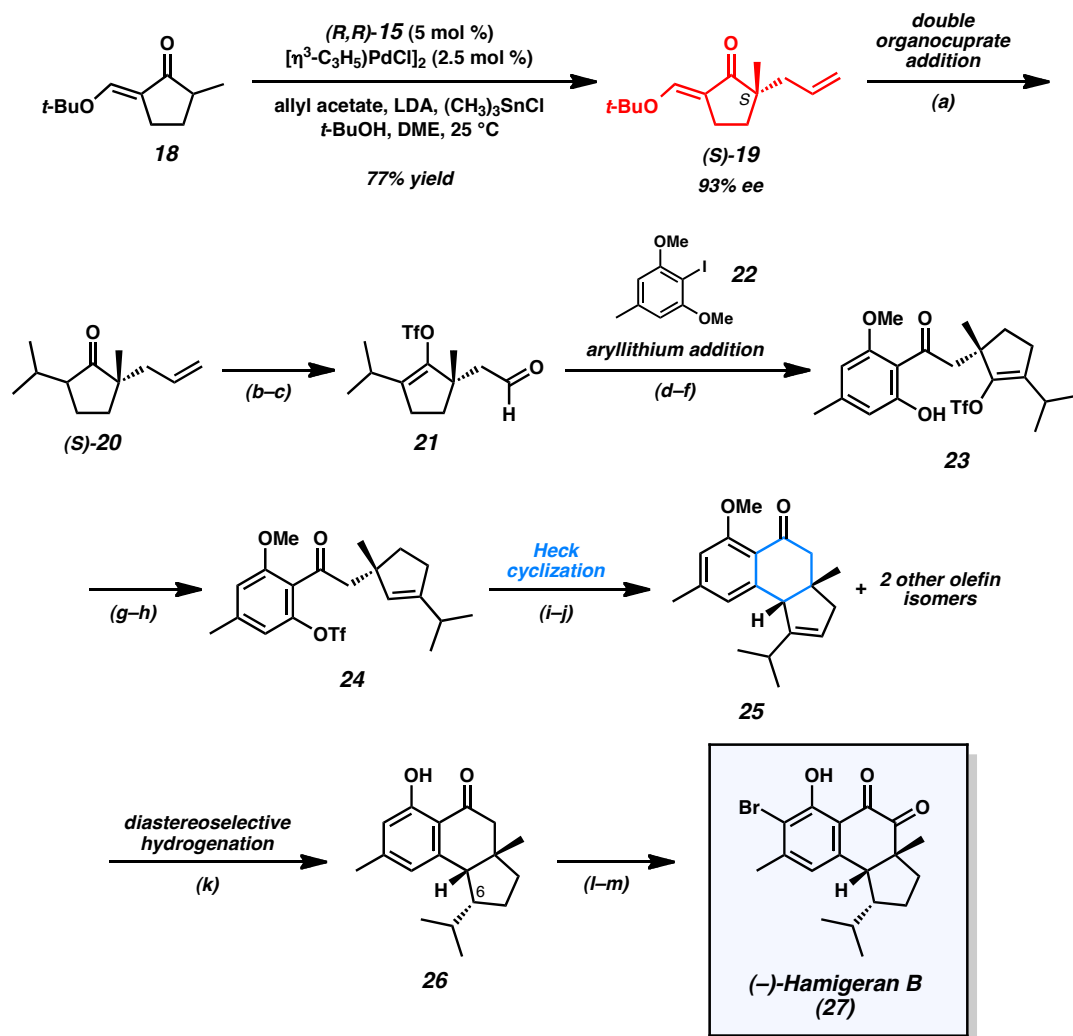
The synthetic potential of Pd-catalyzed allylic alkylation reactions for the assembly of all-carbon quaternary stereocenters was illustrated by the early enantioselective syntheses of hamigeran B (**27**)²² and allocyathin B₂ (**37**)²³ by the Trost group (Scheme 1.5 and Scheme 1.6). The common component for both of these syntheses was enantioenriched exocyclic vinylogous ester **19**. In order to form the requisite quaternary stereocenter, the development of an effective asymmetric allylic alkylation reaction for exocyclic vinylogous ester **18** was needed. The treatment of this compound with allyl acetate as the allyl source, LDA as base, trimethyltin chloride as Lewis acid, and $[(\eta^3\text{-C}_3\text{H}_5)\text{PdCl}]_2$ and

chiral ligand (*S,S*)-**15** as catalyst precursors in DME at 0 °C provided α -quaternary ketone (*R*)-**19** in 93% yield but only 12% ee. Extensive reaction optimization revealed that the use of *t*-BuOH as an additive greatly improved asymmetric induction and provided optimized reaction conditions leading to the formation of product **19** in 87% yield and 91% ee. Additionally, it was found that reduced catalyst loadings could also be employed to obtain similar results. The exocyclic vinylogous ester functionality not only served an important purpose as an α' -blocking group to prevent the formation of isomeric enolates, but also enabled subsequent transformations later in the synthetic sequence.

The convergent synthetic approach to hamigeran B (**27**)²² sought to unite an aryl fragment with a cyclopentenyl fragment containing an all-carbon quaternary stereocenter (Scheme 1.5). Subsequent formation of the central six-membered ring would provide the core of the target. In order to proceed toward hamigeran B (**27**), it was necessary to obtain the (*S*)-enantiomer of **19** generated from the optimization studies. By application of Trost ligand (*R,R*)-**15** under otherwise identical reaction conditions, vinylogous ester (*S*)-**19** was obtained in 77% yield and 93% ee. Subsequent treatment with lithium dimethylcuprate in Et₂O led to the formation of cyclopentanone **20** bearing an all-carbon quaternary stereocenter. Triflate formation and oxidative cleavage of the allyl group provided aldehyde **21**. Nucleophilic addition of the aryllithium of **22** followed by oxidation of the intermediate alcohol with Dess–Martin periodinane and selective monodemethylation with BCl₃ gave ketone **23**. Enol triflate reduction under palladium catalysis, formation of the aryl triflate **24**, and application of Heck cyclization conditions using Pd(OAc)₂, dppb, and K₂CO₃ in toluene afforded a mixture of isomeric disubstituted, trisubstituted, and tetrasubstituted olefinic tricycles. Following BBr₃-

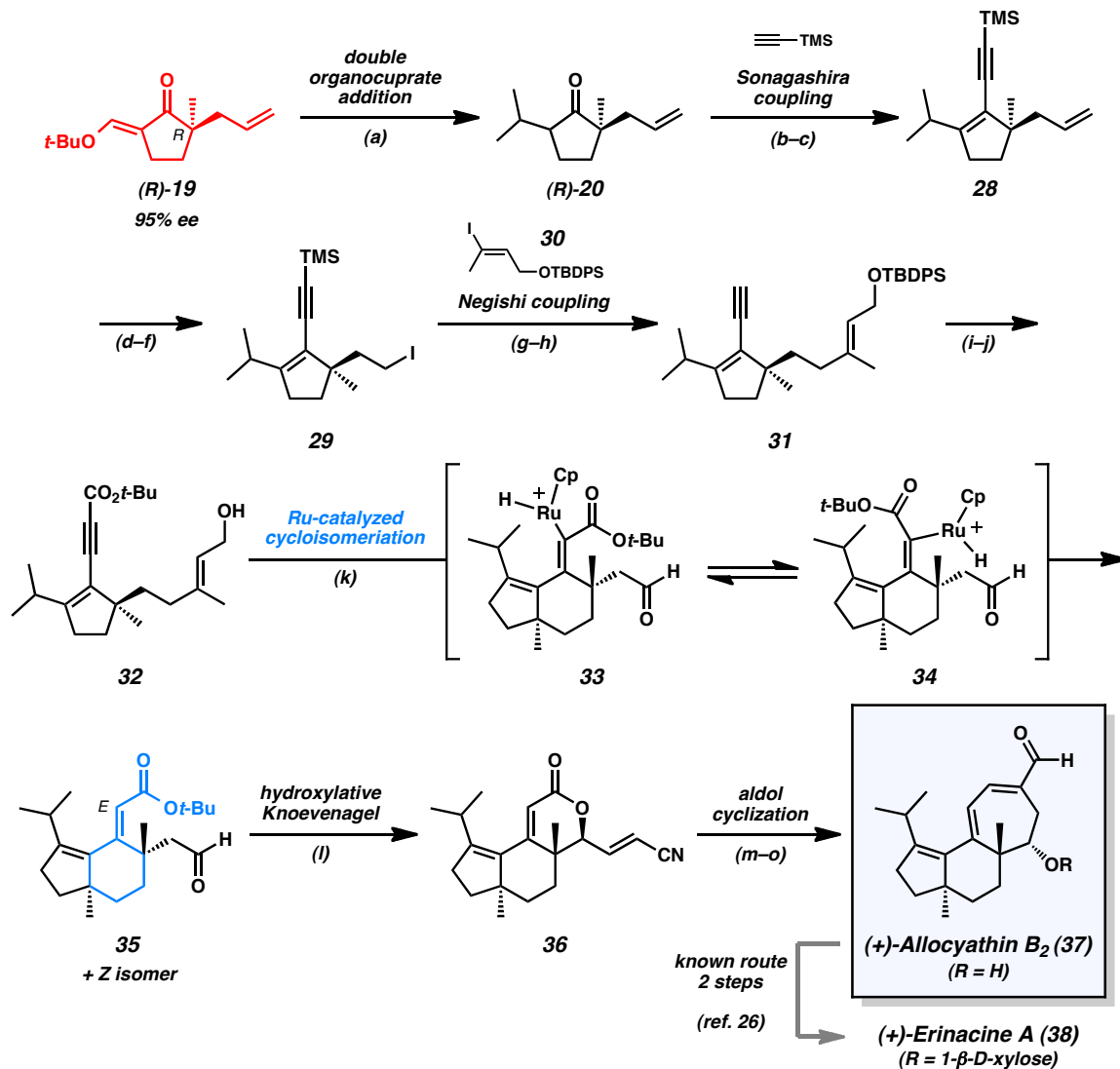
induced demethylation, phenolic trisubstituted olefin **25** could be isolated from the mixture in 51% yield over 2 steps. The selection of appropriate hydrogenation conditions proved crucial to the formation of the remaining stereocenter. Treatment of alkene **25** with Pd/C in ethanol with 1500 psi H₂ led to the undesired C(6)-epimer, while hydrogenation with Ir black in ethanol directly provided desired tricycle **26**. Late stage diketone formation with SeO₂ and acetic acid in *p*-dioxane followed by regioselective arene bromination led to hamigeran B (**27**).

Scheme 1.5. Total Synthesis of Hamigeran B



Reaction Conditions: (a) $(\text{CH}_3)_2\text{CuLi}$, Et_2O , -20°C (89% yield). (b) LDA, THF, $-78 \rightarrow 0^\circ\text{C}$; then $\text{PhN}(\text{Tf})_2$ (87% yield). (c) OsO_4 (3.77 mol %), NMO, THF, H_2O ; then NaIO_4 . (d) iodoarene **22**, DME, -55°C ; then aldehyde **21**. (e) Dess–Martin periodinane, NaHCO_3 , CH_2Cl_2 , 75% yield (3 steps). (f) BCl_3 , CH_2Cl_2 , -20°C (85% yield). (g) $\text{Pd}(\text{OAc})_2$ (10 mol %), dppf (20 mol %), HCO_2H , Et_3N , DMF, 70°C (94% yield). (h) Tf_2O , CH_2Cl_2 , pyridine, 0°C (94% yield). (i) $\text{Pd}(\text{OAc})_2$, dppb, K_2CO_3 , PhCH_3 . (j) BBr_3 , CH_2Cl_2 , -78°C (51% yield, 2 steps). (k) Ir black, H_2 (1500 psi), EtOH (>99% yield). (l) SeO_2 , cat. AcOH, p-dioxane (90% yield). (m) NBS, $i\text{-Pr}_2\text{NH}$ (5 mol %), CH_2Cl_2 (85% yield).

By employing the enantiomeric chiral intermediate (*R*)-**19**, the Trost group completed the synthesis of allocyathin B₂ (**37**) shortly after their investigations of hamigeran B (**27**) (Scheme 1.6). The challenging central cyclohexane ring bearing two all-carbon quaternary stereocenters presented an opportunity to test the group's methods for Ru-catalyzed enyne cycloisomerizations. Exocyclic vinylogous ester **19** underwent a double organocuprate addition to give ketone **20** as in the earlier synthesis of hamigeran B (**27**). Triflation and Sonagashira coupling provided alkyne **28**. Oxidative olefin cleavage, aldehyde reduction, and terminal alcohol substitution provided iodide **29**. Lithium-halogen exchange and zincation enabled a Negishi coupling with iodide **30**. Esterification of the alkyne and alcohol deprotection provided enyne **32**. Treatment of this compound with the group's previously developed conditions for Ru-catalyzed cycloisomerization²⁴ provided a mixture of *E* and *Z* olefin isomers. An investigation of various ester groups found that the *tert*-butyl ester provided the best ratio of *E*:*Z* olefin isomers. Ultimately, the *E* isomer could be isolated and advanced to unsaturated lactone **35** by a hydroxylative Knoevenagel reaction with phenylsulfinyl acetonitrile.²⁵ Hydrogenation of the least hindered disubstituted double bond, hydride reduction, and aldol cyclization completed the total synthesis of allocyathin B₂ (**37**). The preparation of this compound also constituted a formal synthesis of erinacine A (**38**) based on the prior work of Snider.²⁶ By applying their asymmetric alkylation methodology, the Trost group achieved the divergent total syntheses of hamigeran B (**27**) and allocyathin B₂ (**37**) with exocyclic vinylogous ester **19** as the common precursor.

Scheme 1.6. Total Synthesis of Allocyathin B₂ and Formal Synthesis of Erinacine A

Reaction Conditions: (a) (CH₃)₂CuLi, Et₂O, -20 °C (89% yield). (b) LDA, THF, -78→0 °C; then PhN(Tf)₂ (96% yield). (c) Pd₂(dba)₃·CHCl₃ (2.5 mol %), PPh₃ (20 mol %), CuI (5 mol %), TMS-acetylene, n-BuNH₂, 50 °C (85% yield). (d) OsO₄ (1 mol %), NMO; then NaIO₄ (87% yield). (e) NaBH₄, MeOH (94% yield). (f) PPh₃, I₂, imidazole, (97% yield). (g) t-BuLi, ZnCl₂, THF, -78 °C→rt; then Pd(PPh₃)₄ (5 mol %), vinyl iodide **30**. (h) K₂CO₃, MeOH (74% yield, 2 steps). (i) n-BuLi, THF, -78 °C; then Boc₂O, -78→rt (99% yield). (j) TBAF, THF, (52–55% yield). (k) CpRu(CH₃CN)₃PF₆ (20 mol %), DMF (1 equiv), 2-butanone, rt (48% yield of **35**, or 55% combined yield, 6.7:1 E:Z ratio). (l) PhS(O)CH₂CN, piperidine, PhH (75% yield). (m) 10% Pd/C,

EtOAc, H_2 (1 atm) (83% yield). (n) DIBAL, CH_2Cl_2 , $-78\text{ }^\circ\text{C}$. (o) KOH, MeOH, $60\text{ }^\circ\text{C}$ (51% yield, 2 steps).

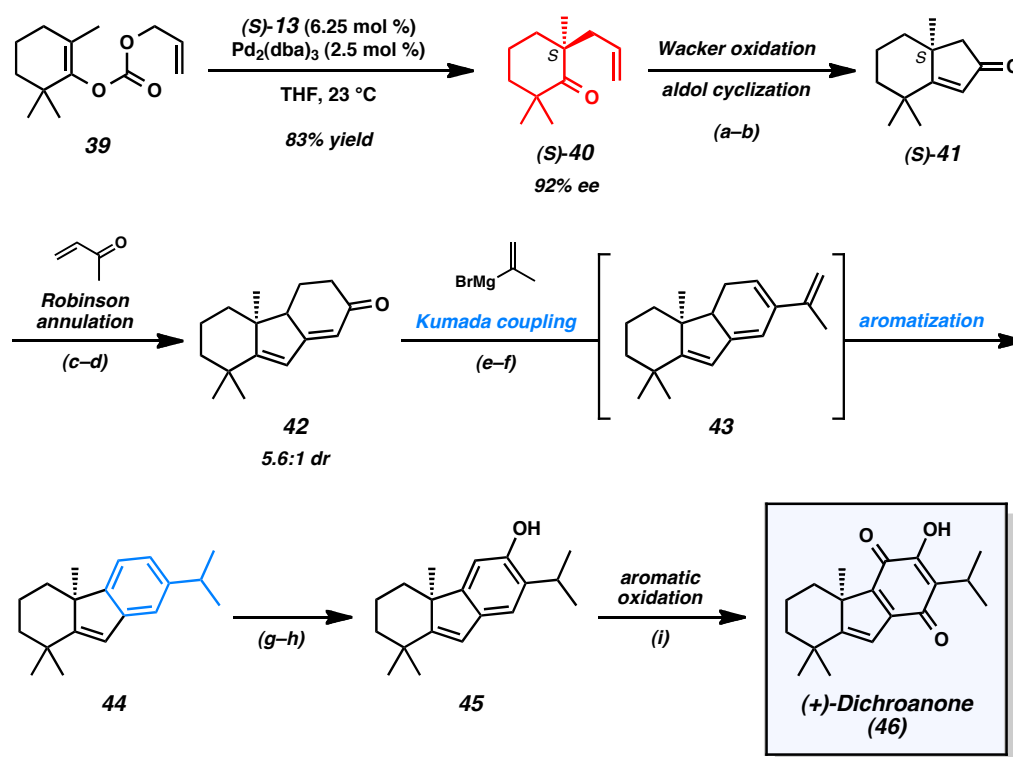
1.3.2 TOTAL SYNTHESSES OF DICHROANONE AND LIPHAGAL

Following the development of a Pd·PHOX catalyst system for the catalytic construction of α -quaternary cyclic ketones,^{17a} the Stoltz group sought to prepare the unique and highly substituted carbocyclic structures of dichroanone (**46**)²⁷ and liphagal (**56**)²⁸ (Scheme 1.7 and Scheme 1.8). Central to their divergent synthetic approach to these natural products was the preparation of bicyclic enone **41**, which contains two quaternary carbons in close proximity in the cyclohexane ring (Scheme 1.7). The synthetic routes toward both of these natural products began with the Pd-catalyzed asymmetric decarboxylative allylic alkylation of cyclic enol carbonate **39**. The addition of this compound to a solution of $Pd_2(dba)_3$ and (*S*)-*t*-Bu-PHOX (**13**) in THF (or TBME) led to enantioenriched ketone **40** in 83% yield and 92% ee. The presence of the α' -methyl groups in the substrate did not appear to impede catalysis. By performing Wacker oxidation and intramolecular aldol cyclization according to previously developed protocols,^{17a} bicyclic ketone **41** could be obtained in 74% yield over 2 steps. The key enone possesses a prevalent substitution pattern found in not only dichroanone (**46**) and liphagal (**56**), but also many other terpenoid natural products.

The (*S*)-enantiomer of bicyclic enone **41** was advanced toward dichroanone (**46**) by the de novo construction of the fully substituted quinone nucleus. A Robinson annulation sequence followed by vinyl triflate formation and Pd-catalyzed Kumada coupling with isopropenyl magnesium bromide led to isopropyl arene **44**. The reaction likely proceeds

through coupling product **43**, which can undergo facile aromatization to give the benzannulated ring system. Titanium-mediated formylation of the aromatic ring proceeded smoothly to give an intermediate aldehyde, which was converted to the corresponding phenol **45** by means of a Baeyer–Villiger oxidation. Careful generation of a reactive intermediate *o*-quinone could be achieved by the treatment of the tricycle with IBX. Subsequent trapping of the reactive intermediate with pentafluorothiophenol, reoxidation with NaOH/MeOH/O₂, and hydrolysis with aqueous HCl completed the synthesis of dichroanone (**46**). Notably, the total synthesis proceeded without the use of protecting groups and provided an asymmetric route to this family of quinone norditerpenoids.

Scheme 1.7. Total Synthesis of Dichroanone

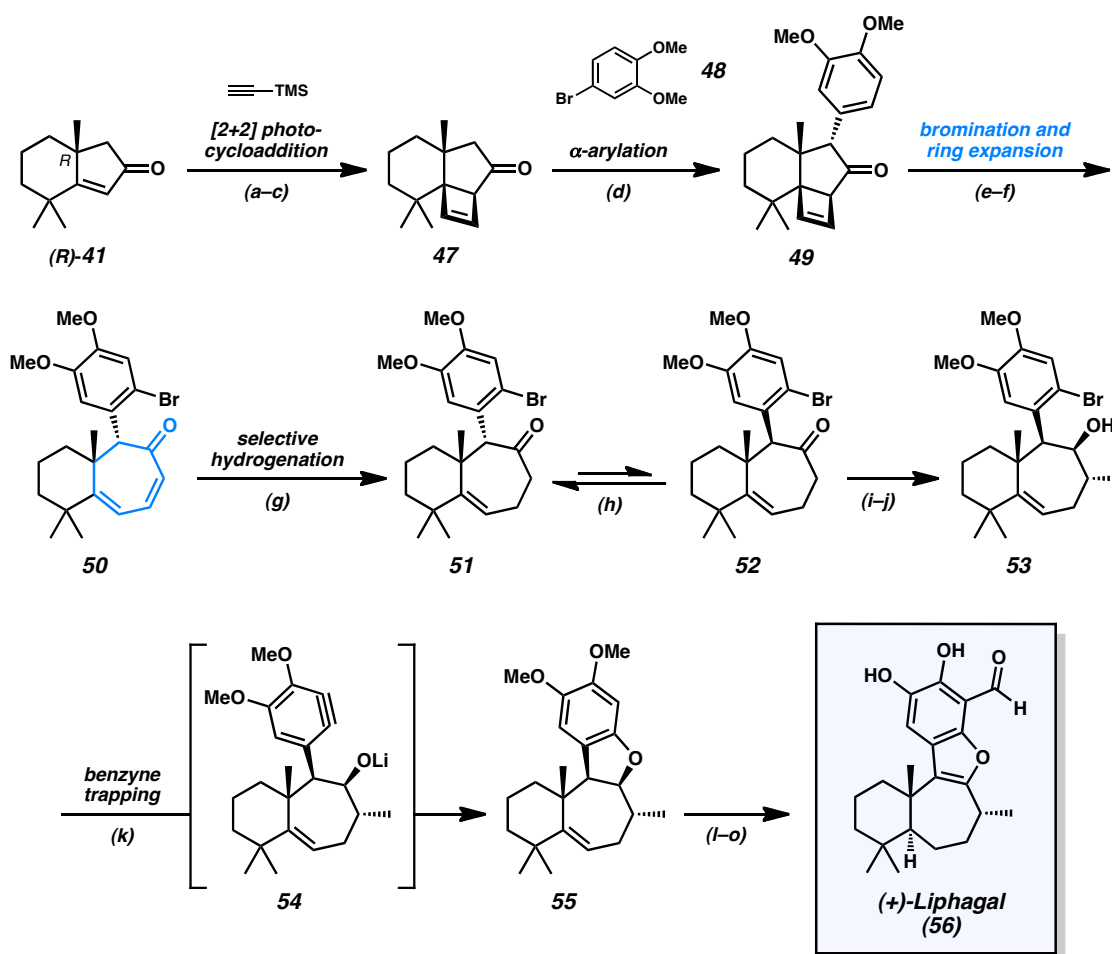


Reaction Conditions: (a) PdCl_2 (5 mol %), $\text{Cu}(\text{OAc})_2 \cdot \text{H}_2\text{O}$ (25 mol %), O_2 (1 atm), $\text{DMA}/\text{H}_2\text{O}$ (7:1), 23 °C, Parr-shaker (77% yield). (b) KOH (0.45 equiv), xylenes, 110 °C, Dean–Stark (96% yield). (c) LiHMDS , THF, 0→23 °C; then methyl vinyl ketone, –78 °C; then aq NH_4Cl , –78→23 °C (72% yield). (d) powdered KOH (2 equiv), xylenes, 110 °C, Dean–Stark (80% yield). (e) LDA , THF, –78 °C; then $\text{PhN}(\text{Tf})_2$, –78→23 °C. (f) isopropenylmagnesium bromide (2 equiv), $\text{Pd}(\text{PPh}_3)_4$ (5 mol %), THF, 23 °C; then 6 M aq HCl , 23 °C (65% yield, 2 steps). (g) $\text{Cl}_2\text{HCOCH}_3$, TiCl_4 , CH_2Cl_2 , –78→23 °C (79% yield). (h) aq H_2O_2 , aq H_2SO_4 , THF/MeOH/ H_2O (2:5:1), 23 °C (74% yield). (i) IBX (1.2 equiv), CHCl_3 , 23 °C; then $\text{C}_6\text{F}_5\text{SH}$ (4 equiv), 23 °C; then O_2 (1 atm), NaOH (10 equiv), MeOH, 23→75 °C; then 6 M aq HCl , 23 °C (35% yield).

While the route toward dichroanone demonstrated the utility of bicyclic enone **41** in α -functionalization reactions, the synthesis of liphagal²⁸ (**56**) demonstrated further synthetic applications for this bicyclic scaffold. With enone (*R*)-**41** available by allylic alkylation of substrate **39** with (*R*)-*t*-Bu-PHOX (**13**), a photoinduced [2+2] cycloaddition with TMS-acetylene was performed (Scheme 1.8). Treatment of the crude cycloadduct with $\text{BF}_3 \cdot \text{OEt}_2$, followed by TBAF, led to cyclobutene **47**. The strained ketone underwent α -arylation with 4-bromoveratrole (**48**) under microwave irradiation to give highly functionalized tricycle **49**. Arene bromination of this compound proved to be remarkably chemoselective as the strained cyclobutene remained intact during the transformation. Subsequent microwave-assisted thermal ring expansion provided conjugated cycloheptadienone **50**. Selective hydrogenation of the less substituted double bond followed by base-mediated epimerization led to bicycle **52** after two equilibration cycles. LDA -mediated methylation of the non-conjugated cycloheptenone and DIBAL reduction provided alcohol **53**. Treatment of this compound with LDA led to a reactive aryne

intermediate, which could react intramolecularly with the adjacent lithium alkoxide to provide dihydrobenzofuran **55**. Hydrogenation of the remaining olefin provided the necessary stereochemistry at the junction of the six- and seven-membered rings. Dihydrobenzofuran oxidation followed by arene formylation and phenol demethylation provided liphagal (**56**). Taken together, the two syntheses demonstrate the unique synthetic utility of bicyclic enone **41**, which is formed from the decarboxylative asymmetric allylic alkylation of enol carbonate **39**.

Scheme 1.8. Total Synthesis of Liphagal



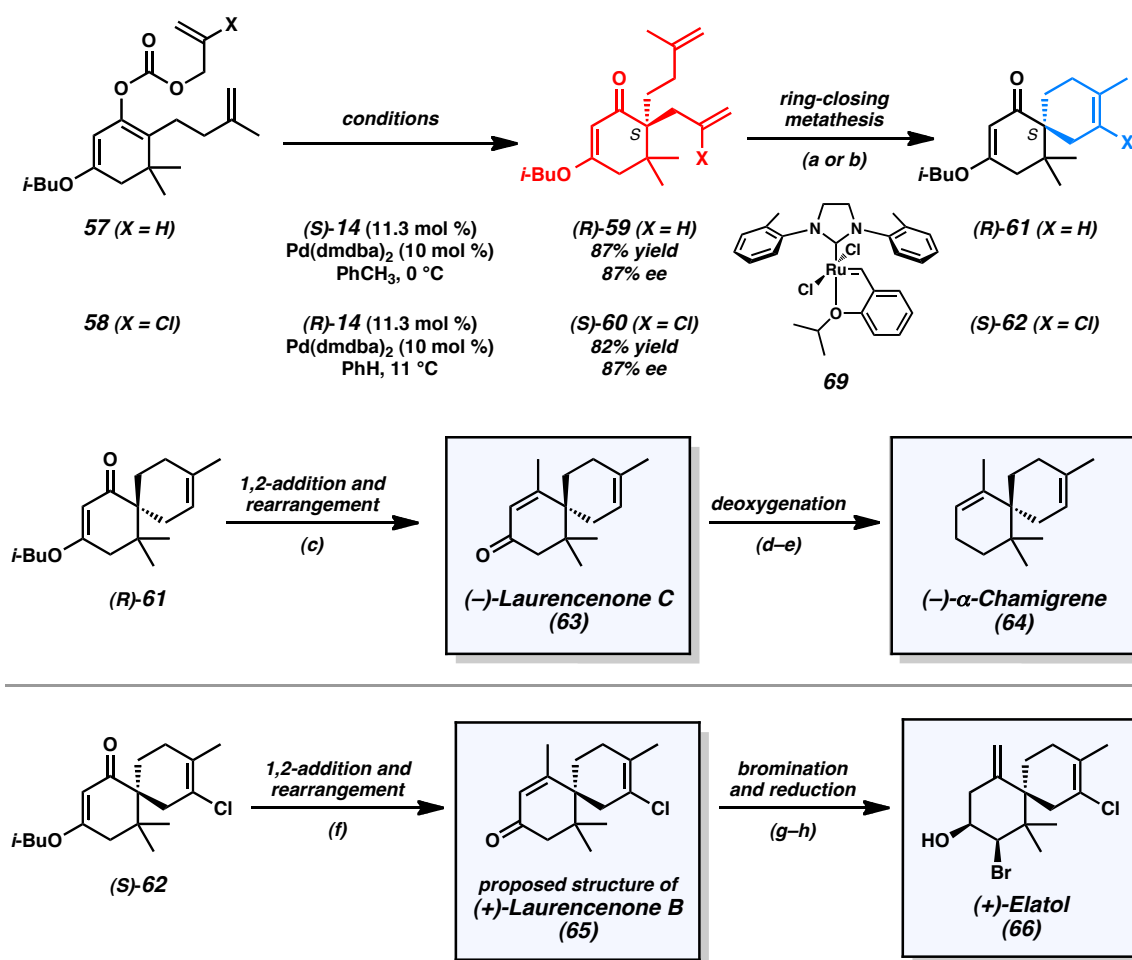
Reaction Conditions: (a) TMS-acetylene, UV-B lamps, acetone. (b) $\text{BF}_3 \cdot \text{OEt}_2$, CH_2Cl_2 . (c) TBAF, THF (68% yield, 3 steps). (d) $\text{Pd}(\text{P}(\text{t-Bu})_3)_2$ (5 mol %), 4-bromoveratrole, NaOt-Bu , THF, μwaves , 120 °C (67% yield). (e) Br_2 (1.8 equiv), CHCl_3 (65% yield). (f) μwaves , *o*-dichlorobenzene, 250 °C (68% yield). (g) PtO_2 (20 mol %), H_2 (1 atm), EtOAc (69% yield). (h) NaOMe, MeOH, 65 °C (78% yield, 3 cycles). (i) LDA, THF, $-78 \rightarrow 0$ °C; then CH_3I , $-78 \rightarrow 0$ °C (68% yield). (j) DIBAL, PhCH_3 (91% yield). (k) LDA (3 equiv), THF, -20 °C (83% yield). (l) Pd/C (19 mol %), H_2 (1 atm), EtOH, 21 °C (97% yield). (m) NO^+BF_4^- , CH_3CN , 0 °C (70% yield). (n) *n*-BuLi, TMEDA, THF, 0 °C; then DMF, $0 \rightarrow 21$ °C (70 % yield). (o) BI_3 , CH_2Cl_2 (45% yield).

1.3.3 TOTAL SYNTHESIS OF ELATOL, α -CHAMIGRENE, LAURENCENONE C

After successfully demonstrating the utility of the allyl enol carbonate approach^{17a} for enolate generation in the asymmetric construction of quaternary stereocenters, the Stoltz group sought to extend the scope of the asymmetric decarboxylative allylic alkylation reactions in order to gain access to the chamigrene family of natural products²⁹ (Scheme 1.9). These compounds are distinguished by the central all-carbon quaternary stereocenter connecting two highly substituted six-membered rings, as evidenced by the structures of laurencenone C (**63**) and α -chamigrene (**64**). The halogenation patterns for members such as elatol (**66**) presented additional synthetic challenges. In order to arrive at these natural products, a flexible synthetic route was needed.

The *gem*-dimethyl group adjacent to the desired site of alkylation in substrates **57** and **58** presented a formidable challenge for the decarboxylative allylic alkylation methodology with the Pd·PHOX catalyst system. The investigation of enol carbonate and

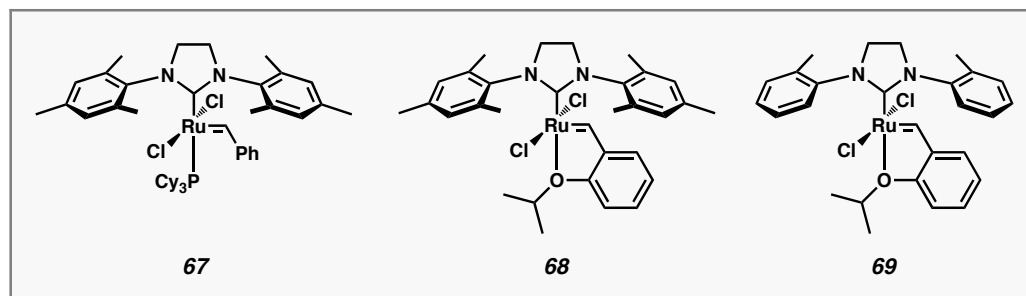
β -ketoester substrates with (*S*)-*t*-Bu-PHOX (**13**) led to product in 81% ee, but conversions were consistently poor in both cases. Faced with these synthetic difficulties, ligand modifications were explored to promote the desired C–C bond forming step in the catalytic cycle. By employing the electron-deficient PHOX derivative **14**, it was reasoned that the increased electrophilicity of the derived Pd π -allyl complex could override the steric constraints imposed by the substrate. The combination of electron-deficient PHOX ligand **14** with Pd(dmdba)₂ in toluene or benzene ultimately provided the most effective conditions. Vinylogous ester **59** could be obtained in 87% yield and 87% ee while the analogous chlorinated vinylogous ester **60** could be obtained in 82% yield and 87% ee. In the presence of catalyst, these substrates could be converted to product below ambient temperature. In addition to these two substrates, the reaction conditions could be applied to numerous α -substituted analogs as well.

Scheme 1.9. Total Syntheses of Laurencenone C, α -Chamigrene, the Proposed Structure of Laurencenone B, and Elatol

Reaction Conditions: (a) substrate **59**, Grubbs–Hoveyda 3rd generation catalyst (**69**) (5 mol %), PhH , 60 °C (97% yield). (b) substrate **60**, Grubbs–Hoveyda 3rd generation catalyst (**69**) (5 mol %), PhH , 60 °C (97% yield). (c) $MeLi$, $CeCl_3$, THF , $-78 \rightarrow 0$ °C; then 10% aq HCl , $0 \rightarrow 23$ °C (80% yield). (d) $BF_3 \cdot OEt_2$, $HSCH_2CH_2SH$, $MeOH$, 23 °C (92% yield). (e) $Na(0)$, $Et_2O/NH_3(l)$, $-60 \rightarrow reflux$ (44% yield). (f) $MeLi$, $CeCl_3$, THF , $-78 \rightarrow 0$ °C; then 10% aq HCl , $0 \rightarrow 23$ °C (89% yield). (g) Br_2 , 48% aq HBr , $AcOH$, 23 °C. (h) $DIBAL$, THF , $-78 \rightarrow 60$ °C (32% yield, 2 steps).

From enantioenriched vinylogous esters **59** and **60**, it was envisioned that a ring-closing metathesis to a trisubstituted or tetrasubstituted olefin would provide the spirobicyclic core of the chamigrene natural products (Scheme 1.9). Unfortunately, the application of commonly used ruthenium metathesis catalysts **67** and **68** (Figure 1.3) provided unsatisfactory results. The use of the metathesis catalyst **69**,³⁰ which was concurrently developed by the Grubbs laboratory, proved to be an effective solution. Trisubstituted olefin **61** and chlorinated tetrasubstituted olefin **62** were both formed in excellent yields. Notably, the advances enabled by ruthenium complex **69** provided one of the first examples of the effective ring-closing metathesis to form highly substituted halogenated olefins.

Figure 1.3. Ruthenium Olefin Metathesis Catalysts



With the spirocyclic core of the target natural products secured, short sequences enabled the synthesis of various chamigrene natural products. The addition of methyllithium to spirocycle **61** in the presence of CeCl_3 activator followed by acid workup provided laurencenone C (**63**). Formation of the corresponding thioketal followed by dissolving metal reduction provided α -chamigrene (**64**) in only two additional steps. The application of the same methyllithium addition and acidic workup

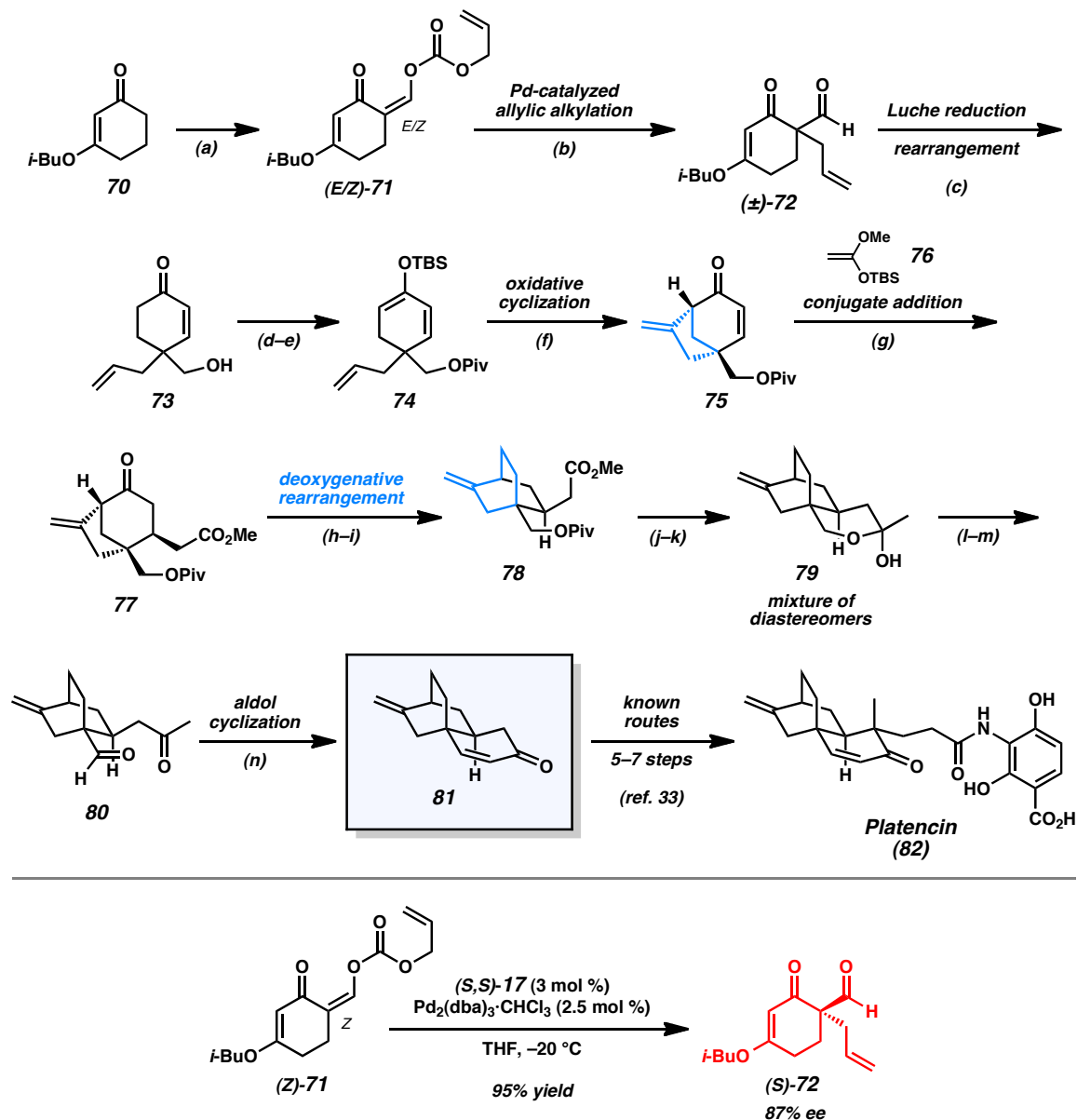
conditions to vinylogous ester **62** enabled the formation of enone **65**, which represents a chlorinated analog of **63**. Although this structure was reported as laurencenone B, the spectra did not match those of the published compound. Nevertheless, the compound was brominated and reduced with DIBAL to obtain elatol (**66**). Overall, three spirocyclic natural products in the family were prepared using this unified asymmetric alkylation/ring-closing metathesis strategy.

1.3.4 FORMAL SYNTHESIS OF PLATENCIN

Maier completed a formal synthesis of platencin (**82**)³¹ by employing a decarboxylative allylic alkylation reaction to build the substitution around a central quaternary carbon atom that joins three different rings (Scheme 1.10). Beginning from vinylogous ester **70**, formylation and allyl enol carbonate construction provided rapid access to allylic alkylation substrate **71** as a mixture of *E* and *Z* isomers. Treatment with catalytic Pd(OAc)₂ and PPh₃ provided allylation product (±)-**72**. Subsequent Luche reduction and rearrangement under acidic conditions provided enone **73**. Esterification of the primary alcohol and silylation provided silyl dienol ether **74**. Aerobic oxidative cyclization according to Toyota's conditions³² afforded [3.2.1] bicycle **75**. The addition of silyl ketene acetal **76** provided conjugate adduct **77**. Subsequent tosylhydrazone formation and skeletal rearrangement led to [2.2.2] bicycle **78**. Weinreb amide formation and treatment with methyllithium gave hemiacetal **79** as an inconsequential mixture of diastereomers. Reduction and oxidation of this compound provided the ring-opened ketoaldehyde **80**. A straightforward aldol cyclization completed the advanced intermediate **81** employed in numerous syntheses of platencin (**82**).³³

In order to provide asymmetric entry into this route, Maier returned to the allylic alkylation step with a focus on the development of an enantioselective variant. Treatment of (Z)-**71** with catalytic $\text{Pd}_2(\text{dba})_3 \cdot \text{CHCl}_3$ and ligand (S,S)-**17** in THF at 0 °C provided access to α -quaternary product **72** in 78% ee. Further optimization revealed that decreasing the reaction temperature to –20 °C provided improved results with the desired compound isolable in 95% yield and 87% ee. As observed in Trost's initial studies on decarboxylative alkylations of allyl enol carbonates,¹⁸ the chiral diamine scaffold of ligand **17** proved effective for quaternary stereocenter formation. As a demonstration of the essentially neutral conditions of the decarboxylative alkylation reaction, the potentially sensitive aldehyde functionality underwent minimal side reactions following quaternary stereocenter formation.

Scheme 1.10. Formal Synthesis of Platencin



Reaction Conditions: (a) NaH, $\text{HCO}_2i\text{-Bu}$, 0 $^{\circ}\text{C}$; then $\text{ClCO}_2\text{allyl}$, cat. KH, THF, 0 $^{\circ}\text{C}$. (b) $\text{Pd}(\text{OAc})_2$ (1.3 mol %), PPh_3 , THF, 20 $^{\circ}\text{C}$ (92% yield, 2 steps). (c) NaBH_4 , $\text{CeCl}_3\cdot 7\text{H}_2\text{O}$, MeOH, 0 $^{\circ}\text{C}$; then $p\text{-TsOH}$, $\text{H}_2\text{O}/\text{Et}_2\text{O}$, rt. (d) PivCl (2 equiv), pyridine (4 equiv), DMAP (0.05 equiv), CH_2Cl_2 , rt (94% yield, 2 steps). (e) LDA (1.5 equiv), TBSCl (2 equiv), HMPA (1 equiv), THF, $-80\text{ }^{\circ}\text{C} \rightarrow \text{rt}$ (88% yield). (f) O_2 , $\text{Pd}(\text{OAc})_2$ (5.8 mol %), DMSO (85% yield). (g) $\text{H}_2\text{C}=\text{C}(\text{OMe})\text{OTBS}$ (**76**) (1.5 equiv), TiCl_4 (1.2 equiv), CH_2Cl_2 , $-80\text{ }^{\circ}\text{C}$, (88% yield).

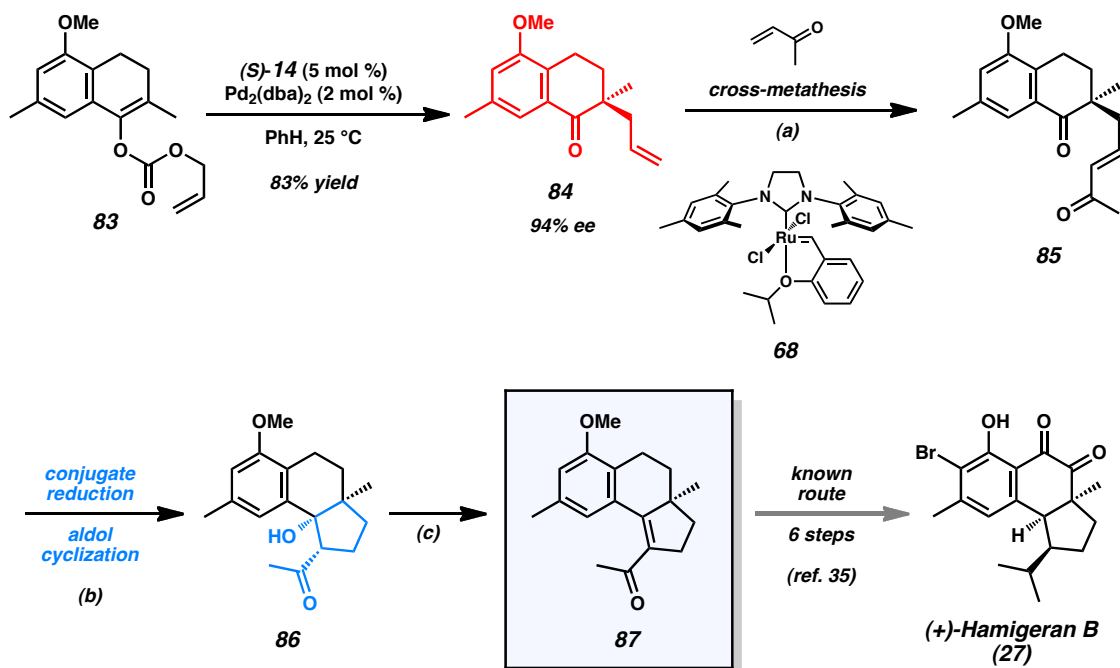
(h) $TsNHNH_2$ (1.3 equiv), MeOH, 60 °C (95% yield). (i) $NaCNBH_3$, $ZnCl_2$, MeOH, 60 °C (60% yield). (j) $HCl\cdot NH(OMe)Me$ (6 equiv), Me_3Al (5 equiv), CH_2Cl_2 , 0 °C. (k) $MeLi$ (6 equiv), Et_2O , $-80 \rightarrow -30$ °C. (l) $LiAlH_4$ (1 equiv), Et_2O , $-80 \rightarrow 0$ °C (85% yield, 2 steps). (m) $(COCl)_2$ (5.8 equiv), DMSO (9 equiv), -80 °C, Et_3N (73% yield). (n) $NaOH$ (6.5 equiv), $EtOH$, 20 °C, 20 h, 87% yield).

1.3.5 FORMAL SYNTHESIS OF HAMIGERAN B

A report from the Stoltz group outlined an intramolecular aldol strategy for the construction of the tricyclic framework of hamigeran B (**27**).³⁴ The synthetic plan targeted the early construction of an α -quaternary tetralone fragment through a Pd-catalyzed decarboxylative allylic alkylation reaction^{17a} (Scheme 1.11). Facile access to enol carbonate **83** enabled rapid evaluation of reaction conditions for the construction of the key quaternary stereocenter. The initial evaluation of (*S*)-*t*-Bu-PHOX (**13**) and $Pd_2(dba)_3$ as catalyst precursors in THF provided functionalized tetralone **84** in 71% yield and 88% ee. The application of the electron-deficient ligand **14** provided greater levels of asymmetric induction with the product isolable in 83% yield and 94% ee. Subsequent olefin cross-metathesis with methyl vinyl ketone provided enone **85** for the evaluation of the planned tandem conjugate reduction and aldol cyclization. Treatment of the compound with Stryker's reagent ($[Ph_3PCuH]_6$) gave desired β -hydroxyketone **86** along with the uncyclized reduction product. Dehydration of compound **86** led to a tricyclic enone **87**, which was previously reported by Miesch,³⁵ and completed an asymmetric formal synthesis of hamigeran B (**27**). The synthesis provides another example of the beneficial effect of electron-deficient PHOX ligand **14** in enantioselective allylic

alkylation reactions. When taken together with Trost's earlier total synthesis,²² the value of asymmetric allylic alkylation reactions can be seen in the different chiral ketone synthons available for the construction a common natural product target.

Scheme 1.11. Formal Synthesis of Hamigeran B



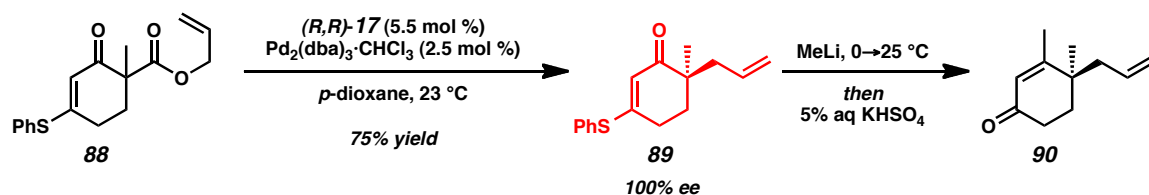
Reaction Conditions: (a) methyl vinyl ketone (10 equiv), Grubbs-Hoveyda 2nd generation catalyst (**68**) (10 mol %), PhH , 35°C (66% yield). (b) $[\text{Ph}_3\text{PCuH}]_6$ (0.5 equiv), PhCH_3 , -40°C . (c) SOCl_2 (15 equiv), DMAP (30 mol %), pyridine, 0°C (62% yield).

1.3.6 TOTAL SYNTHESIS OF CARISSONE AND CASSIOL

The dual syntheses of carissone (**99**)³⁶ and cassiol (**105**)³⁷ by the Stoltz group were enabled by the unique synthetic potential of vinylogous thioester-derived β -ketoester substrates (Scheme 1.13 and Scheme 1.14). While Stoltz developed the first asymmetric

allylic alkylation reactions for cycloalkanone-derived β -ketoester substrates^{17b} (Scheme 1.4), Trost succeeded in extending the substrate scope to vinylogous thioester-derived β -ketoester substrates (Scheme 1.12).³⁸ Under the influence of chiral ligand **17**, α -quaternary vinylogous thioesters such as **89** were prepared in high ee. These products could be readily converted to γ -quaternary enone derivatives through Stork–Danheiser-type transformations. While vinylogous ester derived β -ketoester substrates were also evaluated, conversion was typically sluggish due to the greater orbital overlap of oxygen relative to sulfur.

Scheme 1.12. Extension of β -Ketoester Substrate Scope to Vinylogous Thioester Scaffolds

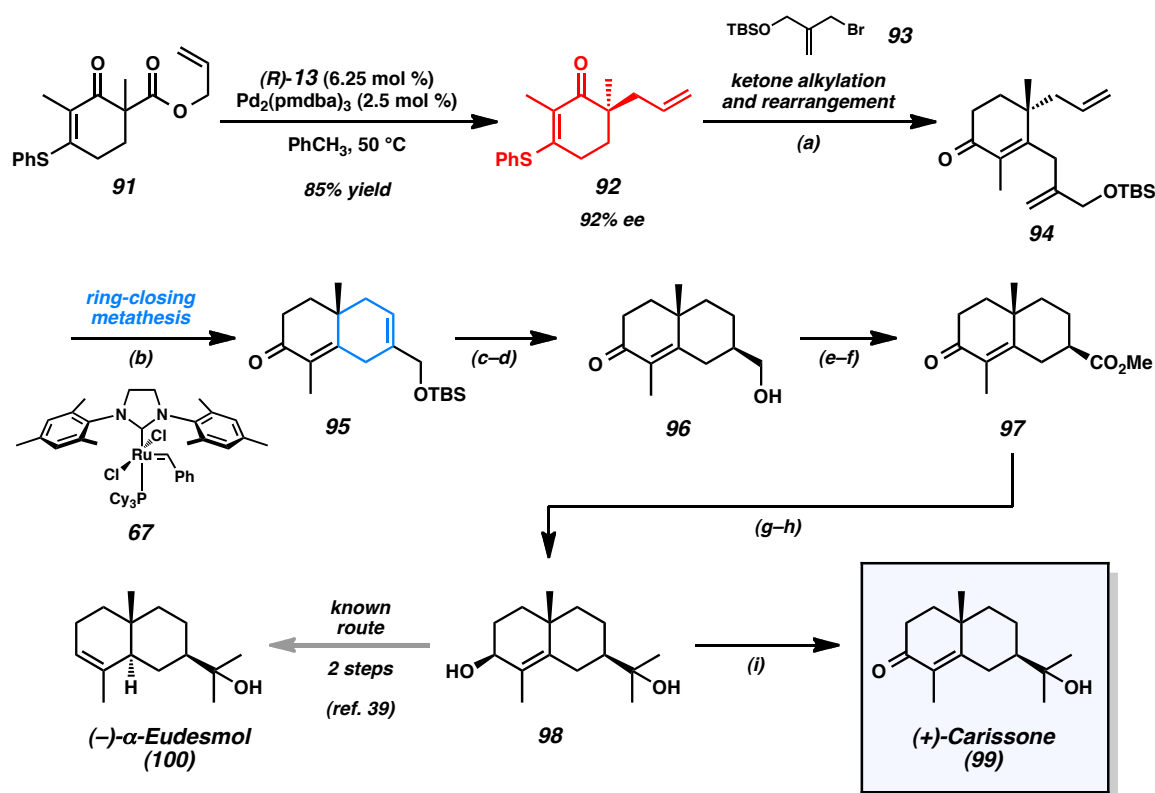


Concurrent work in the Stoltz group sought to develop a PHOX-based catalyst system for the preparation of these useful compounds and their further application in the total synthesis of natural products. While the investigation of β -ketoester and enol carbonate derivatives of α' -substituted isobutyl vinylogous esters provided low conversions and unsatisfactory ee values, the asymmetric allylic alkylation of vinylogous thioester-derived β -ketoester substrate **91** with $\text{Pd}_2(\text{pmdba})_3$ and (*S*)-*t*-Bu-PHOX (**13**) in toluene led to enantioenriched product **92** in 85% yield and 92% ee.

Further manipulations provided a novel asymmetric synthetic route toward eudesmane sesquiterpenoids such as carissone and α -eudesmol³⁶ (Scheme 1.13). The

addition of Grignard reagent of bromide **93** followed by acid-promoted ketone transposition led to enone **94**. Ring-closing metathesis with Grubbs 2nd generation catalyst (**67**) led to fused bicycle **95**. Selective hydrogenation of the less-substituted double bond and desilylation provided hydroxy enone **96**. Oxidation of the alcohol followed by carboxylate methylation led to enone **97**. Subsequent Luche reduction of the enone and dimethylation of the ester led to diol **98**. Allylic alcohol oxidation provided carissone (**99**). Notably, the assembly of diol **98** also completed a formal synthesis of (–)- α -eudesmol (**100**) by interception of Aoyama's route.³⁹

Scheme 1.13. Total Synthesis of Carissone and Formal Synthesis of α -Eudesmol

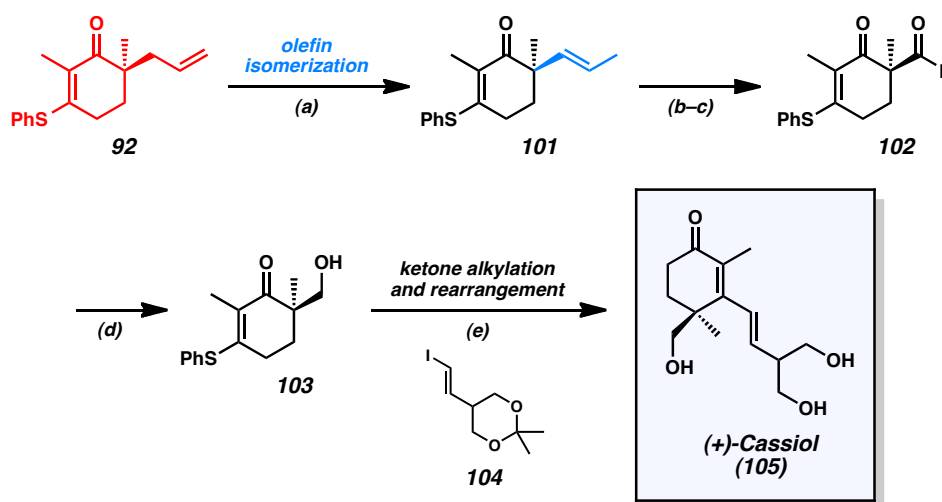


Reaction Conditions: (a) allylic bromide **93**, $\text{Mg}(0)$, I_2 , 0→23 °C (94% yield). (b) Grubbs 2nd generation catalyst (**67**) (3 mol %), PhH , 40 °C (99% yield). (c) $\text{Rh}/\text{Al}_2\text{O}_3$ (5 mol %), H_2 (1 atm),

MeOH. (d) HCl, THF (56% yield, 2 steps). (e) Dess–Martin periodinane, CH₂Cl₂, 0→23 °C. (f) NaClO₂, NaH₂PO₄, 2-methyl-2-butene, *t*-BuOH/H₂O; then CH₂N₂ (87% yield, 2 steps). (g) CeCl₃·7H₂O, NaBH₄, MeOH, –45 °C. (h) MeMgBr, THF, 0→26 °C (73% yield, 2 steps). (i) MnO₂, 4Å MS, CH₂Cl₂, (100% yield).

The concise synthesis of cassiol (**105**)³⁷ also illustrated the utility of α-quaternary vinylogous thioesters formed from decarboxylative asymmetric allylic alkylation reactions (Scheme 1.14). The key enantioenriched vinylogous thioester **92** was subjected to palladium-catalyzed olefin isomerization, oxidative olefin cleavage, and aldehyde reduction steps to provide alcohol **103**. Treatment of this compound with the vinyl lithium of **104** followed by aqueous acid workup led to cassiol (**105**) in a concise sequence. Both of the syntheses completed by the Stoltz group illustrate the conversion of α-quaternary vinylogous thioesters to γ-quaternary cyclohexenones in a unified catalytic asymmetric strategy toward natural products.

Scheme 1.14. Total Synthesis of Cassiol



Reaction Conditions: (a) $\text{PdCl}_2(\text{CH}_3\text{CN})_2$ (10 mol %), PhH , 60 °C (99% yield, 13:1 ratio **101**:**92**). (b) OsO_4 (10 mol %), DABCO, $\text{K}_3\text{Fe}(\text{CN})_6$, K_2CO_3 , $t\text{-BuOH}/\text{H}_2\text{O}$ (1:1), 35 °C. (c) $\text{Pb}(\text{OAc})_4$, PhH , 30 °C (70 % yield). (d) $\text{Li}(\text{Ot-Bu})_3\text{AlH}$, THF, 0 °C (85% yield). (e) vinyl iodide **104**, $t\text{-BuLi}$, Et_2O , –78 °C; then vinylogous thioester **103**; then aq HCl, TBME (36% yield).

1.3.7 TOTAL SYNTHESSES OF FLUSTRAMIDES A AND B, FLUSTRAMINES A AND B

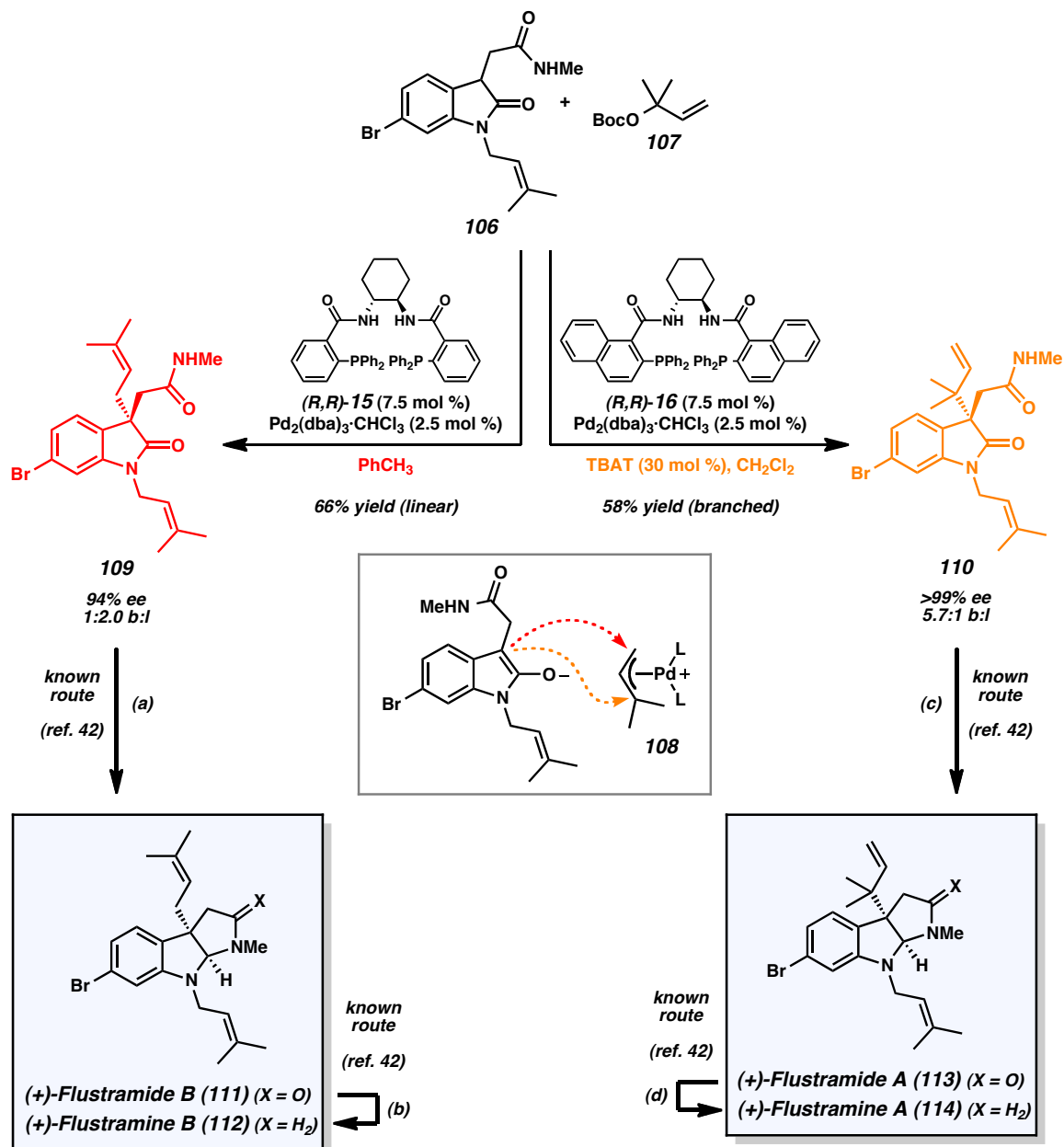
Trost devised a novel and concise strategy for the synthesis of highly substituted pyrroloindoline and pyrroloindolone-type alkaloids such as flustramines A and B and flustramides A and B (**111–114**) (Scheme 1.15).⁴⁰ His group sought to develop reactions based on chiral Pd π -prenyl complex **108**, which can undergo regioselective asymmetric alkylation by an oxindole enolate to forge either the linear prenylated product or the branched reverse prenylated product. Past work has shown that C–C bond formation predominantly occurs at the less substituted allyl terminus,⁴¹ favoring linear product **109**, but the successful modification of reaction conditions would provide branched isomer **110**, which would be difficult to form by alternative means given the proximity of two quaternary carbons.

With this overall problem in mind, a variety of reaction conditions were evaluated to provide potential access to the linear or branched prenylated products. Carbonate **107** was identified as an excellent prenyl source and masked alkoxide base, generating one equivalent of each following oxidative addition and decarboxylation of the substrate by Pd(0). With carbonate **107**, chiral phenyl bis-phosphine ligand **15**, and $\text{Pd}_2(\text{dba})_3\cdot\text{CHCl}_3$ in toluene, a 1:2 ratio of branched:linear products was observed, and the linear product

109 could be isolated in 66% yield and 94% ee. Conversely, combination of the naphthyl bis-phosphine ligand **16**, $\text{Pd}_2(\text{dba})_3 \cdot \text{CHCl}_3$, and catalytic TBAT in CH_2Cl_2 led to a 5.7:1 ratio of branched:linear products with the branched product **110** isolable in 58% yield and greater than 99% ee. These results show that the careful choice and modification of the chiral ligand can greatly influence the regioselectivity of the asymmetric alkylation event leading to all-carbon quaternary stereocenters. Additionally, the general method could be extended to geranylation reactions,⁴⁰ providing impressive access to vicinal all-carbon quaternary stereocenters. The studies performed by Trost show that it is possible to exert control over the regioselectivity, enantioselectivity, and diastereoselectivity of asymmetric alkylation reactions with their chiral ligand systems.

The adoption of Kawasaki's reductive amide cyclization route⁴² provided access to the highly substituted flustramine and flustramide alkaloids. Oxindole reduction of linear alkylation product **109** and branched alkylation product **110** with an alane-dimethylethylamine complex at low temperature provided (+)-flustramide A (**111**) and (+)-flustramide B (**113**). Treatment of these compounds with additional reductant at ambient temperature effected lactam reduction to give (+)-flustramine A (**112**) and (+)-flustramine B (**114**). The synthetic route powerfully enables divergent access to C(3)-quaternary prenylated and reverse prenylated oxindole scaffolds by appropriate choice of chiral ligand. In general, examples of the catalytic, asymmetric synthesis of vicinal quaternary stereocenters are quite rare.

Scheme 1.15. Total Syntheses of Flustramides A and B, Flustramines A and B



Reaction Conditions: (a) $\text{AlH}_3 \cdot \text{NMe}_2\text{Et}$, THF, -15°C (95% yield). (b) $\text{AlH}_3 \cdot \text{NMe}_2\text{Et}$, THF, rt (97% yield). (c) $\text{AlH}_3 \cdot \text{NMe}_2\text{Et}$, THF, -15°C (92% yield). (d) $\text{AlH}_3 \cdot \text{NMe}_2\text{Et}$, THF, rt (90% yield).

1.3.8 TOTAL SYNTHESSES OF CYANTHIWIGINS B, F, AND G

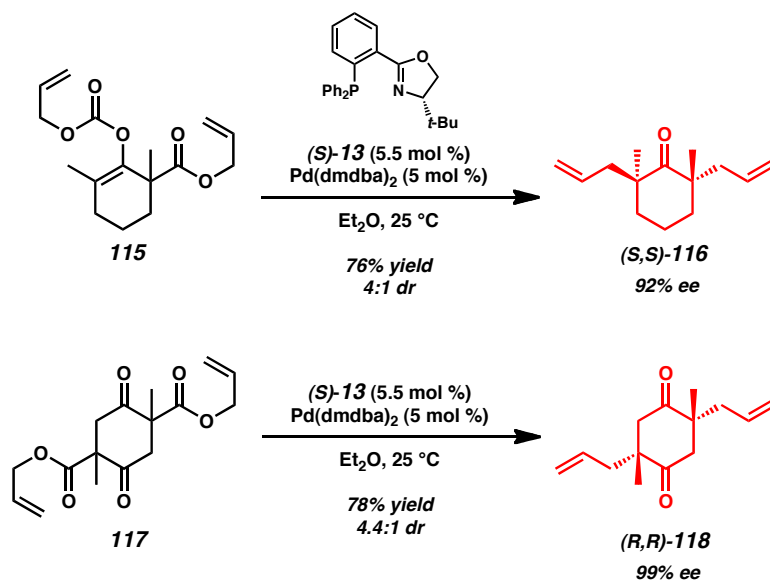
The previously described investigations of Pd-catalyzed allylic alkylations in total synthesis sought to establish one quaternary stereocenter at a time. The highly substituted cyclohexane core of the cyathane diterpenoids motivated the Stoltz group to develop novel double asymmetric decarboxylative allylic alkylation reactions for efficient construction of multiple all-carbon quaternary stereocenters on a single molecule of substrate. These efforts culminated in the efficient total syntheses of cyanthiwigins B, F, and G (**124**, **126**, and **127**) (Scheme 1.17).⁴³

The Stoltz group investigated reactions of substrate **115** in a mixture of catalytic Pd(dmdba)₂ and (*S*)-*t*-Bu-PHOX (**13**) in Et₂O (Scheme 1.16).^{17b} After two sequential asymmetric alkylation events, diketone **116** could be obtained in 76% yield, 92% ee, and 4:1 dr. Studies on the related bis-β-ketoester double alkylation substrate **117** provided product **118** in 78% yield, 99% ee, and 4.4:1 dr.⁴³ These impressive levels of asymmetric induction can be explained by statistical amplification resulting from multiple asymmetric transformations occurring in sequence.^{44,45} The efficiency of these transformations for the assembly of two all-carbon quaternary stereocenters within the same ring system provided an excellent foundation for further synthetic efforts toward the cyathane diterpenoids.

With double alkylation product **118** in hand, the synthesis of numerous members of the cyanthiwigin family could be completed (Scheme 1.17). Desymmetrization of the diketone was achieved by triflation and Negishi coupling to give enone **120**. Subsequent ring-closing metathesis and cross-metathesis with Grubbs–Hoveyda 3rd generation catalyst (**69**) in the presence of vinylboronate **121** provided aldehyde **122**. Radical

cyclization completed the remaining cyclopentane ring. Subsequent triflation and Kumada coupling afforded cyanthiwigin F (**124**).

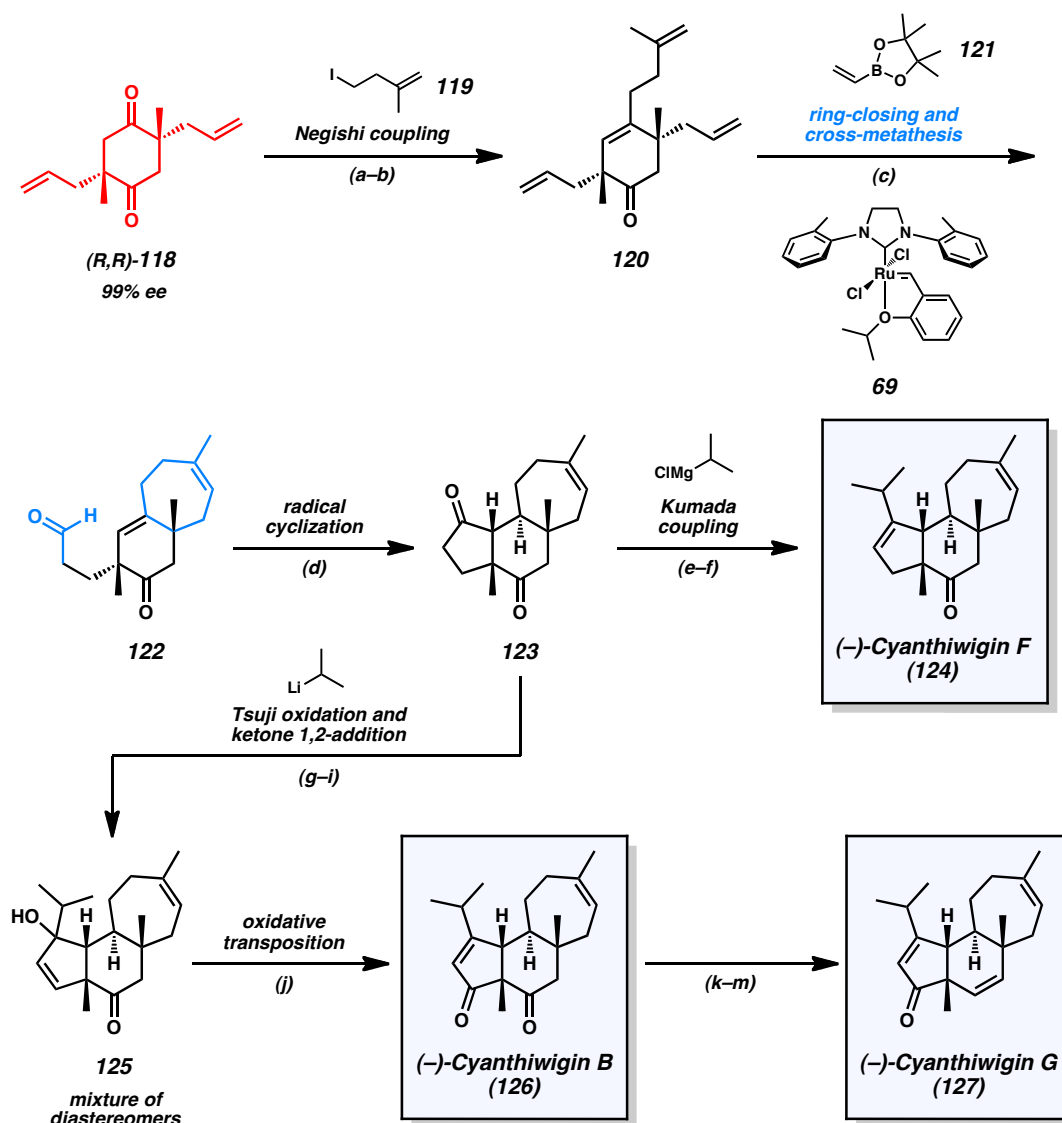
Scheme 1.16. Double Enantioselective Decarboxylative Allylic Alkylation Reactions



Diketone **123** was further functionalized to related natural products cyanthiwigin B (**126**) and cyanthiwigin G (**127**) in a short, concise sequence (Scheme 1.17). By performing a Tsuji oxidation⁴⁶ and treating the intermediate enone with isopropyllithium in the presence of a CeCl_3 activator, adduct **125** could be formed as an inconsequential mixture of diastereomers. Oxidative transposition of the tertiary allylic alcohol enabled the completion of cyanthiwigin B (**126**). Reduction of the ketone and enone moieties with NaBH_4 followed by reoxidation of the allylic alcohol afforded an intermediate alcohol, which could be eliminated using Martin's sulfurane to give cyanthiwigin G (**127**). The unified approach to these natural products was enabled by the development of a doubly enantioselective and diastereoselective allylic alkylation of a single molecule of

substrate. The efficient synthetic route provided unique access to the highly substituted cyclohexanoid core of the cyathane diterpenoids.

Scheme 1.17. Total Syntheses of Cyanthiwigins B, F, and G



Reaction Conditions: (a) KHMDs , PhN(Tf)_2 , THF, -78°C (73% yield). (b) Zn(0) , TMSCl , 1,2-dibromoethane, alkyl iodide **119**, THF, 65°C ; then $\text{Pd(PPh}_3)_4$ (5 mol %) (78% yield). (c) vinylboronic ester **121**, Grubbs–Hoveyda 3rd generation catalyst (**69**) (10 mol %), PhH , 60°C ; then NaBO_3 , THF/ H_2O (51% yield). (d) $t\text{-BuSH}$, AIBN , PhH , 80°C . (e) KHMDs , PhN(Tf)_2 , THF,

–78 °C (60% yield). (f) *i*-PrMgCl, CuCN, THF; Pd(dppf)Cl₂ (10 mol %) (41% yield). (g) KHMDS, THF –78 °C; then allyl chloroformate. (h) Pd₂(pmdba)₃ (5 mol %), CH₃CN, 80 °C (57% yield, 2 steps). (i) CeCl₃, *i*-PrLi, THF, –78 °C (76% yield, mixture of diastereomers). (j) PCC, CH₂Cl₂ (86% yield). (k) NaBH₄, MeOH/CH₂Cl₂, 25 °C. (l) MnO₂, CH₂Cl₂ (15% yield, 2 steps). (m) Martin's sulfurane, CDCl₃ (48% yield).

1.4 CONCLUSION AND OUTLOOK

The pursuit of complex targets has provided inspiration for the development of Pd-catalyzed asymmetric allylic alkylation reactions for the construction of challenging all-carbon quaternary stereocenters. The synthetic methods developed in the past ten years have provided chemists with useful tools for the assembly of densely substituted ring systems, and consequently, the total synthesis of complex natural products. While major advances have been made, broader examination of reaction scope, development of novel catalyst systems, and coupling of palladium enolate chemistry to other powerful bond-forming processes can reshape the future of the field.

1.5 NOTES AND REFERENCES

- (1) For a review discussing our strategy of using natural-product structures to drive the development of enantioselective catalysis, see: Mohr, J. T.; Krout, M. R.; Stoltz, B. M. *Nature* **2008**, *455*, 323–332.
- (2) For excellent general reviews on the catalytic enantioselective generation of quaternary stereocenters, see: (a) Martin, S. F. *Tetrahedron* **1980**, *36*, 419–460. (b) Fuji, K. *Chem. Rev.* **1993**, *93*, 2037–2066. (c) Corey, E. J.; Guzman-Perez, A. *Angew. Chem. Int. Ed.* **1998**, *37*, 388–401. (d) Christoffers, J.; Mann, A. *Angew. Chem. Int. Ed.* **2001**, *40*, 4591–4597. (e) Denissova, I.; Barriault, L. *Tetrahedron* **2003**, *59*, 10105–10146. (f) Douglas, C. J.; Overman, L. E. *Proc. Natl. Acad. Sci. U.S.A.* **2004**, *101*, 5363–5367. (g) Christoffers, J.; Baro, A. *Adv. Synth. Catal.* **2005**, *347*, 1473–1482. (h) *Quaternary Stereocenters: Challenges and Solutions for Organic Synthesis*, Christoffers, J., Baro, A., Eds.; Wiley: Weinheim, 2005. (i) Trost, B. M.; Jiang, C. *Synthesis* **2006**, 369–396. (j) Cozzi, P. G.; Hilgraf, R.; Zimmermann, N. *Eur. J. Org. Chem.* **2007**, 5969–5994. (k) Das, J. P.; Marek, I. *Chem. Commun.* **2011**, *47*, 4593–4623.
- (3) For general reviews discussing palladium-catalyzed asymmetric allylic alkylation, see: (a) Trost, B. M. *Acc. Chem. Res.* **1996**, *29*, 355–364. (b) Trost, B. M.; Van Vranken, D. L. *Chem. Rev.* **1996**, *96*, 395–422. (c) Helmchen, G. *J. Organomet. Chem.* **1999**, *576*, 203–214. (d) Pfaltz, A.; Lautens, M. In *Comprehensive Asymmetric Catalysis*; Jacobsen, E. N., Pfaltz, A., Yamamoto, H., Eds.; Springer: New York, 1999; Vol. 2, pp 833–884. (e) Trost, B. M.; Lee, C. In *Catalytic Asymmetric Synthesis*, 2nd ed.; Ojima, I., Ed.; Wiley-VCH: New York, 2000; pp 593–649. (f) Trost, B. M. *Chem. Pharm. Bull.* **2002**, *50*, 1–14. (g) Trost, B. M. *J.*

- Org. Chem.* **2004**, *69*, 5813–5837. (h) Lu, Z.; Ma, S. *Angew. Chem. Int. Ed.* **2008**, *47*, 258–297. (i) Trost, B. M. *Org. Process Res. Dev.* **2012**, *16*, 185–194.
- (4) For reviews discussing Pd-catalyzed decarboxylative allylic alkylation reactions, see: (a) Tunge, J. A.; Burger, E. C. *Eur. J. Org. Chem.* **2005**, 1715–1726. (b) Mohr, J. T.; Stoltz, B. M. *Chem. Asian J.* **2007**, *2*, 1476–1491. (c) Weaver, J. D.; Recio, III, A.; Grenning, A. J.; Tunge, J. A. *Chem. Rev.* **2011**, *111*, 1846–1913.
- (5) For an earlier review discussing the application of Pd-catalyzed allylic alkylation reactions in total synthesis, see: Trost, B. M.; Crawley, M. L. *Chem. Rev.* **2003**, *103*, 2921–2944.
- (6) For some recent examples of Pd-catalyzed enantioselective allylic alkylation reactions of ketone enolates leading to the formation of chiral tertiary centers at the nucleophile in the context of total synthesis, see: (a) Nigellamine A₂: Bian, J.; Van Wingerden, M.; Ready, J. M. *J. Am. Chem. Soc.* **2006**, *128*, 7428–7429. (b) Hyperolactone C and Biyouyanagin A: Du, C.; Li, L.; Li, Y.; Xie, Z. *Angew. Chem. Int. Ed.* **2009**, *48*, 7853–7856. (c) Tekturna (Aliskiren): Hanessian, S.; Chénard, E. *Org. Lett.* **2012**, *14*, 3222–3225.
- (7) For some recent examples of catalyst-controlled Pd-catalyzed diastereoselective allylic alkylation reactions in the context of total synthesis, see: (a) Spirotryprostatin B: Trost, B. M.; Stiles, D. T. *Org. Lett.* **2007**, *9*, 2763–2766. (b) Epothilone D: Prantz, K.; Mulzer, J. *Chem. Eur. J.* **2010**, *16*, 485–506. (c) Drechslerines A and B: Hagiwara, H.; Fukushima, M.; Kinugawa, K.; Matsui, T.; Hoshi, T.; Suzuki, T. *Tetrahedron* **2011**, *67*, 4061–4068.

- (8) Hayashi, T.; Kanehira, K.; Hagihara, T.; Kumada, M. *J. Org. Chem.* **1988**, *53*, 113–120.
- (9) (a) Sawamura, M.; Nagata, H.; Sakamoto, H.; Ito, Y. *J. Am. Chem. Soc.* **1992**, *114*, 2586–2592. (b) Sawamura, M.; Sudoh, M.; Ito, Y. *J. Am. Chem. Soc.* **1996**, *118*, 3309–3310. (c) Kuwano, R.; Ito, Y. *J. Am. Chem. Soc.* **1999**, *121*, 3236–3237. (d) Kuwano, R.; Uchida, K.; Ito, Y. *Org. Lett.* **2003**, *5*, 2177–2179.
- (10) (a) Trost, B. M.; Ariza, X. *Angew. Chem. Int. Ed. Engl.* **1997**, *36*, 2635–2637. (b) Trost, B. M.; Radinov, R.; Grenzer, E. M. *J. Am. Chem. Soc.* **1997**, *119*, 7879–7880. (c) Trost, B. M.; Schroeder, G. M. *J. Am. Chem. Soc.* **1999**, *121*, 6759–6760. (d) Trost, B. M.; Schroeder, G. M.; Kristensen, J. *Angew. Chem. Int. Ed.* **2002**, *41*, 3492–3495. (e) Trost, B. M.; Schroeder, G. M. *Chem. Eur. J.* **2005**, *11*, 174–184.
- (11) (a) You, S.-L.; Hou, X.-L.; Dai, L.-X.; Cao, B.-X.; Sun, J. *Chem. Commun.* **2000**, 1933–1934. (b) You, S.-L.; Hou, X.-L.; Dai, L.-X.; Zhu, X.-Z. *Org. Lett.* **2001**, *3*, 149–151.
- (12) Tsuji, J.; Minami, I.; Shimizu, I. *Tetrahedron Lett.* **1983**, *24*, 4713–4714.
- (13) Tsuji, J.; Minami, I.; Shimizu, I. *Chem. Lett.* **1983**, 1325–1326.
- (14) Tsuji, J.; Minami, I.; Shimizu, I. *Tetrahedron Lett.* **1983**, *24*, 1793–1796.
- (15) Shimizu, I.; Yamada, T.; Tsuji, J. *Tetrahedron Lett.* **1980**, *21*, 3199–3202.

- (16) Saegusa published very similar work with β -ketoesters simultaneous to Tsuji's work, see: Tsuda, T.; Chujo, Y.; Nishi, S.; Tawara, K.; Saegusa, T. *J. Am. Chem. Soc.* **1980**, *102*, 6381–6384.
- (17) (a) Behenna, D. C.; Stoltz, B. M. *J. Am. Chem. Soc.* **2004**, *126*, 15044–15045. (b) Mohr, J. T.; Behenna, D. C.; Harned, A. M.; Stoltz, B. M. *Angew. Chem. Int. Ed.* **2005**, *44*, 6924–6927. (c) Behenna, D. C.; Mohr, J. T.; Sherden, N. H.; Marinescu, S. C.; Harned, A. M.; Tani, K.; Seto, M.; Ma, S.; Novák, Z.; Krout, M. R.; McFadden, R. M.; Roizen, J. L.; Enquist, Jr., J. A.; White, D. E.; Levine, S. R.; Petrova, K. V.; Iwashita, A.; Virgil, S. C.; Stoltz, B. M. *Chem. Eur. J.* **2011**, *17*, 14199–14223.
- (18) (a) Trost, B. M.; Xu, J. *J. Am. Chem. Soc.* **2005**, *127*, 2846–2847. (b) Trost, B. M.; Xu, J.; Schmidt, T. *J. Am. Chem. Soc.* **2009**, *131*, 18343–18357.
- (19) For a review discussing catalytic enantioselective stereoablative processes, see: Mohr, J. T.; Ebner, D. C.; Stoltz, B. M. *Org. Biomol. Chem.* **2007**, *5*, 3571–3576.
- (20) For an early report of Trost ligands in Pd-catalyzed asymmetric alkylation reactions, see: Trost, B. M.; Van Vranken, D. L.; Bingel, C. *J. Am. Chem. Soc.* **1992**, *114*, 9327–9343.
- (21) For early reports of PHOX ligands, see: (a) von Matt, P.; Pfaltz, A. *Angew. Chem. Int. Ed. Engl.* **1993**, *32*, 566–568. (b) Sprinz, J.; Helmchen, G. *Tetrahedron Lett.* **1993**, *34*, 1769–1772. (c) Dawson, G. J.; Frost, C. G.; Williams, J. M. J.; Coote, S. J. *Tetrahedron Lett.* **1993**, *34*, 3149–3150.

- (22) (a) Trost, B. M.; Pissot-Soldermann, C.; Chen, I.; Schroeder, G. M. *J. Am. Chem. Soc.* **2004**, *126*, 4480–4481. (b) Trost, B. M.; Pissot-Soldermann, C.; Chen, I. *Chem. Eur. J.* **2005**, *11*, 951–959.
- (23) (a) Trost, B. M.; Dong, L.; Schroeder, G. M. *J. Am. Chem. Soc.* **2005**, *127*, 2844–2845. (b) Trost, B. M.; Dong, L.; Schroeder, G. M. *J. Am. Chem. Soc.* **2005**, *127*, 10259–10268.
- (24) (a) Trost, B. M.; Toste, F. D. *J. Am. Chem. Soc.* **1999**, *121*, 9728–9729. (b) Trost, B. M.; Toste, F. D. *J. Am. Chem. Soc.* **2000**, *122*, 714–715. (c) Trost, B. M.; Toste, F. D. *J. Am. Chem. Soc.* **2002**, *124*, 5025–5036.
- (25) (a) Nokami, J.; Mandai, T.; Imakura, Y.; Nishiuchi, K.; Kawada, M.; Wakabayashi, S. *Tetrahedron Lett.* **1981**, *22*, 4489–4490. (b) Ono, T.; Tamaoka, T.; Yuasa, Y.; Matsuda, T.; Nokami, J.; Wakabayashi, S. *J. Am. Chem. Soc.* **1984**, *106*, 7890–7893. (c) Trost, B. M.; Mallart, S. *Tetrahedron Lett.* **1993**, *34*, 8025–8028.
- (26) Snider, B. B.; Vo, N. H.; O’Neil, S. V.; Foxman, B. M. *J. Am. Chem. Soc.* **1996**, *118*, 7644–7645.
- (27) McFadden, R. M.; Stoltz, B. M. *J. Am. Chem. Soc.* **2006**, *128*, 7738–7739.
- (28) Day, J. J.; McFadden, R. M.; Virgil, S. C.; Kolding, H.; Alleva, J. L.; Stoltz, B. M. *Angew. Chem. Int. Ed.* **2011**, *50*, 6814–6818.
- (29) (a) White, D. E.; Stewart, I. C.; Grubbs, R. H.; Stoltz, B. M. *J. Am. Chem. Soc.* **2008**, *130*, 810–811. (b) White, D. E.; Stewart, I. C.; Seashore-Ludlow, B. A.; Grubbs, R. H.; Stoltz, B. M. *Tetrahedron* **2010**, *66*, 4668–4686.

- (30) Stewart, I. C.; Ung, T.; Pletnev, A. A.; Berlin, J. M.; Grubbs, R. H.; Schrodi, Y. *Org. Lett.* **2007**, *9*, 1589–1592.
- (31) Varseev, G. N.; Maier, M. E. *Angew. Chem. Int. Ed.* **2009**, *48*, 3685–3688.
- (32) Toyota, M.; Wada, T.; Fukumoto, K.; Ihara, M. *J. Am. Chem. Soc.* **1998**, *120*, 4916–4925.
- (33) (a) Nicolaou, K. C.; Tria, G. S.; Edmonds, D. J. *Angew. Chem. Int. Ed.* **2008**, *47*, 1780–1783. (b) Hayashida, J.; Rawal, V. H. *Angew. Chem. Int. Ed.* **2008**, *47*, 4373–4376. (c) Yun, S. Y.; Zheng, J.-C.; Lee, D. *Angew. Chem. Int. Ed.* **2008**, *47*, 6201–6203. (d) Tiefenbacher, K.; Mulzer, J. *Angew. Chem. Int. Ed.* **2008**, *47*, 6199–6200. (e) Waalboer, D. C. J.; Schaapman, M. C.; van Delft, F. L.; Rutjes, F. P. J. T. *Angew. Chem. Int. Ed.* **2008**, *47*, 6576–6578. (f) Nicolaou, K. C.; Toh, Q.-Y.; Chen, D. Y.-K. *J. Am. Chem. Soc.* **2008**, *130*, 11292–11293; Nicolaou, K. C.; Toh, Q.-Y.; Chen, D. Y.-K. *J. Am. Chem. Soc.* **2008**, *130*, 14016. (g) Austin, K. A. B.; Banwell, M. G.; Willis, A. C. *Org. Lett.* **2008**, *10*, 4465–4468.
- (34) Mukherjee, H.; McDougal, N. T.; Virgil, S. C.; Stoltz, B. M. *Org. Lett.* **2011**, *13*, 825–827.
- (35) Miesch, L.; Welsch, T.; Rietsch, V.; Miesch, M. *Chem. Eur. J.* **2009**, *15*, 4394–4401.
- (36) Levine, S. R.; Krout, M. R.; Stoltz, B. M. *Org. Lett.* **2009**, *11*, 289–292.
- (37) Petrova, K. V.; Mohr, J. T.; Stoltz, B. M. *Org. Lett.* **2009**, *11*, 293–295.
- (38) Trost, B. M.; Bream, R. N.; Xu, J. *Angew. Chem. Int. Ed.* **2006**, *45*, 3109–3112.

- (39) Aoyama, Y.; Araki, Y.; Konoike, T. *Synlett* **2001**, 9, 1452–1454.
- (40) Trost, B. M.; Malhotra, S.; Chan, W. H. *J. Am. Chem. Soc.* **2011**, *133*, 7328–7331.
- (41) Kazmaier, U.; Stolz, D.; Krämer, K.; Zumpe, F. L. *Chem. Eur. J.* **2008**, *14*, 1322–1329.
- (42) Kawasaki, T.; Shinada, M.; Kamimura, D.; Ohzono, M.; Ogawa, A. *Chem. Commun.* **2006**, 420–422.
- (43) (a) Enquist, Jr., J. A.; Stoltz, B. M. *Nature* **2008**, *453*, 1228–1231. (b) Enquist, Jr., J. A.; Virgil, S. C.; Stoltz, B. M. *Chem. Eur. J.* **2011**, *17*, 9957–9969.
- (44) Langenbeck, W.; Triem, G. Z. *Phys. Chem. Abt. A* **1936**, *117*, 401–409.
- (45) (a) Vigneron, J. P.; Dhaenens, M.; Horeau, A. *Tetrahedron* **1973**, *29*, 1055–1059. (b) Rautentrauch, V. *Bull. Soc. Chim. Fr.* **1994**, *131*, 515–524. (c) Baba, S. E.; Sartor, K.; Poulin, J.; Kagan, H. *Bull. Soc. Chim. Fr.* **1994**, *131*, 525–533.
- (46) (a) Shimizu, I.; Tsuji, J. *J. Am. Chem. Soc.* **1982**, *104*, 5844–5846. (b) Shimizu, I.; Minami, I.; Tsuji, J. *Tetrahedron Lett.* **1983**, *24*, 1797–1800. (c) Minami, I.; Takahashi, K.; Shimizu, I.; Kimura, T.; Tsuji, J. *Tetrahedron* **1986**, *42*, 2971–2977.

CHAPTER 2

Catalytic Asymmetric Synthesis of Cyclopentanoid and Cycloheptanoid Core Structures Using Pd-Catalyzed Asymmetric Alkylation[†]

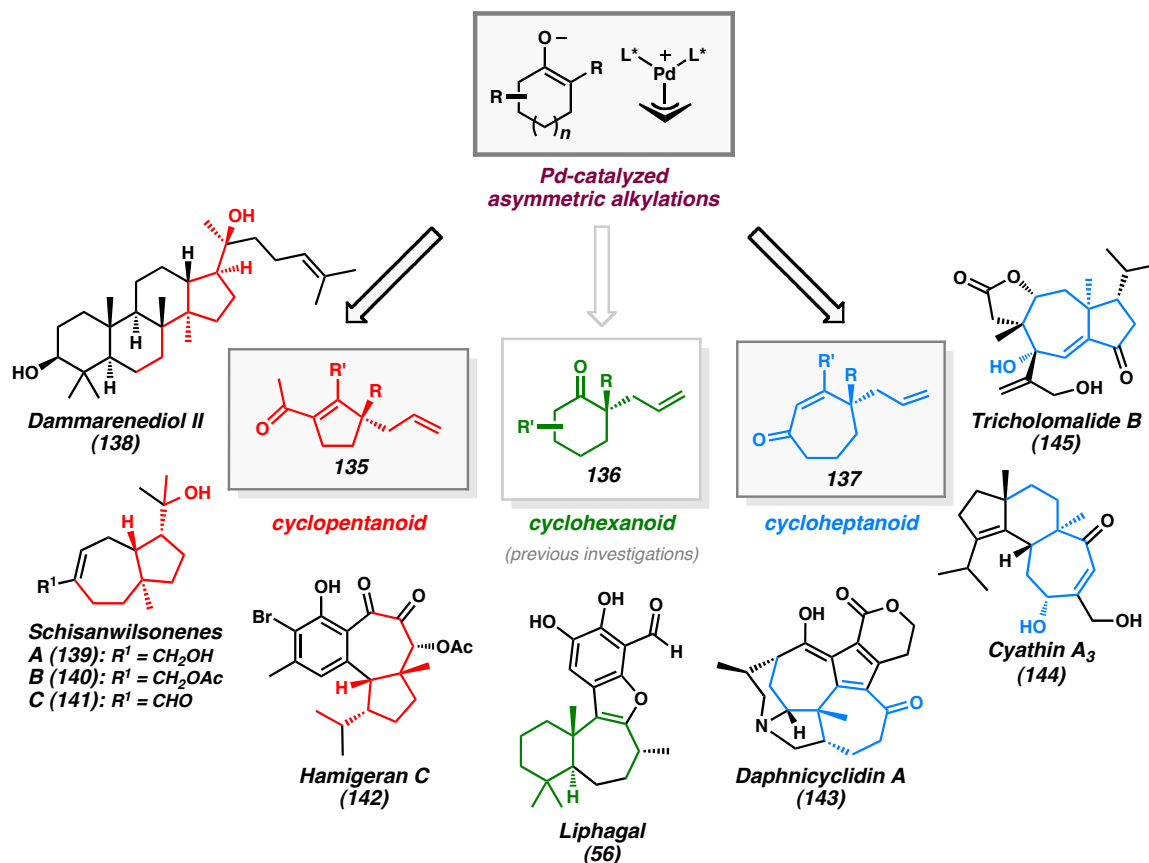
2.1 INTRODUCTION AND BACKGROUND

The stereoselective total synthesis of polycyclic natural products depends greatly on the available tools for the efficient preparation of small and medium sized rings in enantioenriched form.¹ Facile means to elaborate these monocyclic intermediates to fused, bridged, and spirocyclic architectures found within many natural ring systems would significantly contribute to modern synthetic methods. While many strategies have been developed for the preparation of six-membered rings and their corresponding polycyclic derivatives, approaches toward the synthesis of five- and seven-membered rings would benefit from further development.

[†] This work was performed in collaboration with Dr. Michael R. Krout, Dr. Thomas Jensen, Nathan B. Bennett, and Dr. Andrew M. Harned. These works have been published. See: (a) Hong, A. Y.; Krout, M. R.; Jensen, T.; Bennett, N. B.; Harned, A. M.; Stoltz, B. M. *Angew. Chem. Int. Ed.* **2011**, *50*, 2756–2760. (b) Bennett, N. B.; Hong, A. Y.; Harned, A. M.; Stoltz, B. M. *Org. Biomol. Chem.* **2012**, *10*, 56–59. (c) Hong, A. Y.; Bennett, N. B.; Krout, M. R.; Jensen, T.; Harned, A. M.; Stoltz, B. M. *Tetrahedron* **2011**, *67*, 10234–10248.

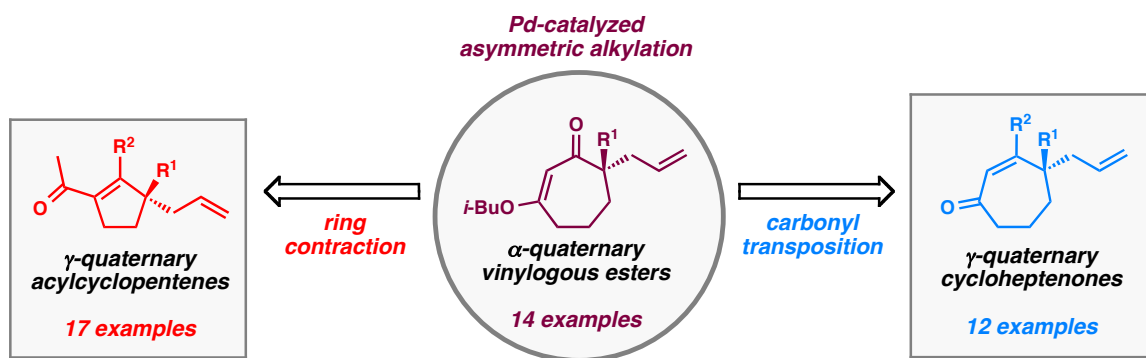
Guided by our continuing interest in the preparation of polycyclic systems bearing all-carbon quaternary stereocenters using Pd-catalyzed asymmetric alkylation chemistry,^{2,3,4,5,6} we sought to prepare various chiral cyclic ketone building blocks for total synthesis (Figure 2.1). Our investigation of six-membered ring substrates has allowed us to achieve the enantioselective total syntheses of a number of complex natural products.⁷ Given our earlier success, we aimed to generalize our approach and gain access to natural products containing chiral cyclopentanoid and cycloheptanoid ring systems as a part of a broader synthetic strategy.

Figure 2.1. Application of Cyclopentanoid, Cyclohexanoid, and Cycloheptanoid Cores Toward Stereoselective Natural Product Synthesis



Our efforts led to the development of general strategies for the preparation of α -quaternary vinylogous esters and their conversion to γ -quaternary cycloheptenones using Stork–Danheiser transformations (Figure 2.2).⁸ During the course of this work, we observed the unusual reactivity of β -hydroxycycloheptanones and exploited a two-carbon ring contraction to provide a general synthesis of γ -quaternary acylcyclopentenones.⁹ With access to the isomeric five- and seven-membered enones, we prepared diverse synthetic derivatives and polycyclic systems that can potentially provide different entry points for synthetic routes toward complex natural products.

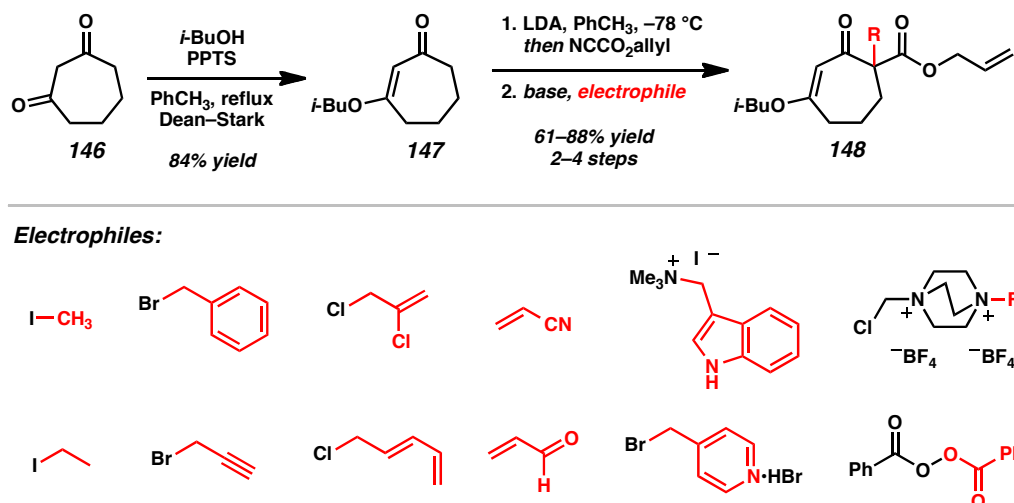
Figure 2.2. General Access to Enantioenriched Cyclopentanoid and Cyclohexanoid Cores



2.2 β -KETOESTER SYNTHESIS AND Pd-CATALYZED ASYMMETRIC ALKYLATION REACTIONS

Much of our past research on the asymmetric alkylation of cyclic ketones^{2,3,7a,c,g-i,10d} and vinylogous esters^{7b,d-f,10a-c,e} focused on six-membered rings, while transformations of larger rings were less thoroughly investigated. We hoped to extend our work by

exploring asymmetric alkylations of seven-membered vinylogous esters. The feasibility of various types of substrates for our asymmetric alkylation chemistry suggested that vinylogous ester **147** could be transformed into silyl enol ether, enol carbonate, or β -ketoester substrates, but we chose to prepare β -ketoesters due to their relative stability and ease of further functionalization. To access a variety of racemic α -quaternary β -ketoester substrates for Pd-catalyzed asymmetric alkylation reactions, we required multi-gram quantities of 1,3-cycloheptanedione (**146**). Dione **146** is commercially available,¹¹ but we typically prepare it from cyclopentanone by the route of Ragan and co-workers to facilitate large scale synthesis.¹² Treatment of **146** with *i*-BuOH and catalytic PPTS under Dean–Stark conditions produced vinylogous ester **147** (Scheme 2.1).¹¹ Acylation of **5** with allyl cyanoformate following deprotonation with LDA enabled facile installation of the requisite allyl ester functionality. Subsequent enolate trapping with a variety of electrophiles under basic conditions provided substrates containing alkyl, alkyne, alkene, 1,3-diene, vinyl chloride, nitrile, heteroarene, aldehyde, fluoride, silyl ether, and ester functionalities in 61–88% yield over two to four steps (**148a–n**). With these quaternary β -ketoesters in hand, we evaluated the scope of Pd-catalyzed asymmetric alkylation reactions on seven-membered ring vinylogous ester substrates, focusing on methyl/allyl substituted **148a** for our optimization efforts.

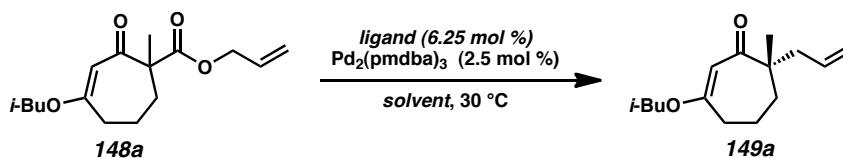
Scheme 2.1. Synthesis of Parent Vinylogous Ester **147** and β -Ketoester Substrates **148**

A survey of several electronically differentiated PHOX ligands combined with $\text{Pd}_2(\text{pmdba})_3$ ^{13,14} in a number of different solvents using methyl-substituted β -ketoester **148a** identified the optimal parameters for this transformation (Table 2.1). Initial conditions employed (*S*)-*t*-Bu-PHOX^{2,15} (**13**, 6.25 mol %) and $\text{Pd}_2(\text{pmdba})_3$ (2.5 mol %) in THF and gave vinylogous ester **149a** in 94% yield and 84% ee (entry 1).¹⁶ Application of the same catalyst system in other ethereal solvents, such as *p*-dioxane, 2-methyl THF, TBME, and Et_2O led to only slight improvements in the enantioselectivity of the reaction to give the desired product in up to 86% ee (entries 2–5). Switching to aromatic solvents provided modest increases in asymmetric induction, furnishing **149a** in 91% yield and 88% ee in the case of toluene (entries 6 and 7).

We next examined the impact of other PHOX ligands (**14** and **150**) in this medium. Electron-deficient ligand **14**^{7b,f,17} improved enantioselectivity at the cost of higher catalyst loading and lower yield (entry 8). Structural modification of the aryl phosphine

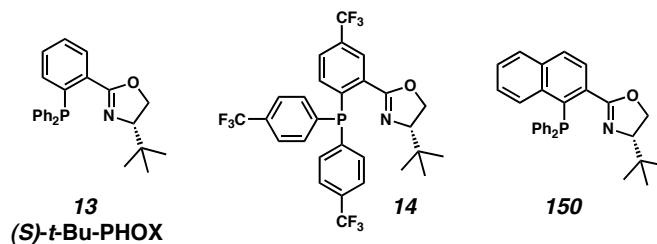
backbone was evaluated with ligand **150**, but this proved to be less effective, giving reduced yield and ee (entry 9). Of the three ligands, **13** furnished the best overall results.

Table 2.1. Solvent and Ligand Effects on Enantioselective Decarboxylative Allylation^a



entry	ligand	solvent	yield (%) ^b	ee (%) ^c
1	13	THF ^e	94	84
2	13	<i>p</i> -dioxane	86	84
3	13	2-methyl THF ^e	75	85
4	13	TBME ^e	88	85
5	13	Et ₂ O	93	86
6	13	PhH	84	86
7	13	PhCH ₃	91	88
8 ^d	14	PhCH ₃	57	90
9	150	PhCH ₃	77	72

^a Conditions: β -ketoester **148a** (1.0 equiv), Pd₂(pmdba)₃ (2.5 mol %), ligand (6.25 mol %) in solvent (0.1 M) at 30 °C; pmdba = 4,4'-methoxydibenzylideneacetone. ^b Isolated yield. ^c Determined by chiral HPLC. ^d Increased catalyst loadings were required to achieve full conversion: Pd₂(pmdba)₃ (5 mol %), **14** (12.5 mol %). ^e THF = tetrahydrofuran, 2-methyl THF = 2-methyl tetrahydrofuran, TBME = *tert*-butyl methyl ether.



With optimal ligand and solvent conditions in hand, we explored asymmetric alkylation reactions of a variety of α -substituted β -ketoesters (Table 2.2). Simple alkyl substitution performed well under our standard conditions (entries 1 and 2). A variety of aromatic and heteroaromatic functionality was well tolerated by the reaction (entries 3, 9–10). Additionally, unsaturated functionality such as alkynes, alkenes, and 1,3-dienes

did not suffer from competitive reaction pathways (entries 4–6). In the case of vinyl chloride **148g**, no products derived from oxidative addition into the C–Cl bond were observed (entry 7). Gratifyingly, *N*-basic functionality such as nitriles and pyridines could be carried through the reaction without noticeable catalyst poisoning (entries 8 and 9). Perhaps the most intriguing result was the observation that substrate **148k** with an unprotected aldehyde could be converted to the enantioenriched product **149k** in 90% yield and 80% ee, highlighting the essentially neutral character of the reaction conditions (entry 11). Tertiary fluoride products could also be obtained efficiently in 94% yield and 91% ee (entry 12). Although most substrates underwent smooth asymmetric alkylation, several substrates such as silyl ether **148m**¹⁸ and benzoate ester **148n**¹⁹ were not formed as efficiently due to unproductive side reactions (entries 13–14).

Table 2.2. Scope of the Pd-Catalyzed Enantioselective Alkylation of Cyclic Vinylogous Esters^a

entry	substrate 148	R	product 149	yield (%) ^b	ee (%) ^c
1	148a	–CH ₃	149a	91	88
2	148b	–CH ₂ CH ₃	149b	89	92
3	148c	–CH ₂ Ph	149c	98	86
4	148d	–CH ₂ C≡CH	149d	88	89
5	148e	–CH ₂ CH ₂ CH=CH ₂	149e	95	87
6	148f		149f	90	90
7	148g		149g	99	86
8	148h	–CH ₂ CH ₂ CN	149h	96	87
9	148i		149i	97	85
10	148j		149j	98	83
11	148k		149k	90	80
12	148l	–F	149l	94	91
13	148m	–CH ₂ OTBDPS ^d	149m	66	58
14	148n		149n	75	57

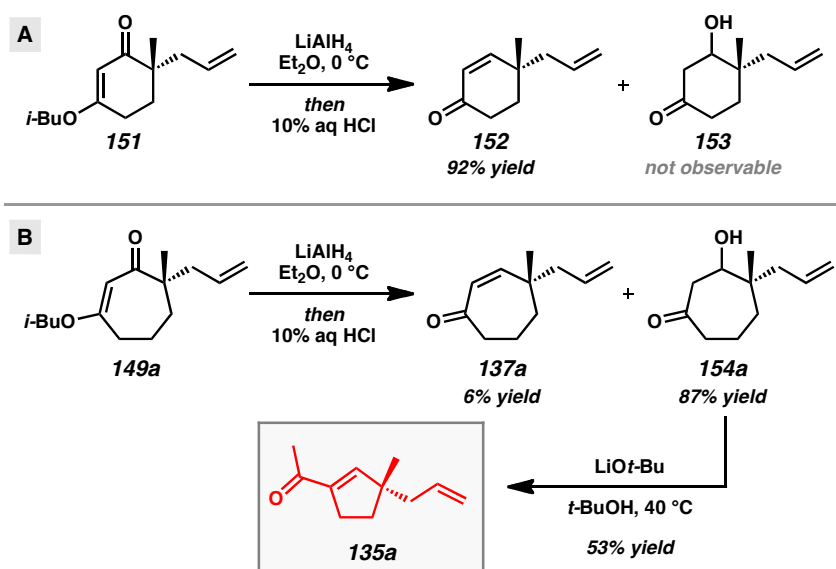
^a Conditions: β -ketoester **148** (1.0 equiv), Pd₂(pmdba)₃ (2.5 mol %), (S)-t-Bu-PHOX (**13**) (6.25 mol %) in PhCH₃ (0.1 M) at 30 °C; pmdba = 4,4'-methoxydibenzylideneacetone. ^b Isolated yield. ^c Determined by chiral HPLC or SFC. ^d Ts = 4-toluenesulfonyl, TBDPS = *tert*-butyldiphenylsilyl.

2.3 OBSERVATION OF THE UNUSUAL REACTIVITY OF β -HYDROXYCYCLOHEPTANONES

With an assortment of asymmetric alkylation products in hand, we next sought to perform a carbonyl transposition using methods developed by Stork and Danheiser.²⁰

Earlier experiments on the hydride reduction of six-membered vinylogous ester **151** with subsequent acid treatment gave enone **152** as expected (Scheme 2.2A). To our surprise, application of identical reaction conditions to the seven-membered analog (**149a**) gave poor yields of cycloheptenone **137a** (Scheme 2.2B). Only minor quantities of elimination product were observed even after prolonged stirring with 10% aqueous HCl. Closer inspection of the reaction mixture revealed β -hydroxyketone **154a** as the major product, suggesting that these seven-membered ring compounds display unique and unusual reactivity compared to their six-membered ring counterparts.^{21,22,23}

Scheme 2.2. Observation of the Unusual Reactivity of β -Hydroxycycloheptanone **154a**

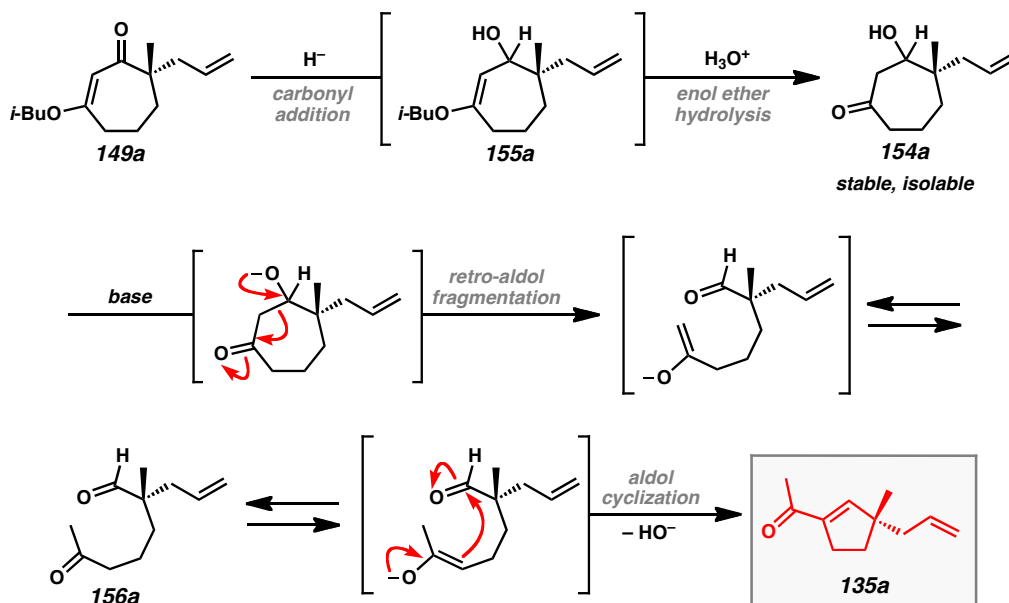


Without initial success using acidic conditions, we reasoned that β -hydroxyketone **154a**²⁴ could potentially provide cycloheptenone **137a** under basic conditions through a β -elimination pathway (Scheme 2.2B). However, attempts in this regard did not produce enone **137a**, but instead gave isomeric enone **135a** that appeared to be formed through an

unexpected ring contraction pathway. Notably, this transformation serves as a rare example of a two-carbon ring contraction.^{22,25,26}

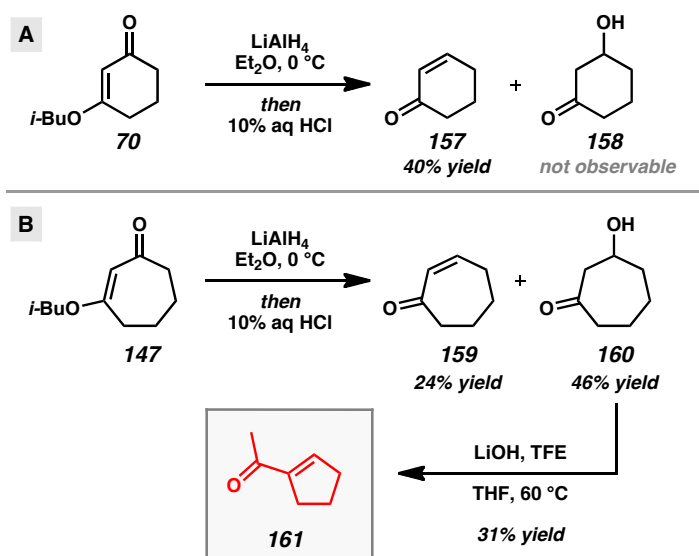
Upon consideration of the reaction mechanism, we believed that this process occurred through an initial deprotonation of the hydroxy moiety, followed by retro-aldol ring fragmentation to a ketoaldehyde enolate (Scheme 2.3). Subsequent isomerization to the more substituted enolate and aldol cyclization could lead to the observed two-carbon ring contraction product **135a**. Attempts to isolate the intermediate ketoaldehyde **156a** were unsuccessful, but aldehyde peaks could be observed by ¹H NMR in reactions that did not proceed to full conversion. Subsequent experiments on more substituted β-hydroxyketones enabled isolation of linear uncyclized intermediates and provided additional support for this reaction mechanism (Scheme 2.6).

Scheme 2.3. Proposed Ring Contraction Mechanism



To explore the general stability and reactivity of β -hydroxycycloheptanones, we briefly examined simplified analogs that do not possess the α -quaternary stereocenter (Scheme 2.4). Following hydride reduction, elimination to cyclohexenone **157** was observed for the six-membered vinylogous ester **70**, while β -hydroxycycloheptanone **160** and volatile cycloheptenone **159** were observed for seven-membered analog **147**. In the seven-membered ring case, a higher proportion of elimination product was observed when compared to the substituted analog **149a**. A milder aqueous acid work-up may suffice to hydrolyze the isobutyl enol ether and enable isolation of the β -hydroxyketone in higher yield in this case. The ring contraction of β -hydroxycycloheptanone **160** under basic conditions proceeded smoothly to give volatile acylcyclopentene **161**. These observations suggest that the unusual two-carbon ring contraction appears to be a reactivity trend associated seven-membered rings and motivated the development of the ring contraction chemistry as a general approach to obtaining chiral acylcyclopentenones.

Scheme 2.4. Attempted Stork–Danheiser Manipulations on Unsubstituted Rings



2.4 RING CONTRACTION STRATEGY FOR PREPARING γ -QUATERNARY ACYLCYCLOPENTENES

Intrigued by our findings, we sought to develop a robust route to γ -quaternary acylcyclopentenones with many substitution patterns. Exploring a number of bases, additives, solvents, and temperatures for the ring contraction of β -hydroxyketone **154a** provided insight into the optimal parameters for the transformation (Table 2.3). Given our early result using LiOt-Bu, we examined numerous aldol cyclization conditions with a variety of non-nucleophilic bases. We observed that several *tert*-butoxides in *t*-BuOH and THF gave conversion to the desired product (**135a**) in good yields (entries 1–4), but noted that the rate of product formation was comparatively slower with LiOt-Bu than with NaOt-Bu or KOt-Bu. The use of various hydroxides revealed a similar trend, where NaOH and KOH generated acylcyclopentene **135a** in 4 hours with improved yields over their respective *tert*-butoxides (entries 5 and 6). The relatively sluggish reactivity of LiOH may be due to the lower solubility of this base in THF, providing **135a** in low yield with the formation of various intermediates (entry 7).

To improve the yield of the reaction with LiOH as base, we investigated the effect of alcohol additives to facilitate the production of mild, organic-soluble bases under the reaction conditions to increase the efficiency of the transformation. The combination of *t*-BuOH and LiOH in THF increased the yield of **135a** to a similar level as that observed with LiOt-Bu, although the reaction still proceeded slowly (entry 8). Application of more acidic, non-nucleophilic alcohols such as hexafluoroisopropanol (HFIP) and trifluoroethanol (TFE) demonstrated exceptional reactivity in combination with LiOH

and efficiently afforded **135a** in high yields (entries 9 and 10).²⁷ In particular, TFE enabled the production of **135a** in 96% yield. Comparable results with preformed $\text{LiOCH}_2\text{CF}_3$ ²⁸ suggest that this alkoxide could be the active base under the LiOH/TFE ring contraction conditions (entry 11).

Concurrent investigation of cesium bases reinforced the importance of alcohol additives for the in situ formation of organic-soluble bases in ring contraction reactions. With $\text{CsOH}\cdot\text{H}_2\text{O}$ and Cs_2CO_3 , product formation was inefficient due to low yield or sluggish reactions (entries 12 and 13). The addition of TFE afforded acylcyclopentene **135a** in yields comparable to those of the LiOH/TFE conditions (entry 14). Notably, ring contraction with Cs_2CO_3 /TFE can also be performed in acetonitrile as an alternative, non-ethereal solvent with high efficiency (entry 15). Additional combinations of bases, additives, solvents, and temperatures were evaluated, but these conditions were generally less effective (entries 16–21).²⁹

Table 2.3. Ring Contraction Reaction Optimization^a

CC(C)C1CCC(=O)CC1O (154a) $\xrightarrow{\text{conditions}}$ CC(C)C1CCC(=O)C1 (135a) + CC(C)C1CCC(=O)CC1 (137a, not observed)

entry	base	additive	solvent	T (°C)	conversion (%)	time (h)	yield (%) ^b
1	LiO <i>t</i> -Bu	—	<i>t</i> -BuOH	40	100	9	71
2	LiO <i>t</i> -Bu	—	THF	40	100	8	60
3	NaO <i>t</i> -Bu	—	THF	40	100	5	81
4	KO <i>t</i> -Bu	—	THF	40	100	5	85
5	NaOH	—	THF	60	100	4	89
6	KOH	—	THF	60	100	4	87
7	LiOH	—	THF	60	78	24	19 ^d
8	LiOH	<i>t</i> -BuOH	THF	60	98	24	78
9	LiOH	HFIP ^c	THF	60	99	12.5	87
10	LiOH	TFE ^c	THF	60	99	12.5	96
11	LiOCH ₂ CF ₃	—	THF	60	—	10	90 ^e
12	CsOH·H ₂ O	—	THF	60	100	4	48
13	Cs ₂ CO ₃	—	THF	60	67	24	61 ^f
14	Cs ₂ CO ₃	TFE ^c	THF	60	100	12.5	86
15	Cs ₂ CO ₃	TFE ^c	CH ₃ CN	60	100	12.5	100
16	NaO <i>t</i> -Bu	<i>t</i> -BuOH	THF	40	100	8	52
17	KO <i>t</i> -Bu	<i>t</i> -BuOH	THF	40	100	8	57
18	LiOH	<i>t</i> -BuOH	THF	40	87	24	77
19	LiOH	TFE ^c	THF	40	73	24	73
20	LiOH	HFIP ^c	THF	40	84	24	81
21	CsF	—	CH ₃ CN	60	86	24	10

^a Conditions: β -hydroxyketone **154a** (1.0 equiv), additive (1.5 equiv), base (1.5 equiv), solvent (0.1 M) at indicated temperature for 9–24 h. ^b GC yield using an internal standard at $\geq 98\%$ conversion unless otherwise stated. ^c HFIP = 1,1,1,3,3,3-hexafluoro-2-propanol; TFE = 2,2,2-trifluoroethanol. ^d Several reaction intermediates observed by TLC and GC analysis; proceeded to 78% conversion. ^e Isolated yield. ^f Reaction did not reach completion at 24 h; proceeded to 67% conversion.

While a number of bases are effective for the production of **135a** in excellent yields, we selected the combination of LiOH/TFE as our standard conditions for reaction scope investigation due to the lower cost and greater availability of base. The data from our study further recognize the unique properties of these mild bases and suggest their application may be examined in a broader context.^{30,31} Importantly, none of the

conditions surveyed for the ring contraction studies generated the β -elimination product, cycloheptenone **137a**.

With the optimal base-promoted conditions in hand, we investigated the scope of the ring contraction chemistry with a variety of substitution patterns²³ (Table 2.4). Simple alkyl, aromatic, heteroaromatic substitution performed well under our standard conditions (Method A) in 84–95% yield (entries 1–6, 10). Additionally, vinyl chlorides, nitriles, and indoles could be incorporated into the target acylcyclopentenones in 85–92% yield (entries 7 and 8). Further studies revealed that alternative aluminum hydrides such as DIBAL could be employed in the generation of the intermediate β -hydroxyketone by enabling more precise control of hydride stoichiometry. The use of these modified conditions followed by oxalic acid work-up in methanol (Method B) facilitated the preparation of pyridine-containing acylcyclopentene **135i** in higher yield compared to Method A (entry 9).

While various compounds could undergo the ring contraction sequence with high efficiency, other substrates with more sensitive functionality required slight modification of the reaction conditions. To this end, we investigated the use of milder reduction conditions developed by Luche³² to further increase the reaction scope. Silyl ether substrate **149m**³³ could be converted to the corresponding acylcyclopentene **135m** in 86% yield using the LiAlH_4 protocol (Method A), but application of Luche reaction conditions using (Method C) enabled an improvement to 91% yield (entry 11). The same conditions provided the related silyl ether-containing acylcyclopentene **135o** with a longer carbon chain in 85% yield (entry 12).

Table 2.4. Ring Contraction Reaction Substrate Scope^{a–e}

entry	substrate 149	reduction conditions	R ¹	R ²	product 135 ^g	yield (%) ^f
1	149a	A	–CH ₃	–CH ₂ CH=CH ₂	135a	84
2	149b	A	–CH ₂ CH ₃	–CH ₂ CH=CH ₂	135b	90
3	149c	A	–CH ₂ Ph	–CH ₂ CH=CH ₂	135c	86
4	149d	A	–CH ₂ C≡CH	–CH ₂ CH=CH ₂	135d	95
5	149e	A	–CH ₂ CH ₂ CH=CH ₂	–CH ₂ CH=CH ₂	135e	87
6	149f	A		–CH ₂ CH=CH ₂	135f	91
7	149g	A		–CH ₂ CH=CH ₂	135g	92
8	149h	A	–CH ₂ CH ₂ CN	–CH ₂ CH=CH ₂	135h	85
9	149i	B		–CH ₂ CH=CH ₂	135i	80
10	149j	A		–CH ₂ CH=CH ₂	135j	87
11	149m	C	–CH ₂ OTBDPS ⁱ	–CH ₂ CH=CH ₂	135m	91
12	149o ^g	C	–(CH ₂) ₃ OTBDPS ⁱ	–CH ₂ CH=CH ₂	135o	85
13	149p ^h	A			135p	81
14	149q ^g	A			135q	87
15	149n	D	–OH	–CH ₂ CH=CH ₂	135n	25
16	149l	A	–F	–CH ₂ CH=CH ₂	135l	0

^a Reduction Conditions A: vinyllogous ester **149** (1.0 equiv), LiAlH₄ (0.55 equiv) in Et₂O (0.2 M) at 0 °C, then 10% aqueous HCl quench. ^b Reduction Conditions B: (1) vinyllogous ester **149** (1.0 equiv), DIBAL (1.2 equiv) in PhCH₃ (0.03 M) at –78 °C; (2) oxalic acid·2H₂O in MeOH (0.02 M). ^c Reduction Conditions C: vinyllogous ester **149** (1.0 equiv), CeCl₃·7H₂O (1.0 equiv), NaBH₄ (3.0 equiv) in MeOH (0.02 M) at 0 °C, then 10% aqueous HCl in Et₂O at 0 °C. ^d Reduction Conditions D: (1) vinyllogous ester **149** (1.0 equiv), DIBAL (3.3 equiv) in PhCH₃ (0.03 M) at –78 °C; (2) 10% aqueous HCl in Et₂O at 0 °C. ^e Ring Contraction Conditions E: β-hydroxyketone **154** (1.0 equiv), CF₃CH₂OH (1.5 equiv), LiOH (1.5 equiv) in THF (0.1 M) at 60 °C. ^f Isolated yield over 2–3 steps. ^g Prepared from **149k**. See Experimental Section. ^h Prepared from **149a**. See Experimental Section. ⁱ Ts = 4-toluenesulfonyl, TBDPS = *tert*-butyldiphenylsilyl, DIBAL = diisobutylaluminum hydride.

Our success in performing ring contractions with a variety of substituents at the quaternary stereocenter encouraged studies aimed at determining whether additional substitution patterns could be introduced into the acylcyclopentene products. While most substrates involved a variable group and an allyl fragment positioned on the quaternary center, we were intrigued by the possibility of performing the ring contraction chemistry with other groups. Investigation of methyl and *trans*-propenyl substituted vinylogous ester **149p** using the standard LiOH/TFE conditions showed that the chemistry was unaffected by modification of the allyl fragment, giving product in 81% yield (entry 13). Additionally, the reaction of spirocycle **149q** also proceeded without complications and afforded the desired product in 87% yield (entry 14).

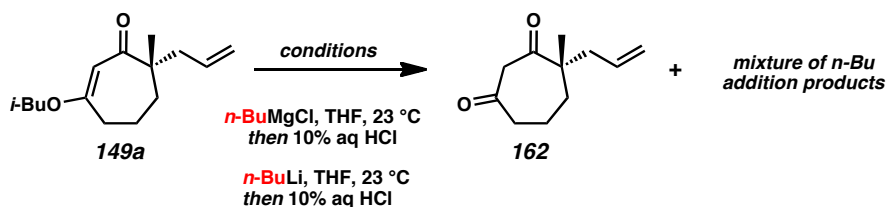
Although many compounds performed well in the ring contraction sequence, certain substrates posed significant challenges. Application of DIBAL reduction conditions with 10% aqueous HCl work-up (Method D) and ring contraction of α -benzoate ester **149n** enabled access to tertiary hydroxyl acylcyclopentene **135n**, but the yield was relatively low compared to other substrates (entry 15). Attempts to prepare the corresponding tertiary fluoride **149l** were unsuccessful as no desired product was observed (entry 16). Under the reaction conditions, both vinylogous esters led to more complex product mixtures from unproductive side reactions in contrast to the typically high yielding transformations observed for other substrates.

To obtain more functionalized acylcyclopentene products and extend our methodology, we sought access to β -substituted acylcyclopentenones by replacing the hydride reduction step with the addition of an organometallic reagent and applying the ring contraction chemistry on the resulting tertiary β -hydroxyketones. We selected a

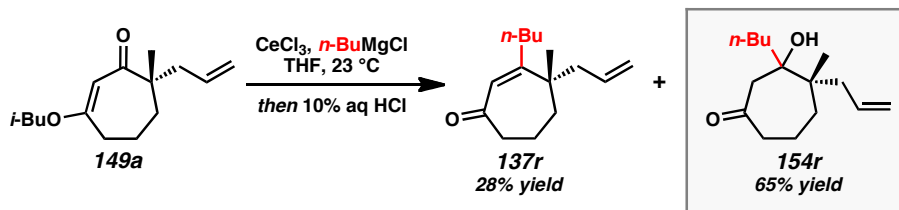
simple system for our initial investigations and evaluated the reaction of *n*-butyl nucleophiles with vinylogous ester **149a**. Unfortunately, the addition of *n*-BuMgCl or *n*-BuLi afforded a complex mixture of products and proceeded slowly without reaching completion, consequently converting unreacted starting material to dione **162** upon work-up with strong acid (Scheme 2.5A).³⁴ This low reactivity could be understood from the electron-rich and sterically-crowded nature of the carbonyl electrophile. Gratifyingly, excellent reactivity was achieved by introducing CeCl₃ to the reaction with the Grignard reagent,³⁵ although a fair amount of the corresponding enone was produced in the transformation (Scheme 2.5B).³⁶ Nevertheless, the CeCl₃-supplemented addition furnished a significantly improved overall yield of addition products with good selectivity for β -hydroxyketone **154r**.

Scheme 2.5. Organometallic Addition to Vinylogous Ester **149a**

A Organometallic Addition Product Distribution

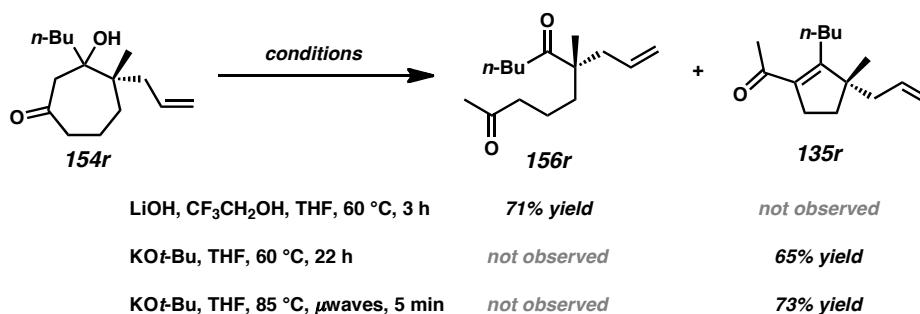


B CeCl₃ Activated Reaction



We next examined the ring contraction sequence with β -hydroxyketone **154r** (Scheme 2.6). Treatment of alcohol **154r** with the optimized ring contraction conditions using LiOH/TFE yielded linear dione **156r** without any of the β -substituted acylcyclopentene. Even though the conditions did not afford the desired product, the isolation of stable uncyclized intermediate **156r** supports our proposed retro-aldol fragmentation/aldol cyclization mechanism (Scheme 2.3). By employing a stronger base such as KO t -Bu, both steps of the rearrangement could be achieved to give acylcyclopentene **135r**. Furthermore, significantly higher yields and reduced reaction times were achieved with microwave irradiation.

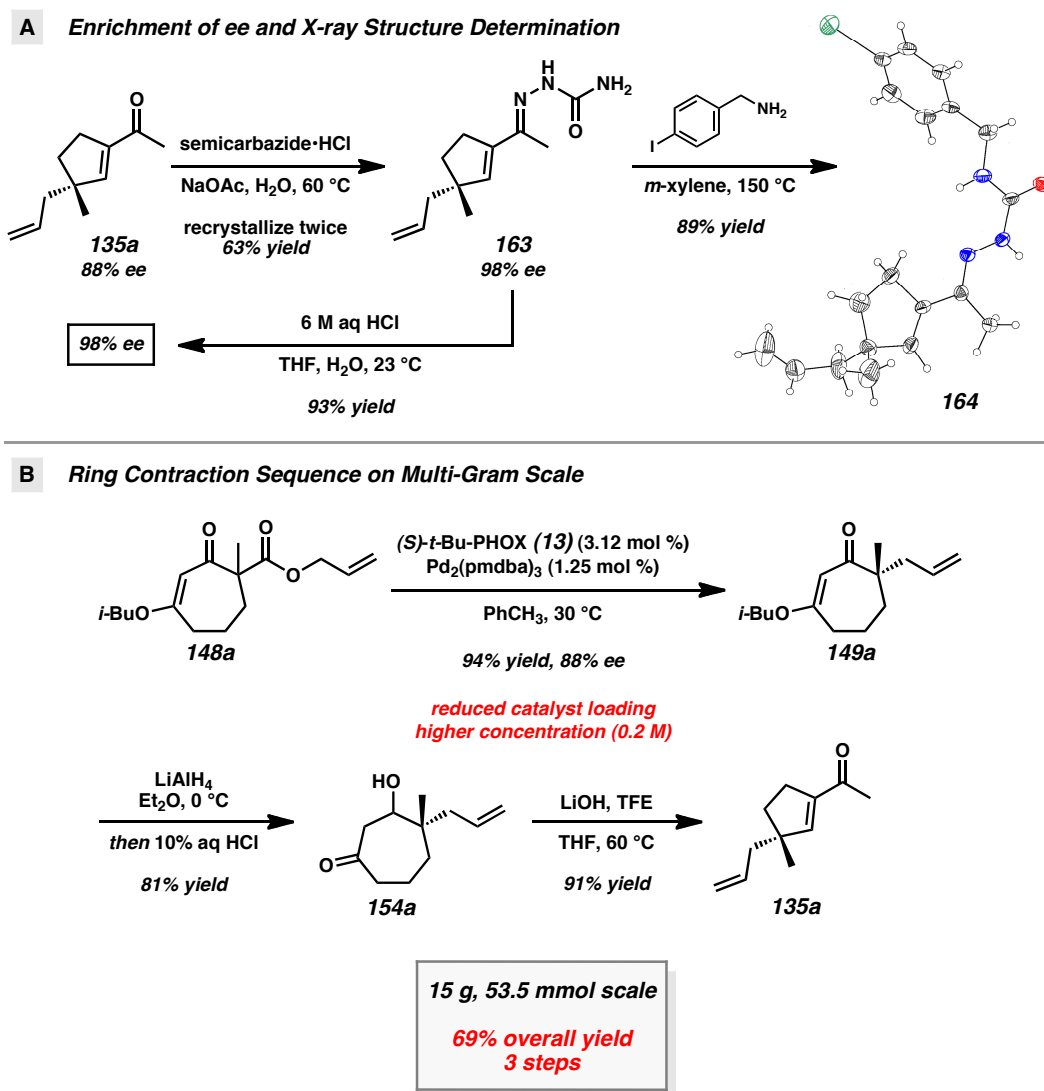
Scheme 2.6. Ring Contraction Screen on β -Hydroxyketone **154r**



With a route to form a variety of acylcyclopentenones that possess different substitution patterns, we were interested in increasing the enantiopurity of these potentially useful intermediates. Formation of the corresponding semicarbazone **163** enabled us to obtain material in 98% ee after two recrystallizations (Scheme 2.7A). A high yielding hydrolysis afforded enantioenriched acylcyclopentene **135a**. Further functionalization of semicarbazone **163** with 4-iodobenzylamine provided crystals that allowed verification of

absolute stereochemistry by X-ray crystallography.³⁷ To demonstrate the viability of our method for large-scale enantioselective synthesis, we performed the asymmetric alkylation and ring contraction transformations on multi-gram scale (Scheme 2.7B). Gratifyingly, our route proved to be robust and reliable. Using 50 mmol of substrate (15 g), we were able to achieve a 94% yield and 88% ee of our desired asymmetric alkylation product. Notably, the increased reaction scale permitted reduced catalyst loadings (1.25 mol % $\text{Pd}_2(\text{pmdba})_3$ and 3.12 mol % (*S*)-*t*-Bu-PHOX, **13**) and higher substrate concentrations (0.2 M). β -Ketoester **148a** underwent the asymmetric alkylation and ring contraction protocol to furnish the desired acylcyclopentene in 69% overall yield over the three step sequence.

Scheme 2.7. Confirmation of Absolute Stereochemistry and Multi-Gram Scale Reactions



2.5 SYNTHESIS OF ACYLCYCLOPENTENE DERIVATIVES USING SITE-SELECTIVE TRANSFORMATIONS

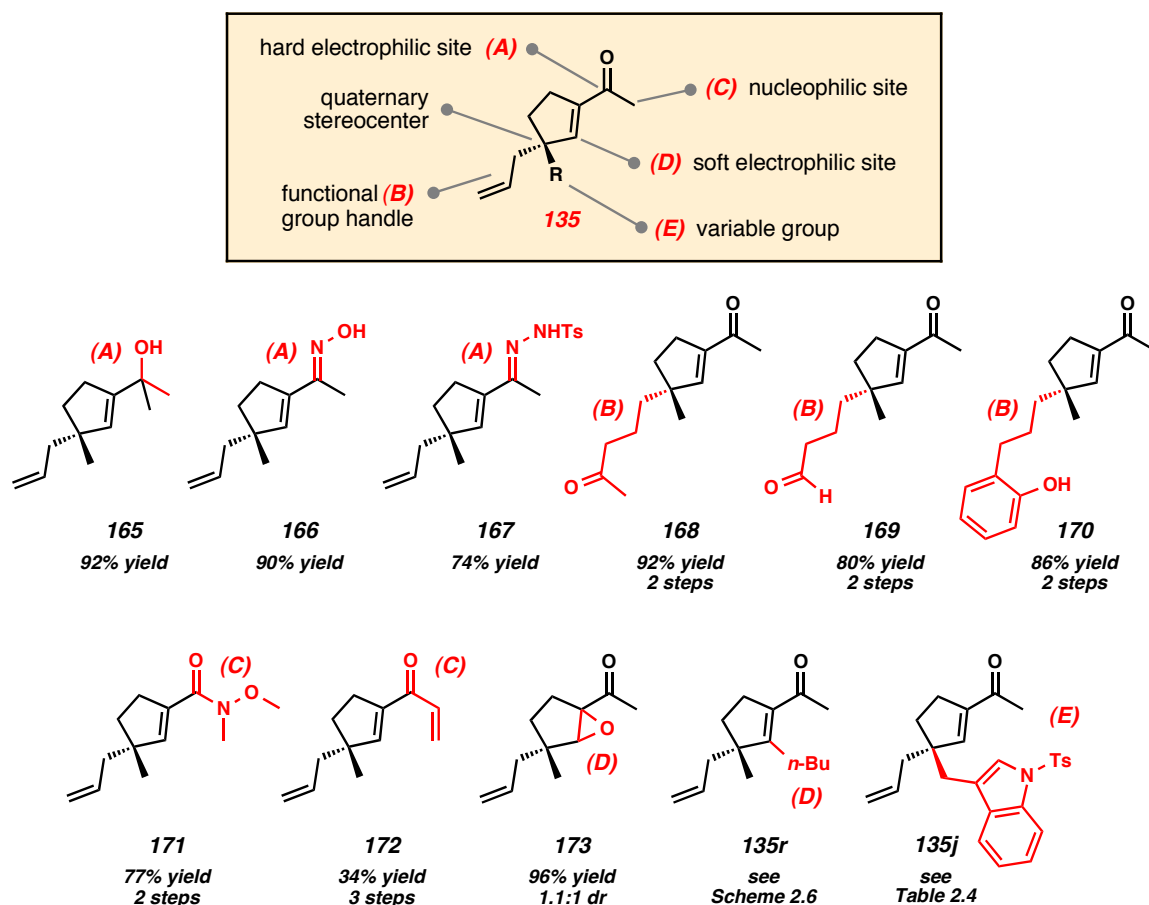
With the ultimate goal of applying our methodology toward the total synthesis of complex natural products, we set out to probe the synthetic utility of various

acylcyclopentenenes prepared using our ring contraction strategy. While acylcyclopentenenes **135** are chiral fragments with low molecular weights, they possess an array of useful functionality that can be exploited for synthetic applications through site-selective functionalizations (Figure 2.3). Acylcyclopentenenes **135** possess hard and soft electrophilic sites, a nucleophilic site, a functional group handle in the form of an allyl group, and a variable group which can be installed through asymmetric alkylation. Additionally, all of the acylcyclopentenenes we have prepared bear an all-carbon quaternary stereocenter or a fully substituted tertiary center.

We aimed to perform site-selective functionalizations to demonstrate that a variety of derivatives could be prepared by recognizing the rich functionality present in acylcyclopentene **135** (Figure 2.3). Selective functionalization of site A enabled access to tertiary alcohols, oximes, and hydrazones in 74–92% yield (**165–167**). Manipulation of site B through olefin metathesis reactions with methyl vinyl ketone or crotonaldehyde provided intermediate bis-enone or enone-enal compounds in 90–95% yield as *trans* olefin isomers. Chemoselective hydrogenation with Wilkinson’s catalyst reduced the less substituted and less sterically hindered olefin in these systems to form mono-enones **168** and **169** in 90–93% yield. Using the insights gathered from these manipulations, we found it was possible to perform chemoselective Heck and hydrogenation reactions to provide acylcyclopentene **170** bearing a pendant phenol in 86% yield over two steps. Through modification of site C, access to Weinreb amides and divinyl ketones could be achieved (**171–172**). Additionally, functionalization of site D gave rise to epoxide **173**. Functionalization of this site was also demonstrated with β -substituted acylcyclopentene **135r** (Scheme 2.6). Lastly, variations at site E were accomplished by installing the

appropriate groups at an early stage during the asymmetric alkylation step (Scheme 2.1 and Table 2.2).

Figure 2.3. Selective Functionalizations on Sites A–E of Acylcyclopentenones **135**

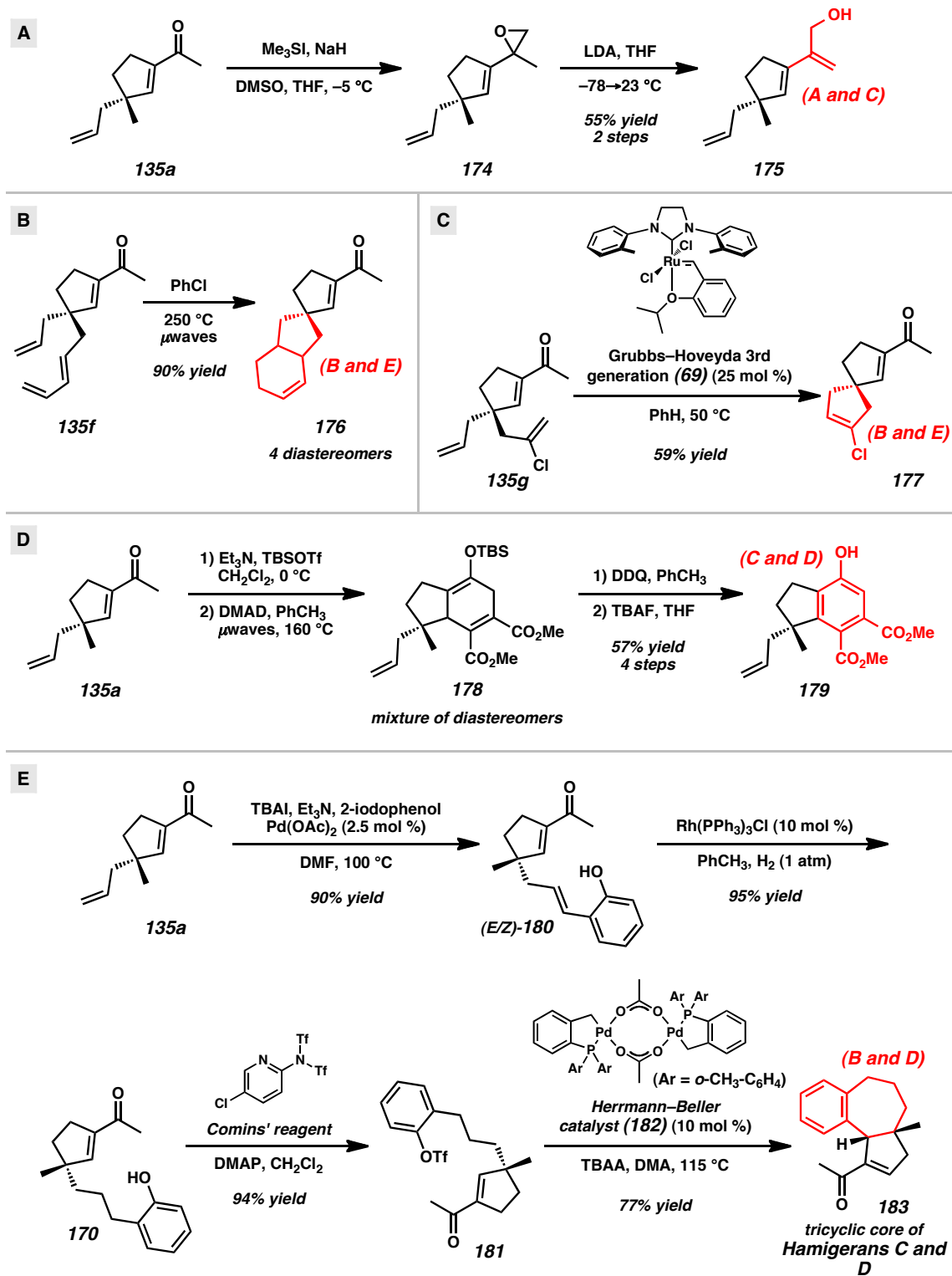


To further increase the potential of these chiral building blocks, we performed manipulations on a combination of reactive sites to arrive at more advanced synthetic intermediates (Scheme 2.8). Hydroxydiene **175** was obtained from acylcyclopentene **135a** by performing a carbonyl epoxidation followed by fragmentation in 55% yield over two steps (Scheme 2.8A). Spirocyclic systems such as enones **176** and **177** can be

obtained by performing an intramolecular Diels–Alder using **135f** or a ring-closing metathesis of **135g** using Grubbs–Hoveyda 3rd generation catalyst (Scheme 2.8B and Scheme 2.8C). Additionally, phenolic indane **179** was generated in 57% yield over four steps by exploiting an intermolecular Diels–Alder reaction with DMAD (Scheme 2.8D). To arrive at synthetic intermediates that bear a stronger resemblance to natural products, we formed the triflate of Heck product **170** using Comins' reagent³⁸ and subjected the compound to a subsequent intramolecular Heck reaction using the Herrmann–Beller palladacycle **182**³⁹ to obtain tricycle **183** with the *cis*-ring fusion (Scheme 2.8E). This key tricycle contains all of the carbocyclic core of hamigerans C and D with correct stereochemistry at the ring fusions.

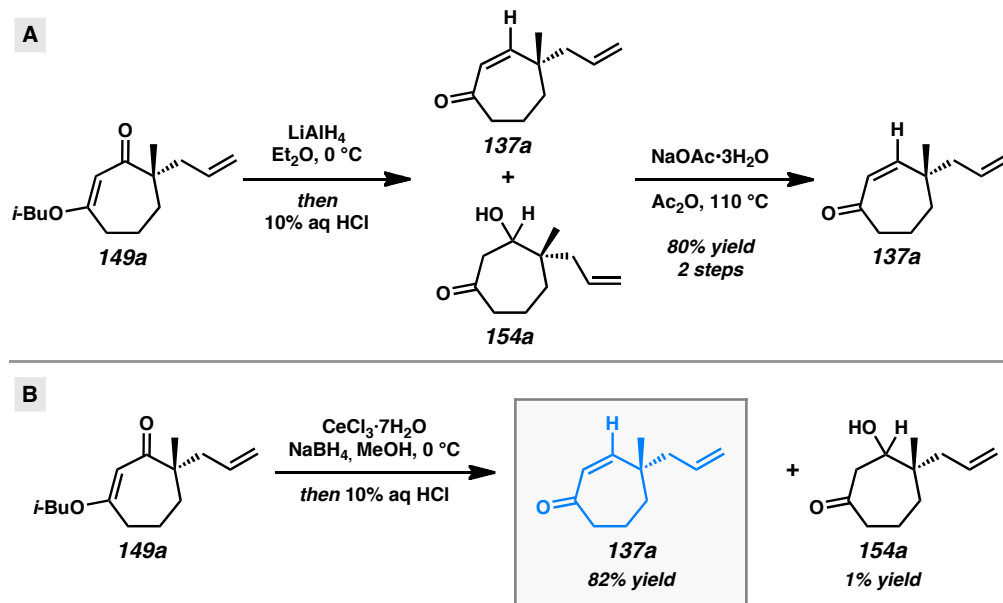
Overall, our general strategy has enabled the synthesis of valuable chiral building blocks by taking advantage of the rich functional group content embedded in acylcyclopentenones **135**. Site-selective manipulations at regions A–E can produce monocyclic and polycyclic compounds with a large degree of structural variation. Our studies have provided valuable insight into the nature of these compounds and we aim to apply our knowledge of these promising synthetic intermediates in the total synthesis of complex natural products.

Scheme 2.8. Functionalization of Multiple Acylcyclopentene Reactive Sites



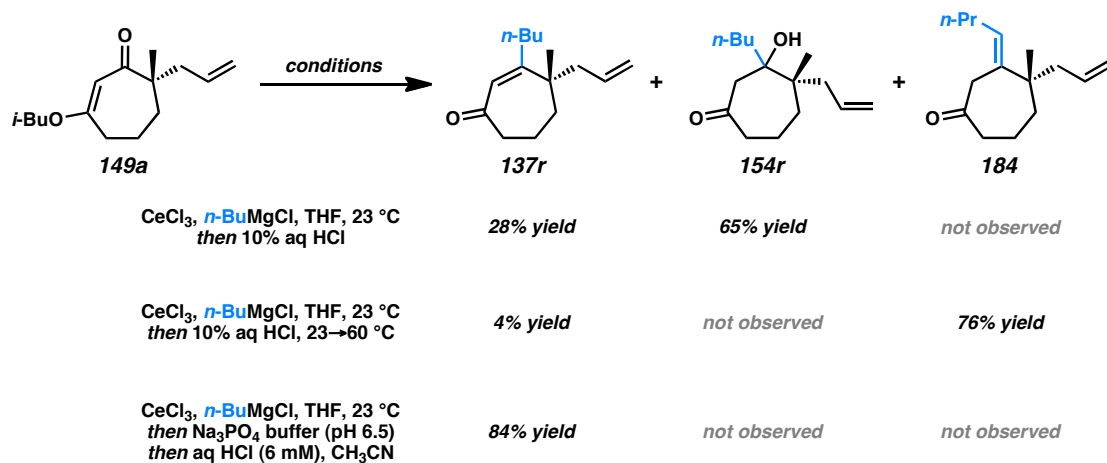
2.6 CARBONYL TRANSPOSITION APPROACH TO γ -QUATERNARY CYCLOHEPTENONES

While pleased to discover the unusual reactivity of vinylogous esters **149** that led to the synthesis of various acylcyclopentenones, we maintained our original interest in preparing enantioenriched γ -quaternary cycloheptenones **137** and began reexamining reaction parameters to this end. Initially, we identified conditions to obtain cycloheptenone **137a** in two steps by activation and elimination of the hydroxy group at elevated temperatures, but ultimately desired a more direct route from vinylogous ester **149a** (Scheme 2.9A). After considerable experimentation, we fortuitously discovered that reduction and elimination using Luche conditions effectively furnished enone **137a** with minimal β -hydroxyketone **154a** (Scheme 2.9B). A number of factors may contribute to the reversed product distribution, with methanol solvent likely playing a large role.⁴⁰ With an effective route to enone **137a**, we also sought to prepare β -substituted cycloheptenones through the 1,2-addition of organometallic reagents.

Scheme 2.9. Stepwise and One-Pot Formation of Cycloheptenone **137a**

We again investigated the addition of *n*-BuMgCl to vinylogous ester **149a** with CeCl₃ additive, focusing on the impact of various quenching parameters. While our previous studies showed that the formation of β -hydroxyketone **154r** was favored over cycloheptenone **137r** (Scheme 2.10, and Scheme 2.11, path a vs path b), we reasoned that elevated temperatures would promote dehydration of β -hydroxyketone **154** to form cycloheptenone **137** as the major product and simplify the product mixture (Scheme 2.11, path c). Subsequent heating of the reaction to 60 °C after acid quench led to complete consumption of β -hydroxyketone (Scheme 2.10). However, the desired cycloheptenone **137r** was isolated as a minor product along with the non-conjugated enone **184** in 76% yield as a single olefin isomer. The prevalence of non-conjugated enone **184** again emphasizes the unusual reactivity of these seven-membered ring systems. To revise our approach, we extensively screened mild acidic work-up conditions to minimize the formation of side products such as isomer **184**. We ultimately discovered that a sodium

phosphate buffer quench followed by treatment of the crude enol ether⁴¹ with dilute HCl in acetonitrile exclusively afforded desired cycloheptenone **137r** (Scheme 2.10). Gratifyingly, a number of sp^3 -hybridized carbon nucleophiles can be employed under these conditions, permitting the preparation of allyl,⁴² homoallyl, and pentenyl substituted cycloheptenones (Table 2.5, entries 1–6, Method F).

Scheme 2.10. Synthesis of β -Substituted Cycloheptenones

Scheme 2.11. General Reaction Mechanism for Carbonyl Transposition

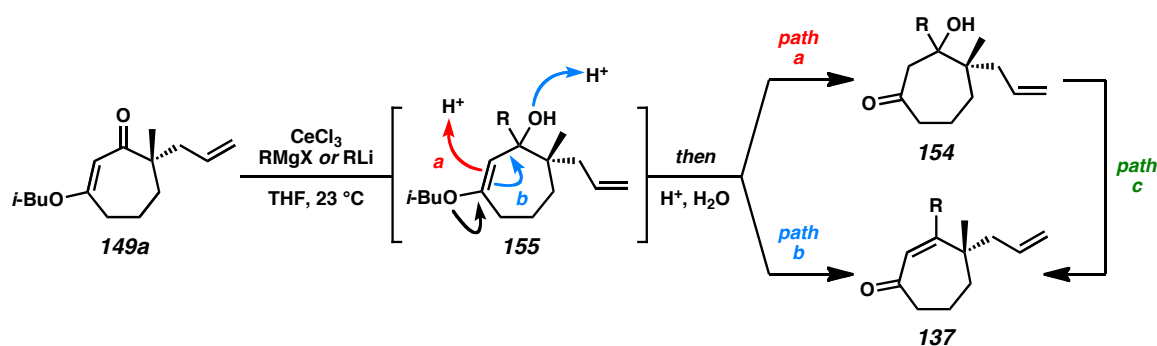


Table 2.5. Scope of Organometallic Addition/Elimination^a

Reaction scheme: **149a** (vinyllogous ester) $\xrightarrow[\text{then work-up conditions}]{\text{CeCl}_3, \text{R-M, THF, 23 } ^\circ\text{C}}$ **137** (unsaturated cycloheptenone).

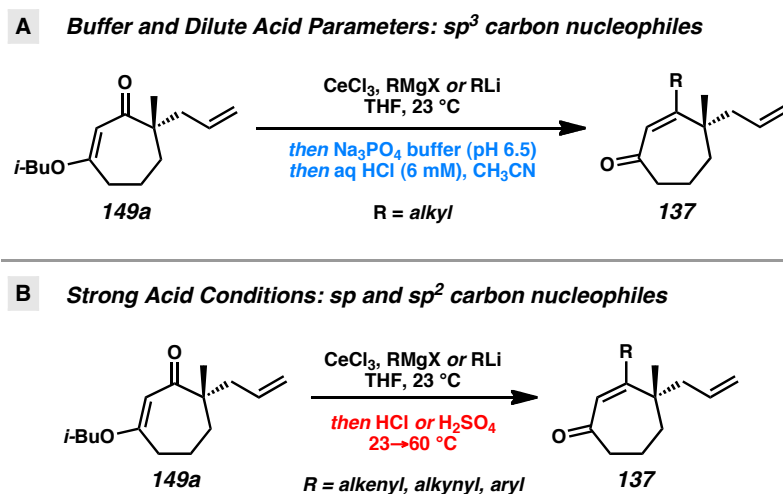
entry	R	M	work-up conditions ^b	product 137	yield (%) ^c
1		–MgCl	F	137r	84
2		–MgBr	F	137s	73
3		–MgBr	F	137t	93
4		–MgBr	F	137u	90
5		–MgBr	F	137v	82
6		–MgBr	F	137w	92
7 ^d		–Li	G	137x	84
8		–MgBr	H	137y	97
9 ^e		–MgBr	H	137z	66
10		–Li	G	137aa	72
11		–MgCl	G	137ab	84

^a Conditions: vinyllogous ester **149a** (1.0 equiv), CeCl₃ (2.5 equiv), RMgX or RLi (3.0 equiv) in THF, 23 °C then work-up by Method F, G, or H. ^b Method F: (1) pH 6.5 Na₃PO₄ buffer; (2) 6 mM HCl, CH₃CN; Method G: 10% w/w aqueous HCl, 60 °C; Method H: 2 M H₂SO₄, 60 °C. ^c Yield of isolated product. ^d Performed without CeCl₃ additive. ^e Product was a 1.9:1 mixture of atropisomers.

We then turned our attention to sp- and sp²-hybridized carbon nucleophiles as part of our goal to prepare variably substituted cycloheptenones **137**. Attempts to apply the buffer and dilute acid quenching parameters provided poor selectivity and often led to complex mixtures of products. A thorough evaluation of work-up conditions revealed that the desired unsaturated β-substituted cycloheptenones could be obtained by quenching the reactions with concentrated strong acid followed by stirring at elevated

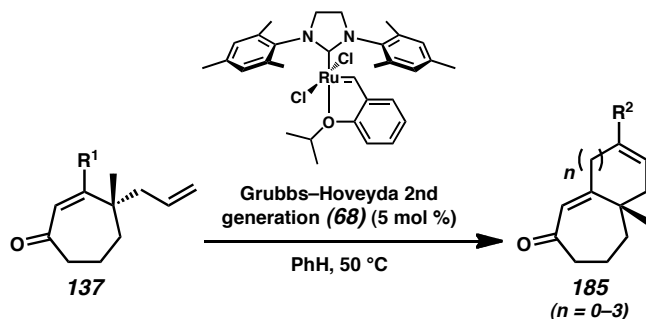
temperatures. Although investigated for sp^3 -hybridized carbon nucleophiles, the strong acid work-up conditions are more suitable for these reactions because the only possible elimination pathway leads to conjugated enone **137**. In this manner, the initial mixture of enone and β -hydroxyketone could be funneled to the desired product (Scheme 2.11, paths b and c). By employing a HCl (Method G) or H_2SO_4 quench (Method H), the synthesis of vinyl,⁴³ alkynyl,⁴⁴ aryl, and heteroaryl substituted enones was achieved in moderate to excellent yield (Table 2.5, entries 7–11). Particularly noteworthy was entry 9, where addition of an *ortho*-substituted Grignard reagent produced sterically congested cycloheptenone **137z**.⁴⁵

These results demonstrate that application of the appropriate quenching parameters based on the type of carbon nucleophile employed is required for successful carbonyl transposition to β -substituted γ -quaternary cycloheptenones (Scheme 2.12). For sp^3 -hybridized carbon nucleophiles, reaction work-up with buffer and dilute acid maximizes enone yield and minimizes formation of non-conjugated enone isomers. In contrast, reactions using sp - and sp^2 -hybridized carbon nucleophiles require strong acidic work-up with heating for best results. Careful application of these general protocols (Methods F–H) provides access to diverse β -substituted γ -quaternary cycloheptenones **137**.

Scheme 2.12. Different Work-Up Conditions for Carbonyl Transposition Reactions Employing sp^3 versus sp/sp^2 Carbon Nucleophiles

2.7 SYNTHESIS OF CYCLOHEPTENONE DERIVATIVES USING TRANSITION-METAL CATALYZED CYCLIZATIONS

Having produced a variety of cycloheptenones, we next turned our attention to the preparation of a series of bi- and tricyclic structures that would be valuable for total synthesis applications. The incorporation of alkene functionality at the β -position allowed rapid access to a series of [7- n] fused ring systems through ring-closing metathesis with the γ -allyl fragment (Table 2.6). This transformation enables the formation of disubstituted bicycles (**185x**, **185s**, **185u**, and **185w**) from terminal alkenes in excellent yields (entries 1, 3, 5, and 8). Trisubstituted bicycles (**185y**, **185t**, and **185v**) are also accessible through enyne ring-forming metathesis (entry 2) and ring-closing metathesis with 1,1-disubstituted alkene β -substituents (entries 4 and 6). Additionally, both atropisomers of cycloheptenone **137z** converge to the [7-7-6] tricyclic enone (**185z**) under the reaction conditions (entry 7).

Table 2.6. Formation of Bi- and Tricyclic Systems Through Ring-Closing Metathesis^a

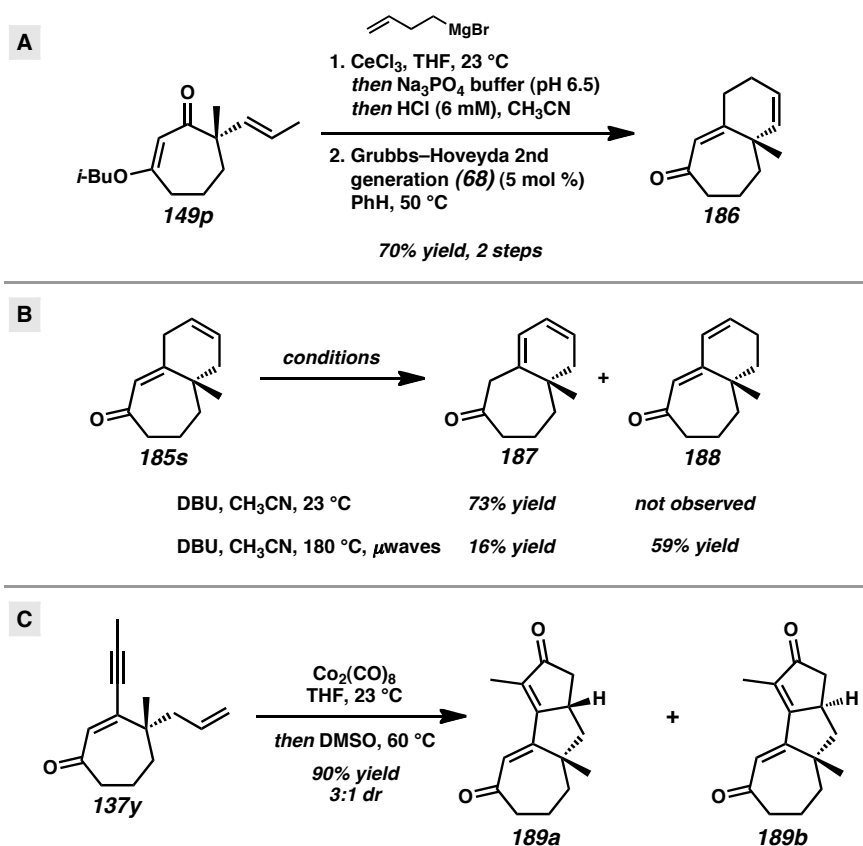
entry	substrate 137	R ¹	product 185	R ²	yield (%) ^b	
1 ^c	137x			185x	R ² = H	93
2	137y			185y	R ² =	99
3 ^d	137s			185s	R ² = H	91
4 ^d	137t			185t	R ² = CH ₃	90
5	137u			185u	R ² = H	90
6	137v			185v	R ² = CH ₃	98
7 ^e	137z			185z	—	96
8	137w			185w	—	99

^a Conditions: cycloheptenone **137** (1.0 equiv) and Grubbs-Hoveyda 2nd generation catalyst (**68**, 5.0 mol %) in PhH, 50 °C. ^b Yield of isolated product. ^c Conditions: cycloheptenone **137** (1.0 equiv) and Grubbs 2nd generation catalyst (**68**, 0.2 mol %) in CH₂Cl₂, reflux. ^d 1,4-benzoquinone (10 mol %) added. ^e Performed in PhCH₃.

With two [7–6] bicyclic structures in hand, we next investigated the preparation of other such bicycles with variable olefin positions. Addition of 3-butenylmagnesium

bromide to *trans*-propenyl vinylogous ester **149p** followed by ring-closing metathesis furnished bicycle **186** with the alkene adjacent to the quaternary stereocenter (Scheme 2.13A). Following the precedent of Fuchs,⁴⁶ we envisioned accessing bicycle **188** through a base-mediated migration from enone **185s**. However, treatment of skipped diene **185s** with an amine base at ambient temperature unexpectedly afforded diene **187** instead (Scheme 2.13B). In the end, the alkene could be migrated in the desired direction to generate diene **188** by performing the reaction in the presence of microwave irradiation. Overall, these methods allow for the preparation of [7–6] bicycles with variable olefin substitution.

Scheme 2.13. Synthesis of Additional [7–6] Bicycles and [7–5–5] Tricycles



Recognition of the proximal enyne functionality of cycloheptenone **137y** prompted an investigation of a Pauson–Khand reaction to form more complex ring systems. Treatment of enone **137y** with dicobalt octacarbonyl in the presence of dimethylsulfoxide⁴⁷ generated the [7–5–5] tricycle in a 3:1 diastereomeric ratio of **189a** to **189b** (Scheme 2.13C). Overall, our organometallic addition and elimination strategy combined with the appropriate work-up conditions facilitated the preparation of numerous bi- and tricyclic systems with a wide array of substitution patterns that may prove useful in the context of natural product synthesis.

2.8 UNIFIED STRATEGY FOR THE SYNTHESIS OF COMPLEX POLYCYCLIC NATURAL PRODUCTS

Our divergent approaches to the synthesis of acylcyclopentenones **135** and cycloheptenones **137** from enantioenriched vinylogous esters **149** have provided the foundation for the preparation of complex polycyclic molecules based on cyclopentanoid and cycloheptanoid core structures (Figure 2.4). Both [5–6] and [5–6–7] fused polycyclic structures could be obtained from acylcyclopentenones. Synthetic elaboration of cycloheptenones provided access to [7–5], [7–6], [7–7], [7–8], [7–7–6], and [7–5–5] fused structures. Additionally, [5–5], [5–6], and [7–6] spirocyclic structures could be obtained using our synthetic approaches. These examples significantly add to the collection of polycyclic architectures accessible by elaboration of chiral six-membered ring carbocycles or heterocycles **136**.^{2,3} We have applied previously developed methodology toward a number of polycyclic cyclohexanoid natural products⁷ (Figure 2.5)

and similarly plan to exploit the ring contraction and ketone transposition methodology in future efforts toward cyclopentanoid and cycloheptanoid natural products. The work presented in this chapter will provide the foundation for future efforts and enable a broader synthetic approach to complex natural product targets.

Figure 2.4. Chiral Fused and Spirocyclic Structures Prepared by Asymmetric Allylic Alkylation

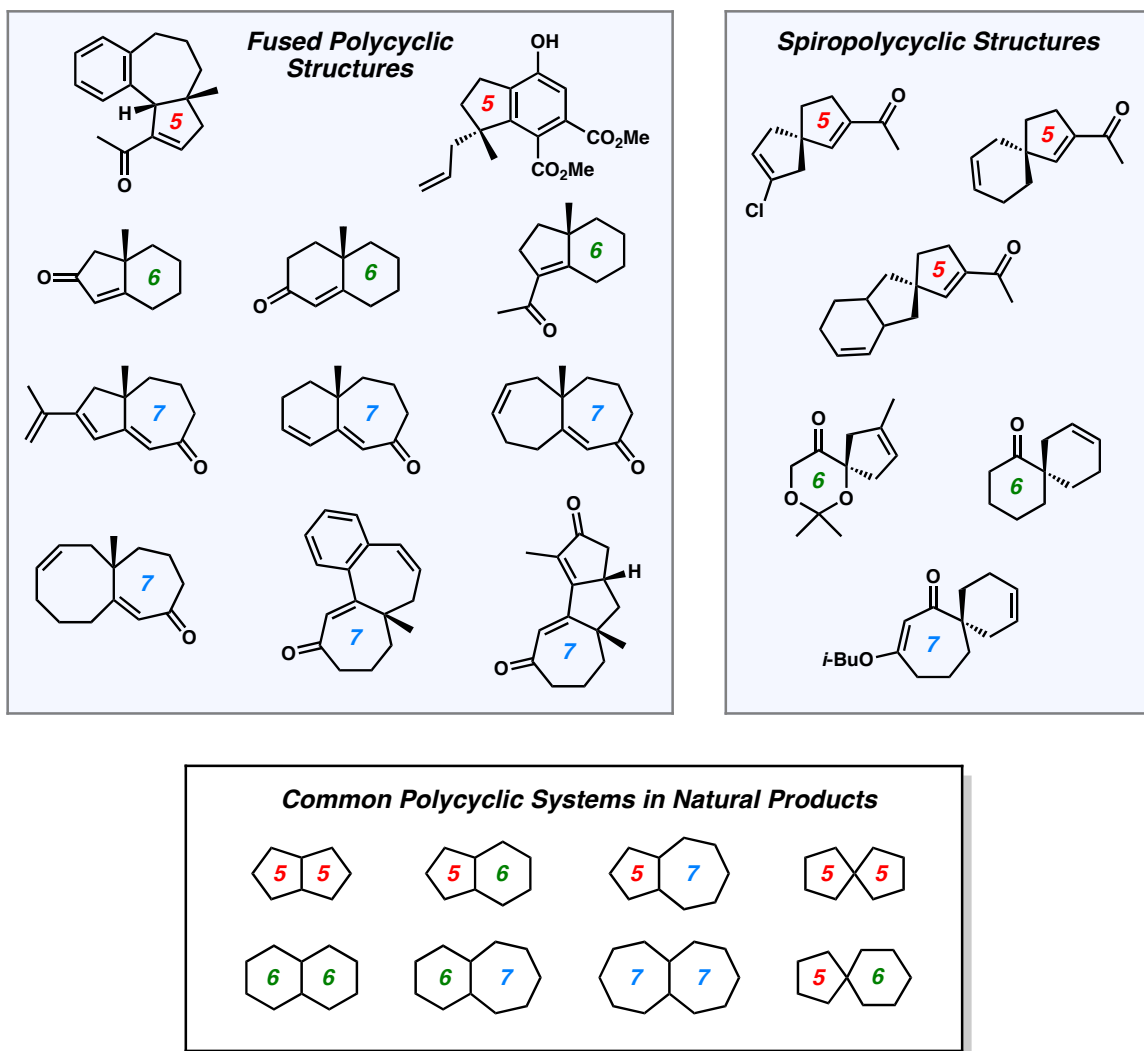
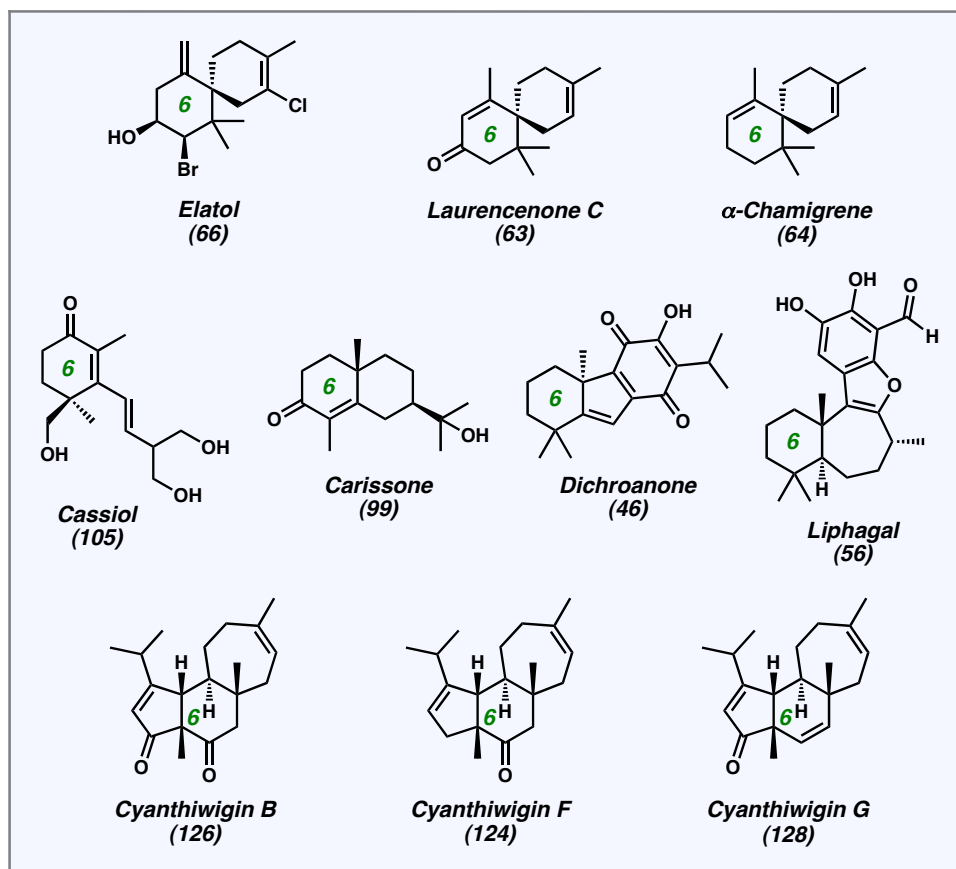


Figure 2.5. Pd-Catalyzed Asymmetric Allylic Alkylation in the Total Synthesis of Natural Products



2.9 CONCLUSION

We have successfully developed general, enantioselective synthetic routes toward γ -quaternary acylcyclopentenones (**135**) and γ -quaternary cycloheptenones (**137**). The key stereoselective component unifying this chemistry is the Pd-catalyzed asymmetric allylation of seven-membered vinylogous ester substrates to form α -quaternary vinylogous esters, for which we have demonstrated a broad substrate scope with a variety of all-carbon and heteroatom-containing functionality. These enantioenriched products were transformed in a divergent manner to either facilitate a two-carbon ring contraction

to acylcyclopentenes or a carbonyl transposition to cycloheptenones. Further synthetic elaboration of these products has enabled access to five- and seven-membered ring systems that are poised for further functionalization to bi- and tricyclic ring systems. Overall, the described strategies provide broader access to polycyclic ring systems and thus complement our previous work with six-membered ring building blocks. Efforts to expand the scope of these reactions, understand the key reaction mechanisms, and apply the chiral products to the total synthesis of natural products are the subject of future studies.

2.10 EXPERIMENTAL SECTION

2.10.1 MATERIALS AND METHODS

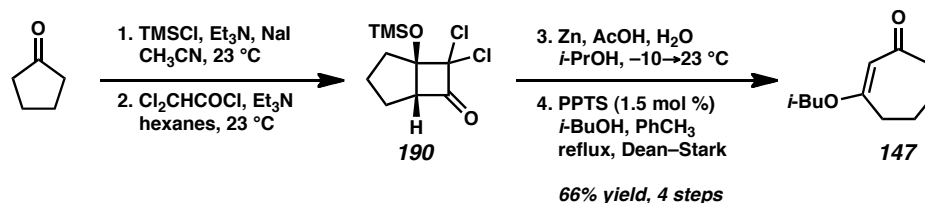
Unless otherwise stated, reactions were performed in flame-dried glassware under an argon or nitrogen atmosphere using dry, deoxygenated solvents. Reaction progress was monitored by thin-layer chromatography (TLC). THF was distilled over sodium/fluorenone or dried by passage through an activated alumina column under argon⁴⁸ prior to use. *p*-Dioxane was distilled over sodium or dried by passage through an activated alumina column under argon prior to use. Methanol was distilled over Mg(OMe)₂ prior to use. Other solvents were dried by passage through an activated alumina column under argon. Diisopropylamine and triethylamine were distilled over CaH₂ prior to use. Iodomethane, iodoethane, acrylonitrile, methyl vinyl ketone, and acrolein were distilled prior to use. Furan was distilled over KOH and hydroquinone prior to use. Purified water was obtained using a Barnstead NANOpure Infinity UV/UF system. Brine solutions are saturated aqueous solutions of sodium chloride. MePh₃PBr was purchased from Sigma-Aldrich and stored in a glove box prior to use. NaH (60% wt. dispersion in mineral oil) was purchased from Sigma-Aldrich and purified by trituration with hexanes under a N₂ atmosphere and removal of residual solvent under vacuum. Grignard and organolithium reagents were purchased from Sigma-Aldrich unless otherwise stated and titrated according to the method of Love.⁴⁹ LiOCH₂CF₃ was prepared according to the method of Shreeve.⁵⁰ Allyl cyanoformate was prepared according to the method of Mander^{51a} or Rattigan.^{51b} Gramine methiodide was prepared according to the method of Armen.⁵² The procedure of Maruyama and Naruta was used

to prepare 1-chloro-2,4-pentadiene (92:8 *E:Z*).⁵³ Phosphinooxazoline (PHOX) ligands (*S*)-*t*-Bu-PHOX (**13**)⁵⁴ and (*S*)-*p*-(CF₃)₃-*t*-Bu-PHOX (**14**)⁵⁵ were prepared by methods described in our previous work. Tris(4,4'-methoxydibenzylideneacetone)dipalladium(0) (Pd₂(pmdba)₃) was prepared according to the method of Ibers⁵⁶ or Fairlamb.^{56b} Herrmann–Beller's catalyst (**182**) was prepared according to a literature procedure.⁵⁷ All other reagents were purchased from Sigma-Aldrich, Acros Organics, Strem, or Alfa Aesar and used as received unless otherwise stated. Reaction temperatures were controlled by an IKA Mag temperature modulator. Microwave-assisted reactions were performed in a Biotage Initiator 2.5 microwave reactor. Glove box manipulations were performed under a N₂ atmosphere. TLC was performed using E. Merck silica gel 60 F254 precoated glass plates (0.25 mm) and visualized by UV fluorescence quenching, *p*-anisaldehyde, or KMnO₄ staining. SiliaFlash P60 Academic Silica gel (particle size 0.040–0.063 mm) or ICN silica gel (particle size 0.032–0.0653 mm) was used for flash column chromatography. Automated flash column chromatography was performed on a Teledyne Isco CombiFlash R_f system. ¹H NMR spectra were recorded on a Varian Mercury 300 MHz, a Varian 400 MR 400 MHz, or a Varian Inova 500 MHz spectrometer and are reported relative to residual CHCl₃ (δ 7.26 ppm) or C₆H₆ (δ 7.16 ppm). Variable temperature ¹H NMR experiments were performed on a Varian Inova 500 MHz spectrometer and are reported relative to residual DMSO (δ 2.50 ppm). ¹³C NMR spectra were recorded on a Varian Mercury 300 MHz, a Varian 400 MR 400 MHz, or a Varian Inova 500 MHz spectrometer (at 75 MHz, 100 MHz, and 125 MHz respectively) and are reported relative to CHCl₃ (δ 77.16 ppm) or C₆H₆ (δ 128.06 ppm). ¹⁹F spectra were recorded on a Varian Mercury 300 MHz or a Varian Inova 500 MHz

spectrometer (at 282 MHz and 470 MHz respectively) and are reported without the use of a reference peak. Data for ^1H NMR are reported as follows: chemical shift (δ ppm) (multiplicity, coupling constant (Hz), integration. Multiplicities are reported as follows: s = singlet, d = doublet, t = triplet, q = quartet, p = pentet, sept = septuplet, m = multiplet, dm = doublet of multiplets, br s = broad singlet, br d = broad doublet, app = apparent. Data for ^{13}C and ^{19}F NMR are reported in terms of chemical shifts (δ ppm). IR spectra were obtained using a Perkin Elmer Paragon 1000 or Perkin Elmer Spectrum BXII spectrometer using thin films deposited on NaCl plates and reported in frequency of absorption (cm^{-1}). Optical rotations were measured with a Jasco P-1010 or Jasco P-2000 polarimeter operating on the sodium D-line (589 nm) using a 100 mm path-length cell and are reported as follows: $[\alpha]_D^{25}$ (concentration in g/100 mL, solvent, ee). Melting points were measured using a Thomas-Hoover capillary melting point apparatus and the reported values are uncorrected. Analytical chiral HPLC was performed with an Agilent 1100 Series HPLC utilizing a Chiralcel AD or OD-H column (4.6 mm x 25 cm) obtained from Daicel Chemical Industries Ltd. with visualization at 254 nm. Analytical chiral SFC was performed with a Mettler Toledo SFC supercritical CO_2 analytical chromatography system with a Chiralcel AD-H column (4.6 mm x 25 cm) with visualization at 254 nm/210 nm. Analytical chiral GC was performed with an Agilent 6850 GC utilizing a G-TA (30 m x 0.25 mm) column (1.0 mL/min carrier gas flow). High-resolution mass spectra (HRMS) were obtained from the Caltech Mass Spectral Facility (EI+ or FAB+) or on an Agilent 6200 Series TOF with an Agilent G1978A Multimode source in electrospray ionization (ESI+), atmospheric pressure chemical ionization (APCI+), or mixed ionization mode (MM: ESI-APCI+).

2.10.2 PREPARATIVE PROCEDURES

2.10.2.1 PREPARATION PARENT VINYLOGOUS ESTER 147



Vinylogous ester 147. NaI (157 g, 1.05 mol, 1.25 equiv) was placed in a 3 L 3-neck round-bottom flask, dried under high vacuum at $90\text{ }^\circ\text{C}$ for 12 h, and allowed to cool to ambient temperature under N_2 . CH_3CN (1.3 L) was added to dissolve the NaI. To the solution was added cyclopentanone (74.3 mL, 0.84 mol, 1.00 equiv), followed by Et_3N (146 mL, 1.05 mol, 1.25 equiv). The flask was fitted with an addition funnel, and the funnel was charged with TMSCl (122 mL, 0.96 mmol, 1.14 equiv), which was added dropwise over 30 min. The resulting suspension was stirred for an additional 1 h at ambient temperature. Pentane (1.0 L) was added, and the biphasic system was stirred vigorously for 10 min. The phases were separated and the CH_3CN layer was extracted with pentane (3 x 400 mL). The combined pentane phases were washed with H_2O (2 x 500 mL) and brine (500 mL), dried over Na_2SO_4 , filtered, and concentrated under reduced pressure to afford the desired product (131 g, quantitative) as a colorless oil.

A portion of the above trimethylsilyl ether (89.7 g, 0.57 mol, 1.00 equiv) was placed in a 3 L 3-neck round-bottom flask fitted with a stopper, an addition funnel, and an overhead stirrer. Hexanes (900 mL) was added, followed by Et_3N (111 mL, 0.80 mol, 1.39 equiv). Dichloroacetyl chloride (66.4 mL, 0.69 mol, 1.21 equiv) was dissolved in hexanes (400 mL) and added dropwise over 9.5 h. After 18 h of stirring at ambient

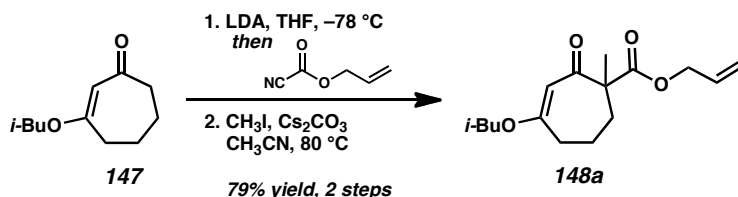
temperature, the brown suspension was filtered, rinsing with EtOAc (3 x 500 mL). The clear brown solution was concentrated under reduced pressure and then filtered through a pad of Al_2O_3 (7 x 18 cm, neutral) using EtOAc as eluent. The solution was concentrated under reduced pressure to afford the desired product (125 g, 0.47 mol, 82% yield) as a brown oil that crystallized in the freezer ($-20\text{ }^\circ\text{C}$).

A portion of the above dichlorocyclobutanone (53.4 g, 0.20 mol, 1.00 equiv) was placed in a 3 L 3-neck round-bottom flask fitted with a thermometer, an addition funnel, and an overhead stirrer. Isopropyl alcohol and purified water (170 mL each) were added and the suspension was cooled to $-10\text{ }^\circ\text{C}$ (internal temperature) using a MeOH/ice bath. Zn dust (58.8 g, 0.90 mol, 4.50 equiv) was added in four portions (5 min between each) and AcOH (63 mL, 1.10 mol, 5.50 equiv) dissolved in H_2O (130 mL) was added dropwise while keeping the internal temperature below $0\text{ }^\circ\text{C}$ (usually added over 1.5 h). The reaction was stirred for an additional 30 min at $-10\text{ }^\circ\text{C}$ (internal temperature) before the cooling bath was removed and the reaction was allowed to warm to ambient temperature. After 8.5 h, the reaction was filtered, rinsing with isopropyl alcohol (100 mL). The mixture was cooled to $0\text{ }^\circ\text{C}$ and neutralized by portionwise addition of K_2CO_3 (74.6 g, 0.54 mol, 5.50 equiv). The viscous suspension was filtered, rinsing with H_2O (100 mL) and EtOAc (300 mL). The biphasic system was concentrated under reduced pressure to ca. 200 mL and extracted with CH_2Cl_2 . The combined organics were dried over MgSO_4 , filtered, and concentrated under reduced pressure to afford the desired product (24.2 g, 0.19 mol, 96% yield) as a pale orange oil.

To a solution of 1,3-cycloheptanedione (35.8 g, 0.28 mol, 1.00 equiv) in toluene (280 mL) in a 1 L flask fitted with a reflux condenser and Dean–Stark trap was added

isobutanol (208 mL, 2.27 mol, 8.11 equiv) and pyridinium *p*-toluenesulfonate (1.07 g, 4.26 mmol, 1.50 mol %). The solution was immersed in an oil bath at 130 °C and monitored by TLC. When the starting material was consumed (typically within 4–6 h), the reaction was allowed to cool to ambient temperature. The resulting dark orange solution was washed with sat. aqueous NaHCO₃ (200 mL). The aqueous phase was extracted with EtOAc (3 x 150 mL) and the combined organics were washed with brine, dried over MgSO₄, filtered, and concentrated under reduced pressure to afford a thick dark orange oil. The crude oil was flushed through a silica gel plug (SiO₂, 7 x 9 cm, 1:4→3:7→1:1 Et₂O-hexanes) to afford vinylogous ester **147** (43.5 g, 0.24 mol, 84% yield, 66% yield over 4 steps) as a pale orange oil; *R*_f = 0.22 (2:1 hexanes:EtOAc); ¹H NMR (500 MHz, CDCl₃) δ 5.37 (s, 1H), 3.49 (d, *J* = 6.6 Hz, 2H), 2.60–2.56 (m, 4H), 2.00 (sept, *J* = 6.6 Hz, 1H), 1.88–1.77 (m, 4H), 0.96 (d, *J* = 6.8 Hz, 6H); ¹³C NMR (125 MHz, CDCl₃) δ 202.5, 176.6, 106.0, 75.0, 41.9, 33.1, 27.9, 23.7, 21.5, 19.3; IR (Neat Film NaCl) 2958, 2872, 1646, 1607, 1469, 1237, 1190, 1174 cm⁻¹; HRMS (EI+) *m/z* calc'd for C₁₁H₁₈O₂ [M]⁺: 182.1307; found 182.1310.

2.10.2.2 PREPARATION OF β-KETOESTERS 148

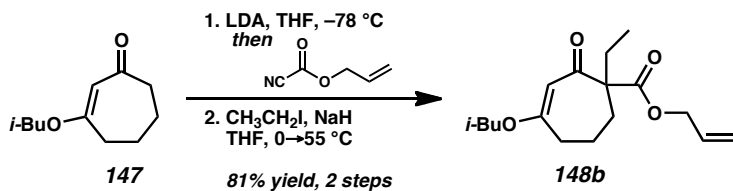


β-Ketoester 148a. To a solution of diisopropylamine (6.46 mL, 46.1 mmol, 1.20 equiv) in THF (180 mL) in a 500 mL round-bottom flask at 0 °C was added *n*-BuLi (17.2 mL,

44.2 mmol, 2.57 M in hexanes, 1.15 equiv) dropwise over 15 min using a syringe pump. After 15 min of stirring at 0 °C, the mixture was cooled to –78 °C using an acetone/CO₂(s) bath. A solution of vinylogous ester **147** (7.01 g, 38.4 mmol, 1.00 equiv) in THF (20 mL) was added dropwise over 20 min using a syringe pump. After an additional 1 h of stirring at –78 °C, allyl cyanofornate (4.60 mL, 42.2 mmol, 1.10 equiv) was added dropwise over 10 min. The mixture was stirred at –78 °C for 2.5 h, quenched by addition of sat. aqueous NH₄Cl and H₂O (30 mL each), and allowed to warm to ambient temperature. The reaction was diluted with Et₂O (100 mL) and the phases were separated. The aqueous phase was extracted with Et₂O (2 x 100 mL). The combined organic phases were dried over MgSO₄, filtered, and concentrated under reduced pressure to afford a pale orange oil.

The crude oil was dissolved in CH₃CN (130 mL) in a 500 mL round-bottom flask and treated with CH₃I (7.2 mL, 115 mmol, 3.00 equiv) and Cs₂CO₃ (16.76 g, 49.9 mmol, 1.30 equiv). The flask was fitted with a condenser, immersed in an oil bath, and heated to 80 °C with vigorous stirring. After 12 h of stirring at 80 °C, the reaction was allowed to cool to ambient temperature, diluted with EtOAc (100 mL), dried over MgSO₄, filtered, and concentrated under reduced pressure to afford an orange oil. The crude product was purified by flash column chromatography (SiO₂, 5 x 15 cm, 19:1→9:1 hexanes:EtOAc, dry-loaded using Celite) to afford β-ketoester **148a** (8.51 g, 30.4 mmol, 79% yield over 2 steps) as a pale yellow oil; *R*_f = 0.43 (4:1 hexanes:EtOAc); ¹H NMR (500 MHz, CDCl₃) δ 5.86 (dddd, *J* = 17.1, 10.7, 5.6, 5.6 Hz, 1H), 5.39 (s, 1H), 5.29 (app dq, *J* = 17.1, 1.5 Hz, 1H), 5.20 (app dq, *J* = 10.5, 1.4 Hz, 1H), 4.62 (dddd, *J* = 13.3, 5.6, 1.2, 1.2 Hz, 1H), 4.56 (dddd, *J* = 13.4, 5.6, 1.2, 1.2 Hz, 1H), 3.54–3.42 (m, 2H), 2.59 (ddd, *J* = 17.8, 9.8,

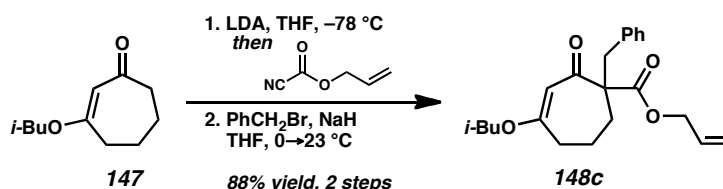
3.9 Hz, 1H), 2.45–2.38 (m, 2H), 2.02–1.94 (m, 2H), 1.84–1.75 (m, 1H), 1.70 (ddd, $J = 14.4, 7.3, 4.4$ Hz, 1H), 1.43 (s, 3H), 0.94 (d, $J = 6.6$ Hz, 6H); ^{13}C NMR (125 MHz, CDCl_3) δ 199.1, 174.0, 173.5, 132.0, 118.4, 105.2, 74.8, 65.8, 59.1, 34.3, 33.9, 27.9, 24.2, 21.4, 19.3; IR (Neat Film NaCl) 2959, 2936, 2875, 1734, 1650, 1613, 1456, 1384, 1233, 1170, 1115, 994 cm^{-1} ; HRMS (EI+) m/z calc'd for $\text{C}_{16}\text{H}_{24}\text{O}_4$ $[\text{M}]^+$: 280.1675; found 280.1686.



β -Ketoester 148b. To a solution of diisopropylamine (0.92 mL, 6.58 mmol, 1.20 equiv) in THF (27 mL) in a 100 mL round-bottom flask at 0°C was added n -BuLi (2.56 mL, 6.30 mmol, 2.46 M in hexanes, 1.15 equiv) dropwise over 10 min. After 15 min of stirring at 0°C , the mixture was cooled to -78°C using an acetone/ $\text{CO}_2(\text{s})$ bath. A solution of vinylogous ester **147** (1.00 g, 5.48 mmol, 1.00 equiv) in THF (2 mL) was added dropwise using positive pressure cannulation. After an additional 1 h of stirring at -78°C , allyl cyanoformate (0.67 mL, 6.02 mmol, 1.10 equiv) was added dropwise over 10 min. The mixture was stirred at -78°C for 2.5 h, quenched by addition of 50% sat. aqueous NH_4Cl (8 mL), and allowed to warm to ambient temperature. The reaction was diluted with Et_2O (25 mL) and the phases were separated. The aqueous phase was extracted with Et_2O (3 x 25 mL). The combined organic phases were dried over Na_2SO_4 , filtered, and concentrated under reduced pressure to afford a pale orange oil.

The crude oil was dissolved in THF (8 mL) in a 100 mL round-bottom flask, cooled to 0 °C, and stirred vigorously as hexane-washed NaH (158 mg, 6.58 mmol, 1.20 equiv) was added in one portion. Evolution of gas was observed and the reaction was stirred at 0 °C for 30 min to give a yellow-orange solution. CH₃CH₂I (1.31 mL, 16.4 mmol, 3.00 equiv) was added dropwise. The reaction was allowed to warm to ambient temperature and stirred for 4.5 h. The mixture was heated to 45 °C and stirred for 1.5 h. Additional CH₃CH₂I (0.65 mL, 8.22 mmol, 1.50 equiv) was added dropwise and the mixture was stirred at 45 °C for 6 h. A third portion of CH₃CH₂I (0.33 mL, 4.11 mmol, 0.75 equiv) was added dropwise and the reaction was warmed to 55 °C and stirred for 1.5 h. The flask was cooled to ambient temperature and quenched by addition of 50% sat. aqueous NH₄Cl (10 mL). The phases were separated and the aqueous layer was extracted with Et₂O (3 x 15 mL). The combined organic phases were washed with brine, dried over Na₂SO₄, filtered, and concentrated under reduced pressure. The crude product was purified by flash column chromatography (SiO₂, 5 x 20 cm, 9:1→6:1→3:1→2:1 hexanes:EtOAc) to afford β-ketoester **148b** (1.31 g, 4.44 mmol, 81% yield over 2 steps) as a yellow oil; *R*_f = 0.53 (4:1 hexanes:EtOAc); ¹H NMR (300 MHz, CDCl₃) δ 5.85 (dddd, *J* = 17.5, 10.2, 5.7, 5.7 Hz, 1H), 5.35 (s, 1H), 5.29 (app dq, *J* = 17.2, 1.5 Hz, 1H), 5.19 (app dq, *J* = 10.4, 1.3 Hz, 1H), 4.62 (dddd, *J* = 13.2, 5.7, 1.4, 1.4 Hz, 1H), 4.54 (dddd, *J* = 13.2, 5.7, 1.4, 1.4 Hz, 1H), 3.57–3.34 (m, 2H), 2.60 (dddd, *J* = 17.9, 9.9, 3.7, 1.2 Hz, 1H), 2.49–2.26 (m, 2H), 2.12–1.85 (m, 4H), 1.85–1.57 (m, 2H), 0.93 (d, *J* = 6.7 Hz, 6H), 0.84 (t, *J* = 7.5 Hz, 3H); ¹³C NMR (75 MHz, CDCl₃) δ 198.7, 173.7, 173.2, 132.0, 118.5, 105.5, 74.7, 65.7, 63.1, 34.1, 31.0, 30.6, 27.9, 22.0, 19.3, 9.0; IR (Neat Film NaCl) 3085, 2960, 2937, 2876, 1731, 1663, 1613, 1471, 1461, 1453, 1424, 1383,

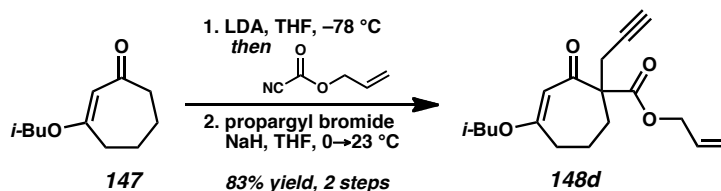
1369, 1328, 1304, 1278, 1229, 1199, 1170, 1121, 1006, 988, 931, 875, 858, 813 cm^{-1} ;
 HRMS (MM: ESI-APCI+) m/z calc'd for $\text{C}_{17}\text{H}_{27}\text{O}_4$ $[\text{M}+\text{H}]^+$: 295.1904; found 295.1918.



β -Ketoester 148c. To a solution of diisopropylamine (0.92 mL, 6.58 mmol, 1.20 equiv) in THF (27 mL) in a 100 mL round-bottom flask at 0 $^{\circ}\text{C}$ was added *n*-BuLi (2.56 mL, 6.30 mmol, 2.46 M in hexanes, 1.15 equiv) dropwise over 10 min. After 15 min of stirring at 0 $^{\circ}\text{C}$, the mixture was cooled to $-78\text{ }^{\circ}\text{C}$ using an acetone/ $\text{CO}_2(\text{s})$ bath. A solution of vinylogous ester **147** (1.00 g, 5.48 mmol, 1.00 equiv) in THF (2 mL) was added dropwise using positive pressure cannulation. After an additional 1 h of stirring at $-78\text{ }^{\circ}\text{C}$, allyl cyanofornate (0.67 mL, 6.02 mmol, 1.10 equiv) was added dropwise over 10 min. The mixture was stirred at $-78\text{ }^{\circ}\text{C}$ for 2.5 h, quenched by addition of 50% sat. aqueous NH_4Cl (8 mL), and allowed to warm to ambient temperature. The reaction was diluted with Et_2O (25 mL) and the phases were separated. The aqueous phase was extracted with Et_2O (3 x 25 mL). The combined organic phases were dried over Na_2SO_4 , filtered, and concentrated under reduced pressure to afford a pale orange oil.

The crude oil was dissolved in THF (8 mL) in a 100 mL round-bottom flask, cooled to 0 $^{\circ}\text{C}$, and stirred vigorously as hexane-washed NaH (197 mg, 8.22 mmol, 1.50 equiv) was added in one portion. Evolution of gas was observed and the reaction was stirred at 0 $^{\circ}\text{C}$ for 30 min to give a yellow-orange solution. Benzyl bromide (1.96 mL, 16.44 mmol, 3.00 equiv) was added dropwise. The reaction was allowed to warm to ambient

temperature and stirred for 3 h. The reaction was quenched by addition of 50% sat. aqueous NH_4Cl (10 mL). The phases were separated and the aqueous layer was extracted with Et_2O (3 x 15 mL). The combined organic phases were washed with brine, dried over MgSO_4 , filtered, and concentrated under reduced pressure. The crude product was purified by flash column chromatography (SiO_2 , 3 x 23 cm, hexanes \rightarrow 10:1 hexanes:EtOAc) to afford β -ketoester **148c** (1.72 g, 4.83 mmol, 88% yield over 2 steps) as a pale yellow oil; $R_f = 0.26$ (10:1 hexanes:EtOAc); ^1H NMR (300 MHz, CDCl_3) δ 7.30–7.15 (m, 3H), 7.15–7.06 (m, 2H), 5.85 (dddd, $J = 17.1, 10.4, 5.8, 5.8$ Hz, 1H), 5.36 (s, 1H), 5.30 (app dq, $J = 17.2, 1.5$ Hz, 1H), 5.21 (app dq, $J = 10.4, 1.3$ Hz, 1H), 4.63 (dddd, $J = 13.2, 5.7, 1.3, 1.3$ Hz, 1H), 4.52 (dddd, $J = 13.2, 5.8, 1.3, 1.3$ Hz, 1H), 3.42 (d, $J = 6.5$ Hz, 2H), 3.30 (d, $J = 13.5$ Hz, 1H), 3.23 (d, $J = 13.5$ Hz, 1H), 2.54 (ddd, $J = 12.1, 10.0, 3.5$ Hz, 1H), 2.38–2.18 (m, 2H), 2.04–1.83 (m, 2H), 1.81–1.64 (m, 2H), 0.92 (d, $J = 6.7$ Hz, 6H); ^{13}C NMR (75 MHz, CDCl_3) δ 198.0, 174.0, 172.7, 137.0, 131.8, 130.7, 128.1, 126.8, 118.8, 105.7, 74.8, 66.0, 64.0, 43.1, 34.0, 31.3, 27.9, 22.0, 19.2; IR (Neat Film NaCl) 3085, 3062, 3029, 2959, 2934, 2873, 1736, 1732, 1661, 1652, 1611, 1495, 1471, 1454, 1423, 1383, 1368, 1270, 1235, 1173, 1088, 1007, 957, 992, 930, 862, 815, 741 cm^{-1} ; HRMS (APCI+) m/z calc'd for $\text{C}_{22}\text{H}_{29}\text{O}_4$ $[\text{M}+\text{H}]^+$: 357.2060; found 357.2051.

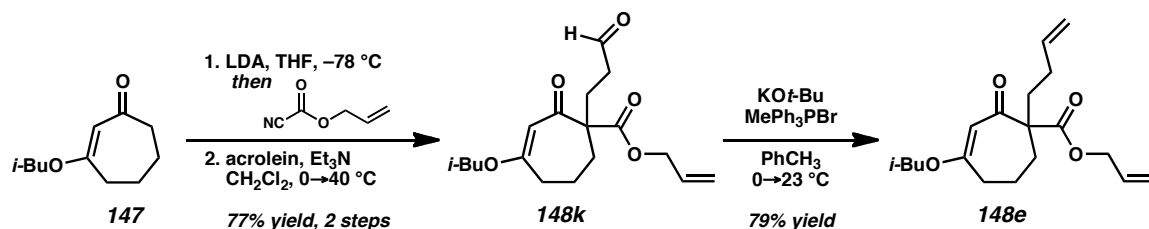


β -Ketoester 148d. To a solution of diisopropylamine (0.92 mL, 6.58 mmol, 1.20 equiv) in THF (27 mL) in a 100 mL round-bottom flask at 0 $^\circ\text{C}$ was added n -BuLi (2.56 mL,

6.30 mmol, 2.46 M in hexanes, 1.15 equiv) dropwise over 10 min. After 15 min of stirring at 0 °C, the mixture was cooled to –78 °C using an acetone/CO₂(s) bath. A solution of vinylogous ester **147** (1.00 g, 5.48 mmol, 1.00 equiv) in THF (2 mL) was added dropwise using positive pressure cannulation. After an additional 1 h of stirring at –78 °C, allyl cyanoformate (0.67 mL, 6.02 mmol, 1.10 equiv) was added dropwise over 10 min. The mixture was stirred at –78 °C for 2.5 h, quenched by addition of 50% sat. aqueous NH₄Cl (8 mL), and then allowed to warm to ambient temperature. The reaction was diluted with Et₂O (25 mL) and the phases were separated. The aqueous phase was extracted with Et₂O (3 x 25 mL). The combined organic phases were dried over Na₂SO₄, filtered, and concentrated under reduced pressure to afford a pale orange oil.

The crude oil was dissolved in THF (8 mL) in a 100 mL round-bottom flask, cooled to 0 °C, and stirred vigorously as hexane-washed NaH (197 mg, 8.22 mmol, 1.5 equiv) was added in one portion. Evolution of gas was observed and the reaction was stirred at 0 °C for 30 min to give a yellow-orange solution. Propargyl bromide (1.22 mL, 10.96 mmol, 80% wt in toluene, 2.00 equiv) was added dropwise and the reaction was allowed to warm to ambient temperature and stirred for 5.5 h. The reaction was quenched by addition of 50% sat. aqueous NH₄Cl (10 mL). The phases were separated and the aqueous layer was extracted with Et₂O (3 x 15 mL). The combined organic phases were washed with brine, dried over Na₂SO₄, filtered, and concentrated under reduced pressure. The crude product was purified by flash column chromatography (SiO₂, 3 x 24 cm, hexanes→20:1→15:1→10:1 hexanes:EtOAc) to afford β-ketoester **148d** (1.38 g, 4.53 mmol, 83% yield over 2 steps) as a pale yellow oil; *R*_f = 0.55 (4:1 hexanes:EtOAc); ¹H NMR (300 MHz, CDCl₃) δ 5.85 (dddd, *J* = 17.2, 10.4, 5.7, 5.7 Hz, 1H), 5.38 (s, 1H), 5.29

(app dq, $J = 17.2, 1.5$ Hz, 1H), 5.19 (app dq, $J = 10.4, 1.3$ Hz, 1H), 4.63 (dddd, $J = 13.2, 5.6, 1.4, 1.4$ Hz, 1H), 4.56 (dddd, $J = 13.2, 5.7, 1.4, 1.4$ Hz, 1H), 3.56–3.38 (m, 2H), 2.79 (dd, $J = 2.7, 0.6$ Hz, 1H), 2.72–2.32 (m, 4H), 2.15–1.89 (m, 4H), 1.89–1.71 (m, 1H), 0.93 (d, $J = 6.7$ Hz, 6H); ^{13}C NMR (75 MHz, CDCl_3) δ 196.5, 174.8, 171.7, 131.7, 118.7, 105.0, 80.2, 74.9, 71.4, 66.1, 62.0, 34.3, 31.2, 27.9, 27.5, 21.7, 19.2; IR (Neat Film NaCl) 3289, 3085, 2959, 2933, 2874, 2120, 1740, 1735, 1654, 1649, 1470, 1452, 1424, 1402, 1384, 1369, 1309, 1291, 1272, 1232, 1187, 1173, 1133, 1085, 1066, 1007, 968, 930, 863, 820 cm^{-1} ; HRMS (EI+) m/z calc'd for $\text{C}_{18}\text{H}_{25}\text{O}_4$ $[\text{M}+\text{H}]^+$: 305.1753; found 305.1746.



β -Ketoester 148k. To a solution of diisopropylamine (1.49 mL, 10.63 mmol, 1.20 equiv) in THF (43 mL) in a 250 mL round-bottom flask at 0 $^\circ\text{C}$ was added *n*-BuLi (4.74 mL, 10.19 mmol, 2.51 M in hexanes, 1.15 equiv) dropwise over 10 min. After 15 min of stirring at 0 $^\circ\text{C}$, the mixture was cooled to $-78\text{ }^\circ\text{C}$ using an acetone/ $\text{CO}_2(\text{s})$ bath. A solution of vinylogous ester **147** (1.61 g, 8.86 mmol, 1.00 equiv) in THF (3 mL) was added dropwise using positive pressure cannulation. After an additional 1 h of stirring at $-78\text{ }^\circ\text{C}$, allyl cyanoformate (1.06 mL, 9.74 mmol, 1.10 equiv) was added dropwise over 10 min. The mixture was stirred at $-78\text{ }^\circ\text{C}$ for 2.5 h, quenched by addition of 50% sat. aqueous NH_4Cl (12.9 mL), and then allowed to warm to ambient temperature. The reaction was diluted with Et_2O (50 mL) and the phases were separated. The aqueous

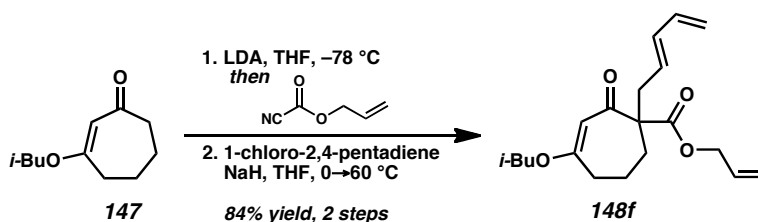
phase was extracted with Et₂O (3 x 100 mL). The combined organic phases were dried over Na₂SO₄, filtered, and concentrated under reduced pressure to afford a pale orange oil. The crude oil was purified by automated flash column chromatography using a Teledyne Isco CombiFlash R_f (SiO₂, 25 g loading cartridge, 330 g column, hold 0% [3 min]→ramp to 20% [10 min]→hold 20% [10 min]→ramp to 50% [4 min]→hold 50% EtOAc in hexanes [5 min]) to afford the intermediate β-ketoester (2.02 g, 7.58 mmol, 86% yield).

A portion of the intermediate β-ketoester (990 mg, 3.72 mmol, 1.00 equiv) was dissolved in CH₂Cl₂ (10 mL) in a 100 mL round-bottom flask, cooled to 0 °C, and treated with Et₃N (0.518 mL, 3.72 mmol, 1.00 equiv). Acrolein (0.248 mL, 3.72 mmol, 1.00 equiv) was added dropwise and the reaction was allowed to warm to ambient temperature. After 51 h, the reaction was cooled to 0 °C and an additional portion of acrolein (0.125 mL, 1.86 mmol, 0.50 equiv) was added. After 100 h, the reaction was concentrated under reduced pressure, dissolved in Et₂O, and filtered through a cotton plug to remove salts. The filtrate was concentrated under reduced pressure and the crude product was purified by flash column chromatography (SiO₂, 3 x 25 cm, 10:1→6:1→4:1 hexanes:EtOAc) to afford β-ketoester **148k** (1.07 g, 3.34 mmol, 90% yield, 77% yield over 2 steps) as a clear oil; *R*_f = 0.23, broad (4:1 hexanes:EtOAc); ¹H NMR (300 MHz, CDCl₃) δ 9.73 (t, *J* = 1.3 Hz, 1H), 5.86 (dddd, *J* = 17.1, 10.4, 5.8, 5.8 Hz, 1H), 5.36 (s, 1H), 5.30 (app dq, *J* = 17.2, 1.5 Hz, 1H), 5.22 (app dq, *J* = 10.4, 1.2 Hz, 1H), 4.63 (dddd, *J* = 13.1, 5.7, 1.3, 1.3 Hz, 1H), 4.55 (dddd, *J* = 13.2, 5.8, 1.3, 1.3 Hz, 1H), 3.55–3.40 (m, 2H), 2.66–2.29 (m, 5H), 2.29–2.08 (m, 2H), 2.08–1.89 (m, 2H), 1.89–1.59 (m, 2H), 0.94 (d, *J* = 6.7 Hz, 6H); ¹³C NMR (75 MHz, CDCl₃) δ 201.6, 197.9, 173.9, 172.7, 131.7,

119.0, 105.3, 74.9, 66.0, 61.8, 39.7, 34.2, 32.1, 29.6, 27.9, 21.5, 19.2; IR (Neat Film NaCl) 3084, 2960, 2936, 2875, 2829, 2723, 1727, 1649, 1611, 1471, 1454, 1422, 1403, 1385, 1369, 1306, 1270, 1234, 1191, 1173, 1104, 1004, 990, 931, 877, 862, 822 cm^{-1} ; HRMS (FAB+) m/z calc'd for $\text{C}_{18}\text{H}_{27}\text{O}_5$ $[\text{M}+\text{H}]^+$: 323.1858; found 323.1860.

β -Ketoester **148e.** MePh_3PBr (1.33 g, 3.72 mmol, 1.26 equiv) was suspended in toluene (20 mL) in 100 mL round-bottom flask and cooled to 0 °C. $\text{KO}t\text{-Bu}$ (0.348 g, 3.10 mmol, 1.05 equiv) was added in one portion and the bright yellow mixture was stirred at 0 °C for 30 min, warmed to ambient temperature, and stirred for an additional 2 h. The mixture was cooled to 0 °C and a solution of aldehyde **148k** (0.95 g, 2.94 mmol, 1.00 equiv) in toluene (2 mL) was added to the reaction using positive pressure cannulation. The mixture turned brown. The reaction was maintained at 0 °C for 1.5 h, warmed to ambient temperature, and stirred for 4 h. The reaction was quenched by addition of 50% sat. aqueous NH_4Cl (4 mL). The phases were separated and the aqueous phase was extracted with Et_2O (3 x 100 mL). The combined organic phases were dried over Na_2SO_4 , filtered, and concentrated under reduced pressure. The crude product was purified by flash column chromatography (SiO_2 , 3 x 25 cm, 20:1→15:1 hexanes: EtOAc) to afford β -ketoester **148e** (747 mg, 2.33 mmol, 79% yield) as a pale yellow oil; R_f = 0.66 (4:1 hexanes: EtOAc); ^1H NMR (300 MHz, CDCl_3) δ 5.85 (dddd, J = 17.2, 10.4, 5.7, 5.7 Hz, 1H), 5.84–5.69 (m, 1H), 5.35 (s, 1H), 5.29 (app dq, J = 17.2, 1.5 Hz, 1H), 5.20 (app dq, J = 10.4, 1.3 Hz, 1H), 5.08–4.96 (m, 1H), 4.96–4.87 (m, 1H), 4.62 (dddd, J = 13.1, 5.7, 1.4, 1.4 Hz, 1H), 4.54 (dddd, J = 13.1, 5.7, 1.4, 1.4 Hz, 1H), 3.53–3.38 (m, 2H), 2.59 (dddd, J = 17.9, 9.8, 3.7, 1.1 Hz, 1H), 2.51–2.29 (m, 2H), 2.09–1.87 (m, 6H), 1.87–

1.66 (m, 2H), 0.94 (d, $J = 6.7$, 3H), 0.94 (d, $J = 6.7$, 3H); ^{13}C NMR (75 MHz, CDCl_3) δ 198.4, 173.7, 173.0, 138.2, 131.9, 118.6, 114.9, 105.4, 74.8, 65.8, 62.6, 36.8, 34.1, 31.5, 28.8, 27.9, 22.0, 19.3; IR (Neat Film NaCl) 3078, 2959, 2935, 2874, 1732, 1662, 1612, 1471, 1453, 1423, 1401, 1384, 1369, 1307, 1270, 1231, 1194, 1170, 1091, 993, 913, 874, 817, 766 cm^{-1} ; HRMS (EI+) m/z calc'd for $\text{C}_{19}\text{H}_{28}\text{O}_4$ $[\text{M}]^{+}$: 320.1988; found 320.1977.

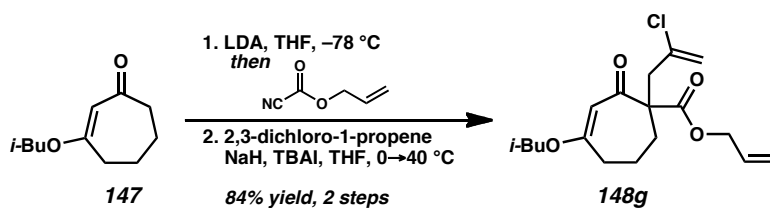


β -Ketoester 148f. To a solution of diisopropylamine (0.406 mL, 2.90 mmol, 1.20 equiv) in THF (12 mL) in a 50 mL round-bottom flask at 0 $^{\circ}\text{C}$ was added n -BuLi (1.10 mL, 2.77 mmol, 2.51 M in hexanes, 1.15 equiv) dropwise over 10 min. After 15 min of stirring at 0 $^{\circ}\text{C}$, the mixture was cooled to $-78\text{ }^{\circ}\text{C}$ using an acetone/ $\text{CO}_2(\text{s})$ bath. A solution of vinylogous ester **147** (0.44 g, 2.41 mmol, 1.00 equiv) in THF (2 mL) was added dropwise using positive pressure cannulation. After an additional 1 h of stirring at $-78\text{ }^{\circ}\text{C}$, allyl cyanoformate (0.288 mL, 2.65 mmol, 1.10 equiv) was added dropwise over 10 min. The mixture was stirred at $-78\text{ }^{\circ}\text{C}$ for 2.5 h, quenched by addition of 50% sat. aqueous NH_4Cl (4 mL), and then allowed to warm to ambient temperature. The reaction was diluted with Et_2O (15 mL) and the phases were separated. The aqueous phase was extracted with Et_2O (3 x 15 mL). The combined organic phases were dried over Na_2SO_4 , filtered, and concentrated under reduced pressure to afford a pale orange oil. The crude oil was purified by automated flash column chromatography using a Teledyne Isco CombiFlash R_f (SiO_2 , 5 g loading cartridge, 40 g column, hold 0% [1 min] \rightarrow ramp to 20% [8

min]→hold 20% [5 min]→ramp to 50% [4 min]→50% EtOAc in hexanes [6 min]) to afford the intermediate β -ketoester (590 mg, 2.21 mmol, 92% yield).

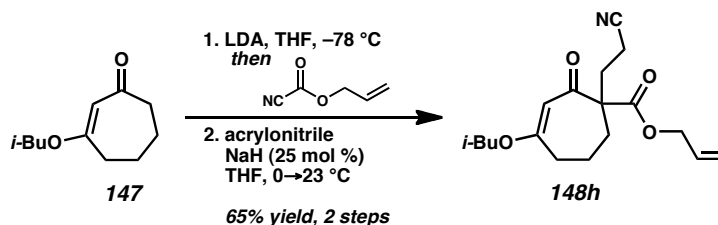
A portion of the intermediate β -ketoester (250 mg, 0.94 mmol, 1.00 equiv) was dissolved in THF (5 mL) in a 50 mL round-bottom flask, cooled to 0 °C, and stirred vigorously as hexane-washed NaH (33.8 mg, 6.58 mmol, 1.50 equiv) was added in one portion. Evolution of gas was observed and the reaction was stirred at 0 °C for 30 min to give a yellow-orange solution. 1-chloro-2,4-pentadiene⁵³ (144 mg, 1.41 mmol, 1.50 equiv) was added dropwise and the reaction was allowed to warm to ambient temperature and then heated to 40 °C. After 10.5 h, an additional portion of 1-chloro-2,4-pentadiene (144 mg, 1.41 mmol, 1.50 equiv) was added and the reaction was heated at 50 °C for 11.5 h. The flask was cooled to ambient temperature and the reaction was quenched by addition of 50% sat. aqueous NH₄Cl (2 mL). The phases were separated and the aqueous layer was extracted with Et₂O (3 x 10 mL). The combined organic phases were washed with brine, dried over Na₂SO₄, filtered, and concentrated under reduced pressure. The crude product was purified by flash column chromatography (SiO₂, 3 x 25 cm, 20:1→15:1→10:1 hexanes:EtOAc) to afford β -ketoester **148f** (286 mg, 0.86 mmol, 91% yield, 84% yield over 2 steps) as a pale yellow oil; R_f = 0.59 (4:1 hexanes:EtOAc); ¹H NMR (300 MHz, CDCl₃) δ 6.25 (ddd, J = 16.7, 10.3, 10.3 Hz, 1H), 6.11–5.98 (m, 1H), 5.83 (dddd, J = 17.2, 10.4, 5.7, 5.7 Hz, 1H), 5.58 (ddd, J = 15.1, 7.7, 7.7 Hz, 1H), 5.36 (s, 1H), 5.27 (app dq, J = 17.2, 1.5 Hz, 1H), 5.18 (app dq, J = 10.4, 1.2 Hz, 1H), 5.08 (dd, J = 16.9, 1.6 Hz, 1H), 4.96 (dd, J = 16.9, 1.6 Hz, 1H), 4.60 (dddd, J = 13.2, 5.8, 1.4, 1.4 Hz, 1H), 4.52 (dddd, J = 13.2, 5.8, 1.4, 1.4 Hz, 1H), 3.57–3.35 (m, 2H), 2.65 (d, J = 7.7 Hz, 2H), 2.56 (ddd, J = 12.7, 6.8, 2.3 Hz, 1H), 2.48–2.19 (m, 2H), 2.10–1.85 (m, 2H),

1.85–1.63 (m, 2H), 0.92 (d, $J = 6.7$, 3H), 0.92 (d, $J = 6.7$, 3H); ^{13}C NMR (75 MHz, CDCl_3) δ 197.9, 174.0, 172.7, 136.9, 134.6, 131.9, 129.7, 118.6, 116.1, 105.4, 74.8, 65.9, 62.9, 41.0, 34.1, 31.4, 27.9, 21.8, 19.2; IR (Neat Film NaCl) 3085, 2959, 2933, 2874, 1733, 1650, 1612, 1471, 1453, 1434, 1402, 1384, 1369, 1307, 1272, 1234, 1194, 1171, 1093, 1006, 968, 955, 929, 900, 864, 822, 761 cm^{-1} ; HRMS (FAB+) m/z calc'd for $\text{C}_{20}\text{H}_{29}\text{O}_4$ $[\text{M}+\text{H}]^+$: 333.2066; found 333.2052.



β -Ketoester 148g. To a solution of diisopropylamine (0.92 mL, 6.58 mmol, 1.20 equiv) in THF (27 mL) in a 100 mL round-bottom flask at $0\text{ }^{\circ}\text{C}$ was added n -BuLi (2.56 mL, 6.30 mmol, 2.46 M in hexanes, 1.15 equiv) dropwise over 10 min. After 15 min of stirring at $0\text{ }^{\circ}\text{C}$, the mixture was cooled to $-78\text{ }^{\circ}\text{C}$ using an acetone/ $\text{CO}_2(\text{s})$ bath. A solution of vinylogous ester **147** (1.00 g, 5.48 mmol, 1.00 equiv) in THF (2 mL) was added dropwise using positive pressure cannulation. After an additional 1 h of stirring at $-78\text{ }^{\circ}\text{C}$, allyl cyanofornate (0.67 mL, 6.02 mmol, 1.10 equiv) was added dropwise over 10 min. The mixture was stirred at $-78\text{ }^{\circ}\text{C}$ for 2.5 h, quenched by addition of 50% sat. aqueous NH_4Cl (8 mL), and allowed to warm to ambient temperature. The reaction was diluted with Et_2O (25 mL) and the phases were separated. The aqueous phase was extracted with Et_2O (3 x 25 mL). The combined organic phases were dried over Na_2SO_4 , filtered, and concentrated under reduced pressure to afford a pale orange oil.

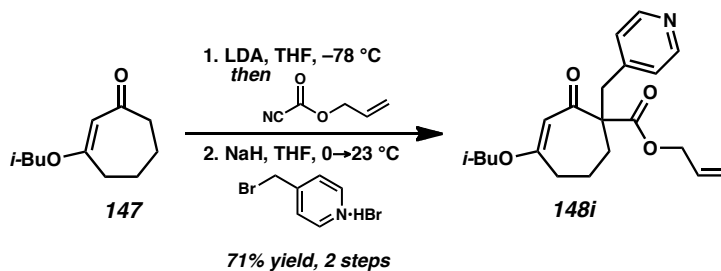
The crude oil was dissolved in THF (8 mL) in a 100 mL round-bottom flask, cooled to 0 °C, and stirred vigorously as hexane-washed NaH (197 mg, 8.22 mmol, 1.50 equiv) was added in one portion. Evolution of gas was observed and the reaction was stirred at 0 °C for 30 min to give a yellow-orange solution. 2,3-dichloro-1-propene (1.00 mL, 10.96 mmol, 2.0 equiv) was added dropwise and the reaction was allowed to warm to ambient temperature. After 10 h, TBAI (202 mg, 0.548 mmol, 0.10 equiv) was added and the reaction was heated to 40 °C. After 41 h, the reaction was cooled to ambient temperature and quenched by addition of 50% sat. aqueous NH₄Cl (10 mL). The phases were separated and the aqueous layer was extracted with Et₂O (3 x 15 mL). The combined organic phases were washed with brine, dried over Na₂SO₄, filtered, and concentrated under reduced pressure. The crude product was purified by flash column chromatography (SiO₂, 3 x 25 cm, 20:1→15:1 hexanes:EtOAc) to afford β -ketoester **148g** (1.57 g, 4.61 mmol, 84% yield over 2 steps) as a yellow oil; R_f = 0.60 (4:1 hexanes:EtOAc); ¹H NMR (300 MHz, CDCl₃) δ 5.87 (dddd, J = 17.1, 10.4, 5.8, 5.8 Hz, 1H), 5.38–5.25 (m, 3H), 5.25–5.16 (m, 2H), 4.65 (dddd, J = 13.2, 5.8, 1.3, 1.3 Hz, 1H), 4.52 (dddd, J = 13.1, 5.8, 1.3, 1.3 Hz, 1H), 3.45 (ddd, J = 21.1, 9.3, 6.5 Hz, 2H), 3.04 (s, 2H), 2.71 (dddd, J = 18.2, 10.2, 3.0, 1.3 Hz, 1H), 2.62–2.47 (m, 1H), 2.39 (ddd, J = 17.2, 6.9, 2.6 Hz, 1H), 2.10–1.90 (m, 2H), 1.89–1.65 (m, 2H), 0.94 (d, J = 6.7 Hz, 3H), 0.94 (d, J = 6.7 Hz, 3H); ¹³C NMR (75 MHz, CDCl₃) δ 196.6, 174.8, 172.1, 138.1, 131.7, 118.8, 117.1, 104.9, 74.8, 66.2, 62.2, 46.1, 33.9, 30.7, 27.8, 22.6, 19.2; IR (Neat Film NaCl) 3085, 2960, 2935, 2875, 1737, 1662, 1610, 1471, 1452, 1427, 1384, 1369, 1298, 1272, 1229, 1198, 1171, 1153, 1079, 1008, 967, 930, 890, 862, 813 cm⁻¹; HRMS (EI+) m/z calc'd for C₁₈H₂₅O₄ [M–Cl]⁺: 305.1753; found 305.1742.



β -Ketoester 148h. To a solution of diisopropylamine (1.53 mL, 10.93 mmol, 1.20 equiv) in THF (45 mL) in a 250 mL round-bottom flask at $0\text{ }^{\circ}\text{C}$ was added *n*-BuLi (4.17 mL, 10.47 mmol, 2.51 M in hexanes, 1.15 equiv) dropwise over 10 min. After 15 min of stirring at $0\text{ }^{\circ}\text{C}$, the mixture was cooled to $-78\text{ }^{\circ}\text{C}$ using an acetone/ $\text{CO}_2(\text{s})$ bath. A solution of vinylogous ester **147** (1.66 g, 9.11 mmol, 1.00 equiv) in THF (2 mL) was added dropwise over 10 min. After an additional 1 h of stirring at $-78\text{ }^{\circ}\text{C}$, allyl cyanoformate (1.09 mL, 10.0 mmol, 1.10 equiv) was added dropwise over 10 min. The mixture was stirred at $-78\text{ }^{\circ}\text{C}$ for 2.5 h, quenched by addition of 50% sat. aqueous NH_4Cl (13.5 mL), and then allowed to warm to ambient temperature. The reaction was diluted with Et_2O (50 mL) and the phases were separated. The aqueous phase was extracted with Et_2O (3 x 100 mL). The combined organic phases were dried over Na_2SO_4 , filtered, and concentrated under reduced pressure to afford a pale orange oil. The crude oil was purified by automated flash column chromatography using a Teledyne Isco CombiFlash R_f (SiO_2 , 25 g loading cartridge, 80 g column, multi-step gradient, hold 0% [2 min] \rightarrow ramp to 20% [4 min] \rightarrow hold 20% [15 min] \rightarrow ramp to 50% [7 min] \rightarrow hold 50% EtOAc in hexanes [5 min]) to afford the intermediate β -ketoester (2.08 g, 7.80 mmol, 86% yield).

One third of the intermediate β -ketoester (694 mg, 2.60 mmol, 1.00 equiv) was dissolved in THF (5 mL) in a 50 mL round-bottom flask, cooled to $0\text{ }^{\circ}\text{C}$, and stirred

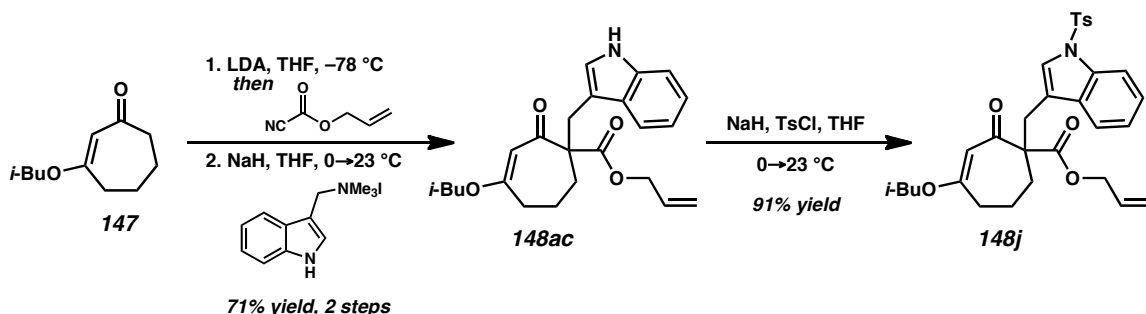
vigorously as hexane-washed NaH (15.6 mg, 0.65 mmol, 0.25 equiv) was added in one portion. Evolution of gas was observed and the reaction was stirred at 0 °C for 30 min to give a yellow-orange solution. Acrylonitrile (0.256 mL, 3.90 mmol, 1.50 equiv) was added dropwise and the reaction was allowed to warm to ambient temperature. After 40 h, the reaction was diluted with Et₂O (30 mL) and washed with H₂O (5 mL) and brine (5 mL). The aqueous layer was extracted with Et₂O (3 x 20 mL). The combined organic phases were washed with brine, dried over Na₂SO₄, filtered, and concentrated under reduced pressure. The crude product was purified by flash column chromatography (SiO₂, 3 x 25 cm, 10:1→6:1→4:1 hexanes:EtOAc) to afford β-ketoester **148h** (620 mg, 1.94 mmol, 75% yield, 65% yield over 2 steps) as a clear, colorless oil; *R*_f = 0.29 (4:1 hexanes:EtOAc); ¹H NMR (300 MHz, CDCl₃) δ 5.87 (dddd, *J* = 16.2, 10.4, 5.8, 5.8 Hz, 1H), 5.38 (s, 1H), 5.32 (app dq, *J* = 17.2, 1.4 Hz, 1H), 5.25 (app dq, *J* = 10.4, 1.1 Hz, 1H), 4.67 (dddd, *J* = 13.0, 5.8, 1.2, 1.2 Hz, 1H), 4.58 (dddd, *J* = 13.1, 5.9, 1.2, 1.2 Hz, 1H), 3.57–3.39 (m, 2H), 2.58 (ddd, *J* = 13.1, 9.6, 3.9 Hz, 1H), 2.51–2.32 (m, 4H), 2.32–2.11 (m, 2H), 2.11–1.90 (m, 2H), 1.90–1.64 (m, 2H), 0.95 (d, *J* = 6.7 Hz, 6H); ¹³C NMR (75 MHz, CDCl₃) δ 196.9, 174.4, 172.0, 131.4, 119.7, 119.3, 105.1, 75.0, 66.3, 61.5, 34.1, 33.1, 32.0, 27.9, 21.4, 19.2, 13.3; IR (Neat Film NaCl) 3081, 2959, 2936, 2875, 2247, 1733, 1648, 1609, 1471, 1454, 1423, 1403, 1385, 1369, 1297, 1269, 1235, 1192, 1173, 1096, 996, 932, 874, 824, 764 cm⁻¹; HRMS (EI+) *m/z* calc'd for C₁₈H₂₅O₄N [M]⁺: 319.1784; found 319.1777.



β -Ketoester 148i. To a solution of diisopropylamine (3.54 mL, 25.27 mmol, 1.20 equiv) in THF (108 mL) in a 250 mL round-bottom flask at 0 °C was added *n*-BuLi (10.26 mL, 24.22 mmol, 2.36 M in hexanes, 1.15 equiv) dropwise over 10 min. After 15 min of stirring at 0 °C, the mixture was cooled to –78 °C using an acetone/CO₂(s) bath. A solution of vinylogous ester **147** (3.84 g, 21.06 mmol, 1.00 equiv) in THF (10 mL) was added dropwise using positive pressure cannulation. After an additional 1 h of stirring at –78 °C, allyl cyanoformate (2.52 mL, 9.74 mmol, 1.10 equiv) was added dropwise over 10 min. The mixture was stirred at –78 °C for 2.5 h, quenched by addition of 50% sat. aqueous NH₄Cl (30.7 mL), and then allowed to warm to ambient temperature. The reaction was diluted with Et₂O (100 mL) and the phases were separated. The aqueous phase was extracted with Et₂O (3 x 100 mL). The combined organic phases were dried over Na₂SO₄, filtered, and concentrated under reduced pressure to afford a pale orange oil. The crude oil was purified by automated flash column chromatography using a Teledyne Isco CombiFlash R_f (SiO₂, 32 g loading cartridge, 330 g column, multi-step gradient, hold 0% [2 min]→ramp to 20% [10 min]→hold 20% [6 min]→ramp to 50% [3 min]→hold 50% EtOAc in hexanes [11 min]) to afford the intermediate β -ketoester (4.66 g, 17.50 mmol, 83% yield) as a pale orange oil.

A portion of the intermediate β -ketoester (1.00 g, 3.75 mmol, 1.00 equiv) was dissolved in THF (25 mL) in a 100 mL round-bottom flask, cooled to 0 °C, and stirred

vigorously as hexane-washed NaH (90 mg, 3.75 mmol, 1.00 equiv) was added in one portion. Evolution of gas was observed and the reaction was stirred at 0 °C for 30 min to give a yellow-orange solution. Additional NaH (202 mg, 8.43 mmol, 2.25 equiv) was added, giving a thick yellow suspension. After 5 min, 4-(bromomethyl)pyridine hydrogen bromide (996 mg, 3.94 mmol, 1.05 equiv) was added portionwise and the reaction was allowed to warm to ambient temperature. After 14 h, the reaction was quenched by addition of 50% sat. aqueous NH₄Cl (16 mL) to give a brown biphasic mixture. The phases were separated and the aqueous layer was extracted with Et₂O (3 x 25 mL). The combined organic phases were dried over Na₂SO₄, filtered, and concentrated under reduced pressure. The crude product was purified by flash column chromatography (SiO₂, 3 x 25 cm, 1:1→1:4 hexanes:EtOAc→EtOAc) to afford β -ketoester **148i** (1.16 g, 3.23 mmol, 86% yield, 71% yield over 2 steps) as a yellow oil; *R*_f = 0.28, broad (1:2 hexanes:EtOAc); ¹H NMR (300 MHz, CDCl₃) δ 8.44 (dd, *J* = 4.4, 1.6 Hz, 2H), 7.06 (dd, *J* = 4.4, 1.6 Hz, 2H), 5.82 (dddd, *J* = 17.1, 10.4, 5.8, 5.8 Hz, 1H), 5.37 (s, 1H), 5.28 (app dq, *J* = 17.2, 1.5 Hz, 1H), 5.21 (app dq, *J* = 10.4, 1.2 Hz, 1H), 4.61 (dddd, *J* = 13.1, 5.9, 1.3, 1.3 Hz, 1H), 4.50 (dddd, *J* = 13.1, 5.9, 1.3, 1.3 Hz, 1H), 3.42 (d, *J* = 6.5 Hz, 2H), 3.27 (d, *J* = 13.3 Hz, 1H), 3.18 (d, *J* = 13.3 Hz, 1H), 2.54 (ddd, *J* = 17.2, 9.3, 3.0 Hz, 1H), 2.38–2.21 (m, 2H), 2.03–1.86 (m, 2H), 1.83–1.59 (m, 2H), 0.91 (d, *J* = 6.7 Hz, 6H); ¹³C NMR (75 MHz, CDCl₃) δ 197.0, 174.3, 172.3, 149.6, 146.1, 131.4, 126.0, 119.2, 105.6, 74.9, 66.1, 63.5, 42.4, 33.9, 31.5, 27.8, 21.8, 19.2; IR (Neat Film NaCl) 3072, 3026, 2959, 2935, 2874, 1733, 1660, 1608, 1557, 1496, 1470, 1452, 1415, 1384, 1369, 1293, 1272, 1232, 1201, 1172, 1095, 1074, 1005, 994, 956, 935, 862, 823, 773 cm⁻¹; HRMS (EI+) *m/z* calc'd for C₂₁H₂₇O₄N [M]⁺: 357.1940; found 357.1945.



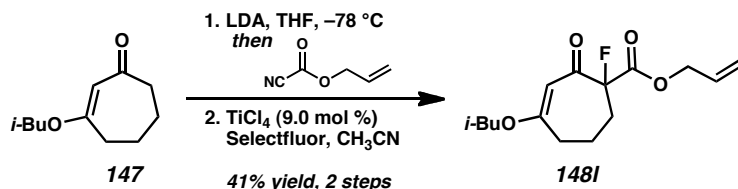
Indolyl β -Ketoester 148ac. To a solution of diisopropylamine (3.54 mL, 25.27 mmol, 1.20 equiv) in THF (108 mL) in a 250 mL round-bottom flask at 0 °C was added *n*-BuLi (10.26 mL, 24.22 mmol, 2.36 M in hexanes, 1.15 equiv) dropwise over 10 min. After 15 min of stirring at 0 °C, the mixture was cooled to –78 °C using an acetone/CO₂(s) bath. A solution of vinylogous ester **147** (3.84 g, 21.06 mmol, 1.00 equiv) in THF (10 mL) was added dropwise using positive pressure cannulation. After an additional 1 h of stirring at –78 °C, allyl cyanoformate (2.52 mL, 9.74 mmol, 1.10 equiv) was added dropwise over 10 min. The mixture was stirred at –78 °C for 2.5 h, quenched by addition of 50% sat. aqueous NH₄Cl (30.7 mL), and then allowed to warm to ambient temperature. The reaction was diluted with Et₂O (100 mL) and the phases were separated. The aqueous phase was extracted with Et₂O (3 x 100 mL). The combined organic phases were dried over Na₂SO₄, filtered, and concentrated under reduced pressure to afford a pale orange oil. The crude oil was purified by automated flash column chromatography using a Teledyne Isco CombiFlash R_f (SiO₂, 32 g loading cartridge, 330 g column, multi-step gradient, hold 0% [2 min]→ramp to 20% [10 min]→hold 20% [6 min]→ramp to 50% [3 min]→hold 50% EtOAc in hexanes [11 min]) to afford the intermediate β -ketoester (4.66 g, 17.50 mmol, 83% yield) as a pale orange oil.

A portion of the intermediate β -ketoester (0.85 g, 3.19 mmol, 1.00 equiv) was dissolved in THF (32 mL) in a 100 mL round-bottom flask, cooled to 0 °C, and stirred vigorously as hexane-washed NaH (84 mg, 3.51 mmol, 1.10 equiv) was added in one portion. Evolution of gas was observed and the reaction was stirred at 0 °C for 30 min to give a yellow-orange solution. Gramine methiodide⁵² (1.06 g, 3.35 mmol, 1.05 equiv) was added portionwise to give a suspension. After 11.5 h, the reaction was a brown-orange solution. Additional gramine methiodide (212 mg, 0.67 mmol, 0.31 equiv) was added. After 30 min, the reaction was quenched by addition of 50% sat. aqueous NH_4Cl (4.3 mL) to give a brown biphasic mixture. Volatiles were removed under reduced pressure. The residue was extracted with EtOAc (3 x 40 mL), dried over Na_2SO_4 , filtered, and concentrated under reduced pressure. The residue was dissolved in a minimal amount of 1:1 hexanes:EtOAc and filtered through a silica gel pad (1.5 x 10 cm, 1:1 hexanes:EtOAc). The filtrate was concentrated under reduced pressure. The crude product was purified by flash column chromatography (SiO_2 , 5 x 20 cm, 6:1→4:1→2:1 hexanes:EtOAc) to afford β -ketoester **148ac** (1.09 g, 2.75 mmol, 86% yield, 71% yield over 2 steps) as an orange-brown semi-solid; R_f = 0.21 (4:1 hexanes:EtOAc); ^1H NMR (300 MHz, CDCl_3) δ 8.08 (s, 1H), 7.67–7.54 (m, 1H), 7.38–7.29 (m, 1H), 7.21–7.04 (m, 2H), 7.00 (d, J = 2.4 Hz, 1H), 5.84 (dddd, J = 17.2, 10.4, 5.7, 5.7 Hz, 1H), 5.37 (s, 1H), 5.29 (app dq, J = 17.2, 1.5 Hz, 1H), 5.20 (app dq, J = 10.4, 1.3 Hz, 1H), 4.60 (dddd, J = 13.2, 5.6, 1.4, 1.4 Hz, 1H), 4.50 (dddd, J = 13.2, 5.8, 1.4, 1.4 Hz, 1H), 3.52 (dd, J = 14.3, 0.5 Hz, 1H), 3.47–3.31 (m, 3H), 2.63–2.34 (m, 2H), 2.28 (ddd, J = 17.8, 7.7, 4.0 Hz, 1H), 2.02–1.63 (m, 4H), 0.90 (d, J = 6.7 Hz, 6H); ^{13}C NMR (75 MHz, CDCl_3) δ 198.8, 173.7, 173.2, 135.8, 131.9, 128.8, 124.3, 121.8, 119.5, 119.2, 118.6, 111.1, 111.0, 106.0, 74.7,

65.9, 64.3, 34.0, 32.8, 31.6, 27.8, 21.7, 19.2; IR (Neat Film NaCl) 3785, 3584, 3392, 3079, 3057, 2958, 2930, 2874, 1729, 1641, 1607, 1457, 1457, 1433, 1423, 1384, 1368, 1341, 1233, 1191, 1174, 1127, 1085, 1010, 932, 879, 863, 822, 742 cm^{-1} ; HRMS (EI+) m/z calc'd for $\text{C}_{24}\text{H}_{29}\text{O}_4\text{N}$ $[\text{M}]^+$: 395.2097; found 395.2097.

Tosylindolyl β -Ketoester **148j.** To a solution of indole **148ac** (250 mg, 0.63 mmol, 1.00 equiv) in THF (9 mL) in a 100 mL round-bottom flask was added TsCl (241 mg, 1.26 mmol, 2.00 equiv). The mixture was cooled to 0 °C and stirred vigorously as hexane-washed NaH (61 mg, 2.53 mmol, 4.00 equiv) was added in one portion. The reaction was maintained at 0 °C for 5 min before warming to ambient temperature. After 24 h, the white suspension was cooled to 0 °C and additional TsCl (241 mg, 1.26 mmol, 2.00 equiv) was added, followed by hexane-washed NaH (121 mg, 5.06 mmol, 8.00 equiv) in one portion. The reaction was allowed to warm to ambient temperature. After 46 h, the reaction was quenched by addition of 50% sat. aqueous NH_4Cl (3 mL). The phases were separated and the aqueous phase was extracted with Et_2O (3 x 15 mL). The combined organic phases were dried over Na_2SO_4 , filtered, and concentrated under reduced pressure. The crude product was purified by flash column chromatography (SiO_2 , 3 x 25 cm, 10:1→6:1→4:1 hexanes:EtOAc) to afford β -ketoester **148j** (317 mg, 5.76 mmol, 91% yield) as a yellow foam; R_f = 0.40 (4:1 hexanes:EtOAc); ^1H NMR (300 MHz, CDCl_3) δ 7.97–7.89 (m, 1H), 7.75–7.66 (m, 2H), 7.53–7.44 (m, 1H), 7.35 (s, 1H), 7.31–7.13 (m, 4H), 5.77 (dddd, J = 17.1, 10.4, 5.8 Hz, 1H), 5.39 (s, 1H), 5.25 (app dq, J = 17.2, 1.5 Hz, 1H), 5.18 (app dq, J = 10.4, 1.2 Hz, 1H), 4.52 (dddd, J = 13.1, 5.7, 1.3, 1.3 Hz, 1H), 4.42 (dddd, J = 13.2, 5.9, 1.3, 1.3 Hz, 1H), 3.48–3.32 (m, 3H), 3.26 (d, J = 14.4

Hz, 1H), 2.52 (ddd, $J = 17.7, 9.2, 3.3$ Hz, 1H), 2.41–2.19 (m, 5H), 2.02–1.82 (m, 2H), 1.78–1.58 (m, 2H), 0.92 (d, $J = 6.7$ Hz, 6H); ^{13}C NMR (75 MHz, CDCl_3) δ 197.8, 174.0, 172.8, 144.8, 135.4, 134.9, 132.1, 131.6, 129.9, 127.0, 125.8, 124.6, 123.2, 119.9, 118.9, 118.0, 113.7, 105.9, 74.8, 66.1, 63.6, 34.1, 32.2, 31.7, 27.9, 21.7, 21.6, 19.2; IR (Neat Film NaCl) 3854, 3401, 2959, 2931, 2874, 1731, 1657, 1650, 1609, 1448, 1368, 1279, 1233, 1188, 1173, 1121, 1098, 1087, 1019, 1007, 992, 976, 938, 864, 813, 748 cm^{-1} ; HRMS (FAB+) m/z calc'd for $\text{C}_{31}\text{H}_{36}\text{O}_6\text{N}$ $[\text{M}+\text{H}]^+$: 550.2263; found 550.2250.

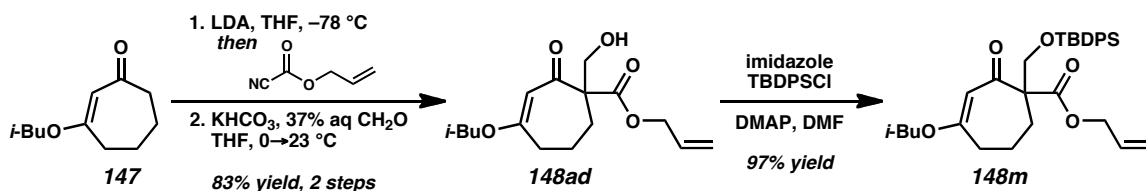


β -Ketoester 148l. To a solution of diisopropylamine (0.92 mL, 6.58 mmol, 1.20 equiv) in THF (27 mL) in a 100 mL round-bottomed flask at 0 $^\circ\text{C}$ in an ice/water bath was added *n*-BuLi (2.56 mL, 2.46 M in hexanes, 6.30 mmol, 1.15 equiv) dropwise over 10 min. After 15 min of stirring at 0 $^\circ\text{C}$, the mixture was cooled to $-78\text{ }^\circ\text{C}$ using an acetone/ $\text{CO}_2(\text{s})$ bath. A solution of vinylogous ester **147** (1.00 g, 5.48 mmol, 1.00 equiv) in THF (2 mL) was added dropwise using positive pressure cannulation. After an additional 1 h of stirring at $-78\text{ }^\circ\text{C}$, allyl cyanoformate (0.67 mL, 6.02 mmol, 1.10 equiv) was added dropwise over 10 min. The mixture was stirred at $-78\text{ }^\circ\text{C}$ for 2.5 h, quenched by addition of 50% sat. aqueous NH_4Cl (8 mL), and then allowed to warm to ambient temperature. The reaction mixture was diluted with Et_2O (25 mL) and the layers were separated. The aqueous phase was extracted with Et_2O (3 x 25 mL). The combined

organic layers were dried over Na₂SO₄, filtered, and concentrated under reduced pressure to afford a pale orange oil.

The crude oil was dissolved in CH₃CN (55 mL) in a 100 mL round-bottomed flask under N₂ and TiCl₄ (53.7 μL, 0.49 mmol, 9.0 mol %) was added dropwise, giving a dark purple-brown mixture. After 10 min, Selectfluor (2.33 g, 6.58 mmol, 1.20 equiv) was added in one portion. After 3.5 h, the reaction mixture was an orange suspension. The reaction was concentrated under reduced pressure and the orange residue was partitioned between water (25 mL) and Et₂O (25 mL). The layers were separated and the aqueous layer was extracted with Et₂O (3 x 25 mL). The combined organic layers were washed with brine, dried over Na₂SO₄, filtered, and concentrated under reduced pressure. The crude product was purified by automated flash column chromatography using Teledyne Isco CombiFlash R_f (SiO₂, 25 g loading cartridge, 120 g column, 10% EtOAc in hexanes) to afford β-ketoester **148I** (639 mg, 2.25 mmol, 41% yield over 2 steps) as a pale yellow oil; R_f = 0.44 (4:1 hexanes:EtOAc); ¹H NMR (500 MHz, CDCl₃) δ 5.86 (dddd, *J* = 17.1, 10.7, 5.6, 5.6 Hz, 1H), 5.39 (s, 1H), 5.29 (ddd, *J* = 17.1, 2.9, 1.5 Hz, 1H), 5.20 (app d, *J* = 10.5 Hz, 1H), 4.59 (dddd, *J* = 19.0, 13.2, 5.6, 1.2 Hz, 2H), 3.50 (dd, *J* = 9.3, 6.8 Hz, 1H), 3.47 (dd, *J* = 9.3, 6.6 Hz, 1H), 2.59 (ddd, *J* = 17.8, 9.8, 3.9 Hz, 1H), 2.45–2.38 (m, 2H), 2.02–1.94 (m, 1H), 1.84–1.75 (m, 1H), 1.70 (ddd, *J* = 14.4, 7.3, 4.4 Hz, 1H), 1.43 (s, 3H), 0.94 (d, *J* = 6.6 Hz, 6H); ¹³C NMR (75 MHz, CDCl₃) δ 192.1 (d, *J*_{CF} = 24.1 Hz), 178.0, 167.6 (d, *J*_{CF} = 25.4 Hz), 131.3, 119.0, 102.0 (d, *J*_{CF} = 1.1 Hz), 99.3 (d, *J*_{CF} = 193.5 Hz), 75.3, 66.6, 34.0 (d, *J*_{CF} = 2.1 Hz), 31.9 (d, *J*_{CF} = 22.5 Hz), 27.8, 20.7 (d, *J*_{CF} = 1.7 Hz), 19.1; ¹⁹F NMR (282 MHz, CDCl₃) δ –148.54 (dd, *J* = 35.4, 20.7 Hz); IR (Neat Film NaCl) 3086, 2960, 2938, 2876, 1752, 1654, 1649, 1603, 1471, 1453, 1422, 1403, 1385,

1369, 1282, 1249, 1229, 1204, 1176, 1137, 1095, 1045, 991, 953, 927, 874, 862, 843, 829, 795, 758 cm^{-1} ; HRMS (EI+) m/z calc'd for $\text{C}_{15}\text{H}_{21}\text{O}_4\text{F}$ $[\text{M}]^{+}$: 284.1425; found 284.1424.



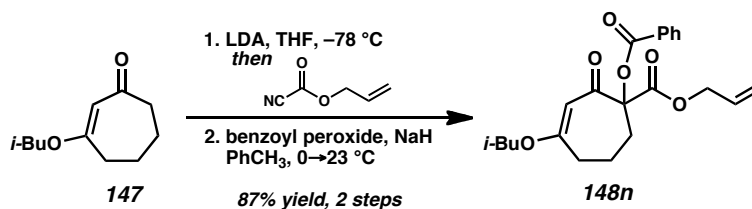
Hydroxy β -Ketoester 148ad. To a solution of diisopropylamine (1.84 mL, 13.15 mmol, 1.20 equiv) in THF (54 mL) in a 250 mL round-bottom flask at $0\text{ }^{\circ}\text{C}$ was added *n*-BuLi (5.12 mL, 12.60 mmol, 2.51 M in hexanes, 1.15 equiv) dropwise over 10 min. After 15 min of stirring at $0\text{ }^{\circ}\text{C}$, the mixture was cooled to $-78\text{ }^{\circ}\text{C}$ using an acetone/ $\text{CO}_2(\text{s})$ bath. A solution of vinylogous ester **147** (2.00 g, 10.96 mmol, 1.00 equiv) in THF (4 mL) was added dropwise using positive pressure cannulation. After an additional 1 h of stirring at $-78\text{ }^{\circ}\text{C}$, allyl cyanofornate (1.34 mL, 12.06 mmol, 1.10 equiv) was added dropwise over 10 min. The mixture was stirred at $-78\text{ }^{\circ}\text{C}$ for 2.5 h, quenched by addition of 50% sat. aqueous NH_4Cl (16 mL), and then allowed to warm to ambient temperature. The reaction was diluted with Et_2O (200 mL) and the phases were separated. The aqueous phase was extracted with Et_2O (3 x 100 mL). The combined organic phases were dried over Na_2SO_4 , filtered, and concentrated under reduced pressure to afford a pale orange oil (2.92 g).

Half of the crude oil (1.46 g) was dissolved in THF (10 mL) in a 50 mL round-bottom flask and cooled to $0\text{ }^{\circ}\text{C}$. KHCO_3 (1.65 g, 16.44 mmol, 3.00 equiv) and 37% wt. aqueous formaldehyde (2.81 mL, 37.73 mmol, 6.9 equiv) were added. The reaction was allowed

to warm to ambient temperature. After 11 h, the reaction was diluted with H₂O and CH₂Cl₂ (25 mL each). The phases were separated and the aqueous layer was extracted with CH₂Cl₂ (4 x 12 mL). The combined organic phases were dried over Na₂SO₄, filtered, and concentrated under reduced pressure. The crude product was purified by flash column chromatography (SiO₂, 3 x 25 cm, 4:1→2:1→1:1 hexanes:EtOAc) to afford β -ketoester **148ad** (1.35 g, 4.55 mmol, 83% yield over 2 steps) as a pale yellow oil; R_f = 0.21 (4:1 hexanes:EtOAc); ¹H NMR (300 MHz, CDCl₃) δ 5.89 (dddd, J = 17.2, 10.4, 5.7, 5.7 Hz, 1H), 5.43 (s, 1H), 5.32 (app dq, J = 17.2, 1.5 Hz, 1H), 5.23 (app dq, J = 10.4, 1.3 Hz, 1H), 4.76–4.54 (m, 2H), 3.93–3.72 (m, 2H), 3.51 (d, J = 6.5 Hz, 2H), 3.59–3.45 (m, 1H), 2.68–2.50 (m, 1H), 2.50–2.35 (m, 1H), 2.31–2.12 (m, 1H), 2.10–1.91 (m, 2H), 1.91–1.71 (m, 2H), 0.96 (d, J = 6.7 Hz, 6H); ¹³C NMR (75 MHz, CDCl₃) δ 200.2, 175.1, 171.9, 131.6, 118.9, 105.6, 75.1, 68.7, 66.1, 63.6, 33.7, 28.6, 27.9, 20.9, 19.2; IR (Neat Film NaCl) 3448, 3083, 2959, 2937, 2875, 1733, 1646, 1608, 1471, 1457, 1420, 1404, 1385, 1369, 1298, 1235, 1195, 1171, 1099, 1044, 998, 928, 869, 825 cm⁻¹; HRMS (FAB+) m/z calc'd for C₁₆H₂₅O₅ [M+H]⁺: 297.1702; found 297.1715.

Siloxy β -Ketoester 148m. Alcohol **148ad** (895 mg, 3.02 mmol, 1.00 equiv), DMAP (553 mg, 4.53 mmol, 1.50 equiv), and imidazole (308 mg, 4.53 mmol, 1.50 equiv) were dissolved in DMF (11 mL) in a 20 mL scintillation vial with magnetic stir bar and septum fitted screw cap. TBDPSCl (0.942 mL, 3.62 mmol, 1.20 equiv) was added dropwise. The stirred mixture turned into a turbid white suspension within 5 min. After 54 h, the reaction was poured into H₂O (35 mL) and 2:1 CH₂Cl₂/hexanes (75 mL). The phases were separated and the aqueous layer was further extracted with 2:1 CH₂Cl₂/hexanes (4 x

35 mL). The combined organics were dried over Na₂SO₄, filtered, and concentrated under reduced pressure. The crude product was purified by flash column chromatography (SiO₂, 5 x 25 cm, 40:1→20:1 hexanes:EtOAc) to afford siloxy β -ketoester **148m** (1.567 g, 2.93 mmol, 97% yield) as a clear, colorless oil; R_f = 0.58 (4:1 hexanes:EtOAc); ¹H NMR (300 MHz, CDCl₃) δ 7.70–7.61 (m, 4H), 7.47–7.32 (m, 6H), 5.86 (dddd, J = 17.1, 10.5, 5.7, 5.7 Hz, 1H), 5.39 (s, 1H), 5.29 (app dq, J = 17.2, 1.5 Hz, 1H), 5.19 (app dq, J = 10.4, 1.2 Hz, 1H), 4.65 (dddd, J = 13.2, 5.7, 1.3, 1.3 Hz, 1H), 4.52 (dddd, J = 13.3, 5.7, 1.3, 1.3 Hz, 1H), 4.15 (d, J = 9.6 Hz, 1H), 4.05 (d, J = 9.6 Hz, 1H), 3.47 (d, J = 6.5 Hz, 2H), 2.80–2.51 (m, 2H), 2.43 (ddd, J = 11.0, 7.4, 2.9 Hz, 1H), 2.17–1.89 (m, 3H), 1.89–1.68 (m, 1H), 1.04 (s, 9H), 0.95 (d, J = 6.7 Hz, 6H); ¹³C NMR (75 MHz, CDCl₃) δ 197.5, 174.8, 171.6, 135.8, 135.7, 133.3, 133.2, 131.89, 129.8, 129.7, 127.8, 127.7, 118.5, 105.8, 74.8, 69.0, 65.9, 65.1, 34.5, 30.0, 27.8, 26.8, 21.9, 19.4, 19.2; IR (Neat Film NaCl) 3460, 3071, 3049, 2958, 2931, 2890, 2857, 1738, 1650, 1609, 1472, 1429, 1384, 1362, 1299, 1236, 1200, 1173, 1113, 1007, 998, 936, 864, 822, 740 cm⁻¹; HRMS (FAB+) m/z calc'd for C₃₂H₄₃O₅Si [M+H]⁺: 535.2880; found 535.2880.



β -Ketoester 148n. To a solution of diisopropylamine (1.84 mL, 13.15 mmol, 1.20 equiv) in THF (54 mL) in a 250 mL round-bottomed flask at 0 °C in an ice/water bath was added *n*-BuLi (5.12 mL, 2.51 M in hexanes, 12.60 mmol, 1.15 equiv) dropwise over 10 min. After 15 min of stirring at 0 °C, the mixture was cooled to –78 °C using an

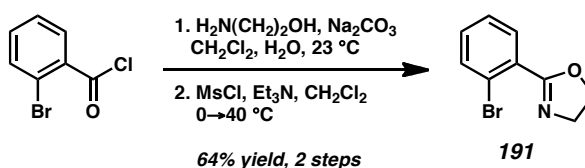
acetone/CO₂(s) bath. A solution of vinylogous ester **147** (2.00 g, 10.96 mmol, 1.00 equiv) in THF (4 mL) was added dropwise using positive pressure cannulation. After an additional 1 h of stirring at –78 °C, allyl cyanoformate (1.34 mL, 12.06 mmol, 1.10 equiv) was added dropwise over 10 min. The mixture was stirred at –78 °C for 2.5 h, quenched by addition of 50% sat. aqueous NH₄Cl (16 mL), and then allowed to warm to ambient temperature. The reaction mixture was diluted with Et₂O (20 mL) and the layers were separated. The aqueous phase was extracted with Et₂O (3 x 10 mL). The combined organic layers were dried over Na₂SO₄, filtered, and concentrated under reduced pressure to afford a pale orange oil (2.92 g).

Half of the crude oil (1.46 g) was dissolved in toluene (30 mL) in a 100 mL round-bottomed flask, cooled to 0 °C, and stirred vigorously as hexane-washed NaH (197 mg, 8.22 mmol, 1.50 equiv) was added in one portion. Evolution of gas was observed and the reaction mixture was stirred at 0 °C for 30 min. Benzoyl peroxide (1.99 g, 8.22 mmol, 1.50 equiv) was added slowly portionwise, giving a thick, pasty suspension. The reaction was warmed to ambient temperature and diluted with toluene (20 mL) to give a more freely stirring turbid yellow mixture. After 30 min, the reaction was diluted with toluene (50 mL) and washed with H₂O (2 x 5 mL) and brine (2 x 5 mL). The aqueous layers were combined and extracted with EtOAc (2 x 25 mL). The combined organic layers were dried over Na₂SO₄, filtered, and concentrated under reduced pressure. The crude product was purified by flash column chromatography (SiO₂, 5 x 13 cm, 10:1 hexanes:EtOAc) to afford β-ketoester **148n** (1.85 g, 4.79 mmol, 87% yield over 2 steps) as a pale yellow oil; *R_f* = 0.46 (4:1 hexanes:EtOAc); ¹H NMR (300 MHz, CDCl₃) δ 8.09–7.99 (m, 2H), 7.64–7.53 (m, 1H), 7.50–7.38 (m, 2H), 5.89 (dddd, *J* = 17.2, 10.5,

5.7, 5.7 Hz, 1H), 5.42 (s, 1H), 5.31 (app dq, $J = 17.2, 1.5$ Hz, 1H), 5.20 (app dq, $J = 10.4, 1.3$ Hz, 1H), 4.80–4.62 (m, 2H), 3.57 (d, $J = 6.5$ Hz, 2H), 2.87–2.46 (m, 4H), 2.12–1.85 (m, 3H), 0.96 (d, $J = 6.7$ Hz, 6H); ^{13}C NMR (75 MHz, CDCl_3) δ 192.1, 175.9, 168.0, 165.1, 133.6, 131.7, 130.0, 129.6, 128.6, 118.7, 102.2, 88.8, 75.2, 66.6, 33.8, 31.2, 27.9, 21.2, 19.2, 19.2; IR (Neat Film NaCl) 3070, 2960, 2937, 2875, 1753, 1727, 1661, 1605, 1471, 1452, 1423, 1384, 1369, 1315, 1280, 1222, 1206, 1175, 1107, 1097, 1070, 1044, 1026, 1002, 933, 849, 792 cm^{-1} ; HRMS (EI+) m/z calc'd for $\text{C}_{22}\text{H}_{26}\text{O}_6$ $[\text{M}]^{+}$: 386.1733; found 386.1729.

2.10.2.3 SYNTHESIS OF PHOX LIGANDS

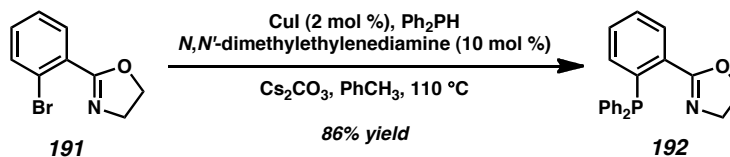
Ligands (*S*)-*t*-Bu-PHOX (**13**)⁵⁴ and (*S*)-*p*-(CF_3)₃-*t*-Bu-PHOX (**14**)⁵⁵ were prepared according to previously reported procedures. The preparation of ligands **192** and **150** are described below.



2-(2-Bromo-phenyl)-4,5-dihydrooxazole 191. To a solution of ethanolamine (1.32 mL, 21.9 mmol, 1.20 equiv) in CH_2Cl_2 (60 mL) in a 250 mL round-bottom flask was added a solution of Na_2CO_3 (5.80 g, 54.7 mmol, 3.00 equiv) in H_2O (45 mL). Neat 2-bromobenzoyl chloride (4.00 g, 2.38 mL, 18.2 mmol, 1.00 equiv) was added dropwise via syringe to the vigorously stirred biphasic system. The reaction flask was capped with a yellow plastic stopper and stirred for 7.5 h at 23 °C. The layers were separated and the

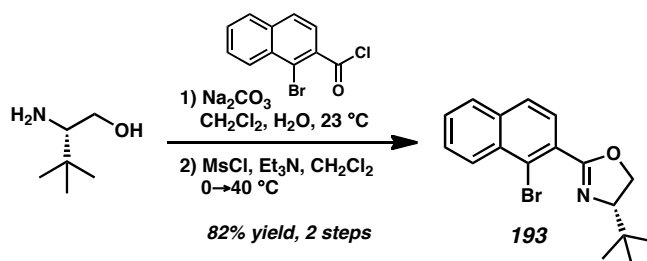
aqueous phase was extracted with CH_2Cl_2 (2 x 25 mL). The combined organics were dried over Na_2SO_4 , filtered, and concentrated under reduced pressure to afford a white solid. The crude product was dissolved in CH_2Cl_2 (50 mL) and hexanes (10 mL) was added. The solution was concentrated to ca. 25 mL under reduced pressure resulting in precipitation of the intermediate amide (4.02 g, 16.4 mmol, 90% yield) as a white solid.

The intermediate amide (2.0 g, 8.2 mmol, 1.00 equiv) was dissolved in CH_2Cl_2 (62 mL) in a 100 mL round-bottom flask equipped with a reflux condenser. Et_3N (3.43 mL, 24.5 mmol, 3.00 equiv) was added and the solution was cooled to 0 °C by use of an ice/water bath. Methanesulfonyl chloride (952 μL , 12.3 mmol, 1.50 equiv) was added dropwise. The reaction mixture was stirred at 0 °C for 30 min and heated to 40 °C in an oil bath. After 5 h of stirring, the resulting yellow solution was allowed to cool to ambient temperature, diluted with CH_2Cl_2 (25 mL), and washed with H_2O (2 x 25 mL) and brine (25 mL). The organic layer was dried over Na_2SO_4 , filtered, and concentrated under reduced pressure to afford a thick, pale yellow oil. The crude oil was purified by flash chromatography (SiO_2 , 5 x 10 cm, 6:2:2 hexanes:EtOAc:toluene) to afford 2-(2-bromo-phenyl)-4,5-dihydrooxazole **191** (1.31 g, 5.79 mmol, 71% yield); R_f = 0.45 (9:1 CHCl_3 :MeOH); ^1H NMR (500 MHz, CDCl_3) δ 7.72 (dd, J = 7.8, 2.0 Hz, 1H), 7.65 (dd, J = 8.1, 1.0 Hz, 1H), 7.35 (app dt, J = 7.6, 1.2 Hz, 1H), 7.29 (app dt, J = 7.6, 1.7 Hz, 1H), 4.46 (t, J = 9.6 Hz, 2H), 4.12 (t, J = 9.6 Hz, 2H); ^{13}C NMR (125 MHz, CDCl_3) δ 164.0, 134.1, 131.8, 131.5, 129.8, 127.2, 122.0, 67.8, 55.5; IR (Neat Film NaCl) 3390, 3070, 2966, 2904, 2868, 1729, 1646, 1589, 1432, 1362, 1328, 1272, 1243, 1093, 1026, 938 cm^{-1} ; HRMS (EI+) m/z calc'd for $\text{C}_9\text{H}_8\text{BrNO}$ $[\text{M}]^+$: 224.9789; found 224.9779.



PHOX Ligand 192. A 250 mL Schlenk flask was charged with CuI (66.7 mg, 0.35 mmol, 2 mol %), Ph₂PH (3.85 mL, 22.1 mmol, 1.25 equiv), *N,N'*-dimethylethylenediamine (191 mL, 1.77 mmol, 10 mol %), and toluene (18 mL). The solution was stirred at 23 °C for 20 min. 2-(2-Bromo-phenyl)-4,5-dihydrooxazole **191** (4.0 g, 17.7 mmol, 1.00 equiv) was azeotroped with toluene (2 x 5 mL) under reduced pressure, dissolved in toluene (18 mL), and transferred quantitatively to the Schlenk flask by use of positive pressure cannulation. Cs₂CO₃ (8.65 g, 26.5 mmol, 1.50 equiv) was added in one portion and the flask was evacuated/backfilled with Ar (three cycles). The teflon valve was sealed and the yellow heterogeneous reaction mixture was stirred vigorously, immersed in an oil bath, and heated to 110 °C. After 20 h of stirring at 110 °C, the mixture was allowed to cool to ambient temperature and filtered through a pad of Celite using CH₂Cl₂ (2 x 50 mL). The filtrate was concentrated under reduced pressure to afford a clear orange oil. The crude oil was flushed through a plug of silica gel (SiO₂, 5 x 10 cm, hexanes→9:1 CH₂Cl₂:Et₂O) to afford PHOX ligand **192** (5.03 g, 15.2 mmol, 86% yield) as a colorless viscous oil that crystallized upon standing; *R*_f = 0.50 (7:3 hexanes:EtOAc); ¹H NMR (500 MHz, CDCl₃) δ 7.85 (dd, *J* = 7.6, 3.4 Hz, 1H), 7.37–7.26 (comp. m, 12H), 6.89 (dd, *J* = 4.1, 7.6 Hz, 1H), 4.08 (t, *J* = 9.5 Hz, 2H), 3.78 (t, *J* = 9.5 Hz, 2H); ¹³C NMR (125 MHz, CDCl₃) δ 164.5 (d, *J*_{CP} = 2.8 Hz), 139.1 (d, *J*_{CP} = 24.9 Hz), 138.0 (d, *J*_{CP} = 11.5 Hz), 134.1 (d, *J*_{CP} = 20.7 Hz), 133.7 (d, *J*_{CP} = 1.8 Hz), 131.9 (d, *J*_{CP} = 18.9 Hz), 130.5, 129.9 (d, *J*_{CP} = 2.8 Hz), 128.7, 128.5 (d, *J*_{CP} = 7.4 Hz), 128.1, 67.2, 55.0; ³¹P NMR (121 MHz, CDCl₃) δ –3.99 (s); IR (Neat Film NaCl) 3053, 3000, 2971,

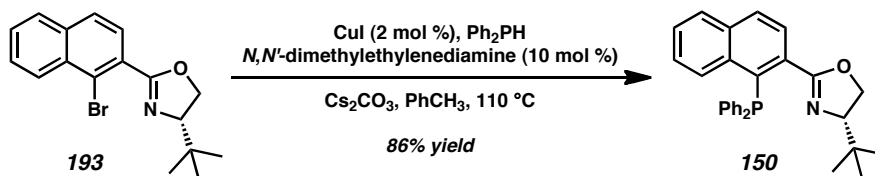
2901, 2876, 1650, 1585, 1562, 1478, 1434, 1354, 1326, 1248, 1133, 1089, 1070, 1041, 974, 942, 898, 743 cm^{-1} ; HRMS (FAB+) m/z calc'd for $\text{C}_{21}\text{H}_{19}\text{NOP}$ $[\text{M}+\text{H}]^+$: 332.1204; found 332.1218; mp = 99–101 °C.



Dihydrooxazole 193. (*S*)-*tert*-Leucinol (1.02 g, 8.66 mmol, 1.00 equiv) was placed in a 250 mL round-bottom flask and dissolved in CH_2Cl_2 (14 mL). Na_2CO_3 (2.75 g, 26.0 mmol, 3.00 equiv) in H_2O (27.0 mL) was added dropwise via syringe to the vigorously stirred biphasic system. To the biphasic mixture was added a solution of 1-bromonaphthalene-2-carbonyl chloride (2.68 g, 9.96 mmol, 1.15 equiv) in CH_2Cl_2 (15 mL). The reaction was stirred vigorously at 23 °C for 9.5 h. The phases were separated and the aqueous phase was extracted with CH_2Cl_2 (4 x 50 mL). The combined organics were stirred with KOH (10 mL, 10 mmol, 1.0 N in MeOH) for 30 min then transferred to a separatory funnel. H_2O (10 mL) was added and the mixture was neutralized with HCl (6.0 M in H_2O). The phases were separated and the aqueous phase was extracted with CH_2Cl_2 (4 x 50 mL). The combined organics were dried over MgSO_4 and concentrated under reduced pressure to afford the intermediate amide (3.03 g) as a pale yellow solid.

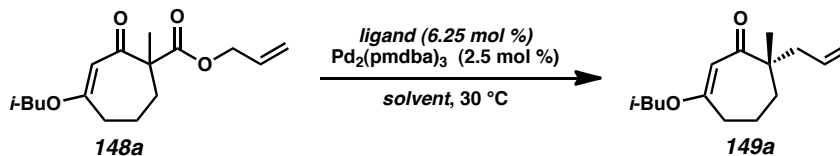
The intermediate amide (3.03 g) was dissolved in CH_2Cl_2 (43.3 mL) in a 100 mL 3-neck round-bottom flask fitted with a reflux condenser. The solution was cooled to 0 °C by use of an ice/water bath and Et_3N (2.90 mL, 20.8 mmol, 2.40 equiv) was added.

Methanesulfonyl chloride (0.77 mL, 9.96 mmol, 1.15 equiv) was added dropwise. The reaction mixture was stirred at 0 °C for 30 min and heated to 40 °C in a water bath. After 21 h of stirring, the mixture was allowed to cool to ambient temperature and saturated aqueous NaHCO₃ was added. The biphasic system was stirred vigorously for 5 min and the layers were separated. The aqueous phase was extracted with CH₂Cl₂ (2 x 50 mL). The combined organics were washed with brine (50 mL), dried over MgSO₄, and concentrated under reduced pressure to afford a pale yellow oil. The crude oil was purified by flash chromatography (SiO₂, 3 x 15 cm, 9:1 hexanes:EtOAc) to afford **193** (2.36 g, 7.12 mmol, 82% yield over two steps) as a pale yellow oil that solidifies when placed in a –20 °C freezer; *R_f* = 0.73 (9:1 CHCl₃:MeOH); ¹H NMR (300 MHz, CDCl₃) δ 8.41 (dd, *J* = 7.7, 0.5 Hz, 1H), 7.85–7.81 (m, 2H), 7.64 (d, *J* = 8.5 Hz, 1H), 7.60 (app dt, *J* = 8.2, 1.3 Hz, 1H), 7.56 (app dt, *J* = 6.9, 1.3 Hz, 1H), 4.46 (dd, *J* = 10.4, 8.5 Hz, 1H), 4.33 (dd, *J* = 8.5, 8.0 Hz, 1H), 4.17 (dd, *J* = 10.4, 8.2 Hz, 1H), 1.05 (s, 9H); ¹³C NMR (125 MHz, CDCl₃) δ 163.8, 134.9, 132.3, 128.8, 128.3, 128.3, 128.0, 127.8, 127.7, 126.9, 123.2, 76.9, 69.2, 34.1, 26.1; IR (Neat Film NaCl) 3065, 2956, 2899, 2863, 1667, 1620, 1594, 1556, 1499, 1476, 1463, 1393, 1372, 1362, 1339, 1321, 1300, 1238, 1264, 1210, 1161, 1104, 1024, 977, 956, 920, 817, 752 cm^{–1}; HRMS (EI+) *m/z* calc'd for C₁₇H₁₈ONBr [M]⁺: 331.0572; found 331.0583; [α]_D^{20.0} –64.0 (c 0.92, CHCl₃); mp = 66–68 °C.



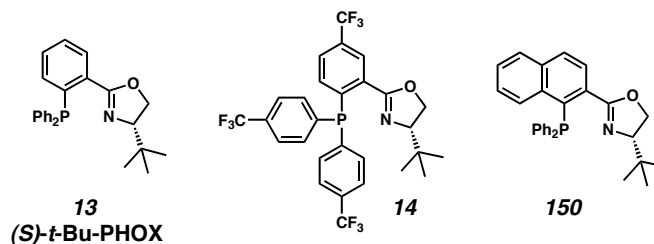
PHOX Ligand 150. Prepared by the typical method as described for **192** above by employing **193** (830.6 mg, 2.50 mmol). After 24 h of stirring, the reaction mixture was filtered through a plug of Celite, eluted with CH_2Cl_2 (2 x 25 mL), and concentrated under reduced pressure. The crude oil was passed through a short plug of silica (SiO_2 , 2.5 x 8 cm, hexanes→9:1 CH_2Cl_2 : Et_2O) to afford a bright yellow oil. The crude oil was purified by flash chromatography (SiO_2 , 2.5 x 25 cm, 19:1 hexanes:acetone and then 2.5 x 21 cm, 9:1→6:1 hexanes: EtOAc) to afford PHOX ligand **150** (950.8 mg, 2.17 mmol, 87% yield) as a bright yellow foam; R_f = 0.21 (9:1 hexanes: EtOAc); ^1H NMR (500 MHz, CDCl_3) δ 7.97 (d, J = 8.1 Hz, 1H), 7.96 (d, J = 8.0 Hz, 2H), 7.72 (dd, J = 8.3, 2.9 Hz, 1H), 7.45 (app dt, J = 7.8, 1.7 Hz, 2H), 7.41–7.38 (m, 3H), 7.29–7.22 (m, 6H), 7.16 (ddd, J = 8.3, 6.9, 1.0 Hz, 1H), 4.17–4.15 (m, 2H), 3.91 (dd, J = 9.8, 8.8 Hz, 1H), 0.97 (s, 9H); ^{13}C NMR (125 MHz, CDCl_3) δ 165.6 (d, J_{CP} = 5.1 Hz), 137.5 (d, J_{CP} = 33.1 Hz), 136.8, (d, J_{CP} = 14.7 Hz), 136.5 (d, J_{CP} = 14.7), 134.9, 134.7 (d, J_{CP} = 33.6 Hz), 133.1 (d, J_{CP} = 26.7 Hz), 132.2 (d, J_{CP} = 17.5 Hz), 132.1 (d, J_{CP} = 17.5 Hz), 131.5 (d, J_{CP} = 0.9 Hz), 129.1 (d, J_{CP} = 7.4 Hz), 129.0, 128.4 (d, J_{CP} = 6.0 Hz), 127.8 (d, J_{CP} = 8.3 Hz), 126.6 (d, J_{CP} = 8.7 Hz), 126.4 (d, J_{CP} = 40.5 Hz), 76.8, 69.0, 34.1, 26.3; ^{31}P NMR (121 MHz, CDCl_3) δ -9.33 (s); IR (Neat Film NaCl) 3054, 2954, 2867, 1665, 1584, 1478, 1434, 1364, 1244, 1094, 1026, 986, 962, 922, 824 cm^{-1} ; HRMS (FAB+) m/z calc'd for $\text{C}_{29}\text{H}_{28}\text{NOP}$ $[\text{M}]^{+}$: 437.1908; found 437.1908; $[\alpha]_{\text{D}}^{26.1}$ -38.2 (c 1.59, n -hexane).

2.10.2.4 ENANTIOSELECTIVE Pd-CATALYZED DECARBOXYLATIVE ALKYLATION SCREENING PROTOCOL^a



entry	ligand	solvent	yield (%) ^b	ee (%) ^c
1	13	THF ^e	94	84
2	13	<i>p</i> -dioxane	86	84
3	13	2-methyl THF ^e	75	85
4	13	TBME ^e	88	85
5	13	Et ₂ O	93	86
6	13	PhH	84	86
7	13	PhCH ₃	91	88
8 ^d	14	PhCH ₃	57	90
9	150	PhCH ₃	77	72

^a Conditions: β -ketoester **148a** (1.0 equiv), $\text{Pd}_2(\text{pmdba})_3$ (2.5 mol %), ligand (6.25 mol %) in solvent (0.1 M) at 30 °C; pmdba = 4,4'-methoxydibenzylideneacetone. ^b Isolated yield. ^c Determined by chiral HPLC. ^d Increased catalyst loadings were required to achieve full conversion: $\text{Pd}_2(\text{pmdba})_3$ (5 mol %), **14** (12.5 mol %). ^e THF = tetrahydrofuran, 2-methyl THF = 2-methyl tetrahydrofuran, TBME = *tert*-butyl methyl ether.

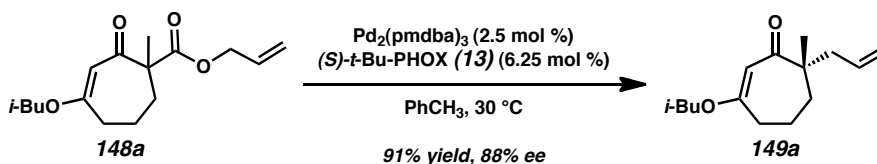


Enantioselective Allylation Screen to Produce Vinylous Ester **149a (0.20 mmol scale).** To a 25 mL flask was added $\text{Pd}_2(\text{pmdba})_3$ (5.00 μmol , 2.5 mol %) and ligand (12.5 μmol , 6.25 mol %). The flask was evacuated/backfilled with N_2 (3 cycles, 5 min evacuation per cycle). Solvent (most of total volume, 0.1 M final concentration) was added and the black suspension was stirred for 30 min at 30 °C using an oil bath. A solution of β -ketoester **148a** (0.20 mmol, 1.00 equiv) in solvent (remainder of total volume) was transferred to the catalyst solution using positive pressure cannulation.

When judged complete by TLC analysis, the reaction was filtered through a small plug of SiO₂, eluted with Et₂O, and concentrated under reduced pressure. Purification by flash column chromatography (SiO₂, 1.5 x 15 cm, 9:1→6:1 hexanes:EtOAc) or preparative TLC (SiO₂, 2:1 hexanes:EtOAc) provided vinylogous ester **149a** for analysis. HPLC conditions: 1% IPA in hexanes, 1.0 mL/min, OD-H column, *t_R* (min): major = 6.30, minor = 7.26. (For characterization data, see p. 124)

2.10.2.5 PREPARATION OF CHIRAL VINYLOGOUS ESTERS 149

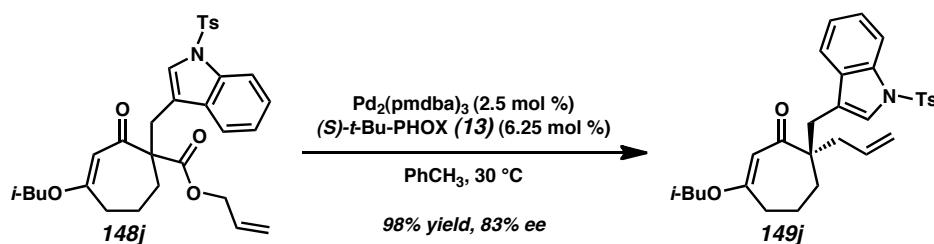
Non-enantioselective reactions were performed using Pd(PPh₃)₄ (5 mol %) or achiral PHOX ligand **192** (6.25 mol %) and Pd₂(pmdba)₃ (2.5 mol %) in toluene at 30 °C. For the synthesis of ligand **192**, see p. 115–117.



Schlenk Manifold Method: Asymmetric Allylic Alkylation

Vinylogous Ester 149a. Pd₂(pmdba)₃ (5.0 mg, 4.5 μmol, 2.5 mol %) and (*S*)-*t*-Bu-PHOX (4.4 mg, 11 μmol, 6.25 mol %) were placed in a 1 dram vial. The flask was evacuated/backfilled with N₂ (3 cycles, 10 min evacuation per cycle). Toluene (1.3 mL, sparged with N₂ for 1 h immediately before use) was added and the black suspension was immersed in an oil bath preheated to 30 °C. After 30 min of stirring, β-ketoester **148a** (50.7 mg, 0.181 mmol, 1.00 equiv) was added as a solution in toluene (0.5 mL, sparged with N₂ immediately before use) using positive pressure cannulation. The dark orange

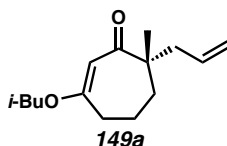
catalyst solution turned olive green immediately upon addition of β -ketoester **148a**. The reaction was stirred at 30 °C for 21 h, allowed to cool to ambient temperature, filtered through a silica gel plug (2 x 2 cm, Et₂O), and concentrated under reduced pressure. The crude oil was purified by preparative TLC (SiO₂, 4:1 hexanes:EtOAc) to afford vinylogous ester **149a** (38.8 mg, 0.164 mmol, 91% yield, 88% ee) as a pale yellow oil. (For characterization data, see p. 124).



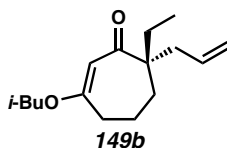
Glove Box Method: Asymmetric Allylic Alkylation

Vinylogous Ester 149j. A 20 mL scintillation vial was loaded with β -ketoester **148j** (447 mg, 0.81 mmol, 1.00 equiv). A separate 20 mL scintillation vial was loaded with $\text{Pd}_2(\text{pmdba})_3$ (19.7 mg, 0.051 mmol, 6.25 mol %), $(S)\text{-}t\text{-Bu-PHOX}$ (22.3 mg, 0.020 mmol, 2.5 mol %), and magnetic stir bar. The two vials and a teflon-lined hard cap were evacuated/backfilled with N₂ in a glove box antechamber (3 cycles, 5 min evacuation per cycle) before being transferred into the glove box. Toluene (5 mL) was added to the vial containing $\text{Pd}_2(\text{pmdba})_3$ and $(S)\text{-}t\text{-Bu-PHOX}$. The vial was capped and heated to 30 °C for 30 min. During this time, the mixture developed a dark orange color. β -Ketoester **148j** was dissolved in toluene (3 mL) and added to the catalyst solution dropwise, causing the solution to turn olive green. The solution was stirred at 30 °C in a heating block. The capped vial was removed from the glove box after 29 h of stirring. The crude

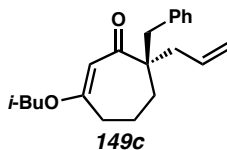
product was concentrated under reduced pressure and purified by flash column chromatography (SiO₂, 5 x 25 cm, 15:1→10:1→8:1→6:1 hexanes:EtOAc) to afford vinylogous ester **149j** (403 mg, 0.796 mmol, 98% yield, 82.9% ee) as a thick, white semi-solid. (For characterization data, see p. 131).



Vinylogous Ester 149a (*Table 2.1, entry 1*). Prepared using Schlenk Manifold Method. 38.8 mg, 0.164 mmol, 91% yield. Preparative TLC (SiO₂, 4:1 hexanes:EtOAc). R_f = 0.31 (3:1 hexanes:Et₂O); ¹H NMR (500 MHz, CDCl₃) δ 5.72 (dddd, J = 16.6, 10.5, 7.3, 7.3 Hz, 1H), 5.31 (s, 1H), 5.05–5.00 (m, 2H), 3.50 (dd, J = 9.3, 6.6 Hz, 1H), 3.47 (dd, J = 9.3, 6.6 Hz, 1H), 2.53–2.42 (m, 2H), 2.38 (dd, J = 13.7, 7.1 Hz, 1H), 2.20 (dd, J = 13.7, 7.8 Hz, 1H), 1.98 (app sept, J = 6.6 Hz, 1H), 1.86–1.70 (m, 3H), 1.62–1.56 (m, 1H), 1.14 (s, 3H), 0.95 (d, J = 6.6 Hz, 6H); ¹³C NMR (125 MHz, CDCl₃) δ 206.7, 171.3, 134.6, 117.9, 105.0, 74.5, 51.5, 45.4, 36.1, 35.2, 28.0, 25.2, 19.9, 19.3, 19.3; IR (Neat Film NaCl) 2960, 2933, 2873, 1614, 1470, 1387, 1192, 1171, 998, 912 cm⁻¹; HRMS (EI+) m/z calc'd for C₁₅H₂₄O₂ [M]⁺: 236.1776; found 236.1767; $[\alpha]_D^{25.6}$ –69.04 (c 1.08, CHCl₃, 88.0% ee); HPLC conditions: 1% IPA in hexanes, 1.0 mL/min, OD-H column, t_R (min): major = 6.30, minor = 7.26.

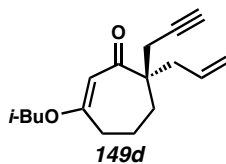


Vinyllogous Ester 149b (*Table 2.1, entry 2*). Prepared using Schlenk Manifold Method. 226.3 mg, 0.90 mmol, 89% yield. Flash column chromatography (SiO₂, 3 x 24 cm, 20:1→15:1→10:1 hexanes:EtOAc). R_f = 0.43 (10:1 hexanes:EtOAc); ¹H NMR (300 MHz, CDCl₃) δ 5.82–5.62 (m, 1H), 5.29 (s, 1H), 5.06–4.98 (m, 2H), 3.48 (dd, J = 11.1, 6.6 Hz, 1H), 3.45 (dd, J = 11.2, 6.6 Hz, 1H), 2.49–2.42 (m, 2H), 2.40 (dddd, J = 13.8, 7.1, 1.2 Hz, 1H), 2.23 (dddd, J = 13.8, 7.7, 1.1, 1.1 Hz, 1H), 1.97 (app sept, J = 6.7 Hz, 1H), 1.84–1.44 (m, 6H), 0.98–0.91 (d, J = 6.7 Hz, 6H), 0.79 (t, J = 7.5 Hz, 3H); ¹³C NMR (75 MHz, CDCl₃) δ 206.2, 171.0, 135.1, 117.6, 105.5, 74.4, 54.8, 41.9, 36.1, 32.3, 31.3, 28.0, 20.0, 19.3, 8.6; IR (Neat Film NaCl) 3073, 2960, 2933, 2876, 1617, 1613, 1459, 1400, 1387, 1369, 1314, 1220, 1190, 1173, 996, 969, 954, 912, 883, 873, 856, 782 cm⁻¹; HRMS (EI+) m/z calc'd for C₁₆H₂₆O₂ [M]⁺: 250.1933; found 250.1909; $[\alpha]_D^{25.0}$ +25.83 (c 1.04, CHCl₃, 91.6% ee); HPLC conditions: 0.25% IPA in hexanes, 1.0 mL/min, AD column, t_R (min): minor = 16.23, major = 18.08.



Vinyllogous Ester 149c (*Table 2.1, entry 3*). Prepared using Schlenk Manifold Method. 172.5 mg, 0.552 mmol, 98% yield. Flash column chromatography (SiO₂, 3 x 24 cm, 20:1→15:1→10:1 hexanes:EtOAc). R_f = 0.50 (10:1 hexanes:EtOAc); ¹H NMR (300 MHz, CDCl₃) δ 7.28–7.14 (m, 3H), 7.14–7.08 (m, 2H), 5.85–5.68 (m, 1H), 5.31 (s, 1H),

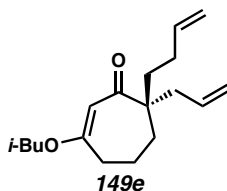
5.10–4.99 (m, 2H), 3.44 (dd, $J = 14.7, 6.6$ Hz, 1H), 3.41 (dd, $J = 14.7, 6.6$ Hz, 1H), 3.14 (d, $J = 13.3$ Hz, 1H), 2.71 (d, $J = 13.3$ Hz, 1H), 2.51 (dddd, $J = 13.7, 6.8, 1.2, 1.2$ Hz, 1H), 2.45–2.32 (m, 2H), 2.16 (dddd, $J = 13.7, 7.9, 1.1, 1.1$ Hz, 1H), 1.93 (app sept, $J = 6.7$ Hz, 1H), 1.83–1.56 (m, 4H), 0.92 (d, $J = 6.7$ Hz, 6H); ^{13}C NMR (75 MHz, CDCl_3) δ 205.5, 171.4, 138.3, 134.5, 130.8, 128.0, 126.3, 118.2, 106.3, 74.5, 56.2, 44.1, 43.9, 36.3, 31.3, 27.9, 19.5, 19.3; IR (Neat Film NaCl) 3072, 3061, 3027, 3002, 2957, 2931, 2871, 1610, 1495, 1471, 1454, 1422, 1403, 1387, 1368, 1318, 1280, 1217, 1189, 1173, 1081, 1031, 1007, 969, 957, 913, 875, 856, 831, 760, 746, 733 cm^{-1} ; HRMS (EI+) m/z calc'd for $\text{C}_{21}\text{H}_{28}\text{O}_2$ $[\text{M}]^{+}$: 312.2089; found 312.2083; $[\alpha]_{\text{D}}^{25.0} +2.91$ (c 0.98, CHCl_3 , 86.3% ee); HPLC conditions: 0.5% IPA in hexanes, 1.0 mL/min, OD-H column, t_{R} (min): minor = 13.96, major = 15.70.



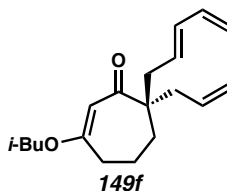
Vinyllogous Ester 149d (*Table 2.1, entry 4*). Prepared using Schlenk Manifold Method.

224.7 mg, 0.86 mmol, 88% yield. Flash column chromatography (SiO_2 , 3 x 25 cm, 20:1→15:1 hexanes:EtOAc). $R_f = 0.44$ (10:1 hexanes:EtOAc); ^1H NMR (300 MHz, CDCl_3) δ 5.74–5.59 (m, 1H), 5.32 (s, 1H), 5.12–5.02 (m, 2H), 3.50 (dd, $J = 14.9, 6.5$ Hz, 1H), 3.47 (dd, $J = 14.7, 6.6$ Hz, 1H), 2.53–2.48 (m, 4H), 2.46 (dddd, $J = 13.7, 7.3, 1.2, 1.2$ Hz, 1H), 2.35 (dddd, $J = 13.7, 7.6, 1.1, 1.1$ Hz, 1H), 2.09–1.67 (m, 5H), 1.57 (s, 1H), 0.95 (d, $J = 6.7$ Hz, 6H); ^{13}C NMR (75 MHz, CDCl_3) δ 204.0, 171.7, 133.7, 118.5, 105.0, 81.7, 74.6, 70.8, 54.2, 42.9, 36.1, 32.5, 28.0, 27.1, 20.0, 19.3; IR (Neat Film NaCl) 3301,

3075, 2957, 2930, 2873, 2116, 1612, 1471, 1457, 1435, 1423, 1402, 1387, 1368, 1320, 1221, 1191, 1175, 995, 969, 916, 874, 845 cm^{-1} ; HRMS (EI+) m/z calc'd for $\text{C}_{17}\text{H}_{24}\text{O}_2$ $[\text{M}]^+$: 260.1776; found 260.1737; $[\alpha]_{\text{D}}^{25.0}$ -26.51 (c 1.03, CHCl_3 , 88.5% ee); HPLC conditions: 0.5% IPA in hexanes, 1.0 mL/min, OD-H column, t_{R} (min): major = 12.35, minor = 13.43.

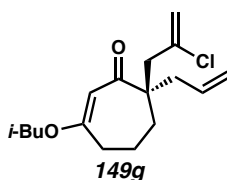


Vinyllogous Ester 149e (*Table 2.1, entry 5*). Prepared using Glove Box Method. 287.5 mg, 1.04 mmol, 95% yield. Flash column chromatography (SiO_2 , 2 x 25 cm, 20:1 hexanes:EtOAc). R_f = 0.44 (10:1 hexanes:EtOAc); ^1H NMR (300 MHz, CDCl_3) δ 5.84–5.64 (m, 2H), 5.30 (s, 1H), 5.09–4.87 (m, 4H), 3.49 (dd, J = 11.2, 6.6 Hz, 1H), 3.46 (dd, J = 11.1, 6.6 Hz, 1H), 2.54–2.37 (m, 3H), 2.27 (dddd, J = 13.8, 7.7, 1.2, 1.2 Hz, 1H), 2.07–1.89 (m, 3H), 1.86–1.45 (m, 6H), 0.95 (d, J = 6.7 Hz, 6H); ^{13}C NMR (75 MHz, CDCl_3) δ 205.8, 171.1, 138.9, 134.8, 117.9, 114.5, 105.5, 74.8, 54.4, 42.3, 38.0, 36.1, 32.7, 28.6, 28.0, 19.9, 19.3; IR (Neat Film NaCl) 3076, 2958, 2932, 2874, 1639, 1614, 1471, 1455, 1434, 1424, 1402, 1387, 1368, 1317, 1280, 1216, 1190, 1174, 1086, 996, 969, 955, 910, 878, 853, 829, 771 cm^{-1} ; HRMS (EI+) m/z calc'd for $\text{C}_{18}\text{H}_{28}\text{O}_2$ $[\text{M}]^+$: 276.2089; found 276.2060; $[\alpha]_{\text{D}}^{25.0}$ $+15.28$ (c 0.97, CHCl_3 , 86.9% ee); HPLC conditions: 0.8% IPA in hexanes, 2.0 mL/min, AD column, t_{R} (min): major = 5.03, minor = 6.06.



Vinyllogous Ester 149f (*Table 2.1, entry 6*). Prepared using Schlenk Manifold Method.

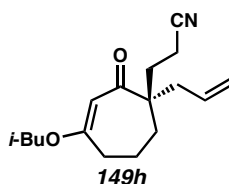
232.9 mg, 0.81 mmol, 90% yield. Flash column chromatography (SiO₂, 3 x 25 cm, 20:1→15:1 hexanes:EtOAc). *R_f* = 0.45 (10:1 hexanes:EtOAc); ¹H NMR (300 MHz, CDCl₃) δ 6.30 (dt, *J* = 16.9, 10.3 Hz, 1H), 6.04 (dd, *J* = 15.1, 10.4 Hz, 1H), 5.82–5.53 (m, 2H), 5.31 (s, 1H), 5.15–4.92 (m, 4H), 3.48 (d, *J* = 6.5 Hz, 2H), 2.55–2.36 (m, 4H), 2.30–2.16 (m, 2H), 1.98 (app sept, *J* = 6.7 Hz, 1H), 1.84–1.67 (m, 4H), 0.95 (d, *J* = 6.7 Hz, 6H); ¹³C NMR (75 MHz, CDCl₃) δ 205.3, 171.4, 137.2, 134.5, 134.1, 130.8, 118.0, 115.5, 105.5, 74.5, 55.1, 43.1, 41.6, 36.1, 32.5, 28.0, 19.9, 19.3; IR (Neat Film NaCl) 3075, 3036, 3007, 2958, 2931, 2873, 1726, 1635, 1611, 1471, 1456, 1436, 1402, 1387, 1368, 1312, 1277, 1219, 1190, 1173, 1085, 1005, 954, 911, 874, 831 cm⁻¹; HRMS (FAB+) *m/z* calc'd for C₁₉H₂₉O₂ [M+H]⁺: 289.2168; found 289.2172; [α]_D^{25.0} –20.62 (*c* 1.05, CHCl₃, 89.6% ee); SFC conditions: 5.0% IPA in hexanes, 2.5 mL/min, AD-H column, *t_R* (min): minor = 6.31, major = 6.99.



Vinyllogous Ester 149g (*Table 2.1, entry 7*). Prepared using Schlenk Manifold Method.

259.5 mg, 0.87 mmol, 99% yield. Flash column chromatography (SiO₂, 3 x 25 cm, 20:1→15:1 hexanes:EtOAc). *R_f* = 0.36 (10:1 hexanes:EtOAc); ¹H NMR (300 MHz,

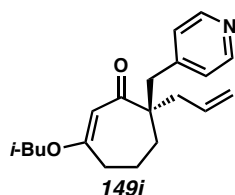
CDCl₃) δ 5.78–5.62 (m, 1H), 5.36 (s, 1H), 5.25 (s, 1H), 5.14 (s, 1H), 5.11–5.01 (m, 2H), 3.54–3.43 (m, 2H), 2.95 (dd, J = 14.4, 0.7 Hz, 1H), 2.54–2.41 (m, 4H), 2.25 (dddd, J = 13.9, 7.9, 1.1, 1.1 Hz, 1H), 2.07–1.89 (m, 2H), 1.88–1.70 (m, 3H), 0.95 (d, J = 6.7 Hz, 6H); ¹³C NMR (75 MHz, CDCl₃) δ 204.3, 171.6, 139.4, 133.9, 118.7, 116.6, 105.9, 74.6, 54.7, 46.7, 43.7, 36.3, 31.5, 28.0, 19.6, 19.3; IR (Neat Film NaCl) 3075, 2958, 2934, 2874, 1612, 1471, 1458, 1424, 1403, 1388, 1368, 1339, 1321, 1297, 1222, 1192, 1175, 1082, 1010, 995, 968, 956, 916, 875, 847, 746 cm⁻¹; HRMS (FAB+) m/z calc'd for C₁₇H₂₆O₂Cl [M+H]⁺: 297.1621; found 297.1623; $[\alpha]_D^{25.0}$ +4.20 (c 1.02, CHCl₃, 85.7% ee); HPLC conditions: 0.1% IPA in hexanes, 1.0 mL/min, OD-H column, t_R (min): minor = 24.19, major = 27.22.



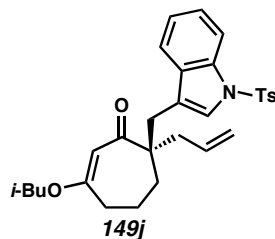
Vinyllogous Ester 149h (Table 2.1, entry 8). Prepared using Schlenk Manifold Method.

292.8 mg, 1.06 mmol, 96% yield. Flash column chromatography (SiO₂, 3 x 25 cm, 20:1→10:1→8:1→6:1 hexanes:EtOAc). R_f = 0.39 broad (4:1 hexanes:EtOAc); ¹H NMR (300 MHz, CDCl₃) δ 5.75–5.58 (m, 1H), 5.31 (s, 1H), 5.15–5.04 (m, 2H), 3.48 (d, J = 6.5 Hz, 2H), 2.51 (t, J = 6.1 Hz, 2H), 2.40 (dddd, J = 14.0, 7.0, 1.2, 1.2 Hz, 1H), 2.35–2.22 (m, 3H), 2.11–1.93 (m, 2H), 1.93–1.62 (m, 5H), 0.96 (d, J = 6.7 Hz, 6H); ¹³C NMR (75 MHz, CDCl₃) δ 203.9, 172.1, 133.1, 120.3, 119.2, 104.9, 74.7, 53.6, 41.8, 36.1, 33.9, 32.8, 28.0, 19.8, 19.3, 12.8; IR (Neat Film NaCl) 3076, 2958, 2933, 2874, 2246, 1635, 1609, 1472, 1458, 1420, 1404, 1388, 1368, 1319, 1281, 1214, 1192, 1175, 1084, 1003,

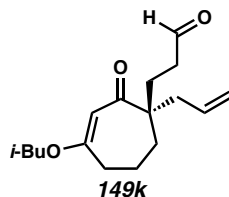
917, 880, 854, 827, 766 cm^{-1} ; HRMS (EI+) m/z calc'd for $\text{C}_{17}\text{H}_{25}\text{O}_2\text{N}$ $[\text{M}]^{+}$: 275.1885; found 275.1893; $[\alpha]_{\text{D}}^{25.0} -20.97$ (c 1.06, CHCl_3 , 87.4% ee); HPLC conditions: 5.0% IPA in hexanes, 1.0 mL/min, OD-H column, t_{R} (min): major = 10.67, minor = 14.66.



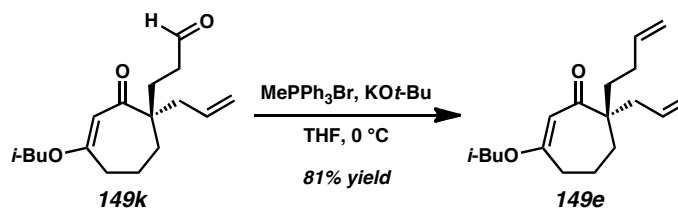
Vinylogous Ester 149i (*Table 2.1, entry 9*). Prepared using Glove Box Method. 339.6 mg, 1.08 mmol, 97% yield. Flash column chromatography (SiO_2 , 3 x 20 cm, 1:1→1:4 hexanes:EtOAc→EtOAc). R_f = 0.28, broad (1:2 hexanes:EtOAc); ^1H NMR (300 MHz, CDCl_3) δ 8.45 (dd, J = 4.5, 1.5 Hz, 2H), 7.05 (dd, J = 4.5, 1.6 Hz, 2H), 5.84–5.66 (m, 1H), 5.31 (s, 1H), 5.15–5.02 (m, 2H), 3.44 (dd, J = 15.1, 6.3 Hz, 1H), 3.41 (dd, J = 15.0, 6.3 Hz, 1H), 3.20 (d, J = 12.9 Hz, 1H), 2.60 (d, J = 12.9 Hz, 1H), 2.48 (dddd, J = 13.8, 6.9, 1.2, 1.2 Hz, 1H), 2.43–2.29 (m, 2H), 2.23 (dddd, J = 13.8, 7.8, 1.1, 1.1 Hz, 1H), 1.94 (app sept, J = 6.7 Hz, 1H), 1.84–1.67 (m, 2H), 1.67–1.51 (m, 2H), 0.92 (d, J = 6.7 Hz, 6H); ^{13}C NMR (75 MHz, CDCl_3) δ 204.4, 171.8, 149.5, 147.6, 133.7, 126.2, 118.9, 106.0, 74.6, 55.8, 43.8, 43.5, 36.2, 31.5, 27.9, 19.4, 19.3; IR (Neat Film NaCl) 3072, 3024, 2957, 2931, 2873, 1608, 1558, 1496, 1471, 1458, 1438, 1415, 1388, 1368, 1320, 1220, 1190, 1173, 1072, 994, 957, 916, 876, 844, 796 cm^{-1} ; HRMS (EI+) m/z calc'd for $\text{C}_{20}\text{H}_{27}\text{O}_2\text{N}$ $[\text{M}]^{+}$: 313.2042; found 313.2045; $[\alpha]_{\text{D}}^{25.0} +22.44$ (c 1.16, CHCl_3 , 84.6% ee); HPLC conditions: 5.0% EtOH in hexanes, 1.0 mL/min, AD column, t_{R} (min): major = 13.22, minor = 15.13.



Vinylogous Ester 149j (*Table 2.1, entry 10*). Prepared using Glove Box Method. 403 mg, 0.796 mmol, 98% yield. Flash column chromatography (SiO₂, 5 x 25 cm, 15:1→10:1→8:1→6:1 hexanes:EtOAc). R_f = 0.49 (4:1 hexanes:EtOAc); ¹H NMR (300 MHz, CDCl₃) δ 7.96 (dm, J = 8.4 Hz, 1H), 7.70 (dm, J = 8.4 Hz, 2H), 7.48 (dm, J = 7.9 Hz, 1H), 7.31–7.13 (m, 5H), 5.86–5.68 (m, 1H), 5.32 (s, 1H), 5.13–5.00 (m, 2H), 3.42 (dd, J = 17.0, 7.7 Hz, 1H), 3.38 (dd, J = 17.0, 7.6 Hz, 1H), 3.20 (dd, J = 14.2, 0.7 Hz, 1H), 2.73 (d, J = 14.1 Hz, 1H), 2.51 (dddd, J = 13.7, 6.9, 1.3, 1.3 Hz, 1H), 2.44–2.15 (m, 6H), 1.92 (app sept, J = 6.7 Hz, 1H), 1.76–1.46 (m, 4H), 0.92 (d, J = 6.7 Hz, 6H); ¹³C NMR (75 MHz, CDCl₃) δ 205.2, 171.7, 144.8, 135.4, 135.0, 134.1, 132.4, 129.8, 126.9, 125.4, 124.5, 123.2, 120.1, 119.6, 118.6, 113.8, 106.4, 74.6, 55.9, 44.1, 36.3, 33.0, 31.9, 27.9, 21.7, 19.5, 19.3; IR (Neat Film NaCl) 3584, 3401, 2068, 2958, 2930, 2873, 1609, 1494, 1470, 1448, 1422, 1402, 1368, 1306, 1279, 1215, 1188, 1174, 1120, 1097, 1020, 975, 916, 876, 813, 782, 747 cm⁻¹; HRMS (FAB+) m/z calc'd for C₃₀H₃₆O₄NS [M+H]⁺: 506.2365; found 506.2358; $[\alpha]_D^{25.0}$ +9.10 (c 1.00, CHCl₃, 82.9% ee); HPLC conditions: 5.0% EtOH in hexanes, 1.0 mL/min, AD column, t_R (min): major = 11.11, minor = 16.64.

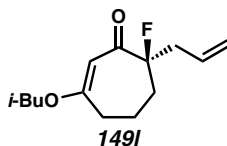


Vinylogous Ester 149k (*Table 2.1, entry 11*). Prepared using Glove Box Method. 77.3 mg, 0.278 mmol, 90% yield. Flash column chromatography (SiO₂, 2 x 25 cm, 6:1→4:1 hexanes:EtOAc). R_f = 0.35, broad (4:1 hexanes:EtOAc); ¹H NMR (300 MHz, CDCl₃) δ 9.73 (t, J = 1.5 Hz, 1H), 5.78–5.61 (m, 1H), 5.29 (s, 1H), 5.11–5.02 (m, 2H), 3.47 (m, 2H), 2.54–2.33 (m, 5H), 2.28 (dddd, J = 14.0, 7.6, 1.2, 1.2 Hz, 1H), 2.07–1.73 (m, 5H), 1.73–1.56 (m, 2H), 0.95 (d, J = 6.7 Hz, 6H); ¹³C NMR (75 MHz, CDCl₃) δ 205.0, 202.3, 171.7, 134.0, 118.5, 105.2, 74.6, 53.6, 42.1, 39.4, 36.1, 33.1, 30.3, 28.0, 19.9, 19.3; IR (Neat Film NaCl) 3075, 2958, 2931, 2719, 1724, 1611, 1471, 1458, 1421, 1403, 1388, 1368, 1213, 1191, 1175, 998, 915, 878 cm⁻¹; HRMS (FAB+) m/z calc'd for C₁₇H₂₇O₃ [M+H]⁺: 279.1960; found 279.1969; $[\alpha]_D^{25.0}$ +15.37 (c 1.03, CHCl₃, 79.5% ee); Compound **149k** was derivatized using procedure below to determine ee using the corresponding chiral HPLC assay for vinylogous ester **149e**.



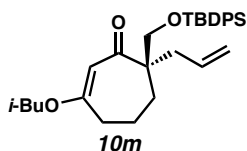
Vinylogous Ester 149e. To a solution of MePh₃PBr (323.2 mg, 0.905 mmol, 0.84 equiv) in THF (14.0 mL) in a 50 mL round-bottom flask at 0 °C was added KO t -Bu (84.6 mg, 0.754 mmol, 0.699 equiv) to give a bright yellow suspension. Aldehyde **149k** (299.9 mg, 1.078 mmol, 1.00 equiv) in THF (2 mL) was added to the suspension using positive

pressure cannulation and maintained at 0 °C. The reaction faded to an off-white suspension. After 1.5 h of stirring, an additional portion of Wittig reagent was prepared in a 20 mL scintillation vial. MePPh₃Br (323.2 mg, 0.905 mmol, 0.84 equiv) was added to the vial. The vial was sealed with a septum, evacuated/backfilled with N₂ (3 cycles, 5 min evacuation per cycle). Anhydrous THF (3 mL) was added and the vial was cooled to 0 °C. KO^t-Bu (84.6 mg, 0.754 mmol, 0.699 equiv) was added in one portion, giving a bright yellow suspension which was added to the reaction flask using positive pressure cannulation. The tan suspension was stirred at 0 °C for 1 h. An additional portion of Wittig reagent using MePPh₃Br (323.2 mg, 0.905 mmol, 0.84 equiv), KO^t-Bu (84.6 mg, 0.754 mmol, 0.699 equiv) and THF (3 mL) was prepared at 0 °C and added using positive pressure cannulation as previously described. The reaction showed a persistent yellow color. After 30 min of stirring at 0 °C, the reaction was quenched by addition of sat. aqueous NH₄Cl (5 mL) and stirred for 30 min while the mixture was allowed to warm to ambient temperature. The mixture was extracted with Et₂O (3 x 20 mL), dried over Na₂SO₄, filtered, and concentrated under reduced pressure. The residue was purified by flash column chromatography (SiO₂, 3 x 25 cm, 1%→2%→3%→5% EtOAc in hexanes) to afford vinylogous ester **149e** (243.7 mg, 0.882 mmol, 81% yield) as a yellow liquid; HPLC conditions: 0.8% IPA in hexanes, 2.0 mL/min, AD column, t_R (min): major = 4.39, minor = 3.17. (For characterization data, see p. 127).



Vinyllogous Ester 149l (*Table 2.1, entry 12*). Prepared using Schlenk Manifold Method.

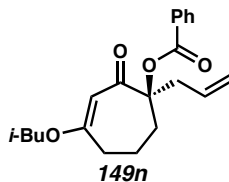
172.5 mg, 0.552 mmol, 98% yield. Flash column chromatography (SiO₂, 3 x 24 cm, 20:1→15:1→10:1 hexanes:EtOAc). R_f = 0.59 (4:1 hexanes:EtOAc); ¹H NMR (300 MHz, CDCl₃) δ 5.89–5.72 (m, 1H), 5.28 (s, 1H), 5.18–5.08 (m, 2H), 3.53 (dd, J = 10.6, 6.5 Hz, 1H), 3.50 (dd, J = 10.6, 6.6 Hz, 1H), 2.80–2.46 (m, 3H), 2.46–2.33 (m, 1H), 2.22–1.67 (m, 5H), 0.97 (d, J = 6.7 Hz, 3H), 0.96 (d, J = 6.7 Hz, 3H); ¹³C NMR (75 MHz, CDCl₃) δ 198.2 (d, J_{CF} = 24.9 Hz), 176.9 (d, J_{CF} = 1.8 Hz), 131.9 (d, J_{CF} = 4.4 Hz), 119.3, 101.7, 101.2 (d, J_{CF} = 180.6 Hz), 75.0, 42.1 (d, J_{CF} = 23.2 Hz), 34.4 (d, J_{CF} = 23.2 Hz), 34.1 (d, J_{CF} = 2.4 Hz), 27.9, 21.7 (d, J_{CF} = 2.1 Hz), 19.3, 19.2; ¹⁹F NMR (282 MHz, CDCl₃) δ –145.81 (m); IR (Neat Film NaCl) 3086, 2960, 1752, 1654, 1649, 1603, 1471, 1453, 1422, 1403, 1385, 1369, 1282, 1249, 1229, 1204, 1176, 1137, 1095, 1066, 145, 991, 927, 873, 843, 795, 758 cm^{–1}; HRMS (EI+) m/z calc'd for C₁₄H₂₁O₂F [M]⁺: 240.1526; found 240.1524; $[\alpha]_D^{25.0}$ +0.61 (c 1.02, CHCl₃, 91.2% ee); HPLC conditions: 1.0% IPA in hexanes, 1.0 mL/min, OD-H column, t_R (min): minor = 8.05, major = 8.80.



Vinyllogous Ester 149m (*Table 2.1, entry 13*). Prepared using Glove Box Method.

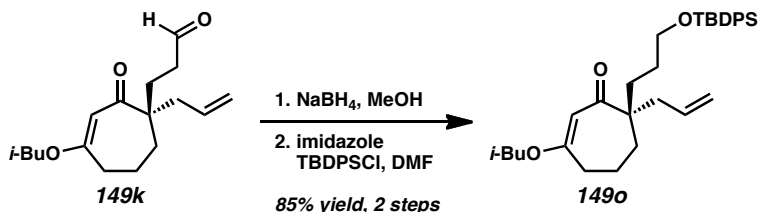
242.0 mg, 0.493 mmol, 66% yield. Flash column chromatography (SiO₂, 3 x 25 cm, 2%→5%→10% EtOAc in hexanes). R_f = 0.44 (10:1 hexanes:EtOAc); ¹H NMR (300

MHz, CDCl₃) δ 7.67–7.61 (m, 4H), 7.46–7.33 (m, 6H), 5.78–5.60 (m, 1H), 5.32 (s, 1H), 5.08–4.96 (m, 2H), 3.78 (d, J = 9.7 Hz, 1H), 3.67 (d, J = 9.7 Hz, 1H), 3.46 (dd, J = 14.7, 6.5 Hz, 1H), 3.43 (dd, J = 14.6, 6.5 Hz, 1H), 2.49 (dddd, J = 13.7, 6.6, 1.3, 1.3 Hz, 1H), 2.48–2.41 (m, 2H), 2.33 (dddd, J = 13.8, 7.8, 1.2, 1.2 Hz, 1H), 2.09–1.88 (m, 2H), 1.82–1.65 (m, 3H), 1.04 (s, 9H), 0.95 (d, J = 6.7 Hz, 6H); ¹³C NMR (75 MHz, CDCl₃) δ 204.5, 171.5, 135.9, 135.8, 134.7, 133.7, 133.5, 129.7, 127.8, 127.7, 117.8, 106.1, 74.5, 69.0, 57.4, 41.0, 36.3, 30.3, 28.0, 27.0, 20.0, 19.5, 19.3; IR (Neat Film NaCl) 3071, 3050, 2957, 2930, 2857, 1731, 1614, 1472, 1428, 1402, 1388, 1368, 1315, 1261, 1222, 1190, 1174, 1112, 1007, 998, 969, 955, 938, 914, 880, 824, 810, 740 cm⁻¹; HRMS (FAB+) m/z calc'd for C₃₁H₄₃O₃Si [M+H]⁺: 491.2982; found 491.2993; $[\alpha]_D^{25.0}$ –6.72 (c 1.09, CHCl₃, 57.8% ee); HPLC conditions: 0.2% IPA in hexanes, 1.0 mL/min, OD-H column, t_R (min): major = 21.74, minor = 25.53.



Vinyllogous Ester 149n (*Table 2.1, entry 14*). Prepared using Schlenk Manifold Method. 589.8 mg, 1.72 mmol, 75% yield. Flash column chromatography (SiO₂, 5 x 13 cm, 20:1→15:1→10:1→6:1 hexanes:EtOAc). R_f = 0.57 (4:1 hexanes:EtOAc); ¹H NMR (300 MHz, CDCl₃) δ 8.03–7.96 (m, 2H), 7.55 (t, J = 7.4 Hz, 1H), 7.42 (t, J = 7.5 Hz, 2H), 5.96–5.78 (m, 1H), 5.27 (s, 1H), 5.19–5.08 (m, 2H), 3.42 (dd, J = 9.4, 6.6 Hz, 1H), 3.39 (dd, J = 9.4, 6.5 Hz, 1H), 3.06 (dddd, J = 14.8, 6.7, 1.4, 1.4 Hz, 1H), 2.83–2.67 (m, 2H), 2.55–2.34 (m, 2H), 2.10–1.74 (m, 4H), 0.80 (dd, J = 6.6, 4.7 Hz, 6H); ¹³C NMR (75

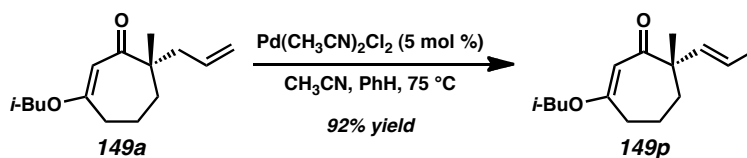
MHz, CDCl₃) δ 198.1, 174.3, 165.5, 133.1, 132.5, 130.6, 129.7, 128.5, 119.2, 102.1, 88.6, 74.9, 40.8, 34.0, 27.7, 21.9, 19.1, 19.0; IR (Neat Film NaCl) 3073, 2959, 2934, 2873, 1718, 1672, 1649, 1613, 1479, 1451, 1421, 1382, 1368, 1315, 1291, 1258, 1231, 1199, 1174, 1108, 1070, 1026, 1004, 919, 866, 820, 801, 762, 715 cm⁻¹; HRMS (EI+) m/z calc'd for C₂₁H₂₆O₄ [M]⁺: 342.1815; found 342.1831; $[\alpha]_D^{25.0}$ +79.72 (c 1.02, CHCl₃, 57.1% ee); HPLC conditions: 1.0% IPA in hexanes, 1.0 mL/min, OD-H column, t_R (min): major = 18.28, minor = 22.01.



Vinylogous Ester 149o. A round-bottom flask with magnetic stir bar was charged with aldehyde **149o** (40.2 mg, 0.14 mmol, 1.00 equiv) and MeOH (3.0 mL). The flask was cooled to 0 °C and NaBH₄ (5.5 mg, 0.14 mmol, 1.00 equiv) was added slowly portionwise. The mixture was stirred for 1 h at 0 °C. Sat. aqueous NaHCO₃ (3 mL) was added, followed by CH₂Cl₂ (10 mL). The mixture was stirred vigorously for 5 min. The phases were separated and the aqueous layer was extracted with CH₂Cl₂ (3 x 10 mL). Combined organic phases were dried over Na₂SO₄, filtered, and concentrated under reduced pressure. The crude alcohol was used directly in the next step without further purification. R_f = 0.29 (2:1 hexanes:EtOAc).

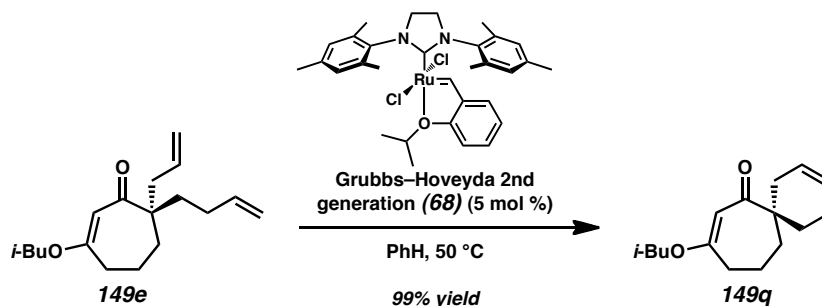
To a 2 dram vial with a solution of crude alcohol and imidazole (11.8 mg, 0.17 mmol, 1.20 equiv) in DMF (0.7 mL) at 0 °C was added TBDPSCl (39.6 μ L, 0.14 mmol, 1.00 equiv) dropwise. After 2 h of stirring, the reaction was quenched by addition of H₂O (0.3

mL) and extracted with Et₂O (5 x 5 mL). The combined organics were dried over MgSO₄, filtered, and concentrated under reduced pressure. The residue was purified by automated flash column chromatography using a Teledyne Isco CombiFlash R_f (SiO₂, 12 g loading cartridge, 80 g column, multi-step gradient, hold 2% [2 min]→ramp to 5% [10 min]→hold 5% [10 min]→ramp to 10% [32 min]→hold 10% Et₂O in hexanes [5 min]) to afford vinylogous ester **149o** (63.3 mg, 0.12 mmol, 85% yield over 2 steps) as a pale, white oil; R_f = 0.42 (10:1 hexanes:EtOAc); ¹H NMR (300 MHz, CDCl₃) δ 7.69–7.62 (m, 4H), 7.46–7.33 (m, 6H), 5.82–5.62 (m, 1H), 5.29 (s, 1H), 5.08–4.96 (m, 2H), 3.61 (t, *J* = 6.1 Hz, 2H), 3.48 (dd, *J* = 13.7, 6.6 Hz, 1H), 3.45 (dd, *J* = 13.7, 6.6 Hz, 1H), 2.50–2.43 (m, 2H), 2.40 (dddd, *J* = 13.8, 7.0, 1.2 Hz, 1H), 2.25 (dddd, *J* = 13.9, 7.8, 1.1 Hz, 1H), 1.98 (app sept, *J* = 6.7 Hz, 1H), 1.86–1.38 (m, 8H), 1.04 (s, 9H), 0.95 (d, *J* = 6.7 Hz, 6H); ¹³C NMR (75 MHz, CDCl₃) δ 206.0, 171.0, 135.7, 134.9, 134.1, 129.6, 127.7, 117.7, 105.2, 74.4, 64.4, 54.2, 42.1, 36.1, 34.8, 32.8, 28.0, 27.3, 27.0, 20.0, 19.3; IR (Neat Film NaCl) 3071, 3051, 3013, 2998, 2956, 2930, 2858, 1614, 1471, 1428, 1401, 1387, 1368, 1311, 1214, 1188, 1174, 1111, 1028, 1007, 998, 966, 913, 872, 823, 780, 740, 725 cm⁻¹; HRMS (FAB+) *m/z* calc'd for C₃₃H₄₇O₃Si [M+H]⁺: 519.3295; found 519.3275; [α]_D^{25.0} +9.06 (*c* 0.95, CHCl₃, 78.4% ee).



Vinylogous Ester 149p. Pd(CH₃CN)₂Cl₂ (49.1 mg, 0.189 mmol, 5 mol %) was placed in a 50 mL round-bottom Schlenk flask and evacuated/backfilled with N₂ (3 cycles, 5 min

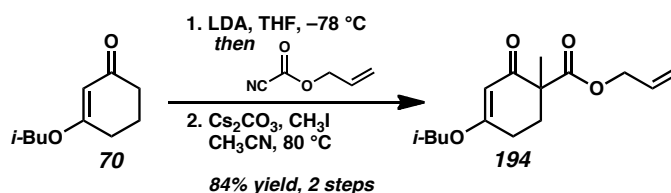
per cycle). Benzene (10 mL) was added, followed by acetonitrile (90 μ L). A solution of vinylogous ester **149a** (895 mg, 3.79 mmol, 1.00 equiv) in benzene (5.0 mL) was added using positive pressure cannulation. The resulting orange solution was heated to 75 °C in an oil bath. After 11 h of stirring, the reaction was cooled to ambient temperature, filtered through a Celite plug (eluted with Et₂O), and concentrated carefully under reduced pressure, allowing for a film of ice to form on the outside of the flask, to afford a pale yellow oil. The crude oil was purified by automated flash column chromatography using a Teledyne Isco CombiFlash R_f (SiO₂, 25 g loading cartridge, 80 g column, linear gradient, 0→10% EtOAc in hexanes [33 min]) to afford vinylogous ester **149p** (823.6 mg, 3.48 mmol, 92% yield) in a 20:1 ratio to isomeric starting material **149a**. Analytically pure samples could be obtained using the above column conditions; R_f = 0.56 (4:1 hexanes:EtOAc); ¹H NMR (300 MHz, CDCl₃) δ 5.56 (dq, *J* = 15.7, 1.4 Hz, 1H), 5.41 (dq, *J* = 15.7, 6.2, Hz, 1H), 5.34 (s, 1H), 3.48 (d, *J* = 6.5 Hz, 2H), 2.63–2.33 (m, 2H), 2.04–1.91 (m, 1H), 1.90–1.70 (m, 4H), 1.67 (dd, *J* = 6.2, 1.4 Hz, 3H), 1.22 (s, 3H), 0.95 (d, *J* = 6.7 Hz, 6H); ¹³C NMR (75 MHz, CDCl₃) δ 205.3, 171.6, 136.5, 123.9, 105.2, 74.5, 53.9, 36.2, 33.3, 28.0, 27.2, 20.2, 19.3, 18.4; IR (Neat Film NaCl) 3022, 2960, 2873, 1614, 1471, 1455, 1423, 1402, 1387, 1370, 1212, 1192, 1173, 1120, 967, 883, 858, 827 cm⁻¹; HRMS (MM: ESI-APCI+) *m/z* calc'd for C₁₅H₂₅O₂ [M+H]⁺: 237.1849; found 237.1848; [α]_D^{25.0} +4.05 (*c* 1.39, CHCl₃, 88.0 % ee).



Vinylogous Ester 149q. Vinylogous ester **149e** (100 mg, 0.362 mmol, 1.00 equiv) was added to a 50 mL 2-neck flask fitted with a rubber septum and oven-dried reflux condenser. The flask was evacuated/backfilled with Ar (3 cycles, 5 min evacuation per cycle). Dry degassed benzene (36.2 mL, sparged with N₂ for 1 h immediately before use) was added. Grubbs-Hoveyda 2nd generation catalyst (11.3 mg, 18.1 μ mol, 5 mol %) was added to the reaction, giving the solution an olive green color. The mixture was kept under Ar, stirred until homogeneous, and heated to 50 $^{\circ}$ C using an oil bath. After 30 min of stirring, the reaction was cooled to ambient temperature and several drops of ethyl vinyl ether were added. After 30 min, the reaction developed a deep brown color. The mixture was concentrated under reduced pressure and filtered through a silica gel plug (3 x 5 cm, 1:1 hexanes:Et₂O). The solvents were removed under reduced pressure and the residue was purified by flash column chromatography (SiO₂, 3 x 25 cm, 20:1 \rightarrow 15:1 \rightarrow 10:1 hexanes:EtOAc) to afford vinylogous ester **149q** (89.2 mg, 0.359 mmol, 99% yield) as a white solid. R_f = 0.39 (10:1 hexanes:EtOAc); ¹H NMR (300 MHz, CDCl₃) δ 5.69–5.58 (m, 2H), 5.30 (s, 1H), 3.49 (dd, J = 14.4, 6.5 Hz, 1H), 3.46 (dd, J = 14.3, 6.5 Hz, 1H), 2.70–2.57 (m, 1H), 2.54–2.44 (m, 2H), 2.08–1.91 (m, 3H), 1.91–1.57 (m, 7H), 0.95 (d, J = 6.7 Hz, 6H); ¹³C NMR (75 MHz, CDCl₃) δ 207.2, 171.3, 125.6, 125.4, 104.0, 74.4, 50.5, 35.9, 33.9, 32.3, 32.2, 28.0, 22.4, 20.6, 19.3; IR (Neat Film NaCl) 3050, 3023, 2981, 2958, 2928, 2890, 2874, 2837, 1726, 1633, 1610, 1470,

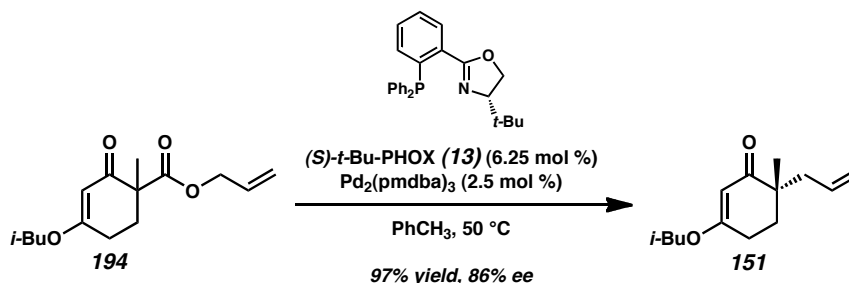
1457, 1435, 1416, 1406, 1392, 1364, 1327, 1295, 1270, 1218, 1178, 1189, 1117, 1096, 1045, 1028, 1003, 953, 935, 917, 888, 850, 837, 807, 758, 731 cm^{-1} ; HRMS (EI+) m/z calc'd for $\text{C}_{16}\text{H}_{24}\text{O}_2$ $[\text{M}]^+$: 248.1776; found 248.1774; $[\alpha]_{\text{D}}^{25.0}$ -32.18 (c 0.97, CHCl_3 , 78.4% ee).

2.10.2.6 SYNTHETIC STUDIES ON THE REDUCTION/REARRANGEMENT OF SIX- AND SEVEN-MEMBERED VINYLOGOUS ESTERS



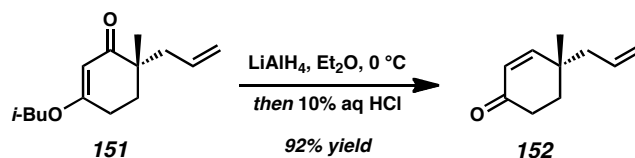
β -Ketoester 194. To a solution of diisopropylamine (0.49 mL, 3.47 mmol, 1.17 equiv) in THF (10 mL) in a 50 mL round-bottom flask at $0\text{ }^{\circ}\text{C}$ was added *n*-BuLi (1.70 mL, 3.40 mmol, 2.1 M in hexanes, 1.15 equiv) dropwise over 10 min. After 15 min of stirring at $0\text{ }^{\circ}\text{C}$, the reaction was cooled to $-78\text{ }^{\circ}\text{C}$ using an acetone/ $\text{CO}_2(\text{s})$ bath. A solution of vinylogous ester **70**⁵⁸ (0.50 g, 2.97 mmol, 1.00 equiv) in THF (5.0 mL) was added dropwise using positive pressure cannulation. After an additional 1 h of stirring at $-78\text{ }^{\circ}\text{C}$, allyl cyanoformate (0.37 mL, 3.40 mmol, 1.15 equiv) was added dropwise. The reaction was stirred at $-78\text{ }^{\circ}\text{C}$ for 2.5 h, quenched by addition of sat. aqueous NH_4Cl and H_2O (5 mL each), and then allowed to warm to ambient temperature. The reaction was diluted with Et_2O (25 mL) and the phases were separated. The aqueous phase was extracted with Et_2O (2 x 25 mL) and the combined organic phases were dried over MgSO_4 , filtered, and concentrated under reduced pressure to afford a pale red oil.

The crude oil was added to a 25 mL Schlenk flask and dissolved in CH₃CN (10 mL). CH₃I (0.56 mL, 8.90 mmol, 3.00 equiv) was added, followed by Cs₂CO₃ (1.26 g, 3.90 mmol, 1.30 equiv). The flask was sealed with a teflon valve, immersed in an oil bath, and heated to 80 °C. After 14 h of vigorous stirring, the suspension was allowed to cool to ambient temperature, diluted with EtOAc (25 mL), dried over MgSO₄, filtered, and concentrated under reduced pressure. The crude product was purified by flash column chromatography (SiO₂, 3 x 20 cm, 19:1→9:1→4:1, hexanes:EtOAc) to afford β-ketoester **194** (0.67 g, 2.52 mmol, 84% yield over 2 steps) as a pale yellow oil; *R*_f = 0.36 (4:1 hexanes:EtOAc); ¹H NMR (300 MHz, CDCl₃) δ 5.81 (dddd, *J* = 17.2, 10.7, 5.5, 5.5 Hz, 1H), 5.30 (s, 1H), 5.22 (app dq, *J* = 17.2, 1.5 Hz, 1H), 5.14 (app dq, *J* = 10.5, 1.3 Hz, 1H), 4.65–4.46 (m, 2H), 3.55 (d, *J* = 6.5 Hz, 2H), 2.60–2.23 (m, 3H), 1.97 (app sept, *J* = 6.6 Hz, 1H), 1.89–1.70 (m, 1H), 1.35 (s, 3H), 0.91 (d, *J* = 6.7 Hz, 6H); ¹³C NMR (75 MHz, CDCl₃) δ 196.4, 176.7, 172.5, 131.9, 118.0, 101.7, 74.9, 65.5, 52.3, 31.7, 27.7, 26.3, 20.6, 19.0; IR (Neat Film NaCl) 2961, 2937, 2876, 1733, 1660, 1608, 1457, 1427, 1406, 1385, 1369, 1346, 1319, 1248, 1199, 1176, 1113, 1039, 991, 928, 837, 818, 772, 751 cm⁻¹; HRMS (EI+) *m/z* calc'd for C₁₅H₂₂O₄ [M]⁺: 266.1518; found 266.1510.

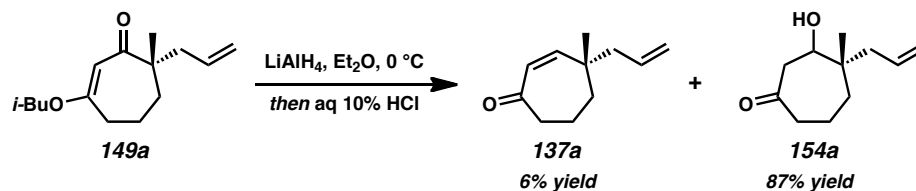


Vinyllogous Ester 151. β-Ketoester **194** (180 mg, 0.68 mmol, 1.00 equiv) in a 20 mL scintillation vial and a septum-fitted screw cap were evacuated/backfilled with N₂ (3

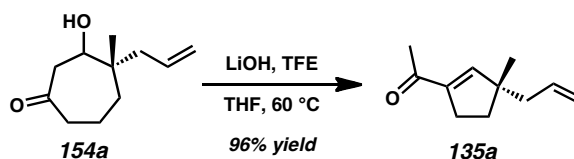
cycles, 5 min evacuation per cycle) in a glove box antechamber before being transferred into a glove box. A separate 20 mL scintillation vial in the glove box was loaded with (*S*)-*t*-Bu-PHOX (16.4 mg, 0.042 mmol, 6.25 mol %), Pd₂(pmdba)₃ (18.5 mg, 0.017 mmol, 2.5 mol %), and a magnetic stir bar. Toluene (4 mL) was added and the black suspension was stirred at 30 °C in a heating block for 30 min. β-Ketoester **194** was dissolved in toluene (2.8 mL) and added to the orange catalyst solution, causing an immediate color change to olive green. The vial was capped with the septum-fitted screw cap and the edges were sealed with electrical tape. The vial was removed from the glove box, connected to a N₂-filled Schlenk manifold, and immersed in a 50 °C oil bath. After 22 h, the reaction was an orange-brown solution. The mixture was concentrated under reduced pressure and purified by flash column chromatography (SiO₂, 2 x 25 cm, 20:1→10:1, hexanes:EtOAc) to afford vinylogous ester **151** (146 mg, 0.66 mmol, 97% yield) as a clear, colorless oil; *R*_f = 0.57 (4:1 hexanes:EtOAc); ¹H NMR (300 MHz, CDCl₃) δ 5.81–5.63 (m, 1H), 5.22 (s, 1H), 5.08–4.98 (m, 2H), 3.56 (d, *J* = 6.5 Hz, 2H), 2.40 (app t, *J* = 6.4 Hz, 2H), 2.33 (dddd, *J* = 13.8, 7.6, 1.0, 1.0 Hz, 1H), 2.16 (dddd, *J* = 13.8, 7.6, 1.0, 1.0 Hz, 1H), 2.00 (app sept, *J* = 6.7 Hz, 1H), 1.90 (ddd, *J* = 13.4, 6.6, 6.6 Hz, 1H), 1.68 (ddd, *J* = 13.6, 6.2, 6.2 Hz, 1H), 1.06 (s, 3H), 0.95 (d, *J* = 6.7 Hz, 6H); ¹³C NMR (75 MHz, CDCl₃) δ 203.5, 176.1, 134.4, 117.9, 101.4, 74.8, 43.3, 41.6, 31.9, 27.9, 26.0, 22.3, 19.2; IR (Neat Film NaCl) 3074, 2962, 2932, 2875, 1655, 1611, 1470, 1464, 1429, 1404, 1384, 1368, 1327, 1307, 1299, 1240, 1195, 1178, 1123, 1080, 1032, 996, 968, 951, 913, 862, 840, 806, 786, 736 cm⁻¹; HRMS (EI+) *m/z* calc'd for C₁₄H₂₂O₂ [M]⁺: 222.1620; found 222.1627; [α]_D^{25.0} –10.67 (*c* 0.98, CHCl₃, 86.3% ee); HPLC conditions: 5% IPA in hexanes, OD-H column, *t*_R (min): major = 5.80, minor = 6.53.



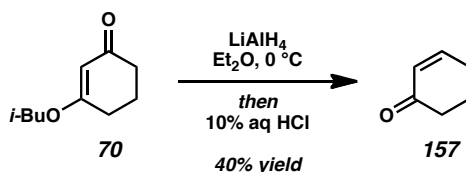
Cyclohexenone 152. A 50 mL round-bottom flask was charged with Et₂O (11.1 mL) and cooled to 0 °C in an ice/water bath. LiAlH₄ (13.6 mg, 0.36 mmol, 0.55 equiv) was added in one portion. After 10 min, a solution of vinyllogous ester **151** (146 mg, 0.66 mmol, 1.00 equiv) in Et₂O (2.0 mL) was added dropwise using positive pressure cannulation. After 30 min of stirring at 0 °C, an additional portion of LiAlH₄ (2.5 mg, 0.066 mmol, 0.10 equiv) was added. After 60 min of stirring, the reaction was quenched by slow addition of aqueous HCl (1.0 mL, 10% w/w). The resulting biphasic system was allowed to warm to ambient temperature and stirred vigorously for 8.5 h. The phases were separated and the aqueous phase was extracted with Et₂O (3 x 15 mL). The combined organic phases were dried over Na₂SO₄, filtered, and concentrated under reduced pressure. The crude product was purified using flash column chromatography (SiO₂, 2 x 25 cm, 10:1→4:1→1:1→1:2 hexanes:Et₂O) to afford cyclohexenone **152** (90.5 mg, 0.60 mmol, 92% yield) as a yellow oil; *R*_f = 0.51 (4:1 hexanes:EtOAc); ¹H NMR (300 MHz, CDCl₃) δ 6.67 (d, *J* = 10.2 Hz, 1H), 5.88 (d, *J* = 10.2 Hz, 1H), 5.79 (dddd, *J* = 16.8, 10.3, 7.4, 7.4 Hz, 1H), 5.20–5.01 (m, 2H), 2.54–2.36 (m, 2H), 2.29–2.10 (m, 2H), 2.05–1.89 (m, 1H), 1.85–1.69 (m, 1H), 1.14 (s, 3H); ¹³C NMR (75 MHz, CDCl₃) δ 199.4, 158.4, 133.4, 127.6, 118.6, 45.2, 35.7, 34.1, 33.6, 24.7; IR (Neat Film NaCl) 3077, 3005, 2960, 2917, 2868, 2849, 1682, 1639, 1616, 1459, 1419, 1390, 1373, 1332, 1250, 1223, 1193, 1115, 996, 961, 918, 871, 803, 757 cm⁻¹; HRMS (EI+) *m/z* calc'd for C₁₀H₁₄O [M]⁺: 150.1045; found 150.1056; [α]_D^{25.0} +26.72 (*c* 1.02, CHCl₃, 86.3% ee).



Cycloheptenone 137a and **β -Hydroxyketone 154a**. For procedure and characterization data, see General Method A (Section 2.10.2.8, p. 155–155).

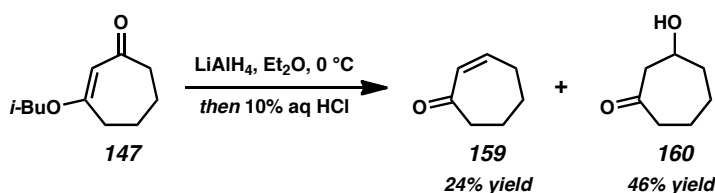


Acylcyclopentene 135a. For procedure and characterization data, see General Method E (Section 2.10.2.8, p. 156).



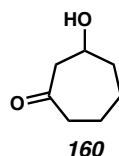
Cyclohexenone 157. A 25 mL round-bottom flask with magnetic stir bar and LiAlH_4 (22.8 mg, 0.60 mmol, 0.60 equiv) was charged with Et_2O (4 mL) and cooled to 0°C in an ice/water bath. After 10 min, a solution of vinylogous ester **70** (168.23 mg, 1.00 mmol, 1.00 equiv) in Et_2O (1 mL) was added dropwise using positive pressure cannulation. After 30 min of stirring at 0°C , the reaction was quenched by slow addition of aqueous HCl (2.60 mL, 10% w/w). The resulting biphasic system was allowed to warm to ambient temperature. The phases were separated and the aqueous phase was extracted with Et_2O (3 x 10 mL). The combined organic phases were dried over MgSO_4 , filtered,

and concentrated carefully under reduced pressure in an ice/water bath. The crude product purified using flash column chromatography (SiO₂, 2 x 25 cm, 5:1→4:1 hexanes:EtOAc) to afford cyclohexenone **157** (39.4 mg, 0.41 mmol, 40% yield) as a volatile pale yellow oil. Spectra for the compound match data for commercially available material.

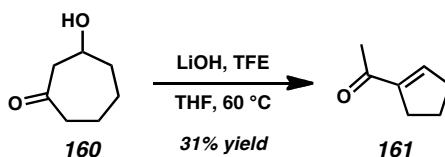


Cycloheptenone 159 and β-Hydroxyketone 160. A 50 mL round-bottom flask with magnetic stir bar and LiAlH₄ (806 mg, 21.2 mmol, 0.60 equiv) was charged with Et₂O (8 mL) and cooled to 0 °C in an ice/water bath. After 10 min, a solution of vinylogous ester **147** (328.2 mg, 1.80 mmol, 1.00 equiv) in Et₂O (2 mL) was added dropwise using positive pressure cannulation. After 30 min of stirring at 0 °C, the reaction was quenched by slow addition of aqueous HCl (4.73 mL, 10% w/w). The resulting biphasic system was allowed to warm to ambient temperature. The phases were separated and the aqueous phase was extracted with EtOAc (3 x 10 mL). The combined organic phases were dried over Na₂SO₄, filtered, and concentrated carefully under reduced pressure in an ice/water bath. The crude product purified using flash column chromatography (SiO₂, 2 x 25 cm, 6:1→4:1→2:1→1:1→1:2→1:4 hexanes:EtOAc) to afford β-hydroxyketone **160** (107.1 mg, 0.84 mmol, 46% yield) as a pale yellow oil and cycloheptenone **159** (47.9 mg, 0.44 mmol, 24% yield) as a colorless oil.

Cycloheptenone 159: Spectra for the compound match data for commercially available material.



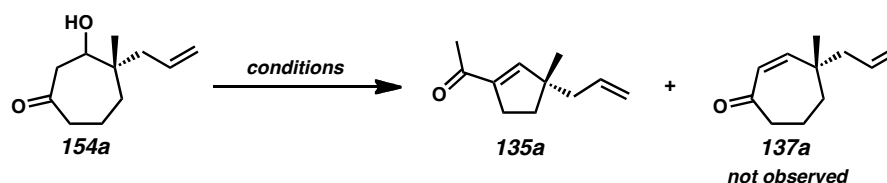
β -Hydroxyketone 160: R_f = 0.26 (1:1 hexanes:EtOAc); ^1H NMR (500 MHz, CDCl_3) δ 4.18–3.97 (m, 1H), 2.89–2.67 (m, 2H), 2.55–2.35 (m, 2H), 2.10 (br s, 1H), 1.95–1.69 (m, 5H), 1.65–1.49 (m, 1H); ^{13}C NMR (125 MHz, CDCl_3) δ 212.6, 67.5, 51.8, 44.4, 38.8, 24.4, 23.8; IR (Neat Film NaCl) 3420, 2930, 2861, 1696, 1449, 1410, 1349, 1263, 1196, 1157, 1109, 1043, 1016, 929, 878, 829, 752, 710 cm^{-1} ; HRMS (EI+) m/z calc'd for $\text{C}_7\text{H}_{12}\text{O}_2$ $[\text{M}]^+$: 128.0837; found 128.0828.



Acylcyclopentene 161. Alcohol **160** (101.3 mg, 0.79 mmol, 1.00 equiv) was dissolved in THF (7.9 mL) in a 20 mL scintillation vial with magnetic stir bar. The solution was treated with 2,2,2-trifluoroethanol (86.4 μL , 1.19 mmol, 1.50 equiv) and anhydrous LiOH (28.4 mg, 1.19 mmol, 1.50 equiv). The headspace of the vial was purged with N_2 and the vial was capped with a teflon-lined hard cap and stirred at 60 $^\circ\text{C}$ in a heating block. After 16 h of stirring, the suspension was allowed to cool to ambient temperature, diluted with Et_2O (150 mL), dried over Na_2SO_4 (30 min of stirring), filtered, and concentrated carefully under reduced pressure in an ice/water bath. The crude product was purified

using flash column chromatography (SiO₂, 2 x 20 cm, 15:1→10:1 hexanes:Et₂O) to afford acylcyclopentene **161** (27 mg, 0.25 mmol, 31% yield) as a colorless fragrant oil. Spectra for the compound match data for commercially available material.

2.10.2.7 RING CONTRACTION SCREENING PROTOCOL^a



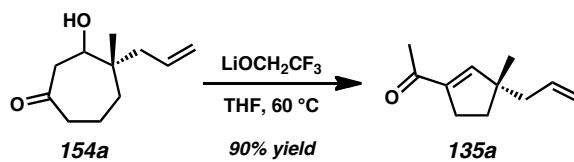
entry	base	additive	solvent	T (°C)	conversion (%)	time (h)	yield (%) ^b
1	LiO <i>t</i> -Bu	—	<i>t</i> -BuOH	40	100	9	71
2	LiO <i>t</i> -Bu	—	THF	40	100	8	60
3	NaO <i>t</i> -Bu	—	THF	40	100	5	81
4	KO <i>t</i> -Bu	—	THF	40	100	5	85
5	NaOH	—	THF	60	100	4	89
6	KOH	—	THF	60	100	4	87
7	LiOH	—	THF	60	78	24	19 ^d
8	LiOH	<i>t</i> -BuOH	THF	60	98	24	78
9	LiOH	HFIP ^c	THF	60	99	12.5	87
10	LiOH	TFE ^c	THF	60	99	12.5	96
11	LiOCH ₂ CF ₃	—	THF	60	—	10	90 ^e
12	CsOH·H ₂ O	—	THF	60	100	4	48
13	Cs ₂ CO ₃	—	THF	60	67	24	61 ^f
14	Cs ₂ CO ₃	TFE ^c	THF	60	100	12.5	86
15	Cs ₂ CO ₃	TFE ^c	CH ₃ CN	60	100	12.5	100
16	NaO <i>t</i> -Bu	<i>t</i> -BuOH	THF	40	100	8	52
17	KO <i>t</i> -Bu	<i>t</i> -BuOH	THF	40	100	8	57
18	LiOH	<i>t</i> -BuOH	THF	40	87	24	77
19	LiOH	TFE ^c	THF	40	73	24	73
20	LiOH	HFIP ^c	THF	40	84	24	81
21	CsF	—	CH ₃ CN	60	86	24	10

^a Conditions: β -hydroxyketone **154a** (1.0 equiv), additive (1.5 equiv), base (1.5 equiv), solvent (0.1 M) at indicated temperature for 9–24 h. ^b GC yield using an internal standard at $\geq 98\%$ conversion unless otherwise stated. ^c HFIP = 1,1,1,3,3,3-hexafluoro-2-propanol; TFE = 2,2,2-trifluoroethanol. ^d Several reaction intermediates observed by TLC and GC analysis; proceeded to 78% conversion. ^e Isolated yield. ^f Reaction did not reach completion at 24 h; proceeded to 67% conversion.

Ring Contraction Screen to Produce Acylcyclopentene **135a** (0.10 mmol scale, Table

2.3, entries 1–15). A benzene solution of β -hydroxyketone **154a** was transferred to a dry

1 dram vial and concentrated under reduced pressure to obtain a starting mass. To this vial was added a magnetic stir bar and 1,4-diisopropylbenzene (internal standard). The contents were solvated in either *t*-BuOH or THF (0.1 M). After complete solvation, an appropriate additive (*t*-BuOH, TFE, or HFIP; 1.50 equiv) was added, followed by base (1.50 equiv). The head space of the vial was purged with N₂ and the vial was capped with a teflon-lined hard cap and stirred at the appropriate temperature (40 or 60 °C) in a heating block. Reaction progress was initially followed by TLC analysis and when necessary, aliquots were removed and flushed through a small SiO₂ plug with EtOAc for GC analysis. GC conditions: 90 °C isothermal for 5 min, then ramp 10 °C/min to 250 °C, DB-WAX column, *t_R* (min): 1,4-diisopropylbenzene = 5.3, acylcyclopentene **135a** = 9.3, β-hydroxyketone **154a** = 17.1 and 17.2 (two diastereomers). (For characterization data, see p. 155–156).



Ring Contraction using LiOCH₂CF₃ (Table 2.3, entry 11). β-Hydroxyketone **154a** (30.0 mg, 0.16 mmol, 1.00 equiv) was measured into a 1 dram vial with magnetic stir bar with a septum-fitted screw cap. LiOCH₂CF₃⁵⁰ (26.0 mg, 0.25 mmol, 1.50 equiv) was measured into a separate 1 dram vial, capped with a septum, evacuated/backfilled with N₂ (3 cycles, 5 min evacuation per cycle), and dissolved in THF (0.5 mL). The solution was cannulated into the vial containing β-hydroxyketone along with additional THF rinses (2 x 0.5 mL). The yellow solution was stirred at 60 °C in a heating block. After 10 h, the reaction was cooled to ambient temperature. The turbid brown solution was diluted with

Et₂O and stirred with Na₂SO₄ for 30 min. The reaction was filtered and concentrated under reduced pressure at 0 °C in an ice/water bath. The residue was purified by flash column chromatography (SiO₂, 1 x 20 cm, 15:1 hexanes:Et₂O) to afford acylcyclopentene **135a** (24.4 mg, 0.149 mmol, 90% yield) as a clear, colorless oil. (For characterization data, see p. 156).

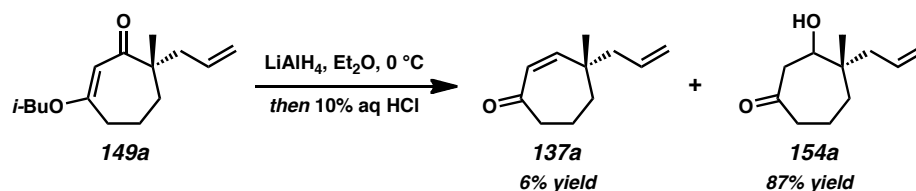
Additional Conditions. Additional reaction conditions are listed in Table 2.3, entries 16–21.

Unsuccessful Conditions. No reaction was observed using the following bases, with or without TFE additive: DBU, TMG, Na₂CO₃, K₂CO₃, BaCO₃, CaH₂. DBU = 1,8-diazabicyclo [5.4.0]undec-7-ene, TMG = 1,1,3,3-tetramethylguanidine.

2.10.2.8 PREPARATION OF β -HYDROXYKETONES AND ACYLCYCLOPENTENES

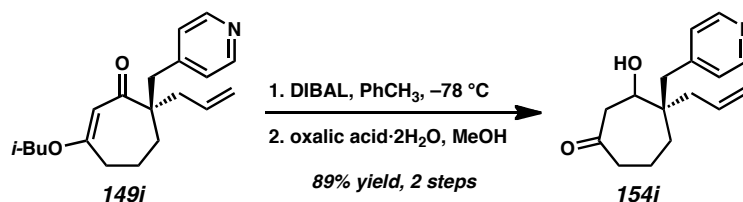
Full characterization data is reported for acylcyclopentenenes **135**, cycloheptenone **137a**, and β -hydroxyketone intermediate **154a** (mixture of diastereomers). For all other β -hydroxyketone intermediates (**154b–j**, **1–o**, mixtures of diastereomers), R_f, IR, and HRMS data are reported and ¹H NMR and IR spectra are provided for reference in Figures A1.130–A1.160. For acylcyclopentenenes **135a**, the ee value was unchanged from corresponding vinylogous ester **149a**. For all other acylcyclopentenenes (**135**), ee values

are assumed to be unchanged from the corresponding vinylogous esters (**149**). Representative procedures for General Methods A–E are described below.



General Method A: LiAlH_4 Hydride Reduction / 10% Aq. HCl Hydrolysis

Cycloheptenone 137a and **β -Hydroxyketone 154a**. A 500 mL round-bottom flask with magnetic stir bar was charged with Et_2O (150 mL) and cooled to $0\text{ }^\circ\text{C}$ in an ice/water bath. LiAlH_4 (806 mg, 21.2 mmol, 0.55 equiv) was added in one portion. After 10 min, a solution of vinylogous ester **149a** (9.13 g, 38.6 mmol, 1.00 equiv) in Et_2O (43 mL) was added dropwise using positive pressure cannulation. The grey suspension was stirred for 40 min and additional LiAlH_4 (148 mg, 3.9 mmol, 0.10 equiv) was added in one portion. After an additional 30 min of stirring at $0\text{ }^\circ\text{C}$, the reaction was quenched by slow addition of aqueous HCl (110 mL, 10% w/w). The resulting biphasic system was allowed to warm to ambient temperature and stirred vigorously for 8.5 h. The phases were separated and the aqueous phase was extracted with Et_2O (3 x 100 mL). The combined organic phases were dried over Na_2SO_4 , filtered, and concentrated under reduced pressure. The crude product was azeotroped with toluene (3 x 20 mL) and purified using flash column chromatography (SiO_2 , 5 x 15 cm, 9:1→3:1 hexanes: EtOAc , dry-loaded using Celite) to afford β -hydroxyketone **154a** (6.09 g, 33.41 mmol, 87% yield, 1.3:1 dr) as a colorless semi-solid and cycloheptenone **137a** (387 mg, 2.36 mmol, 6% yield) as a colorless oil. (For characterization data, see p. 155–155).

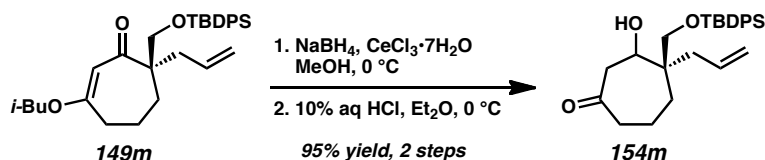


General Method B: DIBAL Reduction / Oxalic Acid Hydrolysis

β -Hydroxyketone 154i. A 25 mL pear-shaped flask was charged with vinylogous ester **149i** (29.4 mg, 0.094 mmol, 1.00 equiv) and toluene (3.0 mL). The solution was cooled to -78°C using an acetone/ $\text{CO}_2(\text{s})$ bath. A 1.0 M solution of DIBAL in toluene (112.6 μL , 0.113 mmol, 1.00 equiv) was added dropwise and the solution was stirred for 10 min. MeOH (180 μL), $\text{Na}_2\text{SO}_4 \cdot 10\text{H}_2\text{O}$ (1.08 g), and Celite (360 mg) were added. The reaction was stirred vigorously and allowed to warm slowly to ambient temperature. The mixture was filtered through a Celite plug (3 x 3 cm, EtOAc), and concentrated under reduced pressure. $R_f = 0.28$, broad (1:2 hexanes:EtOAc).

The crude hydroxy isobutyl enol ether was added to a 25 mL round-bottom flask and dissolved in MeOH (4.0 mL). Oxalic acid dihydrate (354.9 mg, 2.82 mmol, 30.0 equiv) was added in one portion. After 1 h of stirring, the reaction was neutralized to pH 7 with 1 M aqueous pH 7 $\text{NaH}_2\text{PO}_4/\text{Na}_2\text{HPO}_4$ buffer (6 mL). The biphasic mixture was stirred vigorously for 10 min and the phases were separated. The aqueous layer was extracted with Et_2O (4 x 15 mL). The combined organic phases were dried over Na_2SO_4 , filtered, and concentrated under reduced pressure. The crude product was purified using flash column chromatography (SiO_2 , 1.5 x 25 cm, 4:1 \rightarrow 2:1 \rightarrow 1:2 hexanes:acetone) to afford β -hydroxyketone **154i** as a mixture of diastereomers (21.6 mg, 0.083 mmol, 89% yield over

2 steps, 2.8:1 dr) as a clear, colorless residue which solidified upon standing. (For characterization data, see p. 165).

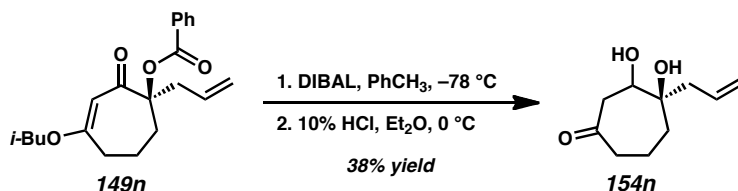


General Method C: Luche Reduction / 10% Aq. HCl Hydrolysis

β -Hydroxyketone 154m. A 100 mL round-bottom flask with magnetic stir bar was charged with vinylogous ester **149m** (65.6 mg, 0.134 mmol, 1.00 equiv) and anhydrous MeOH (8.3 mL). The solution was cooled to 0 °C in an ice/water bath. $\text{CeCl}_3 \cdot 7\text{H}_2\text{O}$ (78.2 mg, 0.21 mmol, 1.56 equiv) was added in one portion and the mixture was stirred for 5 min. Addition of NaBH_4 (23.8 mg, 0.63 mmol, 4.70 equiv) led to the evolution of gas and a turbid solution that became clear after several minutes. The reaction was stirred at 0 °C. After 15 min, the reaction was diluted with CH_2Cl_2 (20 mL) until turbid, filtered through a Celite plug (3 x 3 cm, CH_2Cl_2), and concentrated under reduced pressure. The residue was taken up in CH_2Cl_2 , filtered through a Celite plug (3 x 5 cm, CH_2Cl_2), and concentrated under reduced pressure a second time. $R_f = 0.33$ (10:1 hexanes:EtOAc).

The crude hydroxy isobutyl enol ether was added to a 25 mL round-bottom flask with a magnetic stir bar and dissolved in Et_2O (3.8 mL). The vigorously stirred solution was cooled to 0 °C and aqueous HCl (384 μL , 10% w/w) was added dropwise via syringe. After 30 min, the reaction was allowed to warm to ambient temperature and extracted with Et_2O (3 x 5 mL). The combined organic phases were dried over Na_2SO_4 , filtered,

and concentrated under reduced pressure. The crude product was purified using flash column chromatography (SiO₂, 1.5 x 25 cm, 6:1→4:1 hexanes:EtOAc) to afford β -hydroxyketone **154m** as a mixture of diastereomers (55.6 mg, 0.13 mmol, 95% yield over 2 steps, 3.5:1 dr) as a colorless oil. (For characterization data, see p. 168).

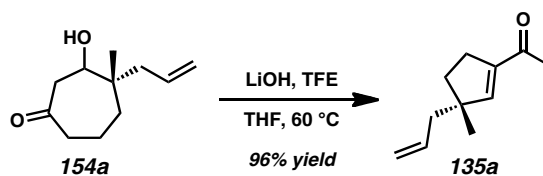


General Method D: DIBAL Reduction / 10% Aq. HCl Hydrolysis

β -Hydroxyketone 154n. A 50 mL pear-shaped flask was charged with vinylogous ester **149n** (100 mg, 0.292 mmol, 1.00 equiv) and toluene (9.5 mL). The solution was cooled to $-78\text{ }^\circ\text{C}$ using an acetone/CO₂(s) bath. A 1.0 M solution of DIBAL in toluene (963 μL , 0.963 mmol, 1.00 equiv) was added dropwise and the mixture was stirred for 15 min. MeOH (1.0 mL), Na₂SO₄·10 H₂O (6.0 g), and Celite (1.2 g) were added and the mixture was stirred vigorously and allowed to warm slowly to ambient temperature. The mixture was filtered through a Celite plug (3 x 3 cm, EtOAc), and concentrated under reduced pressure. $R_f = 0.30$ (2:1 hexanes:EtOAc).

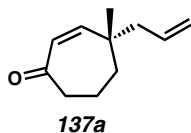
The crude hydroxy isobutyl enol ether was added to a 50 mL pear-shaped flask, dissolved in Et₂O (10 mL), and cooled to $0\text{ }^\circ\text{C}$ in an ice/water bath. Aqueous HCl (0.835 mL, 10% w/w) was added dropwise and the biphasic mixture was stirred vigorously at $0\text{ }^\circ\text{C}$. After 40 min of stirring, additional aqueous HCl (0.835 mL, 10% w/w) was added. After 1.5 h, the layers were separated and the aqueous layer was extracted with Et₂O (5 x 15 mL). The combined organic layers were dried over Na₂SO₄, filtered, and concentrated

under reduced pressure. The crude product was purified using flash column chromatography (SiO₂, 1.5 x 25 cm, 10:1→6:1→4:1→2:1→1:1→1:2 hexanes:EtOAc) to afford β -hydroxyketone **154n** as a mixture of diastereomers (20.3 mg, 0.110 mmol, 38% yield over 2 steps) as a clear, colorless oil. (For characterization data, see p. 172).

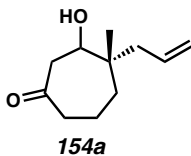


General Method E: β -Hydroxyketone Ring Contraction

Acylcyclopentene 135a. Alcohol **154a** (6.09 g, 33.4 mmol, 1.00 equiv) was dissolved in THF (334 mL) in a 500 mL round-bottom flask. The solution was treated with 2,2,2-trifluoroethanol (3.67 mL, 50.1 mmol, 1.50 equiv) and anhydrous LiOH (1.20 g, 50.1 mmol, 1.50 equiv). The flask was fitted with a condenser, purged with N₂, and heated to 60 °C using an oil bath. After 18 h of stirring, the suspension was allowed to cool to ambient temperature, diluted with Et₂O (150 mL), dried over Na₂SO₄ (30 min of stirring), filtered, and concentrated carefully under reduced pressure, allowing for a film of ice to form on the outside of the flask. The crude product was purified using flash column chromatography (SiO₂, 5 x 15 cm, 15:1 hexanes:Et₂O) to afford acylcyclopentene **135a** (5.29 g, 32.2 mmol, 96% yield) as a colorless fragrant oil. (For characterization data, see p. 156).

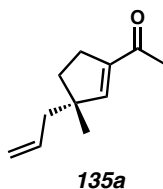


Cycloheptenone 137a. Prepared using General Method A. 387 mg, 2.36 mmol, 6% yield. Flash column chromatography (SiO₂, 5 x 15 cm, 9:1→3:1 hexanes:EtOAc, dry-loaded using Celite). R_f = 0.54 (7:3 hexanes:EtOAc); ¹H NMR (500 MHz, CDCl₃) δ 6.04 (dd, J = 12.9, 0.7 Hz, 1H), 5.82 (d, J = 12.9 Hz, 1H), 5.75 (dddd, J = 17.1, 10.3, 7.8, 7.1 Hz, 1H), 5.10 (dddd, J = 10.3, 1.2, 1.2, 1.2 Hz, 1H), 5.08–5.03 (m, 1H), 2.65–2.52 (m, 2H), 2.19 (app dd, J = 13.7, 6.8 Hz, 1H), 2.11 (app dd, J = 13.7, 8.1 Hz, 1H), 1.84–1.76 (m, 3H), 1.68–1.63 (m, 1H), 1.10 (s, 3H); ¹³C NMR (75 MHz, CDCl₃) δ 204.7, 152.5, 133.8, 128.6, 118.6, 47.2, 45.1, 42.7, 38.2, 27.1, 18.4; IR (Neat Film NaCl) 3076, 3011, 2962, 2934, 2870, 1659, 1454, 1402, 1373, 1349, 1335, 1278, 1208, 1172, 997, 916, 874, 822, 772 cm⁻¹; HRMS (EI+) m/z calc'd for C₁₁H₁₆O [M]⁺: 164.1201; found 164.1209; $[\alpha]_D^{21.0}$ -9.55 (c 1.07, CHCl₃, 88.0% ee).



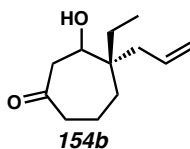
β-Hydroxyketone 154a (Table 2.4, entry 1). Prepared using General Method A. 6.09 g, 33.41 mmol, 87% yield, 1.3:1 dr. Flash column chromatography (SiO₂, 5 x 15 cm, 9:1→3:1 hexanes:EtOAc, dry-loaded using Celite). R_f = 0.23 (7:3 hexanes:EtOAc); ¹H NMR (500 MHz, CDCl₃) δ **major epimer:** 5.88 (dddd, J = 15.1, 9.0, 7.6, 7.6 Hz, 1H), 5.12–5.08 (m, 2H), 3.70 (dd, J = 4.9, 3.9 Hz, 1H), 2.86 (dd, J = 15.6, 1.7 Hz, 1H), 2.65 (dd, J = 15.6, 7.3 Hz, 1H), 2.54–2.43 (m, 2H), 2.24 (dd, J = 13.7, 7.8 Hz, 1H), 2.07 (dd, J

= 13.4, 7.3 Hz, 1H), 1.99 (dd, J = 15.9, 4.4 Hz, 1H), 1.82–1.69 (m, 2H), 1.45–1.41 (m, 1H), 0.96 (s, 3H); **minor epimer**: 5.83 (dddd, J = 14.9, 10.3, 7.6, 7.6 Hz, 1H), 5.12–5.06 (m, 2H), 3.68 (dd, J = 4.1, 2.4 Hz, 1H) 2.80 (dd, J = 15.4, 2.4 Hz, 1H), 2.74 (dd, J = 15.4, 8.1 Hz 1H), 2.46–2.38 (m, 2H), 2.18 (dd, J = 13.9, 7.3 Hz, 1H), 2.09 (dd, J = 12.9, 7.8 Hz, 1H), 1.82–1.65 (m, 3H), 1.50–1.47 (m, 1H), 1.02 (s, 3H); ^{13}C NMR (75 MHz, CDCl_3) δ **major epimer**: 213.2, 135.0, 118.1, 72.9, 46.7, 44.9, 44.2, 41.0, 36.3, 21.9, 18.9; **minor epimer**: 212.6, 134.2, 118.3, 73.3, 47.2, 42.8, 41.0, 35.9, 22.6, 18.7; IR (Neat Film NaCl) 3436, 3074, 2932, 1692, 1638, 1443, 1403, 1380, 1352, 1318, 1246, 1168, 1106, 1069, 999, 913, 840 cm^{-1} ; HRMS (EI+) m/z calc'd for $\text{C}_{11}\text{H}_{18}\text{O}_2$ $[\text{M}]^{+}$: 182.1313; found 182.1307; $[\alpha]_{\text{D}}^{22.8}$ –57.10 (c 2.56, CHCl_3 , 88.0% ee).

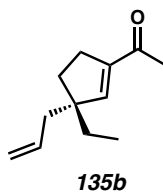


Acylcyclopentene 135a (Table 2.4, entry 1). Prepared using General Method E. 5.29 g, 32.2 mmol, 96% yield. Flash column chromatography (SiO_2 , 5 x 15 cm, 15:1 hexanes: Et_2O). R_f = 0.67 (8:2 hexanes: EtOAc); ^1H NMR (500 MHz, CDCl_3) δ 6.45 (app t, J = 1.7 Hz, 1H), 5.76 (dddd, J = 16.4, 10.7, 7.3, 7.3 Hz, 1H), 5.07–5.03 (m, 2H), 2.59–2.48 (m, 2H), 2.30 (s, 3H), 2.21–2.14 (m, 2H), 1.85 (ddd, J = 12.9, 8.3, 6.3 Hz, 1H), 1.64 (ddd, J = 12.9, 8.5, 6.1 Hz, 1H), 1.11 (s, 3H); ^{13}C NMR (125 MHz, CDCl_3) δ 197.5, 151.9, 143.8, 134.9, 117.8, 50.0, 45.3, 36.0, 29.7, 26.8, 25.6; IR (Neat Film NaCl) 3077, 2956, 2863, 1668, 1635, 1616, 1454, 1435, 1372, 1366, 1309, 1265, 1213, 1177, 993, 914, 862 cm^{-1} ; HRMS (EI+) m/z calc'd for $\text{C}_{11}\text{H}_{17}\text{O}$ $[\text{M}+\text{H}]^{+}$: 165.1279; found 165.1281;

$[\alpha]_D^{21.4} +17.30$ (c 0.955, CHCl_3 , 88.0% ee); GC conditions: 80 °C isothermal, GTA column, t_R (min): major = 54.7, minor = 60.2.

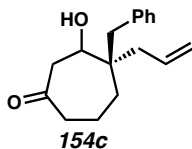


β -Hydroxyketone 154b (*Table 2.4, entry 2*). Prepared using General Method A. 111.5 mg, 0.57 mmol, 95% yield. Flash column chromatography (SiO_2 , 2 x 25 cm, 10:1→3:1 hexanes:EtOAc). R_f = 0.36 (2:1 hexanes:EtOAc); ^1H NMR (300 MHz, CDCl_3) mixture of two diastereomers, see Figure A1.133; IR (Neat Film NaCl) 3448, 3073, 2965, 2933, 1832, 1696, 1691, 1673, 1459, 1413, 1381, 1352, 1334, 1323, 1306, 1269, 1252, 1269, 1252, 1172, 1138, 1111, 1084, 1071, 1050, 997, 955, 930, 912, 876, 825, 777, 737 cm^{-1} ; HRMS (EI+) m/z calc'd for $\text{C}_{12}\text{H}_{20}\text{O}_2$ $[\text{M}]^{+}$: 196.1463; found 196.1480.

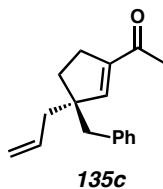


Acylcyclopentene 135b (*Table 2.4, entry 2*). Prepared using General Method E. 21.8 mg, 0.12 mmol, 95% yield. Flash column chromatography (SiO_2 , 1 x 20 cm, 15:1 hexanes:Et₂O). R_f = 0.73 (2:1 hexanes:EtOAc); ^1H NMR (300 MHz, CDCl_3) δ 6.44 (dd, J = 1.8, 1.8 Hz, 1H), 5.80–5.64 (m, 1H), 5.08–5.04 (m, 1H), 5.03–5.00 (m, 1H), 2.55–2.46 (m, 2H), 2.30 (s, 3H), 2.19–2.16 (m, 2H), 1.81–1.68 (m, 2H), 1.52–1.41 (m, 2H), 0.85 (dd, J = 7.5, 7.5 Hz, 3H); ^{13}C NMR (75 MHz, CDCl_3) δ 197.4, 150.7, 144.6, 134.8,

117.7, 54.0, 43.1, 32.9, 31.3, 30.1, 26.9, 9.1; IR (Neat Film NaCl) 3075, 2962, 2922, 2878, 2855, 1669, 1639, 1617, 1459, 1437, 1372, 1319, 1266, 1207, 1052, 995, 913, 868, 784 cm^{-1} ; HRMS (EI+) m/z calc'd for $\text{C}_{12}\text{H}_{19}\text{O}$ $[\text{M}+\text{H}]^+$: 179.1436; found 179.1401; $[\alpha]_{\text{D}}^{25.0} +7.06$ (c 0.98, CHCl_3 , 91.6% ee).

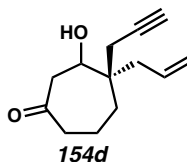


β -Hydroxyketone 154c (*Table 2.4, entry 3*). Prepared using General Method A. 109.9 mg, 0.43 mmol, 89% yield. Flash column chromatography (SiO_2 , 2 x 25 cm, 10:1 \rightarrow 3:1 hexanes:EtOAc). R_f = 0.11 (4:1 hexanes:EtOAc); ^1H NMR (300 MHz, CDCl_3) mixture of two diastereomers, see Figure A1.135; IR (Neat Film NaCl) 3443, 3072, 3028, 3003, 2930, 2865, 1696, 1692, 1685, 1636, 1601, 1582, 1495, 1453, 1413, 1400, 1352, 1340, 1255, 1182, 1163, 1118, 1058, 1031, 995, 970, 916, 885, 848, 809, 754 cm^{-1} ; HRMS (EI+) m/z calc'd for $\text{C}_{17}\text{H}_{22}\text{O}_2$ $[\text{M}]^{+}$: 258.1620; found 258.1642.

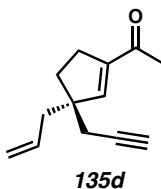


Acylcyclopentene 135c (*Table 2.4, entry 3*). Prepared using General Method E. 22.7 mg, 0.094 mmol, 97% yield. Flash column chromatography (SiO_2 , 1 x 20 cm, 15:1 hexanes:Et₂O). R_f = 0.54 (4:1 hexanes:EtOAc); ^1H NMR (300 MHz, CDCl_3) δ 7.30–7.18 (m, 3H), 7.14–7.08 (m, 2H), 6.45 (dd, J = 1.8, 1.8 Hz, 1H), 5.78 (dddd, J = 16.3, 10.8, 7.7, 7.0 Hz, 1H), 5.13–5.10 (m, 1H), 5.07 (dddd, J = 9.1, 2.2, 1.2, 1.2 Hz, 1H), 2.79 (d, J

= 13.3 Hz, 1H), 2.73 (d, J = 13.3 Hz, 1H), 2.43 (dddd, J = 16.5, 8.6, 5.7, 1.7 Hz, 1H), 2.27–2.17 (m, 3H), 2.21 (s, 3H), 1.91–1.75 (m, 2H); ^{13}C NMR (75 MHz, CDCl_3) δ 197.1, 150.1, 144.9, 138.2, 134.7, 130.4, 128.1, 126.4, 118.3, 54.6, 45.2, 43.3, 33.3, 30.0, 26.9; IR (Neat Film NaCl) 3061 3027, 3002, 2920, 2853, 1668, 1638. 1617, 1495, 1453, 1442, 1371, 1314, 1264, 1197, 1089, 1030, 995, 914, 861, 734 cm^{-1} ; HRMS (EI+) m/z calc'd for $\text{C}_{17}\text{H}_{20}\text{O}$ $[\text{M}]^{+}$: 240.1514; found 240.1530; $[\alpha]_{\text{D}}^{25.0}$ –20.63 (c 0.83, CHCl_3 , 86.3% ee).

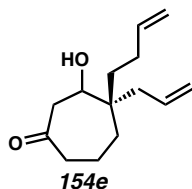


β -Hydroxyketone 154d (*Table 2.4, entry 4*). Prepared using General Method A. 117 mg, 0.56 mmol, 98% yield. Flash column chromatography (SiO_2 , 2 x 25 cm, 10:1→3:1 hexanes:EtOAc). R_f = 0.35 (10:1 hexanes:EtOAc); ^1H NMR (300 MHz, CDCl_3) mixture of two diastereomers, see Figure A1.137; IR (Neat Film NaCl) 3434, 3295, 3074, 3002, 2932, 2114, 1690, 1684, 1637, 1447, 1354, 1252, 1166, 1124, 1064, 977, 917, 886, 838 cm^{-1} ; HRMS (EI+) m/z calc'd for $\text{C}_{13}\text{H}_{18}\text{O}_2$ $[\text{M}]^{+}$: 206.1307; found 206.1311.

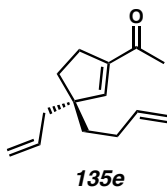


Acylcyclopentene 135d (*Table 2.4, entry 4*). Prepared using General Method E. 22.5 mg, 0.12 mmol, 97% yield. Flash column chromatography (SiO_2 , 1 x 20 cm, 15:1

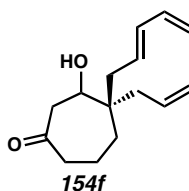
hexanes:Et₂O). $R_f = 0.74$ (2:1 hexanes:EtOAc); ¹H NMR (300 MHz, CDCl₃) δ 6.51 (dd, $J = 1.8, 1.8$ Hz, 1H), 5.73 (dddd, $J = 16.9, 10.2, 7.4, 7.4$ Hz, 1H), 5.13 (dm, $J = 10.2$ Hz, 1H), 5.10–5.07 (m, 1H), 2.66–2.46 (m, 2H), 2.34–2.33 (m, 1H), 2.33–2.32 (m, 1H), 2.32 (s, 3H), 2.32–2.30 (m, 2H), 1.99 (dd, $J = 2.7, 2.7$ Hz, 1H), 1.93–1.75 (m, 2H); ¹³C NMR (75 MHz, CDCl₃) 197.3, 148.6, 145.2, 133.9, 118.6, 81.4, 70.3, 53.2, 42.4, 33.4, 30.0, 28.5, 26.9; IR (Neat Film NaCl) 3298, 3075, 3001, 2924, 2857, 2116, 1669, 1639, 1617, 1457, 1437, 1372, 1318, 1265, 1222, 1204, 996, 919, 867 cm⁻¹; HRMS (EI+) m/z calc'd for C₁₃H₁₆O [M]⁺: 188.1201; found 188.1211; $[\alpha]_D^{25.0} -58.65$ (c 0.71, CHCl₃, 88.5% ee).



β -Hydroxyketone 154e (*Table 2.4, entry 5*). Prepared using General Method A. 116.7 mg, 0.52 mmol, 97% yield. Flash column chromatography (SiO₂, 2 x 25 cm, 10:1→3:1 hexanes:EtOAc). $R_f = 0.15$ (4:1 hexanes:EtOAc); ¹H NMR (300 MHz, CDCl₃) mixture of two diastereomers, see Figure A1.139; IR (Neat Film NaCl) 3447, 3075, 3001, 2975, 2931, 2866, 1827, 1693, 1639, 1456, 1415, 1352, 1336, 1250, 1169, 1116, 1073, 995, 910, 855, 763, 714 cm⁻¹; HRMS (EI+) m/z calc'd for C₁₈H₂₈O₂ [M]⁺: 276.2089; found 276.2060.

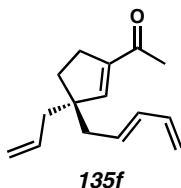


Acylcyclopentene 135e (*Table 2.4, entry 5*). Prepared using General Method E. 19.1 mg, 0.093 mmol, 90% yield. Flash column chromatography (SiO₂, 1 x 20 cm, 15:1 hexanes:Et₂O). R_f = 0.62 (4:1 hexanes:EtOAc); ¹H NMR (300 MHz, CDCl₃) δ 6.45 (dd, J = 1.8, 1.8 Hz, 1H), 5.79 (dddd, J = 16.8, 10.2, 6.5, 6.5 Hz, 1H), 5.72 (dddd, J = 16.8, 9.5, 7.3, 7.3 Hz, 1H), 5.09–5.07 (m, 1H), 5.05–4.97 (m, 2H), 4.94 (dm, J = 10.2 Hz, 1H), 2.56–2.49 (m, 2H), 2.30 (s, 3H), 2.23–2.17 (m, 2H), 2.15–1.91 (m, 2H), 1.85–1.70 (m, 2H), 1.58–1.50 (m, 2H); ¹³C NMR (75 MHz, CDCl₃) δ 197.3, 150.4, 144.6, 138.8, 134.6, 117.9, 114.6, 53.5, 43.6, 38.1, 33.3, 30.1, 29.2, 26.9; IR (Neat Film NaCl) 3076, 3001, 2976, 2919, 2854, 1670, 1640, 1618, 1437, 1372, 1314, 1265, 1204, 995, 911, 865 cm⁻¹; HRMS (EI+) m/z calc'd for C₁₄H₂₁O [M+H]⁺: 205.1592; found 205.1588; [α]_D^{25.0} –30.08 (*c* 0.92, CHCl₃, 86.9% ee).

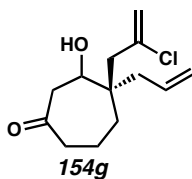


β -Hydroxyketone 154f (*Table 2.4, entry 6*). Prepared using General Method A. 117.5 mg, 0.50 mmol, 96% yield. Flash column chromatography (SiO₂, 2 x 25 cm, 10:1→3:1 hexanes:EtOAc). R_f = 0.19 (4:1 hexanes:EtOAc); ¹H NMR (300 MHz, CDCl₃) mixture of two diastereomers, see Figure A1.141; IR (Neat Film NaCl) 3448, 3075, 3035, 3007, 2972, 2929, 2865, 1700, 1696, 1691, 1685, 1648, 1637, 1600, 1449, 1415, 1352, 1333,

1245, 1171, 1120, 1068, 1052, 1005, 969, 954, 912, 855, 838, 817, 720 cm^{-1} ; HRMS (FAB+) m/z calc'd for $\text{C}_{15}\text{H}_{23}\text{O}_2$ $[\text{M}+\text{H}]^+$: 235.1698; found 235.1697.

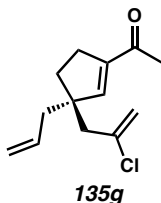


Acylcyclopentene 135f (*Table 2.4, entry 6*). Prepared using General Method E. 25.2 mg, 0.12 mmol, 95% yield. Flash column chromatography (SiO_2 , 1 x 20 cm, 15:1 hexanes: Et_2O). R_f = 0.65 (4:1 hexanes: EtOAc); ^1H NMR (300 MHz, CDCl_3) δ 6.45 (dd, J = 1.8, 1.8 Hz, 1H), 6.30 (ddd, J = 16.9, 10.2, 10.2 Hz, 1H), 6.08 (dd, J = 15.0, 10.4 Hz, 1H), 5.73 (dddd, J = 16.4, 11.6, 8.9, 7.5 Hz, 1H), 5.63 (ddd, J = 15.0, 7.6, 7.6 Hz, 1H), 5.14–5.09 (m, 2H), 5.06–5.02 (m, 1H), 5.00 (dm, J = 10.1 Hz, 1H), 2.54–2.46 (m, 2H), 2.30 (s, 3H), 2.25–2.17 (m, 4H), 1.80–1.74 (m, 2H); ^{13}C NMR (75 MHz, CDCl_3) δ 197.3, 150.0, 144.8, 137.0, 134.5, 134.3, 130.4, 118.1, 115.9, 54.0, 43.3, 42.0, 33.2, 30.0, 26.9; IR (Neat Film NaCl) 3079, 3006, 2929, 2857, 1735, 1670, 1640, 1617, 1439, 1371, 1318, 1267, 1201, 1175, 1084, 1004, 952, 912 cm^{-1} ; HRMS (FAB+) m/z calc'd for $\text{C}_{15}\text{H}_{21}\text{O}$ $[\text{M}+\text{H}]^+$: 217.1592; found 217.1568; $[\alpha]_{\text{D}}^{25.0}$ -32.14 (c 1.26, CHCl_3 , 89.6% ee).

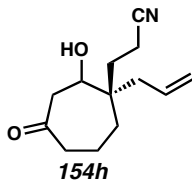


β -Hydroxyketone 154g (*Table 2.4, entry 7*). Prepared using General Method A. 114.9 mg, 0.47 mmol, 93% yield. Flash column chromatography (SiO_2 , 2 x 25 cm, 10:1→3:1

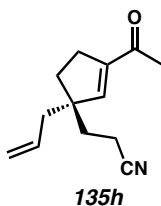
hexanes:EtOAc). $R_f = 0.15$ (4:1 hexanes:EtOAc); ^1H NMR (300 MHz, CDCl_3) mixture of two diastereomers, see Figure A1.143; IR (Neat Film NaCl) 3436, 3075, 2931, 2869, 1695, 1627, 1452, 1414, 1352, 1297, 1251, 1222, 1151, 1064, 1021, 997, 974, 915, 887, 839 cm^{-1} ; HRMS (EI+) m/z calc'd for $\text{C}_{13}\text{H}_{19}\text{O}_2\text{Cl}$ $[\text{M}]^+$: 242.1074; found 242.1063.



Acylcyclopentene 135g (*Table 2.4, entry 7*). Prepared using General Method E. 23.8 mg, 0.11 mmol, 99% yield. Flash column chromatography (SiO_2 , 1 x 20 cm, 15:1 hexanes:Et₂O). $R_f = 0.55$ (4:1 hexanes:EtOAc); ^1H NMR (300 MHz, CDCl_3) δ 6.61 (dd, $J = 1.8, 1.8\text{ Hz}$, 1H), 5.73 (dddd, $J = 15.9, 11.1, 7.9, 7.3\text{ Hz}$, 1H), 5.29 (d, $J = 1.2\text{ Hz}$, 1H), 5.15–5.14 (m, 1H), 5.11–5.10 (m, 1H), 5.08–5.04 (m, 1H), 2.56–2.48 (m, 4H), 2.31 (s, 3H), 2.28–2.25 (m, 2H), 1.93 (ddd, $J = 13.3, 8.4, 6.6\text{ Hz}$, 1H), 1.84 (ddd, $J = 13.3, 8.1, 6.4\text{ Hz}$, 1H); ^{13}C NMR (75 MHz, CDCl_3) δ 197.3, 149.6, 144.4, 139.4, 134.0, 118.7, 116.4, 53.4, 48.0, 43.4, 33.3, 29.8, 26.9; IR (Neat Film NaCl) 3076, 2946, 2857, 1669, 1629, 1434, 1372, 1320, 1266, 1230, 1206, 1167, 996, 917, 886 cm^{-1} ; HRMS (EI+) m/z calc'd for $\text{C}_{13}\text{H}_{18}\text{OCl}$ $[\text{M}+\text{H}]^+$: 225.1046; found 225.1053; $[\alpha]_{\text{D}}^{25.0} +46.29$ (c 1.06, CHCl_3 , 85.7% ee).

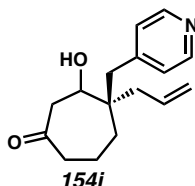


β -Hydroxyketone 154h (*Table 2.4, entry 8*). Prepared using General Method A. 72.4 mg, 0.33 mmol, 90% yield. Flash column chromatography (SiO_2 , 2 x 25 cm, 4:1 \rightarrow 2:1 \rightarrow 1:1 hexanes:EtOAc). R_f = 0.40, broad (1:1 hexanes:EtOAc); ^1H NMR (300 MHz, CDCl_3) mixture of two diastereomers, see Figure A1.145; IR (Neat Film NaCl) 3468, 3075, 2932, 2871, 2247, 1696, 1458, 1437, 1420, 1352, 1319, 1252, 1169, 1122, 1070, 999, 921, 853, 754 cm^{-1} ; HRMS (EI+) m/z calc'd for $\text{C}_{13}\text{H}_{19}\text{O}_2\text{N}$ $[\text{M}]^{+}$: 221.1416; found 221.1411.

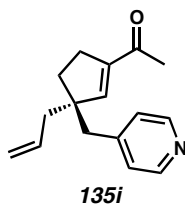


Acylcyclopentene 135h (*Table 2.4, entry 8*). Prepared using General Method E. 19.4 mg, 0.095 mmol, 94% yield. Flash column chromatography (SiO_2 , 1 x 20 cm, 2:1 \rightarrow 3:2 \rightarrow 1:1 hexanes:Et₂O). R_f = 0.84, broad (1:1 hexanes:EtOAc); ^1H NMR (300 MHz, CDCl_3) δ 6.42 (dd, J = 1.8, 1.8 Hz, 1H), 5.70 (dddd, J = 16.4, 10.6, 7.4, 7.4 Hz, 1H), 5.15–5.12 (m, 1H), 5.15–5.06 (m, 1H), 2.60–2.52 (m, 2H), 2.37–2.22 (m, 2H), 2.32 (s, 3H), 2.23–2.20 (m, 2H), 1.93–1.82 (m, 3H), 1.73 (ddd, J = 13.6, 8.2, 7.0 Hz, 1H); ^{13}C NMR (75 MHz, CDCl_3) δ 196.8, 147.2, 146.0, 133.3, 120.0, 119.0, 53.2, 43.5, 34.2, 32.7, 30.2, 27.0, 13.1; IR (Neat Film NaCl) 3074, 2923, 2857, 2245, 1667, 1640, 1618, 1423,

1373, 1308, 1264, 1202, 1090, 996, 918, 867 cm^{-1} ; HRMS (EI+) m/z calc'd for $\text{C}_{13}\text{H}_{18}\text{NO}$ $[\text{M}+\text{H}]^+$: 204.1388; found 204.1385; $[\alpha]_{\text{D}}^{25.0} -31.11$ (c 0.90, CHCl_3 , 87.4% ee).

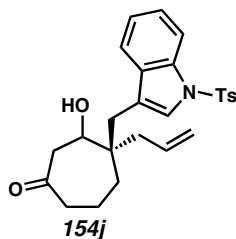


β -Hydroxyketone 154i (*Table 2.4, entry 9*). Prepared using General Method B. 21.6 mg, 0.083 mmol, 89% yield over 2 steps. Flash column chromatography (SiO_2 , 1.5 x 25 cm, 4:1 \rightarrow 2:1 \rightarrow 1:2 hexanes:acetone). R_f = 0.10 (2:1 hexanes:acetone); ^1H NMR (300 MHz, CDCl_3) mixture of two diastereomers, see Figure A1.147; IR (Neat Film NaCl) 3391, 3201, 3073, 2929, 2865, 1699, 1636, 1603, 1557, 1497, 1456, 1418, 1352, 1332, 1297, 1258, 1222, 1187, 1161, 1113, 1069, 1005, 995, 972, 915, 886, 851, 802, 735 cm^{-1} ; HRMS (FAB+) m/z calc'd for $\text{C}_{16}\text{H}_{22}\text{O}_2\text{N}$ $[\text{M}+\text{H}]^+$: 260.1650; found 260.1649.

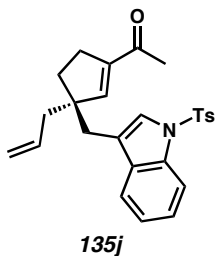


Acylcyclopentene 135i (*Table 2.4, entry 9*). Prepared using General Method E. 15.7 mg, 0.065 mmol, 90% yield. Flash column chromatography (SiO_2 , 1.5 x 16 cm, 2:1 \rightarrow 1:1 hexanes:acetone). R_f = 0.47 (2:1 hexanes:acetone); ^1H NMR (300 MHz, CDCl_3) δ 8.49 (br d, J = 3.8 Hz, 2H), 7.04 (d, J = 5.7 Hz, 2H), 6.40 (dd, J = 1.7, 1.7 Hz, 1H), 5.75 (dddd, J = 17.3, 10.3, 7.3, 7.3 Hz, 1H), 5.16–5.04 (m, 2H), 2.77 (d, J = 13.0 Hz, 1H), 2.71 (d, J = 13.0 Hz, 1H), 2.52–2.39 (m, 1H), 2.33–2.35 (m, 1H), 2.28 (s, 3H), 2.24–2.20

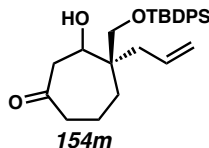
(m, 2H), 1.85–1.80 (m, 2H); ^{13}C NMR (75 MHz, CDCl_3) δ 196.8, 149.6, 148.6, 147.3, 145.4, 134.0, 125.7, 118.8, 54.2, 44.4, 43.3, 33.3, 30.0, 27.0; IR (Neat Film NaCl) 3401, 3071, 3025, 2922, 2856, 1668, 1640, 1618, 1600, 1557, 1495, 1441, 1415, 1373, 1318, 1277, 1265, 1220, 1194, 1071, 994, 917, 874, 844, 810, 763 cm^{-1} ; HRMS (EI+) m/z calc'd for $\text{C}_{16}\text{H}_{19}\text{ON}$ $[\text{M}]^+$: 176.1467; found 176.1458; $[\alpha]_{\text{D}}^{25.0}$ -8.58 (c 0.77, CHCl_3 , 84.6% ee).



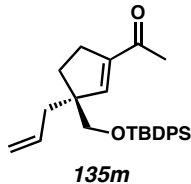
β -Hydroxyketone 154j (*Table 2.4, entry 10*). Prepared using General Method A. 300.1 mg, 0.67 mmol, 94% yield. Flash column chromatography (SiO_2 , 3 x 25 cm, 4:1 \rightarrow 3:1 \rightarrow 2:1 \rightarrow 1:1 hexanes:EtOAc). R_f = 0.20, 0.26 (two diastereomers) (2:1 hexanes:EtOAc); ^1H NMR (300 MHz, CDCl_3) mixture of two diastereomers, see Figure A1.149; IR (Neat Film NaCl) 3436, 3068, 2930, 2873, 1693, 1639, 1597, 1494, 1447, 1365, 1402, 1365, 1279, 1211, 1188, 1172, 1133, 1121, 1095, 1063, 1020, 995, 975, 913, 813, 778, 747 cm^{-1} ; HRMS (FAB+) m/z calc'd for $\text{C}_{26}\text{H}_{30}\text{O}_4\text{NS}$ $[\text{M}+\text{H}]^+$: 452.1896; found 452.1896.



Acylcyclopentene 135j (*Table 2.4, entry 10*). Prepared using General Method E. 55.7 mg, 0.10 mmol, 93% yield. Flash column chromatography (SiO₂, 2 x 25 cm, 10:1→8:1→6:1→4:1 hexanes:EtOAc). R_f = 0.67 (2:1 hexanes:EtOAc); ¹H NMR (300 MHz, CDCl₃) δ 7.98 (br d, J = 8.2 Hz, 1H), 7.63 (dm, J = 8.4 Hz, 2H), 7.40 (dd, J = 7.3, 0.8 Hz, 1H), 7.33 (br s, 1H), 7.30 (ddd, J = 8.2, 8.2, 1.3 Hz, 1H), 7.21 (ddd, J = 7.5, 7.5, 1.1 Hz, 1H), 7.17 (dm, J = 8.2 Hz, 2H), 6.35 (dd, J = 1.8, 1.8 Hz, 1H), 5.75 (dddd, J = 16.9, 10.3, 7.7, 6.9 Hz, 1H), 5.13–5.10 (m, 1H), 5.10–5.04 (m, 1H), 2.82 (s, 3H), 2.44 (dddd, J = 14.7, 8.8, 5.9, 1.7 Hz, 1H), 2.33 (br s, 2H), 2.31–2.18 (m, 3H), 2.16 (s, 3H), 1.86 (ddd, J = 14.6, 8.6, 6.1 Hz, 1H), 1.79 (ddd, J = 14.8, 7.6, 5.8 Hz, 1H); ¹³C NMR (75 MHz, CDCl₃) δ 196.9, 149.9, 145.1, 144.9, 135.2, 135.1, 134.3, 131.9, 130.0, 126.7, 124.8, 124.7, 123.2, 119.9, 119.4, 118.5, 113.9, 54.5, 43.5, 33.8, 33.4, 30.0, 26.8, 21.7; IR (Neat Film NaCl) 3316, 3129, 3101, 3068, 3001, 2974, 2922, 2855, 1667, 1639, 1618, 1597, 1562, 1493, 1448, 1400, 1372, 1307, 1293, 1277, 1211, 1188, 1174, 1121, 1094, 1020, 978, 916, 853, 813, 747 cm⁻¹; HRMS (EI+) m/z calc'd for C₂₆H₂₇O₃NS [M]⁺: 433.1712; found 433.1694; $[\alpha]_D^{25.0}$ +0.35 (*c* 1.09, CHCl₃, 82.9% ee).

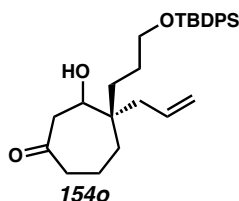


β -Hydroxyketone 154m (*Table 2.4, entry 11*). Prepared using General Method C. 55.6 mg, 0.13 mmol, 95% yield over 2 steps. Flash column chromatography (SiO_2 , 1.5 x 25 cm, 6:1→4:1 hexanes:EtOAc). R_f = 0.22, 0.28 (two diastereomers) (4:1 hexanes:EtOAc); ^1H NMR (300 MHz, CDCl_3) mixture of two diastereomers, see Figure A1.151; IR (Neat Film NaCl) 3468, 3072, 3050, 2999, 3013, 2931, 2895, 2858, 2248, 1960, 1891, 1823, 1772, 1698, 1638, 1590, 1472, 1462, 1446, 1428, 1391, 1361, 1337, 1260, 1222, 1186, 1172, 1158, 1113, 1088, 1030, 1006, 999, 976, 914, 841, 823, 810, 740 cm^{-1} ; HRMS (FAB+) m/z calc'd for $\text{C}_{27}\text{H}_{37}\text{O}_3\text{Si}$ $[\text{M}+\text{H}]^+$: 437.2512; found 437.2517.

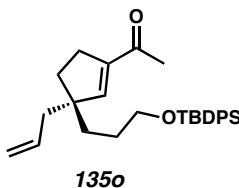


Acylcyclopentene 135m (*Table 2.4, entry 11*). Prepared using General Method E. 32.6 mg, 0.078 mmol, 96% yield. Flash column chromatography (SiO_2 , 1 x 20 cm, 15:1 hexanes:Et₂O). R_f = 0.60 (4:1 hexanes:EtOAc); ^1H NMR (300 MHz, CDCl_3) δ 7.67–7.60 (m, 4H), 7.47–7.34 (m, 6H), 6.50 (dd, J = 1.8, 1.8 Hz, 1H), 5.71 (dddd, J = 17.0, 10.1, 7.8, 6.9 Hz, 1H), 5.12–5.08 (m, 1H), 5.06–5.02 (m, 1H), 3.57 (d, J = 9.8 Hz, 1H), 3.53 (d, J = 9.8 Hz, 1H), 2.54–2.48 (m, 2H), 2.38 (ddd, J = 13.8, 6.9, 1.1 Hz, 1H), 2.31–2.25 (m, 1H), 2.29 (s, 3H), 1.81–1.72 (m, 2H), 1.07 (s, 9H); ^{13}C NMR (75 MHz, CDCl_3) δ 197.2, 148.5, 145.7, 135.8, 135.7, 134.5, 133.6, 133.6, 129.9, 129.9, 127.8, 118.0, 69.1, 56.5, 40.4, 30.7, 30.0, 27.0, 26.8, 19.5; IR (Neat Film NaCl) 3072, 3050, 2999, 2956, 2931,

2896, 2857, 1671, 1639, 1618, 1472, 1463, 1427, 1367, 1320, 1266, 1232, 1188, 1112, 998, 936, 915, 864, 824, 740 cm^{-1} ; HRMS (EI+) m/z calc'd for $\text{C}_{27}\text{H}_{34}\text{O}_2\text{Si}$ $[\text{M}]^{+}$: 433.1712; found 433.1694; $[\alpha]_{\text{D}}^{25.0} -17.58$ (c 0.94, CHCl_3 , 51.4% ee).

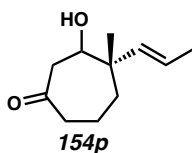


β -Hydroxyketone 154o (Table 2.4, entry 12). Prepared using General Method C. 110.6 mg, 0.24 mmol, 92% yield over 2 steps. Flash column chromatography (SiO_2 , 2 x 25 cm, 6:1 \rightarrow 4:1 hexanes:EtOAc). R_f = 0.15 (4:1 hexanes:EtOAc); ^1H NMR (300 MHz, CDCl_3) mixture of two diastereomers, see Figure A1.153; IR (Neat Film NaCl) 3436, 3071, 3050, 3013, 2999, 2931, 2896, 2859, 1960, 1891, 1826, 1694, 1638, 1589, 1472, 1461, 1428, 1390, 1360, 1325, 1307, 1251, 1218, 1188, 1168, 1111, 1092, 1007, 998, 973, 934, 914, 823, 798, 740 cm^{-1} ; HRMS (FAB+) m/z calc'd for $\text{C}_{29}\text{H}_{41}\text{O}_3\text{Si}$ $[\text{M}+\text{H}]^{+}$: 465.2825; found 465.2810.

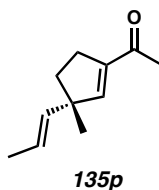


Acylcyclopentene 135o (Table 2.4, entry 12). Prepared using General Method E. 92.2 mg, 0.21 mmol, 92% yield. Flash column chromatography (SiO_2 , 2 x 25 cm, 15:1 hexanes:Et₂O). R_f = 0.64 (4:1 hexanes:EtOAc); ^1H NMR (300 MHz, CDCl_3) δ 7.71–7.64 (m, 4H), 7.48–7.35 (m, 6H), 6.44 (dd, J = 1.7, 1.7 Hz, 1H), 5.81–5.65 (m, 1H), 5.10–5.07

(m, 1H), 5.05–5.02 (m, 1H), 3.69–3.64 (m, 2H), 2.55–2.49 (m, 2H), 2.31 (s, 3H), 2.20–2.18 (m, 2H), 1.84–1.67 (m, 2H), 1.53–1.48 (m, 4H), 1.07 (s, 9H); ^{13}C NMR (75 MHz, CDCl_3) δ 197.3, 150.7, 144.4, 135.7, 134.7, 134.0, 129.7, 127.7, 117.8, 64.3, 53.3, 43.5, 34.8, 33.3, 30.0, 28.0, 27.0, 26.8, 19.3; IR (Neat Film NaCl) 3071, 3050, 3013, 2999, 2931, 2897, 2857, 1670, 638, 1618, 1589, 1472, 1461, 1448, 1428, 1388, 1372, 1316, 1263, 1201, 1157, 1111, 1093, 1030, 1008, 998, 937, 915, 865, 823, 803, 741, 726 cm^{-1} ; HRMS (FAB+) m/z calc'd for $\text{C}_{25}\text{H}_{29}\text{O}_2\text{Si}$ $[\text{M}-\text{C}_4\text{H}_9]^+$: 389.1968; found 389.1958; $[\alpha]_{\text{D}}^{25.0}$ –14.19 (c 0.92, CHCl_3 , 78.4% ee).

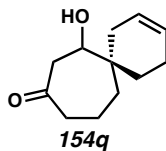


β -Hydroxyketone 154p (Table 2.4, entry 13). Prepared using General Method A. 429.5 mg, 2.36 mmol, 87% yield. Flash column chromatography (SiO_2 , 3 x 20 cm, 9:1→3:1 hexanes:EtOAc). R_f = 0.14 (4:1 hexanes:EtOAc); ^1H NMR (400 MHz, CDCl_3) mixture of two diastereomers, see Figure A1.155; IR (Neat Film NaCl) 3449, 3027, 2963, 2928, 2873, 1694, 1454, 1404, 1350, 1320, 1251, 1170, 1066, 969 cm^{-1} ; HRMS (MM: ESI-APCI+) m/z calc'd for $\text{C}_{11}\text{H}_{19}\text{O}_2$ $[\text{M}+\text{H}]^+$: 165.1274; found 165.1278.

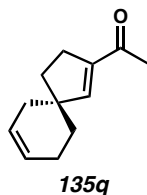


Acylcyclopentene 135p (Table 2.4, entry 13). Prepared using General Method E. Due to the volatility of acylcyclopentene **135p**, the work-up solvent (Et_2O) was removed using

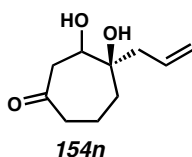
ambient pressure distillation (50→80 °C). 323.8 mg, 1.97 mmol, 93% yield. The crude oil was purified by automated flash column chromatography using a Teledyne Isco CombiFlash R_f (SiO₂, 32 g loading cartridge, 80 g column, linear gradient, 0→30% Et₂O in pentane [33 min]) and solvent was removed using ambient pressure distillation (60 °C). R_f = 0.55 (4:1 hexanes:EtOAc); ¹H NMR (400 MHz, CDCl₃) δ 6.41 (dd, *J* = 1.7, 1.7 Hz, 1H), 5.50 (dq, *J* = 15.5, 1.3 Hz, 1H), 5.39 (dq, *J* = 15.6, 6.2 Hz, 1H), 2.58–2.52 (m, 2H), 2.31–2.28 (m, 1H), 2.30 (s, 3H), 1.91 (ddd, *J* = 12.8, 7.4, 7.4 Hz, 1H), 1.74 (ddd, *J* = 12.8, 7.2, 7.2 Hz, 1H), 1.68–1.64 (m, 2H), 1.19 (s, 3H); ¹³C NMR (100 MHz, CDCl₃) δ 197.5, 151.4, 143.8, 137.5, 122.3, 51.5, 38.1, 29.6, 26.8, 25.4, 18.2; IR (Neat Film NaCl) 3022, 2958, 2859, 1674, 1617, 1451, 1377, 1365, 1310, 1271, 1229, 1165, 967 cm⁻¹; HRMS (MM: ESI-APCI+) *m/z* calc'd for C₁₁H₁₇O [M+H]⁺: 165.1279; found 165.1278; [α]_D^{25.0} +89.82 (*c* 1.04, CHCl₃, 88.0 % ee).



β-Hydroxyketone 154q (*Table 2.4, entry 14*). Prepared using General Method A. 29.1 mg, 0.150 mmol, 96% yield. Flash column chromatography (SiO₂, 2 x 20 cm, 9:1→3:1 hexanes:EtOAc). R_f = 0.09 (4:1 hexanes:EtOAc); ¹H NMR (300 MHz, CDCl₃) mixture of two diastereomers, see Figure A1.157; IR (Neat Film NaCl) 3436, 3021, 2922, 2873, 2842, 2697, 1692, 1656, 1436, 1402, 1353, 1318, 1256, 1202, 1184, 1172, 1152, 1093, 1071, 1050, 1000, 981, 970, 949, 932, 876, 850, 834, 798, 750 cm⁻¹; HRMS (EI+) *m/z* calc'd for C₁₂H₁₈O₂ [M]⁺: 194.1307; found 194.1315.

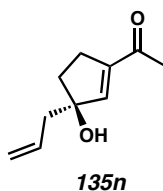


Acylcyclopentene 135q (*Table 2.4, entry 14*). Prepared using General Method E. 21.7 mg, 0.123 mmol, 91% yield. Flash column chromatography (SiO₂, 1 x 20 cm, 15:1 hexanes:Et₂O). R_f = 0.65 (4:1 hexanes:EtOAc); ¹H NMR (300 MHz, CDCl₃) δ 6.58 (dd, J = 1.8, 1.8 Hz, 1H), 5.72 (dm, J = 10.0 Hz, 1H), 5.65 (dm, J = 10.0 Hz, 1H), 2.59–2.52 (m, 2H), 2.30 (s, 3H), 2.13–2.04 (m, 2H), 2.02–1.98 (m, 2H), 1.77–1.70 (m, 2H), 1.69 (ddd, J = 12.8, 6.3, 6.3 Hz, 1H), 1.56 (ddd, J = 12.8, 6.5, 6.5 Hz, 1H); ¹³C NMR (75 MHz, CDCl₃) δ 197.8, 151.4, 143.9, 127.0, 125.5, 48.7, 35.8, 35.8, 32.5, 28.9, 26.8, 23.1; IR (Neat Film NaCl) 3320, 3023, 2918, 2856, 1704, 1669, 1616, 1436, 1371, 1436, 1371, 1316, 1269, 1231, 11945, 1116, 1086, 1045, 1020, 980, 962, 935, 864, 763 cm⁻¹; HRMS (EI+) m/z calc'd for C₁₂H₁₆O [M]⁺: 176.1201; found 176.1234; $[\alpha]_D^{25.0}$ -10.42 (c 1.08, CHCl₃, 78.4% ee).

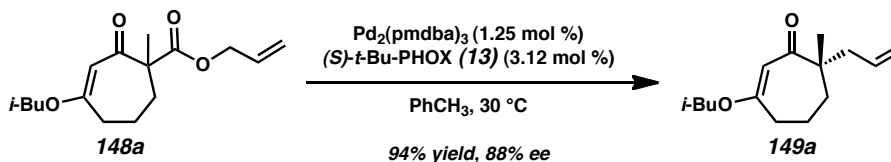


β -Hydroxyketone 154n (*Table 2.4, entry 15*). Prepared using General Method D. 20.3 mg, 0.110 mmol, 38% yield over 2 steps. Flash column chromatography (SiO₂, 1.5 x 25 cm, 10:1→6:1→4:1→2:1→1:1→1:2 hexanes:EtOAc). R_f = 0.19 (1:1 hexanes:EtOAc); ¹H NMR (300 MHz, CDCl₃) mixture of two diastereomers, see Figure A1.159; IR (Neat Film NaCl) 3369, 3077, 3011, 2947, 2924, 1688, 1641, 1469, 1439,

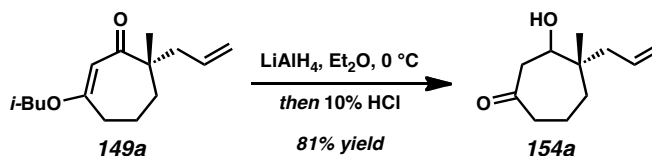
1343, 1268, 1216, 1193, 1128, 1108, 1079, 1052, 1032, 1019, 999, 966, 909, 889, 808, 731 cm^{-1} ; HRMS (MM: ESI-APCI+) m/z calc'd for $\text{C}_{10}\text{H}_{15}\text{O}_2$ $[\text{M}-\text{OH}]^+$: 167.1067; found 167.1066.



Acylcyclopentene 135n (*Table 2.4, entry 15*). Prepared using General Method E. 12.2 mg, 0.073 mmol, 67% yield. Flash column chromatography (SiO_2 , 1.5 x 25 cm, 10:1→4:1→2:1→1:1 hexanes:EtOAc); R_f = 0.44 (1:1 hexanes:EtOAc); ^1H NMR (500 MHz, CDCl_3) δ 6.48 (app t, J = 1.9 Hz, 1H), 5.91–5.77 (dddd, J = 16.5, 10.7, 7.4, 7.4 Hz, 1H), 5.23–5.15 (m, 2H), 2.67 (dddd, J = 17.0, 8.9, 4.1, 1.7 Hz, 1H), 2.50–2.40 (m, 3H), 2.33 (s, 3H), 2.14 (ddd, J = 13.7, 8.5, 4.1 Hz, 1H), 2.03 (br s, 1H), 1.91 (ddd, J = 13.7, 9.0, 5.8 Hz, 1H); ^{13}C NMR (125 MHz, CDCl_3) δ 197.5, 145.9, 145.5, 132.9, 119.8, 85.2, 44.9, 37.4, 29.1, 27.0; IR (Neat Film NaCl) 3400, 3077, 3004, 2961, 2929, 2856, 1841, 1668, 1622, 1428, 1372, 1295, 1267, 1228, 1205, 1173, 1070, 1057, 1016, 998, 966, 935, 917, 862, 831, 776 cm^{-1} ; HRMS (MM: ESI-APCI+) m/z calc'd for $\text{C}_{10}\text{H}_{13}\text{O}$ $[\text{M}-\text{OH}]^+$: 149.0961; found 149.0967; $[\alpha]_{\text{D}}^{25.0}$ –22.45 (c 1.22, CHCl_3 , 57.1% ee).

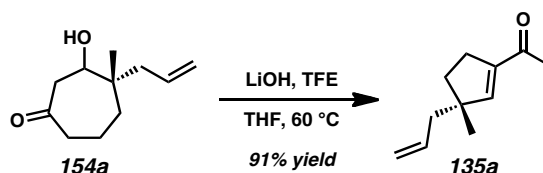
2.10.2.9 LARGE SCALE SYNTHESIS OF ACYLCYCLOPENTENE 135a

Vinylogous Ester 149a. $\text{Pd}_2(\text{pmdba})_3$ (733.1 mg, 0.67 mmol, 0.0125) and (*S*)-*t*-Bu-PHOX (647.0 mg, 1.67 mmol, 0.0312 equiv) were placed in a 500 mL round-bottom flask. The flask was evacuated/backfilled with N_2 (3 cycles, 10 min evacuation per cycle). Toluene (222 mL, sparged with N_2 for 1 h immediately before use) was added and the black suspension was immersed in an oil bath preheated to 30 °C. After 30 min of stirring, β -ketoester **148a** (15.0 g, 53.5 mmol, 1.0 equiv) in toluene (46 mL, sparged with N_2 immediately before use) was added using positive pressure cannulation. The dark orange catalyst solution turned olive green immediately after the addition of β -ketoester **148a**. The solution was stirred at 30 °C for 32 h, allowed to cool to ambient temperature, filtered through a silica gel plug (2 x 5.5 cm SiO_2 , Et_2O), and concentrated under reduced pressure. The crude oil was purified by flash column chromatography (SiO_2 , 8 x 12 cm, 19:1 hexanes: EtOAc , dry-loaded using SiO_2) to afford vinylogous ester **149a** (11.83 g, 50.1 mmol, 94% yield, 88% ee) as a pale yellow oil. (For characterization data, see p. 124).



β -Hydroxyketone 154a. A 500 mL round-bottom flask with magnetic stir bar was charged with Et_2O (150 mL) and cooled to 0 °C. LiAlH_4 (1.04 g, 0.0275 mol, 0.55 equiv)

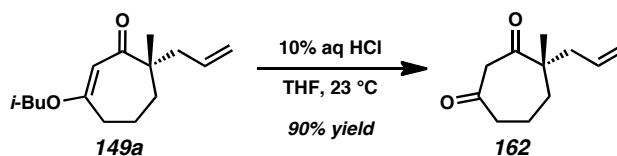
was added in one portion. After 10 min, a solution of vinylogous ester **149a** (11.83 g, 50 mmol, 1.0 equiv) in Et₂O (50 and 25 mL for quantitative transfer) was added dropwise using positive pressure cannulation. The grey suspension was stirred for 60 min after which LiAlH₄ (190 mg, 5.0 mmol, 0.1 equiv) was added in one portion. After an additional 10 min of stirring at 0 °C, the reaction was quenched by slow addition of aqueous HCl (143 mL, 10% w/w). The resulting biphasic system was allowed to warm to ambient temperature and stirred vigorously for 10 h. The reaction was diluted with Et₂O, the phases were separated and the aqueous phase was extracted with Et₂O (3 x 150 mL). The combined organic phases were dried over Na₂SO₄, filtered, and concentrated under reduced pressure. The crude product was azeotroped with toluene (50 mL) and purified using flash column chromatography (SiO₂, 8 x 13 cm, 9:1→3:1 hexanes:EtOAc, dry-loaded using Celite) to afford β-hydroxyketone **154a** (7.25 g, 39.8 mmol, 81% yield) as a colorless semi-solid. (For characterization data, see p. 155).



Acylcyclopentene 135a. Alcohol **154a** (7.25 g, 39.8 mmol, 1.0 equiv) was dissolved in THF (400 mL) in a 1 L round-bottom flask. The solution was treated with 2,2,2-trifluoroethanol (5.99 g, 4.36 mL, 59.7 mmol, 1.5 equiv) and LiOH (1.43 g, 59.7 mmol, 1.5 equiv). The flask was fitted with a reflux condenser, purged with N₂, and heated to 60 °C using an oil bath. After 18 h of stirring, the suspension was allowed to cool to ambient temperature, diluted with Et₂O (200 mL), stirred with Na₂SO₄ for 30 min,

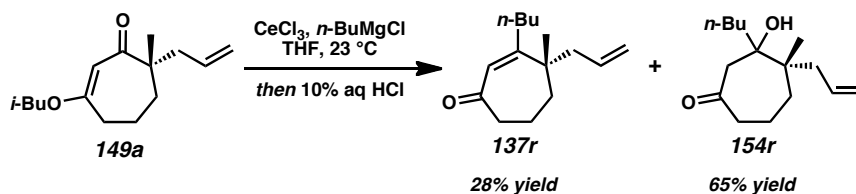
filtered, and concentrated carefully under reduced pressure, allowing for a film of ice to form on the outside of the flask. The crude product was purified using flash column chromatography (SiO₂, 8 x 12 cm, 15:1→9:1 pentane:Et₂O) to afford acylcyclopentene **135a** (5.93 g, 36.1 mmol, 91% yield) as a colorless fragrant oil. (For characterization data, see p. 156).

2.10.2.10 INITIAL SYNTHETIC STUDIES ON THE ORGANOMETALLIC ADDITION/REARRANGEMENT OF 149a



Cyclic Dione 162. A 20 mL scintillation vial equipped with a stir bar was charged with vinylogous ester **149a** (144.6 mg, 0.61 mmol, 1.00 equiv), THF (1 mL), and aqueous HCl (1 mL, 10% w/w, 2.87 mmol, 4.69 equiv). After 4.5 h of vigorous stirring, the solution was diluted with H₂O (5 mL) and transferred to a separatory funnel where the aqueous phase was extracted four times with Et₂O. The combined organics (70 mL) were dried over MgSO₄, filtered, and concentrated. The crude oil was purified by flash chromatography (SiO₂, 27.5 x 2 cm, 100% hexanes→10% EtOAc in hexanes) to afford cyclic dione **162** (99.4 mg, 0.55 mmol, 90% yield) as a pale yellow oil; *R_f* = 0.48 (30% EtOAc in hexanes); ¹H NMR (500 MHz, CDCl₃) δ 5.69 (d, *J* = 14.0 Hz, 1H), 5.12–5.04 (m, 2H), 3.72 (d, *J* = 14.0 Hz, 1H), 3.53 (d, *J* = 14.0 Hz, 1H), 2.48 (t, *J* = 6.6 Hz, 2H), 2.40 (dddd, *J* = 13.9, 7.1, 1.2, 1.2 Hz, 1H), 2.22 (dddd, *J* = 13.9, 7.7, 1.1, 1.1 Hz, 1H), 2.02–1.75 (m, 4H), 1.15 (s, 3H); ¹³C NMR (125 MHz, CDCl₃) δ 208.4, 203.7, 133.1,

119.1, 57.6, 50.9, 43.5, 42.9, 36.7, 21.9, 19.8; IR (Neat Film NaCl) 3076, 2972, 2935, 2871, 1719, 1695, 1639, 1463, 1417, 1378, 1337, 1210, 1160, 1112, 1059, 1026, 921 cm^{-1} ; HRMS (EI+) m/z calc'd for $\text{C}_{11}\text{H}_{16}\text{O}_2$ $[\text{M}]^{+}$: 180.1150; found 180.1165; $[\alpha]_{\text{D}}^{25.0}$ -19.38 (c 1.00, CHCl_3 , 88.0% ee).

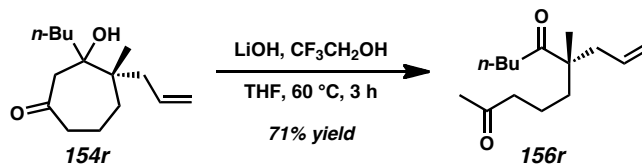


Cycloheptenone 137r and β -Hydroxyketone 154r. $\text{CeCl}_3 \cdot 7\text{H}_2\text{O}$ (419 mg, 1.13 mmol, 2.55 equiv) in a 100 mL round-bottom flask was immersed in a preheated oil bath at 150 °C and placed under vacuum for 4 h while stirring. The flask was cooled to ambient temperature, backfilled with N_2 , and charged with THF (4 mL). After 15 h of stirring, additional THF (4 mL) and n -butylmagnesium chloride solution (1.2 mL, 1.86 M in THF, 2.23 mmol, 5.02 equiv) were added to the flask. The resulting slurry was stirred for 4.25 h before vinylogous ester **149a** (105 mg, 0.444 mmol, 1.00 equiv) dissolved in THF (1 mL) was added using positive pressure cannulation followed by two THF rinses (2 x 0.5 mL). After 45 min of stirring, the reaction was quenched by addition of 10% w/w HCl (10 mL). The phases were separated and the aqueous layer was extracted with ethyl acetate (3 x 15 mL). The combined organic phases were washed with brine, dried over Na_2SO_4 , filtered, and concentrated under reduced pressure. The residue was purified by flash column chromatography using a Teledyne Isco CombiFlash R_f system (SiO_2 , 25 g loading cartridge, 12 g column, multi-step gradient, hold 0% [1 min] \rightarrow ramp to 10% [5 min] \rightarrow hold 10% [31 min] \rightarrow 100% EtOAc in hexanes [10 min]) to afford cycloheptenone

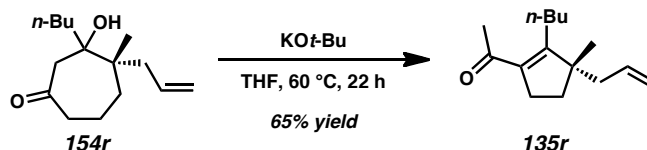
137r (28 mg, 0.13 mmol, 28% yield) and β -hydroxyketone **154r** (69 mg, 0.29 mmol, 65% yield) as pale yellow oils.

Cycloheptenone 137r. $R_f = 0.68$ (30% EtOAc in hexanes); ^1H NMR (500 MHz, CDCl_3) δ 5.89 (s, 1H), 5.63 (dddd, $J = 16.9, 10.3, 7.9, 6.7$ Hz, 1H), 5.10–4.98 (m, 2H), 2.61–2.54 (m, 2H), 2.37 (dddd, $J = 14.1, 6.7, 1.3, 1.3$ Hz, 1H), 2.18–2.03 (m, 3H), 1.85–1.72 (m, 3H), 1.66–1.56 (m, 1H), 1.53–1.43 (m, 2H), 1.37 (app. septuplet, $J = 7.3$ Hz, 2H), 1.15 (s, 3H), 0.92 (t, $J = 7.3$ Hz, 3H); ^{13}C NMR (125 MHz, CDCl_3) δ 205.4, 163.0, 134.2, 128.7, 118.1, 45.7, 45.3, 44.4, 38.8, 34.0, 32.4, 25.7, 23.0, 17.6, 14.1; IR (Neat Film NaCl) 3076, 2957, 2933, 2872, 1652, 1611, 1467, 1414, 1379, 1342, 1263, 1218, 1178, 1109, 1072, 996, 962, 914, 841, 780, 713 cm^{-1} ; HRMS (MM: ESI-APCI+) m/z calc'd for $\text{C}_{15}\text{H}_{25}\text{O}$ $[\text{M}+\text{H}]^+$: 221.1900; found 221.1905; $[\alpha]_{\text{D}}^{25.0} -33.17$ (c 1.17, CHCl_3 , 88.0% ee).

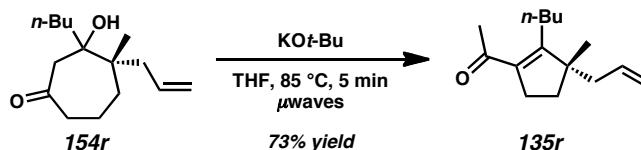
β -Hydroxyketone 154r. $R_f = 0.48$ (30% EtOAc in hexanes); ^1H NMR (500 MHz, CDCl_3) mixture of two diastereomers, see Figure A1.212; IR (Neat Film NaCl) 3502, 3073, 2956, 2871, 1695, 1638, 1468, 1404, 1380, 1341, 1286, 1181, 1125, 1052, 1028, 998, 913, 868, 796, 732 cm^{-1} ; HRMS (MM: ESI-APCI+) m/z calc'd for $\text{C}_{15}\text{H}_{27}\text{O}_2$ $[\text{M}+\text{H}]^+$: 239.2006; found 239.2013.



Linear Dione 156r. A 50 mL round-bottom flask equipped with a magnetic stir and fitted with a water condenser was charged with β -hydroxyketone **154r** (56.9 mg, 0.24 mmol, 1.00 equiv), THF (3 mL), TFE (60 μ L, 0.83 mmol, 3.50 equiv), and LiOH (17.3 mg, 0.72 mmol, 3.03 equiv). The flask was backfilled with argon and lowered into a preheated oil bath (60 $^\circ$ C). After 3 h, the reaction was removed from the bath, allowed to cool to room temperature, dried over Na_2SO_4 , filtered, and concentrated under reduced pressure. The crude oil was purified by flash chromatography (SiO_2 , 3 x 21 cm, 10% \rightarrow 20% \rightarrow 30% EtOAc in hexanes) to afford linear dione **156r** (40.1 mg, 0.17 mmol, 71% yield) as a pale yellow oil; R_f = 0.57 (30% EtOAc in hexanes); ^1H NMR (500 MHz, CDCl_3) δ 5.68–5.57 (m, 1H), 5.06–4.98 (m, 2H), 2.43 (t, J = 7.3 Hz, 2H), 2.39 (t, J = 6.4 Hz, 2H), 2.31 (dddd, J = 14.0, 7.3, 1.2, 1.2 Hz, 1H), 2.18 (dddd, J = 14.0, 7.7, 1.2, 1.2 Hz, 1H), 2.11 (s, 3H), 1.63–1.34 (m, 6H), 1.33–1.24 (m, 2H), 1.10 (s, 3H), 0.89 (t, J = 7.3 Hz, 3H); ^{13}C NMR (125 MHz, CDCl_3) δ 214.9, 208.6, 133.9, 118.1, 50.9, 44.0, 42.6, 37.4, 37.4, 30.1, 25.9, 22.6, 21.1, 18.7, 14.1; IR (Neat Film NaCl) 3076, 2958, 2933, 2873, 1718, 1701, 1639, 1465, 1409, 1378, 1360, 1256, 1230, 1174, 1142, 1120, 1029, 994, 916, 766, 728 cm^{-1} ; HRMS (MM: ESI-APCI+) m/z calc'd for $\text{C}_{15}\text{H}_{27}\text{O}_2$ $[\text{M}+\text{H}]^+$: 239.2006; found 239.2005; $[\alpha]_D^{25.0}$ +5.57 (c 1.17, CHCl_3 , 88.0% ee).

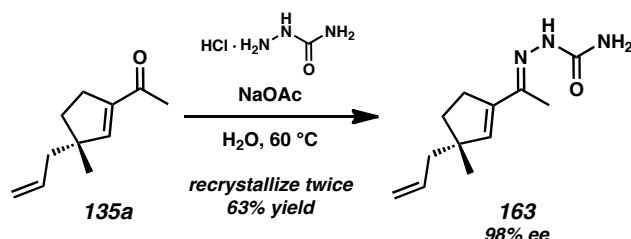


Acylcyclopentene 135r. A 25 mL round-bottom flask equipped with a stir bar and fitted with a water condenser was charged with β -hydroxyketone **154r** (91.5 mg, 0.38 mmol, 1.00 equiv), THF (4 mL), and KO*t*-Bu (66.5 mg, 0.59 mmol, 1.55 equiv). The flask was lowered into a preheated oil bath (60 °C) and stirred overnight. Additional THF (4 mL) was added after 19 h of heating. After an additional 3 h, the reaction was removed from the bath, allowed to cool to room temperature, dried over Na₂SO₄, filtered through a silica gel plug, and concentrated under reduced pressure. The crude oil was purified by flash chromatography (SiO₂, 3 x 27 cm, 100% pentane→2%→5%→10% Et₂O in pentane) to afford acylcyclopentene **135r** (55.1 mg, 0.25 mmol, 65% yield) as a pale yellow oil; R_f = 0.81 (30% EtOAc in hexanes); ¹H NMR (500 MHz, CDCl₃) δ 5.77–5.65 (m, 1H), 5.08–5.00 (m, 2H), 2.60–2.49 (m, 2H), 2.45–2.37 (m, 1H), 2.24–2.17 (m, 4H), 2.15–2.10 (m, 2H), 1.85 (ddd, J = 12.8, 7.7, 6.2 Hz, 1H), 1.60–1.51 (m, 1H), 1.47–1.34 (m, 4H), 1.06 (s, 3H), 0.93 (t, J = 7.1 Hz, 3H); ¹³C NMR (125 MHz, CDCl₃) δ 198.8, 164.2, 135.0, 134.7, 117.6, 52.6, 43.8, 35.0, 32.1, 31.5, 30.4, 27.6, 24.7, 23.8, 14.0; IR (Neat film NaCl) 3075, 3002, 2957, 2930, 2870, 2859, 1677, 1653, 1639, 1602, 1456, 1432, 1373, 1355, 1311, 1275, 1258, 1188, 1141, 1089, 995, 959, 913, 848, 801, 726 cm⁻¹; HRMS (MM: ESI-APCI+) m/z calc'd for C₁₅H₂₅O [M+H]⁺: 221.1900; found 221.1900; [α]_D^{25.0} –1.44 (c 1.35, CHCl₃, 88.0% ee).



Acylcyclopentene 135r. KOt-Bu (32 mg, 0.283 mmol, 1.62 equiv), THF (1.75 mL), and β -hydroxyketone mmol, 1.00 equiv) were added to a 0.5–2.0 mL microwave vial with a magnetic spin vane. The pale yellow solution was subjected to microwave irradiation in a Biotage Initiator microwave reactor (temperature: 85 °C, sensitivity: normal). After 5 min of irradiation, the crimp cap was removed and Na₂SO₄ was added to the vial. The contents were filtered through a silica gel plug with Et₂O, concentrated under reduced pressure, and purified by flash column chromatography (5% Et₂O in pentane) to yield acylcyclopentene **135** (31 mg, 0.14 mmol, 73% yield) as a pale yellow oil.

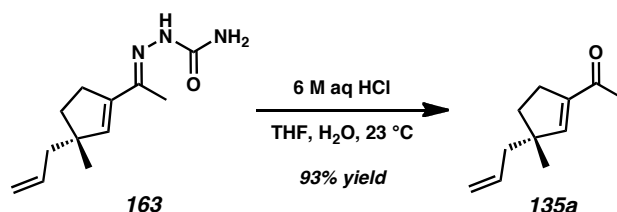
2.10.2.11 PREPARATION OF ACYLCYCLOPENTENE DERIVATIVES



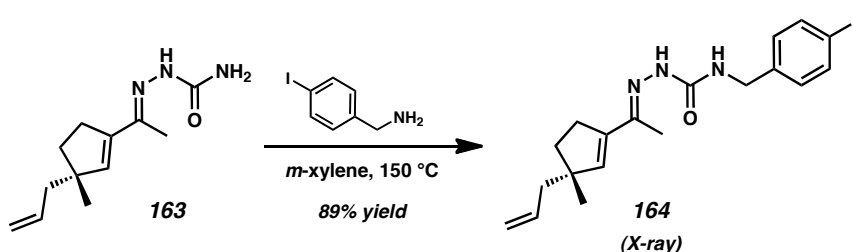
Semicarbazone 163. A 15 mL round-bottom flask was charged with sodium acetate (150 mg, 1.83 mmol, 1.20 equiv), semicarbazide hydrochloride (204 mg, 1.83 mmol, 1.20 equiv), and a magnetic stir bar. Purified water (1.7 mL) was added and the mixture was stirred until all the solids had dissolved. Acylcyclopentene **135a** (250 mg, 1.52 mmol, 1.00 equiv) was added neat and the mixture was heated to 60 °C for 4 h. The slurry was allowed to cool to ambient temperature while stirring and vacuum filtered

(water aspirator). The white solid was dried under reduced pressure to afford semicarbazone **15** (311 mg, 1.40 mmol, 92% yield). The ee of the semicarbazone at this point was found to be 91% (measured by hydrolysis to ketone **135a**, GC conditions: 80 °C isothermal for 90 min, G-TA column, t_R (min): acylcyclopentene **135a** = 54.98).

The semicarbazone **163** (300 mg, 1.36 mmol) was transferred to a round-bottom flask, the solids were suspended in toluene-hexanes (50:50), and the mixture was heated to 90 °C while stirring. After a few min of stirring, the solids had dissolved completely to afford a clear, colorless solution. Heating was discontinued and the stirring mixture was allowed to cool to ambient temperature while still immersed in the oil bath. After 10 h had elapsed, the slurry was vacuum filtered to afford **163** (246 mg, 1.11 mmol, 82% yield, 63% overall yield after recrystallizing twice). The ee at this point was found to be 94.5% (measured by hydrolysis to ketone **135a**). A second recrystallization following the above procedure employing **163** (241 mg, 1.09 mmol) afforded **163** (201 mg, 0.91 mmol, 83% yield). The ee at this point was found to be 97.9% (measured by hydrolysis to ketone **135a**); R_f = 0.30 (9:1 CHCl_3 -MeOH); ^1H NMR (300 MHz, CDCl_3) δ 8.52 (br s, 1H), 6.06 (br s, 1H), 5.85 (app t, J = 1.6 Hz, 1H), 5.76 (dddd, J = 16.7, 9.3, 7.4, 7.4 Hz, 1H), 5.47 (br s, 1H), 5.06–4.98 (m, 2H), 2.67–2.49 (m, 2H), 2.15–2.12 (m, 2H), 1.98 (s, 3H), 1.82 (ddd, J = 12.8, 8.2, 6.9 Hz, 1H), 1.62 (ddd, J = 12.8, 8.5, 6.4 Hz, 1H), 1.07 (s, 3H); ^{13}C NMR (75 MHz, CDCl_3) δ 158.1, 145.0, 141.7, 141.2, 135.6, 117.2, 49.2, 45.9, 36.2, 30.8, 26.3, 12.8; IR (Neat Film NaCl) 3473, 3266, 3189, 2946, 2858, 1698, 1579, 1478, 1437, 1377, 1349, 1321, 1130, 1109, 993, 910, 845, 768 cm^{-1} ; HRMS (ESI+) m/z calc'd for $\text{C}_{12}\text{H}_{20}\text{N}_3\text{O}$ $[\text{M}+\text{H}]^+$: 222.1606; found 222.1610; $[\alpha]_D^{22.6}$ +39.80 (c 0.84, CHCl_3 , 97.9% ee); mp = 145–146 °C (1:1 toluene-hexanes).

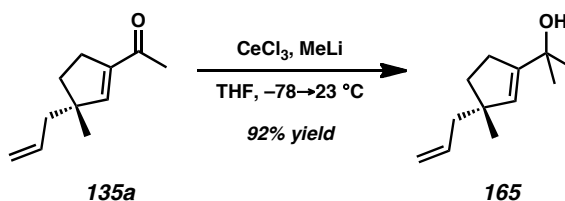


Acylcyclopentene 135a. A solution of semicarbazone **163** (191.8 mg, 0.867 mmol, 1.00 equiv) in THF (1.92 mL) was treated with aqueous HCl (3.84 mL, 6.0 M, in H₂O) was added. The resulting biphasic mixture was stirred vigorously at ambient temperature for 30 h. The reaction was diluted with Et₂O (10 mL), the phases were separated, and the aqueous phase was extracted with Et₂O (2 x 10 mL). The combined organics were dried over MgSO₄, filtered, and concentrated carefully under reduced pressure, allowing for a film of ice to form on the outside of the flask. The residue was filtered through a short silica gel plug (1 x 10 cm SiO₂, 4:1 hexanes:Et₂O) to afford acylcyclopentene **135a** (132.6 mg, 0.81 mmol, 93% yield); $[\alpha]_D^{22.6} +39.80$ (*c* 0.84, CHCl₃, 97.9% ee). (For characterization data, see p. 156).



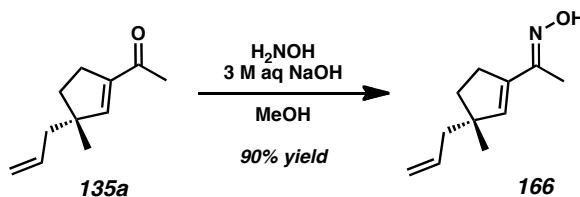
Iodoarene 164. To a solution of semicarbazone **163** (50 mg, 0.23 mmol, 1.00 equiv) in *m*-xylene (2.2 mL) was added 4-iodo-benzylamine (63 mg, 0.27 mmol, 1.17 equiv). The resulting pale yellow solution was immersed in an oil bath and heated to 150 °C. After 9 h of stirring at 150 °C, the reaction was allowed to cool to ambient temperature and

concentrated under reduced pressure to afford a pale yellow solid. The crude solid was purified by flash column chromatography (1.0 x 15 cm SiO₂, 9:1→7:3 hexanes:EtOAc) to afford iodoarene **164** (88 mg, 0.20 mmol, 89% yield) as a white solid. X-ray quality crystals were obtained by slow vapor diffusion of pentane into a chloroform solution of **164**; R_f = 0.52 (9:1 CHCl₃-MeOH); ¹H NMR (500 MHz, CDCl₃) δ 7.88 (s, 1H), 7.66–7.64 (m, 2H), 7.08 (d, J = 8.5 Hz, 2H), 6.50 (t, J = 6.1 Hz, 1H), 5.86 (app t, J = 1.5 Hz, 1H), 5.76 (dddd, J = 16.9, 9.0, 7.6, 7.6 Hz, 1H), 5.04–5.01 (m, 2H), 4.46 (d, J = 6.3 Hz, 2H), 2.60–2.49 (m, 2H), 2.18–2.10 (m, 2H); 1.95 (s, 3H), 1.82 (ddd, J = 12.9, 8.5, 6.3 Hz, 1H), 1.62 (ddd, J = 12.9, 8.5, 6.1 Hz, 1H), 1.07 (s, 3H); ¹³C NMR (125 MHz, CDCl₃) δ 156.3, 144.5, 141.5, 141.4, 139.2, 137.8, 135.6, 129.4, 117.2, 92.6, 49.3, 45.9, 43.2, 36.2, 30.9, 26.3, 12.5; IR (Neat Film NaCl) 3411, 3194, 3075, 2946, 2920, 2863, 1677, 1528, 1486, 1401, 1323, 1259, 1142, 1114, 1057, 1000, 913, 845 cm⁻¹; HRMS (FAB+) m/z calc'd for C₁₉H₂₅N₃OI [M+H]⁺: 438.1043; found 438.1036; $[\alpha]_D^{22.2}$ +31.43 (c 0.36, CHCl₃, 91.0% ee); mp = 123–124 °C (CHCl₃-*n*-pentane).

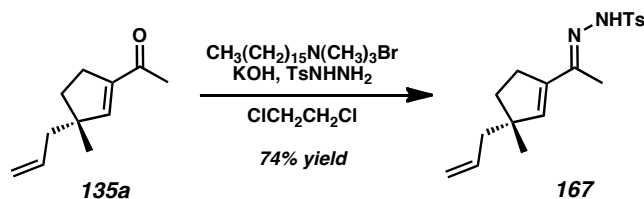


Alcohol 165. CeCl₃ (187 mg, 0.759 mmol, 2.50 equiv) was weighed out in a glove box and placed in a 25 mL round-bottom flask. The flask was sealed with a septum and removed from the glove box. THF (3 mL) was added to the flask, the suspension was cooled to –78 °C using an acetone/CO₂(s) bath, and MeLi (326 μL, 0.912 mmol, 2.80 M in DME, 3.00 equiv) was added in a dropwise manner. The resulting pale brown

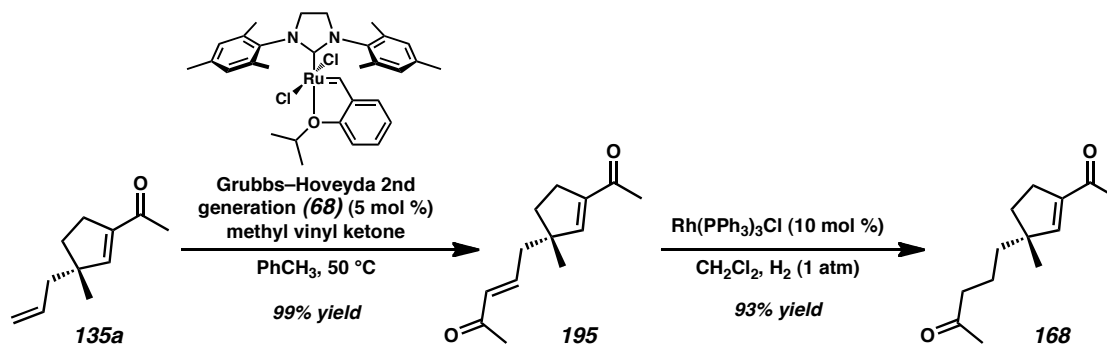
suspension was stirred at $-78\text{ }^{\circ}\text{C}$ for 30 min. Acylcyclopentene **135a** (50.0 mg, 0.304 mmol, 1.00 equiv) was added neat to the reaction in a dropwise manner. After 30 min of stirring at $-78\text{ }^{\circ}\text{C}$, the reaction was quenched by dropwise addition of sat. aqueous NH_4Cl (1.0 mL), the cooling bath was removed, and the reaction was allowed to warm to ambient temperature. The reaction was diluted with Et_2O (10 mL) and H_2O (10 mL), and the phases were separated. The aqueous phase was extracted with Et_2O (3 x 15 mL), and the combined organic phases were washed with brine (10 mL), dried over MgSO_4 , filtered, and concentrated under reduced pressure. The crude product was purified by automated flash column chromatography using a Teledyne Isco CombiFlash R_f (SiO_2 , 5 g loading cartridge, 12 g column, multi-step gradient, 5% [5 min] \rightarrow 10% Et_2O in pentane) to afford alcohol **165** (50.4 mg, 0.280 mmol, 92% yield) as a pale yellow oil; R_f = 0.31 (4:1 hexanes:EtOAc); ^1H NMR (400 MHz, CDCl_3) δ 5.78 (dddd, J = 14.7, 11.8, 9.3, 7.4 Hz, 1H), 5.34 (dd, J = 1.8, 1.8 Hz, 1H), 5.04–5.00 (m, 1H), 5.00–4.97 (m, 1H), 2.45–2.29 (m, 2H), 2.18–2.00 (m, 2H), 1.81 (ddd, J = 12.7, 8.3, 6.0 Hz, 1H), 1.60 (ddd, J = 12.7, 8.5, 6.1 Hz, 1H), 1.44 (br s, 1H), 1.34 (s, 6H), 1.02 (s, 3H); ^{13}C NMR (100 MHz, CDCl_3) δ 149.7, 136.21, 131.6, 116.7, 70.9, 48.2, 46.2, 36.9, 30.9, 29.3, 29.3, 26.5; IR (Neat Film NaCl) 3370, 3077, 2973, 2943, 2859, 1637, 1454, 1412, 1367, 1328, 1254, 1212, 1162, 1137, 997, 960, 940, 910, 853, 806 cm^{-1} ; HRMS (MM: ESI-APCI+) m/z calc'd for $\text{C}_{12}\text{H}_{19}$ $[\text{M}-\text{OH}]^+$: 163.1481; found 163.1482; $[\alpha]_{\text{D}}^{25.0}$ +5.34 (c 1.16, CHCl_3 , 88.0 % ee).



Oxime 166. A 1 dram vial with magnetic stir bar was charged with acylcyclopentene **135a** (40.0 mg, 0.24 mmol, 1.00 equiv), MeOH (0.24 mL), 50% wt aqueous hydroxylamine (47 μL , 0.76 mmol, 3.13 equiv), and 3 M aqueous NaOH (125 μL , 0.376 mmol, 0.51 equiv). After 9 d, the reaction was diluted with Et_2O (10 mL) and H_2O (2 mL) and stirred vigorously for several minutes. The layers were separated and the aqueous layer was extracted with Et_2O (5 x 10 mL). The combined organic layers were dried over MgSO_4 , filtered, and concentrated under reduced pressure. The residue was taken up in CH_2Cl_2 , filtered through a cotton plug, and concentrated under reduced pressure. The residue was purified by flash column chromatography (SiO_2 , 1.5 x 20 cm, 20:1 \rightarrow 15:1 hexanes:EtOAc) to afford oxime **166** (39.3 mg, 0.21 mmol, 90% yield) as a clear oil; R_f = 0.52 (4:1 hexanes:EtOAc); ^1H NMR (300 MHz, CDCl_3) δ 9.73 (br s, 1H), 5.90 (br t, J = 1.5 Hz, 1H), 5.85–5.66 (m, 1H), 5.02 (m, 2H), 2.70–2.45 (m, 2H), 2.14 (m, 2H), 2.05 (s, 3H), 1.85 (ddd, J = 12.9, 8.1, 6.6 Hz, 1H), 1.65 (ddd, J = 12.8, 8.3, 6.3 Hz, 1H), 1.08 (s, 3H); ^{13}C NMR (75 MHz, CDCl_3) δ 154.0, 141.8, 139.1, 135.6, 117.2, 48.9, 45.9, 36.3, 30.6, 26.2, 11.3; IR (Neat Film NaCl) 3272, 3233, 3075, 3003, 2952, 2925, 2864, 1639, 1455, 1437, 1414, 1379, 1322, 1280, 1103, 1010, 995, 913, 850, 828, 756, 715 cm^{-1} ; HRMS (EI+) m/z calc'd for $\text{C}_8\text{H}_{12}\text{NO}$ [$\text{M}-\text{C}_3\text{H}_5$] $^+$: 138.0919; found 138.0960; $[\alpha]_{\text{D}}^{25.0}$ +21.34 (c 1.57, CHCl_3 , 88.0% ee).



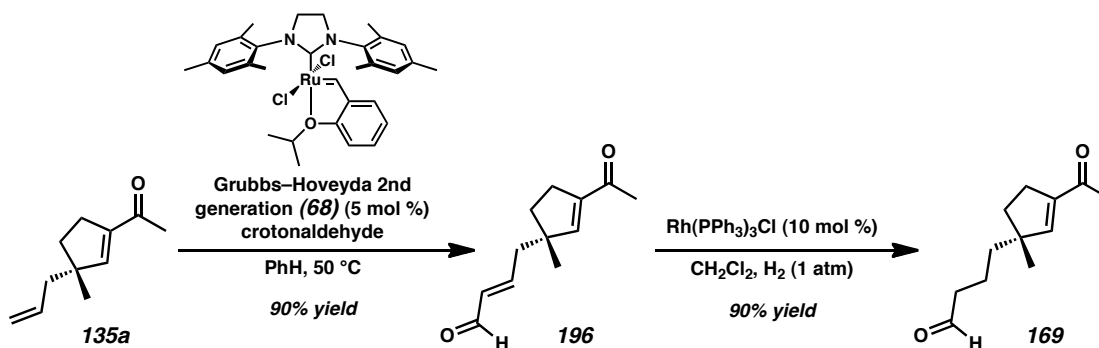
Tosylhydrazone 167. A 25 mL flask with magnetic stir bar was charged with acylcyclopentene **135a** (40.0 mg, 0.24 mmol, 1.00 equiv), 1,2-dichloroethane (2.7 mL), cetyltrimethylammonium bromide (26.6 mg, 0.073 mmol, 0.30 equiv), KOH (136.7 mg, 2.44 mmol, 10.0 equiv), and TsHNNH₂ (271.9 mg, 1.46 mmol, 6.00 equiv), forming a thick white suspension. After 43 h, the reaction was quenched by the addition of sat. aqueous NH₄Cl (5 mL). The mixture was extracted with CH₂Cl₂ (5 x 10 mL) and the combined organic layers were dried over Na₂SO₄, filtered, and concentrated under reduced pressure. The residue was purified by flash column chromatography using a Teledyne Isco CombiFlash R_f system (SiO₂, 3 x 25 cm, 4:1→3:1 hexanes:EtOAc) to afford tosylhydrazone **167** (196.7 mg, 0.94 mmol, 74% yield) as a clear oil; R_f = 0.41 (2:1 hexanes:EtOAc); ¹H NMR (300 MHz, CDCl₃) δ 7.86 (d, *J* = 8.3 Hz, 2H), 7.54 (br s, 1H), 7.31 (d, *J* = 8.0 Hz, 2H), 5.85 (app t, *J* = 1.6 Hz, 1H), 5.81–5.62 (m, 1H), 5.06–4.92 (m, 2H), 2.58–2.48 (m, 2H), 2.43 (s, 3H), 2.19–2.00 (m, 2H), 1.89 (s, 3H), 1.85–1.71 (m, 1H), 1.71–1.50 (m, 1H), 1.03 (s, 3H); ¹³C NMR (75 MHz, CDCl₃) δ 151.5, 144.1, 142.4, 141.6, 135.5, 135.4, 129.5, 128.3, 117.2, 49.3, 45.8, 36.2, 30.7, 26.1, 21.7, 12.9; IR (Neat Film NaCl) 3217, 3072, 2953, 2924, 2864, 1706, 1639, 1618, 1598, 1495, 1454, 1401, 1337, 1307, 1292, 1212, 1185, 1168, 1094, 1059, 1029, 996, 914, 870, 850, 830, 813, 706 cm⁻¹; HRMS (EI+) *m/z* calc'd for C₁₅H₁₉O₂N₂S [M–C₃H₅]⁺: 291.1167; found 291.1181; [α]_D^{25.0} +34.25 (c 1.05, CHCl₃, 88.0% ee).



Bis-enone 195. To an oven-dried reaction tube with magnetic stir bar was added acylcyclopentene **135a** (50 mg, 0.304 mmol, 1.00 equiv). The headspace was purged with N₂ and dry degassed toluene (2.0 mL, sparged with N₂ for 1 h immediately before use) was added, followed by methyl vinyl ketone (124 μ L, 1.53 mmol, 5.03 equiv). Grubbs-Hoveyda 2nd generation catalyst (9.5 mg, 15.2 μ mol, 5 mol %) was quickly added to the reaction, giving the solution an olive green color. A reflux condenser was attached and the reaction was inserted into a 50 °C heating block. The solution quickly developed a dark brown color. After 2 h, the reaction was cooled to ambient temperature. The solution was filtered through a short silica gel plug (2 x 4 cm, Et₂O). The filtrate was concentrated under reduced pressure and the brown residue was purified by flash column chromatography (SiO₂, 2 x 25 cm, 10:1→4:1→2:1→1:1 hexanes:EtOAc) to afford bis-enone **195** (62.3 mg, 0.30 mmol, 99% yield) as a brown liquid; R_f = 0.31 (2:1 hexanes:EtOAc); ¹H NMR (300 MHz, CDCl₃) δ 6.71 (ddd, J = 15.5, 7.6, 7.6 Hz, 1H), 6.42 (s, 1H), 6.10 (d, J = 15.8 Hz, 1H), 2.68–2.40 (m, 2H), 2.33 (dd, J = 7.6, 0.9 Hz, 2H), 2.28 (s, 3H), 2.22 (s, 3H), 1.84 (ddd, J = 14.7, 8.2, 6.6 Hz, 1H), 1.70 (ddd, J = 13.1, 8.4, 6.1 Hz, 1H), 1.14 (s, 3H); ¹³C NMR (75 MHz, CDCl₃) δ 198.1, 197.1, 150.2, 144.3, 143.8, 133.8, 50.1, 43.7, 36.2, 29.8, 27.3, 26.8, 25.7; IR (Neat Film NaCl) 3584, 3318, 2956, 2866, 1697, 1669, 1626, 1454, 1429, 1365, 1308, 1254, 1182, 1098, 1021, 982,

937, 867 cm^{-1} ; HRMS (EI+) m/z calc'd for $\text{C}_{13}\text{H}_{18}\text{O}_2$ $[\text{M}]^{+}$: 206.1307; found 206.1303; $[\alpha]_{\text{D}}^{25.0} +47.61$ (c 1.02, CHCl_3 , 88.0% ee).

Mono-enone 168. An oven-dried 2-neck flask fitted with a magnetic stir bar, rubber septum, and glass T-joint with 14/20 adapter was charged with bis-enone **195** (50.0 mg, 0.24 mmol, 1.00 equiv) and evacuated/backfilled with N_2 in a glove box antechamber (3 cycles, 5 min evacuation per cycle) before being transferred into the glove box. CH_2Cl_2 (2.5 mL) and $\text{Rh}(\text{PPh}_3)_3\text{Cl}$ (22.4 mg, 0.024 mmol, 10 mol %) were added to the flask, giving a red solution. The flask was sealed with a septum on one neck and T-joint (set to the closed position) on the other neck and carefully brought out of the glove box. A H_2 balloon was attached to the T-joint and the flask was gently evacuated/backfilled with H_2 (3 cycles, 2 min evacuation per cycle). After 10 h of stirring, the brown reaction mixture was filtered through a short silica gel plug (2 x 4 cm, Et_2O) and concentrated under reduced pressure. The residue was purified by flash column chromatography (SiO_2 , 2 x 25 cm, 10:1 \rightarrow 4:1 \rightarrow 2:1 hexanes: Et_2O) to afford enone **168** (46.8 mg, 0.23 mmol, 93% yield) as an orange liquid; R_f = 0.40 (2:1 hexanes: EtOAc); ^1H NMR (300 MHz, CDCl_3) δ 6.43 (app t, J = 1.7 Hz, 1H), 2.65–2.46 (m, 2H), 2.40 (t, J = 7.1 Hz, 2H), 2.27 (s, 3H), 2.11 (s, 3H), 1.88–1.72 (m, 1H), 1.71–1.46 (m, 3H), 1.46–1.29 (m, 2H), 1.08 (s, 3H); ^{13}C NMR (75 MHz, CDCl_3) δ 208.8, 197.5, 152.0, 143.6, 50.0, 44.2, 40.4, 36.1, 30.1, 29.7, 26.8, 25.6, 19.4; IR (Neat Film NaCl) 2998, 2953, 2866, 1716, 1667, 1616, 1456, 1427, 1367, 1308, 1270, 1225, 1190, 1170, 1103, 1058, 1021, 841, 871, 726 cm^{-1} ; HRMS (EI+) m/z calc'd for $\text{C}_{13}\text{H}_{20}\text{O}_2$ $[\text{M}]^{+}$: 208.1463; found 208.1460; $[\alpha]_{\text{D}}^{25.0} +25.55$ (c 1.46, CHCl_3 , 88.0% ee).

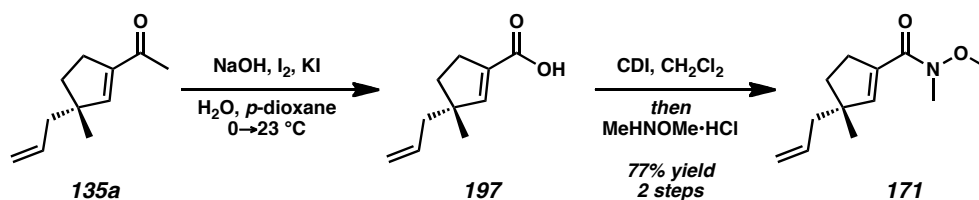


Bis-enone 196. To a 2-neck round-bottomed flask with magnetic stir bar and attached reflux condenser was added acylcyclopentene **135a** (100 mg, 0.608 mmol, 1.00 equiv). The flask was evacuated/backfilled with N₂ (3 cycles, 30 s evacuation per cycle). Dry degassed benzene (8.0 mL, sparged with N₂ for 1 h immediately before use) was added, followed by crotonaldehyde (251 μ L, 3.06 mmol, 5.03 equiv). Grubbs-Hoveyda 2nd generation catalyst (19.0 mg, 30.4 μ mol, 5 mol %) was quickly added to the reaction, giving the solution an olive green color. The flask was immersed in a 50 °C oil bath. The solution quickly developed a dark brown color. After 2 h, the reaction was cooled to ambient temperature. Several drops of ethyl vinyl ether were added and the reaction mixture was stirred for 5 min. The mixture was concentrated under reduced pressure and the brown residue was purified by flash column chromatography (SiO₂, 2 x 25 cm, 10:1→4:1→2:1 hexanes:EtOAc) to afford bis-enone **196** (105.4 mg, 0.55 mmol, 90% yield) as a brown oil; R_f = 0.38 (2:1 hexanes:EtOAc); ¹H NMR (300 MHz, CDCl₃) δ 9.50 (d, J = 7.8 Hz, 1H), 6.76 (app dt, J = 15.4, 7.6 Hz, 1H), 6.42 (app t, J = 1.8 Hz, 1H), 6.13 (app ddt, J = 15.5, 7.8, 1.3 Hz, 1H), 2.68–2.50 (m, 2H), 2.45 (dd, J = 7.6, 1.3 Hz, 2H), 2.28 (s, 3H), 1.85 (ddd, J = 13.1, 8.4, 6.5 Hz, 1H), 1.72 (ddd, J = 13.1, 8.5, 6.0 Hz, 1H), 1.16 (s, 3H); ¹³C NMR (75 MHz, CDCl₃) δ 197.0, 193.5, 154.0, 149.7, 144.5, 135.6,

50.1, 43.9, 36.1, 29.8, 26.8, 25.8; IR (Neat Film NaCl) 3359, 3317, 3041, 2957, 2928, 2867, 2820, 2743, 2708, 1691, 1668, 1636, 1618, 1456, 1431, 1378, 1369, 1341, 1308, 1269, 1203, 1162, 1149, 1109, 1093, 1036, 1013, 978, 936, 893, 868 cm^{-1} ; HRMS (FAB+) m/z calc'd for $\text{C}_{12}\text{H}_{17}\text{O}_2$ $[\text{M}+\text{H}]^+$: 193.1229; found 193.1224; $[\alpha]_{\text{D}}^{25.0} +46.07$ (c 1.13, CHCl_3 , 88.0% ee).

Mono-enone 169. An oven-dried 2-neck flask fitted with a magnetic stir bar, rubber septum, and a glass T-joint with 14/20 adapter was charged with and bis-enone **196** (42.8 mg, 0.22 mmol, 1.00 equiv) and evacuated/backfilled with N_2 in a glove box antechamber (3 cycles, 5 min evacuation per cycle) before being transferred into the glove box. CH_2Cl_2 (2.5 mL) and $\text{Rh}(\text{PPh}_3)_3\text{Cl}$ (10.3 mg, 0.011 mmol, 5 mol %) were added to the flask, giving a red solution. The flask was sealed with a septum on one neck and T-joint (set to the closed position) on the other neck and carefully brought out of the glove box. A H_2 balloon was attached to the T-joint and the flask was gently evacuated/backfilled with H_2 (five cycles, 2 min evacuation per cycle). After 20 h of stirring, an additional portion of $\text{Rh}(\text{PPh}_3)_3\text{Cl}$ (10.3 mg, 0.011 mmol, 5 mol %) in CH_2Cl_2 (0.5 mL) was added to the reaction using positive pressure cannulation. After 1.5 h of stirring, the reaction was diluted with Et_2O , filtered through a short silica gel plug (2 x 4 cm, Et_2O), and concentrated under reduced pressure. The residue was purified by flash column chromatography (SiO_2 , 2 x 25 cm, 10:1→4:1 hexanes: Et_2O) to afford enone **169** (39.2 mg, 0.20 mmol, 90% yield) as a pale colorless oil; R_f = 0.48 (2:1 hexanes: EtOAc); ^1H NMR (300 MHz, CDCl_3) δ 9.75 (t, J = 1.5 Hz, 1H), 6.44 (app t, J = 1.7 Hz, 1H), 2.59–2.48 (m, 2H), 2.43 (td, J = 7.1, 1.4 Hz, 2H), 2.28 (s, 3H), 1.88–1.73 (m, 1H), 1.73–1.51

(m, 3H), 1.51–1.33 (m, 2H), 1.09 (s, 3H); ^{13}C NMR (75 MHz, CDCl_3) δ 202.3, 197.5, 151.7, 143.8, 50.0, 44.5, 40.4, 36.1, 29.8, 26.8, 25.6, 17.8; IR (Neat Film NaCl) 3427, 3314, 3042, 2951, 2865, 2721, 1723, 1665, 1616, 1457, 1411, 1378, 1367, 1340, 1308, 1269, 1193, 1156, 1105, 1060, 1034, 1020, 970, 942, 867, 801 cm^{-1} ; HRMS (EI+) m/z calc'd for $\text{C}_{12}\text{H}_{18}\text{O}_2$ $[\text{M}]^{+}$: 194.1307; found 194.1321; $[\alpha]_{\text{D}}^{25.0} +32.50$ (c 0.69, CHCl_3 , 88.0% ee).

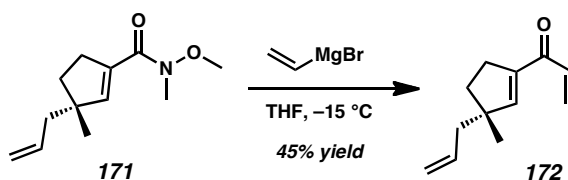


Carboxylic acid 197. A 50 mL round-bottom flask with magnetic stir bar was charged with acylcyclopentene **135a** (200 mg, 1.22 mmol, 1.00 equiv) and *p*-dioxane (10 mL). The solution was cooled to 0 °C and 5 M aqueous NaOH (10 mL) was added dropwise. The white suspension was stirred for 5 min at 0 °C. A dark brown solution of I_2 (1.37 g, 5.40 mmol, 4.40 equiv) and KI (2.09 g, 12.59 mmol, 10.50 equiv) in purified H_2O (10 mL) was added to the reaction dropwise, causing the reaction to become a yellow suspension. After 6.5 h of stirring at 0 °C, an additional portion of I_2 (343 mg, 1.35 mmol, 1.11 equiv) in *p*-dioxane (2 mL) was added to the reaction. After 30 min of stirring at 0 °C, the reaction was acidified to pH 2 using 2 M aqueous HCl. The reaction was extracted with Et_2O (3 x 30 mL) until the organic layer was clear. The combined organic phases were washed with sat. aqueous $\text{K}_2\text{S}_2\text{O}_3$ (2 x 10 mL), H_2O (2 x 10 mL), and brine (2 x 10 mL). The combined organic phases were dried over Na_2SO_4 , filtered, and concentrated under reduced pressure to give a yellow semi-solid. The residue was taken

up in EtOAc, filtered through a silica gel plug (3 x 3 cm, EtOAc), and concentrated to give carboxylic acid **197** as a pale yellow oil which was used directly in the next step; R_f = 0.35, broad (2:1 hexanes:EtOAc); ^1H NMR (300 MHz, CDCl_3) δ 6.69 (app t, J = 1.9 Hz, 1H), 5.89–5.62 (m, 1H), 5.11–4.99 (m, 2H), 2.68–2.47 (m, 2H), 2.26–2.09 (m, 2H), 1.91 (ddd, J = 13.0, 8.2, 7.0 Hz, 1H), 1.69 (ddd, J = 13.0, 8.2, 6.2 Hz, 1H), 1.10 (s, 3H); ^{13}C NMR (75 MHz, CDCl_3) δ 170.7, 154.3, 134.8, 133.9, 117.8, 49.8, 45.2, 36.3, 30.3, 25.5; IR (Neat Film NaCl) 3076, 3004, 2956, 2926, 2865, 2610, 1687, 1634, 1454, 1424, 1374, 1348, 1306, 1280, 1216, 1180, 1083, 995, 915, 745, 720 cm^{-1} ; HRMS (EI+) m/z calc'd for $\text{C}_7\text{H}_9\text{O}_2$ $[\text{M}-\text{C}_3\text{H}_5]^+$: 125.0603; found 125.0629; $[\alpha]_D^{25.0}$ +1.43 (c 0.80, CHCl_3 , 88.0% ee).

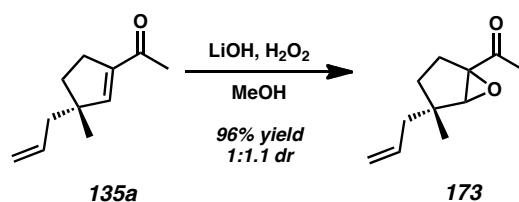
Amide 171. A 50 mL flask with magnetic stir bar was charged with carboxylic acid **197** (202.7 mg, 1.22 mmol, 1.00 equiv) and anhydrous CH_2Cl_2 (4.0 mL). To the vigorously stirred reaction was added 1,1'-carbonyldiimidazole (217 mg, 1.34 mmol, 1.10 equiv) in a portionwise manner. After 15 min, anhydrous *N,O*-dimethylhydroxylamine hydrochloride (143 mg, 1.46 mmol, 1.20 equiv) was added portionwise. The reaction became turbid after several min. After 21 h, an additional portion of *N,O*-dimethylhydroxylamine hydrochloride (14.3 mg, 0.146 mmol, 0.12 equiv) was added. At 23.5 h, the reaction was transferred to a separatory funnel, washed with 0.25 M HCl (2 x 2 mL), sat. aqueous NaHCO_3 , and brine. The combined organic phases were dried over Na_2SO_4 , filtered, and concentrated under reduced pressure. The residue was purified by flash column chromatography (SiO_2 , 3 x 25 cm, 4:1→3:1 hexanes:EtOAc) to afford amide **171** as a clear oil (196.7 mg, 0.94 mmol, 77% yield over 2 steps); R_f = 0.41 (2:1

hexanes:EtOAc); ^1H NMR (300 MHz, CDCl_3) δ 6.26 (app t, $J = 1.9$ Hz, 1H), 5.87–5.68 (m, 1H), 5.09–4.97 (m, 2H), 3.63 (s, 3H), 3.23 (s, 3H), 2.77–2.55 (m, 2H), 2.21–2.11 (m, 2H), 1.83 (ddd, $J = 12.8, 8.3, 6.4$ Hz, 1H), 1.62 (ddd, $J = 12.7, 8.4, 6.0$ Hz, 1H), 1.08 (s, 3H); ^{13}C NMR (75 MHz, CDCl_3) δ 167.5, 147.0, 135.4, 135.3, 117.4, 61.2, 49.4, 45.4, 35.9, 33.3, 32.9, 25.6; IR (Neat Film NaCl) 3584, 3401, 3078, 2954, 2930, 2864, 1641, 1609, 1454, 1441, 1414, 1378, 1329, 1198, 1177, 1152, 1105, 1043, 997, 969, 914, 812, 723 cm^{-1} ; HRMS (EI+) m/z calc'd for $\text{C}_{12}\text{H}_{20}\text{NO}_2$ $[\text{M}+\text{H}]^+$: 210.1494; found 210.1498; $[\alpha]_{\text{D}}^{25.0} +1.41$ (c 0.98, CHCl_3 , 88.0% ee).



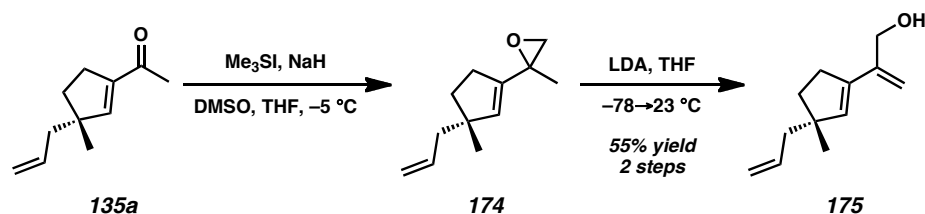
Divinylketone 172. A 25 mL round-bottomed flask with magnetic stir bar was charged with amide **171** (97.0 mg, 0.46 mmol, 1.00 equiv), evacuated/backfilled with N_2 (3 cycles, 5 min evacuation per cycle), dissolved in THF (3.0 mL), and cooled to $-15\text{ }^\circ\text{C}$ using an ethylene glycol/ $\text{CO}_2(\text{s})$ bath. The yellow solution became cloudy. Vinylmagnesium bromide solution (1.38 mL, 1.0 M in THF, 1.38 mmol, 3.00 equiv) was added dropwise. The solution was maintained at $-15\text{ }^\circ\text{C}$ for 20 min before the flask was allowed to warm to ambient temperature. The reaction was quenched by addition into sat. aqueous NH_4Cl (2.0 mL) using positive pressure cannulation. The mixture was extracted with Et_2O (3 x 10 mL), dried over Na_2SO_4 , filtered, and concentrated under reduced pressure. The residue was purified by flash column chromatography (SiO_2 , 2 x 25 cm, 0% \rightarrow 1% \rightarrow 2% \rightarrow 3% Et_2O in hexanes) to afford divinylketone **172** (36.2 mg, 0.21

mmol, 45% yield) as a pale yellow liquid; $R_f = 0.68$ (4:1 hexanes:EtOAc); ^1H NMR (300 MHz, CDCl_3) δ 6.88 (dd, $J = 17.1, 10.5$ Hz, 1H), 6.53 (app t, $J = 1.7$ Hz, 1H), 6.28 (dd, $J = 17.1, 1.9$ Hz, 1H), 5.85–5.65 (m, 1H), 5.69 (dd, $J = 10.5, 1.9$ Hz, 1H), 5.11–4.99 (m, 2H), 2.76–2.50 (m, 2H), 2.29–2.09 (m, 2H), 1.87 (ddd, $J = 12.9, 8.2, 6.8$ Hz, 1H), 1.67 (ddd, $J = 12.9, 8.3, 6.3$ Hz, 1H), 1.13 (s, 3H); ^{13}C NMR (75 MHz, CDCl_3) δ 188.9, 152.1, 143.7, 134.8, 132.6, 127.7, 117.8, 50.3, 45.3, 35.8, 30.1, 25.5; IR (Neat Film NaCl) 3584, 3400, 3078, 2955, 2927, 2866, 1622, 1606, 1453, 1440, 1408, 1374, 1348, 1308, 1255, 1204, 1169, 1059, 981, 956, 915, 783 cm^{-1} ; HRMS (EI+) m/z calc'd for $\text{C}_9\text{H}_{11}\text{O}$ $[\text{M}-\text{C}_3\text{H}_5]^+$: 135.0846; found 135.0810; $[\alpha]_D^{25.0} +0.84$ (c 0.81, CHCl_3 , 88.0% ee).



Epoxide 173. A solution of acylcyclopentene **135a** (100 mg, 0.609 mmol, 1.00 equiv) in MeOH (6.1 mL) in a 25 mL round-bottom flask was treated with LiOH (7.3 mg, 0.30 mmol, 0.50 equiv) in one portion. Aqueous H_2O_2 (75.0 μL , 83.3 mg, 2.00 equiv, 50% in H_2O) was added dropwise. After 12 h of stirring at ambient temperature additional aqueous H_2O_2 (75.0 μL , 83.3 mg, 2.00 equiv, 50% in H_2O) was added. The reaction was stirred for an additional 8 h, diluted with CH_2Cl_2 (10 mL), sat. aqueous NaHCO_3 (1.0 mL), and water (1.0 mL). The phases were separated and the aqueous phase was extracted with CH_2Cl_2 . The combined organic phases were dried over Mg_2SO_4 , filtered, and concentrated carefully under reduced pressure. The crude product was purified by automated flash column chromatography using a Teledyne Isco CombiFlash R_f (SiO_2 , 12

g loading cartridge, 25 g column, linear gradient, 5%→30% Et₂O in pentane [15 min]) to afford epoxide **173** (106 mg, 0.588 mmol, 96% yield) as a colorless fragrant oil and as a 1.1:1 mixture of diastereomers; R_f = 0.54 (4:1 hexanes:EtOAc); ¹H NMR (400 MHz, CDCl₃) δ 5.90–5.68 (m, 2H), 5.14–5.01 (m, 4H), 3.32 (s, 1H), 3.30 (s, 1H), 2.35–2.21 (m, 4H), 2.07 (s, 3H), 2.07 (s, 3H), 2.05–1.99 (m, 2H), 1.96–1.85 (m, 2H), 1.54–1.49 (m, 1H), 1.33–1.29 (m, 2H), 1.20–1.16 (m, 1H), 1.13 (s, 3H), 0.91 (s, 3H); ¹³C NMR (100 MHz, CDCl₃) δ 205.8, 205.6, 134.7, 133.6, 118.4, 117.8, 70.3, 70.2, 69.4, 69.3, 42.7, 42.7, 42.4, 42.3, 41.3, 31.9, 31.4, 25.0, 24.8, 24.1, 21.7, 20.5; IR (Neat Film NaCl) 3072, 3002, 2958, 2878, 1706, 1642, 1459, 1444, 1419, 1397, 1360, 1325, 1286, 1261, 1115, 922, 856, 831 cm⁻¹; HRMS (MM: ESI-APCI+) m/z calc'd for C₁₁H₁₇ [M+H]⁺: 181.1223; found 181.1226; $[\alpha]_D^{25.0}$ –6.94 (*c* 1.40, CHCl₃, 88.0 % ee).

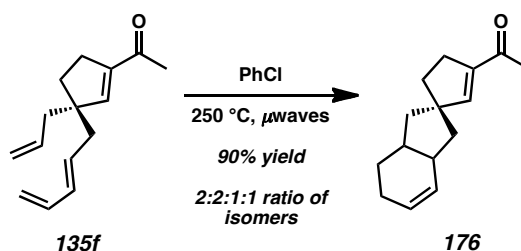


Allylic alcohol 174. NaH (36.5 mg, 0.91 mmol, 3.0 equiv, 60% w/w in mineral oil) was suspended in DMSO (1.2 mL) in a 25 mL round-bottom flask. After 20 min of stirring at ambient temperature, THF (3.7 mL) was added and the resulting mixture was cooled to –5 °C using a water/NaCl/ice bath. Me₃Si (192.3 mg, 0.95 mmol, 3.1 equiv) was dissolved in DMSO (1.2 mL) and added dropwise to the stirred reaction. After an additional 5 min of stirring, acylcyclopentene **135a** (50 mg, 0.30 mmol, 1.0 equiv) was added neat dropwise. After 1.5 h of stirring at –5 °C, the reaction was diluted with Et₂O (15 mL) and quenched by pouring the reaction over 10 g of ice. The phases were

separated and the aqueous layer was extracted with Et₂O (2 x 10 mL). The combined organic phases were washed with brine (10 mL), dried over MgSO₄, filtered, and concentrated carefully under reduced pressure, allowing for a film of ice to form on the outside of the flask, to give the volatile crude epoxide **174** as a colorless oil; R_f = 0.60 (4:1 hexanes:EtOAc); ¹H NMR (500 MHz, CDCl₃) mixture of two diastereomers, see Figure A1.259; ¹³C NMR (100 MHz, CDCl₃) mixture of two diastereomers, see Figure A1.260; IR (Neat Film NaCl) 3072, 3037, 2953, 2923, 2864, 1637, 1451, 1437, 1385, 1370, 1338, 1259, 1140, 1105, 1066, 994, 910, 856, 846, 806, 730 cm⁻¹; HRMS (APCI+) m/z calc'd for C₁₂H₁₉O [M+H]⁺: 179.1435; found 179.1430.

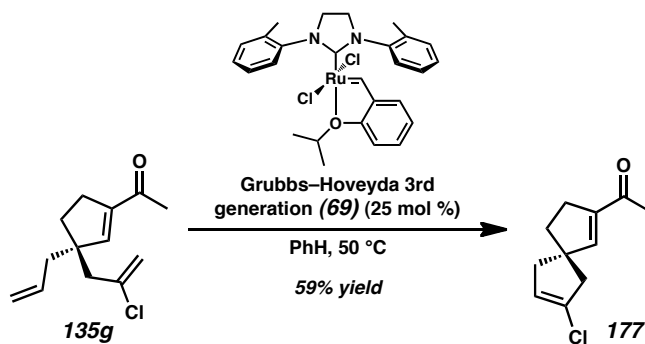
To a solution of diisopropylamine (0.11 mL, 0.76 mmol, 2.5 equiv) in THF (2.0 mL) in a 10 mL round-bottom flask at 0 °C was added *n*-BuLi (370 μL, 0.76 mmol, 2.05 M in cyclohexane, 2.5 equiv) dropwise over 10 min. After 15 min of stirring, the reaction was cooled to -78 °C using an acetone/CO₂(s) bath and crude epoxide **174** in THF (1.0 mL) was added dropwise using positive pressure cannulation. The cooling bath was allowed to warm to ambient temperature and the reaction was stirred for 18 h. The reaction was diluted with Et₂O (10 mL) and quenched by addition of a 50:50 (v/v) mixture of sat. aqueous NH₄Cl and water (2.0 mL each). The phases were separated and the aqueous phase was extracted with Et₂O (2 x 10 mL). The combined organic phases were washed with brine (10 mL), dried over MgSO₄, filtered, and concentrated carefully under reduced pressure, allowing for a film of ice to form on the outside of the flask, to afford a pale yellow oil. The residue was purified by flash column chromatography (SiO₂, 1 x 22 cm, 20% Et₂O in pentane) to afford allylic alcohol **175** (29.9 mg, 0.17 mmol, 55% yield over 2 steps) as a colorless oil; R_f = 0.25 (4:1 hexanes:EtOAc); ¹H NMR (500 MHz, CDCl₃)

δ 5.82–5.72 (m, 1H), 5.60 (dd, $J = 1.7, 1.7$ Hz, 1H), 5.22 (app q, $J = 1.4$ Hz, 1H), 5.05–5.04 (m, 1H), 5.04–5.01 (m, 1H), 5.01–4.99 (m, 1H), 4.33 (br s, 2H), 2.58–2.45 (m, 2H), 2.17–2.08 (m, 2H), 1.82 (ddd, $J = 12.7, 8.8, 5.9$ Hz, 1H), 1.62 (ddd, $J = 12.7, 8.8, 5.8$ Hz, 1H), 1.51 (br s, 1H), 1.06 (s, 3H); ^{13}C NMR (125 MHz, CDCl_3) δ 143.6, 139.1, 136.0, 135.9, 116.9, 111.9, 64.3, 49.3, 46.2, 35.9, 32.0, 26.4; IR (Neat Film NaCl) 3325, 3071, 3032, 2948, 2859, 1639, 1600, 1451, 1437, 1414, 1370, 1320, 1226, 1194, 1078, 1029, 994, 910, 848 cm^{-1} ; HRMS (MM: ESI-APCI+) m/z calc'd for $\text{C}_{12}\text{H}_{17}$ $[\text{M}-\text{OH}]^+$: 161.1325; found 161.1324; $[\alpha]_{\text{D}}^{25.0} +17.59$ (c 1.38, CHCl_3 , 88.0% ee).



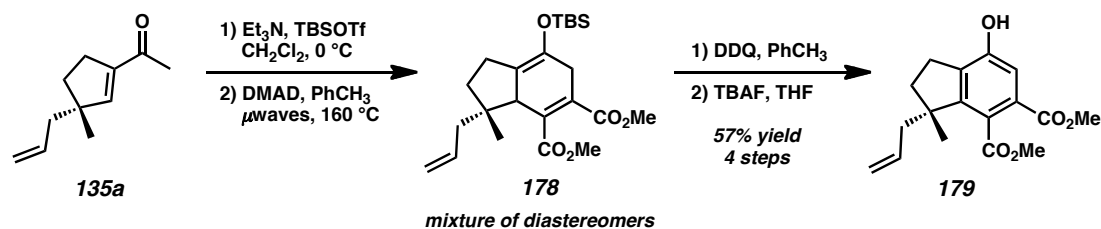
Cyclohexene 176. Acylcyclopentene **135f** (25.2 mg, 0.12 mmol, 1.00 equiv) was added to a 2.0–5.0 mL microwave vial with magnetic stir bar and sealed with a septum-fitted crimp cap. Chlorobenzene (5 mL) was added via syringe. The clear, colorless solution was subjected to microwave irradiation in a Biotage Initiator microwave reactor (temperature: 250 °C, sensitivity: low). After 2 h of irradiation, the vial was uncapped and the solvent was removed under reduced pressure. The yellow residue was purified by flash column chromatography (SiO_2 , 1.5 x 15 cm, 15:1 hexanes: Et_2O) to afford cyclohexene **176** as a yellow oil (22.5 mg, 0.104 mmol, 90% yield); $R_f = 0.65$ (4:1 hexanes: EtOAc); ^1H NMR (500 MHz, CDCl_3) mixture of four diastereomers (2:2:1:1), see Figure A1.265; ^{13}C NMR (125 MHz, CDCl_3) mixture of four diastereomers, see

Figure A1.266; IR (Neat Film NaCl) 3014, 2921, 2855, 1666, 1611, 1448, 1437, 1369, 1339, 1303, 1268, 1190, 1093, 1075, 1051, 1037, 1024, 935, 868, 798, 733, 703 cm^{-1} ; HRMS (EI+) m/z calc'd for $\text{C}_{15}\text{H}_{20}\text{O}$ $[\text{M}]^{+}$: 216.1514; found 216.1518; $[\alpha]_{\text{D}}^{25.0} -15.57$ (c 1.01, CHCl_3 , 88.0% ee).



Spirocycle 177. A 2-neck flask fitted with rubber septum and reflux condenser under N_2 was charged with Grubbs-Hoveyda 3rd generation catalyst (2.2 mg, 0.035 mmol, 6.1 mol %). Dry degassed benzene (4 mL, sparged with N_2 for 1 h immediately before use) was added to give a pale green solution. The flask was evacuated/backfilled with N_2 (3 cycles, 5 min evacuation per cycle). Acylcyclopentene **135g** (14.2 mg, 0.063 mmol, 1.0 equiv) in dry, degassed benzene (4 mL) under N_2 was added to the catalyst solution using positive pressure cannulation. The flask was rinsed with benzene (2 mL) and washes were added into the catalyst solution. The reaction was immersed in a preheated 50 °C oil bath and stirred for 44 h. An additional portion of Grubbs-Hoveyda 3rd generation catalyst (4.4 mg, 0.070 mmol, 12.2 mol %) in degassed benzene (2 mL) was added into the reaction using positive pressure cannulation. After stirring for an additional 15 h, a third portion of Grubbs-Hoveyda 3rd generation catalyst (2.2 mg, 0.035 mmol, 6.1 mol %) in degassed benzene (2 mL) was added into the reaction using positive pressure

cannulation. After 31 h, the reaction was treated with several drops of ethyl vinyl ether and allowed to cool to ambient temperature. The solution was diluted with Et₂O (15 mL) and filtered through a short silica gel plug (2 x 10 cm, Et₂O). The orange filtrate was purified by flash column chromatography (SiO₂, 2 x 25 cm, 1%→3%→5%→6.5% Et₂O in hexanes) to give volatile spirocycle **177** (7.3 mg, 0.0376 mmol, 59% yield); *R_f* = 0.49 (4:1 hexanes:EtOAc); ¹H NMR (500 MHz, CDCl₃) δ 6.61 (app t, *J* = 1.7 Hz, 1H), 5.64 (app p, *J* = 2.2 Hz, 1H), 2.66 (ddd, *J* = 16.2, 4.5, 2.1 Hz, 1H), 2.62–2.53 (m, 3H), 2.51 (ddd, *J* = 16.2, 4.6, 2.4 Hz, 1H), 2.43 (ddd, *J* = 16.3, 4.6, 2.4 Hz, 1H), 2.31 (s, 3H), 2.09–1.95 (m, 2H); ¹³C NMR (125 MHz, CDCl₃) δ 197.3, 150.2, 144.2, 130.7, 125.2, 56.2, 49.7, 44.3, 39.4, 29.6, 26.8; IR (Neat Film NaCl) 2929, 2845, 1726, 1668, 1616, 1436, 1370, 1340, 1314, 1276, 1193, 1079, 1052, 990, 966, 936, 905, 866, 822, 804 cm⁻¹; HRMS (EI+) *m/z* calc'd for C₁₁H₁₃OCl [M]⁺: 196.0655; found 196.0655; [α]_D^{25.0} –19.80 (*c* 0.53, CHCl₃, 88.0% ee).



Phenol 179. A 15 mL flask with magnetic stir bar was charged with acylcyclopentene **135a** (50 mg, 0.274 mmol, 1.00 equiv) and anhydrous CH₂Cl₂ (3.0 mL). The flask was cooled to 0 °C and Et₃N (152.8 μL, 1.096 mmol, 4.00 equiv) was added, followed by dropwise addition of TBSOTf (125.8 μL, 0.548 mmol, 2.00 equiv). The reaction became a pale yellow solution. After 1 h of stirring at 0 °C, the reaction was quenched by the addition of sat. aqueous NaHCO₃ and slowly allowed to warm to ambient temperature.

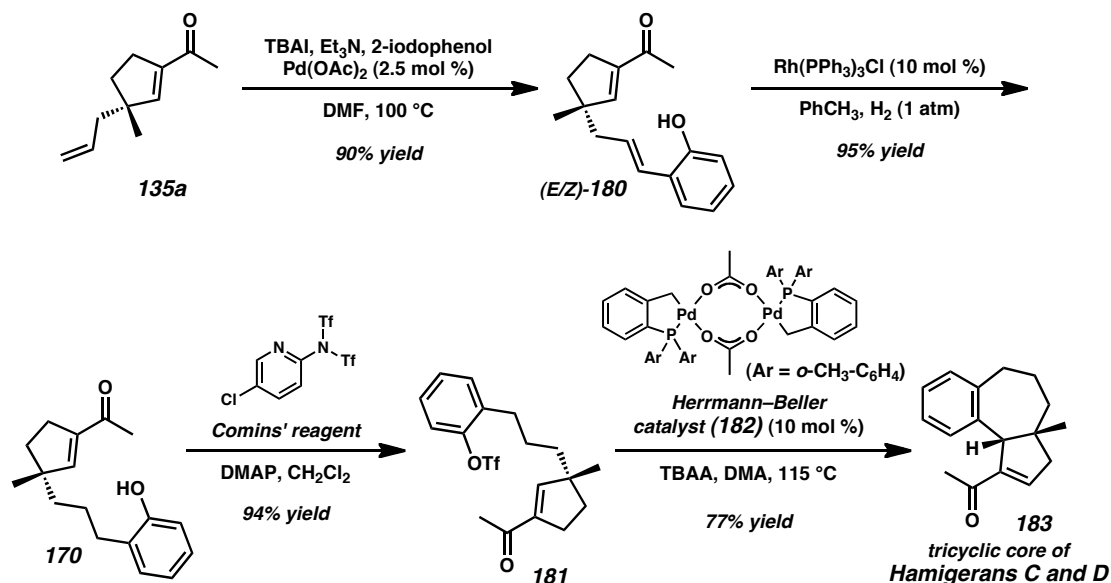
The mixture was extracted with CH_2Cl_2 (3 x 10 mL) and the combined organics were dried over Na_2SO_4 , filtered, and concentrated under reduced pressure. The residue was filtered through a silica gel plug (2 x 3 cm, 5:1 H:Et₂O) and concentrated under reduced pressure to give crude silyl enol ether as a pale yellow oil. $R_f = 0.79$ (10:1 hexanes:EtOAc).

The silyl enol ether was added to a 2.0–5.0 mL microwave vial with magnetic stir bar and sealed with a septum-fitted crimp cap. Toluene (5 mL) was added, followed by dimethyl acetylenedicarboxylate (101 μL , 0.822 mmol, 3.00 equiv). The clear, colorless solution was subjected to microwave irradiation in a Biotage Initiator microwave reactor (temperature: 160 °C, sensitivity: low). After 2.5 h of irradiation, the vial was uncapped and solvent was removed under reduced pressure. The yellow residue was purified by flash column chromatography (SiO_2 , 3 x 25 cm, 15:1→10:1→4:1→2:1 hexanes:EtOAc) to afford siloxydiene **178** as a mixture of diastereomers. $R_f = 0.31$ (10:1 hexanes:EtOAc).

A 20 mL scintillation vial with magnetic stir bar was charged with siloxydiene **178** and toluene (3.0 mL). DDQ (63.5 mg, 0.280 mmol, 1.02 equiv) was added portionwise. Upon complete addition, the solution became a turbid red suspension. After 2 h, the reaction was diluted with CH_2Cl_2 and filtered through a Celite plug (2 x 3 cm, CH_2Cl_2). The clear yellow solution was concentrated under reduced pressure. The residue was purified by flash column chromatography (SiO_2 , 2 x 25 cm, 20:1→15:1→10:1→4:1→2:1 hexanes:EtOAc) to afford the intermediate silyl aryl ether. $R_f = 0.31$ (10:1 hexanes:EtOAc).

A 20 mL scintillation vial with magnetic stir bar was charged with silyl aryl ether. The vial was evacuated, and backfilled with N_2 . Anhydrous THF (3 mL) was added and

a TBAF solution (300 μ L, 1.0 M in THF) was added dropwise, giving a bright red solution. After 10 min, the reaction was quenched by the addition of sat. aqueous NH_4Cl (600 μ L) and H_2O (600 μ L). The mixture was stirred vigorously for 20 min and extracted with Et_2O (3 x 5 mL). The combined organics were dried over Na_2SO_4 , filtered, and concentrated under reduced pressure. The residue was purified by flash column chromatography (SiO_2 , 2 x 25 cm, 5:1 \rightarrow 4:1 hexanes:EtOAc) to afford phenol **179** as a pale yellow oil (52.6 mg, 0.173 mmol, 57% yield over 4 steps); R_f = 0.11 (2:1 hexanes:EtOAc); ^1H NMR (300 MHz, CDCl_3) δ 7.30 (s, 1H), 5.89 (br s, J = 1.9 Hz, 1H), 5.66 (dddd, J = 17.3, 10.2, 7.9, 7.9 Hz, 1H), 5.09–4.91 (m, 2H), 3.88 (s, 3H), 3.83 (s, 3H), 2.76 (t, J = 7.3 Hz, 2H), 2.47–2.26 (m, 2H), 2.24–2.08 (ddd, J = 12.0, 7.0, 7.0 Hz, 1H), 1.85–1.70 (ddd, J = 12.7, 7.6, 7.6 Hz, 1H), 1.26 (s, 3H); ^{13}C NMR (75 MHz, CDCl_3) δ 170.4, 166.7, 152.5, 150.0, 135.8, 135.3, 128.3, 124.0, 117.7, 115.4, 52.7, 52.5, 49.4, 44.1, 38.3, 26.1, 25.6; IR (Neat Film NaCl) 3401, 3075, 2953, 2871, 1723, 1639, 1588, 1435, 1418, 1376, 1330, 1311, 1258, 1192, 1175, 1142, 1047, 995, 964, 916, 884, 857, 794, 769, 738, 719 cm^{-1} ; HRMS (EI+) m/z calc'd for $\text{C}_{17}\text{H}_{20}\text{O}_5$ $[\text{M}]^+$: 304.1311; found 304.1317; $[\alpha]_D^{25.0}$ –45.63 (c 0.91, CHCl_3 , 88.0% ee).

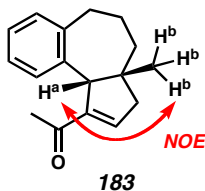


Phenol 180. DMF (1.52 mL) was sparged with N₂ in a 25 mL Schlenk flask for 1 h. Et₃N (0.849 mL, 6.09 mmol, 5.0 equiv), TBAI (450 mg, 1.22 mmol, 1.0 equiv) and 2-iodophenol (282.2 mg, 1.28 mmol, 1.05 equiv) were added, followed by Pd(OAc)₂ (6.84 mg, 0.030 mmol, 2.5 mol %). The flask was carefully evacuated/backfilled with N₂ (3 cycles, 1 min evacuation per cycle) followed by addition of acylcyclopentene **135a** (200 mg, 1.22 mmol, 1.0 equiv). The suspension was immersed in an oil bath at 100 °C. The reaction turned orange within 15 min of stirring. After 5 h of stirring, the reaction was allowed to cool to ambient temperature, diluted with EtOAc (10 mL), and poured into aqueous HCl (10 mL, 1.0 M). The phases were separated and the aqueous phase was extracted with EtOAc (2 x 10 mL). The combined organic phases were washed with brine (10 mL), dried over MgSO₄, filtered, and concentrated under reduced pressure. The crude oil was purified by flash column chromatography using a Teledyne Isco CombiFlash R_f system (SiO₂, 12 g loading cartridge, 40 g column, linear gradient, 5%→30% EtOAc in hexanes [25 min]) to afford styrenyl phenol **180** as a mixture of

olefin isomers (283.0 mg, 1.10 mmol, 90% yield) as a colorless oil. $R_f = 0.17$ (4:1 hexanes:EtOAc).

Rh(PPh₃)₃Cl (22.2 mg, 0.024 mmol, 0.10 equiv) was weighed out in a glove box and added to a long reaction tube with magnetic stir bar. Styrenyl phenol **180** (61.5 mg, 0.240 mmol, 1.0 equiv) was dissolved in toluene (4.8 mL) and added to the reaction tube using positive pressure cannulation. H₂ was bubbled through the suspension for 5 min and the reaction tube was fitted with a balloon containing H₂ (1 atm). The reaction was stirred for an additional 6 h at which point TLC analysis indicated complete conversion of the starting material. The resulting clear orange reaction mixture was adsorbed onto a 12 g Isco loading cartridge and purified by flash column chromatography using a Teledyne Isco CombiFlash R_f system (SiO₂, 12 g loading cartridge, 24 g column, linear gradient, 5%→50% Et₂O in hexanes [40 min]) to afford phenol **170** (58.9 mg, 0.228 mmol, 95% yield) as a pale yellow oil; $R_f = 0.18$ (4:1 hexanes:EtOAc); ¹H NMR (300 MHz, CDCl₃) δ 7.13–7.04 (m, 2H), 6.87 (t, $J = 7.4$ Hz, 1H), 6.75 (d, $J = 7.9$ Hz, 1H), 6.46 (app t, $J = 1.7$ Hz, 1H), 4.82 (bs, 1H), 2.60 (t, $J = 7.3$ Hz, 2H), 2.56–2.50 (m, 2H), 2.29 (s, 3H), 1.87–1.75 (m, 1H), 1.71–1.42 (m, 5H), 1.09 (s, 3H); ¹³C NMR (125 MHz, CDCl₃) δ 197.9, 153.6, 152.8, 143.4, 130.4, 128.4, 127.3, 120.9, 115.3, 50.1, 40.8, 36.2, 30.8, 29.7, 26.8, 25.8, 25.5; IR (Neat Film NaCl) 3344, 3054, 3039, 2951, 2863, 1651, 1610, 1592, 1507, 1455, 1377, 1365, 1313, 1272, 1238, 1179, 1155, 1127, 1106, 1042, 907, 853, 752 cm⁻¹; HRMS (MM: ESI-APCI+) m/z calc'd for C₁₇H₂₃O₂ [M+H]⁺: 259.1693; found 259.1691; $[\alpha]_D^{25.0} +28.73$ (c 0.74, CHCl₃, 88.0% ee).

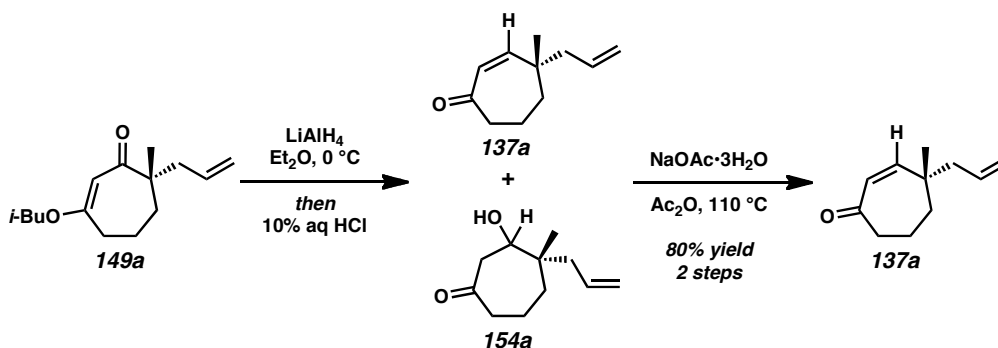
Triflate 181. To a solution of phenol **170** (104.2 mg, 0.40 mmol, 1.00 equiv) in CH₂Cl₂ (8.0 mL) in a 20 mL vial was added DMAP (97.8 mg, 0.80 mmol, 2.0 equiv) in one portion, followed by *N,N*-Bis(trifluoromethylsulfonyl)-5-chloro-2-pyridylamine (172.8 mg, 0.44 mmol, 1.1 equiv). After 15 min of stirring at ambient temperature, TLC revealed full conversion of phenol **170**. The reaction mixture was adsorbed onto a 12 g Isco loading cartridge and purified by flash column chromatography using a Teledyne Isco CombiFlash R_f system (SiO₂, 12 g loading cartridge, 40 g column, linear gradient, 5→20% EtOAc in hexanes [25 min]) to afford triflate **181** (146.2 mg, 0.374 mmol, 94% yield) as a clear, colorless oil; *R*_f = 0.44. (4:1 hexanes:EtOAc); ¹H NMR (500 MHz, CDCl₃) δ 7.32–7.30 (m, 2H), 7.28 (dd, *J* = 8.5, 4.0 Hz, 1H), 7.24 (dm, *J* = 7.8 Hz, 1H), 6.44 (app t, *J* = 1.8 Hz, 1H), 2.69 (t, *J* = 7.7 Hz, 2H), 2.61–2.46 (m, 2H), 2.29 (s, 3H), 1.80 (ddd, *J* = 13.0, 8.7, 6.5 Hz, 1H), 1.66 (ddd, *J* = 11.8, 8.0, 5.2 Hz, 1H), 1.64–1.45 (m, 3H), 1.50 (ddd, *J* = 11.4, 7.5, 5.1 Hz, 1H), 1.10 (s, 3H); ¹³C NMR (125 MHz, CDCl₃) δ 197.6, 152.0, 148.1, 143.7, 135.1, 131.3, 128.5, 128.0, 121.5, 118.7 (q, *J* = 320 Hz, 1C), 50.0, 40.7, 36.1, 30.8, 29.8, 26.8, 25.8, 25.7; IR (Neat Film NaCl) 3032, 2958, 2868, 1671, 1617, 1486, 1454, 1420, 1365, 1303, 1251, 1217, 1140, 1100, 1073, 893, 814, 767 cm⁻¹; HRMS (MM: ESI-APCI+) *m/z* calc'd for C₁₈H₂₂F₃O₄S [M+H]⁺: 391.1188; found 391.1193; [α]_D^{25.0} +22.00 (c 1.31, CHCl₃, 88.0% ee).



Acylcyclopentene 183. To a solution of triflate **181** (30.0 mg, 0.077 mmol, 1.0 equiv) in dry DMA (1.54 mL) in a 4 dram vial was added TBAA (57.9 mg, 0.19 mmol, 2.5 equiv, stored and weighed out in a glove box). The resulting clear, colorless solution was degassed by bubbling Ar through the solution for 1 h. Herrmann's catalyst⁵⁷ (7.2 mg, 7.7 μ mol, 0.10 equiv) was placed in a reaction tube which was subsequently evacuated/backfilled with Ar (3 cycles, 1 min evacuation per cycle). The solution containing triflate **181** was added to the catalyst using positive pressure cannulation. The resulting pale green-yellow solution was immersed in an oil bath at ambient temperature and heated to 115 °C. After 2 h of stirring, the reaction was allowed to cool to ambient temperature, diluted with EtOAc (10 mL), and poured into aqueous HCl (1.0 M, 5.0 mL). The phases were separated and the aqueous phase was extracted with EtOAc (10 mL). The combined organics were washed with brine (5.0 mL), dried over MgSO₄, filtered, and concentrated under reduced pressure. The crude product was purified by flash column chromatography using a Teledyne Isco CombiFlash R_f system (SiO₂, 2.5 g loading cartridge, 4 g column, multi-step gradient, hold 5% [10 min]→hold 10% [4 min]→hold 20% [3 min]→hold 60% EtOAc in hexanes [3 min]) to afford acylcyclopentene **183** (14.3 mg, 0.0595 mmol, 77% yield, 62% yield over 4 steps) as a pale yellow solid. The relative stereochemistry was assigned based on strong NOE interaction between H^a and H^b; R_f = 0.46 (4:1 hexanes:EtOAc); ¹H NMR (500 MHz, CDCl₃) δ 7.17–7.06 (m, 3H), 6.95 (app t, *J* = 2.4 Hz, 1H), 6.63 (bd, *J* = 6.2 Hz, 1H), 3.86

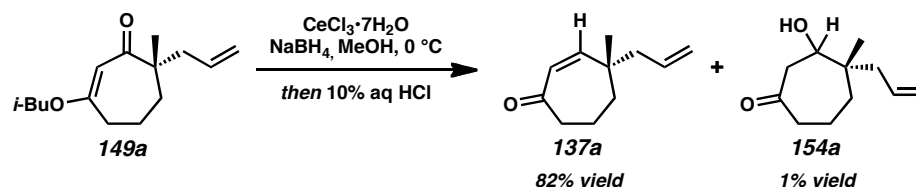
(s, 1H), 2.92–2.84 (m, 1H), 2.66 (app dd, $J = 13.5, 7.9$ Hz, 1H), 2.41 (s, 3H), 2.32–2.18 (m, 2H) 1.84 (app ddt, $J = 13.5, 7.7, 5.6$ Hz, 1H), 1.58–1.43 (m, 1H), 1.30 (ddd, $J = 14.0, 5.1, 2.3$ Hz, 1H), 1.18 (s, 3H), 0.85 (app dt, $J = 13.5, 5.6$ Hz, 1H); ^{13}C NMR (125 MHz, CDCl_3) δ 196.7, 146.2, 144.6, 139.6, 139.2, 128.5, 126.7, 126.2, 125.0, 55.5, 48.4, 43.9, 34.1, 30.6, 26.9, 25.9, 21.4; IR (Neat Film NaCl) 3062, 3012, 2933, 2893, 2859, 1659, 1617, 1476, 1456, 1446, 1370, 1278, 1266, 1244, 1199, 1123, 997, 935, 794, 757, 752, 730 cm^{-1} ; HRMS (MM: ESI-APCI+) m/z calc'd for $\text{C}_{17}\text{H}_{21}\text{O}$ $[\text{M}+\text{H}]^+$: 241.1587; found 241.1591; $[\alpha]_{\text{D}}^{25.0} +3.88$ (c 1.43, CHCl_3 , 88.0% ee).

2.10.2.12 REVISED APPROACH TO THE REDUCTION/REARRANGEMENT AND ORGANOMETALLIC ADDITION/REARRANGEMENT OF **149a**



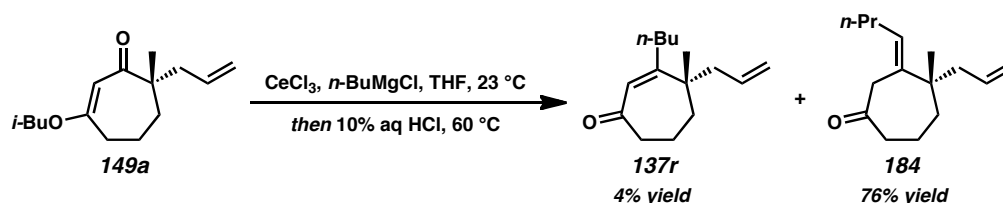
Cycloheptenone 137a. A round-bottom flask charged with vinylogous ester **149a** (367.0 mg, 1.55 mmol, 1.00 equiv) and THF (5 mL, 0.3 M) was cooled in a $0\text{ }^\circ\text{C}$ ice/water bath and LiAlH_4 (34.0 mg, 0.90 mmol, 0.58 equiv) was added. After 25 min of stirring, the reaction was quenched at $0\text{ }^\circ\text{C}$ with the addition of aqueous HCl (10 mL, 10% w/w) and transferred to a separatory funnel where the aqueous phase was extracted with EtOAc (3 x 10 mL). The combined organics were dried over Na_2SO_4 , filtered, and concentrated

under reduced pressure. To the resulting crude oil was added Ac_2O (3.8 mL) and $\text{NaOAc}\cdot 3\text{H}_2\text{O}$ (1.28 g, 9.43 mmol, 6.08 equiv) and the mixture was lowered into a preheated oil bath (110 °C). After 15 h of heating, the reaction was allowed to cool to ambient temperature and quenched with K_2CO_3 (5.59 g, 40.5 mmol) and water (10 mL). After an additional 30 min of stirring, the solution was transferred to a separatory funnel where the aqueous phase was extracted with EtOAc (4 x 10 mL). The combined organics were dried over Na_2SO_4 , filtered, and concentrated under reduced pressure. The crude oil was purified by flash chromatography (SiO_2 , 2 x 16 cm, 20:1 hexanes:EtOAc) to afford cycloheptenone **137a** (203.9 mg, 1.24 mmol, 80% yield) as a pale yellow oil. (For characterization data, see p. 155–155).



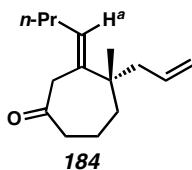
Cycloheptenone 137a and β -Hydroxyketone 154a. A 100 mL round-bottom flask with magnetic stir bar was charged with vinylogous ester **149a** (186.8 mg, 0.79 mmol, 1.00 equiv) and anhydrous MeOH (14 mL). The solution was cooled to 0 °C (water/ice bath). $\text{CeCl}_3\cdot 7\text{H}_2\text{O}$ (294.5 mg, 0.79 mmol, 1.00 equiv) was added in one portion and the mixture was stirred for 5 min. Portionwise addition of NaBH_4 (89.7 mg, 2.37 mmol, 3.00 equiv) at 0 °C led to the evolution of gas and a turbid solution that became clearer after several minutes. TLC analysis indicated that no starting material remained after 2 min. Consequently, the reaction was quenched by dropwise addition of aqueous HCl (2 mL, 10% w/w) at 0 °C. After an additional 10 min of stirring, the reaction was diluted with

CH₂Cl₂ (60 mL) and H₂O (2 mL). The layers were separated. The aqueous layer was extracted with CH₂Cl₂ (6 x 5 mL). The combined organic layers were washed with sat. aqueous NaHCO₃ (2 x 5 mL) and brine (2 x 5 mL), dried over Na₂SO₄, filtered, and evaporated to give a pale yellow oil. The crude mixture was purified using flash chromatography (SiO₂, 2 x 25 cm, 20:1→15:1→3:1 hexanes:EtOAc) to afford volatile enone **137a** (106.9 mg, 0.645 mmol, 82% yield) as a pale yellow oil and β-hydroxyketone **154a** as a mixture of diastereomers (1.4 mg, 0.0077 mmol, 1% yield, 3.5:1 dr) as a colorless oil. (For characterization data of **137a** and **154a**, see p. 155–155).



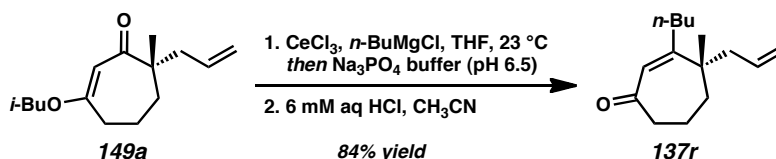
Cycloheptenone 137r and Cycloheptenone Isomer 184. An oven dried 15 mL round-bottom flask equipped with a magnetic stir bar was cycled into a glove box. The flask was loaded with anhydrous cerium chloride (130.4 mg, 0.53 mmol, 2.49 equiv), fitted with a septum, removed from the glove box, and connected to an argon-filled Schlenk manifold. A portion of THF (5.5 mL) was added, rinsing the cerium chloride to the bottom of the flask. As the resulting thick white slurry was stirred, a solution of *n*-butylmagnesium chloride (340 μL, 1.89 M in THF, 0.64 mmol, 3.03 equiv) was added and the mixture turned pale yellow. After 45 min of stirring, neat vinylogous ester **149a** (50.2 mg, 0.21 mmol, 1.00 equiv) was added to the flask. The slurry maintained the yellow color with the addition. TLC analysis indicated that no starting material remained after 5 min. After an additional 10 min of stirring, the reaction was quenched with

aqueous HCl (1 mL, 10% w/w) and lowered into a preheated oil bath (60 °C). After 17 h, the yellow suspension was removed from the bath, cooled to ambient temperature, and transferred to a separatory funnel where the aqueous phase was extracted four times with Et₂O. The combined organics (75 mL) were dried over MgSO₄, filtered, and concentrated under reduced pressure. The crude oil was purified by flash chromatography (SiO₂, 1 x 27 cm, 100% hexanes→2%→10% EtOAc in hexanes) to afford moderately contaminated cycloheptenone **137r** and pure alkene isomer **184** (35.4 mg, 0.16 mmol, 76% yield) as an orange oil. Additional purification by flash chromatography (SiO₂, 1 x 27 cm, 100% hexanes→2%→5% EtOAc in hexanes) furnished cycloheptenone **137r** (1.7 mg at 95% purity, 0.0076 mmol, 4% yield) as a yellow oil. (For characterization data of **137r**, see p. 178).



Cycloheptenone Isomer 184. R_f = 0.76 (30% EtOAc in hexanes); The relative alkene stereochemistry was assigned based on NOE interactions of H^a proton; ¹H NMR (500 MHz, CDCl₃) δ 5.66 (dddd, J = 16.9, 10.6, 7.9, 6.6 Hz, 1H), 5.43 (t, J = 7.1 Hz, 1H), 5.03–4.97 (m, 2H), 3.20 (d, J = 14.6 Hz, 1H), 3.13 (d, J = 14.6 Hz, 1H), 2.47–2.38 (m, 1H), 2.36–2.26 (m, 2H), 2.15–1.95 (m, 3H), 1.82–1.69 (m, 2H), 1.66–1.58 (m, 1H), 1.58–1.50 (m, 1H), 1.40–1.32 (m, 2H), 1.07 (s, 3H), 0.88 (t, J = 7.4 Hz, 3H); ¹³C NMR (125 MHz, CDCl₃) δ 210.0, 136.2, 135.1, 130.0, 117.2, 44.8, 43.3, 43.3, 41.8, 41.1, 30.2, 25.0, 22.9, 19.6, 13.9; IR (Neat Film NaCl) 3074, 3042, 2959, 2929, 2871, 1706, 1638, 1457,

1436, 1378, 1351, 1302, 1262, 1231, 1163, 1098, 1069, 996, 953, 912, 805, 776, 729 cm^{-1} ; HRMS (EI+) m/z calc'd for $\text{C}_{15}\text{H}_{24}\text{O}_2$ $[\text{M}]^{+}$: 220.1827; found 220.1780; $[\alpha]_{\text{D}}^{25.0}$ -10.92 (c 0.76, CHCl_3 , 88.0% ee).

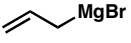
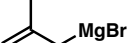
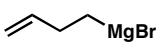
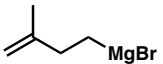
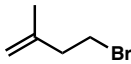
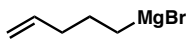
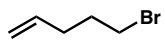
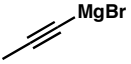
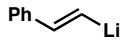
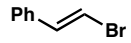
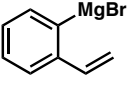
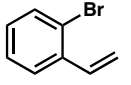
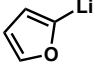

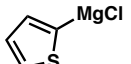
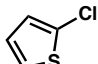


Cycloheptenone 137r. A 50 mL round-bottom flask equipped with a magnetic stir bar was cycled into a glove box. The flask was loaded with anhydrous cerium chloride (260.8 mg, 1.06 mmol, 2.50 equiv), fitted with a septum, removed from the glove box, and connected to an argon-filled Schlenk manifold. A portion of THF (8.5 mL) was added, rinsing the cerium chloride to the bottom of the flask. As the resulting thick white slurry was stirred, a solution of *n*-butylmagnesium bromide (680 μL , 1.87 M in THF, 1.27 mmol, 3.00 equiv) was added and the mixture turned grey. After 30 min of stirring, vinylogous ester **149a** (100.0 mg, 0.42 mmol, 1.00 equiv) was added neat from a Hamilton syringe and the needle was rinsed with a small portion of THF (2 mL; total THF added = 10.5 mL, 0.04 M). The color of the slurry initially transitioned to yellow with the vinylogous ester addition before turning back to grey. TLC analysis indicated that no starting material remained after 15 min. After an additional 10 min of stirring, the reaction was quenched with pH 6.5 Na_3PO_4 buffer (8 mL). A thick grey emulsion formed. The mixture was transferred to a separatory funnel where the aqueous phase was extracted four times with Et_2O . The combined organics (125 mL) were dried over MgSO_4 , filtered, and concentrated under reduced pressure. The crude oil was transferred to a 20 mL scintillation vial and concentrated under reduced pressure. A stir bar, CH_3CN

(1.0 mL), and 6 mM aqueous HCl (1.0 mL) were added to the vial. The resulting cloudy solution was stirred vigorously for 5 min before being transferred to a separatory funnel where the aqueous phase was extracted four times with Et₂O. The combined organics (100 mL) were dried over MgSO₄, filtered, and concentrated under reduced pressure. The crude oil was purified by flash chromatography (SiO₂, 3 x 30 cm, 100% hexanes→2%→5% EtOAc in hexanes) to afford cycloheptenone **137r** (82.4 mg, 0.35 mmol, 84% yield) as a pale yellow oil. (For characterization data of **137r**, see p. 178).

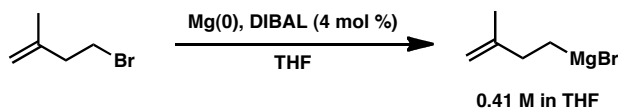
2.10.2.13 GRIGNARD AND ORGANOLITHIUM REAGENTS^a

Table 2.7. Sources of Grignard and Organolithium Reagents

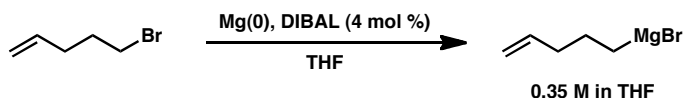
entry	reagent	molarity (M)	obtained from
1	 <chem>CC=C[Mg]Br</chem>	0.86 M in Et ₂ O	Sigma-Aldrich
2	 <chem>CC(C)=C[Mg]Br</chem>	0.39 M in THF	Sigma-Aldrich
3	 <chem>CCCC=C[Mg]Br</chem>	0.44 M in THF	Sigma-Aldrich
4	 <chem>CC(C)CC=C[Mg]Br</chem>	0.41 M in THF	 <chem>CC(C)CCBr</chem>
5	 <chem>CCCCC=C[Mg]Br</chem>	0.35 M in THF	 <chem>CCCCCBr</chem>
6	 <chem>C#C[Mg]Br</chem>	0.25 M in THF	Sigma-Aldrich
7	 <chem>c1ccccc1/C=C/[Li]</chem>	N/A ^b	 <chem>c1ccccc1/C=C/Br</chem>
8	 <chem>c1ccccc1C=C[Mg]Br</chem>	0.40 M in THF	 <chem>c1ccccc1C=CBr</chem>
9	 <chem>c1ccoc1[Li]</chem>	N/A ^b	 <chem>c1ccoc1</chem>
10	 <chem>Cc1ccsc1[Mg]Cl</chem>	0.44 M in THF	 <chem>Cc1ccsc1Cl</chem>

^a Titrated using method of Love (see ref. 49). ^b Not titrated.

Grignard and Organolithium Reagents. Reagents were purchased from Sigma-Aldrich or prepared according to procedures listed below. Reagents were titrated according to the method of Love.⁴⁹

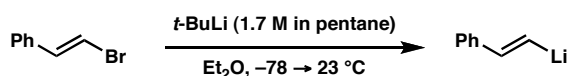


(3-Methylbut-3-enyl)magnesium bromide (*Table 2.7, entry 4*). A 250 mL Schlenk bomb (14/20 joint off of a 12 mm Kontes valve) equipped with a magnetic stir bar, fitted with a rubber septum, and connected to a Schlenk manifold was flame-dried three times, backfilling with argon after each drying cycle. Once cool, magnesium metal (2.04 g, 83.79 mmol, 2.50 equiv) was added. After three argon backfilling cycles, the flask was charged with THF (50 mL, 0.7 M) and neat DIBAL⁵⁹ (150 μ L, 1.29 mmol, 4 mol %) and stirring was initiated. The stirring was stopped after 10 min and 4-bromo-2-methylbut-1-ene⁶⁰ (5.00 g, 33.57 mmol, 1.00 equiv) was added via syringe with the needle in the solution directly above the magnesium. The mixture was heated to reflux, sealed by closing the Schlenk valve, and stirred vigorously. The flask was occasionally heated back to reflux and then allowed to cool to room temperature (23 °C). The reaction color became amber over time. After 30 min, an aliquot was removed and titrated following the procedure of Love (0.41 M in THF).⁴⁹ See p. 227 for use of this reagent.

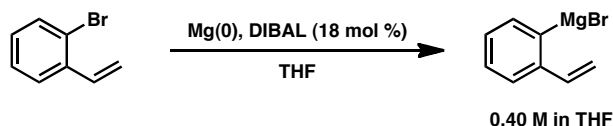


Pent-4-enylmagnesium bromide (*Table 2.7, entry 5*). A 250 mL Schlenk bomb (14/20 joint off of a 12 mm Kontes valve) equipped with a magnetic stir bar, fitted with a rubber septum, and connected to a Schlenk manifold was flame-dried three times, backfilling with argon after each drying cycle. Once cool, magnesium metal (614.4 mg, 25.27 mmol, 2.53 equiv) was added. After three argon backfilling cycles, the flask was charged

with THF (20 mL, 0.5 M) and neat DIBAL⁵⁹ (50 μ L, 0.43 mmol, 4 mol %) and stirring was initiated. The stirring was stopped after 10 min and 5-bromopent-1-ene (1.18 mL, 9.98 mmol, 1.00 equiv) was added via a syringe with the needle in the solution directly above the magnesium. The mixture was heated to reflux, sealed by closing the Schlenk valve, and stirred vigorously. The flask was occasionally heated back to reflux and then allowed to cool to room temperature (23 °C). The reaction color became amber over time. After 30 min, an aliquot was removed and titrated following the procedure of Love (0.35 M in THF).⁴⁹ See p. 217 and p. 229 for use of this reagent.

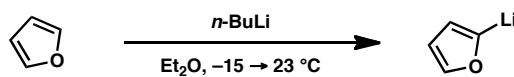


(*E*)-Styryllithium (*Table 2.7, entry 7*). See p. 231 for the synthesis and use of this reagent.

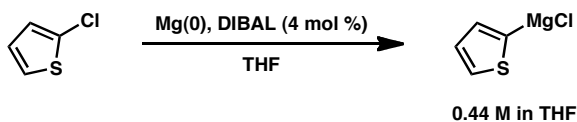


(2-Vinylphenyl)magnesium bromide (*Table 2.7, entry 8*). A 250 mL Schlenk round-bottom flask (14/20 joint off of a 12 mm Kontes valve) equipped with a magnetic stir bar, fitted with a rubber septum, and connected to a Schlenk manifold was flame-dried three times, backfilling with argon after each drying cycle. Once cool, magnesium metal (491.3 mg, 20.21 mmol, 2.53 equiv) was added. After three argon backfilling cycles, the flask was charged with THF (16 mL, 0.5 M) and neat DIBAL⁵⁹ (170 μ L, 1.46 mmol, 18 mol %) and stirring was initiated. The stirring was stopped after 10 min and *o*-

bromostyrene (1.00 mL, 7.98 mmol, 1.00 equiv) was added with the needle in the solution directly above the magnesium. The mixture was heated to reflux, sealed by closing the Schlenk valve, and stirred vigorously. The flask was occasionally heated back to reflux and then allowed to cool to room temperature (23 °C). The reaction became amber over time. After 2 h, a small portion of the reaction was removed and titrated following the procedure of Love.⁴⁹ See p. 234 for use of this reagent.



Furan-2-yl lithium (Table 2.7, entry 9). Prepared following a procedure similar to Sauers and Hagedorn.⁶¹ See p. 236 for the synthesis and use of this reagent.

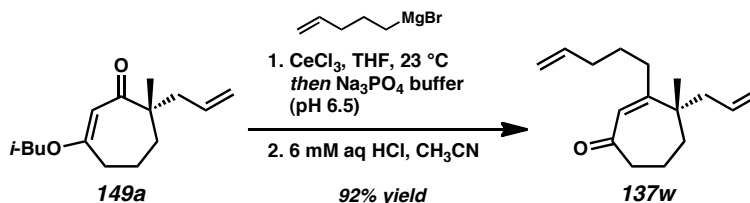


Thiophen-2-ylmagnesium chloride (Table 2.7, entry 10). A two neck 50 mL round-bottom flask equipped with a magnetic stir bar, fitted with a rubber septum on one neck and a water condenser on the other neck, and connected to a Schlenk manifold (through the condenser) was flame-dried three times, backfilling with argon after each drying cycle. Once cool, magnesium metal (635.0 mg, 26.12 mmol, 2.60 equiv) was added. After two argon backfilling cycles, the flask was charged with THF (20 mL) and neat DIBAL⁵⁹ (50 µL, 0.43 mmol, 4 mol %) and stirring was initiated. The stirring was stopped after 10 min and 2-chlorothiophene (930 µL, 10.04 mmol, 1.00 equiv) was added via a syringe with the needle in the solution directly above the magnesium. The mixture was heated to reflux. A small piece of I₂ (size of a spatula tip) dissolved in THF (1 mL)

was cannula-transferred into the mixture after 12 h and 13.5 h. The flask was allowed to cool to room temperature (23 °C). After 15 h, an aliquot was removed and titrated following the procedure of Love (0.44 M in THF).⁴⁹ See p. 218 and p. 238 for use this reagent.

2.10.2.14 CARBONYL TRANSPOSITION TO γ -QUATERNARY CYCLOHEPTENONES

Representative procedures for General Methods F–H are described below.

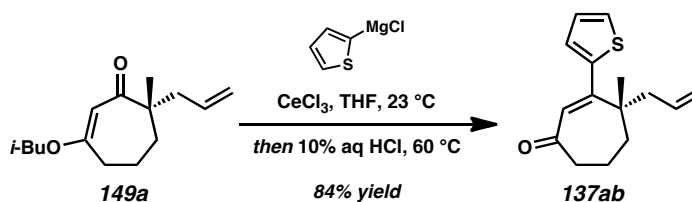


General Method F:

Organometallic Addition / Na_3PO_4 Buffer Quench / Dilute HCl Workup

Cycloheptenone 137w. A 100 mL round-bottom flask equipped with a magnetic stir bar was cycled into a glove box. The flask was loaded with anhydrous cerium chloride (616.2 mg, 2.50 mmol, 2.50 equiv), fitted with a septum, removed from the glove box, and connected to an argon-filled Schlenk manifold. A portion of THF (13 mL) was added, rinsing the cerium chloride to the bottom of the flask. As the resulting thick white slurry was stirred, a solution of pent-4-enylmagnesium bromide (8.6 mL, 0.35 M in THF, 3.01 mmol, 3.01 equiv) was added and the mixture turned grey. After 30 min of stirring, vinylogous ester **149a** (236.3 mg, 1.00 mmol, 1.00 equiv) was cannula-transferred to the

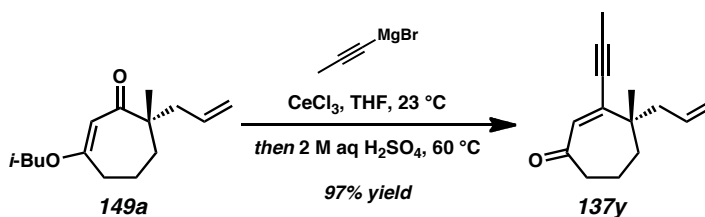
slurry from a flame-dried 10 mL conical flask using several THF rinses (3 x 4 mL; total THF added = 25 mL, 0.04 M). TLC analysis indicated that no starting material remained after 5 min. After an additional 10 min of stirring, the reaction was quenched with pH 6.5 Na₃PO₄ buffer (20 mL). A thick grey emulsion formed. The mixture was transferred to a separatory funnel where the aqueous phase was extracted four times with Et₂O. The combined organic (150 mL) were dried over MgSO₄, filtered, and concentrated under reduced pressure. The crude oil was transferred to a 20 mL scintillation vial and concentrated under reduced pressure. A stir bar, CH₃CN (2.0 mL), and aqueous HCl (2.0 mL, 6 mM) were added to the vial. The resulting cloudy solution was stirred vigorously for 30 min before being transferred to a separatory funnel where the aqueous phase was extracted four times with Et₂O. The combined organics (75 mL) were dried over MgSO₄, filtered, and concentrated under reduced pressure. The crude oil was purified by flash chromatography (SiO₂, 3 x 30 cm, 100% hexanes→1%→2%→5% EtOAc in hexanes) to afford cycloheptenone **137w** (214.2 mg, 0.92 mmol, 92% yield) as a clear colorless oil.



General Method G: Organometallic Addition / Aq. HCl Quench

Cycloheptenone 137ab. A 100 mL round-bottom flask equipped with a magnetic stir bar was cycled into a glove box. The flask was loaded with anhydrous cerium chloride (616.2 mg, 2.50 mmol, 2.50 equiv), fitted with a septum, removed from the glove box, and connected to an argon-filled Schlenk manifold. A portion of THF (13 mL) was

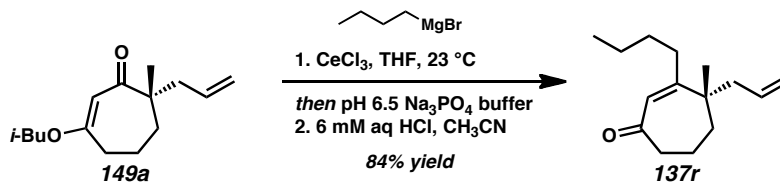
added, rinsing the cerium chloride to the bottom of the flask. As the resulting thick white slurry was stirred, a solution of thiophen-2-ylmagnesium chloride (6.8 mL, 0.44 M in THF, 2.99 mmol, 2.99 equiv) was added and the mixture turned dark grey. After 30 min of stirring, vinylogous ester **149a** (236.4 mg, 1.00 mmol, 1.00 equiv) was cannula-transferred to the slurry from a flame-dried 10 mL conical flask using several THF rinses (3 x 4 mL; total THF added = 25 mL, 0.04 M). TLC analysis indicated that no starting material remained after 25 min. After an additional 5 min of stirring, the reaction was quenched with aqueous HCl (5 mL, 10% w/w) and lowered into a preheated oil bath (60 °C). After 20 h, additional aqueous HCl (5 mL, 10% w/w) was added. After 26 h, the yellow solution was removed from the bath, cooled to ambient temperature, treated with sat. aqueous NaHCO₃ solution (25 mL), and transferred to a separatory funnel where the aqueous phase was extracted four times with Et₂O. The combined organics (150 mL) were rinsed once with sat. aqueous NaHCO₃, dried over MgSO₄, filtered, and concentrated under reduced pressure. The crude oil was purified by flash chromatography (SiO₂, 3 x 30 cm, 100% hexanes→2%→5% EtOAc in hexanes) to afford cycloheptenone **137ab** (206.1 mg, 0.84 mmol, 84% yield) as a yellow/orange oil.



General Method H: Organometallic Addition / Aq. H₂SO₄ Quench

Cycloheptenone 137y. A 100 mL round-bottom flask equipped with a magnetic stir bar was cycled into a glove box. The flask was loaded with anhydrous cerium chloride

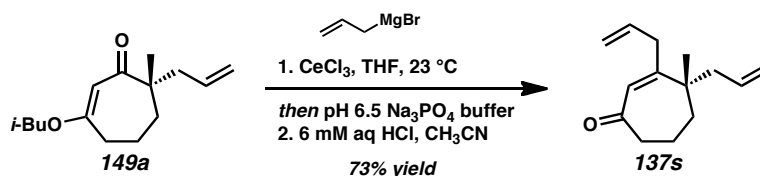
(616.2 mg, 2.50 mmol, 2.50 equiv), fitted with a septum, removed from the glove box, and connected to an argon-filled Schlenk manifold. A portion of THF (13 mL) was added, rinsing the cerium chloride to the bottom of the flask. As the resulting thick white slurry was stirred, a solution of prop-1-ynylmagnesium bromide (12 mL, 0.25 M in THF, 3.00 mmol, 3.00 equiv) was added and the mixture turned yellow. After 30 min of stirring, vinylogous ester **149a** (236.4 mg, 1.00 mmol, 1.00 equiv) was cannula-transferred to the slurry from a flame-dried 10 mL conical flask using several THF rinses (3 x 4 mL; total THF added = 25 mL, 0.04 M). The slurry maintained the yellow color with the addition. TLC analysis indicated that no starting material remained after 5 min. After an additional 10 min of stirring, the reaction was quenched with 2 M H₂SO₄ (5 mL) and lowered into a preheated oil bath (60 °C). A white precipitate formed within several minutes. After 12 h, the yellow suspension was removed from the bath, cooled to ambient temperature, treated with sat. aqueous NaHCO₃ solution (50 mL), and transferred to a separatory funnel where the aqueous phase was extracted four times with Et₂O. The combined organics (175 mL) were rinsed once with sat. aqueous NaHCO₃, dried over MgSO₄, filtered, and concentrated under reduced pressure. The crude oil was purified by flash chromatography (SiO₂, 3 x 30 cm, 100% hexanes→2%→5% EtOAc in hexanes) to afford cycloheptenone **137y** (195.4 mg, 0.97 mmol, 97% yield) as a yellow oil.



Cycloheptenone 137r (Table 2.5, entry 1). Prepared using General Method F. A 50 mL round-bottom flask equipped with a magnetic stir bar, fitted with a rubber septum, and connected to a Schlenk manifold was flame-dried three times, backfilling with argon after each drying cycle. The hot flask was placed into a glove box antechamber, which was evacuated/backfilled with N_2 (3 cycles, 5 min evacuation per cycle) before the flask was brought into the glove box. The flask was loaded with anhydrous cerium chloride (260.8 mg, 1.06 mmol, 2.50 equiv), refitted with the septum, removed from the glove box, and reconnected to the argon-filled Schlenk manifold. A portion of THF (8.5 mL) was added, rinsing the cerium chloride to the bottom of the flask. As the resulting thick white slurry was stirred, a solution of *n*-butylmagnesium bromide (680 μL , 1.87 M in THF, 1.27 mmol, 3.00 equiv) was added and the mixture turned grey. After 30 min of stirring, vinylogous ester **149a** (100.0 mg, 0.42 mmol, 1.00 equiv) was added neat from a Hamilton syringe and the needle was rinsed with a small portion of THF (2 mL; total THF added = 10.5 mL, 0.04 M). The color of the slurry initially transitioned to yellow with the vinylogous ester addition before turning back to grey.

TLC analysis indicated that no starting material remained after 15 min. After an additional 10 min of stirring, the reaction was quenched with pH 6.5 Na_3PO_4 buffer (8 mL). A thick grey emulsion formed. The mixture was transferred to a separatory funnel where the aqueous phase was extracted four times with Et_2O . The combined organics (125 mL) were dried over MgSO_4 , filtered, and concentrated under reduced pressure.

The crude oil was transferred to a 20 mL scintillation vial and concentrated under reduced pressure. A stir bar, CH₃CN (1.0 mL), and 6 mM aqueous HCl (1.0 mL) were added to the vial. The resulting cloudy solution was stirred vigorously for 5 min before being transferred to a separatory funnel where the aqueous phase was extracted four times with Et₂O. The combined organics (100 mL) were dried over MgSO₄, filtered, and concentrated under reduced pressure. The crude oil was purified by flash chromatography (SiO₂, 3 x 30 cm, 100% hexanes→2%→5% EtOAc in hexanes) to afford cycloheptenone **137r** (82.4 mg, 0.35 mmol, 84% yield) as a pale yellow oil. (For characterization data, see p. 178).

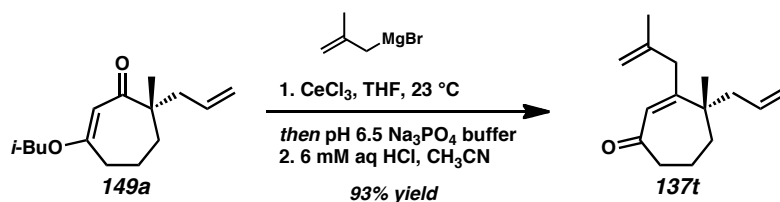


Cycloheptenone 137s (*Table 2.5, entry 2*). Prepared using General Method F. A 100 mL round-bottom flask equipped with a magnetic stir bar, fitted with a rubber septum, and connected to a Schlenk manifold was flame-dried three times, backfilling with argon after each drying cycle. The hot flask was placed into a glove box antechamber, which was evacuated/backfilled with N₂ (3 cycles, 5 min evacuation per cycle) before the flask was brought into the glove box. The flask was loaded with anhydrous cerium chloride (616.3 mg, 2.50 mmol, 2.50 equiv), refitted with the septum, removed from the glove box, and reconnected to the argon-filled Schlenk manifold. A portion of THF (13 mL) was added, rinsing the cerium chloride to the bottom of the flask. As the resulting thick white slurry was stirred, a solution of allylmagnesium bromide (3.49 mL, 0.86 M in Et₂O,

3.00 mmol, 3.00 equiv) was added and the mixture turned initially orange and red over time. After 30 min of stirring, vinylogous ester **149a** (236.6 mg, 1.00 mmol, 1.00 equiv) was cannula-transferred to the slurry from a flame-dried 10 mL conical flask using several THF rinses (3 x 4 mL; total THF added = 25 mL, 0.04 M). The mixture faded back to orange with the addition.

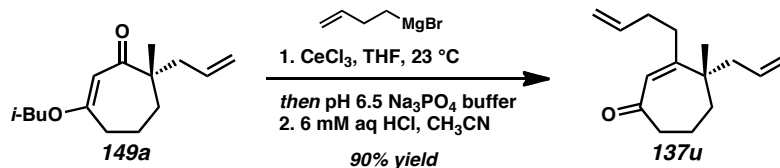
TLC analysis indicated that no starting material remained after 5 min. After an additional 10 min of stirring, the reaction was quenched with pH 6.5 Na₃PO₄ buffer (20 mL). A thick grey emulsion formed. The mixture was transferred to a separatory funnel where the aqueous phase was extracted four times with Et₂O. The combined organics (250 mL) were dried over MgSO₄, filtered, and concentrated under reduced pressure. The crude oil was transferred to a 20 mL scintillation vial and concentrated under reduced pressure. A stir bar, CH₃CN (2.0 mL), and 6 mM aqueous HCl (2.0 mL) were added to the vial. The resulting cloudy solution was stirred vigorously for 30 min before being transferred to a separatory funnel where the aqueous phase was extracted four times with Et₂O. The combined organics (75 mL) were dried over MgSO₄, filtered, and concentrated under reduced pressure. The crude oil was purified by flash chromatography (SiO₂, 3 x 30 cm, 100% hexanes→2%→5% EtOAc in hexanes) to afford cycloheptenone **137s** (148.6 mg, 0.73 mmol, 73% yield) as a pale yellow oil; *R*_f = 0.68 (30% EtOAc in hexanes); ¹H NMR (500 MHz, CDCl₃) δ 5.88 (s, 1H), 5.75 (dddd, *J* = 16.9, 10.1, 6.8, 6.8 Hz, 1H), 5.64 (dddd, *J* = 17.0, 10.3, 7.8, 6.8 Hz, 1H), 5.14–5.00 (m, 4H), 2.96–2.84 (m, 2H), 2.62–2.54 (m, 2H), 2.38 (dddd, *J* = 14.2, 6.8, 1.3, 1.3 Hz, 1H), 2.10 (dddd, *J* = 14.2, 7.8, 1.1, 1.1 Hz, 1H), 1.84–1.76 (m, 3H), 1.67–1.57 (m, 1H), 1.17 (s, 3H); ¹³C NMR (125 MHz, CDCl₃) δ 205.2, 160.3, 136.0, 134.0, 130.0, 118.3, 117.9,

45.5, 45.2, 44.4, 38.8, 38.5, 25.7, 17.6; IR (Neat Film NaCl) 3077, 2976, 2939, 2872, 1654, 1612, 1458, 1412, 1380. 1342, 1290, 1250, 1217, 1177, 1106, 996, 916 cm^{-1} ; HRMS (MM: ESI-APCI+) m/z calc'd for $\text{C}_{14}\text{H}_{21}\text{O}$ $[\text{M}+\text{H}]^+$: 205.1587; found 205.1587; $[\alpha]_{\text{D}}^{25.0} -34.64$ (c 1.55, CHCl_3 , 88% ee).



Cycloheptenone 137t (*Table 2.5, entry 3*). Prepared using General Method F. A 100 mL round-bottom flask equipped with a magnetic stir bar, fitted with a rubber septum, and connected to a Schlenk manifold was flame-dried three times, backfilling with argon after each drying cycle. The hot flask was placed into a glove box antechamber, which was evacuated/backfilled with N_2 (3 cycles, 5 min evacuation per cycle) before the flask was brought into the glove box. The flask was loaded with anhydrous cerium chloride (616.2 mg, 2.50 mmol, 2.50 equiv), refitted with the septum, removed from the glove box, and reconnected to the argon-filled Schlenk manifold. A portion of THF (13 mL) was added, rinsing the cerium chloride to the bottom of the flask. As the resulting thick white slurry was stirred, a solution of (2-methylallyl)magnesium bromide (7.7 mL, 0.39 M in THF, 3.00 mmol, 3.00 equiv) was added and the mixture turned initially yellow and eventually orange with time. After 30 min of stirring, vinylogous ester **149a** (236.2 mg, 1.00 mmol, 1.00 equiv) was cannula-transferred to the slurry from a flame-dried 10 mL conical flask using several THF rinses (3 x 4 mL; total THF added = 25 mL, 0.04 M).

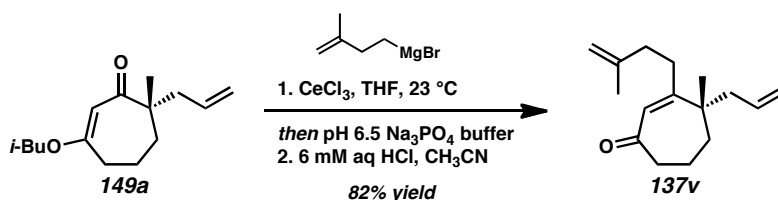
TLC analysis indicated that no starting material remained after 5 min. After an additional 15 min of stirring, the reaction was quenched with pH 6.5 Na_3PO_4 buffer (20 mL). A thick grey emulsion formed. The mixture was transferred to a separatory funnel where the aqueous phase was extracted four times with Et_2O . The combined organics (150 mL) were dried over MgSO_4 , filtered, and concentrated under reduced pressure. The crude oil was transferred to a 20 mL scintillation vial and concentrated under reduced pressure. A stir bar, CH_3CN (2.0 mL), and 6 mM aqueous HCl (2.0 mL) were added to the vial. The resulting cloudy solution was stirred vigorously for 30 min before being transferred to a separatory funnel where the aqueous phase was extracted four times with Et_2O . The combined organics (75 mL) were dried over MgSO_4 , filtered, and concentrated under reduced pressure. The crude oil was purified by flash chromatography (SiO_2 , 3 x 30 cm, 100% hexanes→2%→5% EtOAc in hexanes) to afford cycloheptenone **137t** (202.9 mg, 0.93 mmol, 93% yield) as a pale yellow oil; R_f = 0.65 (30% EtOAc in hexanes); ^1H NMR (500 MHz, CDCl_3) δ 5.89 (s, 1H), 5.65 (dddd, J = 16.9, 10.3, 7.8, 6.8 Hz, 1H), 5.09–5.01 (m, 2H), 4.94–4.91 (m, 1H), 4.78 (dd, J = 1.9, 0.9 Hz, 1H), 2.85 (q, J = 16.2 Hz, 2H), 2.63–2.55 (m, 2H), 2.37 (dddd, J = 14.1, 6.8, 1.3, 1.3 Hz, 1H), 2.10 (dddd, J = 14.2, 7.8, 1.1, 1.1 Hz, 1H), 1.85–1.75 (m, 3H), 1.68 (s, 3H), 1.66–1.59 (m, 1H), 1.16 (s, 3H); ^{13}C NMR (125 MHz, CDCl_3) δ 205.3, 159.1, 142.8, 134.0, 129.5, 118.3, 115.2, 45.4, 45.0, 44.4, 42.7, 38.8, 25.6, 22.2, 17.6; IR (Neat Film NaCl) 3075, 2970, 2939, 2872, 1661, 1652, 1612, 1455, 1376, 1342, 1309, 1249, 1218, 996, 914, 893 cm^{-1} ; HRMS (MM: ESI-APCI+) m/z calc'd for $\text{C}_{15}\text{H}_{23}\text{O}$ $[\text{M}+\text{H}]^+$: 219.1743; found 219.1740; $[\alpha]_{\text{D}}^{25.0}$ –35.09 (c 0.95, CHCl_3 , 88% ee).



Cycloheptenone 137u (*Table 2.5, entry 4*) Prepared using General Method F. A 100 mL round-bottom flask equipped with a magnetic stir bar, fitted with a rubber septum, and connected to a Schlenk manifold was flame-dried three times, backfilling with argon after each drying cycle. The hot flask was placed into a glove box antechamber, which was evacuated/backfilled with N₂ (3 cycles, 5 min evacuation per cycle) before the flask was brought into the glove box. The flask was loaded with anhydrous cerium chloride (616.2 mg, 2.50 mmol, 2.50 equiv), refitted with the septum, removed from the glove box, and reconnected to the argon-filled Schlenk manifold. A portion of THF (13 mL) was added, rinsing the cerium chloride to the bottom of the flask. As the resulting white mixture was stirred, a solution of but-3-enylmagnesium bromide (6.82 mL, 0.44 M in THF, 3.00 mmol, 3.00 equiv) was added, generating a thick grey slurry. After 30 min of stirring, vinylogous ester **149a** (236.4 mg, 1.00 mmol, 1.00 equiv) was cannula-transferred to the slurry from a flame-dried 10 mL conical flask using several THF rinses (3 x 4 mL; total THF added = 25 mL, 0.04 M).

After 20 min, the reaction was quenched with pH 6.5 Na₃PO₄ buffer (20 mL). A thick grey emulsion formed. The mixture was transferred to a separatory funnel where the aqueous phase was extracted four times with Et₂O. The combined organic (150 mL) were dried over MgSO₄, filtered, and concentrated under reduced pressure. The crude oil was transferred to a 20 mL scintillation vial and concentrated under reduced pressure. A stir bar, CH₃CN (2.0 mL), and 6 mM aqueous HCl (2.0 mL) were added to the vial. The

resulting cloudy solution was stirred vigorously for 5 min before being transferred to a separatory funnel where the aqueous phase was extracted four times with Et₂O. The combined organics (80 mL) were dried over MgSO₄, filtered, and concentrated under reduced pressure. The crude oil was purified by flash chromatography (SiO₂, 3 x 30 cm, 100% hexanes→2%→5%→10% EtOAc in hexanes) to afford cycloheptenone **137u** (196.6 mg, 0.90 mmol, 90% yield) as a yellow oil; *R*_f = 0.67 (30% EtOAc in hexanes); ¹H NMR (500 MHz, CDCl₃) δ 5.88 (s, 1H), 5.86–5.77 (m, 1H), 5.63 (dddd, *J* = 16.9, 10.3, 7.8, 6.8 Hz, 1H), 5.08–4.96 (m, 4H), 2.59–2.54 (m, 2H), 2.36 (dddd, *J* = 14.1, 6.7, 1.3, 1.3 Hz, 1H), 2.28–2.17 (m, 4H), 2.08 (dddd, *J* = 14.1, 7.9, 2.1, 1.0 Hz, 1H), 1.83–1.73 (m, 3H), 1.65–1.57 (m, 1H), 1.15 (s, 3H); ¹³C NMR (125 MHz, CDCl₃) δ 205.2, 161.6, 137.7, 134.0, 128.9, 118.2, 115.4, 45.7, 45.2, 44.3, 38.7, 34.0, 33.4, 25.7, 17.6; IR (Neat Film NaCl) 3076, 2975, 2938, 2872, 1652, 1611, 1465, 1452, 1415, 1379, 1342, 1263, 1218, 1177, 1109, 1069, 996, 914, 877, 841, 764, 714 cm⁻¹; HRMS (MM: ESI-APCI+) *m/z* calc'd for C₁₅H₂₃O [M+H]⁺: 219.1743; found 219.1742; [α]_D^{25.0} –34.11 (*c* 1.21, CHCl₃, 88% ee).

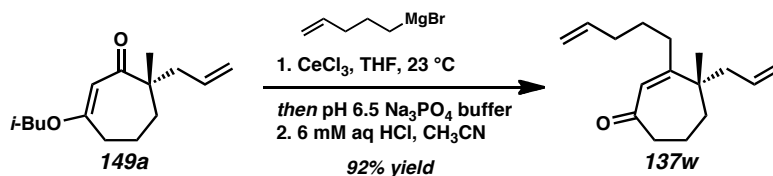


Cycloheptenone 137v (Table 2.5, entry 5). Prepared using General Method F. A 100 mL round-bottom flask equipped with a magnetic stir bar, fitted with a rubber septum, and connected to a Schlenk manifold was flame-dried three times, backfilling with argon after each drying cycle. The hot flask was placed into a glove box antechamber, which

was evacuated/backfilled with N₂ (3 cycles, 5 min evacuation per cycle) before the flask was brought into the glove box. The flask was loaded with anhydrous cerium chloride (616.2 mg, 2.50 mmol, 2.50 equiv), refitted with the septum, removed from the glove box, and reconnected to the argon-filled Schlenk manifold. A portion of THF (13 mL) was added, rinsing the cerium chloride to the bottom of the flask. As the resulting thick white slurry was stirred, a solution of (3-methylbut-3-enyl)magnesium bromide (7.3 mL, 0.41 M in THF, 2.99 mmol, 2.99 equiv) was added and the mixture turned yellow. After 30 min of stirring, vinylogous ester **149a** (236.4 mg, 1.00 mmol, 1.00 equiv) was cannula-transferred to the slurry from a flame-dried 10 mL conical flask using several THF rinses (3 x 4 mL; total THF added = 25 mL, 0.04 M).

TLC analysis indicated that no starting material remained after 5 min. After an additional 10 min of stirring, the reaction was quenched with pH 6.5 Na₃PO₄ buffer (20 mL). A thick grey emulsion formed. The mixture was transferred to a separatory funnel where the aqueous phase was extracted four times with Et₂O. The combined organic (150 mL) were dried over MgSO₄, filtered, and concentrated under reduced pressure. The crude oil was transferred to a 20 mL scintillation vial and concentrated under reduced pressure. A stir bar, CH₃CN (2.0 mL), and 6 mM aqueous HCl (2.0 mL) were added to the vial. The resulting cloudy solution was stirred vigorously for 5 min before being transferred to a separatory funnel where the aqueous phase was extracted four times with Et₂O. The combined organics (75 mL) were dried over MgSO₄, filtered, and concentrated under reduced pressure. The crude oil was purified by flash chromatography (SiO₂, 3 x 30 cm, 100% hexanes→2%→5% EtOAc in hexanes) to afford cycloheptenone **137v** (191.1 mg, 0.82 mmol, 82% yield) as a clear colorless oil; R_f =

0.69 (30% EtOAc in hexanes); ^1H NMR (500 MHz, CDCl_3) δ 5.89 (s, 1H), 5.64 (dddd, J = 16.9, 10.3, 7.8, 6.8 Hz, 1H), 5.09–4.99 (m, 2H), 4.77–4.73 (m, 1H), 4.72–4.69 (m, 1H), 2.59–2.56 (m, 2H), 2.38 (dddd, J = 14.1, 6.7, 1.3, 1.3 Hz, 1H), 2.31–2.14 (m, 4H), 2.10 (dddd, J = 14.1, 7.8, 1.1, 1.1 Hz, 1H), 1.83–1.75 (m, 3H), 1.75–1.74 (m, 3H), 1.66–1.57 (m, 1H), 1.17 (s, 3H); ^{13}C NMR (125 MHz, CDCl_3) δ 205.3, 162.1, 145.1, 134.0, 129.0, 118.3, 110.6, 45.8, 45.3, 44.3, 38.8, 38.3, 32.5, 25.7, 22.7, 17.6; IR (Neat Film NaCl) 3075, 2968, 2938, 2873, 1652, 1611, 1455, 1415, 1377, 1342, 1262, 1218, 1181, 1109, 1069, 996, 915, 887 cm^{-1} ; HRMS (MM: ESI-APCI+) m/z calc'd for $\text{C}_{16}\text{H}_{25}\text{O}$ $[\text{M}+\text{H}]^+$: 233.1900; found 233.1896; $[\alpha]_{\text{D}}^{25.0}$ -32.57 (c 1.32, CHCl_3 , 88% ee).

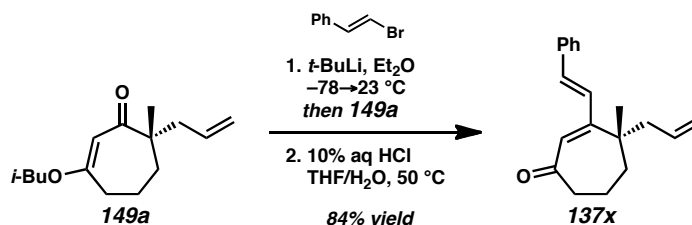


Cycloheptenone 137w (Table 2.5, entry 6). Prepared using General Method F. A 100 mL round-bottom flask equipped with a magnetic stir bar, fitted with a rubber septum, and connected to a Schlenk manifold was flame-dried three times, backfilling with argon after each drying cycle. The hot flask was placed into a glove box antechamber, which was evacuated/backfilled with N_2 (3 cycles, 5 min evacuation per cycle) before the flask was brought into the glove box. The flask was loaded with anhydrous cerium chloride (616.2 mg, 2.50 mmol, 2.50 equiv), refitted with the septum, removed from the glove box, and reconnected to the argon-filled Schlenk manifold. A portion of THF (13 mL) was added, rinsing the cerium chloride to the bottom of the flask. As the resulting thick white slurry was stirred, a solution of pent-4-enylmagnesium bromide (8.6 mL, 0.35 M in

THF, 3.01 mmol, 3.01 equiv) was added and the mixture turned grey. After 30 min of stirring, vinylogous ester **149a** (236.3 mg, 1.00 mmol, 1.00 equiv) was cannula-transferred to the slurry from a flame-dried 10 mL conical flask using several THF rinses (3 x 4 mL; total THF added = 25 mL, 0.04 M).

TLC analysis indicated that no starting material remained after 5 min. After an additional 10 min of stirring, the reaction was quenched with pH 6.5 Na₃PO₄ buffer (20 mL). A thick grey emulsion formed. The mixture was transferred to a separatory funnel where the aqueous phase was extracted four times with Et₂O. The combined organic (150 mL) were dried over MgSO₄, filtered, and concentrated under reduced pressure. The crude oil was transferred to a 20 mL scintillation vial and concentrated under reduced pressure. A stir bar, CH₃CN (2.0 mL), and 6 mM aqueous HCl (2.0 mL) were added to the vial. The resulting cloudy solution was stirred vigorously for 30 min before being transferred to a separatory funnel where the aqueous phase was extracted four times with Et₂O. The combined organics (75 mL) were dried over MgSO₄, filtered, and concentrated under reduced pressure. The crude oil was purified by flash chromatography (SiO₂, 3 x 30 cm, 100% hexanes→1%→2%→5% EtOAc in hexanes) to afford cycloheptenone **137w** (214.2 mg, 0.92 mmol, 92% yield) as a clear colorless oil; *R_f* = 0.65 (30% EtOAc in hexanes); ¹H NMR (500 MHz, CDCl₃) δ 5.88 (s, 1H), 5.79 (dddd, *J* = 16.9, 10.2, 6.7, 6.7 Hz, 1H), 5.67–5.57 (m, 1H), 5.07–4.96 (m, 4H), 2.60–2.53 (m, 2H), 2.35 (dddd, *J* = 14.1, 6.7, 2.5, 1.2 Hz, 1H), 2.20–2.04 (m, 5H), 1.83–1.73 (m, 3H), 1.66–1.53 (m, 3H), 1.14 (s, 3H); ¹³C NMR (125 MHz, CDCl₃) δ 205.3, 162.6, 138.2, 134.1, 128.8, 118.2, 115.3, 45.7, 45.2, 44.3, 38.7, 33.8, 33.5, 29.3, 25.7, 17.6; IR (Neat Film NaCl) 3076, 2975, 2937, 2870, 1652, 1611, 1456, 1415, 1380, 1343, 1257, 1218, 1179,

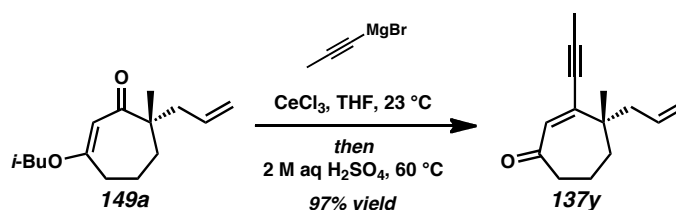
1110, 1071, 994, 913 cm^{-1} ; HRMS (MM: ESI-APCI+) m/z calc'd for $\text{C}_{16}\text{H}_{25}\text{O}$ $[\text{M}+\text{H}]^+$: 233.1900; found 233.1900; $[\alpha]_{\text{D}}^{25.0} -34.96$ (c 1.46, CHCl_3 , 88% ee).



Cycloheptenone 137x (Table 2.5, entry 7). Prepared using General Method G. A flame-dried round-bottom flask equipped with a magnetic stir bar and fitted with a rubber septum was connected to a Schlenk manifold. The flask was charged with (*E*)- β -bromostyrene (1.5 mL, 11.69 mmol, 1.98 equiv) and Et_2O (13 mL) and lowered into a dry ice/acetone bath (-78°C). After dropwise addition of *t*-butyllithium (13.5 mL, 1.7 M in pentane, 22.95 mmol, 3.88 equiv), the solution was stirred for 2 hours (at -78°C), warmed to room temperature (30 min stir at 23°C), and placed back into the dry ice/acetone bath. Vinylogous ester **149a** (1.40 g, 5.92 mmol, 1.00 equiv) was transferred to the round-bottom flask by two Et_2O rinses (2 x 3 mL, total Et_2O added = 19 mL, 0.3 M). The flask was stirred at -78°C for 25 min before being transferred to an ice/water bath (0°C).

TLC analysis indicated that no starting material remained after 2 h. Consequently, the reaction was quenched with 10% w/w aqueous HCl (10 mL). After 20 min of stirring, the mixture was transferred to a separatory funnel where the aqueous phase was extracted three times with Et_2O . The combined organics were dried over MgSO_4 , filtered, and concentrated under reduced pressure. A round-bottom flask was charged with the crude oil, THF (20 mL), and 10% w/w aqueous HCl (0.5 mL) and lowered into a

preheated oil bath (50 °C). After 2 h, the reaction allowed to cool to room temperature, concentrated under reduced pressure, diluted with water (10 mL) and Et₂O (20 mL), and transferred to a separatory funnel where the aqueous layer was extracted twice with Et₂O (2 x 20 mL). The combined organics were dried over MgSO₄, filtered, and concentrated under reduced pressure. The crude oil was purified by flash chromatography (SiO₂, 3 x 23 cm, 20:1→15:1→10:1 hexanes:EtOAc) to afford cycloheptenone **137x** (1.33 g, 4.99 mmol, 84% yield) as a yellow oil; R_f = 0.67 (30% EtOAc in hexanes); ¹H NMR (500 MHz, CDCl₃) δ 7.42 (d, J = 7.3 Hz, 2H), 7.35 (d, J = 7.4 Hz, 2H), 7.28 (d, J = 7.3 Hz, 1H), 6.90 (s, 2H), 6.30 (s, 1H), 5.67 (dddd, J = 16.8, 10.3, 8.1, 6.5 Hz, 1H), 5.09–5.02 (m, 2H), 2.71–2.57 (m, 2H), 2.46 (dddd, J = 14.1, 6.5, 1.3, 1.3 Hz, 1H), 2.14 (dddd, J = 14.1, 8.1, 1.1, 1.1 Hz, 1H), 1.92–1.79 (m, 3H), 1.72–1.64 (m, 1H), 1.27 (s, 3H); ¹³C NMR (125 MHz, CDCl₃) δ 204.7, 158.5, 136.7, 133.9, 133.3, 129.2, 128.9, 128.5, 127.1, 127.1, 118.4, 46.2, 44.5, 44.4, 38.7, 26.8, 17.6; IR (Neat Film NaCl) 3075, 3059, 3002, 2966, 2936, 2869, 1640, 1581, 1573, 1495, 1449, 1414, 1379, 1343, 1303, 1277, 1250, 1217, 1178, 1109, 1082, 1028, 996, 963, 916, 839, 799, 752, 718 cm⁻¹; HRMS (MM: ESI-APCI+) m/z calc'd for C₁₉H₂₃O [M+H]⁺: 267.1743; found 267.1755; $[\alpha]_D^{25.0}$ –44.99 (c 0.81, CHCl₃, 88% ee).

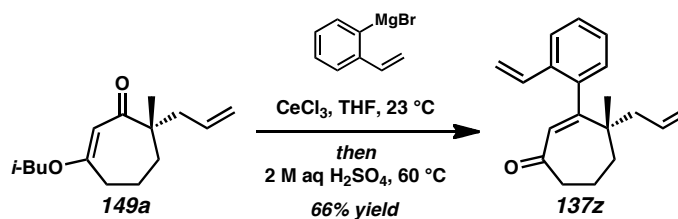


Cycloheptenone 137y (Table 2.5, entry 8). Prepared using General Method H. A 100 mL round-bottom flask equipped with a magnetic stir bar, fitted with a rubber septum,

and connected to a Schlenk manifold was flame-dried three times, backfilling with argon after each drying cycle. The hot flask was placed into a glove box antechamber, which was evacuated/backfilled with N₂ (3 cycles, 5 min evacuation per cycle) before the flask was brought into the glove box. The flask was loaded with anhydrous cerium chloride (616.2 mg, 2.50 mmol, 2.50 equiv), refitted with the septum, removed from the glove box, and reconnected to the argon-filled Schlenk manifold. A portion of THF (13 mL) was added, rinsing the cerium chloride to the bottom of the flask. As the resulting thick white slurry was stirred, a solution of prop-1-ynylmagnesium bromide (12 mL, 0.25 M in THF, 3.00 mmol, 3.00 equiv) was added and the mixture turned yellow. After 30 min of stirring, vinylogous ester **149a** (236.4 mg, 1.00 mmol, 1.00 equiv) was cannula-transferred to the slurry from a flame-dried 10 mL conical flask using several THF rinses (3 x 4 mL; total THF added = 25 mL, 0.04 M). The slurry maintained the yellow color with the addition.

TLC analysis indicated that no starting material remained after 5 min. After an additional 10 min of stirring, the reaction was quenched with 2 M H₂SO₄ (5 mL) and lowered into a preheated oil bath (60 °C). A white precipitate formed within several minutes. After 12 h, the yellow suspension was removed from the bath, cooled to room temperature (23 °C), treated with sat. aqueous NaHCO₃ solution (50 mL), and transferred to a separatory funnel where the aqueous phase was extracted four times with Et₂O. The combined organics (175 mL) were rinsed once with sat. aqueous NaHCO₃, dried over MgSO₄, filtered, and concentrated under reduced pressure. The crude oil was purified by flash chromatography (SiO₂, 3 x 30 cm, 100% hexanes→2%→5% EtOAc in hexanes) to afford cycloheptenone **137y** (195.4 mg, 0.97 mmol, 97% yield) as a yellow oil; R_f = 0.65

(30% EtoAc in hexanes); ^1H NMR (500 MHz, CDCl_3) δ 6.20 (s, 1H), 5.70 (dddd, J = 16.8, 10.5, 8.2, 6.6 Hz, 1H), 5.10–5.01 (m, 2H), 2.65–2.49 (m, 3H), 2.16 (dddd, J = 13.8, 8.2, 1.0, 1.0 Hz, 1H), 2.01 (s, 3H), 1.83–1.75 (m, 3H), 1.66–1.59 (m, 1H), 1.24 (s, 3H); ^{13}C NMR (125 MHz, CDCl_3) δ 203.5, 145.6, 135.0, 134.3, 118.3, 92.9, 80.7, 46.5, 45.4, 44.6, 37.3, 27.0, 17.6, 4.7; IR (Neat Film NaCl) 3076, 2969, 2937, 2219, 1652, 1580, 1455, 1415, 1377, 1346, 1255, 1225, 1184, 1110, 998, 916, 893, 866, 813, 784, 716 cm^{-1} ; HRMS (MM: ESI-APCI+) m/z calc'd for $\text{C}_{14}\text{H}_{19}\text{O}$ $[\text{M}+\text{H}]^+$: 203.1430; found 203.1428; $[\alpha]_{\text{D}}^{25.0}$ -49.25 (c 1.21, CHCl_3 , 88% ee).

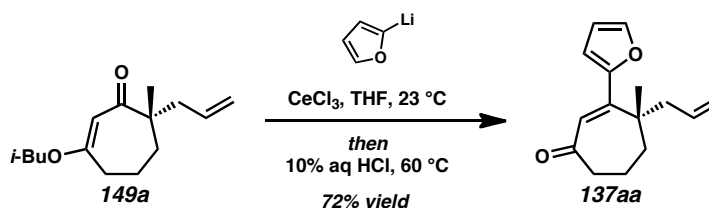


Cycloheptenone 137z (*Table 2.5, entry 9*). Prepared using General Method H. A 100 mL round-bottom flask equipped with a magnetic stir bar, fitted with a rubber septum, and connected to a Schlenk manifold was flame-dried three times, backfilling with argon after each drying cycle. The hot flask was placed into a glove box antechamber, which was evacuated/backfilled with N_2 (4 cycles, 1 min evacuation per cycle) before the flask was brought into the glove box. The flask was loaded with anhydrous cerium chloride (616.4 mg, 2.50 mmol, 2.50 equiv), refitted with the septum, removed from the glove box, and reconnected to the argon-filled Schlenk manifold. A portion of THF (13 mL) was added, rinsing the cerium chloride to the bottom of the flask. As the resulting thick white slurry was stirred, a solution of (2-vinylphenyl)magnesium bromide (7.5 mL, 0.40 M in THF, 3.00 mmol, 3.00 equiv) was added and the mixture turned yellow and green

over time. After 30 min of stirring, vinylogous ester **149a** (236.3 mg, 1.00 mmol, 1.00 equiv) was cannula-transferred to the slurry from a flame-dried 10 mL conical flask using several THF rinses (3 x 4 mL; total THF added = 25 mL, 0.04 M). The reaction color returned to yellow with addition of vinylogous ester **149a**.

TLC analysis indicated that no starting material remained after 40 min. After an additional 30 min of stirring, the reaction was quenched with 2 M H₂SO₄ (5 mL) and lowered into a preheated oil bath (60 °C). A grey precipitate formed within several minutes. After 26 h, the yellow suspension was removed from the bath, cooled to room temperature (23 °C), treated with sat. aqueous NaHCO₃ solution (50 mL), and transferred to a separatory funnel where the aqueous phase was extracted four times with Et₂O. The combined organics (175 mL) were rinsed once with sat. aqueous NaHCO₃, dried over MgSO₄, filtered, and concentrated under reduced pressure. The crude oil was purified first by flash chromatography (SiO₂, 3 x 30 cm, 100% hexanes→2%→5% EtOAc in hexanes) and then by flash chromatography using a Teledyne Isco CombiFlash Rf system (SiO₂, 12 g loading cartridge, 40 g column, multi-step gradient, hold 0% [2 min]→ramp to 85% [17 min]→hold 85% CH₂Cl₂ in hexanes [2.5 min]→ramp to 100% [3 min]→hold 100% CH₂Cl₂ [5 min]) to afford cycloheptenone **137z** (176.7 mg, 0.66 mmol, 66% yield) as a pale yellow oil; *R_f* = 0.74 (30% EtOAc in hexanes); ¹H NMR (500 MHz, CDCl₃) and ¹³C NMR (125 MHz, CDCl₃) mixture of two atropisomers isomers (1.9 : 1 ratio), see Figure A1.307 for ¹H NMR (in CDCl₃) and Figure A1.308 for variable temperature ¹H NMR data (in DMSO-*d*₆ at 25, 50, 75, and 100 °C); IR (Neat Film NaCl) 3060, 3007, 2973, 2936, 2936, 1669, 1626, 1604, 1594, 1476, 1464, 1443, 1413, 1379, 1356, 1338, 1307, 1281, 1251, 1214, 1177, 1136, 1109, 1095, 1057, 1020, 996, 915, 864, 818, 769,

743 cm^{-1} ; HRMS (MM: ESI-APCI+) m/z calc'd for $\text{C}_{19}\text{H}_{23}\text{O}$ $[\text{M}+\text{H}]^+$: 267.1743; found 267.1751.

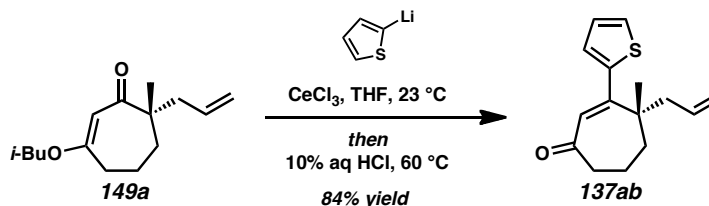


Cycloheptenone 137aa (Table 2.5, entry 10). Prepared using General Method G. A 100 and a 25 mL round-bottom flask each equipped with a magnetic stir bar, fitted with a rubber septum, and connected to a Schlenk manifold were flame-dried three times, backfilling with argon after each drying cycle. The hot 100 mL flask was placed into a glove box antechamber, which was evacuated/backfilled with N_2 (3 cycles, 5 min evacuation per cycle) before the flask was brought into the glove box. The flask was loaded with anhydrous cerium chloride (616.2 mg, 2.50 mmol, 2.50 equiv), refitted with the septum, removed from the glove box, and reconnected to the argon-filled Schlenk manifold.

Once cool, the 25 mL flask was charged with furan (230 μL , 3.16 mmol, 1.05 equiv) and Et_2O (3 mL, 1 M) and lowered into an ethylene glycol/dry ice bath ($-15\text{ }^\circ\text{C}$). To the cooled solution was added $n\text{-BuLi}$ (1.42 mL, 2.12 M in hexanes, 3.01 mmol, 1.00 equiv) dropwise and the flask was warmed to room temperature ($23\text{ }^\circ\text{C}$). The reaction became cloudy and white with time. After 1 h, a portion of THF (13 mL) was added to the 100 mL flask before the contents of the 25 mL flask were cannula-transferred to the 100 mL flask. After 30 min of stirring, vinylogous ester **149a** (236.4 mg, 1.00 mmol, 1.00 equiv)

was cannula-transferred to the 100 mL flask from a flame-dried 10 mL conical flask using several THF rinses (3 x 4 mL; total THF added = 25 mL, 0.04 M).

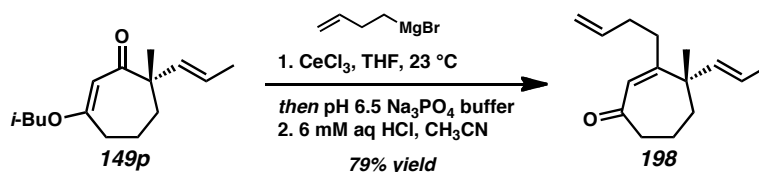
After 35 min, the reaction was quenched with 10% w/w aqueous HCl (5 mL) and lowered into a preheated oil bath (60 °C). After 17 h, the solution was removed from the bath, cooled to room temperature (23 °C), treated with sat. aqueous NaHCO₃ solution (50 mL), and transferred to a separatory funnel where the aqueous phase was extracted four times with Et₂O. The combined organics (250 mL) were rinsed once with sat. aqueous NaHCO₃, dried over MgSO₄, filtered, and concentrated under reduced pressure. The crude oil was purified by flash chromatography (SiO₂, 3 x 30 cm, 100% hexanes→2%→5% EtOAc in hexanes) to afford cycloheptenone **137aa** (164.7 mg, 0.72 mmol, 72% yield) as a yellow oil; *R*_f = 0.70 (30% EtOAc in hexanes); ¹H NMR (500 MHz, CDCl₃) δ 7.45 (dd, *J* = 1.8, 0.6 Hz, 1H), 6.56 (dd, *J* = 3.4, 0.7 Hz, 1H), 6.43 (s, 1H), 6.41 (dd, *J* = 3.4, 1.8 Hz, 1H), 5.65 (dddd, *J* = 16.9, 10.2, 8.1, 6.6 Hz, 1H), 5.01 (dddd, *J* = 10.2, 2.0, 0.9, 0.9 Hz, 1H), 4.97 (dddd, *J* = 16.9, 2.3, 1.4, 1.4 Hz, 1H), 2.71–2.60 (m, 3H), 2.24 (dddd, *J* = 14.1, 8.1, 1.1, 1.1 Hz, 1H), 1.97–1.81 (m, 3H), 1.72–1.64 (m, 1H), 1.38 (s, 3H); ¹³C NMR (125 MHz, CDCl₃) δ 204.7, 155.3, 149.2, 142.9, 134.3, 129.3, 118.1, 111.4, 111.2, 45.9, 44.7, 44.3, 39.8, 26.3, 17.4; IR (Neat Film NaCl) 3118, 3075, 2941, 2871, 1661, 1652, 1645, 1581, 1557, 1455, 1415, 1380, 1341, 1258, 1215, 1173, 1152, 1106, 1080, 1029, 997, 956, 917, 898, 886, 858, 812, 742 cm⁻¹; HRMS (MM: ESI-APCI+) *m/z* calc'd for C₁₅H₁₉O₂ [M+H]⁺: 231.1380; found 231.1374; [α]_D^{25.0} –26.90 (c 1.18, CHCl₃, 88% ee).



Cycloheptenone 137ab (*Table 2.5, entry 11*). Prepared using General Method G. A 100 mL round-bottom flask equipped with a magnetic stir bar, fitted with a rubber septum, and connected to a Schlenk manifold was flame-dried three times, backfilling with argon after each drying cycle. The hot flask was placed into a glove box antechamber, which was evacuated/backfilled with N_2 (3 cycles, 5 min evacuation per cycle) before the flask was brought into the glove box. The flask was loaded with anhydrous cerium chloride (616.2 mg, 2.50 mmol, 2.50 equiv), refitted with the septum, removed from the glove box, and reconnected to the argon-filled Schlenk manifold. A portion of THF (13 mL) was added, rinsing the cerium chloride to the bottom of the flask. As the resulting thick white slurry was stirred, a solution of thiophen-2-ylmagnesium chloride (6.8 mL, 0.44 M in THF, 2.99 mmol, 2.99 equiv) was added and the mixture turned dark grey. After 30 min of stirring, vinylogous ester **149a** (236.4 mg, 1.00 mmol, 1.00 equiv) was cannula-transferred to the slurry from a flame-dried 10 mL conical flask using several THF rinses (3 x 4 mL; total THF added = 25 mL, 0.04 M).

TLC analysis indicated that no starting material remained after 25 min. After an additional 5 min of stirring, the reaction was quenched with 10% w/w aqueous HCl (5 mL) and lowered into a preheated oil bath (60 °C). After 20 h, additional 10% w/w aqueous HCl (5 mL) was added. After 26 h, the yellow solution was removed from the bath, cooled to room temperature (23 °C), treated with sat. aqueous NaHCO_3 solution (25 mL), and transferred to a separatory funnel where the aqueous phase was extracted four

times with Et₂O. The combined organics (150 mL) were rinsed once with sat. aqueous NaHCO₃, dried over MgSO₄, filtered, and concentrated under reduced pressure. The crude oil was purified by flash chromatography (SiO₂, 3 x 30 cm, 100% hexanes→2%→5% EtOAc in hexanes) to afford cycloheptenone **137ab** (206.1 mg, 0.84 mmol, 84% yield) as a yellow/orange oil; *R_f* = 0.70 (30% EtOAc in hexanes); ¹H NMR (500 MHz, CDCl₃) δ 7.27 (dd, *J* = 5.0, 1.5 Hz, 1H), 7.00–6.95 (m, 2H), 6.17 (s, 1H), 5.69 (dddd, *J* = 16.7, 10.2, 8.1, 6.4 Hz, 1H), 5.06 (dddd, *J* = 10.2, 2.0, 1.0, 1.0 Hz, 1H), 5.01 (ddd, *J* = 16.9, 3.4, 1.5 Hz, 1H), 2.74–2.59 (m, 2H), 2.50 (dddd, *J* = 14.1, 6.4, 1.4, 1.4 Hz, 1H), 2.12 (dddd, *J* = 14.1, 8.1, 1.1, 1.1 Hz, 1H), 1.96–1.84 (m, 3H), 1.77–1.68 (m, 1H), 1.29 (s, 3H); ¹³C NMR (125 MHz, CDCl₃) δ 204.2, 154.6, 143.8, 134.0, 133.7, 127.0, 126.7, 125.5, 118.5, 45.6, 45.1, 44.2, 38.8, 26.4, 17.7; IR (Neat Film NaCl) 3103, 3075, 2964, 2938, 2871, 1671, 1655, 1590, 1519, 1454, 1438, 1415, 1378, 1341, 1251, 1234, 1218, 1178, 1134, 1107, 1077, 1045, 996, 917, 849, 836, 761, 708 cm⁻¹; HRMS (MM: ESI-APCI+) *m/z* calc'd for C₁₅H₁₉OS [M+H]⁺: 247.1151; found 247.1152; [α]_D^{25.0} –3.65 (*c* 1.31, CHCl₃, 88% ee).



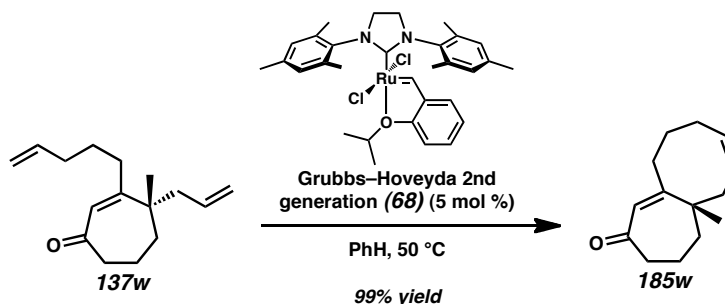
Cycloheptenone 198. Prepared using General Method F. A 100 mL round-bottom flask equipped with a magnetic stir bar, fitted with a rubber septum, and connected to a Schlenk manifold was flame-dried three times, backfilling with argon after each drying cycle. The hot flask was placed into a glove box antechamber, which was

evacuated/backfilled with N₂ (4 cycles, 1 min evacuation per cycle) before the flask was brought into the glove box. The flask was loaded with anhydrous cerium chloride (591.6 mg, 2.40 mmol, 2.50 equiv), refitted with the septum, removed from the glove box, and reconnected to the argon-filled Schlenk manifold. A portion of THF (12 mL) was added, rinsing the cerium chloride to the bottom of the flask. As the resulting thick white slurry was stirred, a solution of but-3-enylmagnesium bromide (6.55 mL, 0.44 M in THF, 2.88 mmol, 3.00 equiv) was added and the mixture turned pale yellow. After 40 min of stirring, vinylogous ester **149p** (226.9 mg, 0.96 mmol, 1.00 equiv) was cannula-transferred to the slurry from a 20 mL scintillation vial using several THF rinses (3 x 4 mL; total THF added = 24 mL, 0.04 M).

TLC analysis indicated that no starting material remained after 5 min. After an additional 10 min, the reaction was quenched with pH 6.5 Na₃PO₄ buffer (20 mL). A thick grey emulsion formed. The mixture was transferred to a separatory funnel where the aqueous phase was extracted four times with Et₂O. The combined organic (125 mL) were dried over MgSO₄, filtered, and concentrated under reduced pressure. The crude oil was transferred to a 20 mL scintillation vial and concentrated under reduced pressure. A stir bar, CH₃CN (2.0 mL), and 6 mM aqueous HCl (2.0 mL) were added to the vial. The resulting cloudy solution was stirred vigorously for 5 min before being transferred to a separatory funnel where the aqueous phase was extracted four times with Et₂O. The combined organics (75 mL) were dried over MgSO₄, filtered, and concentrated under reduced pressure. The crude oil was purified by flash chromatography (SiO₂, 3 x 30.5 cm, 100% hexanes→2%→5% EtOAc in hexanes) to afford cycloheptenone **198** (165.0 mg, 0.76 mmol, 79% yield) as a pale yellow oil; R_f = 0.74 (30% EtOAc in hexanes); ¹H

NMR (500 MHz, CDCl_3) δ 5.93 (s, 1H), 5.83–5.74 (m, 1H), 5.43–5.32 (m, 2H), 5.02 (dm, $J = 17.2$ Hz, 1H), 4.97 (dm, $J = 10.2$ Hz, 1H), 2.66–2.50 (m, 2H), 2.27–2.12 (m, 4H), 1.84–1.71 (m, 4H), 1.69 (dd, $J = 4.8, 0.7$ Hz, 3H), 1.22 (s, 3H); ^{13}C NMR (125 MHz, CDCl_3) δ 204.8, 161.7, 137.8, 137.2, 129.3, 124.4, 115.2, 48.6, 44.1, 41.3, 34.8, 34.1, 26.0, 18.2, 18.0; IR (Neat Film NaCl) 3077, 2962, 2937, 2874, 2856, 1650, 1614, 1451, 1414, 1378, 1342, 1273, 1251, 1224, 1198, 1126, 1069, 974, 911 cm^{-1} ; HRMS (MM: ESI-APCI+) m/z calc'd for $\text{C}_{15}\text{H}_{23}\text{O}$ $[\text{M}+\text{H}]^+$: 219.1743; found 219.1741; $[\alpha]_{\text{D}}^{20.0} +123.43$ (c 1.10, CHCl_3 , 88% ee).

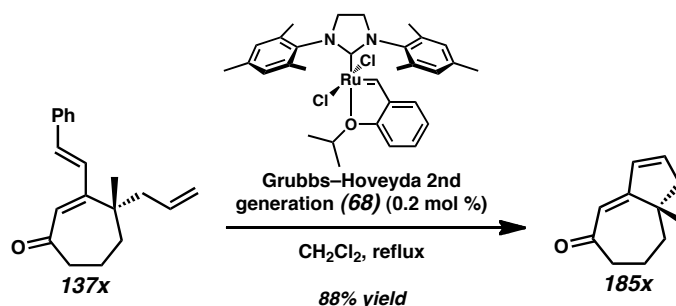
2.10.2.15 PREPARATION OF POLYCYCLIC CYCLOHEPTENONE DERIVATIVES BY RING-CLOSING METATHESIS



General Method I: Ring-Closing Metathesis

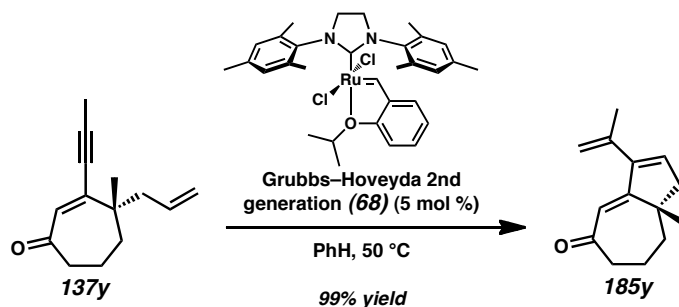
Enone 185w. A 100 mL round-bottom flask equipped with a magnetic stir bar, fitted with a water condenser, and connected to a Schlenk manifold (through the condenser) was flame-dried three times, backfilling with argon after each drying cycle. Once cool, the flask was loaded with neat cycloheptenone **137w** (50.0 mg, 0.22 mmol, 1.00 equiv) and backfilled with argon twice. Benzene (1 h argon sparge before use, 43 mL, 0.005 M) was added to the flask, followed by Grubbs-Hoveyda 2nd generation catalyst (6.7 mg,

0.011 mmol, 5 mol %). The solution color turned pale green with addition of catalyst. The flask was lowered into a preheated oil bath (50 °C). The reaction was removed from the oil bath after 30 min, cooled to room temperature (23 °C), and quenched with ethyl vinyl ether (1 mL). The reaction was filtered through a short silica gel plug rinsing with Et₂O and concentrated under reduced pressure. The crude oil was purified twice by flash chromatography (SiO₂, both columns 2 x 28 cm, 100% hexanes→2%→5% EtOAc in hexanes) to afford cycloheptenone **185w** (43.5 mg, 0.21 mmol, 99% yield) as a yellow oil.



Enone 185x (*Table 2.6, entry 1*). Prepared using General Method I. A 100 mL round-bottom flask equipped with a magnetic stir bar, fitted with a water condenser, and connected to a Schlenk manifold (through the condenser) was flame-dried three times, backfilling with argon after each drying cycle. Once cool, the flask was loaded with neat cycloheptenone **137x** (452.8 mg, 1.70 mmol, 1.00 equiv) and dichloromethane (60 mL, 0.03 M) and the resulting solution was sparged with Ar. After 30 min of degassing, Grubbs 2nd generation catalyst (3.4 mg, 0.0040 mmol, 0.2 mol %) was added to the flask. The solution color turned pale red with addition of catalyst. The flask was lowered into a preheated oil bath (50 °C).

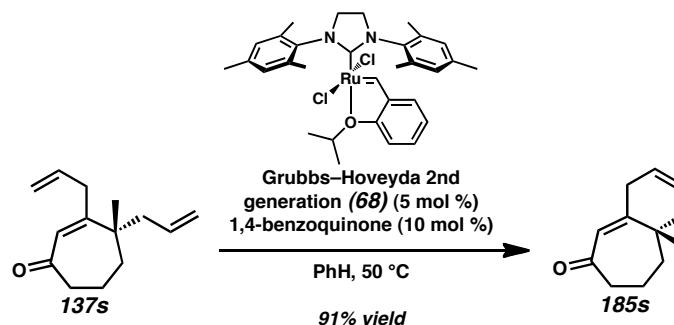
The flask was removed from oil bath after 1 h, cooled to room temperature (23 °C), and charged with DMSO (50 μ L) and silica gel (70 mg). The resulting mixture was concentrated the reaction under reduced pressure and purified by flash chromatography (SiO_2 , 2 x 17 cm, 15:1 hexanes:EtOAc) to afford cycloheptenone **185x** (242.9 mg, 1.50 mmol, 88% yield) as a yellow oil; R_f = 0.52 (30% EtOAc in hexanes); ^1H NMR (500 MHz, CDCl_3) δ 6.35–6.32 (m, 1H), 6.14 (dddd, J = 5.6, 2.5, 1.7, 0.7 Hz, 1H), 5.87 (app s, 1H), 2.70 (dddt, J = 15.1, 6.4, 3.5, 0.9 Hz, 1H), 2.59–2.51 (m, 2H), 2.41 (ddd, J = 17.9, 2.9, 1.6 Hz, 1H), 2.11–2.02 (m, 1H), 2.00–1.82 (m, 3H), 1.23 (s, 3H); ^{13}C NMR (125 MHz, CDCl_3) δ 204.8, 169.2, 142.7, 134.4, 121.7, 51.6, 46.7, 45.1, 37.9, 29.7, 21.2; IR (Neat Film NaCl) 3056, 2930, 2867, 2841, 1651, 1615, 1580, 1449, 1372, 1352, 1293, 1261, 1211, 1190, 1159, 1080, 968, 951, 862, 844, 801, 811, 723 cm^{-1} ; HRMS (MM: ESI–APCI+) m/z calc'd for $\text{C}_{11}\text{H}_{15}\text{O}$ $[\text{M}+\text{H}]^+$: 163.1117; found 163.1120; $[\alpha]_{\text{D}}^{26.0}$ –48.88 (c 1.83, CHCl_3 , 88% ee).



Enone 185y (Table 2.6, entry 2). Prepared using General Method I. A two neck 100 mL round-bottom flask equipped with a magnetic stir bar, fitted with rubber septa and a water condenser, and connected to a Schlenk manifold (through the condenser) was flame-dried three times, backfilling with argon after each drying cycle. Once cool, the flask was loaded with neat cycloheptenone **137y** (50.0 mg, 0.25 mmol, 1.00 equiv) and

backfilled with argon. Benzene (1 h argon sparge before use, 39 mL) was added to the flask, followed by Grubbs–Hoveyda 2nd generation catalyst (7.8 mg, 0.012 mmol, 5 mol %). The solution color turned pale green with addition of catalyst. The flask was rinsed with more benzene (10 mL; total benzene added = 49 mL, 0.005 M) and lowered into a preheated oil bath (50 °C).

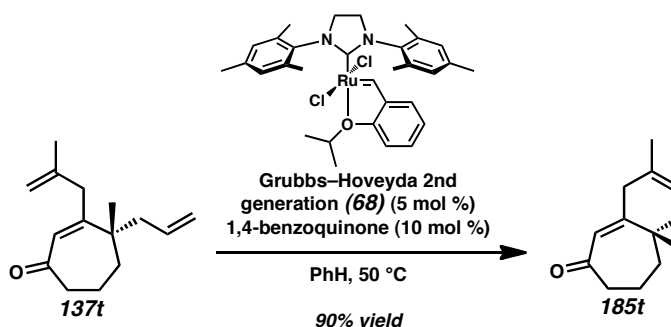
TLC analysis indicated no starting material remained after 3 h. Consequently, the reaction was removed from oil bath, cooled to room temperature (23 °C), and quenched with ethyl vinyl ether (1 mL). The reaction was filtered through a short silica gel plug rinsing with Et₂O and concentrated under reduced pressure. The crude oil was purified by flash chromatography (SiO₂, 2 x 28.5 cm, 100% hexanes→2%→5% EtOAc in hexanes) to afford cycloheptenone **185y** (50 mg, 0.25 mmol, 99% yield) as a yellow oil; *R_f* = 0.64 (30% EtOAc in hexanes); ¹H NMR (500 MHz, CDCl₃) δ 6.16 (t, *J* = 2.8 Hz, 1H), 6.02 (s, 1H), 5.13–5.11 (m, 1H), 4.97 (s, 1H), 2.76 (ddd, *J* = 14.7, 6.7, 4.7 Hz, 1H), 2.56 (ddd, *J* = 14.7, 9.8, 5.1 Hz, 1H), 2.48 (dd, *J* = 17.8, 2.0 Hz, 1H), 2.33 (dd, *J* = 17.8, 3.1 Hz, 1H), 2.09–1.99 (m, 1H), 1.94 (dd, *J* = 9.9, 4.0 Hz, 2H), 1.91–1.89 (m, 3H), 1.89–1.83 (m, 1H), 1.26 (s, 3H); ¹³C NMR (125 MHz, CDCl₃) δ 204.7, 167.2, 146.8, 138.4, 137.5, 122.0, 115.9, 49.5, 48.3, 45.0, 38.2, 28.4, 23.1, 20.9; IR (Neat Film NaCl) 3084, 3052, 2918, 2868, 2845, 1652, 1607, 1450, 1374, 1352, 1311, 1290, 1259, 1210, 1190, 1164, 1117, 1082, 1004, 982, 944, 898, 881, 848, 811, 771, 746 cm⁻¹; HRMS (MM: ESI–APCI+) *m/z* calc'd for C₁₄H₁₉O [M+H]⁺: 203.1430; found 203.11428; [α]_D^{25.0} –55.41 (*c* 1.61, CHCl₃, 88% ee).



Enone 185s (*Table 2.6, entry 3*). Prepared using General Method I. A 250 mL round-bottom flask equipped with a magnetic stir bar, fitted with a water condenser, and connected to a Schlenk manifold (through the condenser) was flame-dried three times, backfilling with argon after each drying cycle. Once cool, cycloheptenone **137s** (174.6 mg, 0.85 mmol, 1.00 equiv) was cannula-transferred from a 20 mL scintillation vial to the 250 mL flask using several benzene rinses (1.5 h argon sparge before use, 5 x 4 mL). Additional benzene (141 mL) was added to the flask followed by 1,4-benzoquinone (9.2 mg, 0.085 mmol, 10 mol %) and Grubbs-Hoveyda 2nd generation catalyst (26.8 mg, 0.043 mmol, 5 mol %). The solution color turned pale green with addition of catalyst. The flask was rinsed with more benzene (10 mL; total benzene added = 171 mL, 0.005 M) and lowered into a preheated oil bath (50 °C).

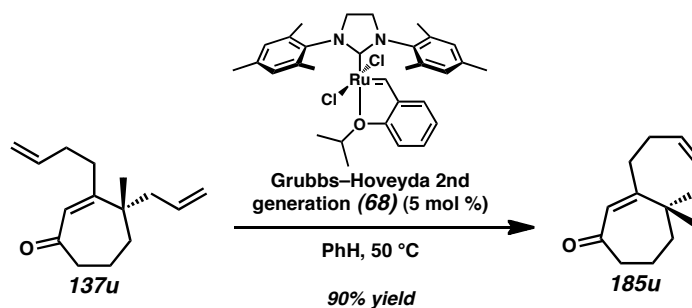
The reaction was removed from oil bath after 2.5 h, cooled to room temperature (23 °C), and quenched with ethyl vinyl ether (2 mL). The reaction color turned dark green with the ethyl vinyl ether addition. The reaction was filtered through a short silica gel plug rinsing with Et₂O and concentrated under reduced pressure. The crude oil was purified by flash chromatography (SiO₂, 3 x 25 cm, 100% hexanes→2%→5% EtOAc in hexanes) to afford cycloheptenone **185s** (47.7 mg, 0.27 mmol, 91% yield) as a yellow oil; *R_f* = 0.58 (30% EtOAc in hexanes); ¹H NMR (500 MHz, C₆D₆) δ 5.95 (d, *J* = 2.1 Hz,

1H), 5.46–5.41 (m, 1H), 5.34 (dddd, $J = 9.9, 4.4, 2.8, 2.8, 1.0$ Hz, 1H), 2.72 (dm, $J = 20.2$ Hz, 1H), 2.44–2.33 (m, 2H), 2.27 (dm, $J = 20.2$ Hz, 1H), 1.97 (dm, $J = 17.6$ Hz, 1H), 1.44 (ddd, $J = 17.5, 5.2, 0.9$ Hz, 1H), 1.33–1.19 (m, 4H), 0.86 (s, 3H); ^{13}C NMR (125 MHz, C_6D_6) δ 202.2, 156.0, 127.2, 125.1, 125.0, 44.3, 41.8, 41.4, 41.2, 36.3, 26.1, 17.6; IR (Neat Film NaCl) 3274, 3029, 2933, 2833, 1720, 1650, 1619, 1452, 1420, 1381, 1345, 1306, 1264, 1239, 1219, 1185, 1125, 1105, 1082, 1004, 976, 952, 938, 924, 892, 884, 871, 836, 775, 733 cm^{-1} ; HRMS (MM: ESI–APCI+) m/z calc'd for $\text{C}_{12}\text{H}_{17}\text{O}$ $[\text{M}+\text{H}]^+$: 177.1274; found 177.1277; $[\alpha]_{\text{D}}^{25.0} -49.94$ (c 0.86, CHCl_3 , 88% ee).



Enone 185t (*Table 2.6, entry 4*). Prepared using General Method I. A three neck 100 mL round-bottom flask equipped with a magnetic stir bar and fitted with rubber septa and a water condenser was connected to a Schlenk manifold (through the condenser). The flask was flame-dried three times, backfilling with argon after each drying cycle. Once cool, the flask was loaded with neat cycloheptenone **137t** (50.0 mg, 0.23 mmol, 1.00 equiv), benzene (1 h argon sparge before use, 46 mL, 0.005 M), 1,4-benzoquinone (2.5 mg, 0.023 mmol, 10 mol %), and Grubbs-Hoveyda 2nd generation catalyst (7.2 mg, 0.011 mmol, 5 mol %). The solution color turned pale green with addition of catalyst. The flask was lowered into a preheated oil bath (50 °C).

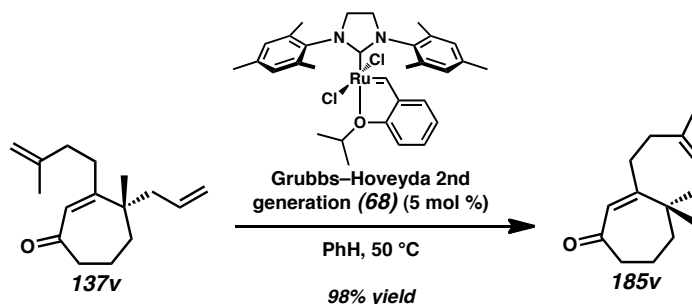
The reaction was removed from oil bath after 1 h, cooled to room temperature (23 °C), and quenched with ethyl vinyl ether (1.5 mL). The reaction color turned dark green with the ethyl vinyl ether addition. The reaction was filtered through a short silica gel plug rinsing with Et₂O and concentrated under reduced pressure. The crude oil was purified by flash chromatography (SiO₂, 2 x 28 cm, 100% hexanes→2%→5% EtOAc in hexanes) to afford cycloheptenone **185t** (39.0 mg, 0.21 mmol, 90% yield) as a yellow oil; *R_f* = 0.56 (30% EtOAc in hexanes); ¹H NMR (500 MHz, CDCl₃) δ 5.87 (d, *J* = 2.0 Hz, 1H), 5.38–5.34 (m, 1H), 3.06 (dm, *J* = 19.7 Hz, 1H), 2.63–2.49 (m, 3H), 2.28 (dm, *J* = 17.2 Hz, 1H), 1.85 (dd, *J* = 17.2, 5.3 Hz, 1H), 1.81–1.75 (m, 2H), 1.74–1.65 (m, 2H), 1.68 (s, 3H), 1.16 (s, 3H); ¹³C NMR (125 MHz, CDCl₃) δ 205.1, 159.4, 131.8, 126.3, 119.5, 44.3, 41.6, 41.5, 41.3, 41.3, 26.6, 22.5, 17.6; IR (Neat Film NaCl) 3273, 3017, 2963, 2930, 1720, 1656, 1651, 1645, 1619, 1616, 1450, 1418, 1378, 1363, 1345, 1268, 1239, 1220, 1191, 1151, 1134, 1104, 1072, 1038, 989, 972, 962, 944, 931, 897, 877, 854, 827, 784, 732 cm⁻¹; HRMS (MM: ESI–APCI+) *m/z* calc'd for C₁₃H₁₉O [M+H]⁺: 191.1430; found 191.1436; [α]_D^{25.0} +9.09 (*c* 0.86, CHCl₃, 88% ee).



Enone 185u (Table 2.6, entry 5). Prepared using General Method I. A two neck 100 mL round-bottom flask equipped with a magnetic stir bar, fitted with rubber septa and a water condenser, and connected to a Schlenk manifold (through the condenser) was

flame-dried three times, backfilling with argon after each drying cycle. Once cool, the flask was loaded with neat cycloheptenone **137u** (50.0 mg, 0.23 mmol, 1.00 equiv), Grubbs–Hoveyda 2nd generation catalyst (7.2 mg, 0.011 mmol, 5 mol %), benzene (1 h argon sparge before use, 46 mL, 0.005 M). The solution color turned pale green with addition of catalyst. The flask was lowered into a preheated oil bath (50 °C).

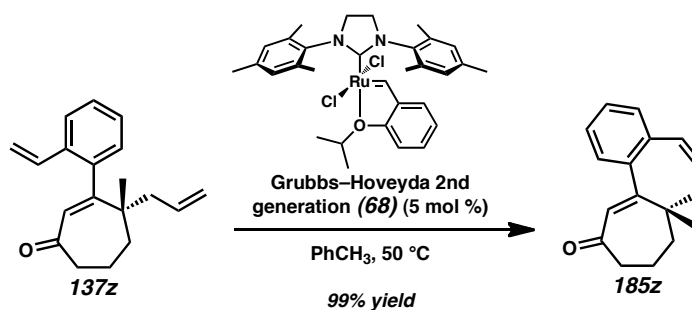
TLC analysis indicated no starting material remained after 15 min. Consequently, the reaction was removed from the oil bath, cooled to room temperature (23 °C), and quenched with ethyl vinyl ether (1 mL). The reaction color turned amber with the ethyl vinyl ether addition. The reaction was filtered through a short silica gel plug rinsing with Et₂O and concentrated under reduced pressure. The crude oil was purified by flash chromatography (SiO₂, 2 x 27.5 cm, 100% hexanes→2%→5% EtOAc in hexanes) to afford cycloheptenone **185u** (39.4 mg, 0.21 mmol, 90% yield) as a yellow oil; *R_f* = 0.58 (30% EtOAc in hexanes); ¹H NMR (500 MHz, CDCl₃) δ 5.87 (s, 1H), 5.65–5.58 (m, 1H), 5.54–5.49 (m, 1H), 2.81–2.74 (m, 1H), 2.66–2.59 (m, 2H), 2.56–2.46 (m, 2H), 2.24–2.13 (m, 2H), 2.07 (ddd, *J* = 14.1, 11.1, 3.1 Hz, 1H), 1.93 (dddd, *J* = 14.1, 11.0, 9.3, 4.8, 2.9 Hz, 1H), 1.85–1.79 (m, 1H), 1.76 (dd, *J* = 14.9, 7.9 Hz, 1H), 1.66 (ddd, *J* = 14.0, 6.9, 2.8 Hz, 1H), 1.16 (s, 3H); ¹³C NMR (125 MHz, CDCl₃) δ 204.8, 165.3, 129.9, 129.7, 126.2, 47.8, 43.9, 40.7, 40.3, 34.5, 32.2, 27.8, 19.6; IR (Neat Film NaCl) 3287, 3017, 2930, 2833, 1652, 1616, 1481, 1450, 1380, 1352, 1342, 1291, 1279, 1262, 1243, 1224, 1204, 1184, 1162, 1084, 1075, 1047, 1021, 984, 963, 921, 896, 877, 846, 834, 788, 755 cm⁻¹; HRMS (MM: ESI–APCI+) *m/z* calc'd for C₁₃H₁₉O [M+H]⁺: 191.1430; found 191.1430; [α]_D^{25.0} –92.01 (*c* 0.82, CHCl₃, 88% ee).



Enone 185v (*Table 2.6, entry 6*). Prepared using General Method I. A two neck 100 mL round-bottom flask equipped with a magnetic stir bar, fitted with rubber septa and a water condenser, and connected to a Schlenk manifold (through the condenser) was flame-dried three times, backfilling with argon after each drying cycle. Once cool, the flask was loaded with neat cycloheptenone **137v** (50.0 mg, 0.22 mmol, 1.00 equiv) and backfilled with argon. Benzene (1 h argon sparge before use, 33 mL) was added to the flask, followed by Grubbs–Hoveyda 2nd generation catalyst (6.7 mg, 0.011 mmol, 5 mol %). The solution color turned pale green with addition of catalyst. The flask was rinsed with more benzene (10 mL; total benzene added = 43 mL, 0.005 M) and lowered into a preheated oil bath (50 °C).

TLC analysis indicated no starting material remained after 30 min. After an additional 10 min of stirring, the reaction was removed from the oil bath, cooled to room temperature (23 °C), and quenched with ethyl vinyl ether (1 mL). The reaction color turned dark brown with the ethyl vinyl ether addition. The reaction was filtered through a short silica gel plug rinsing with Et₂O and concentrated under reduced pressure. The crude oil was purified by flash chromatography (SiO₂, 2 x 28.5 cm, 100% hexanes→2%→5% EtOAc in hexanes) to afford cycloheptenone **185v** (43.2 mg, 0.21 mmol, 98% yield) as a clear colorless oil; *R_f* = 0.63 (30% EtOAc in hexanes); ¹H NMR (500 MHz, CDCl₃) δ 5.87 (s, 1H), 5.41–5.34 (m, 1H), 2.79 (td, *J* = 12.3, 5.3 Hz, 1H),

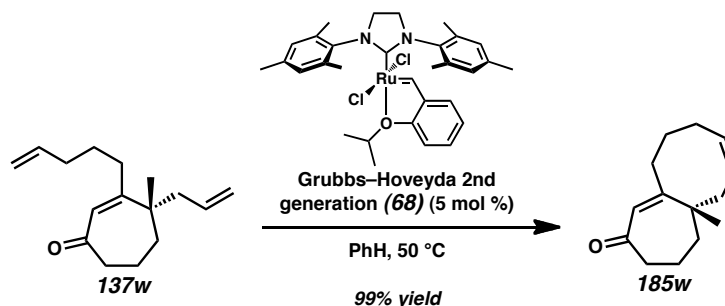
2.66–2.55 (m, 2H), 2.54–2.42 (m, 2H), 2.19 (ddd, $J = 12.5, 6.0, 3.3$ Hz, 1H), 2.14–2.02 (m, 2H), 1.98–1.88 (m, 1H), 1.85–1.76 (m, 1H), 1.71–1.63 (m, 2H), 1.62 (s, 3H), 1.13 (s, 3H); ^{13}C NMR (125 MHz, CDCl_3) δ 204.9, 165.8, 136.9, 129.5, 120.7, 47.7, 43.9, 40.6, 40.2, 36.9, 34.3, 27.5, 25.3, 19.7; IR (Neat Film NaCl) 3300, 3014, 2928, 2828, 1657, 1617, 1480, 1450, 1379, 1353, 1342, 1292, 1259, 1216, 1171, 1131, 1106, 1082, 1050, 1009, 982, 962, 916, 897, 874, 833, 814, 795, 765 cm^{-1} ; HRMS (MM: ESI–APCI+) m/z calc'd for $\text{C}_{14}\text{H}_{21}\text{O}_2$ $[\text{M}+\text{H}]^+$: 205.1587; found 205.1582; $[\alpha]_{\text{D}}^{25.0} -73.66$ (c 0.95, CHCl_3 , 88% ee).



Enone 185z (Table 2.6, entry 7). Prepared using General Method I. A three neck 100 mL round-bottom flask equipped with a magnetic stir bar, fitted with rubber septa and a water condenser, and connected to a Schlenk manifold (through the condenser) was flame-dried three times, backfilling with argon after each drying cycle. Once cool, cycloheptenone **137z** (65.8 mg, 0.25 mmol, 1.00 equiv) was cannula-transferred from a 20 mL scintillation vial to the 100 mL flask using several toluene rinses (1.5 h argon sparge before use, 5 x 4 mL). Additional toluene (20 mL) was added to the flask followed by Grubbs-Hoveyda 2nd generation catalyst (7.7 mg, 0.012 mmol, 5 mol %). The solution color turned pale green with addition of catalyst. The flask was rinsed with

more toluene (9 mL; total toluene added = 49 mL, 0.005 M) and lowered into a preheated oil bath (50 °C).

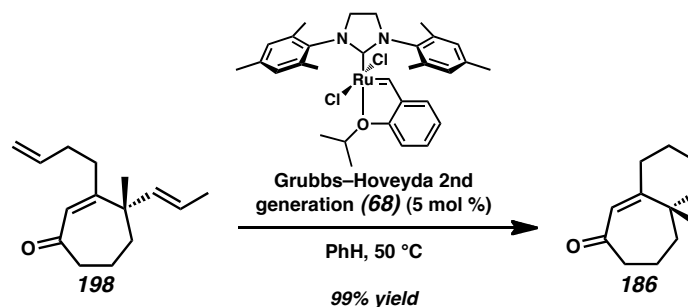
The reaction was removed from the oil bath after 6.5 h, cooled to room temperature (23 °C), and quenched with ethyl vinyl ether (0.5 mL). The reaction color turned dark brown with the ethyl vinyl ether addition. The reaction was filtered through a short silica gel plug rinsing with EtOAc and concentrated under reduced pressure. The crude oil was purified by flash chromatography (SiO₂, 2 x 24.5 cm, 100% hexanes→2%→5% EtOAc in hexanes) to afford cycloheptenone **185z** (56.7 mg, 0.23 mmol, 96% yield) as a yellow oil; R_f = 0.64 (30% EtOAc in hexanes); ¹H NMR (500 MHz, CDCl₃) δ 7.31–7.26 (m, 1H), 7.22–7.19 (m, 2H), 7.10 (d, J = 7.4 Hz, 1H), 6.53 (dm, J = 11.1 Hz, 1H), 6.03 (dt, J = 11.2, 6.0 Hz, 1H), 5.82 (s, 1H), 2.71–2.60 (m, 2H), 2.30 (ddd, J = 15.6, 5.8, 0.8 Hz, 1H), 2.21 (ddd, J = 15.6, 6.3, 1.8 Hz, 1H), 2.15 (ddd, J = 13.9, 7.5, 4.5 Hz, 1H), 2.01–1.85 (m, 3H), 1.14 (s, 3H); ¹³C NMR (125 MHz, CDCl₃) δ 204.3, 162.5, 142.5, 135.5, 132.0, 130.8, 130.0, 128.8, 128.8, 127.9, 127.3, 50.6, 44.2, 42.4, 40.1, 27.8, 19.3; IR (Neat Film NaCl) 3057, 3017, 2933, 2870, 1718, 1665, 1601, 1481, 1445, 1417, 1383, 1354, 1340, 1286, 1258, 1228, 1180, 1125, 996, 984, 936, 890, 828, 780, 757 cm⁻¹; HRMS (MM: ESI–APCI+) m/z calc'd for C₁₇H₁₉O [M+H]⁺: 239.1430; found 239.1432; $[\alpha]_D^{20.0}$ –86.75 (c 0.70, CHCl₃, 88% ee).



Enone 185w (*Table 2.6, entry 8*). Prepared using General Method I. A 100 mL round-bottom flask equipped with a magnetic stir bar, fitted with a water condenser, and connected to a Schlenk manifold (through the condenser) was flame-dried three times, backfilling with argon after each drying cycle. Once cool, the flask was loaded with neat cycloheptenone **137w** (50.0 mg, 0.22 mmol, 1.00 equiv) and backfilled with argon twice. Benzene (1 h argon sparge before use, 43 mL, 0.005 M) was added to the flask, followed by Grubbs-Hoveyda 2nd generation catalyst (6.7 mg, 0.011 mmol, 5 mol %). The solution color turned pale green with addition of catalyst. The flask was lowered into a preheated oil bath (50 °C).

The reaction was removed from the oil bath after 30 min, cooled to room temperature (23 °C), and quenched with ethyl vinyl ether (1 mL). The reaction was filtered through a short silica gel plug rinsing with Et₂O and concentrated under reduced pressure. The crude oil was purified twice by flash chromatography (SiO₂, both columns 2 x 28 cm, 100% hexanes→2%→5% EtOAc in hexanes) to afford cycloheptenone **185w** (43.5 mg, 0.21 mmol, 99% yield) as a yellow oil; *R_f* = 0.56 (30% EtOAc in hexanes); ¹H NMR (500 MHz, CDCl₃) δ 5.77–5.70 (m, 1H), 5.65 (tdt, *J* = 10.4, 6.4, 1.3 Hz, 1H), 2.68–2.55 (m, 2H), 2.54–2.44 (m, 1H), 2.30–2.24 (m, 2H), 2.24–2.15 (m, 1H), 2.13–2.04 (m, 1H), 1.94–1.69 (m, 7H), 1.52–1.41 (m, 1H), 1.22 (s, 3H); ¹³C NMR (125 MHz, CDCl₃) δ 204.2, 165.6, 132.2, 131.9, 128.5, 49.0, 44.2, 39.8, 39.5, 35.5, 31.1, 27.0, 26.5, 17.8; IR

(Neat Film NaCl) 3018, 2928, 2859, 1645, 1608, 1468, 1448, 1411, 1380, 1343, 1327, 1279, 1253, 1214, 1178, 1131, 1102, 1088, 1051, 1015, 987, 965, 937, 920, 899, 880, 845, 796, 777, 747 cm^{-1} ; HRMS (MM: ESI–APCI+) m/z calc'd for $\text{C}_{14}\text{H}_{21}\text{O}$ $[\text{M}+\text{H}]^+$: 205.1587; found 205.1587; $[\alpha]_{\text{D}}^{25.0} -141.99$ (c 1.01, CHCl_3 , 88% ee).

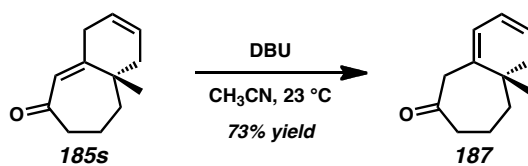


Enone 186. Prepared using General Method I. A 100 mL round-bottom flask equipped with a magnetic stir bar, fitted with a water condenser, and connected to a Schlenk manifold (through the condenser) was flame-dried three times, backfilling with argon after each drying cycle. Once cool, the flask was loaded with neat cycloheptenone **198** (50.0 mg, 0.23 mmol, 1.00 equiv) and backfilled with argon twice. Benzene (1 h argon sparge before use, 44 mL) was added to the flask, followed by Grubbs–Hoveyda 2nd generation catalyst (7.2 mg, 0.011 mmol, 5 mol %). The flask was rinsed with more benzene (2 mL; total benzene added = 46 mL, 0.005 M) and lowered into a preheated oil bath (50 °C). The solution color turned pale green with addition of catalyst and amber over time.

The reaction was removed from the oil bath after 50 min, cooled to room temperature (23 °C), and quenched with ethyl vinyl ether (0.5 mL). The reaction was filtered through a short silica gel plug rinsing with Et_2O and concentrated under reduced pressure. The crude oil was purified twice by flash chromatography (SiO_2 , both columns 2 x 27.5 cm,

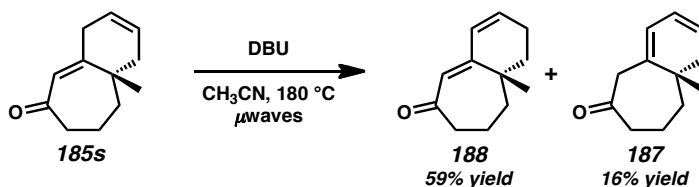
100% hexanes→2%→5% EtOAc in hexanes) to afford cycloheptenone **186** (35.8 mg, 0.23 mmol, 89% yield, 70% yield from vinylogous ester **149p**) as a pale yellow oil; R_f = 0.62 (30% EtOAc in hexanes); ^1H NMR (500 MHz, CDCl_3) δ 5.87 (s, 1H), 5.72–5.67 (m, 1H), 5.28 (dd, J = 9.7, 2.4 Hz, 1H), 2.71–2.64 (m, 1H), 2.62–2.54 (m, 1H), 2.53–2.46 (m, 1H), 2.31–2.11 (m, 3H), 1.92–1.74 (m, 3H), 1.70 (ddd, J = 14.0, 6.6, 2.4 Hz, 1H), 1.27 (s, 3H); ^{13}C NMR (125 MHz, CDCl_3) δ 204.5, 161.3, 137.8, 126.9, 125.3, 44.6, 43.6, 40.6, 33.8, 28.1, 27.7, 18.6; IR (Neat Film NaCl) 3019, 2934, 2866, 2845, 1665, 1653, 1621, 1450, 1414, 1350, 1309, 1281, 1258, 1217, 1181, 1171, 1132, 1087, 1074, 1024, 1013, 973, 938, 902, 881, 865, 783, 767, 716 cm^{-1} ; HRMS (MM: ESI–APCI+) m/z calc'd for $\text{C}_{12}\text{H}_{17}\text{O}$ $[\text{M}+\text{H}]^+$: 177.1274; found 177.1274; $[\alpha]_{\text{D}}^{20.0}$ –188.35 (c 0.72, CHCl_3 , 88% ee).

2.10.2.16 PREPARATION OF POLYCYCLIC CYCLOHEPTENONE DERIVATIVES BY OTHER METHODS



Diene 187. A 20 mL scintillation vial containing enone **185s** (31.5 mg, 0.18 mmol, 1.00 equiv) was equipped with a stir bar and sealed with a screw cap containing a teflon septum. The vial was connected to a Schlenk manifold and backfilled with argon three times. Acetonitrile (1.8 mL, 0.1 M) was added to the vial followed by DBU (30 μL , 0.20 mmol, 1.12 equiv). The solution was stirred at room temperature (23 $^\circ\text{C}$) until no starting material remained by TLC analysis (4 h). The reaction was passed through a short silica

gel plug, rinsed with water, dried over MgSO_4 , filtered through another short silica gel plug, and concentrated under reduced pressure. The resulting crude oil was purified by flash chromatography (SiO_2 , 1 x 28.5 cm, 100% hexanes \rightarrow 2% \rightarrow 5% EtOAc in hexanes) to afford diene **187** (23.1 mg, 0.13 mmol, 73% yield) as a pale yellow oil; $R_f = 0.63$ (30% EtOAc in hexanes); ^1H NMR (500 MHz, CDCl_3) δ 5.86 (ddt, $J = 9.0, 5.3, 1.7$ Hz, 1H), 5.79–5.73 (m, 2H), 3.27 (d, $J = 16.3$ Hz, 1H), 2.93 (d, $J = 16.3$ Hz, 1H), 2.73 (ddd, $J = 12.4, 10.0, 4.7$ Hz, 1H), 2.33–2.23 (m, 2H), 2.08–2.00 (m, 1H), 1.89–1.67 (m, 3H), 1.49–1.41 (m, 1H), 0.99 (s, 3H); ^{13}C NMR (125 MHz, CDCl_3) δ 212.0, 138.6, 125.4, 123.9, 123.6, 49.5, 42.7, 37.6, 37.5, 36.5, 24.1, 20.9; IR (Neat Film NaCl) 3039, 2929, 2865, 2817, 1708, 1645, 1587, 1453, 1424, 1403, 1371, 1356, 1319, 1286, 1263, 1235, 1211, 1143, 1105, 1082, 1039, 987, 969, 940, 925, 851, 817, 761, 704 cm^{-1} ; HRMS (GC-EI+) m/z calc'd for $\text{C}_{12}\text{H}_{16}\text{O}$ $[\text{M}+\cdot]^+$: 176.1201; found 176.1219; $[\alpha]_{\text{D}}^{25.0} -205.54$ (c 0.71, CHCl_3 , 88% ee).

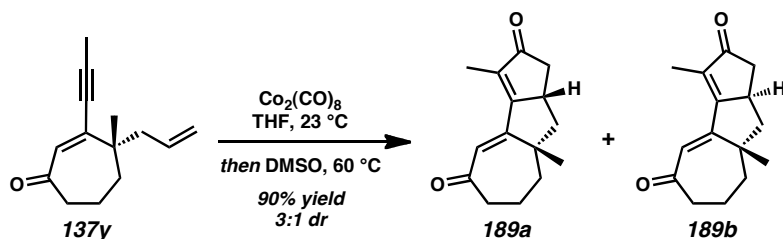


Diene 187 and Diene 188. A 2.0–5.0 mL μwave vial fitted with a stir bar and sealed with a screw cap containing a teflon septum was flame-dried three times, backfilling with argon after each drying cycle. Once cool, diene **185s** (66.7 mg, 0.38 mmol, 1.00 equiv) was cannula-transferred to the vial with several acetonitrile rinses (4 x 1 mL, 0.09 M) and the flask was charged with DBU (66 μL , 0.44 mmol, 1.17 equiv). The pale yellow solution was subjected to microwave irradiation in a Biotage Initiator microwave reactor

(temperature: 180 °C, sensitivity: normal). After 5 h of irradiation, the crimp cap was removed and the reaction was filtered through a silica gel plug. The resulting solution was concentrated under reduced pressure and purified by flash chromatography (SiO₂, 2 x 29 cm, 100% hexanes→10%→30%→50%→80% CH₂Cl₂ in hexanes) to yield diene **188** (39.5 mg, 0.22 mmol, 59% yield) as a yellow oil and diene **187** (10.4 mg, 0.059 mmol, 16% yield) as a pale yellow oil.

Diene 187: Characterization data are identical to the data described above.

Diene 188: R_f = 0.56 (30% EtOAc in hexanes); ¹H NMR (500 MHz, CDCl₃) δ 6.13–6.07 (m, 1H), 6.02 (dd, J = 9.9, 2.8 Hz, 1H), 5.76 (s, 1H), 2.75 (dddt, J = 15.6, 6.6, 5.0, 0.9 Hz, 1H), 2.52 (ddd, J = 15.4, 9.5, 5.6 Hz, 1H), 2.38–2.27 (m, 1H), 2.19 (dtt, J = 19.3, 5.6, 1.3 Hz, 1H), 2.05–1.93 (m, 1H), 1.87–1.77 (m, 2H), 1.74–1.62 (m, 2H), 1.44 (ddt, J = 13.2, 5.4, 1.5 Hz, 1H), 1.13 (s, 3H); ¹³C NMR (125 MHz, CDCl₃) δ 204.1, 156.2, 135.1, 131.4, 129.1, 44.6, 42.2, 38.9, 37.6, 23.1, 22.9, 18.8; IR (Neat Film NaCl) 3026, 2967, 2922, 2868, 2849, 1650, 1621, 1583, 1449, 1428, 1383, 1353, 1338, 1284, 1244, 1225, 1207, 1173, 1163, 1130, 1114, 1090, 1077, 1023, 978, 954, 935, 911, 881, 866, 840, 777, 727 cm⁻¹; HRMS (MM: ESI-APCI+) m/z calc'd for C₁₂H₁₇O [M+H]⁺: 177.1274; found 177.1278; $[\alpha]_D^{25.0}$ –298.04 (c 1.24, CHCl₃, 88% ee).



Enones 189a and 189b. A 20 mL scintillation vial containing cycloheptenone **137y** (185.6 mg, 0.92 mmol, 1.00 equiv) was equipped with a stir bar and sealed with a screw cap containing a teflon septum. The vial was connected to a Schlenk manifold and backfilled with argon three times. The vial was charged with THF (5.0 mL, 0.2 M) and dicobalt octacarbonyl (388.5 mg, 1.14 mmol, 1.24 equiv), generating a dark brown solution. After 12 h of stirring at room temperature (23 °C), DMSO (380 μL , 5.35 mmol, 5.83 equiv) was added and the vial was lowered into a preheated oil bath (60 °C). Reaction turned dark red over time. The vial was removed from the oil bath after 14 h and cooled to room temperature. The reaction mixture was concentrated under reduced pressure and purified by flash chromatography using a Teledyne Isco CombiFlash R_f system (SiO_2 , 25 g loading cartridge, 40 g column, multi-step gradient, hold 0% [5 min]→ramp to 5% [5 min]→hold 5% [50 min]→ramp to 10% [5 min]→hold 10% [15 min]→ramp to 15% [1 min]→hold 15% [7 min]→ramp to 20% [1 min]→hold 20% EtOAc in hexanes [27 min]) to afford a 3:1 diastereomeric mixture of cycloheptenones **189a:189b** (190.2 mg, 0.83 mmol, 90% yield). Analytically pure samples of **189a** and **189b** could be obtained using the above column conditions.

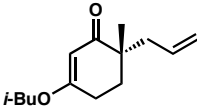
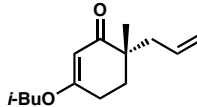
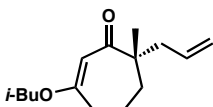
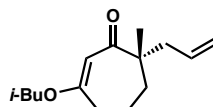
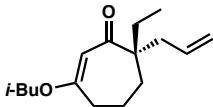
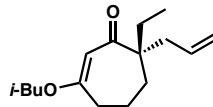
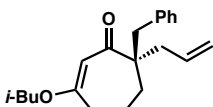
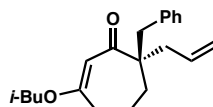
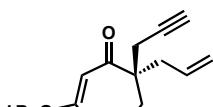
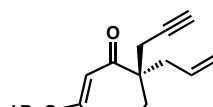
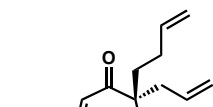
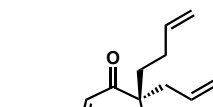
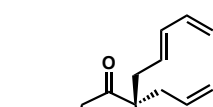
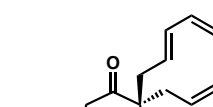
Major diastereomer (189a): yellow oil that solidified upon cooling; R_f = 0.32 (30% EtOAc in hexanes); ^1H NMR (500 MHz, CDCl_3) δ 6.38 (s, 1H), 3.21–3.12 (m, 1H),

2.81–2.75 (m, 1H), 2.75 (dd, $J = 17.8, 6.3$ Hz, 1H), 2.62 (ddd, $J = 14.0, 11.4, 4.6$ Hz, 1H), 2.19–2.09 (m, 1H), 2.11 (dd, $J = 17.8, 3.7$ Hz, 1H), 2.01 (dd, $J = 11.6, 6.9$ Hz, 1H), 1.99–1.90 (m, 2H), 1.89 (d, $J = 2.6$ Hz, 3H), 1.88–1.81 (m, 1H), 1.32 (s, 3H), 1.28 (t, $J = 11.8$ Hz, 1H); ^{13}C NMR (125 MHz, CDCl_3) δ 209.5, 204.8, 172.4, 155.0, 135.6, 128.8, 50.9, 47.2, 45.6, 42.3, 40.5, 39.5, 26.8, 20.9, 9.0; For NOESY correlation data, see Figure A1.351; IR (Neat Film NaCl) 2945, 2917, 2867, 1701, 1662, 1446, 1375, 1332, 1304, 1258, 1219, 1196, 1148, 1099, 1054, 978, 945, 895, 869, 852, 830, 802, 706 cm^{-1} ; HRMS (GC-EI+) m/z calc'd for $\text{C}_{15}\text{H}_{19}\text{O}_2$ $[\text{M}+\text{H}]^+$: 231.1380; found 231.1381; $[\alpha]_{\text{D}}^{20.0} +150.77$ (c 1.01, CHCl_3 , 88% ee).

Minor diastereomer (189b): orange oil that solidified upon cooling; $R_f = 0.25$ (30% EtOAc in hexanes); ^1H NMR (500 MHz, CDCl_3) δ 6.27 (s, 1H), 3.09–2.98 (m, 1H), 2.70 (dd, $J = 18.1, 6.4$ Hz, 1H), 2.71–2.64 (m, 1H), 2.63–2.56 (m, 1H), 2.16 (dd, $J = 12.5, 8.5$ Hz, 1H), 2.11 (dd, $J = 18.1, 3.3$ Hz, 1H), 2.12–1.96 (m, 2H), 1.95–1.87 (m, 2H), 1.87 (d, $J = 2.5$ Hz, 3H), 1.28 (dd, $J = 12.4, 11.6$ Hz, 1H), 1.24 (s, 3H); ^{13}C NMR (125 MHz, CDCl_3) δ 209.7, 206.4, 173.0, 154.6, 133.7, 127.4, 48.9, 48.3, 42.4, 42.3, 41.3, 37.5, 31.9, 22.2, 8.5; For NOESY correlation data, see Figure A1.355; IR (Neat Film NaCl) 2928, 2867, 1703, 1668, 1453, 1410, 1377, 1305, 1285, 1236, 1208, 1157, 1094, 1054, 996, 949, 891, 874, 859, 791, 720 cm^{-1} ; HRMS (GC-EI+) m/z calc'd for $\text{C}_{15}\text{H}_{19}\text{O}_2$ $[\text{M}+\text{H}]^+$: 231.1380; found 231.1372; $[\alpha]_{\text{D}}^{20.0} -407.06$ (c 1.65, CHCl_3 , 88% ee).

2.10.2.17 DETERMINATION OF ENANTIOMERIC EXCESS

Table 2.8. Methods for the Determination of Enantiomeric Excess (Chiral HPLC and SFC)

entry	product	compound assayed	assay conditions	retention time of major isomer (min)	retention time of minor isomer (min)	% ee
1	 151	 151	HPLC Chiralcel OD-H 5% IPA in hexane isocratic, 1.0 mL/min	5.80	6.53	86
2	 149a	 149a	HPLC Chiralcel OD-H 1% IPA in hexane isocratic, 1.0 mL/min	6.30	7.26	88
3	 149b	 149b	HPLC Chiralcel AD 0.25% IPA in hexane isocratic, 1.0 mL/min	18.08	16.23	92
4	 149c	 149c	HPLC Chiralcel OD-H 0.5% IPA in hexane isocratic, 1.0 mL/min	15.70	13.96	86
5	 149d	 149d	HPLC Chiralcel OD-H 0.5% IPA in hexane isocratic, 1.0 mL/min	12.35	13.43	89
6	 149e	 149e	HPLC Chiralcel AD 0.8% IPA in hexane isocratic, 2.0 mL/min	5.03	6.06	87
7	 149f	 149f	SFC Chiralcel AD-H 5% IPA in hexane isocratic, 2.5 mL/min	6.99	6.31	90

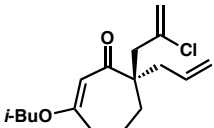
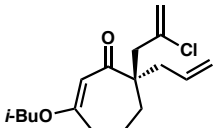
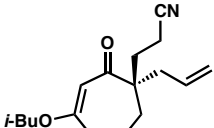
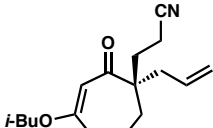
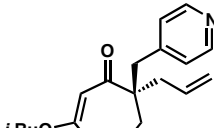
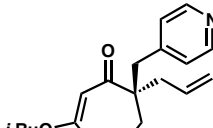
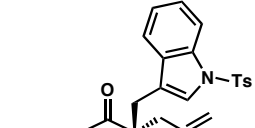
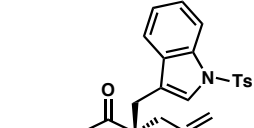
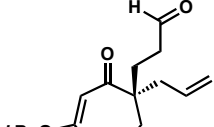
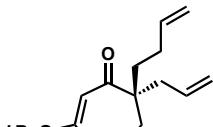
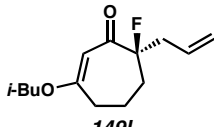
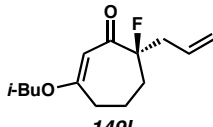
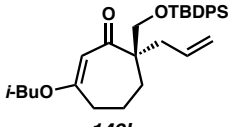
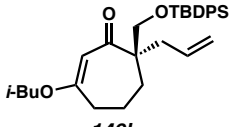
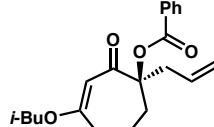
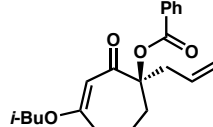
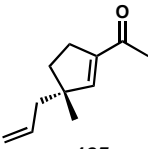
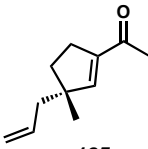
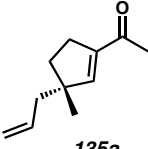
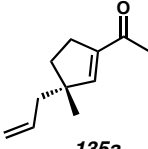
entry	product	compound assayed	assay conditions	retention time of major isomer (min)	retention time of minor isomer (min)	% ee
8	 149g	 149g	HPLC Chiralcel OD-H 0.1% IPA in hexane isocratic, 1.0 mL/min	27.22	24.19	86
9	 149h	 149h	HPLC Chiralcel OD-H 5% IPA in hexane isocratic, 1.0 mL/min	10.67	14.66	87
10	 149i	 149i	HPLC Chiralcel AD 5% EtOH in hexane isocratic, 1.0 mL/min	13.22	15.13	85
11	 149j	 149j	HPLC Chiralcel AD 5% EtOH in hexane isocratic, 1.0 mL/min	11.11	16.64	83
12	 149k	 149e	HPLC Chiralcel AD 0.8% IPA in hexane isocratic, 2.0 mL/min	4.39	5.17	80
13	 149l	 149l	HPLC Chiralcel OD-H 1% IPA in hexane isocratic, 1.0 mL/min	8.80	8.05	91
14	 149l	 149l	HPLC Chiralcel OD-H 0.2% IPA in hexane isocratic, 1.0 mL/min	21.74	25.53	58
15	 149n	 149n	HPLC Chiralcel OD-H 1% IPA in hexane isocratic, 1.0 mL/min	18.28	22.01	57

Table 2.9. Methods for the Determination of Enantiomeric Excess (Chiral GC)

entry	product	compound assayed	assay conditions	retention time of major isomer (min)	retention time of minor isomer (min)	% ee
1	 135a	 135a	GC G-TA 80 °C isotherm	54.98	61.35	88
2	 135a	 135a	GC G-TA 80 °C isotherm	54.74	60.24	98

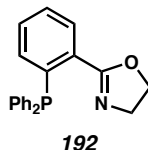
2.11 NOTES AND REFERENCES

- (1) For a review discussing our strategy of using natural product structures to drive the development of enantioselective catalysis, see: Mohr, J. T.; Krout, M. R.; Stoltz, B. M. *Nature* **2008**, *455*, 323–332.
- (2) For examples of asymmetric palladium-catalyzed allylic alkylation reactions of carbocyclic ketone enolates developed by our group, see: (a) Behenna, D. C.; Stoltz, B. M. *J. Am. Chem. Soc.* **2004**, *126*, 15044–15045. (b) Mohr, J. T.; Behenna, D. C.; Harned, A. M.; Stoltz, B. M. *Angew. Chem. Int. Ed.* **2005**, *44*, 6924–6927. (c) Behenna, D. C.; Mohr, J. T.; Sherden, N. H.; Marinescu, S. C.; Harned, A. M.; Tani, K.; Seto, M.; Ma, S.; Novák, Z.; Krout, M. R.; McFadden, R. M.; Roizen, J. L.; Enquist, Jr., J. A.; White, D. E.; Levine, S. R.; Petrova, K. V.; Iwashita, A.; Virgil, S. C.; Stoltz, B. M. *Chem. Eur. J.* **2011**, *17*, 14199–14223.
- (3) For examples of asymmetric palladium-catalyzed allylic alkylation reactions of heterocyclic ketone enolates (such as those derived from dioxanones and lactams) developed by our group, see: (a) Seto, M.; Roizen, J. L.; Stoltz, B. M. *Angew. Chem. Int. Ed.* **2008**, *47*, 6873–6876. (b) Behenna, D. C.; Liu, Y.; Yurino, T.; Kim, J.; White, D. E.; Virgil, S. C.; Stoltz, B. M. *Nature Chem.* **2012**, *4*, 130–133.
- (4) For examples of asymmetric palladium-catalyzed protonation reactions of cyclic ketone enolates, see: (a) Mohr, J. T.; Nishimata, T.; Behenna, D. C.; Stoltz, B. M. *J. Am. Chem. Soc.* **2006**, *128*, 11348–11349. (b) Marinescu, S. C.; Nishimata, T.; Mohr, J. T.; Stoltz, B. M. *Org. Lett.* **2008**, *10*, 1039–1042.

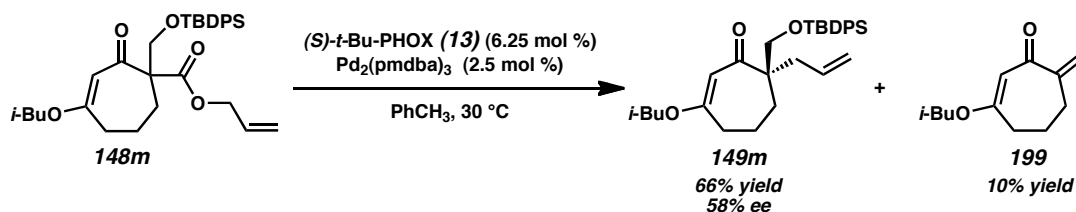
- (5) For an example of an asymmetric palladium-catalyzed conjugate addition/enolate alkylation cascade reaction of cyclic ketone enolates, see: Streuff, J.; White, D. E.; Virgil, S. C.; Stoltz, B. M. *Nature Chem.* **2010**, *2*, 192–196.
- (6) For studies on the computational and experimental studies on the mechanism of palladium-catalyzed asymmetric alkylation using the PHOX ligand scaffold, see: (a) Keith, J. A.; Behenna, D. C.; Mohr, J. T.; Ma, S.; Marinescu, S. C.; Oxgaard, J.; Stoltz, B. M.; Goddard, III, W. A. *J. Am. Chem. Soc.* **2007**, *129*, 11876–11877. (b) Sherden, N. H.; Behenna, D. C.; Virgil, S. C.; Stoltz, B. M. *Angew. Chem. Int. Ed.* **2009**, *48*, 6840–6843. (c) Keith, J. A.; Behenna, D. C.; Sherden, N.; Mohr, J. T.; Ma, S.; Marinescu, S. C.; Nielsen, R. J.; Oxgaard, J.; Stoltz, B. M.; Goddard, III, W. A. *J. Am. Chem. Soc.* **2012**, *134*, 19050–19060.
- (7) For examples of the asymmetric alkylation of cyclic ketone, vinylogous ester, or vinylogous thioester-derived enolates in the context of natural product synthesis, see: (a) Dichroanone: McFadden, R. M.; Stoltz, B. M. *J. Am. Chem. Soc.* **2006**, *128*, 7738–7739. (b) Elatol: White, D. E.; Stewart, I. C.; Grubbs, R. H.; Stoltz, B. M. *J. Am. Chem. Soc.* **2008**, *130*, 810–811. (c) Cyanthiwigin F: Enquist, Jr., J. A.; Stoltz, B. M. *Nature* **2008**, *453*, 1228–1231. (d) Carissone: Levine, S. R.; Krout, M. R.; Stoltz, B. M. *Org. Lett.* **2009**, *11*, 289–292. (e) Cassiol: Petrova, K. V.; Mohr, J. T.; Stoltz, B. M. *Org. Lett.* **2009**, *11*, 293–295. (f) Elatol, Laurencenone C, α -Chamigrene, and the Proposed Structure of Laurencenone B: White, D. E.; Stewart, I. C.; Seashore-Ludlow, B. A.; Grubbs, R. H.; Stoltz, B. M. *Tetrahedron* **2010**, *66*, 4668–4686. (g) Hamigeran B: Mukherjee, H. McDougal, N. T.; Virgil, S. C.; Stoltz, B. M. *Org. Lett.* **2011**, *13*, 825–827. (h) Liphagal: Day, J. J.; McFadden, R. M.; Virgil, S. C.; Kolding, H.; Alleva, J. L.; Stoltz, B.

- M. *Angew. Chem. Int. Ed.* **2011**, *50*, 6814–6818. (i) Cyanthiwiggins B, F, and G: Enquist, Jr., J. A.; Virgil, S. C.; Stoltz, B. M. *Chem. Eur. J.* **2011**, *17*, 9957–9969.
- (8) For our initial communication on the addition of organometallic reagents to chiral vinylogous esters to form γ -quaternary cycloheptenones, see: Bennett, N. B.; Hong, A. Y.; Harned, A. M.; Stoltz, B. M. *Org. Biomol. Chem.* **2012**, *10*, 56–59.
- (9) For our initial communication on the palladium catalyzed asymmetric alkylation and ring contraction studies in the synthesis of γ -quaternary acylcyclopentenones, see: Hong, A. Y.; Krout, M. R.; Jensen, T.; Bennett, N. B.; Harned, A. M.; Stoltz, B. M. *Angew. Chem. Int. Ed.* **2011**, *50*, 2756–2760.
- (10) Concurrent with our efforts, palladium-catalyzed asymmetric allylic alkylations reactions of unstabilized enolates for the synthesis of enantioenriched α -quaternary cyclic ketones, vinylogous esters, and vinylogous thioesters were reported by Trost. See: (a) Trost, B. M.; Pissot-Soldermann, C.; Chen, I.; Schroeder, G. M. *J. Am. Chem. Soc.* **2004**, *126*, 4480–4481. (b) Trost, B. M.; Schroeder, G. M. *Chem. Eur. J.* **2005**, *11*, 174–184. (c) Trost, B. M.; Pissot-Soldermann, C.; Chen, I. *Chem. Eur. J.* **2005**, *11*, 951–959. (d) Trost, B. M.; Xu, J. J. *J. Am. Chem. Soc.* **2005**, *127*, 2846–2847. (e) Trost, B. M.; Bream, R. N.; Xu, J. *Angew. Chem. Int. Ed.* **2006**, *45*, 3109–3112.
- (11) 1,3-Cycloheptanedione (catalog #515981) and 3-isobutoxy-2-cyclohepten-1-one (catalog #T271322) are commercially available from Sigma-Aldrich. The price of 1,3-cycloheptanedione is \$40,000/mol. Adopted from Aldrich August 28th, 2011.

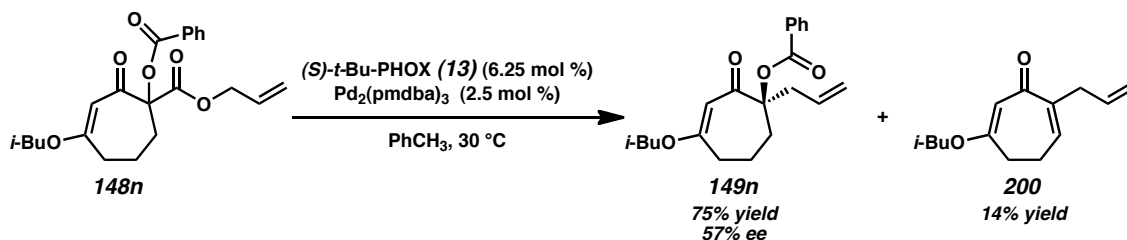
- (12) (a) Ragan, J. A.; Makowski, T. W.; am Ende, D. J.; Clifford, P. J.; Young, G. R.; Conrad, A. K.; Eisenbeis, S. A. *Org. Process Res. Dev.* **1998**, 2, 379–381. (b) Ragan, J. A.; Murry, J. A.; Castaldi, M. J.; Conrad, A. K.; Jones, B. P.; Li, B.; Makowski, T. W.; McDermott, R.; Sitter, B. J.; White, T. D.; Young, G. R. *Org. Process Res. Dev.* **2001**, 5, 498–507. (c) Do, N.; McDermott, R. E.; Ragan, J. A. *Org. Synth.* **2008**, 85, 138–146.
- (13) (a) Ukai, T.; Kawazura, H.; Ishii, Y.; Bonnet, J. J.; Ibers, J. A. *J. Organomet. Chem.* **1974**, 65, 253–266. (b) Fairlamb, I. J. S.; Kapdi, A. R.; Lee, A. F. *Org. Lett.* **2004**, 6, 4435–4438.
- (14) $\text{Pd}_2(\text{pmdba})_3$ is preferable to $\text{Pd}_2(\text{dba})_3$ in this reaction for ease of separation of pmdba from the reaction products during purification. pmdba = 4,4'-methoxydibenzylideneacetone.
- (15) Our group has made improvements to the synthetic route toward PHOX ligands and developed procedures for large-scale synthesis. See: (a) Tani, K.; Behenna, D. C.; McFadden, R. M.; Stoltz, B. M. *Org. Lett.* **2007**, 9, 2529–2531. (b) Krout, M. R.; Mohr, J. T.; Stoltz, B. M. *Org. Synth.* **2009**, 86, 181–193.
- (16) Racemic products were obtained using $\text{Pd}(\text{PPh}_3)_4$ (5 mol %) or achiral PHOX ligand **192** (6.25 mol %) and $\text{Pd}_2(\text{pmdba})_3$ (2.5 mol %) in toluene at 30 °C.



- (17) For a preparation of electron-deficient PHOX ligand **14** ((*S*)-*p*-(CF₃)₃-*t*-Bu-PHOX), see: (a) McDougal, N. T.; Streuff, J.; Mukherjee, H.; Virgil, S. C.; Stoltz, B. M. *Tetrahedron Lett.* **2010**, *51*, 5550–5554. (b) Also see ref. 7b and 7f.
- (18) The reaction with silyl-protected alcohol **148m** afforded alkylation product **149m** and exocyclic enone **199** in 10% yield. A related silyl-protected alcohol substrate did not display this type of elimination during an asymmetric decarboxylative alkylation reaction on a six-membered ring β -ketoester substrate. See ref. 2b.



- (19) The reaction with benzoate ester **148n** afforded alkylation product **149n** and endocyclic enone **200** in 14% yield.

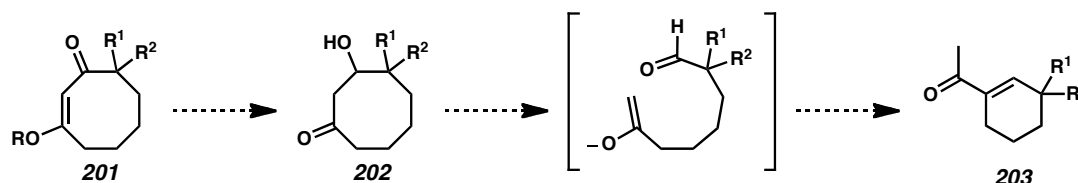


- (20) Stork, G.; Danheiser, R. L. *J. Org. Chem.* **1973**, *38*, 1775–1776.
- (21) Differences in ring conformational preferences can also be observed in the ¹H NMR spectra of 1,3-cyclohexadione (exclusively ketoenol form) and 1,3-cycloheptadione (exclusively diketo form). See ref. 12c.
- (22) For selected examples of the two-carbon ring contraction of seven-membered carbocycles, see: (a) Frankel, J. J.; Julia, S.; Richard-Neuville, C. *Bull. Soc.*

Chim. Fr. **1968**, 4870–4875. (b) Jun, C.-H.; Moon, C. W.; Lim, S.-G.; Lee, H. *Org. Lett.* **2002**, *4*, 1595–1597.

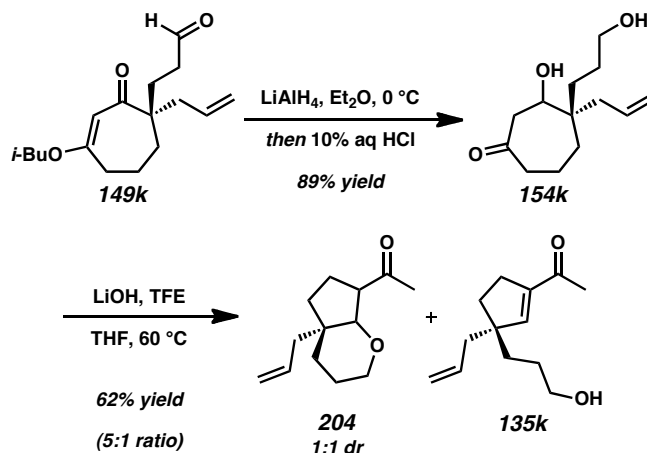
- (23) Notably, **154a** and related β -hydroxyketones appear to undergo minimal decomposition after several months of storage at room temperature by TLC and ^1H NMR analysis, and immediate conversion to acylcyclopentenones **135a** is not necessary to achieve high yields.
- (24) While a recent report shows a single example of a similar β -hydroxyketone, we believe the unusual reactivity and synthetic potential of these compounds has not been fully explored. See: Rinderhagen, H.; Mattay, J. *Chem. Eur. J.* **2004**, *10*, 851–874.
- (25) For an example of a photochemical two-carbon ring contraction of a macrocycle, see: Yang, Z.; Li, Y.; Pattenden, G. *Tetrahedron* **2010**, *66*, 6546–6549.
- (26) For examples of ring contractions of medium-sized ring heterocycles, see:
- (a) Nasveschuk, C. G.; Rovis, T. *Angew. Chem. Int. Ed.* **2005**, *44*, 3264–3267.
 - (b) Nasveschuk, C. G.; Rovis, T. *J. Org. Chem.* **2008**, *73*, 612–617.
 - (c) Nasveschuk, C. G.; Rovis, T. *Org. Biomol. Chem.* **2008**, *6*, 240–254.
 - (d) Baktharaman, S.; Afagh, N.; Vandersteen, A.; Yudin, A. K. *Org. Lett.* **2010**, *12*, 240–243.
 - (e) Dubovyk, I.; Pichugin, D.; Yudin, A. K. *Angew. Chem. Int. Ed.* **2011**, *50*, 5924–5926.
 - (f) Volchkov, I.; Park, S.; Lee, D. *Org. Lett.* **2011**, *13*, 3530–3533.
 - (g) Dubinina, G. G.; Chain, W. J. *Tetrahedron Lett.* **2011**, *52*, 939–942.
- (27) For a discussion of the properties of fluorinated alcohols and their use, see: Begue, J.-P.; Bonnet-Delpon, D.; Crousse, B. *Synlett* **2004**, 18–29.

- (28) A lithium alkoxide species is presumably generated in situ based on the following pK_a values: ($H_2O = 15.7$, $TFE = 12.5$, $HFIP = 9.3$ [water]; $H_2O = 31.2$, $TFE = 23.5$, $HFIP = 18.2$ [DMSO]); Bordwell, F. G. *Acc. Chem. Res.* **1988**, *21*, 456–463.
- (29) No reaction was observed with the following bases (with or without TFE additive): DBU, TMG, Na_2CO_3 , $BaCO_3$, and CaH_2 . DBU = 1,8-diazabicyclo[5.4.0]undec-7-ene, TMG = 1,1,3,3-tetramethylguanidine.
- (30) The two-carbon ring contraction strategy can potentially be extended to β -hydroxyketones of other medium sized rings to provide other useful cyclic enone products. These possibilities are the subject of current investigations.

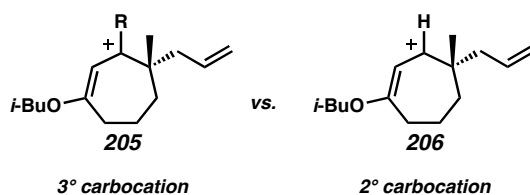


- (31) Fluorinated lithium alkoxides were recently used to promote Horner–Wadsworth–Emmons olefinations of sensitive substrates, demonstrating their mild reactivity. See: Blasdel, L. K.; Myers, A. G. *Org. Lett.* **2005**, *7*, 4281–4283.
- (32) Luche, J. L. *J. Am. Chem. Soc.* **1978**, *100*, 2226–2227.
- (33) Although we had success in preparing silyloxy acylcyclopentene **135p** from vinylogous ester **149p**, we wondered whether it would be possible to perform a ring contraction on aldehyde **149k**. Under our standard conditions, the intermediate ketodiol **154k** can be obtained in 89% yield, however the subsequent

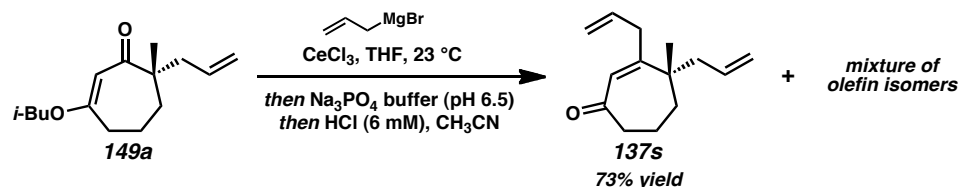
ring contraction proceeded in 62% yield to afford a complex mixture of pyran diastereomers **204** and uncyclized acylcyclopentene **135k**.



- (34) Analytically pure samples of dione **162** can be obtained from vinylogous ester **149a** by treatment with acid. See Experimental Section (Section 2.10.2.10) for details.
- (35) The addition of cerium chloride to reactions with organolithium or Grignard reagents has been shown to increase reactivity and reduce side reactions with vinylogous ester systems, see: Crimmins, M. T.; Dedopoulou, D. *Synth. Commun.* **1992**, 22, 1953–1958.
- (36) The increase in enone formation with the organometallic addition relative to the hydride reduction is likely due to the higher stability of the tertiary carbocation (**205**) compared to the secondary carbocation (**206**) formed along the reduction pathway.



- (37) CCDC 686849 (**164**) contains the supplementary crystallographic data for this chapter. These data can be obtained free of charge from The Cambridge Crystallographic Data Centre via www.ccdc.cam.ac.uk/data_request/cif. The data can also be viewed in Appendix 2.
- (38) Comins, D. L.; Dehghani, A. *Tetrahedron Lett.* **1992**, 33, 6299–6302.
- (39) Herrmann, W. A.; Brossmer, C.; Öfele, K.; Reisinger, C.-P.; Priermeier, T.; Beller, M.; Fischer, H. *Angew. Chem. Int. Ed. Engl.* **1995**, 34, 1845–1848.
- (40) Preferential β -hydroxyketone formation is observed when the acidification of the intermediate isobutyl enol ether is performed in diethyl ether instead of methanol. See Table 2.4.
- (41) Attempts to purify the crude enol ether were challenging due to decomposition to enone **137r** and β -hydroxyketone **154r**.
- (42) The yield of cycloheptenone **137s** is lower than many related enones due to the formation of several side products presumed to be non-conjugated alkene isomers.



- (43) Synthesis of the simple β -vinyl substituted enone proved challenging due to the formation of a complex product mixture.

- (44) Quenching the alkynyl nucleophile addition with hydrochloric acid provided a complex mixture of products, most notably one with an equivalent of HCl added into the molecule. This issue was resolved by instead using sulfuric acid.
- (45) Cycloheptenone **137z** is formed as a 1.9:1 mixture of atropisomers whose isomeric peaks coalesce in a variable temperature ^1H NMR study. See **Figure A1.308**.
- (46) Jin, Z.; Fuchs, P. L. *J. Am. Chem. Soc.* **1994**, *116*, 5995–5996.
- (47) Chung, Y. K.; Lee, B. Y.; Jeong, N.; Hudecek, M.; Pauson, P. L. *Organometallics* **1993**, *12*, 220–223.
- (48) Pangborn, A. B.; Giardello, M. A.; Grubbs, R. H.; Rosen, R. K.; Timmers, F. J. *Organometallics* **1996**, *15*, 1518–1520.
- (49) Love, B. E.; Jones, E. G. *J. Org. Chem.* **1999**, *64*, 3755–3756.
- (50) Mahmood, T.; Shreeve, J. M. *Inorg. Chem.* **1986**, *25*, 3830–3837.
- (51) (a) Mander, L. N.; Sethi, S. P. *Tetrahedron Lett.* **1983**, *24*, 5425–5428.
(b) Donnelly, D. M.; Finet, J. P.; Rattigan, B. A. *J. Chem. Soc., Perkin Trans. 1* **1993**, 1729–1735.
- (52) Geissman, T. A.; Armen, A. *J. Am. Chem. Soc.* **1952**, *74*, 3916–3919.
- (53) Maruyama, K.; Nagai, N.; Naruta, Y. *J. Org. Chem.* **1986**, *51*, 5083–5092.
- (54) (a) Behenna, D. C.; Stoltz, B. M. *J. Am. Chem. Soc.* **2004**, *126*, 15044–15045.
(b) Tani, K.; Behenna, D. C.; McFadden, R. M.; Stoltz, B. M. *Org. Lett.* **2007**, *9*,

- 2529–2531. (c) Krout, M. R.; Mohr, J. T.; Stoltz, B. M. *Org. Synth.* **2009**, 86, 181–193.
- (55) For a preparation of electron-deficient PHOX ligand **14** ((*S*)-*p*-(CF₃)₃-*t*-Bu-PHOX), see: (a) White, D. E.; Stewart, I. C.; Grubbs, R. H.; Stoltz, B. M. *J. Am. Chem. Soc.* **2008**, 130, 810–811. (b) McDougal, N. T.; Streuff, J.; Mukherjee, H.; Virgil, S. C.; Stoltz, B. M. *Tetrahedron Lett.* **2010**, 51, 5550–5554.
- (56) (a) Ukai, T.; Kawazura, H.; Ishii, Y.; Bonnet, J. J.; Ibers, J. A. *J. Organomet. Chem.* **1974**, 65, 253–266. (b) Fairlamb, I. J. S.; Kapdi, A. R.; Lee, A. F. *Org. Lett.* **2004**, 6, 4435–4438.
- (57) Herrmann, W. A.; Brossmer, C.; Öfele, K.; Reisinger, C.-P.; Priermeier, T.; Beller, M.; Fischer, H. *Angew. Chem. Int. Ed. Engl.* **1995**, 34, 1845–1848.
- (58) Bisai, V.; Sarpong, R. *Org. Lett.* **2010**, 12, 2551–2553.
- (59) DIBAL is used to activate the magnesium. See: Tilstam, U.; Weinmann, H. *Org. Proc. Res. Dev.* **2002**, 6, 906–910.
- (60) 4-Bromo-2-methylbut-1-ene is produced from the corresponding alcohol, 3-methyl-3-buten-1-ol. See: Berkowitz, W. F.; Wu, Y. *J. Org. Chem.* **1997**, 62, 1536–1539.
- (61) Sauers, R. R.; Hagedorn, III, A. A.; Van Arnum, S. D.; Gomez, R. P.; Moquin, R. V. *J. Org. Chem.* **1987**, 52, 5501–5505.

APPENDIX 1

Spectra Relevant to Chapter 2:

Catalytic Asymmetric Synthesis of Cyclopentanoid and Cycloheptanoid

Core Structures Using Pd-Catalyzed Asymmetric Alkylation

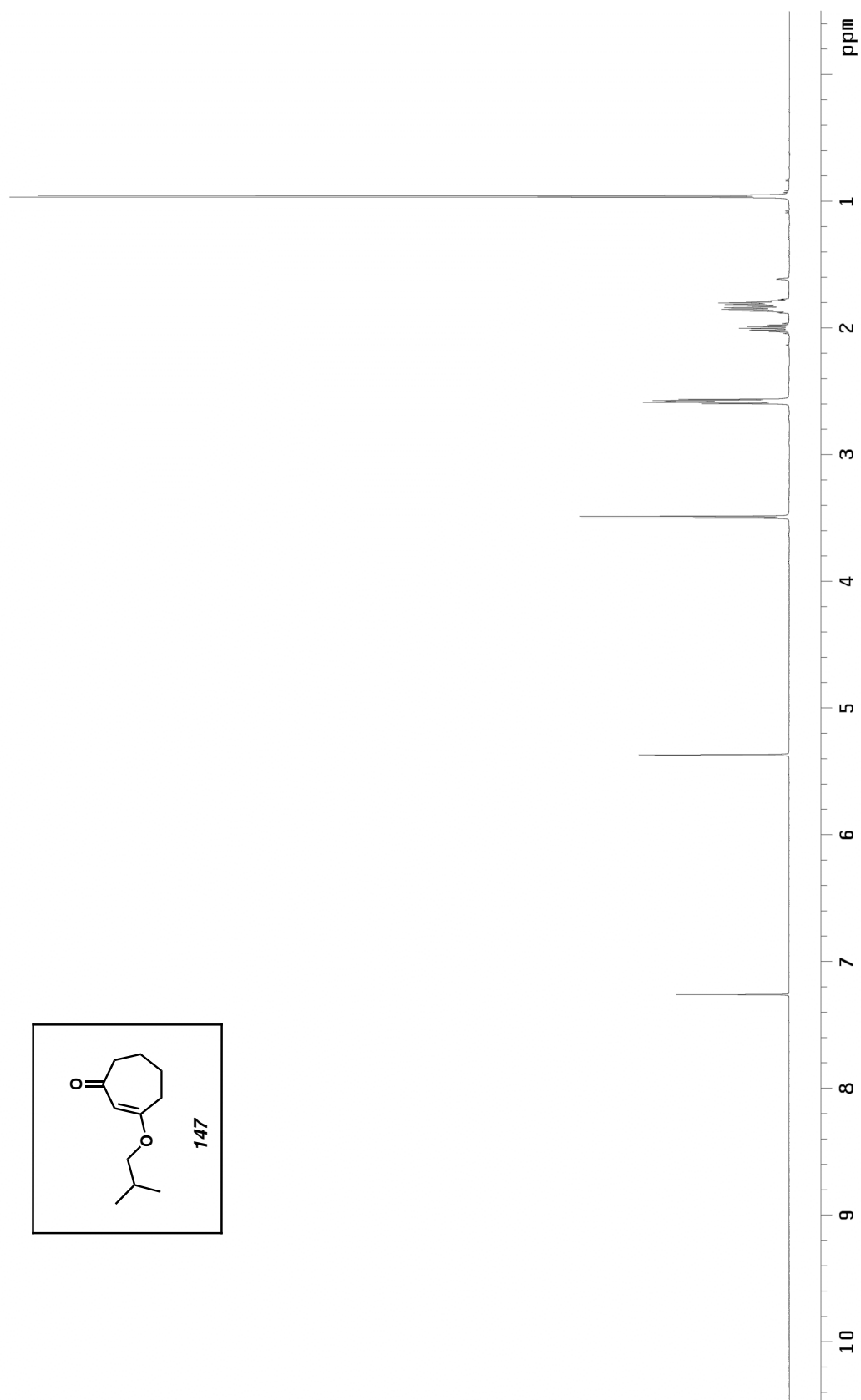


Figure A1.1. ^1H NMR (500 MHz, CDCl_3) of compound **147**.

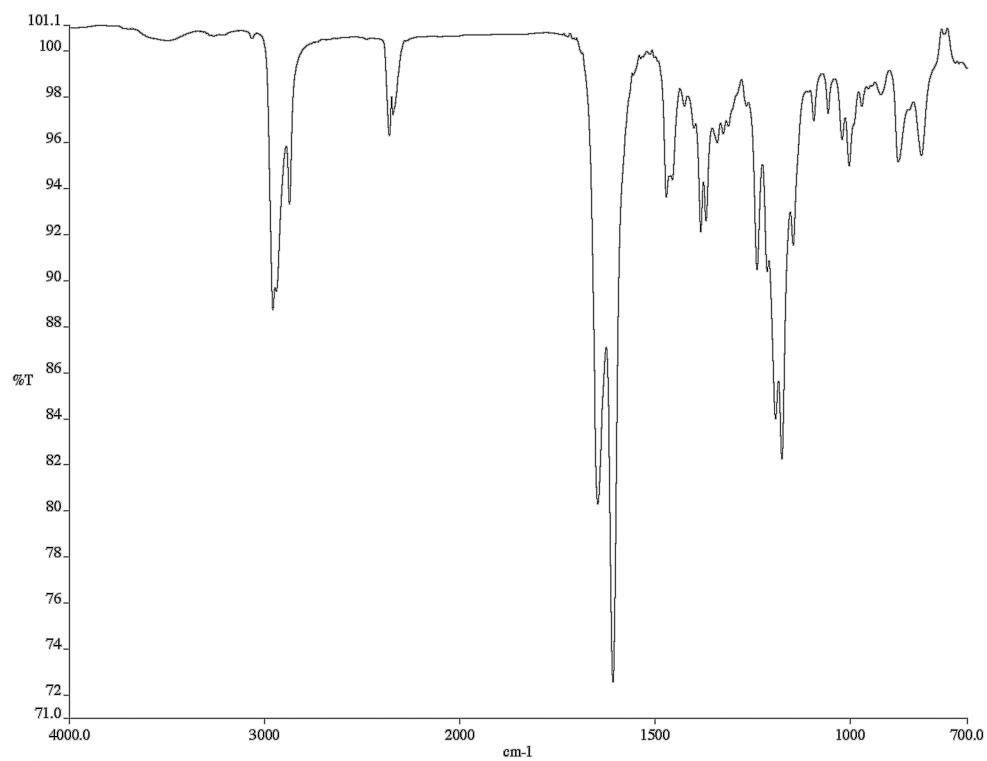


Figure A1.2. Infrared spectrum (thin film/NaCl) of compound **147**.

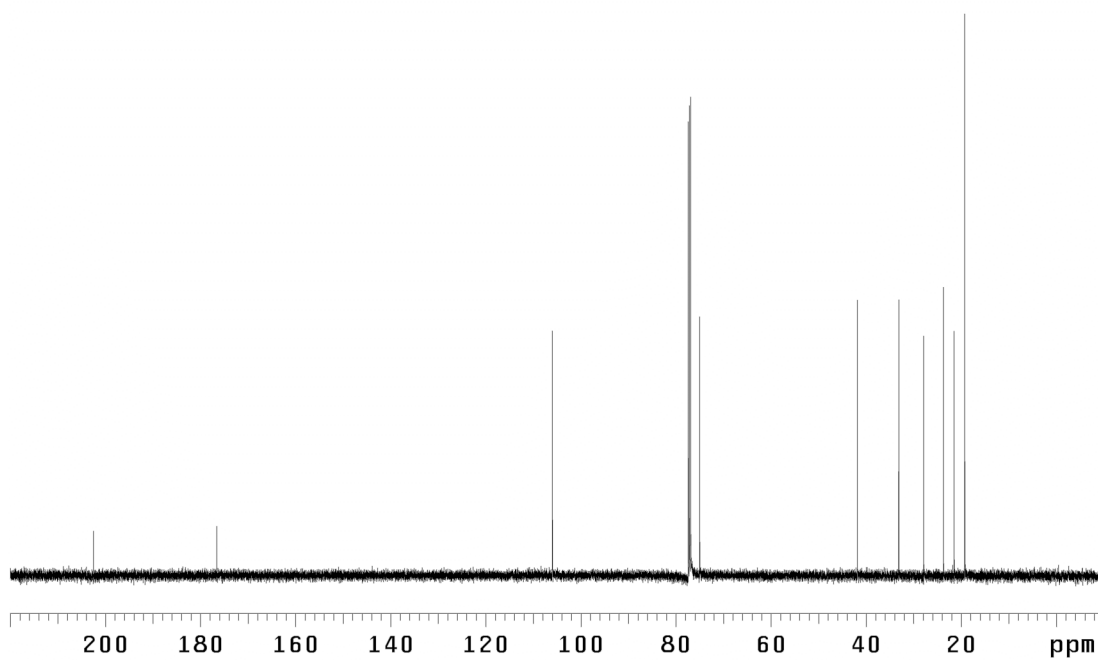
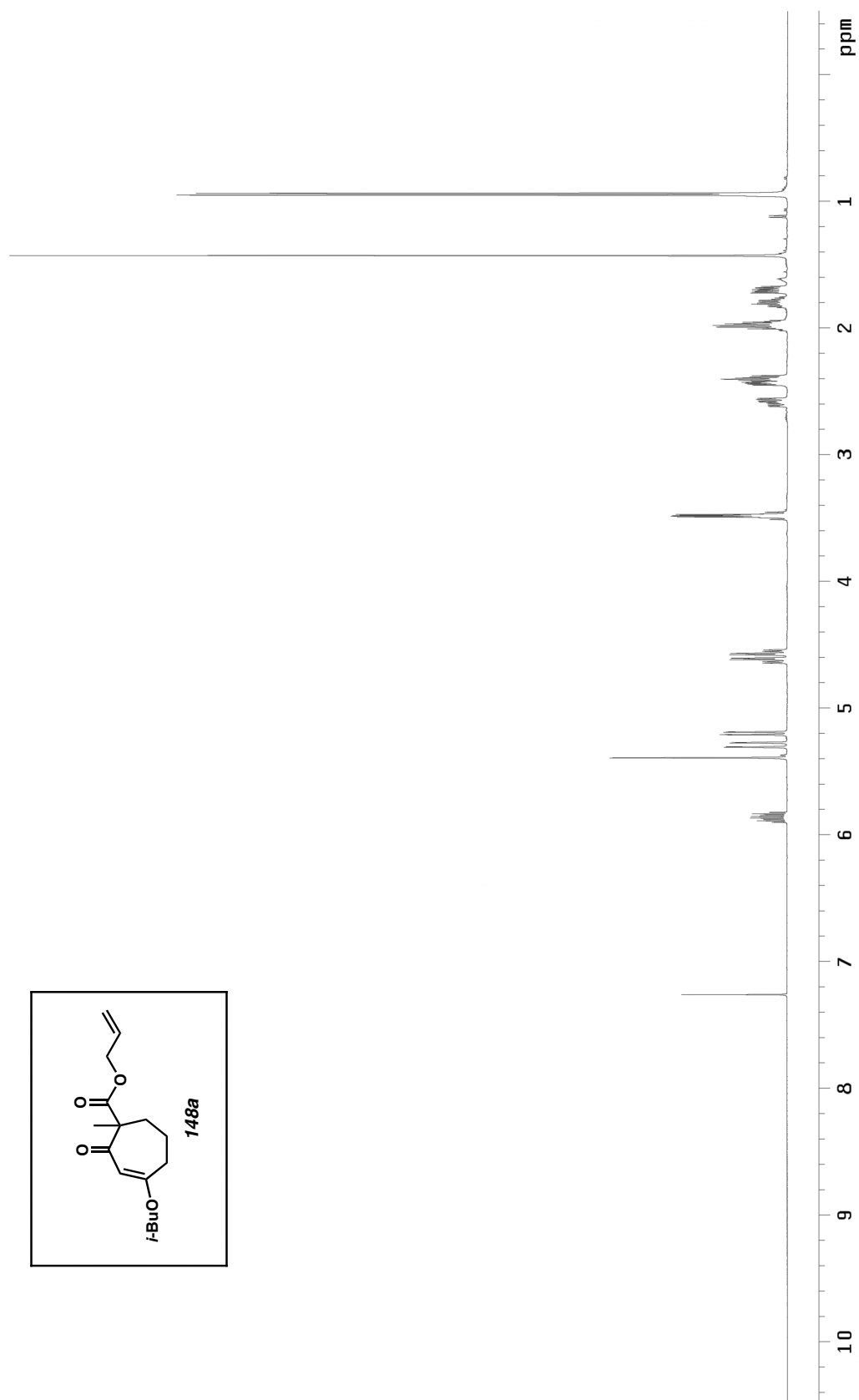


Figure A1.3. ¹³C NMR (125 MHz, CDCl₃) of compound **147**.

Figure A1.4. ^1H NMR (500 MHz, CDCl_3) of compound **148a**.

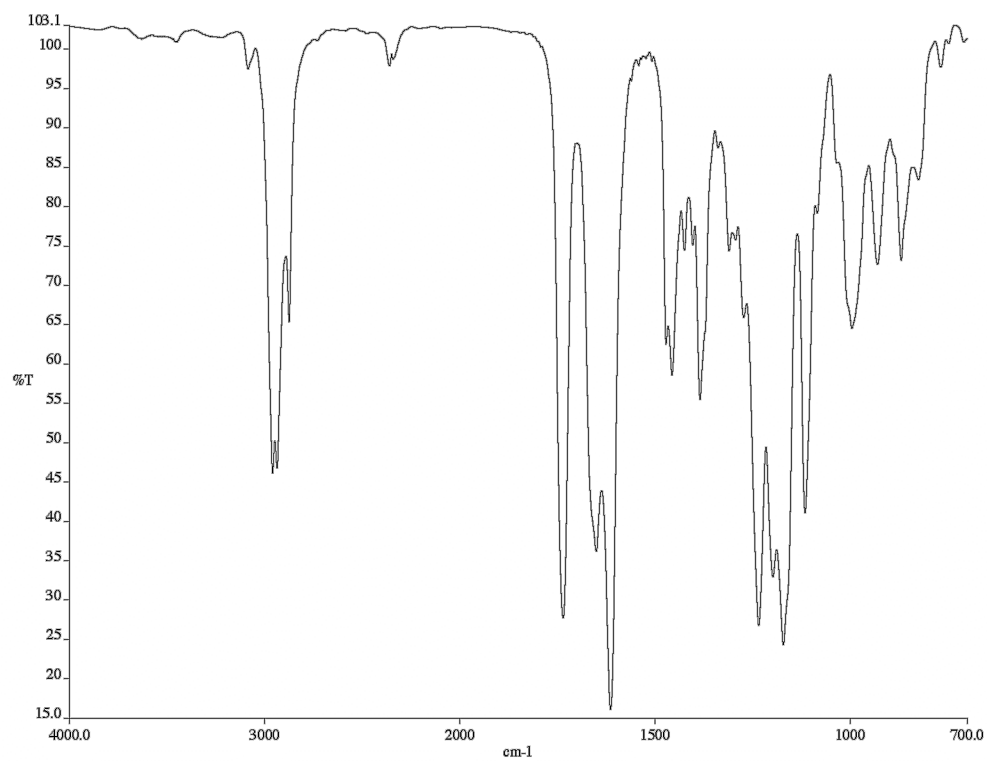


Figure A1.5. Infrared spectrum (thin film/NaCl) of compound **148a**.

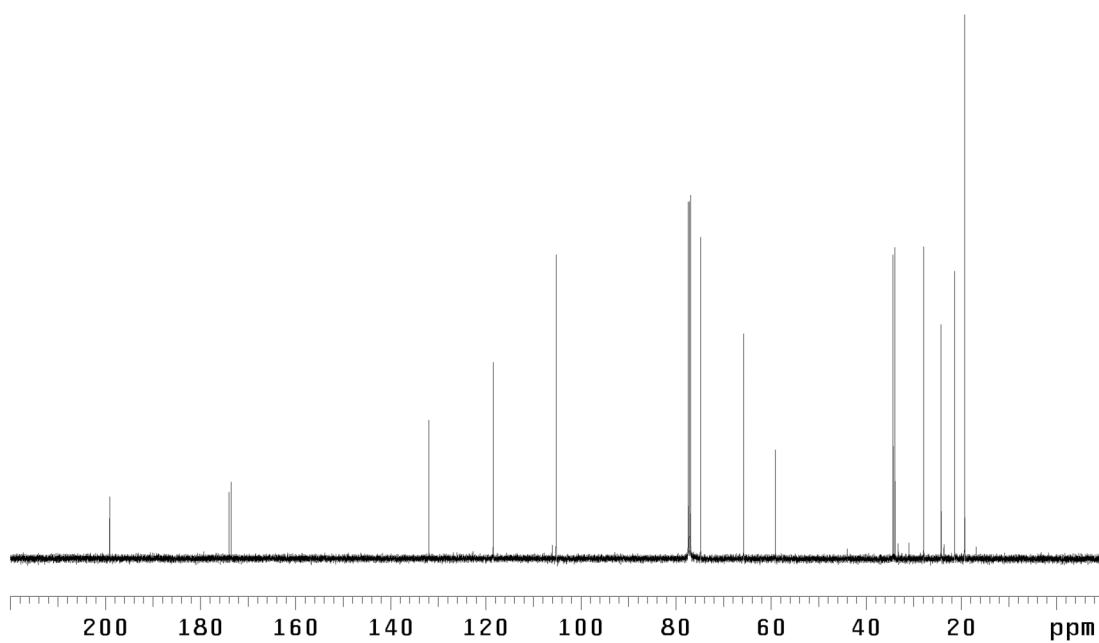


Figure A1.6. ¹³C NMR (125 MHz, CDCl₃) of compound **148a**.

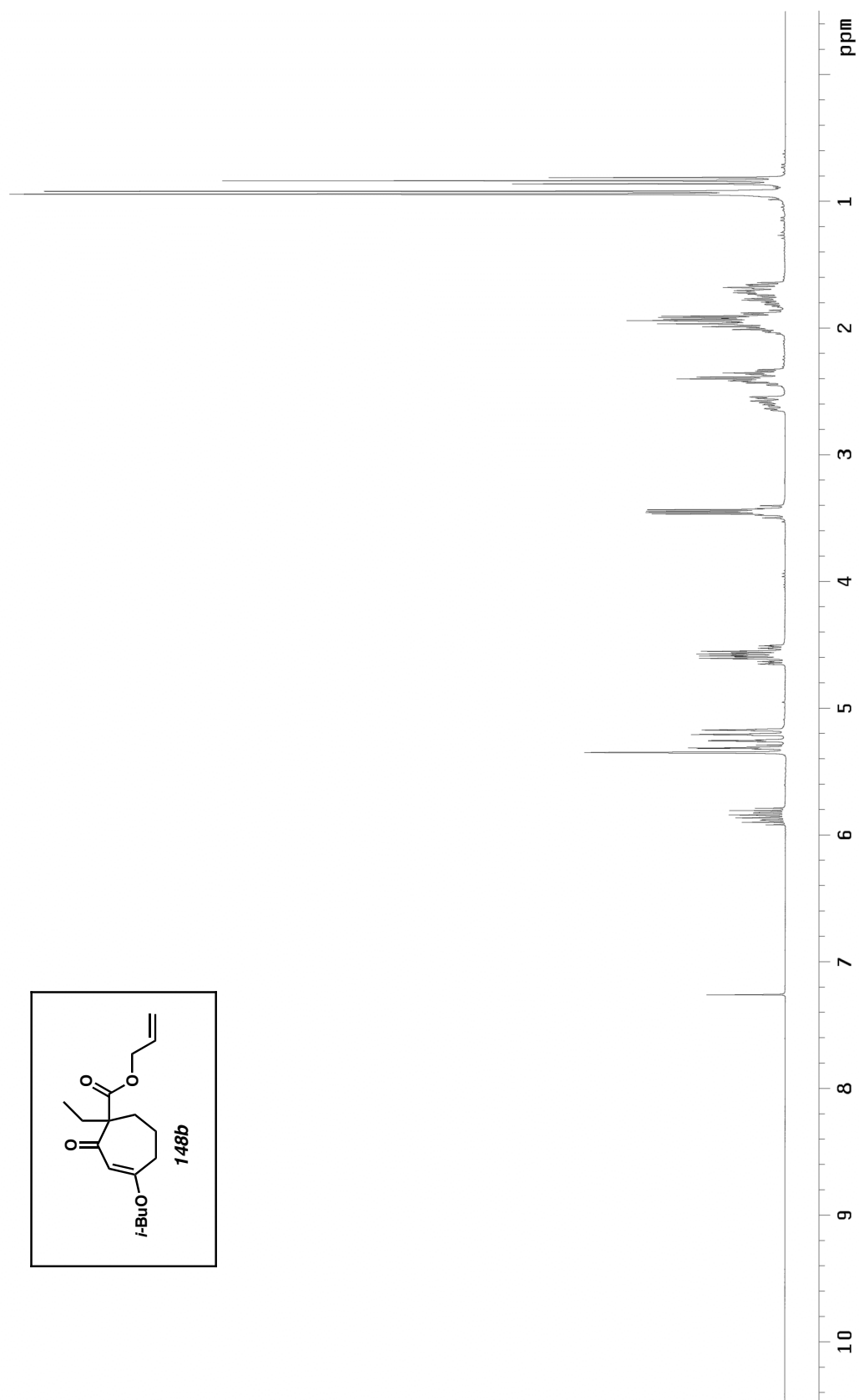


Figure A1.7. ^1H NMR (300 MHz, CDCl_3) of compound **148b**.

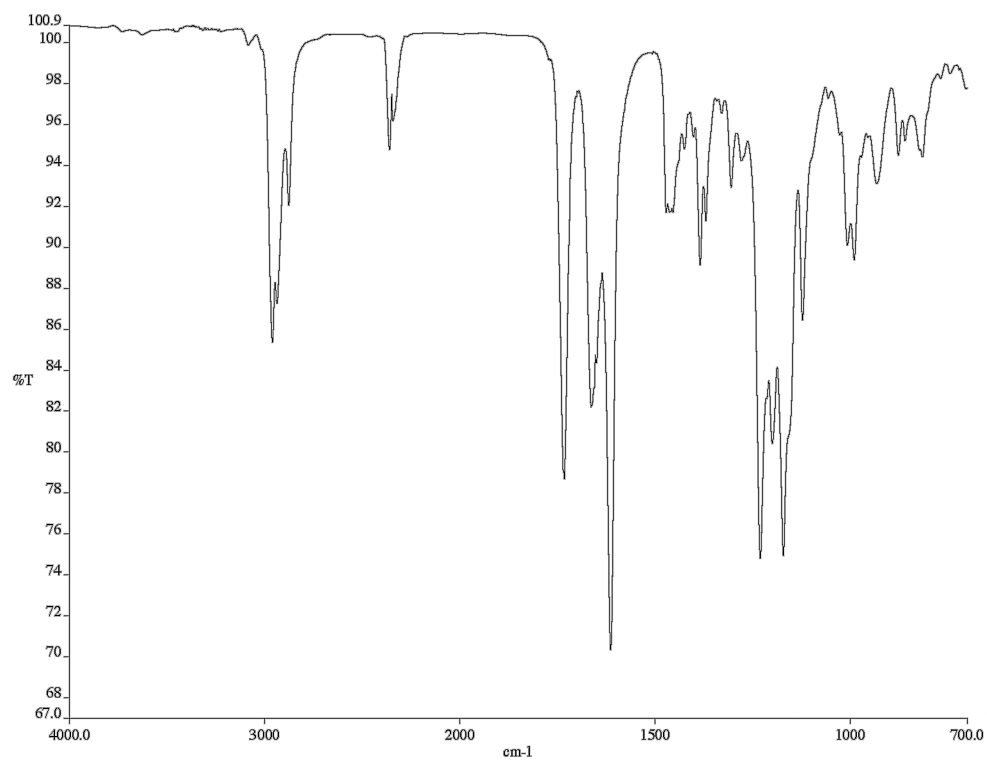


Figure A1.8. Infrared spectrum (thin film/NaCl) of compound **148b**.

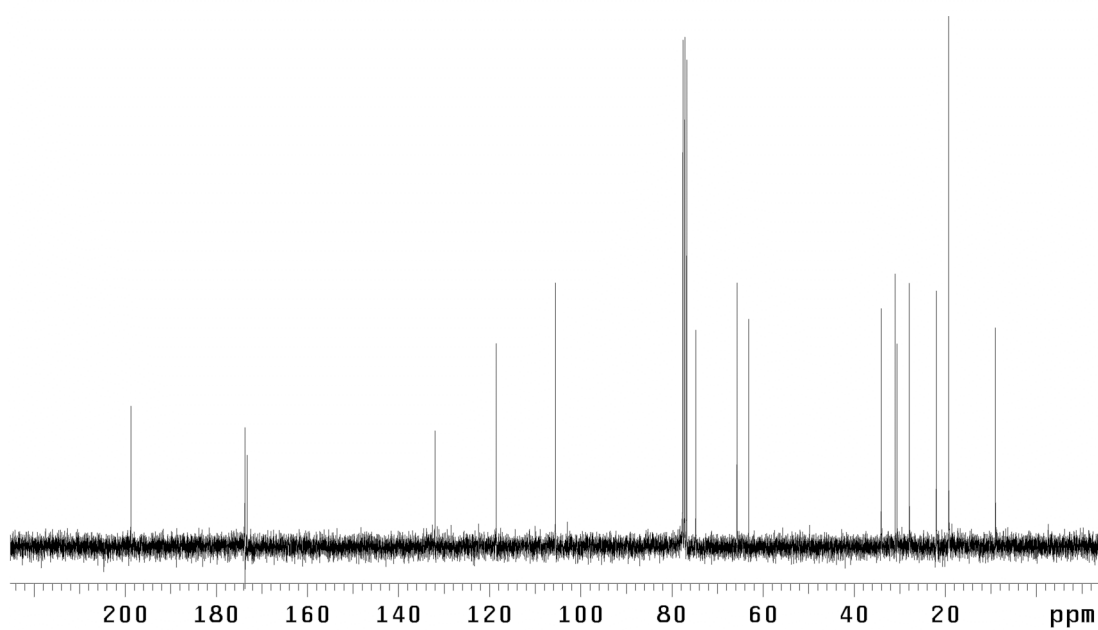
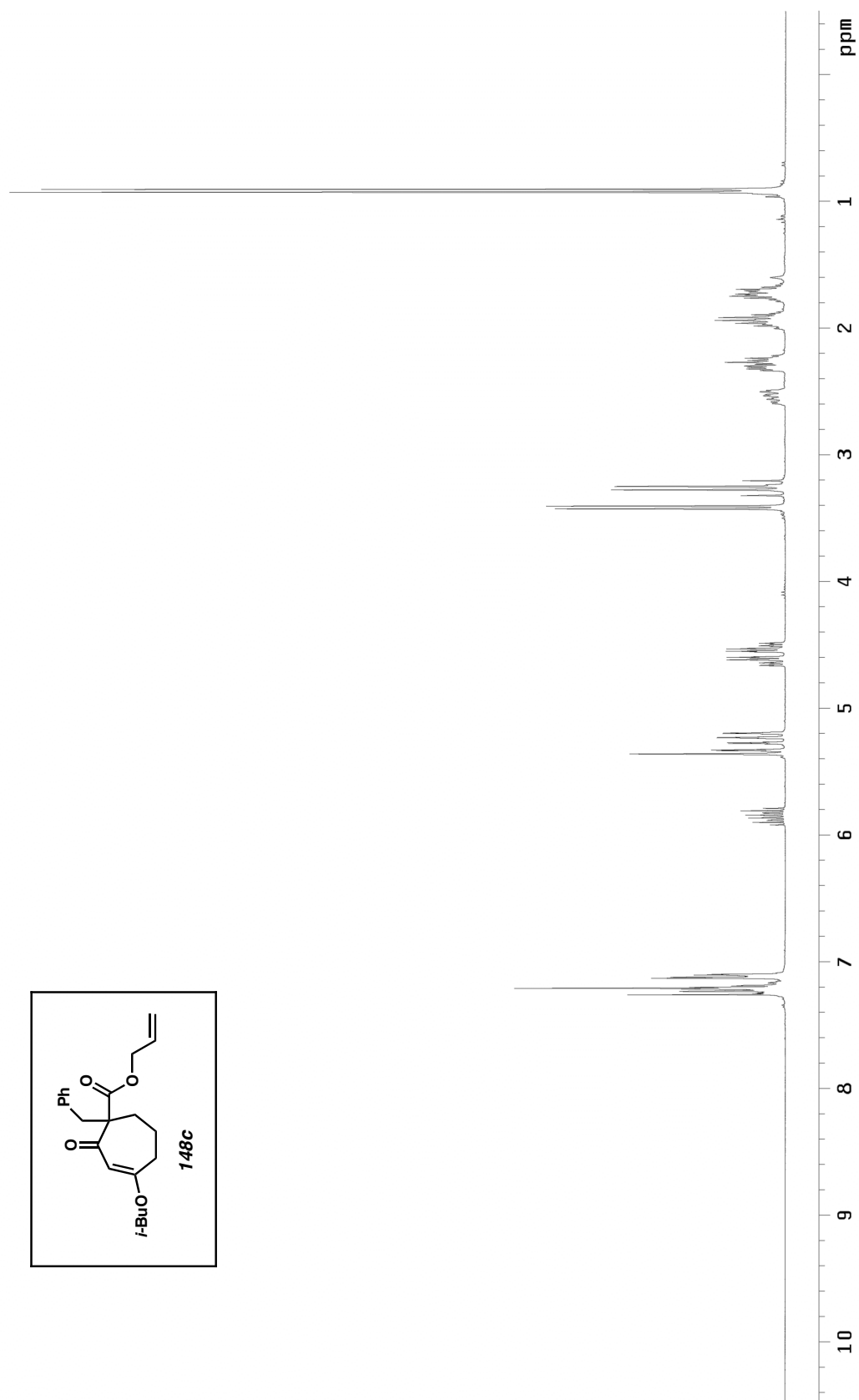


Figure A1.9. ^{13}C NMR (75 MHz, CDCl_3) of compound **148b**.

Figure A1.10. ^1H NMR (300 MHz, CDCl_3) of compound **148c**.

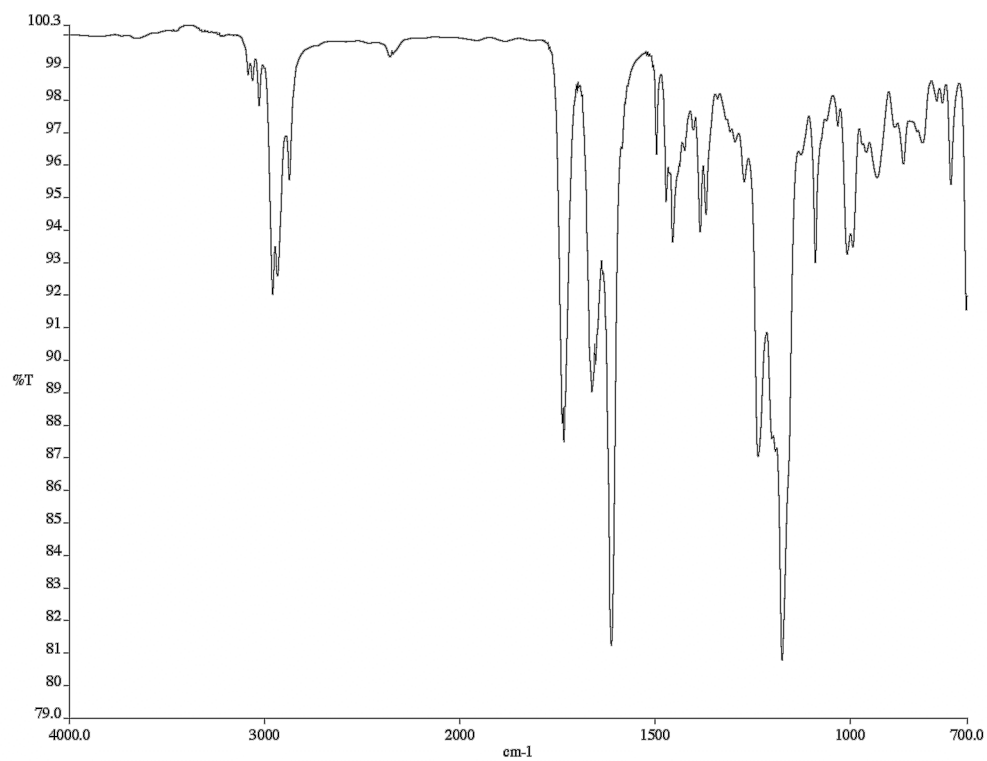


Figure A1.11. Infrared spectrum (thin film/NaCl) of compound **148c**.

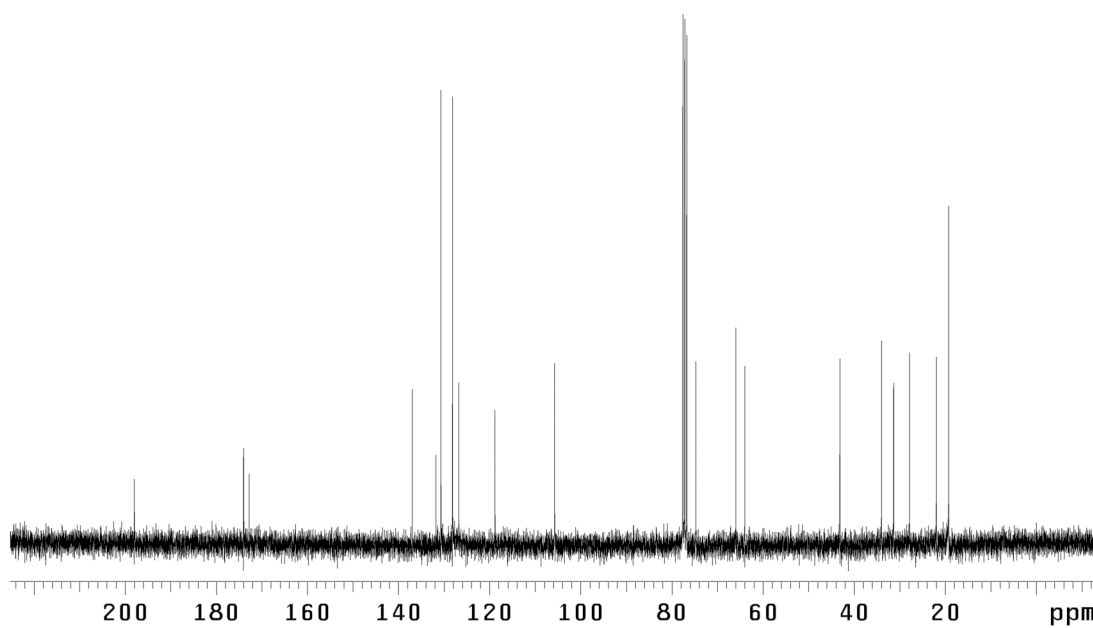


Figure A1.12. ¹³C NMR (75 MHz, CDCl₃) of compound **148c**.

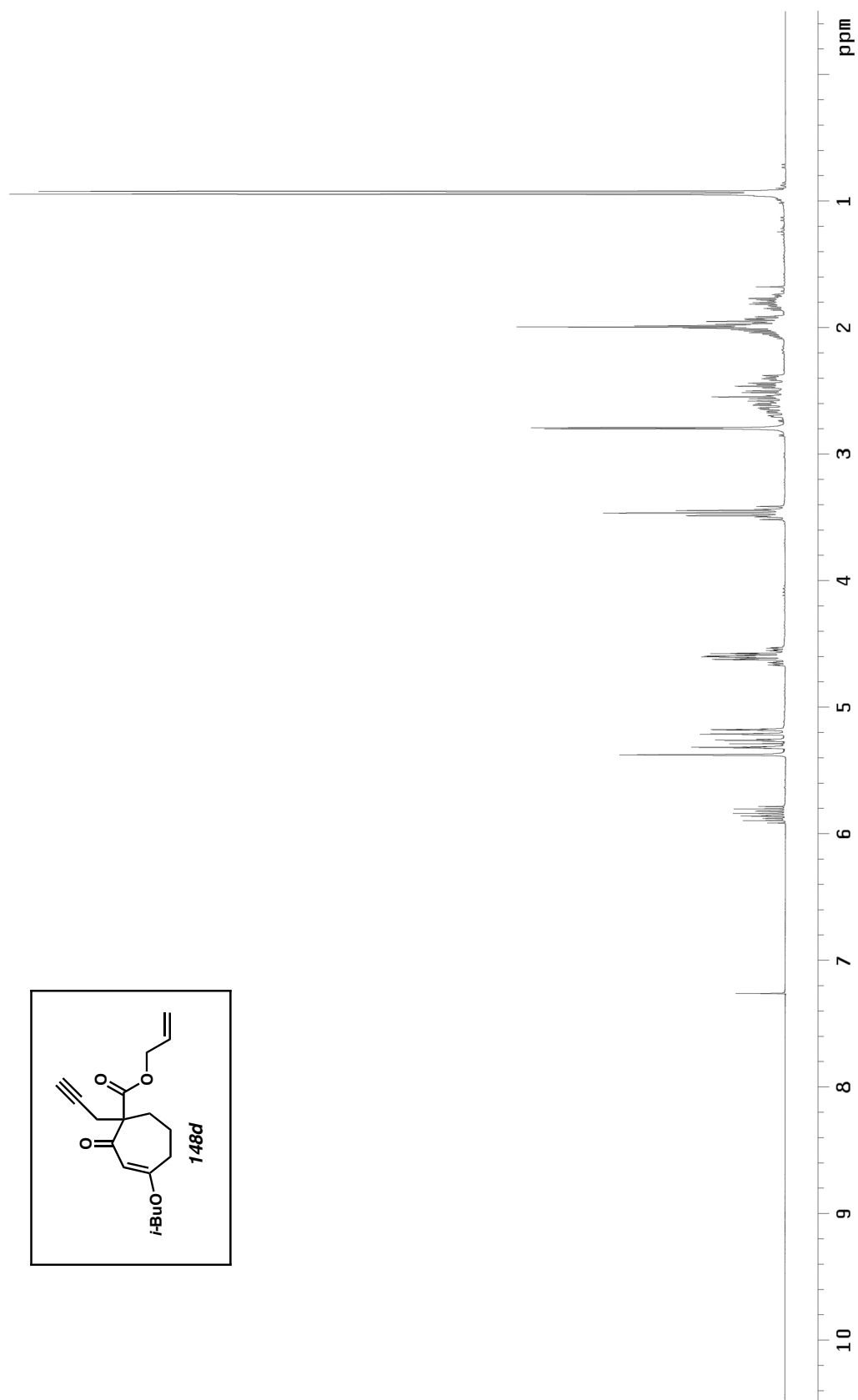


Figure A1.13. ^1H NMR (300 MHz, CDCl_3) of compound **148d**.

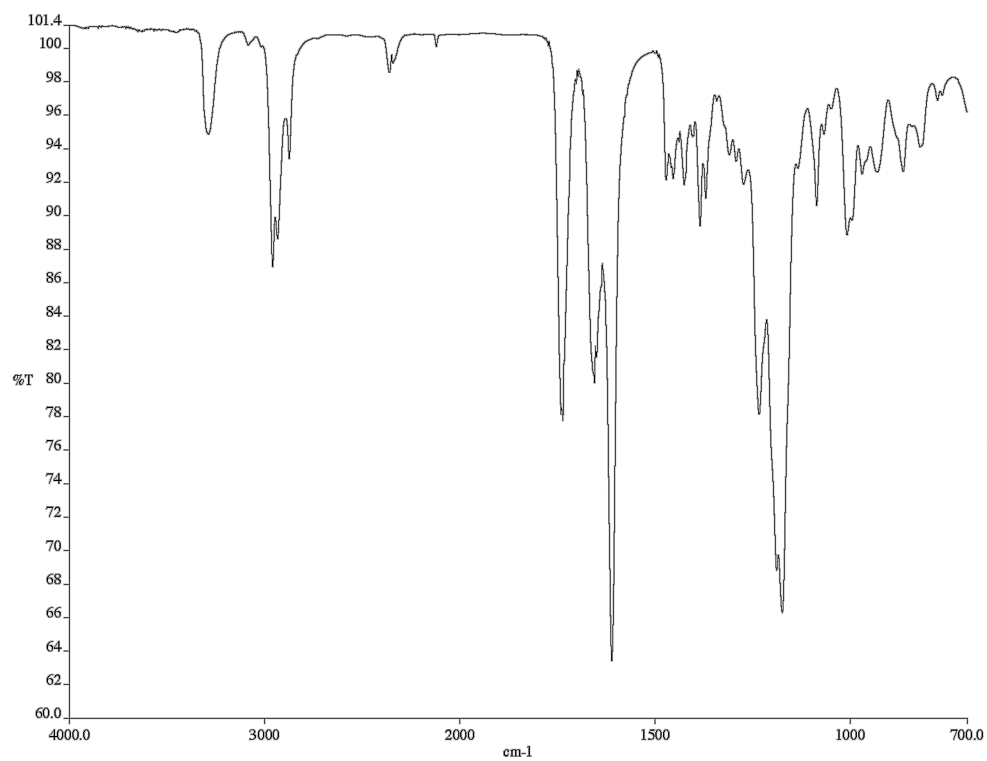


Figure A1.14. Infrared spectrum (thin film/NaCl) of compound **148d**.

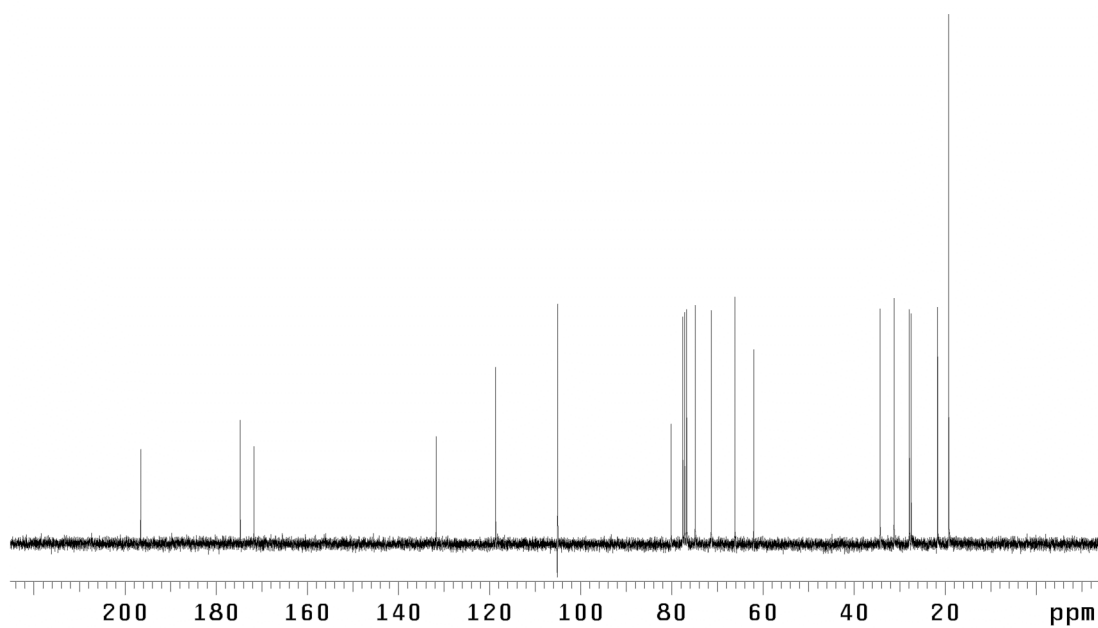


Figure A1.15. ¹³C NMR (75 MHz, CDCl₃) of compound **148d**.

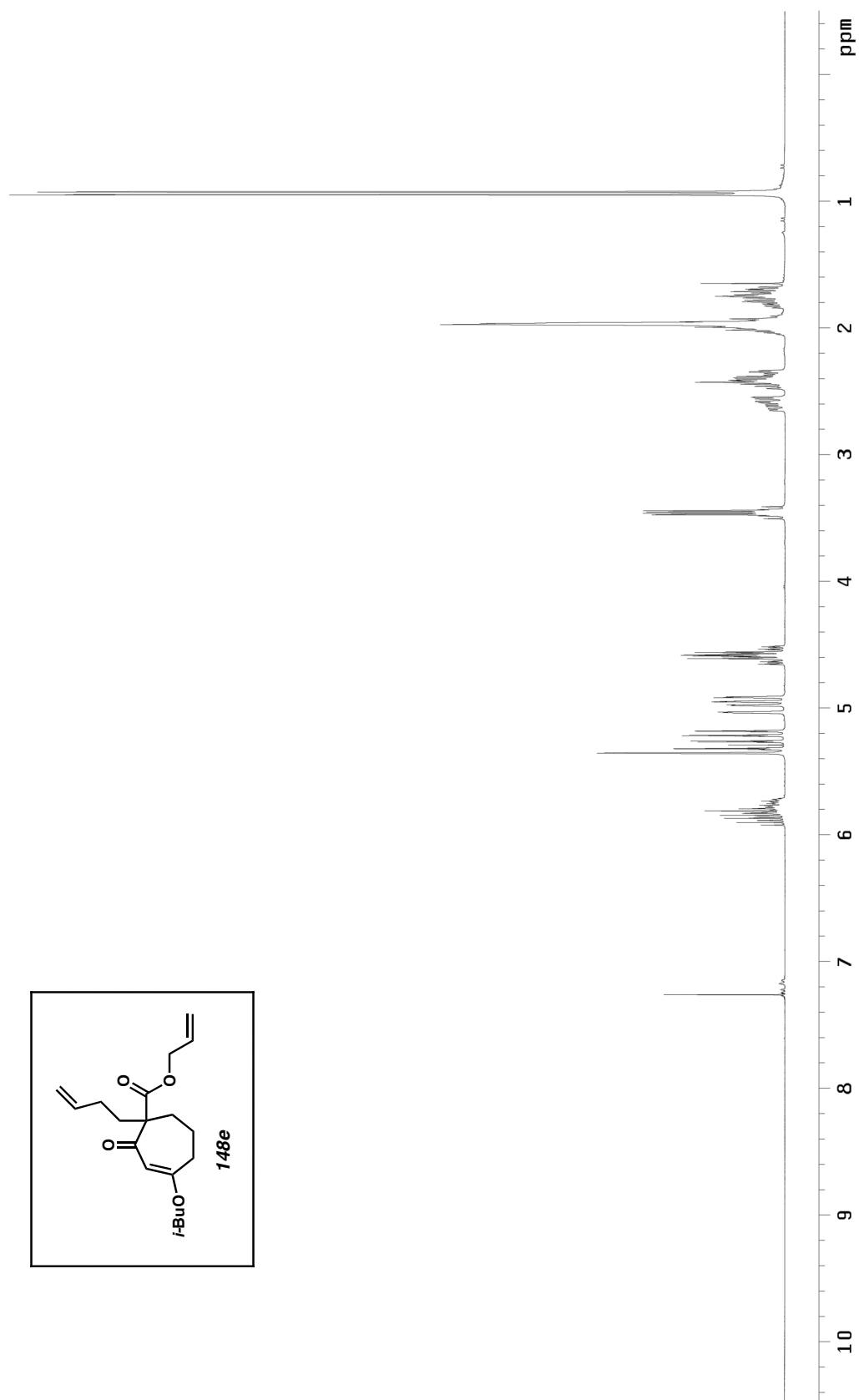


Figure A1.16. ^1H NMR (300 MHz, CDCl_3) of compound **148e**.

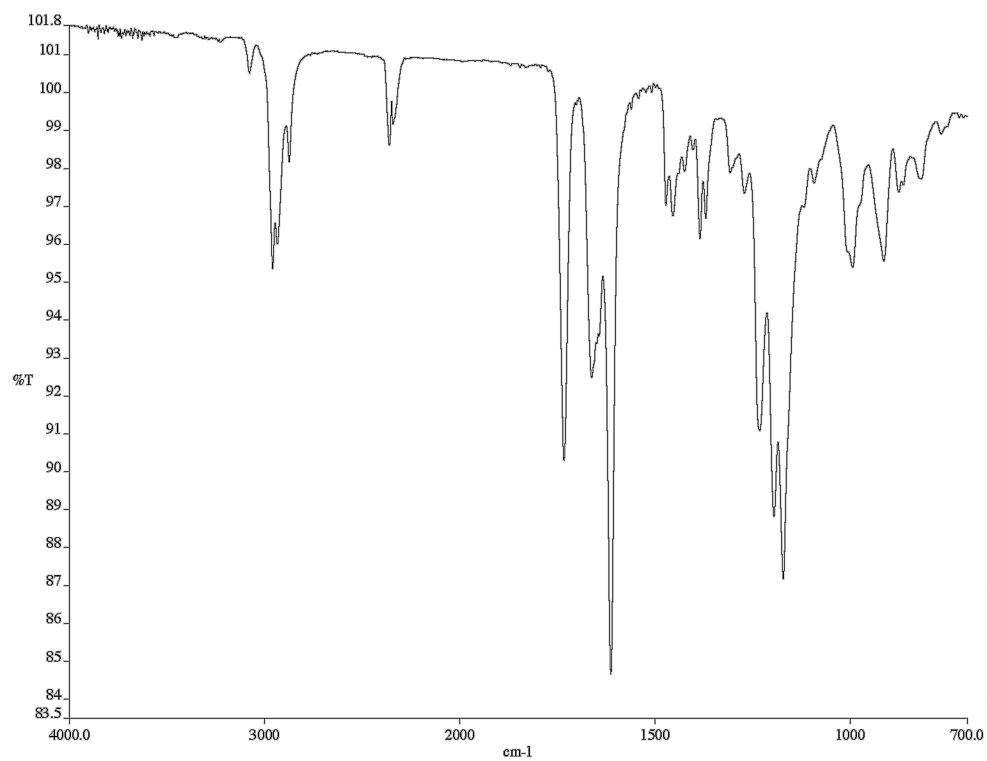


Figure A1.17. Infrared spectrum (thin film/NaCl) of compound **148e**.

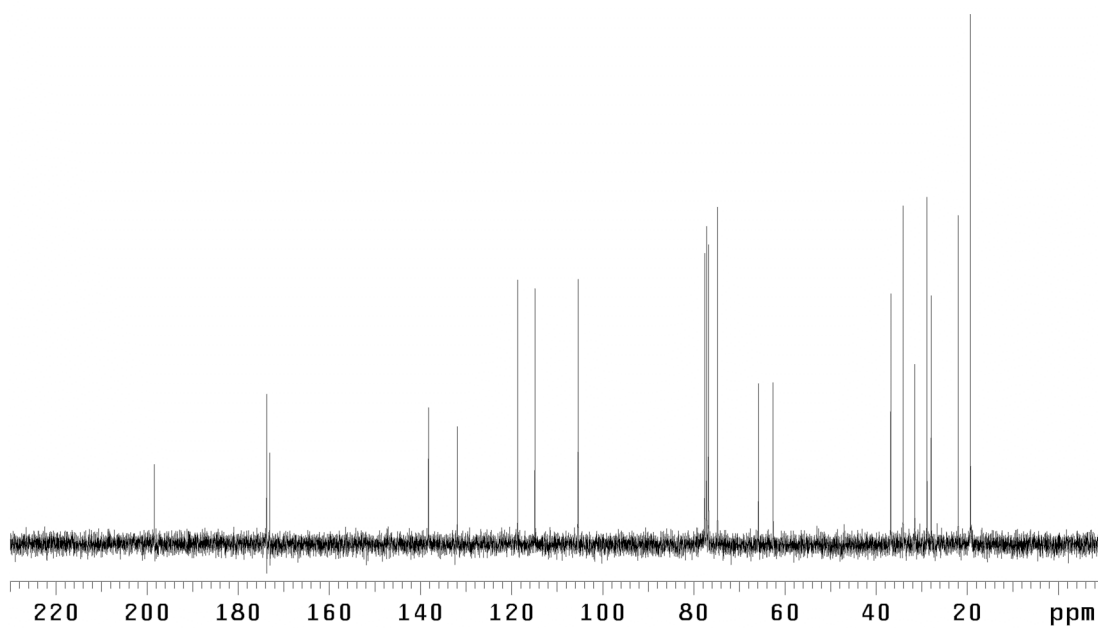
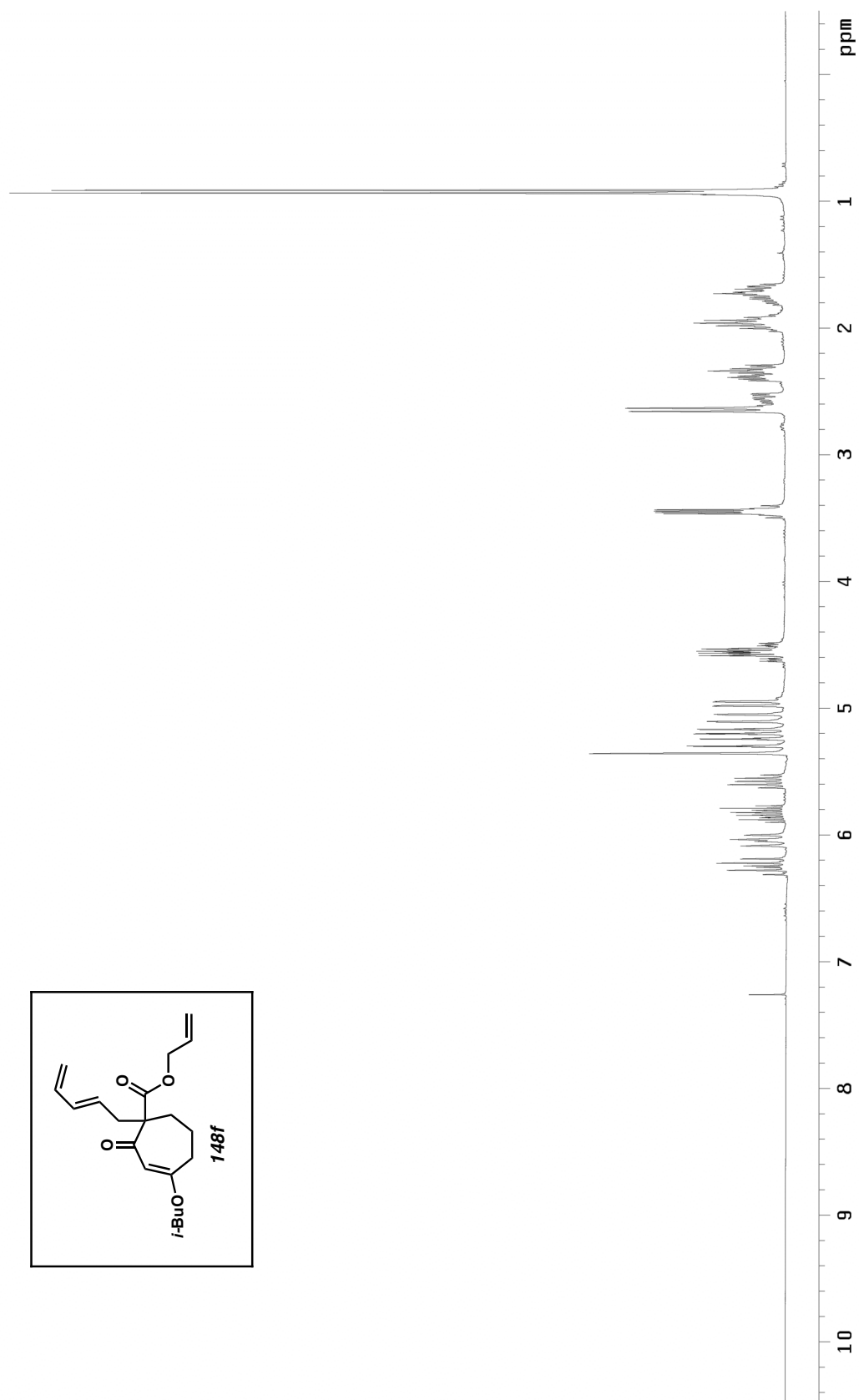


Figure A1.18. ¹³C NMR (75 MHz, CDCl₃) of compound **148e**.

Figure A1.19. ^1H NMR (300 MHz, CDCl_3) of compound **148f**.

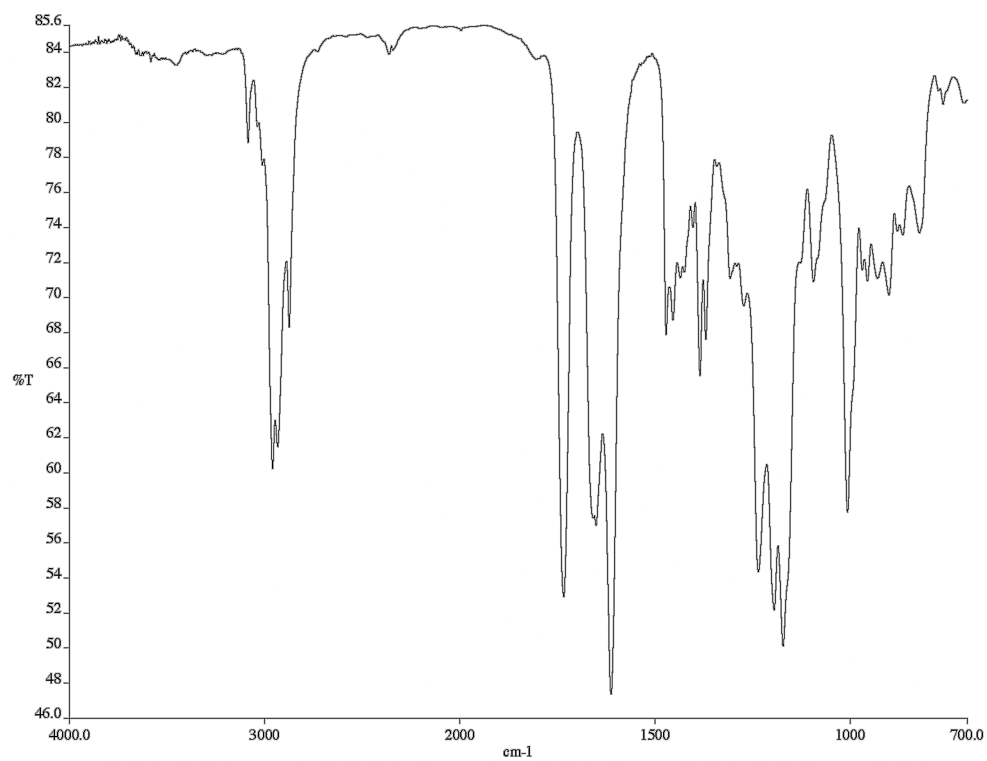


Figure A1.20. Infrared spectrum (thin film/NaCl) of compound **148f**.

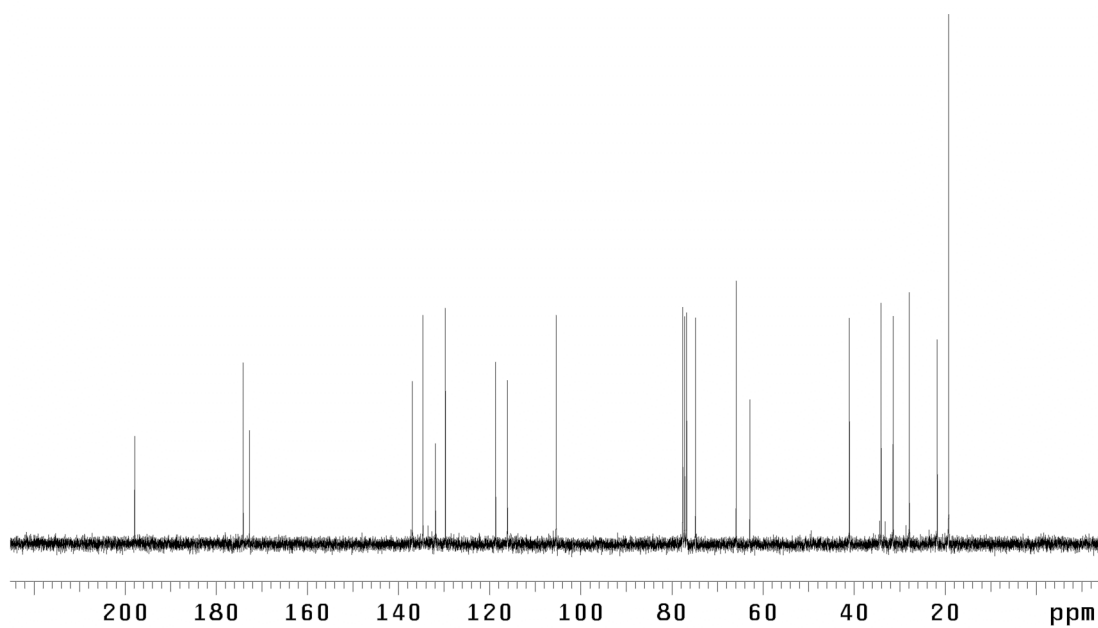
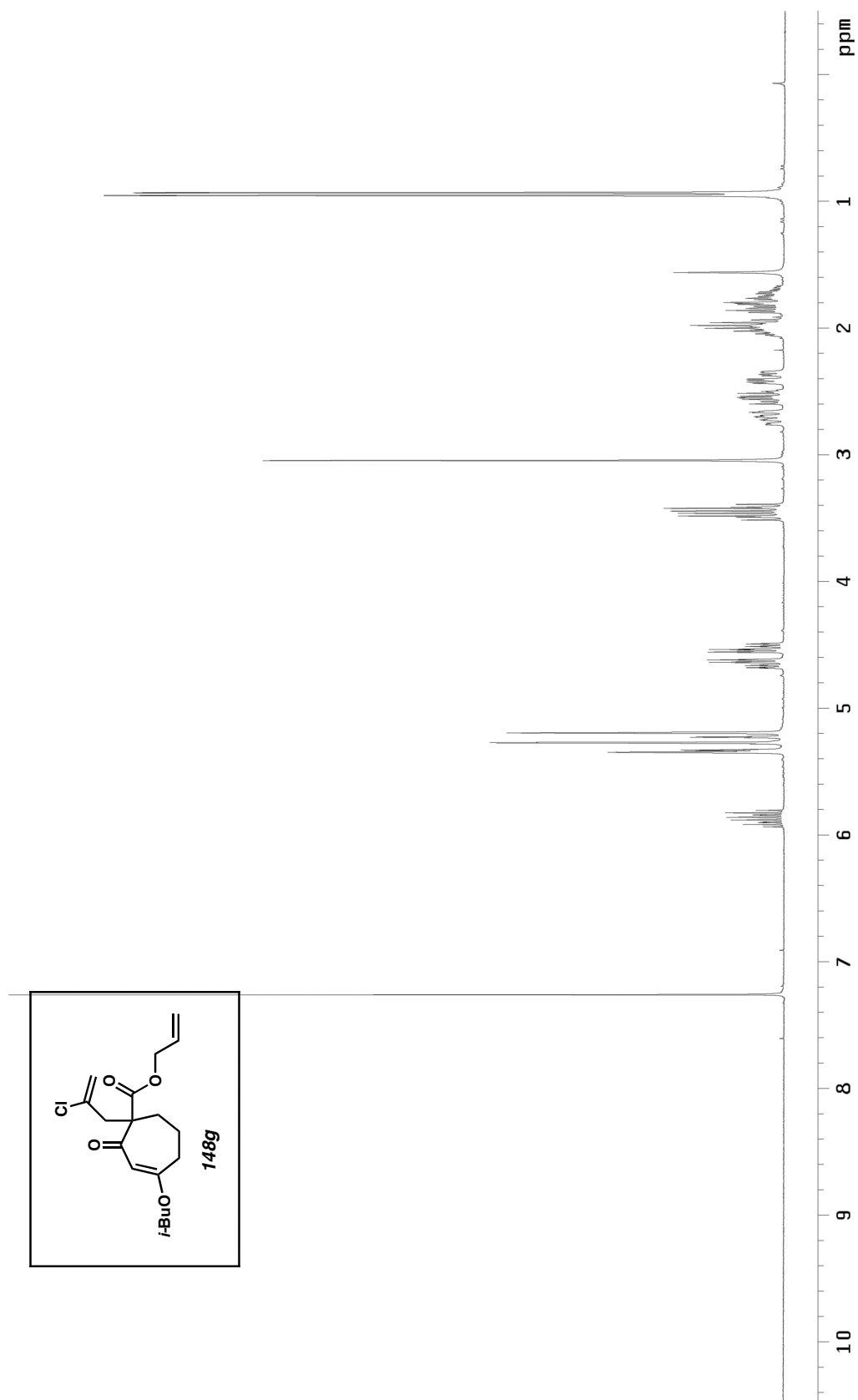


Figure A1.21. ¹³C NMR (75 MHz, CDCl₃) of compound **148f**.

Figure A1.22. ¹H NMR (300 MHz, CDCl₃) of compound **148g**.

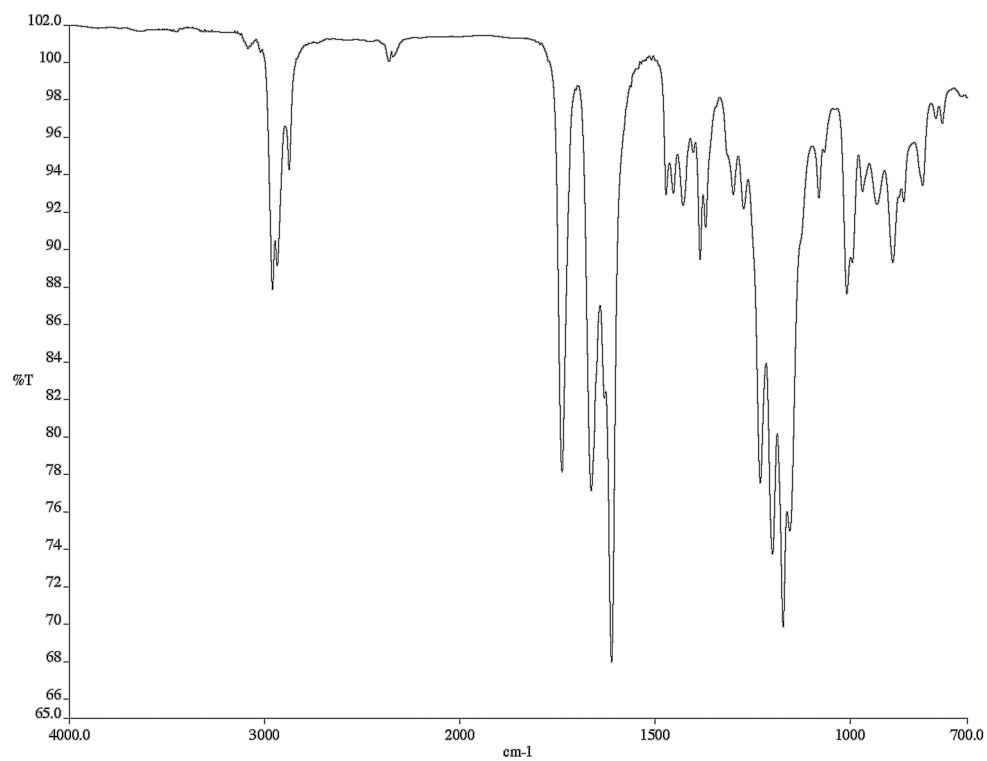


Figure A1.23. Infrared spectrum (thin film/NaCl) of compound **148g**.

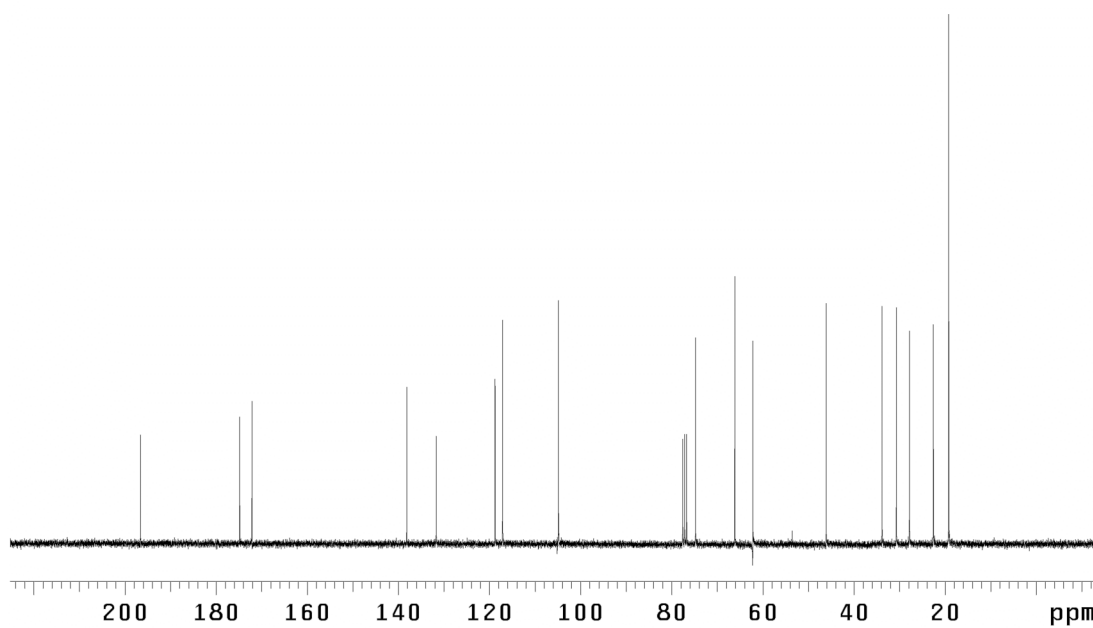


Figure A1.24. ¹³C NMR (75 MHz, CDCl₃) of compound **148g**.

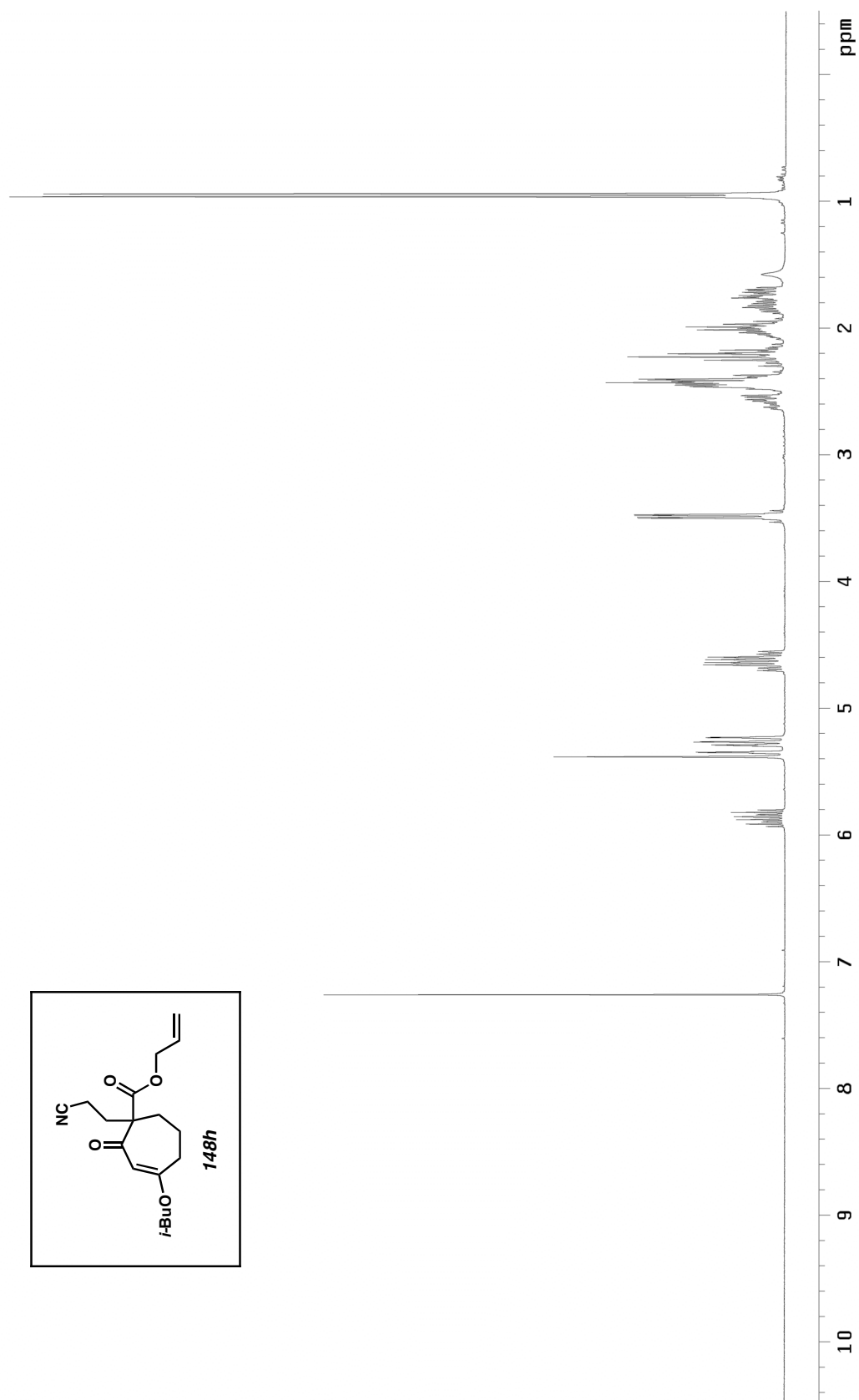


Figure A1.25. ^1H NMR (300 MHz, CDCl_3) of compound **148h**.

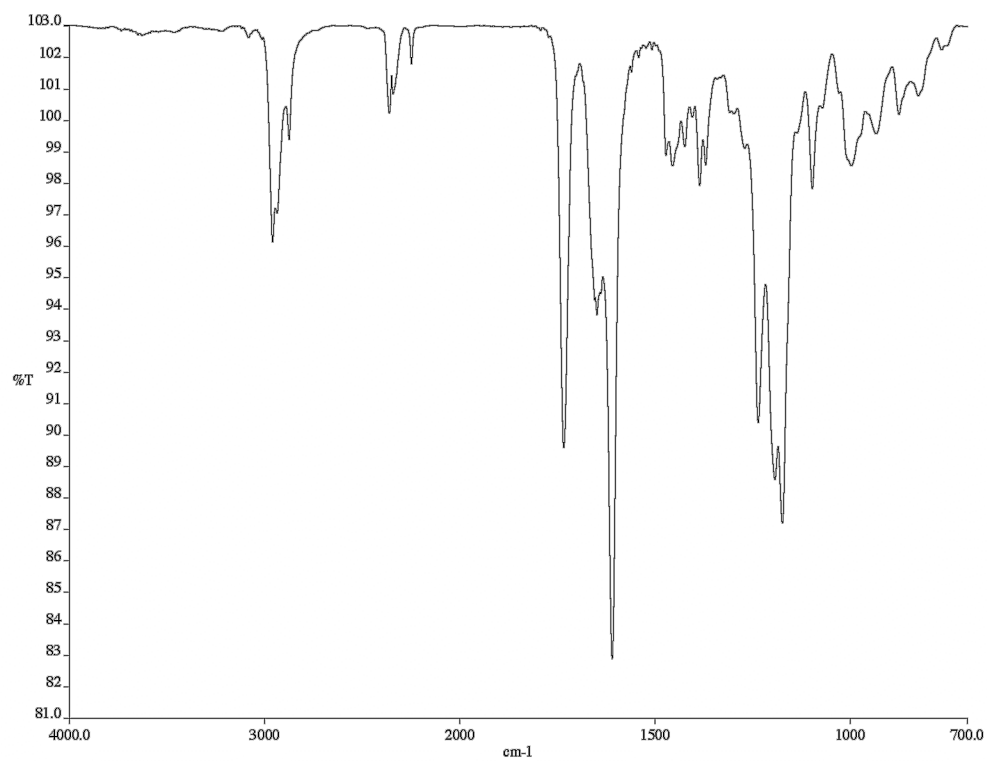


Figure A1.26. Infrared spectrum (thin film/NaCl) of compound **148h**.

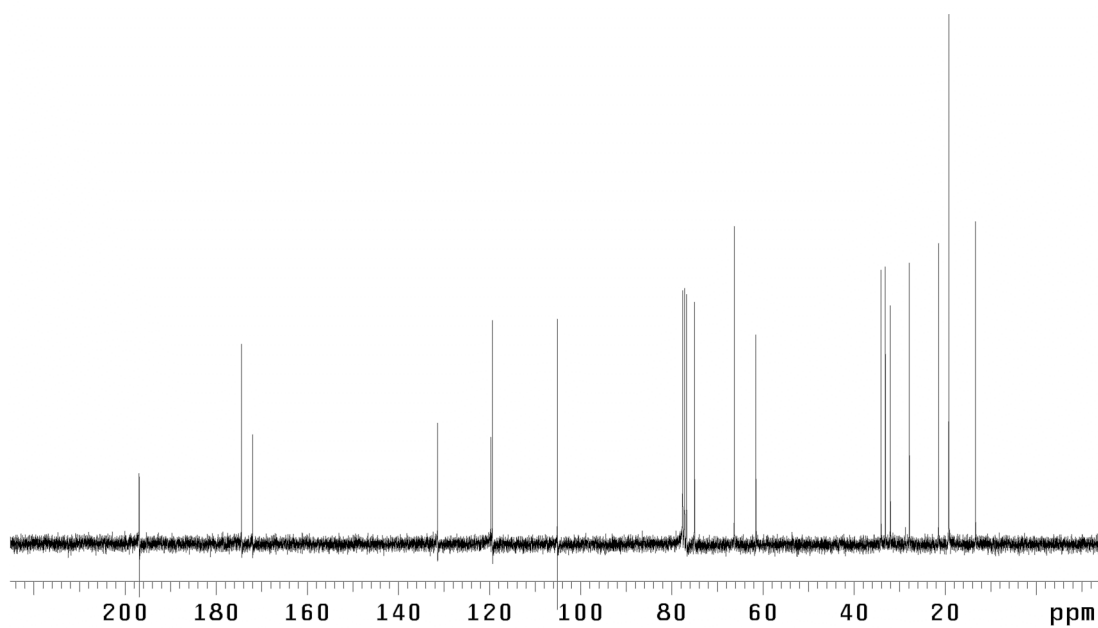
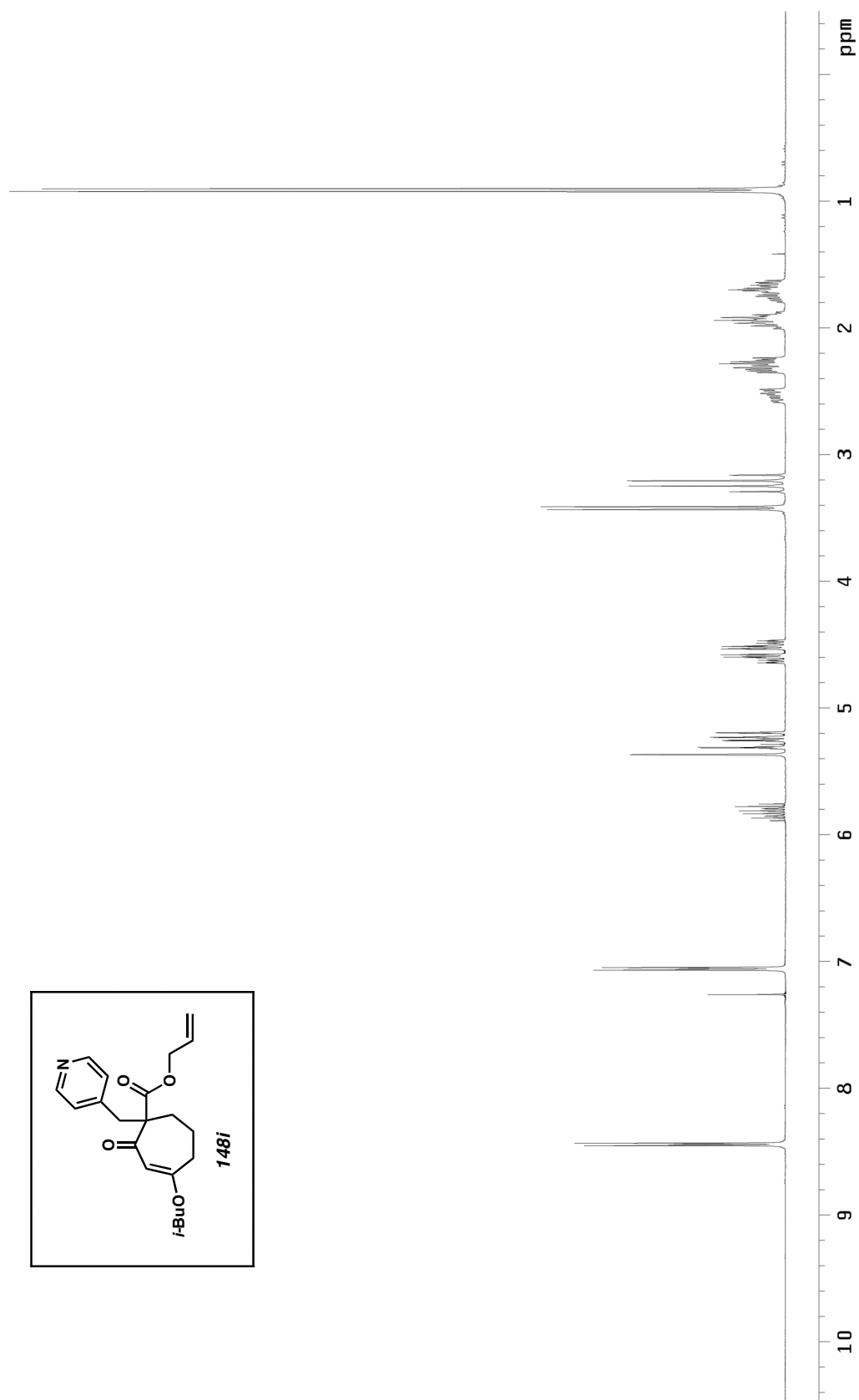


Figure A1.27. ¹³C NMR (75 MHz, CDCl₃) of compound **148h**.

Figure A1.28. ^1H NMR (300 MHz, CDCl_3) of compound **148i**.

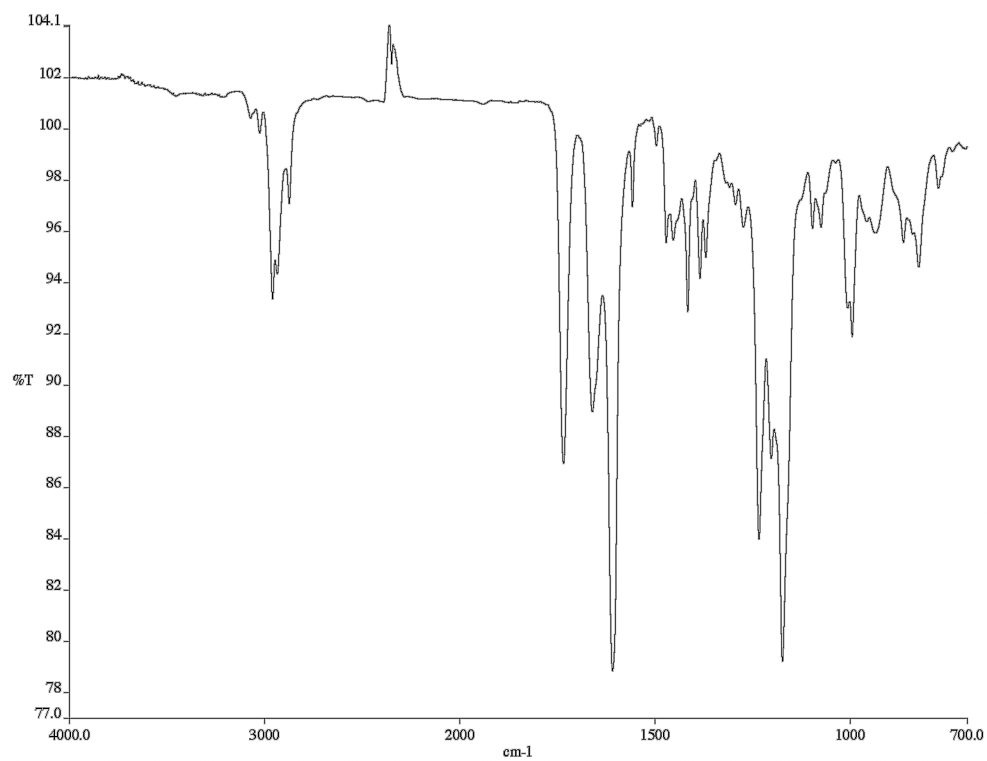


Figure A1.29. Infrared spectrum (thin film/NaCl) of compound **148i**.

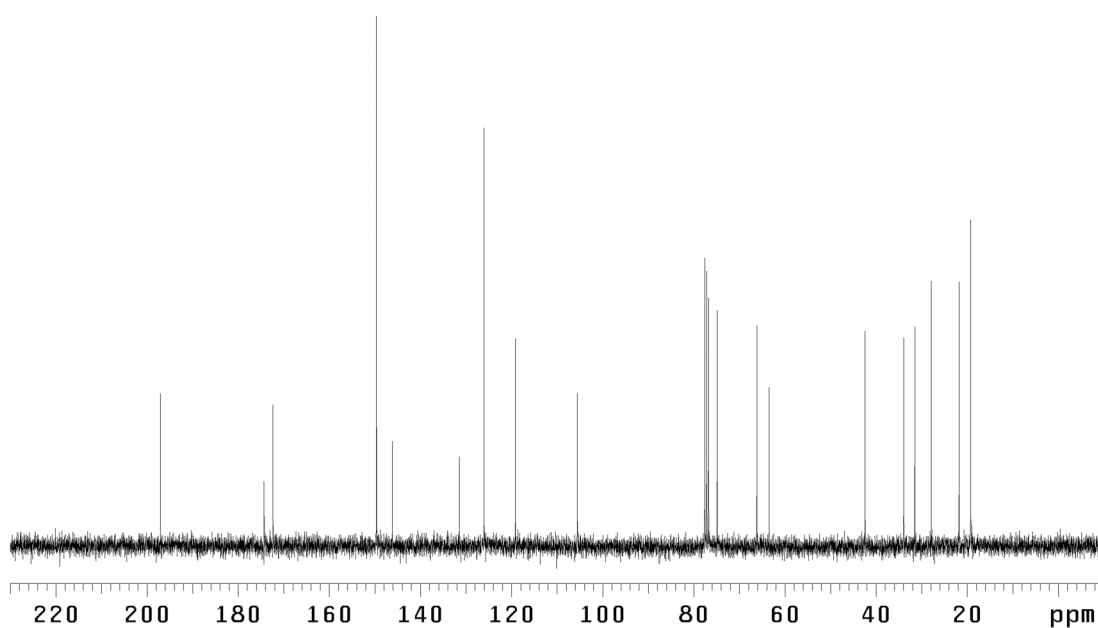
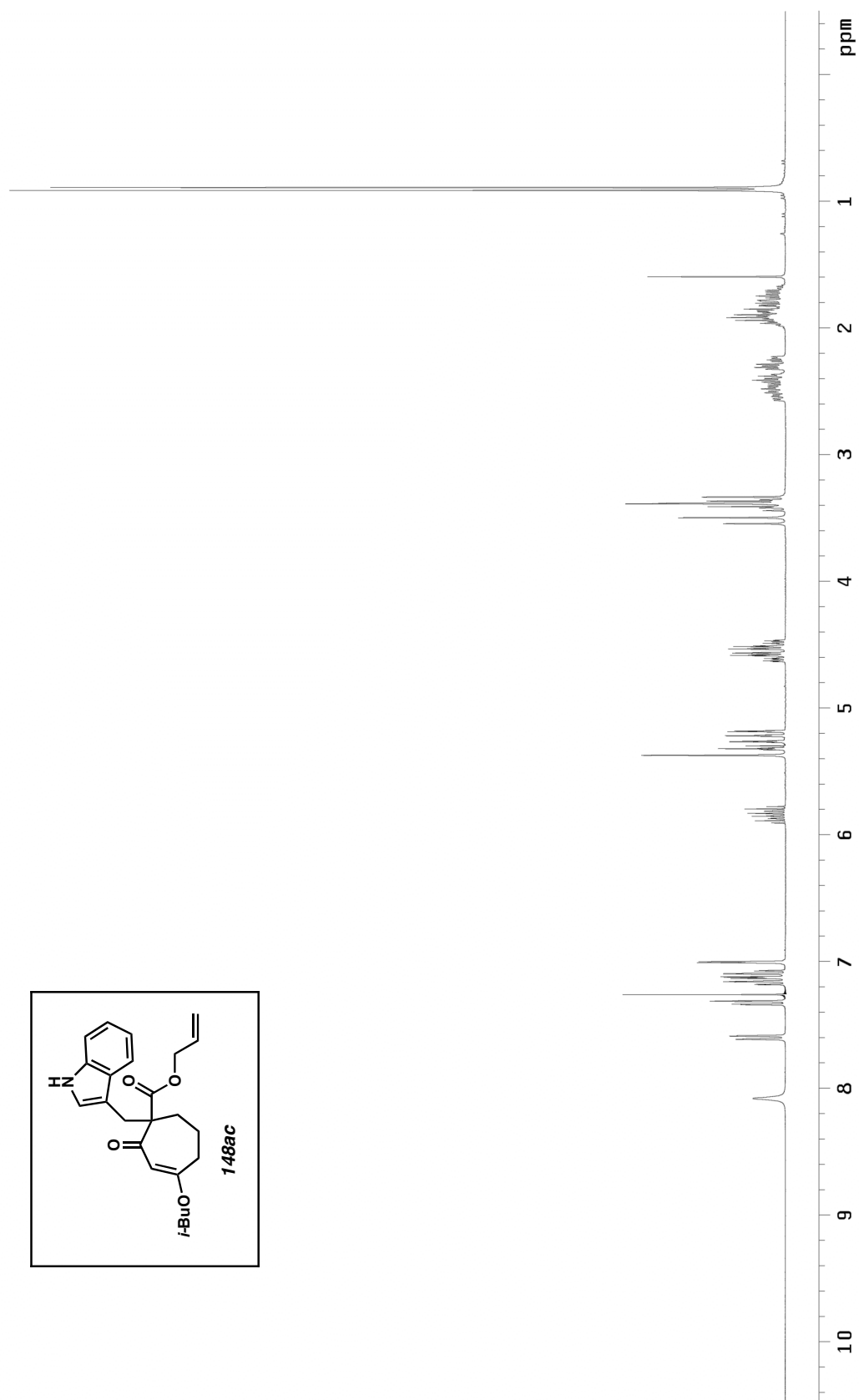


Figure A1.30. ^{13}C NMR (75 MHz, CDCl_3) of compound **148i**.

Figure A1.31. ^1H NMR (300 MHz, CDCl_3) of compound **148ac**.

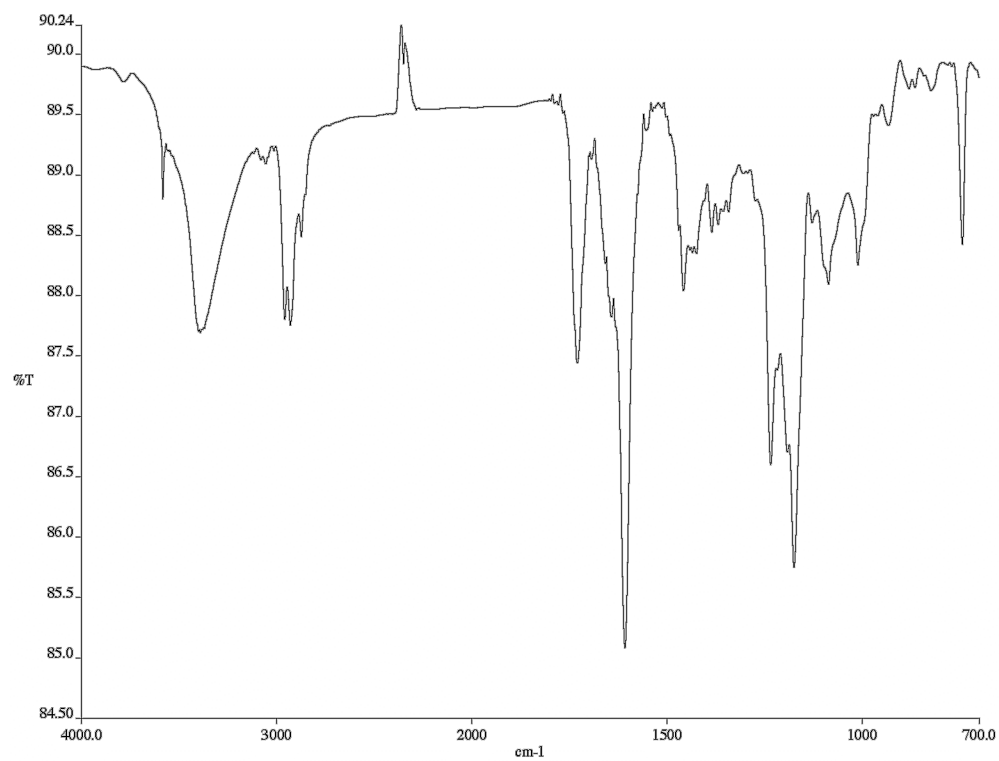


Figure A1.33. Infrared spectrum (thin film/NaCl) of compound **148ac**.

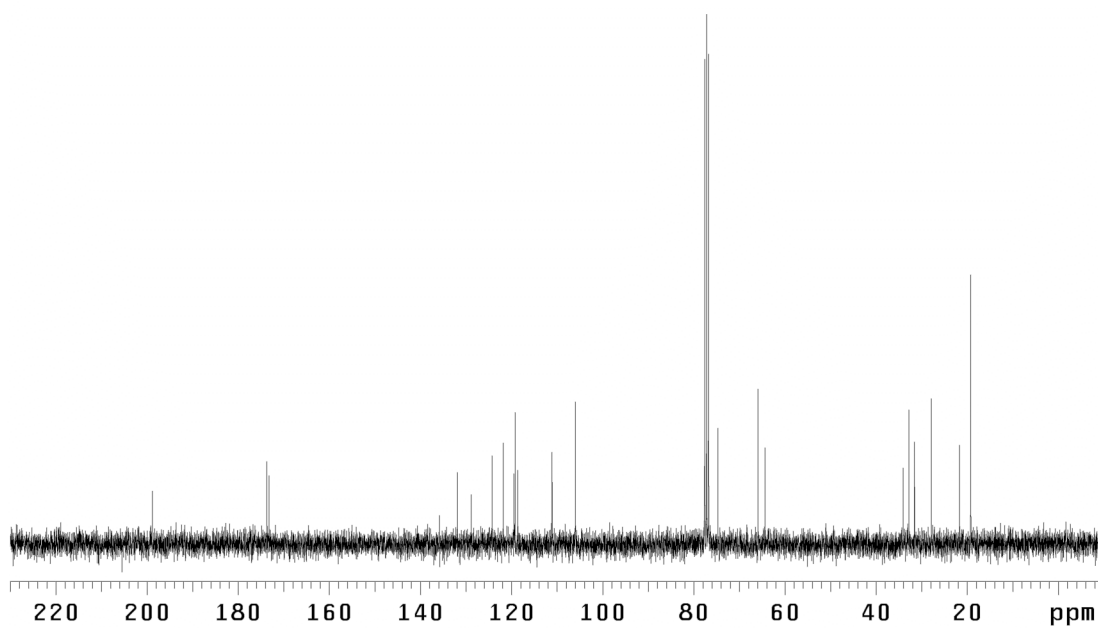
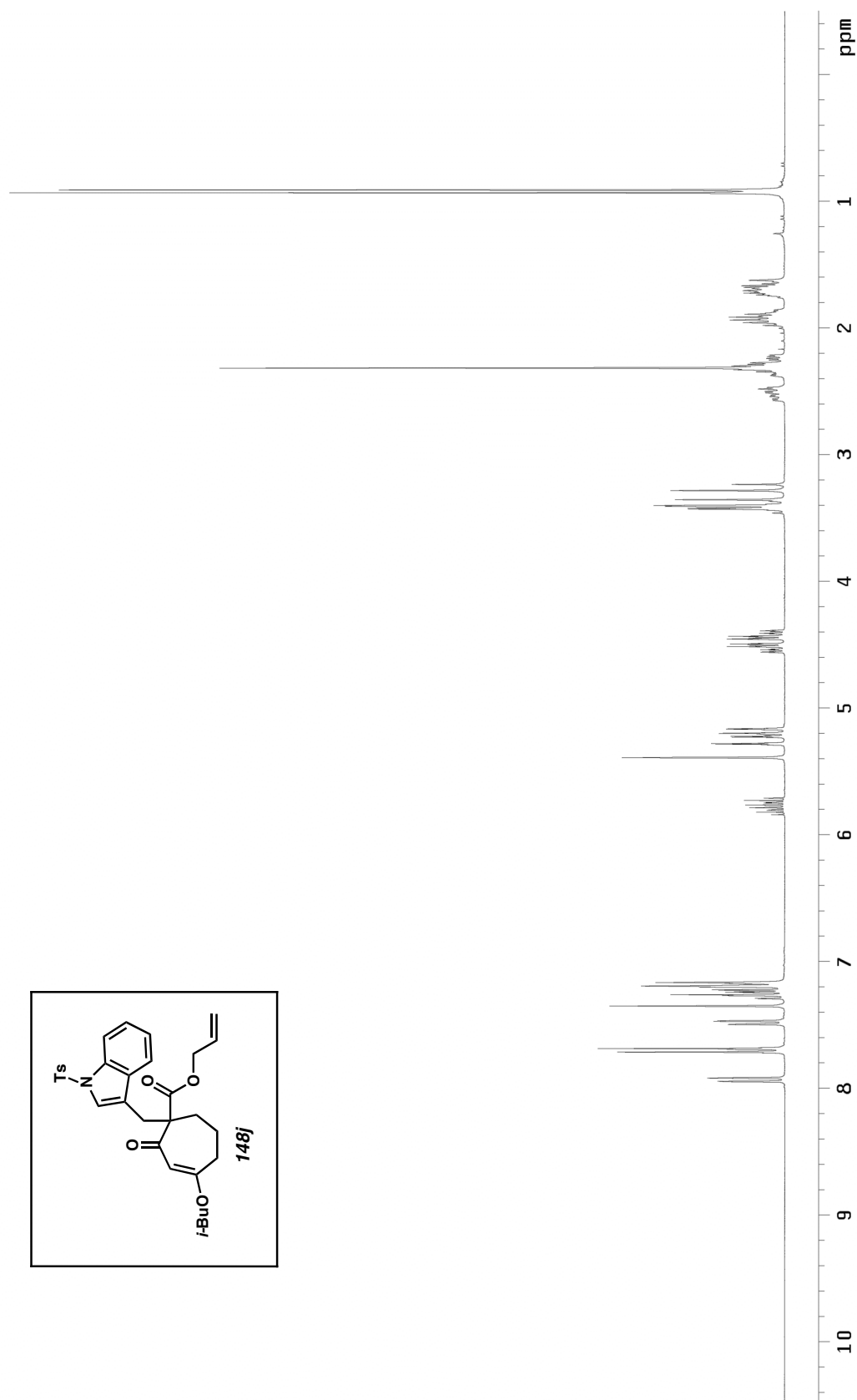


Figure A1.32. ¹³C NMR (75 MHz, CDCl₃) of compound **148ac**.

Figure A1.34. ^1H NMR (300 MHz, CDCl_3) of compound **148j**.

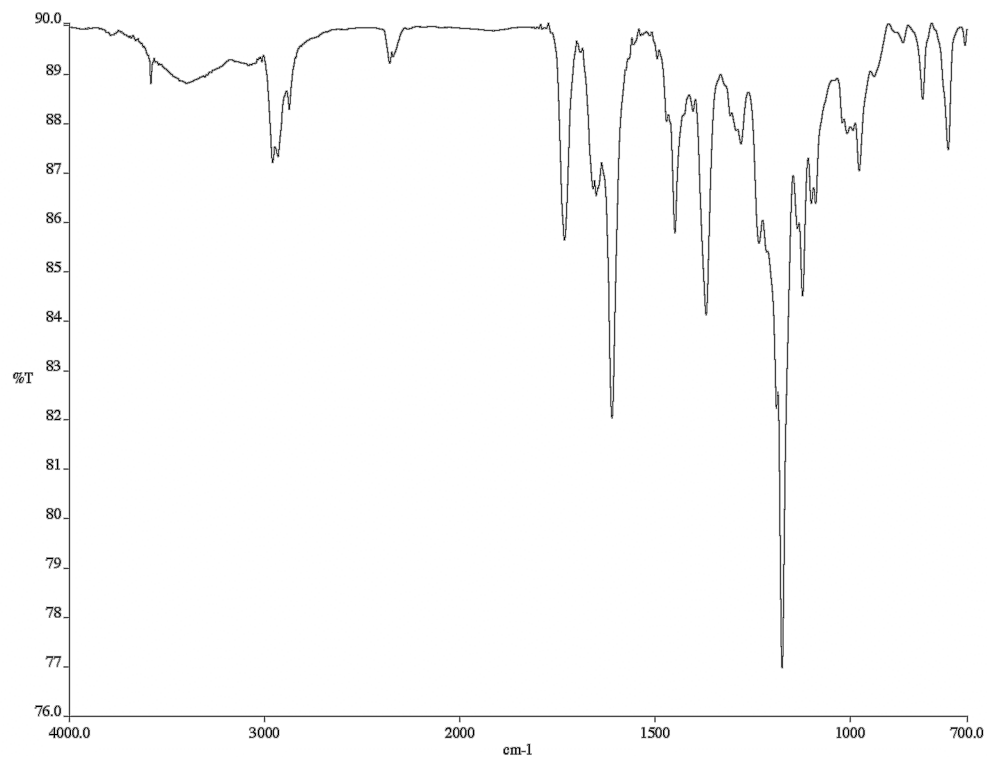


Figure A1.35. Infrared spectrum (thin film/NaCl) of compound **148j**.

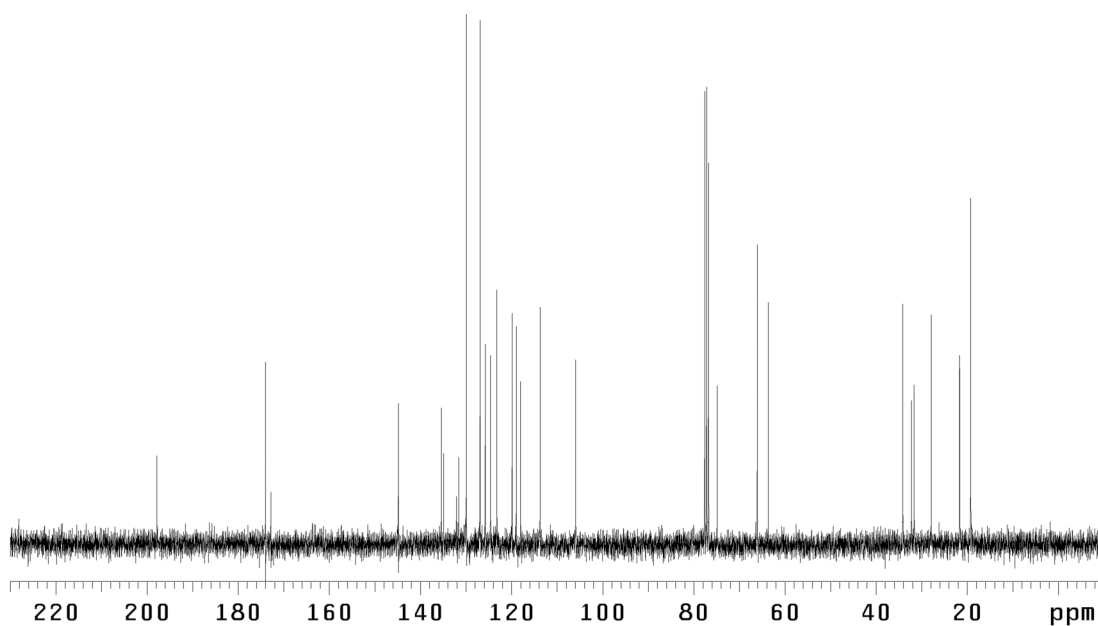
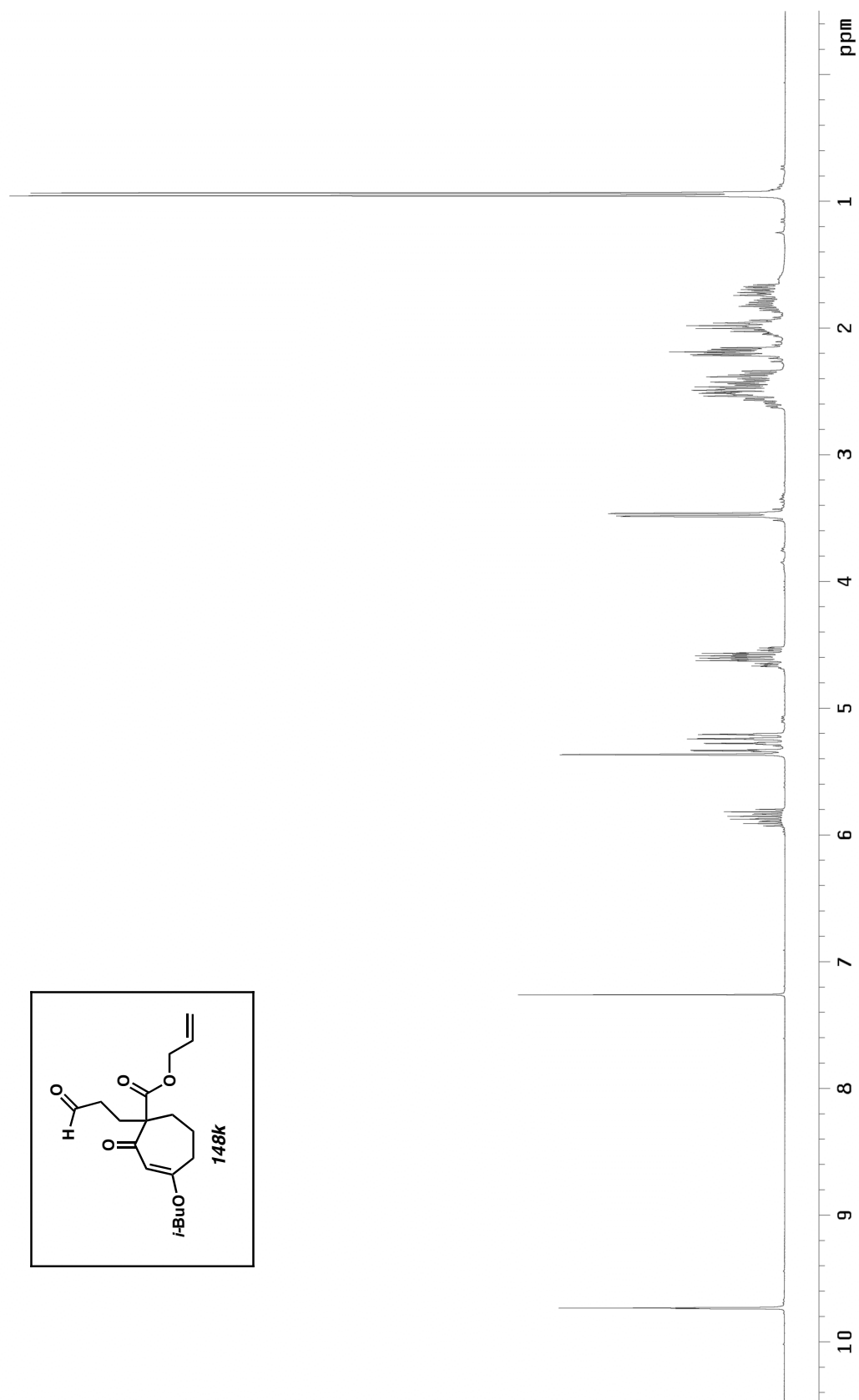


Figure A1.36. ^{13}C NMR (75 MHz, CDCl_3) of compound **148j**.

Figure A1.37. ¹H NMR (300 MHz, CDCl₃) of compound **148k**.

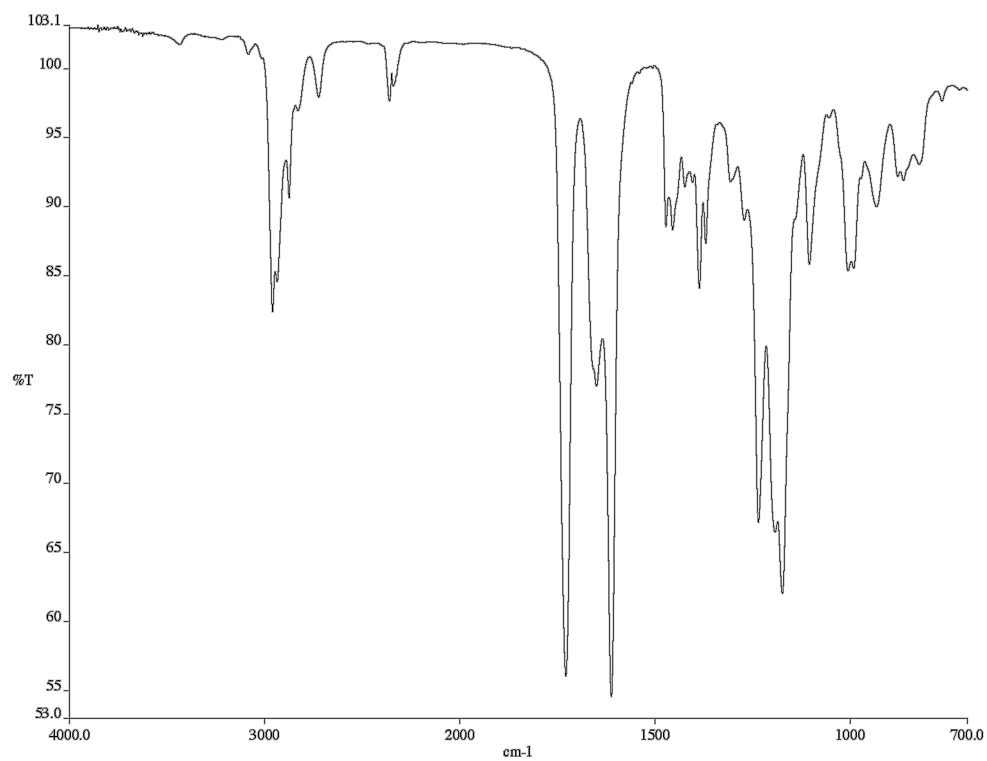


Figure A1.38. Infrared spectrum (thin film/NaCl) of compound **148k**.

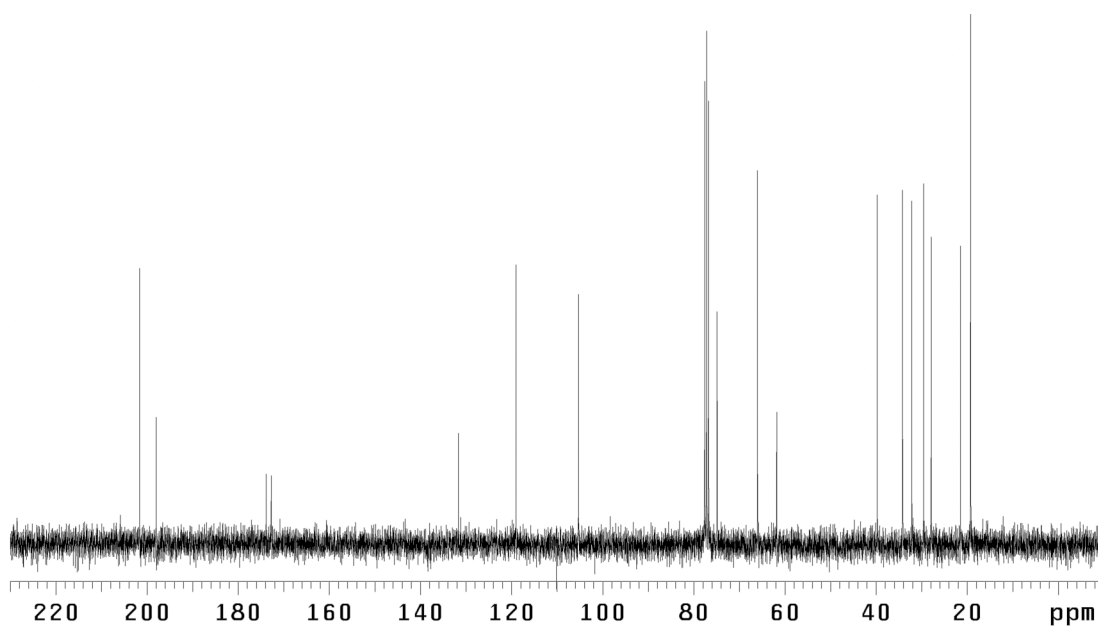
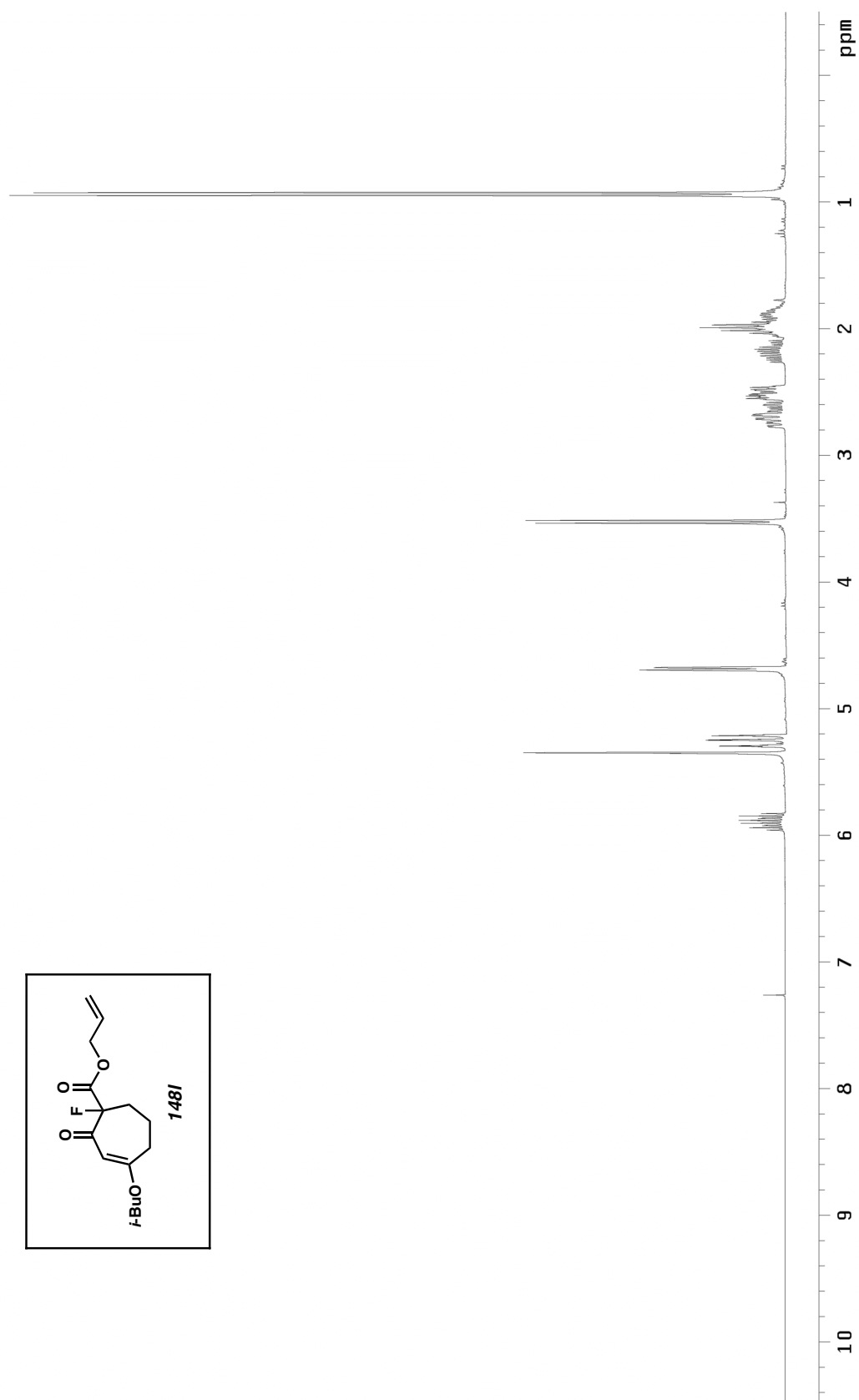
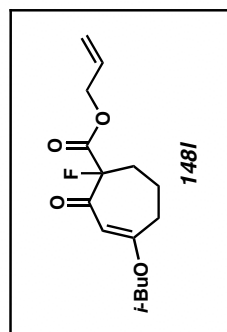


Figure A1.39. ¹³C NMR (75 MHz, CDCl₃) of compound **148k**.

Figure A1.40. ¹H NMR (300 MHz, CDCl₃) of compound **148I**.

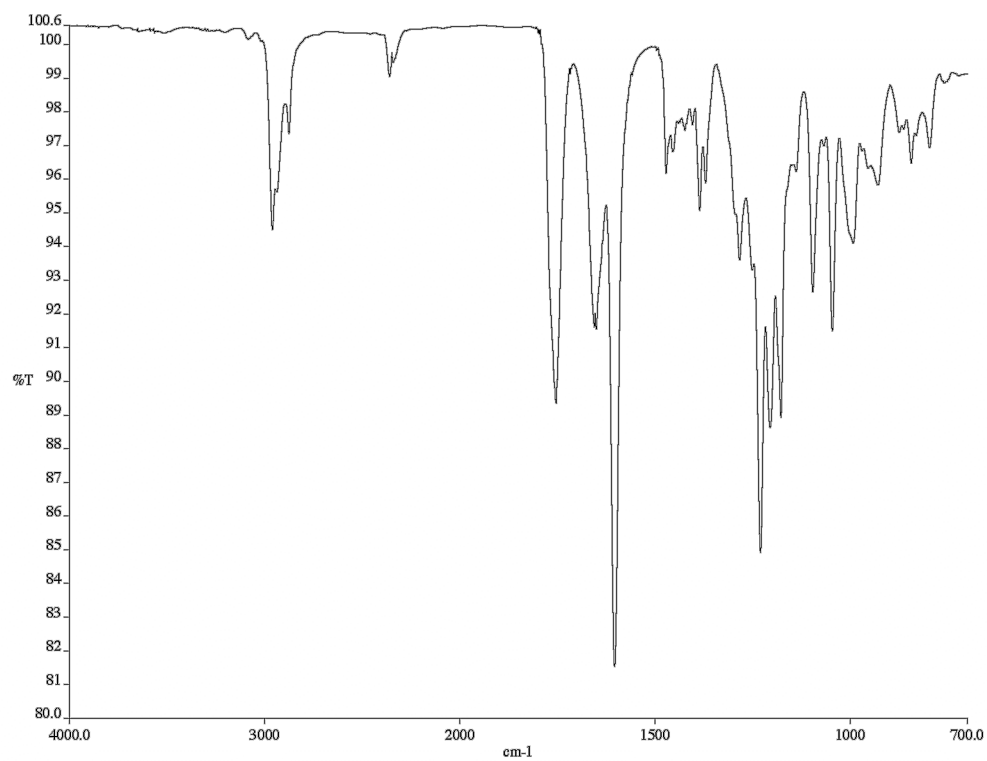


Figure A1.41. Infrared spectrum (thin film/NaCl) of compound **148I**.

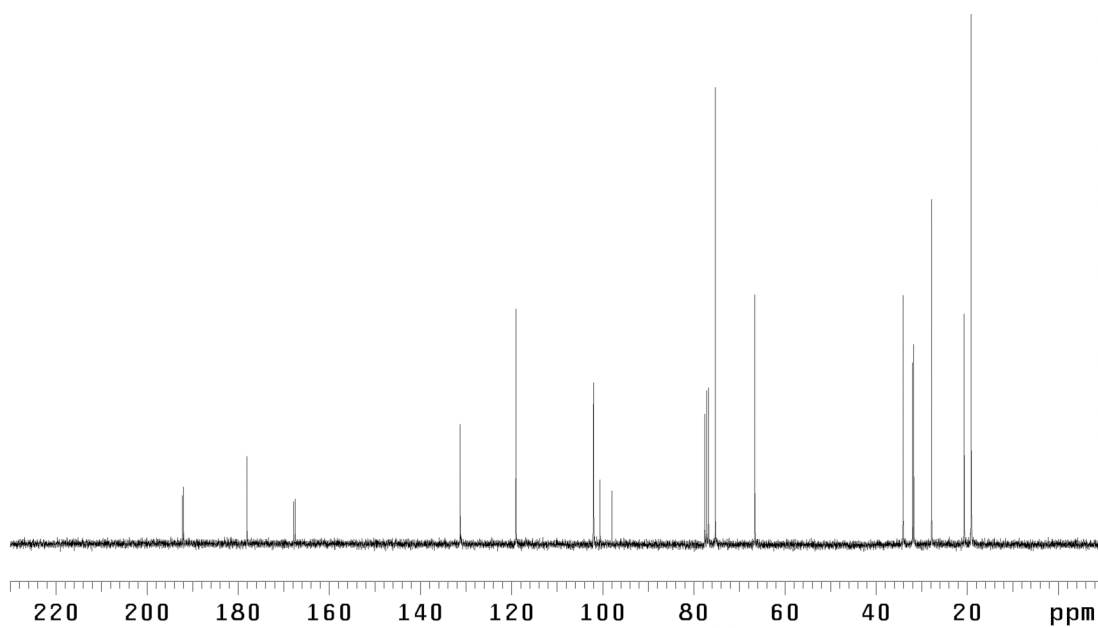
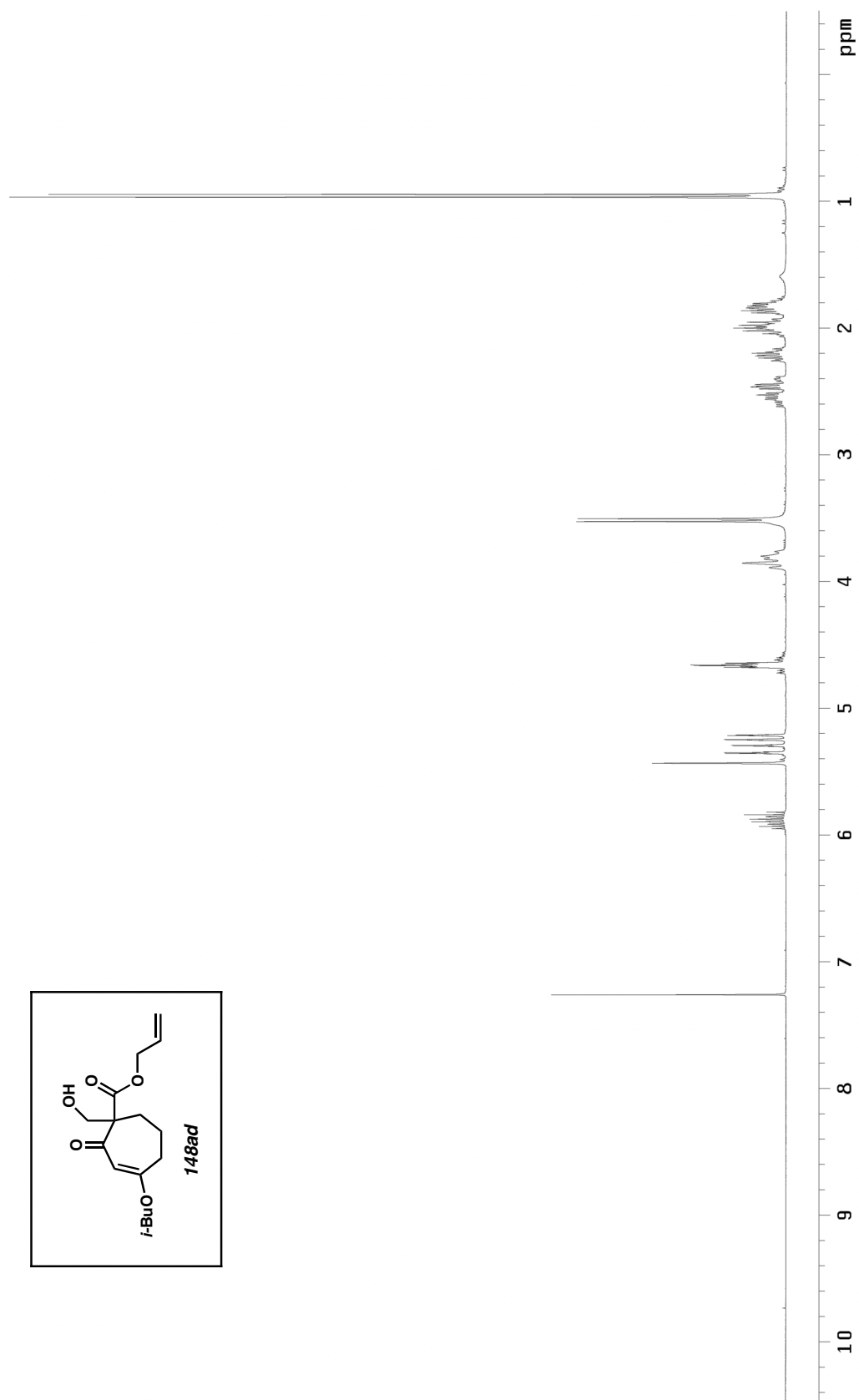


Figure A1.42. ¹³C NMR (75 MHz, CDCl₃) of compound **148I**.

Figure A1.43. ^1H NMR (300 MHz, CDCl_3) of compound **148ad**.

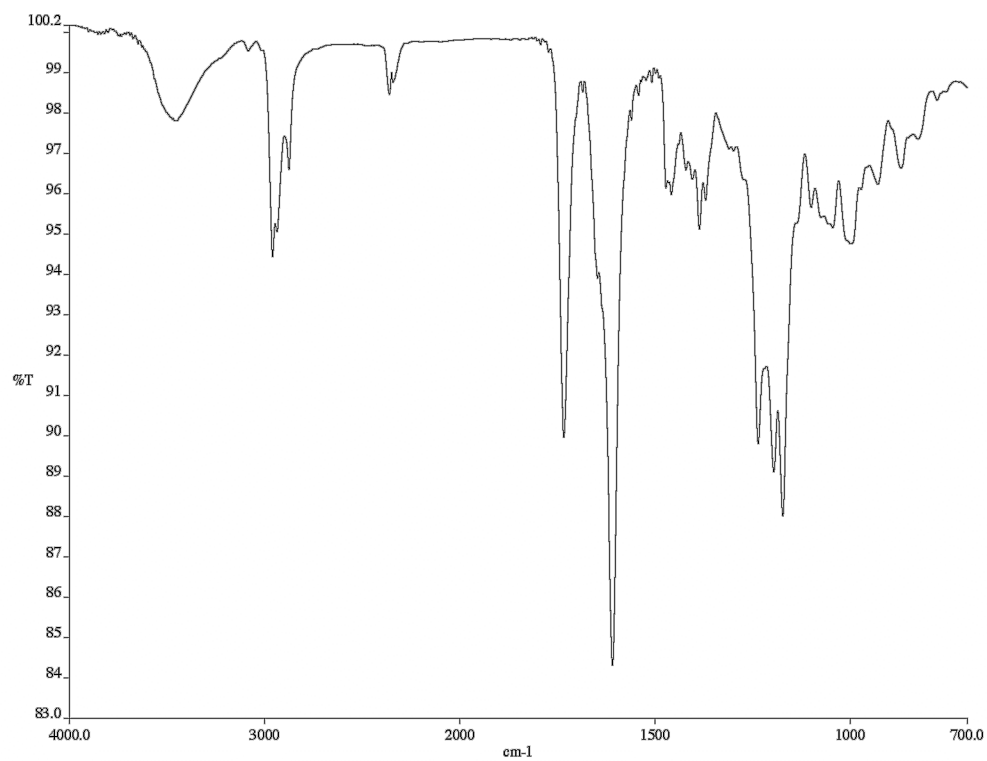


Figure A1.44. Infrared spectrum (thin film/NaCl) of compound **148ad**.

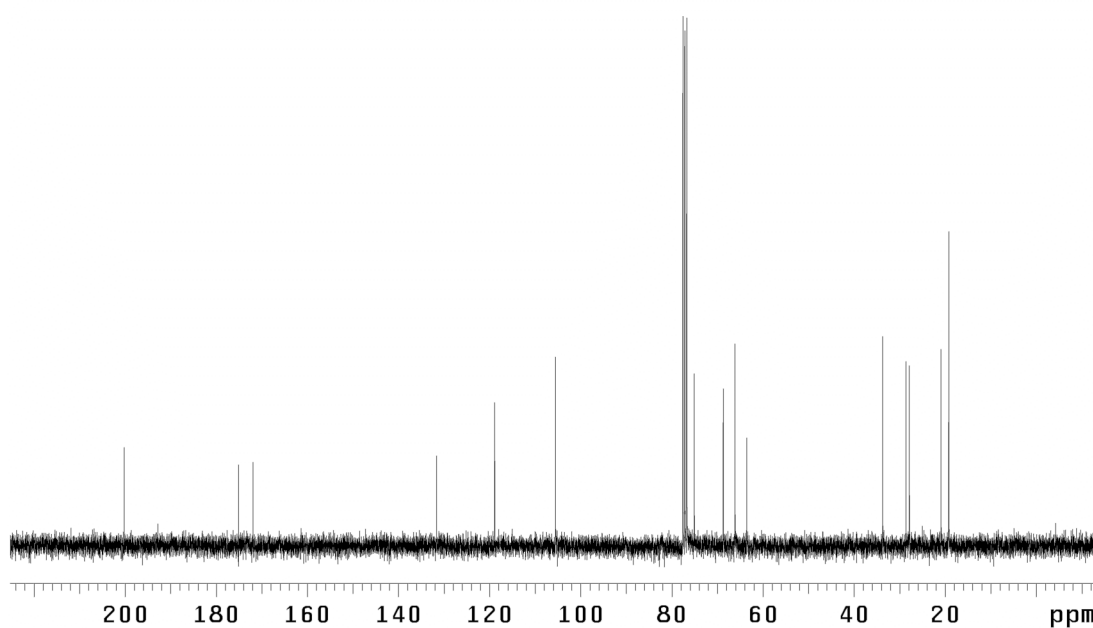
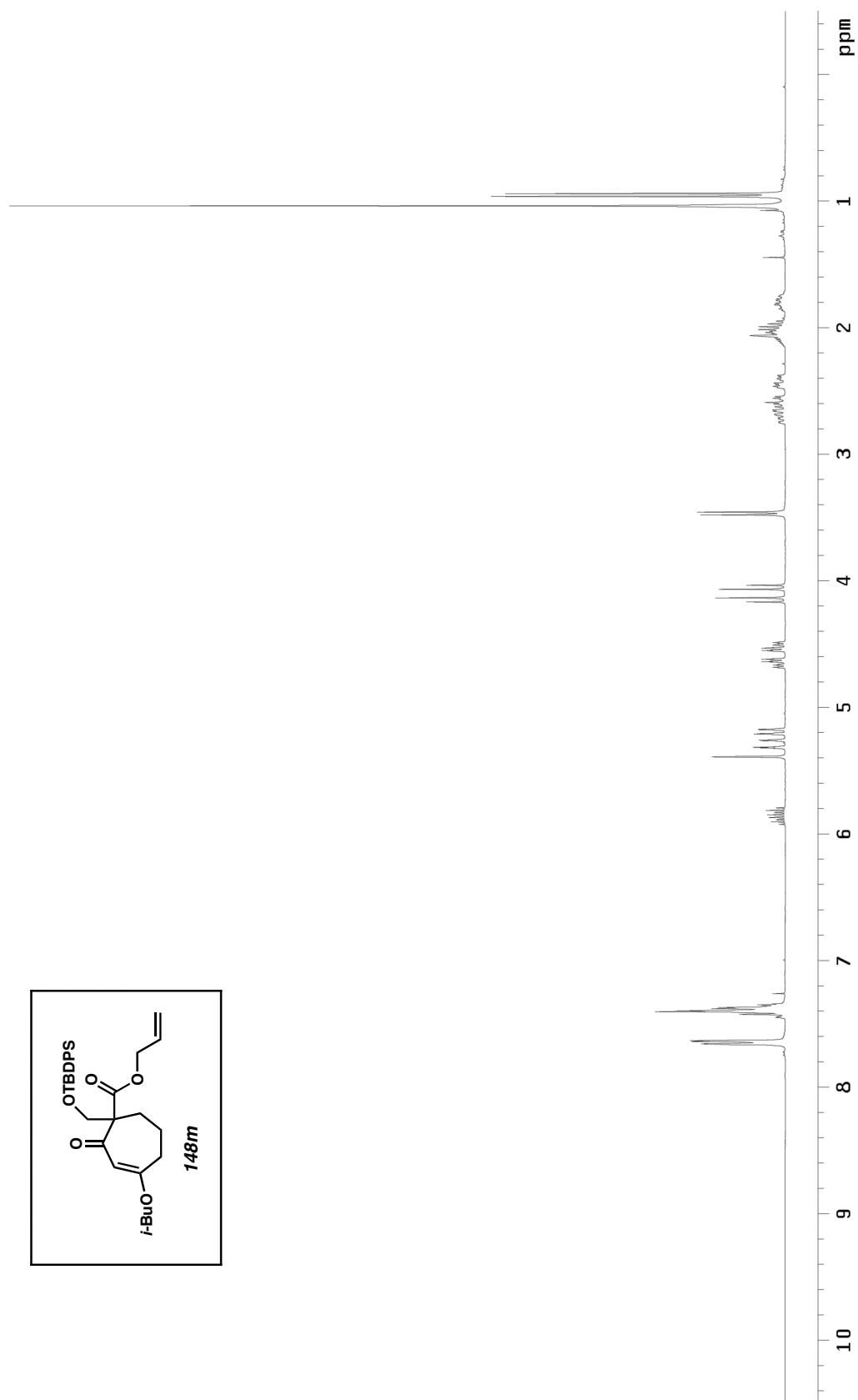


Figure A1.45. ^{13}C NMR (75 MHz, CDCl_3) of compound **148ad**.

Figure A1.46. ^1H NMR (300 MHz, CDCl_3) of compound **148m**.

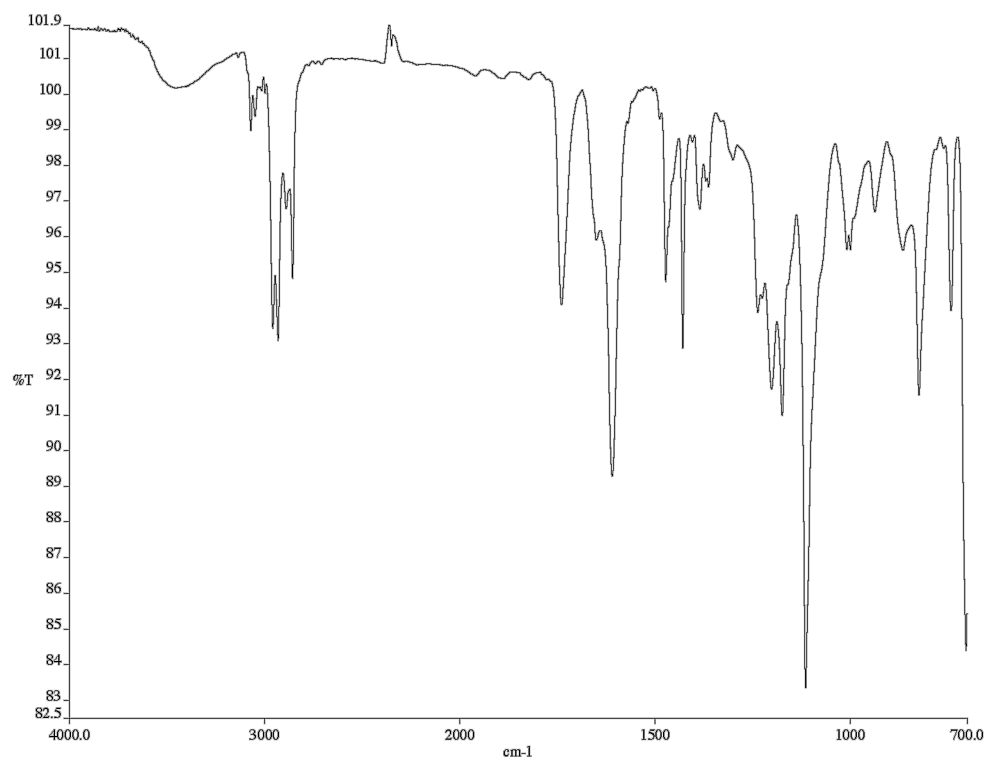


Figure A1.47. Infrared spectrum (thin film/NaCl) of compound **148m**.

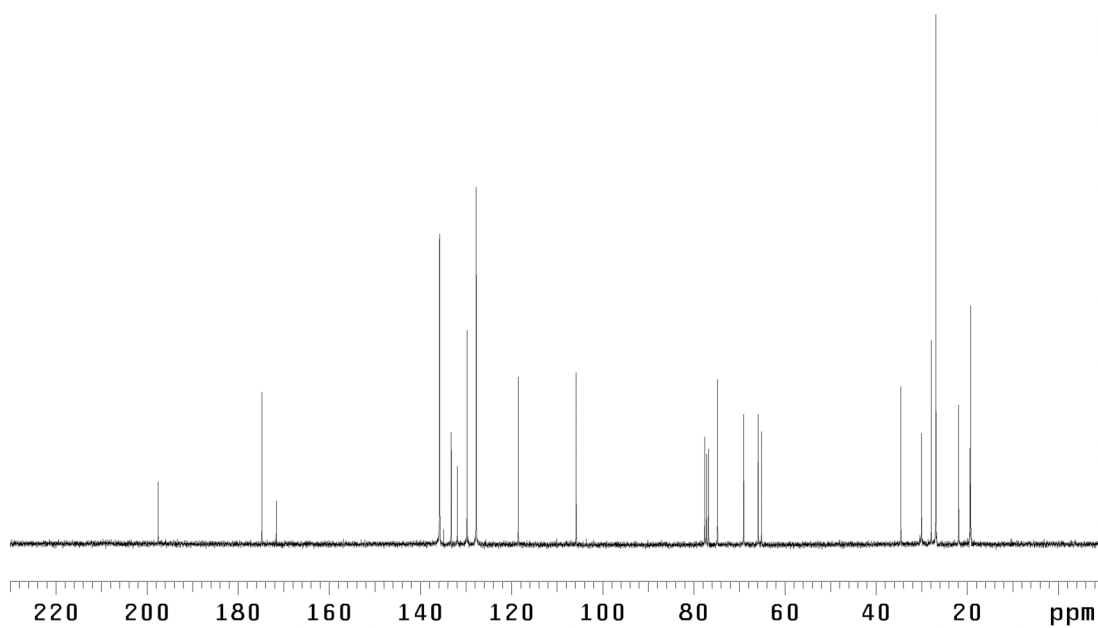
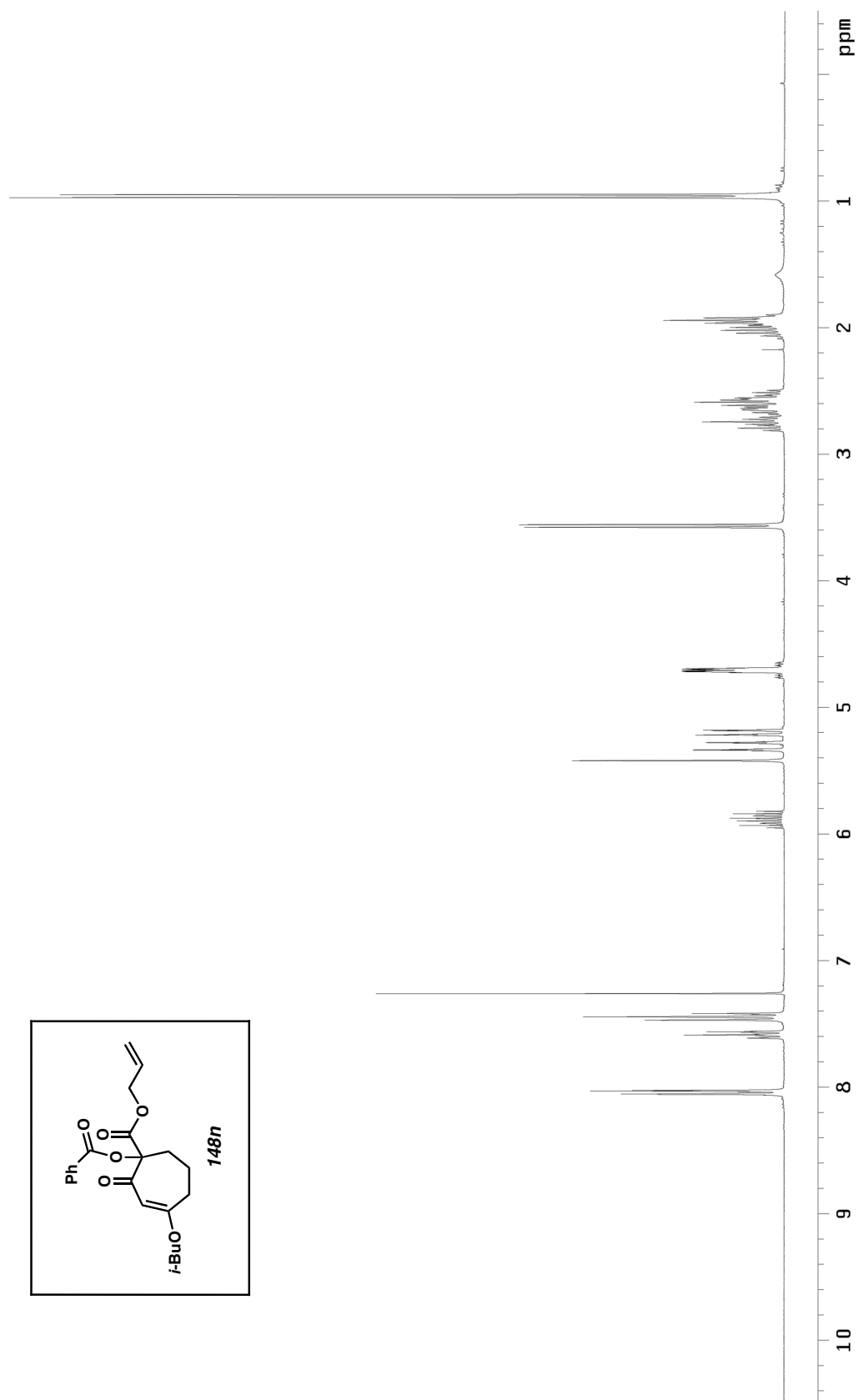


Figure A1.48. ¹³C NMR (75 MHz, CDCl₃) of compound **148m**.

Figure A1.49. ¹H NMR (300 MHz, CDCl₃) of compound **148n**.

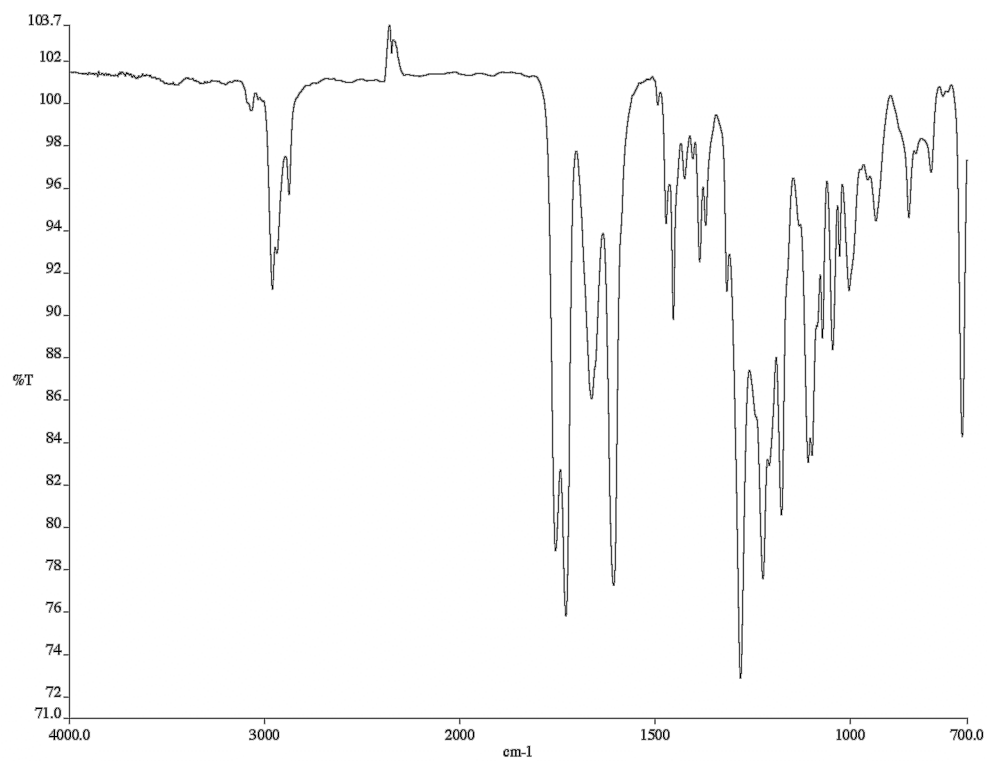


Figure A1.50. Infrared spectrum (thin film/NaCl) of compound **148n**.

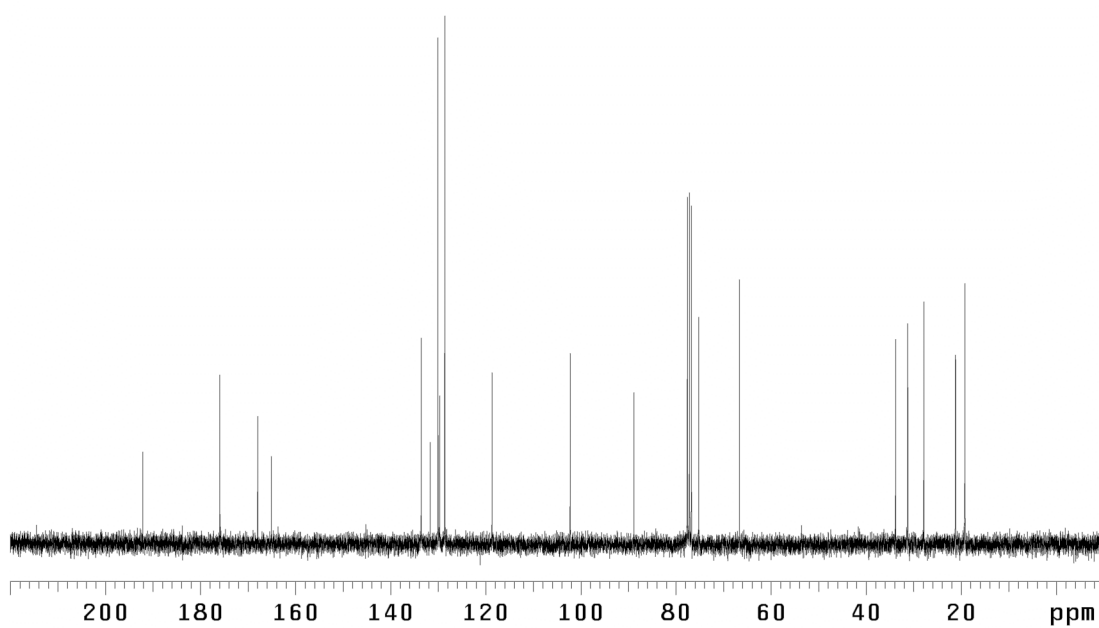


Figure A1.51. ¹³C NMR (75 MHz, CDCl₃) of compound **148n**.

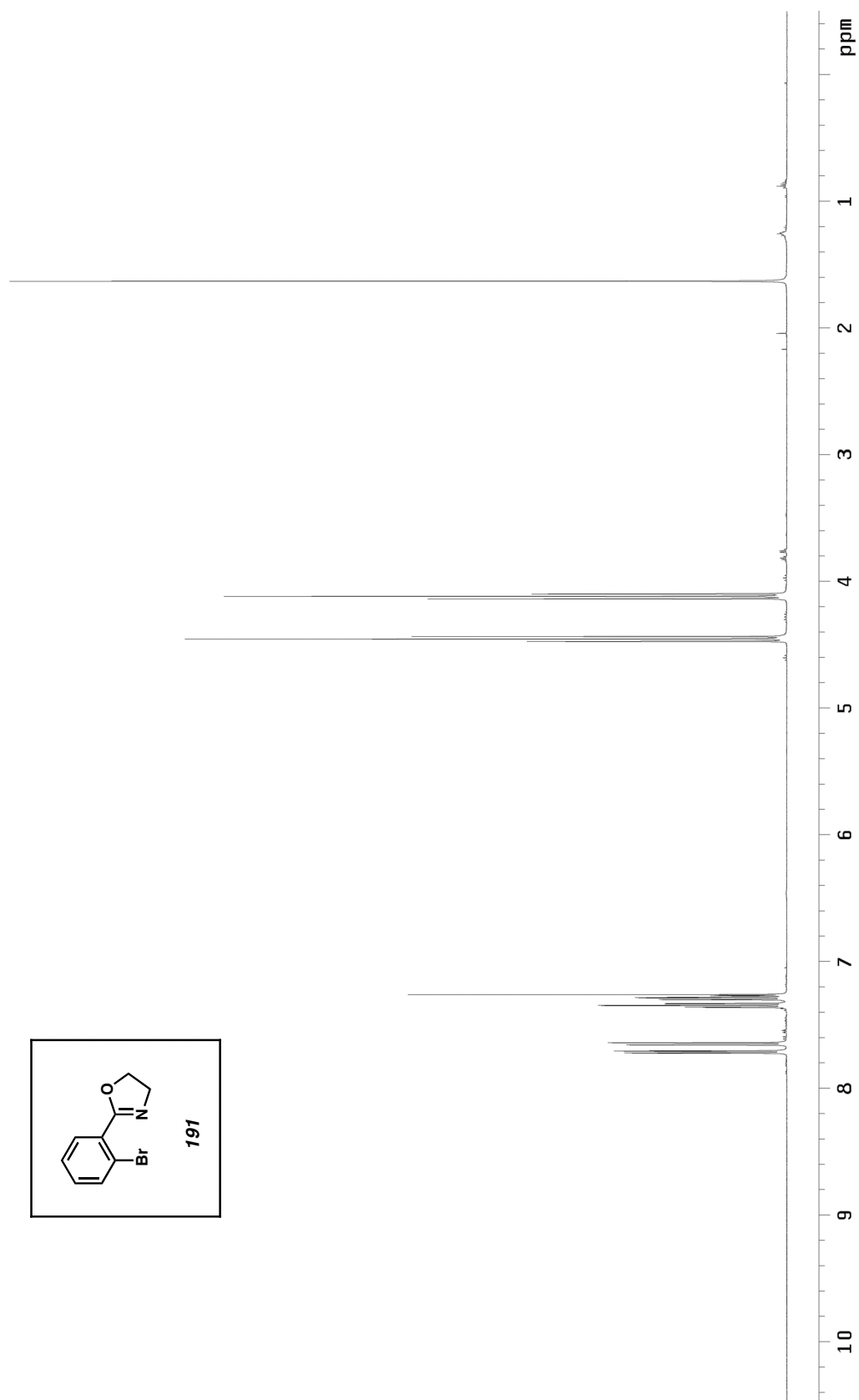


Figure A1.52. ^1H NMR (500 MHz, CDCl_3) of compound **191**.

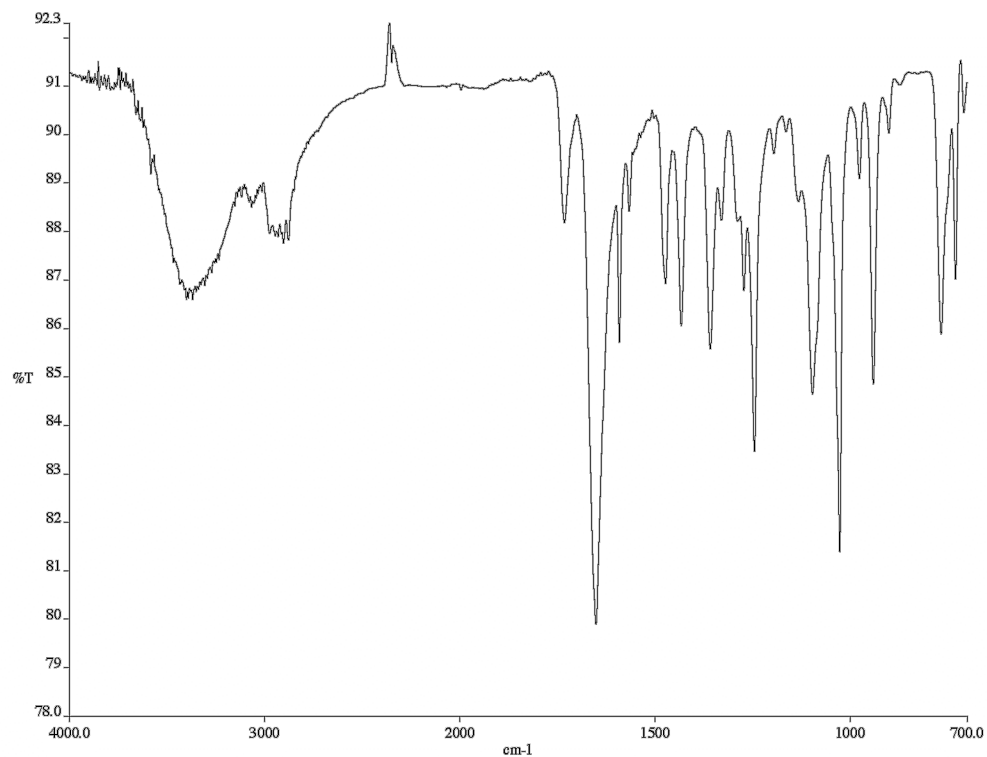


Figure A1.53. Infrared spectrum (thin film/NaCl) of compound **191**.

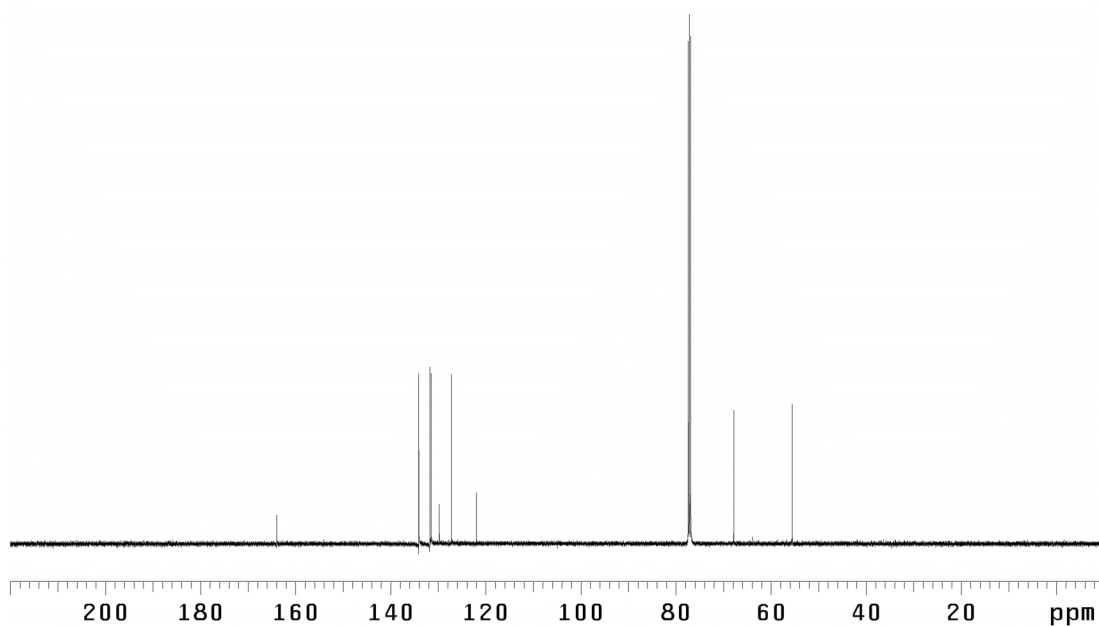
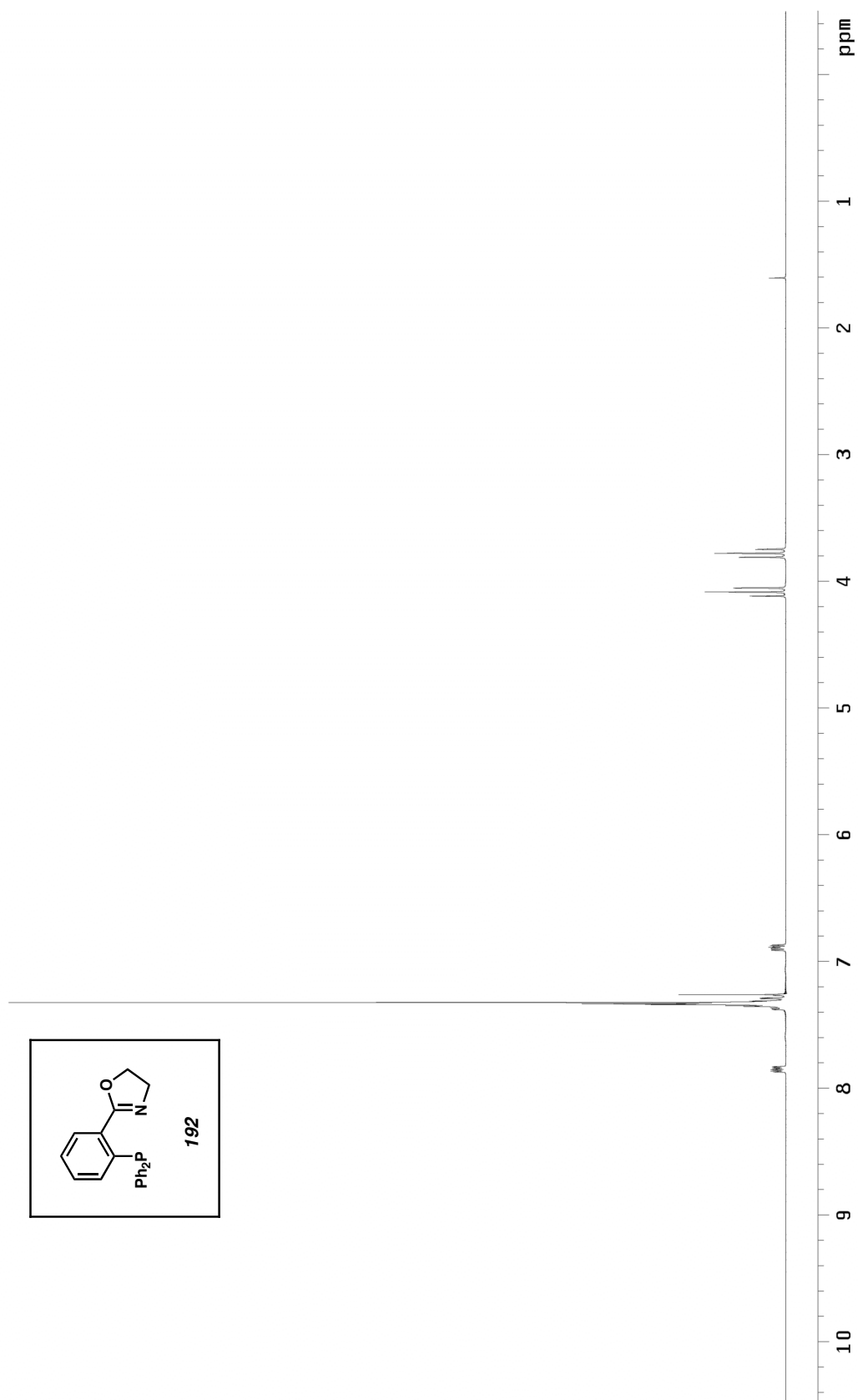


Figure A1.54. ¹³C NMR (125 MHz, CDCl₃) of compound **191**.

Figure A1.55. ^1H NMR (500 MHz, CDCl_3) of compound **192**.

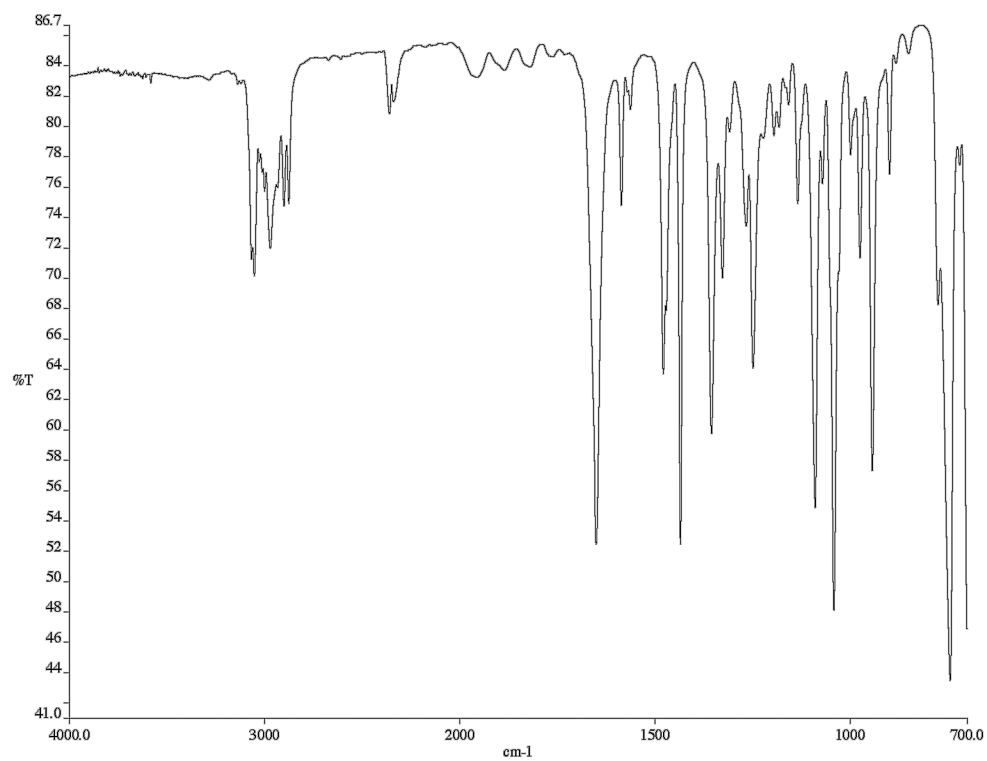


Figure A1.56. Infrared spectrum (thin film/NaCl) of compound **192**.

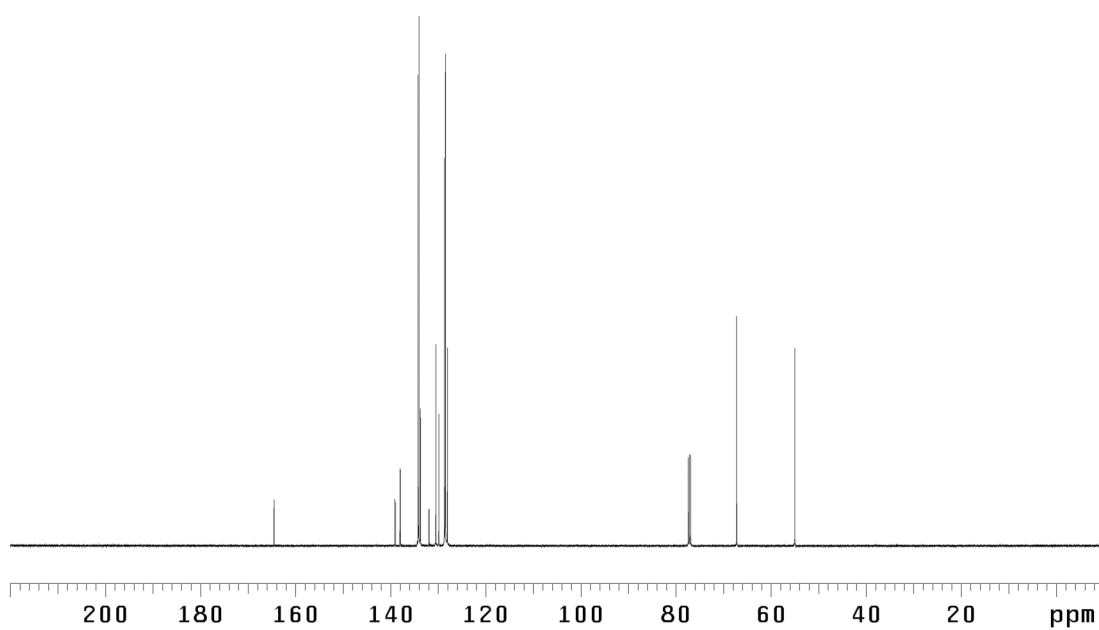


Figure A1.57. ¹³C NMR (125 MHz, CDCl₃) of compound **192**.

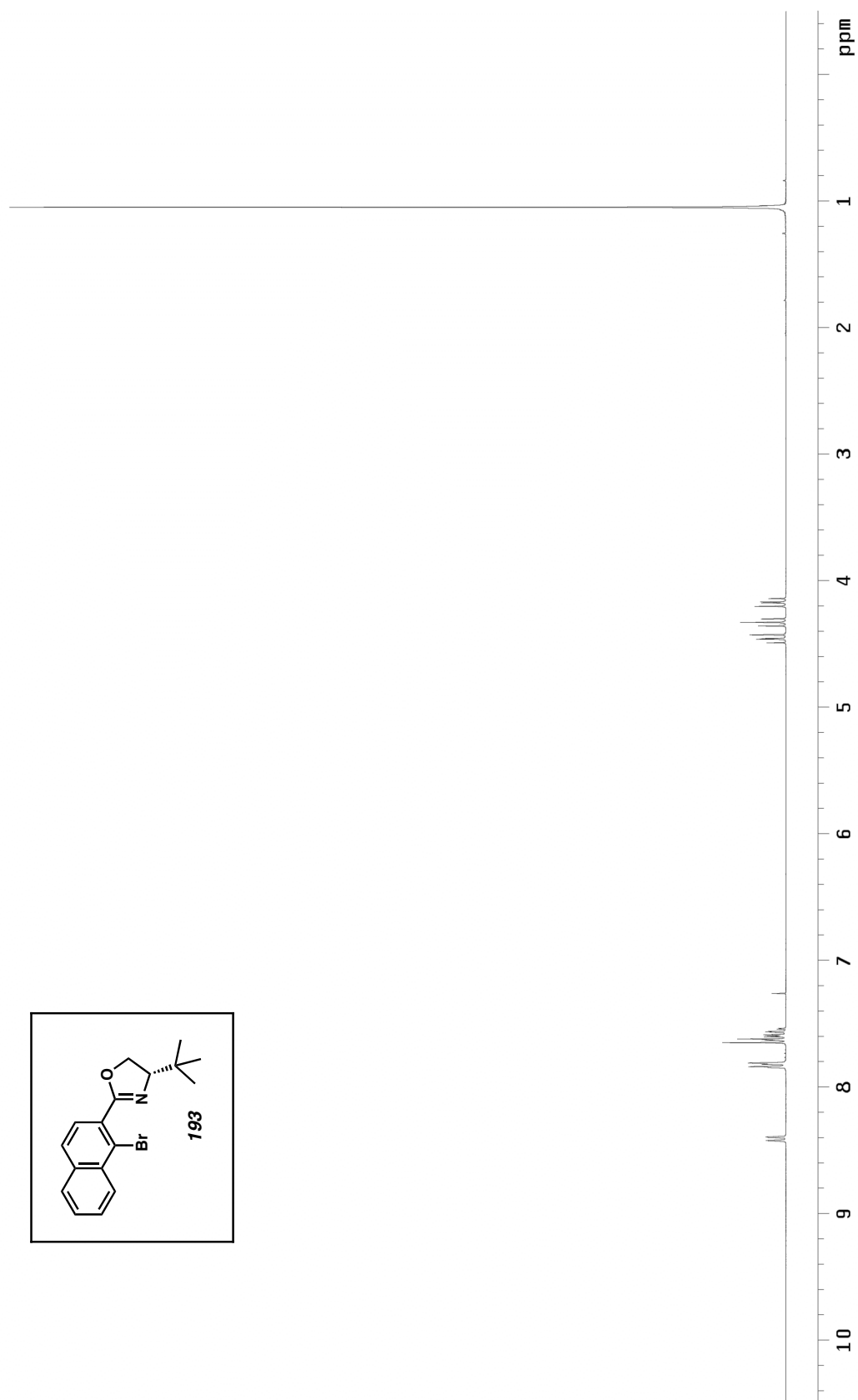


Figure A1.58. ^1H NMR (300 MHz, CDCl_3) of compound **193**.

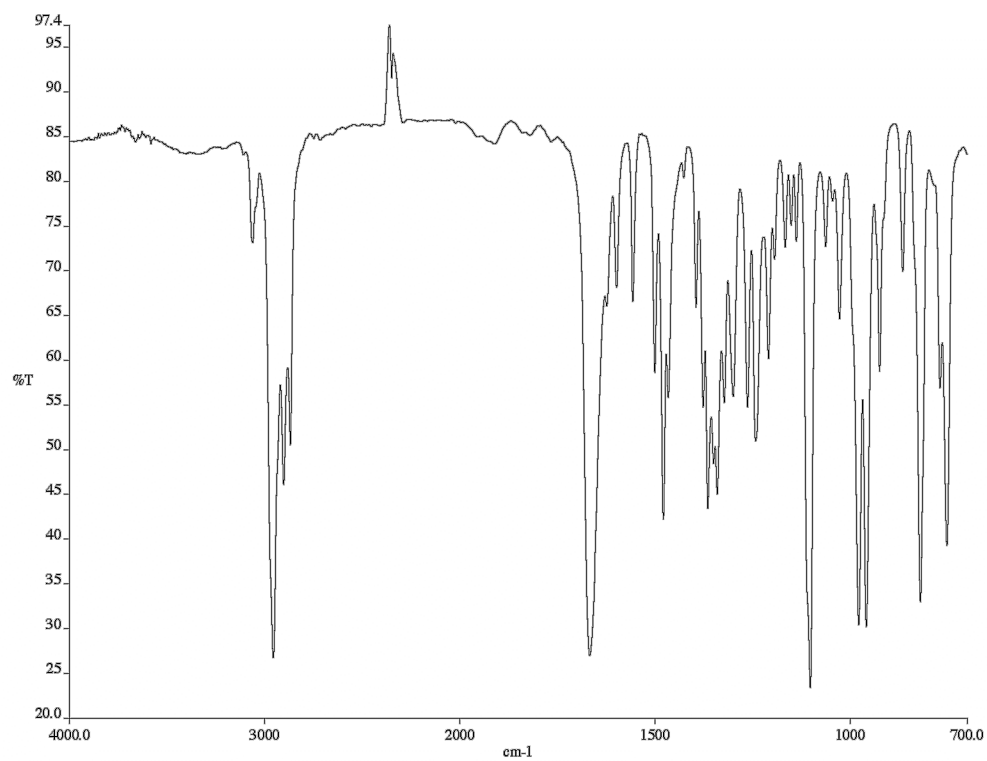


Figure A1.59. Infrared spectrum (thin film/NaCl) of compound **193**.

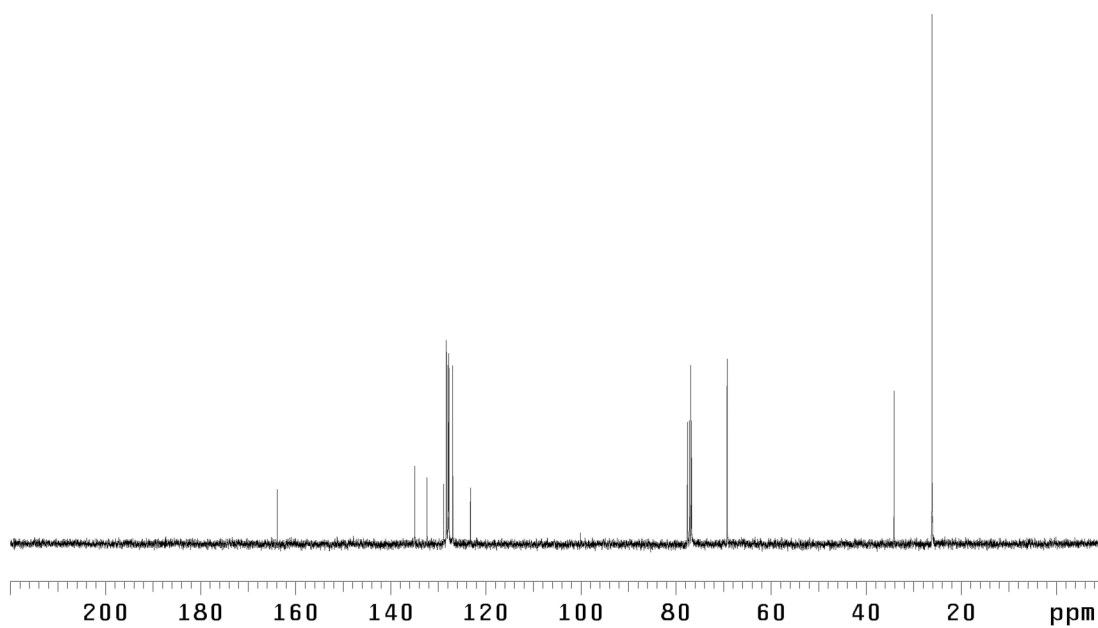


Figure A1.60. ¹³C NMR (75 MHz, CDCl₃) of compound **193**.

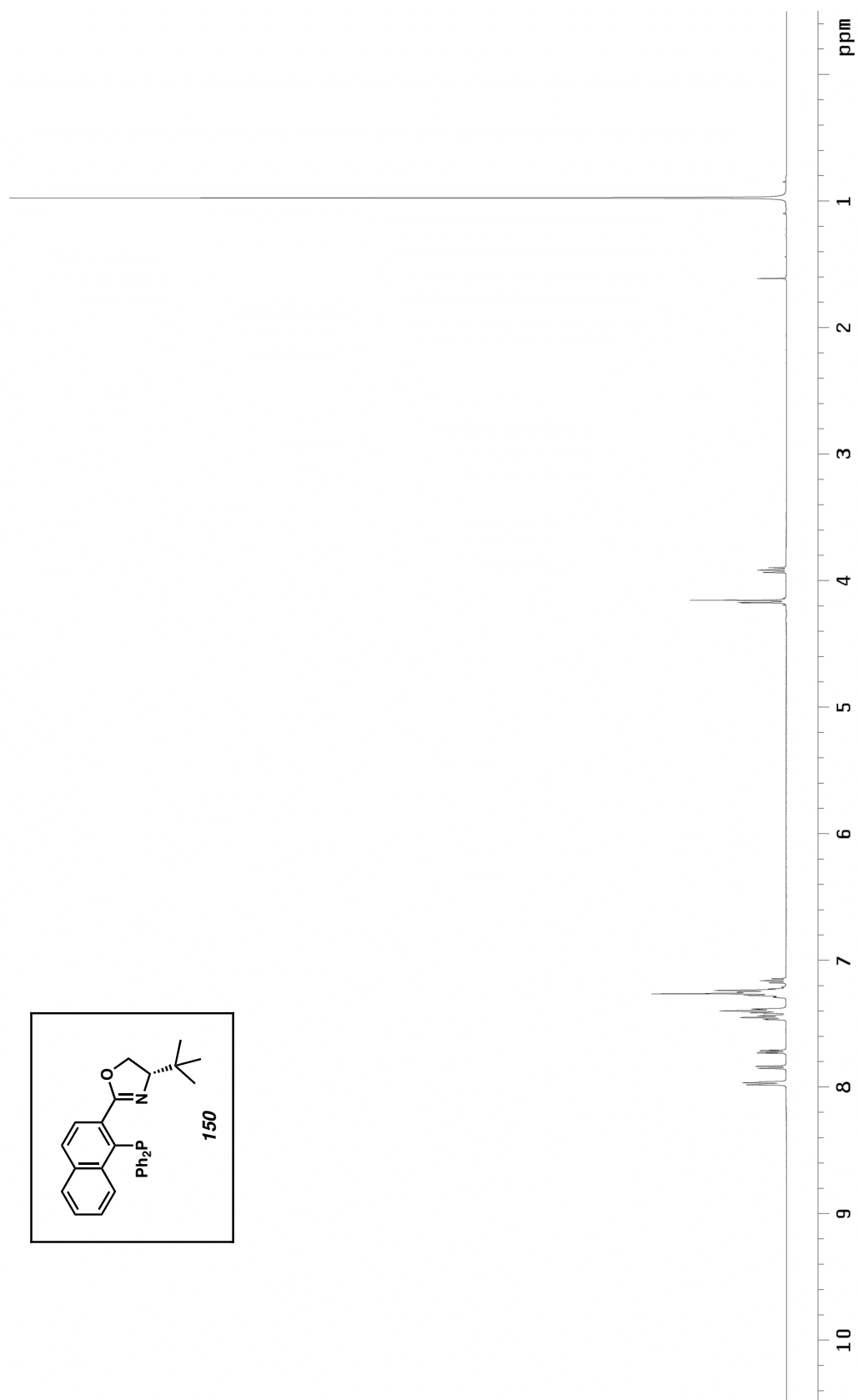


Figure A1.61. ^1H NMR (500 MHz, CDCl_3) of compound **150**.

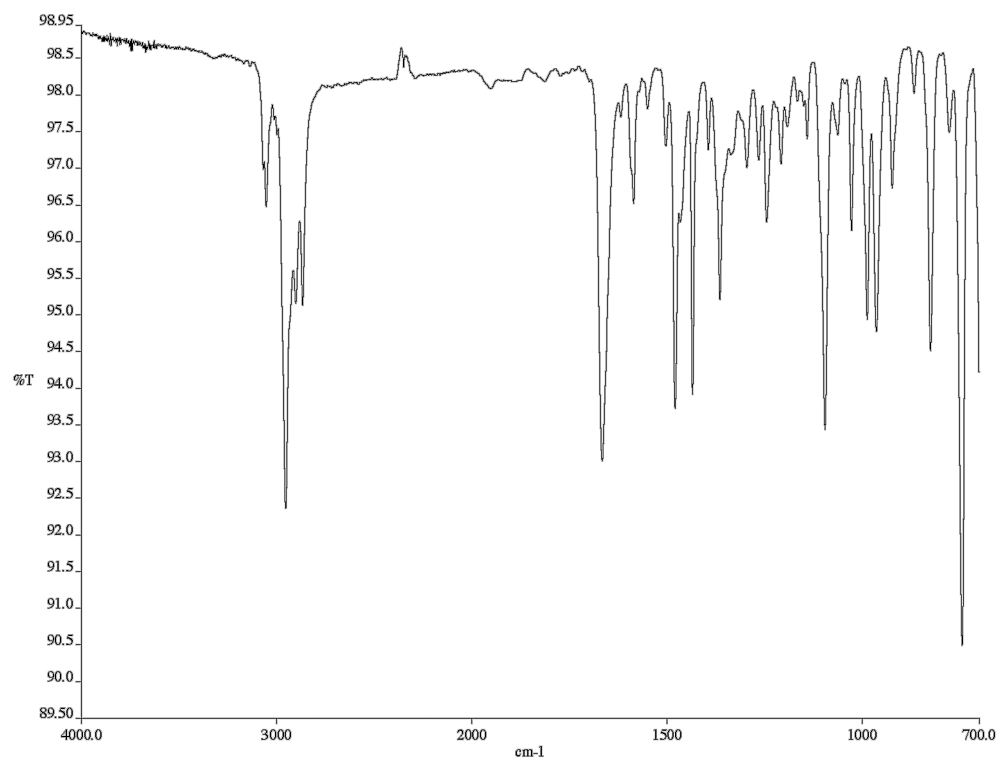


Figure A1.62. Infrared spectrum (thin film/NaCl) of compound **150**.

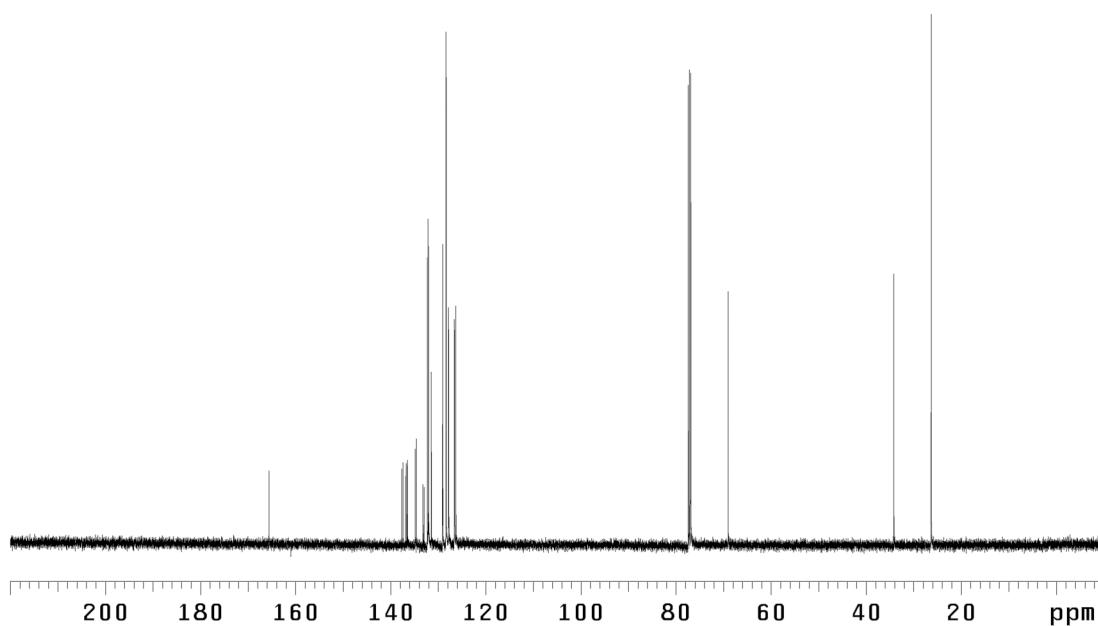


Figure A1.63. ¹³C NMR (125 MHz, CDCl₃) of compound **150**.

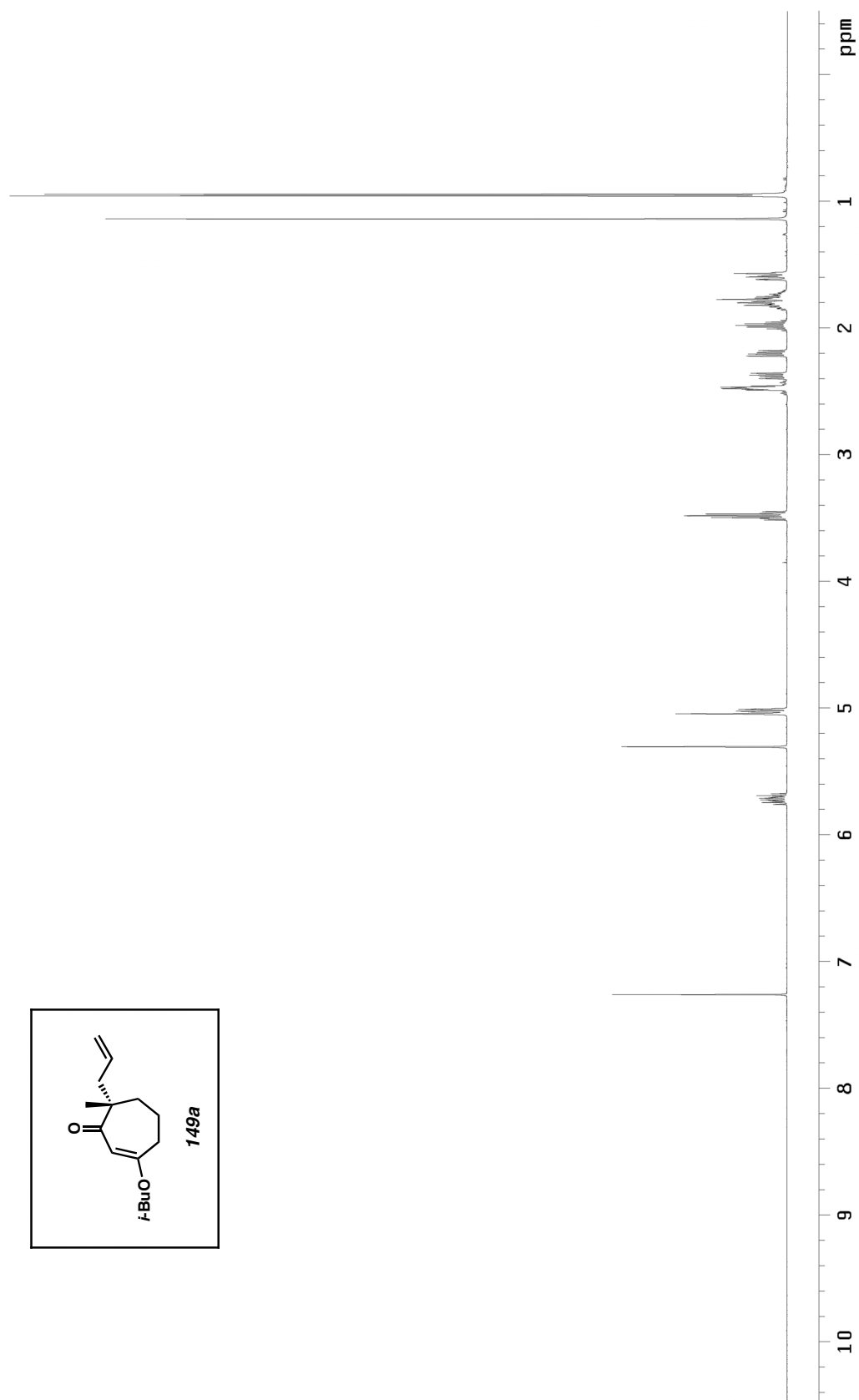


Figure A1.64. ^1H NMR (500 MHz, CDCl_3) of compound **149a**.

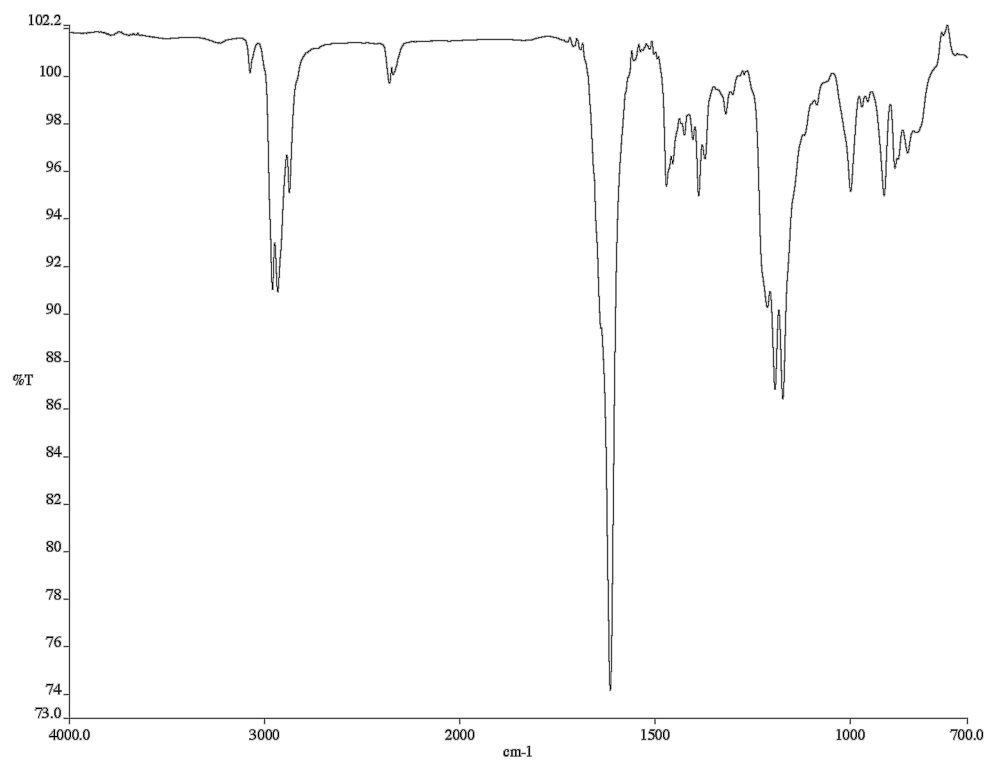


Figure A1.65. Infrared spectrum (thin film/NaCl) of compound **149a**.

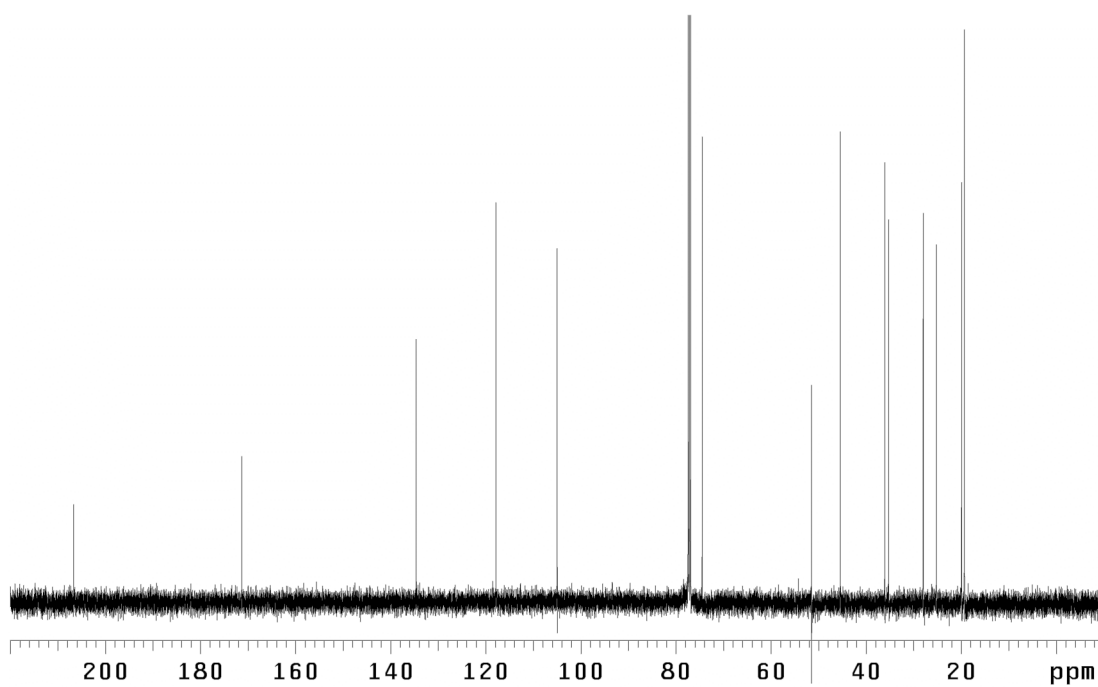


Figure A1.66. ¹³C NMR (125 MHz, CDCl₃) of compound **149a**.

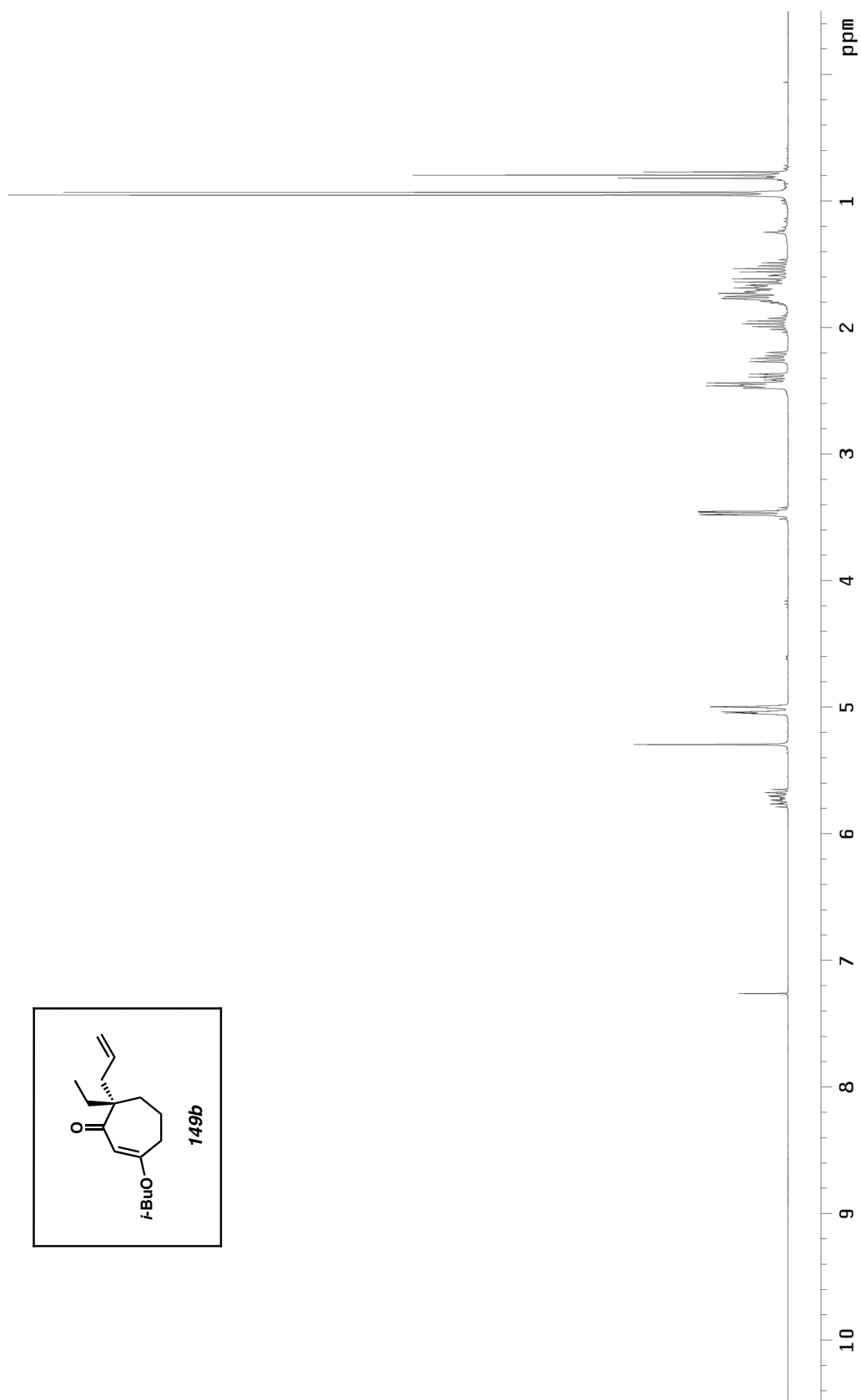


Figure A1.67. ^1H NMR (300 MHz, CDCl_3) of compound **149b**.

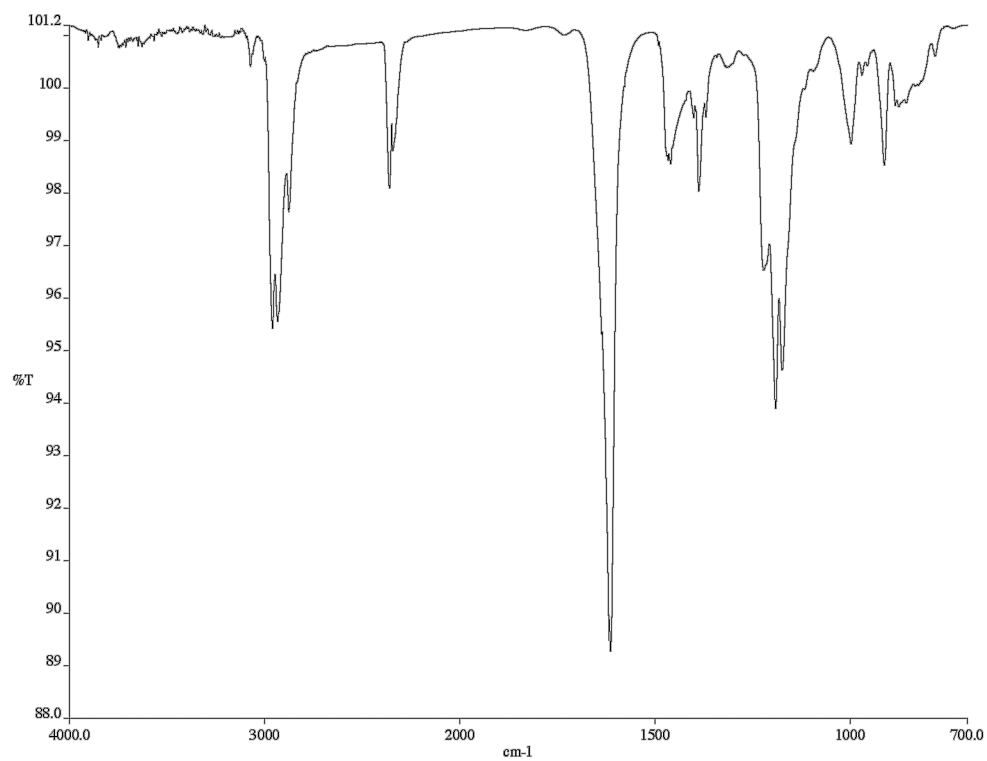


Figure A1.68. Infrared spectrum (thin film/NaCl) of compound **149b**.

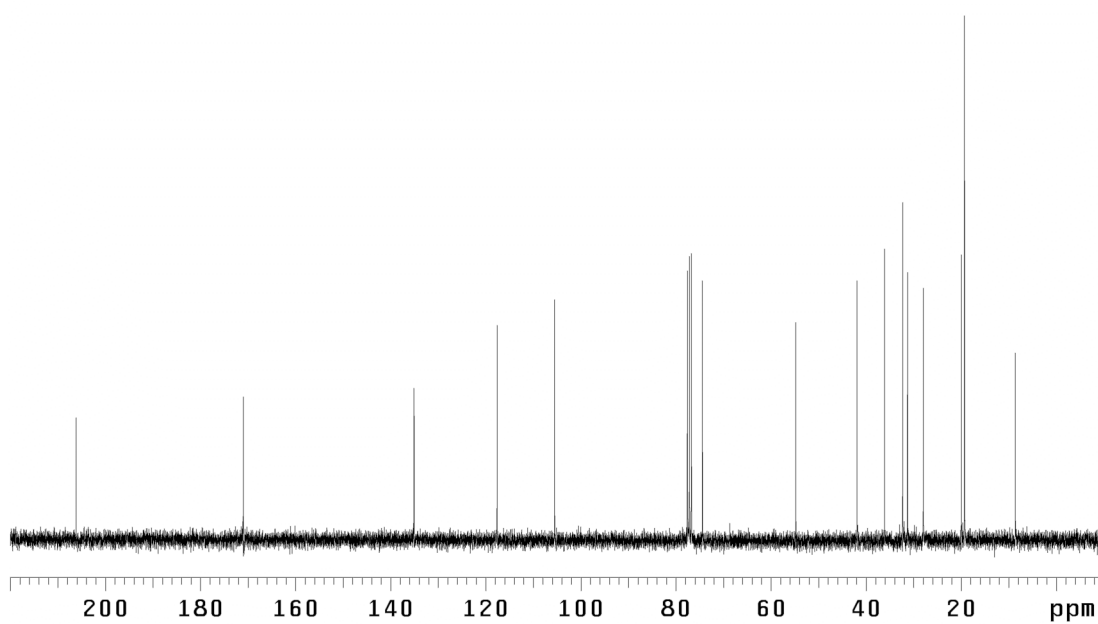


Figure A1.69. ¹³C NMR (75 MHz, CDCl₃) of compound **149b**.

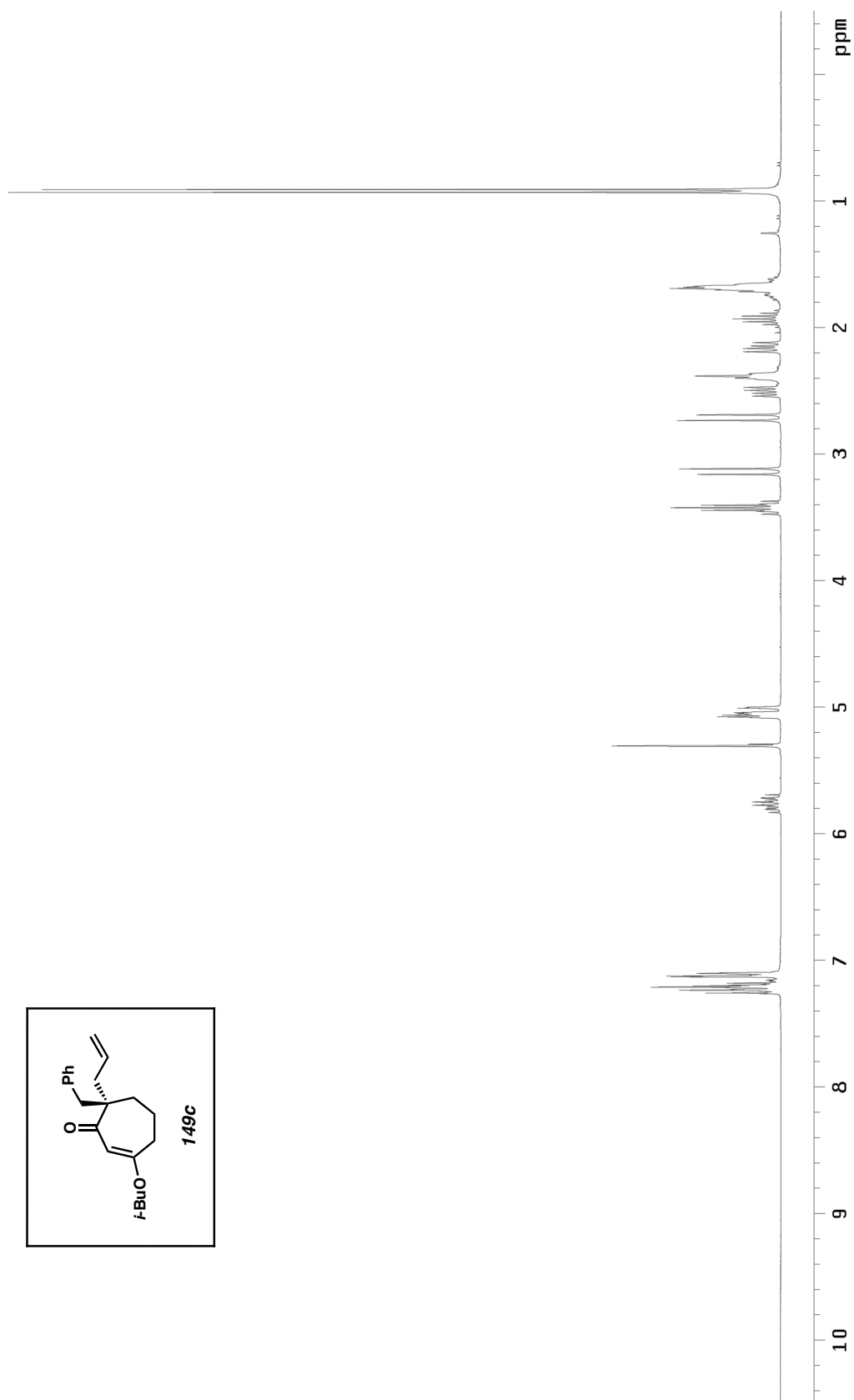


Figure A1.70. ^1H NMR (300 MHz, CDCl_3) of compound **149c**.

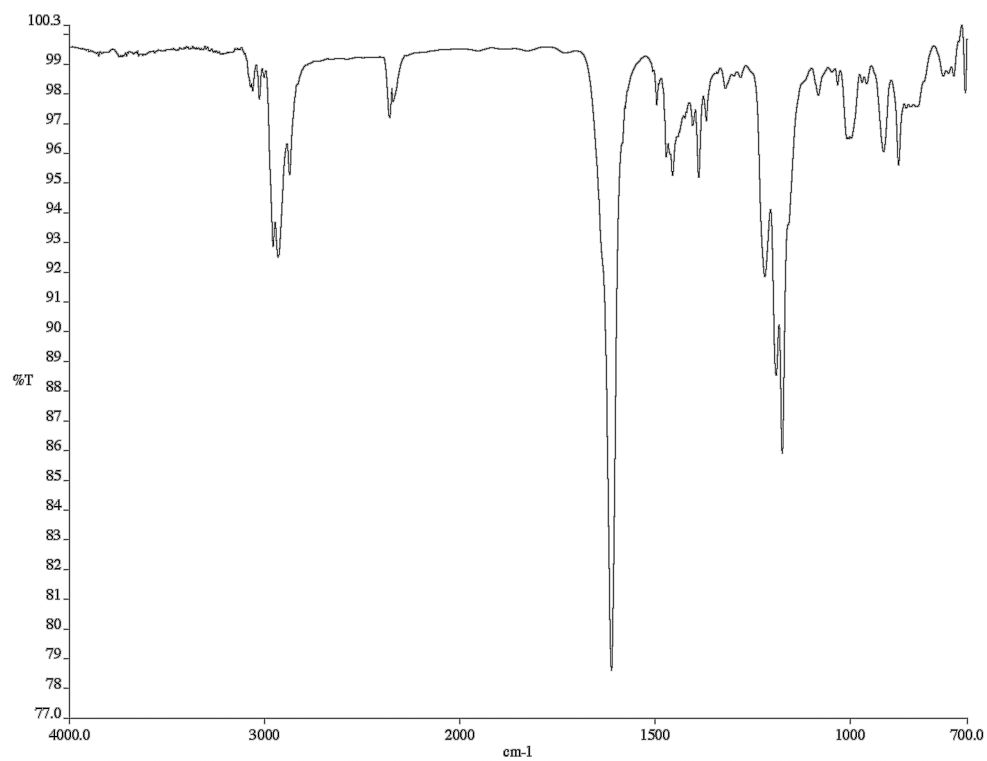


Figure A1.71. Infrared spectrum (thin film/NaCl) of compound **149c**.

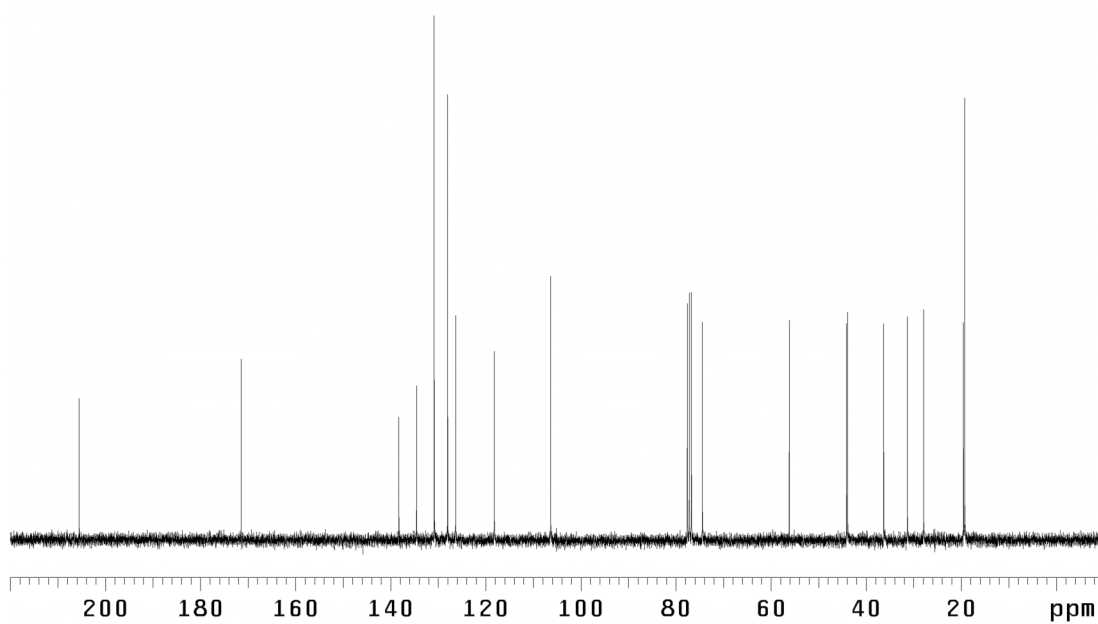
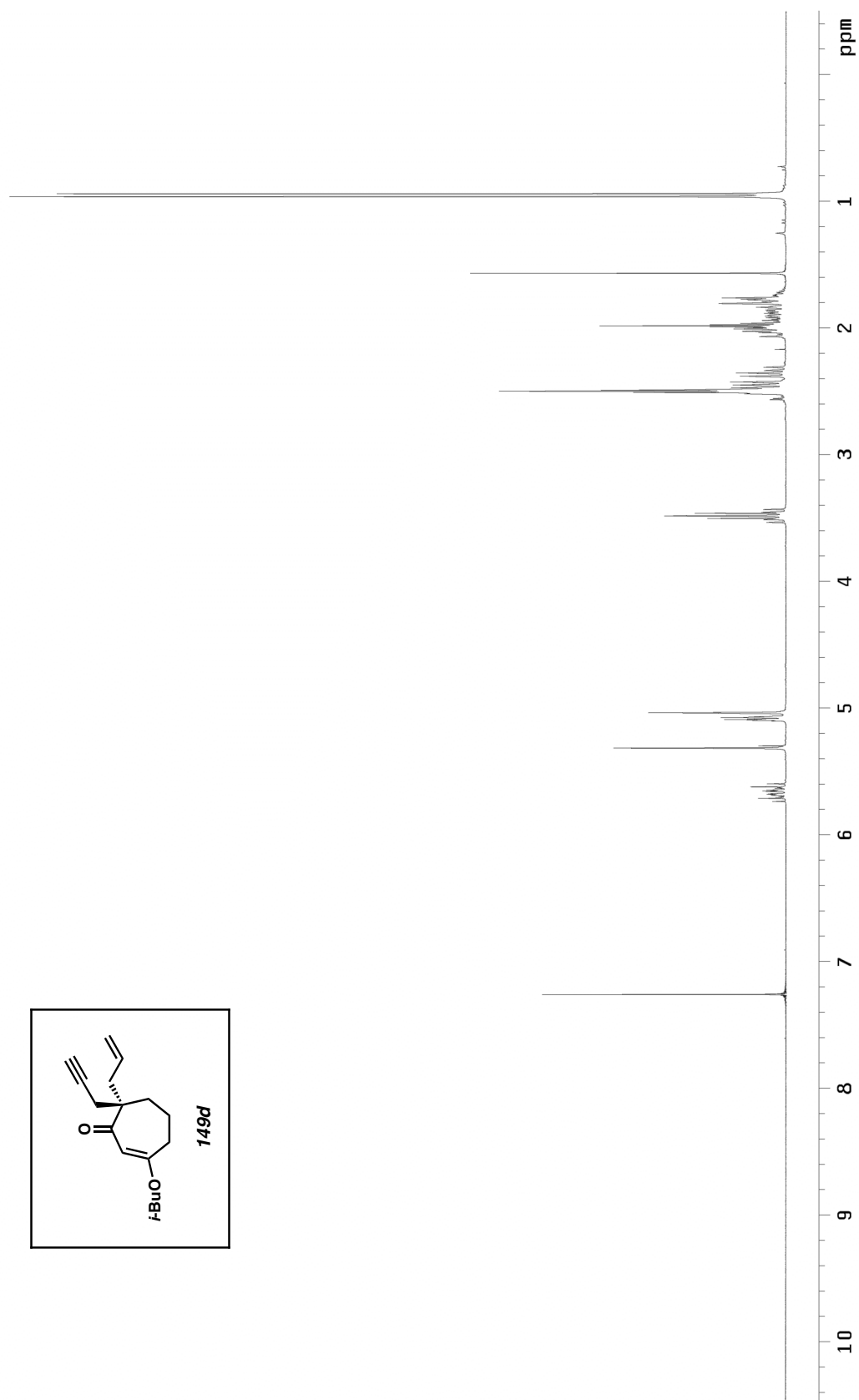


Figure A1.72. ¹³C NMR (75 MHz, CDCl₃) of compound **149c**.



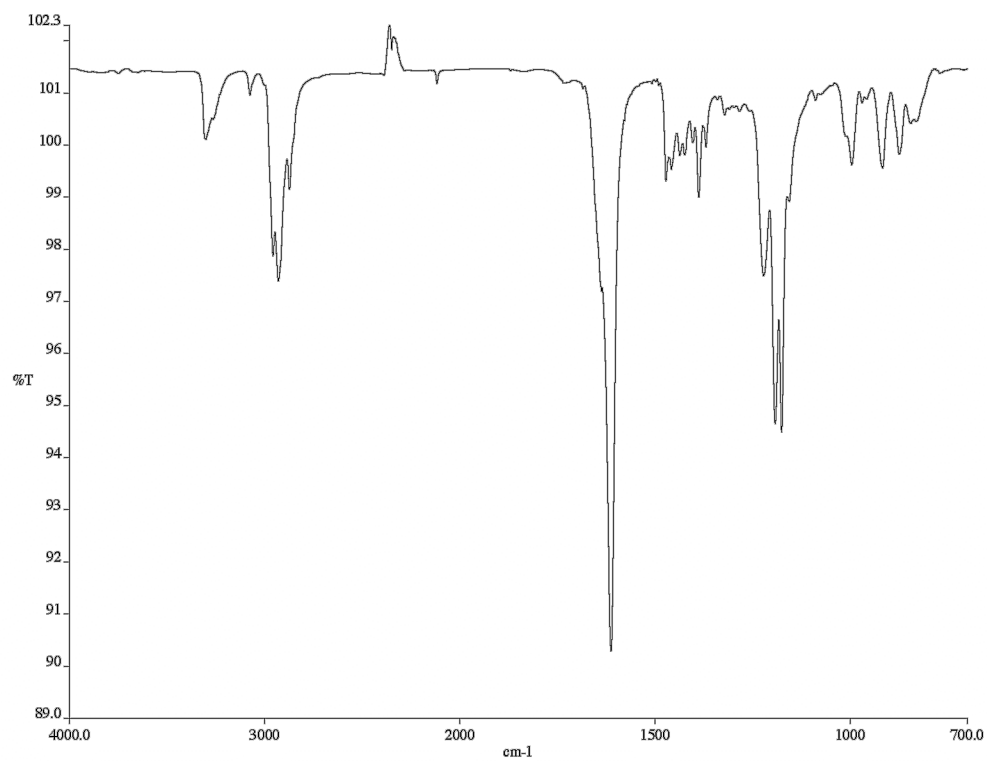


Figure A1.74. Infrared spectrum (thin film/NaCl) of compound **149d**.

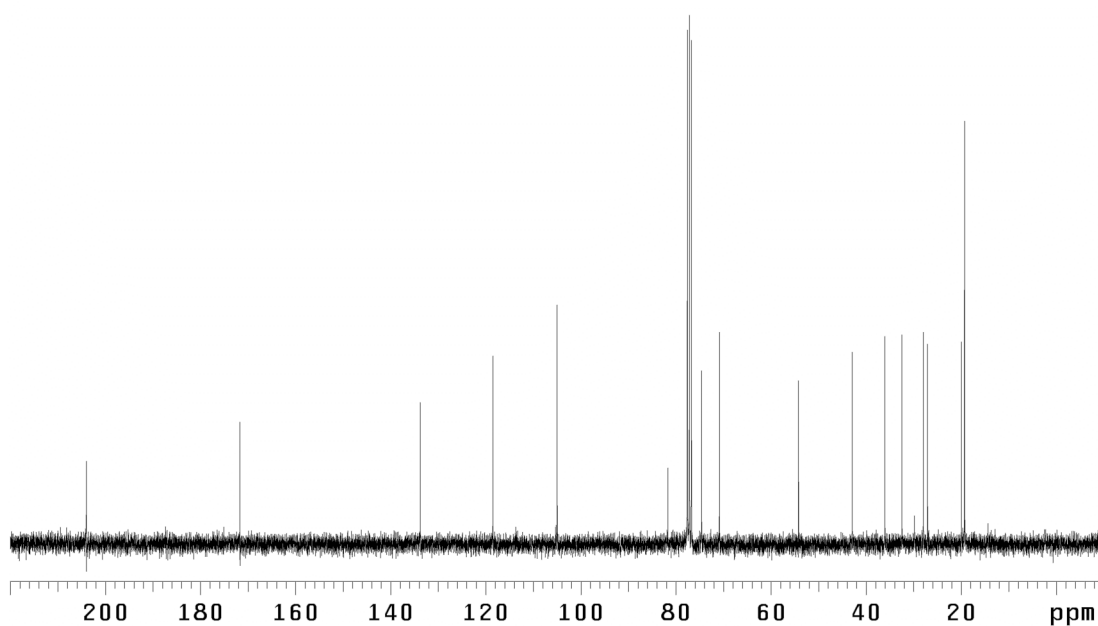


Figure A1.75. ¹³C NMR (75 MHz, CDCl₃) of compound **149d**.

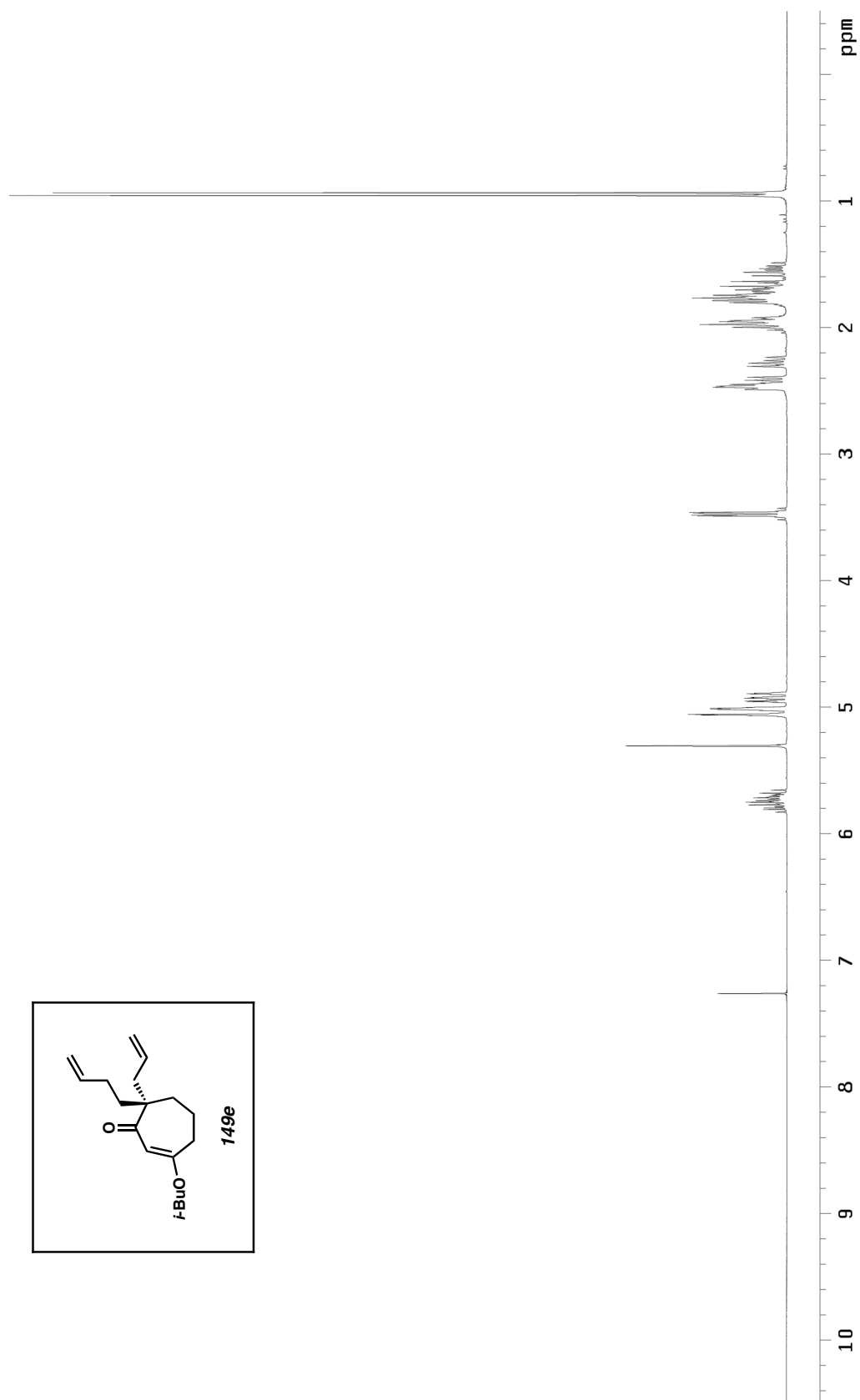


Figure A1.76. ¹H NMR (300 MHz, CDCl₃) of compound **149e**.

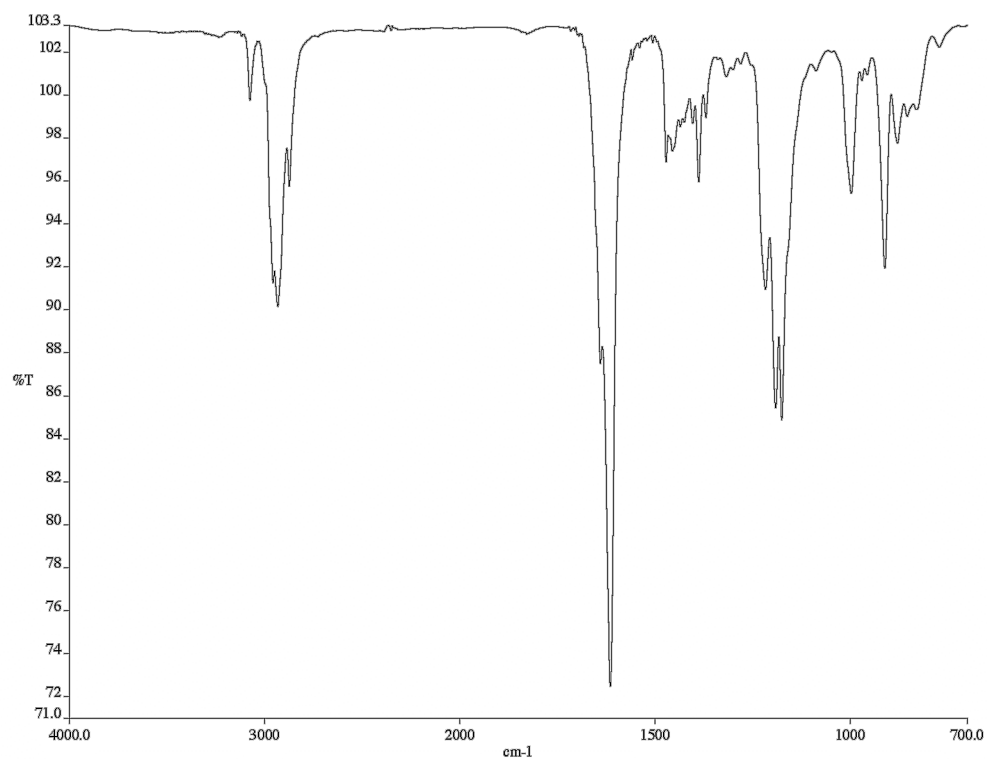


Figure A1.77. Infrared spectrum (thin film/NaCl) of compound **149e**.

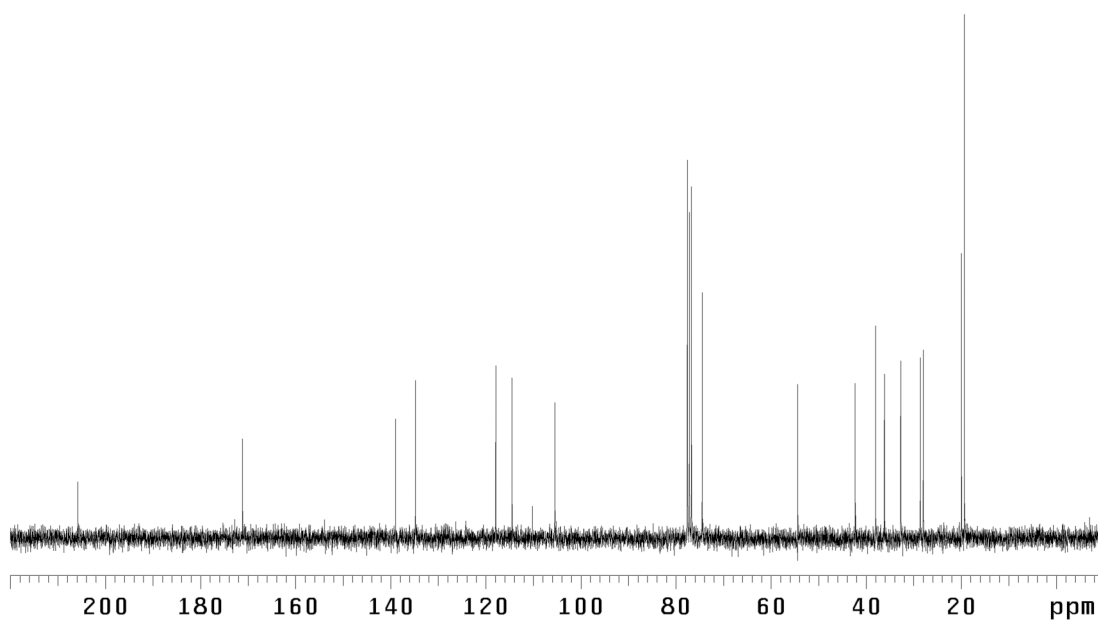


Figure A1.78. ¹³C NMR (75 MHz, CDCl₃) of compound **149e**.

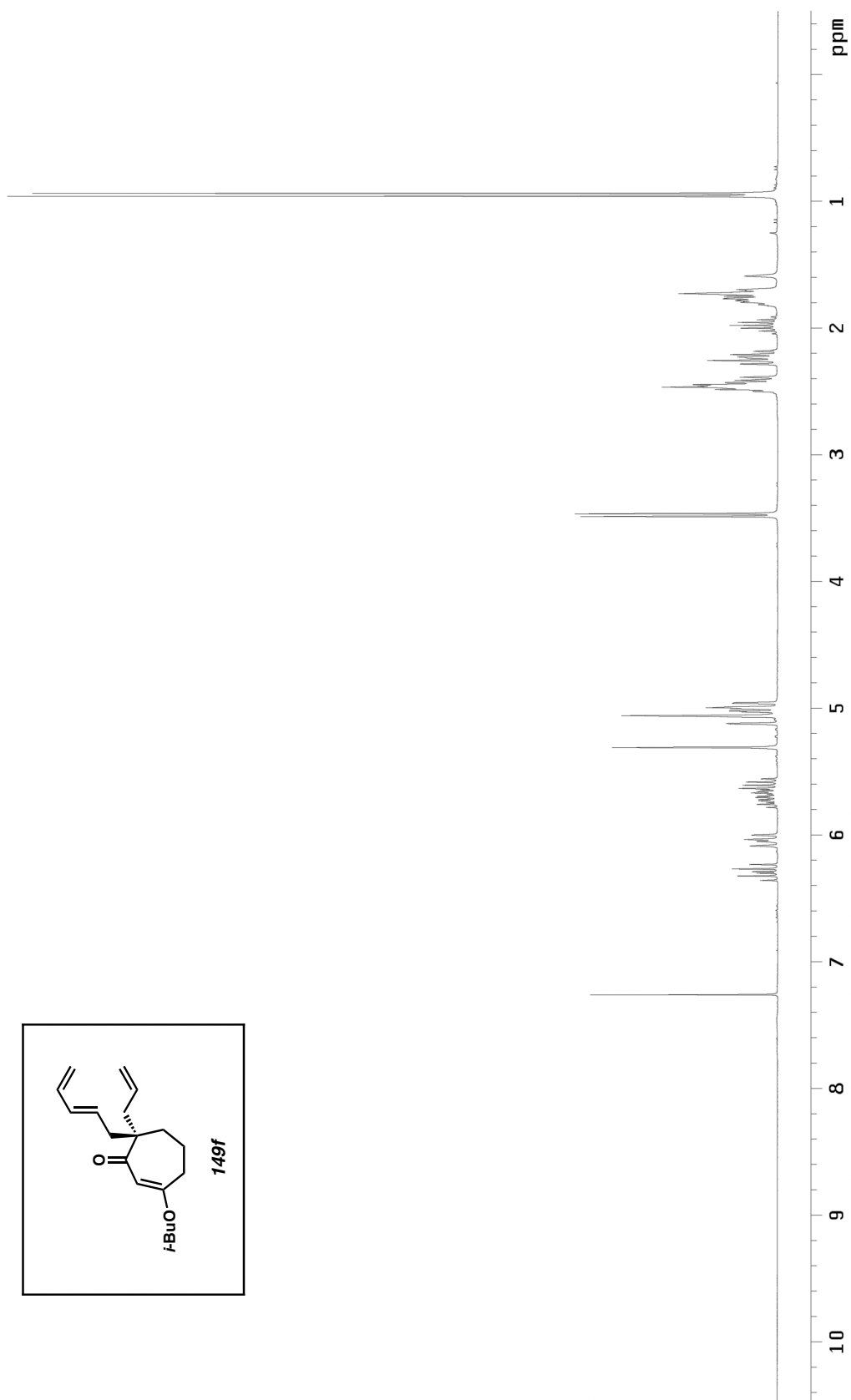


Figure A1.79. ^1H NMR (300 MHz, CDCl_3) of compound **149f**.

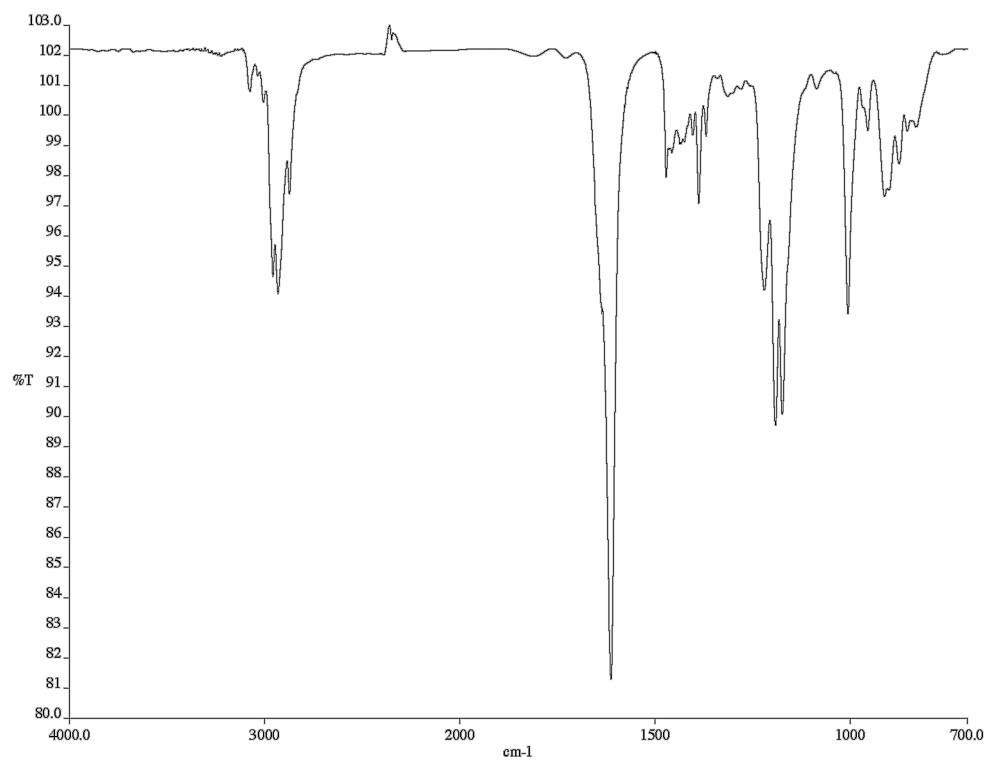


Figure A1.81. Infrared spectrum (thin film/NaCl) of compound **149f**.

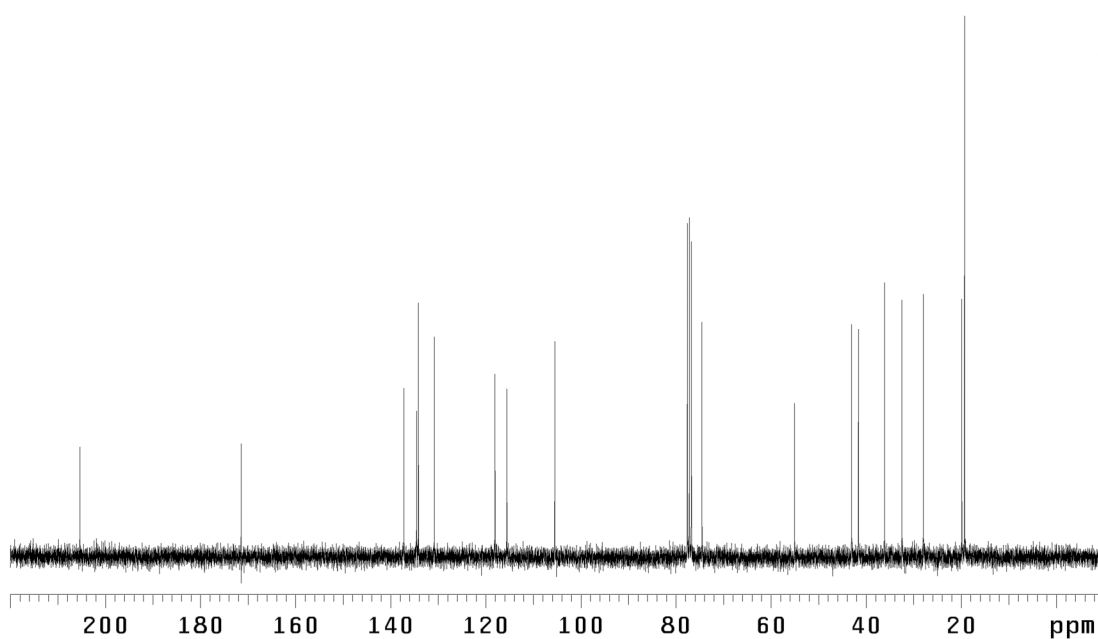


Figure A1.80. ¹³C NMR (75 MHz, CDCl₃) of compound **149f**.

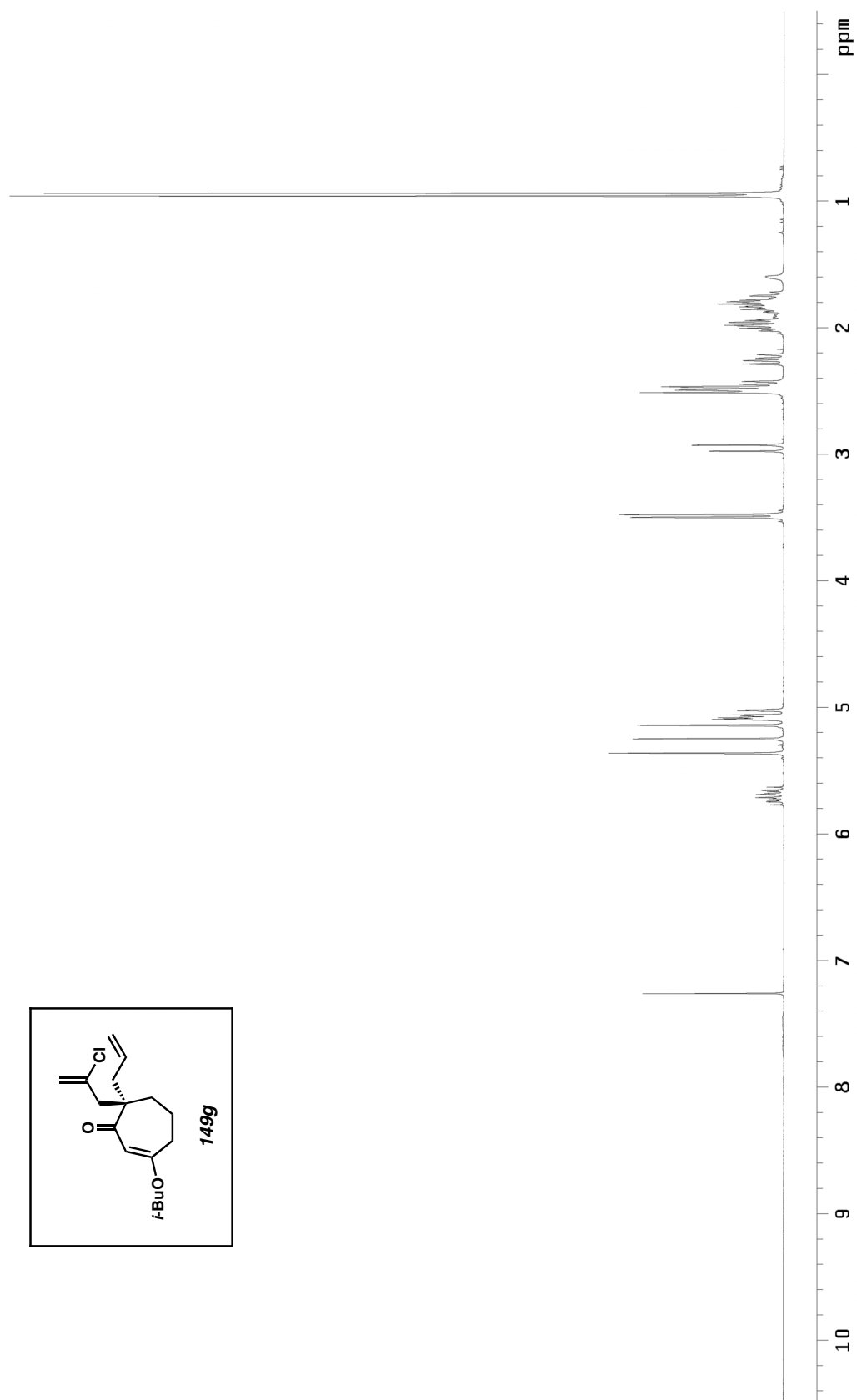


Figure A1.82. ^1H NMR (300 MHz, CDCl_3) of compound **149g**.

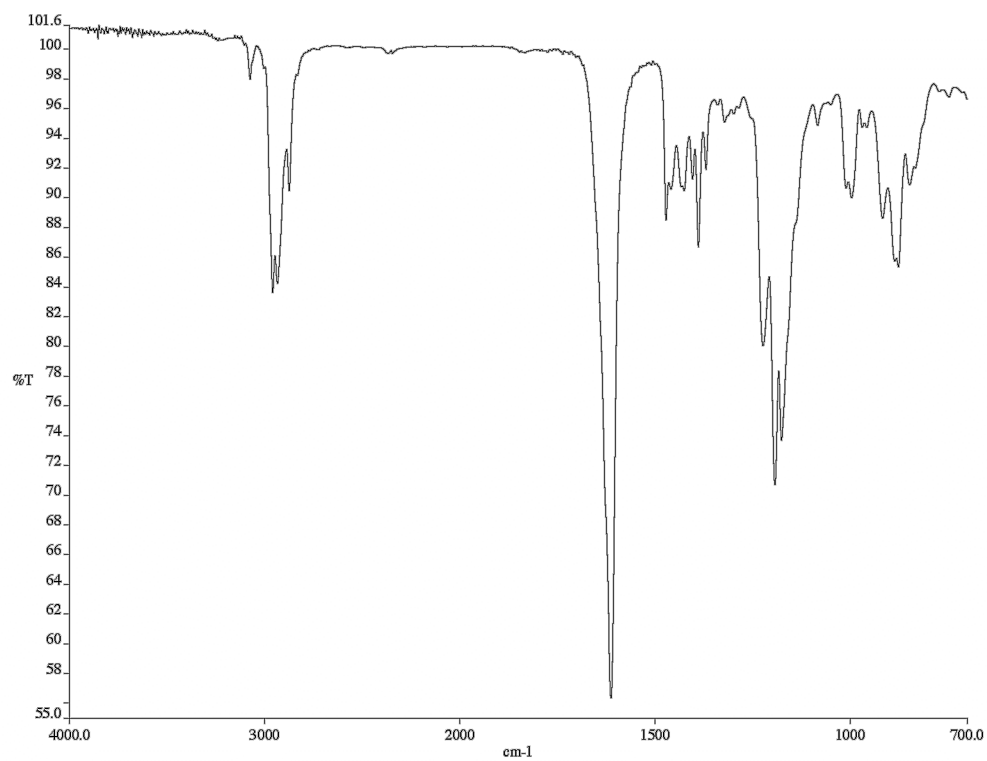


Figure A1.83. Infrared spectrum (thin film/NaCl) of compound **149g**.

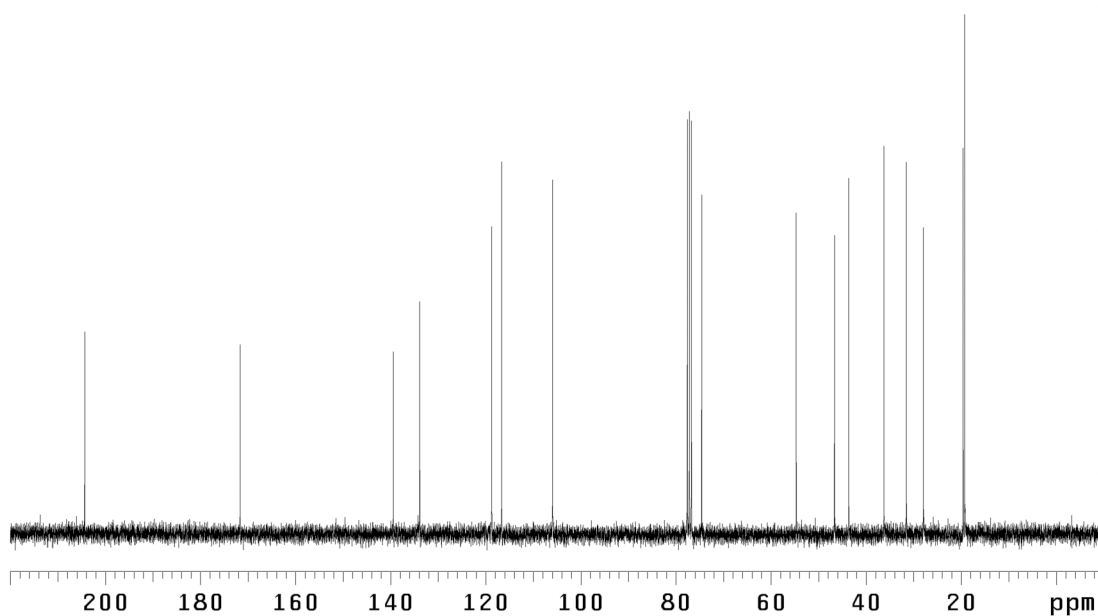


Figure A1.84. ¹³C NMR (75 MHz, CDCl₃) of compound **149g**.

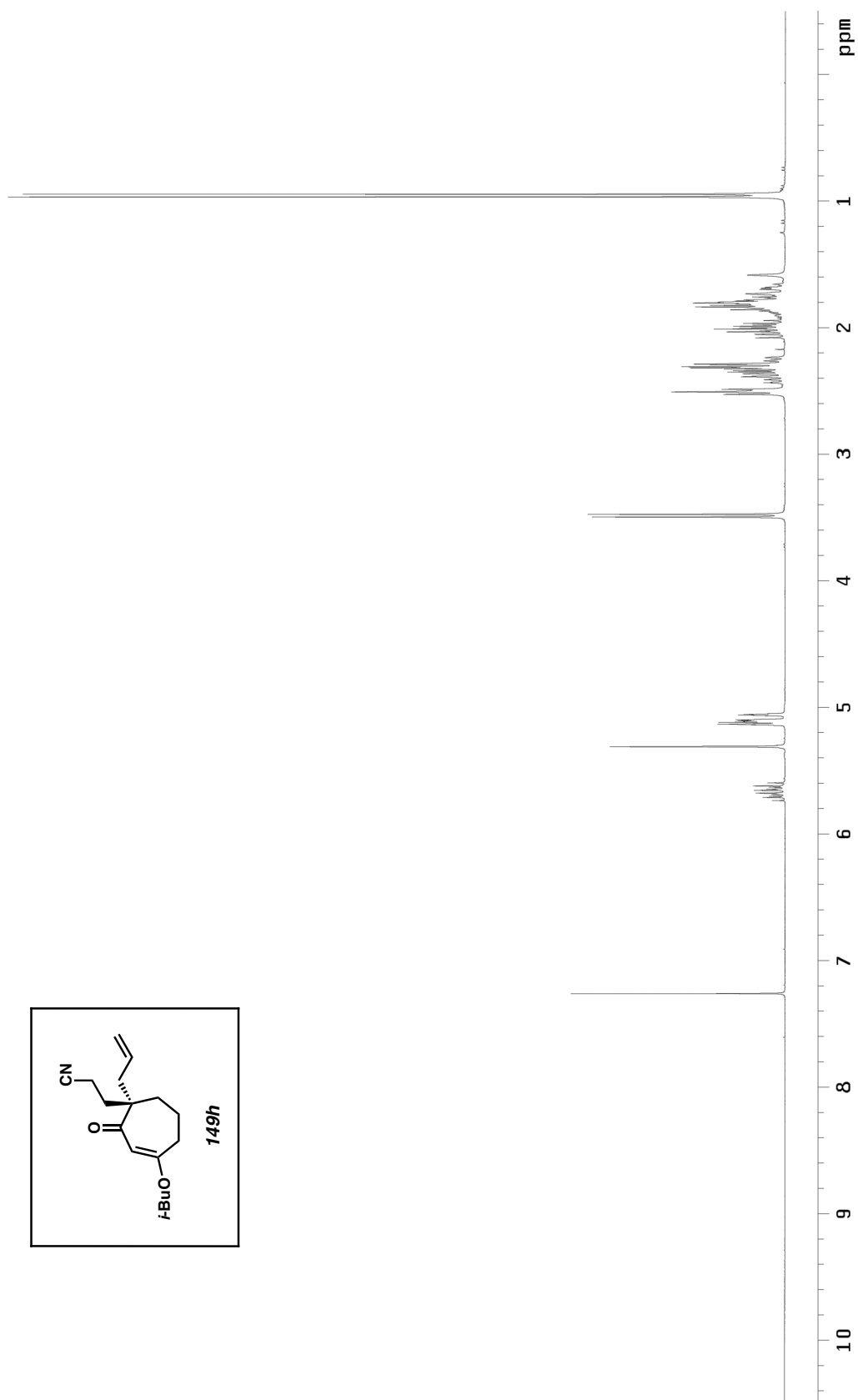


Figure A1.85. ^1H NMR (300 MHz, CDCl_3) of compound **149h**.

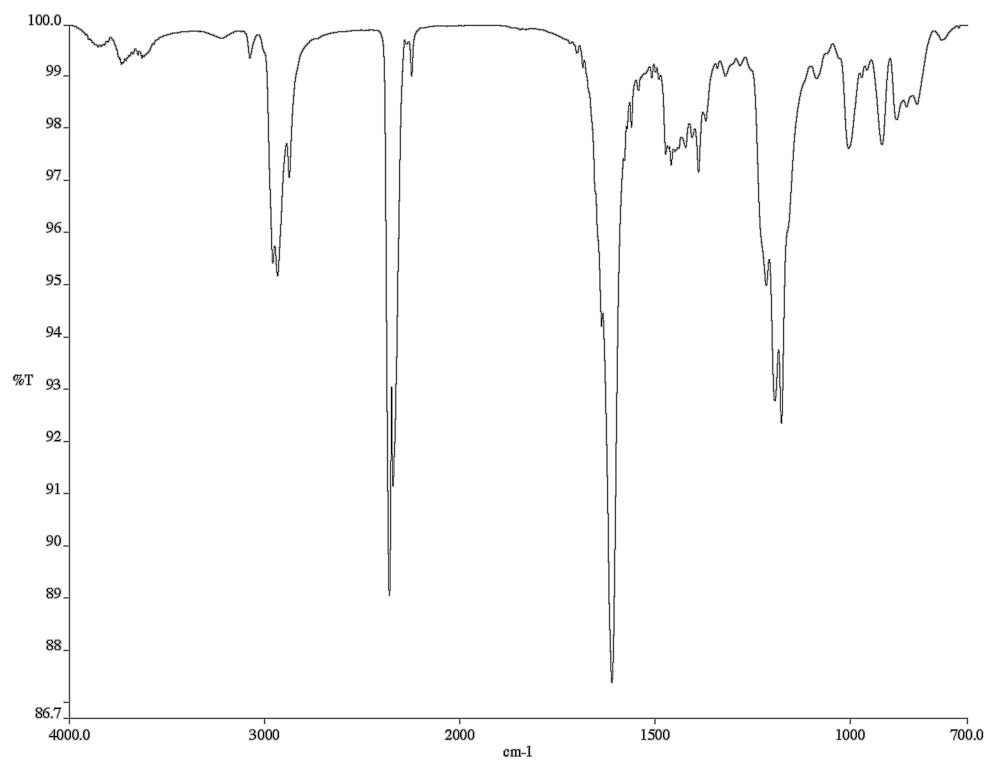


Figure A1.87. Infrared spectrum (thin film/NaCl) of compound **149h**.

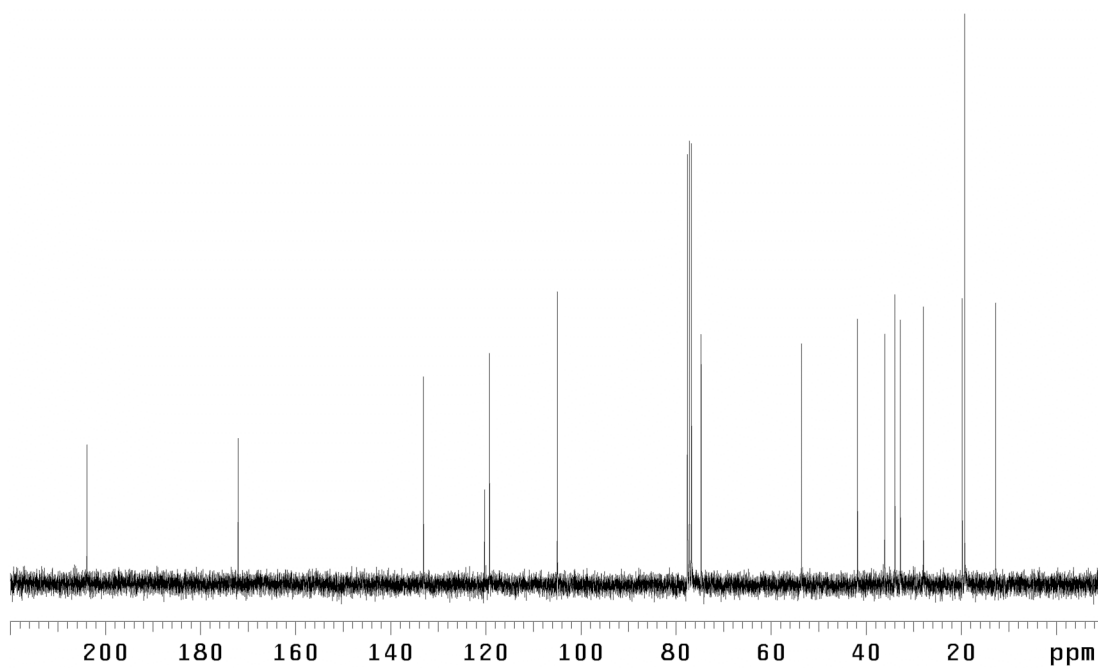
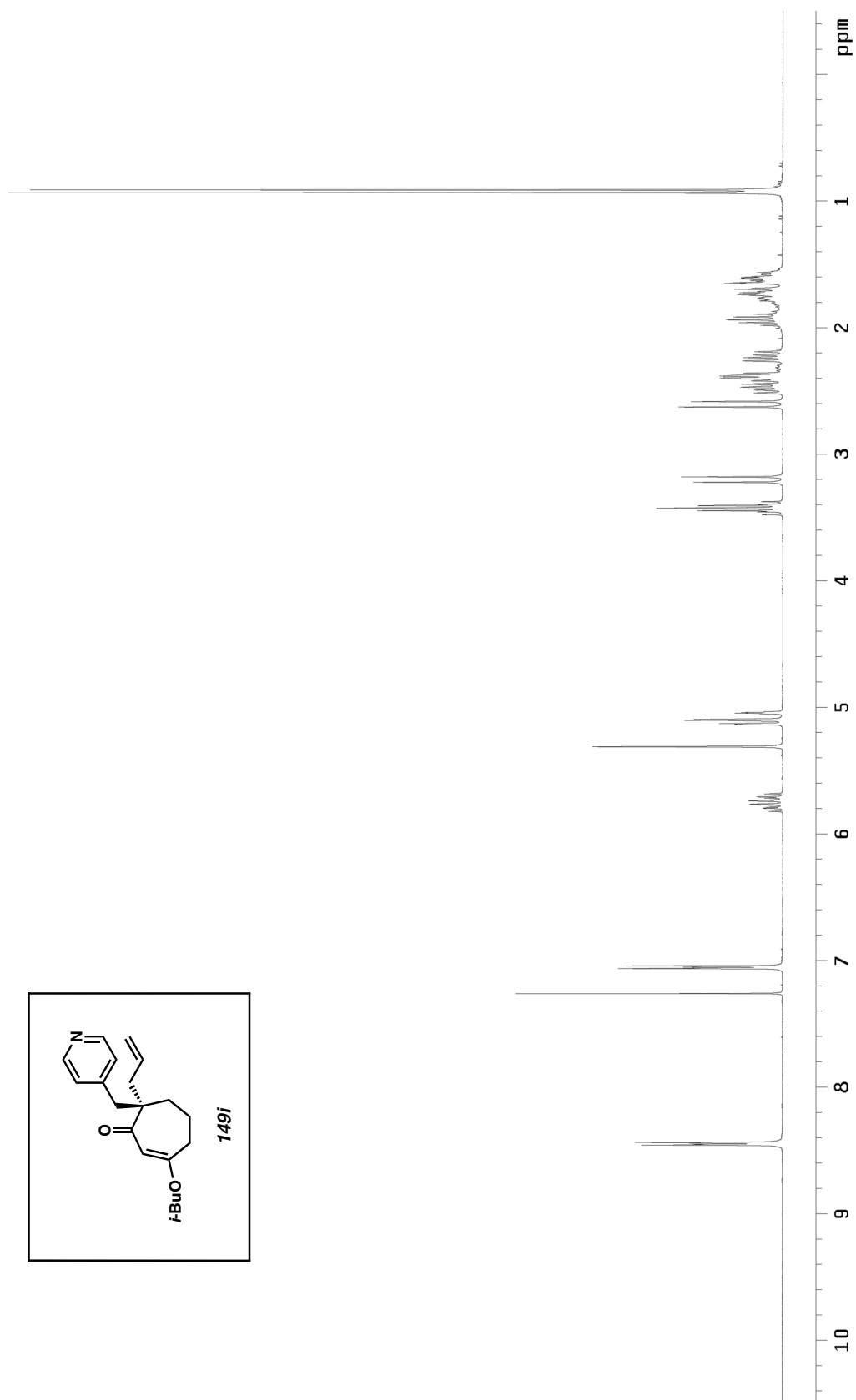


Figure A1.86. ^{13}C NMR (75 MHz, CDCl_3) of compound **149h**.

Figure A1.88. ^1H NMR (300 MHz, CDCl_3) of compound **149i**.

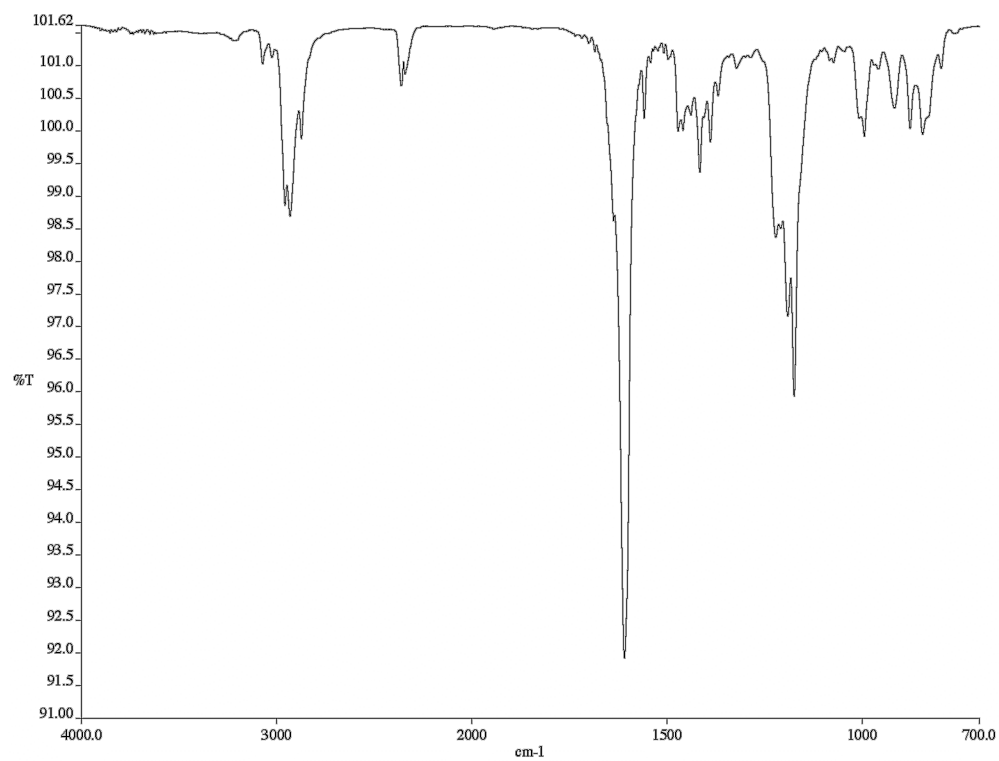


Figure A1.89. Infrared spectrum (thin film/NaCl) of compound **149i**.

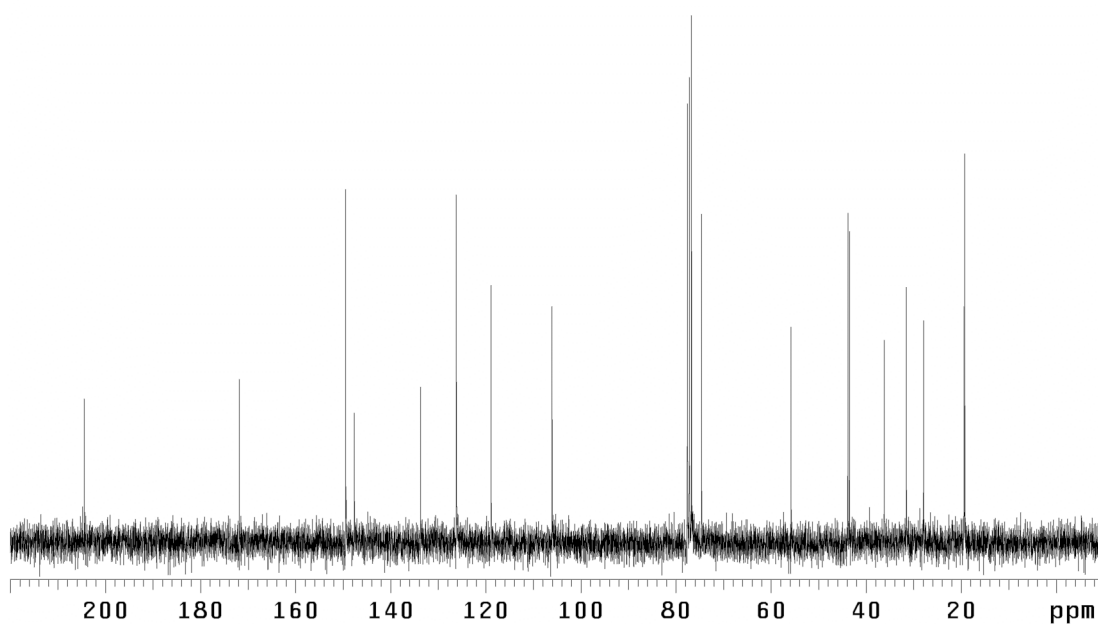
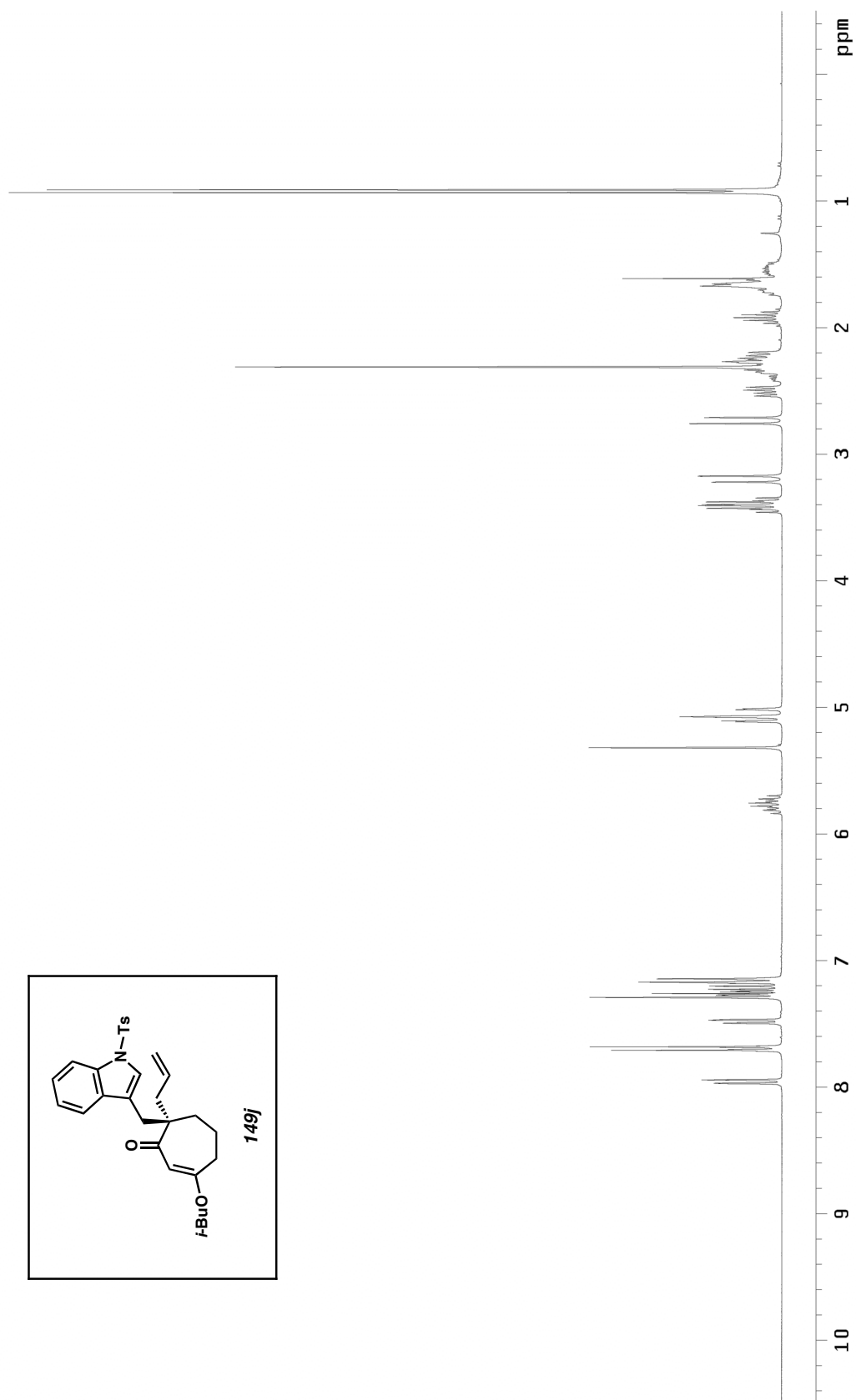


Figure A1.90. ¹³C NMR (75 MHz, CDCl₃) of compound **149i**.

Figure A1.91. ^1H NMR (300 MHz, CDCl_3) of compound **149j**.

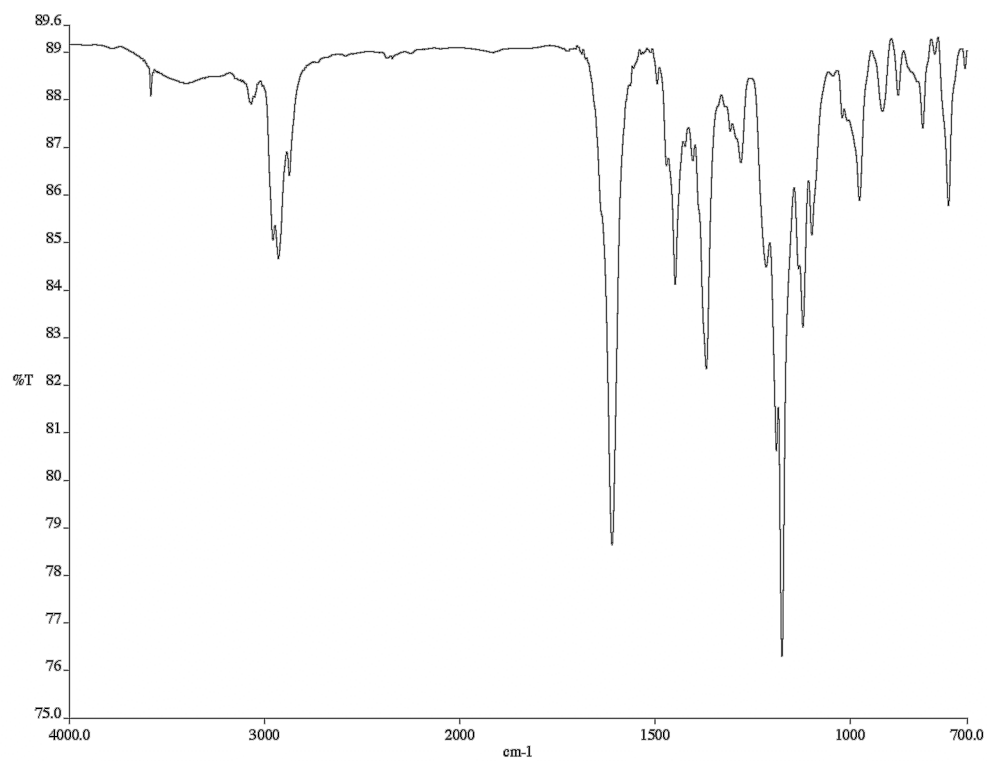


Figure A1.93. Infrared spectrum (thin film/NaCl) of compound **149j**.

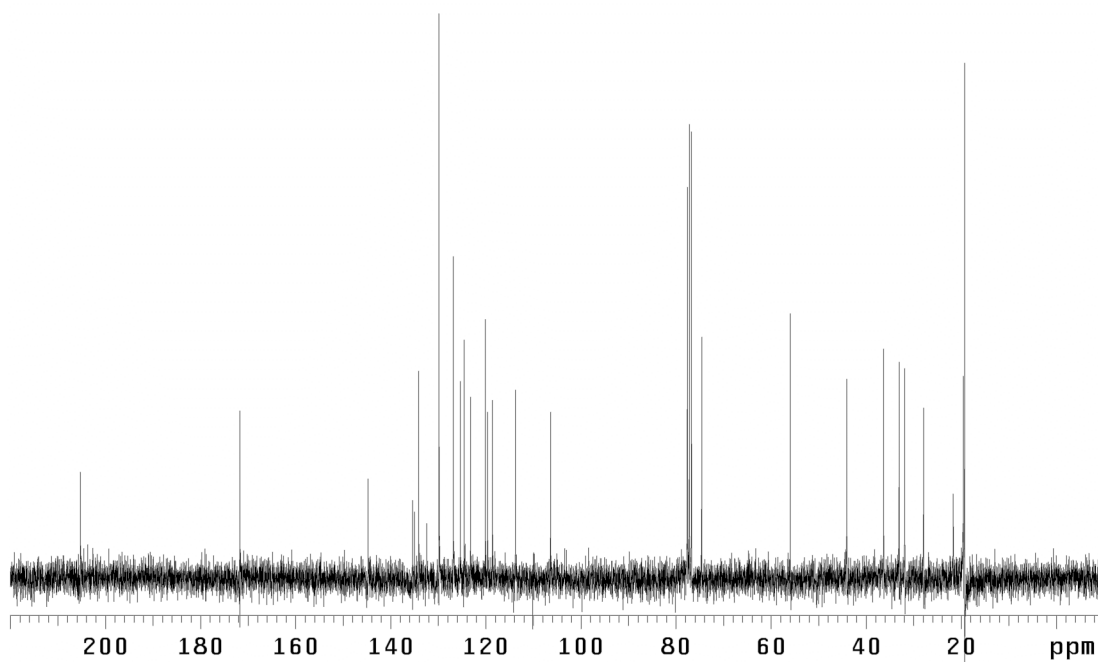


Figure A1.92. ^{13}C NMR (75 MHz, CDCl_3) of compound **149j**.

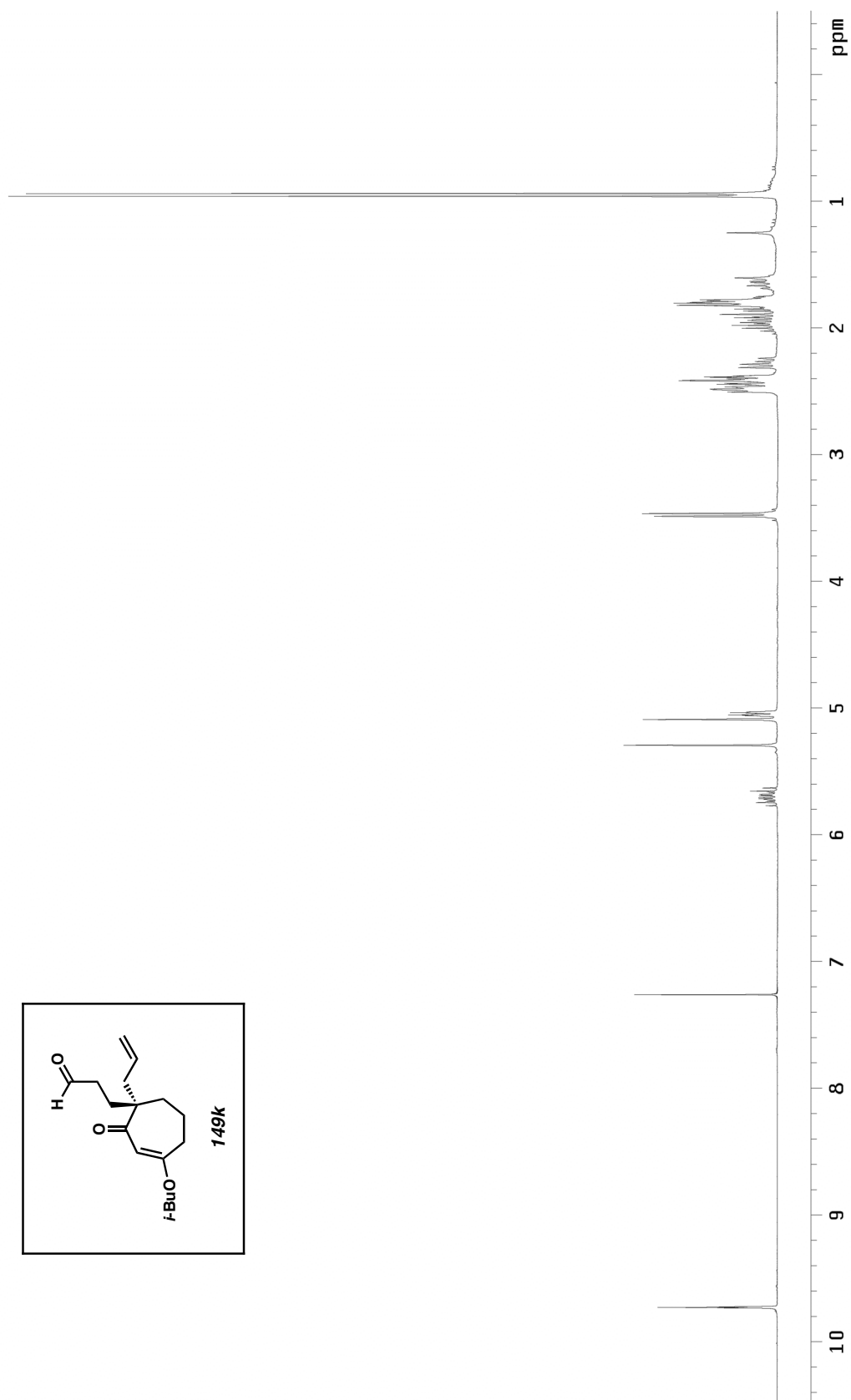


Figure A1.94. ^1H NMR (300 MHz, CDCl_3) of compound **149k**.

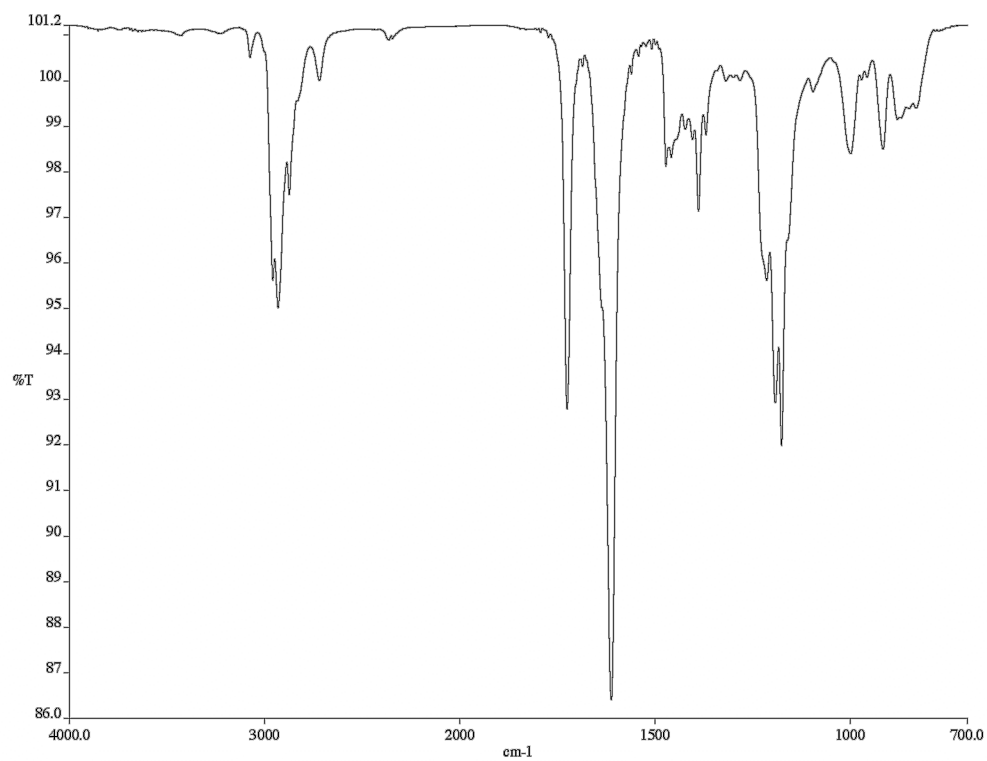


Figure A1.95. Infrared spectrum (thin film/NaCl) of compound **149k**.

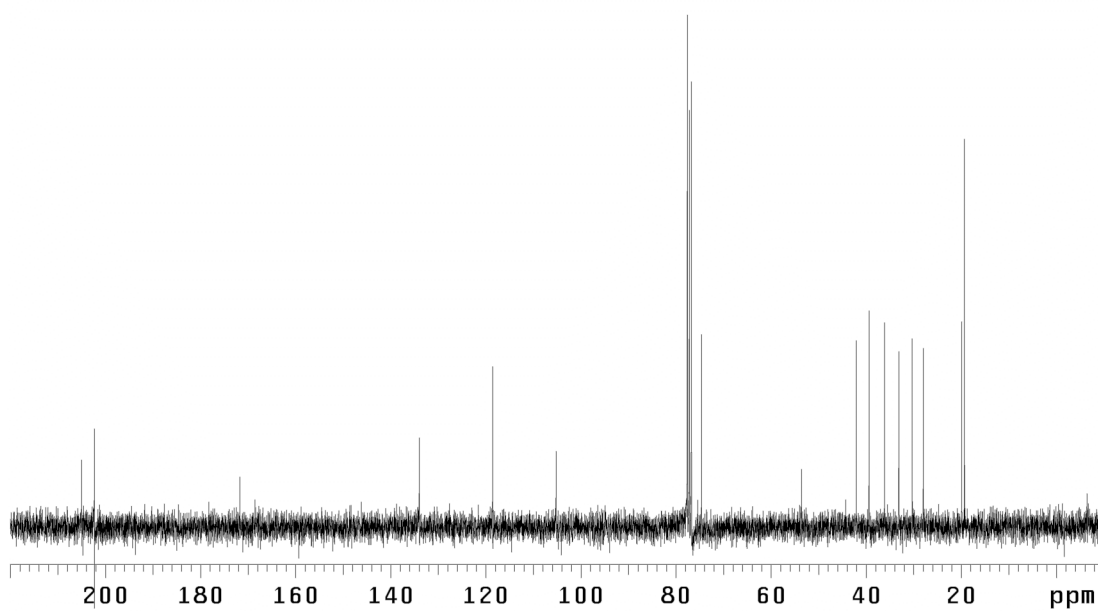
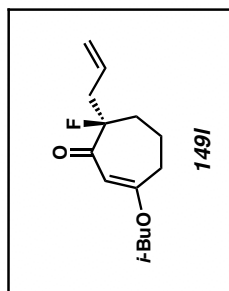
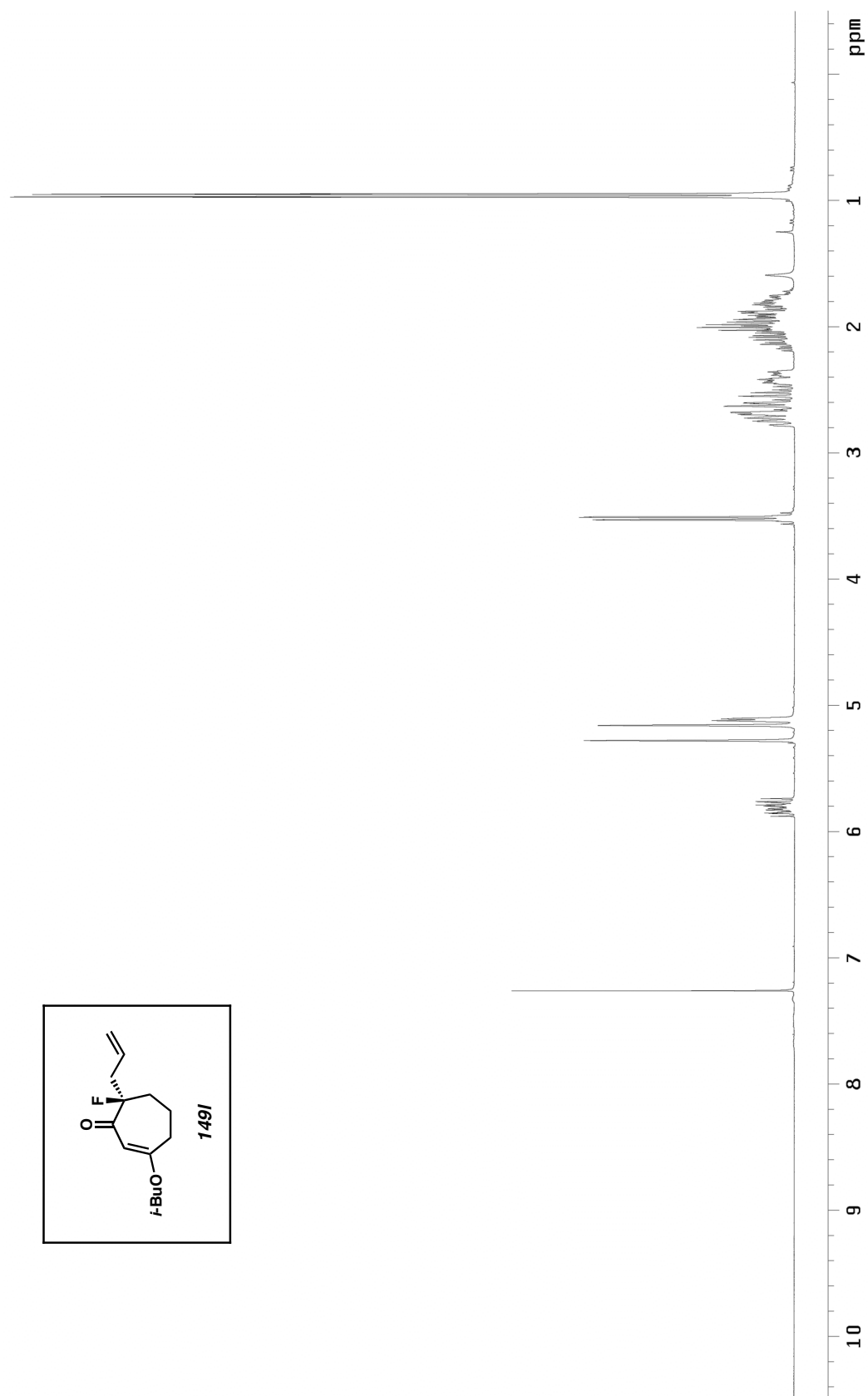


Figure A1.96. ¹³C NMR (75 MHz, CDCl₃) of compound **149k**.

Figure A1.97. ¹H NMR (300 MHz, CDCl₃) of compound **149I**.

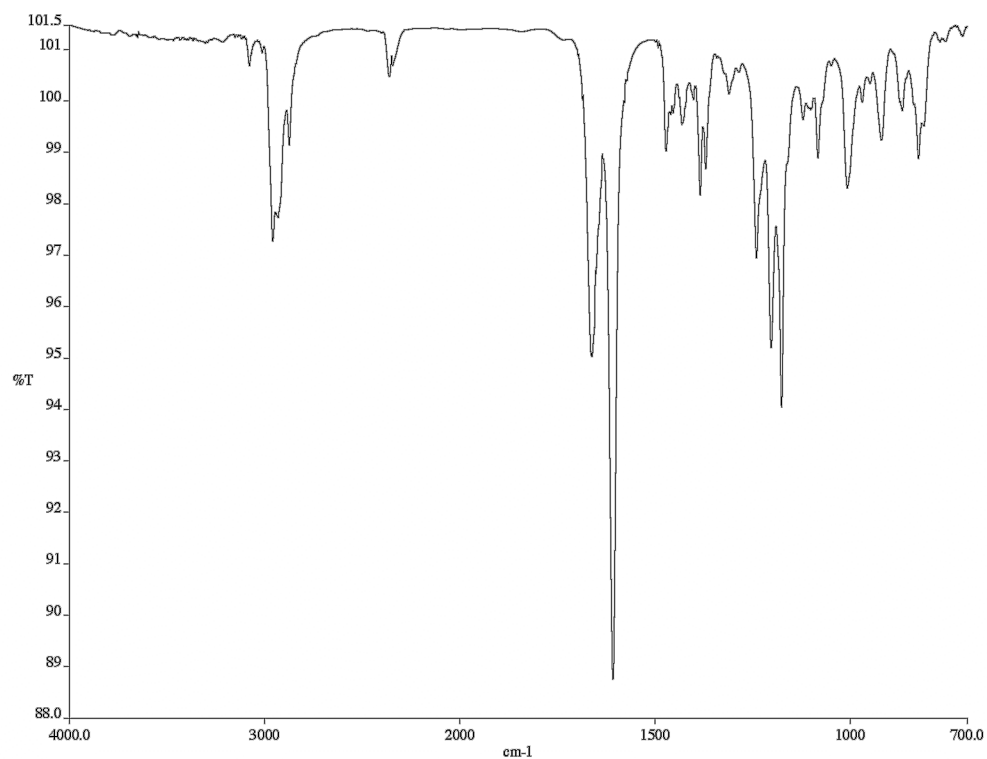


Figure A1.99. Infrared spectrum (thin film/NaCl) of compound **149I**.

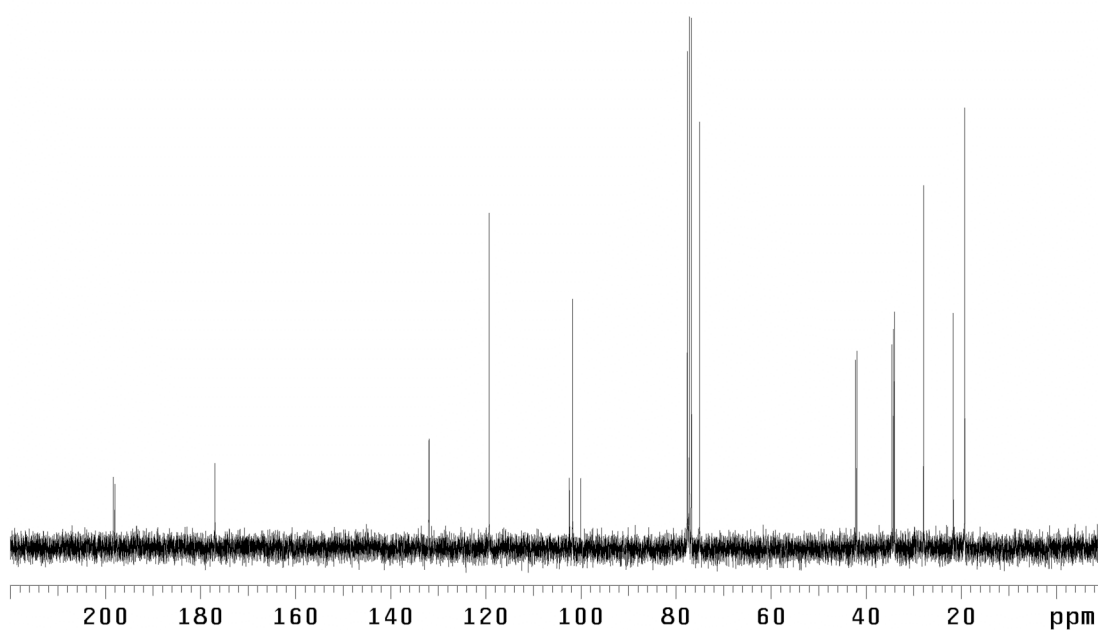
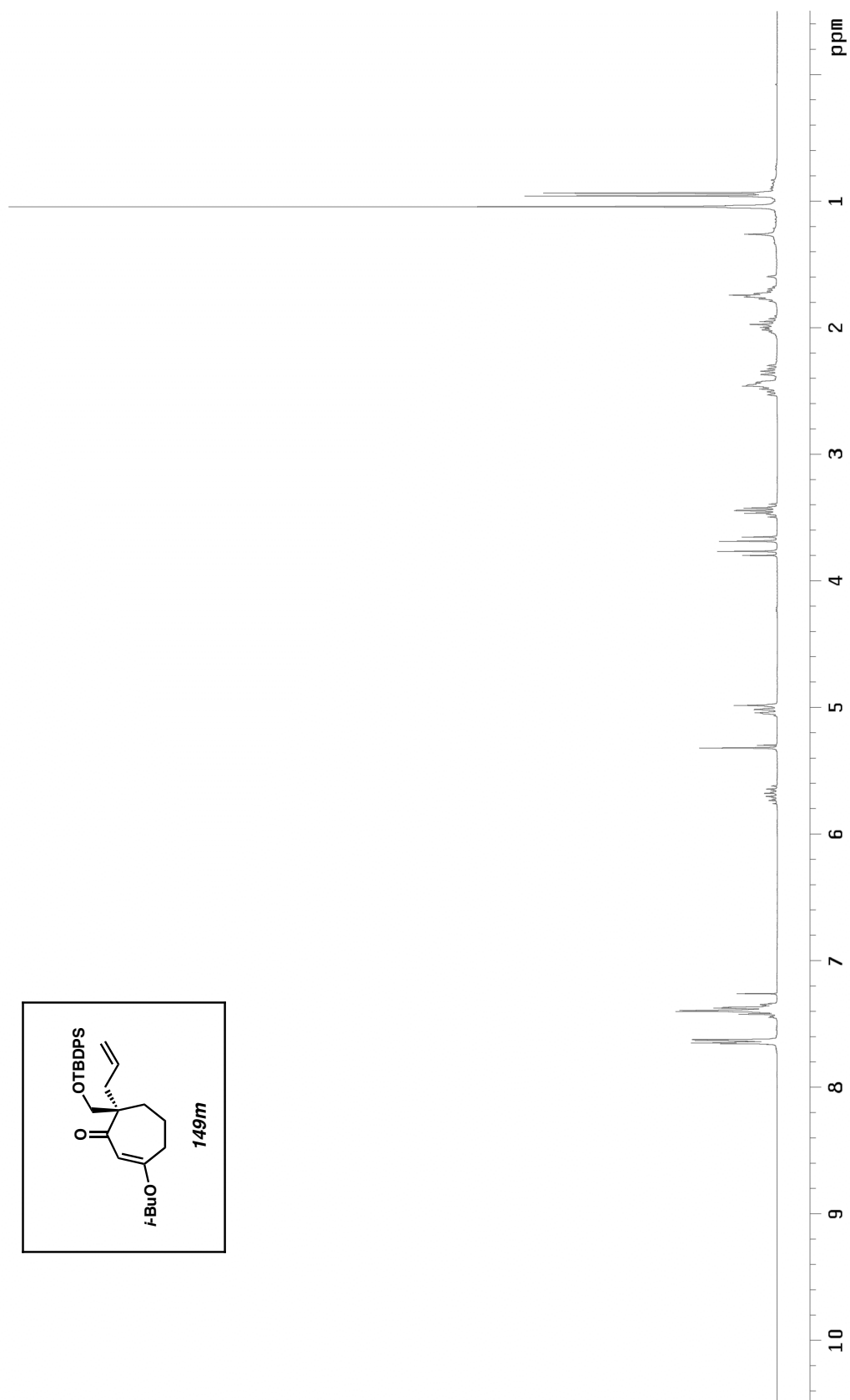


Figure A1.98. ¹³C NMR (75 MHz, CDCl₃) of compound **149I**.

Figure A1.100. ^1H NMR (300 MHz, CDCl_3) of compound **149m**.

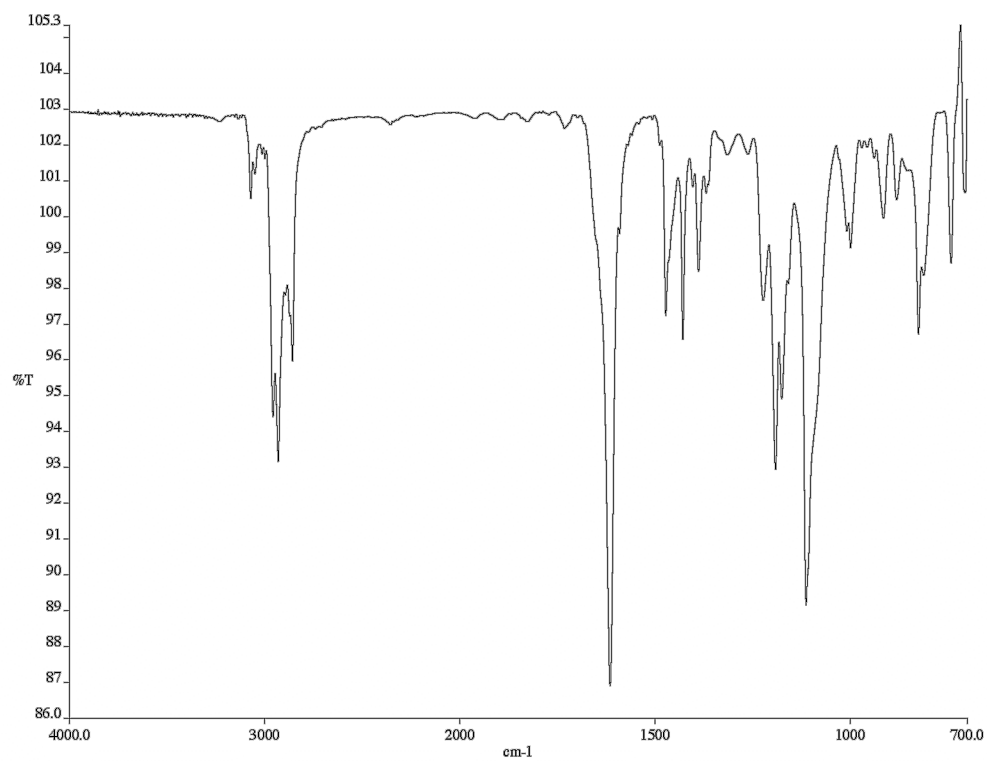


Figure A1.101. Infrared spectrum (thin film/NaCl) of compound **149m**.

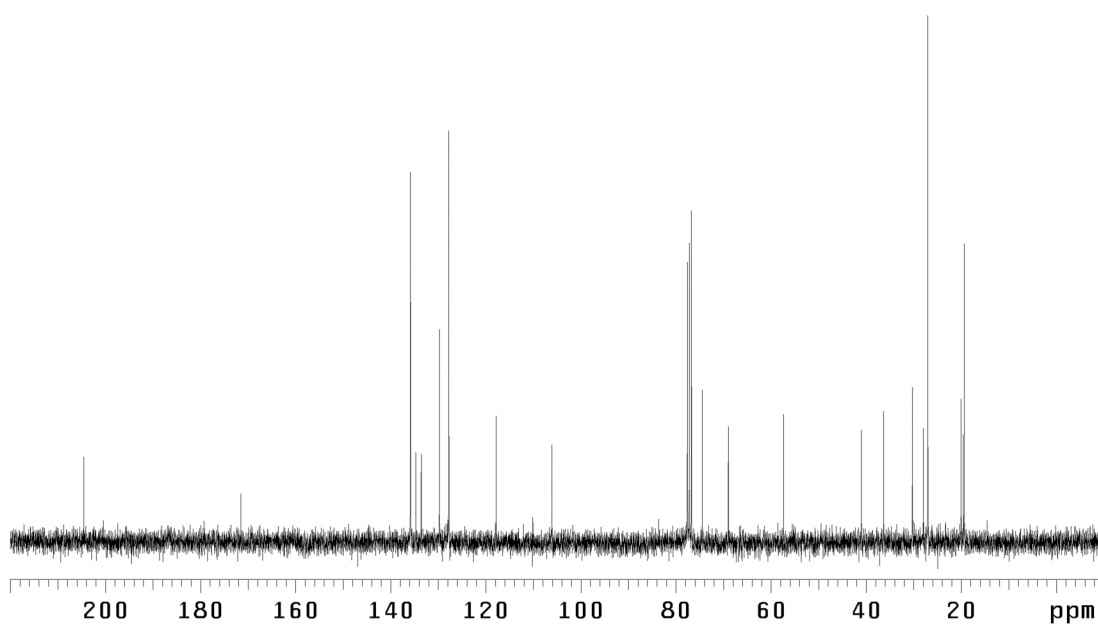
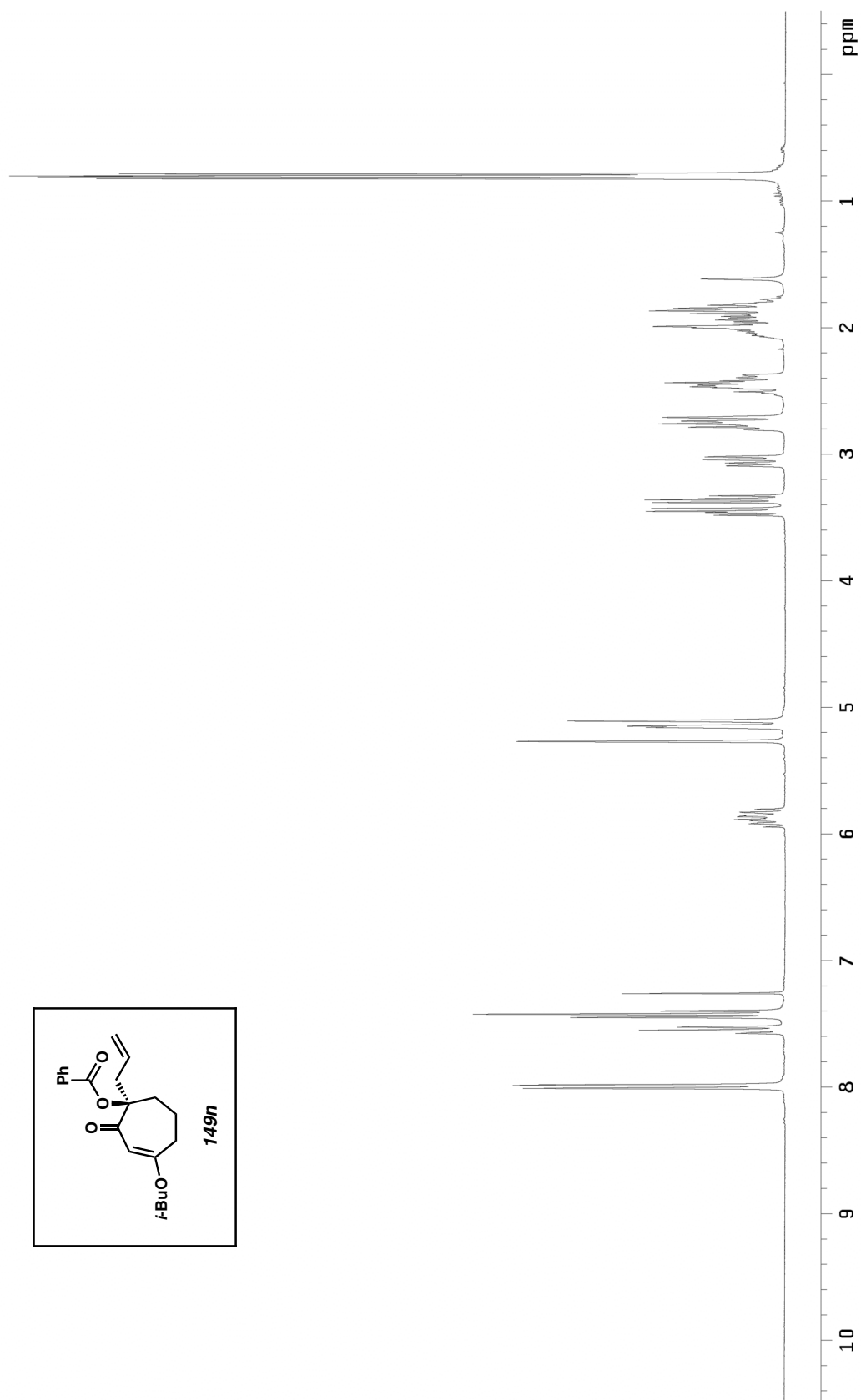


Figure A1.102. ¹³C NMR (75 MHz, CDCl₃) of compound **149m**.

Figure A1.103. ^1H NMR (300 MHz, CDCl_3) of compound **149n**.

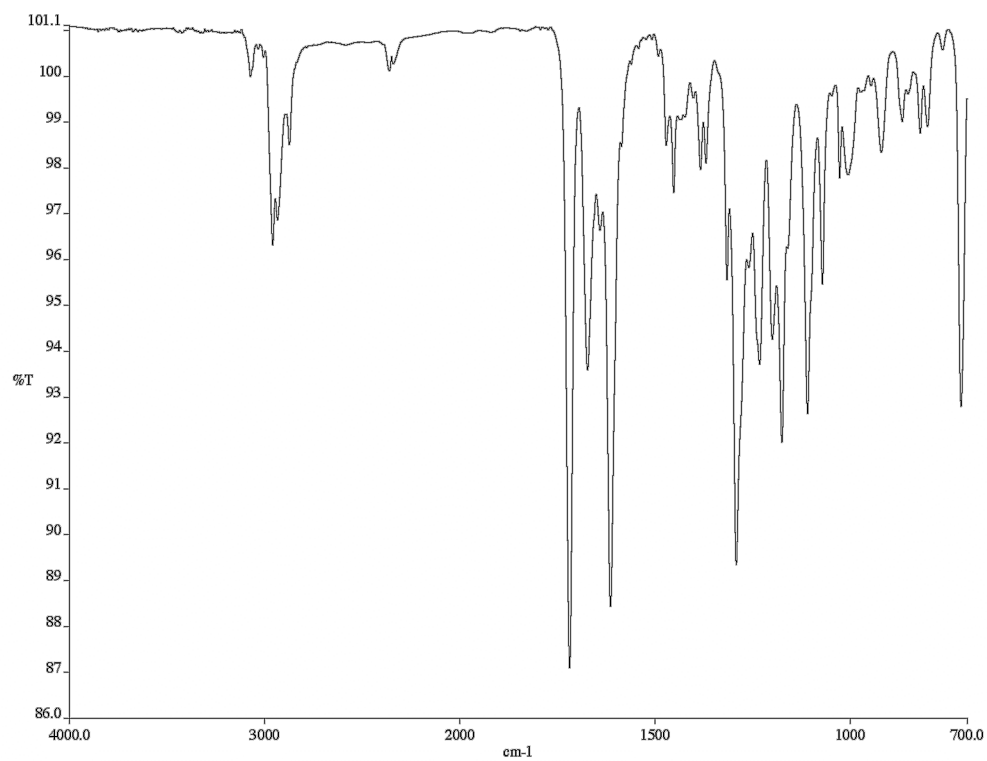


Figure A1.104. Infrared spectrum (thin film/NaCl) of compound **149n**.

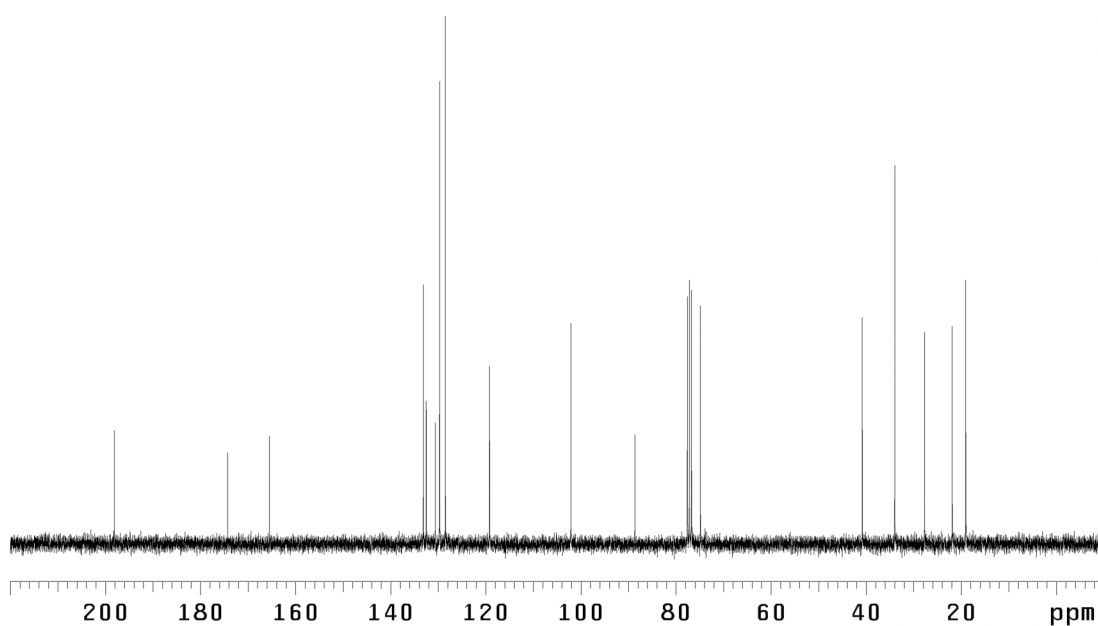
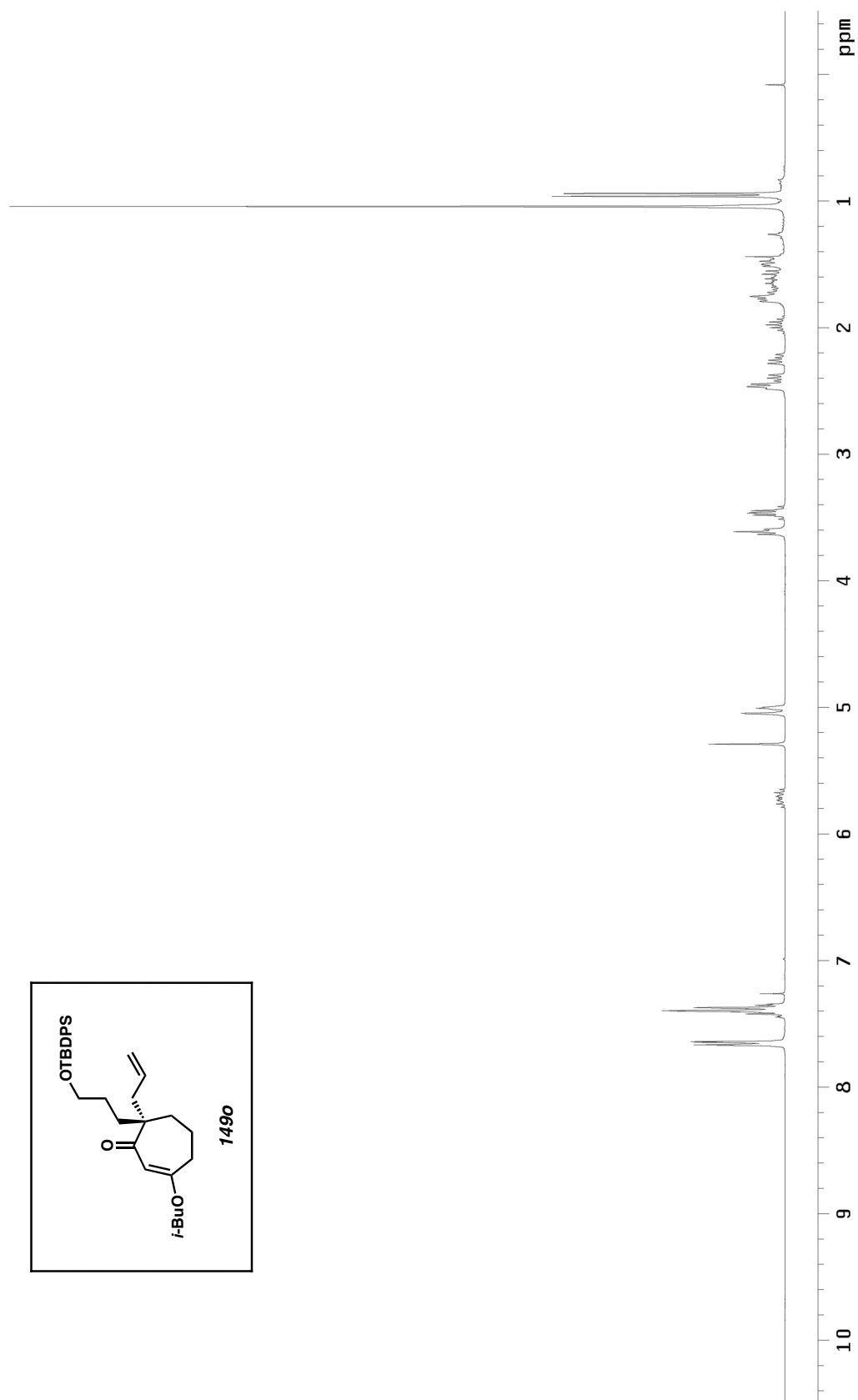


Figure A1.105. ¹³C NMR (75 MHz, CDCl₃) of compound **149n**.

Figure A1.106. ¹H NMR (300 MHz, CDCl₃) of compound **149o**.

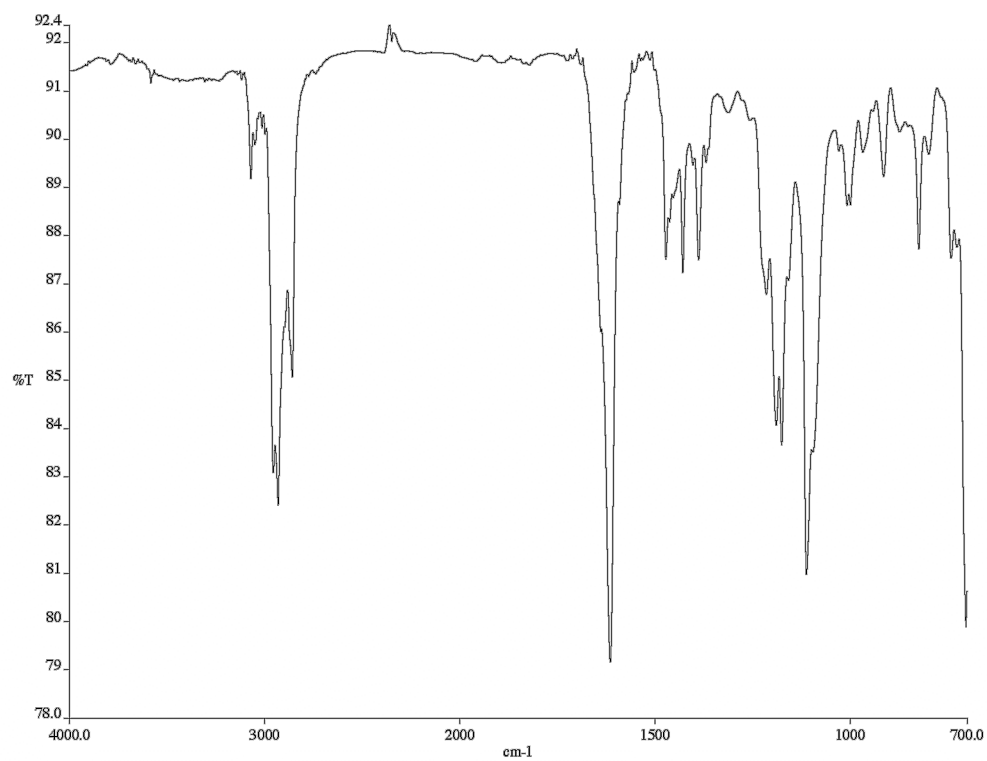


Figure A1.107. Infrared spectrum (thin film/NaCl) of compound **149o**.

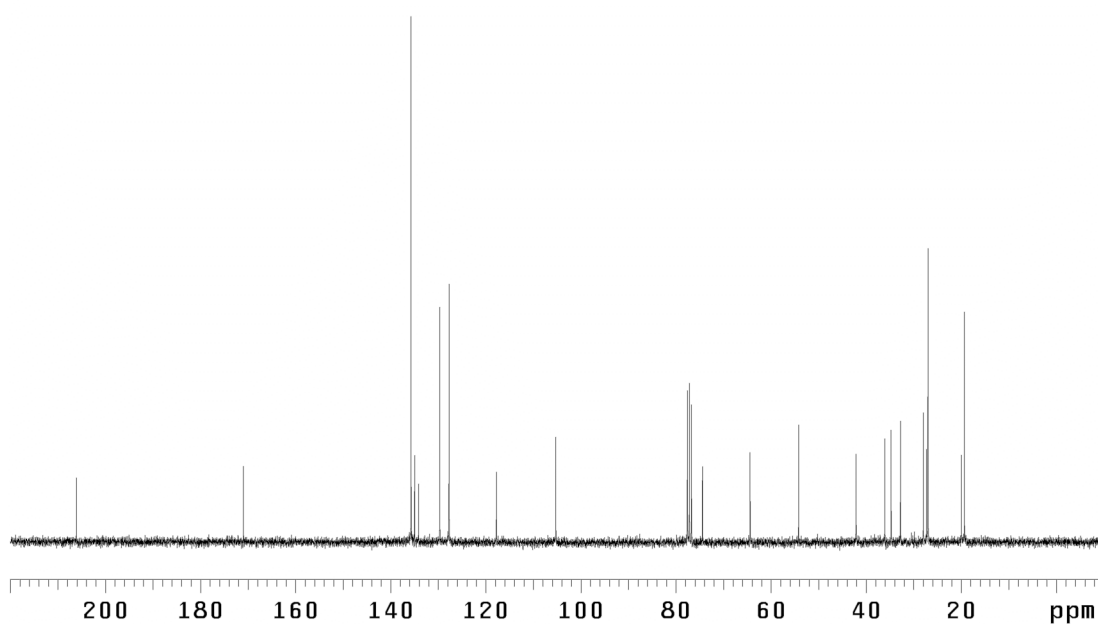
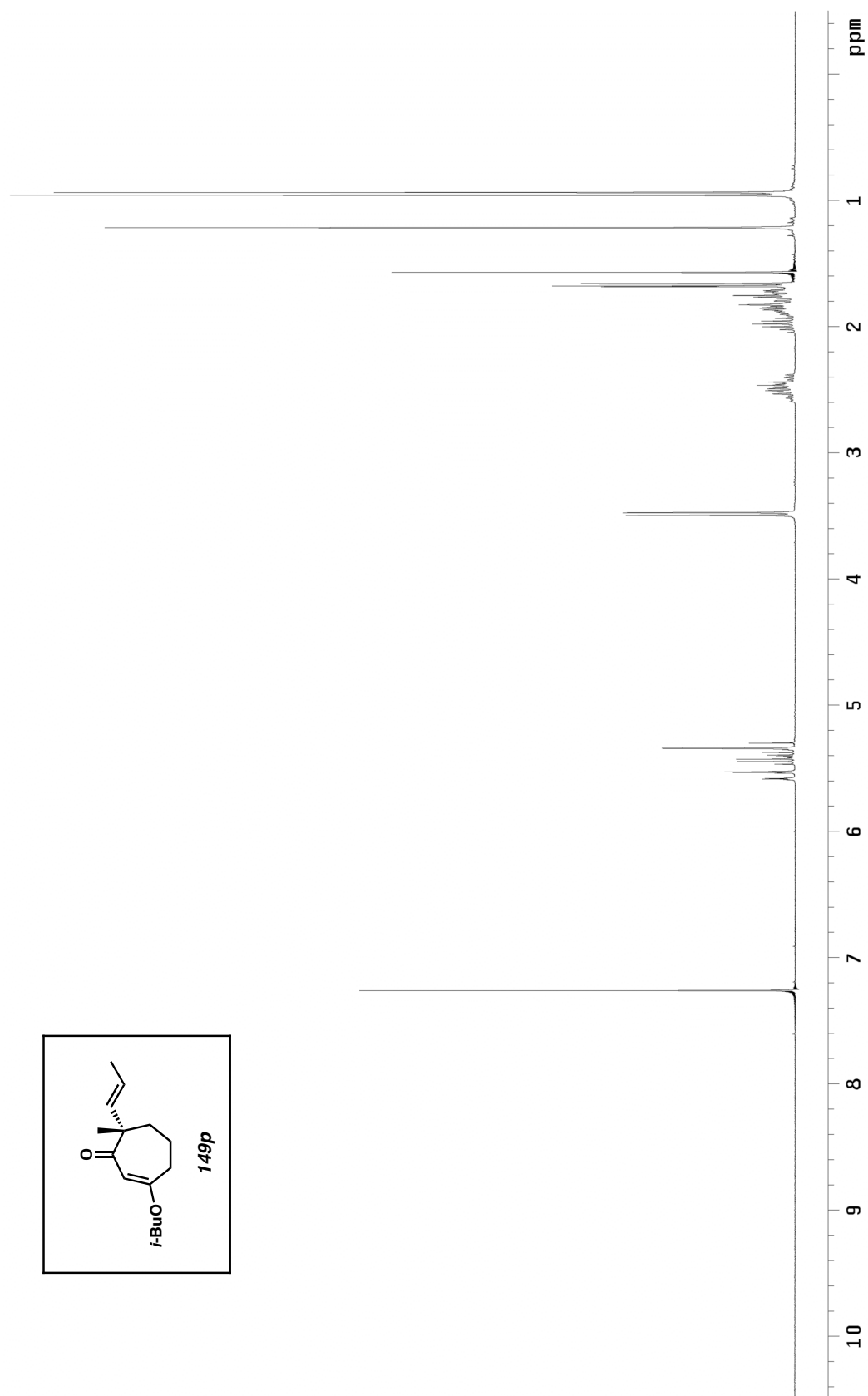


Figure A1.108. ¹³C NMR (75 MHz, CDCl₃) of compound **149o**.

Figure A1.109. ^1H NMR (300 MHz, CDCl_3) of compound **149p**.

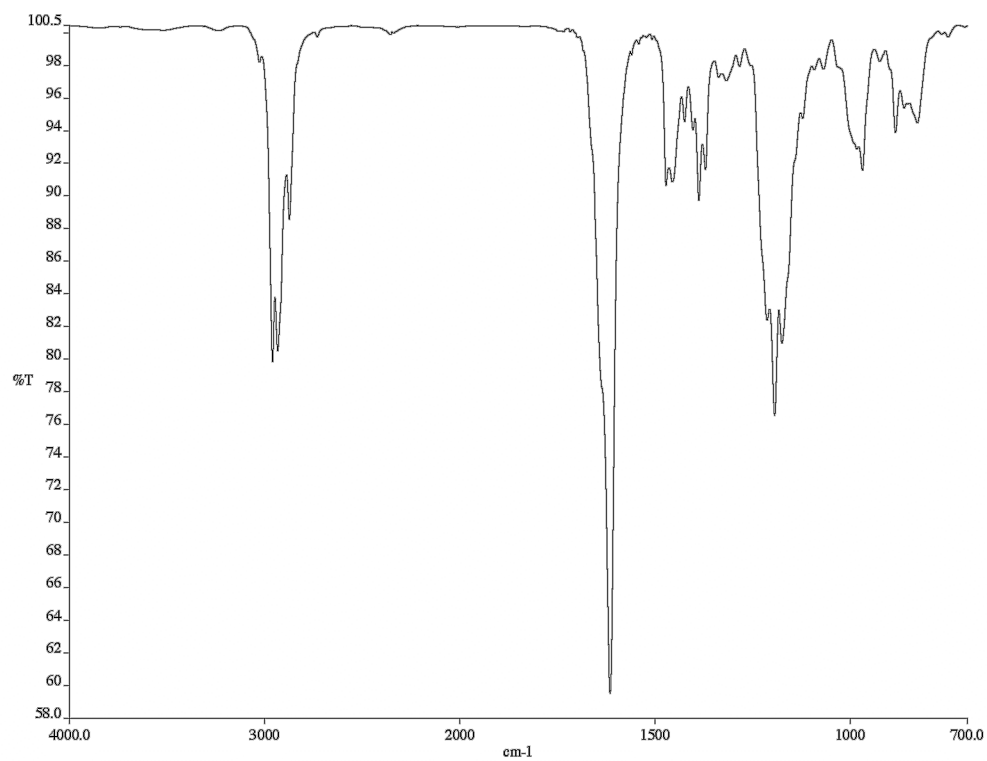


Figure A1.110. Infrared spectrum (thin film/NaCl) of compound **149p**.

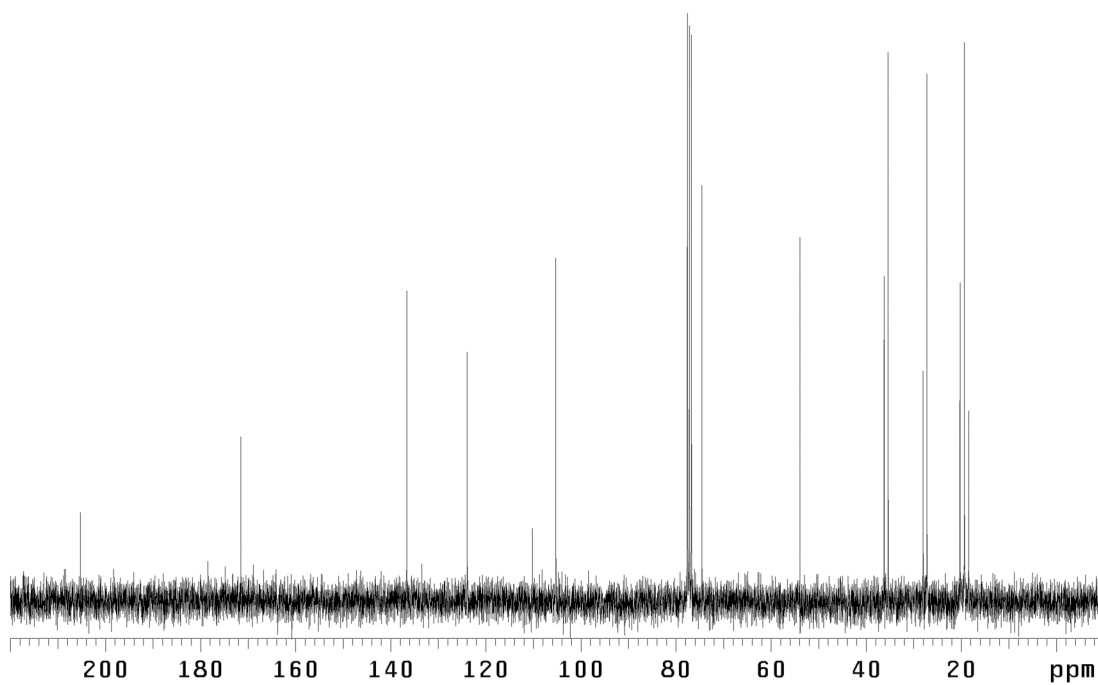
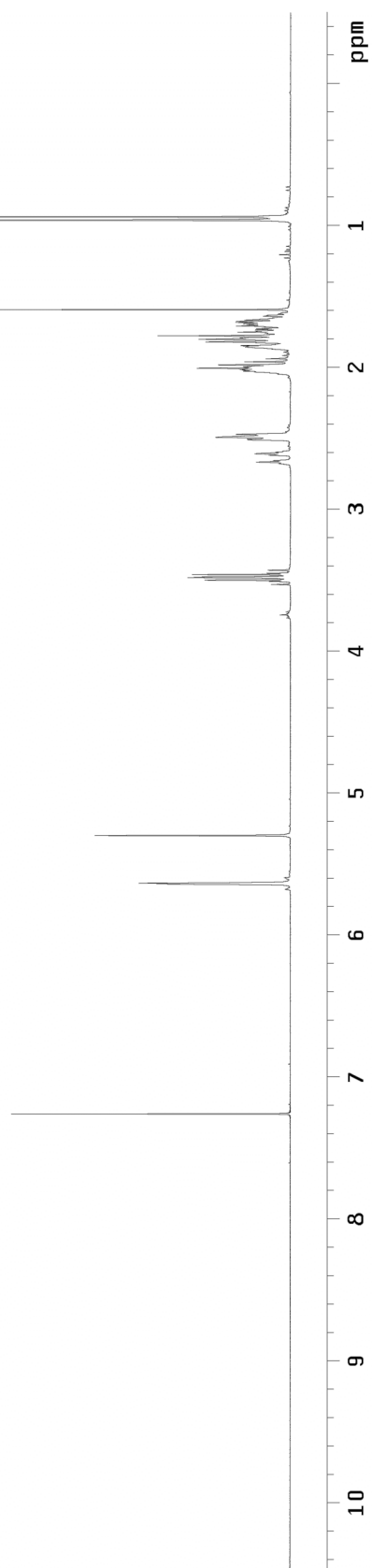
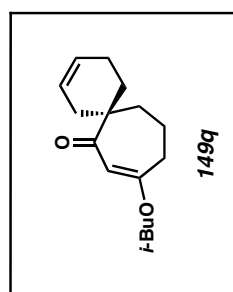


Figure A1.111. ¹³C NMR (75 MHz, CDCl₃) of compound **149p**.

Figure A1.112. ¹H NMR (300 MHz, CDCl₃) of compound **149q**.

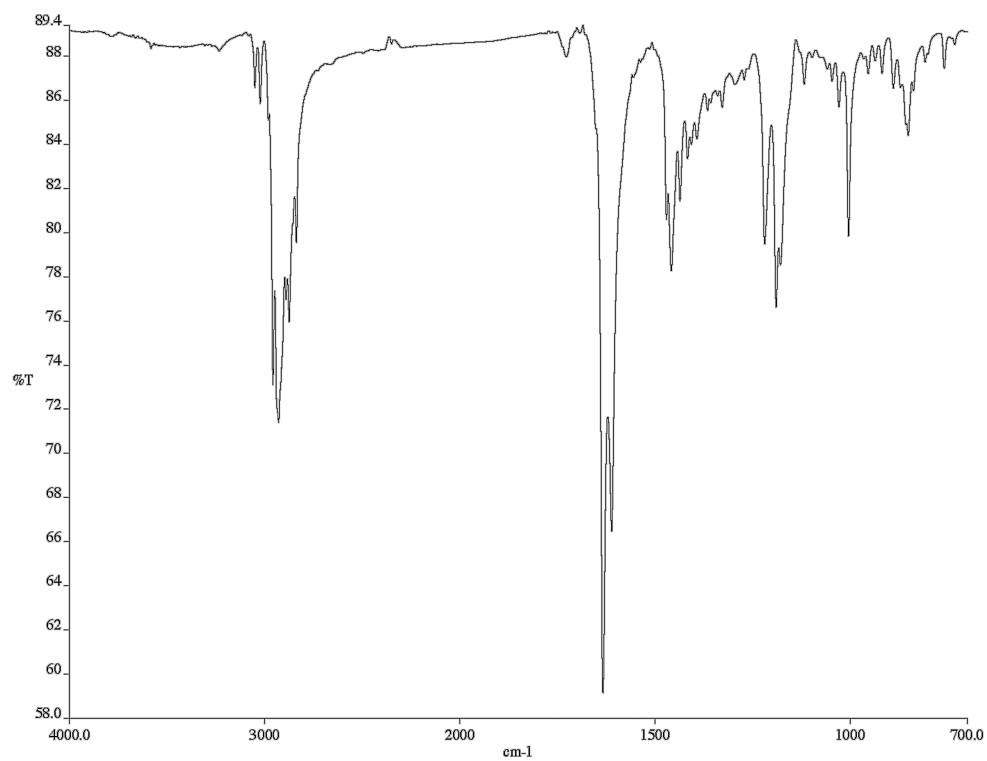


Figure A1.113. Infrared spectrum (thin film/NaCl) of compound **149q**.

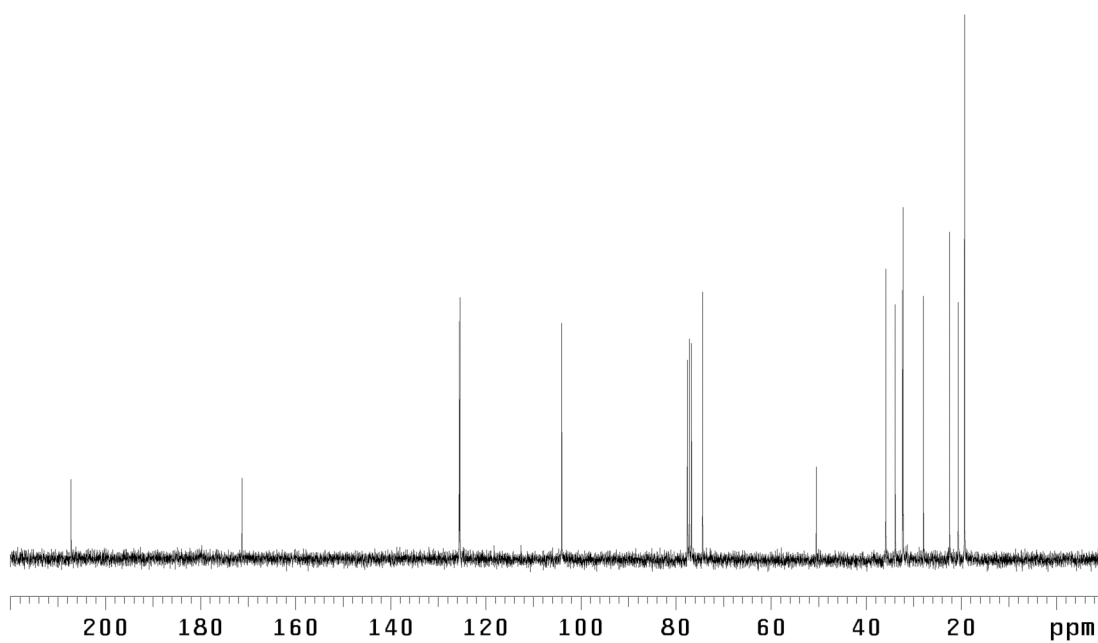


Figure A1.114. ^{13}C NMR (75 MHz, CDCl_3) of compound **149q**.

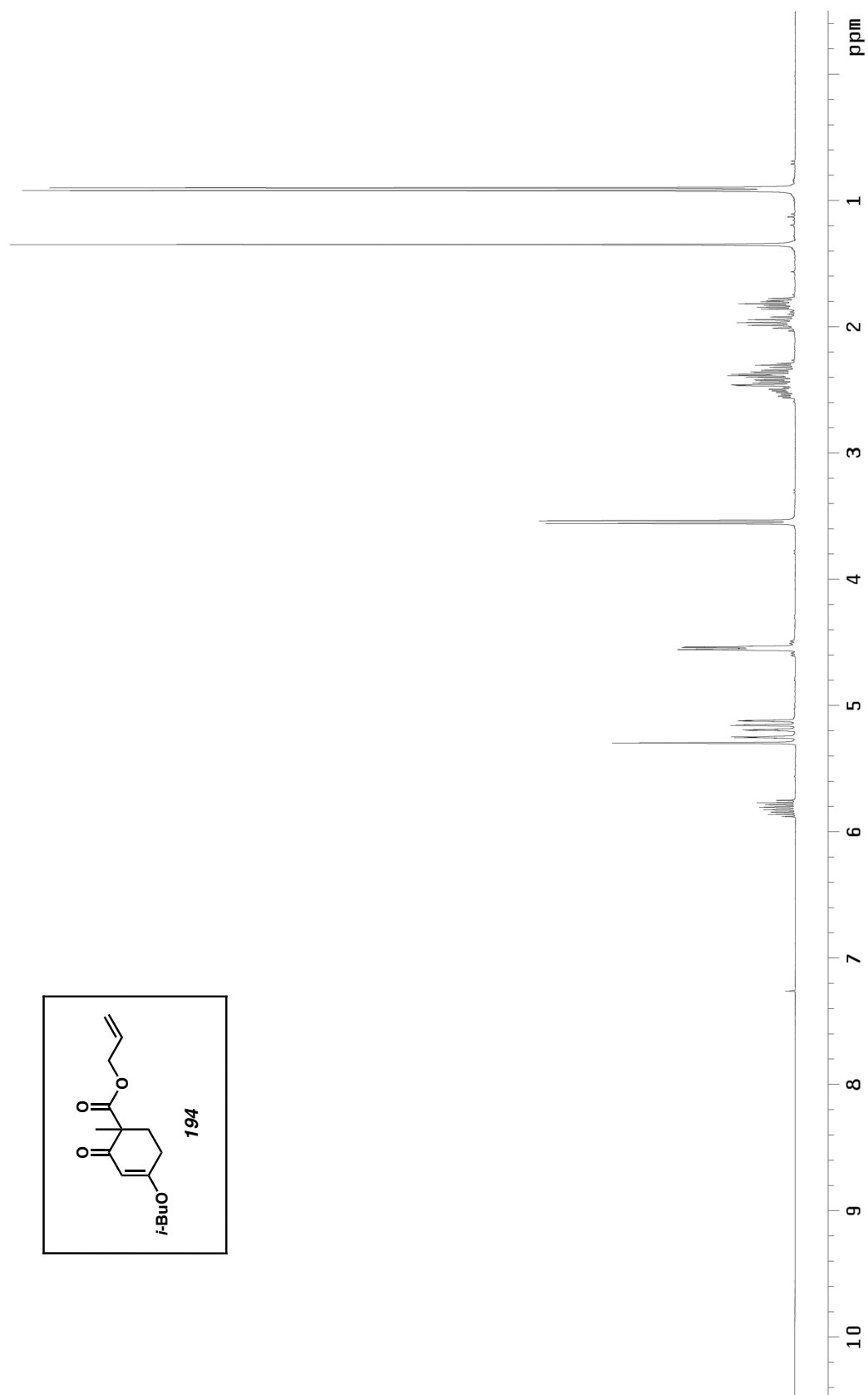


Figure A1.115. ^1H NMR (300 MHz, CDCl_3) of compound **194**.

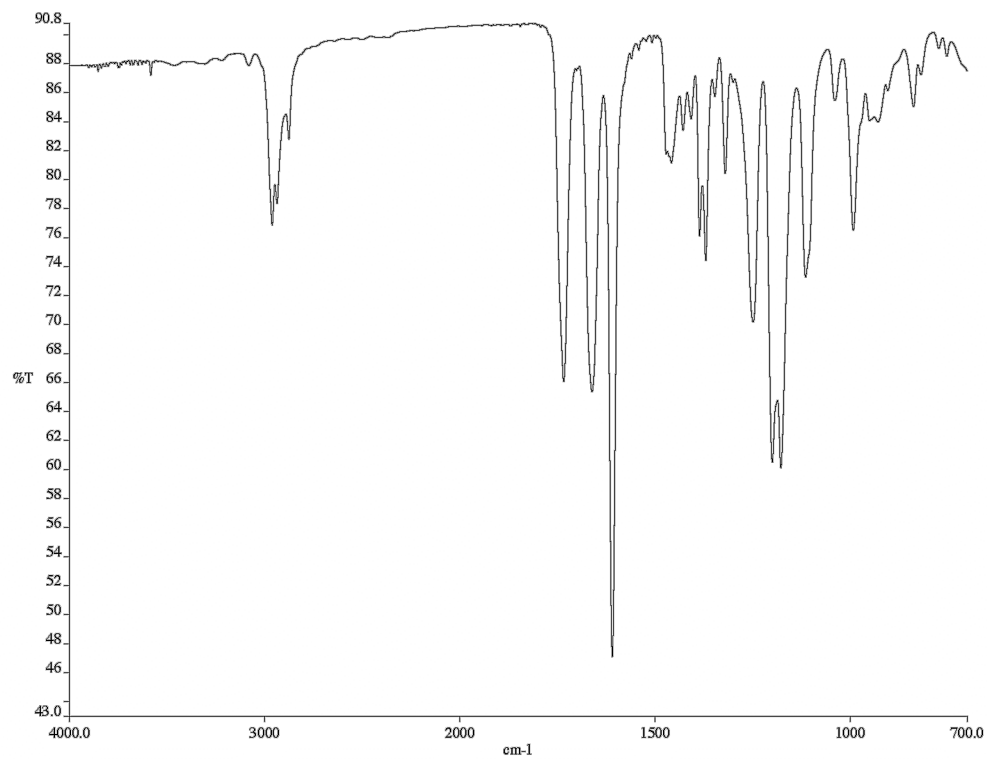


Figure A1.116. Infrared spectrum (thin film/NaCl) of compound **194**.

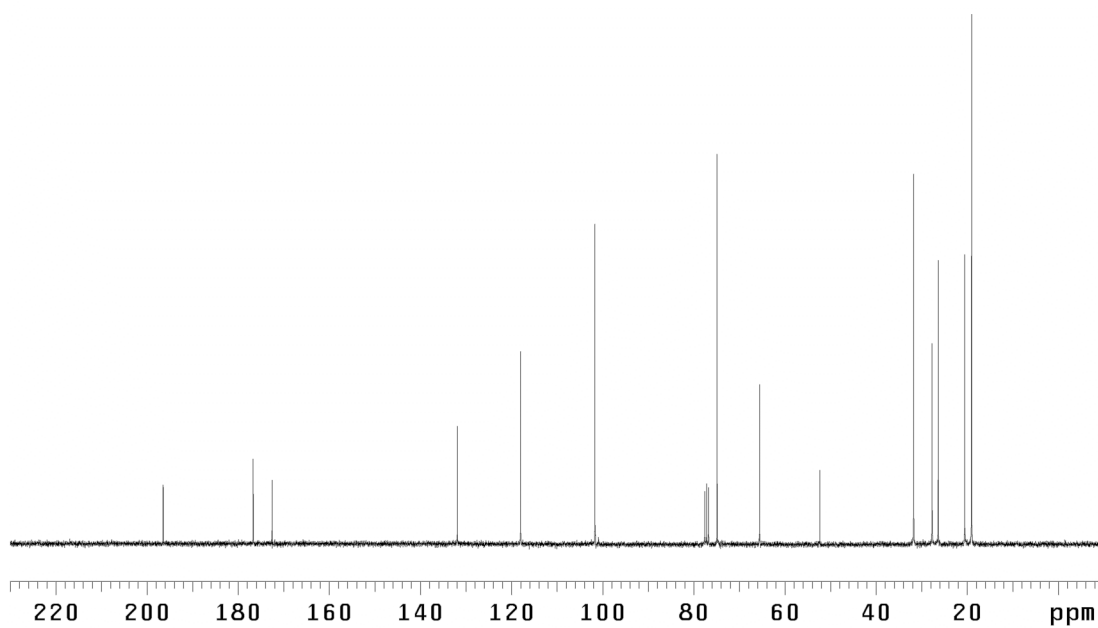


Figure A1.117. ¹³C NMR (75 MHz, CDCl₃) of compound **194**.

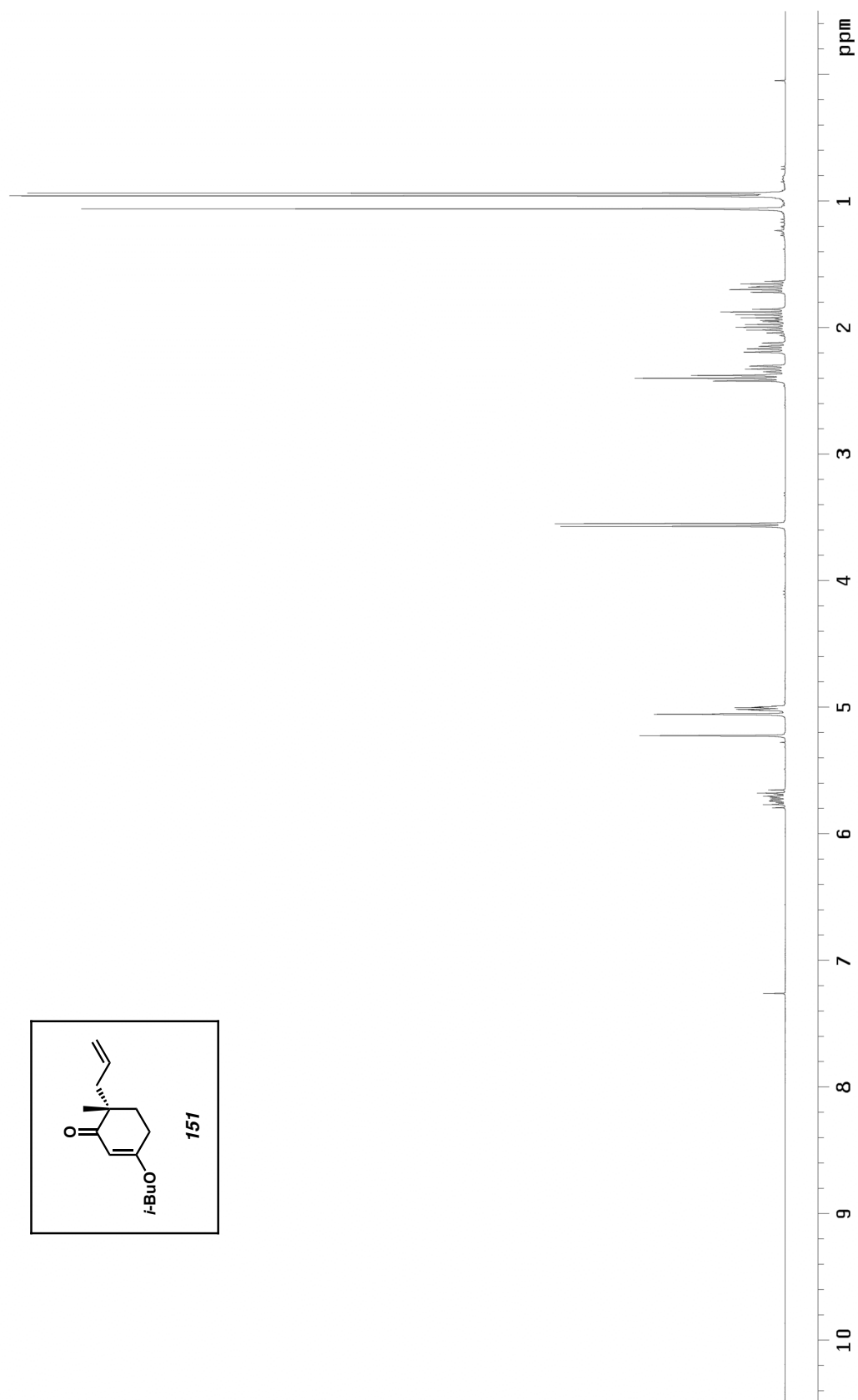


Figure A1.118. ^1H NMR (300 MHz, CDCl_3) of compound **151**.

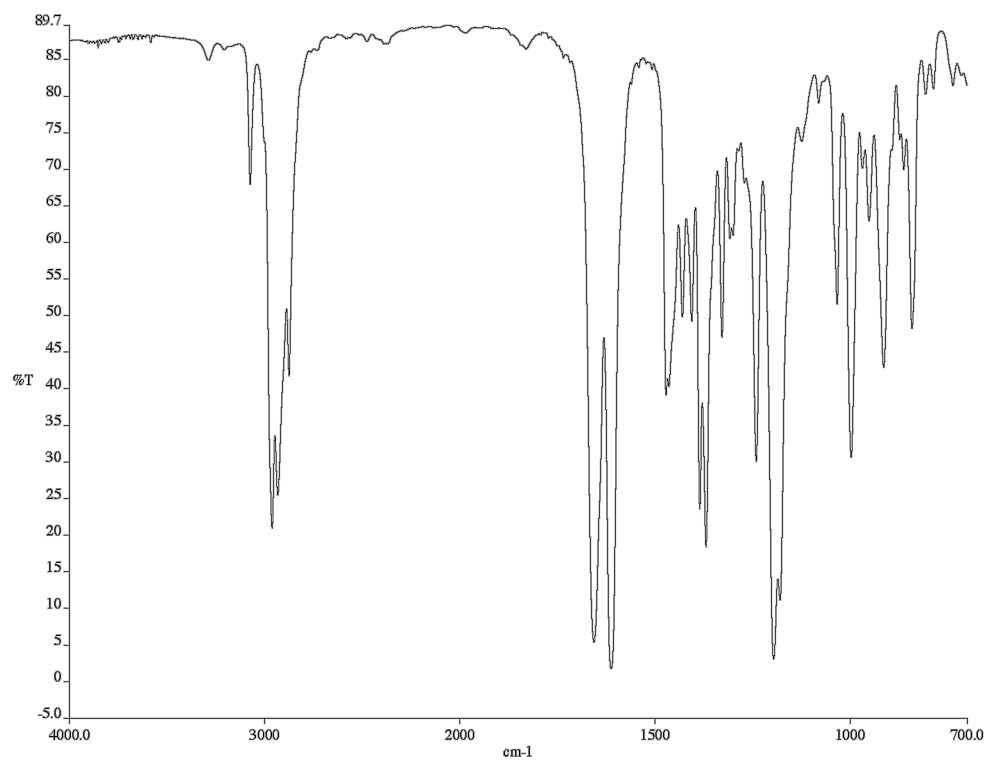


Figure A1.119. Infrared spectrum (thin film/NaCl) of compound **151**.

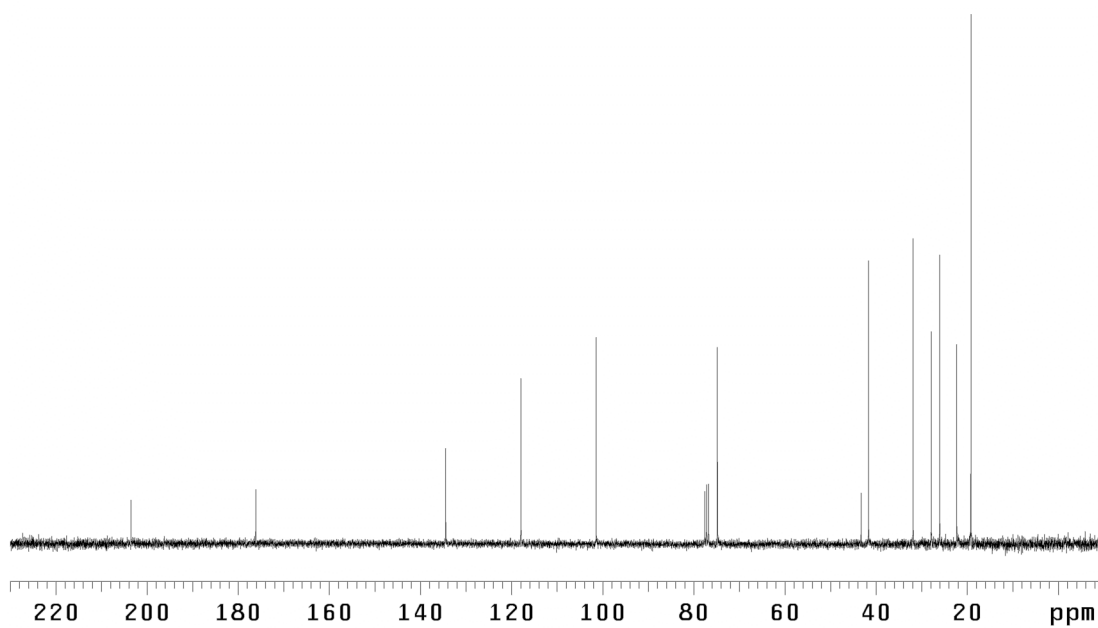


Figure A1.120. ^{13}C NMR (75 MHz, CDCl_3) of compound **151**.

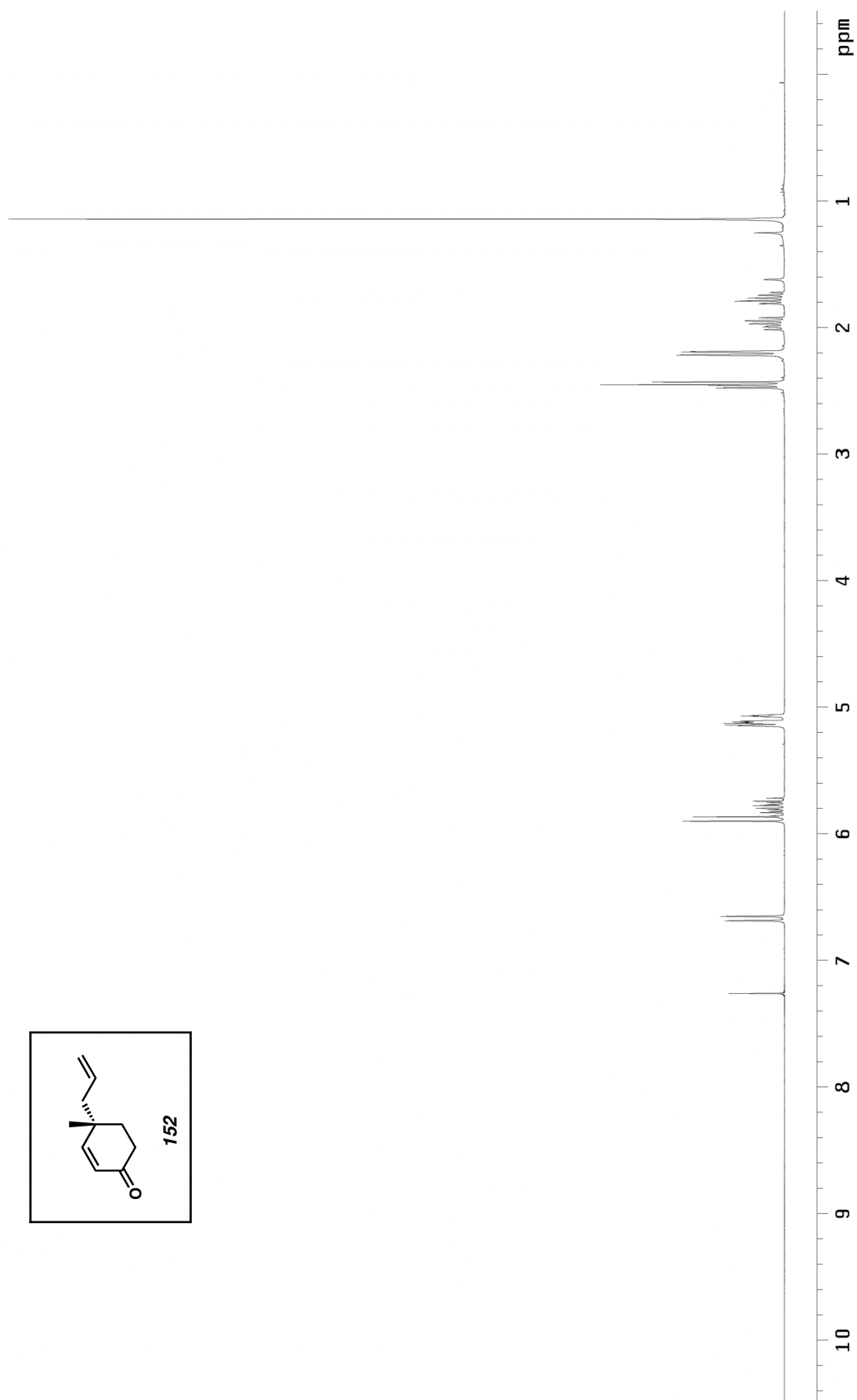


Figure A1.121. ^1H NMR (300 MHz, CDCl_3) of compound **152**.

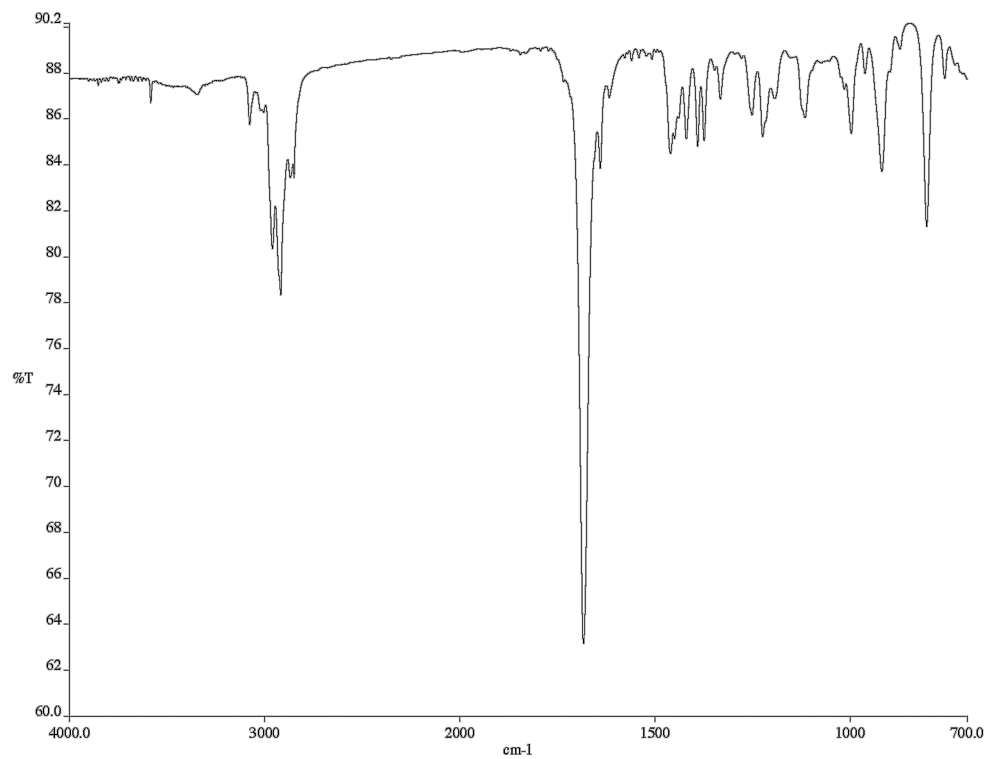


Figure A1.122. Infrared spectrum (thin film/NaCl) of compound **152**.

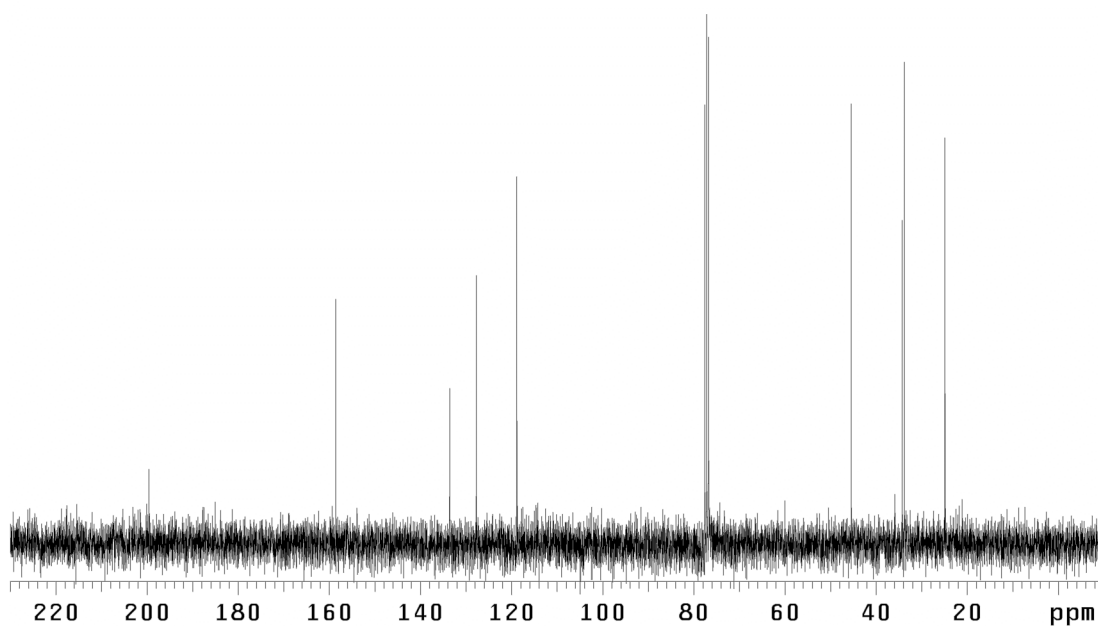


Figure A1.123. ¹³C NMR (75 MHz, CDCl₃) of compound **152**.

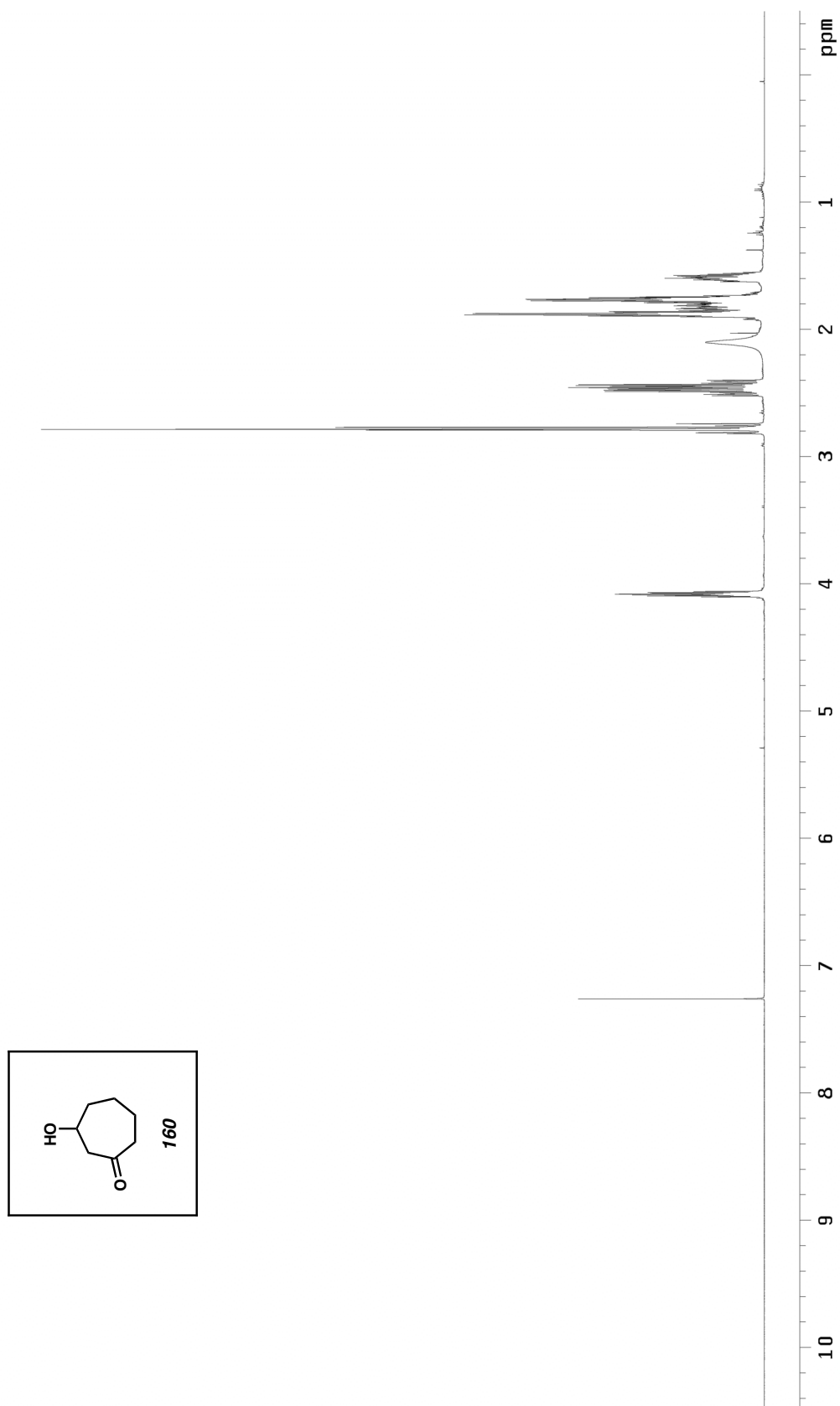


Figure A1.124. ^1H NMR (500 MHz, CDCl_3) of compound **160**.

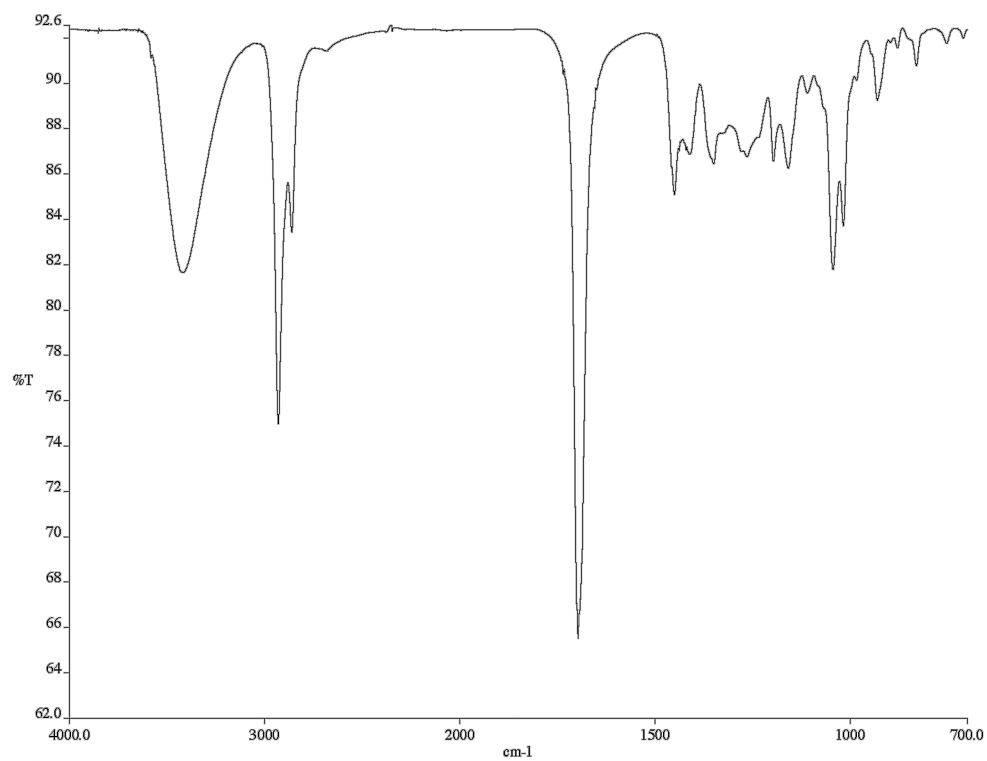


Figure A1.125. Infrared spectrum (thin film/NaCl) of compound **160**.

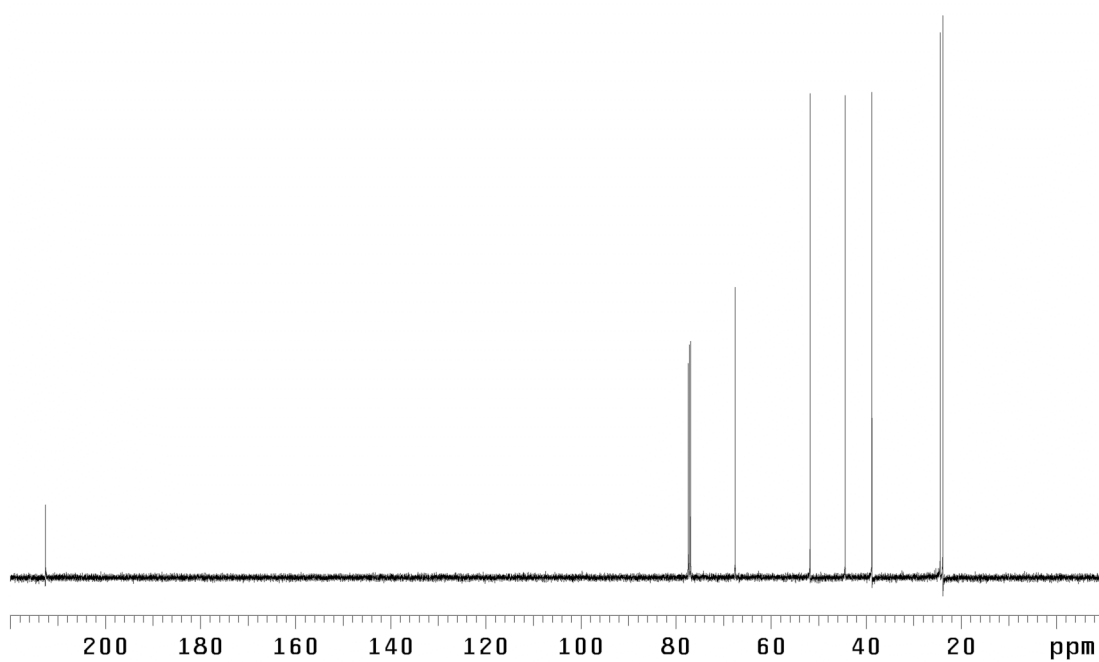


Figure A1.126. ¹³C NMR (125 MHz, CDCl₃) of compound **160**.

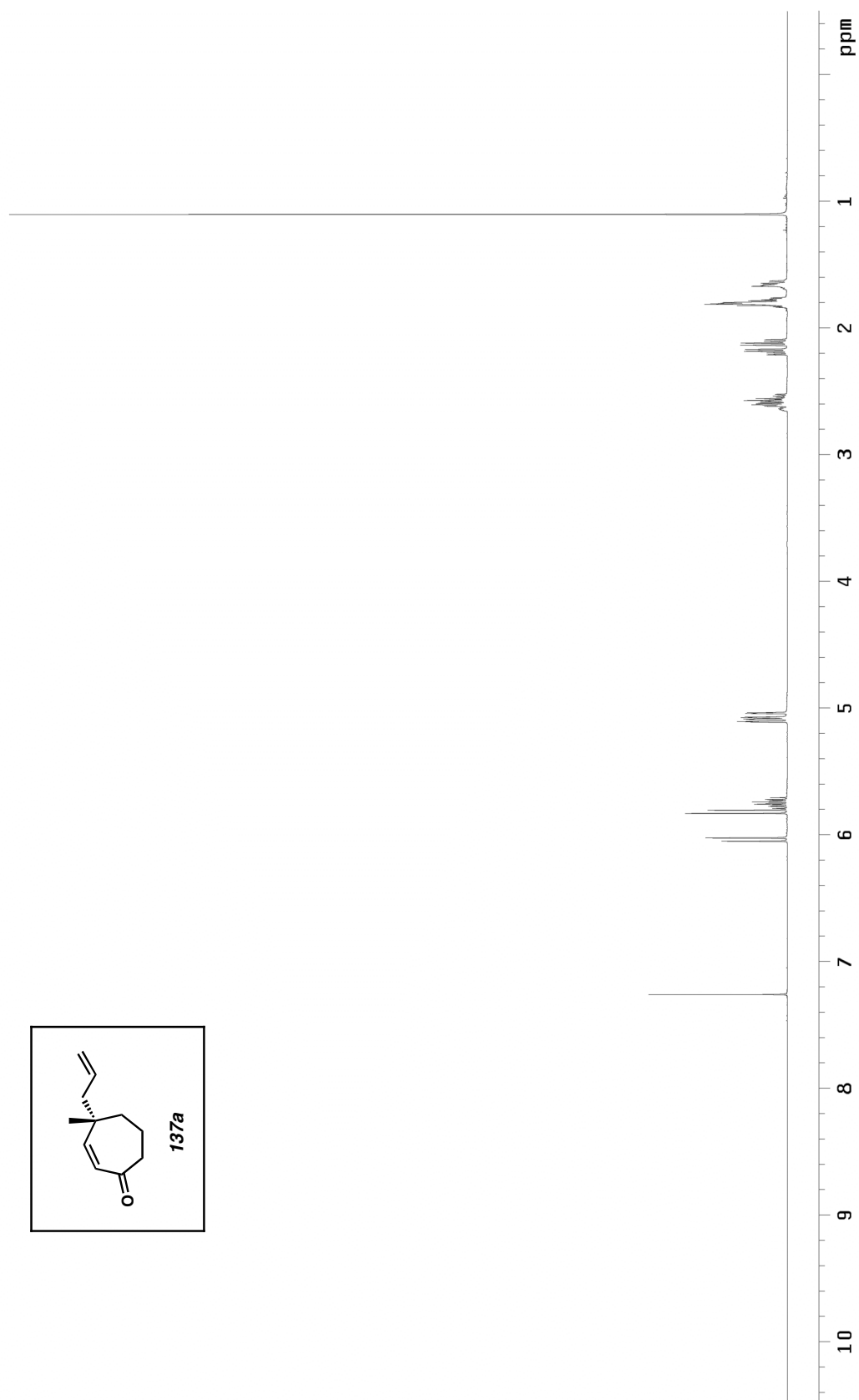


Figure A1.127. ^1H NMR (500 MHz, CDCl_3) of compound **137a**.

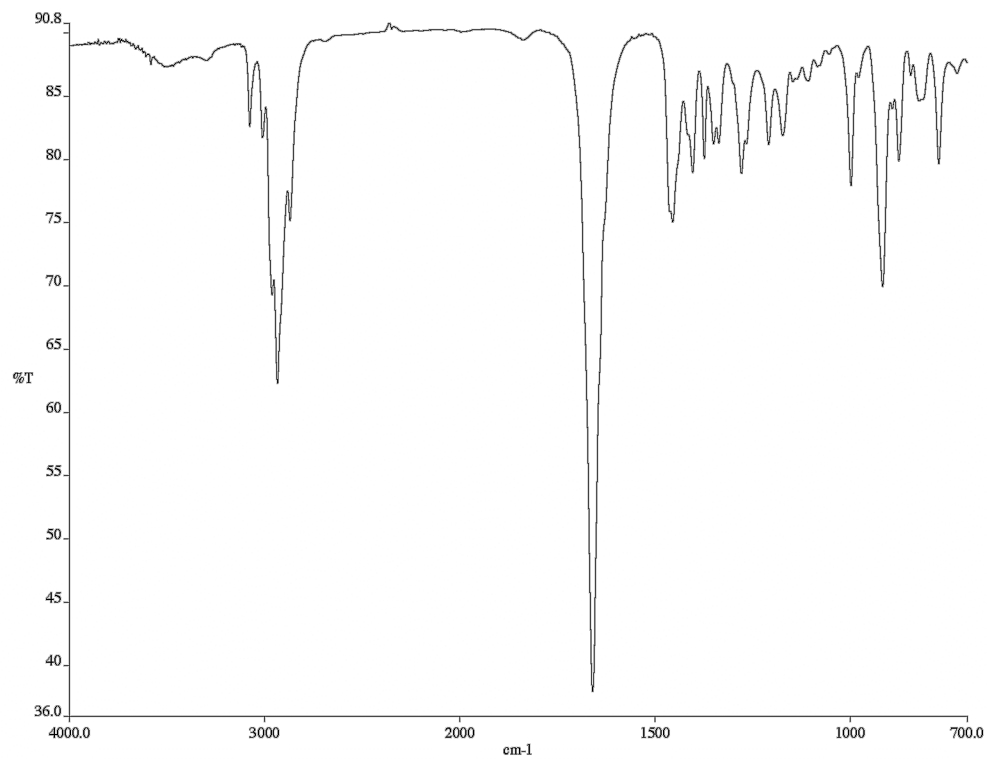


Figure A1.128. Infrared spectrum (thin film/NaCl) of compound **137a**.

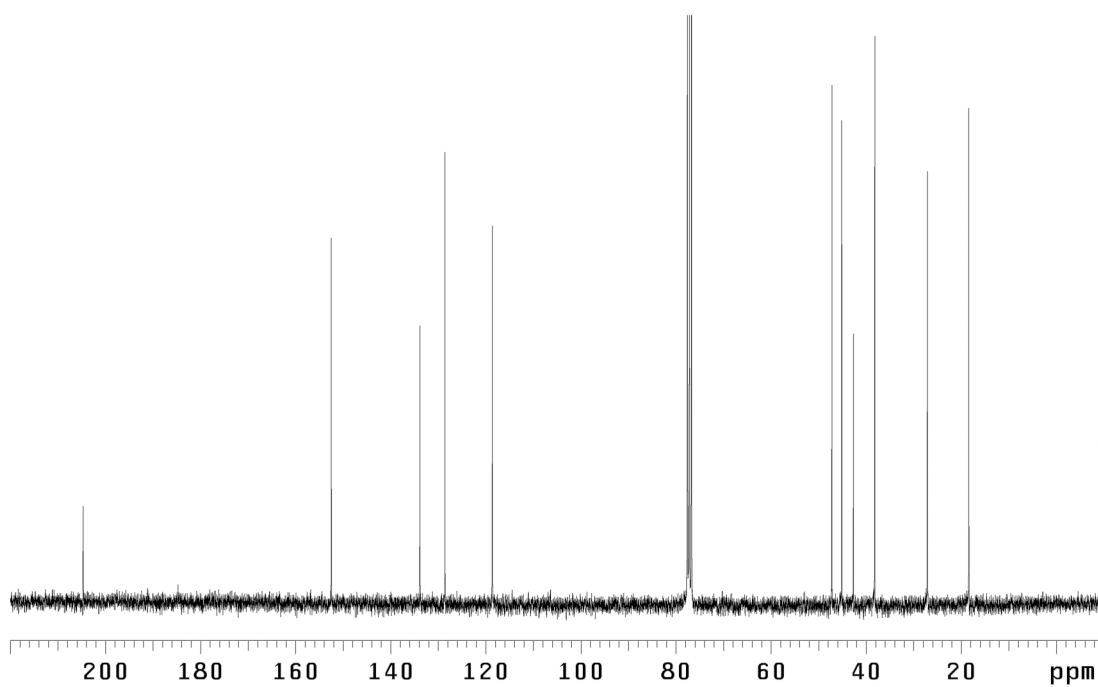


Figure A1.129. ¹³C NMR (125 MHz, CDCl₃) of compound **137a**.

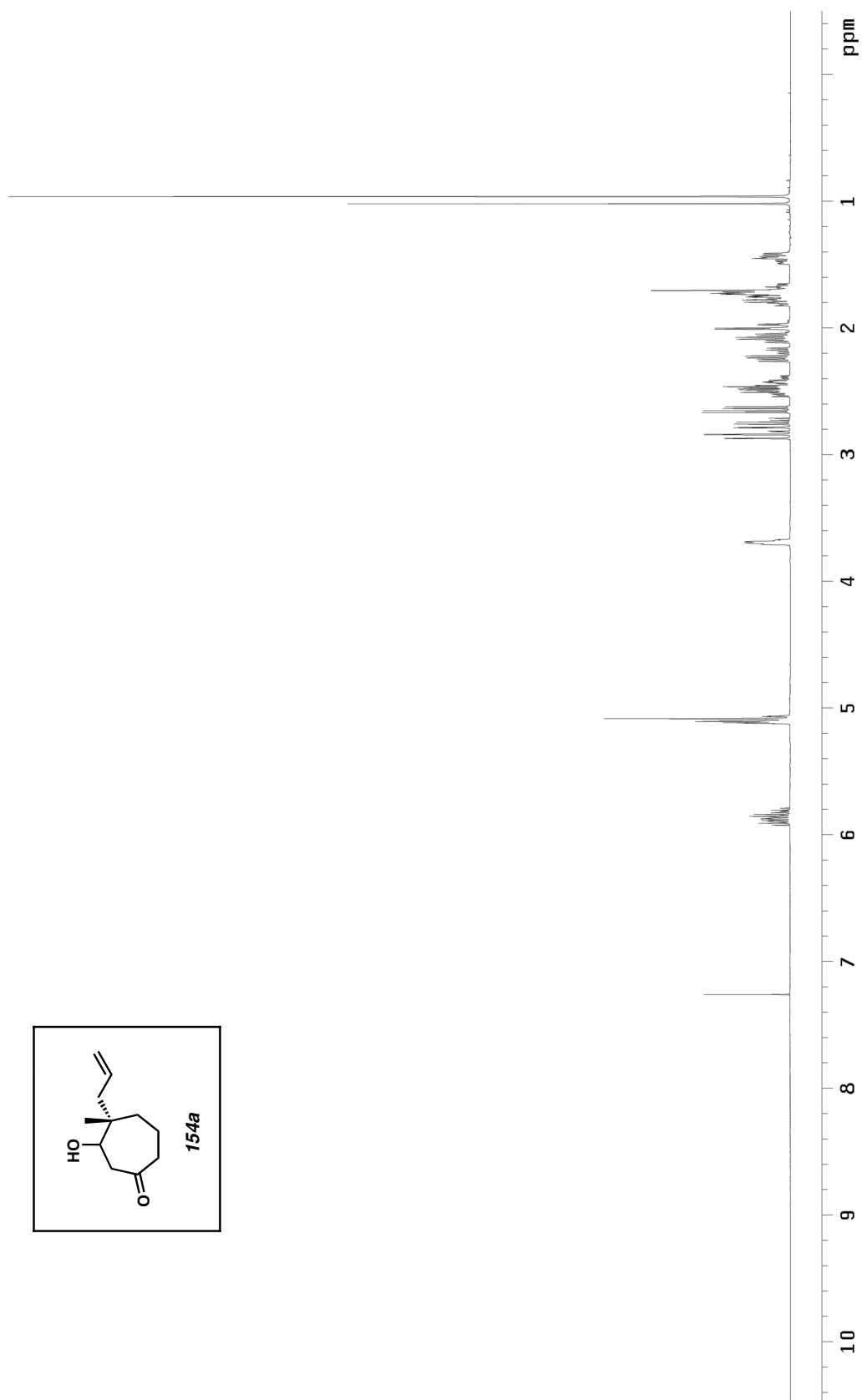


Figure A1.130. ¹H NMR (500 MHz, CDCl₃) of compound **154a**.

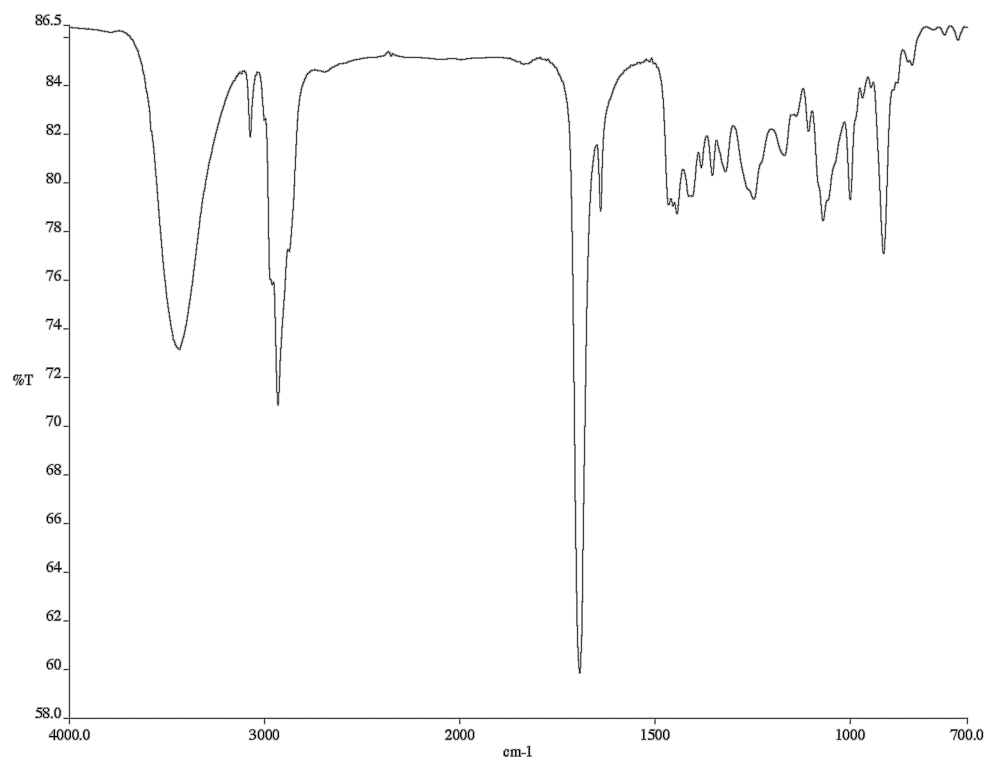


Figure A1.131. Infrared spectrum (thin film/NaCl) of compound **154a**.

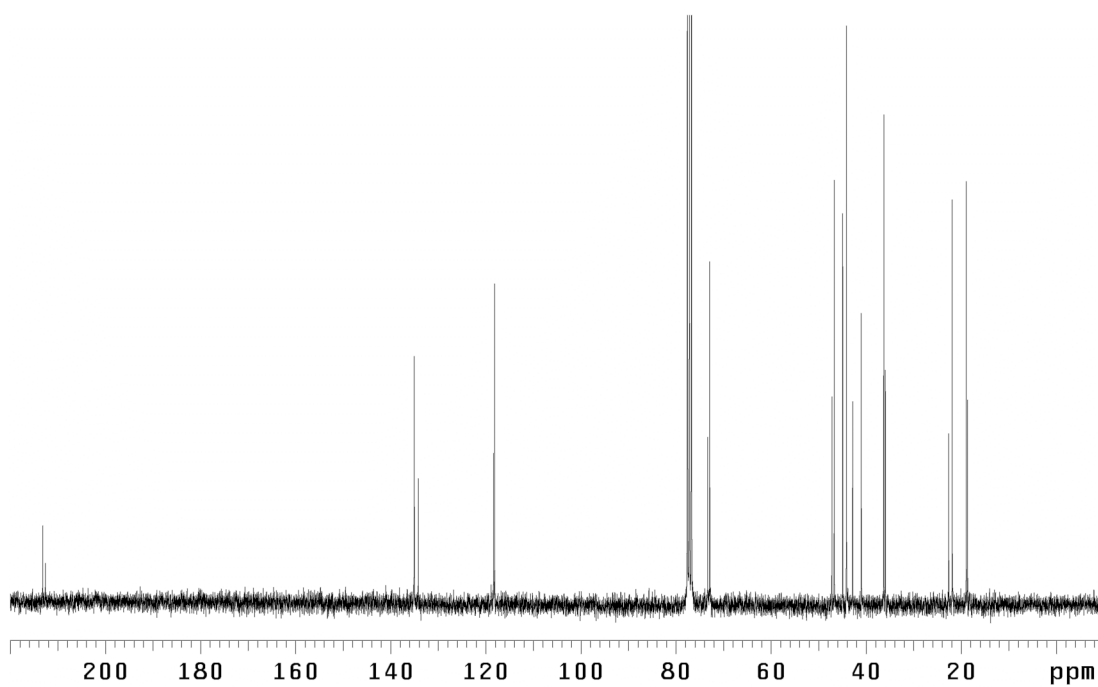
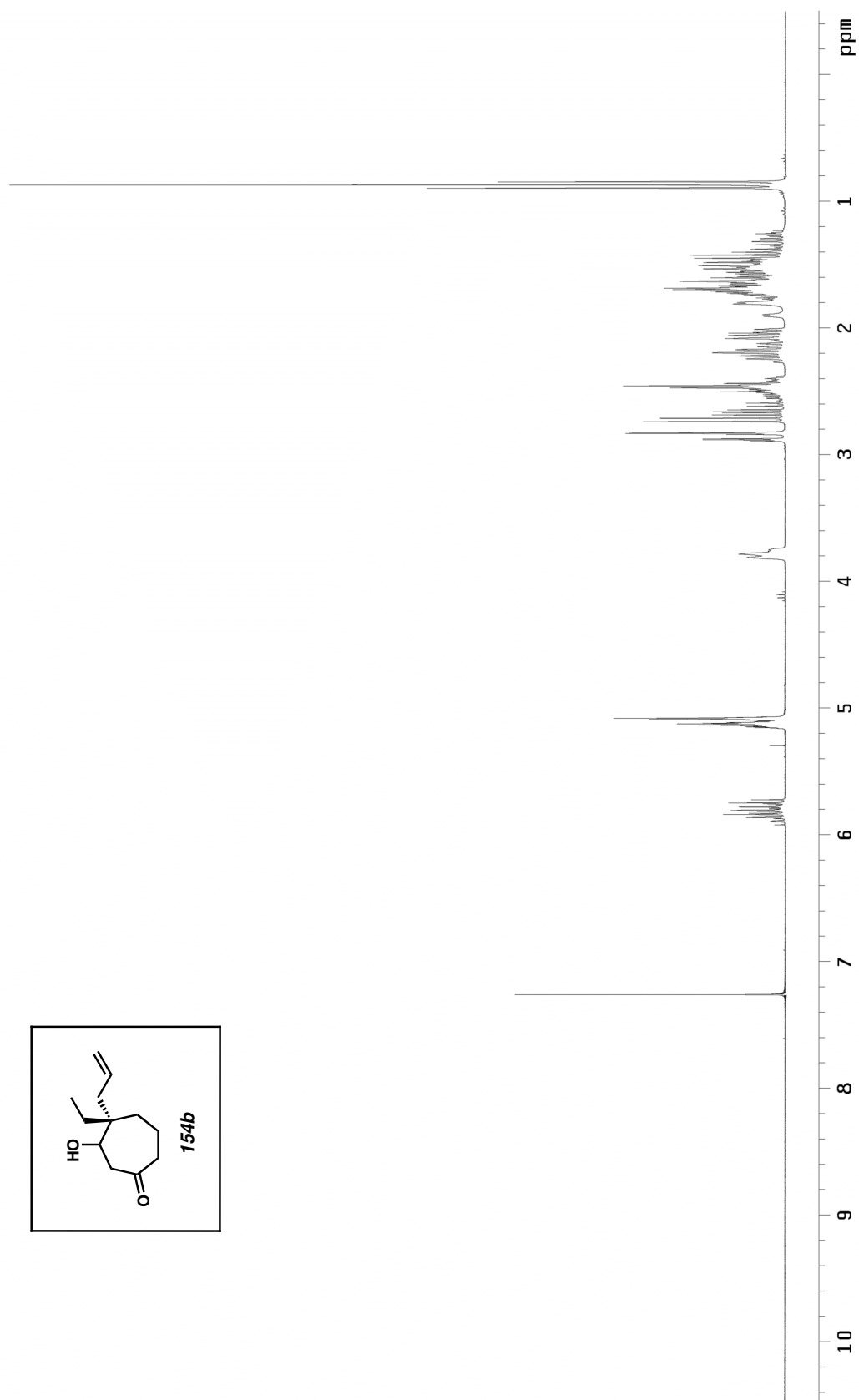


Figure A1.132. ¹³C NMR (125 MHz, CDCl₃) of compound **154a**.

Figure A1.133. ¹H NMR (300 MHz, CDCl₃) of compound **154b**.

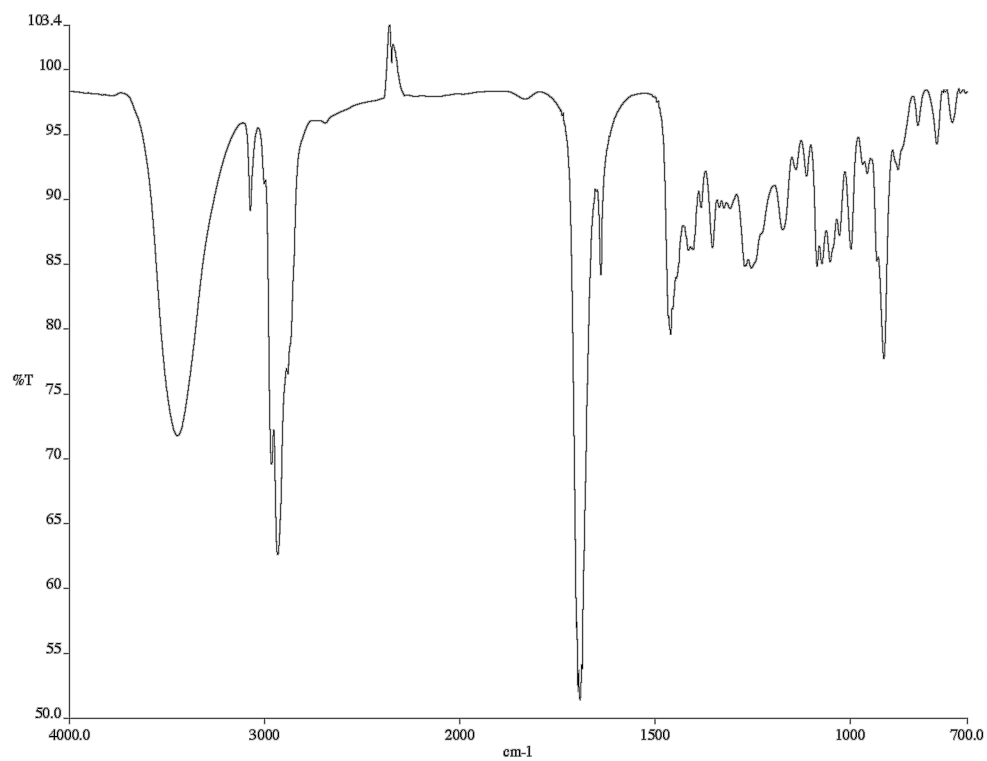
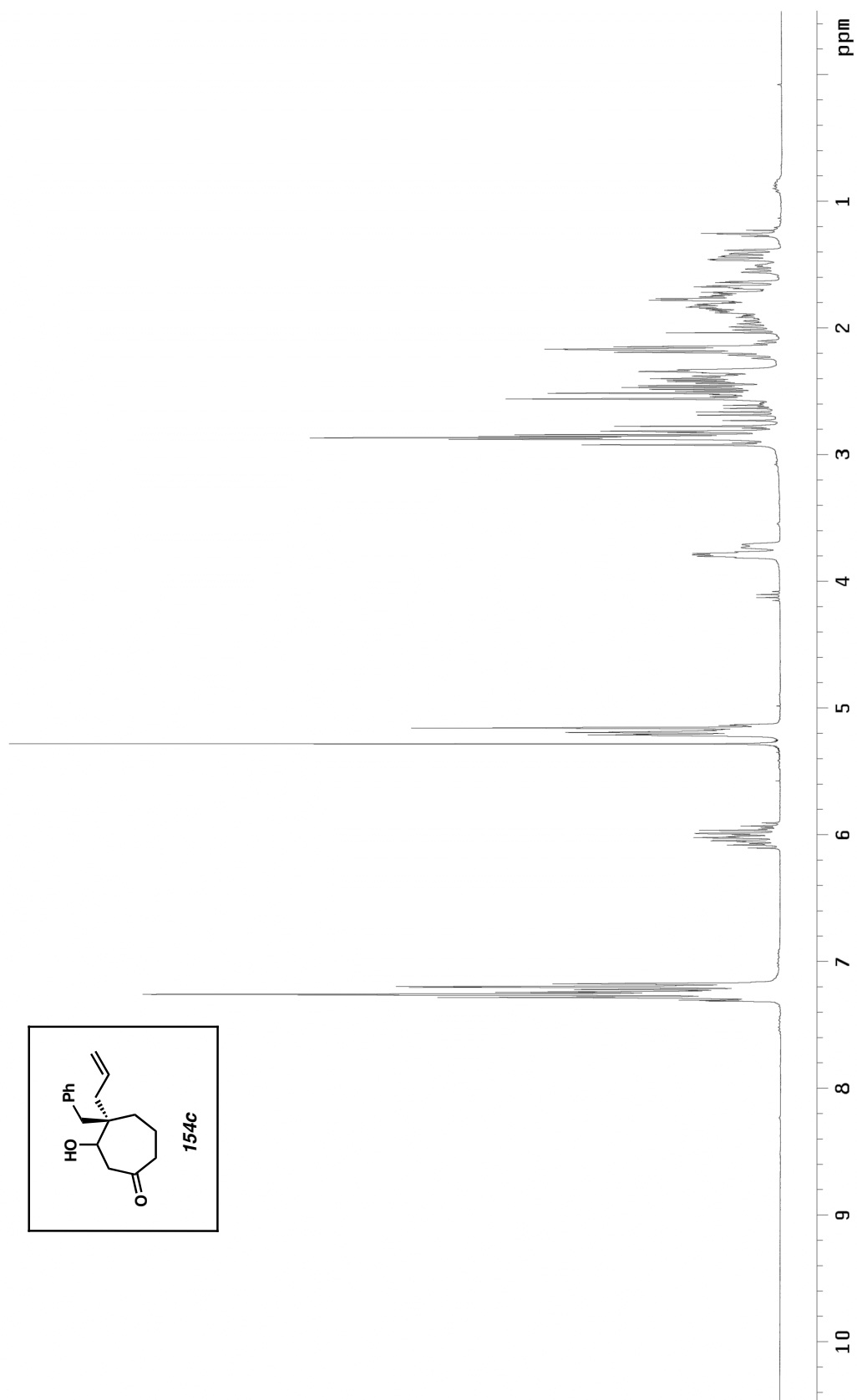


Figure A1.134. Infrared spectrum (thin film/NaCl) of compound **154b**.

Figure A1.135. ¹H NMR (300 MHz, CDCl₃) of compound **154c**.

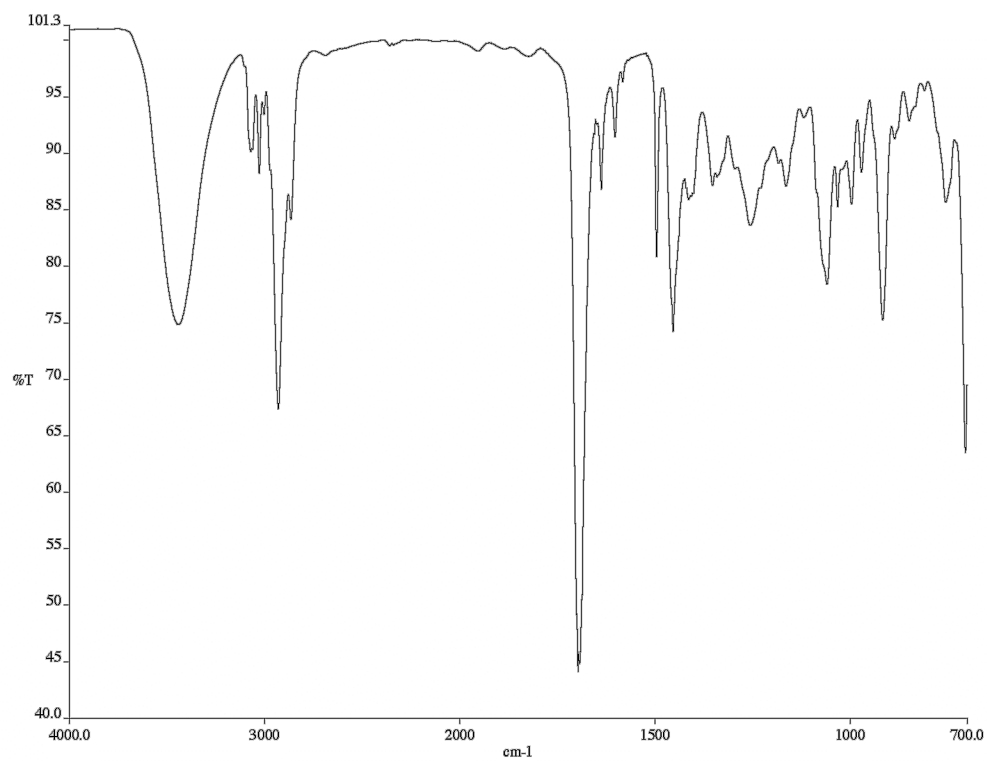
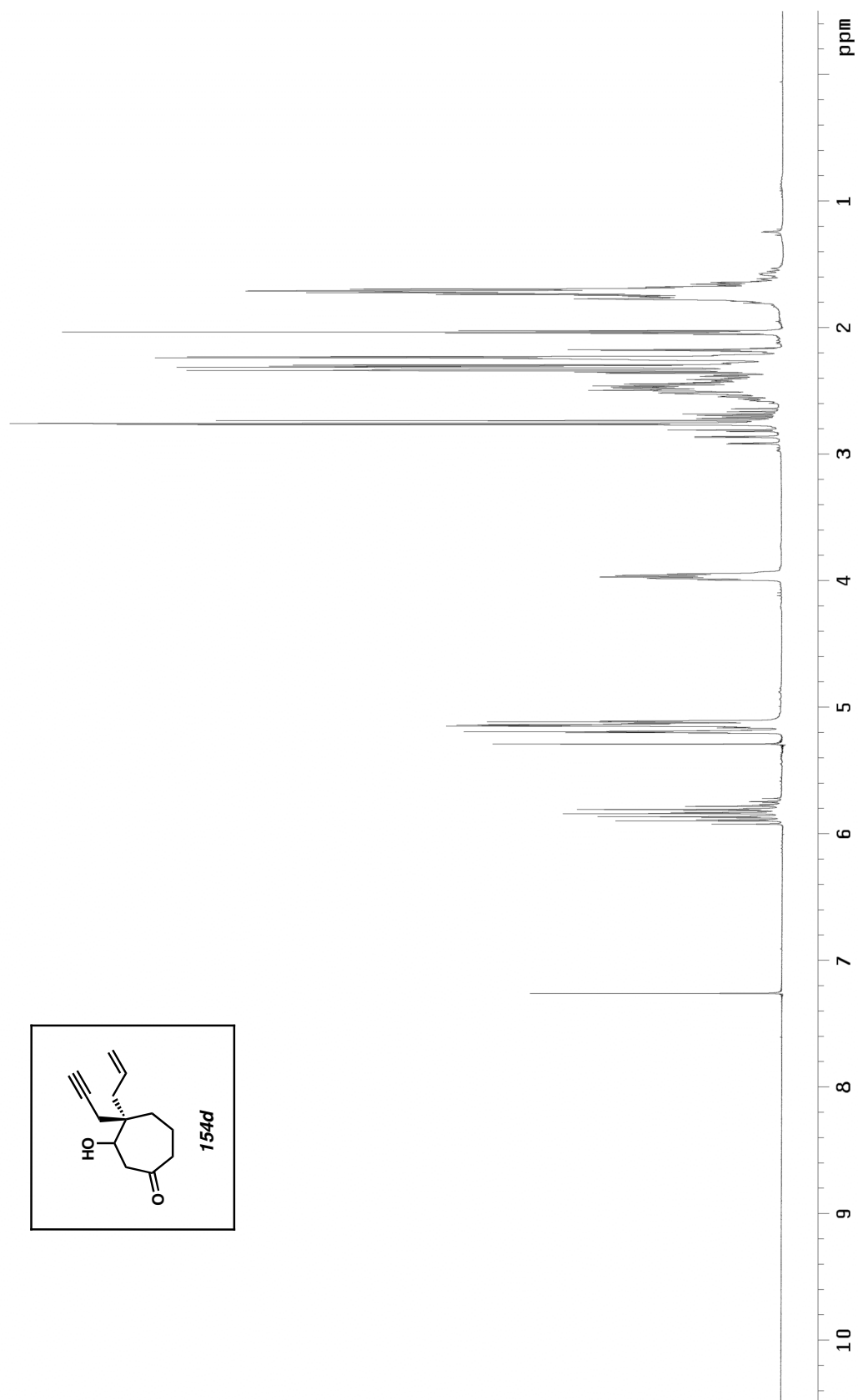


Figure A1.136. Infrared spectrum (thin film/NaCl) of compound **154c**.

Figure A1.137. ^1H NMR (300 MHz, CDCl_3) of compound **154d**.

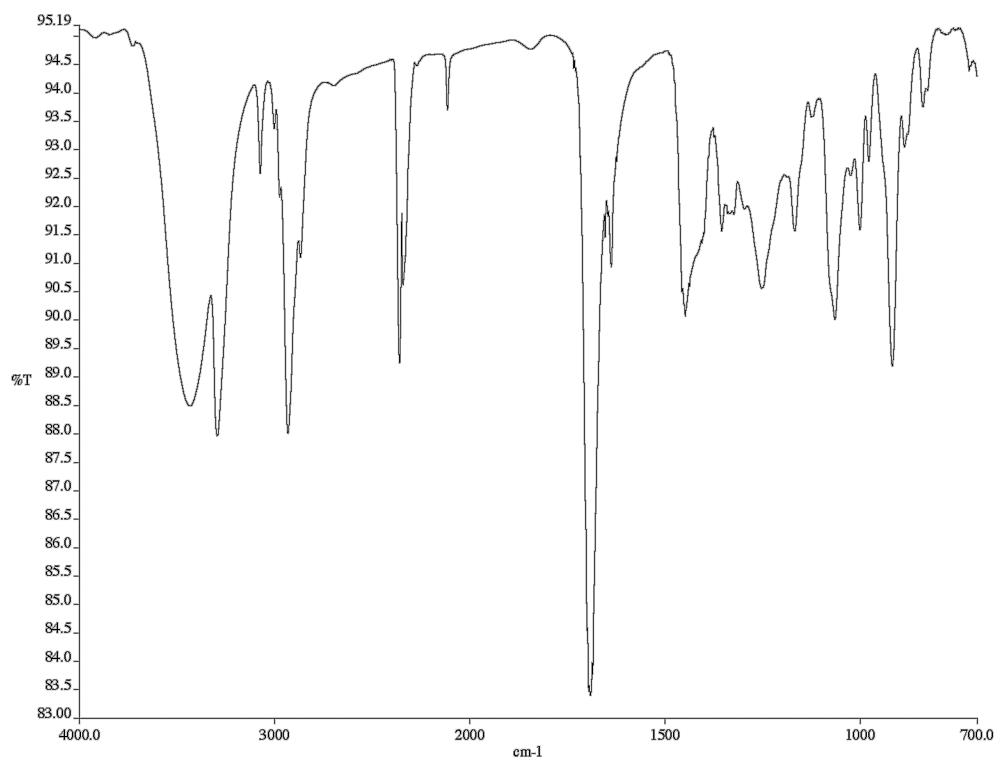


Figure A1.138. Infrared spectrum (thin film/NaCl) of compound **154d**.

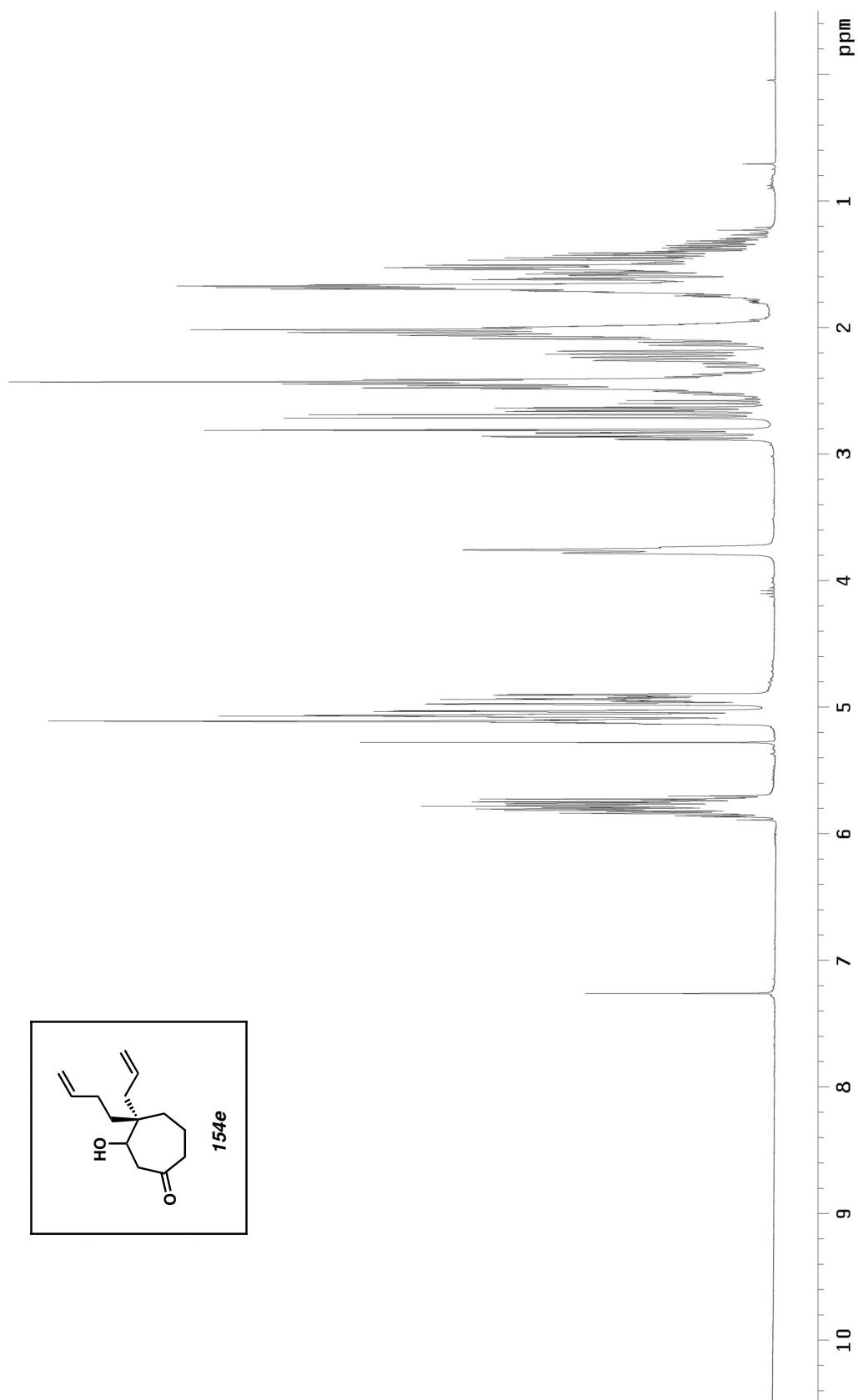


Figure A1.139. ^1H NMR (300 MHz, CDCl_3) of compound **154e**.

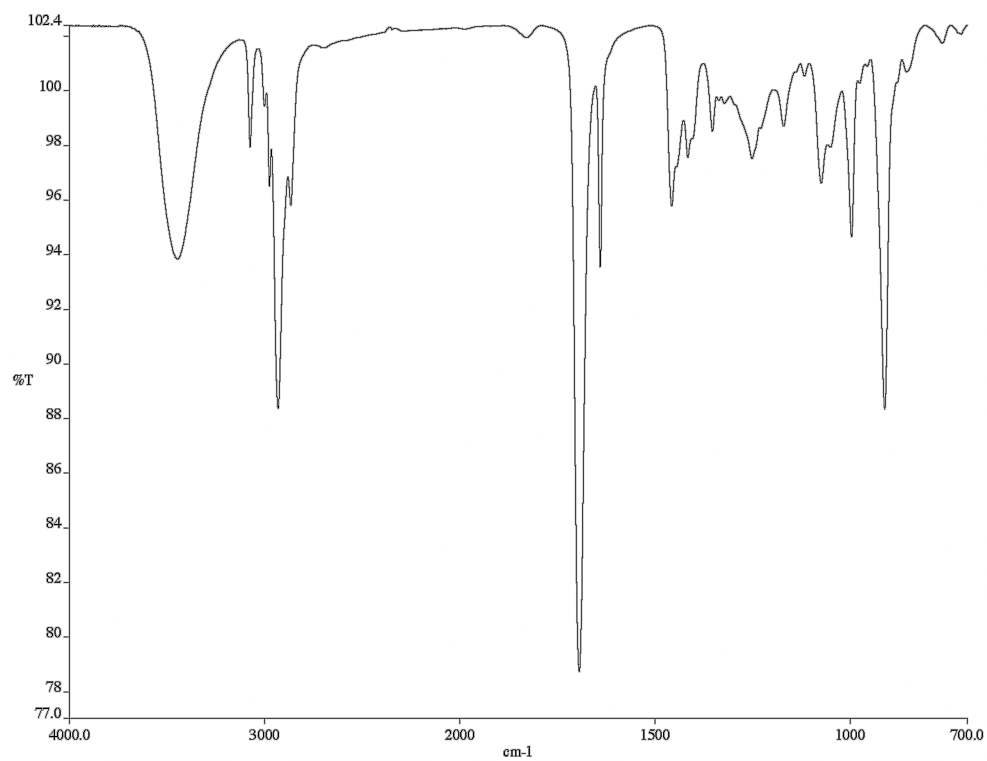


Figure A1.140. Infrared spectrum (thin film/NaCl) of compound **154e**.

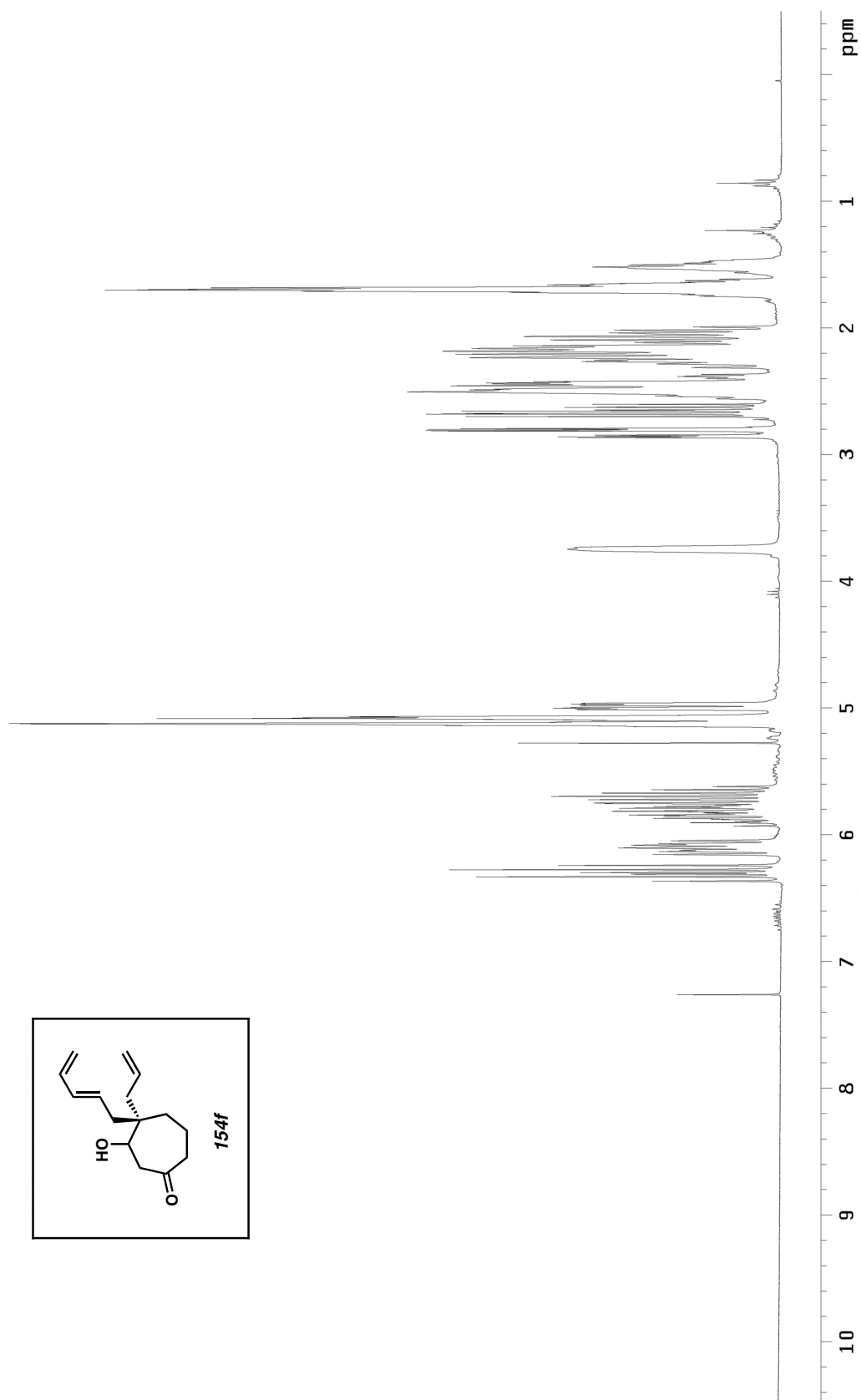


Figure A1.141. ^1H NMR (300 MHz, CDCl_3) of compound **154f**.

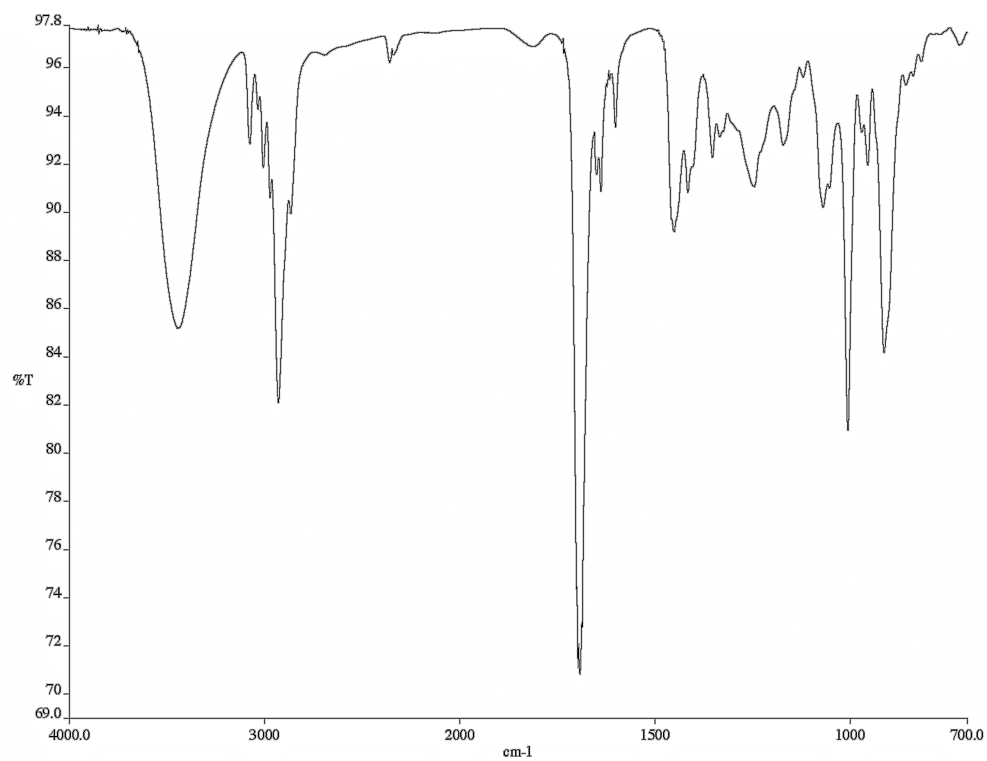
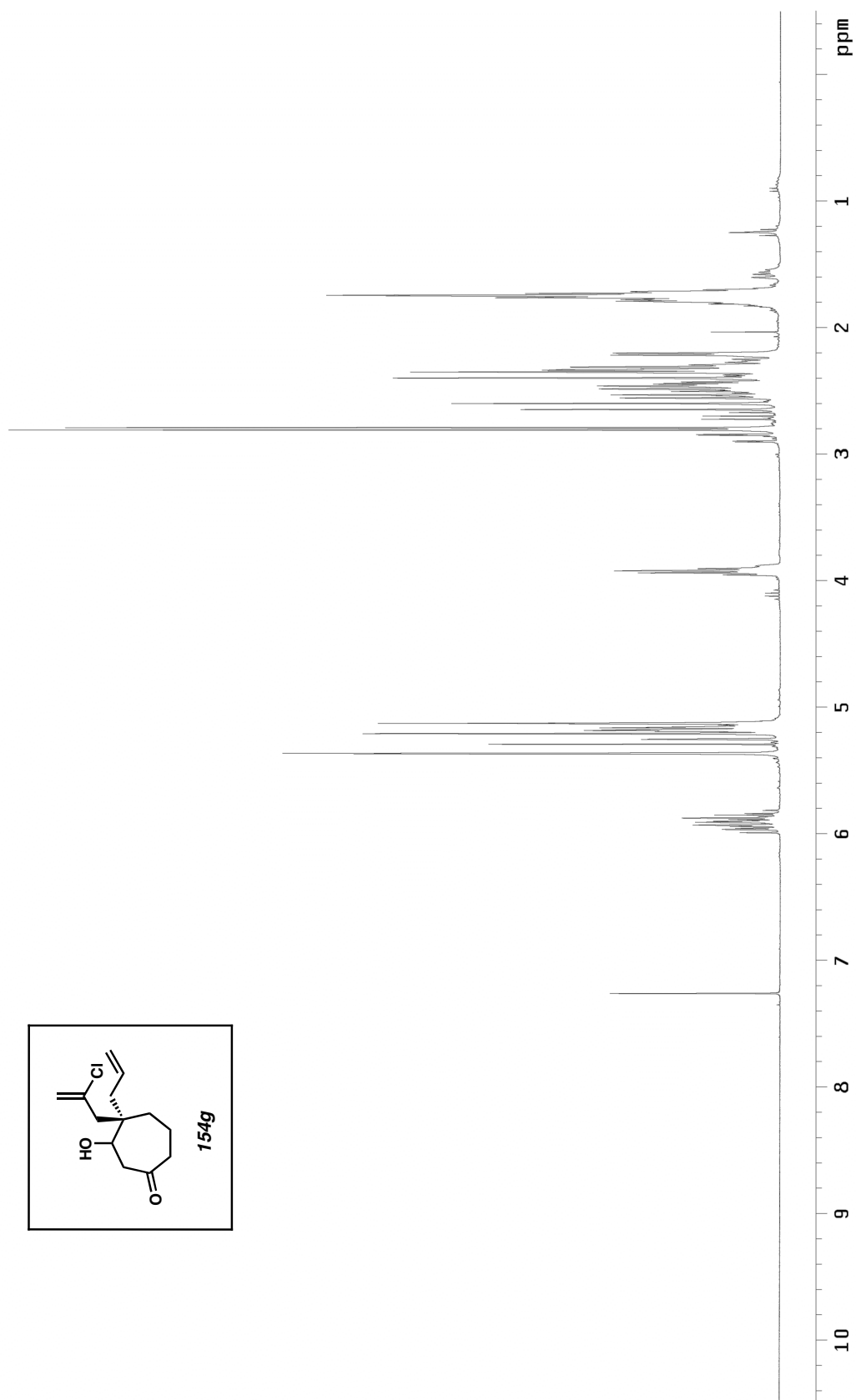


Figure A1.142. Infrared spectrum (thin film/NaCl) of compound **154f**.

Figure A1.143. ^1H NMR (300 MHz, CDCl_3) of compound **154g**.

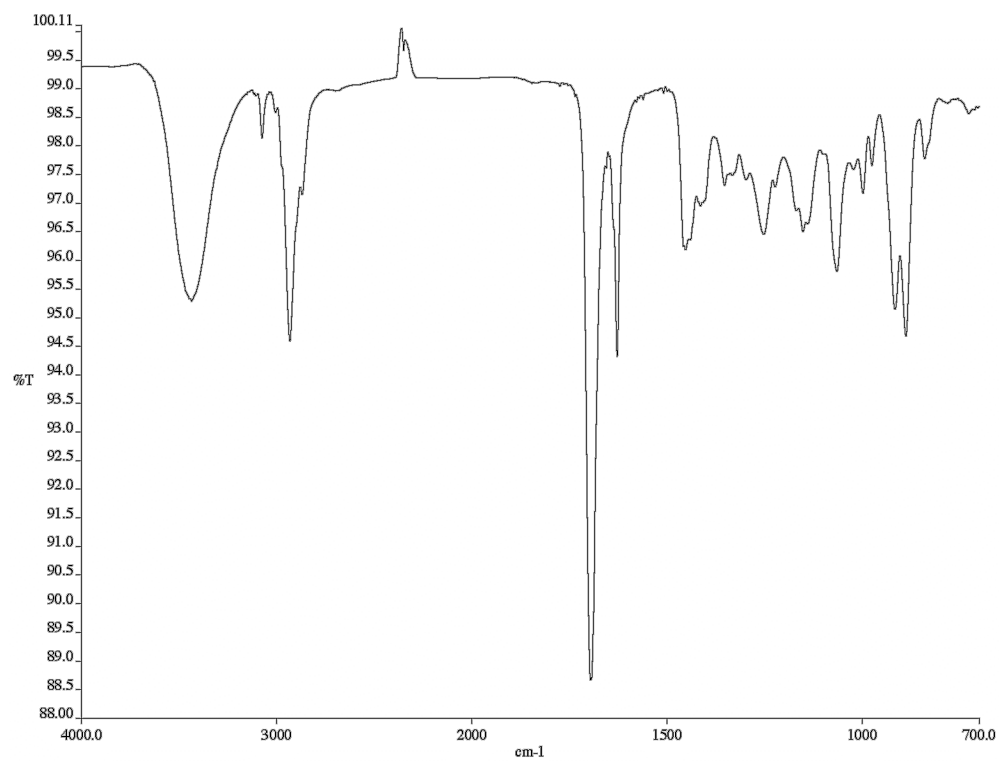
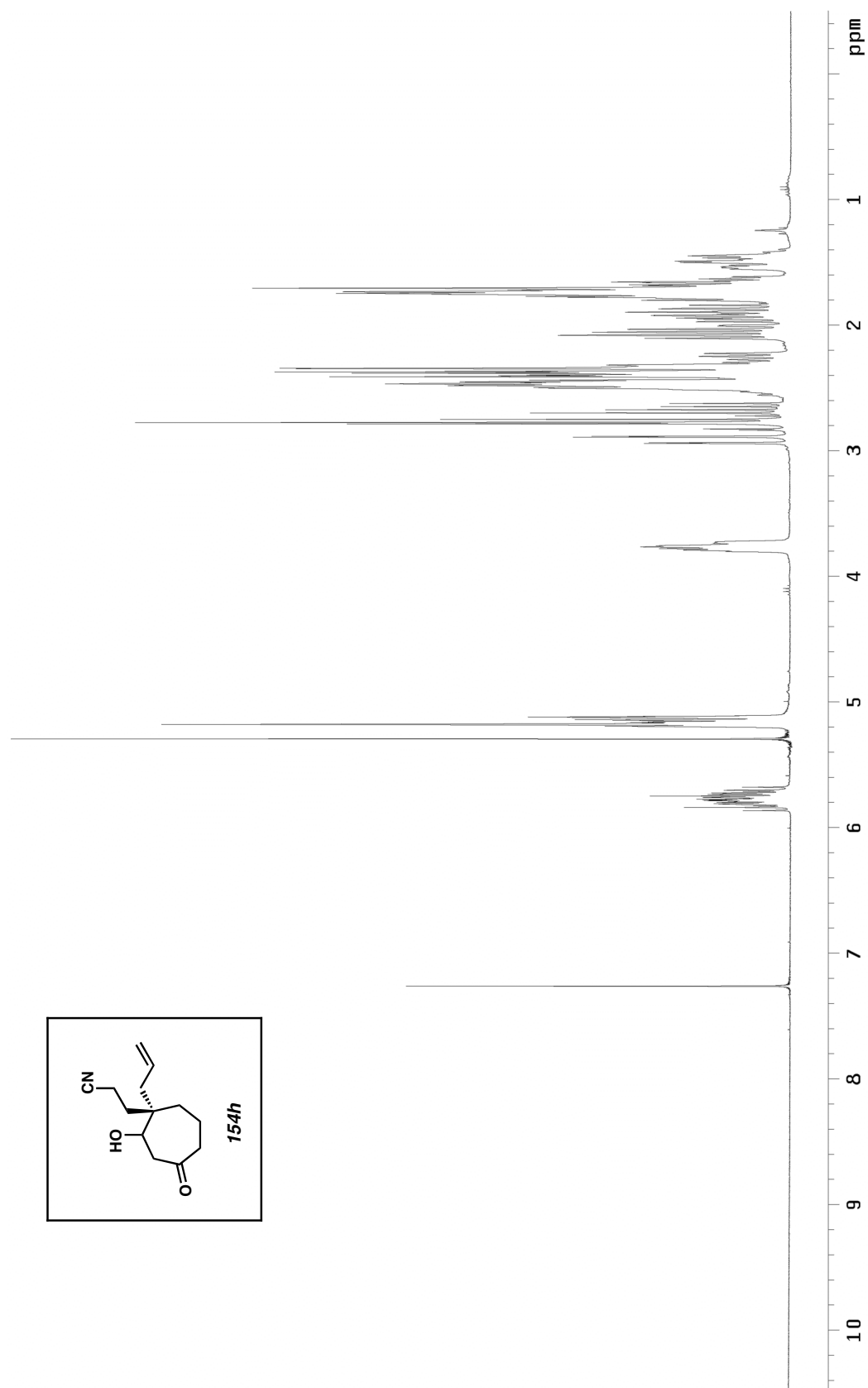


Figure A1.144. Infrared spectrum (thin film/NaCl) of compound **154g**.

Figure A1.145. ¹H NMR (300 MHz, CDCl₃) of compound **154h**.

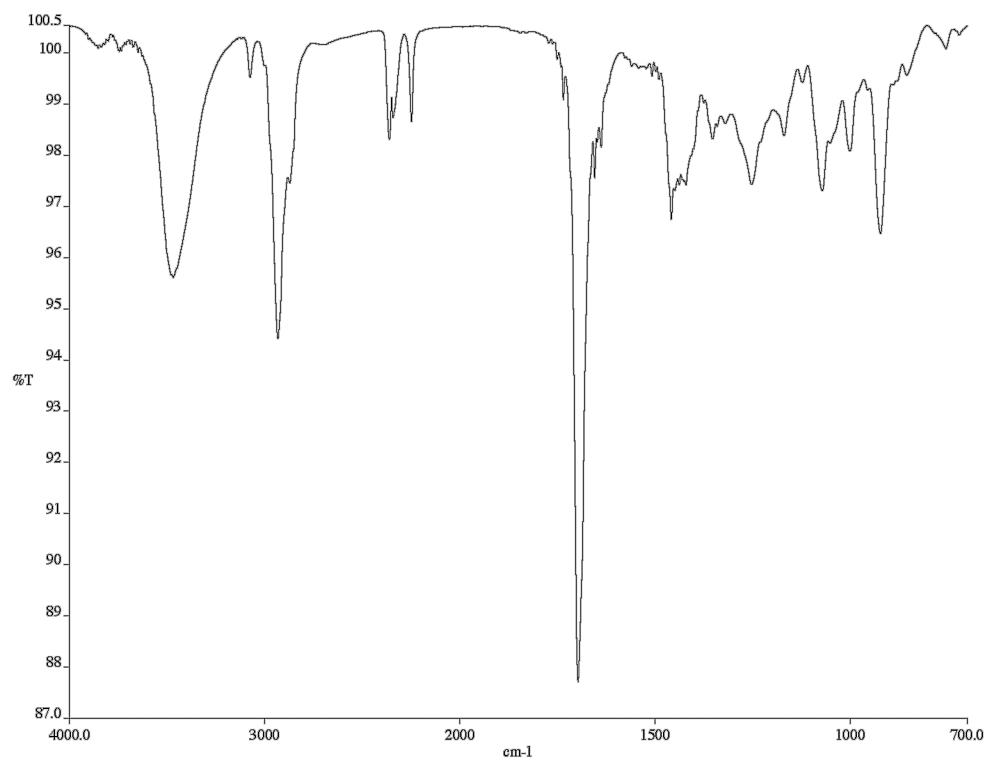


Figure A1.146. Infrared spectrum (thin film/NaCl) of compound **154h**.

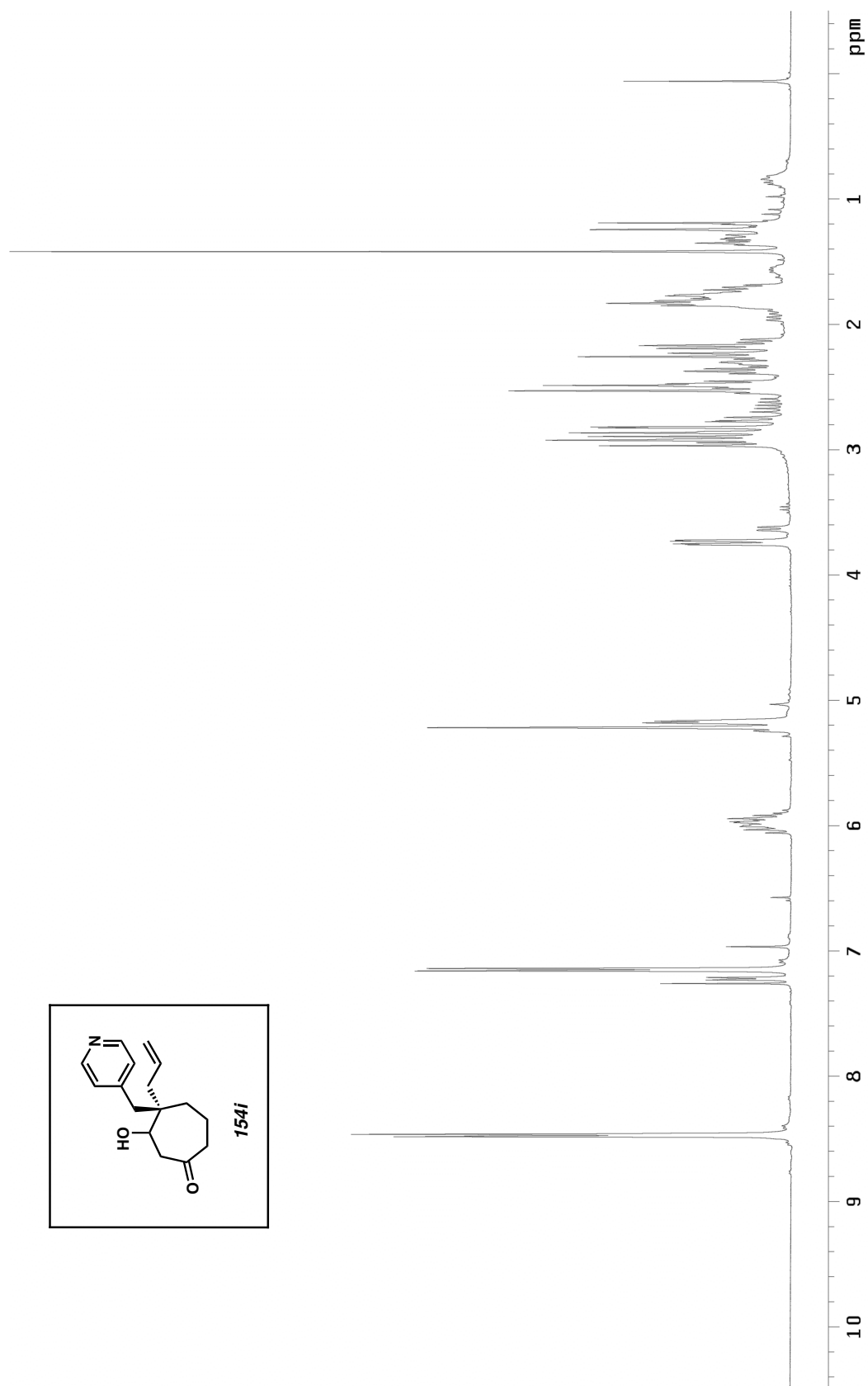


Figure A1.147. ¹H NMR (300 MHz, CDCl₃) of compound **154i**.

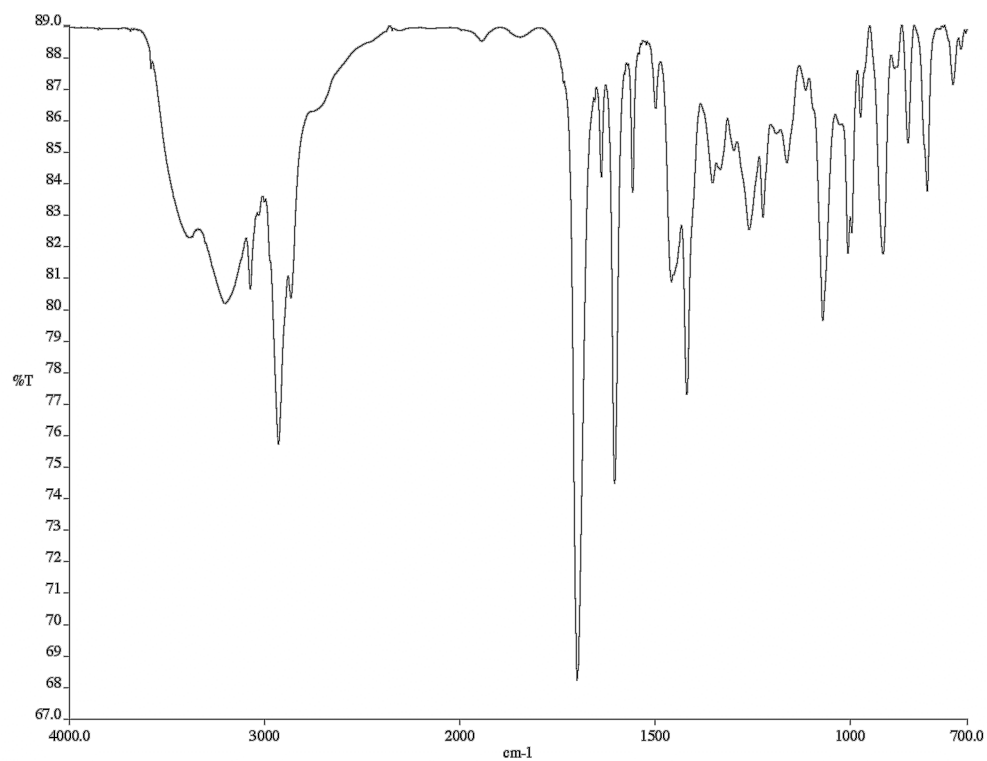


Figure A1.148. Infrared spectrum (thin film/NaCl) of compound **154i**.

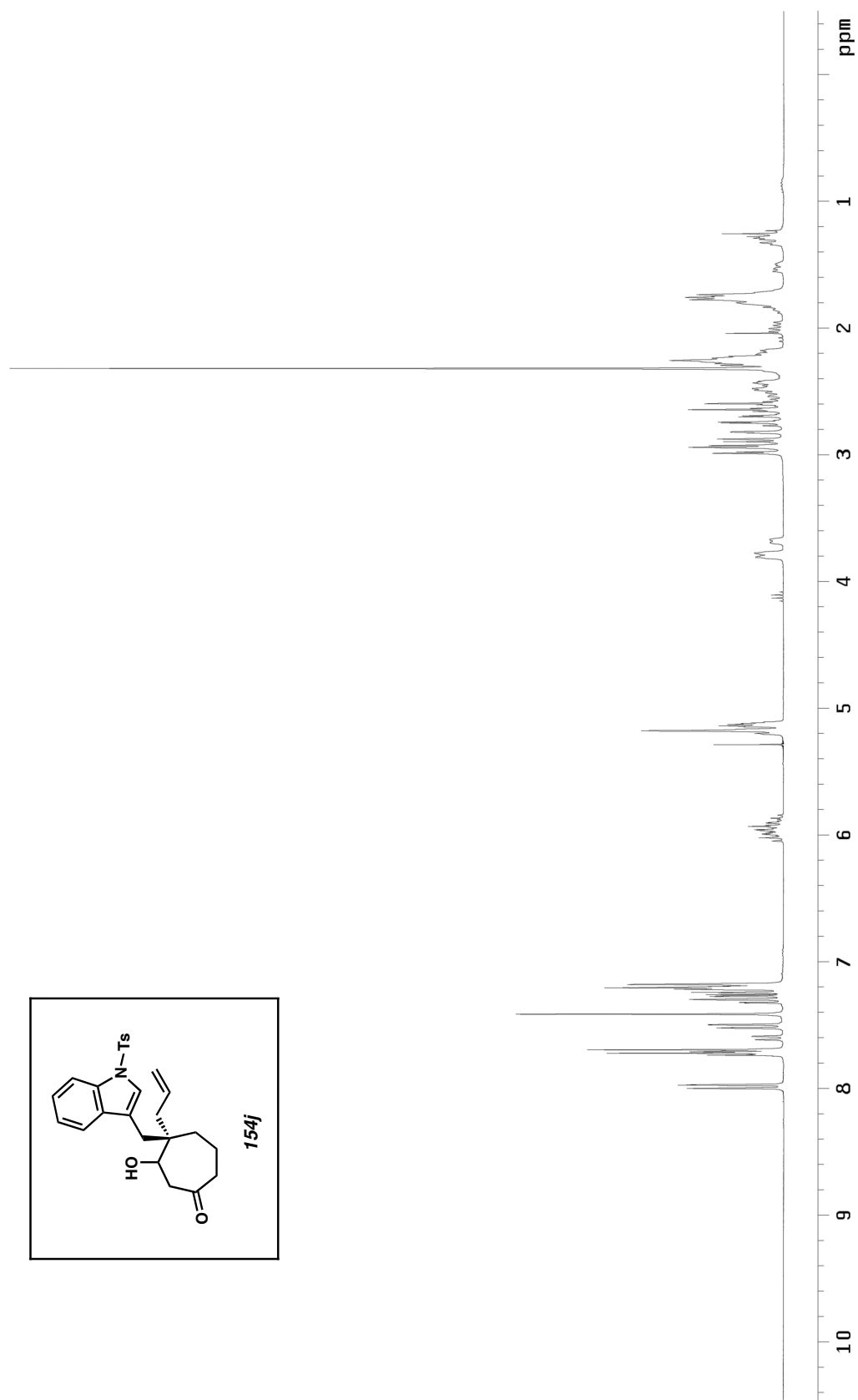


Figure A1.149. ^1H NMR (300 MHz, CDCl_3) of compound **154j**.

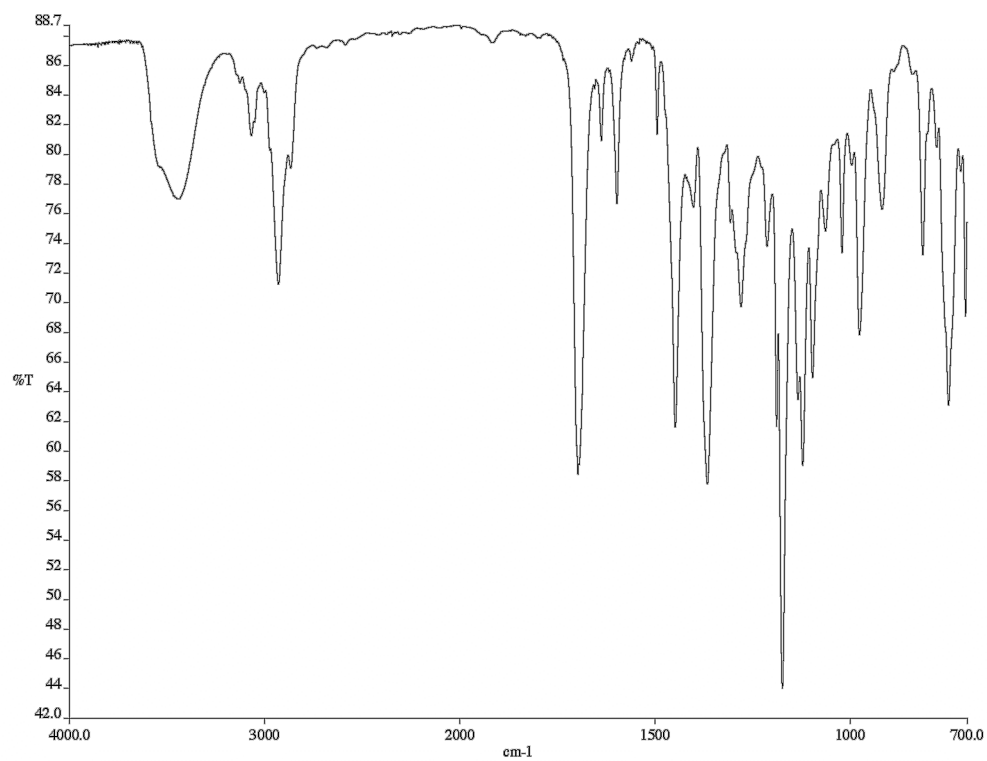


Figure A1.150. Infrared spectrum (thin film/NaCl) of compound **154j**.

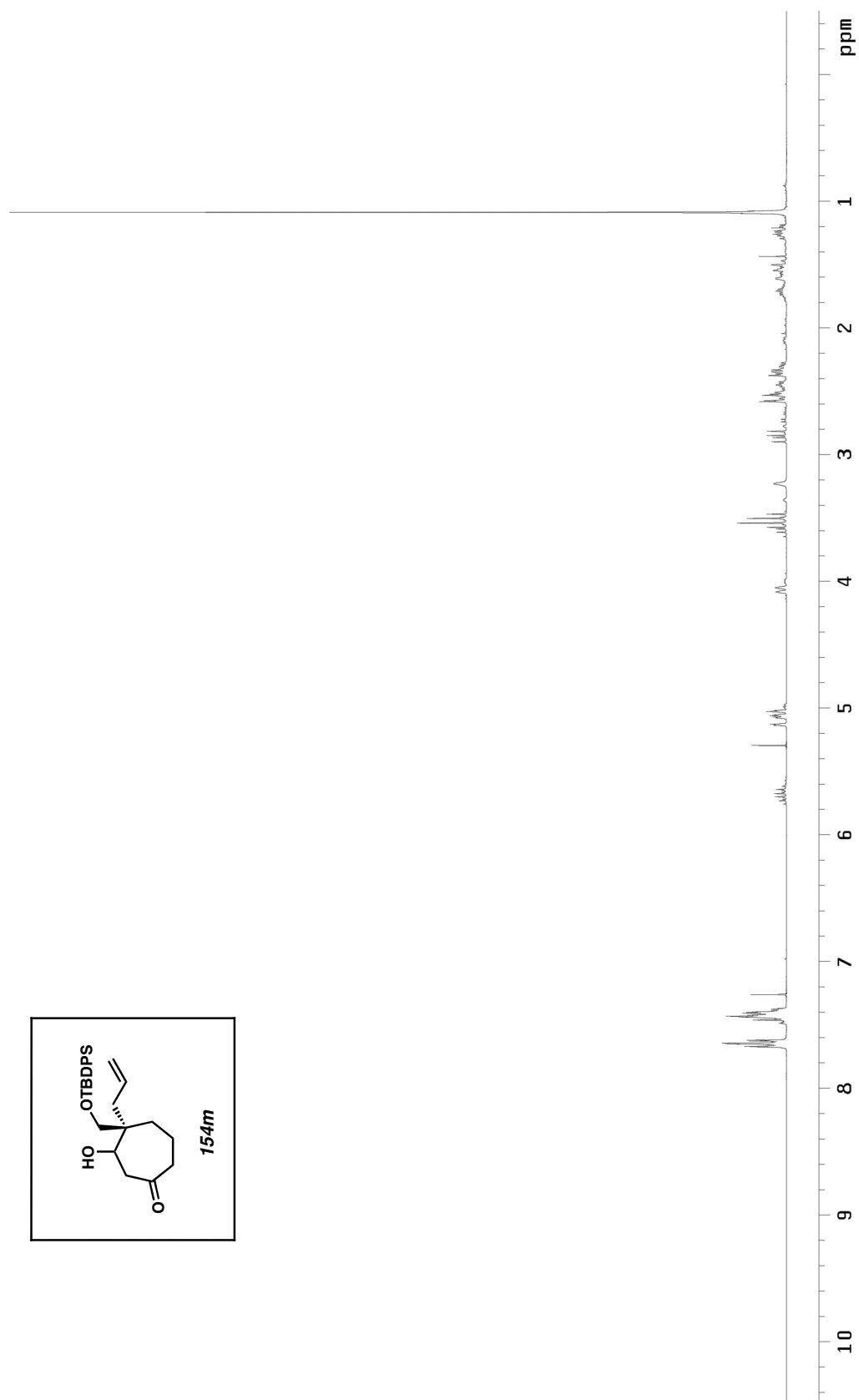


Figure A1.151. ¹H NMR (300 MHz, CDCl₃) of compound **154m**.

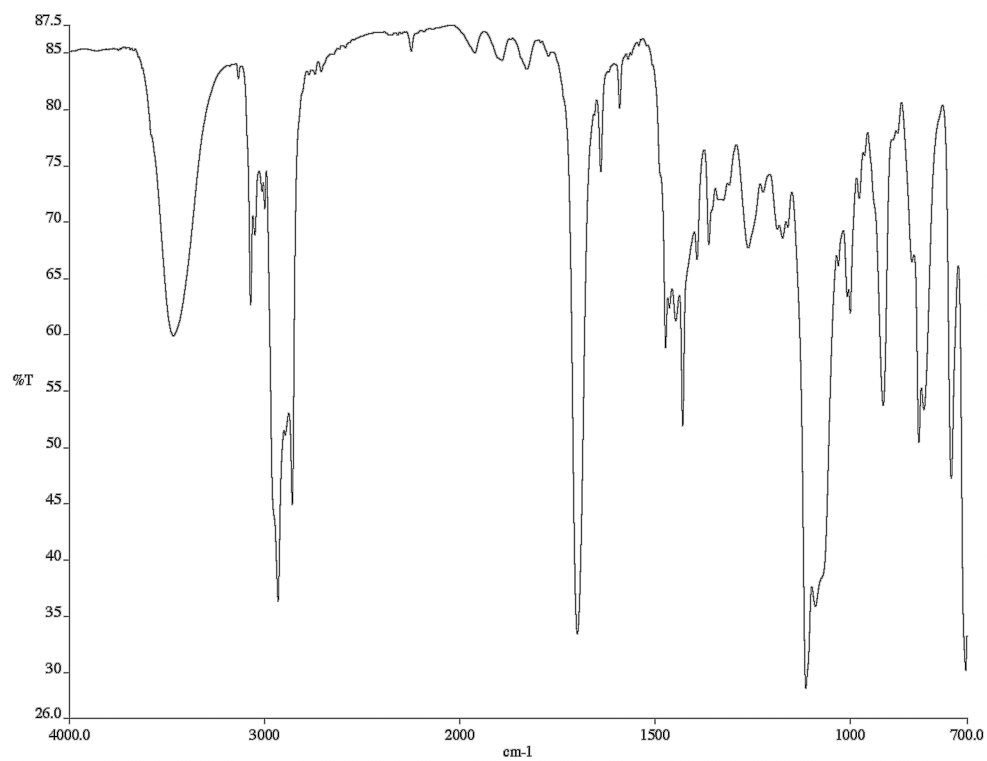
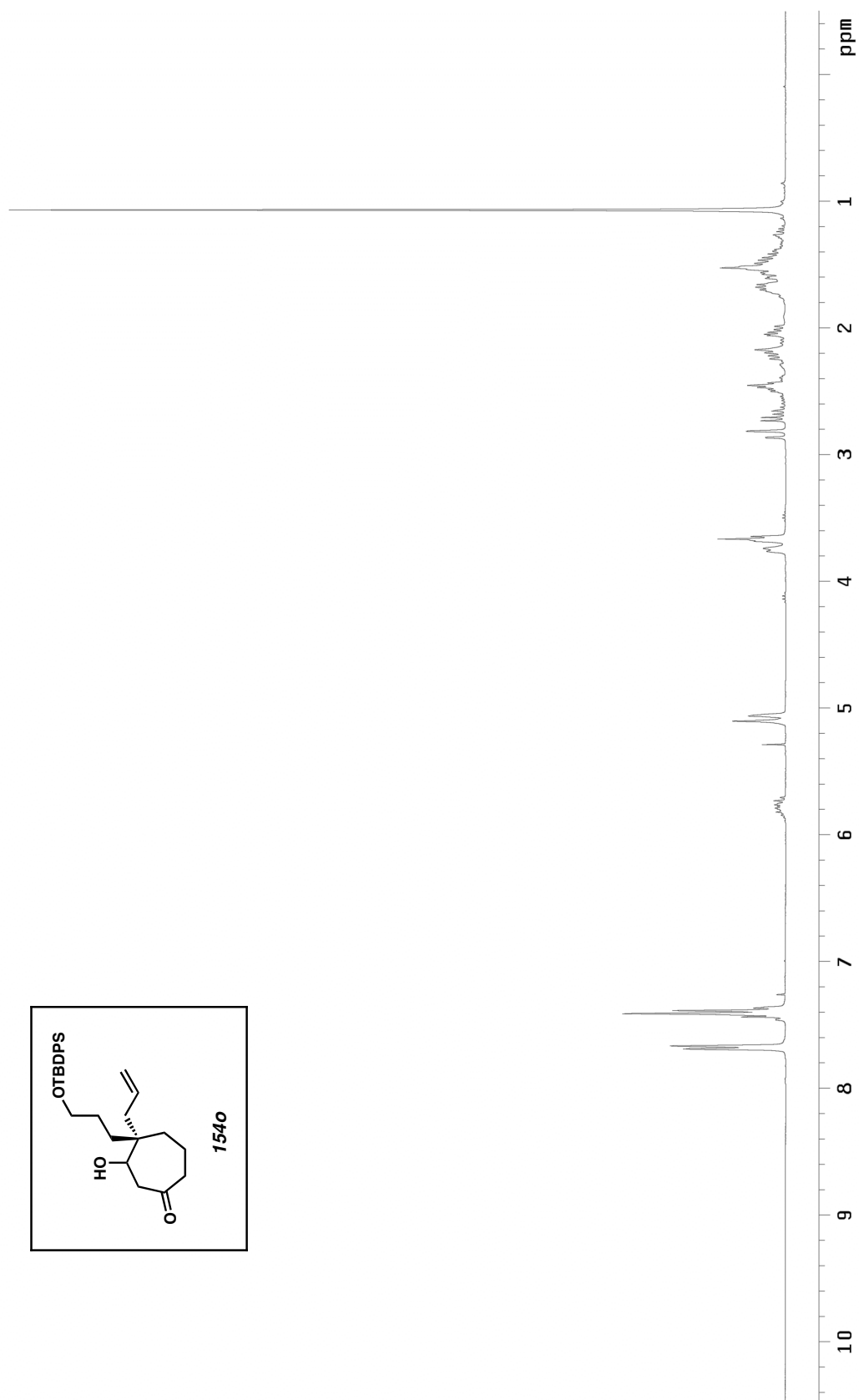


Figure A1.152. Infrared spectrum (thin film/NaCl) of compound **154m**.

Figure A1.153. ¹H NMR (300 MHz, CDCl₃) of compound **154o**.

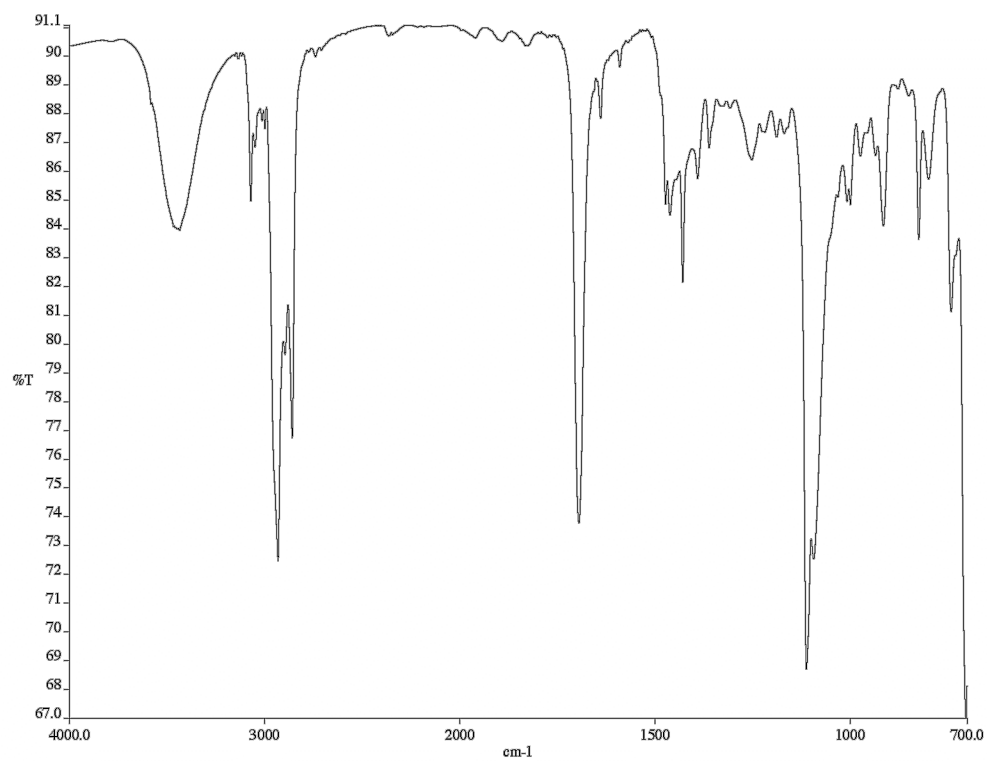


Figure A1.154. Infrared spectrum (thin film/NaCl) of compound **154o**.

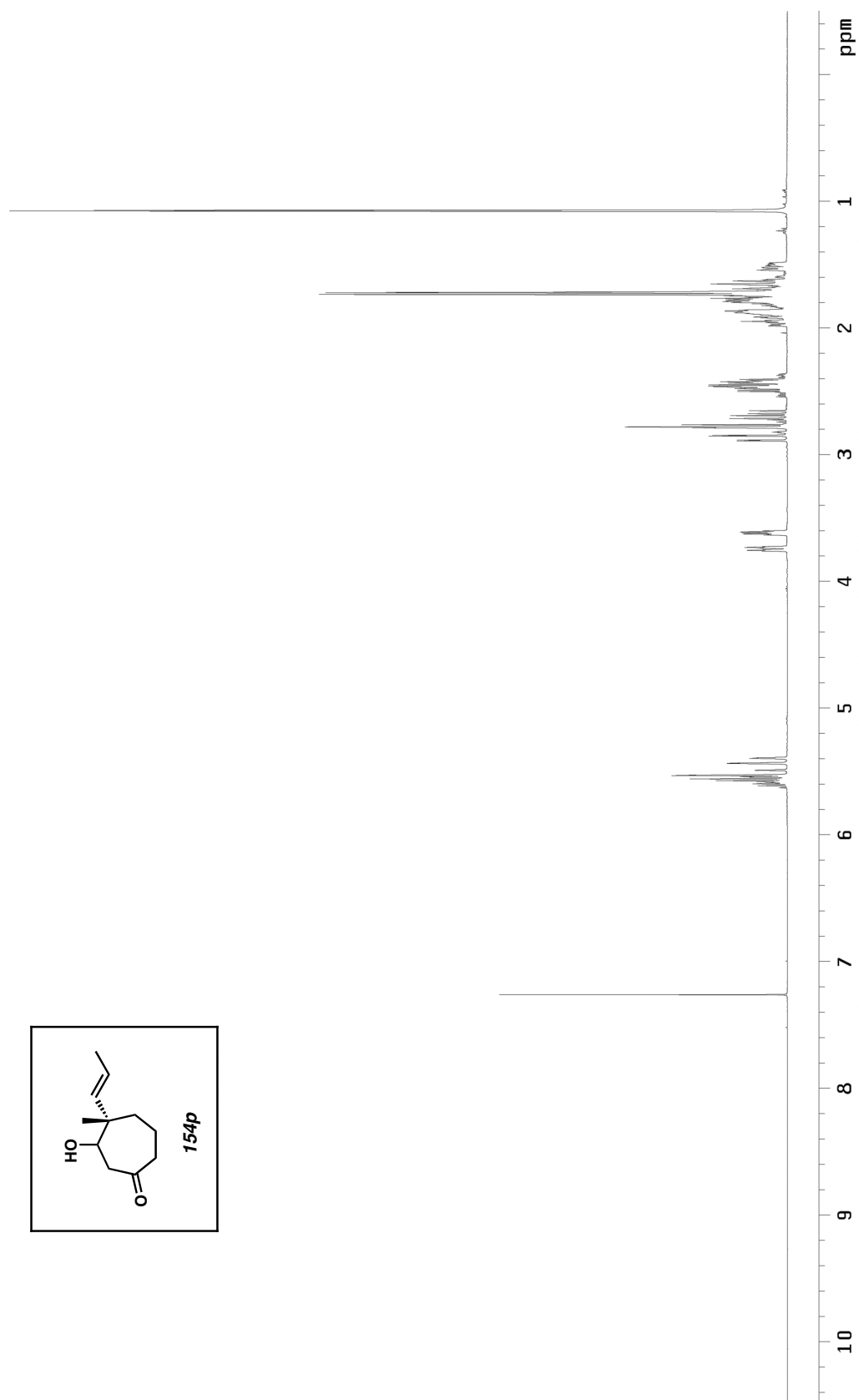


Figure A1.155. ¹H NMR (400 MHz, CDCl₃) of compound **154p**.

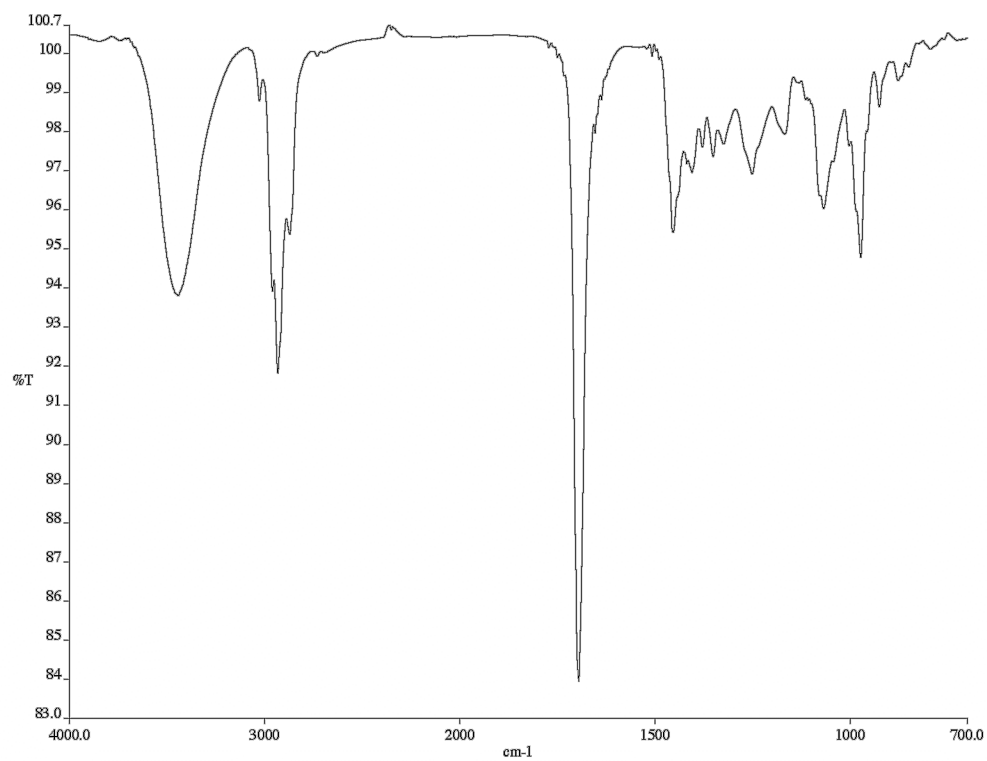
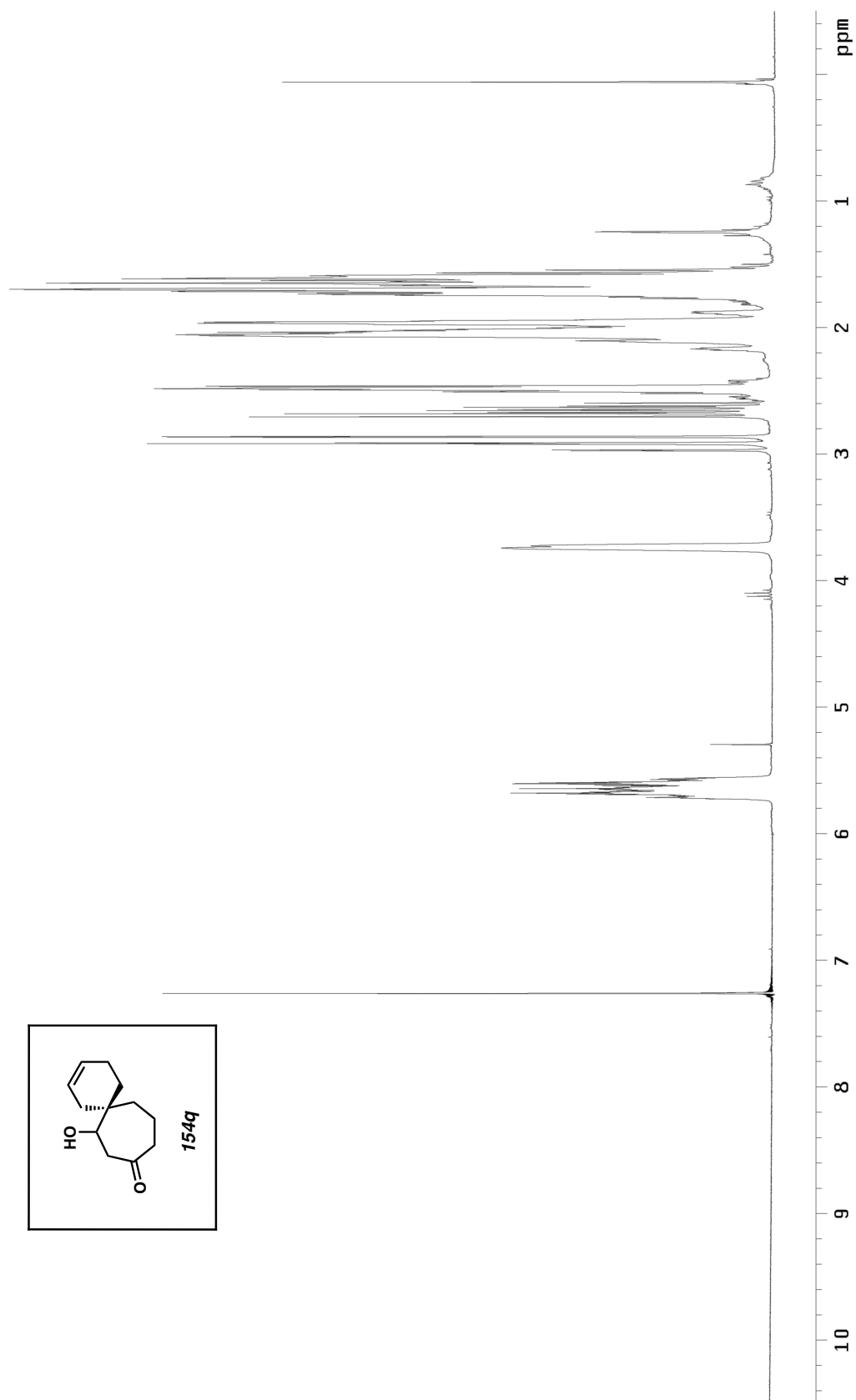


Figure A1.156. Infrared spectrum (thin film/NaCl) of compound **154p**.

Figure A1.157. ^1H NMR (300 MHz, CDCl_3) of compound **154q**.

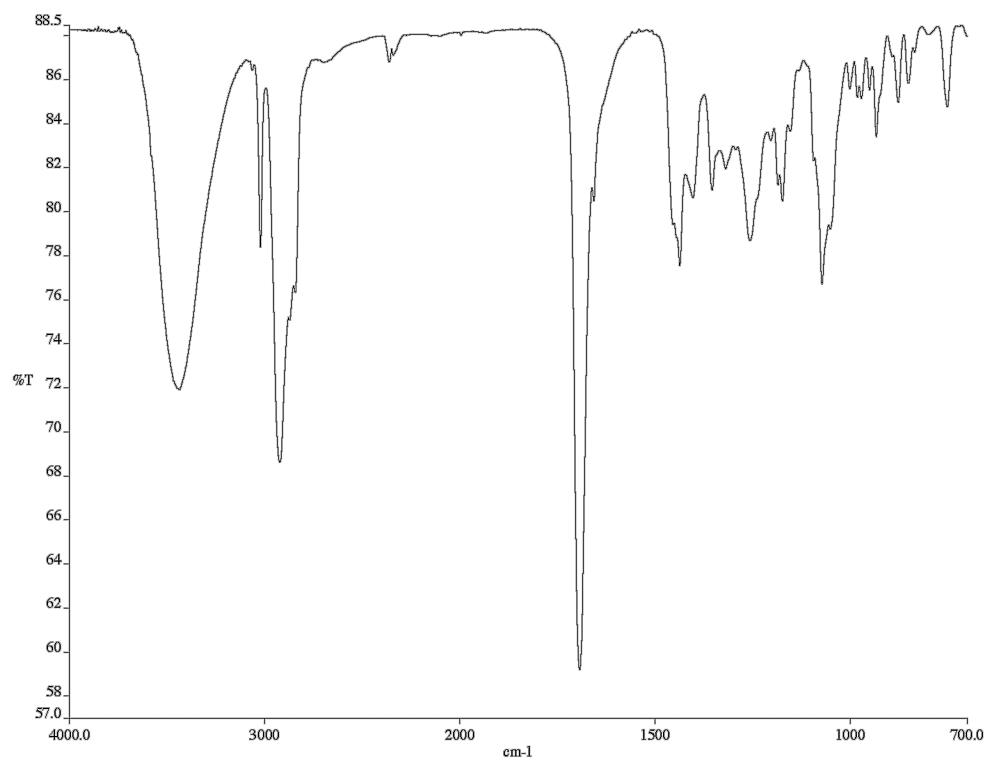


Figure A1.158. Infrared spectrum (thin film/NaCl) of compound **154q**.

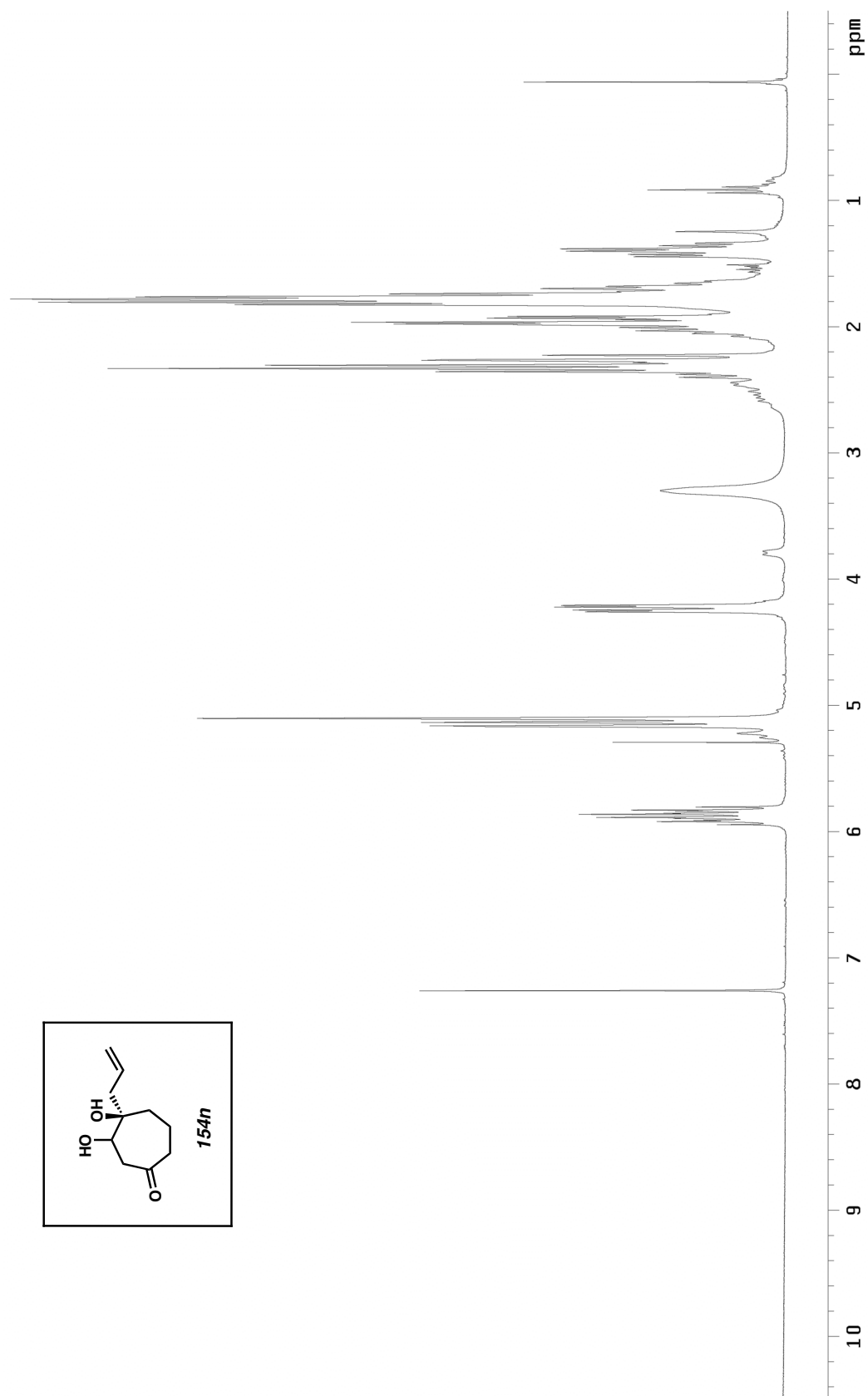


Figure A1.159. ¹H NMR (300 MHz, CDCl₃) of compound **154n**.

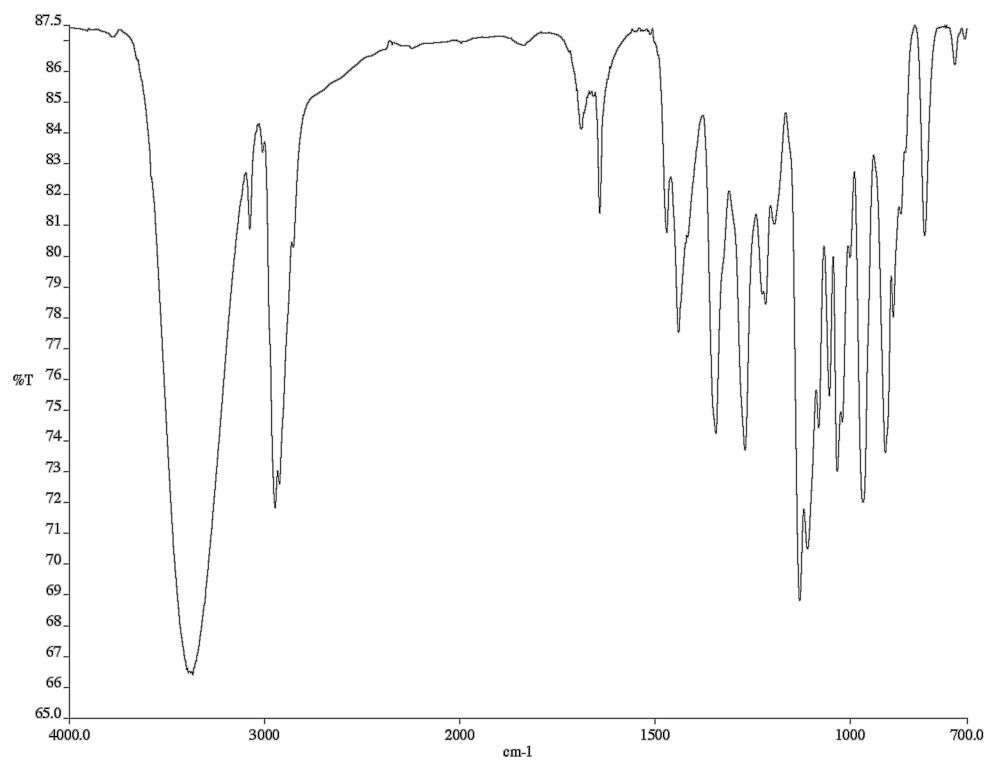


Figure A1.160. Infrared spectrum (thin film/NaCl) of compound **154n**.

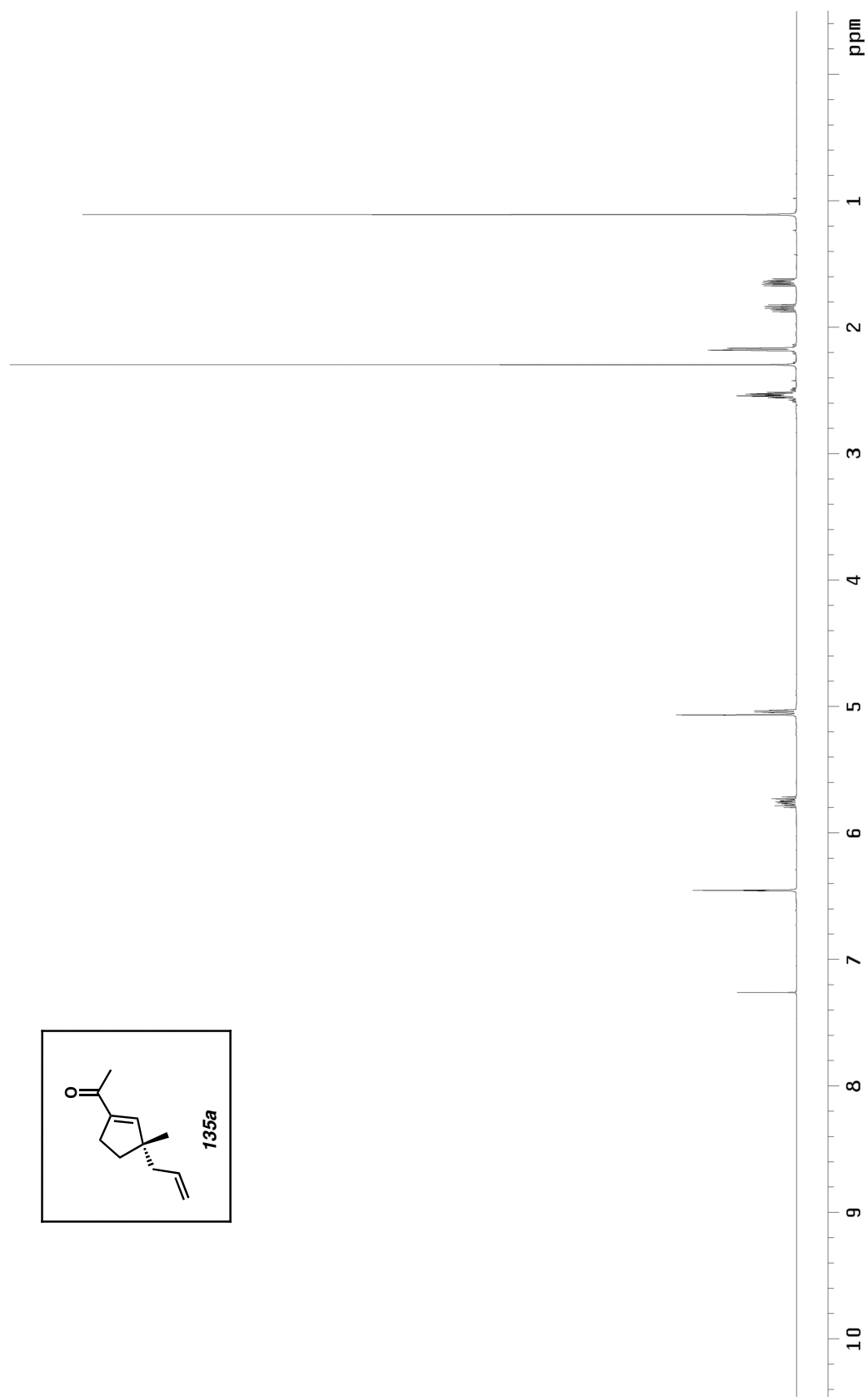


Figure A1.161. ^1H NMR (500 MHz, CDCl_3) of compound **135a**.

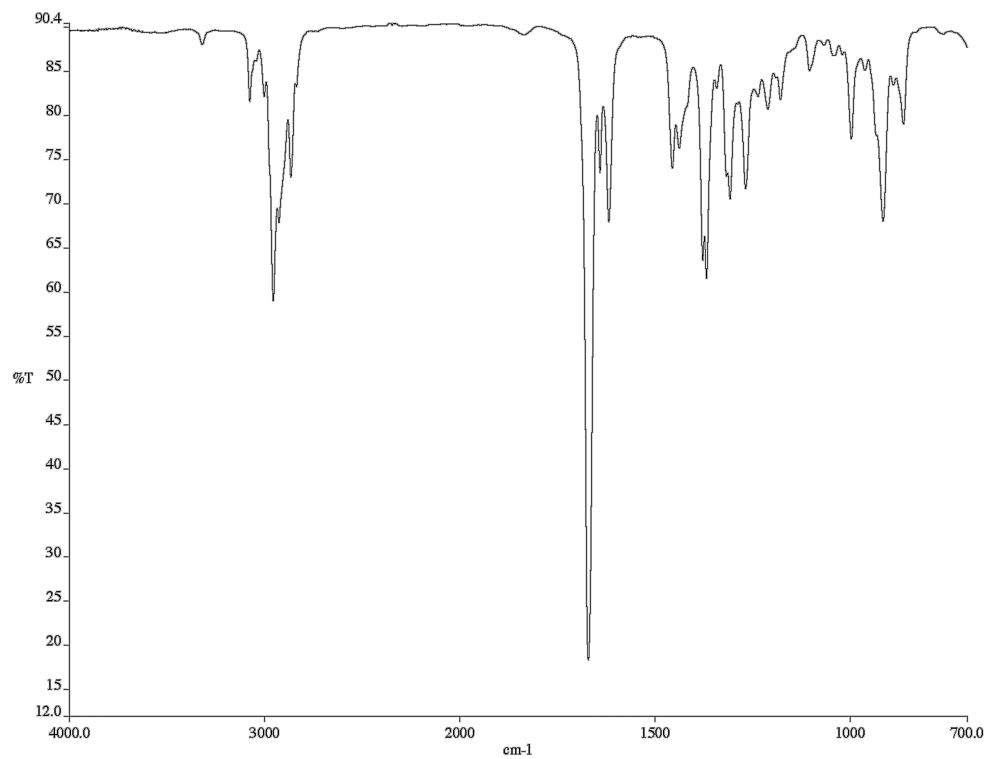


Figure A1.162. Infrared spectrum (thin film/NaCl) of compound **135a**.

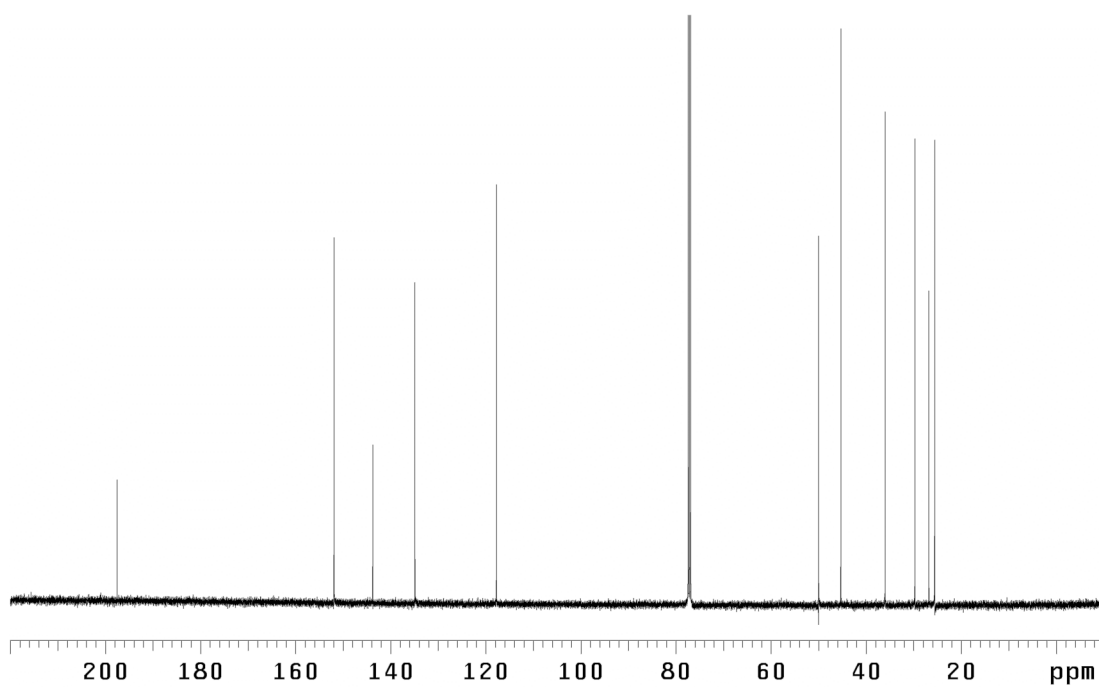


Figure A1.163. ¹³C NMR (125 MHz, CDCl₃) of compound **135a**.

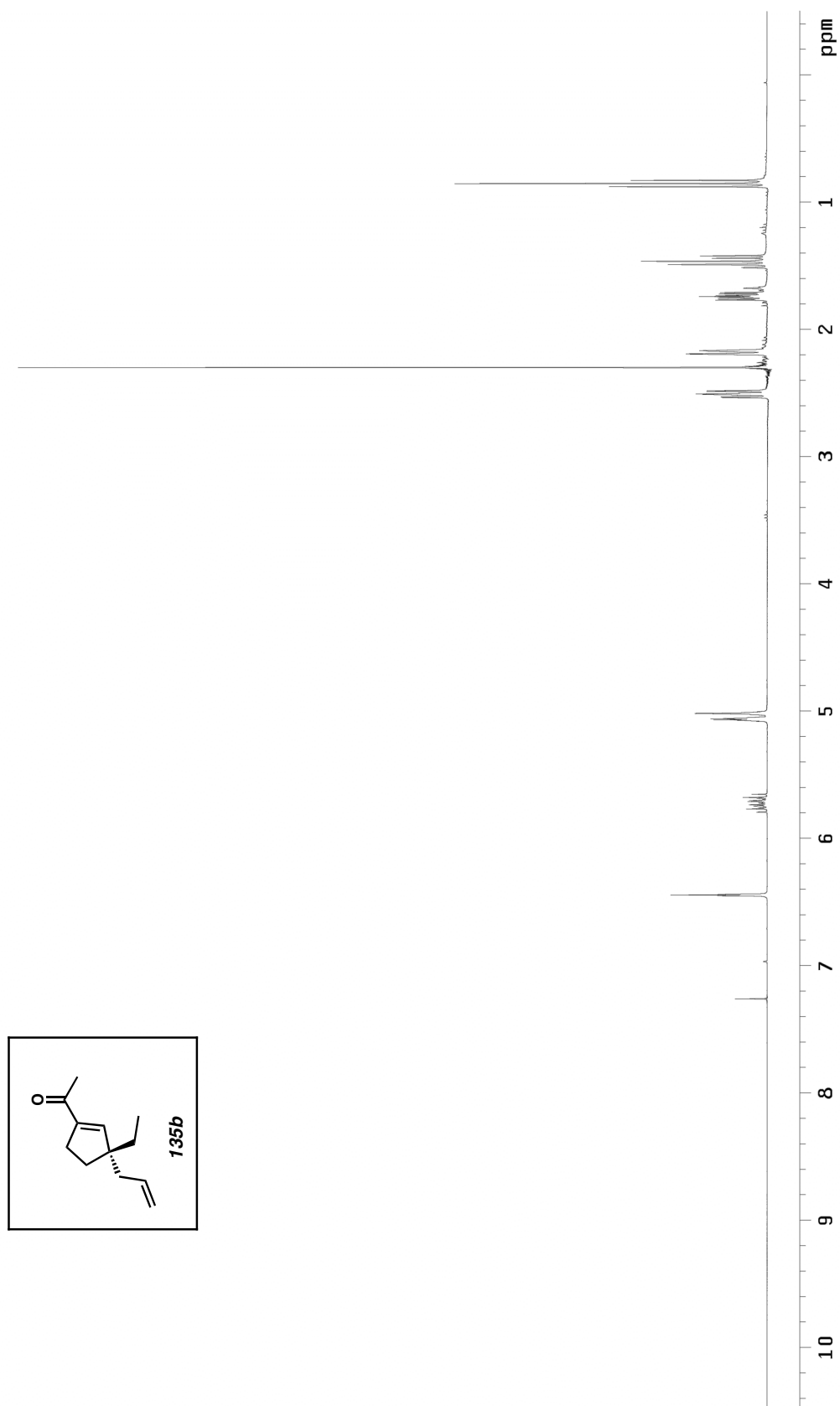


Figure A1.164. ^1H NMR (300 MHz, CDCl_3) of compound **135b**.

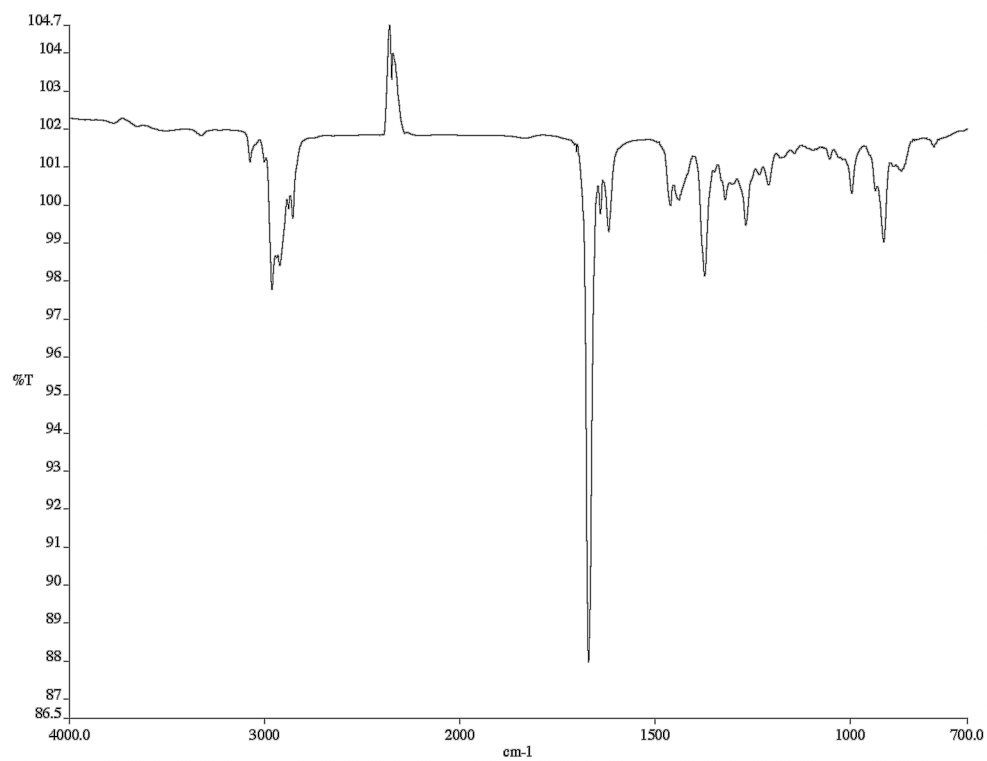


Figure A1.165. Infrared spectrum (thin film/NaCl) of compound **135b**.

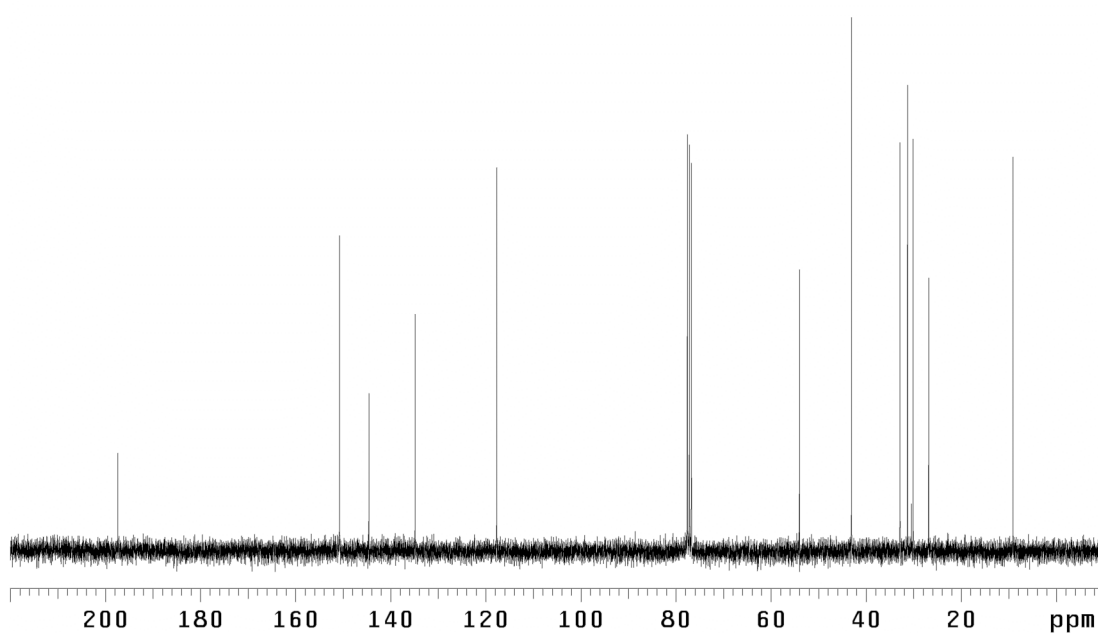


Figure A1.166. ¹³C NMR (75 MHz, CDCl₃) of compound **135b**.

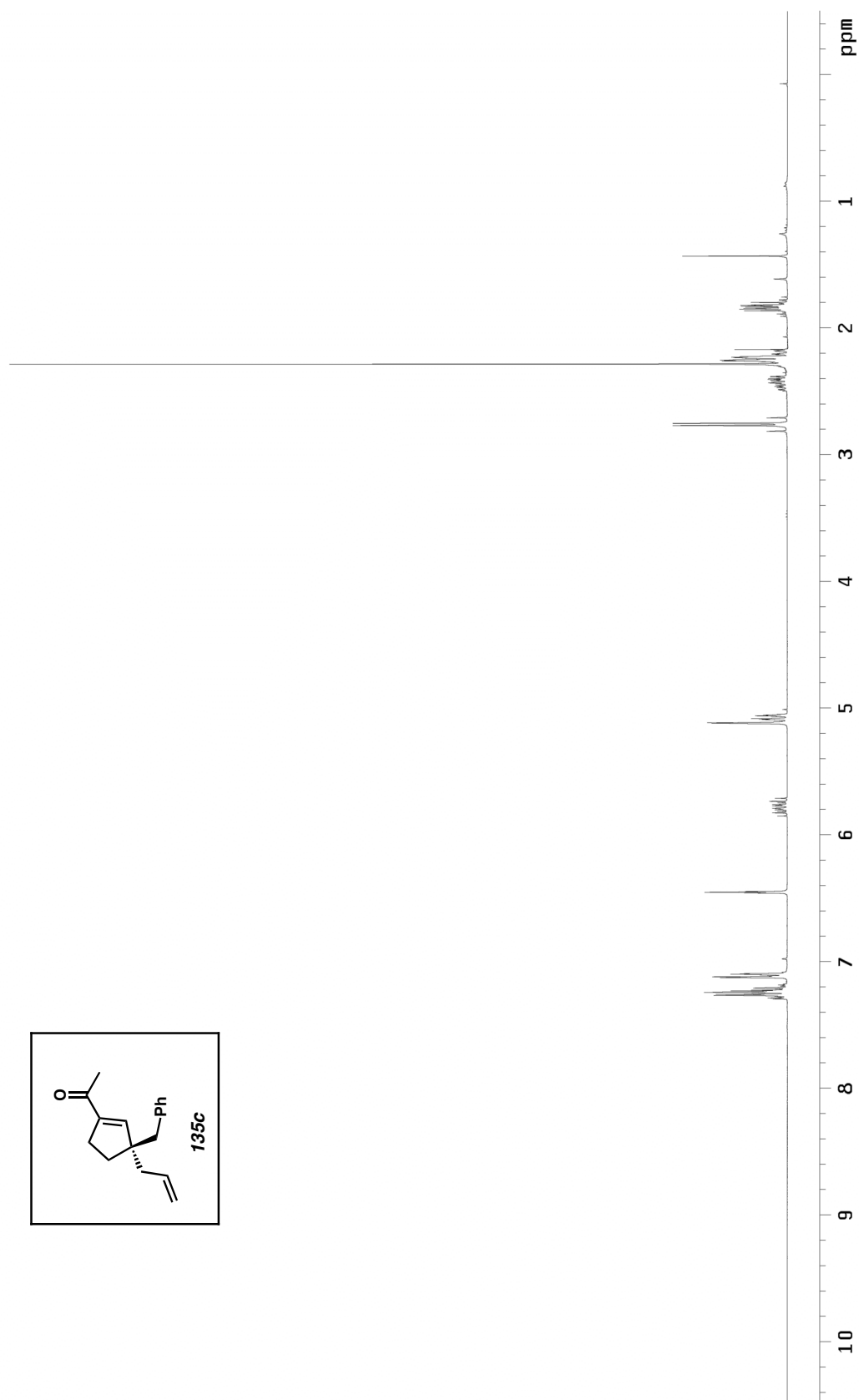


Figure A1.167. ^1H NMR (300 MHz, CDCl_3) of compound **135c**.

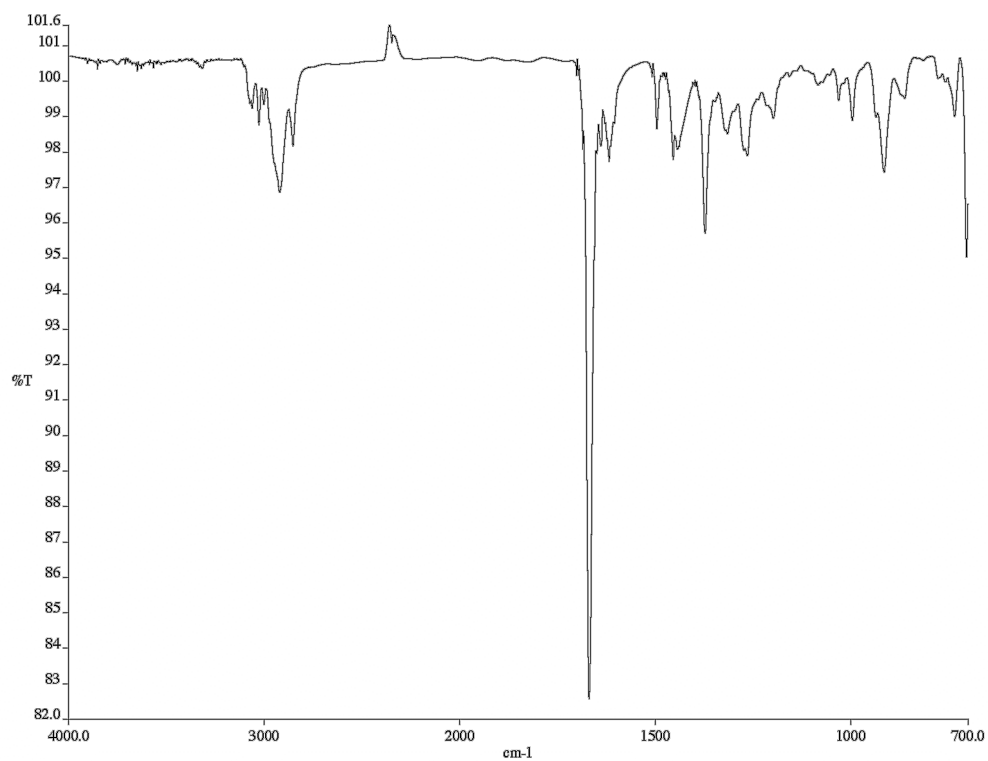


Figure A1.168. Infrared spectrum (thin film/NaCl) of compound **135c**.

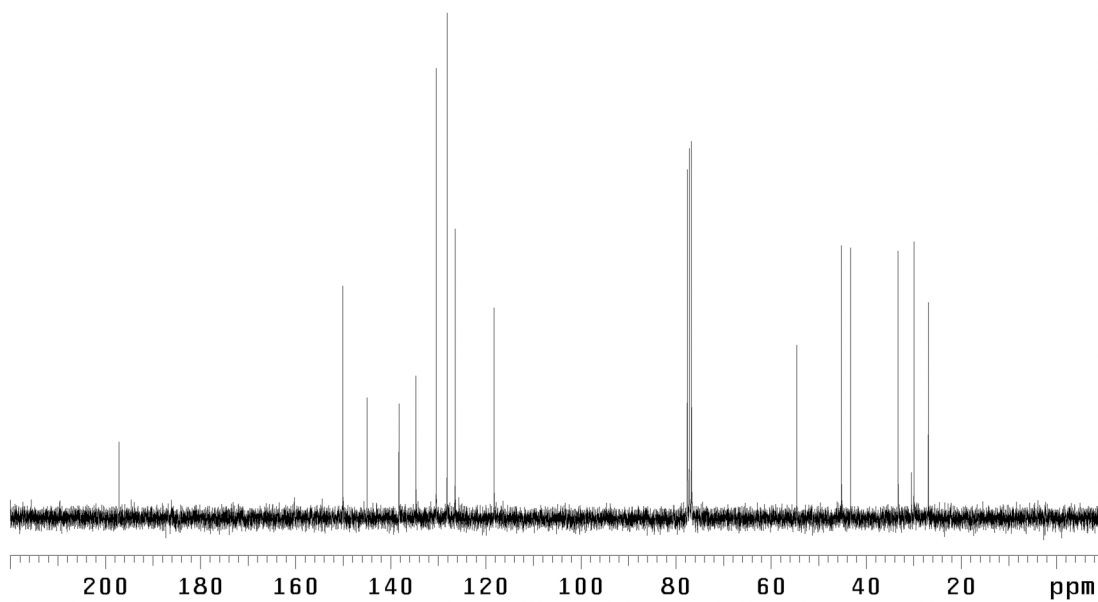


Figure A1.169. ¹³C NMR (75 MHz, CDCl₃) of compound **135c**.

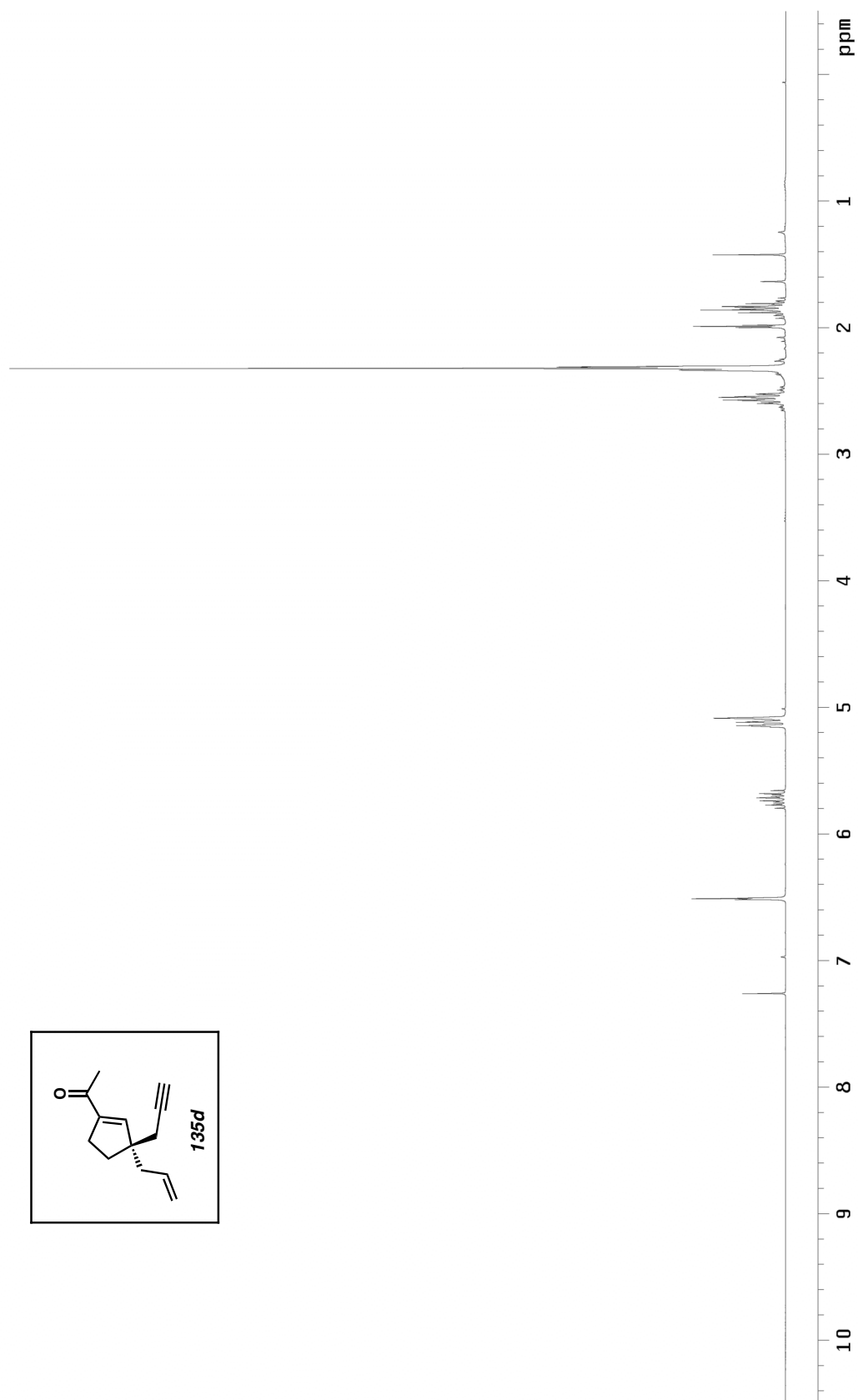


Figure A1.170. ^1H NMR (300 MHz, CDCl_3) of compound **135d**.

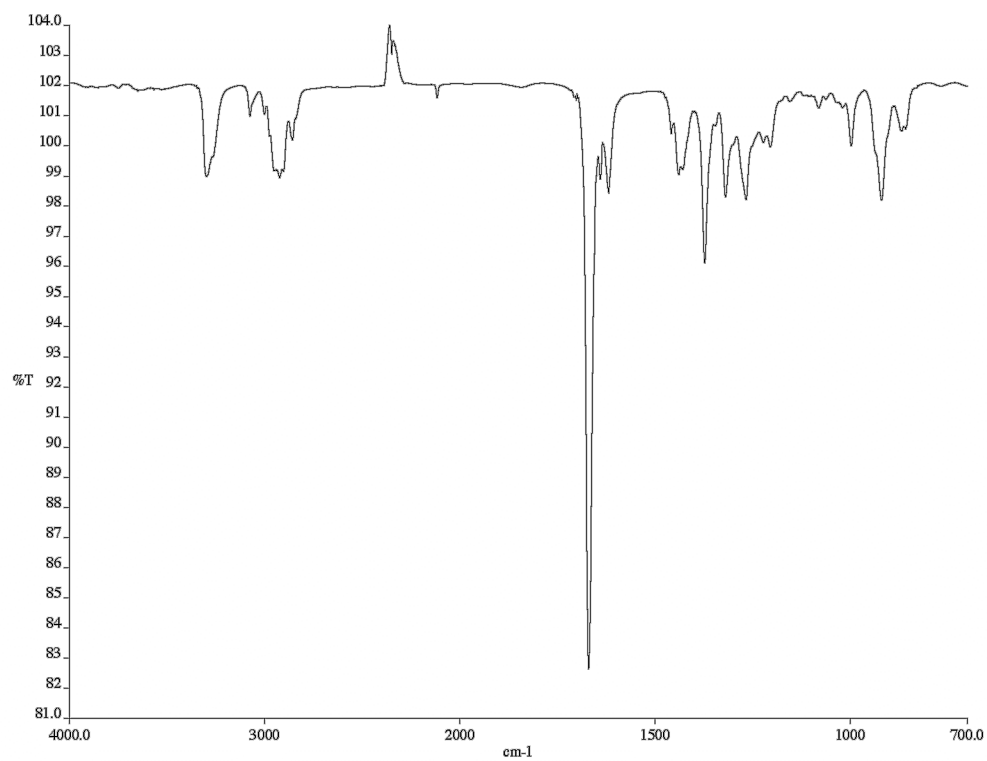


Figure A1.171. Infrared spectrum (thin film/NaCl) of compound **135d**.

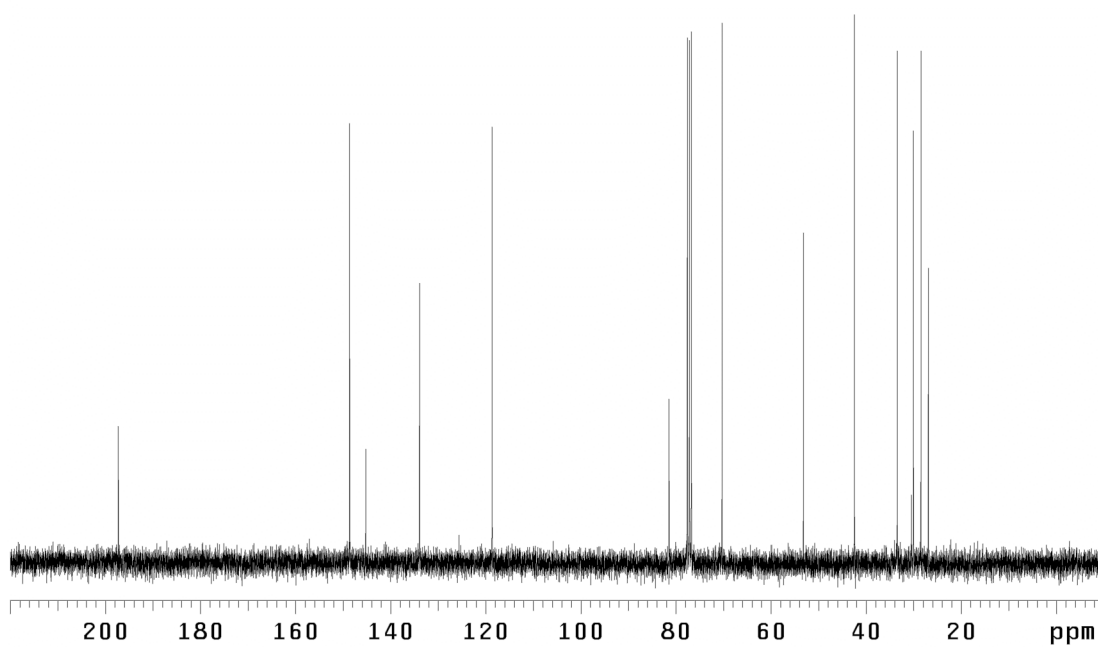


Figure A1.172. ¹³C NMR (75 MHz, CDCl₃) of compound **135d**.

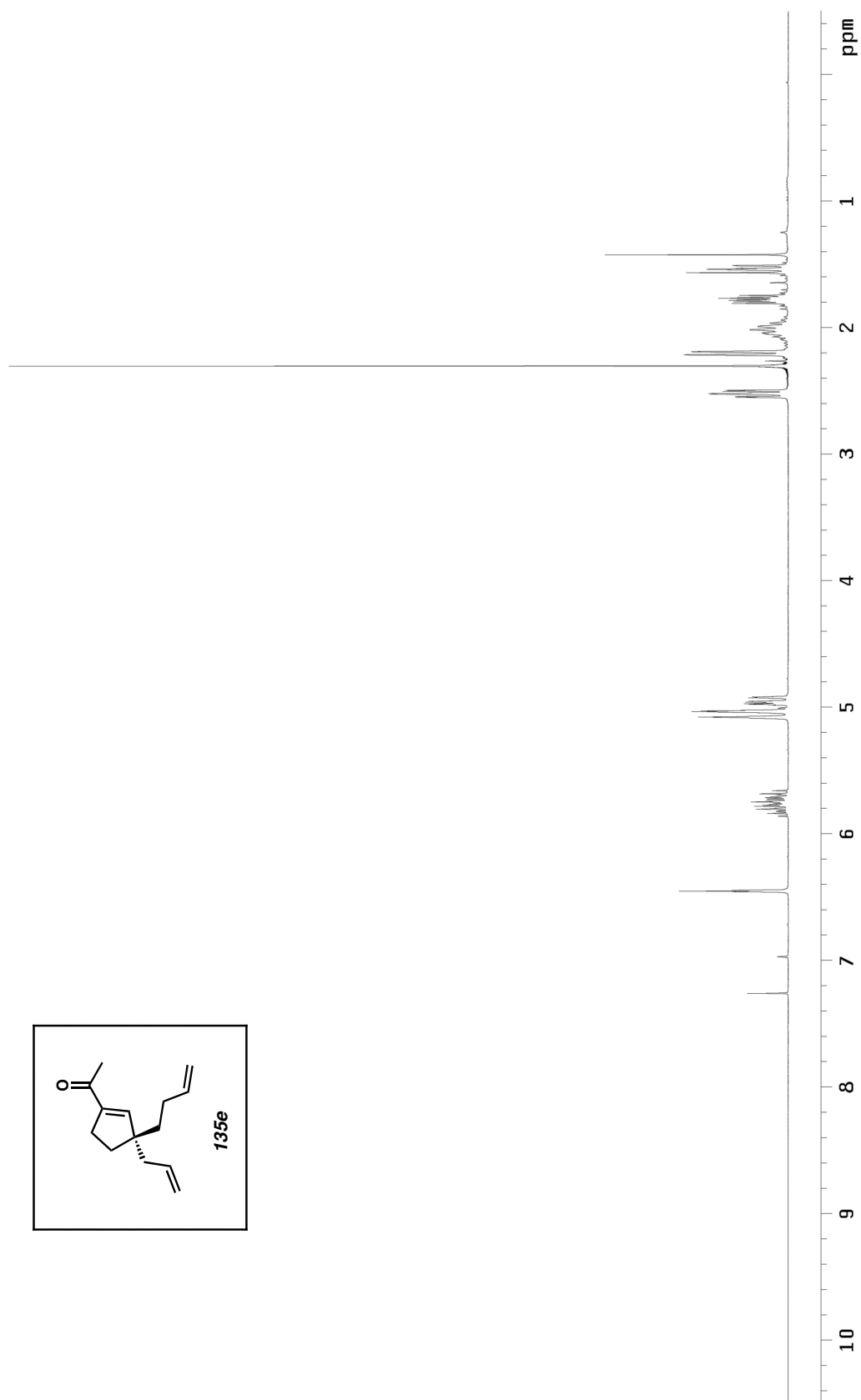


Figure A1.173. ¹H NMR (300 MHz, CDCl₃) of compound **135e**.

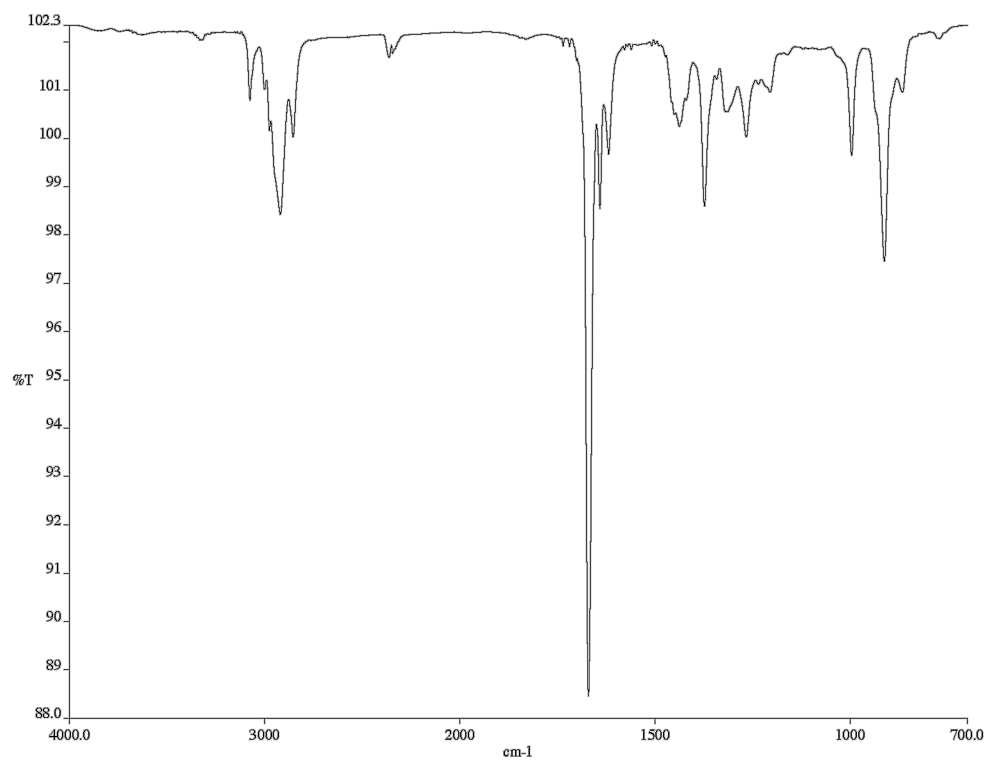


Figure A1.174. Infrared spectrum (thin film/NaCl) of compound **135e**.

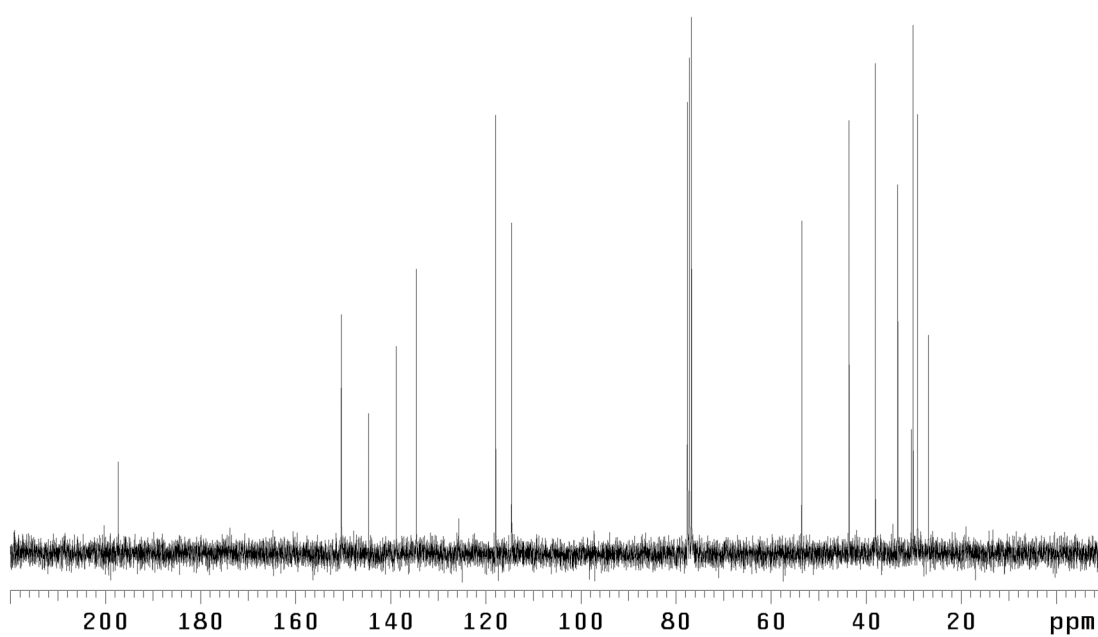


Figure A1.175. ^{13}C NMR (75 MHz, CDCl_3) of compound **135e**.

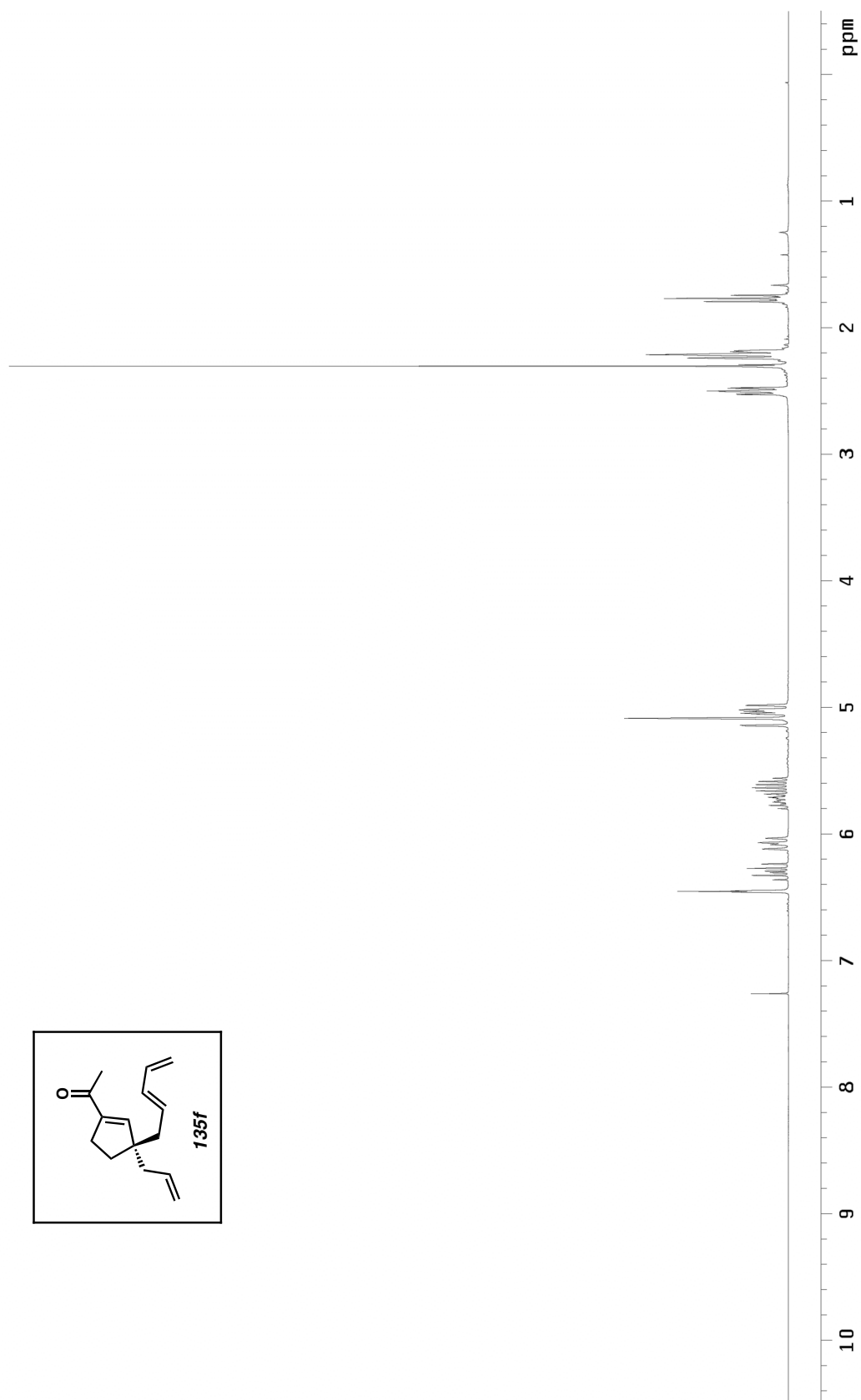


Figure A1.176. ¹H NMR (300 MHz, CDCl₃) of compound **135f**.

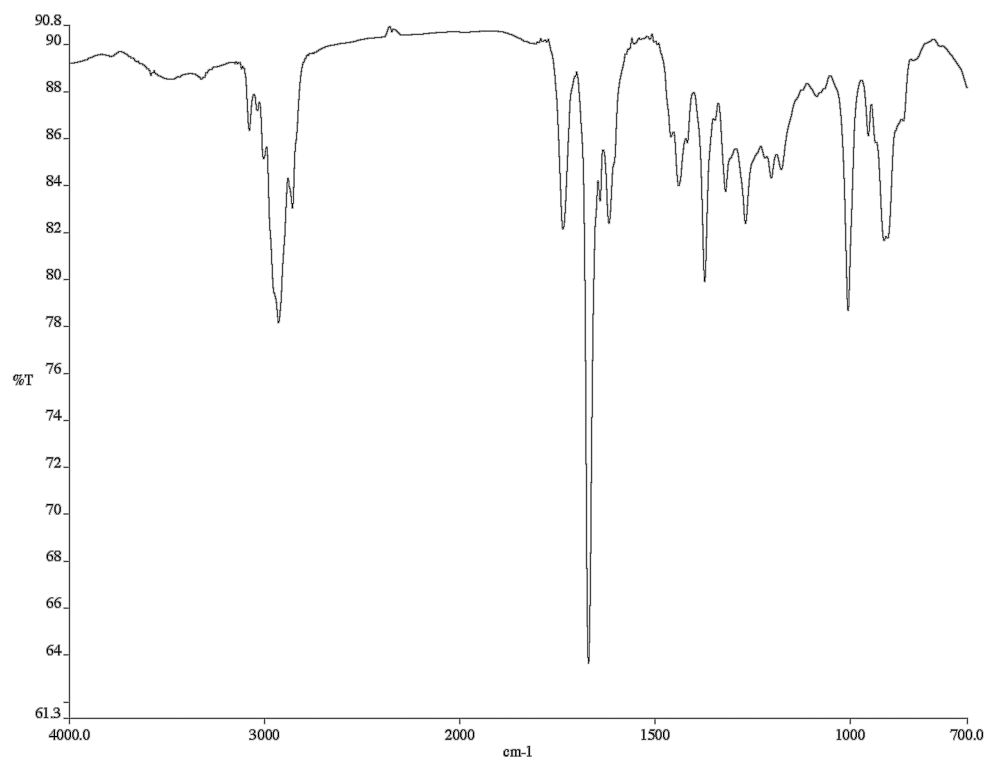


Figure A1.177. Infrared spectrum (thin film/NaCl) of compound **135f**.

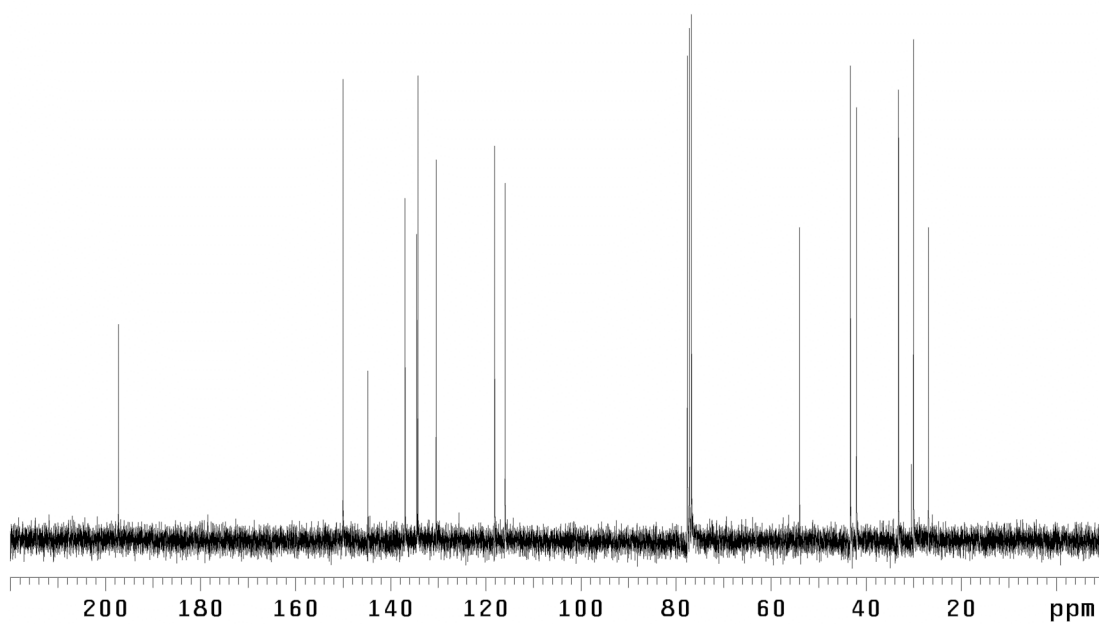


Figure A1.178. ¹³C NMR (75 MHz, CDCl₃) of compound **135f**.

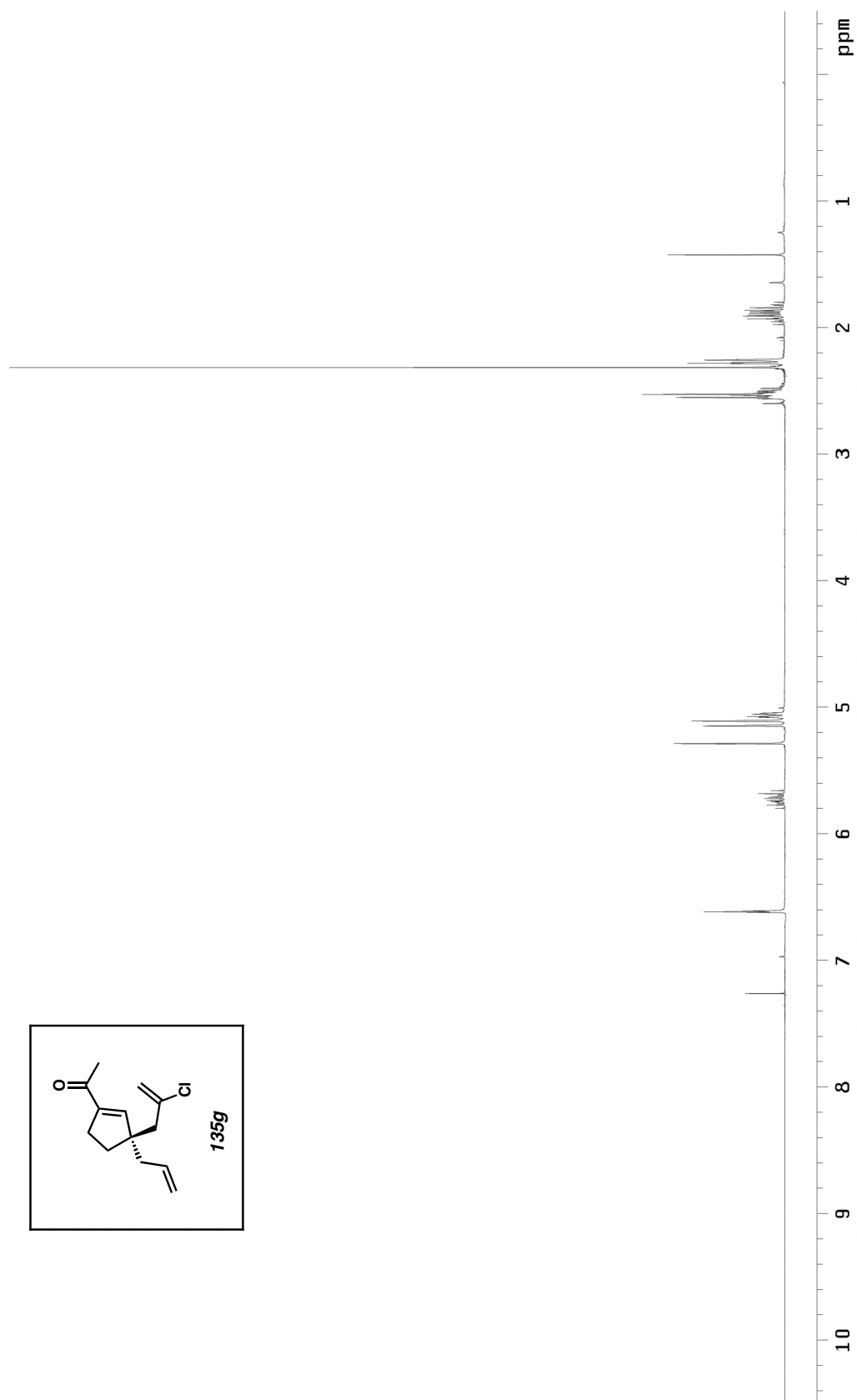


Figure A1.179. ¹H NMR (300 MHz, CDCl₃) of compound **135g**.

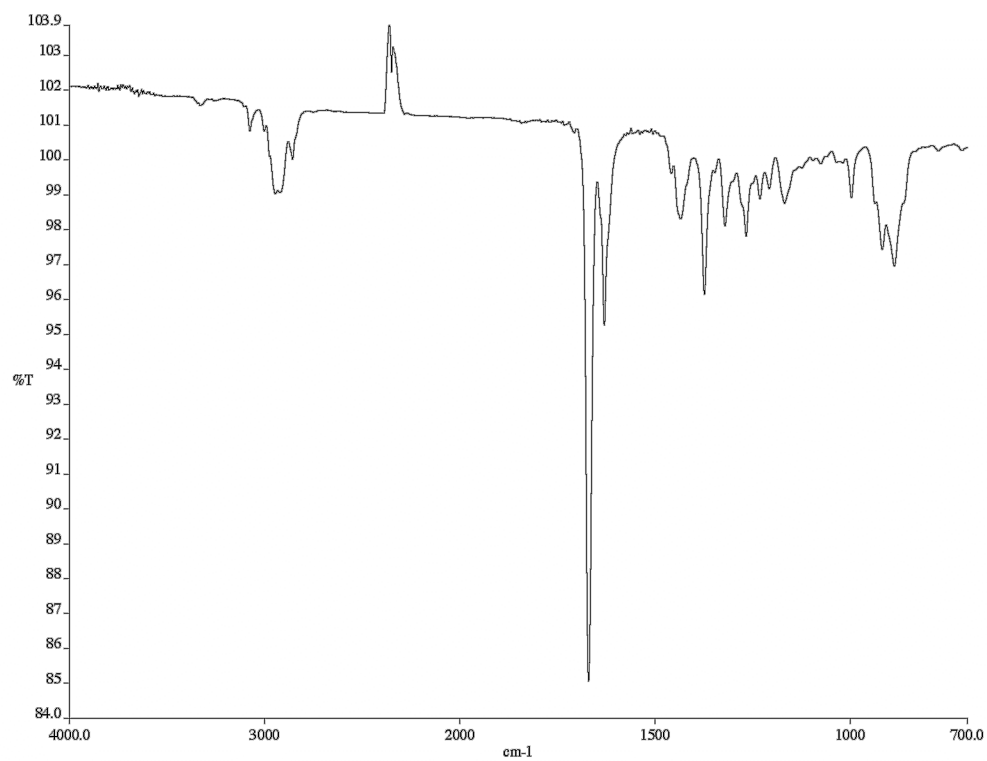


Figure A1.180. Infrared spectrum (thin film/NaCl) of compound **135g**.

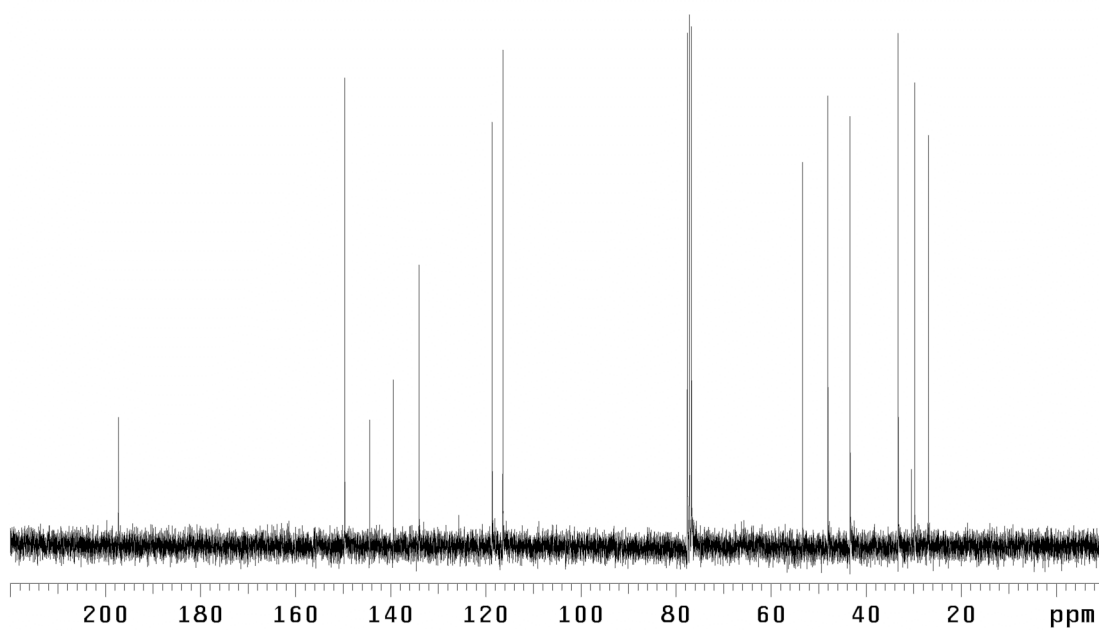


Figure A1.181. ¹³C NMR (75 MHz, CDCl₃) of compound **135g**.

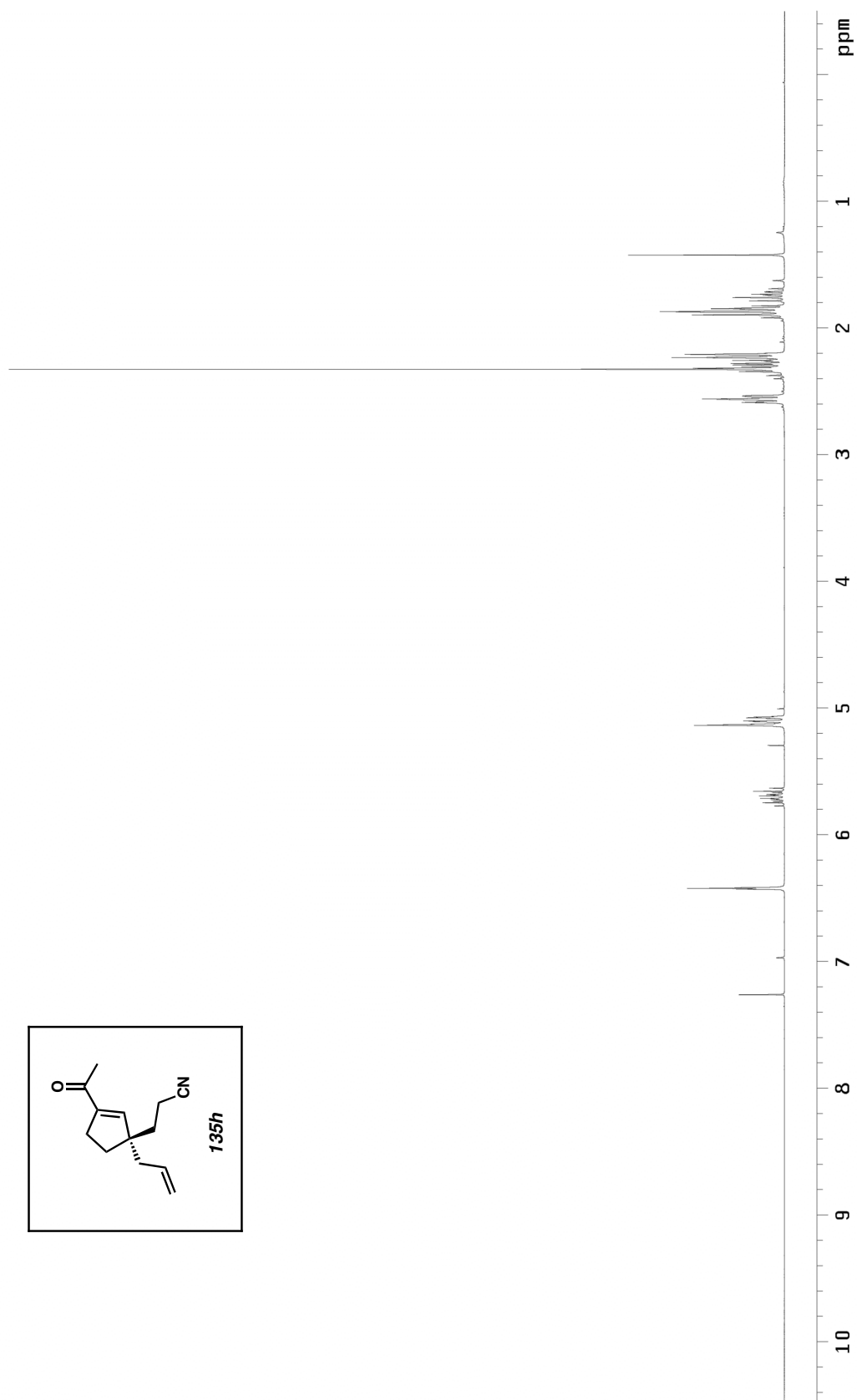


Figure A1.182. ^1H NMR (300 MHz, CDCl_3) of compound **135h**.

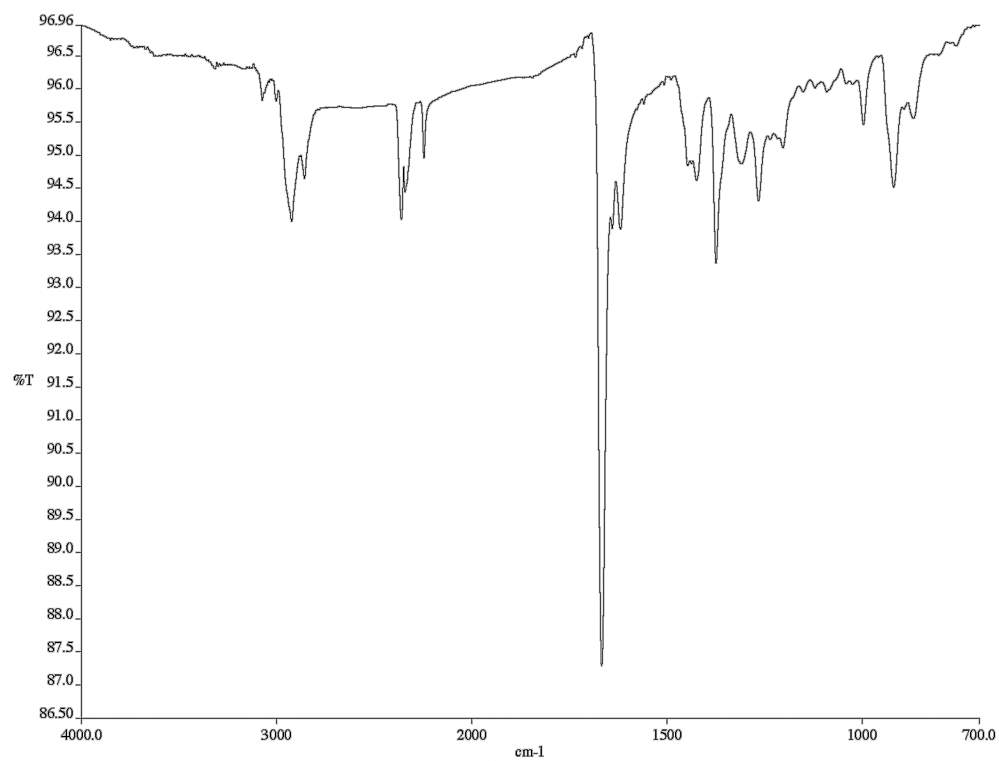


Figure A1.183. Infrared spectrum (thin film/NaCl) of compound **135h**.

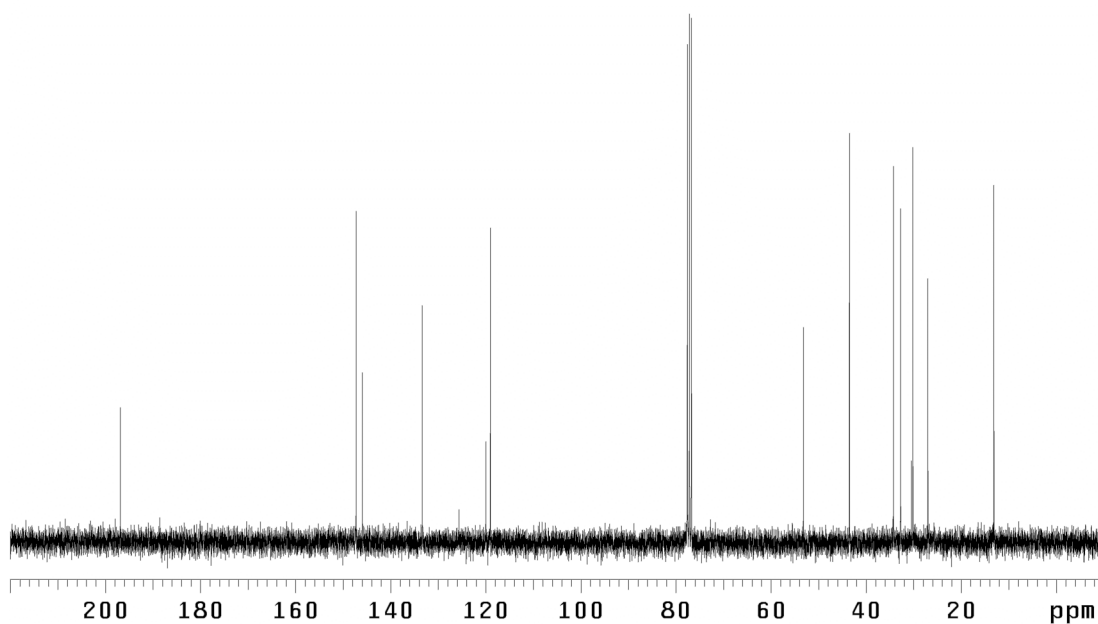


Figure A1.184. ¹³C NMR (75 MHz, CDCl₃) of compound **135h**.

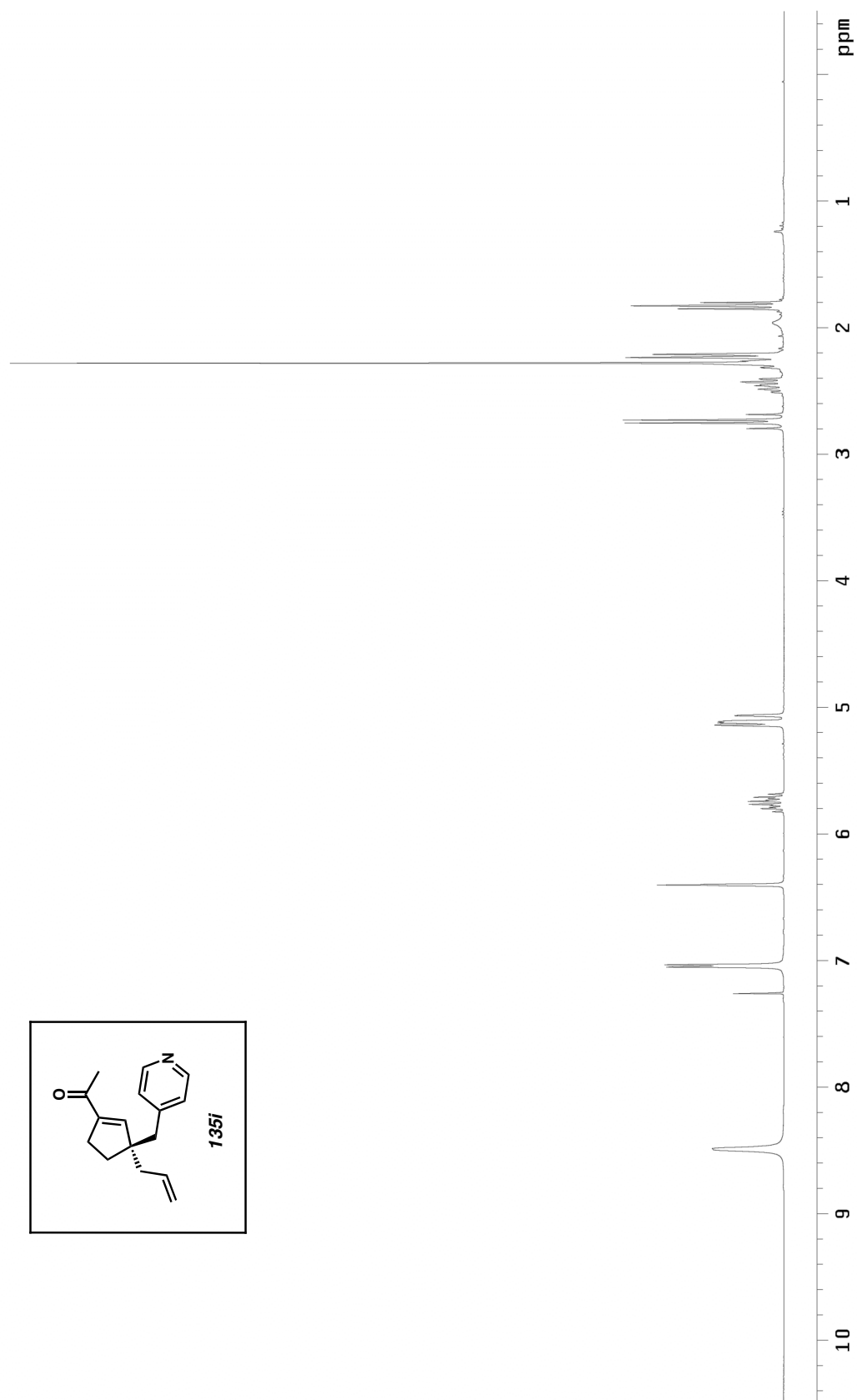


Figure A1.185. ^1H NMR (300 MHz, CDCl_3) of compound **135i**.

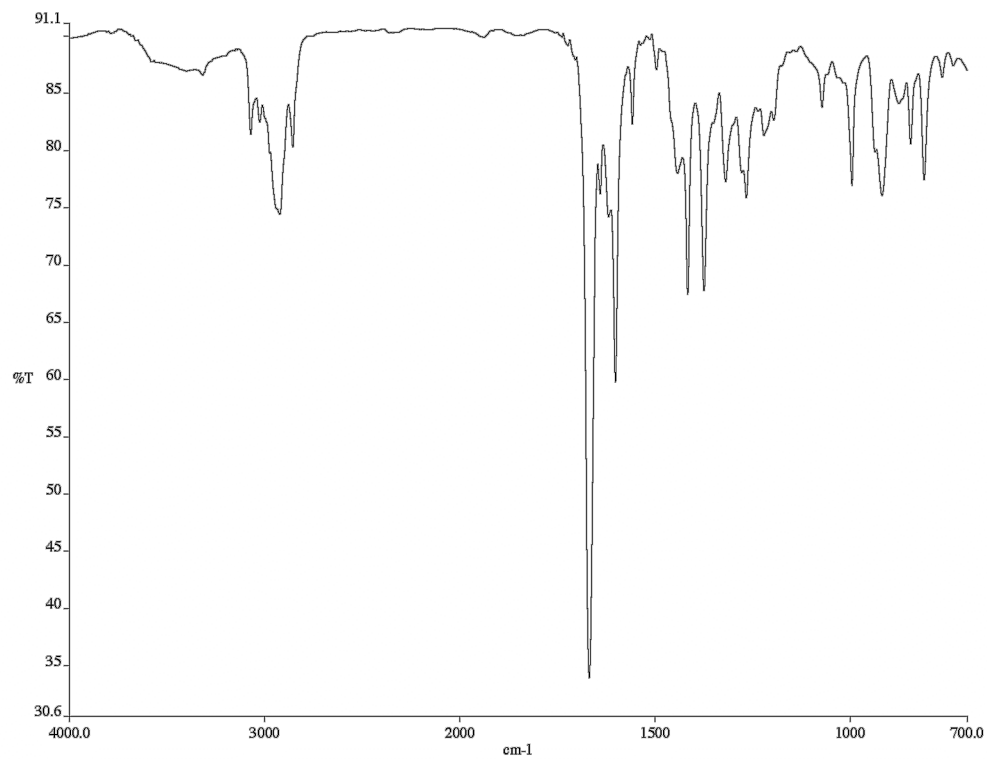


Figure A1.186. Infrared spectrum (thin film/NaCl) of compound **135i**.

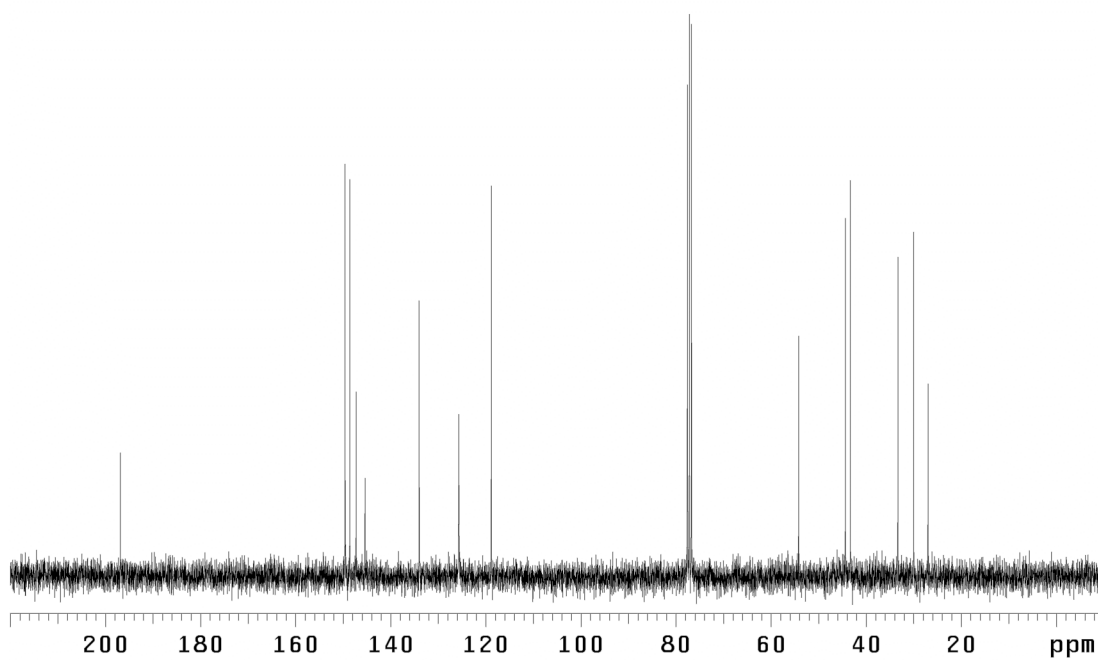


Figure A1.187. ¹³C NMR (75 MHz, CDCl₃) of compound **135i**.

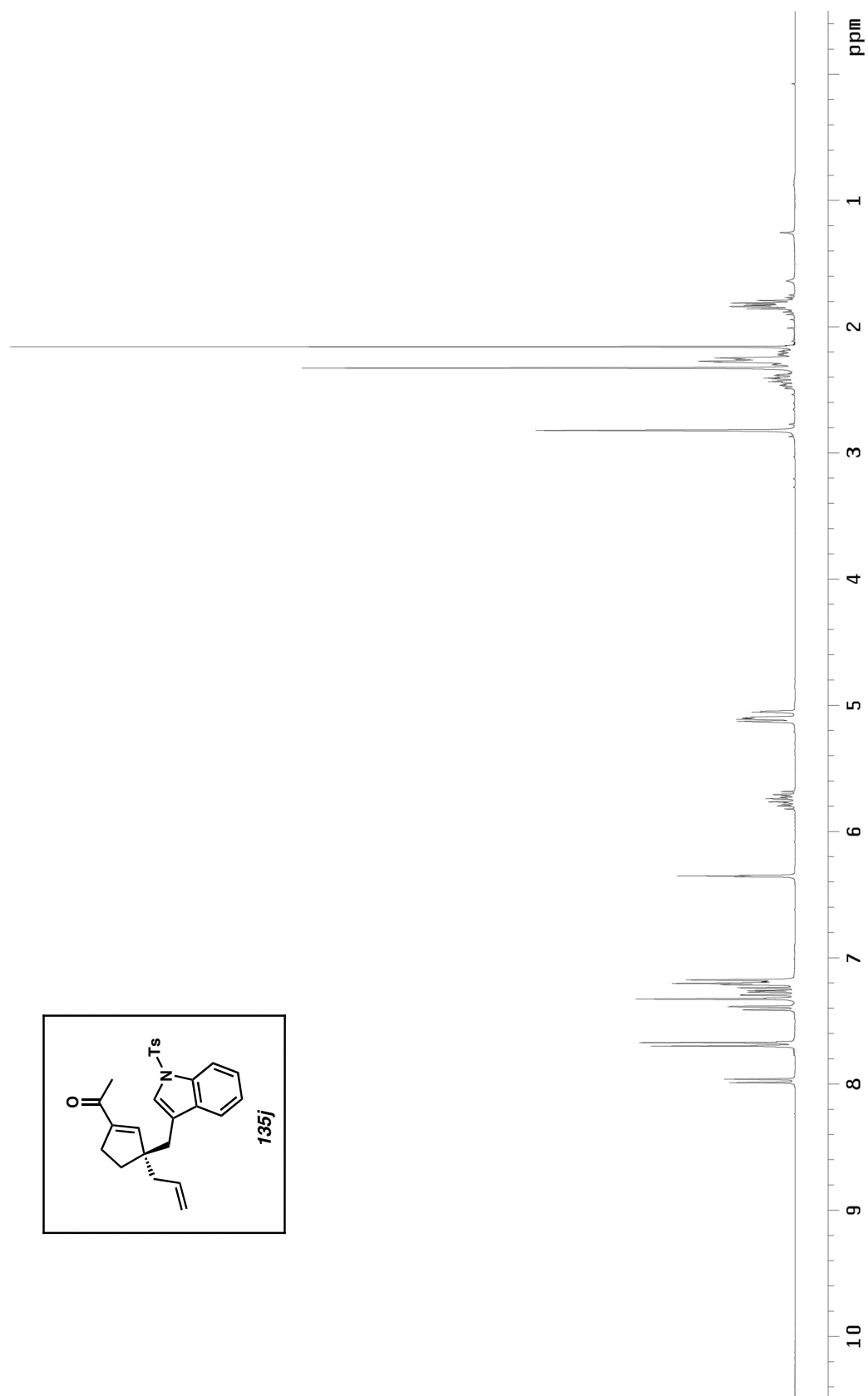


Figure A1.188. ^1H NMR (300 MHz, CDCl_3) of compound **135j**.

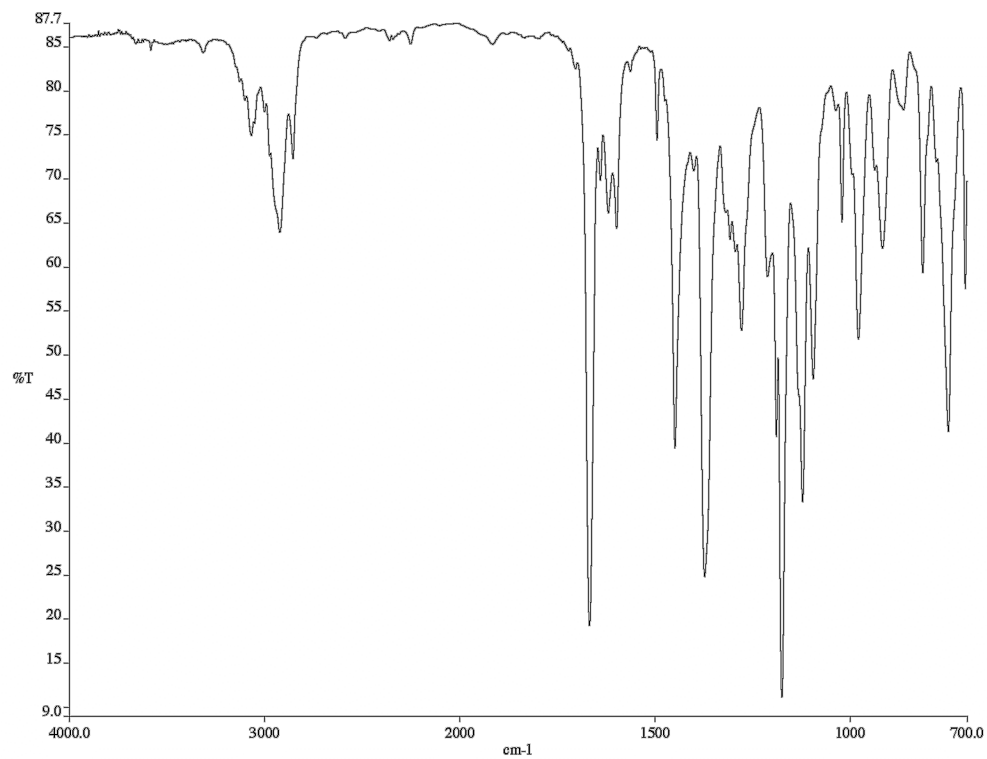


Figure A1.189. Infrared spectrum (thin film/NaCl) of compound **135j**.

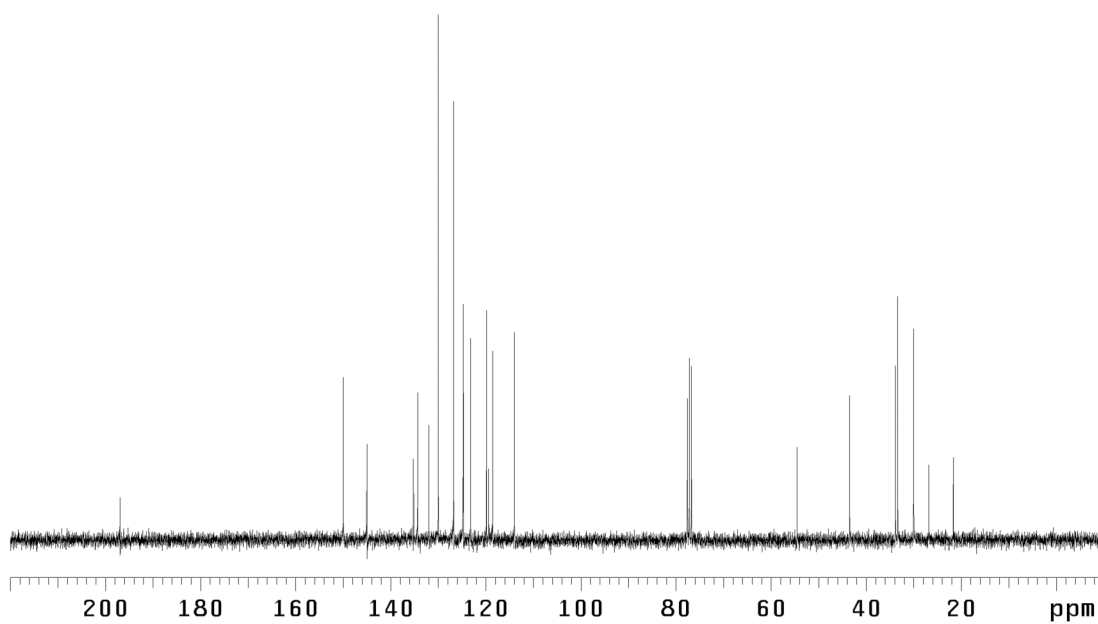


Figure A1.190. ¹³C NMR (75 MHz, CDCl₃) of compound **135j**.

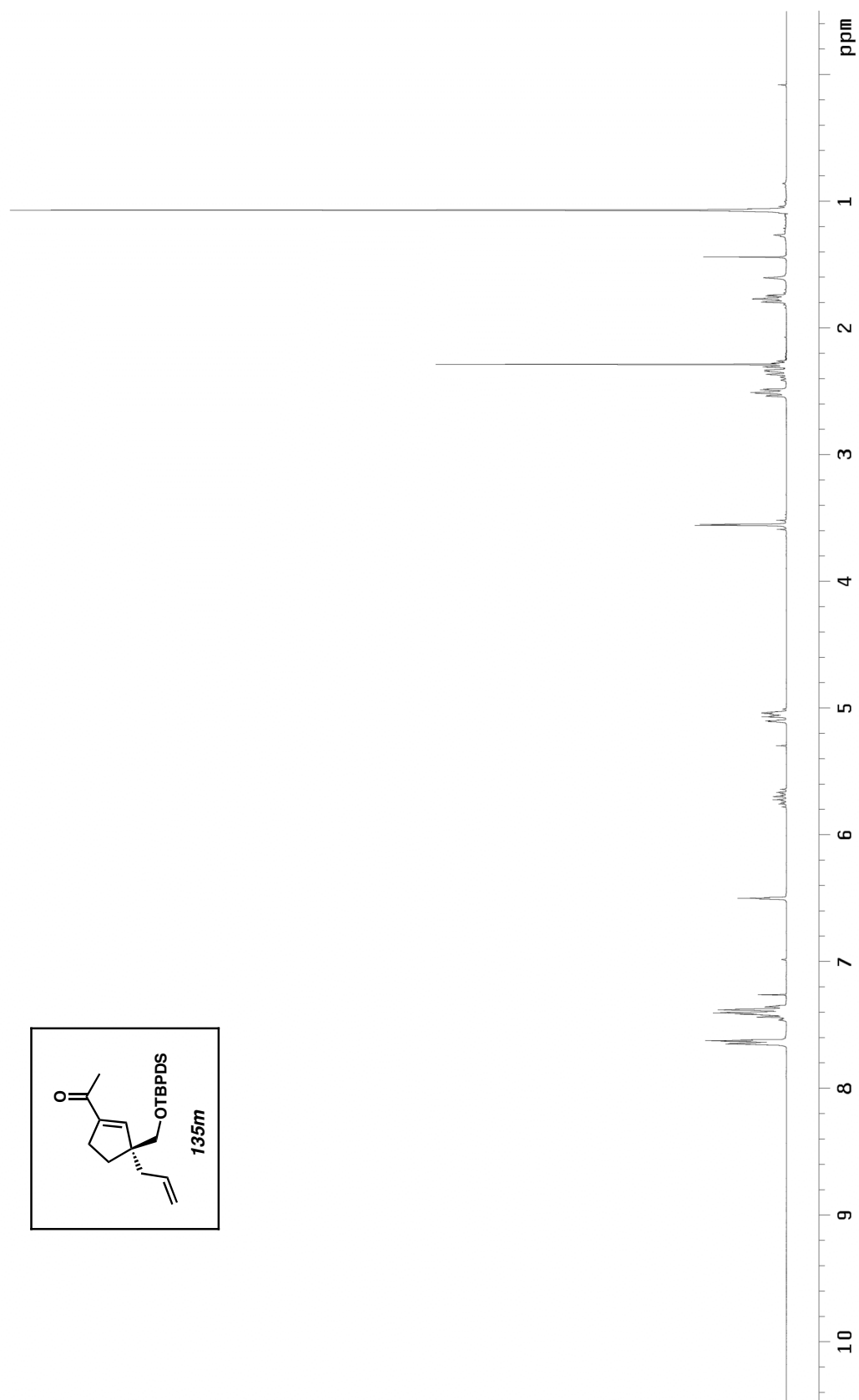


Figure A1.191. ^1H NMR (300 MHz, CDCl_3) of compound **135m**.

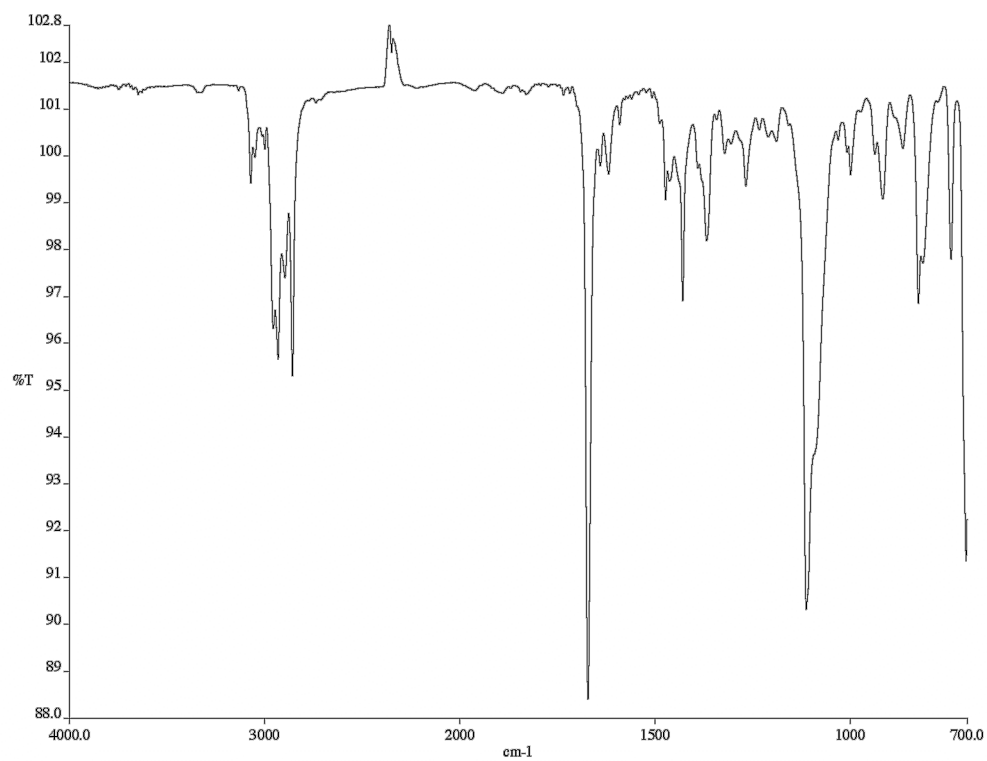


Figure A1.192. Infrared spectrum (thin film/NaCl) of compound **135m**.

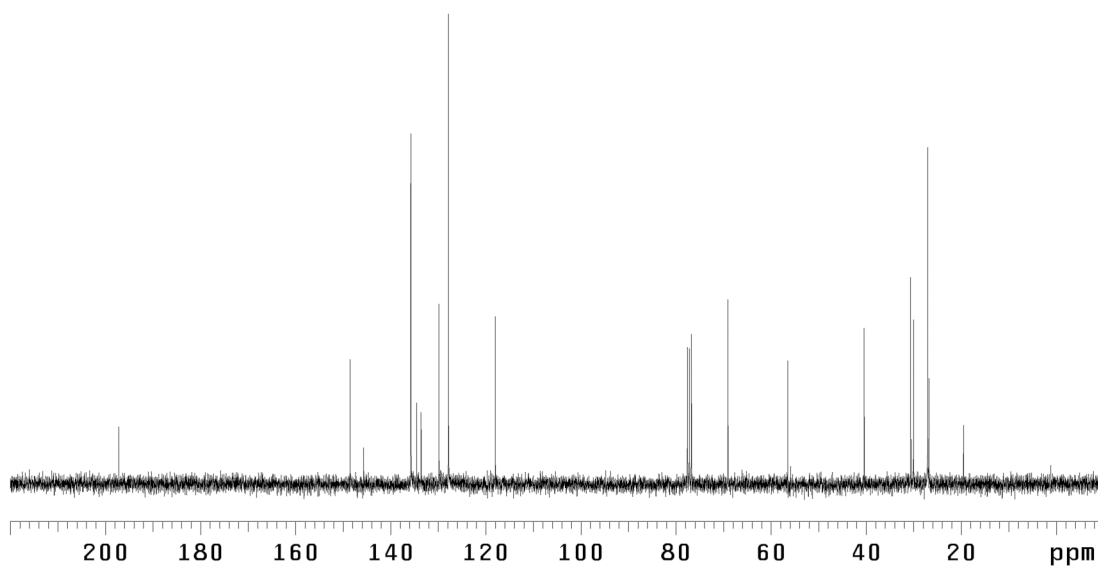


Figure A1.193. ¹³C NMR (75 MHz, CDCl₃) of compound **135m**.

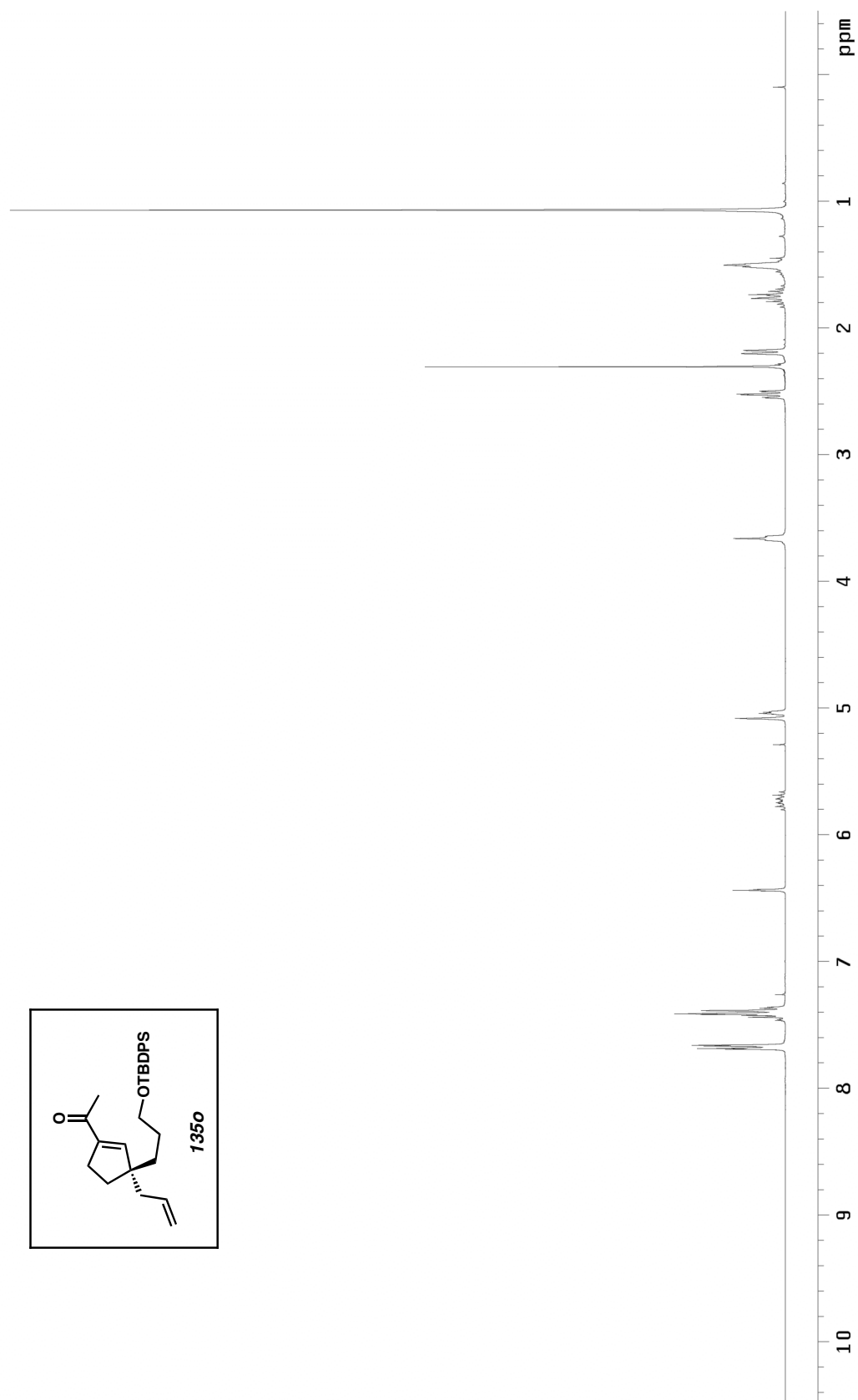


Figure A1.194. ¹H NMR (300 MHz, CDCl₃) of compound **135n**.

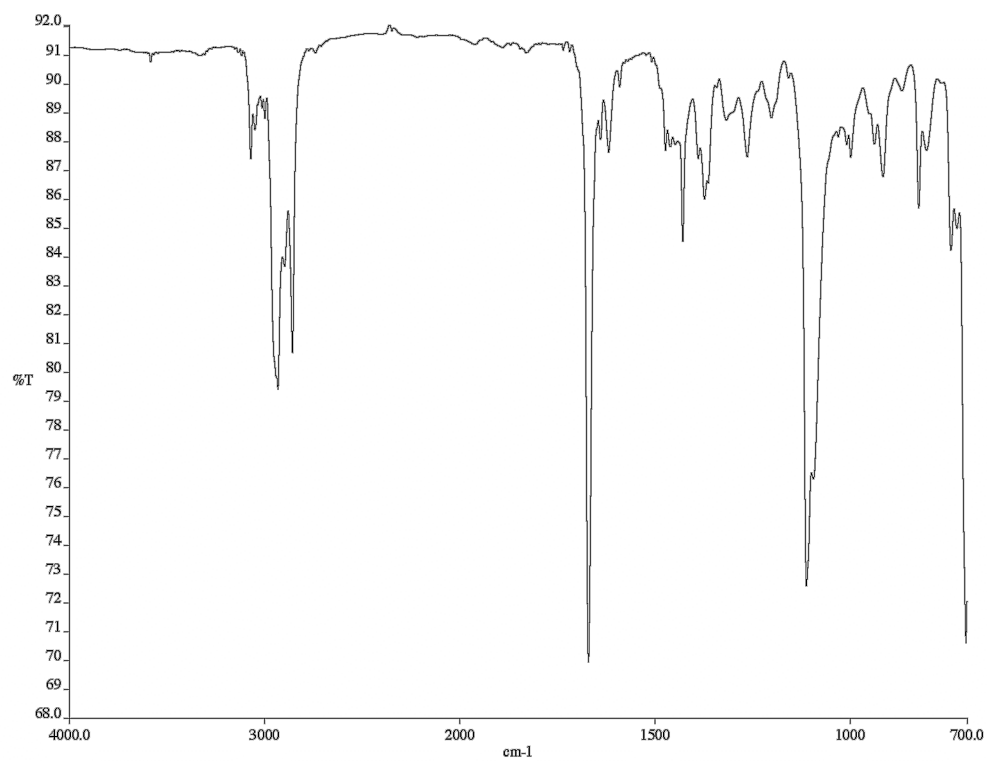


Figure A1.195. Infrared spectrum (thin film/NaCl) of compound **135n**.

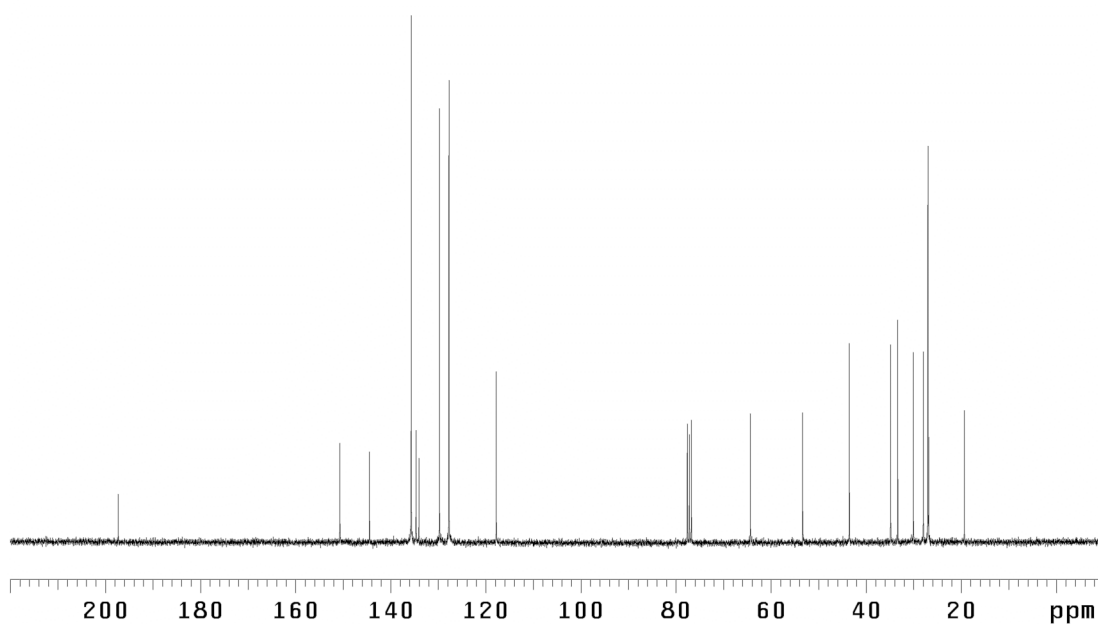


Figure A1.196. ¹³C NMR (75 MHz, CDCl₃) of compound **135n**.

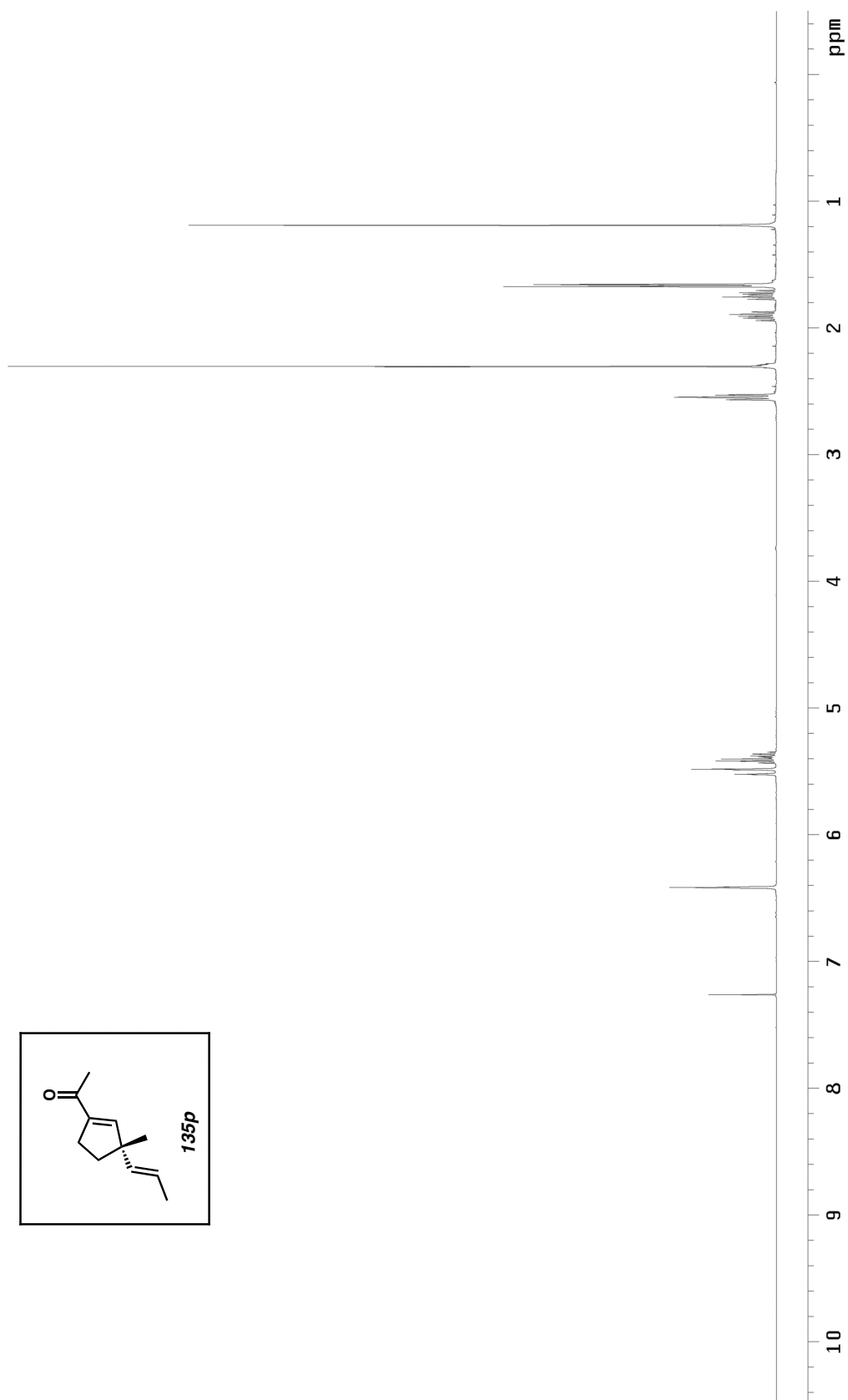


Figure A1.197. ^1H NMR (400 MHz, CDCl_3) of compound **135p**.

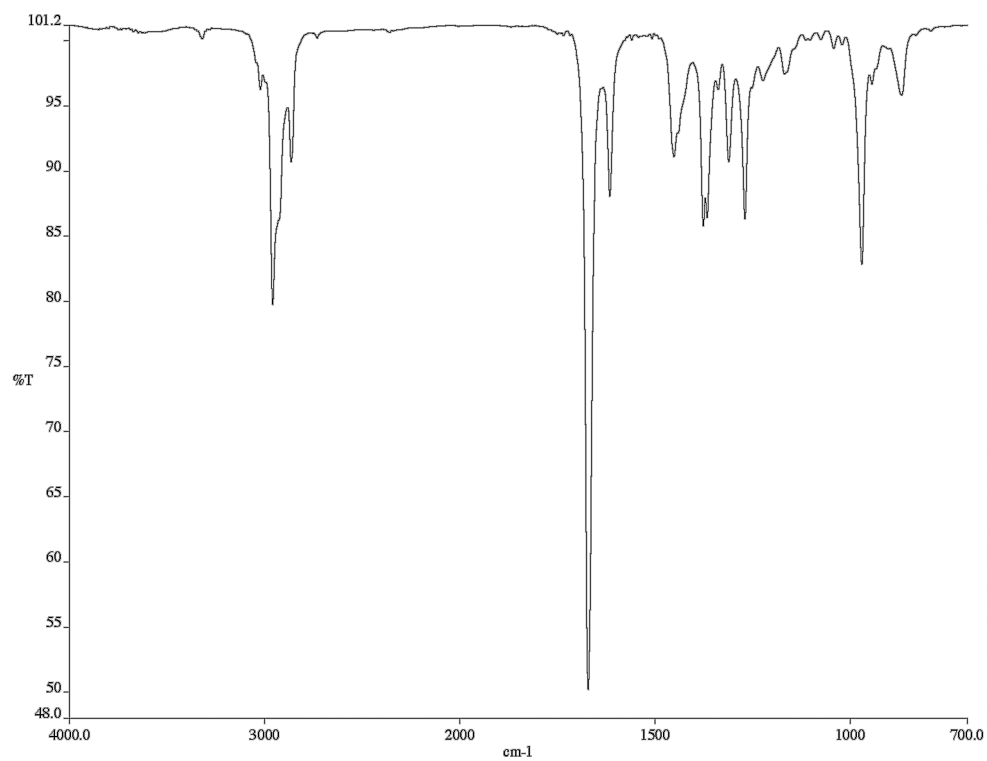


Figure A1.198. Infrared spectrum (thin film/NaCl) of compound **135p**.

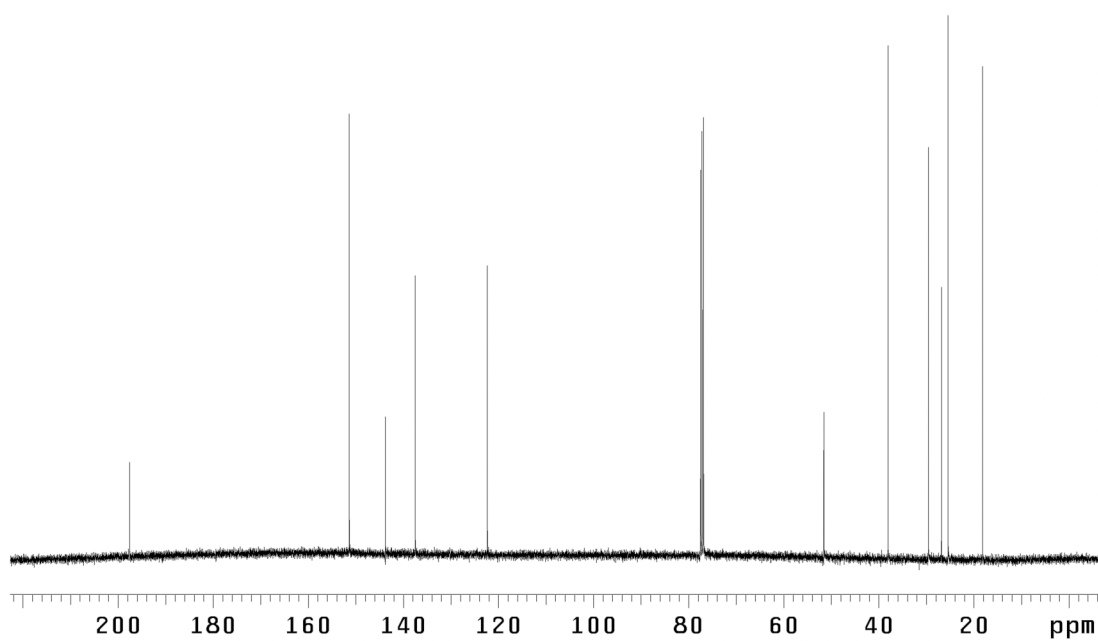


Figure A1.199. ^{13}C NMR (100 MHz, CDCl_3) of compound **135p**.

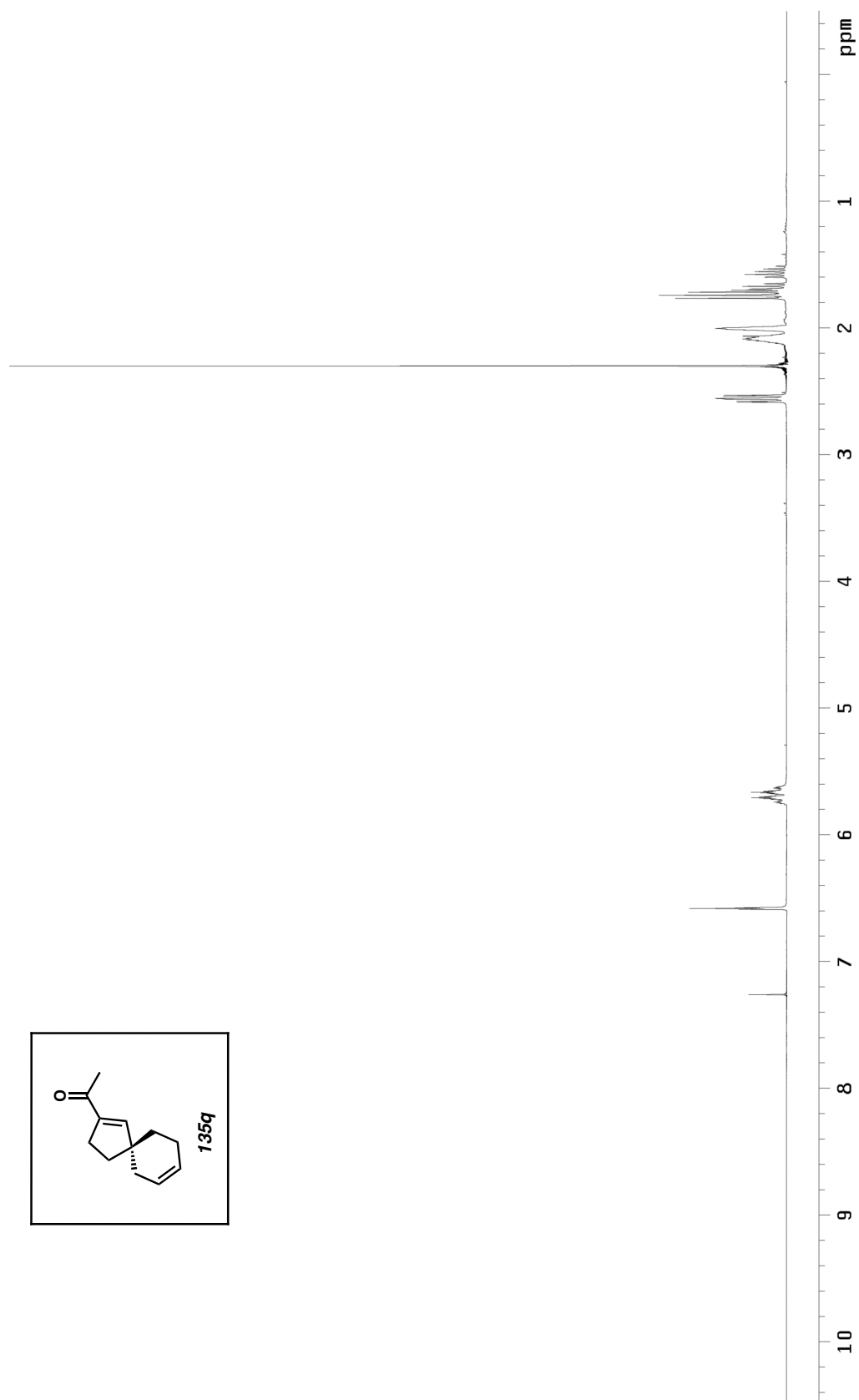


Figure A1.200. ^1H NMR (300 MHz, CDCl_3) of compound **135q**.

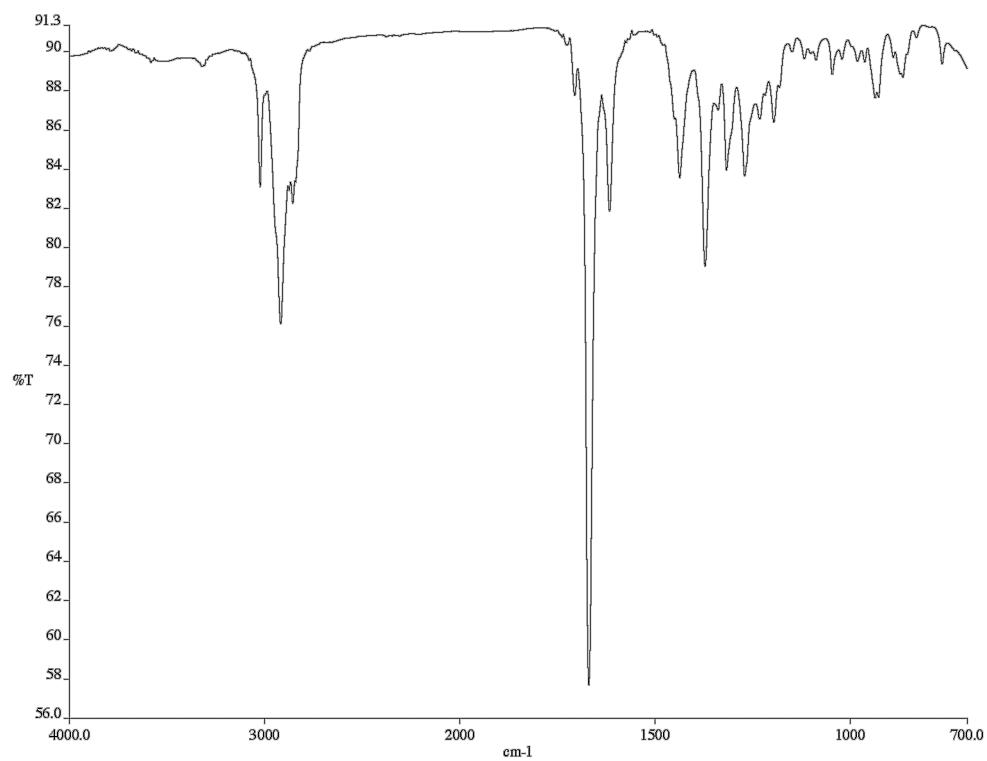


Figure A1.201. Infrared spectrum (thin film/NaCl) of compound **135q**.

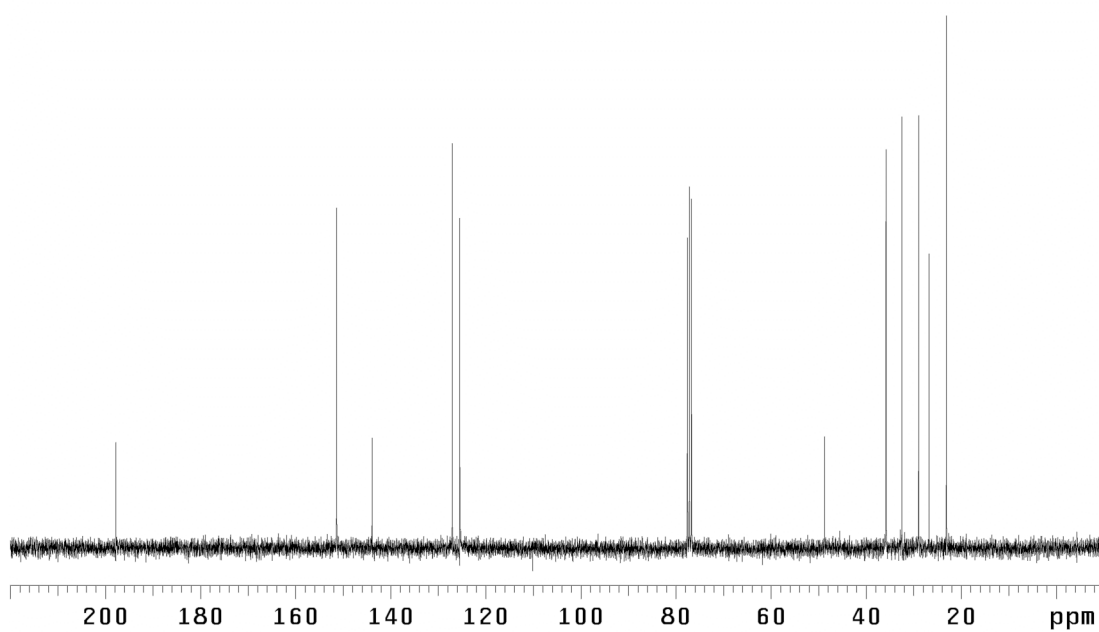


Figure A1.202. ¹³C NMR (75 MHz, CDCl₃) of compound **135q**.

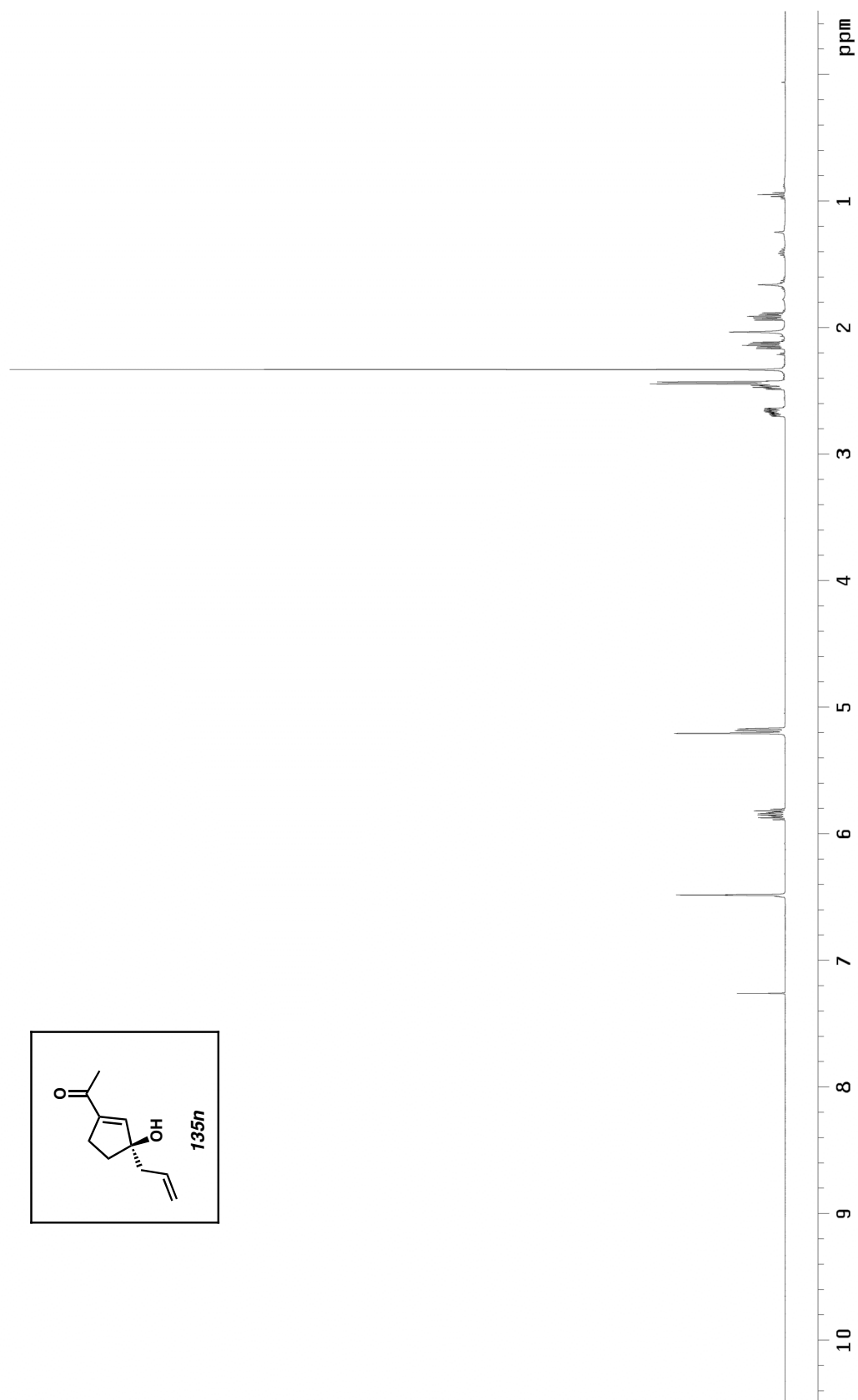


Figure A1.203. ^1H NMR (500 MHz, CDCl_3) of compound **135n**.

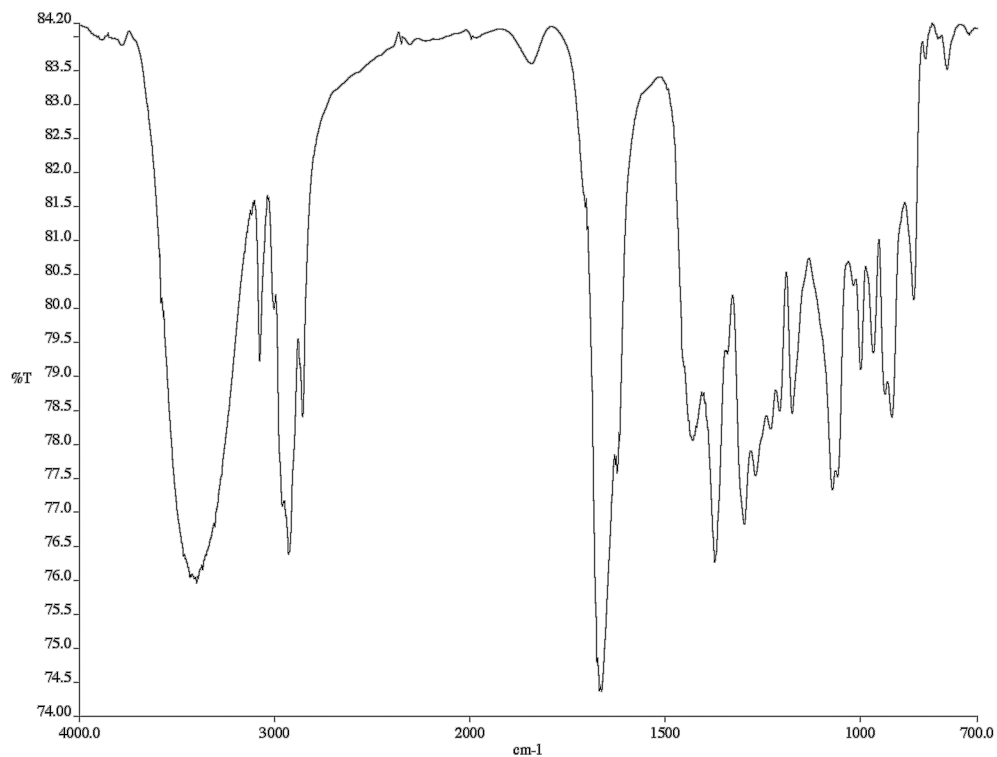


Figure A1.204. Infrared spectrum (thin film/NaCl) of compound **135n**.

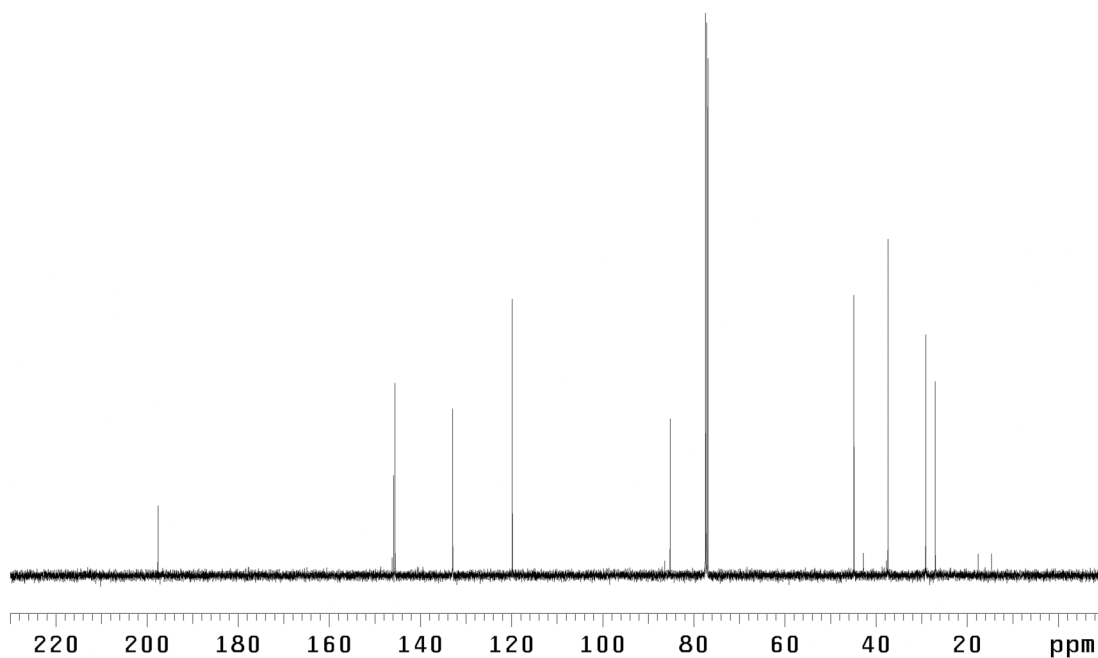


Figure A1.205. ^{13}C NMR (125 MHz, CDCl_3) of compound **135n**.

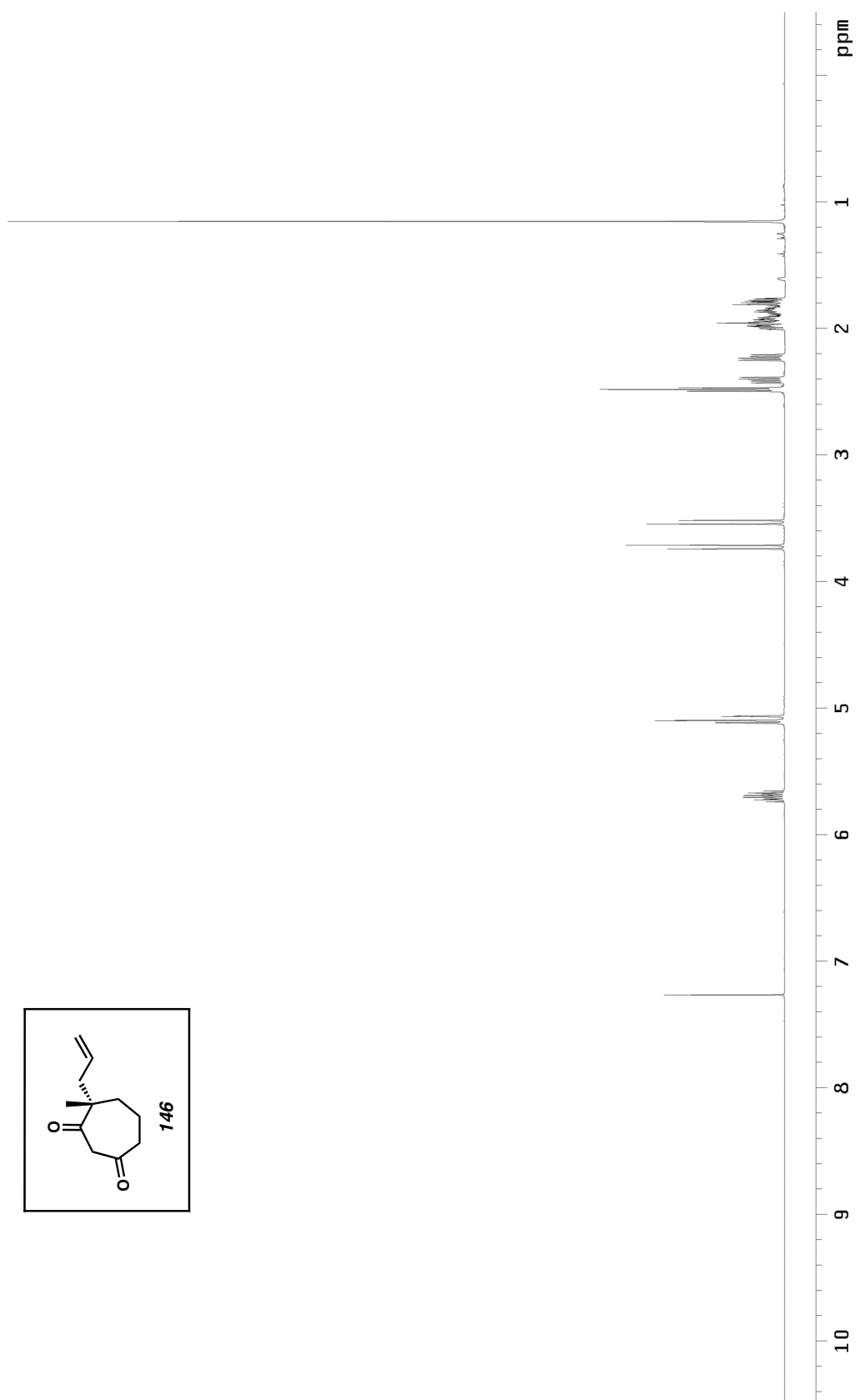


Figure A1.206. ^1H NMR (500 MHz, CDCl_3) of compound **146**.

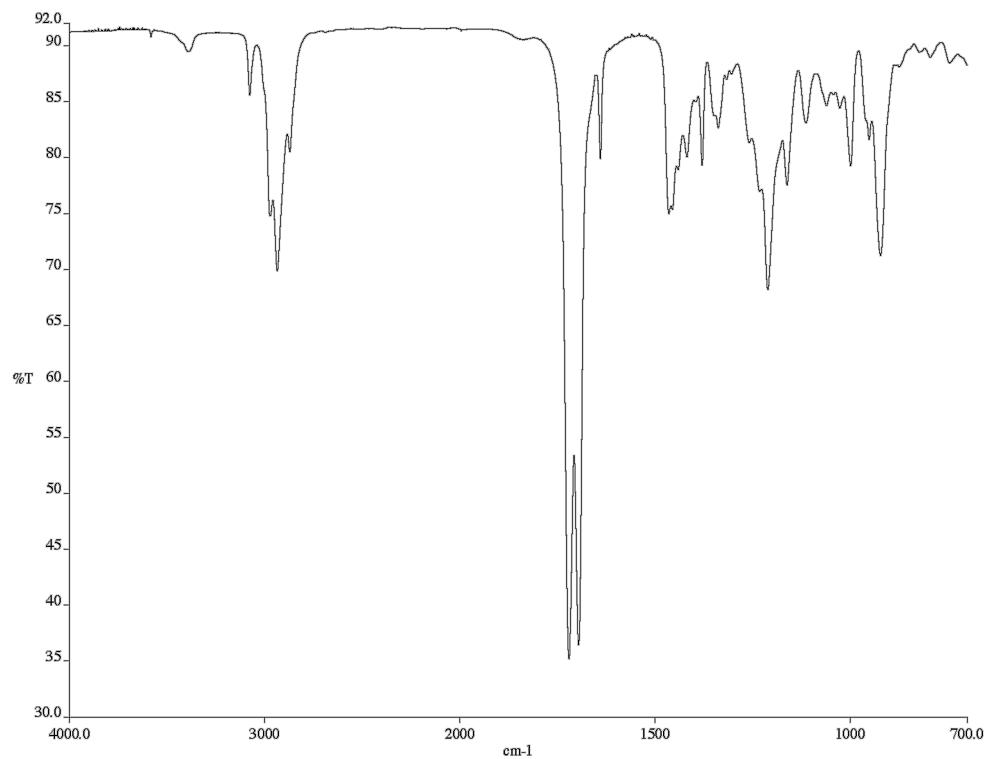


Figure A1.207. Infrared spectrum (thin film/NaCl) of compound **146**.

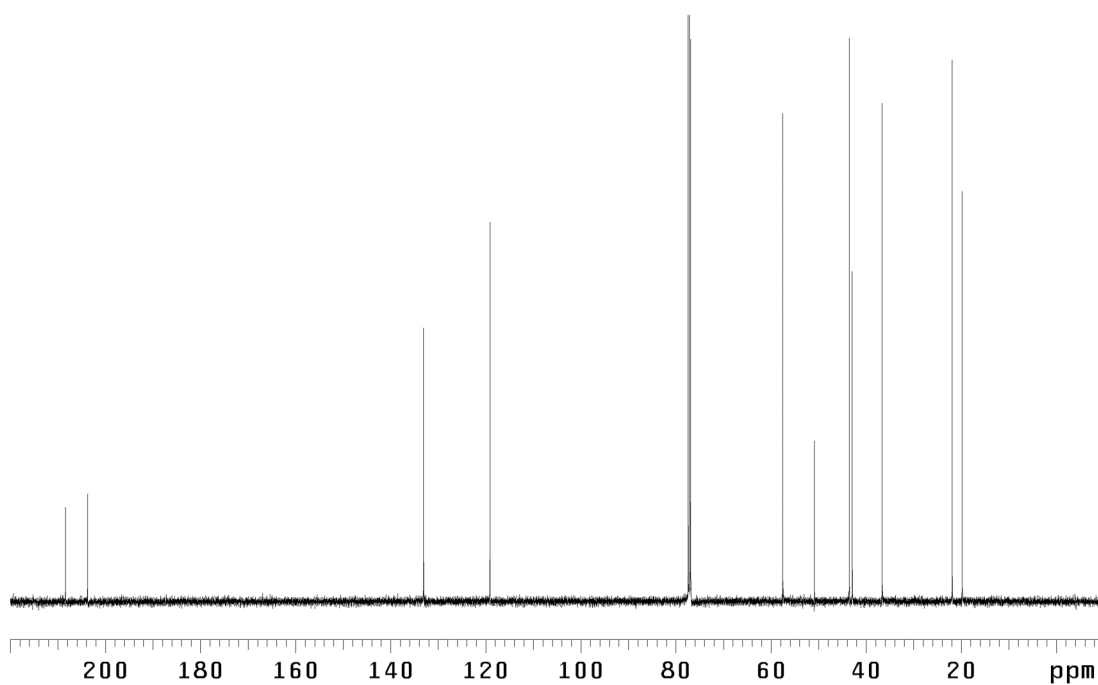
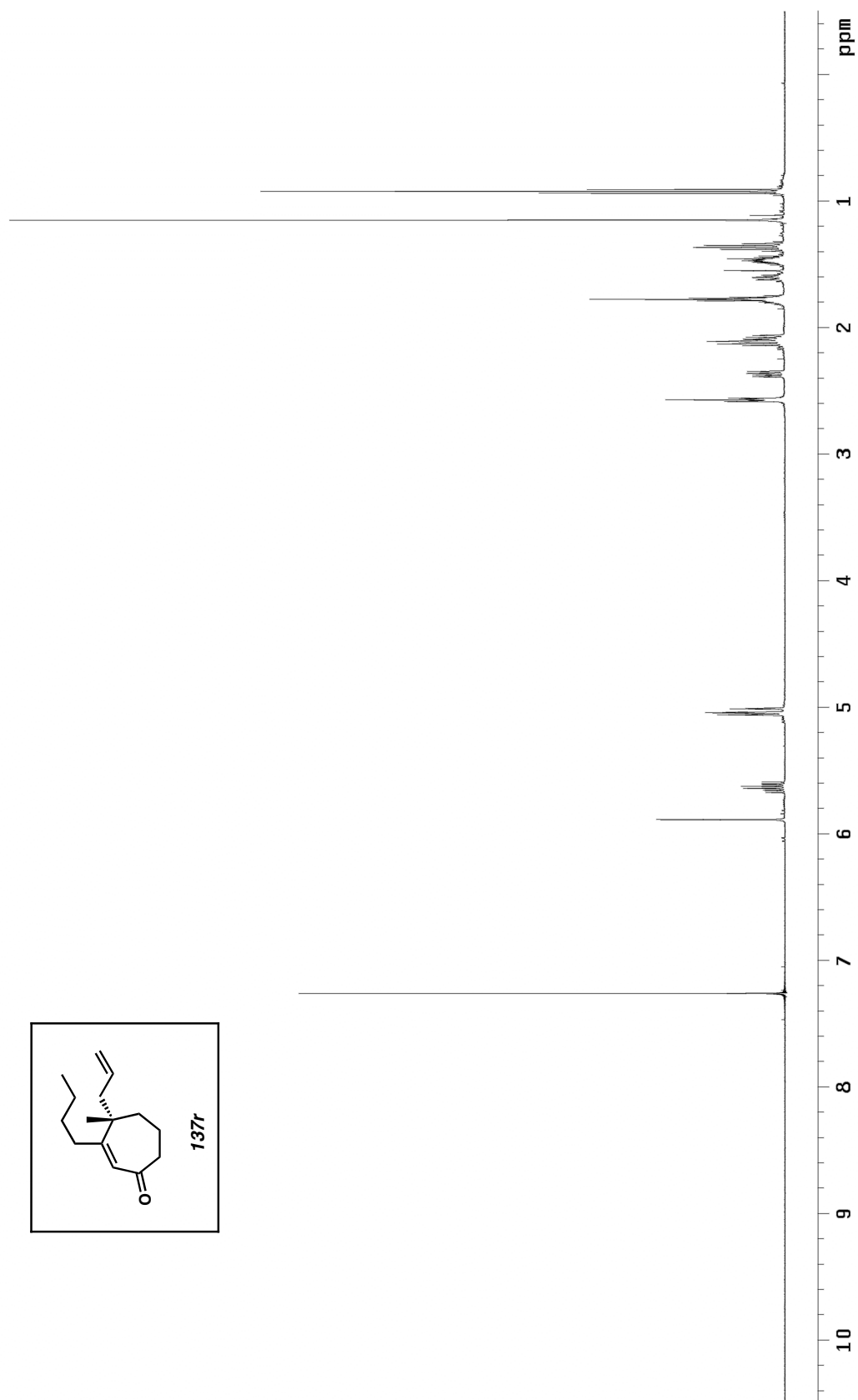


Figure A1.208. ¹³C NMR (125 MHz, CDCl₃) of compound **146**.



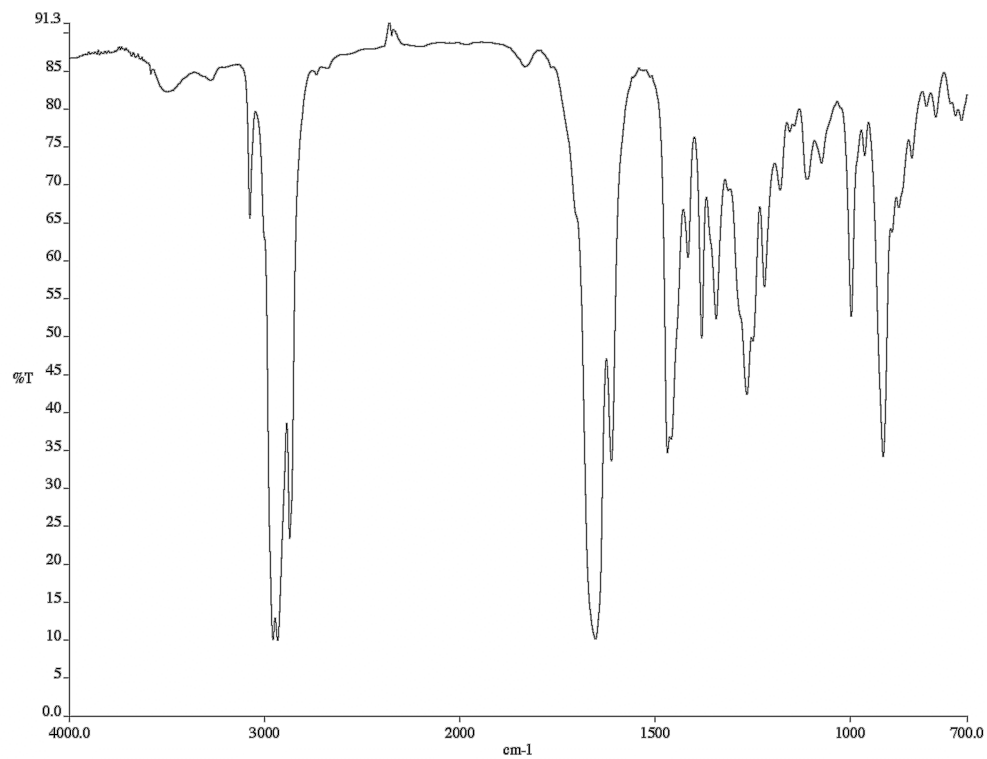


Figure A1.210. Infrared spectrum (thin film/NaCl) of compound **137r**.

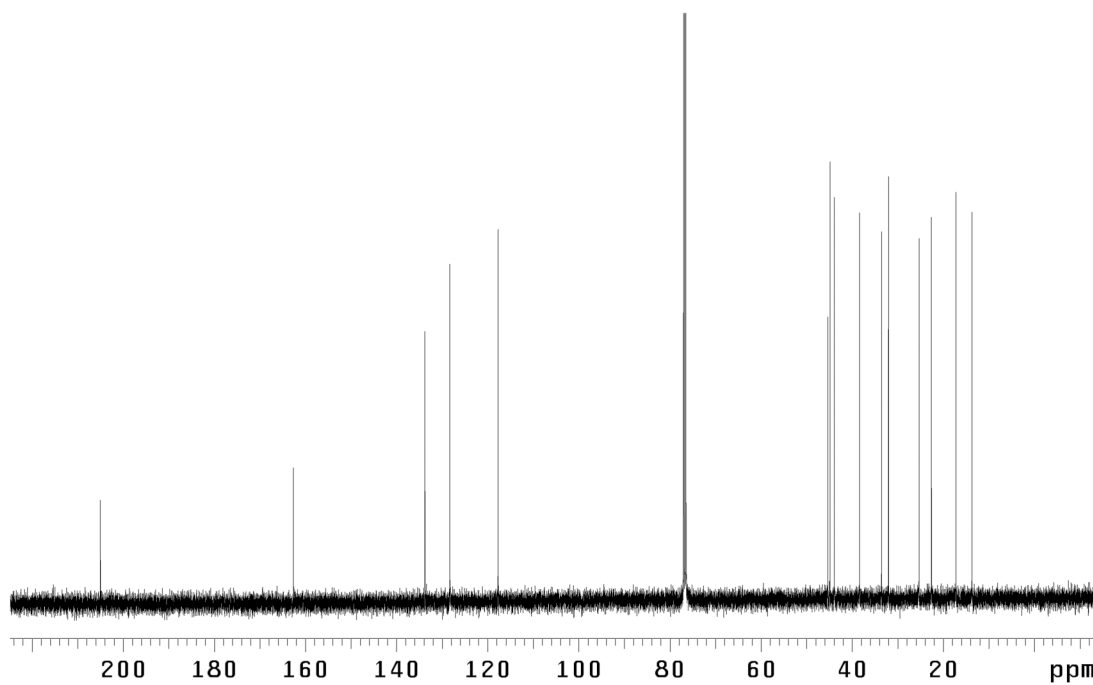


Figure A1.211. ¹³C NMR (125 MHz, CDCl₃) of compound **137r**.

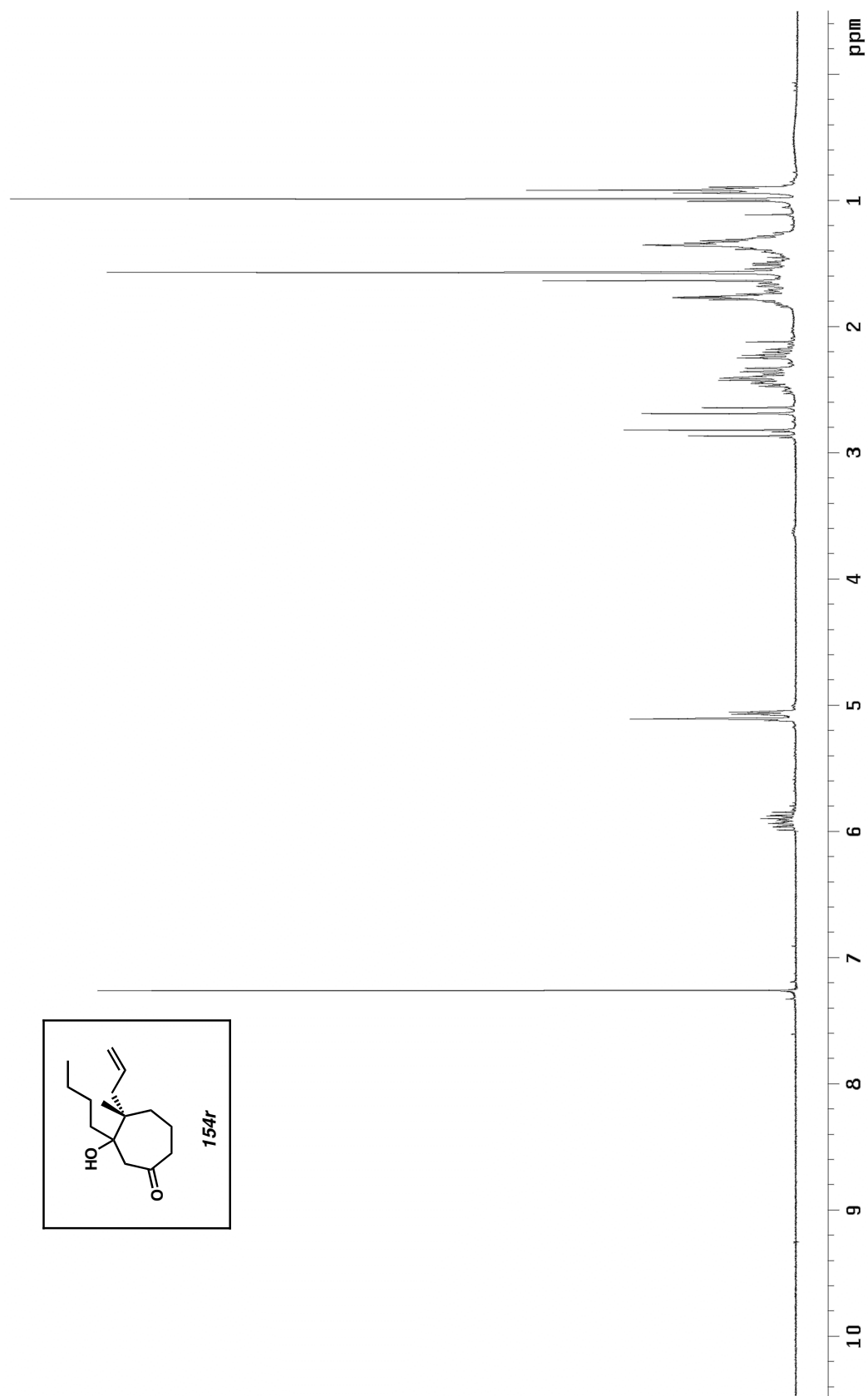


Figure A1.212. ¹H NMR (500 MHz, CDCl₃) of compound **154r**.

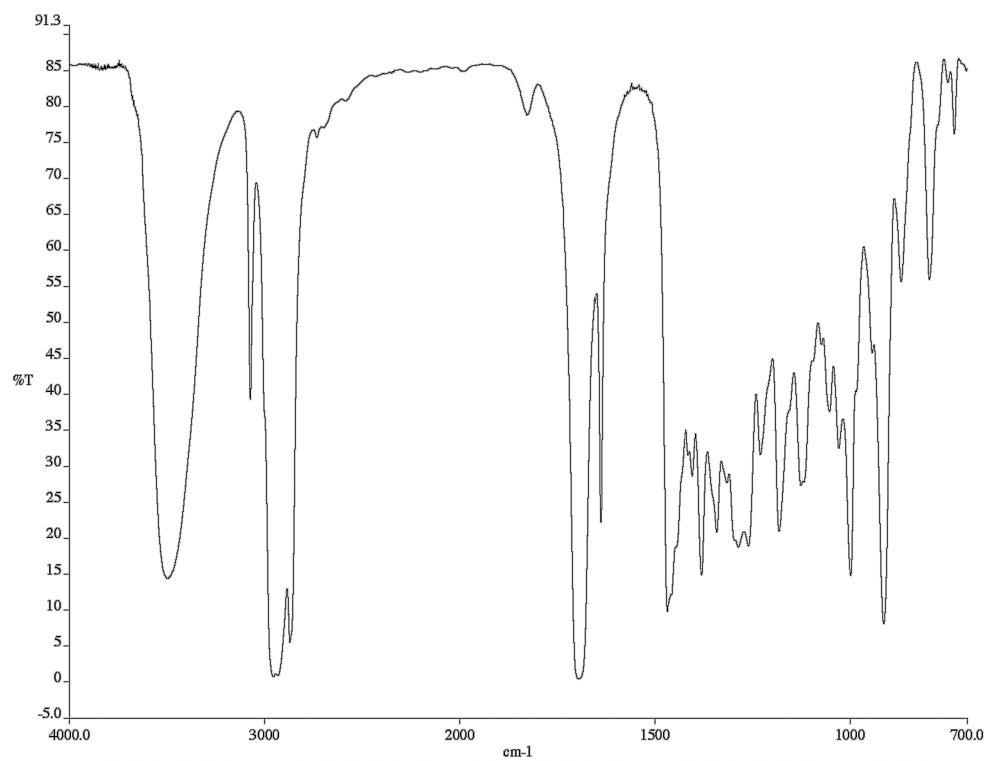


Figure A1.213. Infrared spectrum (thin film/NaCl) of compound **154r**.

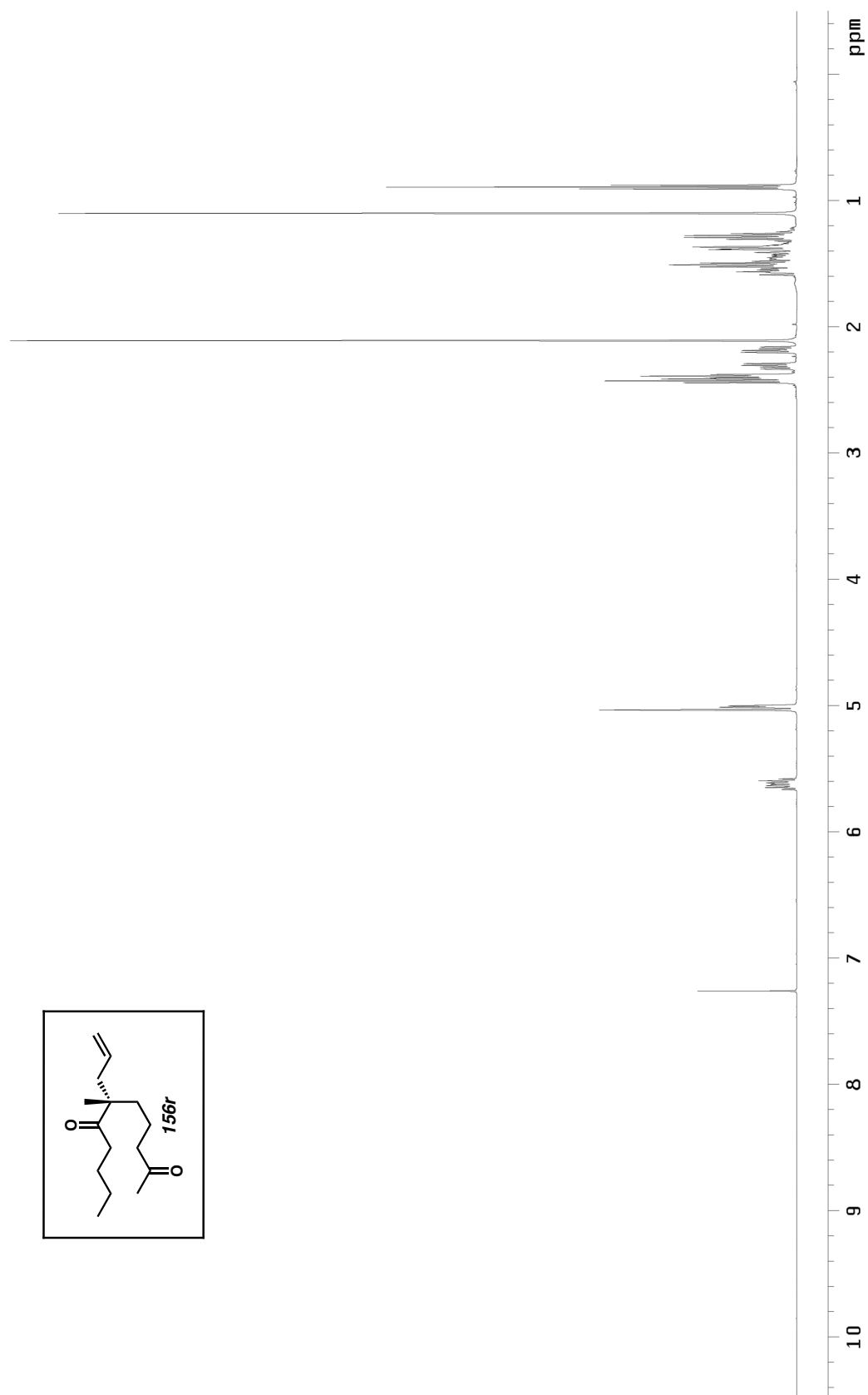


Figure A1.214. ^1H NMR (500 MHz, CDCl_3) of compound **156r**.

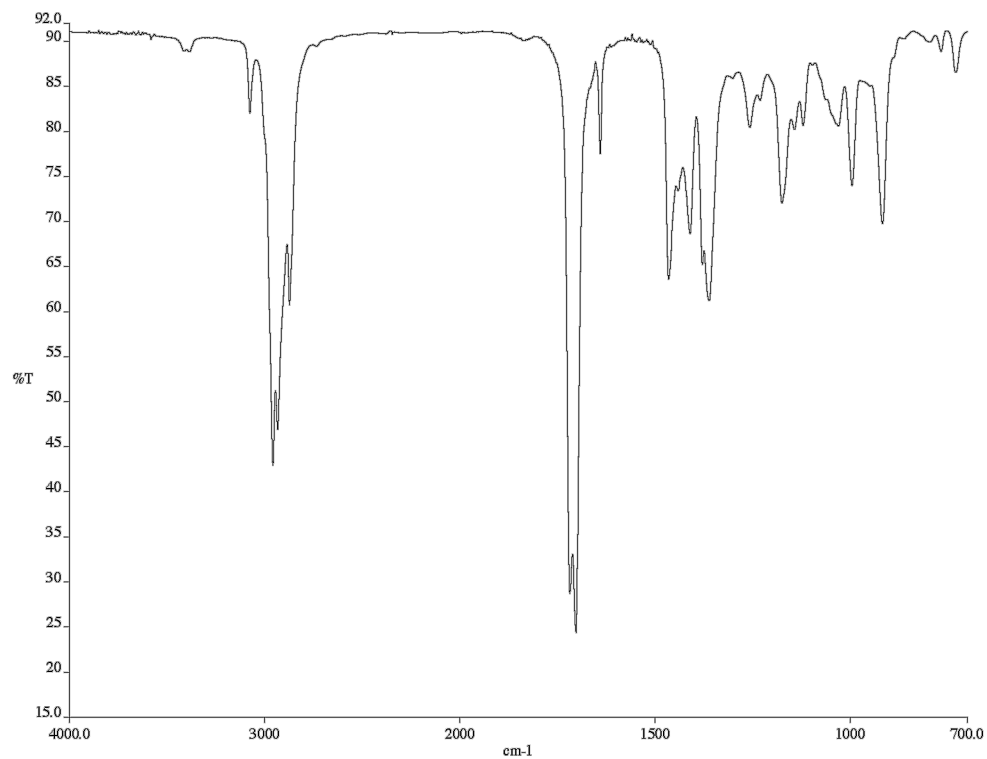


Figure A1.215. Infrared spectrum (thin film/NaCl) of compound **156r**.

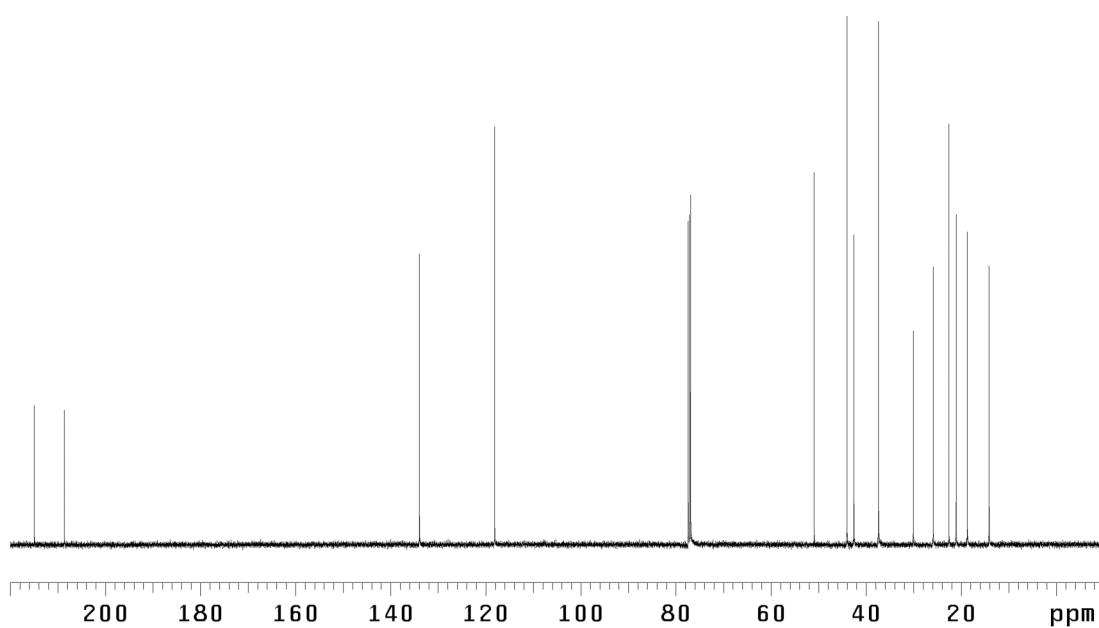


Figure A1.216. ¹³C NMR (125 MHz, CDCl₃) of compound **156r**.

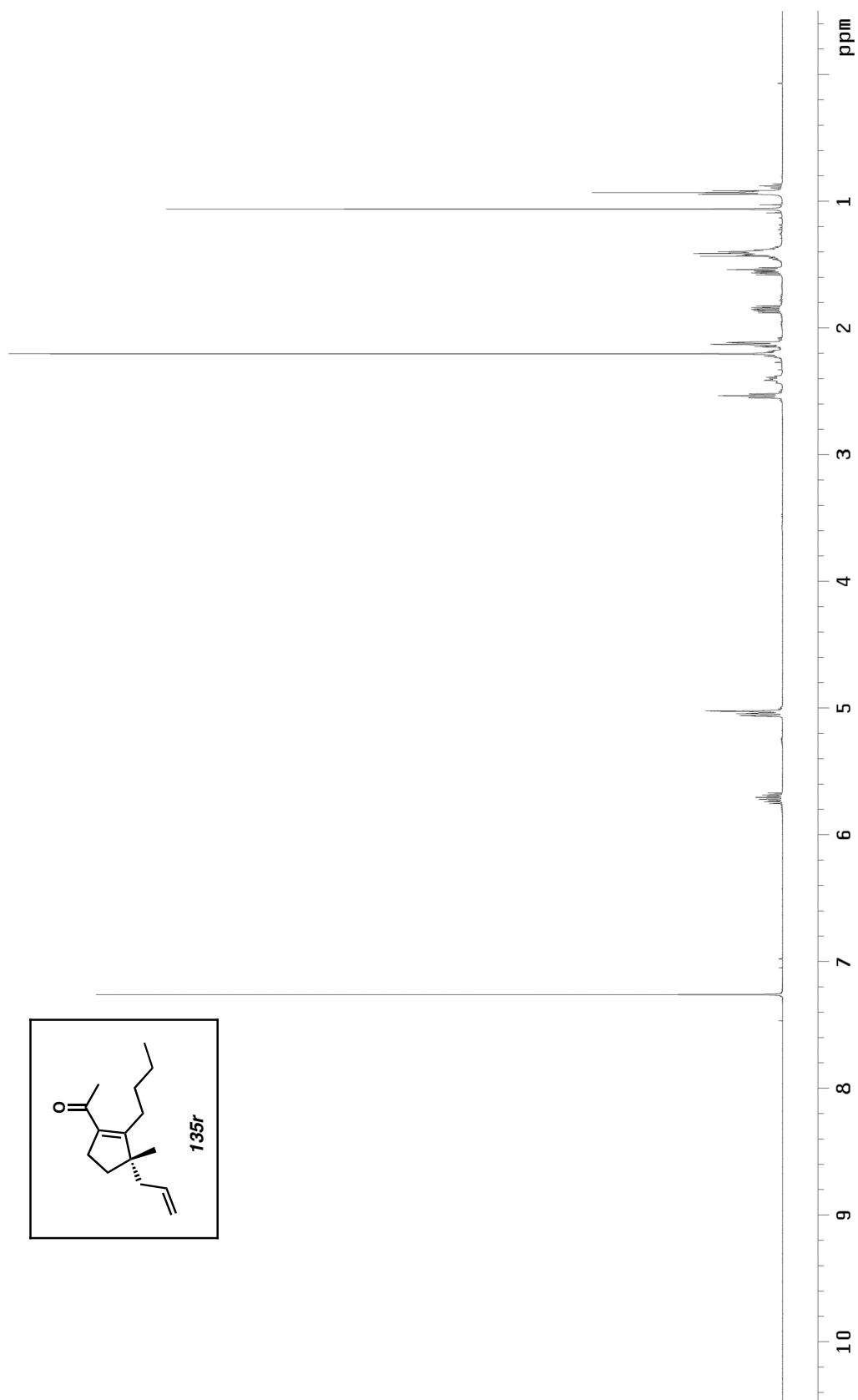


Figure A1.217. ^1H NMR (500 MHz, CDCl_3) of compound **135r**.

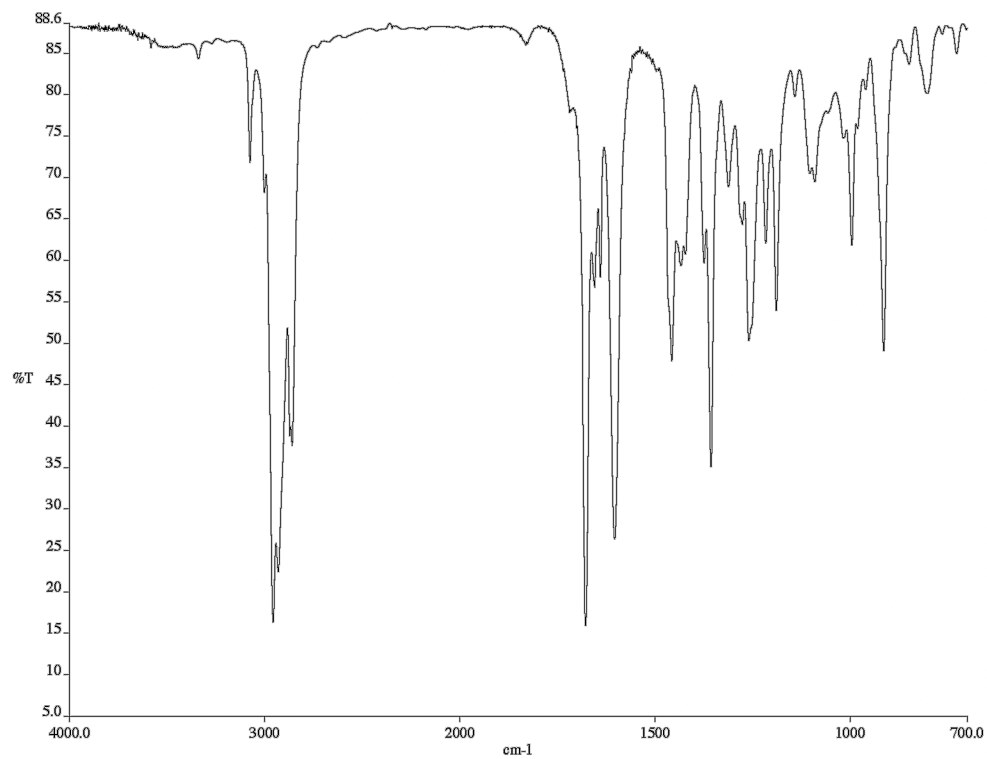


Figure A1.218. Infrared spectrum (thin film/NaCl) of compound **135r**.

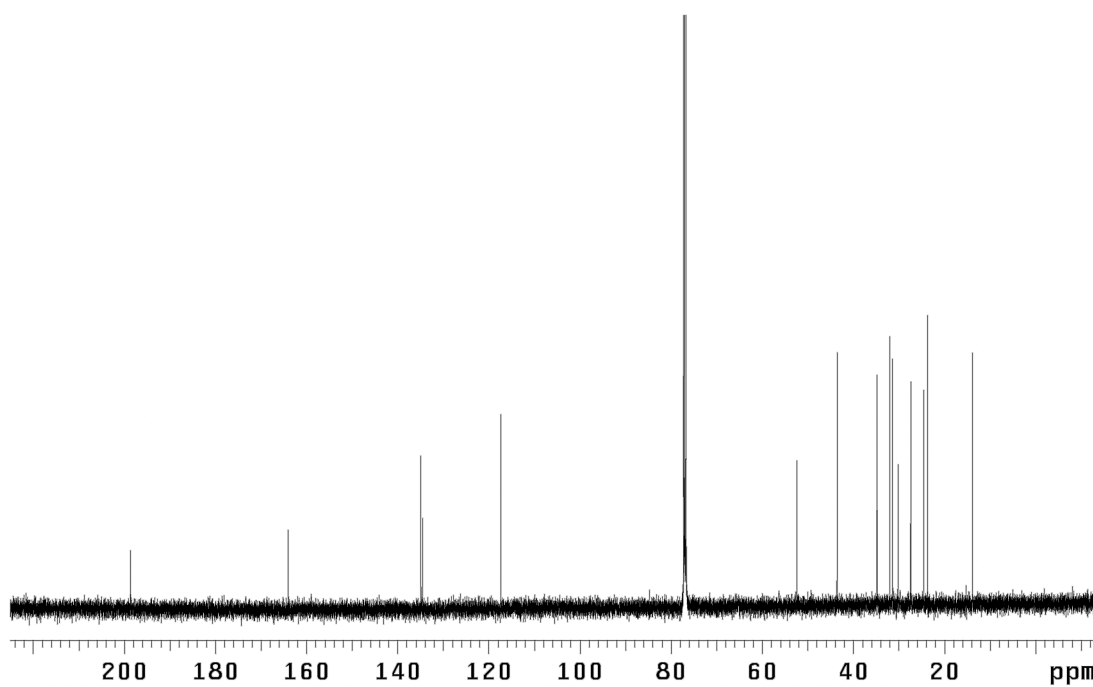


Figure A1.219. ¹³C NMR (125 MHz, CDCl₃) of compound **135r**.

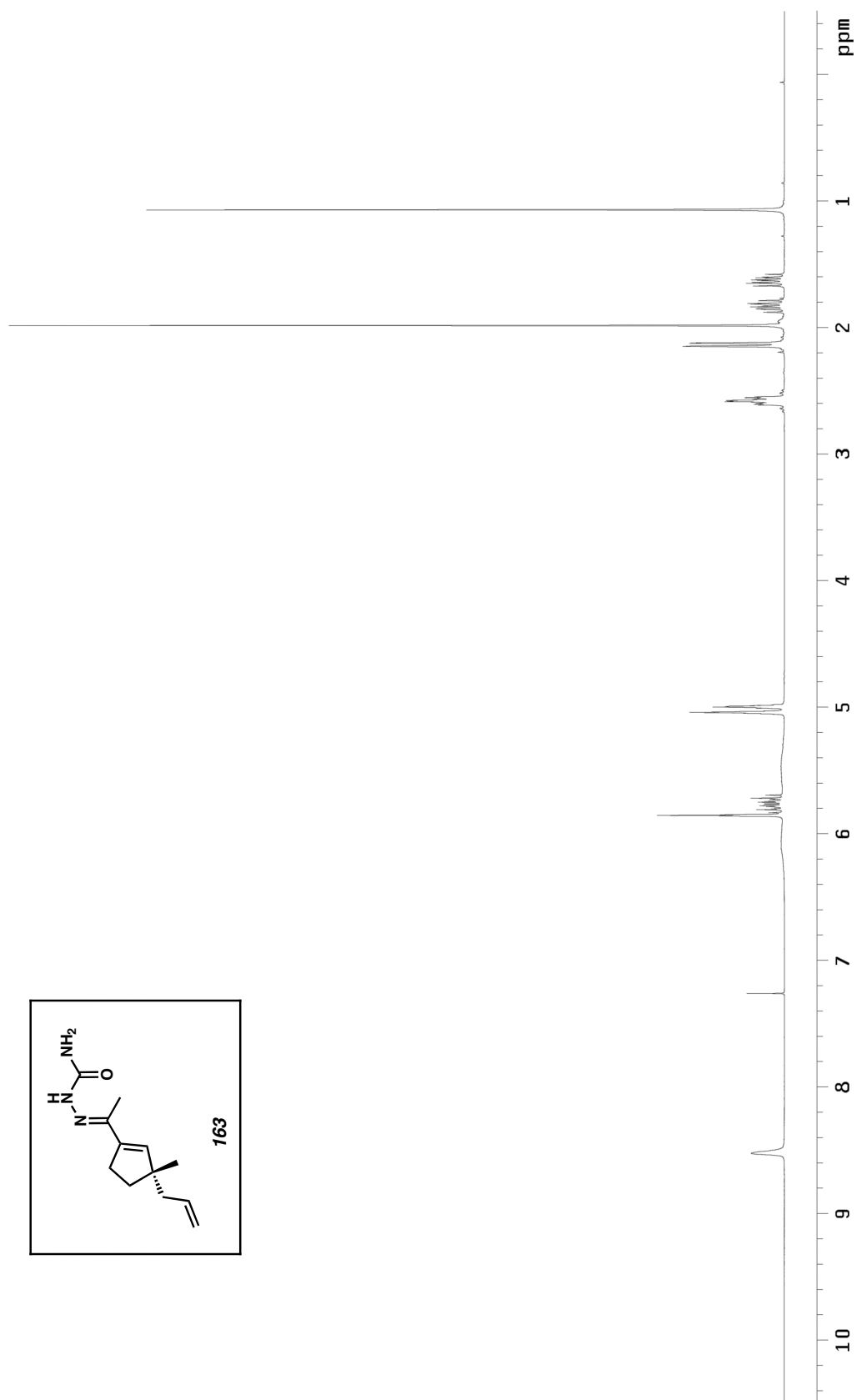


Figure A1.220. ¹H NMR (300 MHz, CDCl₃) of compound **163**.

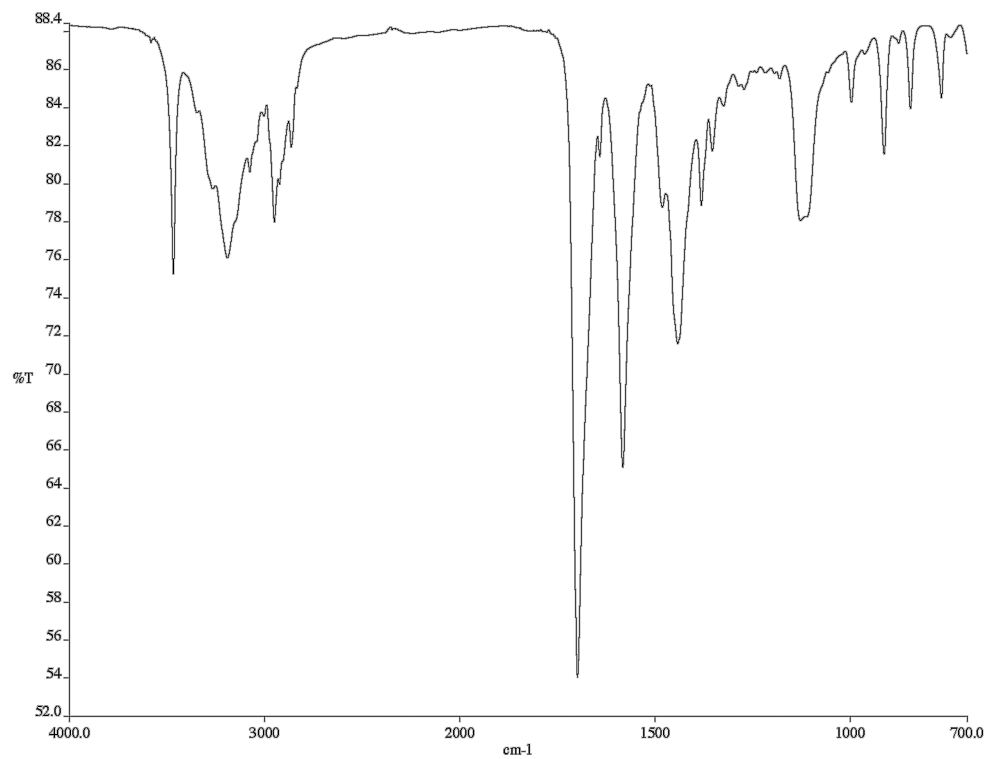


Figure A1.221. Infrared spectrum (thin film/NaCl) of compound **163**.

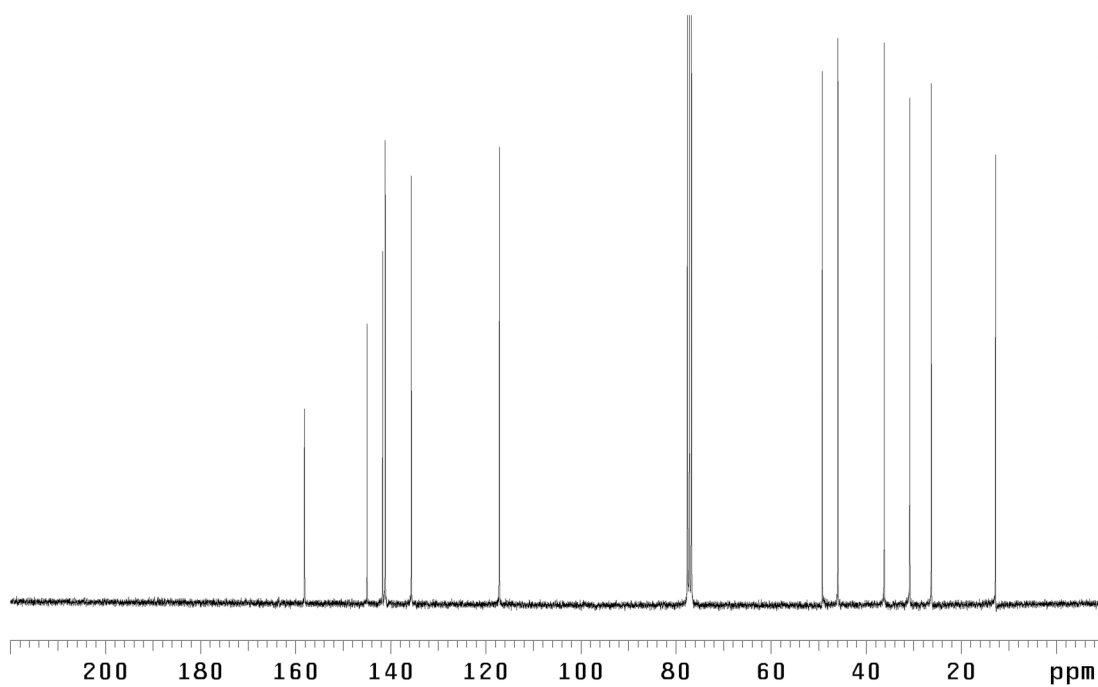


Figure A1.222. ¹³C NMR (75 MHz, CDCl₃) of compound **163**.

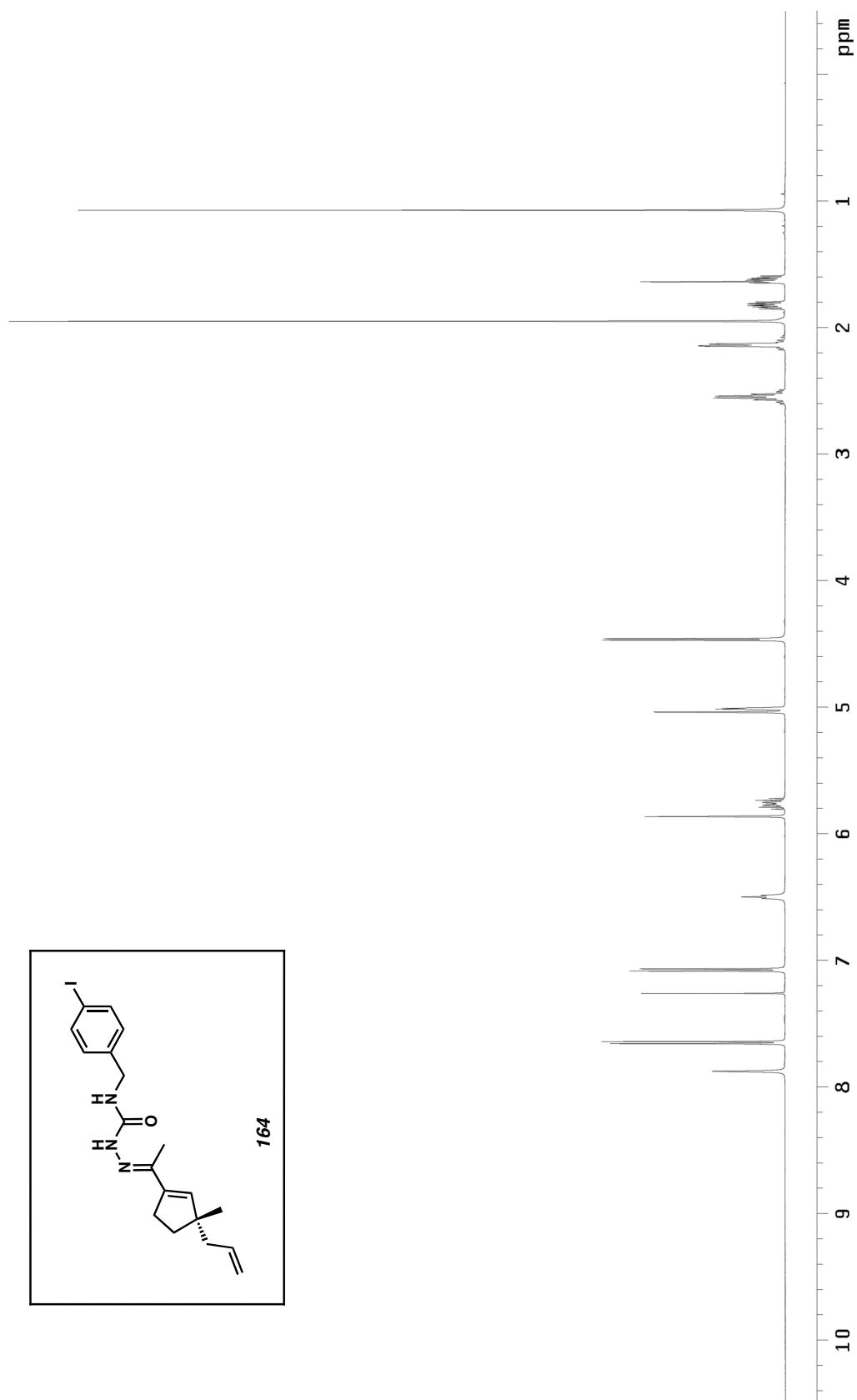


Figure A1.223. ^1H NMR (500 MHz, CDCl_3) of compound **164**.

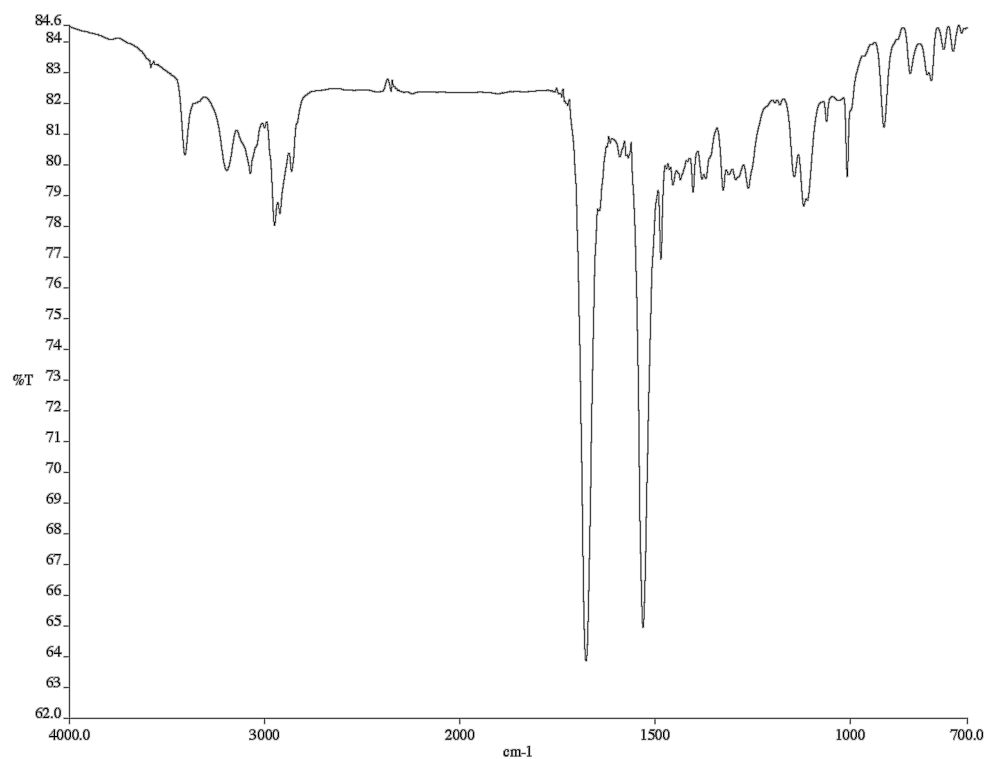


Figure A1.224. Infrared spectrum (thin film/NaCl) of compound **164**.

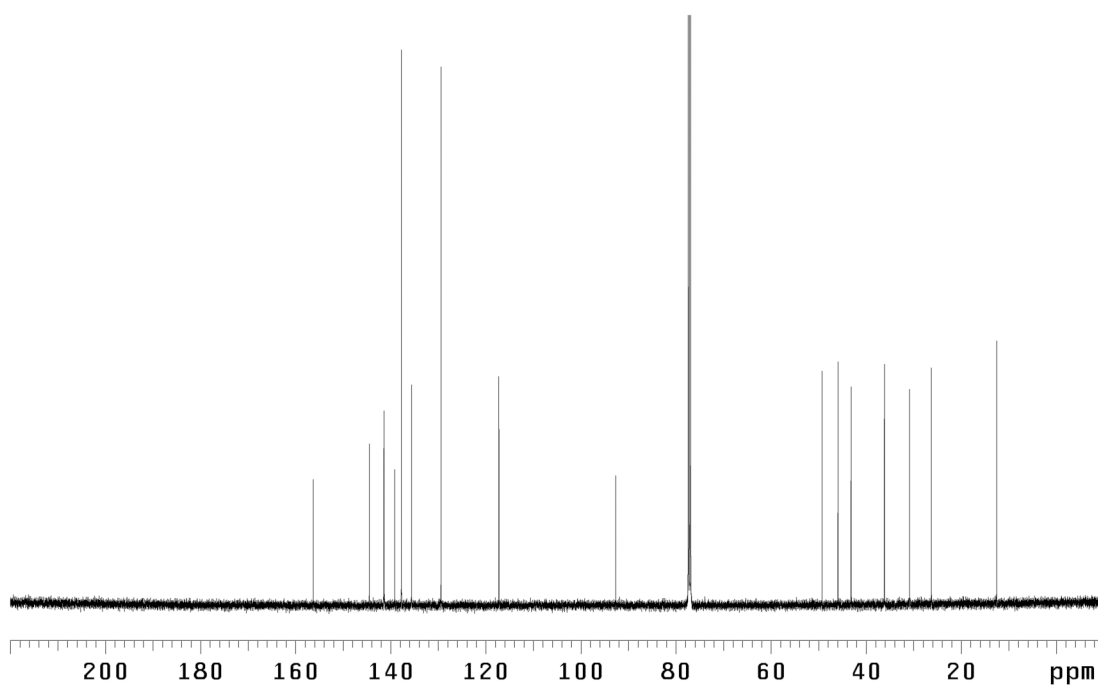


Figure A1.225. ¹³C NMR (125 MHz, CDCl₃) of compound **164**.

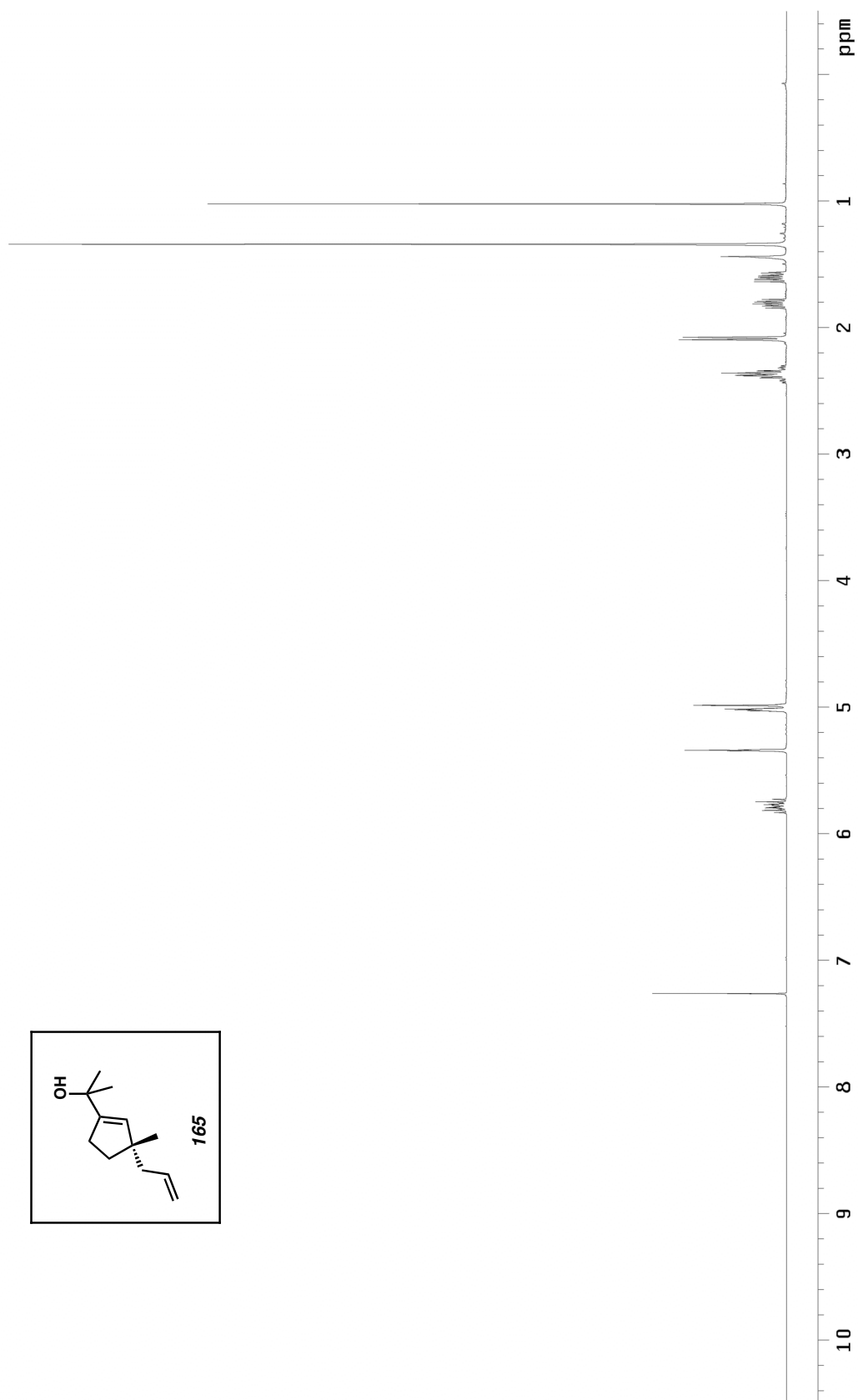


Figure A1.226. ^1H NMR (400 MHz, CDCl_3) of compound **165**.

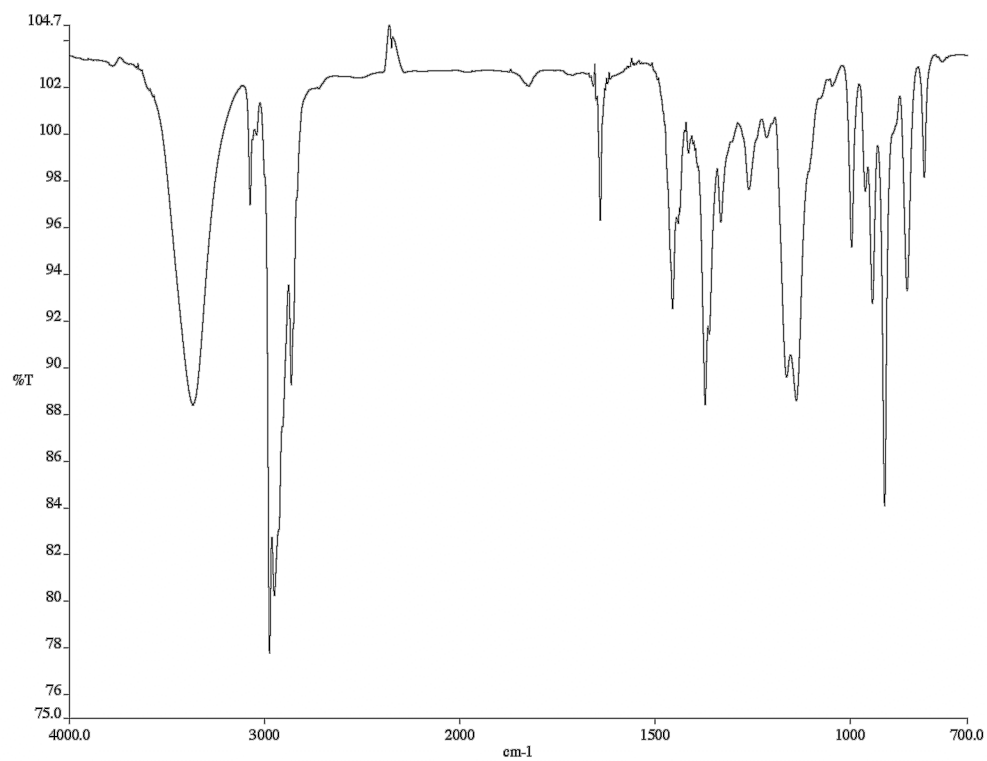


Figure A1.227. Infrared spectrum (thin film/NaCl) of compound **165**.

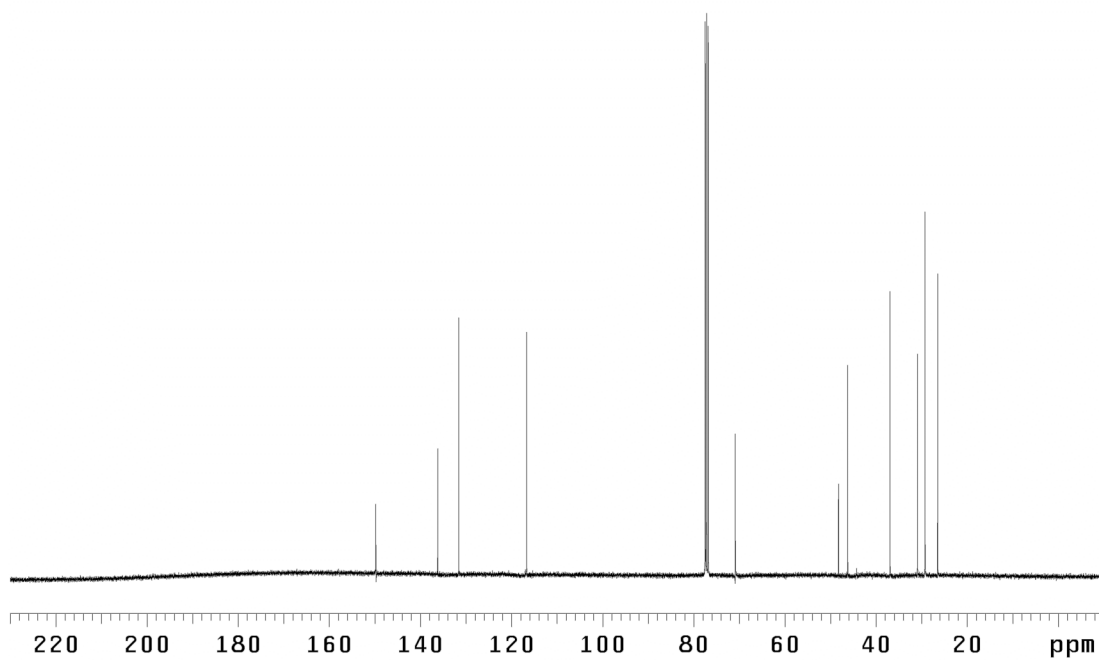


Figure A1.228. ¹³C NMR (100 MHz, CDCl₃) of compound **165**.

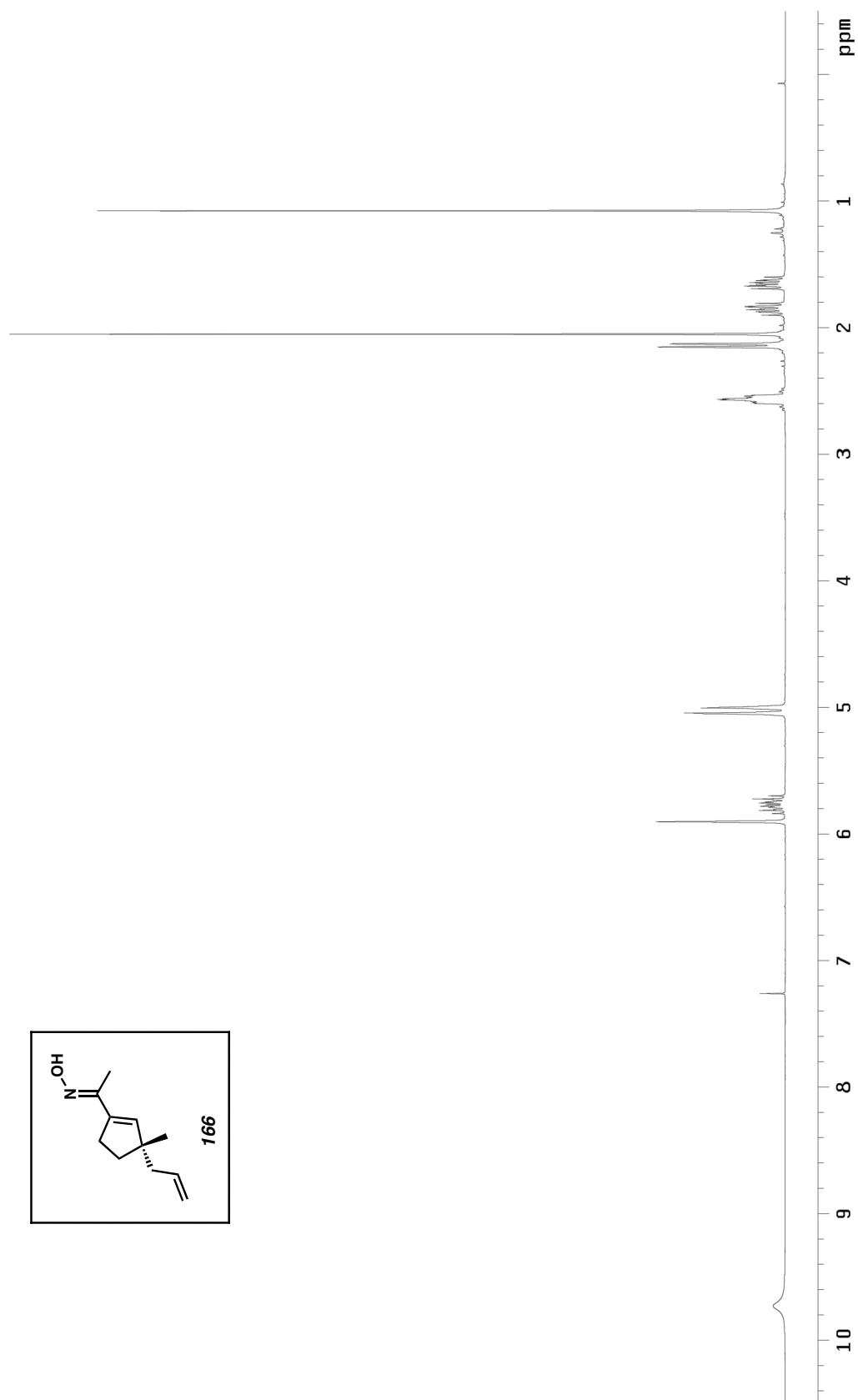


Figure A1.229. ¹H NMR (300 MHz, CDCl₃) of compound **166**.

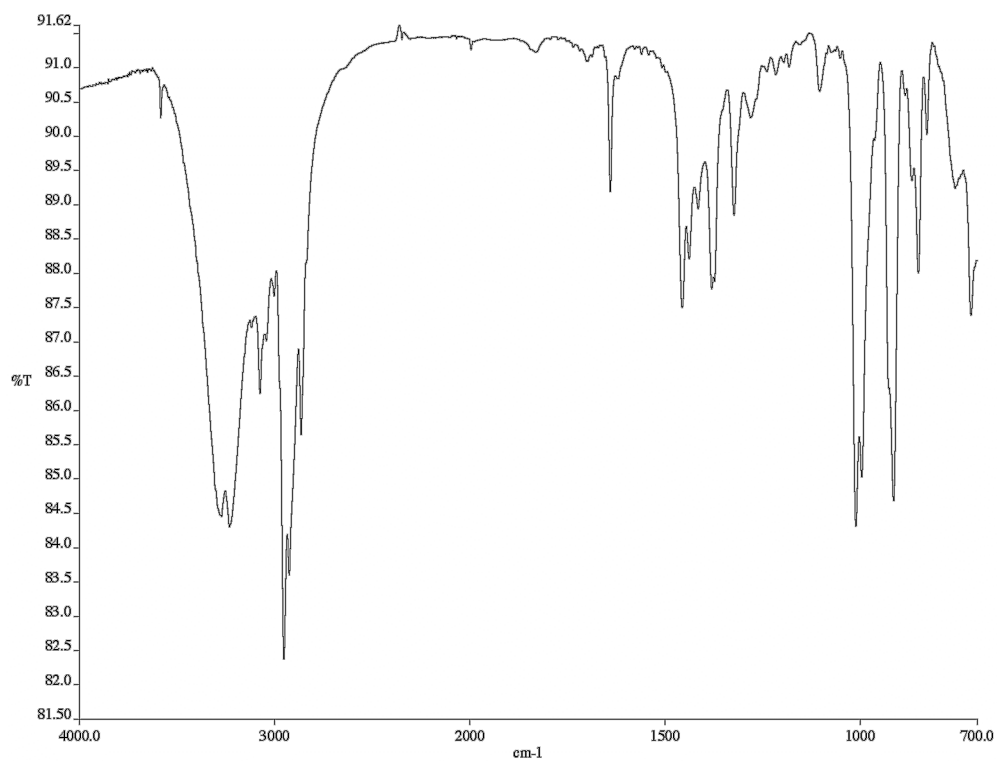


Figure A1.230. Infrared spectrum (thin film/NaCl) of compound **166**.

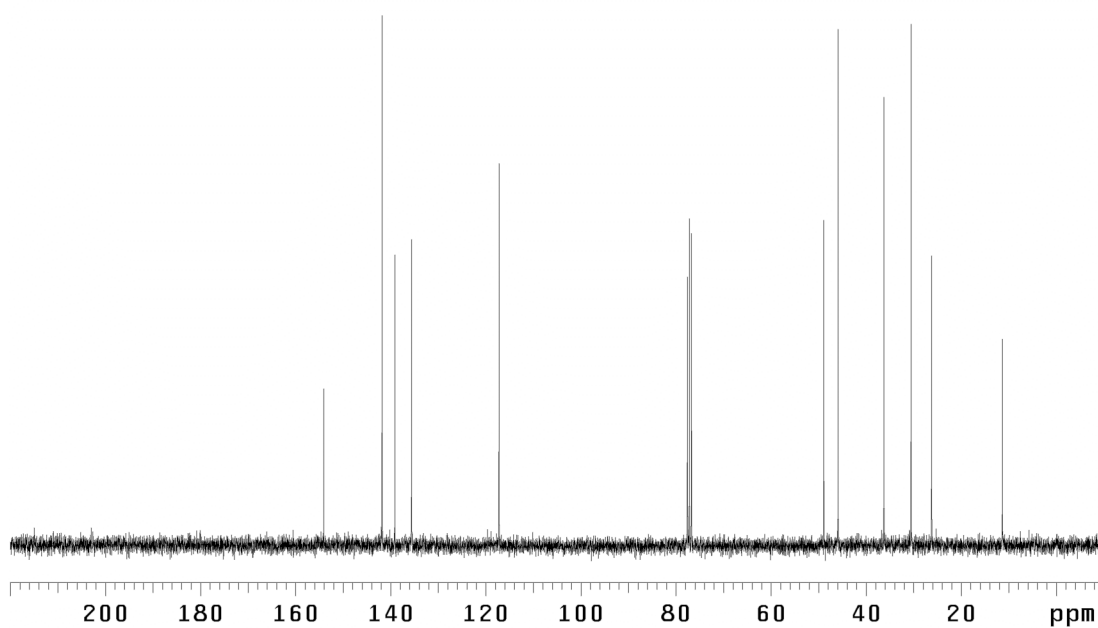


Figure A1.231. ¹³C NMR (75 MHz, CDCl₃) of compound **166**.

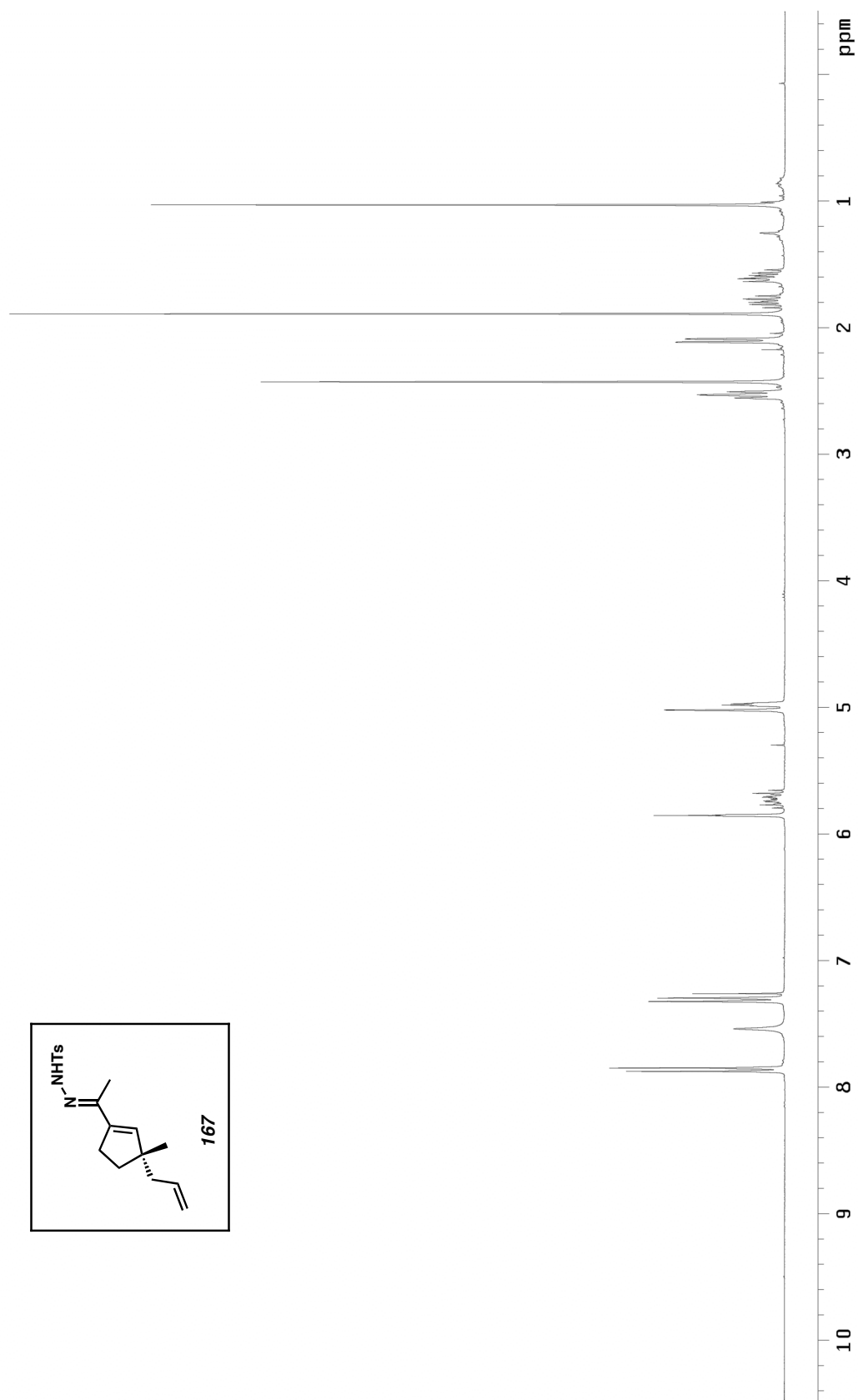


Figure A1.232. ^1H NMR (300 MHz, CDCl_3) of compound **167**.

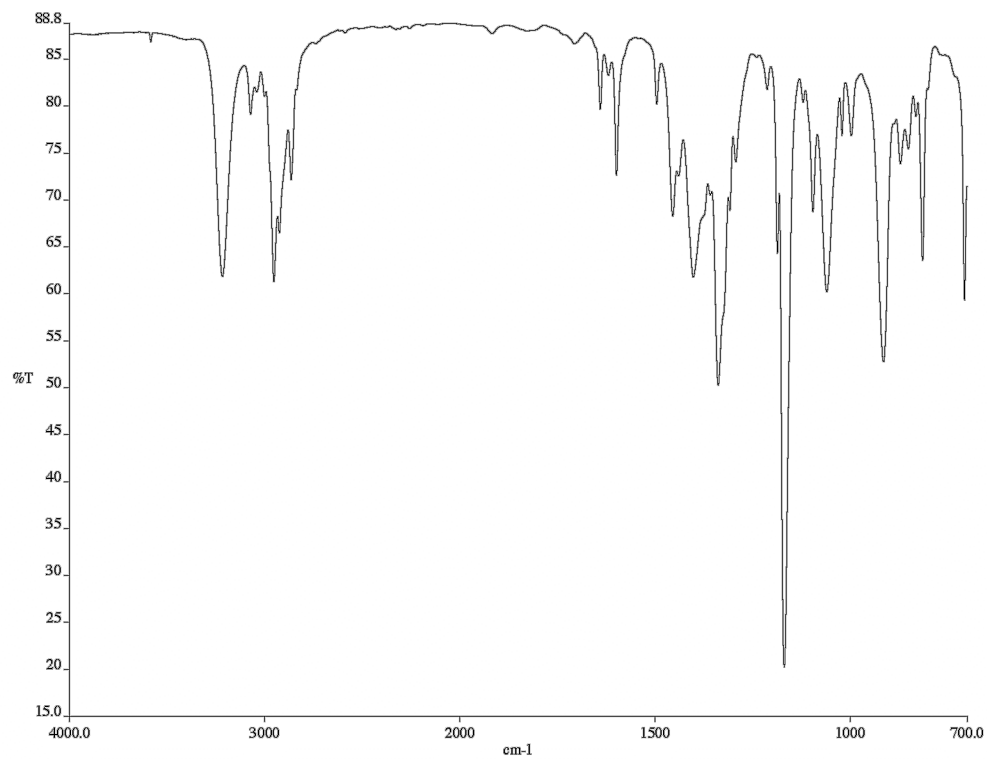


Figure A1.233. Infrared spectrum (thin film/NaCl) of compound **167**.

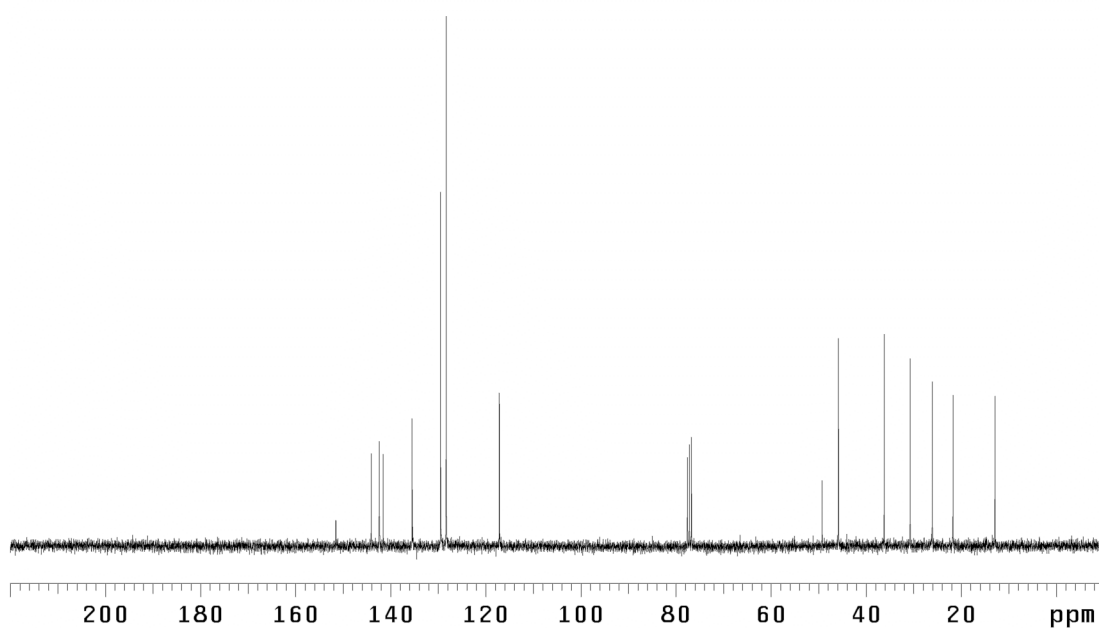


Figure A1.234. ¹³C NMR (75 MHz, CDCl₃) of compound **167**.

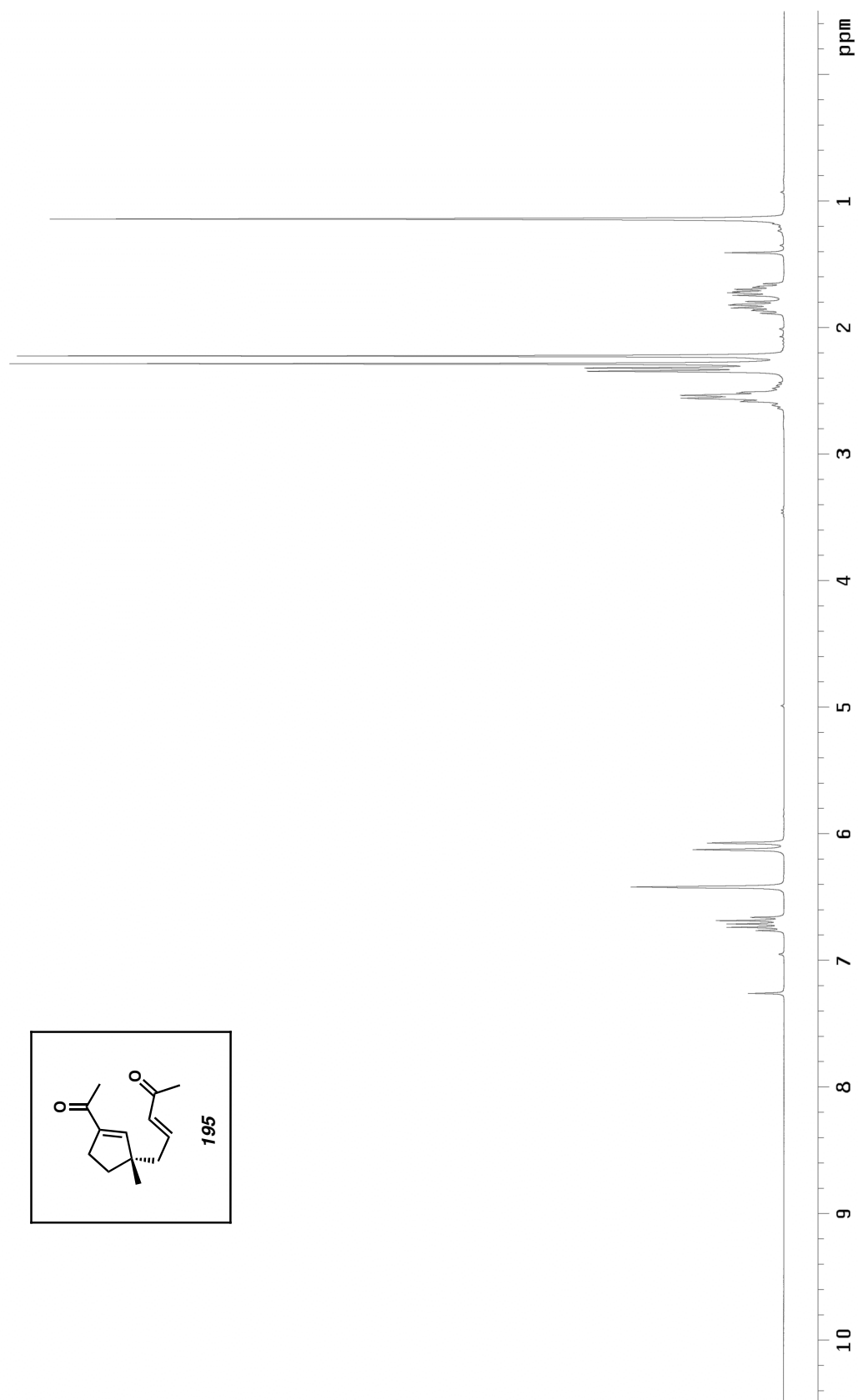


Figure A1.235. ^1H NMR (300 MHz, CDCl_3) of compound **195**.

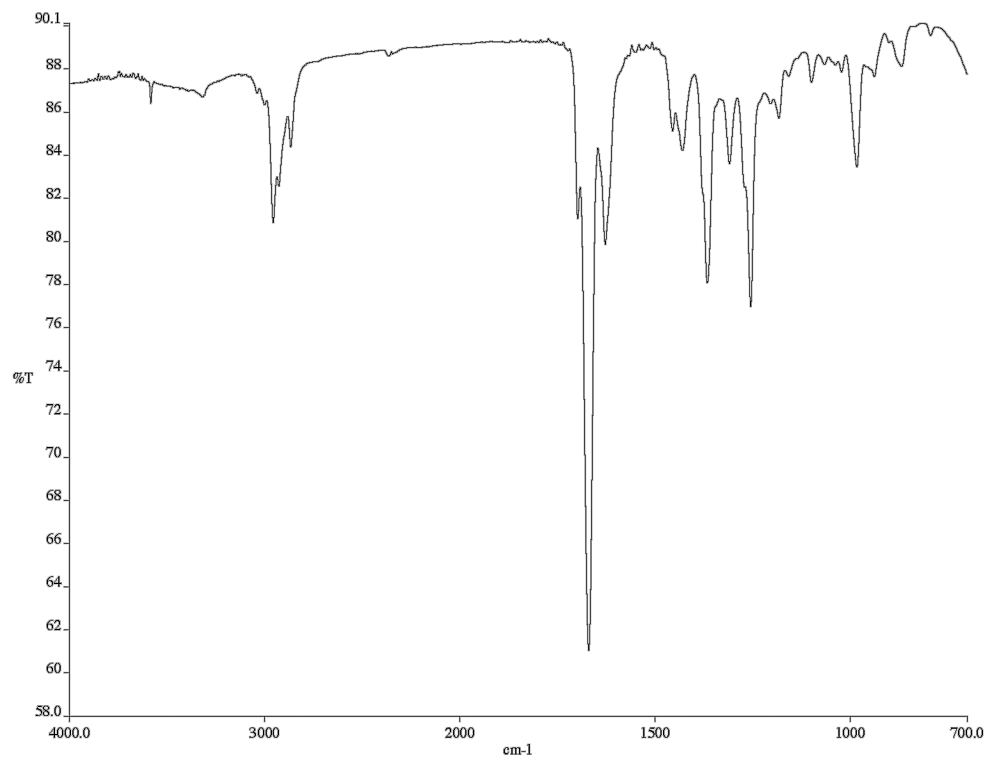


Figure A1.236. Infrared spectrum (thin film/NaCl) of compound **195**.

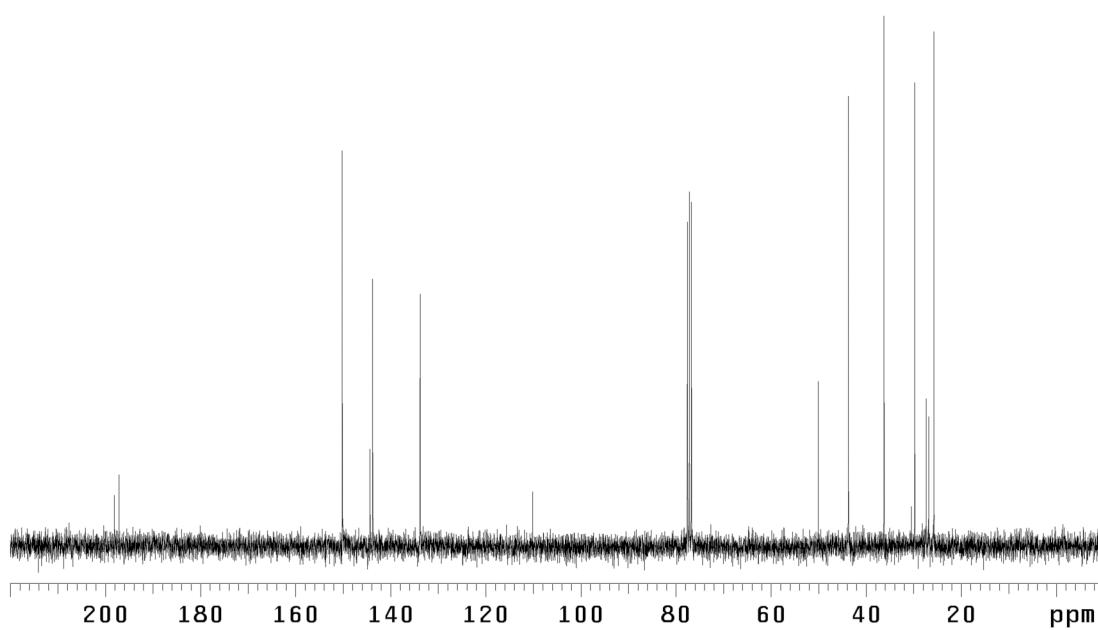


Figure A1.237. ¹³C NMR (75 MHz, CDCl₃) of compound **195**.

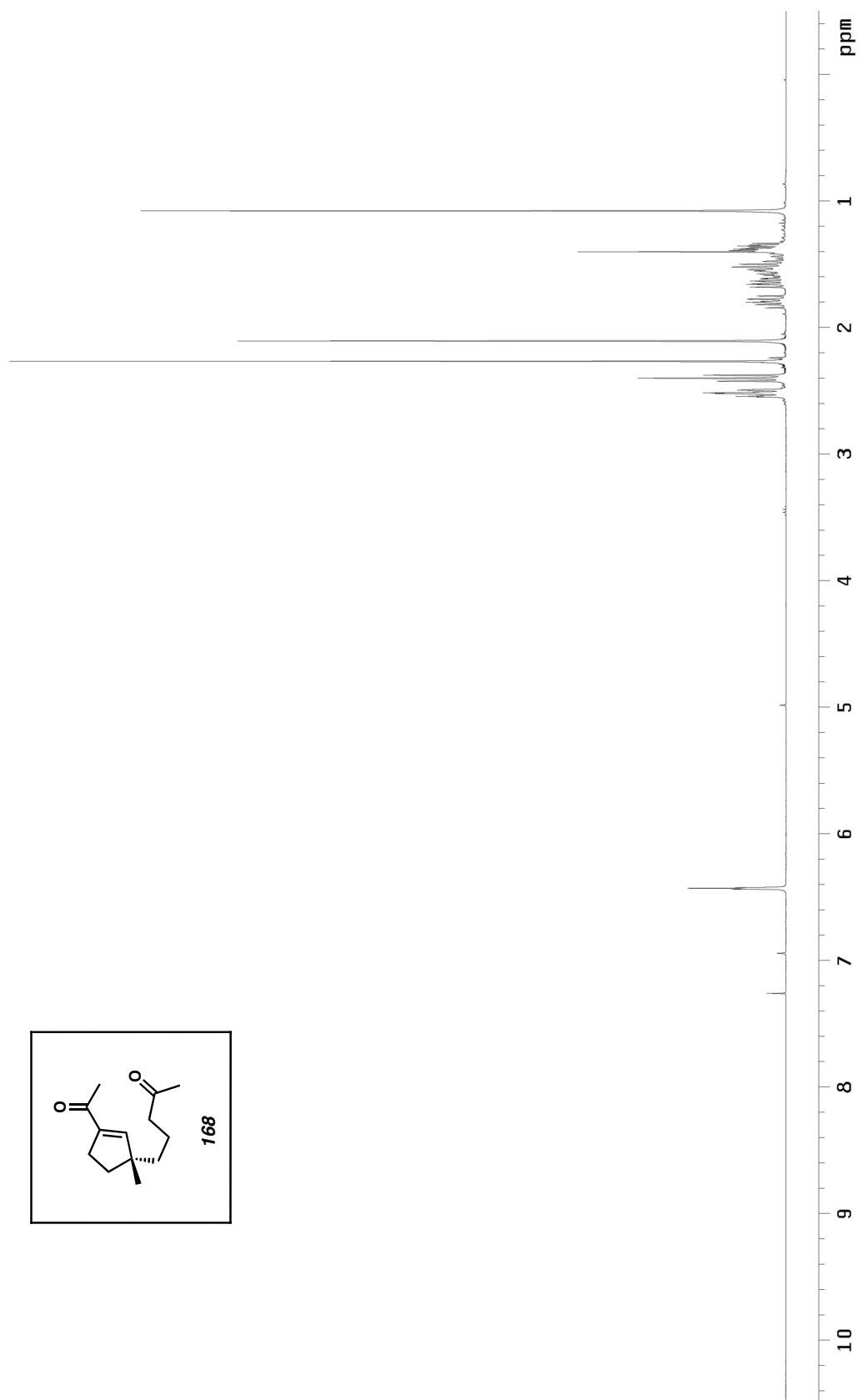


Figure A1.238. ^1H NMR (300 MHz, CDCl_3) of compound **168**.

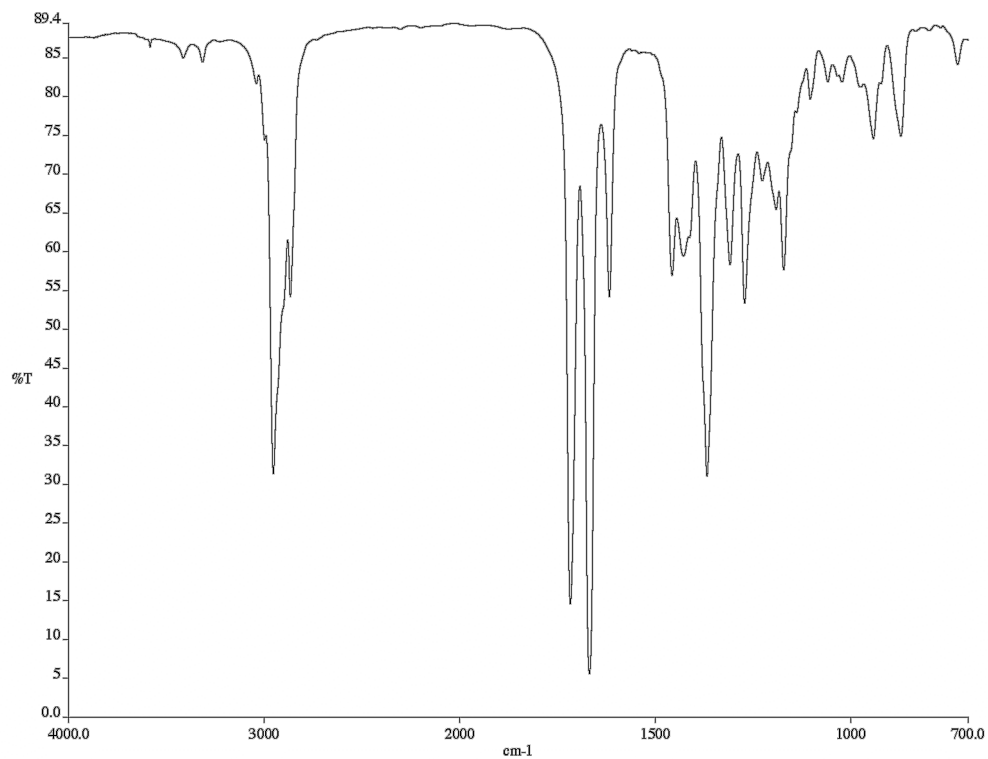


Figure A1.239. Infrared spectrum (thin film/NaCl) of compound **168**.

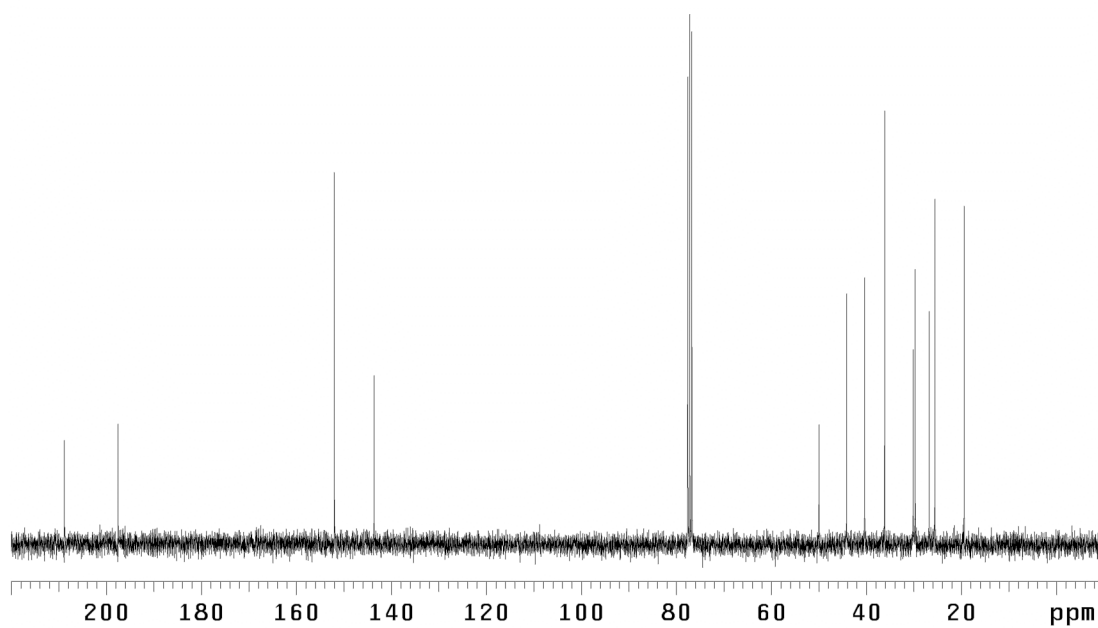


Figure A1.240. ¹³C NMR (75 MHz, CDCl₃) of compound **168**.

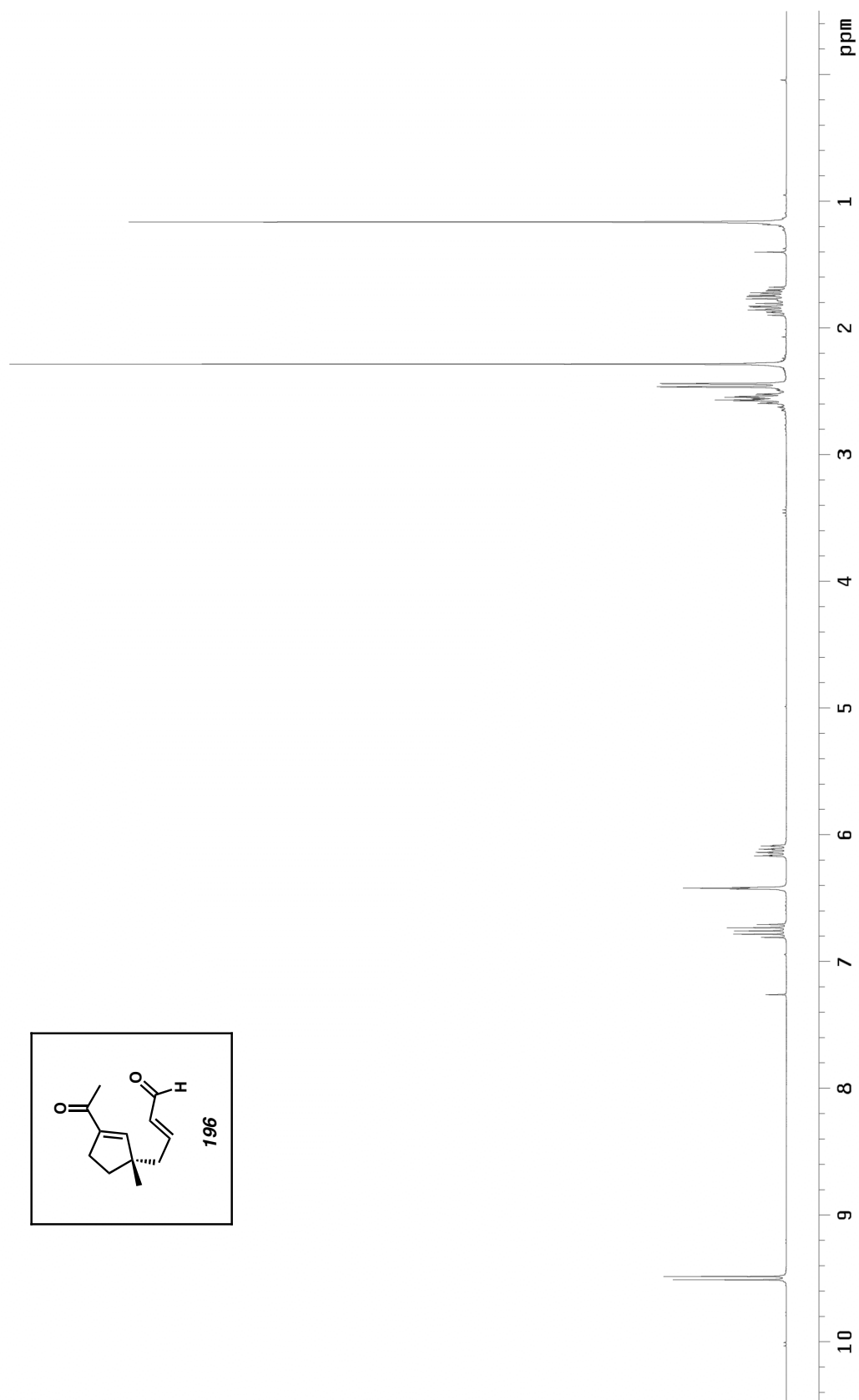


Figure A1.241. ^1H NMR (300 MHz, CDCl_3) of compound **196**.

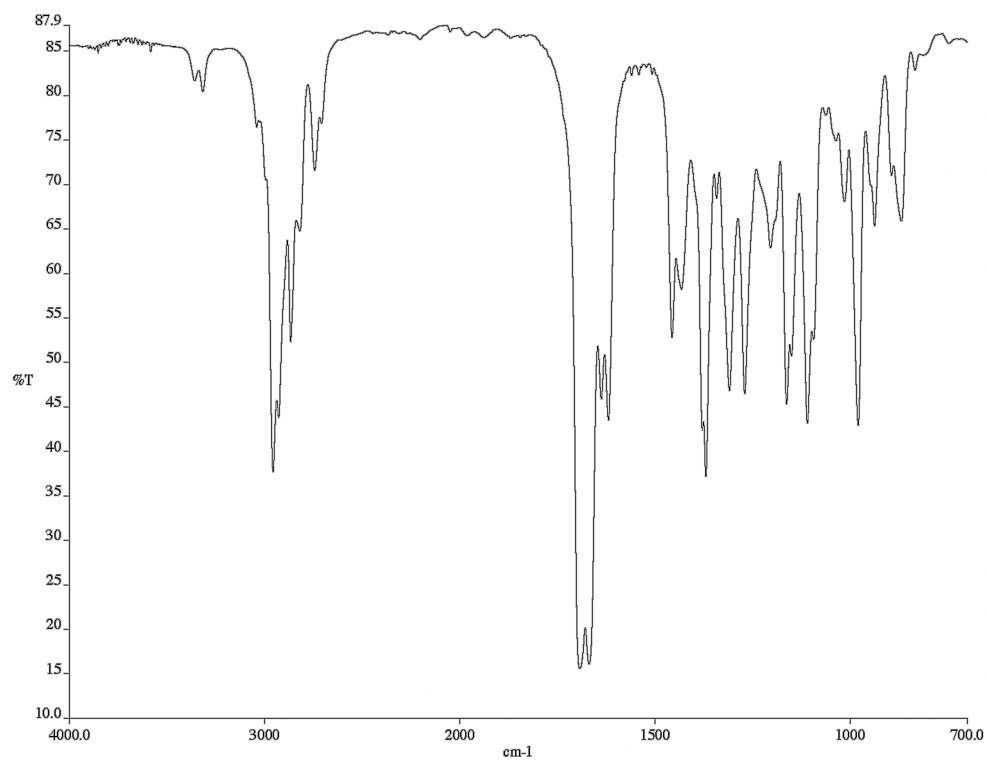


Figure A1.243. Infrared spectrum (thin film/NaCl) of compound **196**.

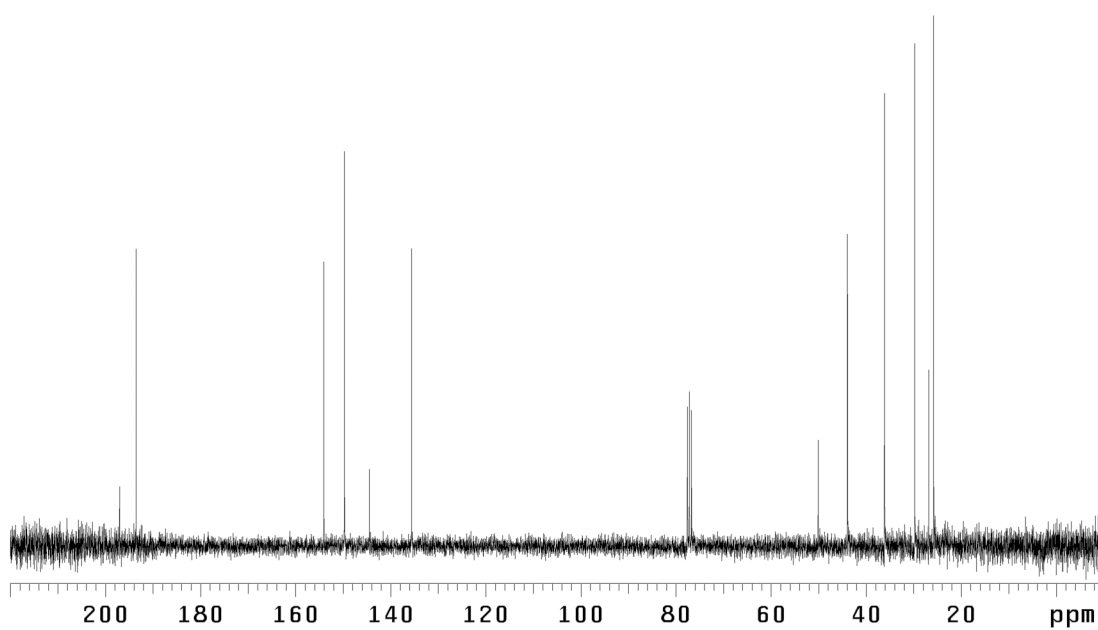


Figure A1.242. ^{13}C NMR (75 MHz, CDCl_3) of compound **196**.

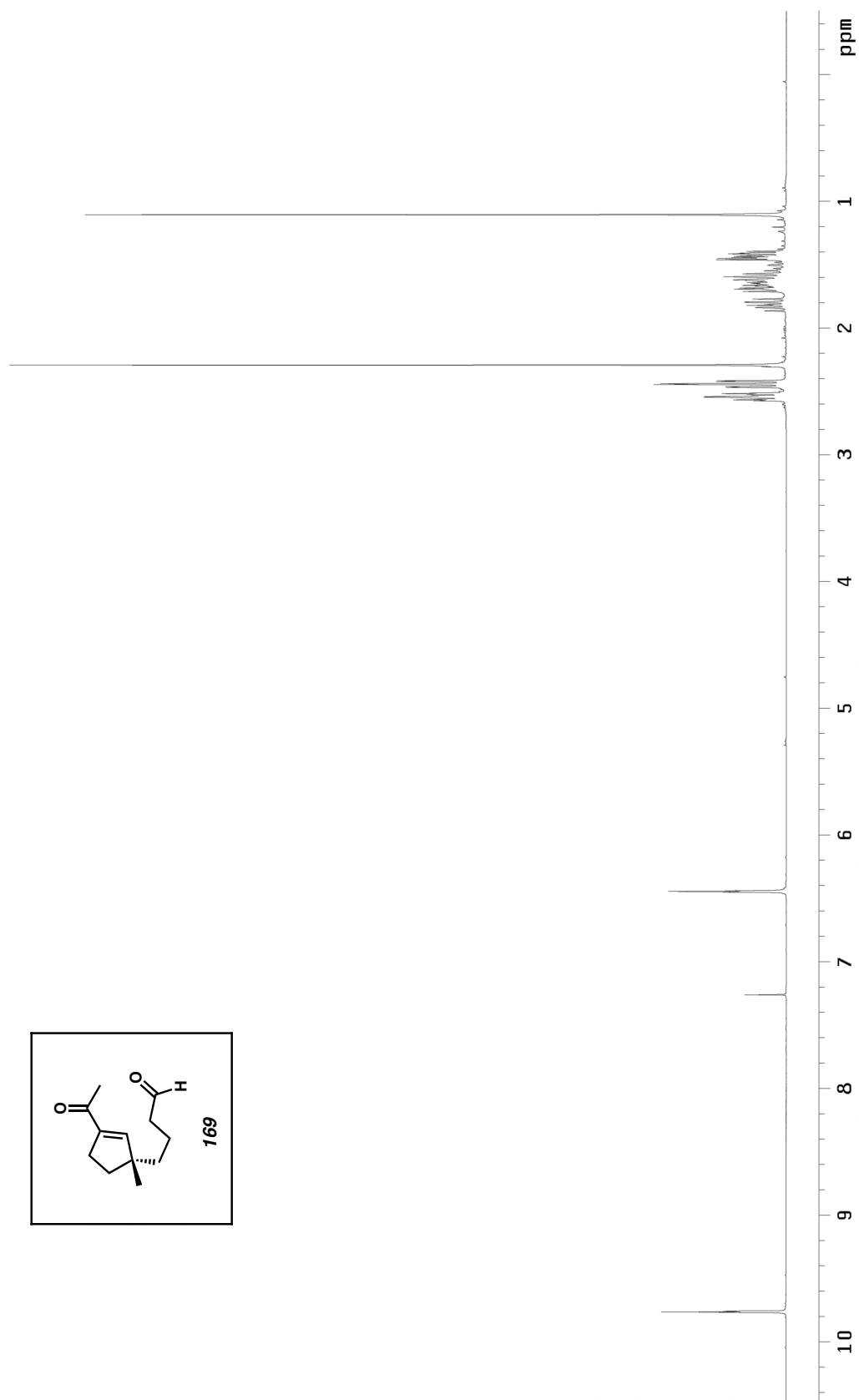


Figure A1.244. ^1H NMR (300 MHz, CDCl_3) of compound **169**.

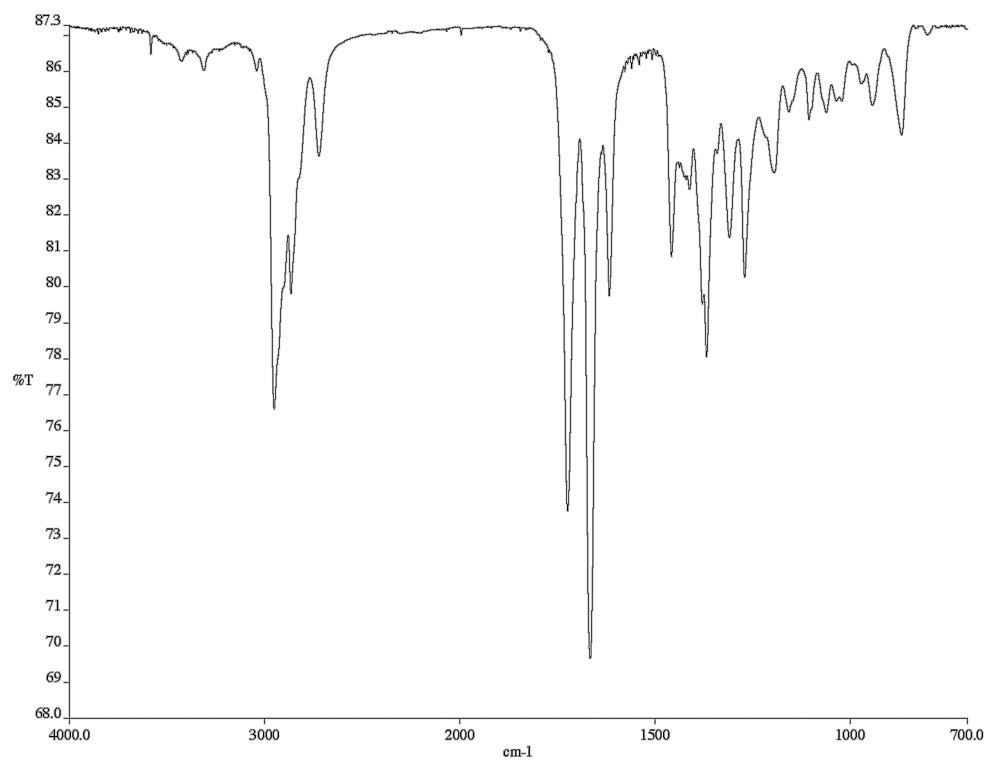


Figure A1.245. Infrared spectrum (thin film/NaCl) of compound **169**.

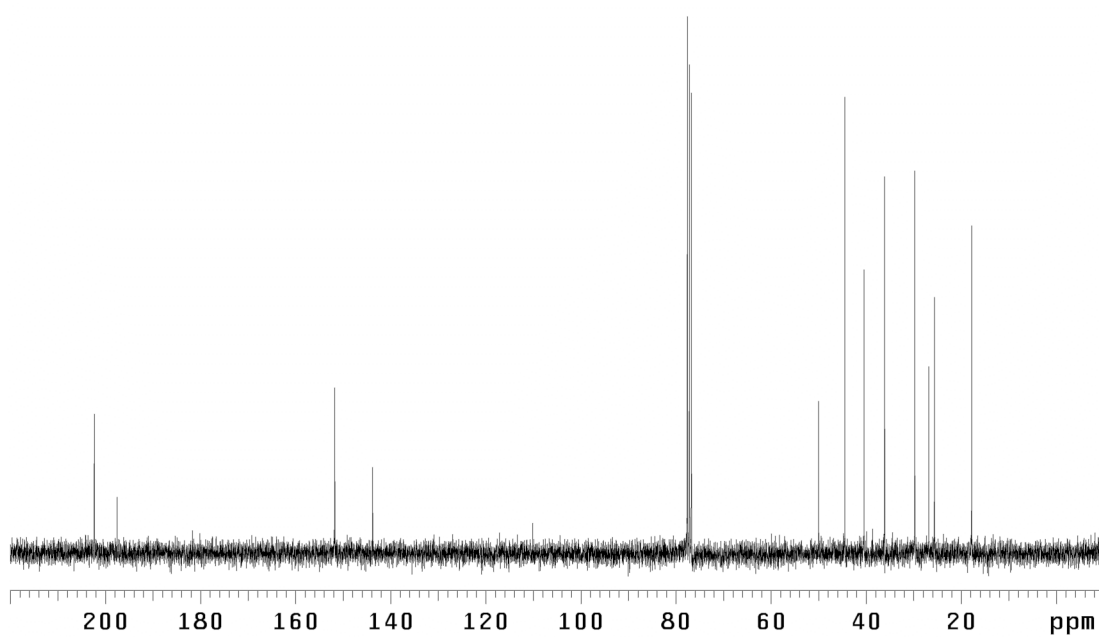


Figure A1.246. ¹³C NMR (75 MHz, CDCl₃) of compound **169**.

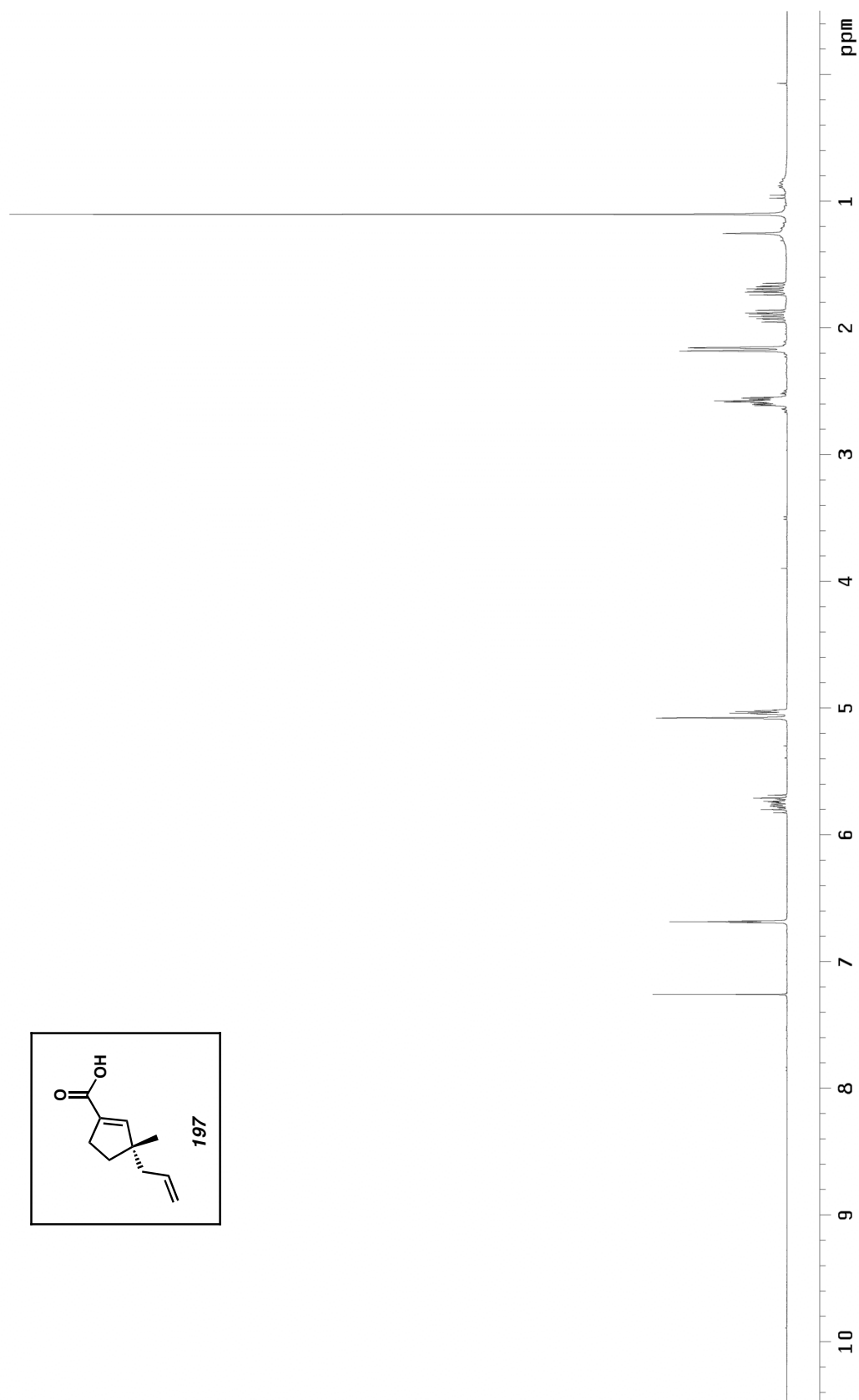


Figure A1.247. ^1H NMR (300 MHz, CDCl_3) of compound **197**.

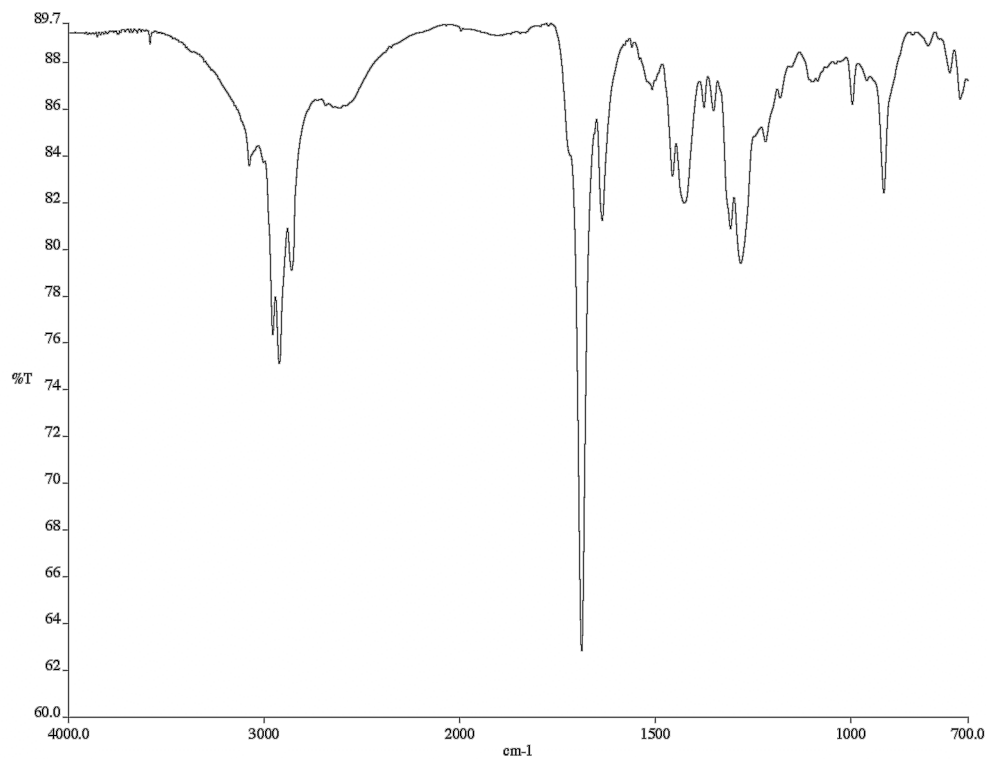


Figure A1.248. Infrared spectrum (thin film/NaCl) of compound **197**.

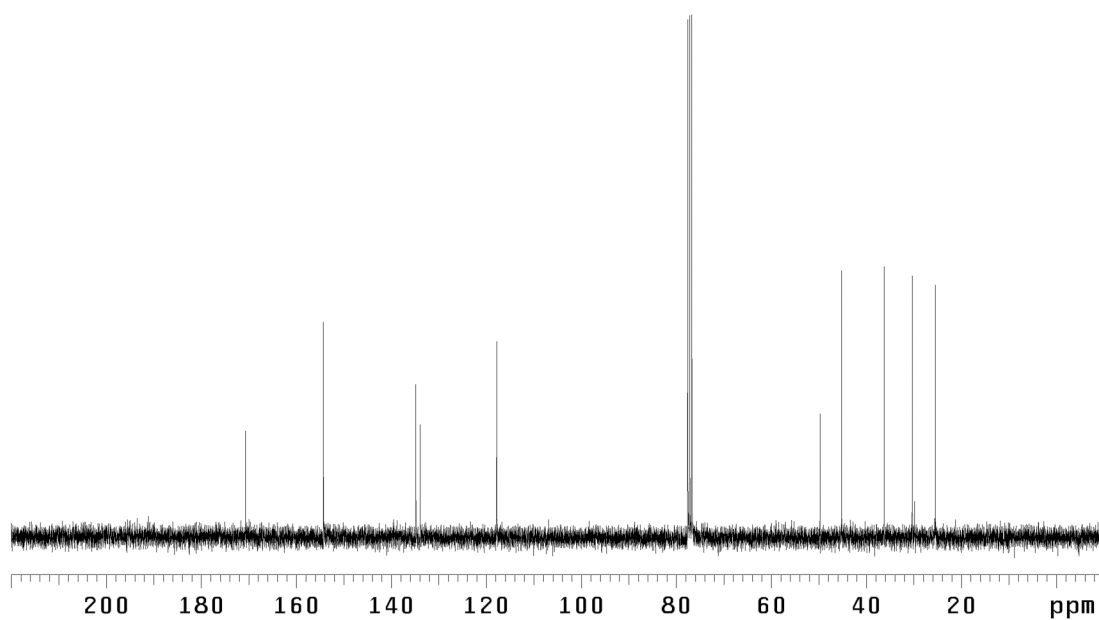


Figure A1.249. ¹³C NMR (75 MHz, CDCl₃) of compound **197**.

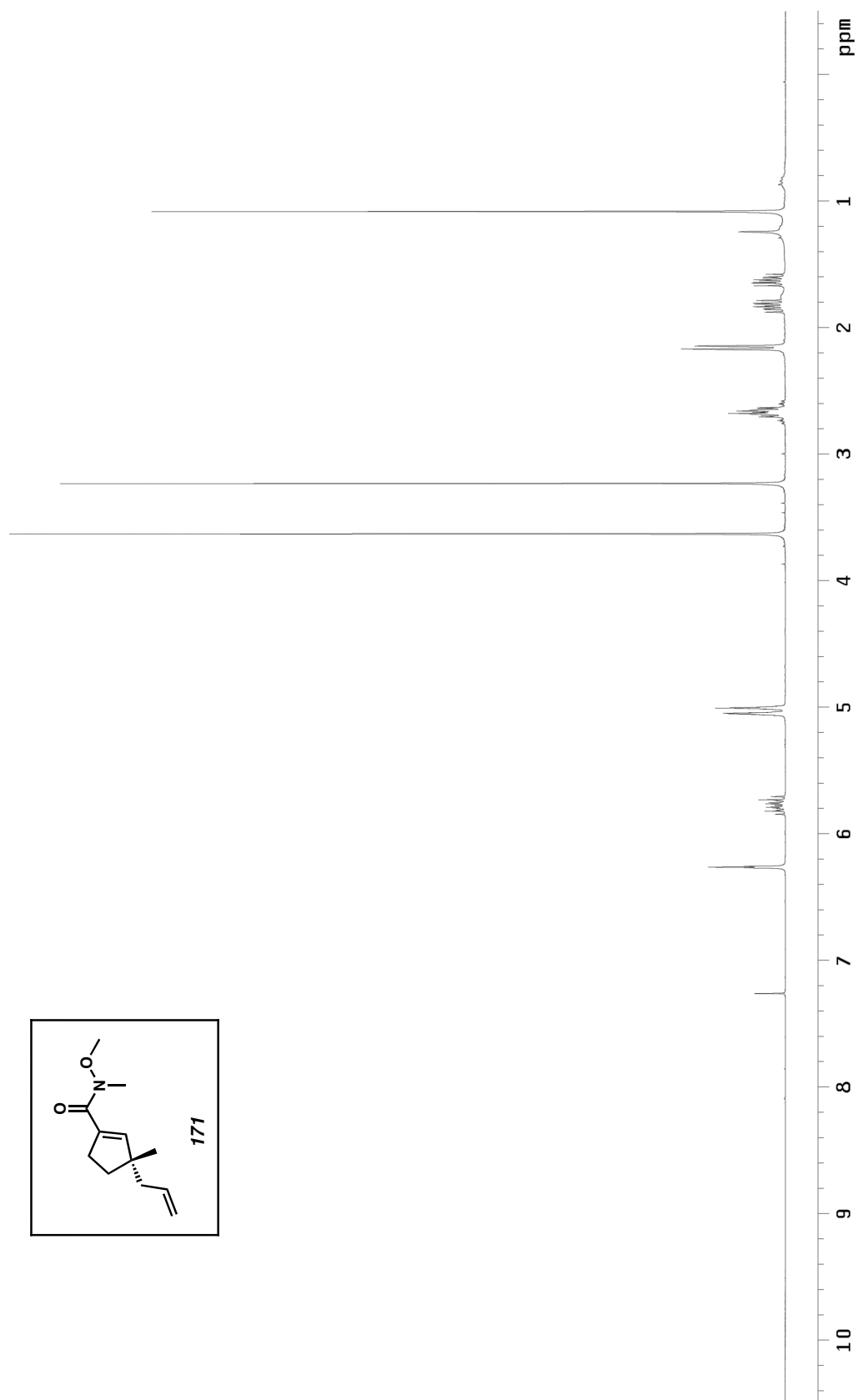


Figure A1.250. ^1H NMR (300 MHz, CDCl_3) of compound **171**.

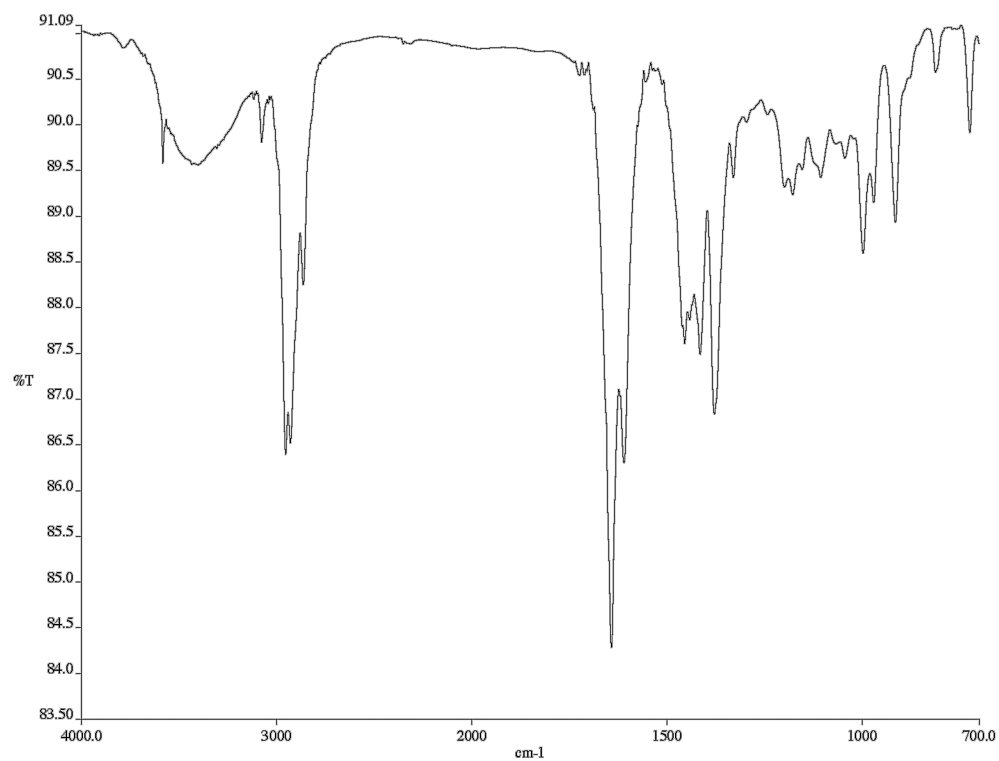


Figure A1.251. Infrared spectrum (thin film/NaCl) of compound **171**.

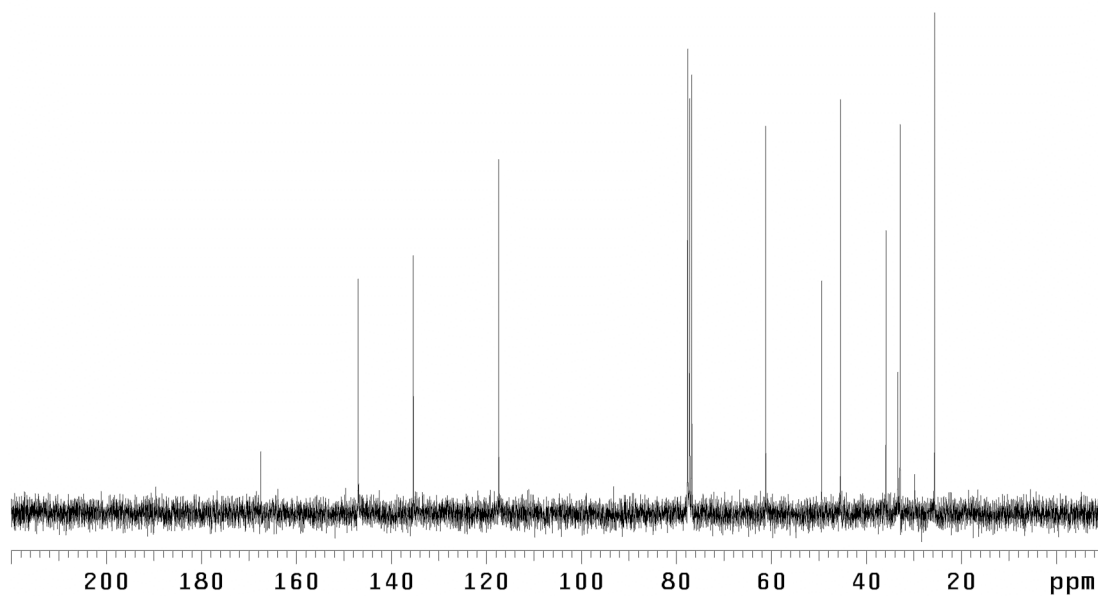


Figure A1.252. ¹³C NMR (75 MHz, CDCl₃) of compound **171**.

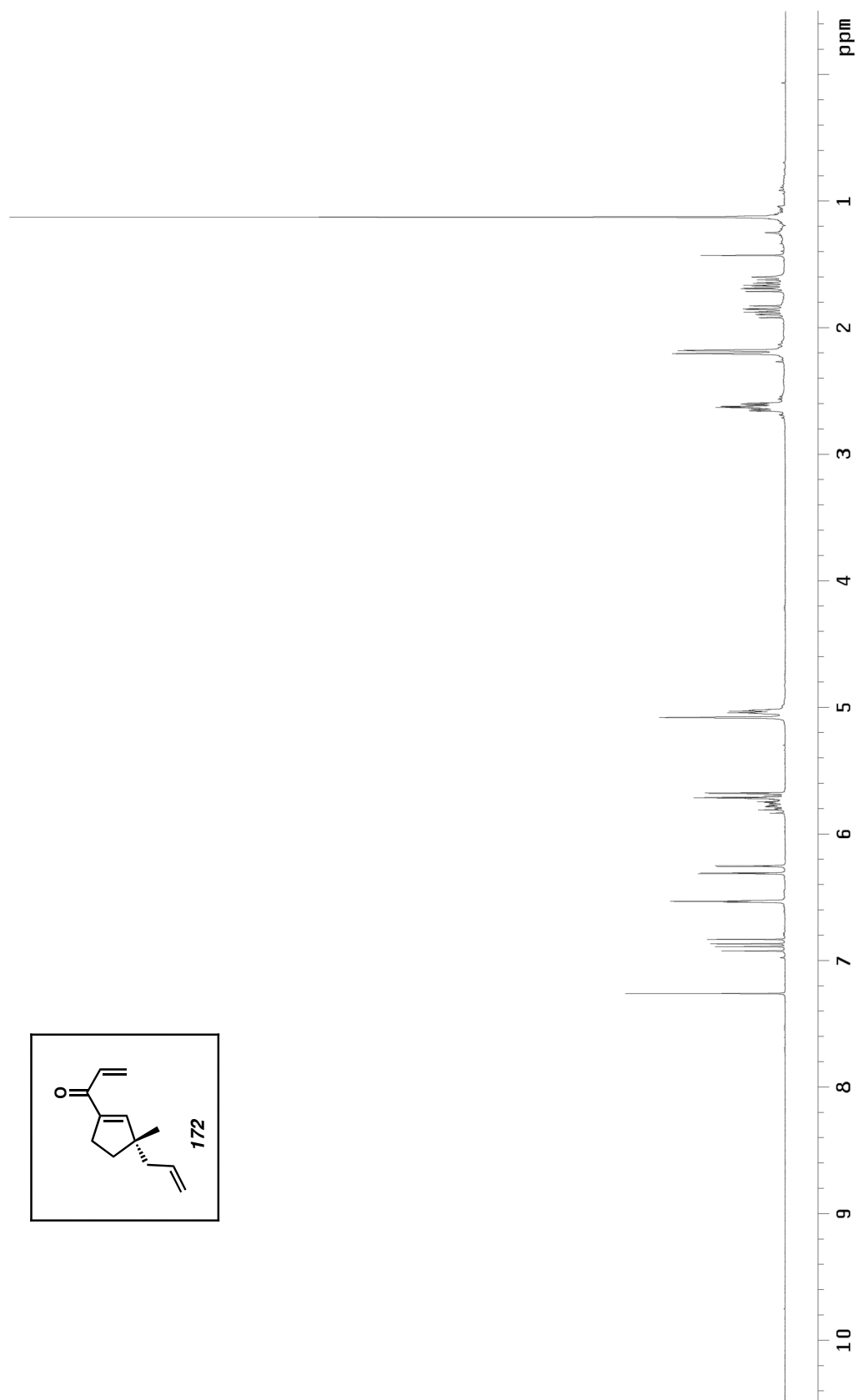


Figure A1.253. ^1H NMR (300 MHz, CDCl_3) of compound **172**.

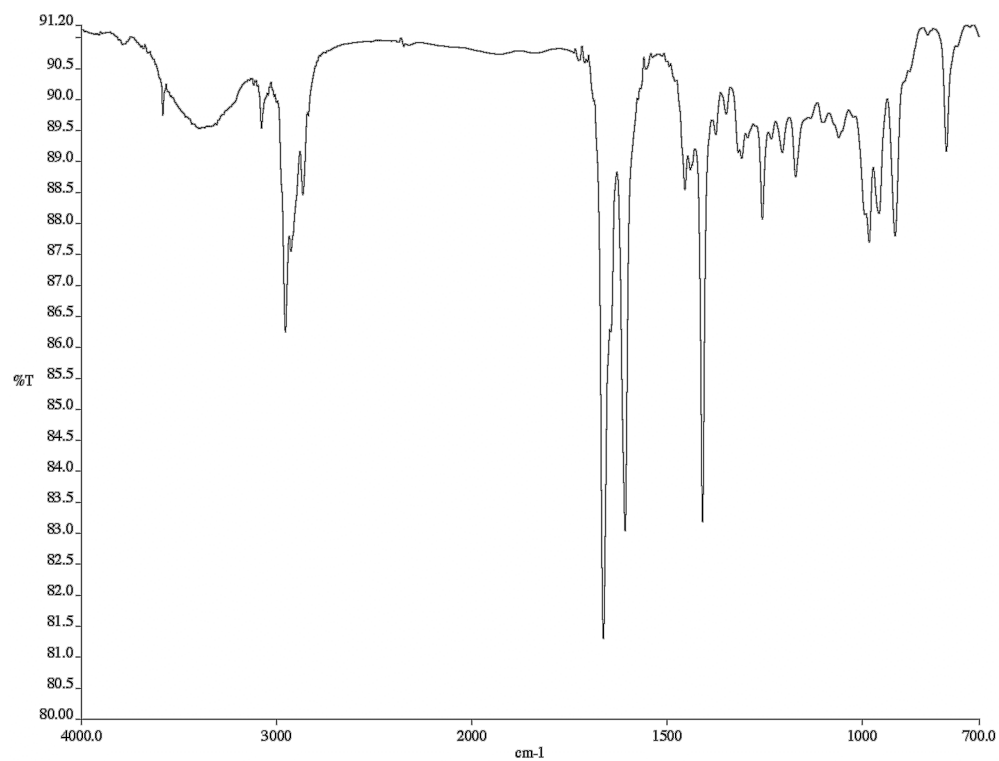


Figure A1.255. Infrared spectrum (thin film/NaCl) of compound **172**.

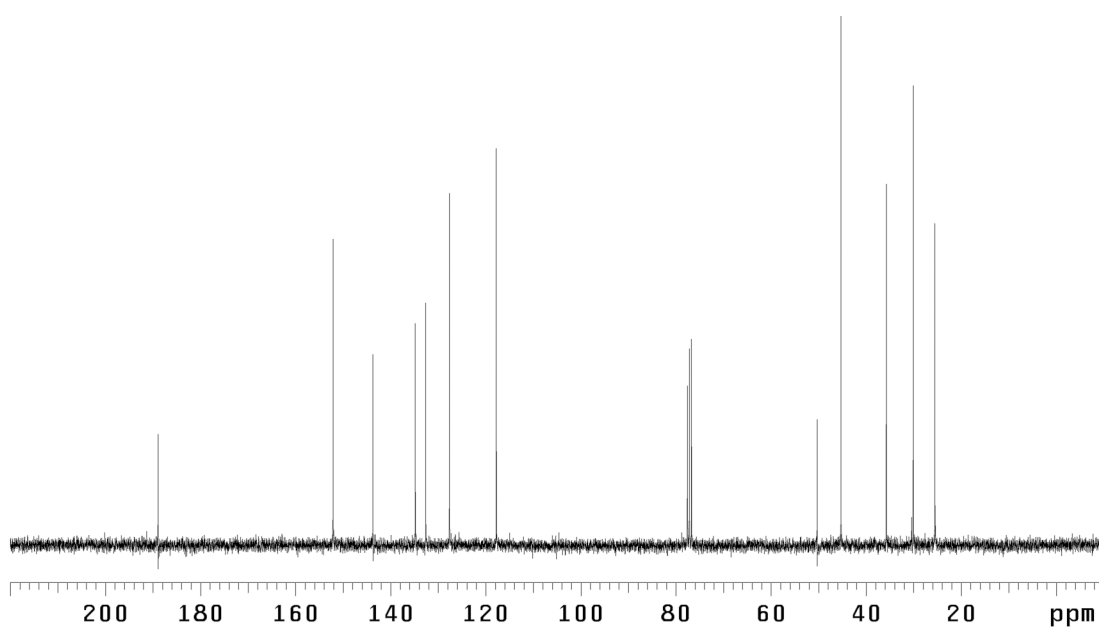


Figure A1.254. ¹³C NMR (75 MHz, CDCl₃) of compound **172**.

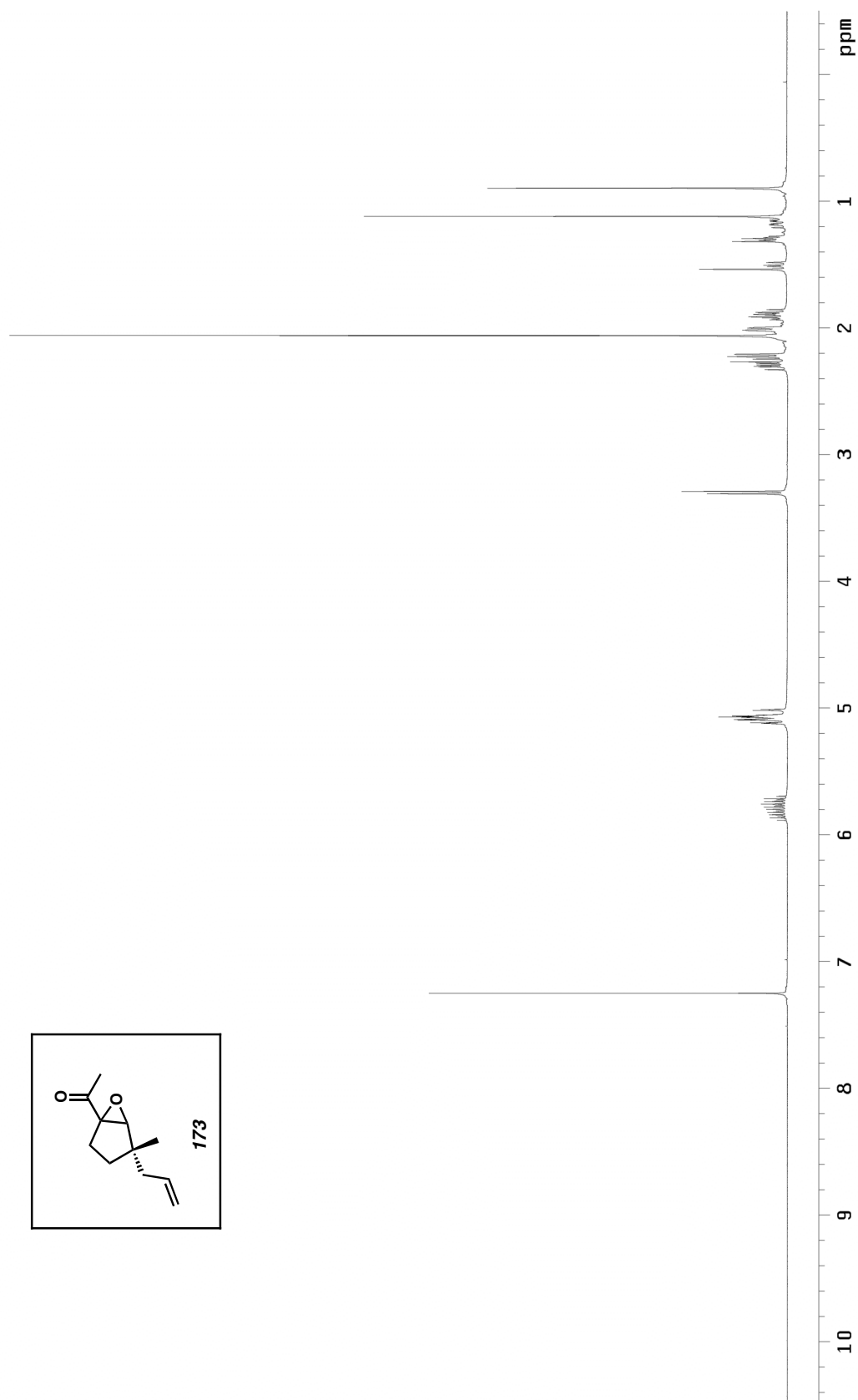


Figure A1.256. ^1H NMR (400 MHz, CDCl_3) of compound **173**.

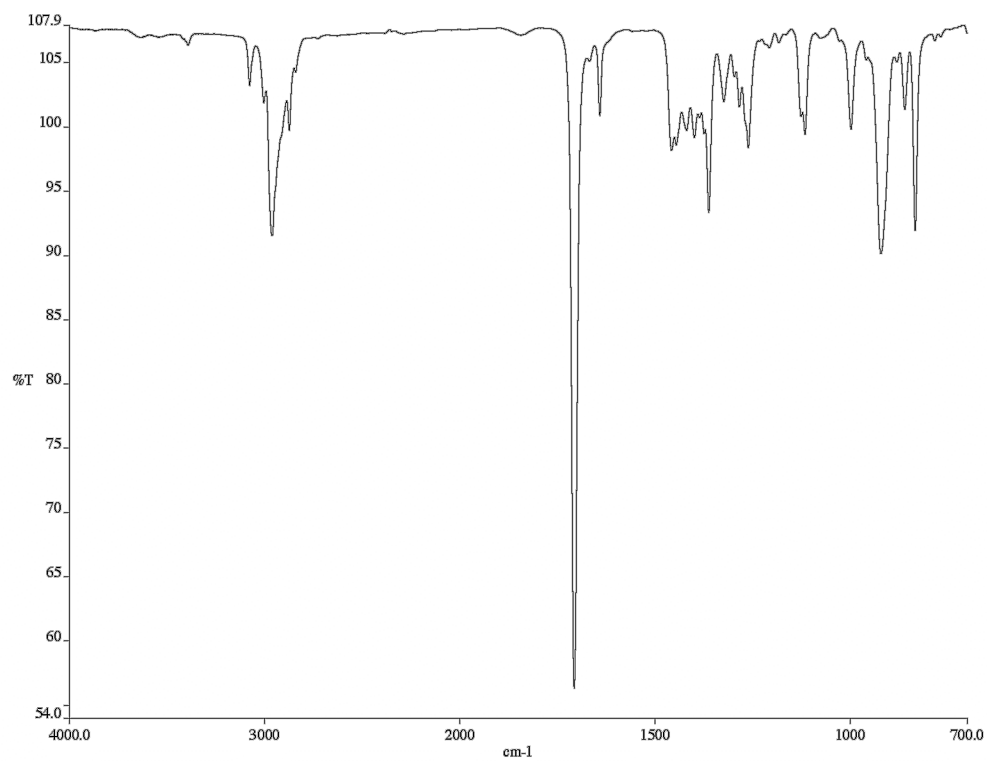


Figure A1.257. Infrared spectrum (thin film/NaCl) of compound **173**.

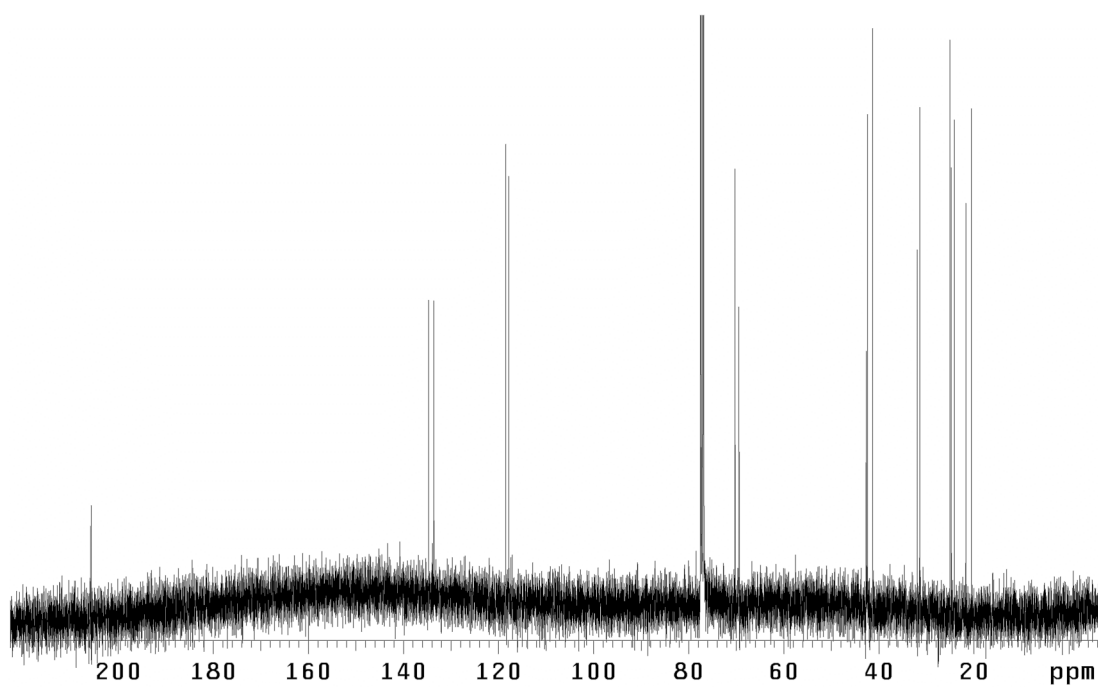


Figure A1.258. ¹³C NMR (100 MHz, CDCl₃) of compound **173**.

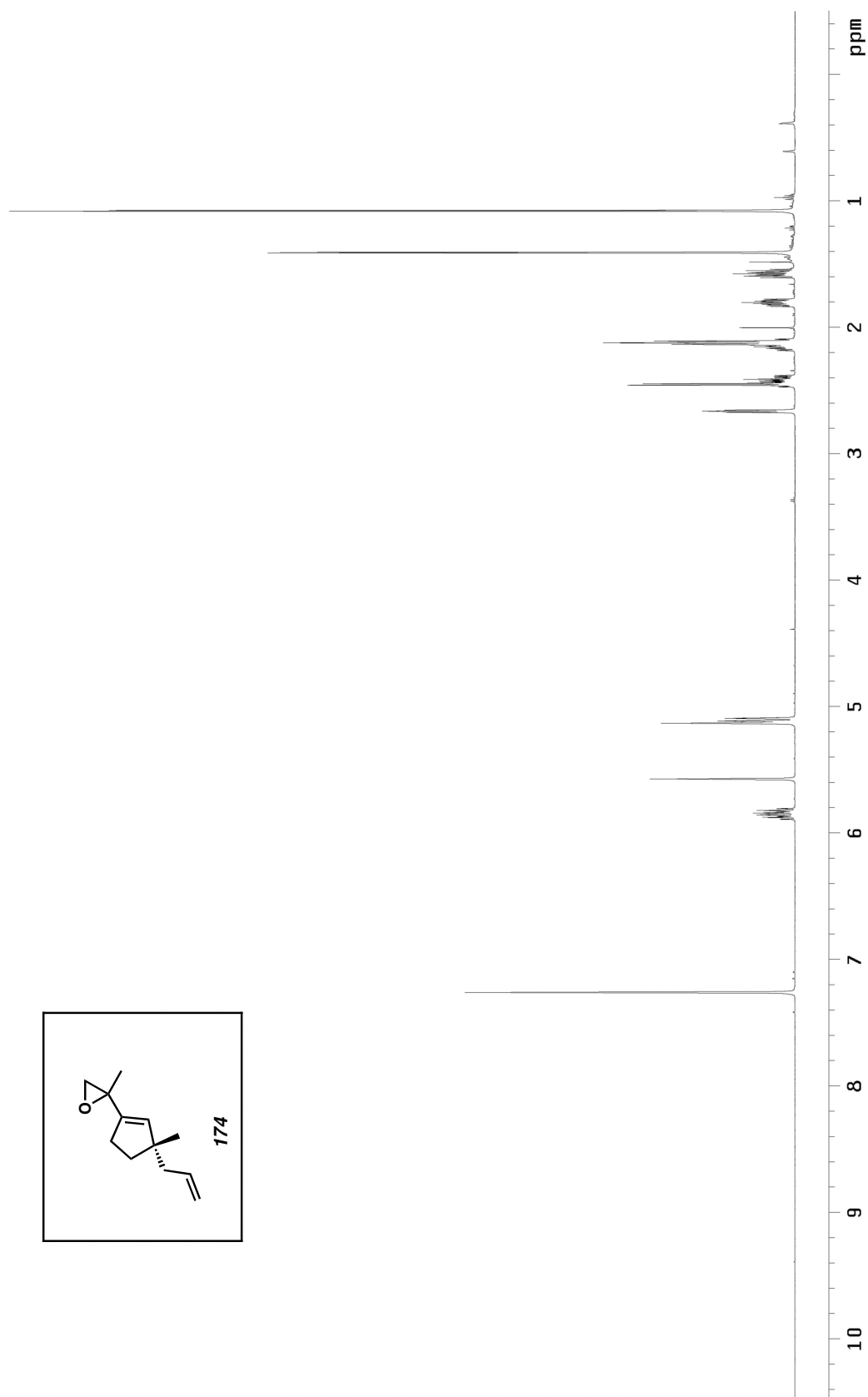


Figure A1.259. ¹H NMR (500 MHz, CDCl₃) of compound **174**.

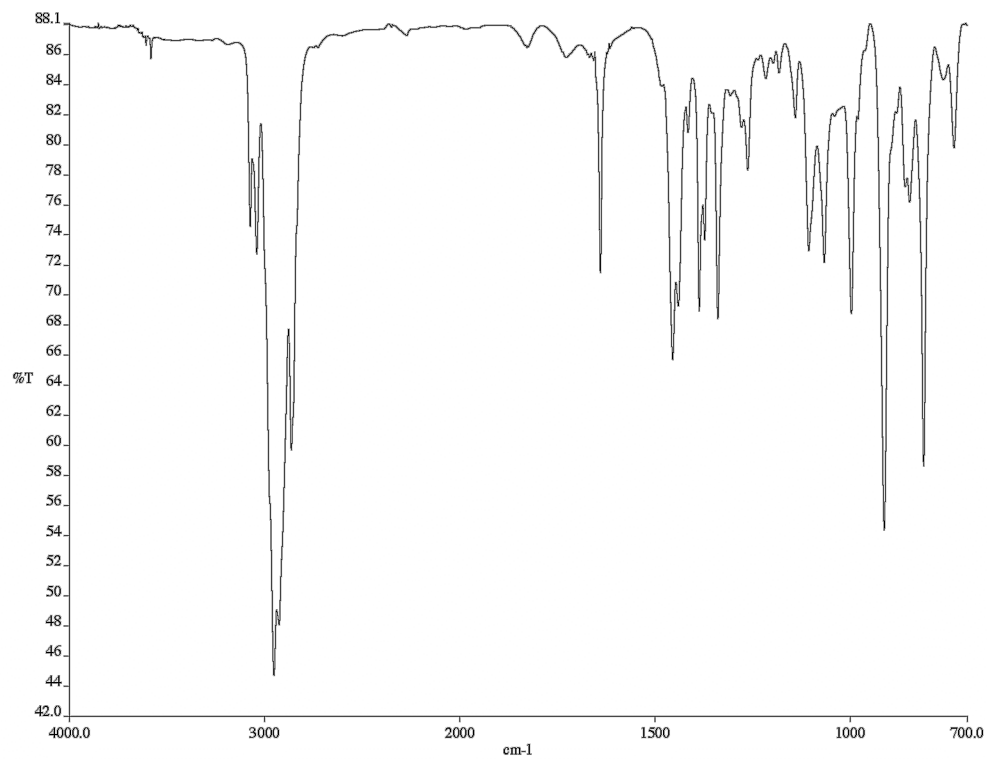


Figure A1.261. Infrared spectrum (thin film/NaCl) of compound **174**.

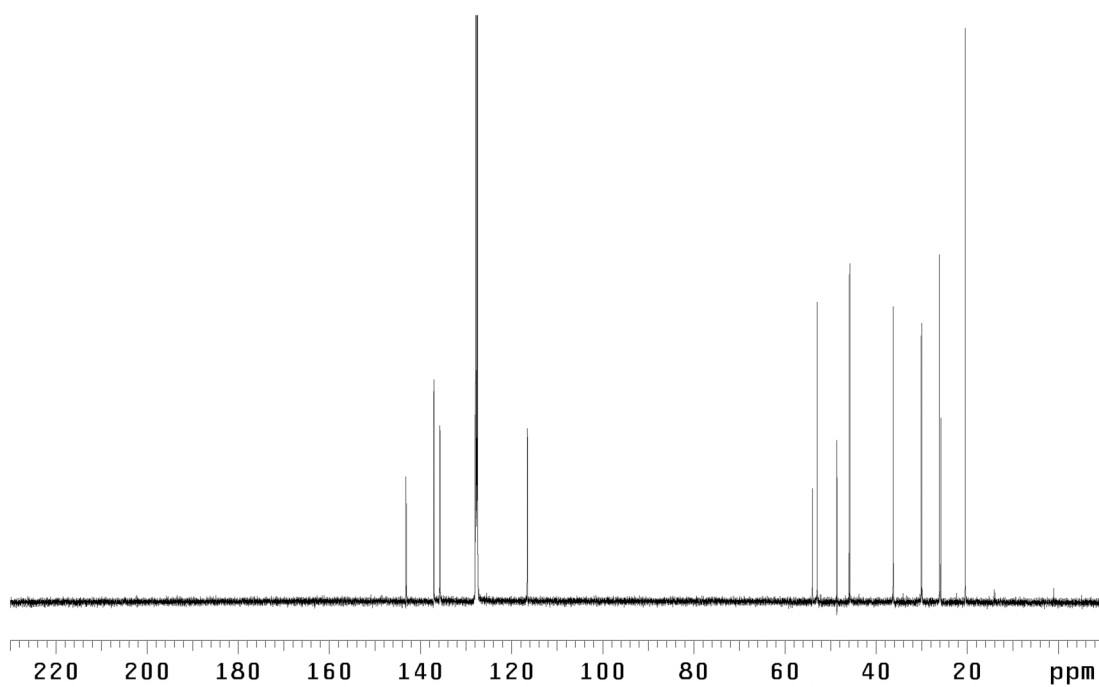


Figure A1.260. ¹³C NMR (125 MHz, CDCl₃) of compound **174**.

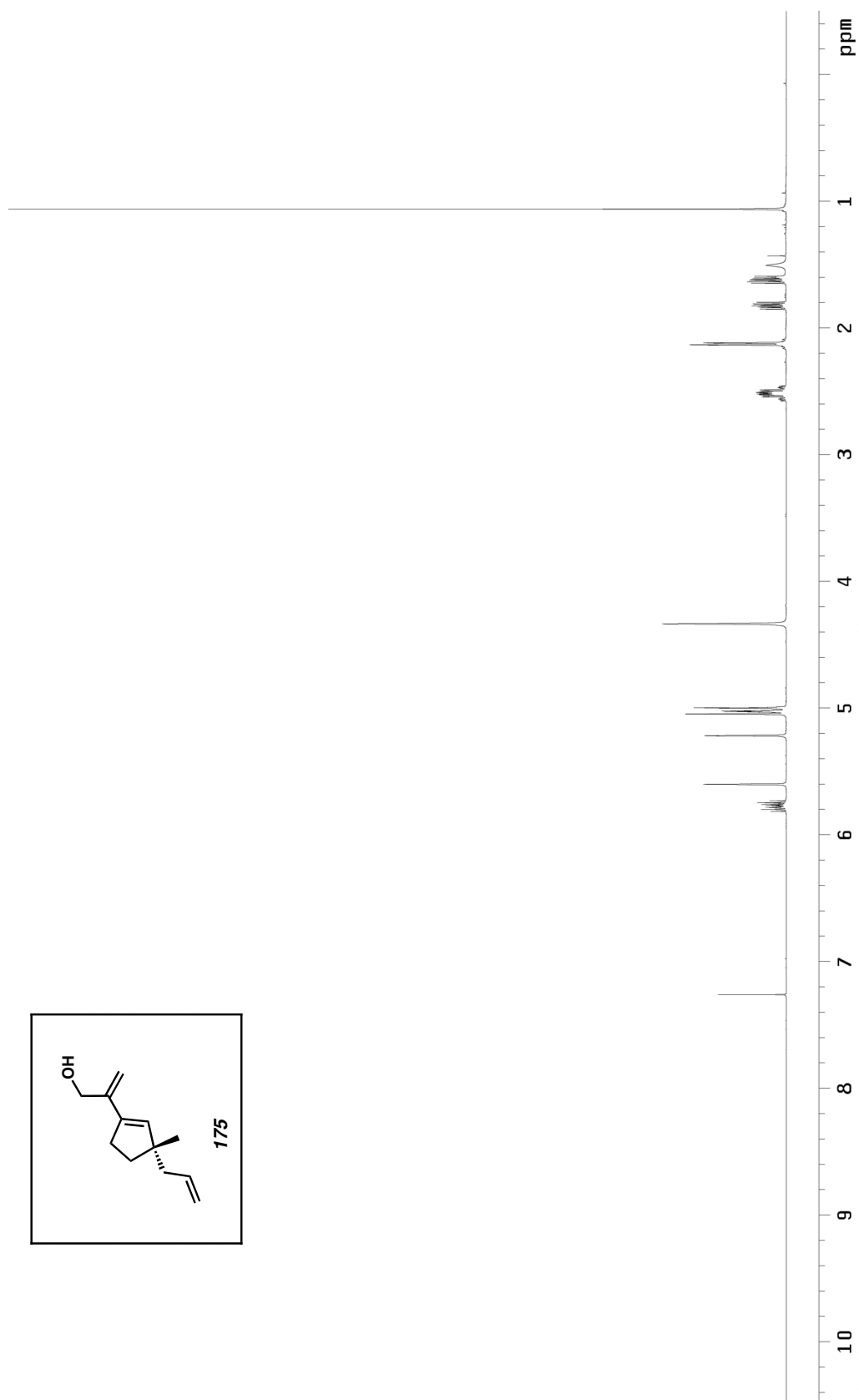


Figure A1.262. ^1H NMR (500 MHz, CDCl_3) of compound **175**.

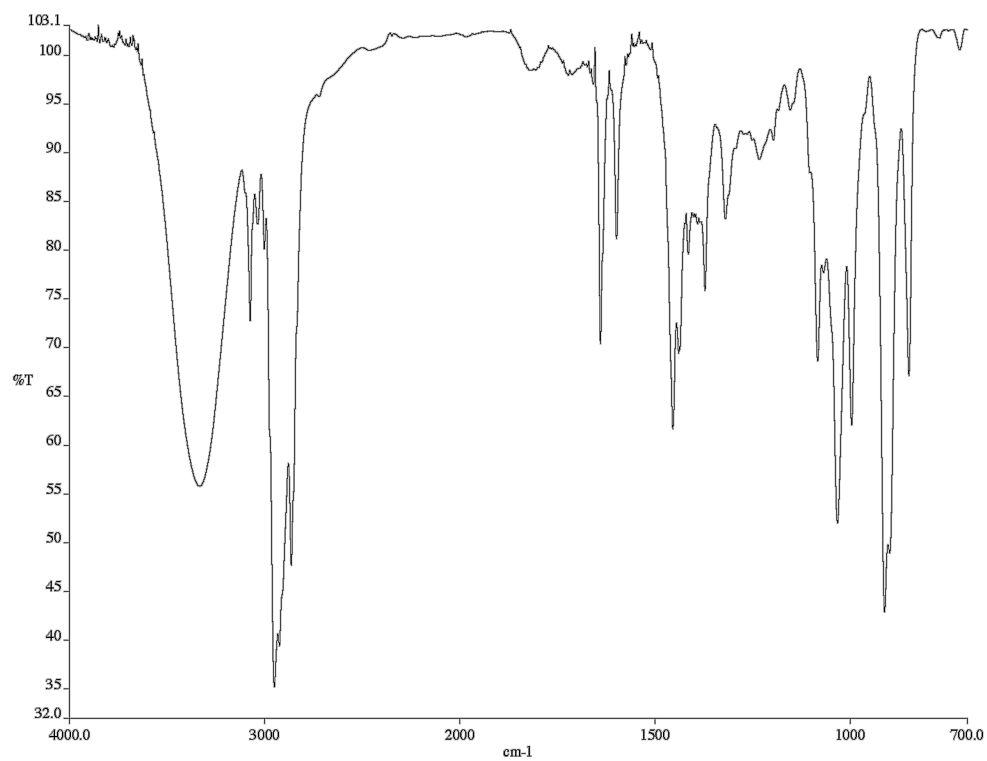


Figure A1.263. Infrared spectrum (thin film/NaCl) of compound **175**.

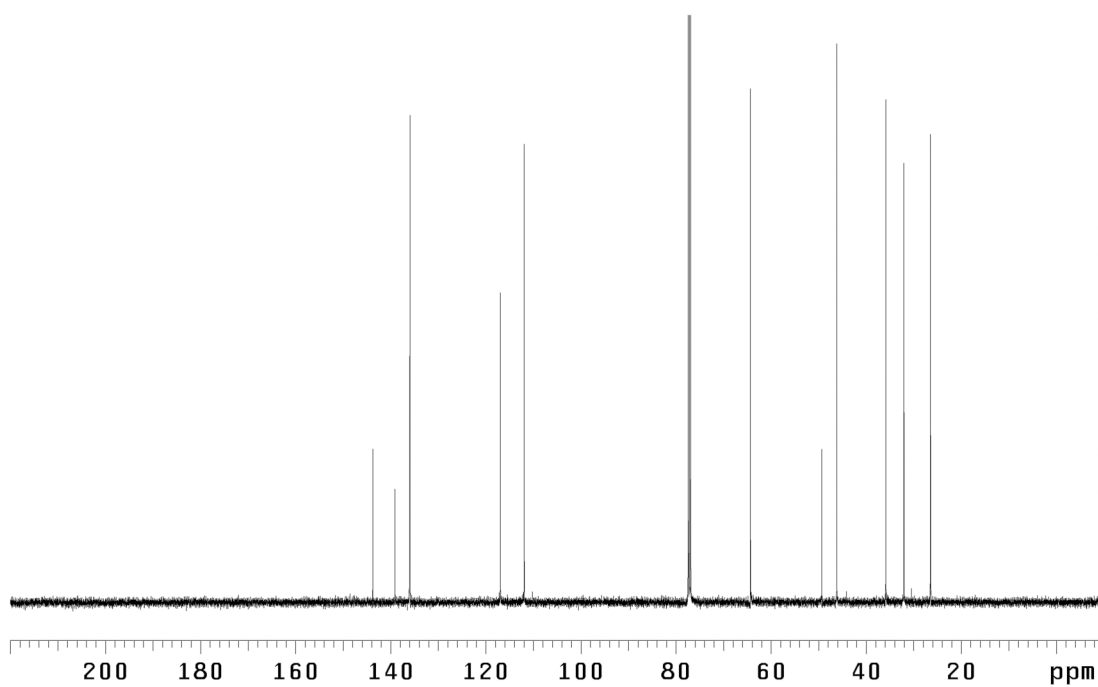


Figure A1.264. ¹³C NMR (125 MHz, CDCl₃) of compound **175**.

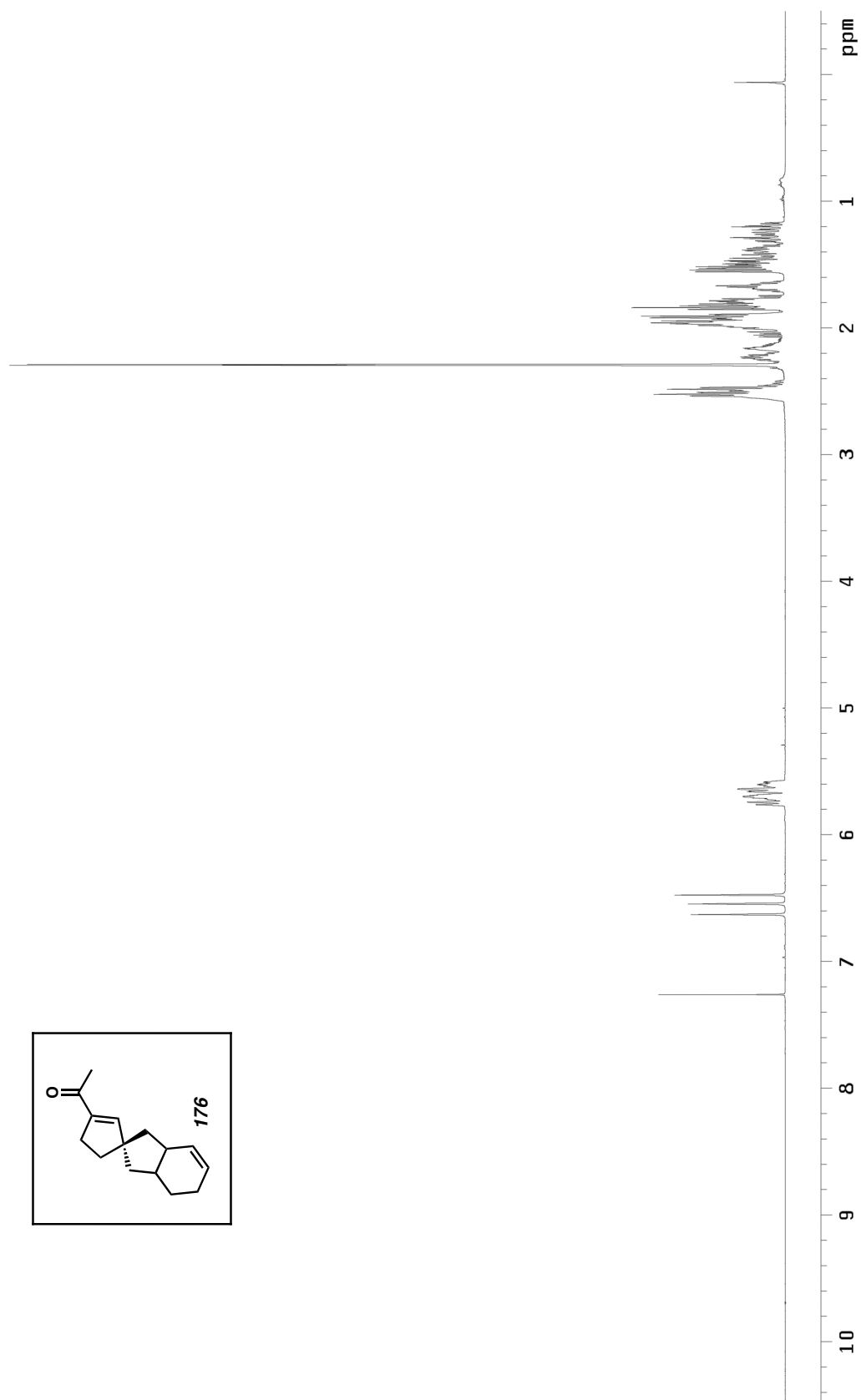


Figure A1.265. ^1H NMR (500 MHz, CDCl_3) of compound **176**.

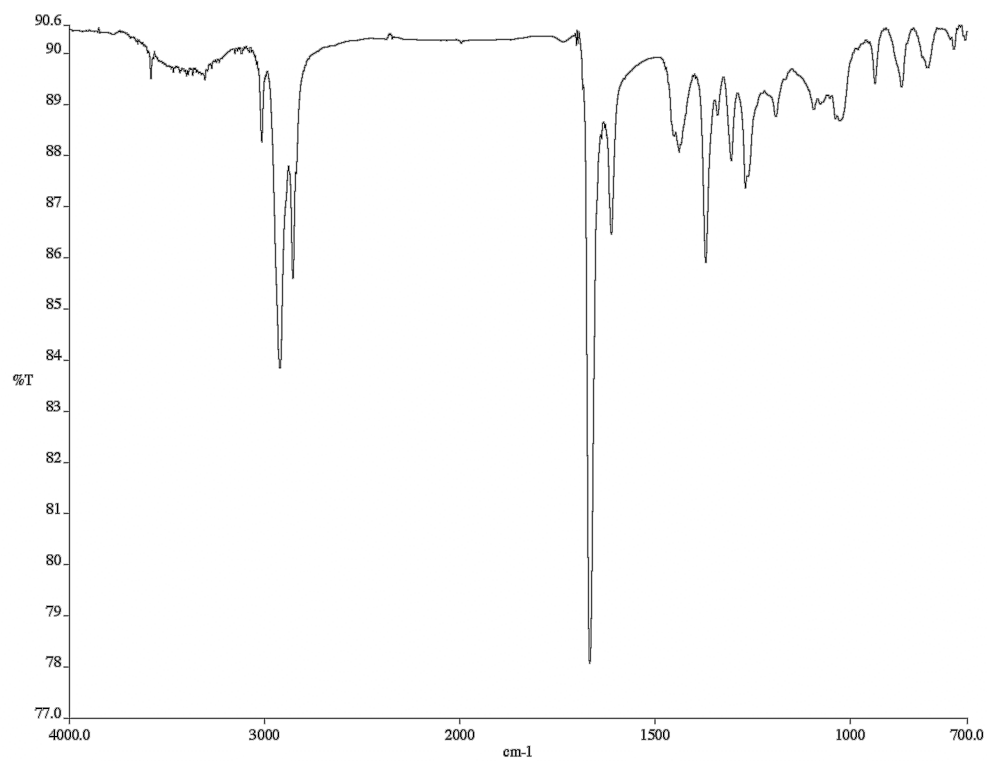


Figure A1.266. Infrared spectrum (thin film/NaCl) of compound **176**.

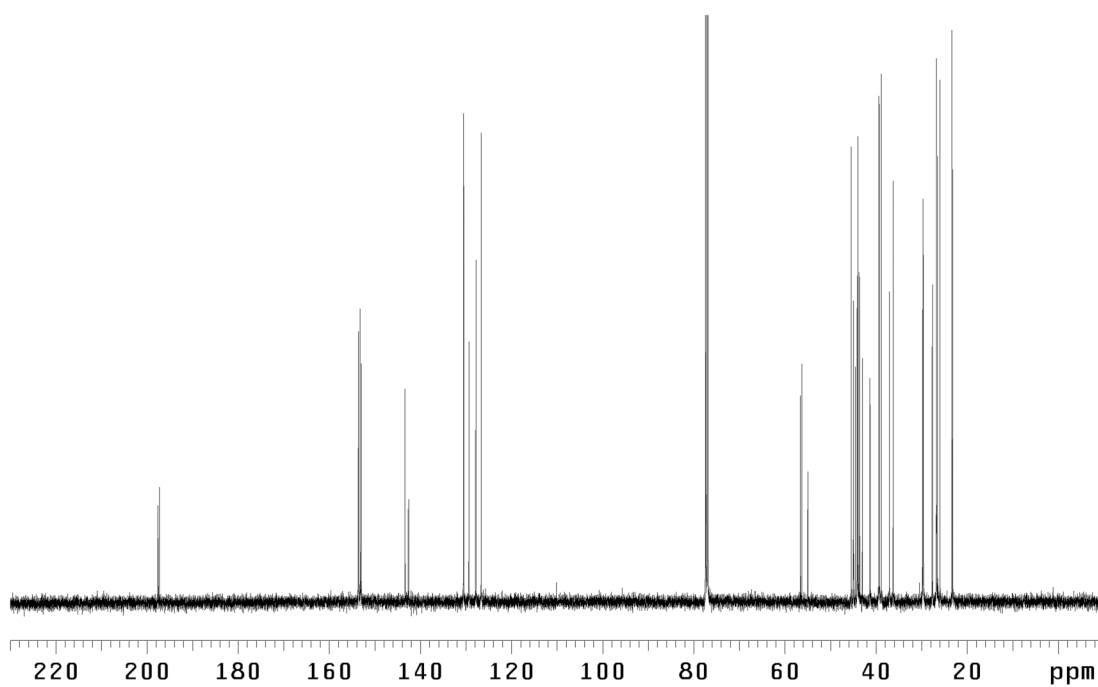


Figure A1.267. ¹³C NMR (125 MHz, CDCl₃) of compound **176**.

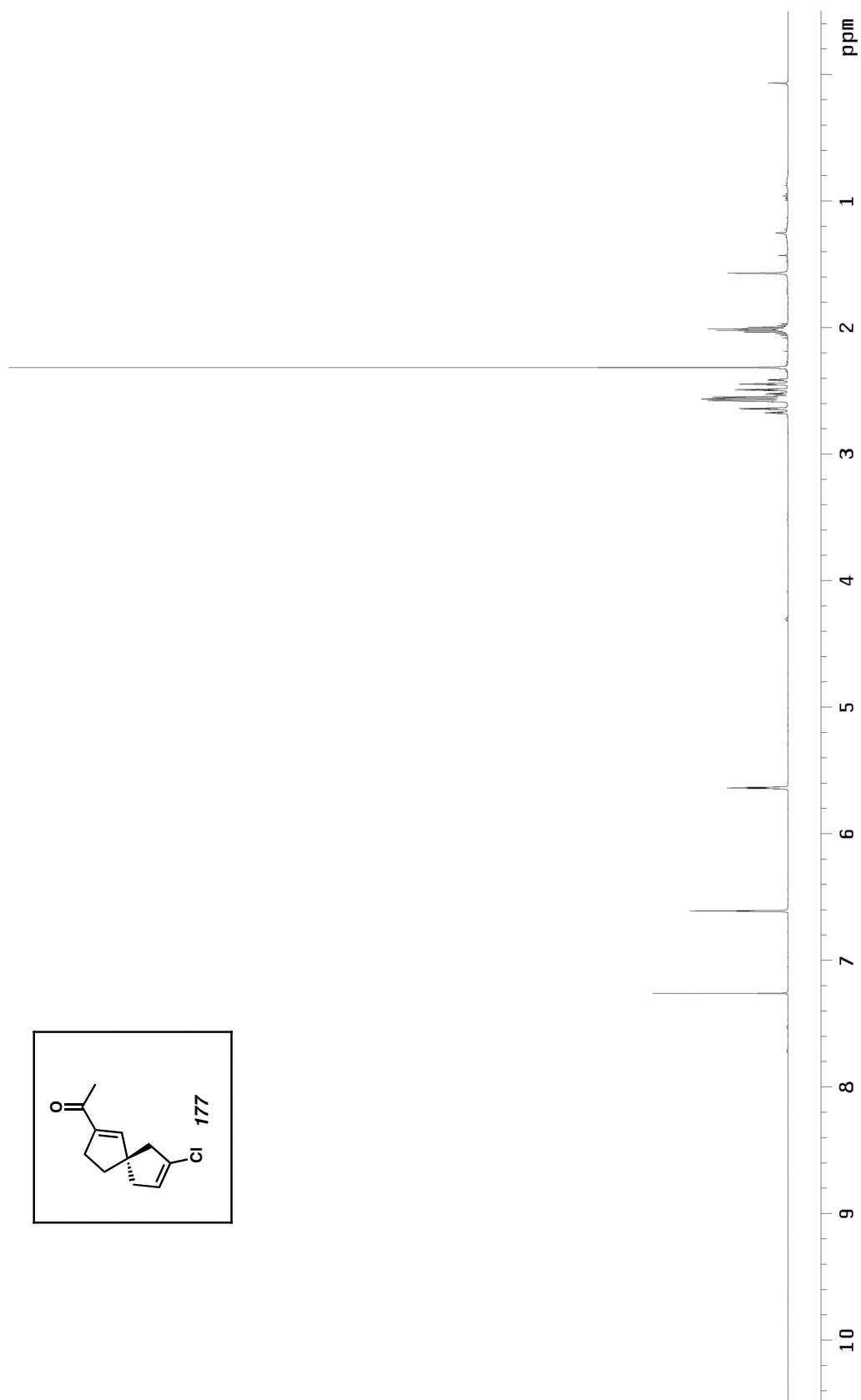


Figure A1.268. ^1H NMR (500 MHz, CDCl_3) of compound **177**.

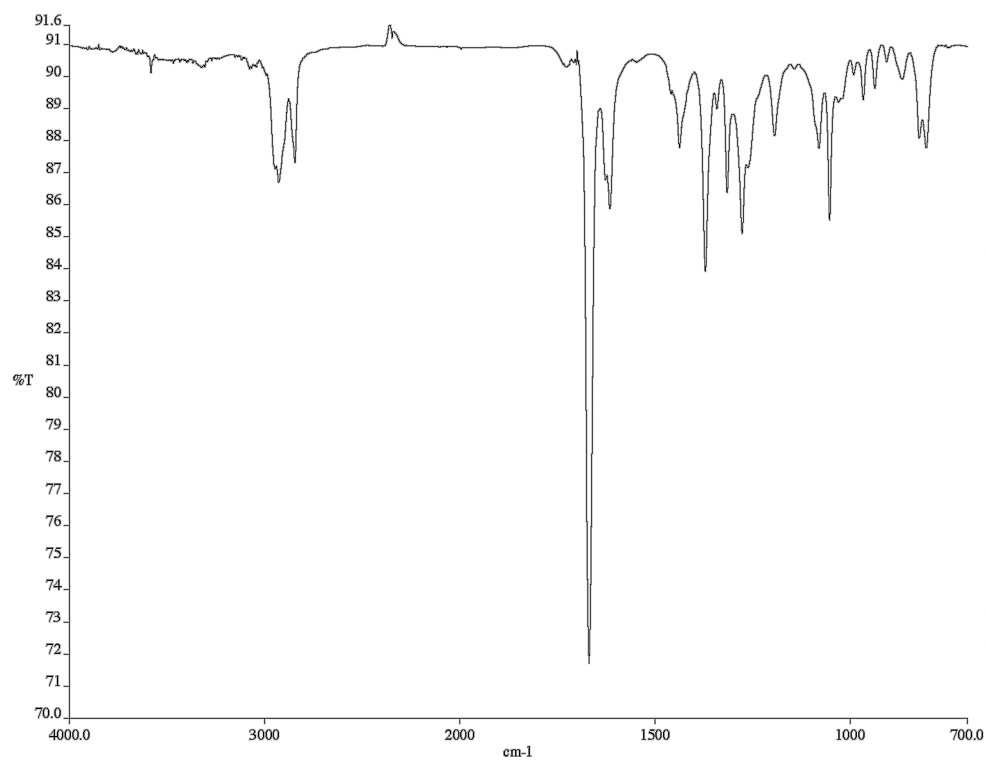


Figure A1.269. Infrared spectrum (thin film/NaCl) of compound **177**.

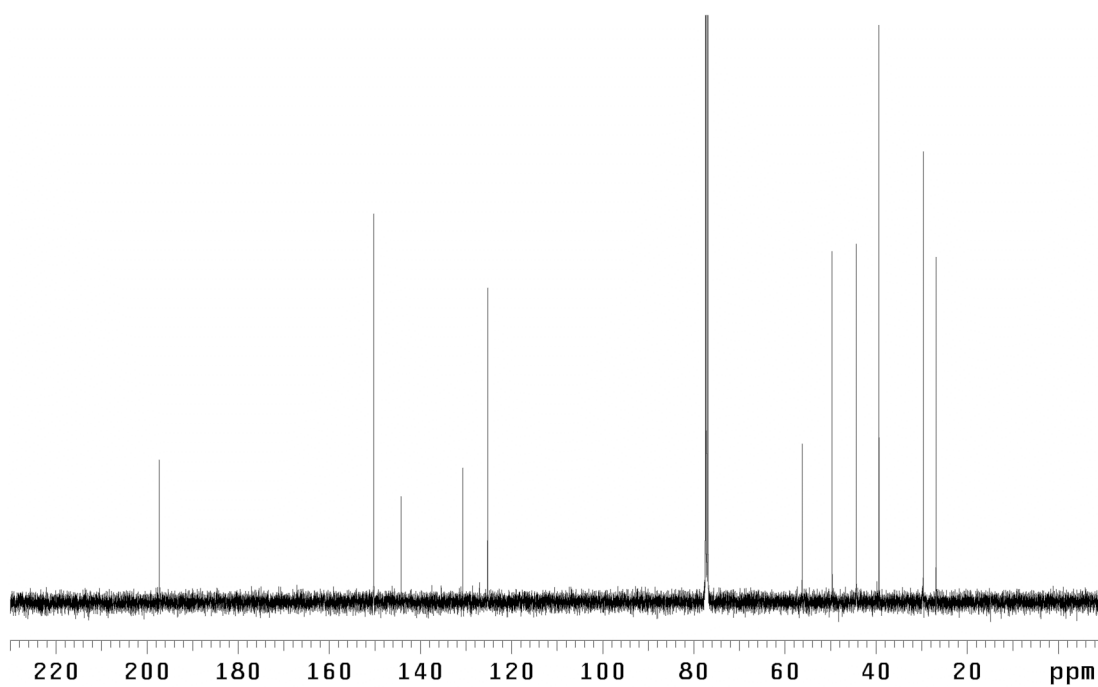


Figure A1.270. ¹³C NMR (125 MHz, CDCl₃) of compound **177**.

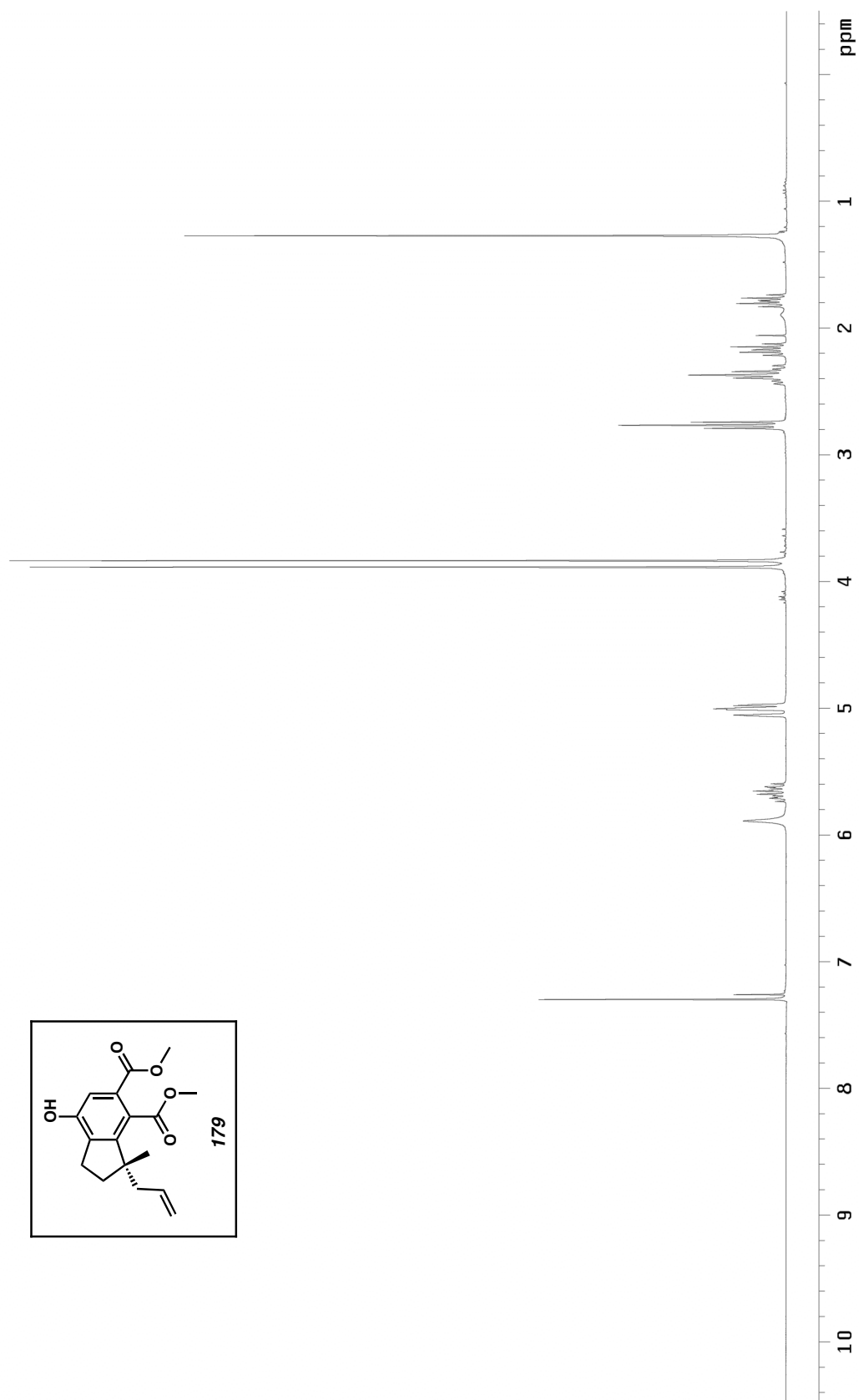


Figure A1.271. ^1H NMR (300 MHz, CDCl_3) of compound **179**.

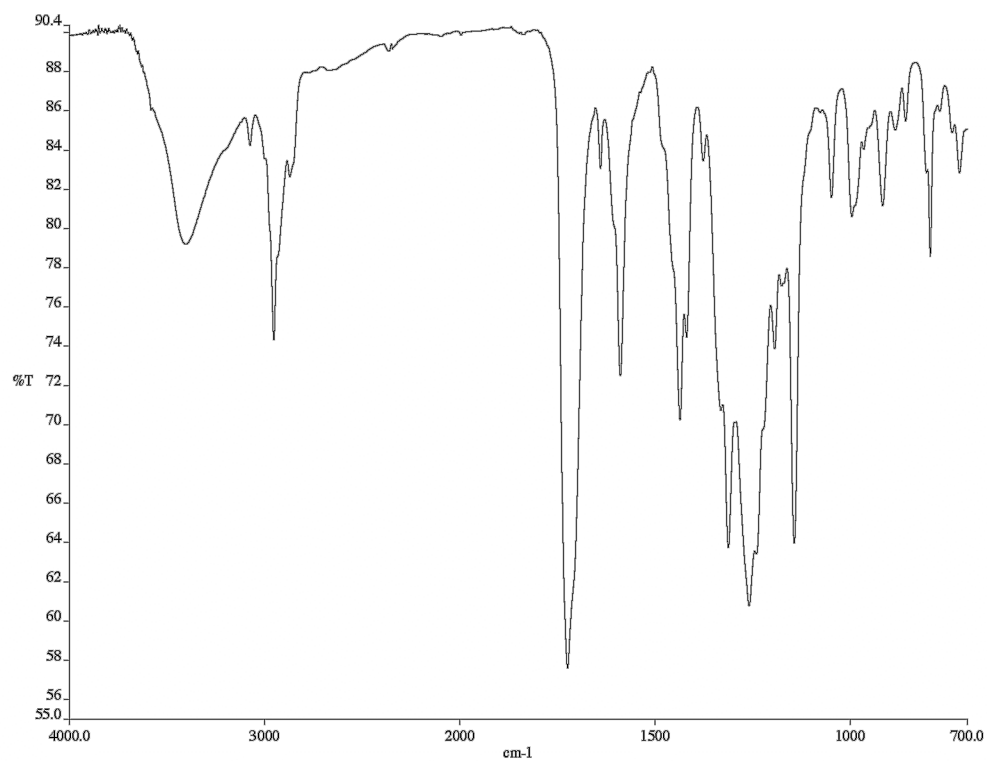


Figure A1.272. Infrared spectrum (thin film/NaCl) of compound **179**.

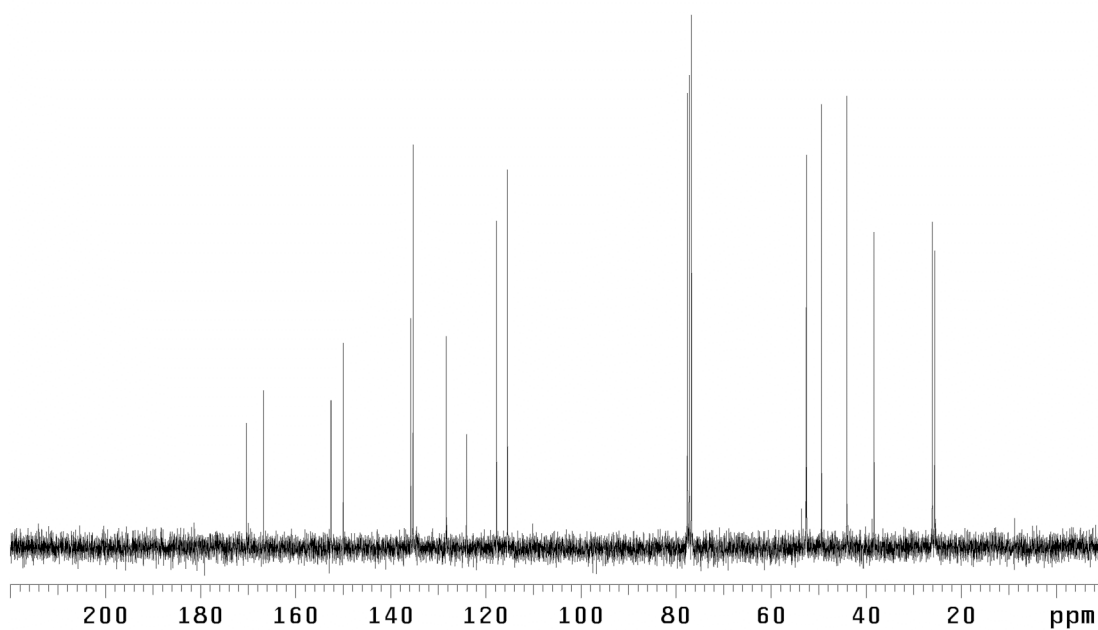


Figure A1.273. ¹³C NMR (75 MHz, CDCl₃) of compound **179**.

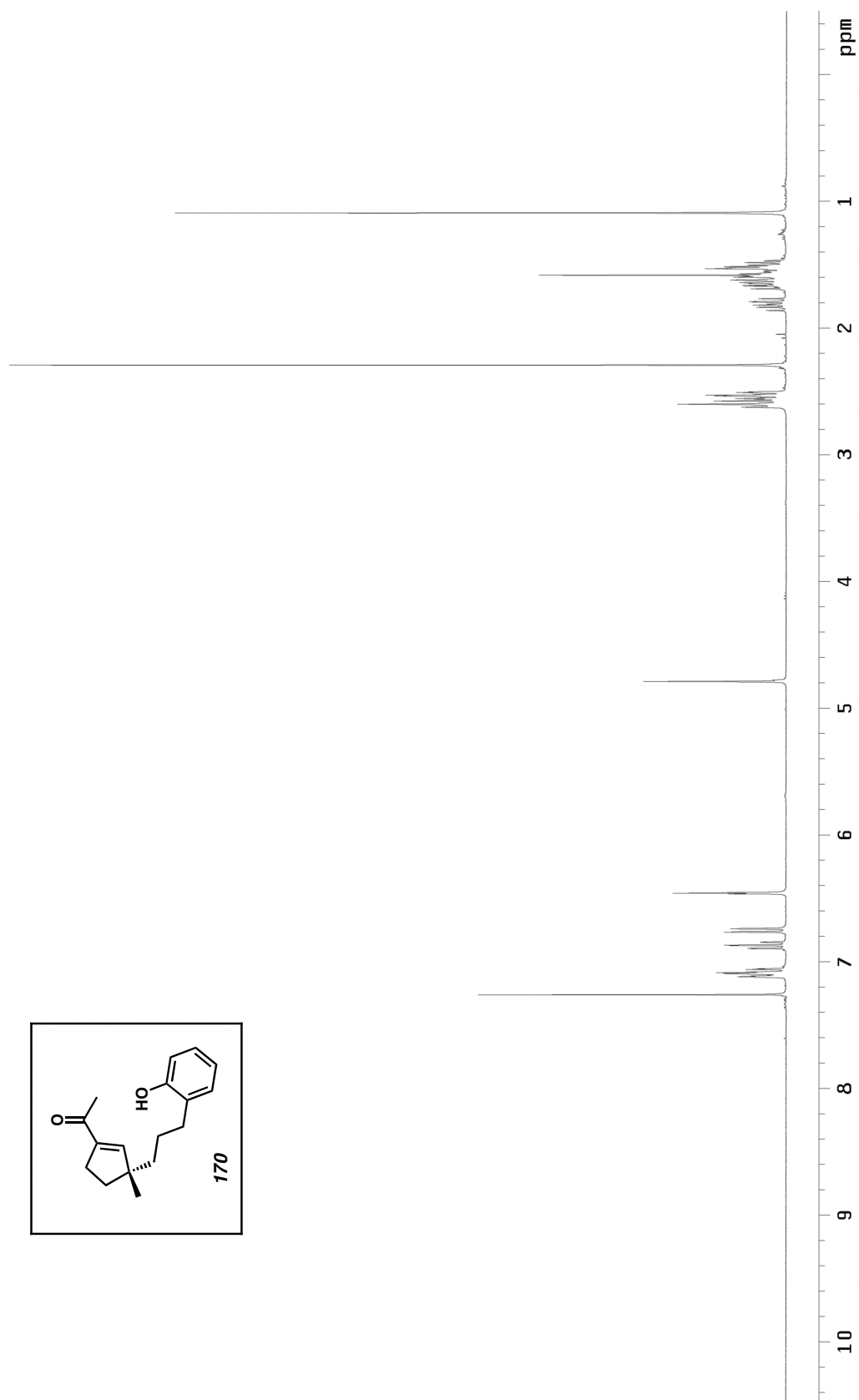


Figure A1.274. ^1H NMR (300 MHz, CDCl_3) of compound **170**.

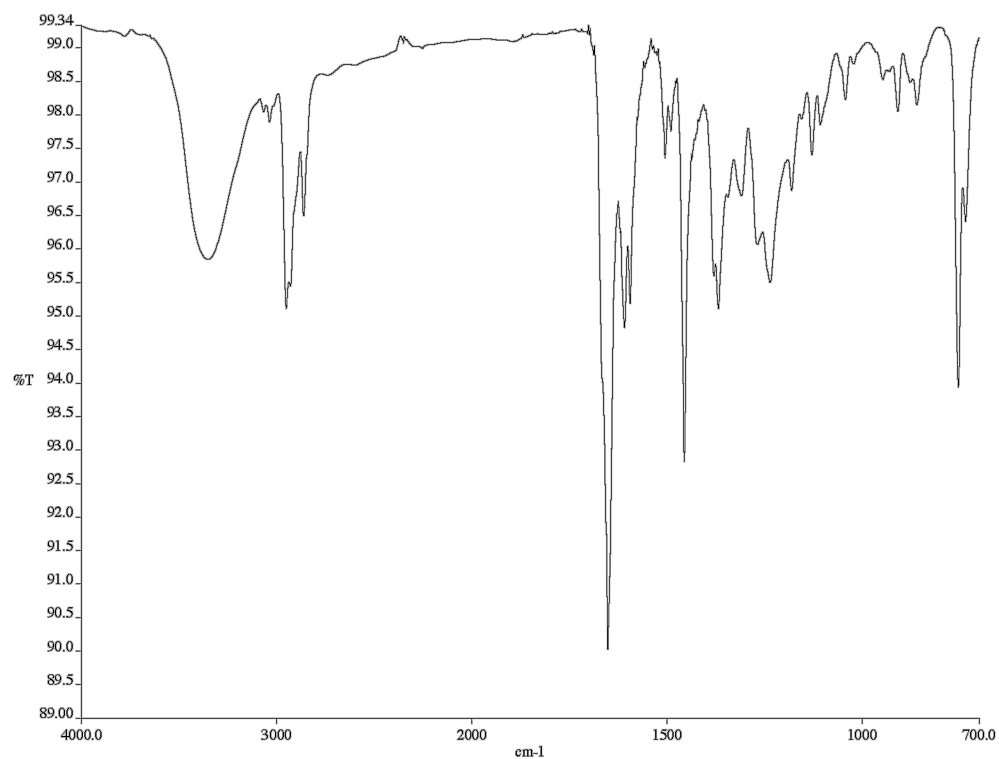


Figure A1.275. Infrared spectrum (thin film/NaCl) of compound **170**.

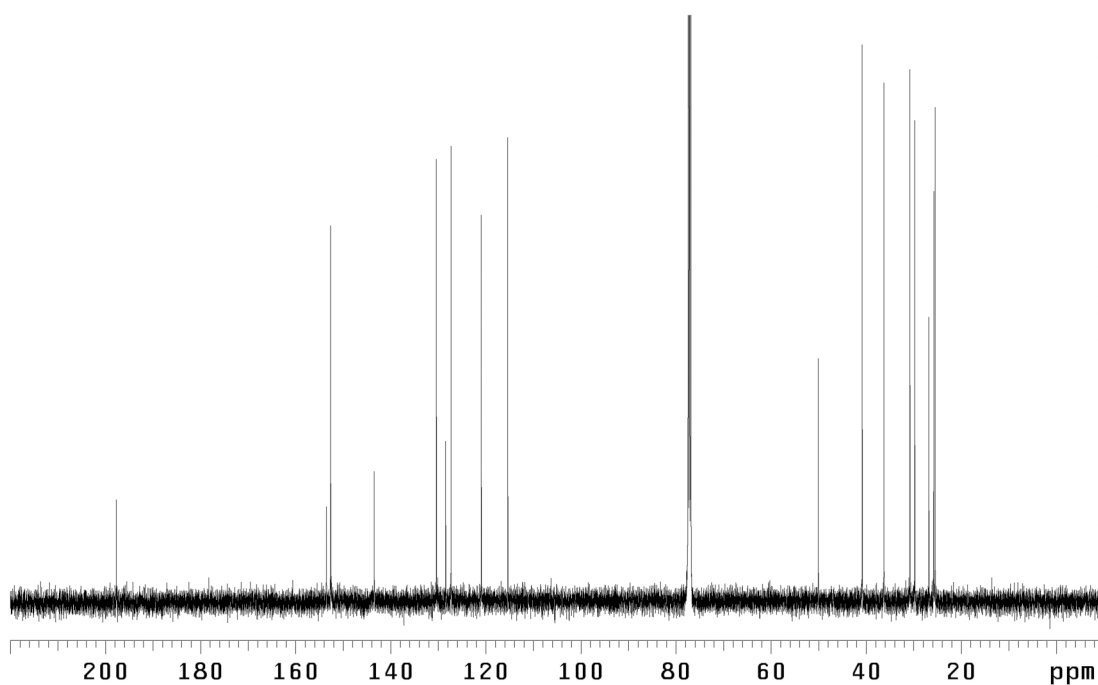


Figure A1.276. ¹³C NMR (125 MHz, CDCl₃) of compound **170**.

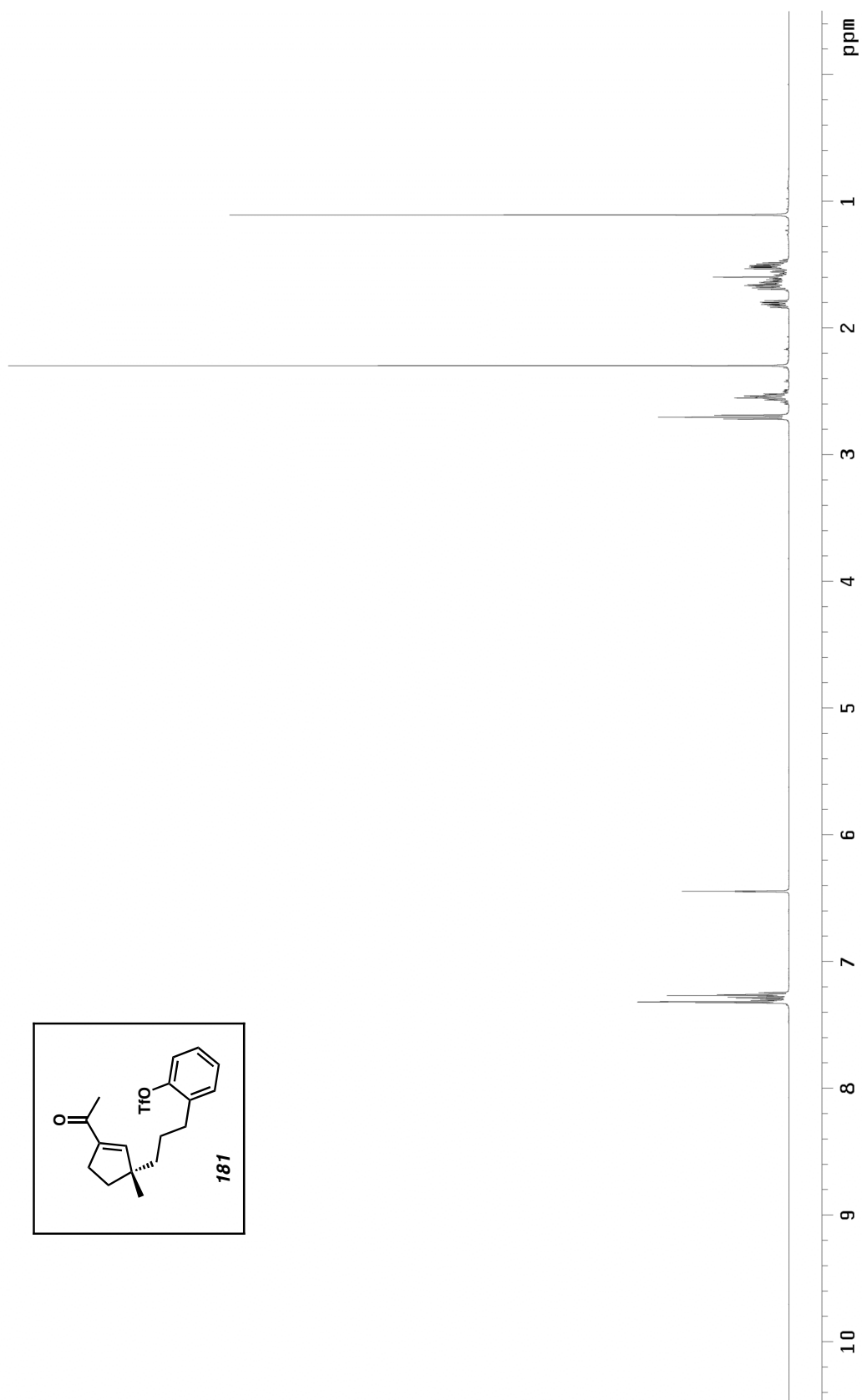


Figure A1.277. ^1H NMR (500 MHz, CDCl_3) of compound **181**.

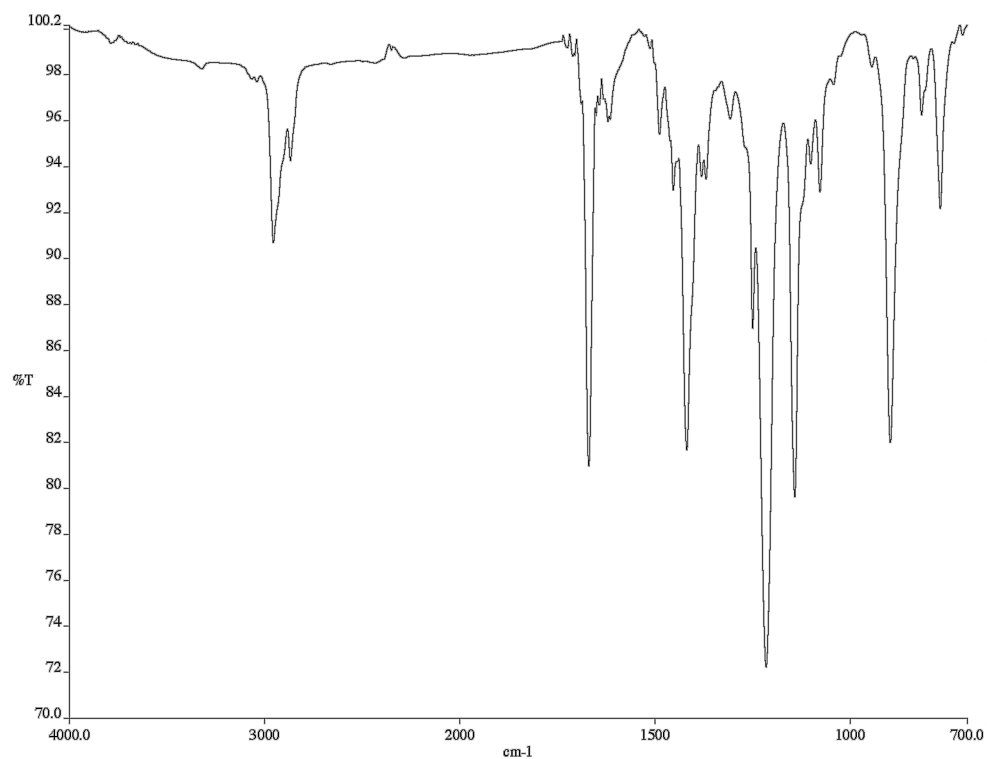


Figure A1.279. Infrared spectrum (thin film/NaCl) of compound **181**.

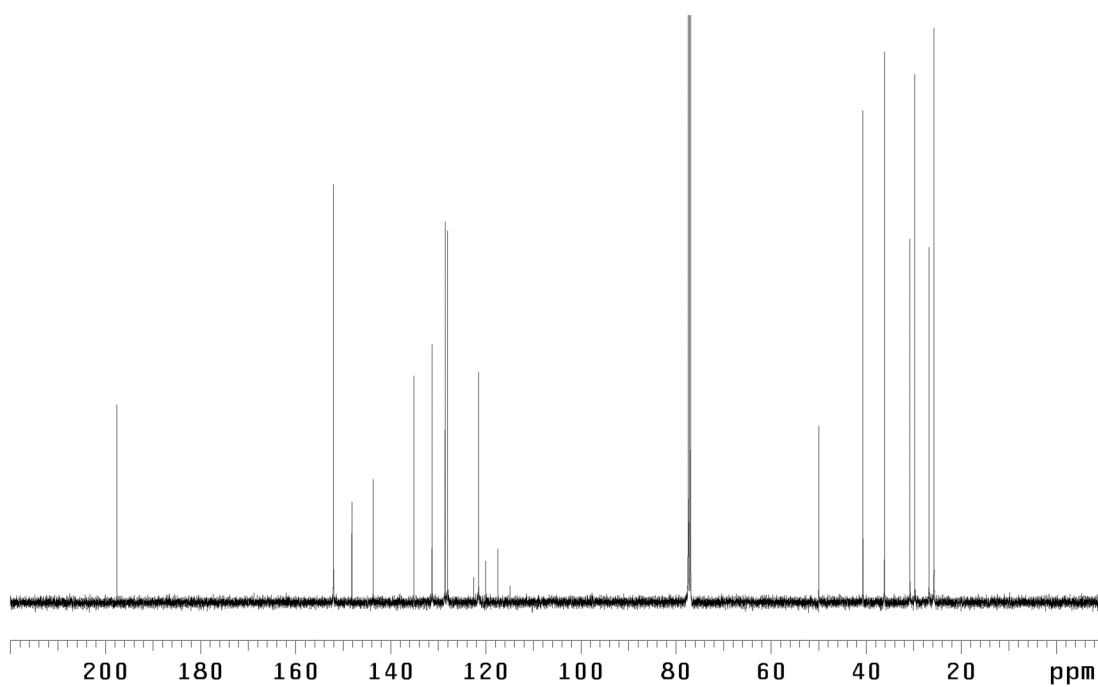


Figure A1.278. ¹³C NMR (125 MHz, CDCl₃) of compound **181**.

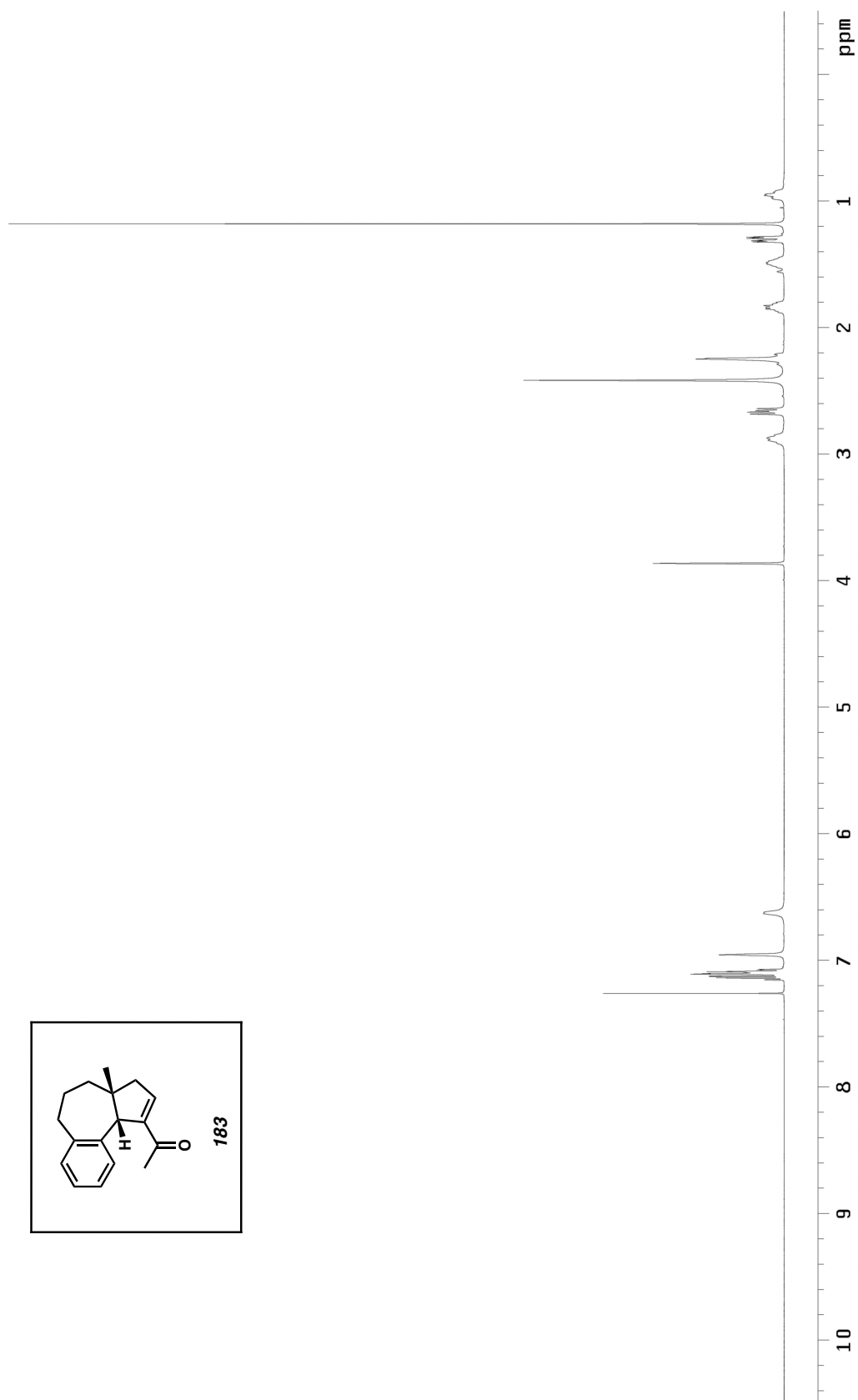


Figure A1.280. ^1H NMR (500 MHz, CDCl_3) of compound **183**.

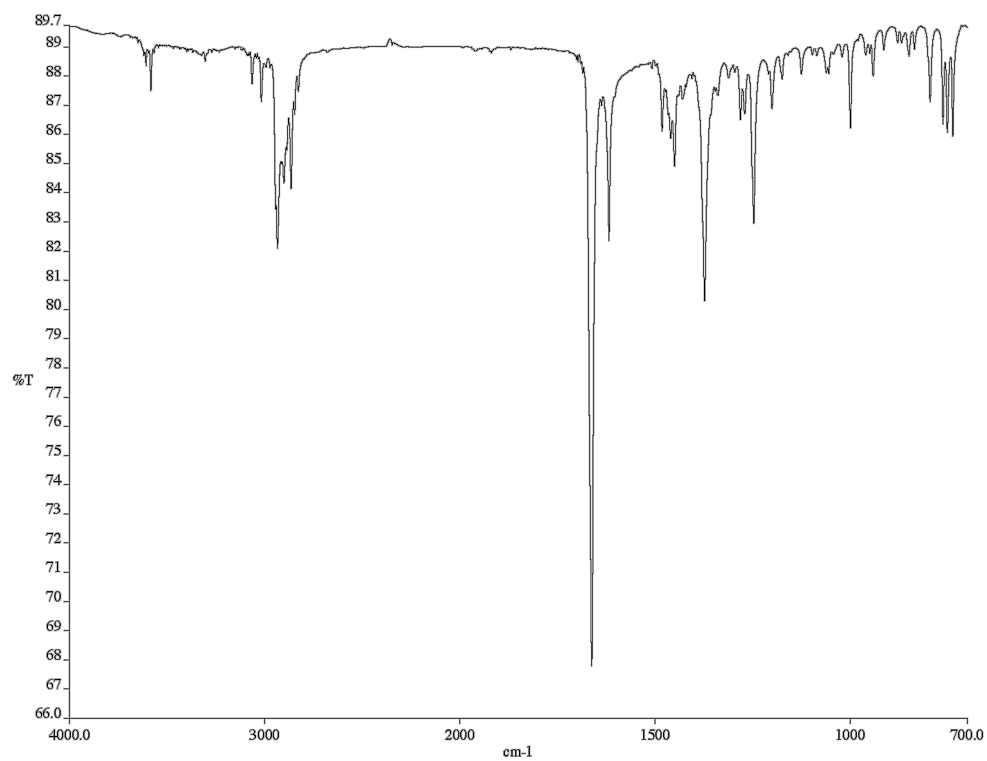


Figure A1.281. Infrared spectrum (thin film/NaCl) of compound **183**.

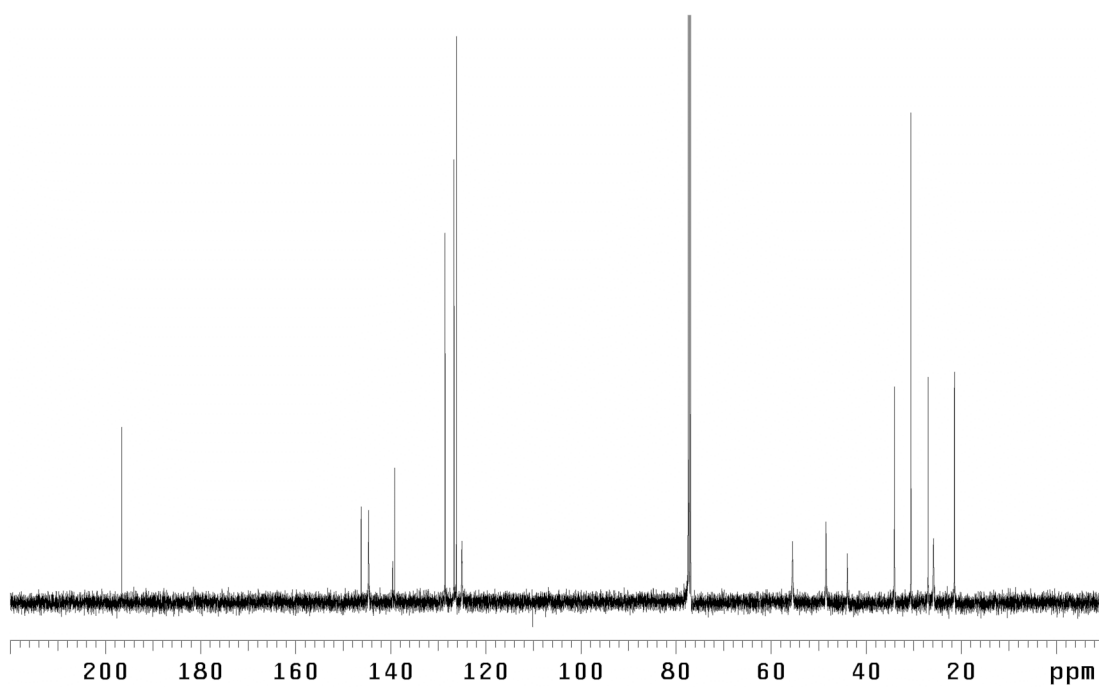
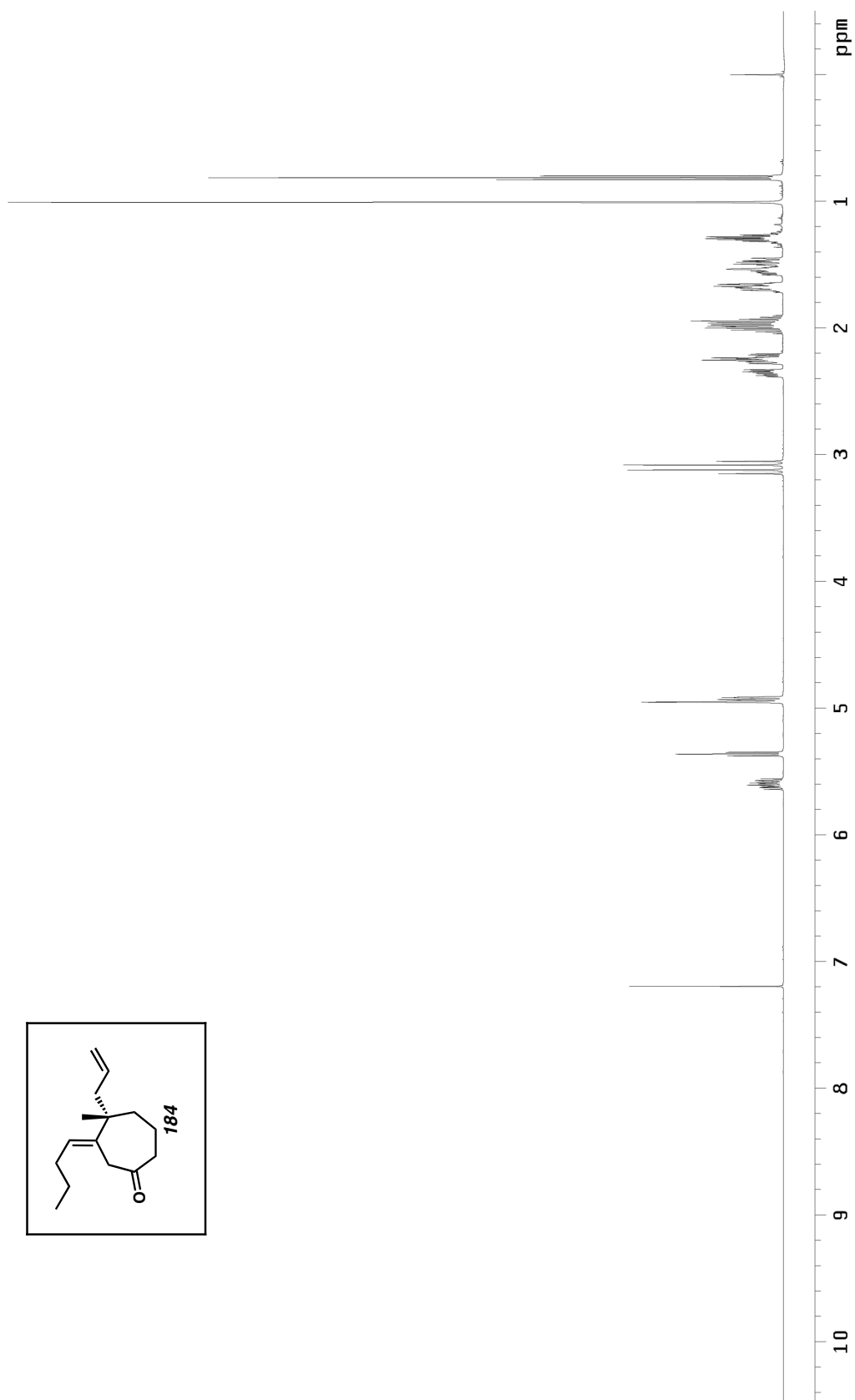


Figure A1.282. ¹³C NMR (125 MHz, CDCl₃) of compound **183**.



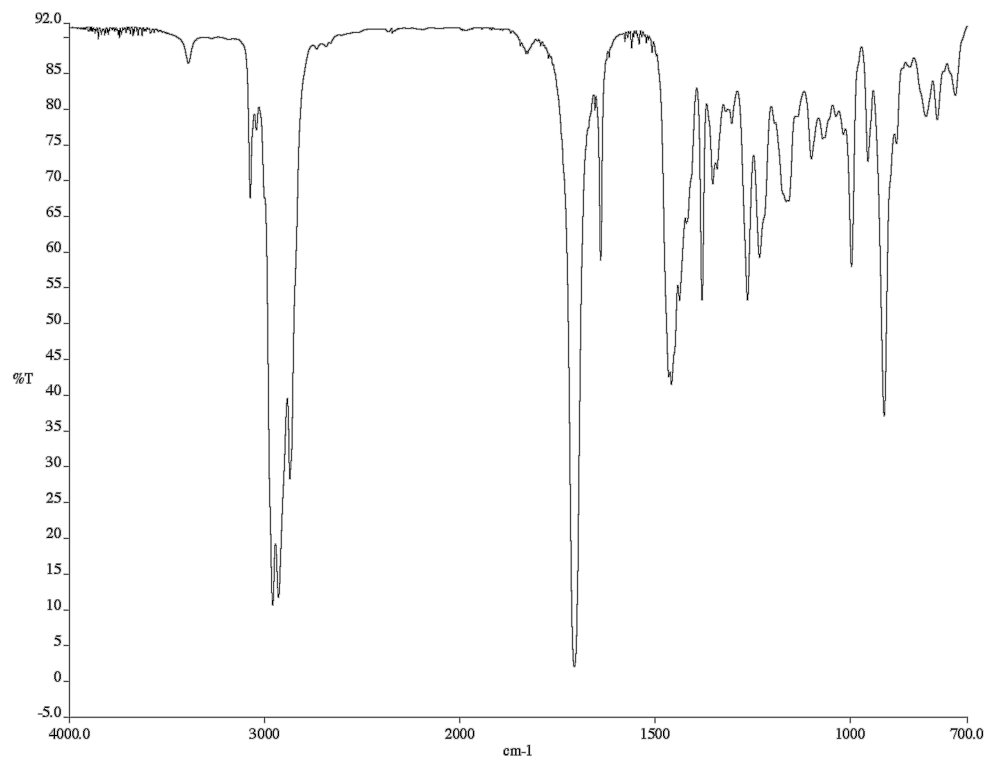


Figure A1.284. Infrared spectrum (thin film/NaCl) of compound **184**.

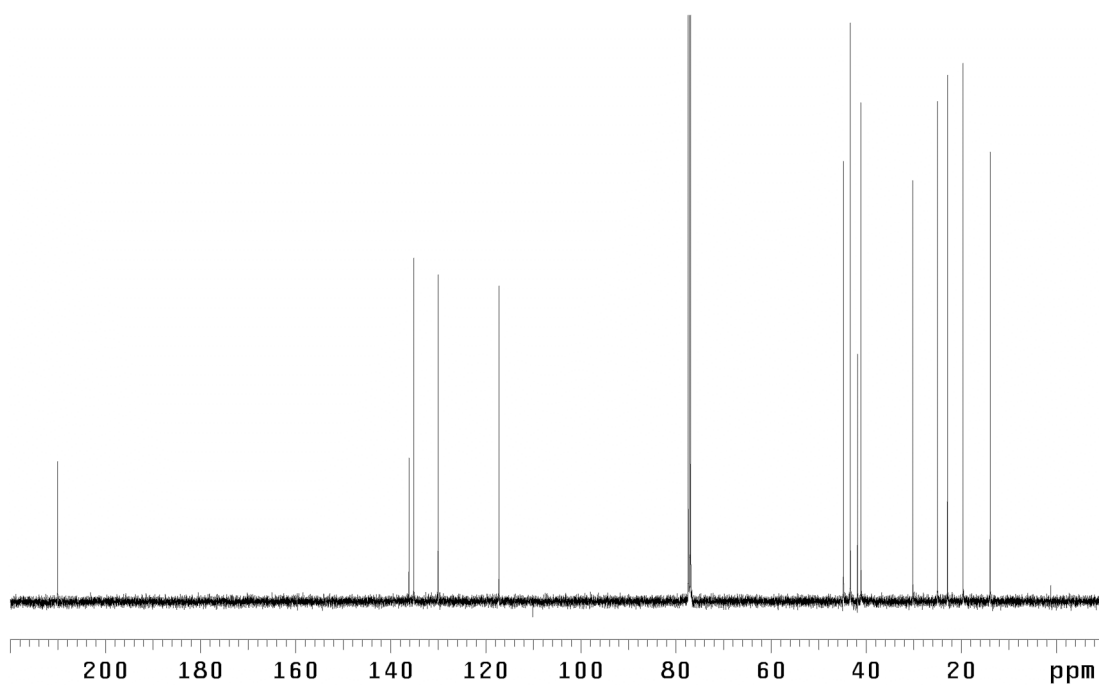


Figure A1.285. ¹³C NMR (125 MHz, CDCl₃) of compound **184**.

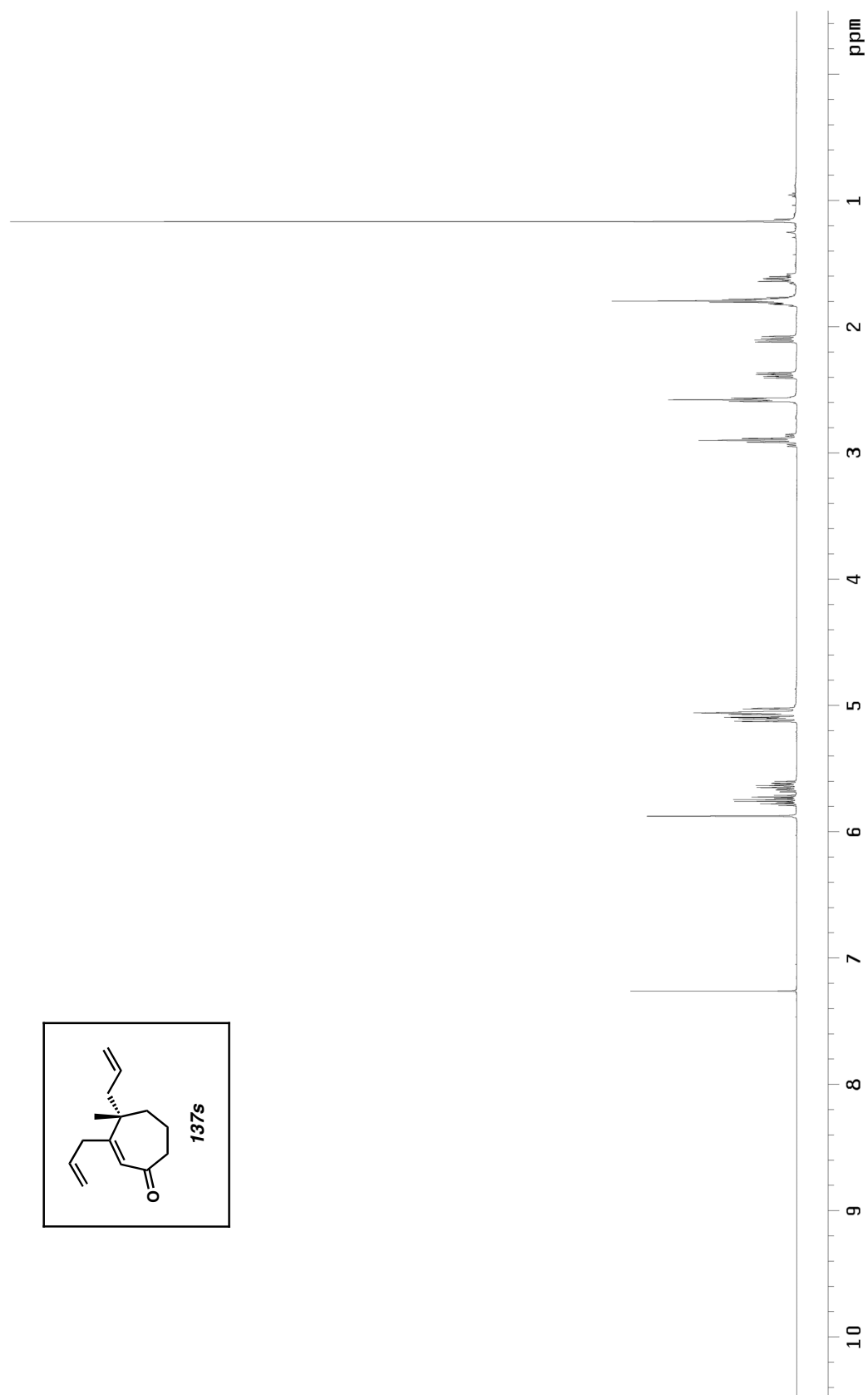


Figure A1.286. ^1H NMR (500 MHz, CDCl_3) of compound **137s**.

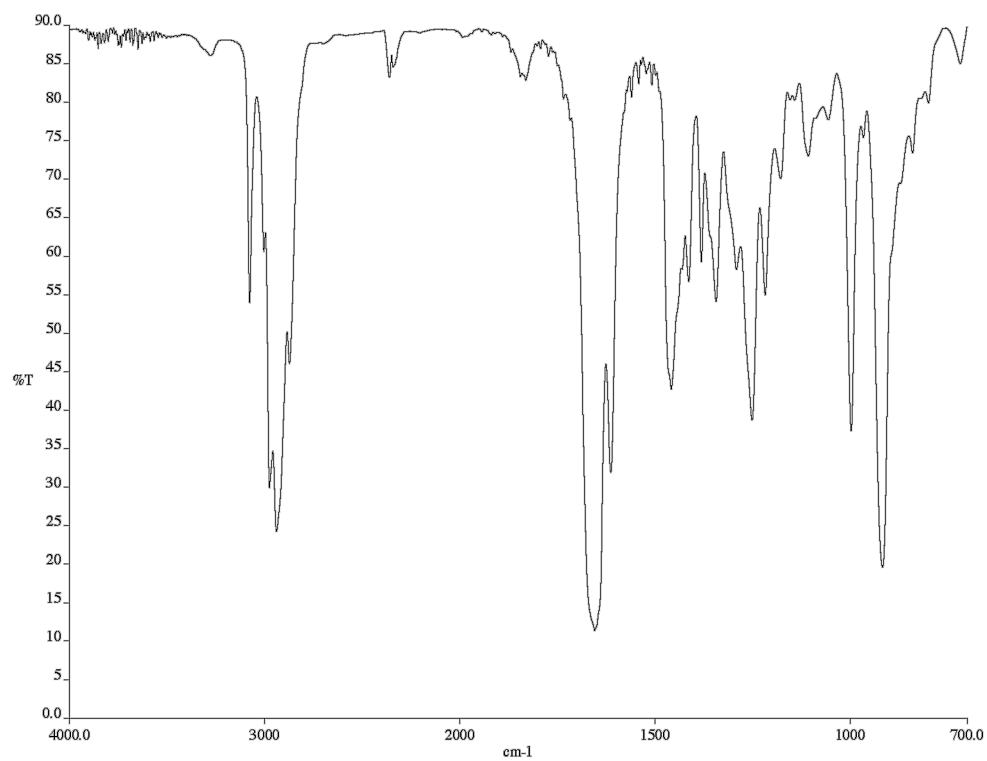


Figure A1.287. Infrared spectrum (thin film/NaCl) of compound **137s**.

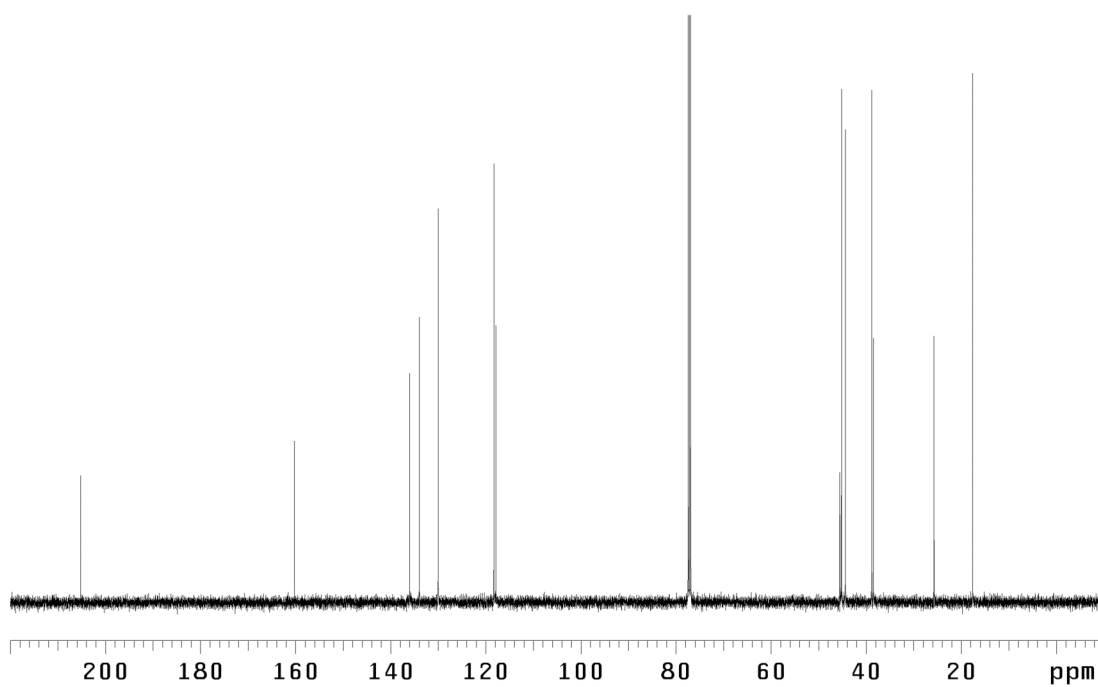


Figure A1.288. ¹³C NMR (125 MHz, CDCl₃) of compound **137s**.

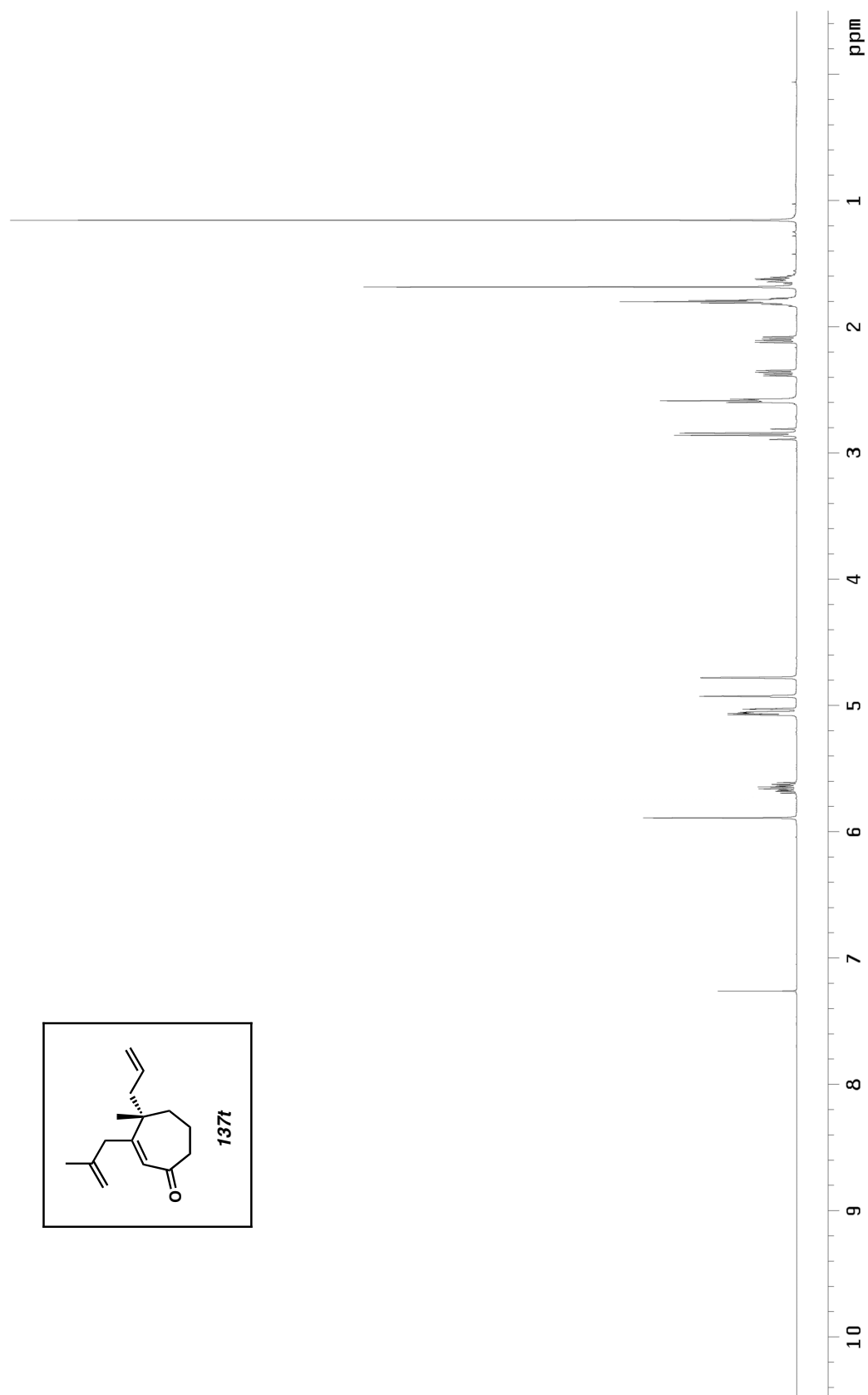


Figure A1.289. ^1H NMR (500 MHz, CDCl_3) of compound **137t**.

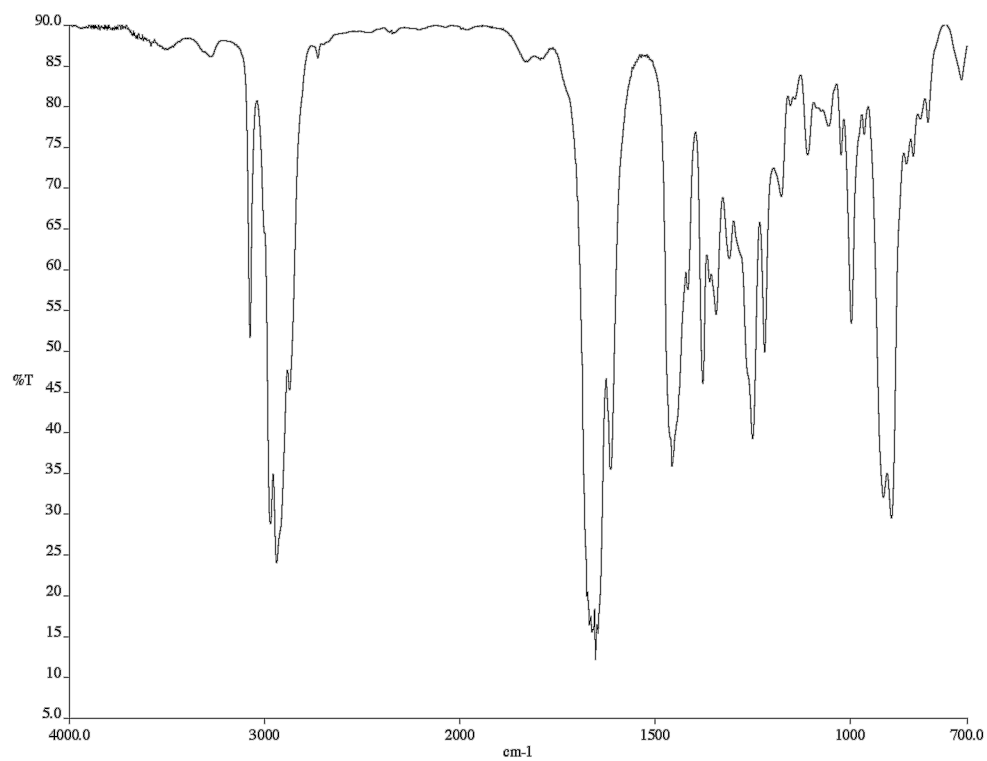


Figure A1.290. Infrared spectrum (thin film/NaCl) of compound **137t**.

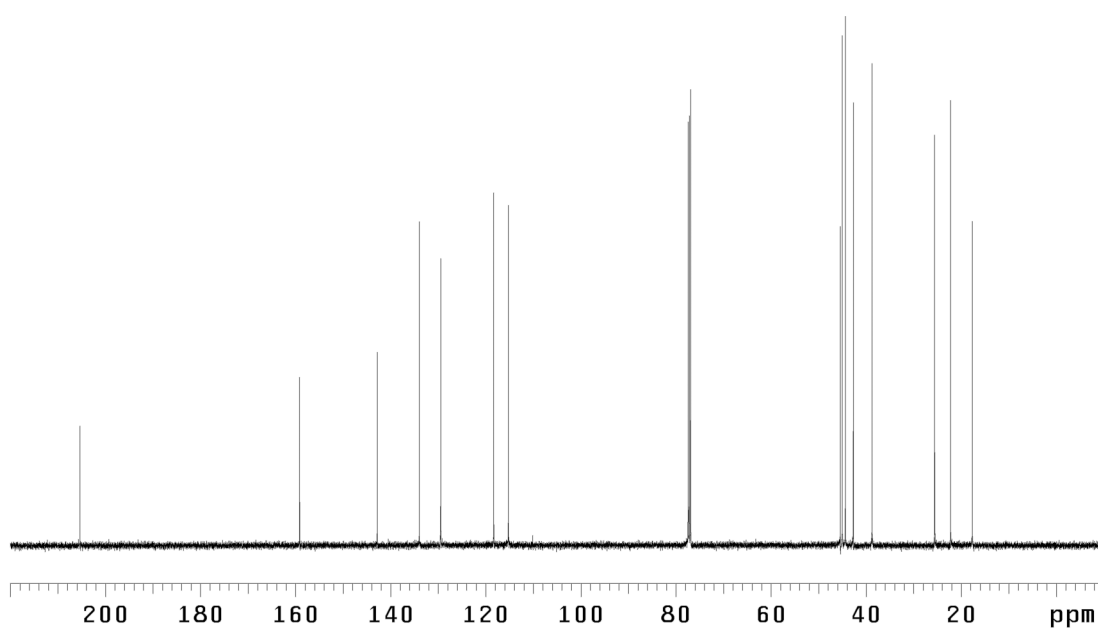


Figure A1.291. ¹³C NMR (125 MHz, CDCl₃) of compound **137t**.

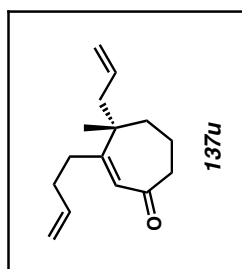
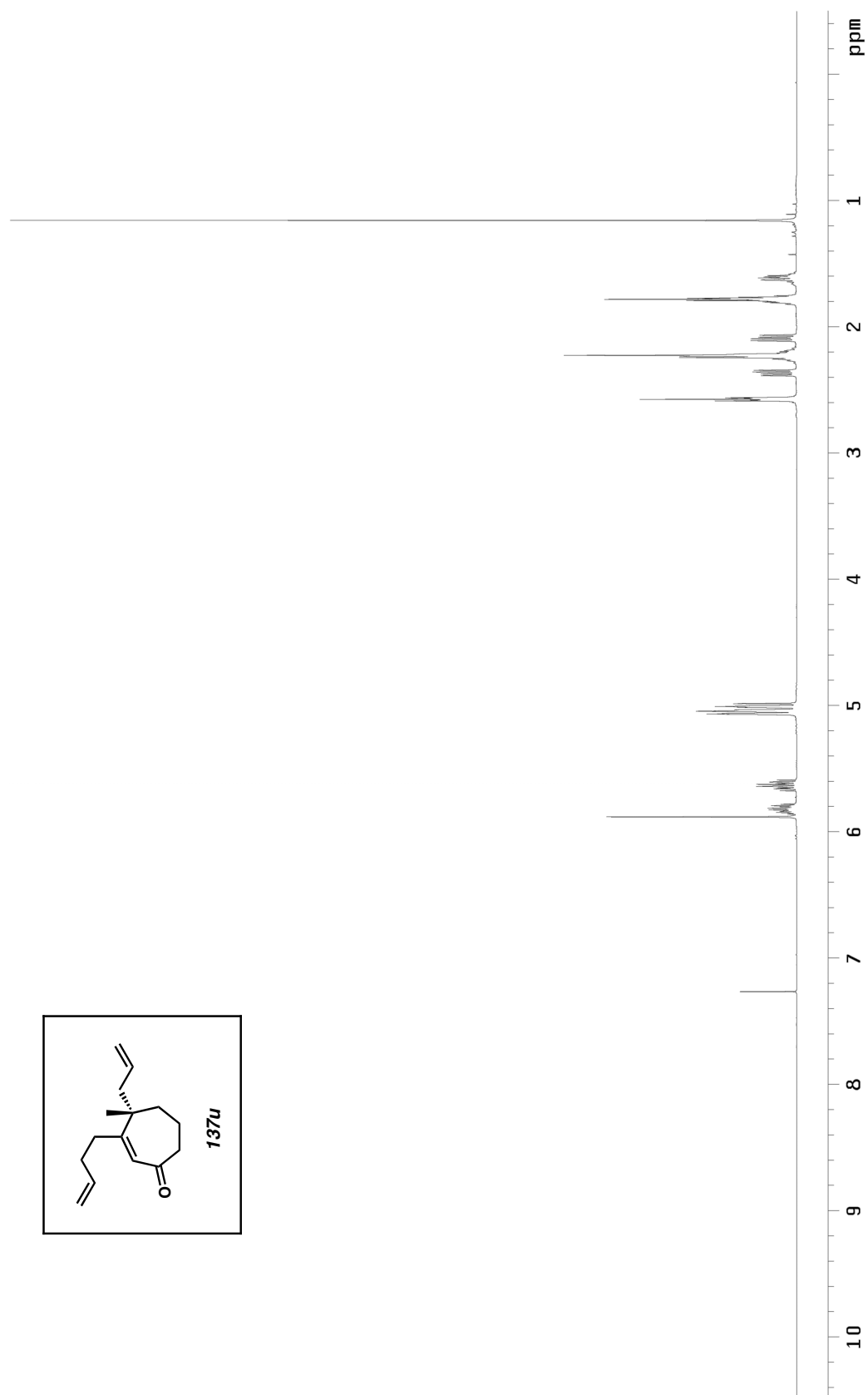


Figure A1.292. ¹H NMR (500 MHz, CDCl₃) of compound **137u**.

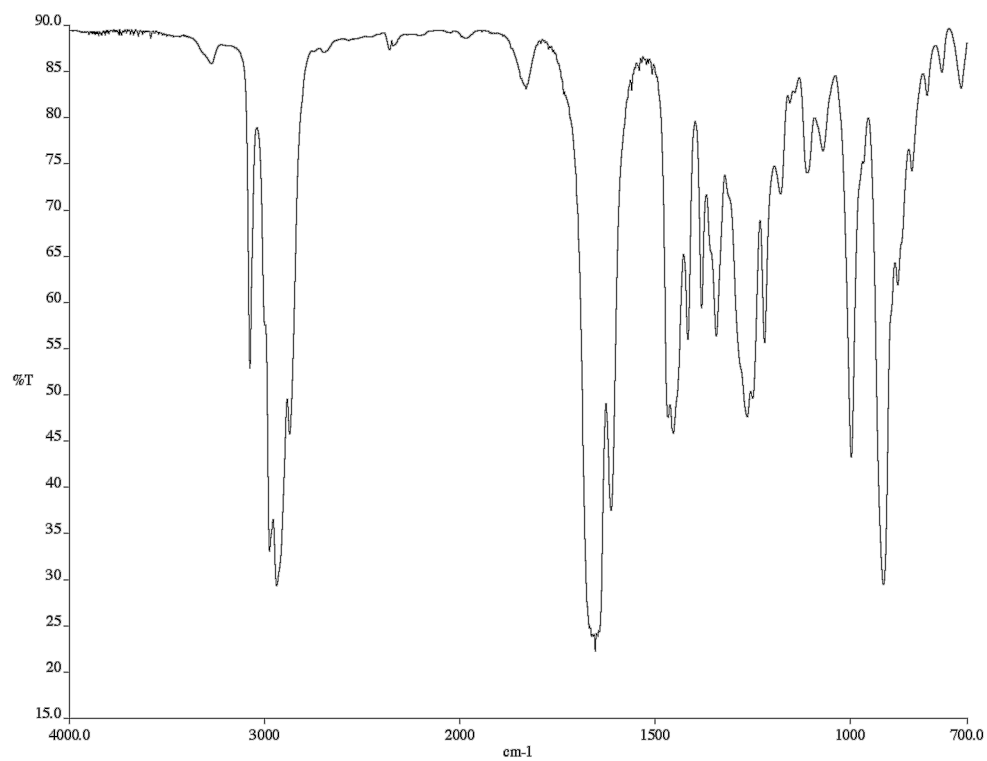


Figure A1.293. Infrared spectrum (thin film/NaCl) of compound **137u**.

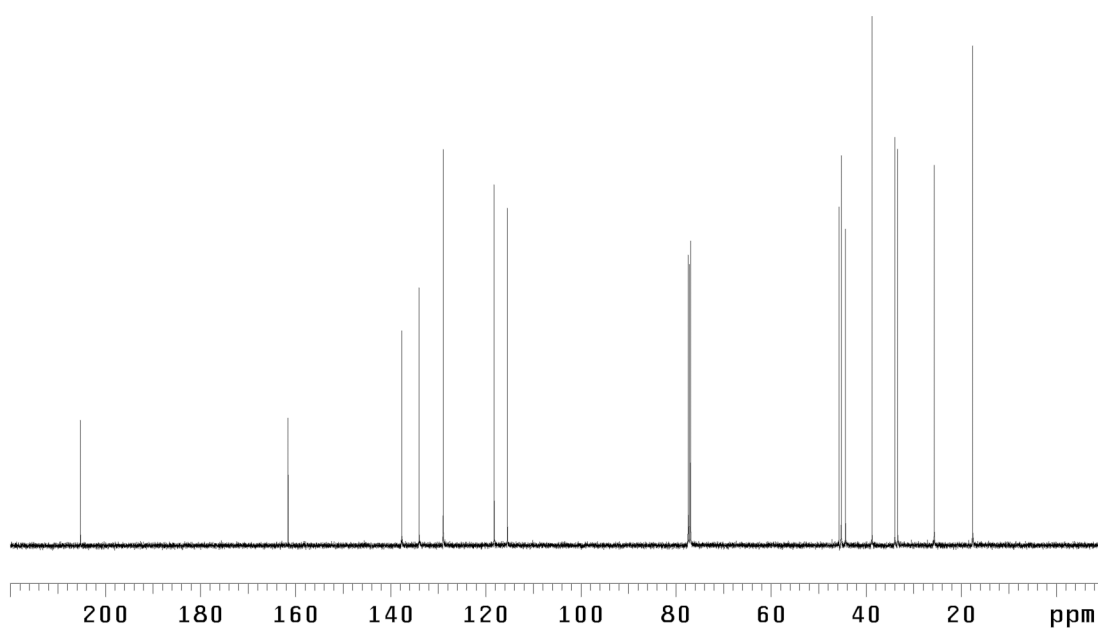
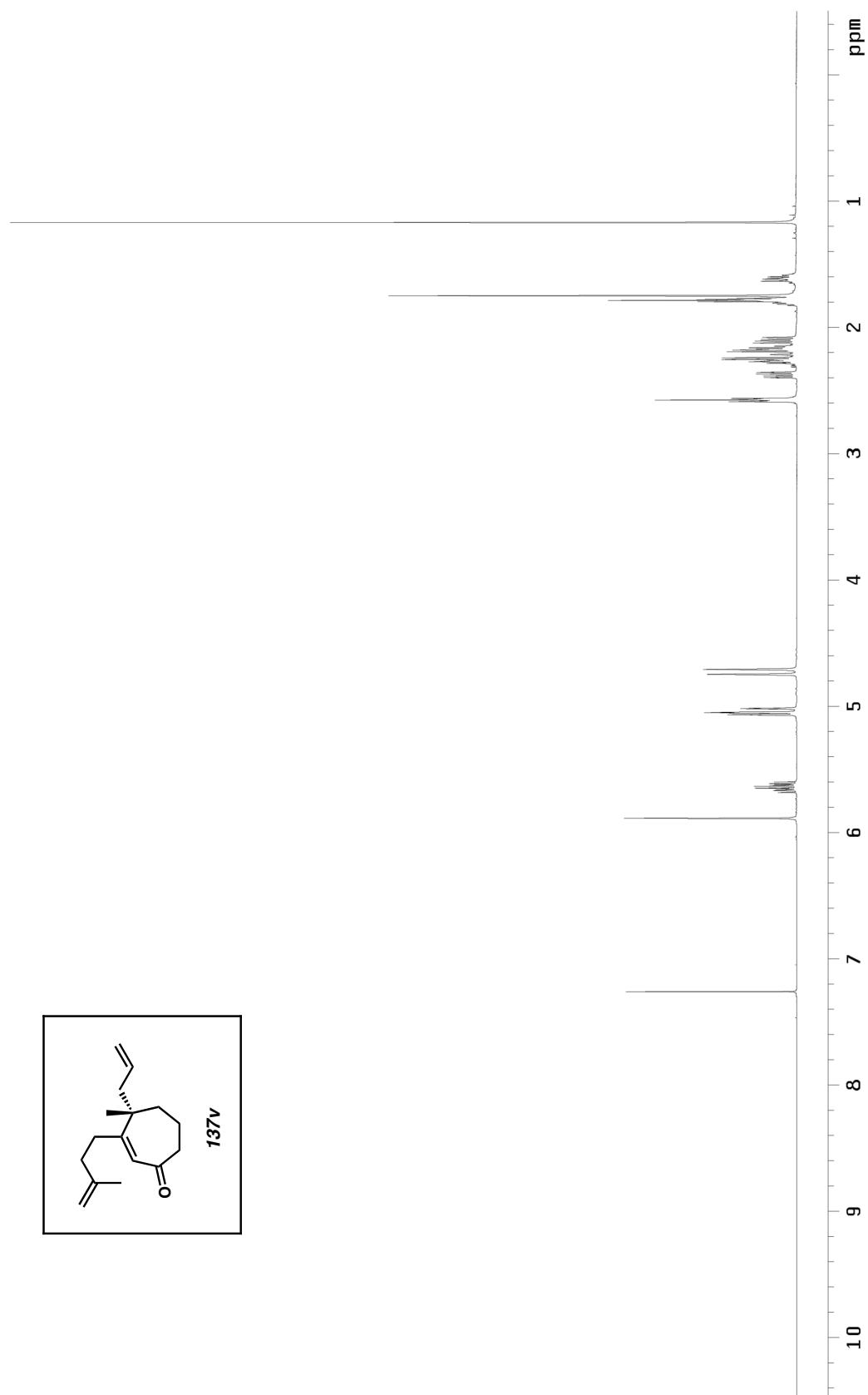


Figure A1.294. ¹³C NMR (125 MHz, CDCl₃) of compound **137u**.

Figure A1.295. ^1H NMR (500 MHz, CDCl_3) of compound **137v**.

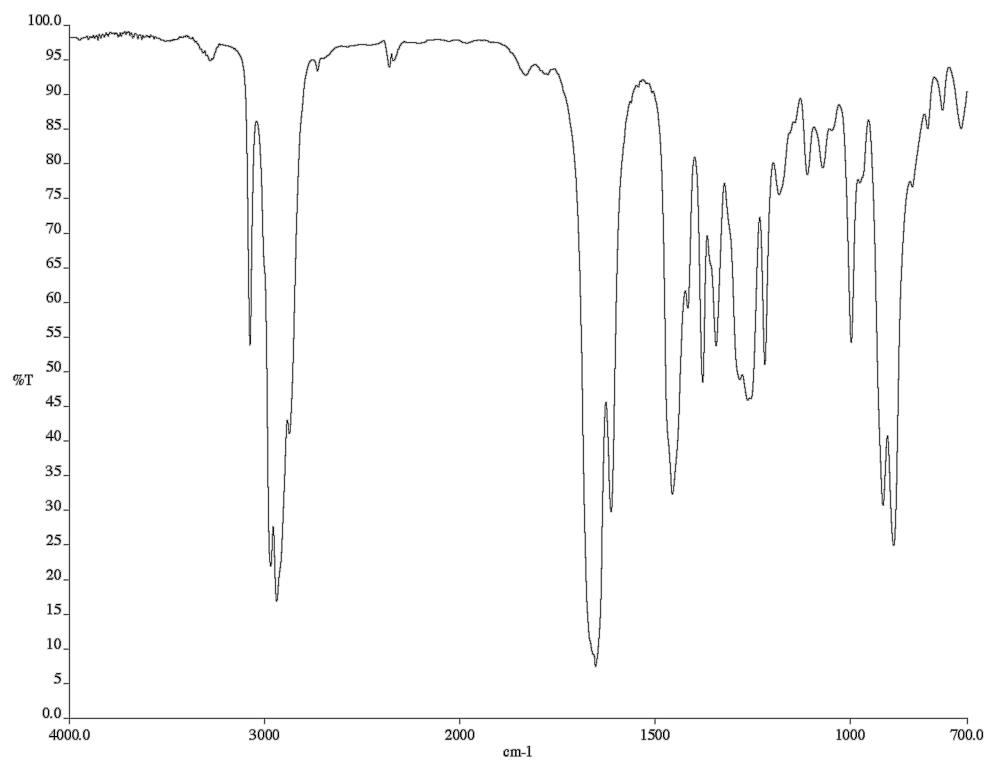


Figure A1.296. Infrared spectrum (thin film/NaCl) of compound **137v**.

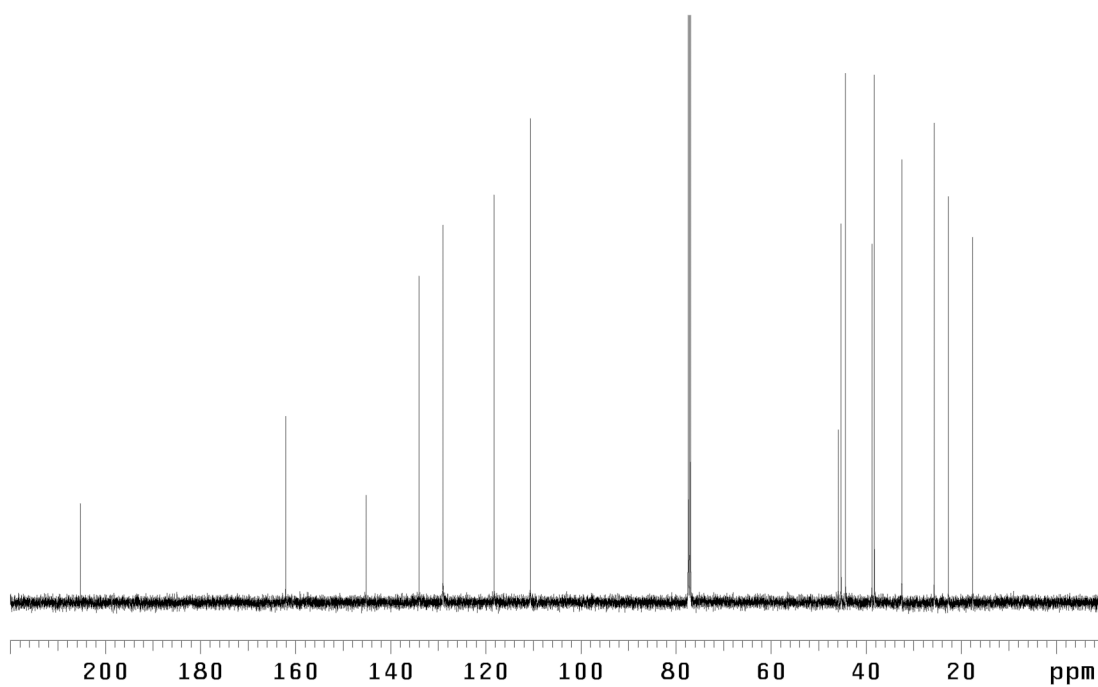


Figure A1.297. ¹³C NMR (125 MHz, CDCl₃) of compound **137v**.

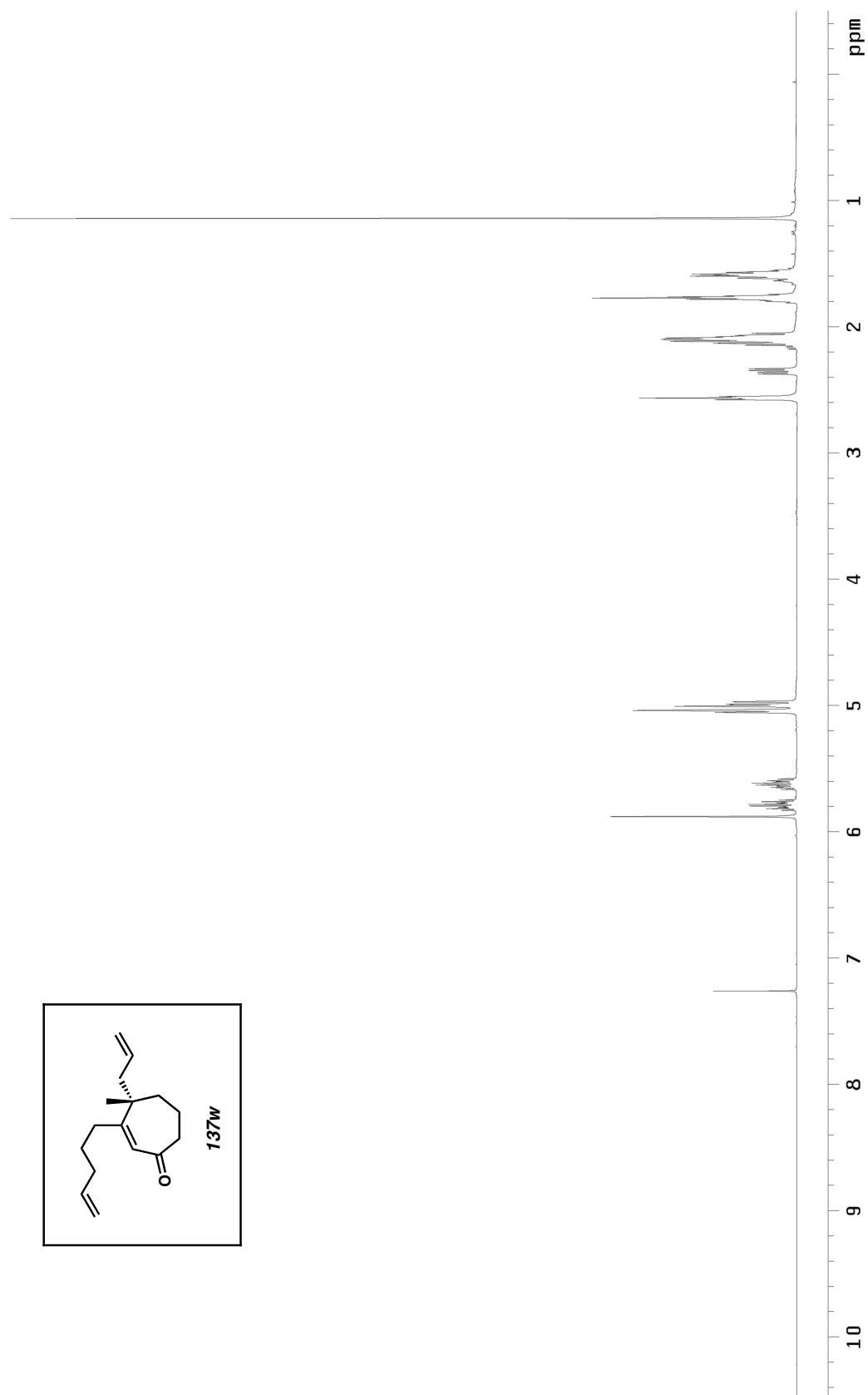


Figure A1.298. ^1H NMR (500 MHz, CDCl_3) of compound **137w**.

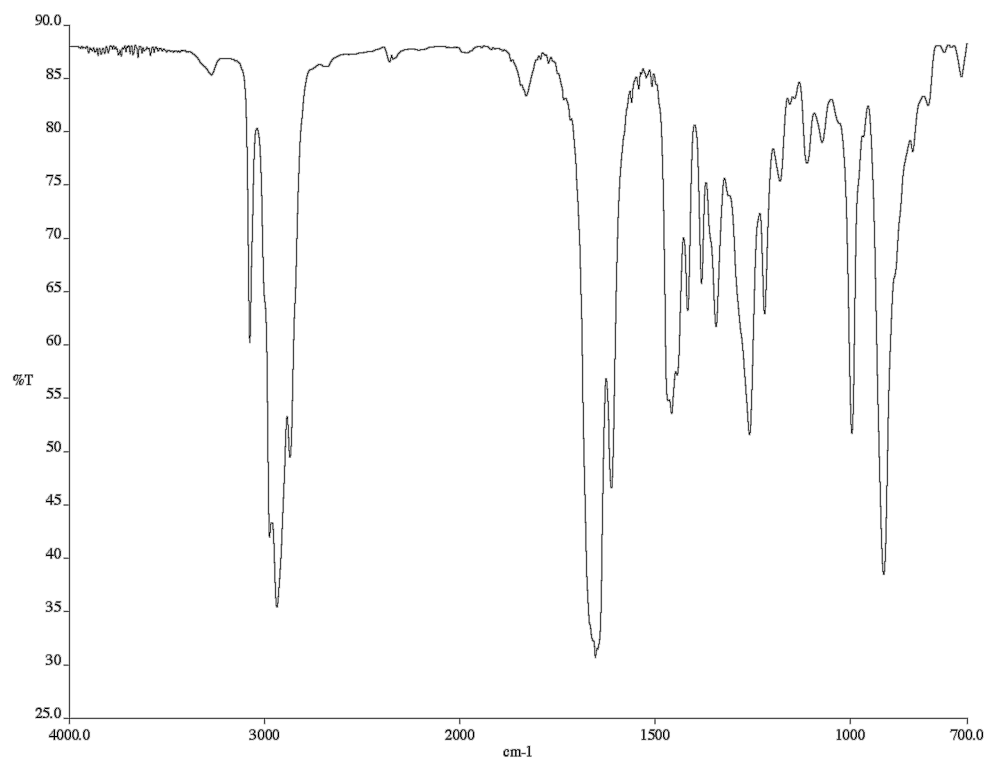


Figure A1.299. Infrared spectrum (thin film/NaCl) of compound **137w**.

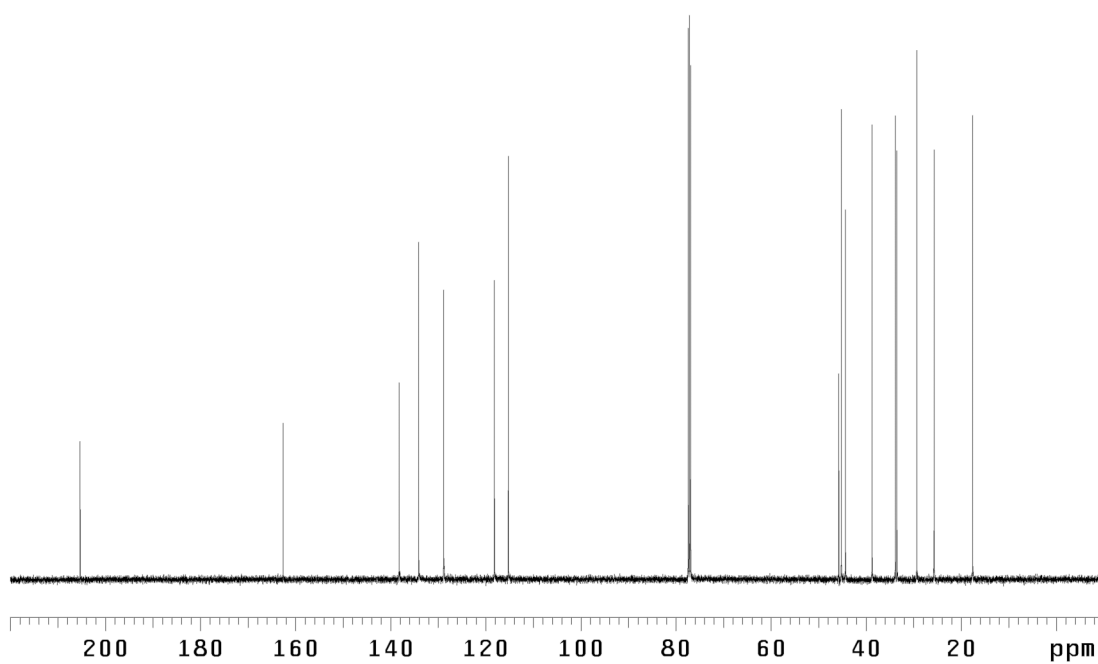
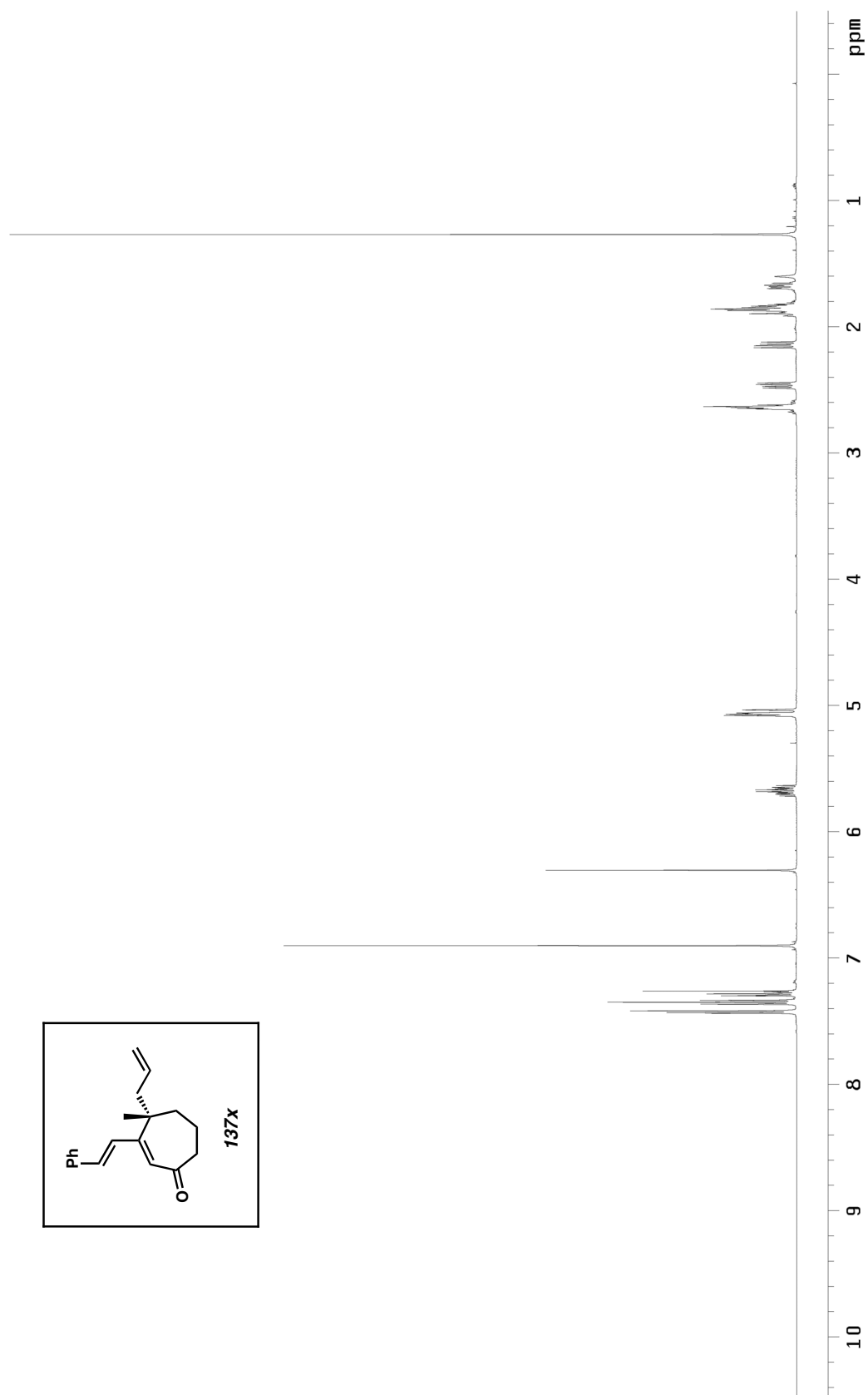


Figure A1.300. ¹³C NMR (125 MHz, CDCl₃) of compound **137w**.

Figure A1.301. ¹H NMR (500 MHz, CDCl₃) of compound **137x**.

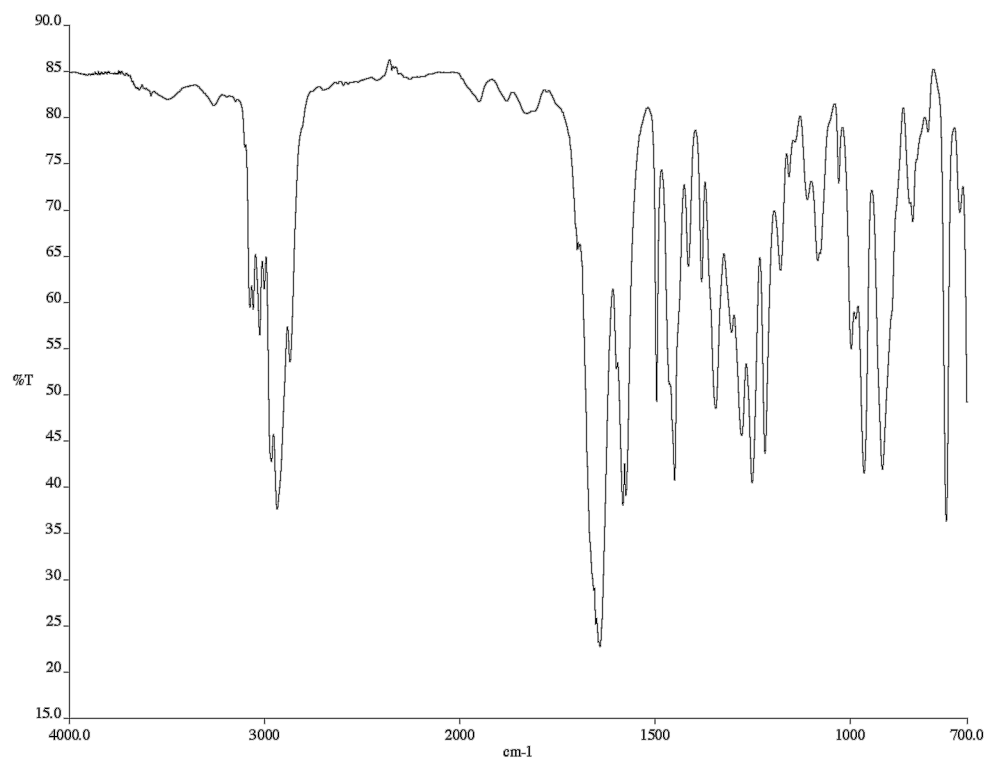


Figure A1.302. Infrared spectrum (thin film/NaCl) of compound **137x**.

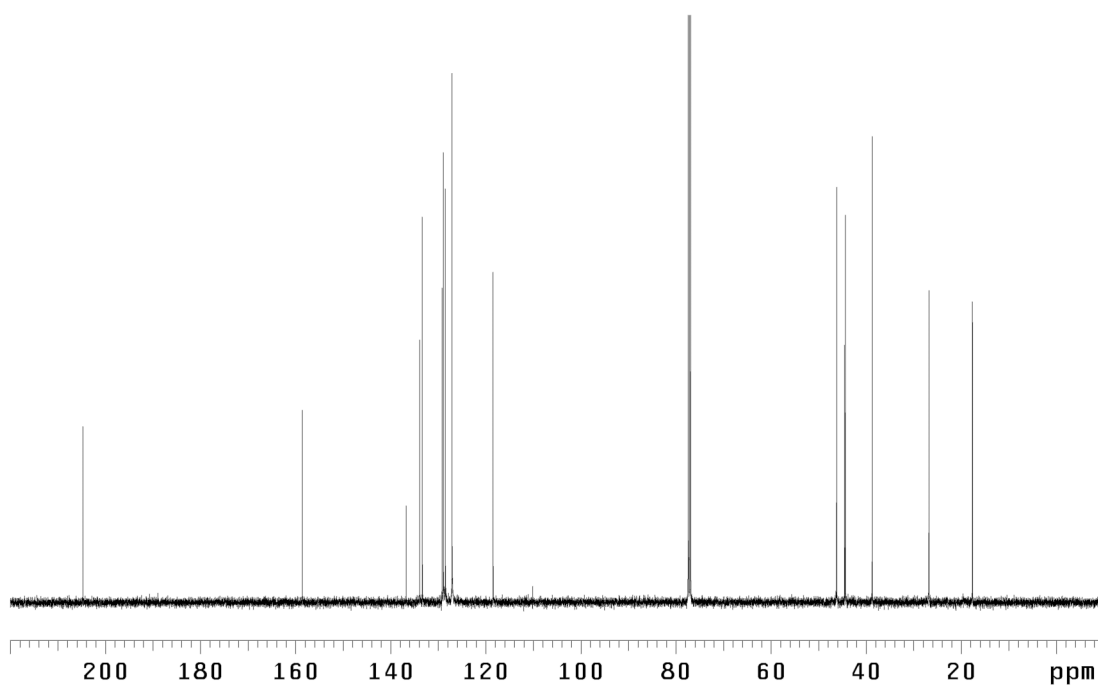
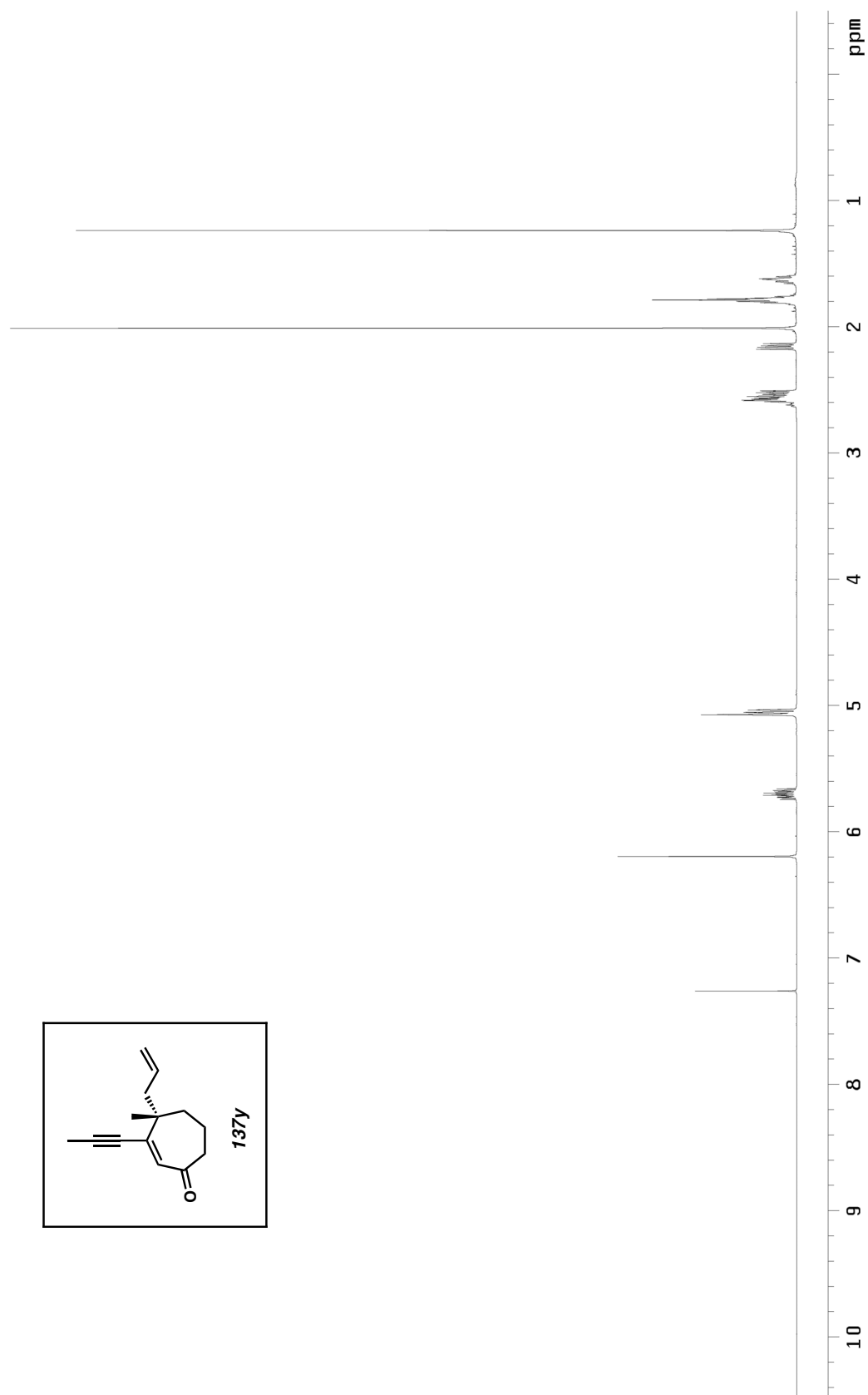


Figure A1.303. ¹³C NMR (125 MHz, CDCl₃) of compound **137x**.

Figure A1.304. ^1H NMR (500 MHz, CDCl_3) of compound **137y**.

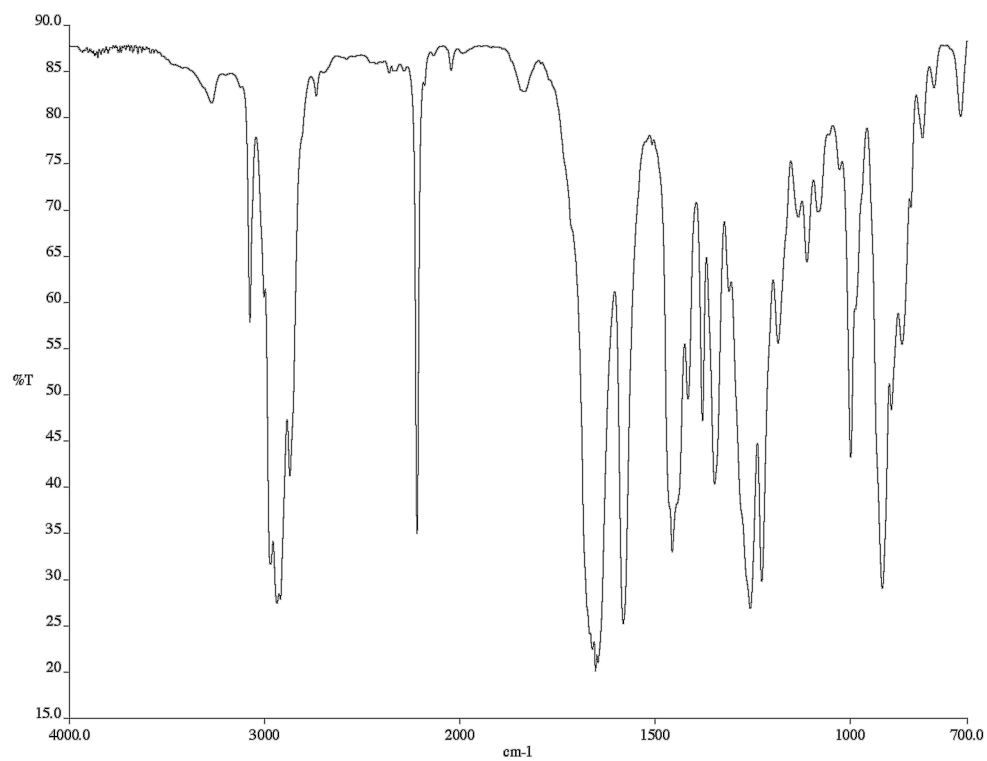


Figure A1.305. Infrared spectrum (thin film/NaCl) of compound **137y**.

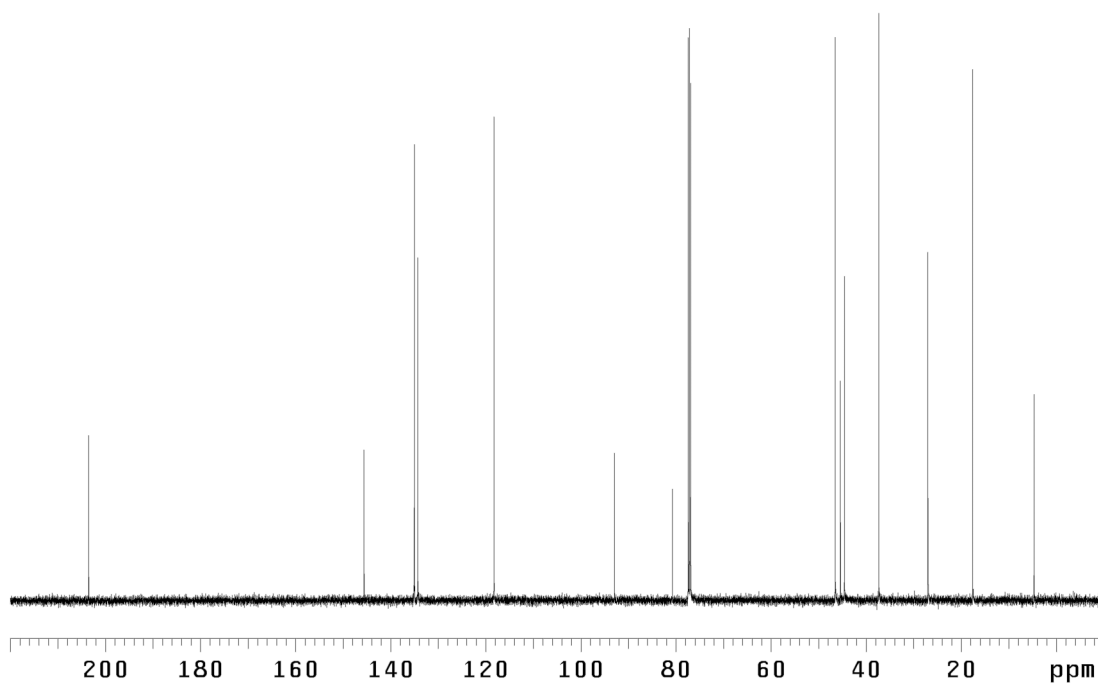
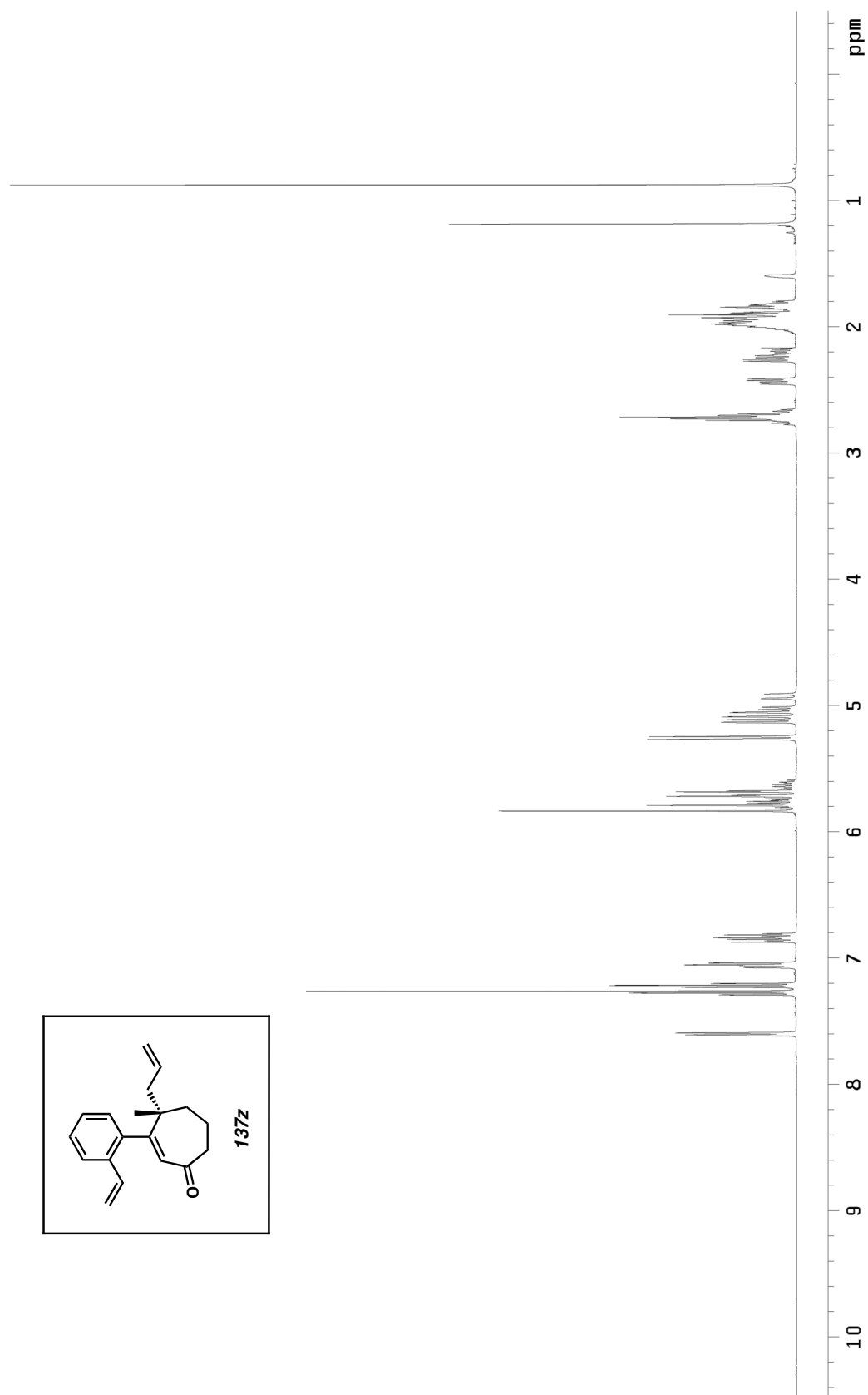


Figure A1.306. ¹³C NMR (125 MHz, CDCl₃) of compound **137y**.

Figure A1.307. ¹H NMR (500 MHz, CDCl₃) of compound **137z**.

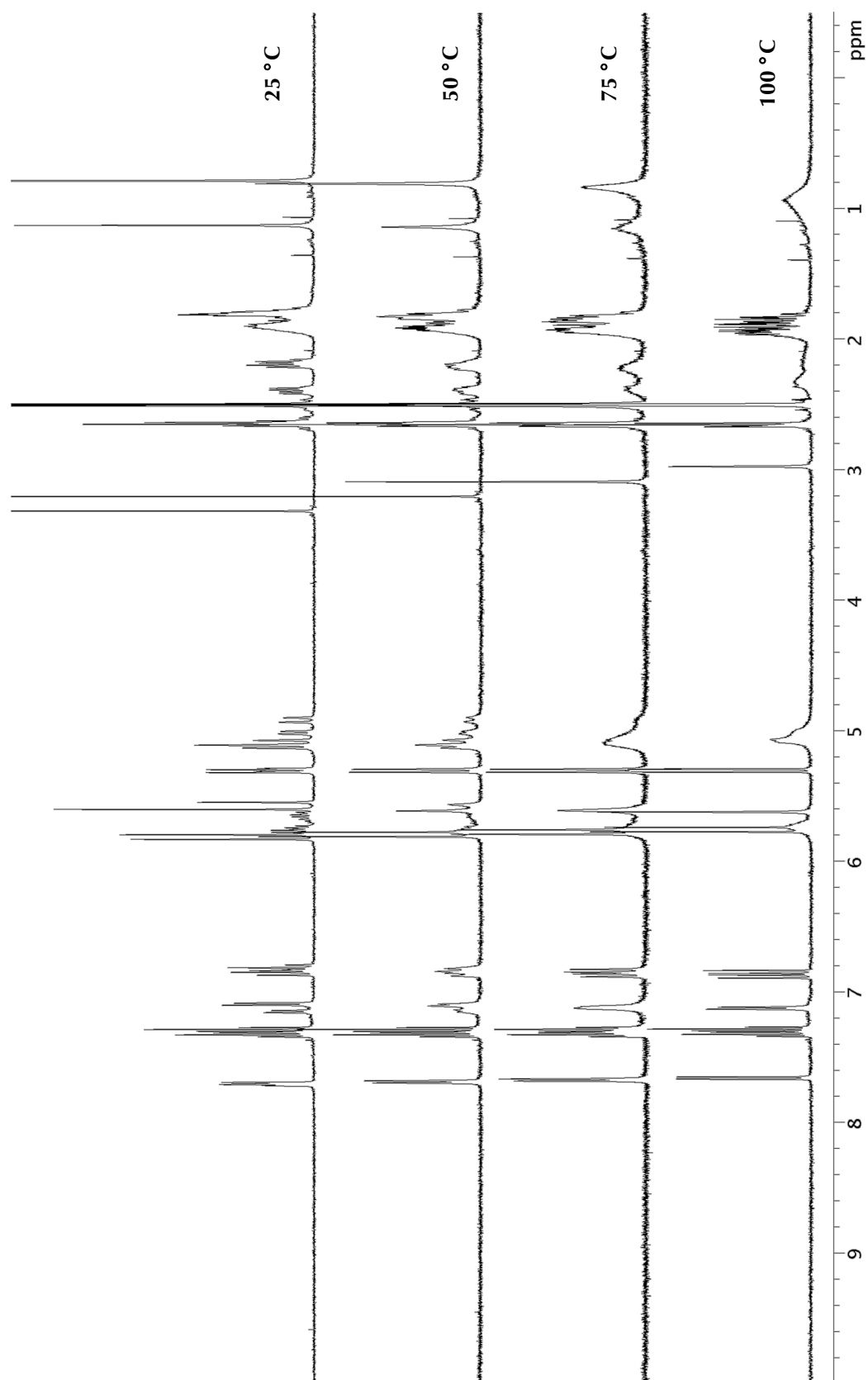


Figure A1.308. Variable Temperature ¹H NMR (500 MHz, DMSO-*d*₆) of compound **137z**.

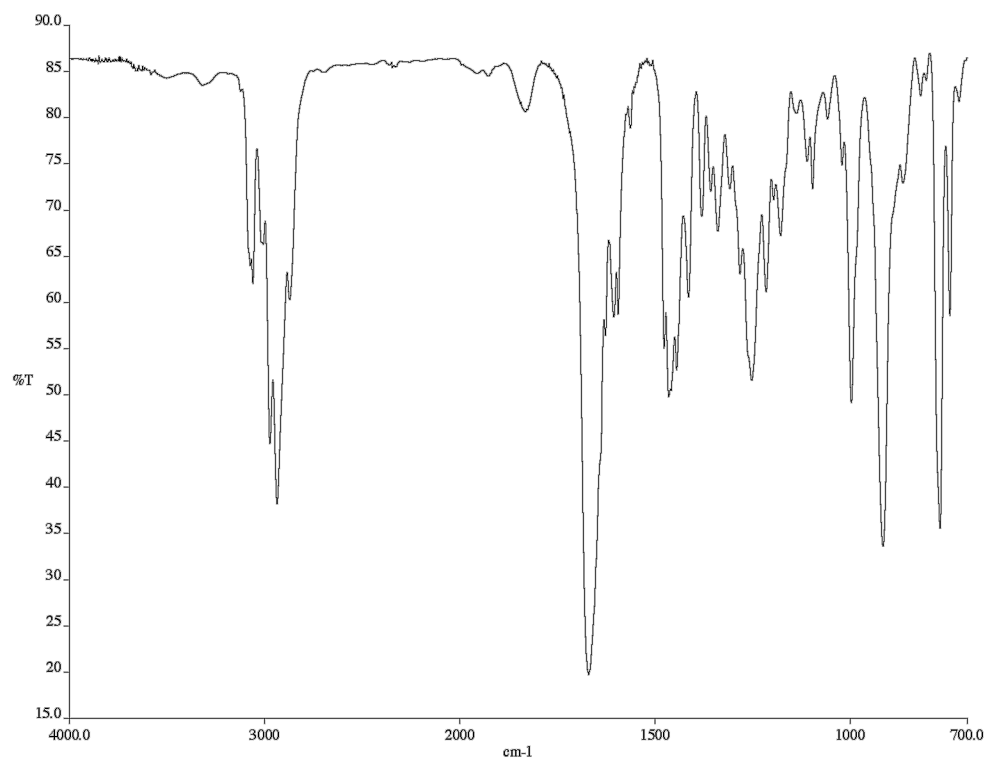


Figure A1.309. Infrared spectrum (thin film/NaCl) of compound **137z**.

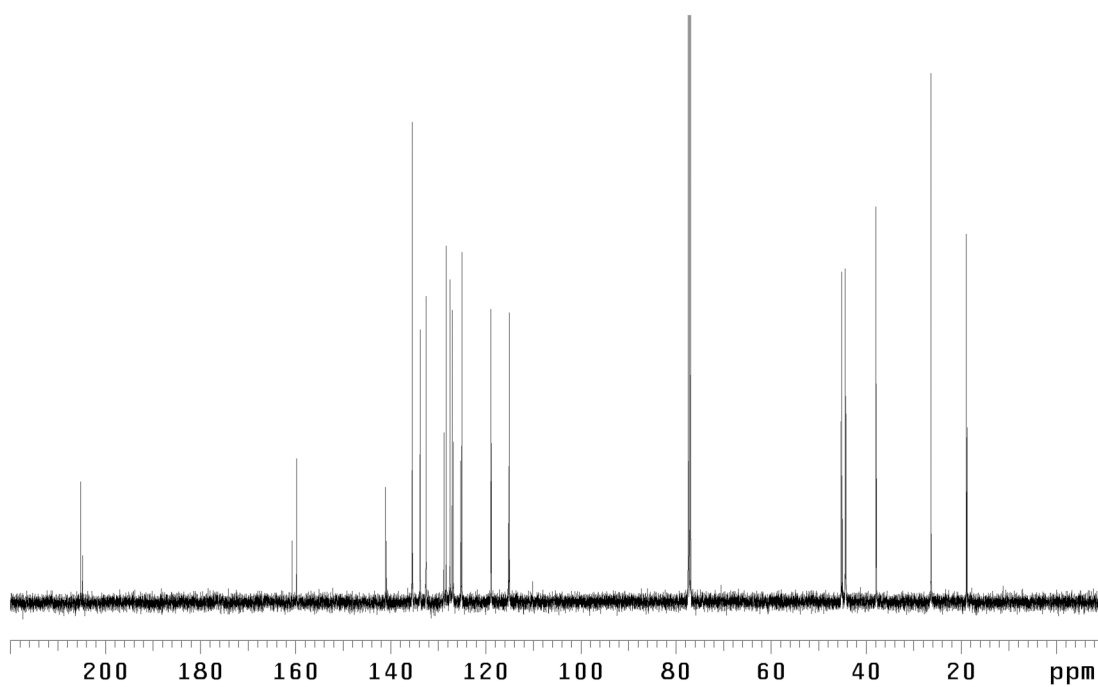


Figure A1.310. ¹³C NMR (125 MHz, CDCl₃) of compound **137z**.

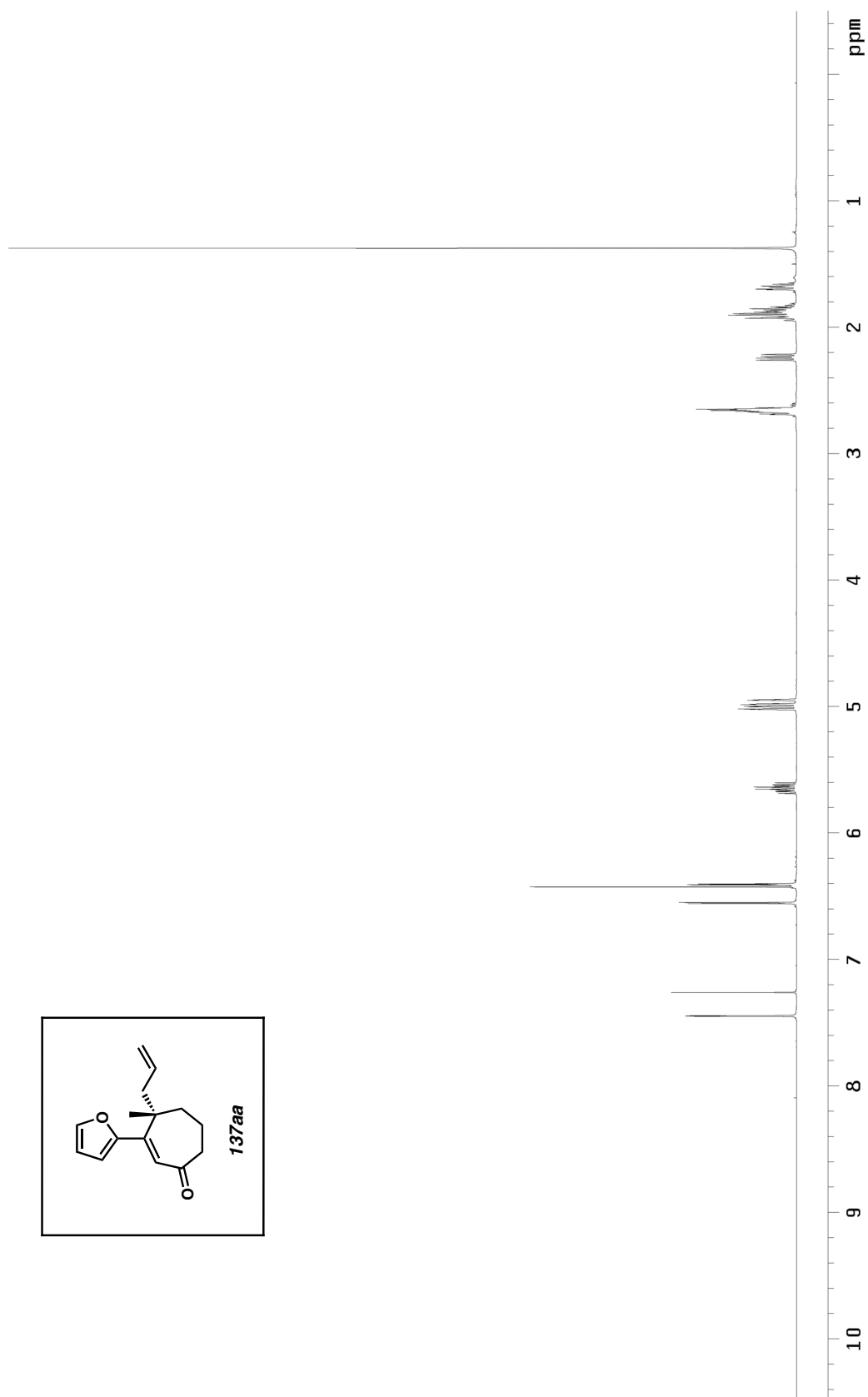


Figure A1.311. ^1H NMR (500 MHz, CDCl_3) of compound **137aa**.

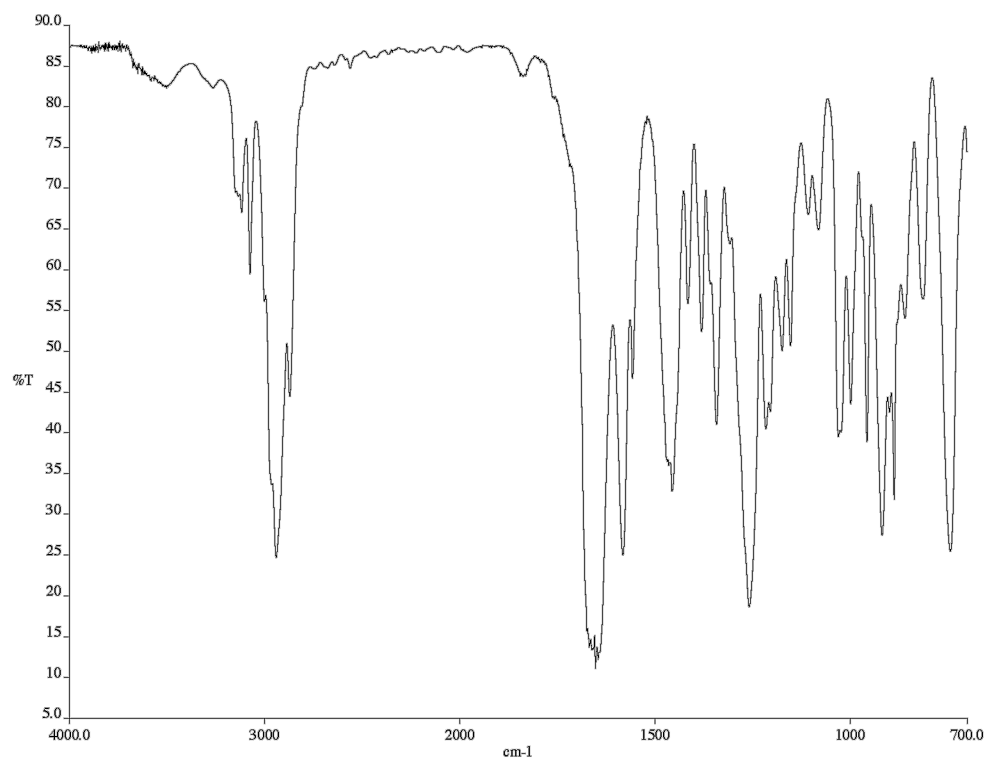


Figure A1.312. Infrared spectrum (thin film/NaCl) of compound **137aa**.

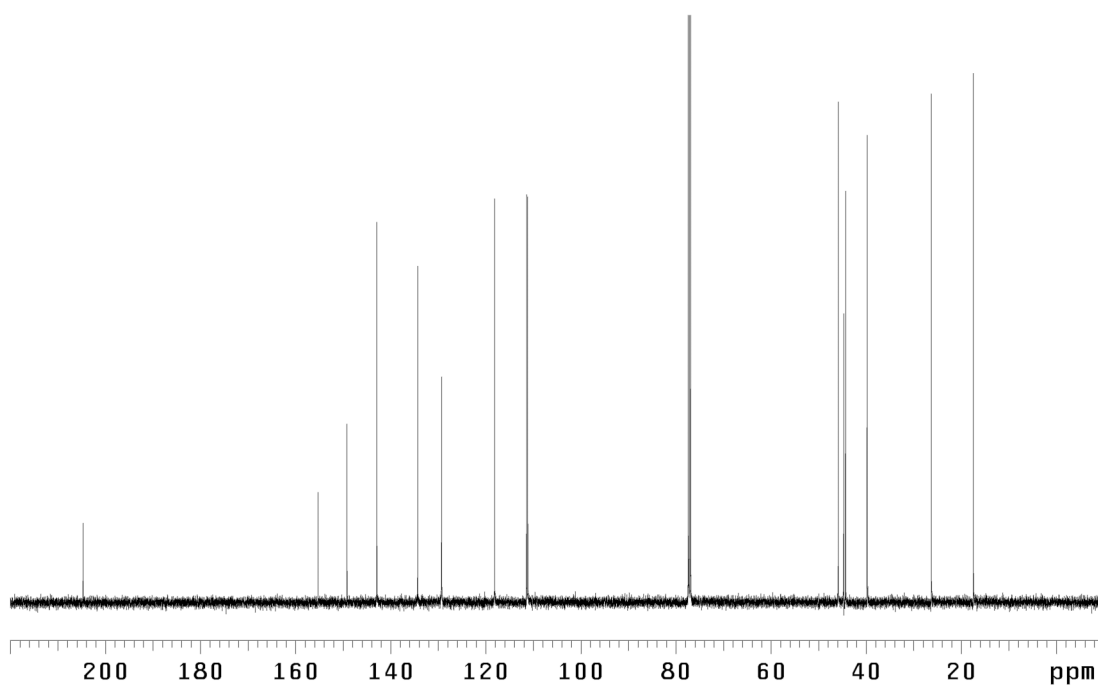


Figure A1.313. ¹³C NMR (125 MHz, CDCl₃) of compound **137aa**.

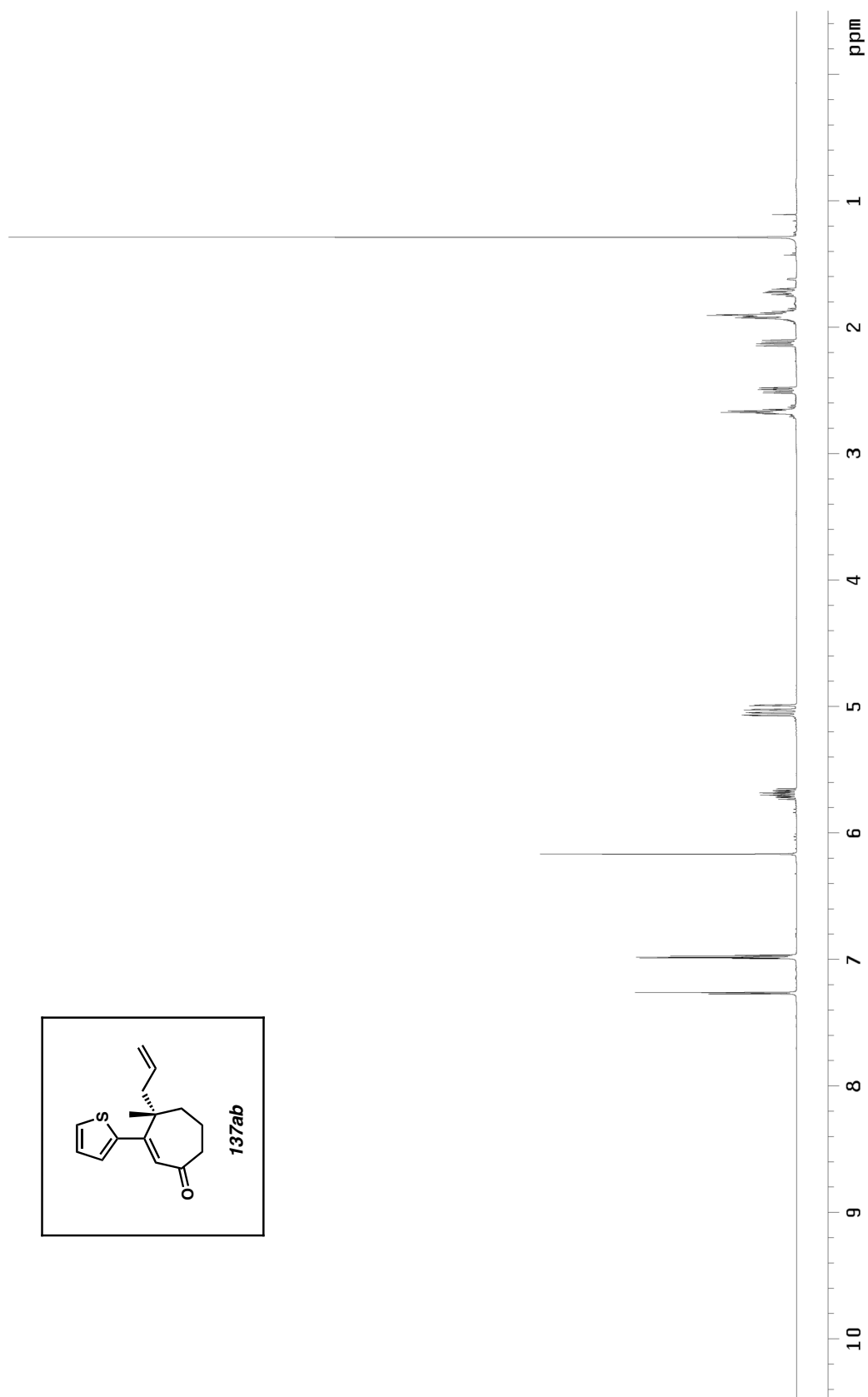


Figure A1.314. ^1H NMR (500 MHz, CDCl_3) of compound **137ab**.

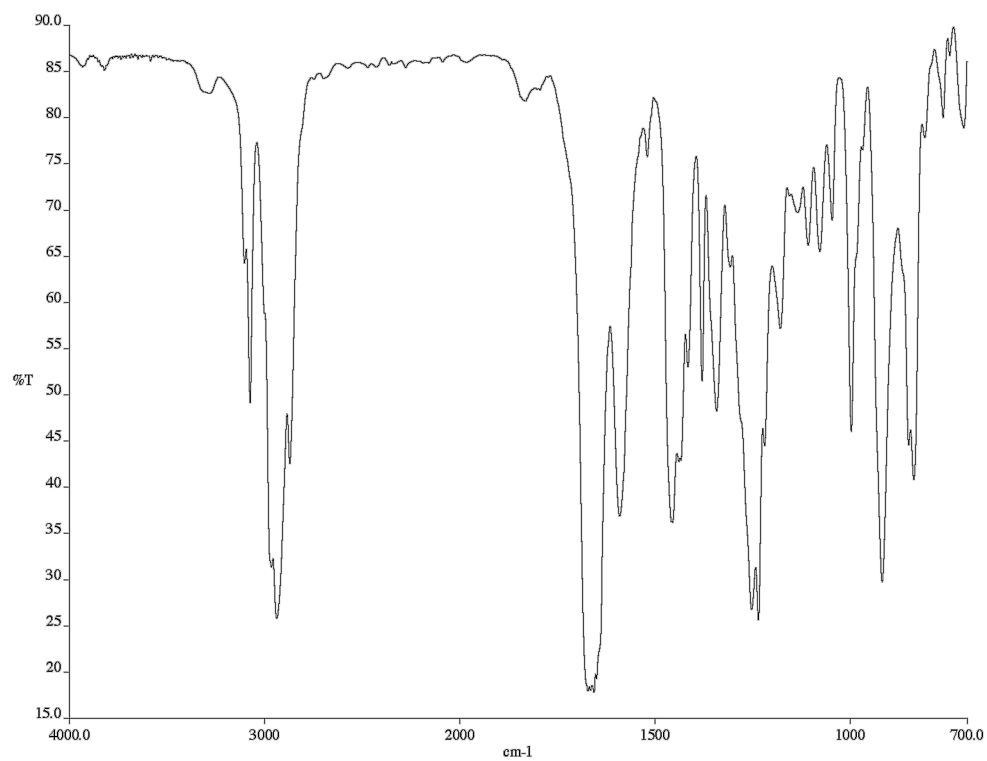


Figure A1.315. Infrared spectrum (thin film/NaCl) of compound **137ab**.

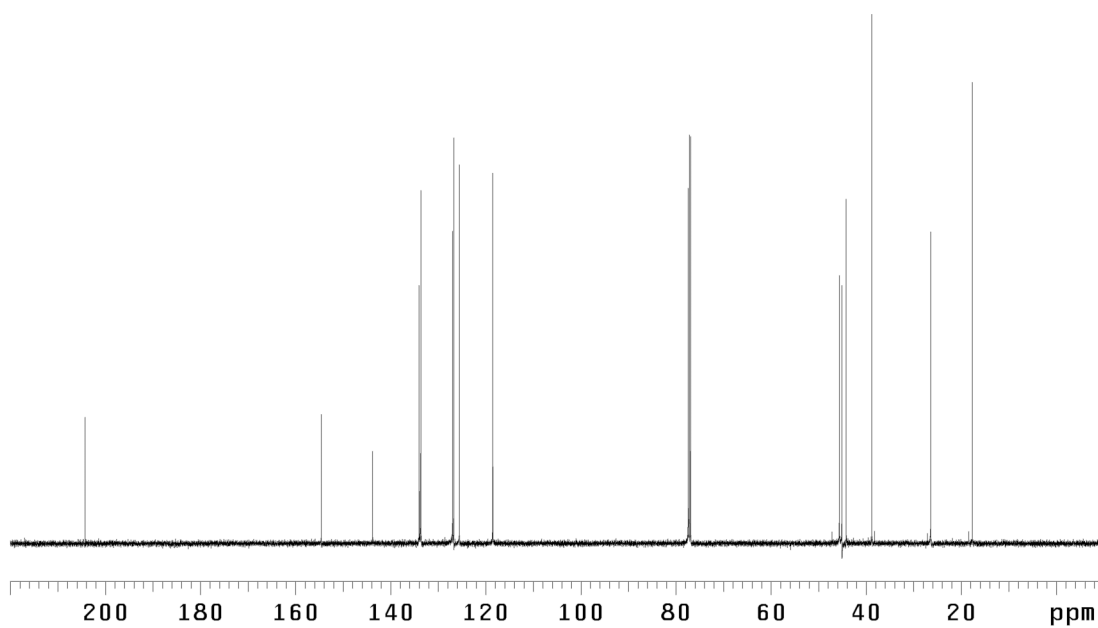


Figure A1.316. ¹³C NMR (125 MHz, CDCl₃) of compound **137ab**.

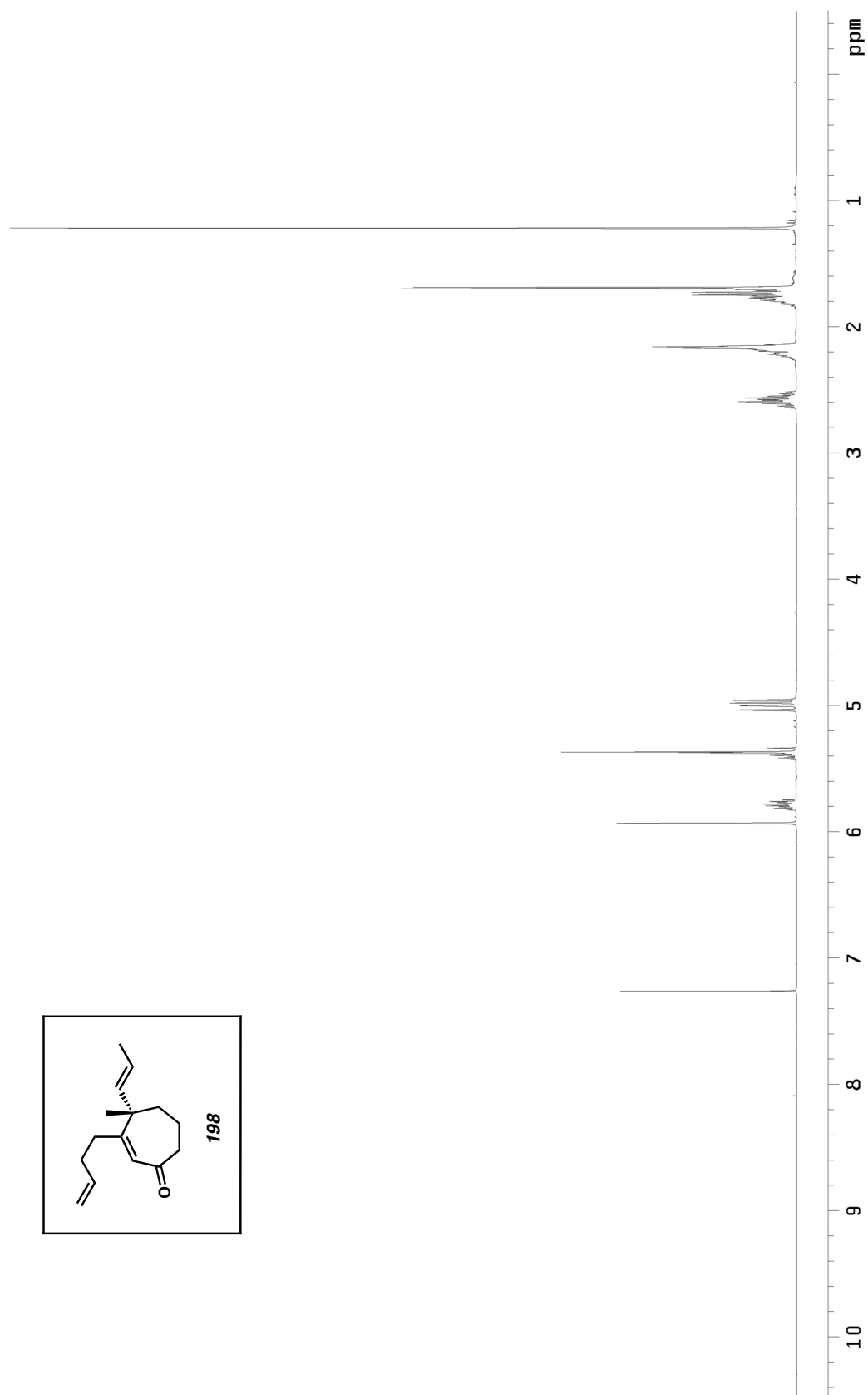


Figure A1.317. ¹H NMR (500 MHz, CDCl₃) of compound **198**.

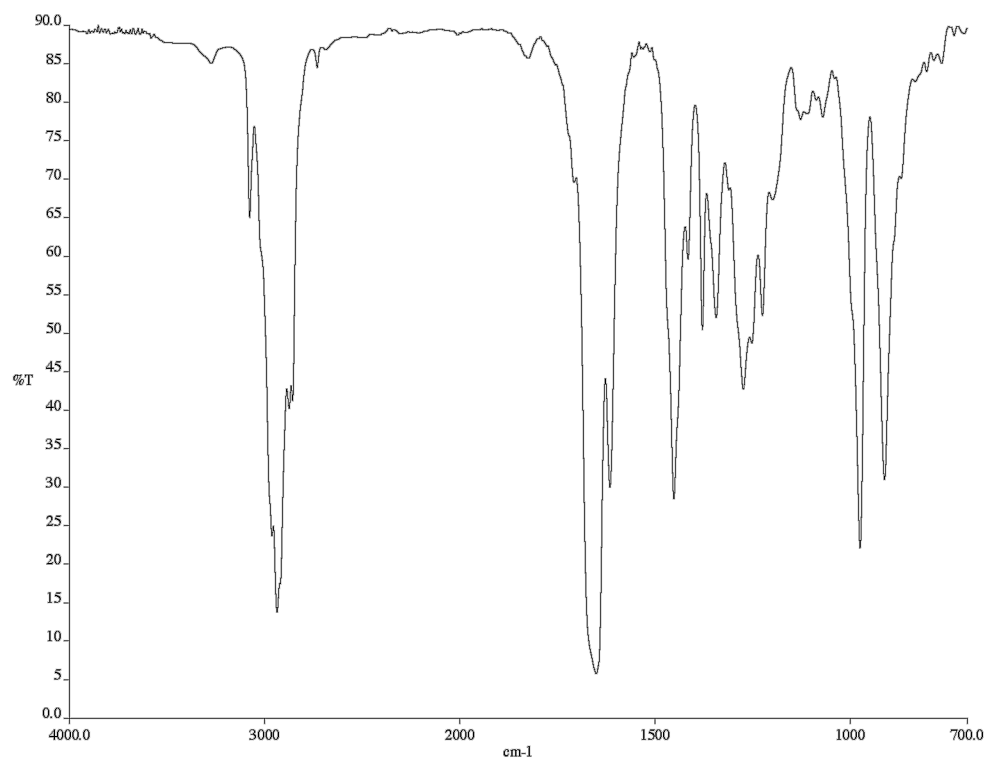


Figure A1.318. Infrared spectrum (thin film/NaCl) of compound **198**.

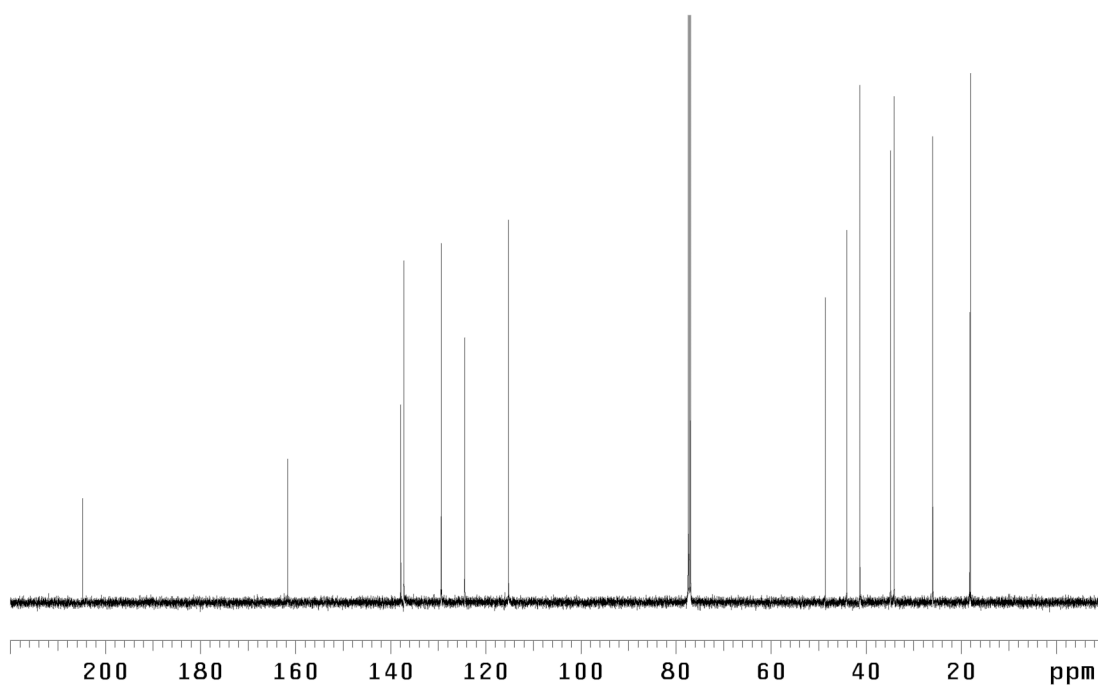


Figure A1.319. ¹³C NMR (125 MHz, CDCl₃) of compound **198**.

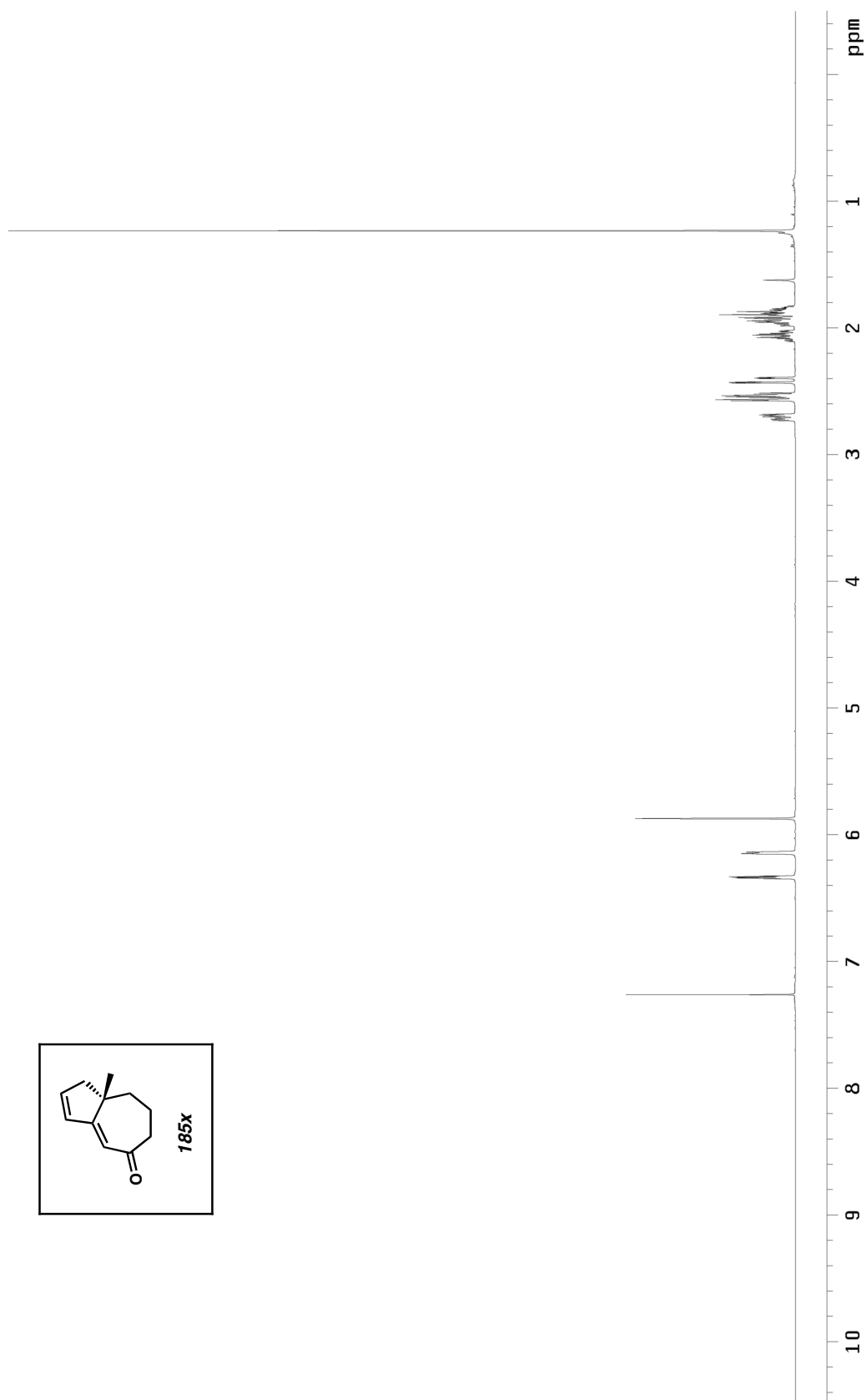


Figure A1.320. ¹H NMR (500 MHz, CDCl₃) of compound **185x**.

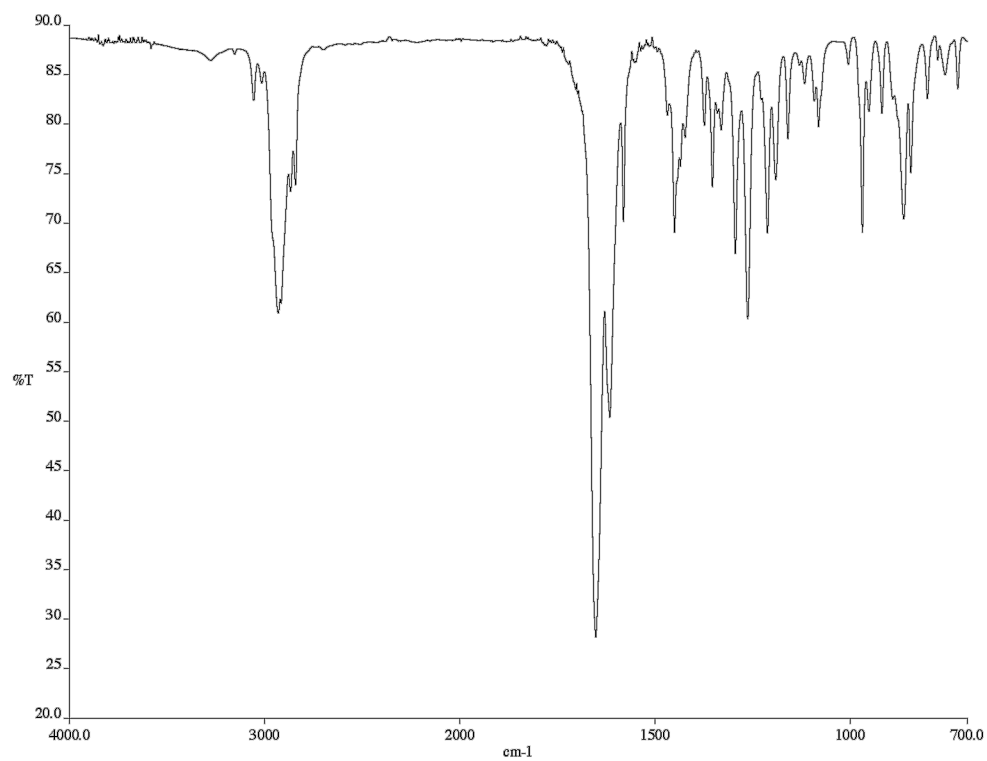


Figure A1.321. Infrared spectrum (thin film/NaCl) of compound **185x**.

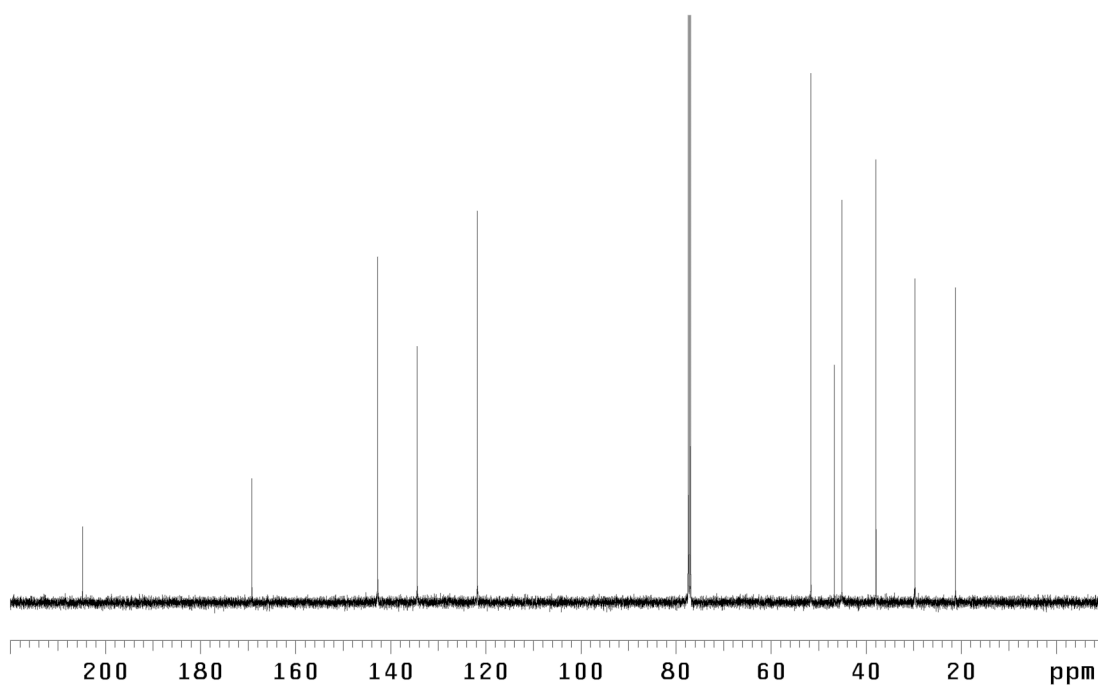
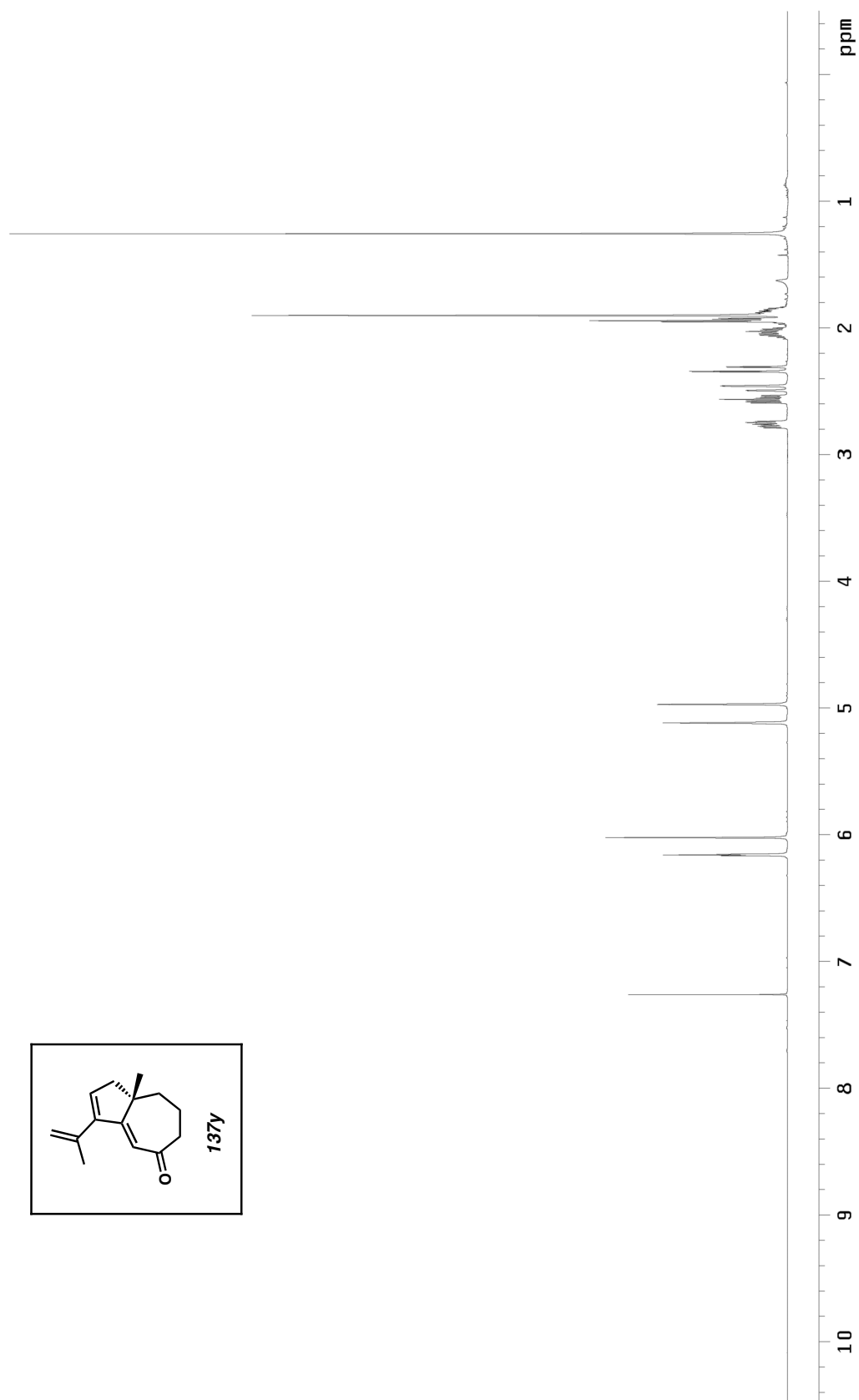


Figure A1.322. ¹³C NMR (125 MHz, CDCl₃) of compound **185x**.

Figure A1.323. ^1H NMR (500 MHz, CDCl_3) of compound **185y**.

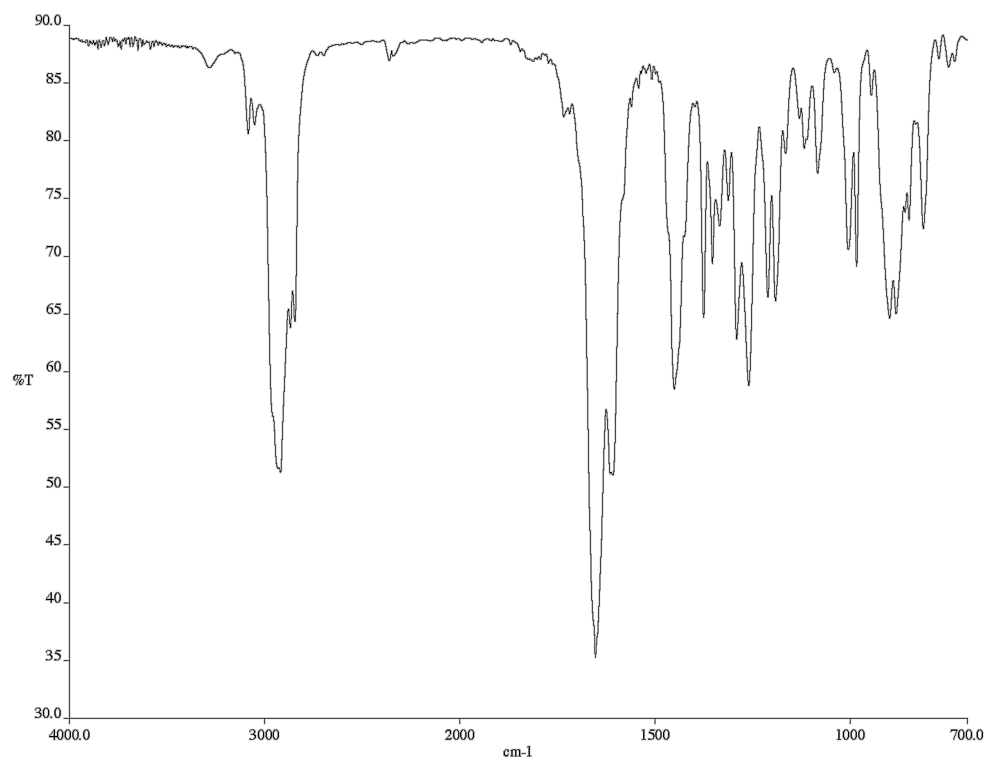


Figure A1.324. Infrared spectrum (thin film/NaCl) of compound **185y**.

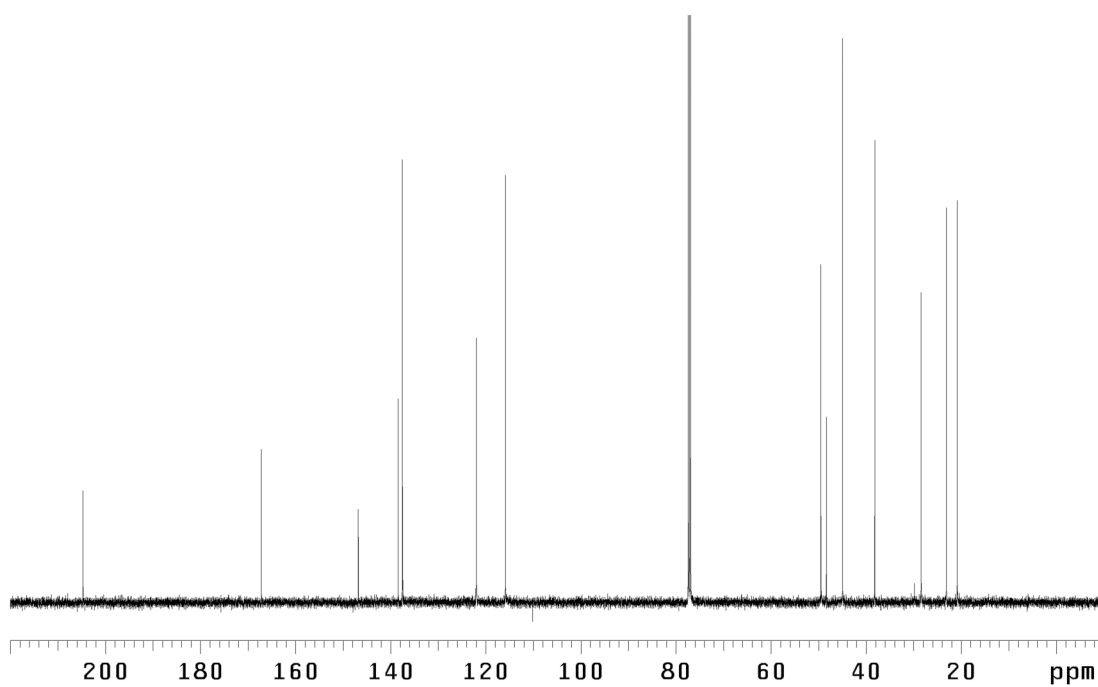
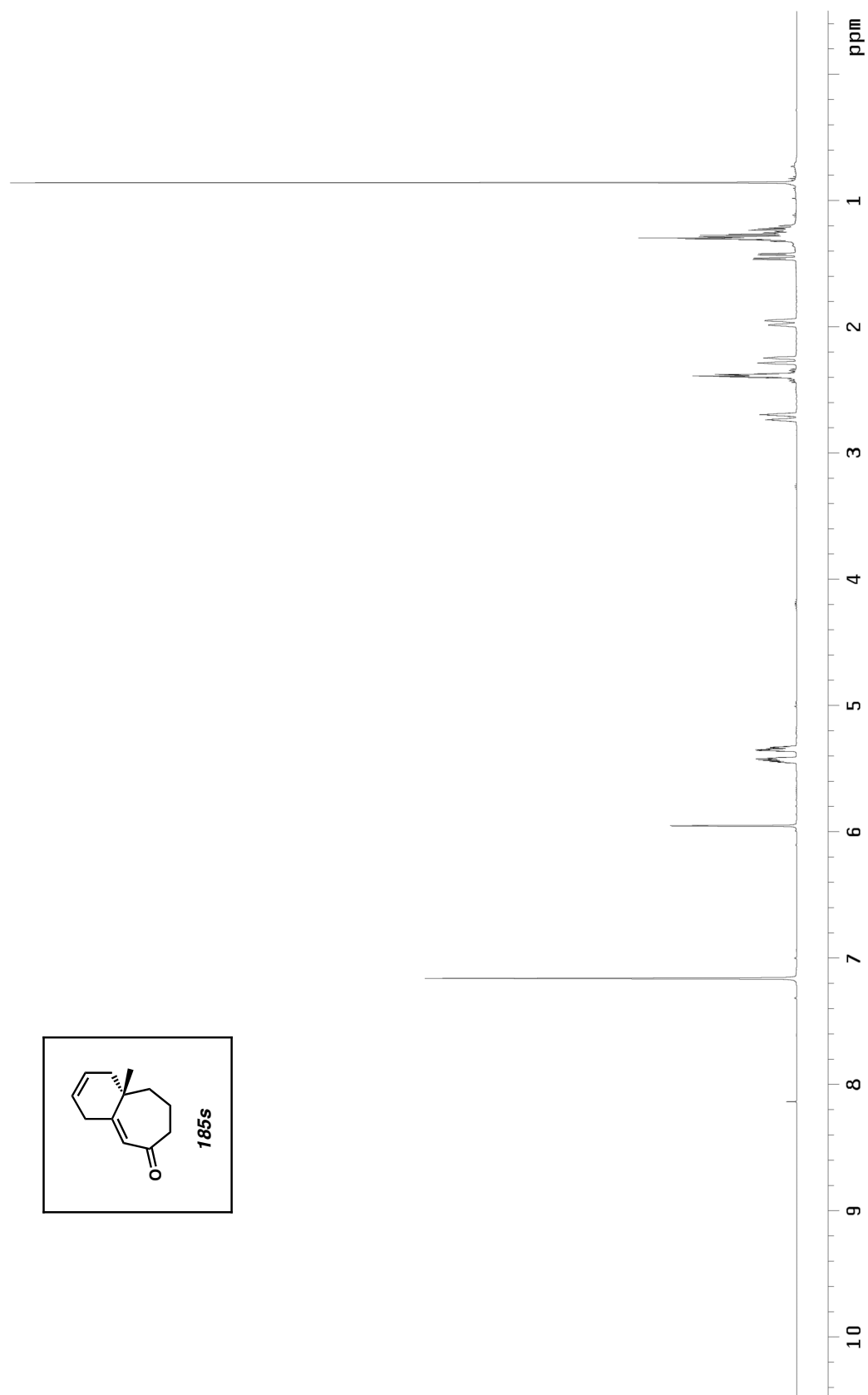


Figure A1.325. ¹³C NMR (125 MHz, CDCl₃) of compound **185y**.

Figure A1.326. ^1H NMR (500 MHz, C_6D_6) of compound **185s**.

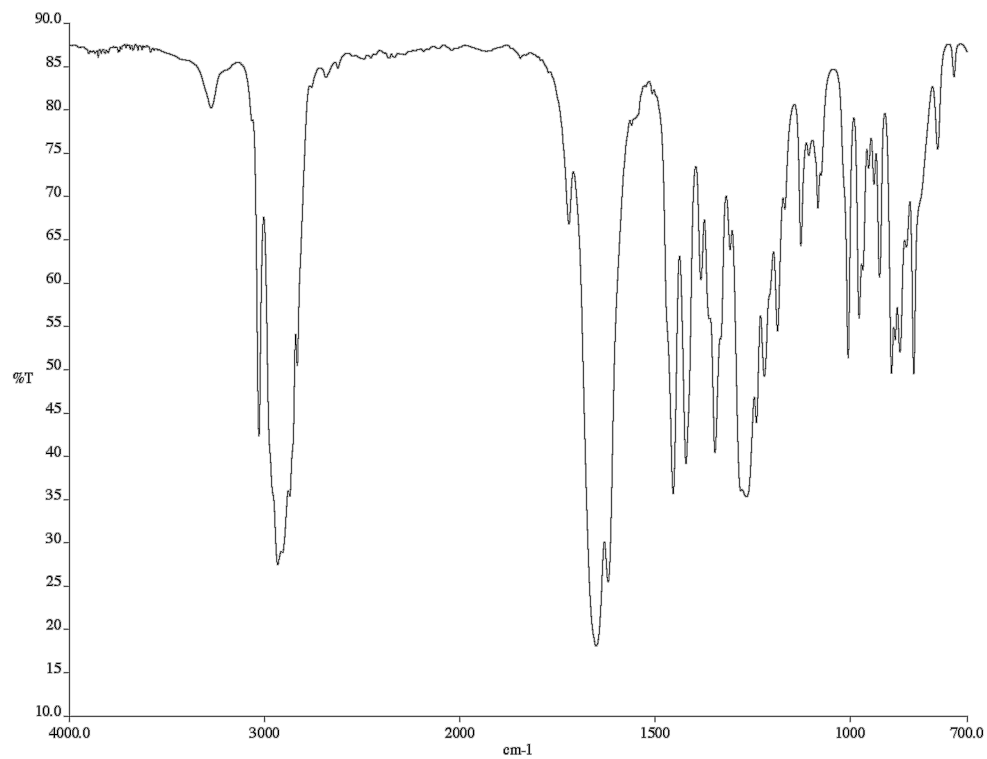


Figure A1.327. Infrared spectrum (thin film/NaCl) of compound **185s**.

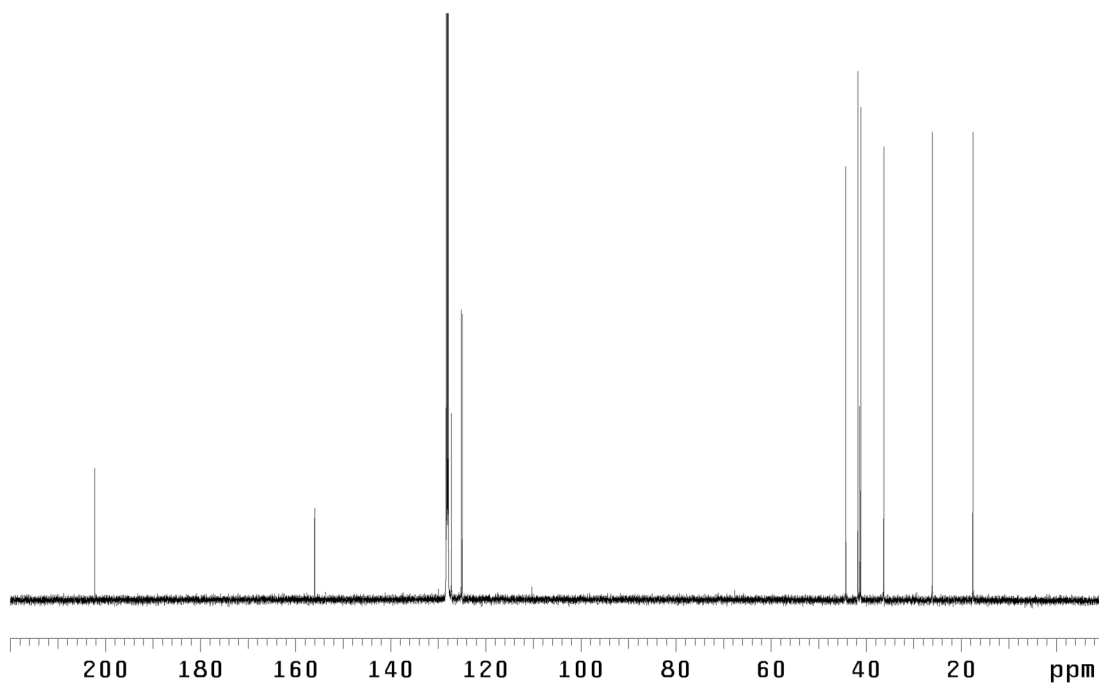
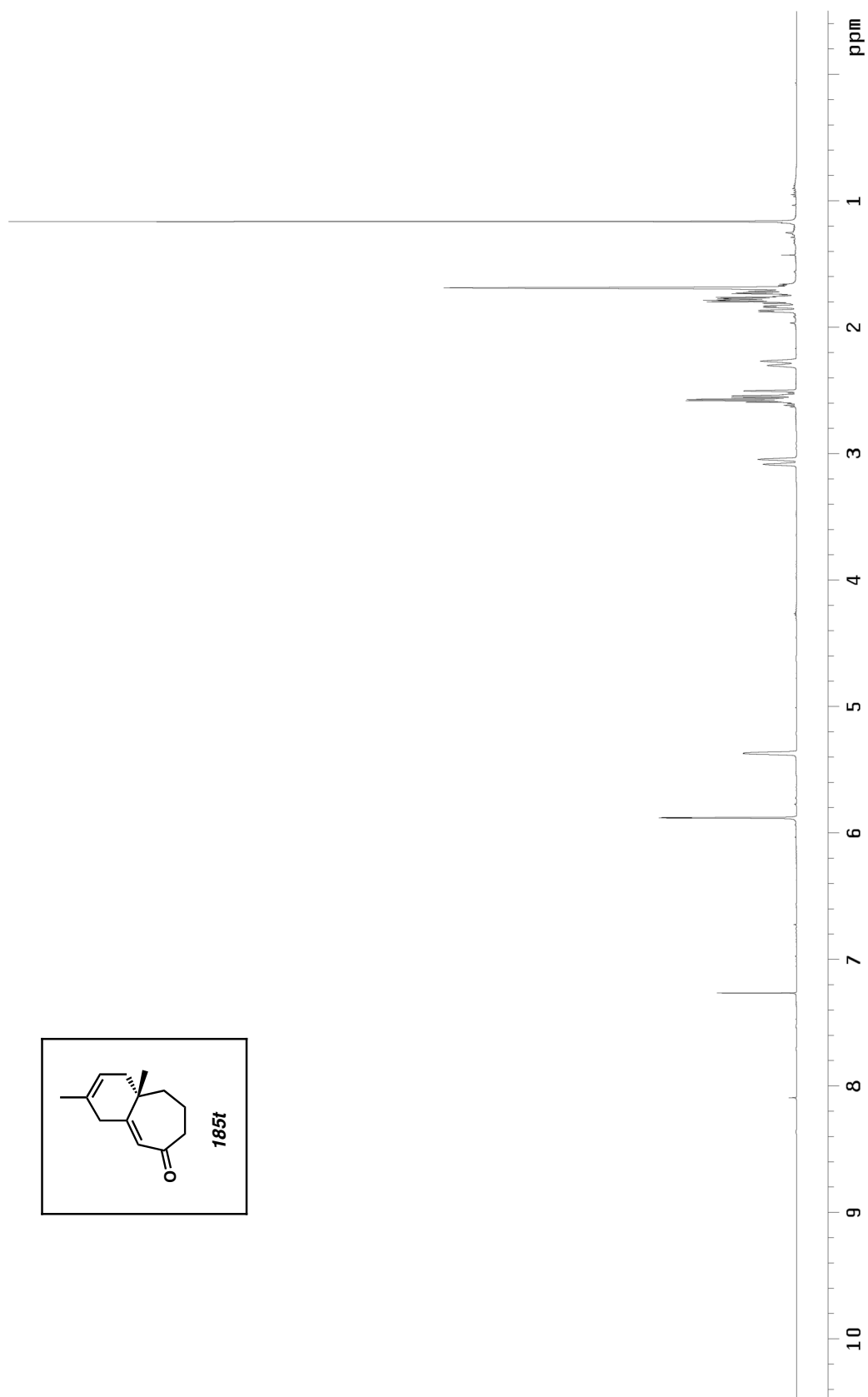


Figure A1.328. ¹³C NMR (125 MHz, C₆D₆) of compound **185s**.

Figure A1.329. ^1H NMR (500 MHz, CDCl_3) of compound **185t**.

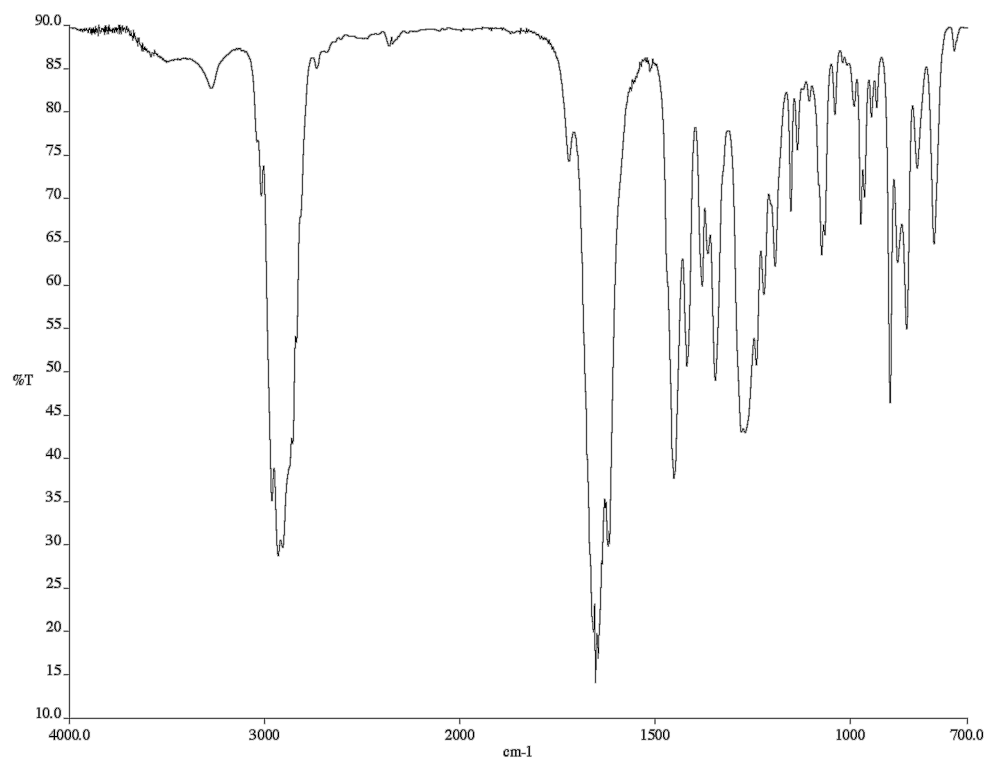


Figure A1.330. Infrared spectrum (thin film/NaCl) of compound **185t**.

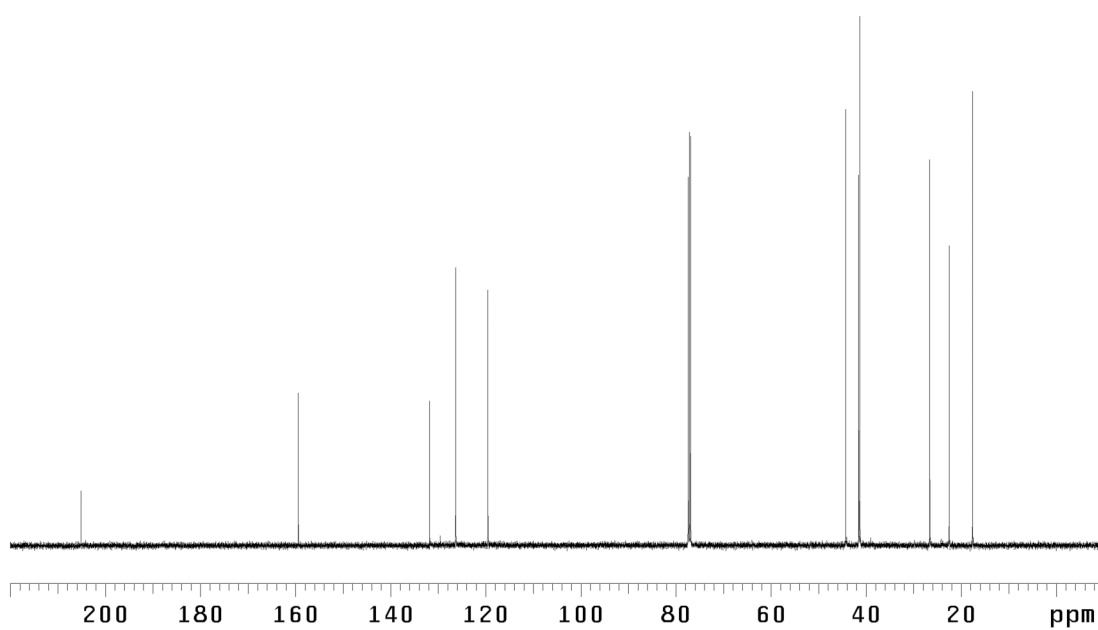


Figure A1.331. ¹³C NMR (125 MHz, CDCl₃) of compound **185t**.

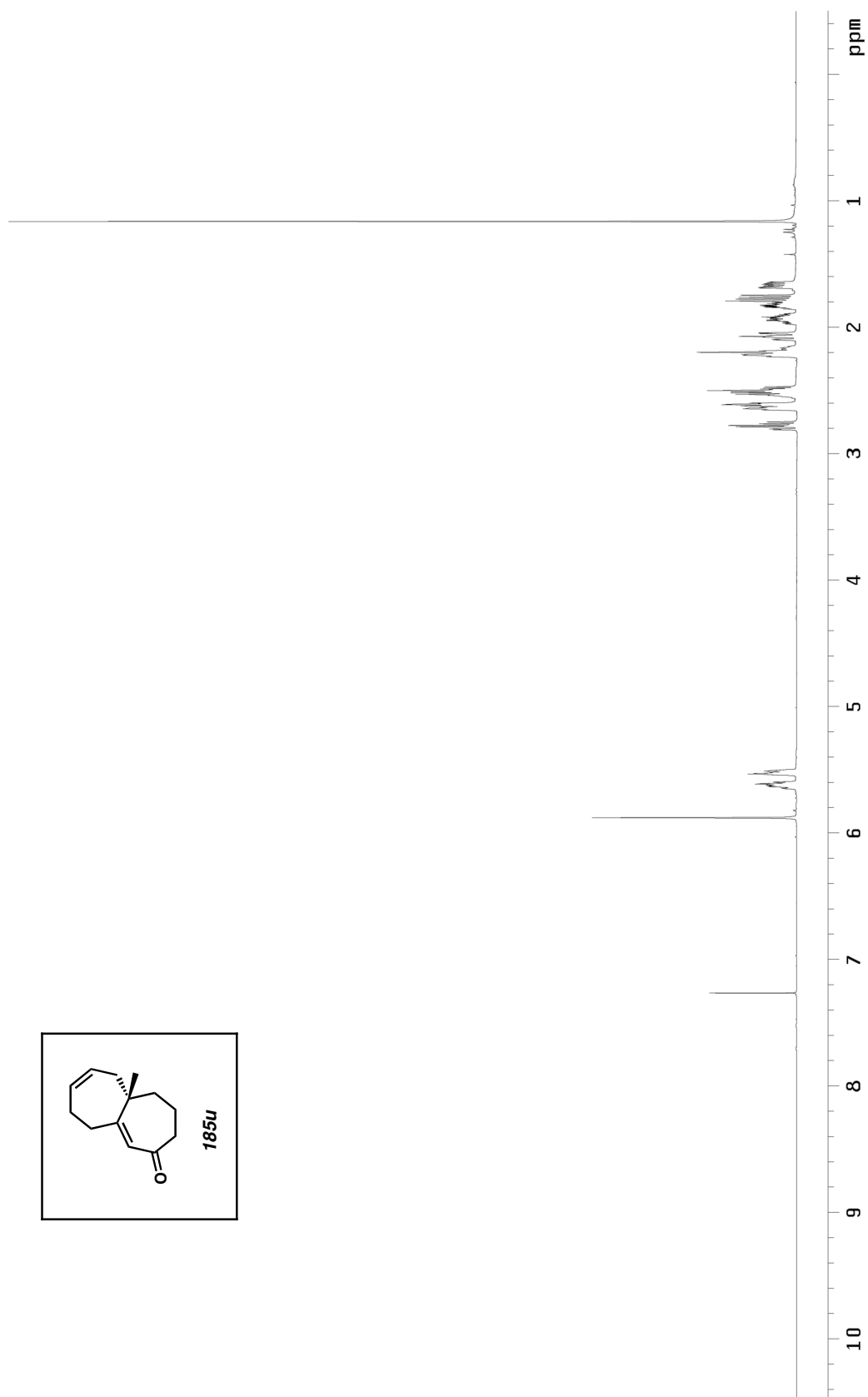


Figure A1.332. ^1H NMR (500 MHz, CDCl_3) of compound **185u**.

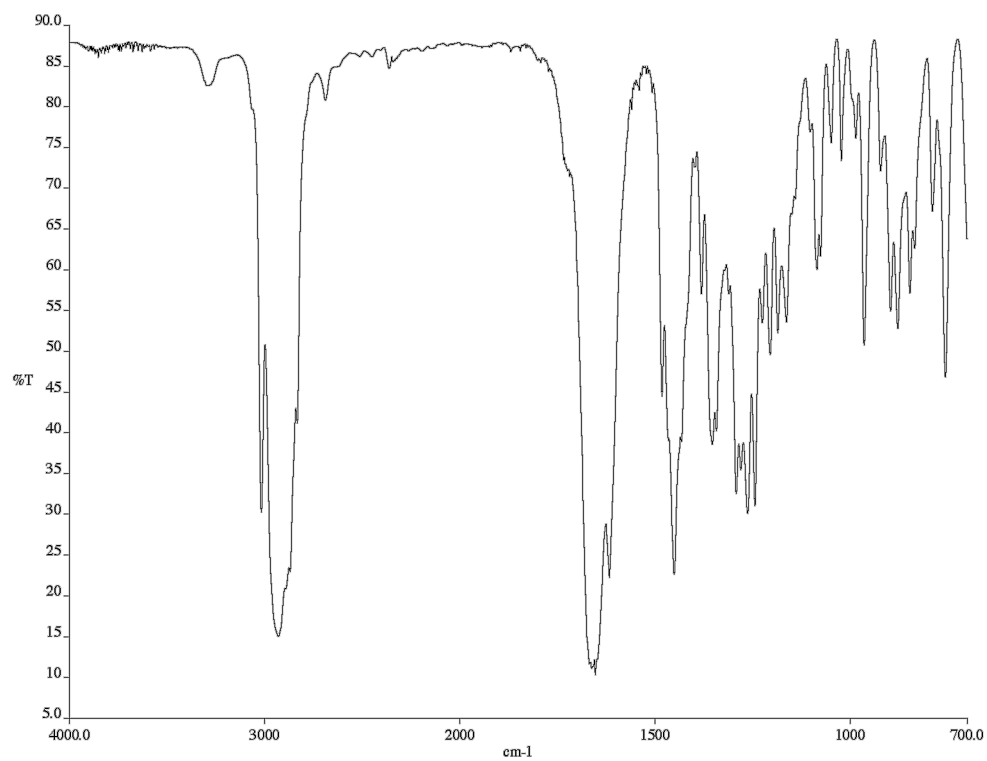


Figure A1.333. Infrared spectrum (thin film/NaCl) of compound **185u**.

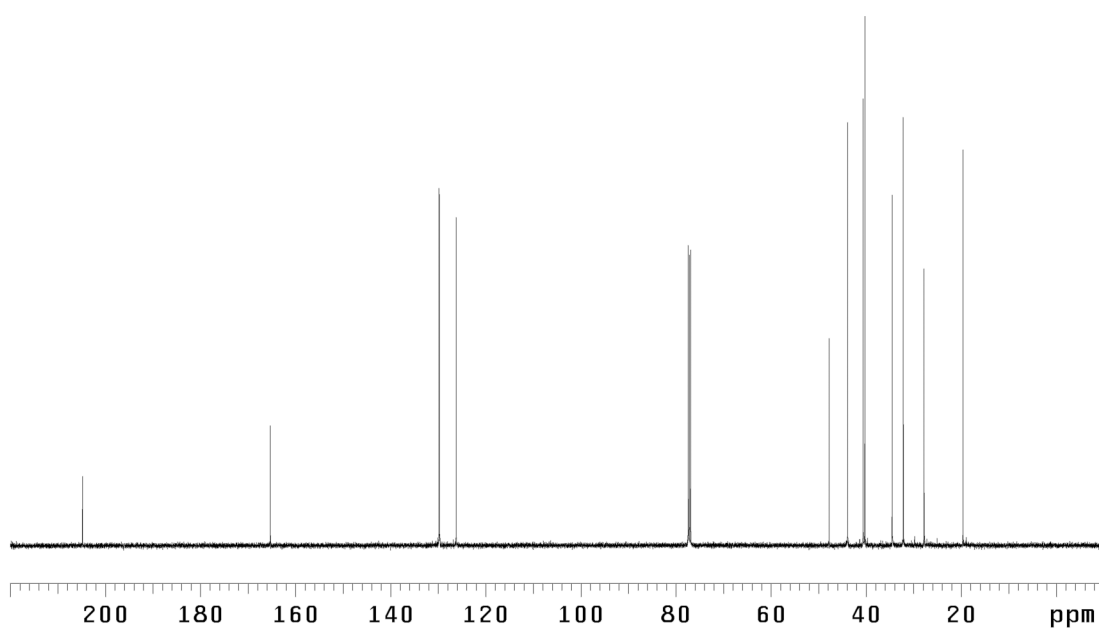


Figure A1.334. ¹³C NMR (125 MHz, CDCl₃) of compound **185u**.

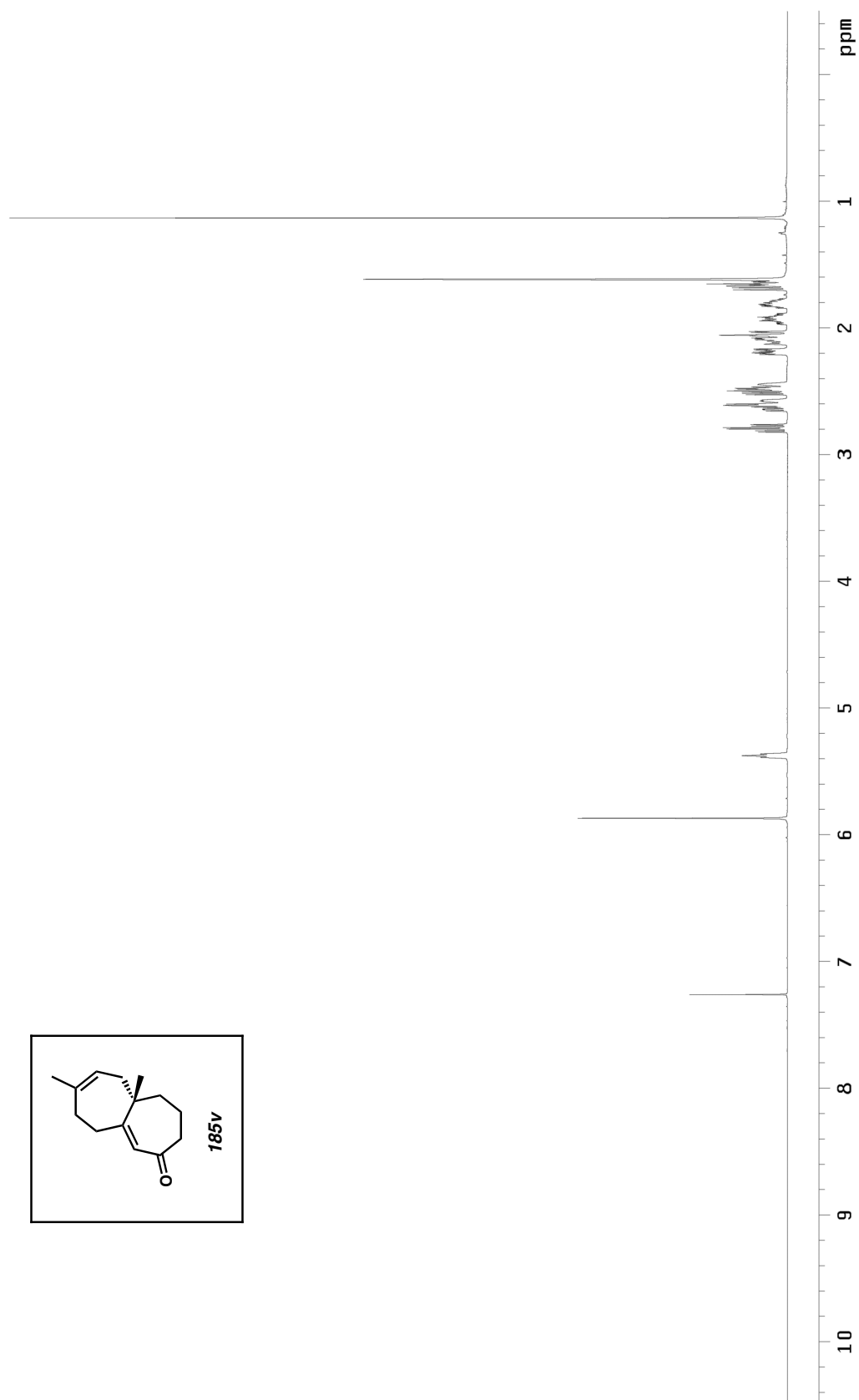


Figure A1.335. ¹H NMR (500 MHz, CDCl₃) of compound **185v**.

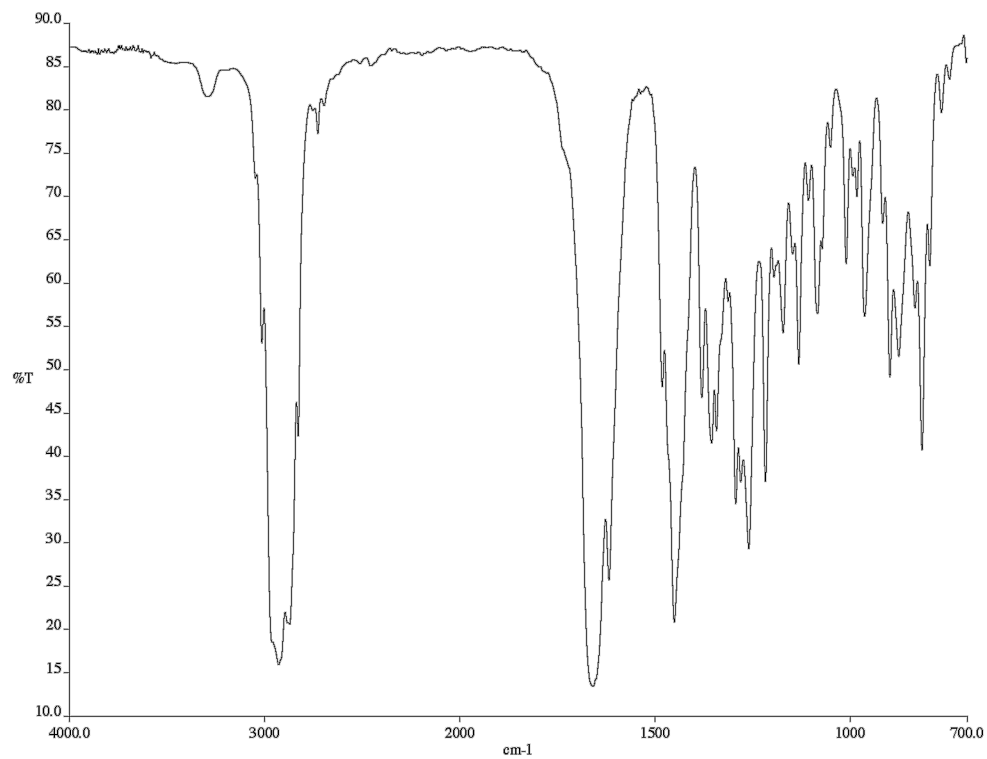


Figure A1.336. Infrared spectrum (thin film/NaCl) of compound **185v**.

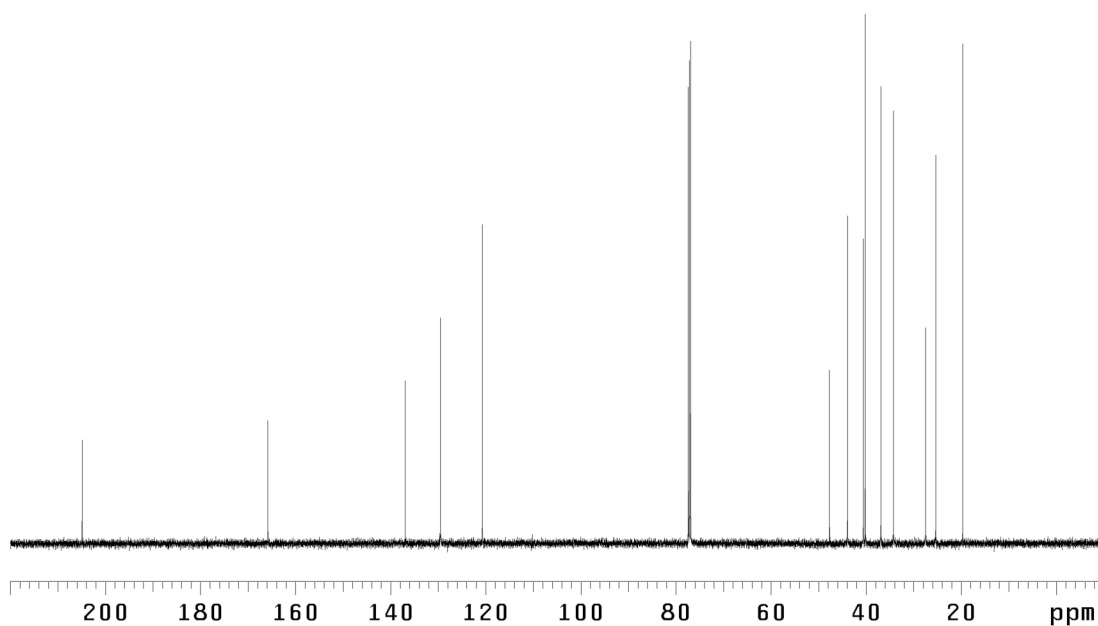


Figure A1.337. ¹³C NMR (125 MHz, CDCl₃) of compound **185v**.

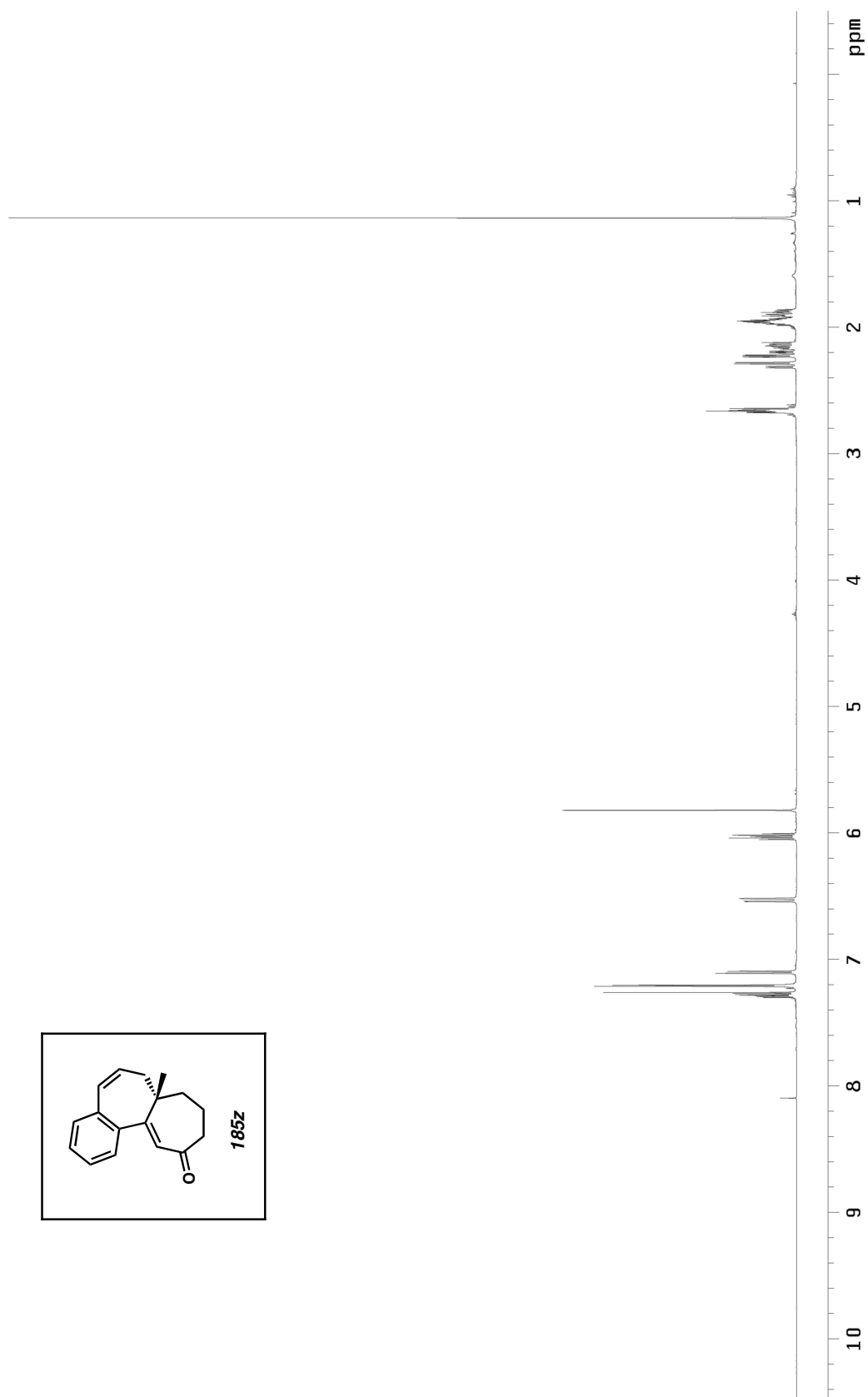


Figure A1.338. ^1H NMR (500 MHz, CDCl_3) of compound **185z**.

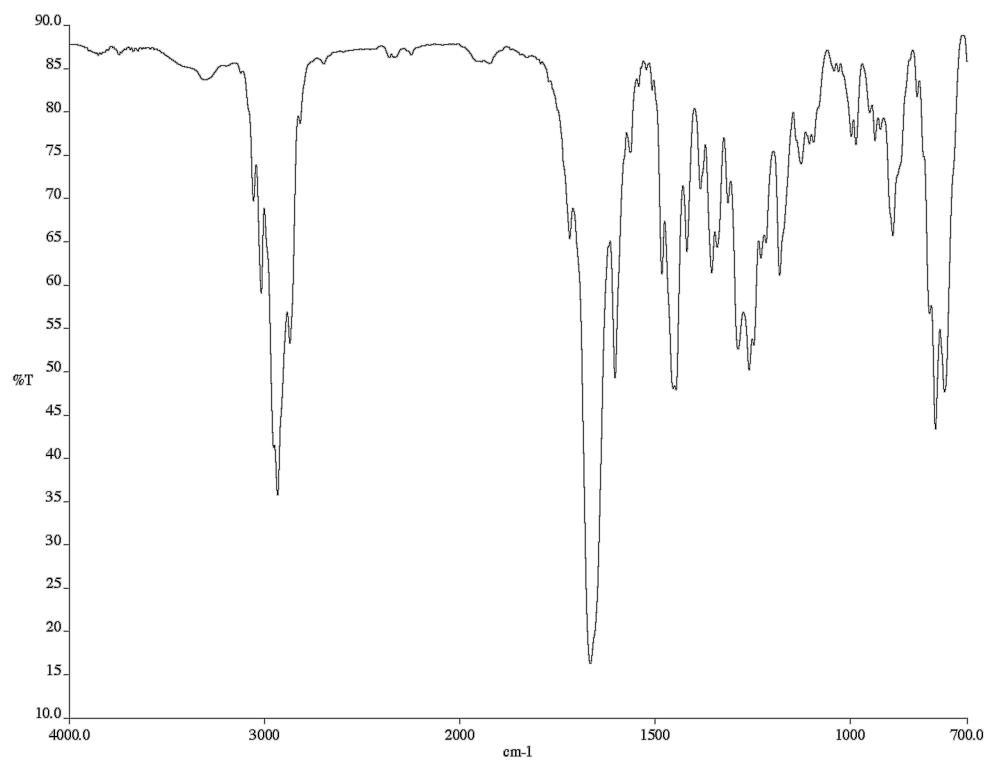


Figure A1.339. Infrared spectrum (thin film/NaCl) of compound **185z**.

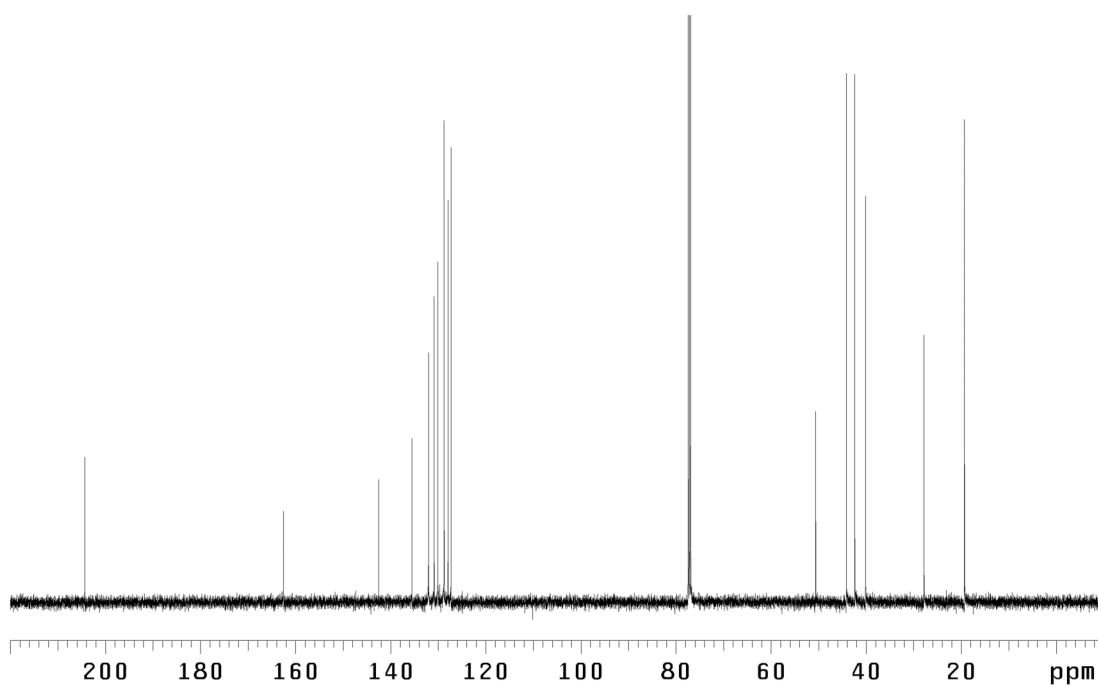


Figure A1.340. ¹³C NMR (125 MHz, CDCl₃) of compound **185z**.

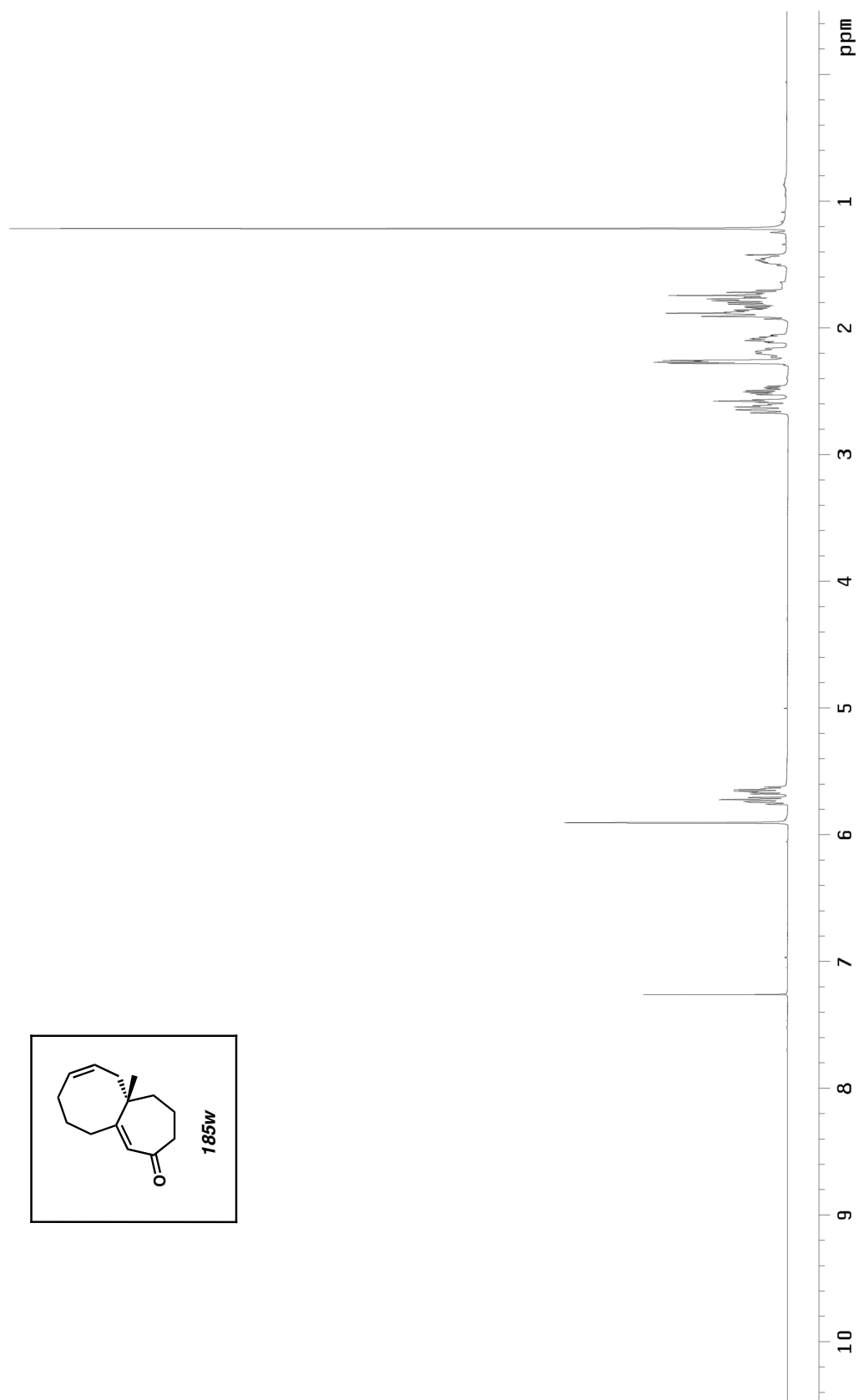


Figure A1.341. ¹H NMR (500 MHz, CDCl₃) of compound **185w**.

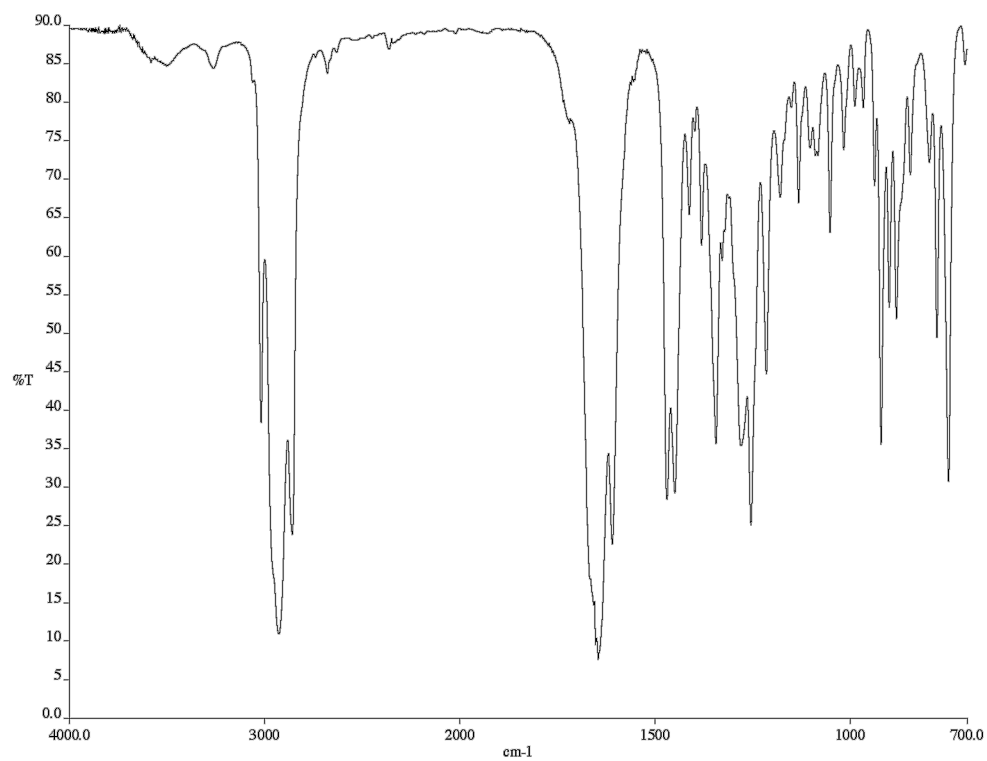


Figure A1.342. Infrared spectrum (thin film/NaCl) of compound **185w**.

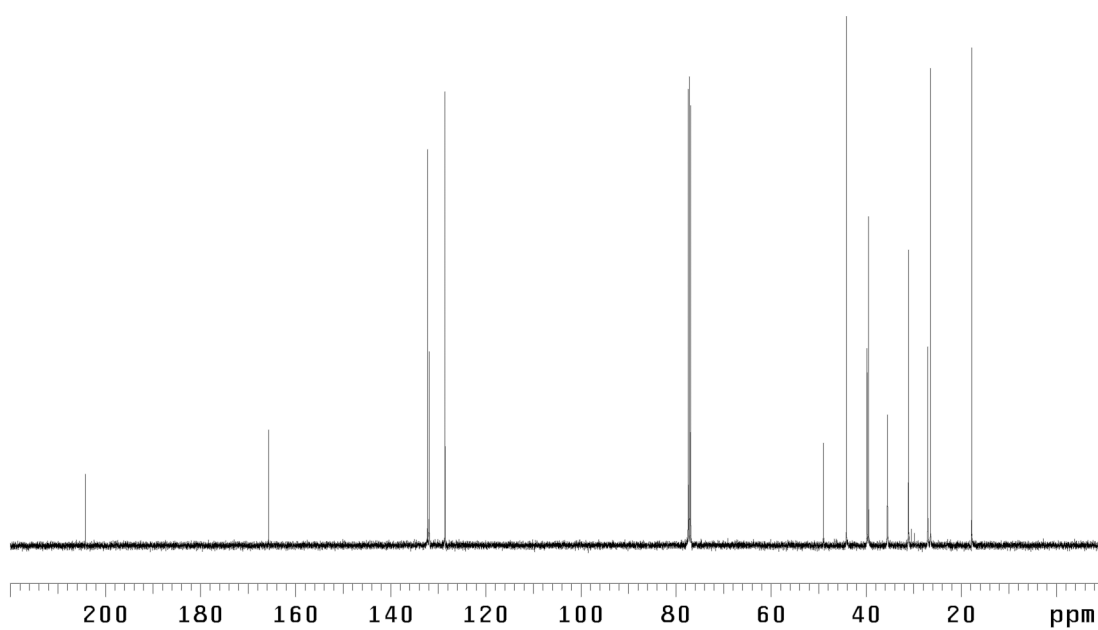


Figure A1.343. ¹³C NMR (125 MHz, CDCl₃) of compound **185w**.

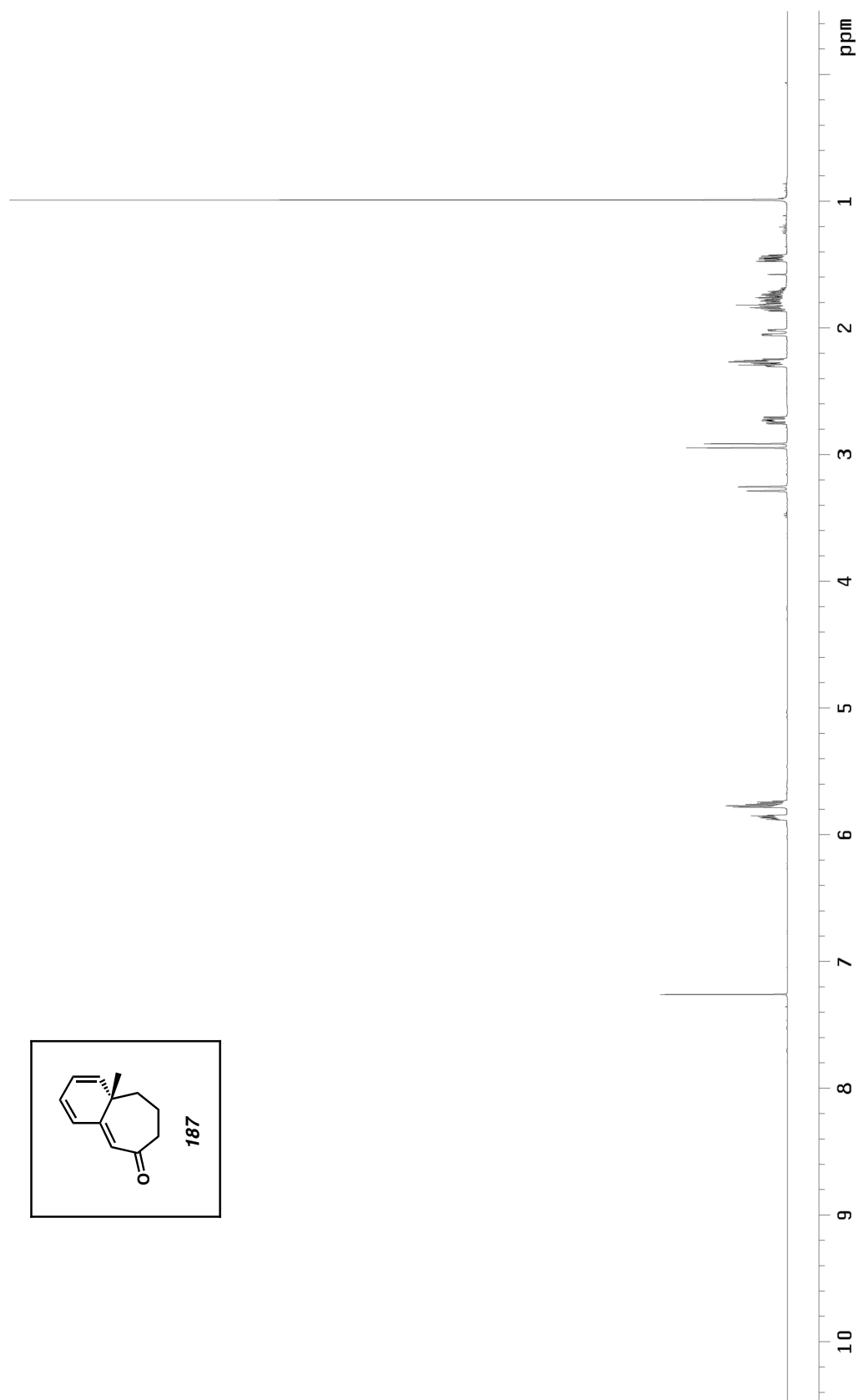


Figure A1.344. ^1H NMR (500 MHz, CDCl_3) of compound **187**.

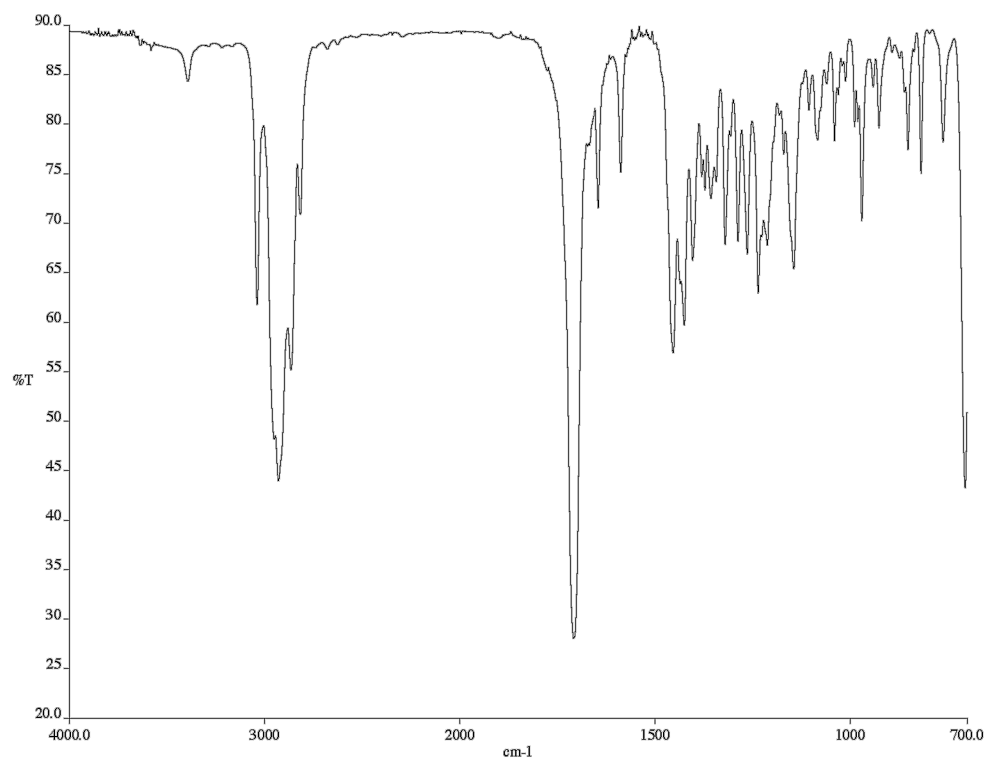


Figure A1.345. Infrared spectrum (thin film/NaCl) of compound **187**.

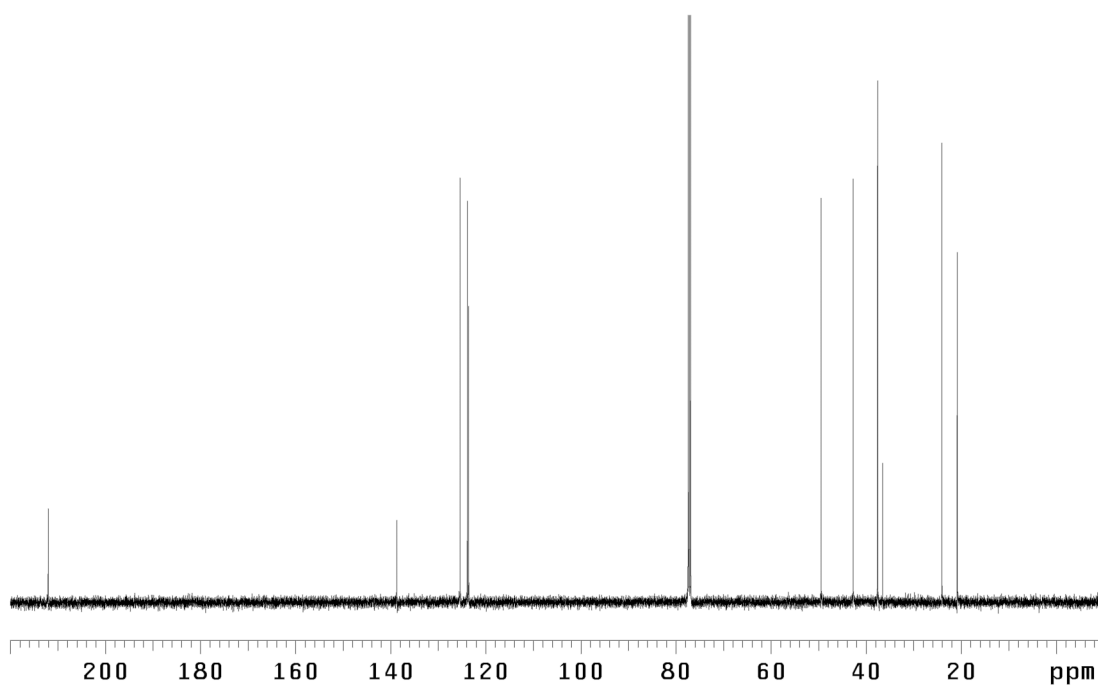


Figure A1.346. ¹³C NMR (125 MHz, CDCl₃) of compound **187**.

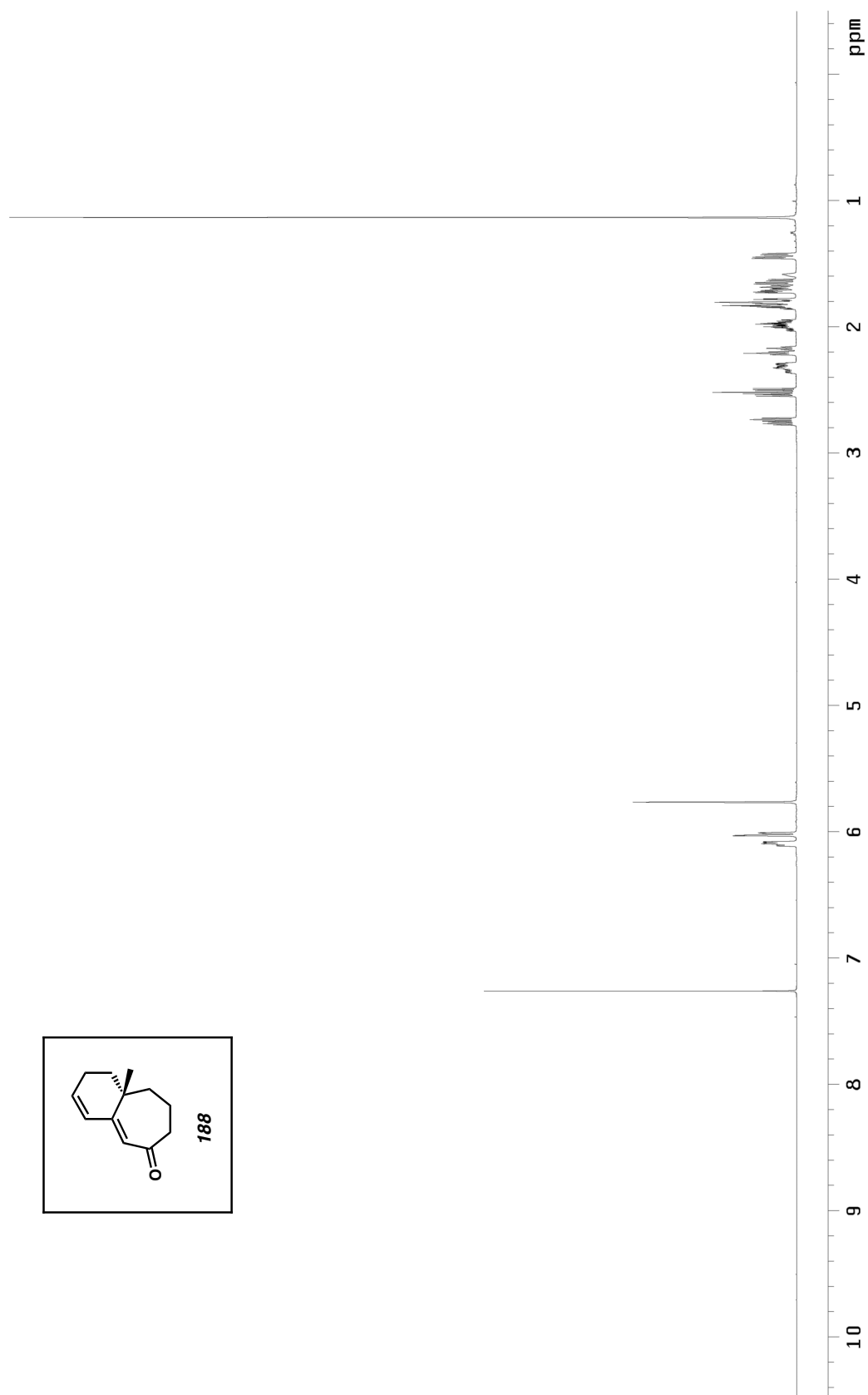


Figure A1.347. ^1H NMR (500 MHz, CDCl_3) of compound **188**.

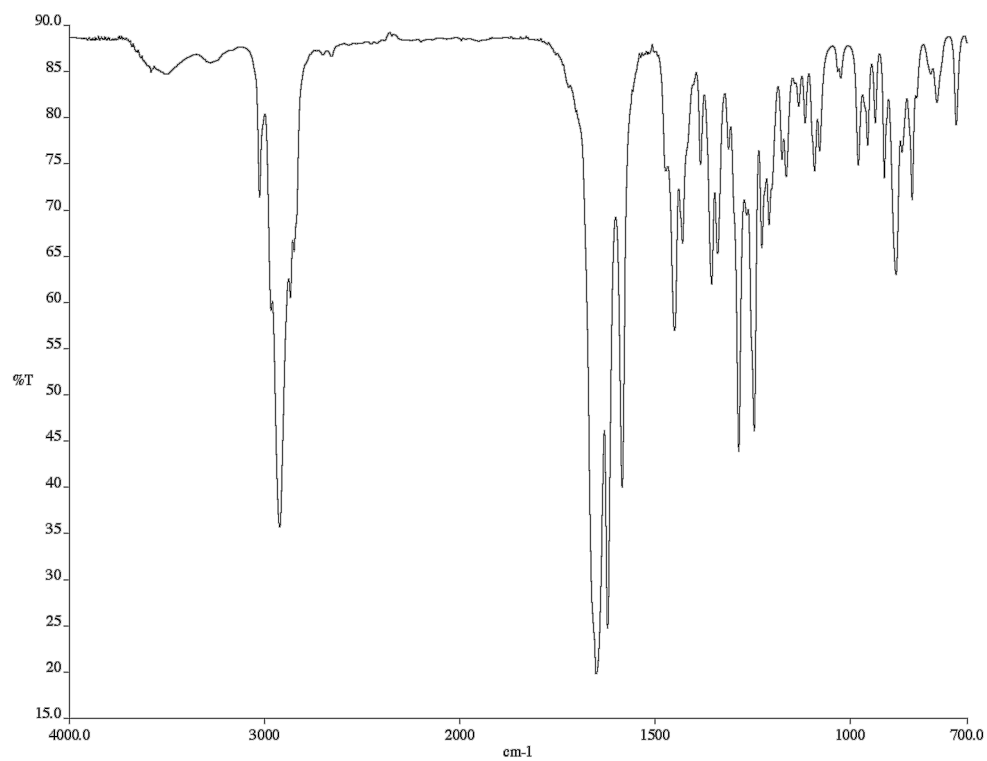


Figure A1.348. Infrared spectrum (thin film/NaCl) of compound **188**.

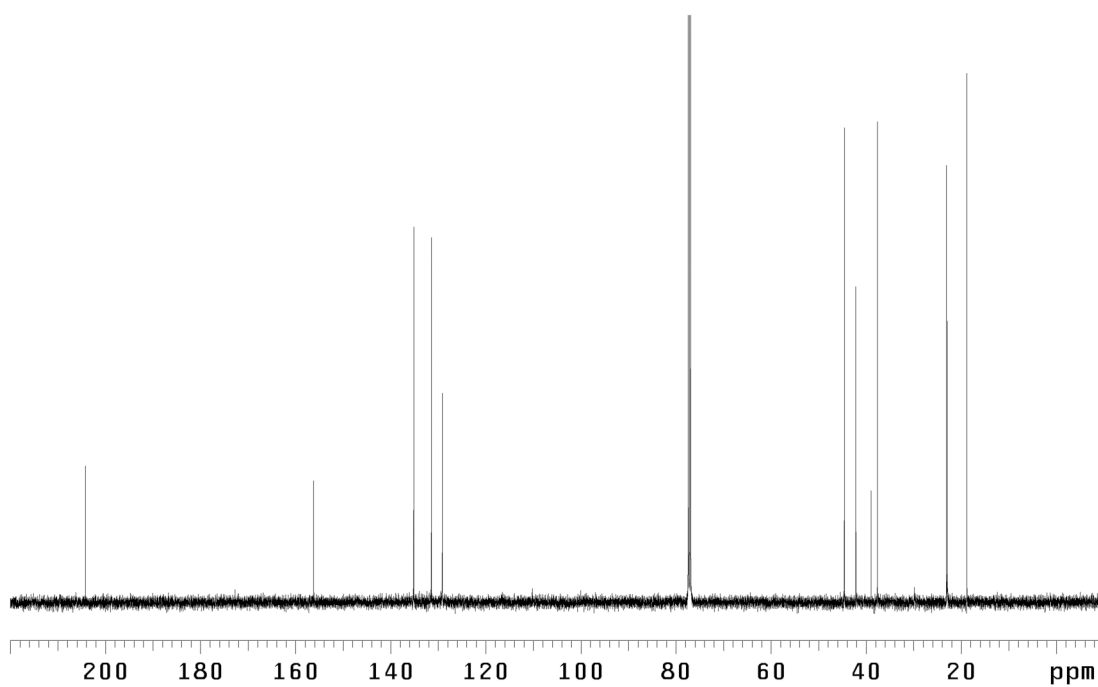


Figure A1.349. ¹³C NMR (125 MHz, CDCl₃) of compound **188**.

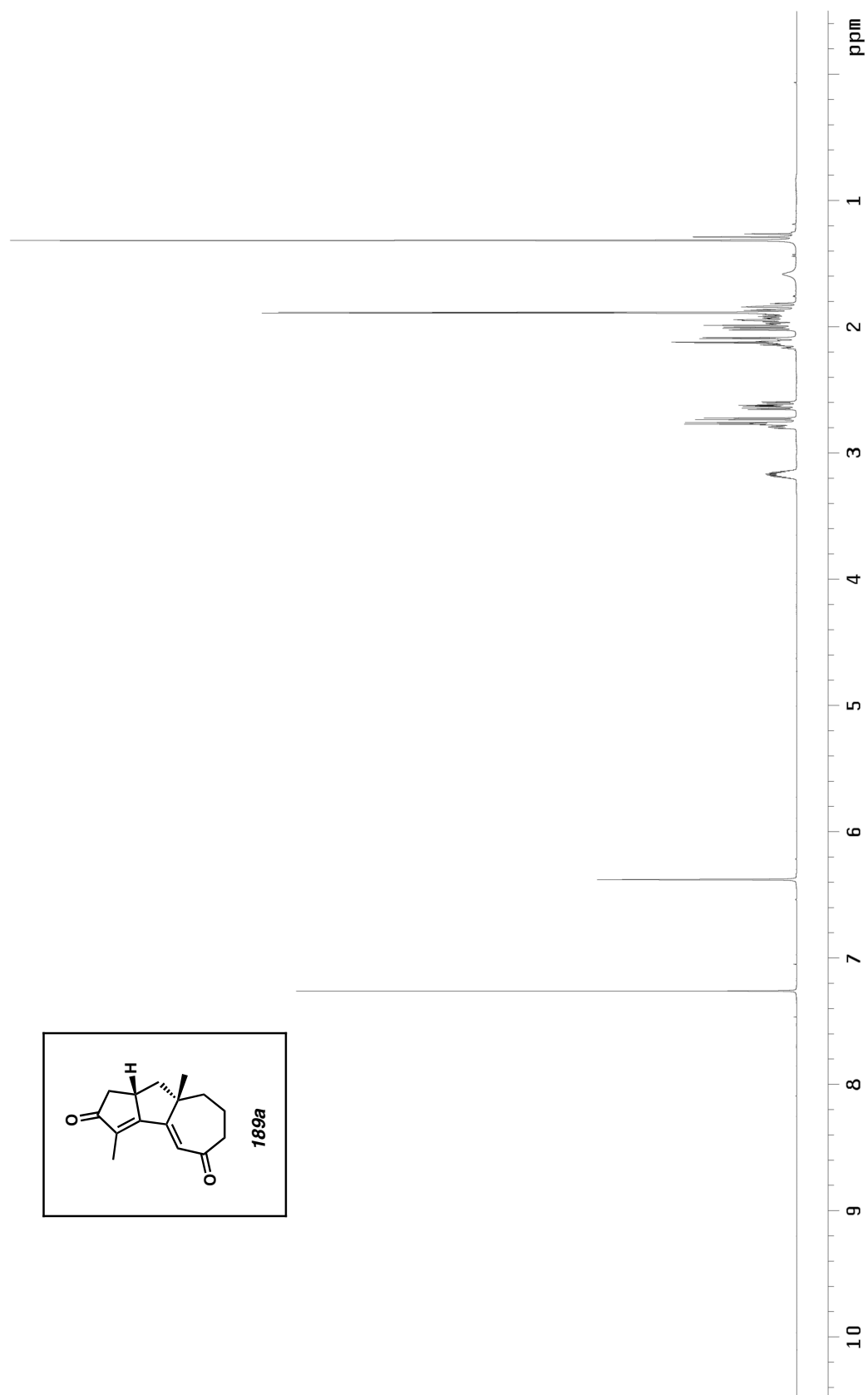


Figure A1.350. ^1H NMR (500 MHz, CDCl_3) of compound **189a**.

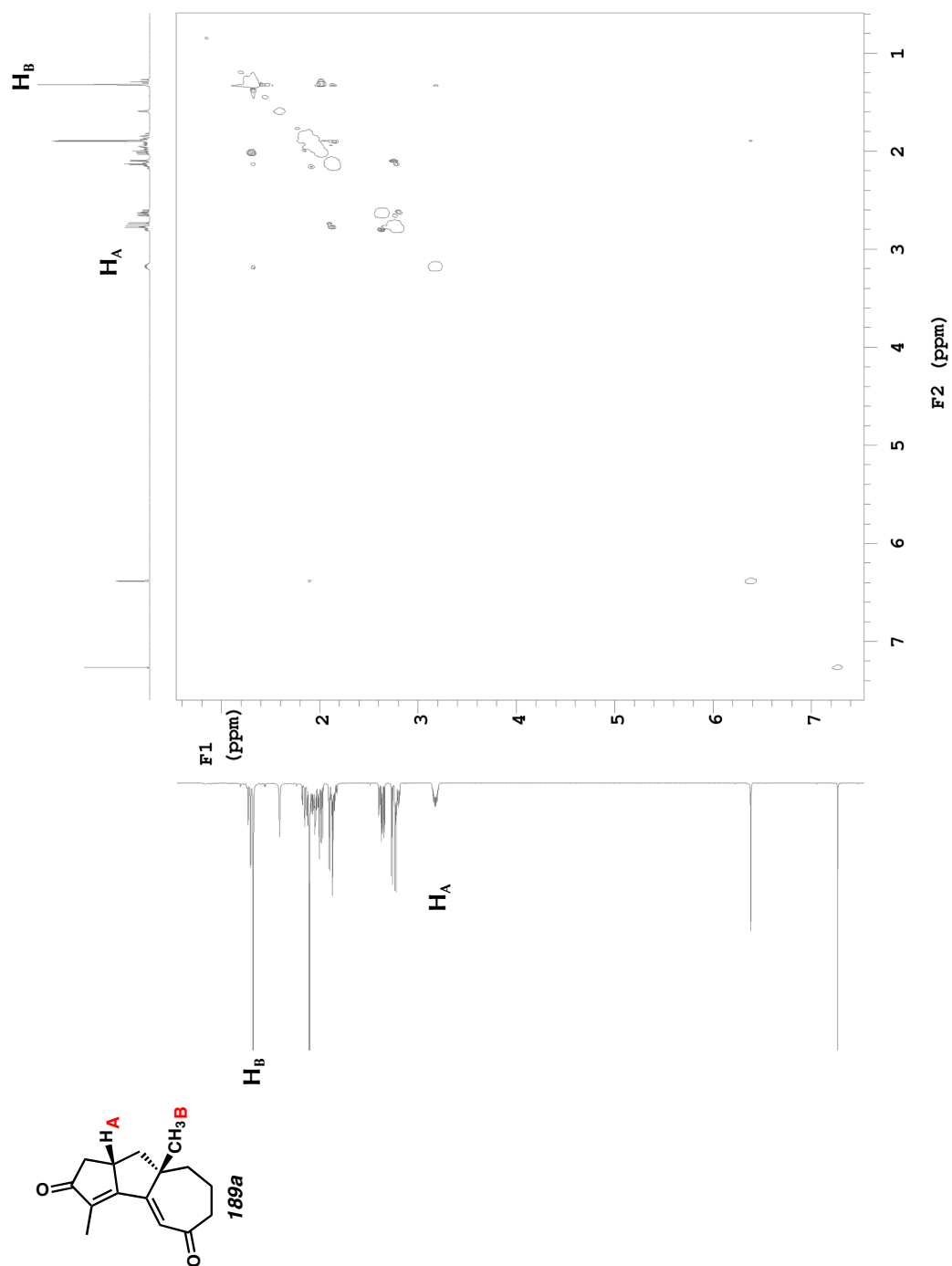


Figure A1.351. NOESY (500 MHz, CDCl₃) of compound **189a**.

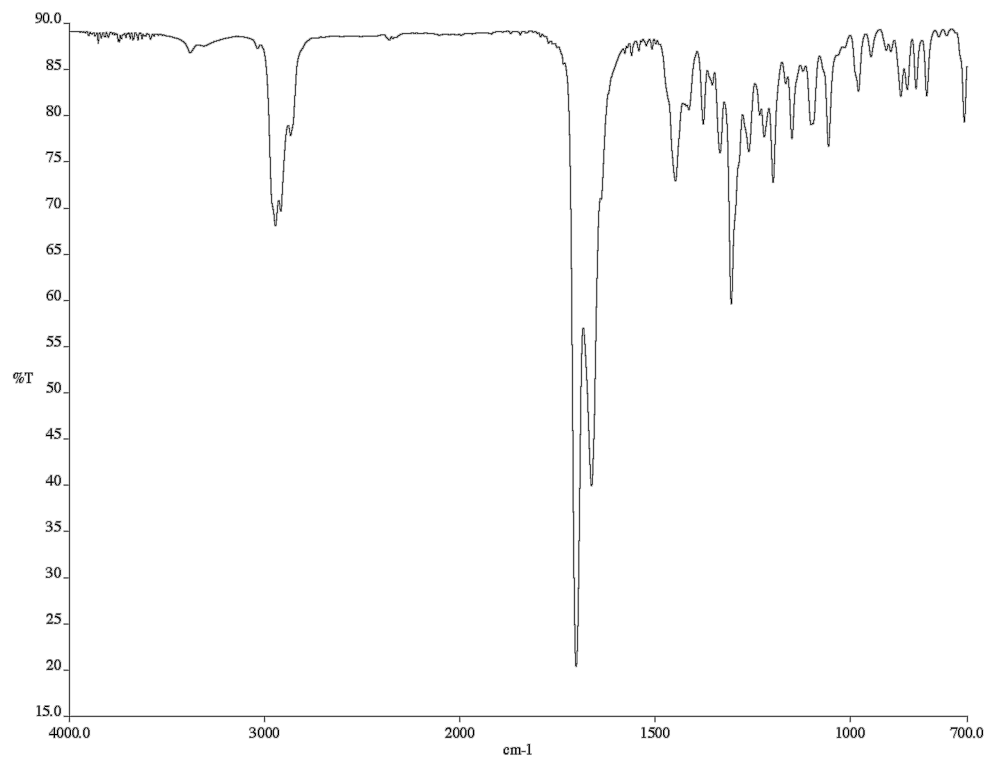


Figure A1.352. Infrared spectrum (thin film/NaCl) of compound **189a**.

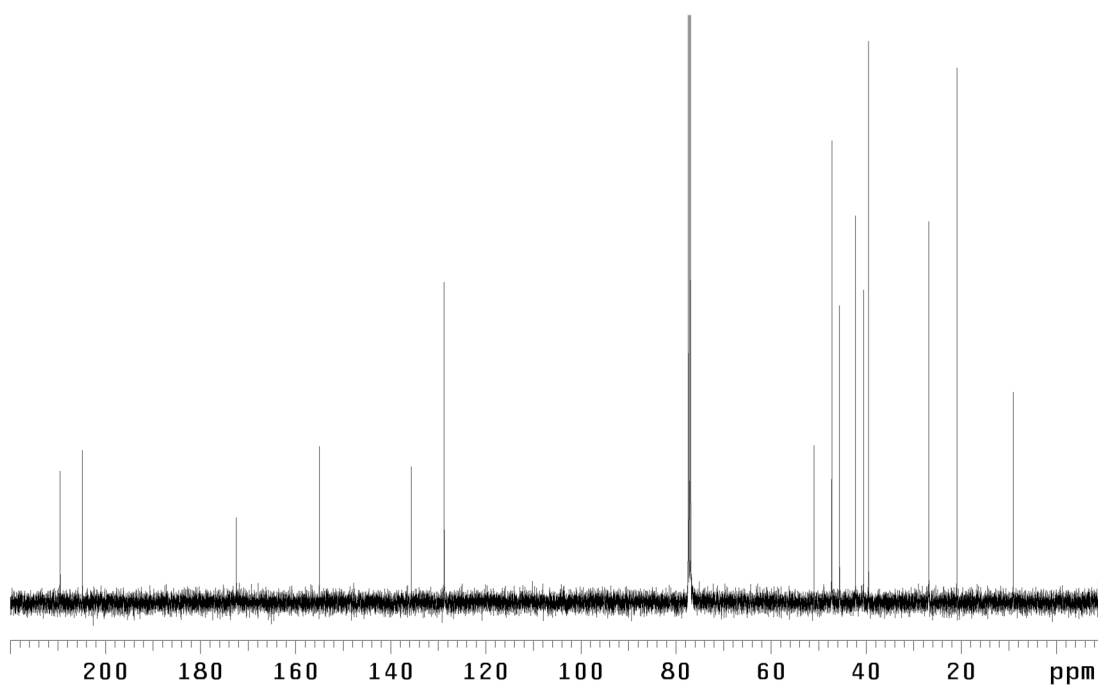


Figure A1.353. ¹³C NMR (125 MHz, CDCl₃) of compound **189a**.

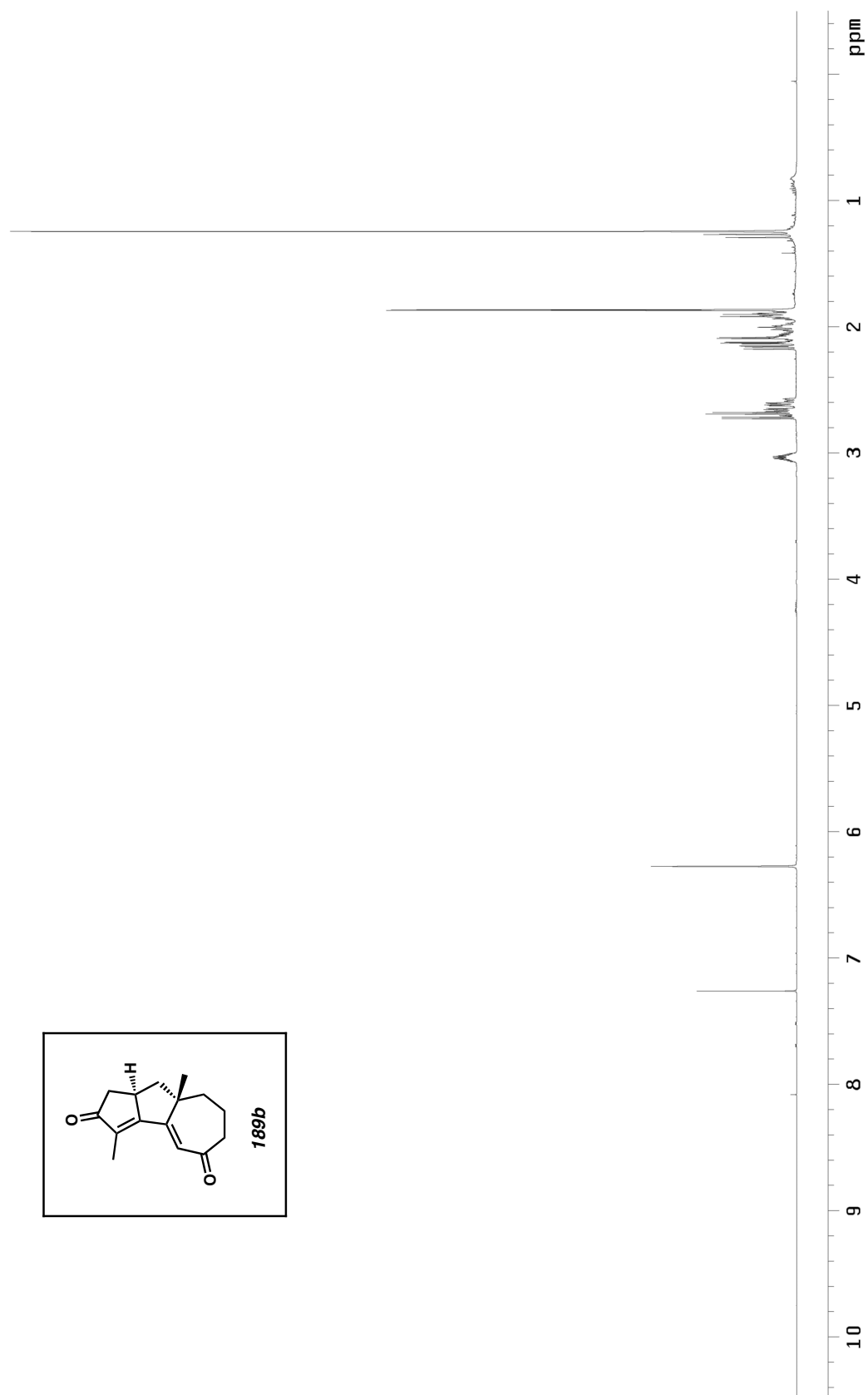


Figure A1.354. ^1H NMR (500 MHz, CDCl_3) of compound **189b**.

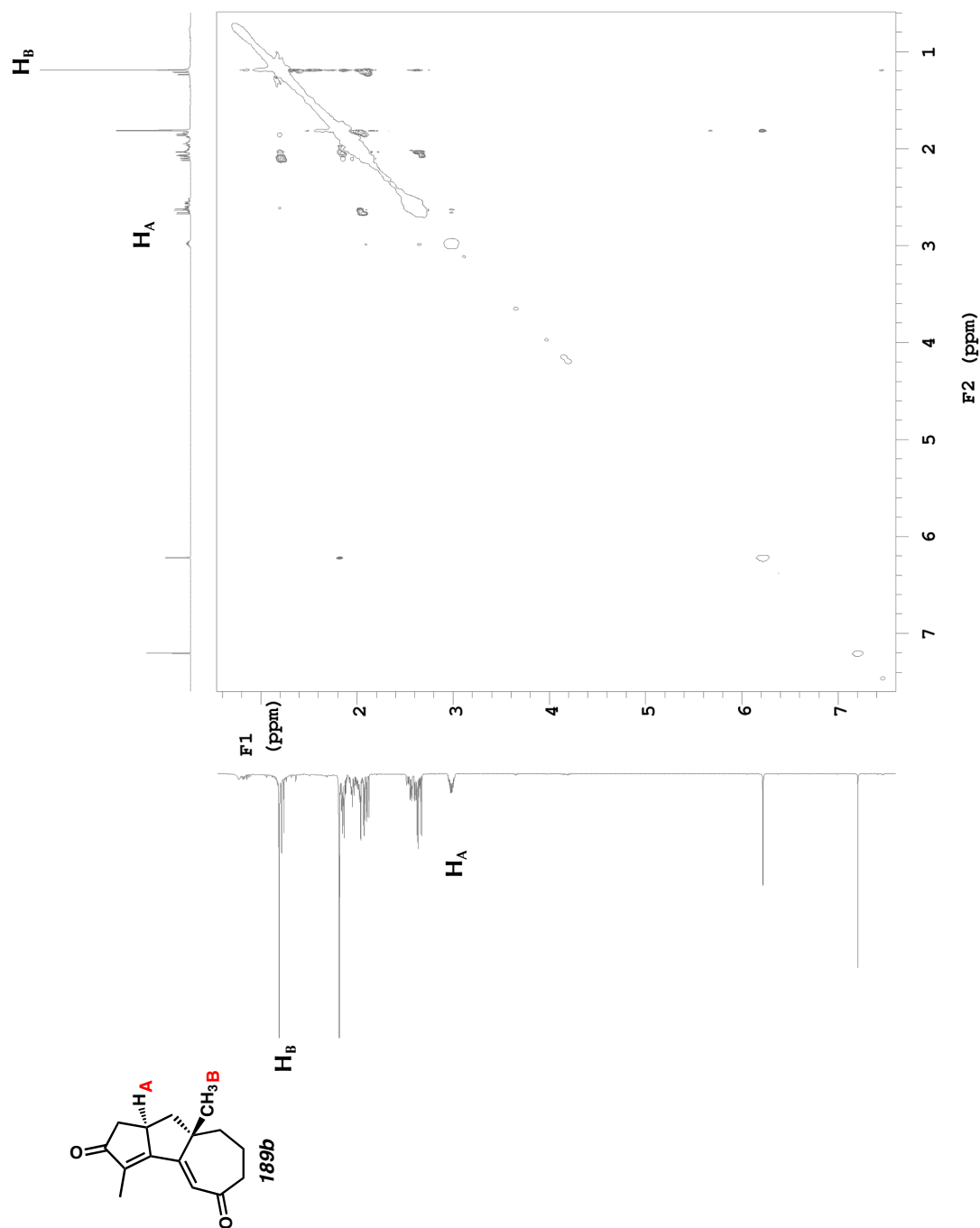


Figure A1.355. NOESY (500 MHz, CDCl₃) of compound **189b**.

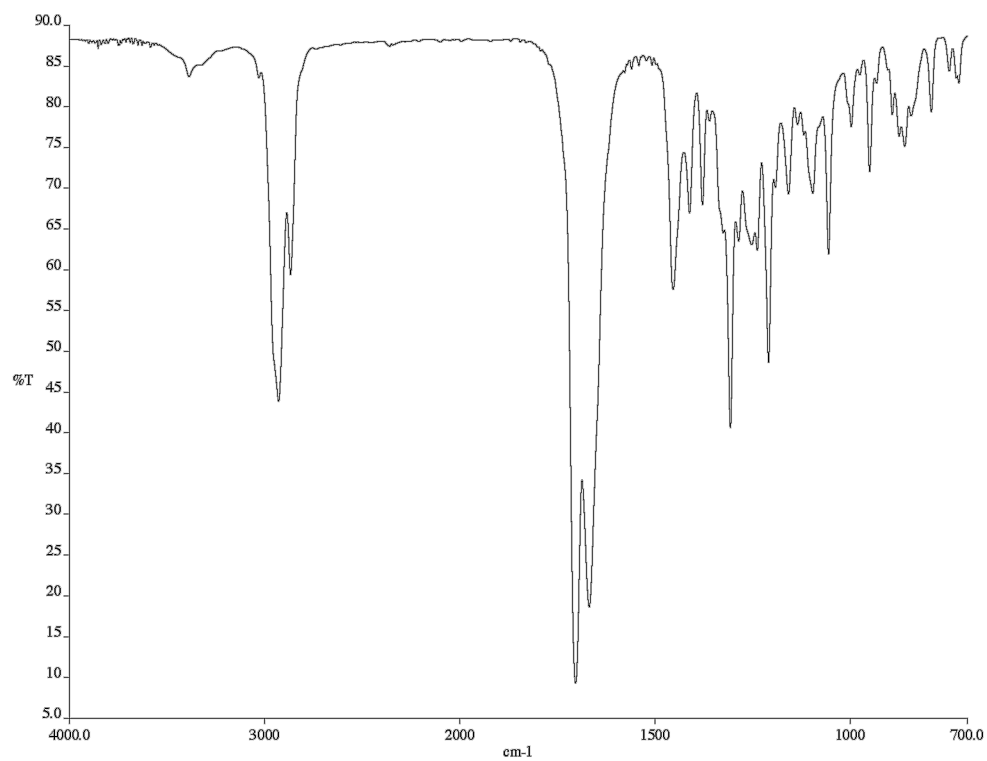


Figure A1.356. Infrared spectrum (thin film/NaCl) of compound **189b**.

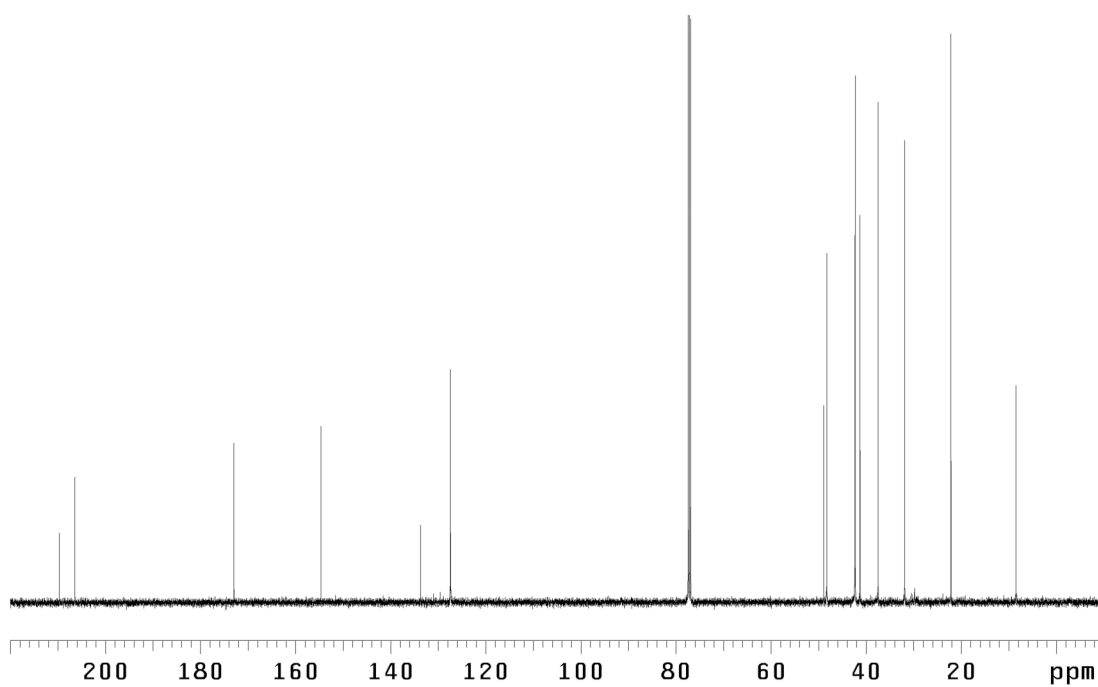


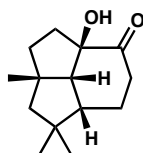
Figure A1.357. ¹³C NMR (125 MHz, CDCl₃) of compound **189b**.

APPENDIX 2

X-Ray Crystallography Reports Relevant to Chapter 2:

Catalytic Asymmetric Synthesis of Cyclopentanoid and Cycloheptanoid

Core Structures Using Pd-Catalyzed Asymmetric Alkylation

A2.1 CRYSTAL STRUCTURE ANALYSIS OF 164Compound **353**

(AYH02) (CCDC 889570)

Contents

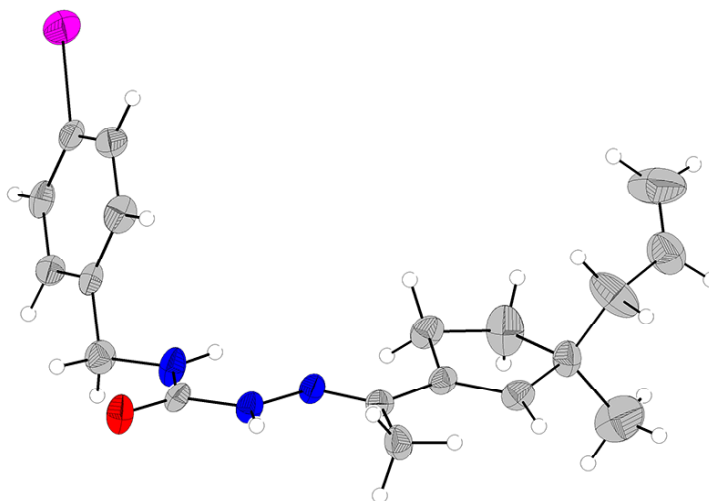
Table A2.1. Crystal data

Table A2.2. Atomic coordinates

Table A2.3. Full bond distances and angles

Table A2.4. Anisotropic displacement parameters

Table A2.5. Hydrogen bond distances and angles

*Figure A2.1. Semicarbazone **164** is shown with 50% probability ellipsoids.*

CCDC 686849 (**164**) contains the supplementary crystallographic data for this appendix. These data can be obtained free of charge from The Cambridge Crystallographic Data Centre via www.ccdc.cam.ac.uk/data_request/cif.

Table A2.1. Crystal data and structure refinement for semicarbazone **164** (CCDC 686849)

Empirical formula	C ₁₉ H ₂₄ N ₃ OI
Formula weight	437.31
Crystallization solvent	Dichloromethane/pentane
Crystal habit	Needle
Crystal size	0.28 x 0.11 x 0.07 mm ³
Crystal color	Colorless

Data Collection

Type of diffractometer	Bruker KAPPA APEX II
Wavelength	0.71073 Å MoK α
Data collection temperature	100(2) K
θ range for 9911 reflections used in lattice determination	2.57 to 28.78°
Unit cell dimensions	a = 17.160(4) Å b = 5.5921(14) Å c = 19.984(5) Å
Volume	1917.6(8) Å ³
Z	4
Crystal system	Monoclinic
Space group	P2 ₁
Density (calculated)	1.515 Mg/m ³
F(000)	880
Data collection program	Bruker APEX2 v2.1-0
θ range for data collection	1.55 to 29.84°
Completeness to $\theta = 29.84^\circ$	88.9 %
Index ranges	$-23 \leq h \leq 23, -7 \leq k \leq 7, -26 \leq l \leq 25$
Data collection scan type	ω scans; 16 settings
Data reduction program	Bruker SAINT-Plus v7.34A
Reflections collected	8962
Independent reflections	8962 [$R_{\text{int}} = 0.0000$]
Absorption coefficient	1.680 mm ⁻¹
Absorption correction	Semi-empirical from equivalents (TWNABS)
Max. and min. transmission	0.7460 and 0.5010

Structure solution and Refinement

Structure solution program	SHELXS-97 (Sheldrick, 2008)
Primary solution method	Direct methods
Secondary solution method	Difference Fourier map
Hydrogen placement	Geometric positions
Structure refinement program	SHELXL-97 (Sheldrick, 2008)
Refinement method	Full matrix least-squares on F^2
Data / restraints / parameters	8962 / 1 / 437
Treatment of hydrogen atoms	Riding
Goodness-of-fit on F^2	1.609
Final R indices [$I > 2\sigma(I)$, 7203 reflections]	$R1 = 0.0409$, $wR2 = 0.0481$
R indices (all data)	$R1 = 0.0619$, $wR2 = 0.0493$
Type of weighting scheme used	Sigma
Weighting scheme used	$w = 1/\sigma^2(F_o^2)$
Max shift/error	0.002
Average shift/error	0.000
Absolute structure determination	Anomalous differences
Absolute structure parameter	0.003(11)
Largest diff. peak and hole	0.807 and $-0.967 \text{ e.}\text{\AA}^{-3}$

Special Refinement Details

The structure was refined as a single component, although the crystals were twins, using an HKLF4 format reflection file prepared with TWINABS (see below). The two orientations were separated using CELL_NOW as follows.

Rotated from first domain by 178.9 degrees about reciprocal axis $-0.032 \ 1.000 \ 0.104$ and real axis $-0.001 \ 1.000 \ 0.007$. Twin law to convert hkl from first to this domain (SHELXL TWIN matrix):

$$\begin{pmatrix} -1.000 & -0.065 & 0.016 \\ -0.003 & 0.998 & 0.014 \\ -0.022 & 0.207 & -0.999 \end{pmatrix}$$

From Saint integration; Twin Law, Sample 1 of 1 transforms $h1.1(1) \rightarrow h1.2(2)$

-0.99897 -0.07583 0.01646
 -0.00750 0.99693 0.01538
 -0.02464 0.19596 -0.99910

Twinabs;

PART 1 - Refinement of parameters to model systematic errors

18757 data (4443 unique) involve domain 1 only, mean I/sigma 13.7

18551 data (4364 unique) involve domain 2 only, mean I/sigma 7.1

10342 data (4106 unique) involve 2 domains, mean I/sigma 19.2

HKLF 4 dataset constructed from all observations involving domains 1..2

8970 Corrected reflections written to file twin4.hkl

Reflections merged according to point-group 2

Minimum and maximum apparent transmission: 0.501007 0.745969

Additional spherical absorption correction applied with $\mu^*r = 0.2000$

Crystals were mounted on a glass fiber using Paratone oil then placed on the diffractometer under a nitrogen stream at 100 K.

Refinement of F^2 against ALL reflections. The weighted R-factor (wR) and goodness of fit (S) are based on F^2 , conventional R-factors (R) are based on F , with F set to zero for negative F^2 . The threshold expression of $F^2 > 2\sigma(F^2)$ is used only for calculating R-factors(gt) etc. and is not relevant to the choice of reflections for refinement. R-factors based on F^2 are statistically about twice as large as those based on F , and R-factors based on ALL data will be even larger.

All esds (except the esd in the dihedral angle between two l.s. planes) are estimated using the full covariance matrix. The cell esds are taken into account individually in the estimation of esds in distances, angles and torsion angles; correlations between esds in cell parameters are only used when they are defined by crystal symmetry. An approximate (isotropic) treatment of cell esds is used for estimating esds involving l.s. planes.

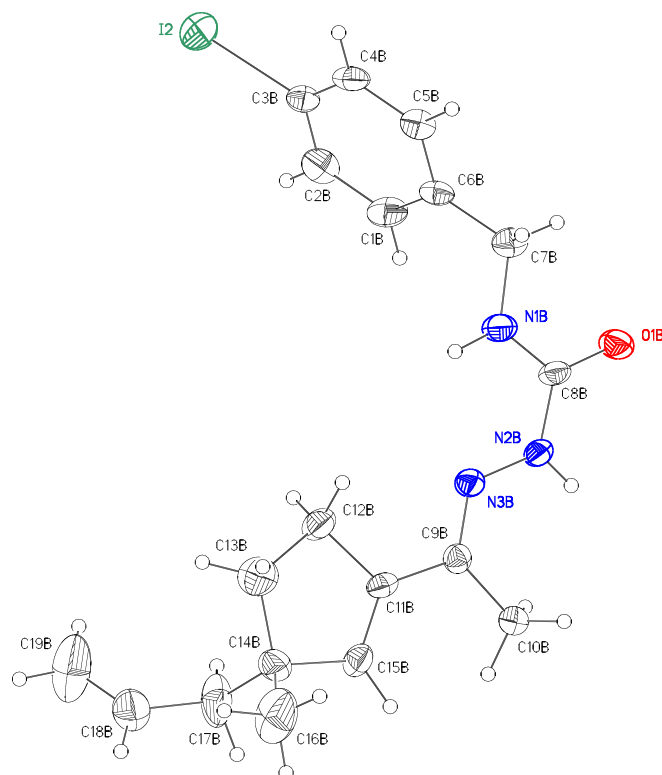
Figure A2.2. Semicarbazone **164** (CCDC 686849).

Table A2.2. Atomic coordinates ($\times 10^4$) and equivalent isotropic displacement parameters ($\text{\AA}^2 \times 10^3$) for semicarbazone **164** (CCDC 686849). $U(\text{eq})$ is defined as the trace of the orthogonalized U^{ij} tensor

	x	y	z	U_{eq}
I(1)	9525(1)	8297(1)	6590(1)	36(1)
O(1A)	7955(1)	941(3)	3051(1)	30(1)
N(1A)	7500(2)	3872(4)	3727(1)	30(1)
N(2A)	6670(2)	1070(4)	3270(1)	28(1)
N(3A)	6059(2)	2296(4)	3562(1)	28(1)
C(1A)	8489(2)	4383(5)	4938(2)	26(1)
C(2A)	8786(2)	5006(6)	5555(2)	27(1)
C(3A)	9158(2)	7186(5)	5637(2)	24(1)
C(4A)	9240(2)	8700(6)	5094(2)	23(1)
C(5A)	8934(2)	8049(6)	4481(2)	24(1)
C(6A)	8541(2)	5886(5)	4389(2)	21(1)
C(7A)	8214(2)	5251(6)	3716(2)	29(1)
C(8A)	7411(2)	1915(5)	3335(2)	24(1)
C(9A)	5356(2)	1676(5)	3411(2)	25(1)
C(10A)	5153(2)	-221(5)	2912(2)	34(1)

Table A2.2 (cont.)

C(11A)	4738(2)	3016(6)	3736(2)	25(1)
C(12A)	4902(2)	5012(5)	4229(2)	30(1)
C(13A)	4096(2)	6199(5)	4302(2)	34(1)
C(14A)	3501(2)	4222(5)	4130(2)	33(1)
C(15A)	3985(2)	2625(5)	3693(2)	32(1)
C(16A)	3271(2)	2838(6)	4771(2)	47(1)
C(17A)	2751(2)	5160(6)	3793(2)	36(1)
C(18A)	2864(2)	6198(6)	3116(2)	39(1)
C(19A)	2612(2)	8233(8)	2900(2)	51(1)
I(2)	5760(1)	351(1)	-1541(1)	52(1)
O(1B)	6661(1)	7118(3)	2275(1)	34(1)
N(1B)	7173(2)	4167(4)	1625(1)	34(1)
N(2B)	7955(2)	7040(4)	2098(1)	27(1)
N(3B)	8578(2)	5882(4)	1807(1)	26(1)
C(1B)	6496(2)	3858(5)	289(2)	33(1)
C(2B)	6341(2)	3322(8)	-374(2)	35(1)
C(3B)	5958(2)	1240(6)	-534(2)	29(1)
C(4B)	5742(2)	-303(6)	-40(2)	31(1)
C(5B)	5895(2)	235(6)	618(2)	28(1)
C(6B)	6287(2)	2329(5)	795(2)	26(1)
C(7B)	6454(2)	2863(6)	1519(2)	32(1)
C(8B)	7233(2)	6143(5)	2016(2)	25(1)
C(9B)	9266(2)	6619(5)	1925(2)	24(1)
C(10B)	9471(2)	8670(6)	2382(2)	33(1)
C(11B)	9892(2)	5325(6)	1586(2)	25(1)
C(12B)	9704(2)	3469(7)	1051(2)	34(1)
C(13B)	10499(2)	2401(6)	903(2)	54(1)
C(14B)	11131(2)	4019(5)	1204(2)	33(1)
C(15B)	10659(2)	5558(6)	1666(2)	30(1)
C(16B)	11736(3)	2543(7)	1600(2)	67(2)
C(17B)	11522(2)	5571(7)	690(2)	58(1)
C(18B)	12017(3)	4302(6)	194(2)	52(1)
C(19B)	11859(3)	3982(7)	-416(2)	77(2)

Table A2.3. Bond lengths [\AA] and angles [$^\circ$] for semicarbazone **164** (CCDC 686849)

I(1)-C(3A)	2.092(3)		
O(1A)-C(8A)	1.226(4)	C(8A)-N(1A)-C(7A)	120.7(3)
N(1A)-C(8A)	1.354(4)	C(8A)-N(2A)-N(3A)	119.8(3)
N(1A)-C(7A)	1.449(4)	C(9A)-N(3A)-N(2A)	118.6(3)
N(2A)-C(8A)	1.361(4)	C(2A)-C(1A)-C(6A)	122.1(3)
N(2A)-N(3A)	1.388(3)	C(1A)-C(2A)-C(3A)	119.6(3)
N(3A)-C(9A)	1.289(4)	C(2A)-C(3A)-C(4A)	119.8(3)
C(1A)-C(2A)	1.375(5)	C(2A)-C(3A)-I(1)	120.1(2)
C(1A)-C(6A)	1.386(4)	C(4A)-C(3A)-I(1)	119.9(2)
C(2A)-C(3A)	1.385(4)	C(5A)-C(4A)-C(3A)	119.7(3)
C(3A)-C(4A)	1.384(4)	C(4A)-C(5A)-C(6A)	121.7(3)
C(4A)-C(5A)	1.376(4)	C(1A)-C(6A)-C(5A)	117.2(3)
C(5A)-C(6A)	1.397(5)	C(1A)-C(6A)-C(7A)	122.8(3)
C(6A)-C(7A)	1.494(4)	C(5A)-C(6A)-C(7A)	120.1(3)
C(9A)-C(11A)	1.457(4)	N(1A)-C(7A)-C(6A)	115.0(3)
C(9A)-C(10A)	1.494(4)	O(1A)-C(8A)-N(1A)	123.1(3)
C(11A)-C(15A)	1.312(4)	O(1A)-C(8A)-N(2A)	121.2(3)
C(11A)-C(12A)	1.514(5)	N(1A)-C(8A)-N(2A)	115.8(3)
C(12A)-C(13A)	1.542(4)	N(3A)-C(9A)-C(11A)	116.2(3)
C(13A)-C(14A)	1.542(5)	N(3A)-C(9A)-C(10A)	123.9(3)
C(14A)-C(15A)	1.505(4)	C(11A)-C(9A)-C(10A)	119.8(3)
C(14A)-C(17A)	1.538(5)	C(15A)-C(11A)-C(9A)	127.4(3)
C(14A)-C(16A)	1.552(5)	C(15A)-C(11A)-C(12A)	109.9(3)
C(17A)-C(18A)	1.487(5)	C(9A)-C(11A)-C(12A)	122.6(3)
C(18A)-C(19A)	1.290(5)	C(11A)-C(12A)-C(13A)	102.6(3)
I(2)-C(3B)	2.096(3)	C(12A)-C(13A)-C(14A)	105.2(2)
O(1B)-C(8B)	1.242(4)	C(15A)-C(14A)-C(17A)	114.4(3)
N(1B)-C(8B)	1.356(4)	C(15A)-C(14A)-C(13A)	100.7(3)
N(1B)-C(7B)	1.447(4)	C(17A)-C(14A)-C(13A)	113.7(3)
N(2B)-C(8B)	1.346(4)	C(15A)-C(14A)-C(16A)	109.3(3)
N(2B)-N(3B)	1.383(3)	C(17A)-C(14A)-C(16A)	108.2(3)
N(3B)-C(9B)	1.270(4)	C(13A)-C(14A)-C(16A)	110.3(3)
C(1B)-C(6B)	1.376(4)	C(11A)-C(15A)-C(14A)	114.4(3)
C(1B)-C(2B)	1.380(5)	C(18A)-C(17A)-C(14A)	114.4(3)
C(2B)-C(3B)	1.373(5)	C(19A)-C(18A)-C(17A)	127.0(3)
C(3B)-C(4B)	1.366(4)	C(8B)-N(1B)-C(7B)	123.6(3)
C(4B)-C(5B)	1.372(4)	C(8B)-N(2B)-N(3B)	119.3(3)
C(5B)-C(6B)	1.394(5)	C(9B)-N(3B)-N(2B)	119.4(3)
C(6B)-C(7B)	1.501(5)	C(6B)-C(1B)-C(2B)	121.4(3)
C(9B)-C(11B)	1.467(4)	C(3B)-C(2B)-C(1B)	119.6(3)
C(9B)-C(10B)	1.504(4)	C(4B)-C(3B)-C(2B)	120.0(3)
C(11B)-C(15B)	1.330(4)	C(4B)-C(3B)-I(2)	120.1(3)
C(11B)-C(12B)	1.522(4)	C(2B)-C(3B)-I(2)	119.8(2)
C(12B)-C(13B)	1.521(5)	C(3B)-C(4B)-C(5B)	120.3(3)
C(13B)-C(14B)	1.530(5)	C(4B)-C(5B)-C(6B)	120.9(3)
C(14B)-C(15B)	1.505(4)	C(1B)-C(6B)-C(5B)	117.7(3)
C(14B)-C(17B)	1.509(5)	C(1B)-C(6B)-C(7B)	122.4(3)
C(14B)-C(16B)	1.537(6)	C(5B)-C(6B)-C(7B)	119.8(3)
C(17B)-C(18B)	1.493(5)	N(1B)-C(7B)-C(6B)	113.3(3)
C(18B)-C(19B)	1.260(5)	O(1B)-C(8B)-N(2B)	121.1(3)

Table A2.3 (cont.)

O(1B)-C(8B)-N(1B)	123.0(3)	C(12B)-C(13B)-C(14B)	108.9(3)
N(2B)-C(8B)-N(1B)	115.9(3)	C(15B)-C(14B)-C(17B)	109.6(3)
N(3B)-C(9B)-C(11B)	116.0(3)	C(15B)-C(14B)-C(13B)	101.3(3)
N(3B)-C(9B)-C(10B)	124.7(3)	C(17B)-C(14B)-C(13B)	112.9(3)
C(11B)-C(9B)-C(10B)	119.3(3)	C(15B)-C(14B)-C(16B)	110.9(3)
C(15B)-C(11B)-C(9B)	128.7(3)	C(17B)-C(14B)-C(16B)	110.8(3)
C(15B)-C(11B)-C(12B)	110.6(3)	C(13B)-C(14B)-C(16B)	110.9(3)
C(9B)-C(11B)-C(12B)	120.7(3)	C(11B)-C(15B)-C(14B)	114.2(3)
C(13B)-C(12B)-C(11B)	102.9(3)	C(18B)-C(17B)-C(14B)	116.1(3)
		C(19B)-C(18B)-C(17B)	126.3(5)

Table A2.4. Anisotropic displacement parameters ($\text{\AA}^2 \times 10^4$) for semicarbazone **164** (CCDC 686849). The anisotropic displacement factor exponent takes the form: $-2\pi^2 [h^2 a^{*2} U^{11} + \dots + 2 h k a^* b^* U^{12}]$

	U ¹¹	U ²²	U ³³	U ²³	U ¹³	U ¹²
I(1)	340(2)	433(1)	310(1)	1(1)	-116(1)	-2(1)
O(1A)	177(14)	294(13)	431(15)	-131(10)	-15(11)	35(10)
N(1A)	166(17)	377(19)	352(17)	-168(12)	3(13)	-6(12)
N(2A)	150(17)	315(15)	378(18)	-133(12)	-22(13)	22(12)
N(3A)	186(19)	310(15)	328(18)	-35(12)	-35(15)	38(13)
C(1A)	190(20)	176(16)	420(20)	13(15)	-22(18)	9(13)
C(2A)	250(20)	237(18)	320(20)	88(15)	-7(16)	-4(16)
C(3A)	170(20)	261(17)	270(20)	-18(14)	-7(16)	69(14)
C(4A)	180(20)	200(20)	310(20)	-23(14)	-29(15)	-13(14)
C(5A)	240(20)	201(19)	275(19)	26(16)	5(15)	34(16)
C(6A)	171(19)	195(18)	269(19)	-26(14)	-8(15)	64(14)
C(7A)	260(20)	280(18)	330(20)	-40(17)	-16(16)	-38(18)
C(8A)	200(20)	257(18)	260(20)	-33(14)	-61(17)	19(16)
C(9A)	200(20)	231(17)	330(20)	-9(14)	-9(18)	-26(15)
C(10A)	200(20)	410(20)	430(20)	-69(17)	3(18)	-44(17)
C(11A)	190(20)	240(20)	330(20)	21(16)	-31(15)	-26(17)
C(12A)	250(20)	283(18)	360(20)	-23(16)	-60(16)	-30(16)
C(13A)	260(20)	305(19)	440(20)	-99(15)	-50(18)	42(16)
C(14A)	190(20)	305(19)	490(30)	-7(15)	9(19)	19(15)
C(15A)	260(20)	240(20)	460(20)	-48(14)	-26(19)	-18(15)
C(16A)	360(30)	500(30)	540(30)	114(18)	30(20)	88(19)
C(17A)	250(20)	390(20)	450(20)	-34(18)	9(18)	40(20)
C(18A)	270(20)	480(20)	420(30)	-75(18)	-70(20)	77(18)
C(19A)	410(30)	600(20)	510(20)	40(20)	-88(19)	120(30)
I(2)	431(2)	791(2)	333(2)	-69(1)	-57(1)	-30(2)
O(1B)	227(16)	346(12)	447(16)	-105(10)	2(13)	9(11)
N(1B)	220(19)	350(17)	440(20)	-151(12)	-38(16)	9(12)
N(2B)	230(20)	301(15)	272(17)	-106(12)	-29(14)	3(13)
N(3B)	208(18)	309(16)	277(16)	-57(12)	-23(14)	26(14)
C(1B)	340(30)	190(20)	470(30)	-9(15)	-50(20)	-62(15)
C(2B)	310(20)	404(19)	350(20)	130(20)	-22(16)	20(20)
C(3B)	190(20)	370(20)	310(20)	-17(16)	-51(17)	17(16)
C(4B)	200(20)	270(20)	450(30)	-58(16)	-50(18)	-39(15)
C(5B)	270(20)	236(18)	340(20)	71(16)	-20(16)	-10(17)
C(6B)	170(20)	246(18)	350(20)	8(15)	-46(17)	-2(14)
C(7B)	300(20)	310(20)	360(20)	-12(15)	-23(17)	-59(16)
C(8B)	200(20)	282(19)	270(20)	-34(14)	-76(16)	-6(16)
C(9B)	250(20)	257(18)	220(20)	11(14)	2(17)	11(16)
C(10B)	260(20)	400(20)	330(20)	-104(16)	37(16)	-60(18)
C(11B)	250(20)	241(17)	253(19)	-25(16)	-45(15)	-52(18)
C(12B)	340(20)	341(18)	330(20)	-105(19)	-60(16)	10(20)
C(13B)	450(30)	450(20)	730(30)	-310(20)	70(30)	-4(19)
C(14B)	250(20)	350(20)	390(20)	-54(15)	20(19)	25(15)

Table A2.4 (cont.)

C(15B)	340(20)	290(18)	266(19)	-75(16)	-25(16)	33(18)
C(16B)	720(40)	680(30)	610(30)	-170(20)	-50(30)	380(30)
C(17B)	840(30)	400(20)	510(30)	-150(20)	330(20)	-90(20)
C(18B)	500(30)	540(30)	520(30)	-104(19)	110(30)	-49(19)
C(19B)	1060(50)	830(40)	420(30)	40(20)	60(30)	500(30)

Table A2.5. Hydrogen bonds for semicarbazone **164** (CCDC 686849) [\AA and $^\circ$]

D-H...A	d(D-H)	d(H...A)	d(D...A)	$\angle(\text{DHA})$
N(2A)-H(2A)...O(1B)#1	0.88	2.13	2.972(3)	159.7
N(2B)-H(2B)...O(1A)#2	0.88	2.04	2.895(3)	163.1

Symmetry transformations used to generate equivalent atoms:

#1 $x, y-1, z$

#2 $x, y+1, z$

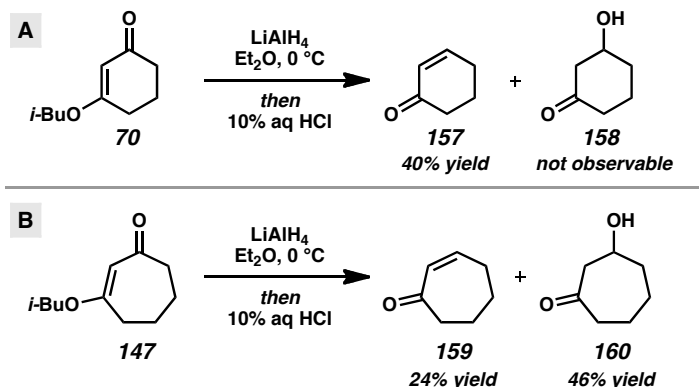
APPENDIX 3

Theoretical Investigation of the Unusual Stability of β -Hydroxycycloheptanones[†]

A3.1 INTRODUCTION AND BACKGROUND

Our group recently investigated the hydride reduction and acid-mediated rearrangement of six- and seven-membered cyclic vinylogous esters according to the Stork–Danheiser procedure.¹ During these studies, we found that β -hydroxycycloheptanones have unusual stability under acidic conditions compared to β -hydroxycyclohexanones.^{2b} As shown in Scheme A3.1, when complex **70** is reduced by LiAlH_4 in Et_2O and processed by 10% aqueous HCl , the only product is enone **157**, and β -hydroxycyclohexanone **158** is not observed. When complex **147** is used as the substrate, both enone **159** and β -hydroxycycloheptanone **160** are formed, but **160** is the major product.

[†] This work was performed in collaboration with Dr. Yu Lan and Prof. Ken N. Houk at UCLA. Calculations were conducted by Dr. Yu Lan. The computational results described in this appendix are unpublished preliminary findings.

Scheme A3.1. Experimental Observations of the Unusual Stability of β -Hydroxycycloheptanone

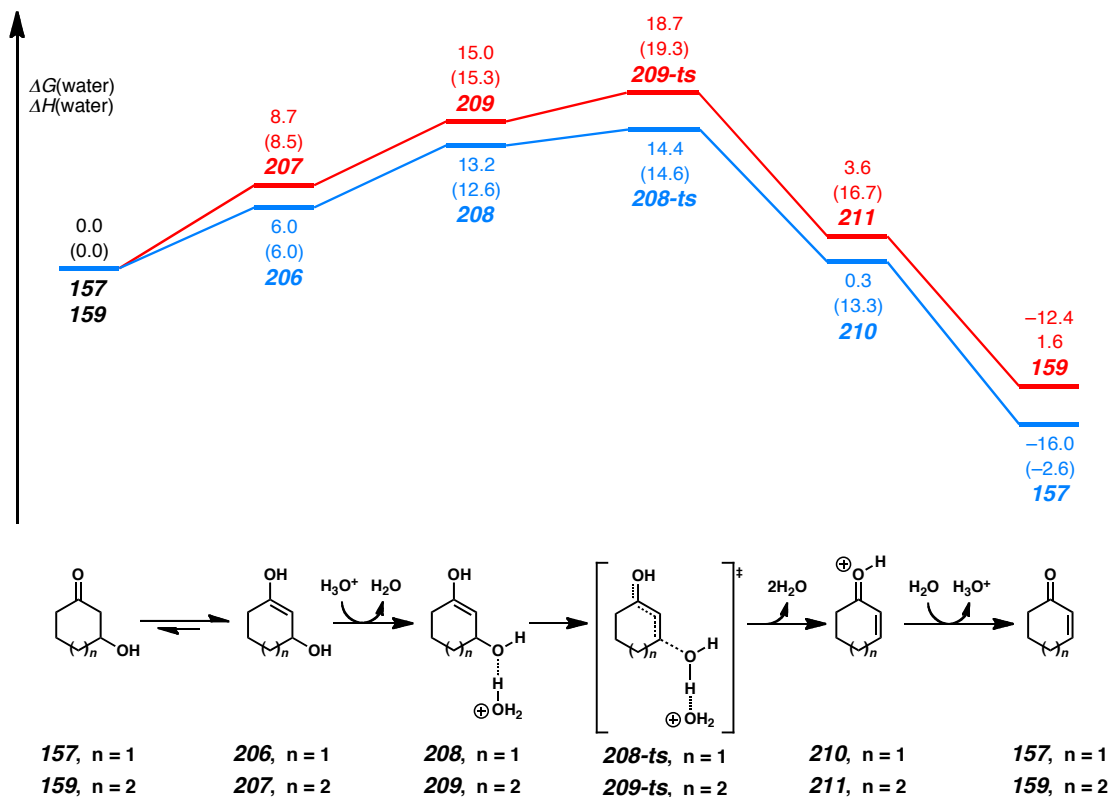
A3.2 QUANTUM CALCULATIONS

A theoretical study was undertaken to understand the mechanism of the hydroxyl elimination and explain the difference of the reactivity. M06-2X/6-311++G(d,p) was used for geometry optimizations. Solvent effects were considered by single point calculations on the gas-phase stationary points with Truhlar's SMD model.

Figure A3.1 gives the proposed mechanism of the hydroxyl elimination, and calculated free energy profiles. β -hydroxycyclohexanone **158** or β -hydroxycycloheptanone **160** isomerize to enol intermediate **206** or **207**, respectively. The keto-enol isomerization energy of **160** is 8.7 kcal/mol, which is 2.7 kcal/mol higher than **158**. The enol can be protonated by hydronium, and complex **208** or **209** are formed with similar free energy increases. The dehydration happens in transition states **208a-ts** or **209b-ts**. The elimination barrier in the seven-membered ring is 4.3 kcal/mol higher than in the six-membered ring. After deprotonation by water, the enone products, **157** or **159**, are formed. The generation of **157** is 3.6 kcal/mol more exergonic than of **159**.

Figure A3.1. The Mechanisms and the Calculated Free Energies of the Dehydration Reaction.

The energies are M06-2X/6-311++G(d,p) calculated free energies in water solvent (SMD). The values in parentheses are relative enthalpies in water.



Ring strain energies explain the reactivities and the product stabilities. The ring strain energies can be calculated by the isomerization from an acyclic molecule plus cyclohexane to the cyclic compound plus hexane. As shown in Table A3.1, the ring strain of cycloheptenol is 3.8 kcal/mol higher than cyclohexenol; the ring strain of cycloheptanone is only 1.9 kcal/mol higher than cyclohexanone. Therefore, the keto-enol isomerization of cyclohexanone is easier than that of cycloheptanone. The ring strain of cycloheptenone is 0.9 kcal/mol higher than cycloheptanone, while the ring strain of cyclohexenone is 2.8 kcal/mol lower than cyclohexanone. Therefore, the generation of six-membered ring enone **157** is more exothermic.

Table A3.1. The Ring Strain Enthalpies of Six- and Seven-Membered Rings.

Values are given by M06-2X/6-311++G(d,p) method.

entry	complex	n = 1	n = 2
1		0.0	5.3
2		-1.3	3.2
3		2.0	3.9
4		-1.1	2.7
5		-0.8	4.8

A3.3 FUTURE DIRECTIONS

In subsequent studies, it will be useful to extend the analyses conducted in this appendix to other medium sized rings. The results from those calculations can help identify other stable β -hydroxycycloalkanones. Such compounds can be prepared by chemical synthesis, and their reactivity in ring contraction reactions can be evaluated.²

A3.4 NOTES AND REFERENCES

- (1) Stork, G.; Danheiser, R. L. *J. Org. Chem.* **1973**, 38, 1775–1776.
- (2) (a) Hong, A. Y.; Krout, M. R.; Jensen, T.; Bennett, N. B.; Harned, A. M.; Stoltz, B. M. *Angew. Chem. Int. Ed.* **2011**, 50, 2756–2760. (b) Hong, A. Y.; Bennett, N. B.; Krout, M. R.; Jensen, T.; Harned, A. M.; Stoltz, B. M. *Tetrahedron* **2011**, 67, 10234–10248.

CHAPTER 3

The Catalytic Asymmetric Total Synthesis of Presilphiperfolanol Natural Products[†]

3.1 INTRODUCTION AND BACKGROUND

Presilphiperfolanols (or prebotrydials) constitute a family of biosynthetically important sesquiterpenes. The natural products have been isolated from several species of plants and fungi and are distinguished by their unique tricyclic structures, which can rearrange to diverse sesquiterpenoid skeletons. The intriguing structures and biosynthetic roles of these compounds provide compelling reasons for their synthesis.

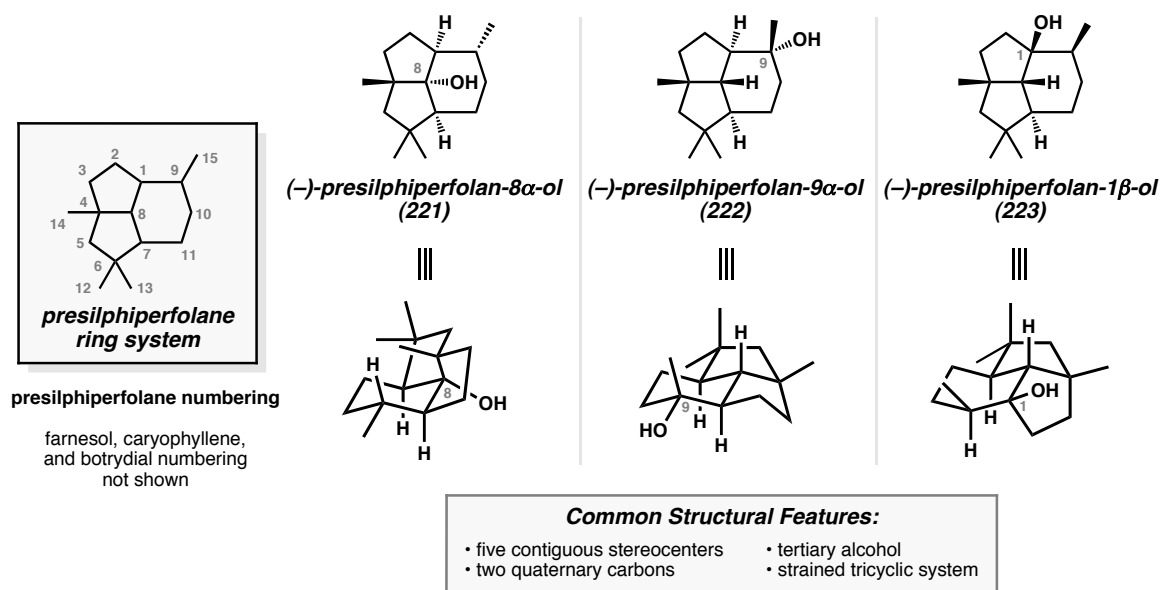
3.1.1 ISOLATION AND STRUCTURAL ELUCIDATION

Currently, three presilphiperfolanols have been isolated and characterized: presilphiperfolan-8 α -ol (**221**)¹ presilphiperfolan-9 α -ol (**222**),² and presilphiperfolan-1 β -

[†] Portions of this work have been published. For the initial communication, see: Hong, A. Y.; Stoltz, B. M. *Angew. Chem. Int. Ed.* **2012**, *51*, 9674–9678. For a review of the presilphiperfolanols, see: Hong, A. Y.; Stoltz, B. M. *Angew. Chem. Int. Ed.* **2014**, *53*, 5248–5260.

ol (**223**)^{3,4} (Figure 3.1). Each of these natural products corresponds to the hydration product of a presilphiperfolanyl cation involved in terpene cyclization pathways. To date, naturally occurring stereoisomers of structures **221–223** have not been reported. The structurally complex presilphiperfolanols are distinguished by their rare, compact tricyclo[5.3.1.0^{4,11}]undecane sesquiterpene skeleton, which bears five contiguous stereocenters, two all-carbon quaternary centers, and a tertiary alcohol. In addition to these readily apparent structural features, considerable ring strain is present in the tricyclic system,^{5,6} allowing these compounds to undergo thermodynamically favorable skeletal rearrangements that lead to structurally diverse polycyclic sesquiterpenes. Computational studies have shown that the heat of formation (ΔH_f) of the presilphiperfolane skeleton is at least 7.1 kcal/mol greater than those for several isomeric sesquiterpene skeletons formed later in the biosynthetic sequence.⁵

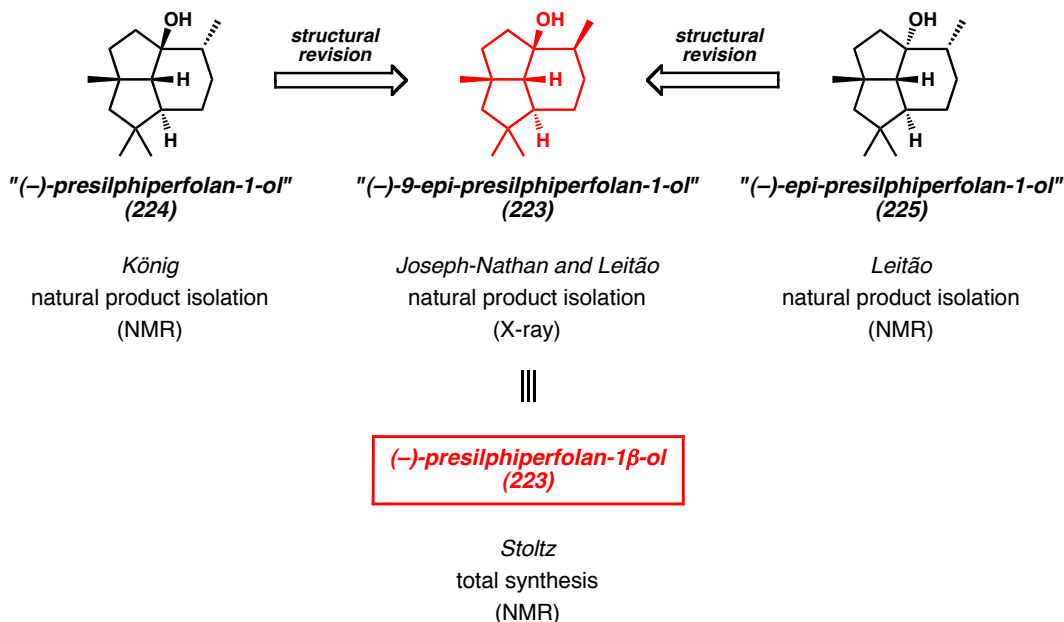
Figure 3.1. Presilphiperfolanol (Prebotrydial) Natural Products



Presilhiperfolan-8 α -ol (**221**) was the first member of the family to be identified.¹ Bohlmann and co-workers isolated the compound from the flowering plants *Eriophyllum staechadifolium* and *Flourensia heterolepis* in 1981. The tricyclic structure and stereochemistry were assigned based on detailed ¹H NMR analysis employing chiral shift reagents. Subsequent work by Coates provided an X-ray crystal structure of the *p*-nitrobenzoate ester derivative.⁷

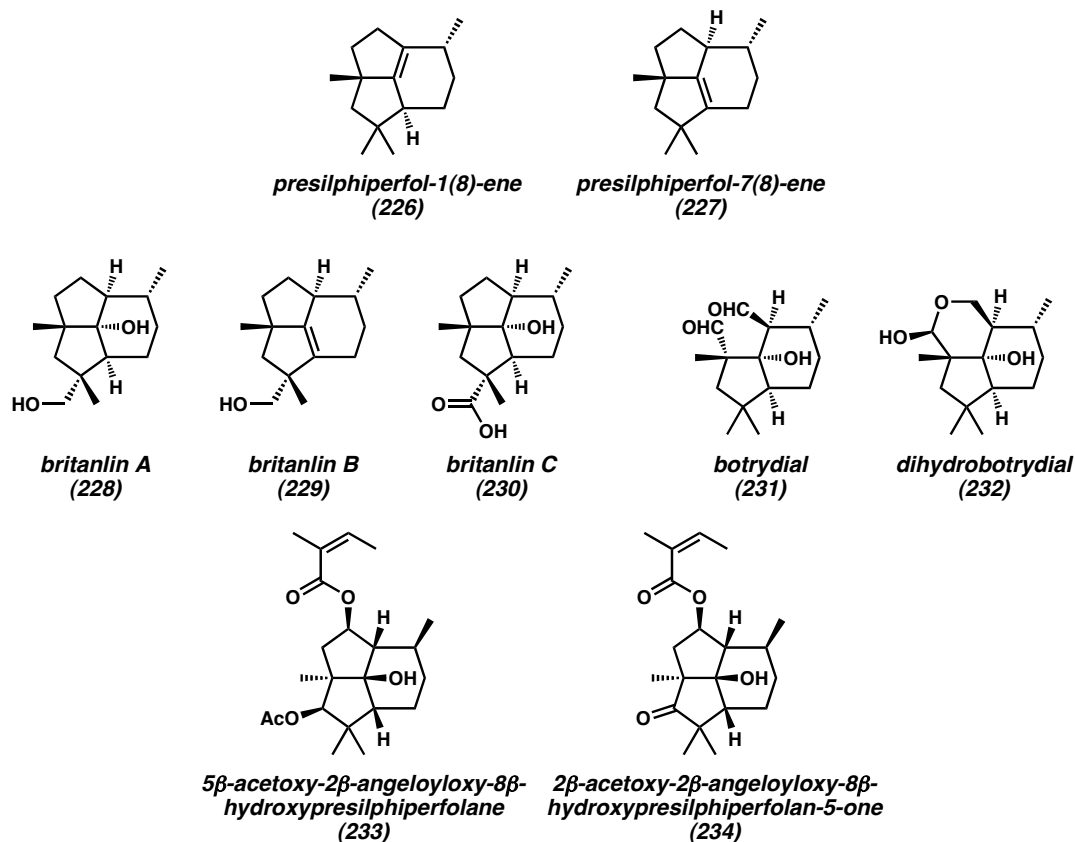
Presilhiperfolan-9 α -ol (**222**)² was later discovered by Weyerstahl in the wormwood *Artemisia lacinata* in 1993, and subsequently by Marco in the related species *Artemisia chamaemelifolia* in 1996. The structure of **222** was determined based on NMR spectroscopic analysis and additionally confirmed by the total synthesis of (\pm)-**222**.⁸

In contrast to presilhiperfolanols **221** and **222**, the structure of presilhiperfolan-1 β -ol (**223**)^{3,4} has been revised several times (Figure 3.2). Alcohol **223** was initially isolated by König in small quantities from the liverwort *Conocephalum conicum* in 1999,³ but was incorrectly assigned structure **224** based on NMR data. The same compound was isolated by Leitão from the fern *Anemia tomentosa* var. *anthriscifolia* and reported as a unique natural product with initial structure **225** from the analysis of NMR spectra.^{4a} Subsequent collaborations between Leitão and Joseph-Nathan unambiguously determined that the isolated compound possessed revised structure **223** by X-ray crystallography.^{4b} Recently, our research group proposed that the compounds isolated by König and Leitão are in fact the same natural product **223** based on synthetic studies, spectroscopic data, and analysis of the likely biosynthetic pathway (see Section 3.4.7).

Figure 3.2. Structural Reassignments of Presilphiperfolan-1 β -ol (**223**)

In addition to the parent presilphiperfolanols, natural products with dehydrated or oxidized tricyclic skeletons have also been reported (Figure 3.3). Presilphiperfol-1(8)-ene (**226**)^{1,7} and presilphiperfol-7(8)-ene (**227**)⁹ presumably arise from the deprotonation of presilphiperfolanyl cation intermediates. Natural products such as the britanlins (**228**–**230**)¹⁰ display additional oxidation at primary carbons in the presilphiperfolane skeleton. Other isolated compounds, such as angelates **233** and **234**, show oxidation at multiple secondary carbons in the tricyclic framework.¹¹ Oxidative ring cleavage is also possible as evidenced by the structures of botrydial (**231**)¹² and dihydrobotrydial (**232**).¹² All of these natural products arise from structural modification of the presilphiperfolanols, which exhibit a low level of oxidation.

Figure 3.3. Natural Products with Dehydrated or Oxidized Presilphiperfolanol Skeletons



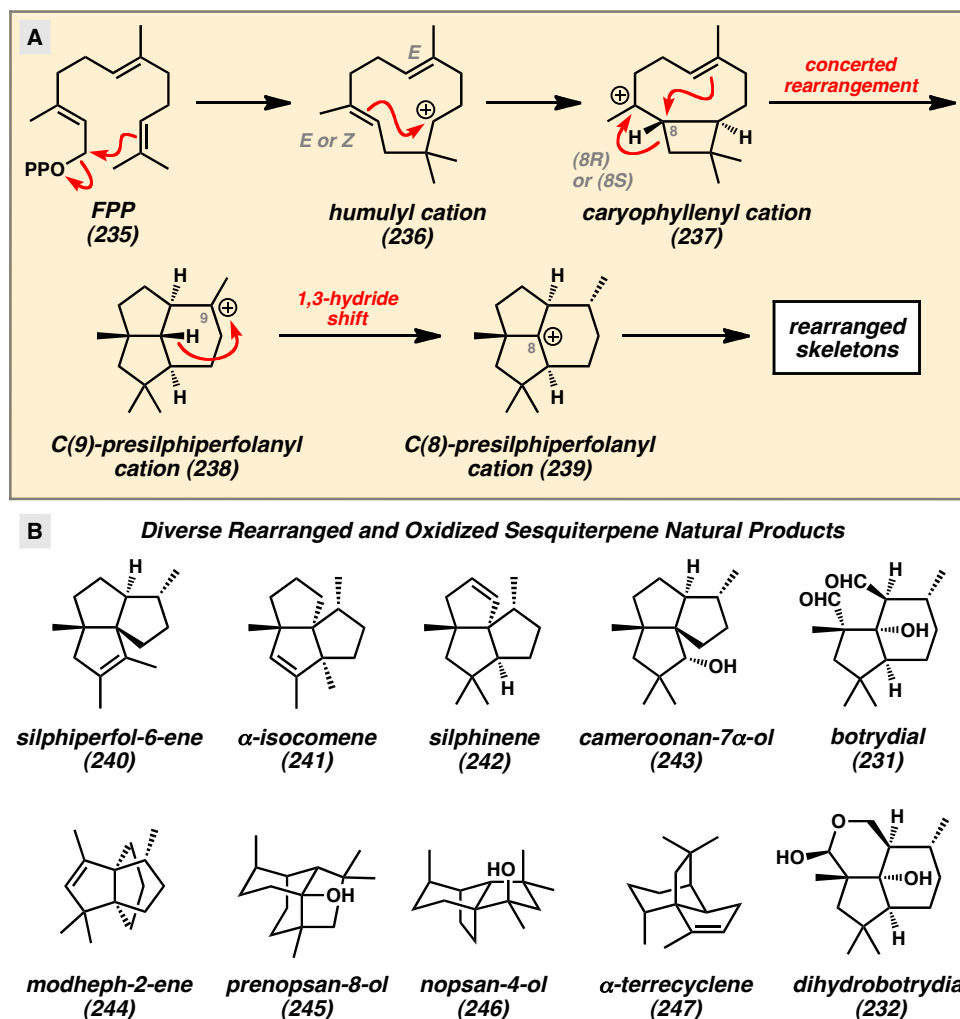
3.1.2 BIOSYNTHESIS OF THE PRESILPHIPERFOLANOLS

The co-isolation of the presilphiperfolanols with structurally related sesquiterpenes provided important clues for their biosynthetic origin. Bohlmann and co-workers observed that presilphiperfolan-8 α -ol (**221**) was often found with various triquinane natural products.^{1,13} Tricyclic alcohol **221** and β -caryophyllene (**248**) (Figure 3.4) were also isolated from the same natural sources in numerous reports.^{9,14} These findings suggested that three classes of polycyclic sesquiterpenes were connected in a common biosynthetic pathway. In 1980, Bohlmann explained these results by proposing that farnesyl pyrophosphate (FPP) (**235**) undergoes enzymatic polycyclization to

caryophyllenyl cation **237** (Scheme 3.1A).¹³ Subsequent cyclobutane ring expansion and cation-alkene cyclization leads to the C(8)-presilphiperfolanyl cation (**239**). From this common intermediate, rearrangement of the carbon skeleton by Wagner–Meerwein shifts can lead to the observed triquinanes.

Concurrent studies by Hanson in 1981 helped to elucidate the presilphiperfolane biosynthetic pathway.¹⁵ In an effort to understand the biogenesis of the downstream metabolite dihydrobotrydial (**232**) from farnesyl pyrophosphate (**235**), his group performed NMR studies with isotopically labeled FPP (**235**). Both ²H and ¹³C labels could be incorporated into these compounds, which were fed to the fungus *Botryis cinerea*. Subsequent analysis of the cyclized and oxidized dihydrobotrydial (**232**) products provided the first evidence for an unusual 1,3-hydride shift linking the initially formed C(9)-presilphiperfolanyl cation (**238**) to the isomeric C(8)-cation (**239**) (Scheme 3.1A). From this intermediate, Hanson reasoned that hydration and enzymatic oxidative cleavage of the less-substituted cyclopentane ring would lead to botrydial (**231**) and dihydrobotrydial (**232**) (Scheme 3.1B).

Scheme 3.1. Modified Bohlmann–Hanson Mechanism for Presilphiperfolane Biosynthesis



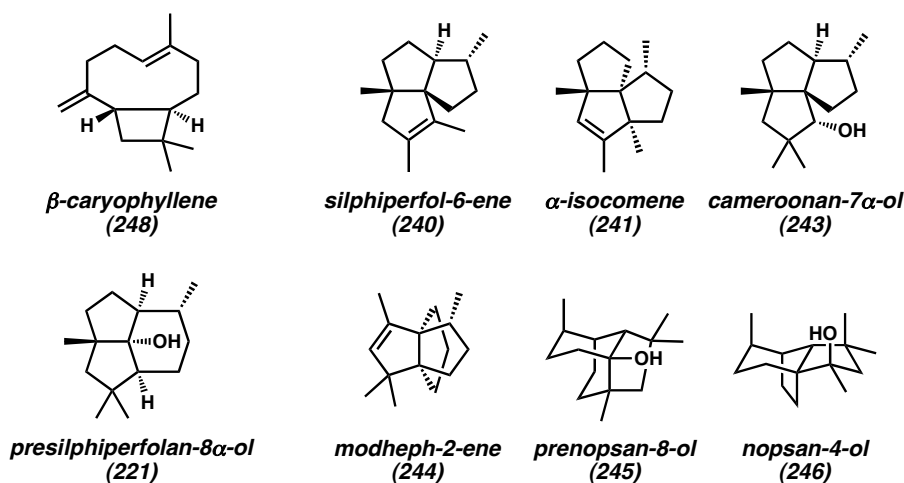
The Bohlmann–Hanson mechanism has been refined and expanded by numerous groups through biochemical, spectroscopic, and computational techniques in recent years. The groups of Collado, Cane, and Viaud worked together to identify the *BcBOT* gene cluster in *B. cinerea* responsible for the enzymatic conversion of FPP (**235**) to botrydial (**231**).¹⁶ In these studies, it was demonstrated that the *BcBOT2* gene encoded an essential sesquiterpene cyclase while other genes in the cluster expressed cytochrome P450 monooxygenases responsible for the oxidation of the presilphiperfolane skeleton to

botrydial (**231**) and related derivatives (Scheme 3.1B). Subsequent work by Cane focused on FPP isotopic labeling with the isolated enzyme. These experiments provided detailed NMR evidence for the stereochemistry of individual cyclization steps.¹⁷

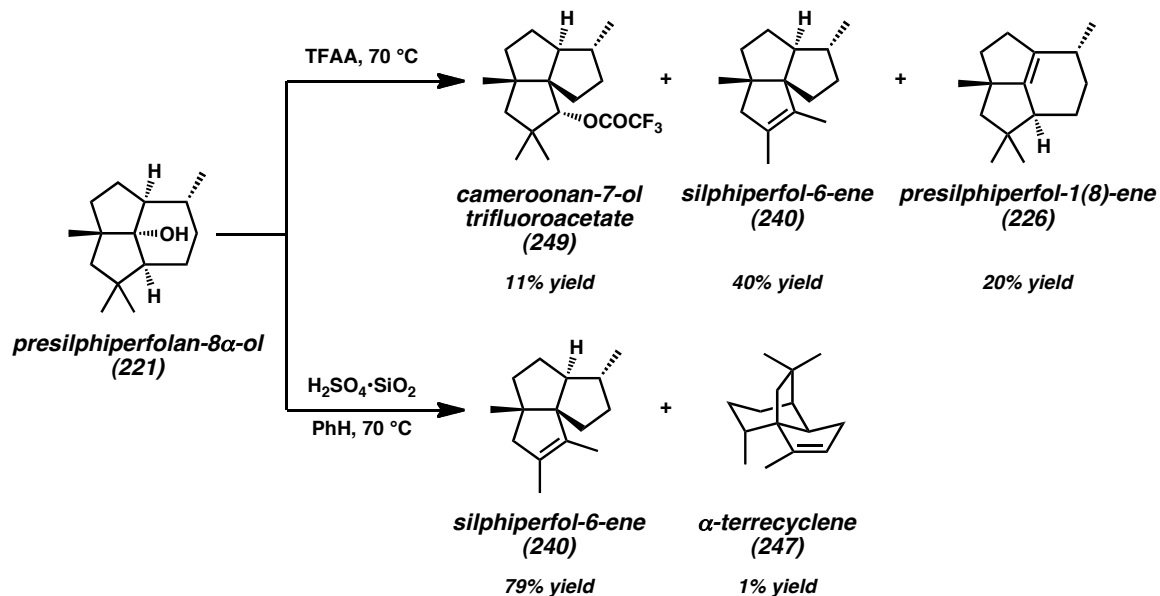
Concurrent work by Tantillo sought to understand the presilphiperfolanol biosynthetic pathway through computational means.¹⁸ Numerous theoretical terpene cyclization pathways were evaluated and a revised mechanism was proposed on the basis of these results (Scheme 3.1A). The key findings were the conformer of caryophyllenyl cation **237** responsible for cyclization, the highly synchronous nature of the cation-alkene cyclizations leading from **237** to **238**, and the feasibility of the 1,3-hydride shift leading from C(9)-cation **238** to C(8)-cation **239**. Barquera-Lozada identified a similar polycyclization pathway for the biosynthetic conversion of FPP (**235**) to α -terrecyclene (**247**) (Scheme 3.1B).¹⁹

3.1.3 BROADER RELEVANCE OF THE PRESILPHIPERFOLANOLS

The importance of the presilphiperfolanols in sesquiterpene biosynthesis has prompted more detailed investigations of the rearrangements leading to other related natural products.^{7,9} A report by Weyerstahl in 1998 described the constituents of the essential oil from the rhizome *Echinops giganteus* var. *lelyi* as containing a rich collection of biogenetically related sesquiterpenes (Figure 3.4).⁹ Along with β -caryophyllene (**248**) and presilphiperfolan-8 α -ol (**221**), 18 unique tricyclic natural products were discovered. All of the tricyclic compounds could be traced to common presilphiperfolanyl cation intermediates through reasonable Wagner–Meerwein shifts. The co-occurrence of these compounds further supports the findings of Bohlmann.^{1,13}

Figure 3.4. Selected Co-isolated Sesquiterpenes from Rhizome *Echinops giganteus* var. *lelyi*

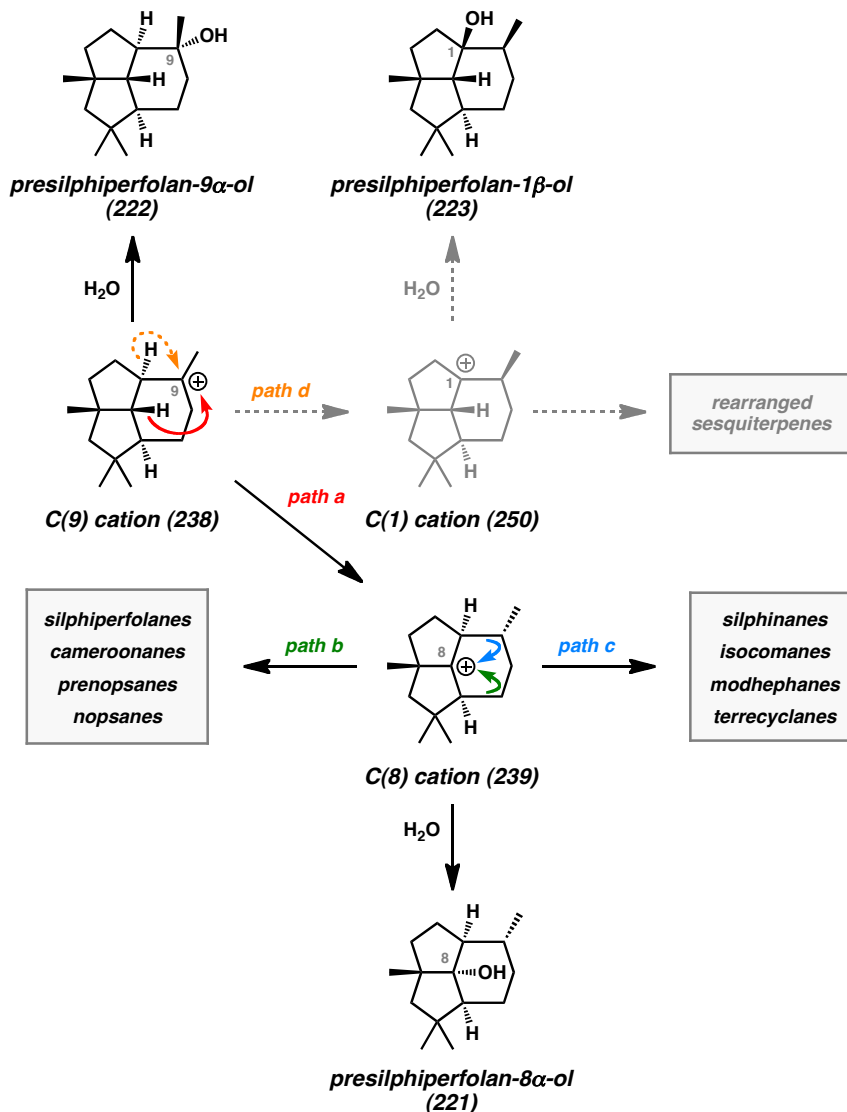
In conjunction with these natural product isolation studies, others have sought to understand the biosynthetic conversion of presilphiperfolane skeletons to those of other sesquiterpene natural products through chemical semi-synthesis. Coates successfully performed the rearrangement of presilphiperfolan-8 α -ol (**221**) with TFAA at 70 °C to obtain cameroonan-7-ol trifluoroacetate (**249**) in 11% yield, silphiperfol-6-ene (**240**) in 40% yield, and presilphiperfol-1(8)-ene (**226**) in 20% yield (Scheme 3.2).^{5,7} Ionization of alcohol **221** with H₂SO₄·SiO₂ in benzene at 70 °C provided silphiperfol-6-ene (**240**) in 79% yield and α -terrecyclene (**247**) in 1% yield. The different distribution of sesquiterpene products obtained under these reaction conditions highlights the strong influence of reaction parameters on competing rearrangement pathways.

Scheme 3.2. Rearrangement of Presilphiperfolan-8 α -ol to Other Sesquiterpene Skeletons

Currently, the presilphiperfolane skeleton is believed to serve as the precursor to silphiperfolane, silphinane, isocomane, modhephane, terrecyclane, prenopsane, nopsane, and cameroonane skeletons (Scheme 3.1B and Scheme 3.3).⁹ The structural diversity of polycyclic skeletons produced from the presilphiperfolane skeleton underscores their fundamental biosynthetic importance in sesquiterpene cyclase pathways.

While past work has explored the formation of presilphiperfolan-9 α -ol (**222**) and presilphiperfolan-8 α -ol (**221**) in great detail, existing biosynthetic proposals have not accounted for the formation of presilphiperfolan-1 β -ol (**223**), the newest discovered member of the family (Scheme 3.3). The understanding of the mechanistic pathway leading to this natural product could additionally provide new insight into the formation of downstream rearranged sesquiterpene natural products.

Scheme 3.3. Rearrangement of Presilphiperfolanols to Other Sesquiterpene Natural Products



3.1.4 BIOLOGICAL ACTIVITY

While the presilphiperfolanols have proven to be important biosynthetic precursors to a number of polycyclic sesquiterpenes, they also exhibit modest biological activity. As a relatively nonpolar low molecular weight alcohol, presilphiperfolan-9 α -ol (**222**) has pleasant olfactory properties and has attracted interest as a possible fragrance

compound.^{2,20} The natural product (–)-**222**² has a pleasantly sweet and woody aroma with hints of coconut and celery. Synthetic (±)-**222**⁸ possesses a slightly different olfactory profile with a strongly radiative, woody, resinous, and amber(gris) notes.

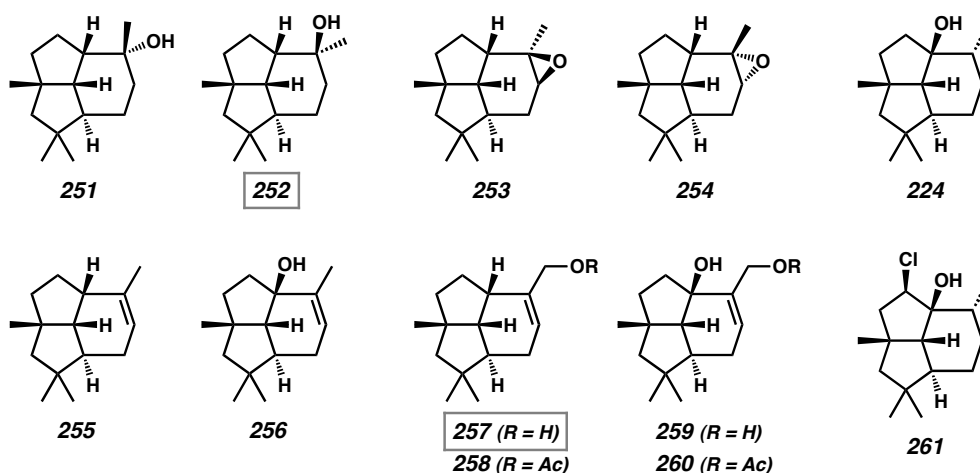
González-Coloma and co-workers discovered the insect antifeedant properties of presilhiperfolan-9 α -ol (**222**) while screening a collection of polycyclic sesquiterpenoids.²¹ The tricyclic alcohol displayed an EC₅₀ of 19.5 nmol/cm² against the Colorado potato beetle *Leptinotarsa decemlineata* and 47.5 nmol/cm² against the aphid species *Diuraphis noxia*. Direct injection or oral dosing of this compound with *L. decemlineata* beetles led to 47% mortality after 72 hours. While the mode of action has not been fully elucidated, alcohol **222** is believed to be toxic to the insect's peripheral and central nervous system.

Leitão and co-workers have found that presilhiperfolan-1 β -ol (**223**) possesses antimycobacterial properties.²² The natural product is active against *Mycobacterium tuberculosis* (H37Rv) and *Mycobacterium smegmatis* (mc²155) strains with minimal inhibitory concentrations (MICs) of 100 μ g/mL and 200 μ g/mL, respectively. Currently, the basis for the observed antimycobacterial activity is unclear.

Unnatural presilhiperfolane analogs have also been investigated for their biological properties. Presilhiperfolane derivatives **224**, **251–261** were investigated as novel antifungal agents by Collado (Figure 3.5).²³ Of these compounds, alcohols **252** and **257** showed the most promising inhibition in fungal growth assays with *Botryis cinerea*. Tertiary alcohol **252** showed complete suppression of fungal growth for four days with continued growth reduction after seven days. Primary alcohol **257** effectively reduced the size of fungal colonies and triggered changes in fungal morphology. For both of

these active tricyclic terpenoid compounds, the hydroxyl groups are believed to be essential for inhibition, as the evaluation of acetylated derivatives such as **258** led to no observable activity.

Figure 3.5. Natural and Unnatural Presilphiperfolanol Analogs Investigated for Antifungal Activity



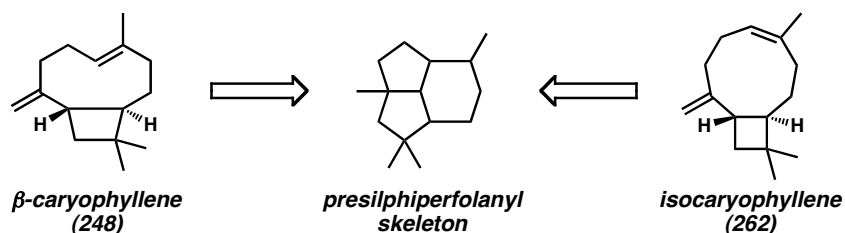
3.2 PREVIOUS SYNTHETIC STUDIES TOWARD PRESILPHIPERFOLANOL NATURAL PRODUCTS

Although the presilphiperfolanols are vitally important to the biosynthesis of numerous polycyclic sesquiterpenes, efforts to synthesize these natural products have been scarce. A number of biomimetic synthetic approaches have aimed to convert advanced biosynthetic precursors to the tricyclic alcohols **221–223**, but these approaches have not been successful. More recently, research directed toward the total synthesis of the presilphiperfolanols has led to compounds that possess the tricyclic core of the targeted natural products.

3.2.1 BIOMIMETIC CATION-POLYENE CYCLIZATIONS OF CARYOPHYLLENE AND ISOCARYOPHYLLENE

Based on the substantial evidence for the biosynthetic conversion of FPP (**235**) to caryophyllenyl cations en route to presilphiperfolanyl cations through cation-polyene cyclizations, many researchers have sought to achieve biomimetic syntheses of the presilphiperfolanols by rearrangement of β -caryophyllene (**248**) or isocaryophyllene (**262**) (Scheme 3.4).²⁴ To date, however, these efforts have not resulted in the formation of any of the naturally occurring tricyclic alcohols **221–223**.

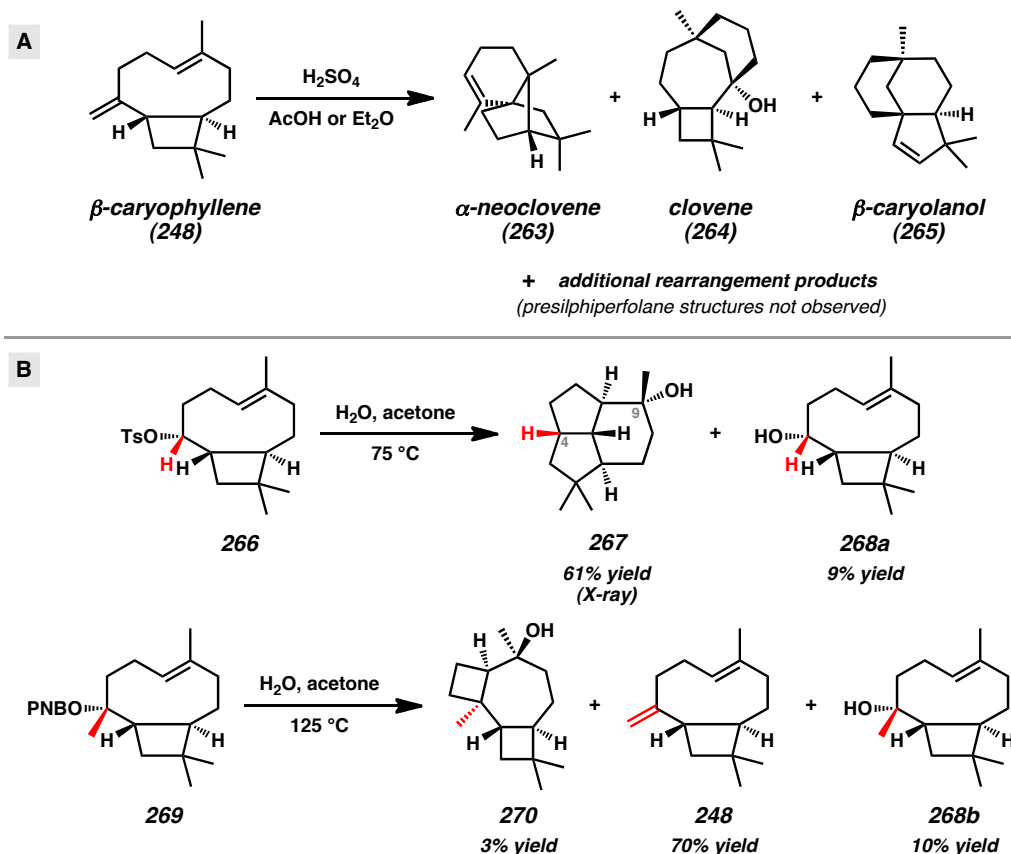
Scheme 3.4. Strategy for the Rearrangement of Caryophyllenyl and Isocaryophyllenyl Skeletons



Research by numerous groups has explored the rearrangement of β -caryophyllene under acidic conditions (Scheme 3.5A).^{25,26} These reactions typically have led to complex mixtures with product distributions that change over time. In this context, numerous rearrangement products such as α -neoclovene (**263**), clovene (**264**), and β -caryolanol (**264**) have been isolated and characterized. A supporting computational study was also performed to help understand the complex nature of the diverse rearrangement pathways.^{26a} To date, however, presilphiperfolane structures have not been observed in any of these detailed studies.

More recently, Coates and co-workers studied the solvolytic rearrangement of β -caryophyllene-derived structures with intriguing results (Scheme 3.5B).^{26b} The ionization and rearrangement β -caryophyllene-derived tosylate **266** in water and acetone at 75 °C provided 12-nor-8 α -presilphiperfolan-9 β -ol (**267**) and alcohol **268a**. Compound **267** resembles presilphiperfolan-9 α -ol (**222**), but notably lacks the C(4) methyl group present in the natural product. Rearrangement reactions employing β -caryophyllenyl precursors with the requisite C(4)-methyl group were also investigated. Subjection of the *p*-nitrobenzoate ester **269** to similar solvolytic rearrangement conditions at slightly higher temperatures did not furnish presilphiperfolan-9 α -ol (**222**), but instead led to 5,8-cyclocaryophyllen-4 α -ol (**270**), β -caryophyllene (**248**), and alcohol **268b**. The different product distributions under nearly identical reaction conditions suggests that the non-enzymatic cyclization is sensitive to the substitution of the caryophyllenyl framework.

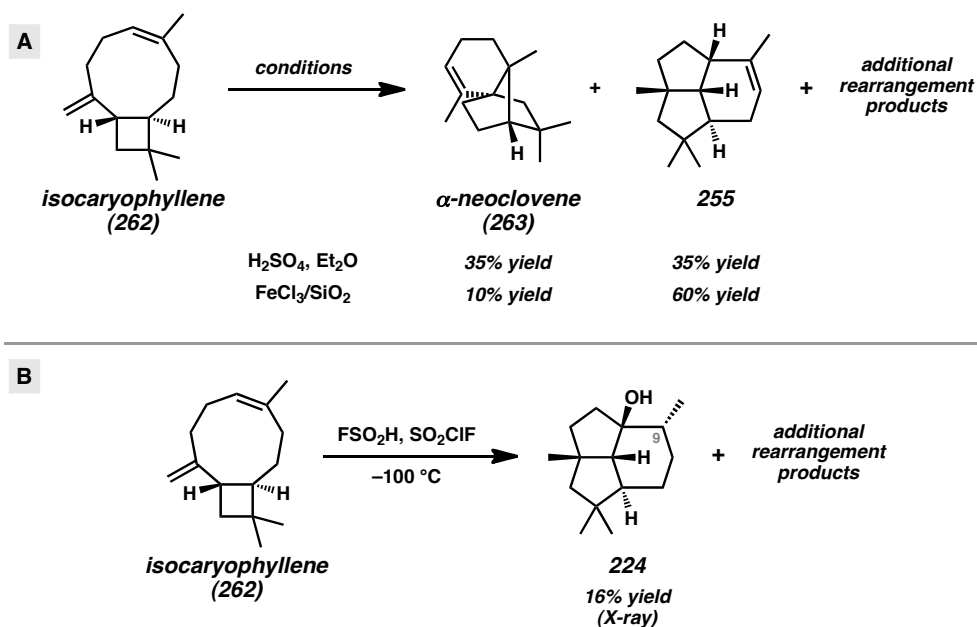
Scheme 3.5. Reported Rearrangements of Caryophyllene Skeletons



The rearrangement of isocaryophyllene (**262**) to presilphiperfolane-type structures has also been investigated.^{23,27,28} Robertson and co-workers treated isocaryophyllene (**262**) with sulfuric acid in diethyl ether to obtain α -neoclovene (**263**) and tricyclic olefin **255**, which resembles the tricyclic core of the presilphiperfolanols (Scheme 3.6A). Since these early studies, Collado was able to favor the formation of olefin **255** by employing silica-supported FeCl_3 .^{23b} Further work by Khomenko and co-workers has produced alcohol-containing tricyclic structures that more closely resemble the presilphiperfolanols.²⁸ Treatment of isocaryophyllene (**262**) with fluorosulfonic acid and sulfonyl fluorochloride at $-100\text{ }^\circ\text{C}$ followed by a careful quenching of the acidic solution

led to the formation of tricyclic alcohol **224** in 16% yield (Scheme 3.6B). The structure was assigned based on ^1H and ^{13}C NMR studies and confirmed by single crystal X-ray diffraction. Notably, this compound is the C(9)-epimer of presilphiperfolan-1 β -ol (**223**) and the structure originally assigned by König as “presilphiperfolan-1-ol” (**224**).

Scheme 3.6. Reported Rearrangements of Isocaryophyllene (**262**)

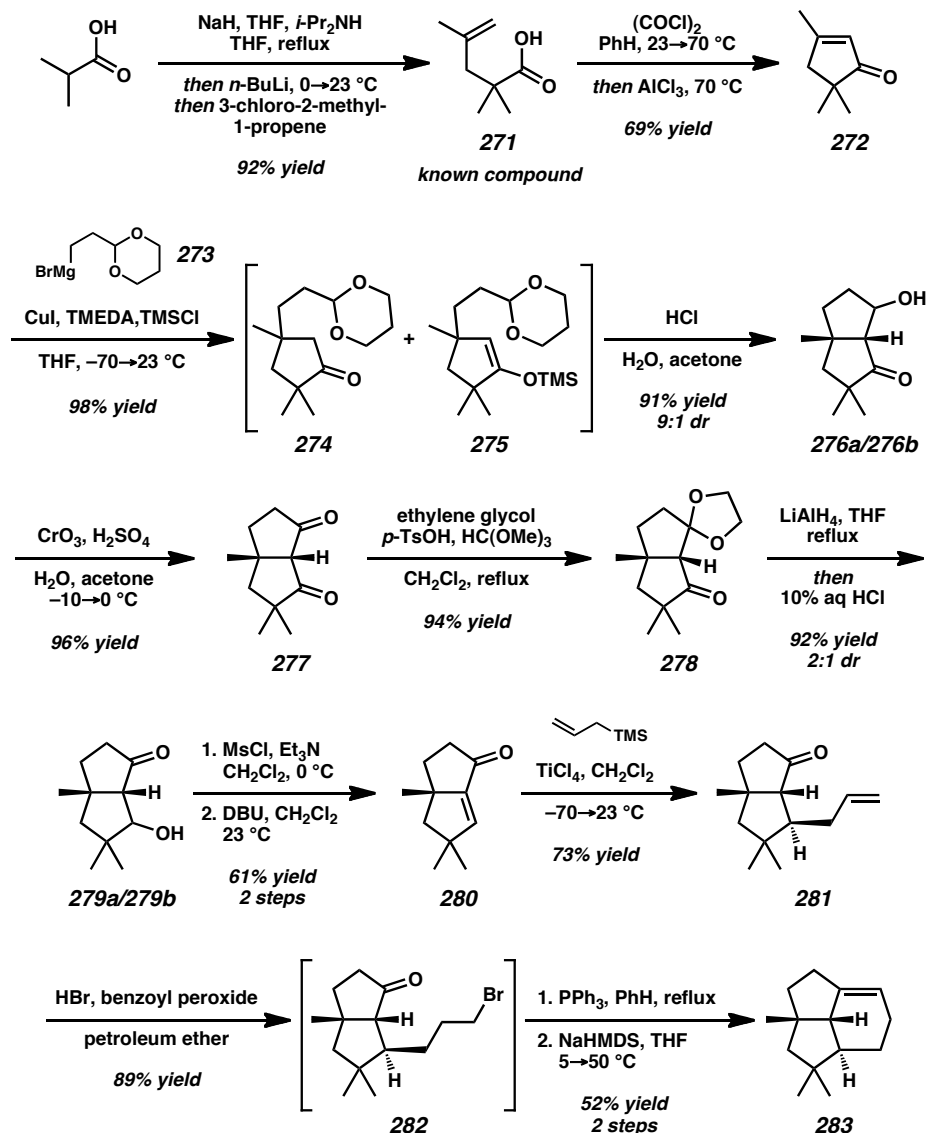


3.2.2 WEYERSTAHL SYNTHESIS OF (\pm)-PRESILPHIPERFOLAN-9 α -OL

Driven by a keen interest in the biosynthetic importance, intriguing polycyclic structure, and olfactory properties of presilphiperfolan-9 α -ol (**222**), Weyerstahl and co-workers aimed to prepare the natural product by total synthesis.⁸

Beginning from isobutyric acid, enolization and alkylation with methallyl chloride provided functionalized pentenoic acid **271** (Scheme 3.7). Subsequent carboxylate activation with oxalyl chloride and cyclization with AlCl_3 provided cyclopentenone **272**

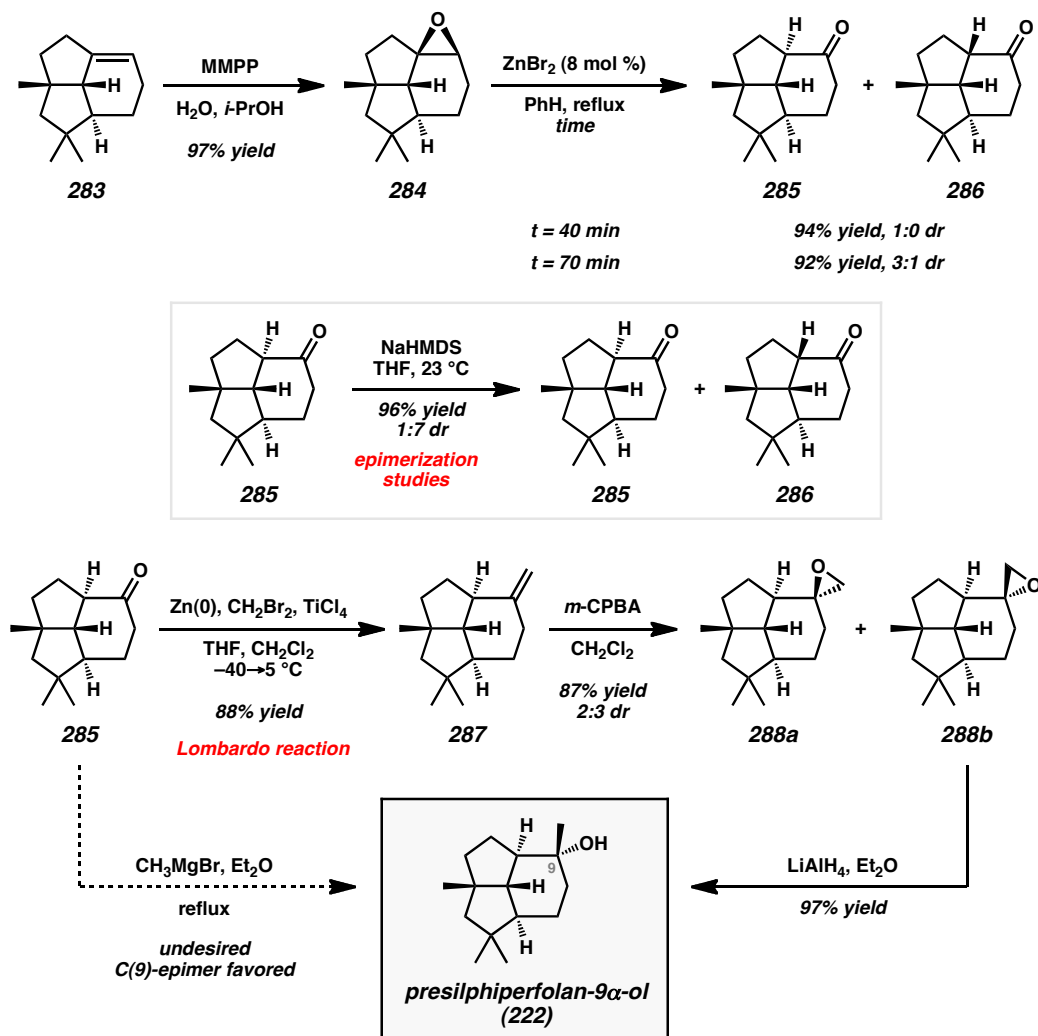
in 69% yield. The conjugate addition of organocuprate **273** with TMSCl as an activator followed by acidic deprotection and aldolization provided a mixture of β -hydroxyketones **276a** and **276b** in 89% yield and 9:1 dr over two steps. A subsequent Jones oxidation afforded diketone **277** in 96% yield. Selective protection of the less hindered carbonyl proceeded smoothly with *p*-TsOH, ethylene glycol, and trimethyl orthoformate in CH_2Cl_2 under reflux conditions. Reduction of the remaining ketone in **278** with LiAlH_4 followed by acidic workup provided β -hydroxyketones **279a** and **279b** in 92% yield and 2:1 dr. Dehydration was achieved by initial mesylation and elimination with DBU to give bicyclic enone **280** in 61% yield over two steps. Alternatively, the elimination was achieved with Burgess' reagent²⁹ in 64% yield. A subsequent diastereoselective Sakurai allylation³⁰ afforded ketone **281** in 73% yield. Regioselective radical hydrobromination of the terminal olefin followed by an intramolecular Wittig reaction completed the tricyclic core of the target tricyclic molecules (**283**) in 52% yield over two steps.

Scheme 3.7. Synthesis of Key Tricyclic Olefin Intermediate **283**

With key tricyclic olefin **283** in hand, a highly diastereoselective epoxidation with magnesium bis(monoperoxyphthalate) (MMPP)³¹ afforded epoxide **284** in 97% yield (Scheme 3.8). The epoxidation could also be achieved with *m*-CPBA, but yields were typically lower. A subsequent stereospecific epoxy-keto rearrangement catalyzed by ZnBr₂ was effective, giving the expected ketone **285** with α-H stereochemistry at C(1) in

94% yield after 40 min. While these reaction conditions proved successful, longer reaction times led to significant C(1)-epimerization to the undesired ketone epimer **286**. The gradual conversion of tricyclic ketone **285** to its epimer **286** over time suggests that the desired ketone is thermodynamically unstable. This hypothesis was also supported by epimerization studies on ketone **285** with NaHMDS, which provided a mixture of **285** and **286** in a 1:7 ratio of diastereomers.

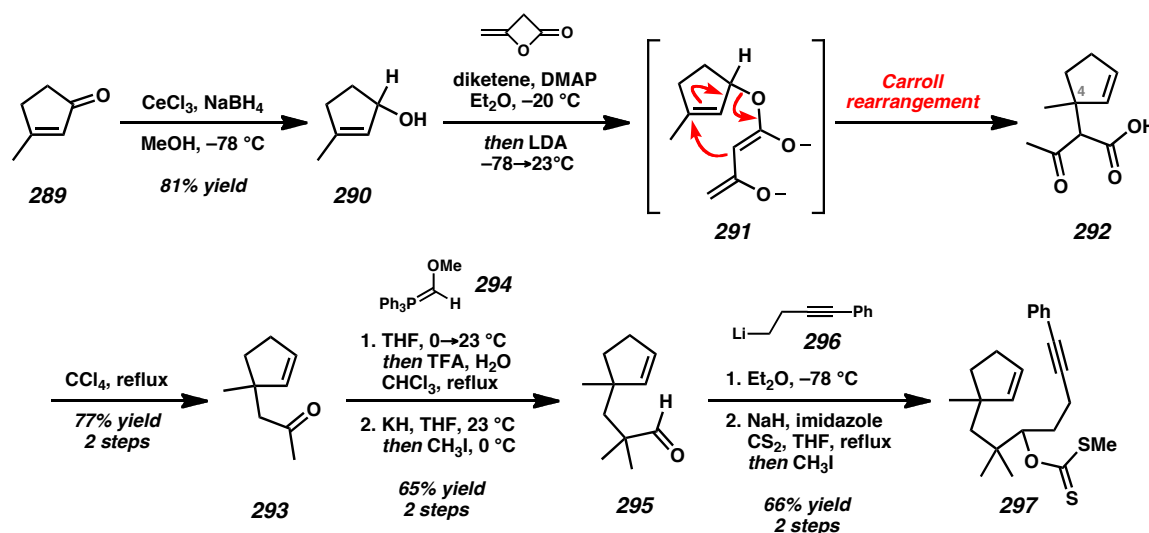
With 14 of the 15 carbons of the target compound installed, it was anticipated that the addition of MeMgBr to **285** could give presilphiperfolan-9 α -ol (**222**) in a direct and straightforward manner. Unfortunately, this transformation predominantly led to the undesired C(9)-epimer with only trace amounts of the desired natural product **222**. The steric environment of the tricycle as well as the favorable Bürgi–Dunitz trajectory from the α -face of the molecule dictated the facial bias of nucleophilic additions into the ketone of **285**. In order to arrive at the natural product through alternative means, a Lombardo reaction was employed to give olefin **287** in 88% yield. A subsequent epoxidation with *m*-CPBA gave a 2:3 ratio of diastereomers **288a** and **288b** in 87% yield. After chromatographic separation, LiAlH₄ reduction of epoxide **288b** finally provided (\pm)-presilphiperfolan-9 α -ol (**222**) in 97% yield. The total synthesis was completed in 17 steps and 4.0% overall yield from commercial starting materials.

Scheme 3.8. Weyerstahl's Completion of (±)-Presilphiperfolan-9α-ol (**222**)

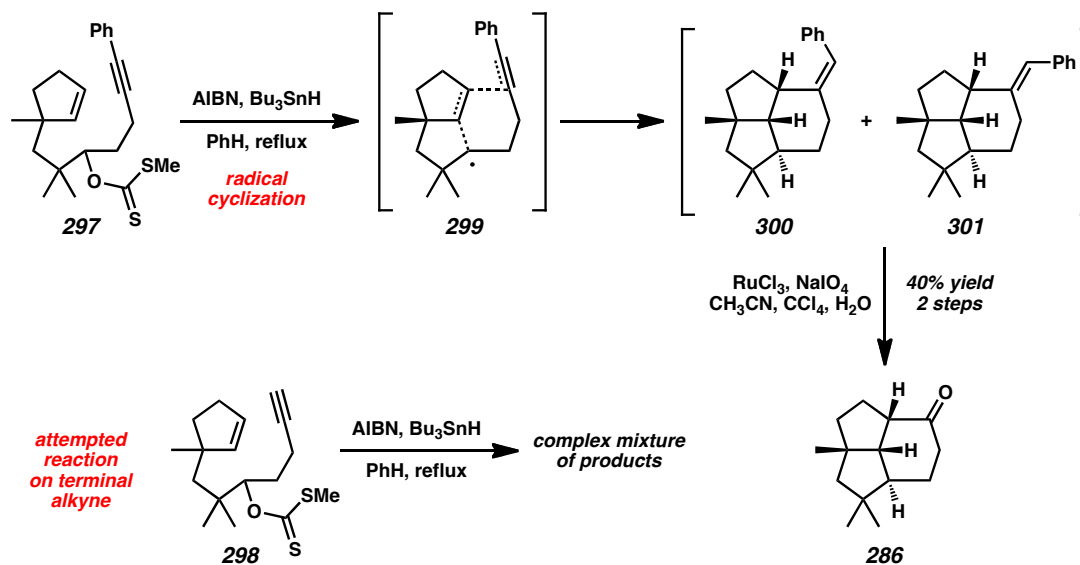
3.2.3 PIERS' RADICAL CYCLIZATION STRATEGY AND SYNTHESIS OF (±)-EPI-9-NORPRESILPHIPERFOLAN-9-ONE

Within a general program directed toward the construction of complex natural products, Piers aimed to complete a concise synthesis of (±)-presilphiperfolan-9α-ol (**222**) using a radical polycyclization strategy.^{32,33} The synthesis proceeded from 3-methyl-2-cyclopentenone (**289**) (Scheme 3.9). An initial Luche reduction³⁴ provided

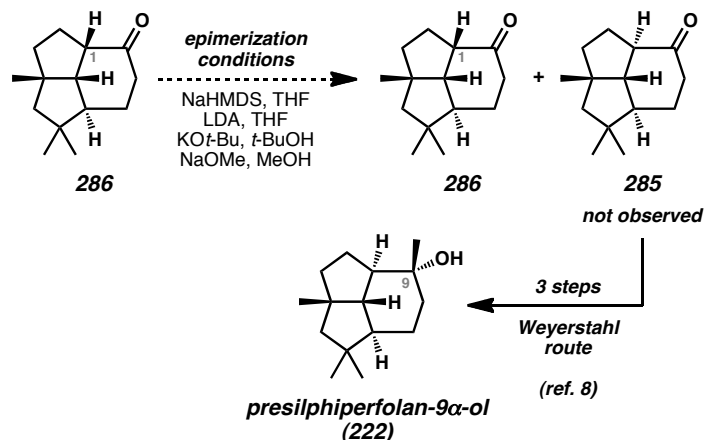
alcohol **290** in excellent yield. By applying the method of Wilson,³⁵ the allylic alcohol was converted to dianionic intermediate **291**, which underwent a thermal Carroll rearrangement³⁶ and decarboxylation to form functionalized cyclopentene **293** in 77% yield over two steps. With the C(4) quaternary carbon installed, a Wittig homologation with ylide **294**³⁷ followed by methyl enol ether hydrolysis provided aldehyde **295** in 72% yield and 1:1 dr. α -Alkylation with methyl iodide, alkyllithium addition with reagent **296**, and xanthate ester formation led to radical cyclization precursor **297**.

Scheme 3.9. Synthesis of Radical Cyclization Precursor **297**

The slow addition of Bu_3SnH and AIBN to xanthate **297** in refluxing benzene provided a mixture of tricyclic olefins **300** and **301** (Scheme 3.10). Oxidative alkene cleavage with RuCl_3 and NaIO_4 ³⁸ afforded (\pm)-*epi*-9-nor-presilphiperfolan-9-one (**286**)⁸ in 40% yield over two steps. The disubstituted alkyne was essential for efficient cyclization since precursor **298** only led to a complex mixture of volatile hydrocarbon products.

Scheme 3.10. Radical Cyclization Cascades with Precursors **297** and **298**

In order to proceed toward presilphiperfolan-9 α -ol (**222**), epimerization of the C(1) methine hydrogen of ketone **286** was necessary (Scheme 3.11). Thermodynamic equilibration according to Weyerstahl's procedure (Scheme 3.8)⁸ failed, returning only starting material. Other strong bases such as LDA, KO t -Bu, and NaOMe provided no trace of the desired ketone **285**. Due to the synthetic difficulties arising from the thermodynamic preferences of the tricyclic scaffold, the synthesis was not advanced further.

Scheme 3.11. Attempted Epimerization of the C(1)-Methine Hydrogen of Ketone **285**

3.2.4 SUMMARY OF PREVIOUS SYNTHETIC STUDIES

The numerous syntheses directed toward the presilphiperfolanols have provided valuable insight into the challenges of achieving diastereoselective reactions due to the steric environment of the congested tricycle. While several promising cation-alkene and radical cyclization approaches have been documented, Weyerstahl's total synthesis of (\pm)-presilphiperfolan-9 α -ol (**222**) was the only completed synthesis of any member of the important sesquiterpene family at the outset of our studies.

3.3 ASYMMETRIC ALKYLATION/RING CONTRACTION APPROACH TO THE PRESILPHIPERFOLANOL NATURAL PRODUCTS

Although the presilphiperfolanol natural products have garnered broad scientific interest in the natural products,^{9,10,11} biosynthesis,^{1,2,5,7,13,14,15,17,18,19} organic synthesis,^{8,33} computation,^{18,19} and fragrance^{2,8,20} literature since their discovery, they have proven to be challenging targets for total synthesis.^{39,40} To date, only **222** has been prepared in

racemic form⁸ and no asymmetric routes toward any of the presilphiperfolanols have been reported. The unique chemical structures and intriguing biosynthetic function of these natural products inspired us to devise an enantioselective total synthesis with an emphasis on asymmetric catalysis.⁴¹ In particular, the further development of our asymmetric alkylation and ring contraction methodology for the preparation of γ -quaternary acylcyclopentenones (**135**)⁴² would provide valuable tools for addressing the long-standing synthetic challenges posed by the presilphiperfolanols. Additionally, a successful synthetic route would enable further exploration of the biosynthetic relationships and biological activity of these important natural products.

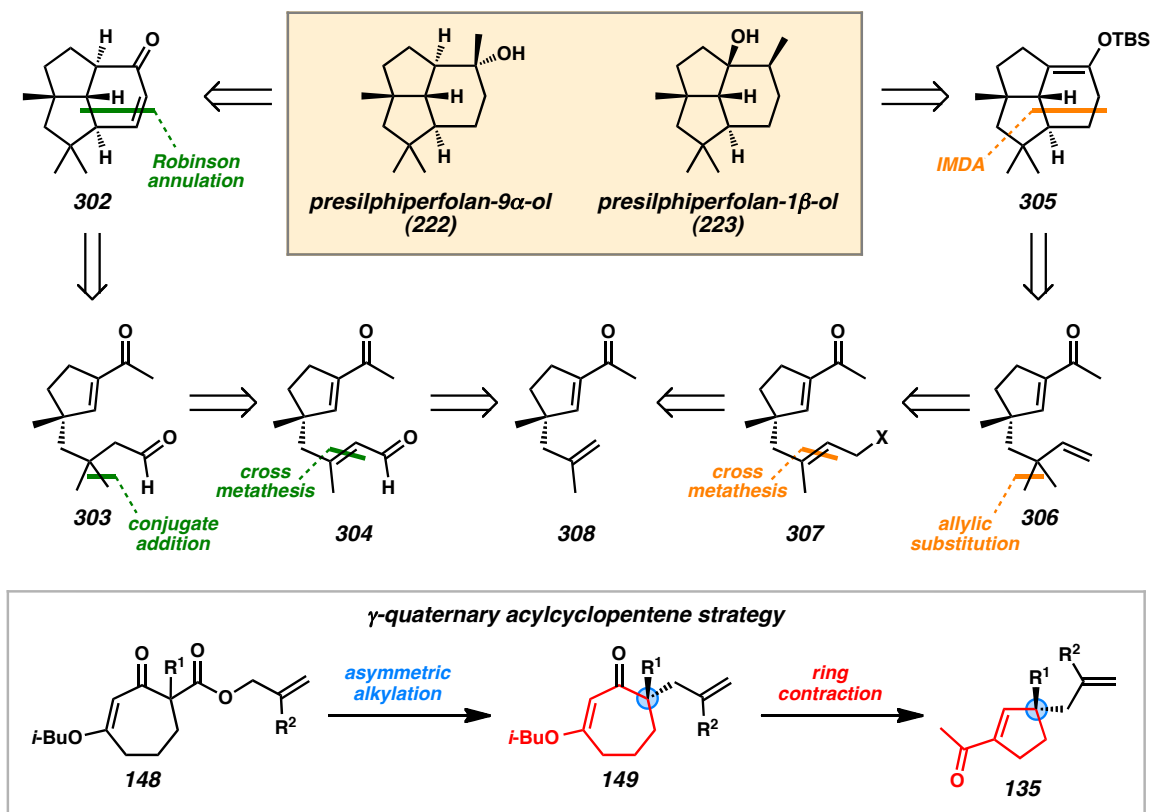
3.3.1 RETROSYNTHETIC ANALYSIS

At the outset of our investigations, the aforementioned discrepancy of the structural assignments of “presilphiperfolan-1-ol” (**224**) and “9-*epi*-presilphiperfolan-1-ol” (**223**) was unknown (Figure 3.2). Therefore, we sought a synthetic route that would not only allow access to presilphiperfolan-9 α -ol **222**, but also 1-hydroxy presilphiperfolanols **223** and **224** as it was believed that each compound was a previously isolated natural product.

Retrosynthetic analysis suggested that tricyclic presilphiperfolanols such as **222** and **223** could be formed by late stage construction of the cyclohexane ring through an intramolecular Robinson annulation or an intramolecular Diels–Alder (IMDA) reaction (Scheme 3.12). Further disconnections along the Robinson annulation route would lead to ketoaldehyde **303**, which would arise from organometallic conjugate addition into enone-enal **304**. Alternatively, the IMDA route would lead to acylcyclopentene precursor **306**, which could be traced to allyl electrophile **307** through an allylic

substitution reaction. Both enone-enal **304** and allyl electrophile **307** could arise from the cross-metathesis of methyl/methallyl acylcyclopentene **308** with appropriate olefinic partners. The strategic application of our newly developed methodology for the synthesis of γ -quaternary acylcyclopentenones (**135**) by means of Pd-catalyzed asymmetric alkylation and two-carbon ring contraction (see Chapter 2) would enable access to common intermediate **308**.⁴² In proceeding forward with this route, it was important to recognize that our acylcyclopentene synthesis demonstrated broad scope for various R^1 substituents, but provided no examples of the R^2 substitution at the allyl fragment. The pursuit of the presilphiperfolanol natural products would provide a valuable opportunity to expand our previously developed reaction methodology.

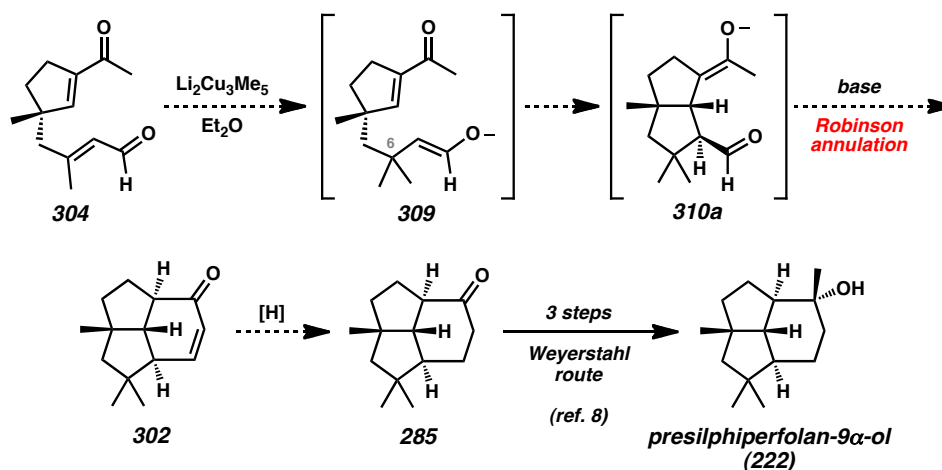
Scheme 3.12. Retrosynthetic Analysis of Presilphiperfolanol Natural Products



3.3.2 CONJUGATE ADDITION/ROBINSON ANNULATION STRATEGY

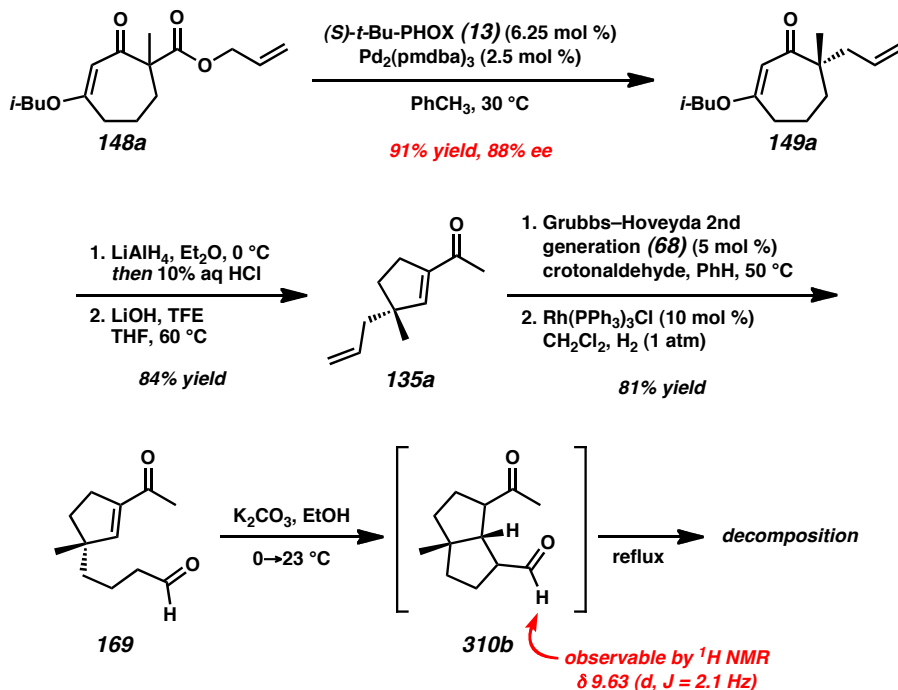
Closer scrutiny of the Robinson annulation approach to the presilphiperfolanols suggested that the conjugate addition reaction could be coupled with cyclohexenone formation in an efficient synthetic approach (Scheme 3.13). This sequence could proceed with the sterically controlled chemoselective conjugate addition into enone-enal **304** using $\text{Li}_2\text{Cu}_3\text{Me}_5$ (Clive's reagent).⁴³ A second intramolecular conjugate addition would take place upon generation of enolate **309**. We envisioned that further treatment with base could afford enone **302** through a Robinson annulation reaction. Olefin reduction could lead to ketone **285**, which can be advanced to presilphiperfolan-9 α -ol (**222**) using the route of Weyerstahl.⁸

Scheme 3.13. Conjugate Addition Cascade and Robinson Annulation Strategy



To evaluate the proposed polycyclization (**309**→**302**), we investigated a simple model cyclization with enone-aldehyde **169** based lacking the C(6) *gem*-dimethyl groups

(Scheme 3.14). This compound was prepared by the straightforward application of our Pd-catalyzed asymmetric alkylation and ring contraction methodology^{42a} for the formation of **135a**. Subsequent olefin cross-metathesis with crotonaldehyde and chemoselective enal hydrogenation provided the model cyclization substrate (see Chapter 2, Section 2.5).^{42c} Treatment of aldehyde **169** with K₂CO₃ in EtOH at 0 °C followed by slow warming to ambient temperature led to the formation of bicyclic ketoaldehyde with general structure **310b** as a single diastereomer as observed by ¹H NMR.⁴⁴ The intermediate was heated in refluxing ethanol to promote formation of the remaining cyclohexane ring, but attempted cyclization failed as the reaction proceeded to decomposition products. Simple molecular modeling studies revealed that the distance between the aldehyde carbon and the nucleophilic terminus of the methyl ketone is about 3.7 Å, making the terminal intramolecular aldol cyclization challenging for this bicyclic system.⁴⁵ On the basis of these findings, the conjugate addition cascade strategy was not pursued further. Importantly, these results provided important experimental clues for the inherent ring strain of the tricyclic presilphiperfolane core.^{5,6}

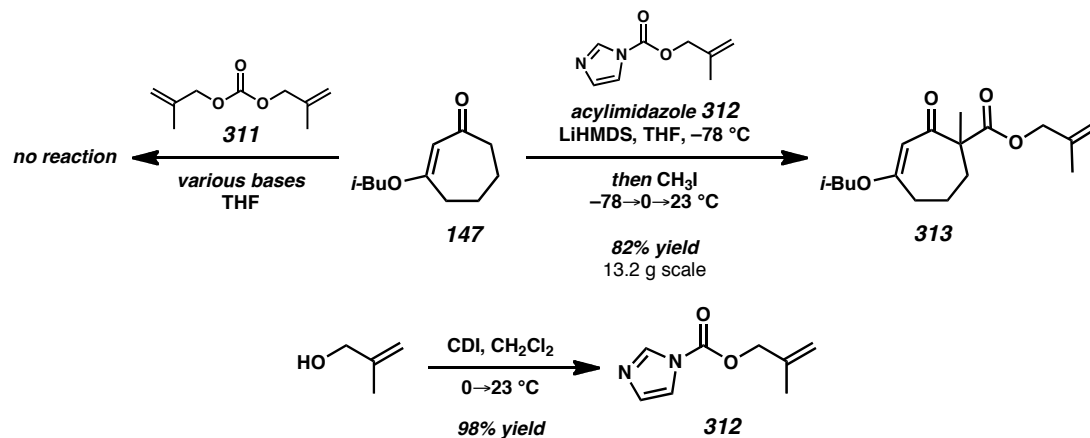
Scheme 3.14. Evaluation of a Simple Model System Based on Acylcyclopentene **135a**

3.3.3 INTRAMOLECULAR DIELS–ALDER STRATEGY

As preliminary experiments began to cast doubt on the proposed Robinson annulation approach, we shifted our attention to the alternative IMDA strategy for the construction of the cyclohexane ring of the presilphiperfolanols. To explore this route, we needed to modify our asymmetric alkylation and ring contraction methodology⁴² to prepare methyl/methallyl-substituted acylcyclopentene **308**. In previous studies, the acylation of parent vinylogous ester **147** was typically performed with allyl cyanoformate, which was prepared from commercial allyl chloroformate.⁴⁶ For our synthesis, the use of methallyl cyanoformate was an option, however the absence of a commercial chloroformate precursor rendered large-scale synthesis inconvenient.

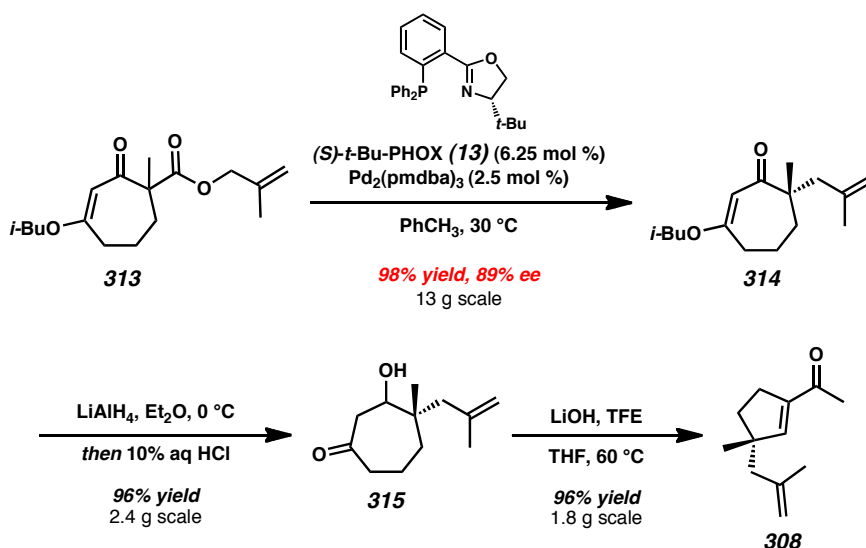
To remedy this situation, alternative reagents were explored for the construction of β -ketoester **314**. Attempted acylations with commercial dimethallyl carbonate (**311**) according to reported procedures^{47b,c} returned only starting material and trace quantities of desired product (Scheme 3.15). The inefficiency of the reaction along with the high cost of carbonate **311** made it necessary to identify more practical reagents. Carbonylimidazole-based compounds were investigated next because of their straightforward preparation.^{48,49} Condensation of methallyl alcohol with CDI according to Sarpong's protocol⁵⁰ provided acylimidazole **312** (Scheme 3.15). The addition of this compound to a solution of the lithium enolate of **147**⁵¹ led to successful installation of the ester functionality. Subsequent addition of methyl iodide to the reaction afforded β -ketoester **313** in 82% yield in an efficient and improved tandem acylation/alkylation process. In this manner, we prepared α,α -difunctionalized β -ketoester **313** on greater than 10 g scale.

Scheme 3.15. Improved Acylation and Alkylation of Vinylogous Ester **147**



With a robust and expedient route to methallyl β -ketoester **313**, the evaluation of the asymmetric alkylation and ring contraction reactions became the next focus (Scheme 3.16). Using our Pd-catalyzed asymmetric alkylation conditions^{42,47,52} with (*S*)-*t*-Bu-PHOX (**13**)^{53,54} and Pd₂(pmdba)₃⁵⁵ in toluene at 30 °C, chiral vinylogous ester **314** could be obtained in 98% yield and 89% ee.^{56,57,58} LiAlH₄ reduction proceeded smoothly to give β -hydroxyketone **315** in 96% yield. Ring contraction with LiOH and TFE in THF at 60 °C led to the desired methyl/methallyl acylcyclopentene **308** in 96% yield. In this manner, multigram quantities of the essential chiral intermediate were readily obtained.

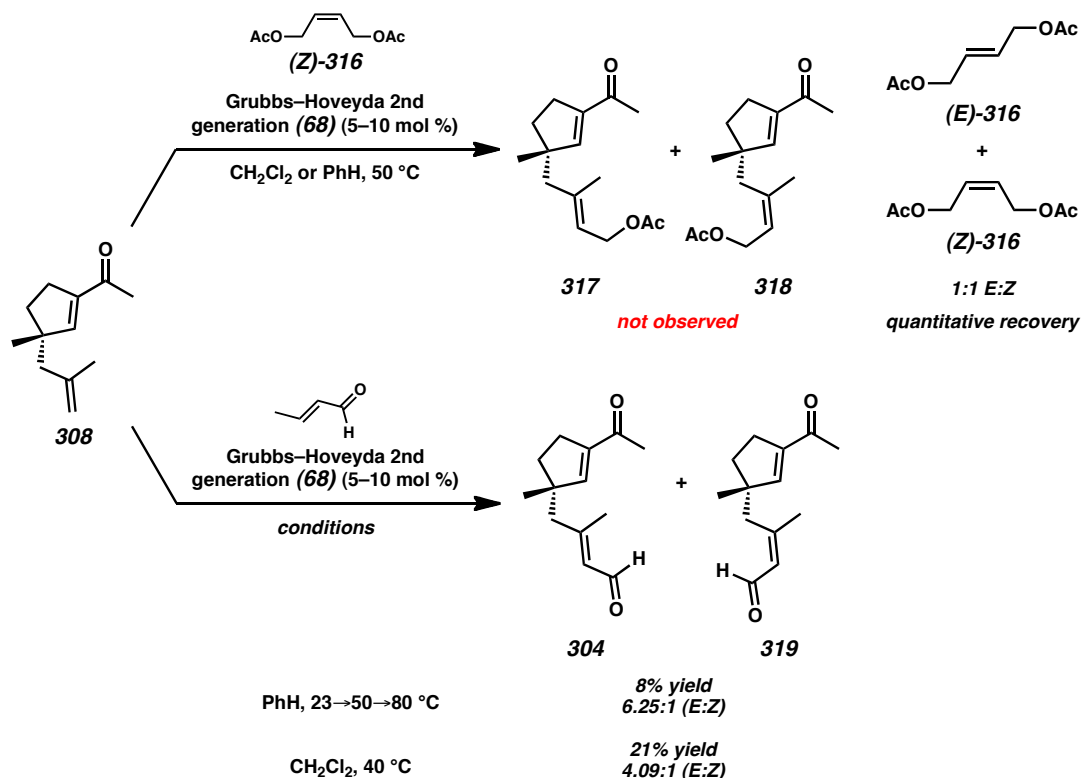
Scheme 3.16. Asymmetric Alkylation and Ring Contraction Sequence with β -Ketoester **313**



To advance toward Diels–Alder precursor **306**, we envisioned that we could perform olefin cross-metathesis with methyl/methallyl acylcyclopentene **308** and *cis*-1,4-diacetoxy-2-butene ((*Z*)-**316**) or crotonaldehyde in a manner analogous to our previous studies (Scheme 3.14). We expected that transformation would be challenging due to the

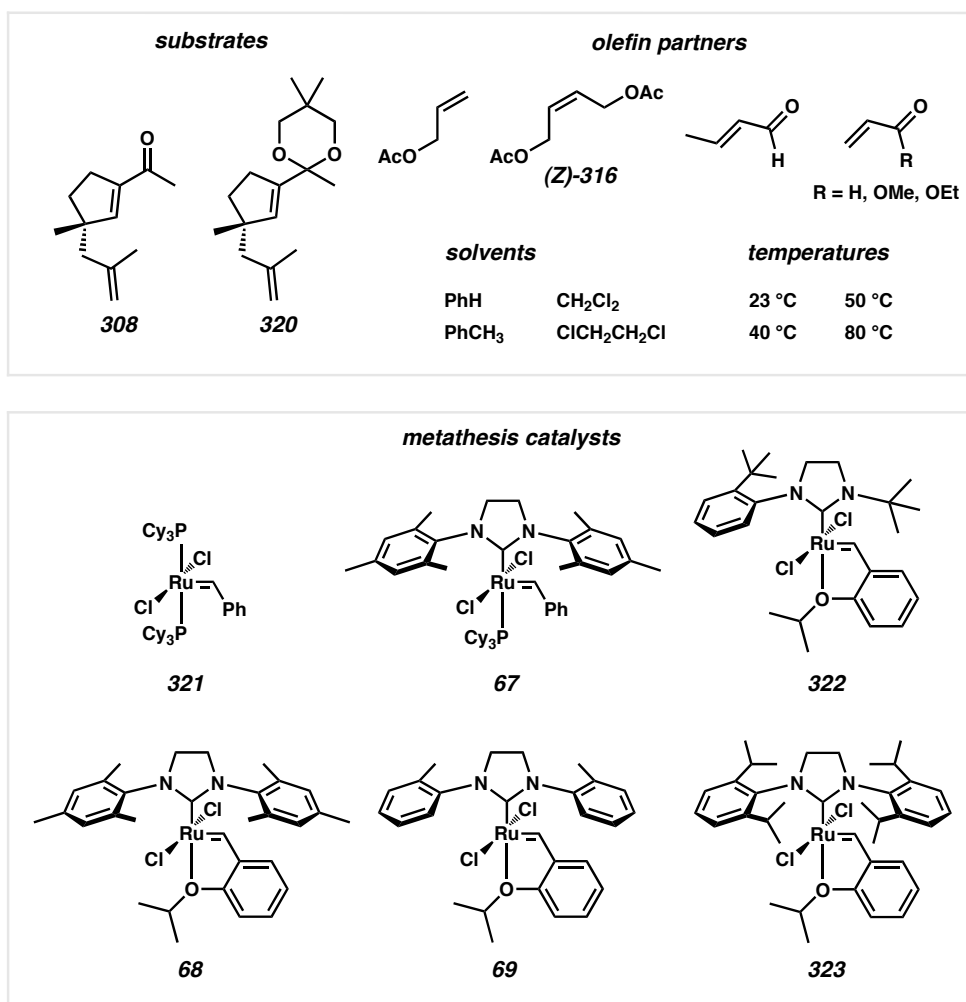
1,1-disubstituted olefin, but relevant examples have been documented⁵⁹ and the simplicity and efficiency of the approach was attractive (Scheme 3.17). Unfortunately, treatment of acylcyclopentene **308** with *cis*-1,4-diacetoxy-2-butene ((*Z*)-**316**) and Grubbs–Hoveyda 2nd generation catalyst (**68**, 5–10 mol %) in CH₂Cl₂ or benzene provided no trace of the desired metathesis products. Under similar reaction conditions with crotonaldehyde as the olefin partner, a mixture of enone-enal olefin isomers **304** and **319** could be obtained in 8% yield and 6.25:1 *E:Z* ratio. The reaction mixture primarily consisted of starting material that could not be separated from overlapping impurities. Employing CH₂Cl₂ as the reaction solvent led to a slight increase in reaction yield, but the efficiency of the transformation remained impractical for synthetic purposes.

Scheme 3.17. Examples of Attempted Cross-Metathesis Reactions with Acylcyclopentene **308**



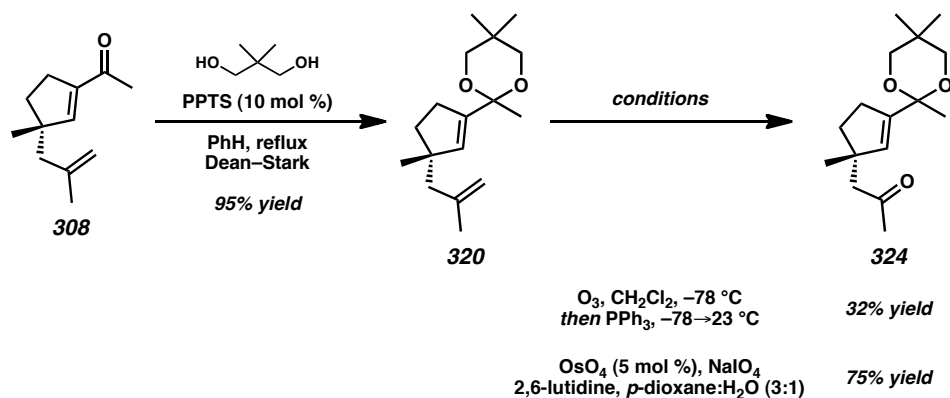
While additional ruthenium-based catalysts (**321–323**) were evaluated in the two cross metathesis reactions, none of these offered any improvement (Figure 3.6). The investigation of carbonyl-protected substrates, alternative olefin partners, and additional solvents and temperatures provided similarly intractable results. Given the difficulty of the desired cross-metathesis reactions with the key 1,1-disubstituted olefin, we refocused our efforts on more traditional olefination strategies to obtain IMDA precursor **306**.

Figure 3.6. Summary of Attempted Cross-Metathesis Reactions



As an alternative approach, we envisioned that olefination reactions could be achieved through a suitable ketone derivative of methallyl acylcyclopentene **308** (Scheme 3.18). Efforts in this regard proceeded with ketalization of the carbonyl functionality with neopentyl glycol and PPTS in benzene under Dean–Stark conditions. Subsequent ozonolysis of the methallyl group was possible, but the results varied with reaction scale and the desired product **324** could not be isolated in greater than 32% yield. Better results were obtained with modified Lemieux–Johnson conditions⁶⁰ for Os-catalyzed oxidative olefin cleavage. Under these conditions, methyl ketone **324** could be obtained in 75% yield.

Scheme 3.18. Synthesis of Methyl Ketone **324**

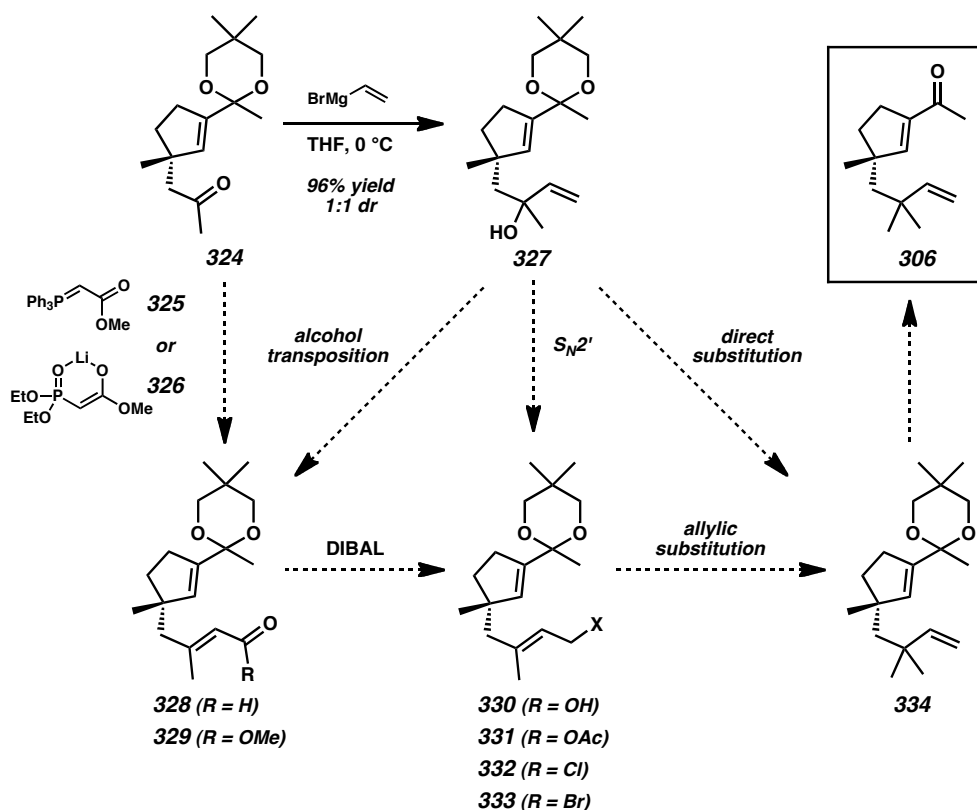


With our desired ketone, we applied a variety of olefination reactions with the goal of obtaining compounds that could be advanced to target acylcyclopentene **306** (Scheme 3.19). The addition of Wittig reagent **325** in excesses of greater than 25 equivalents led to no observable consumption of starting material. A variety of Horner–Wadsworth–

Emmons conditions⁶¹ were also attempted, but the desired product could not be obtained. This lack of reactivity suggests that the highly congested steric environment or competitive deprotonation of methyl ketone in **324** hampers phosphorous ylide olefination reactions.

An alternative organometallic addition strategy⁶² was explored to introduce the necessary carbon fragments for the planned IMDA reaction (Scheme 3.19). Using vinylmagnesium bromide, tertiary allylic alcohol **327** was obtained in 96% yield and 1:1 dr. The installation of the remaining methyl group was needed to proceed toward desired acylcyclopentene **306**.

Scheme 3.19. Various Attempts to Prepare Acylcyclopentene **306**



A variety of redox-neutral and oxidative allylic transposition reactions were attempted to convert tertiary allylic alcohol **327** to acylcyclopentene **306** (Scheme 3.19).^{63,64} The application of Re-catalyzed allylic alcohol isomerization conditions⁶⁵ did not provide any trace of the isomeric primary allylic alcohol **330**. Cr-based oxidative transpositions⁶⁶ with PCC or PDC also failed to give expected rearranged enal products, instead leading to eventual decomposition.⁶⁷ Reported sulfur-mediated transformations⁶⁸ under Parikh–Doering oxidation conditions⁶⁹ also provided no signs of the desired rearrangement.⁶⁷ Attempted oxygen transposition by the action of oxoammonium salts⁷⁰ led to the formation of intractable side products.⁶⁷

To supplement our studies with allylic transposition reactions, we also explored the in situ activation of tertiary alcohol **327** followed by S_N2' reactions with halide⁷¹ or carboxylate nucleophiles⁷² to arrive directly at allyl electrophiles such as **331–333** (Scheme 3.19). Activators such as oxalyl chloride, sulfonyl chloride, acetic anhydride, and trifluoroacetic anhydride were investigated in buffered and non-buffered reaction conditions, but these conditions proved to be incompatible with the sensitive ketal functionality.⁶⁷

Attempts to substitute the tertiary alcohol of **327** with a methyl group and directly obtain *gem*-dimethyl **334** also proved unsuccessful. The application of reported methylations with TiCl₂Me₂⁷³ or AlMe₃⁷⁴ only led to the destruction of starting material.

3.3.4 SUMMARY AND OUTLOOK

The cascade conjugate addition/Robinson annulation approach to the tricyclic core of the presilphiperfolanols was explored with a simple model system based on methyl/allyl

acylcyclopentene **135a**. Preliminary results suggested that the desired transformation would be challenging on the basis of unfavorable conformational restrictions. An alternative intramolecular Diels–Alder strategy was also investigated. The successful extension of our asymmetric alkylation/ring contraction methodology led to methyl/methallyl acylcyclopentene **308**. Numerous attempts to convert this compound to acylcyclopentene **306** proved unsuccessful. In order to arrive at modified acylcyclopentene **306**, a new approach was urgently needed to continue to the synthesis of the presilphiperfolanols.

3.4 TOTAL SYNTHESIS OF (–)-PRESILPHIPERFOLAN-1 β -OL AND RELATED ANALOGS

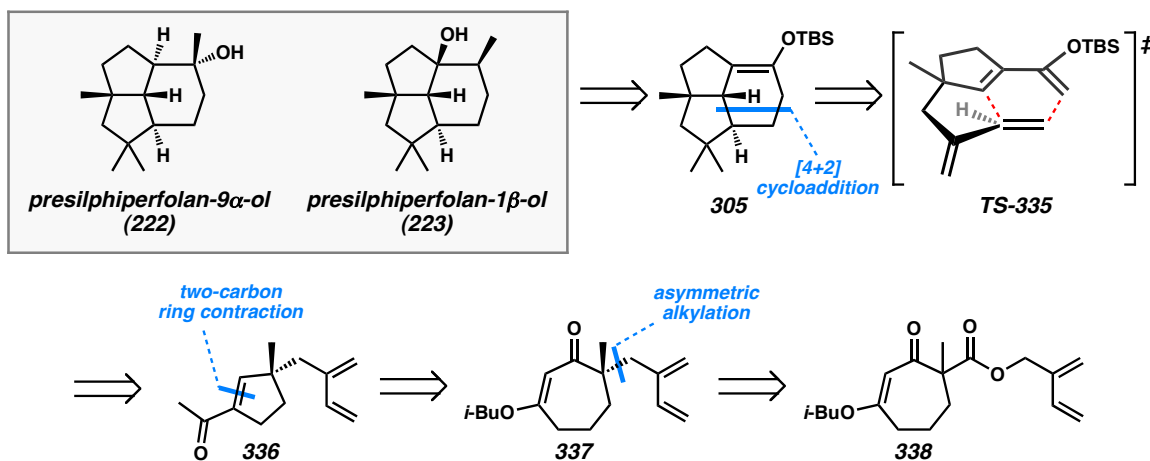
While the application of our asymmetric alkylation and ring contraction strategy for the synthesis of γ -quaternary acylcyclopentenones (**135**)⁴² appeared to be a promising method for the preparation of the presilphiperfolanols, additional modification of our synthetic approach would be necessary to complete the polycyclic natural products.

3.4.1 REVISED RETROSYNTHETIC ANALYSIS

Our synthetic approach based on methyl/methallyl acylcyclopentene **308** proved to be scalable and efficient, but ultimately, attempts to install the necessary carbon fragments for our planned IMDA reaction were unsuccessful. To overcome the obstacles in our previous synthetic route, we envisioned that methyl/isoprenyl acylcyclopentene **336** could allow us to test the key [4+2] cycloaddition reaction through alternative means. By

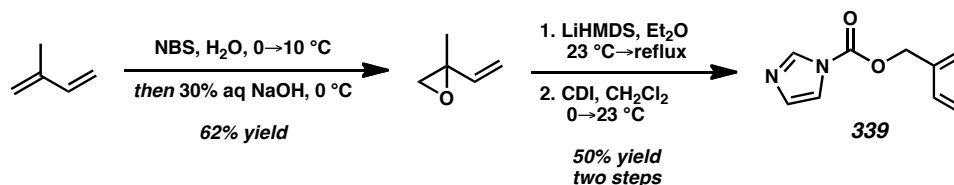
postponing the installation of the *gem*-dimethyl functionality to a later stage of the synthesis, we believed we could pursue simpler, less-substituted cyclization precursors such as acylcyclopentene **336**. The exploration of this modified strategy would require enantioenriched vinylogous ester **337**, which would arise from the unprecedented asymmetric alkylation of a 2-vinyl π -allyl electrophile.⁷⁵

Scheme 3.20. Retrosynthetic Analysis of Presilphiperfolanol Natural Products



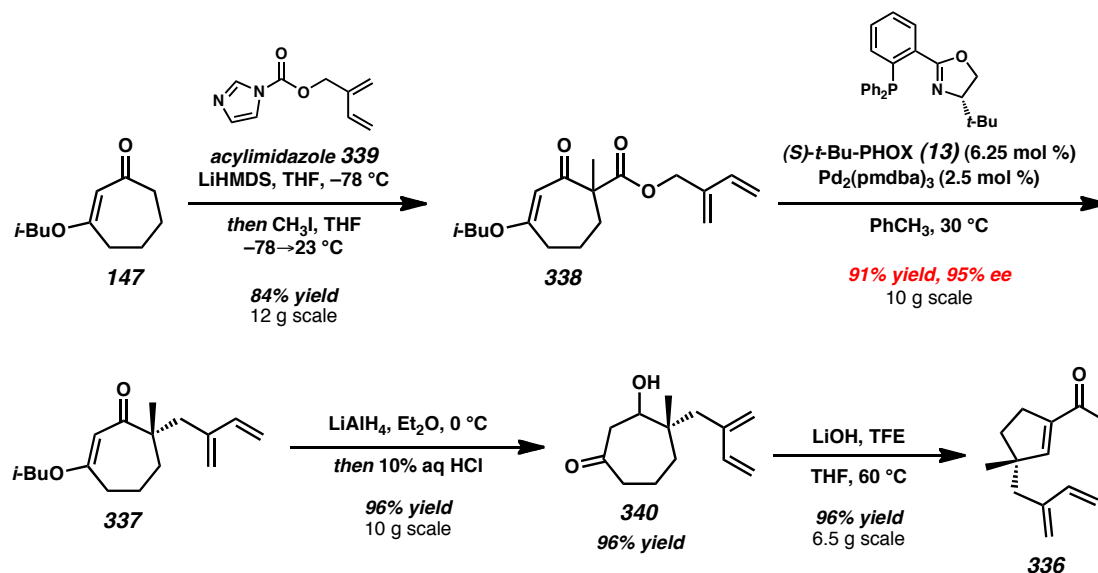
3.4.2 ASYMMETRIC ALKYLATION AND RING CONTRACTION

Our synthetic efforts began with the synthesis of a suitable isoprenol-containing acylating reagent (Scheme 3.21). By adapting the method of Isobe, the selective monoepoxidation of isoprene and base-mediated isomerization to isoprenol was achieved on 10 g scale.⁷⁶ Trapping of the intermediate alcohol with CDI according to the method of Sarpong as before led to the novel acylimidazole **339**.⁵⁰

Scheme 3.21. Synthesis of Isoprenol-Derived Acylimidazole **339**

The successful preparation of isoprenol-derived carbamate **339** enabled us to proceed toward asymmetric alkylation substrate **338** (Scheme 3.22). Commercial 3-isobutoxycycloheptenone **147**⁵¹ underwent acylation/alkylation with reagent **339** and methyl iodide under basic conditions to afford β -ketoester **338** in 84% yield. With the functionalized allyl fragment in place, the asymmetric Pd-catalyzed decarboxylative alkylation^{42,47} of this novel substrate could be performed. Although numerous allyl electrophiles have been employed in these types of reactions, the conjugated diene was recognized as a potential liability for detrimental side reactions under palladium catalysis.⁷⁷

Gratifyingly, treatment of β -ketoester **338** with catalytic Pd₂(pmdba)₃⁵⁵ and (*S*)-*t*-Bu-*PHOX*^{53,54} in toluene afforded isoprenylated vinylogous ester **337** in 91% yield and 95% ee on 10 g scale.^{56,57} Subsequent LiAlH₄ reduction afforded an intermediate β -hydroxyketone, which underwent a base-mediated two-carbon ring contraction to provide acylcyclopentene **336** in 92% yield over two steps.^{42,78}

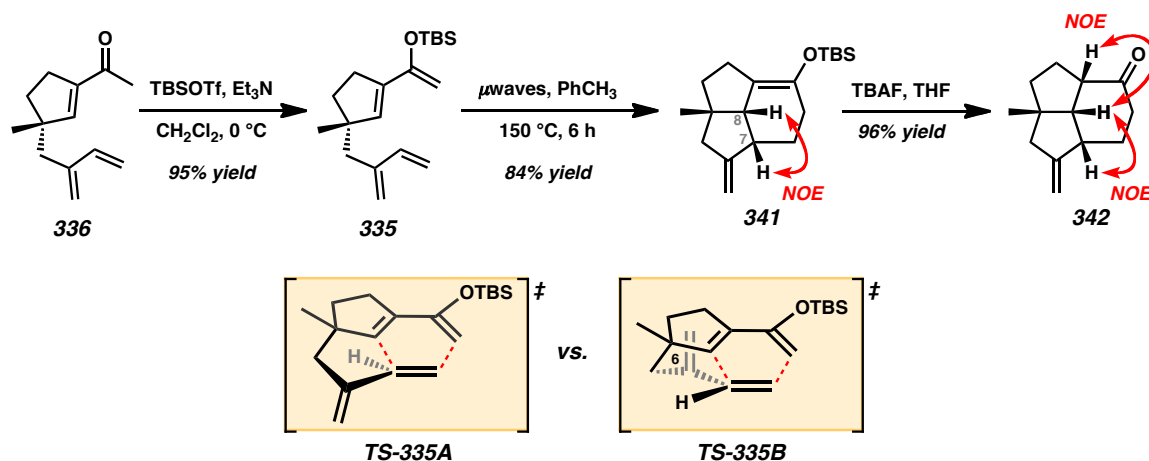
Scheme 3.22. Asymmetric Alkylation and Ring Contraction Sequence with β -Ketoester **338**

3.4.3 INTRAMOLECULAR DIELS–ALDER STUDIES

With methyl/isoprenyl acylcyclopentene **336** in hand, straightforward conversion to the corresponding silyl dienol ether **335** enabled examination of our IMDA strategy^{79,80} (Scheme 3.23). We postulated that the reaction would presumably proceed through transition state **TS-335 A** to minimize steric interactions between the dienophile tether the cyclopentene ring. While this was our desired outcome, we recognized that additional undesired IMDA cycloadducts could be formed due to the presence of two different dienes in the substrate. When silyl dienol ether **335** was subjected to microwave irradiation in toluene at 150 °C, the IMDA reaction proceeded efficiently to give tricycle **341** in 80% yield over two steps as a single diastereomer. The bicyclization notably proceeded without the need for an activated dienophile.⁸¹ Subsequent NOESY experiments on cycloadduct **341** revealed the *cis* relationship of the C(7) and C(8) hydrogens. Desilylation of silyl enol ether **341** provided ketone **342**, which allowed

further stereochemical confirmation. These results suggest that the IMDA primarily proceeds through **TS-335B** rather than the desired and expected **TS-335A**.⁸² Secondary orbital overlap in the IMDA transition state could be a possible reason for the outcome in this case. Unfortunately, in order to advance toward the presilphiperfolanol natural products, a *trans* relationship was needed.

Scheme 3.23. IMDA Reaction on Substrate **335**

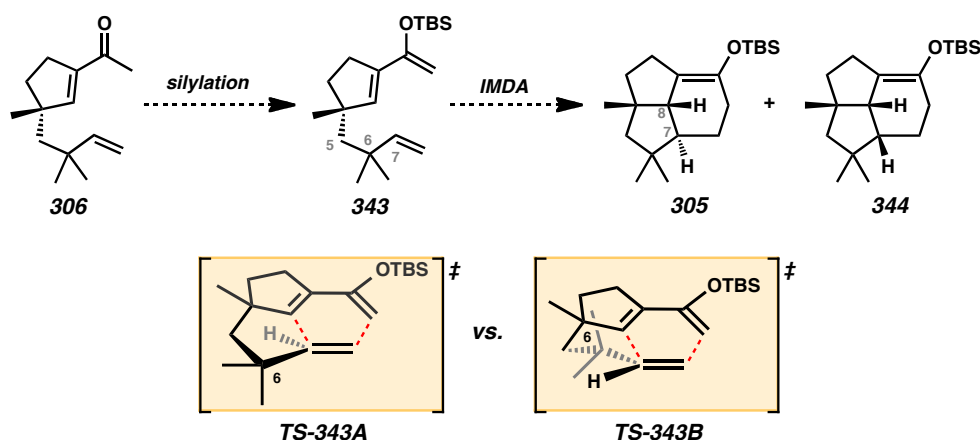


3.4.4 ELABORATION OF METHYL/ISOPRENYL ACYLCYCLOPENTENE

Although we succeeded in constructing the tricyclic framework of the presilphiperfolanols in six steps from commercial materials, we needed to modify our synthetic route to achieve the naturally occurring substitution and stereochemical configurations. Our revised strategy aimed to install the *gem*-dimethyl group at an earlier stage and test our original synthetic approach with acylcyclopentene **306** (Scheme 3.12). Analysis of the possible IMDA transition states of silyl dienol ether **343** suggested that the desired *trans* product should be favored due to the increased steric interactions with

the C(6) *gem*-dimethyl groups (Scheme 3.24).⁸³ In **TS-343A**, the steric elements would be oriented away from the bond-forming centers while cycloaddition through **TS-343B** could only proceed with severe steric clash between the cyclopentene ring and the *gem*-dimethyl functionality. Additionally, the sp^3 hybridization at the C(6) position should decrease the C(5)-C(6)-C(7) bond angle while also providing greater conformational bias⁸⁴ for the desired cyclization. Furthermore, secondary orbital interactions that may be operative in **TS-335B** would no longer apply in the planned IMDA reaction. With these motivating factors, we set out to test our modified IMDA strategy.

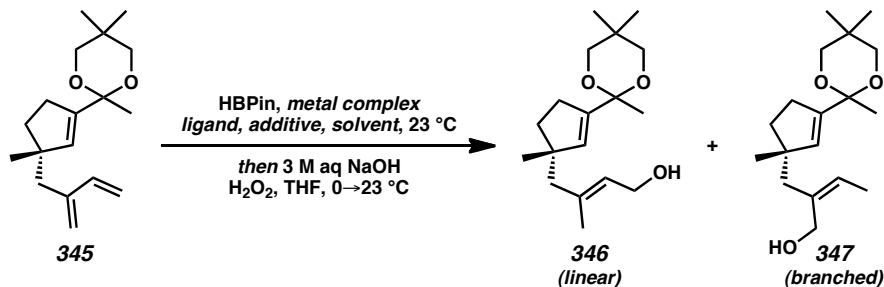
Scheme 3.24. Planned IMDA Reaction on Substrate **343**



The synthesis of the requisite acylcyclopentene **306** proceeded with the ketalization of acylcyclopentene **336** under Dean–Stark conditions (Scheme 3.25). A subsequent regioselective 1,4-hydroboration/oxidation of the sterically hindered substrate **345** was expected to provide desired allylic alcohol **346**. A survey of the chemical literature revealed that Pd,⁸⁵ Fe,^{86a} and Ni⁸⁷ can promote transformation, but iron catalysis demonstrated the best selectivity for our substrate type with 2-substitution of the 1,3-

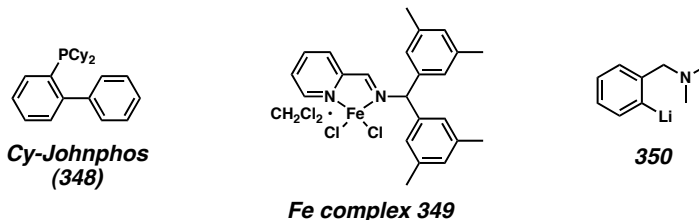
diene. A systematic screen of 1,4-hydroboration reactions with these three transition metals provided the results summarized in Table 3.1.^{88,89} To our surprise, the Ritter $\text{FeCl}_2(\text{py-imine})$ catalyst system provided a disappointing 1.1:1 ratio of linear:branched products **346** and **347** (entries 1 and 2).^{86a} Investigation of Suzuki–Miyaura conditions with $\text{Pd}(\text{PPh}_3)_4$ and HBPIn did not provide any reactivity (entries 3 and 4).⁸⁵ Finally, we turned to Morken's $\text{Ni}(\text{cod})_2/\text{PCy}_3$ catalyst system.⁸⁷ Gratifyingly, these conditions led to a more desirable 3:1 ratio of linear:branched products (entries 5 and 6).⁹⁰ The investigation of other monodentate ligands such as $\text{P}(\text{NMe}_2)_3$ and Cy-JohnPhos led to similar product ratios but in lower combined yields (entries 7 and 8). The bulkier ligand Pt-Bu_3 was the only phosphine that provided improved results, products in a significantly improved 8.3:1 ratio (linear:branched). This result can be rationalized based on the selective formation of the less sterically hindered Ni π -allyl intermediate. Despite this increase in selectivity, the 57% combined yield for the reaction diminished the applicability of the transformation (entries 9 and 10). Based on these results, we proceeded with the $\text{Ni}(\text{cod})_2$ and PCy_3 conditions, which provided the highest quantity of desired allylic alcohol **346**.

Table 3.1. Metal-Catalyzed 1,4-Hydroboration/Oxidation Screen



entry	metal complex (mol %)	ligand or additive (mol %)	solvent	time (h)	yield (%) ^c	<i>l</i> : <i>b</i> ^d
1 ^a	Fe complex 349 (8%)	Mg powder (16%)	Et ₂ O	42	0	n.d.
2 ^a	Fe complex 349 (4%)	aryllithium 350 (8%)	Et ₂ O	10	62	1.1 : 1
3 ^b	Pd(PPh ₃) ₄ (5%)	—	PhH	41	0	n.d.
4 ^b	Pd(P ^{<i>t</i>} -Bu) ₃ (5%)	—	PhH	41	< 5	n.d.
5 ^b	Ni(cod) ₂ (5%)	PCy ₃ (5%)	PhCH ₃	52	89	3.0 : 1
6 ^b	Ni(cod) ₂ (10%)	PCy ₃ (10%)	PhCH ₃	9.5	89	3.2 : 1
7 ^b	Ni(cod) ₂ (5%)	Cy-Johnphos (348) (5%)	PhCH ₃	6.5	50	3.1 : 1
8 ^b	Ni(cod) ₂ (5%)	P(NMe ₂) ₃ (5%)	PhCH ₃	6.5	14	2.8 : 1
9 ^b	Ni(cod) ₂ (5%)	P ^{<i>t</i>} -Bu ₃ (5%)	PhCH ₃	6.5	57	8.3 : 1
10 ^b	Ni(cod) ₂ (10%)	P ^{<i>t</i>} -Bu ₃ (10%)	PhCH ₃	9.5	60	9.0 : 1

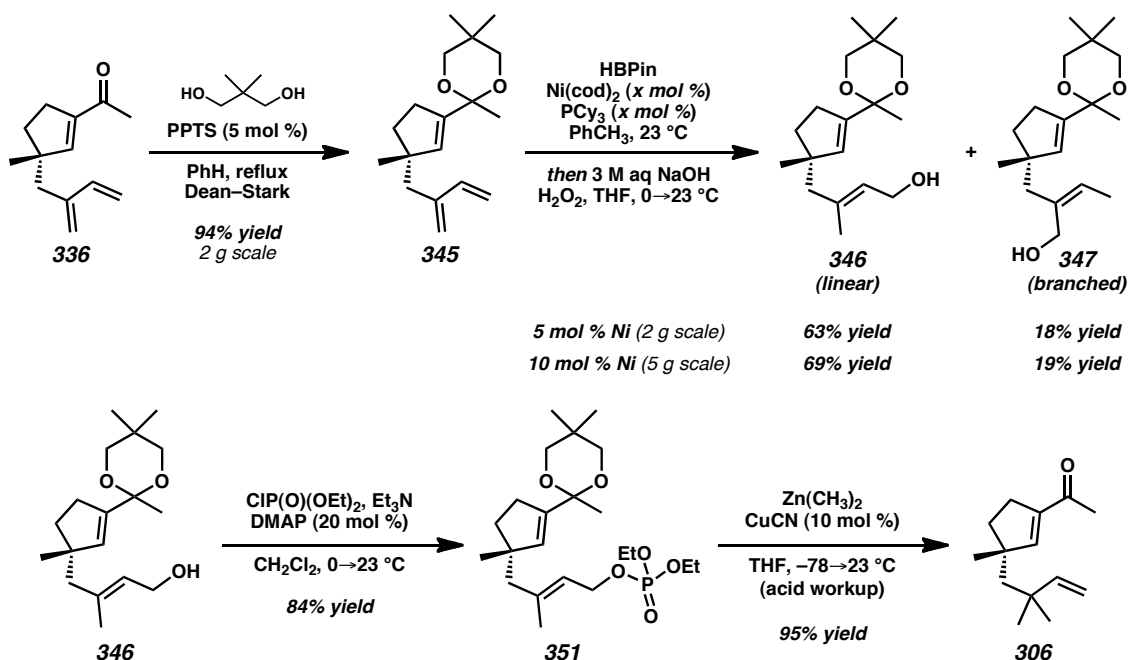
^a Conditions: 1,3-Diene (1.0 equiv), pinacolborane (1.50 equiv), metal complex (x mol %), additive (2x mol %) in solvent (0.15 M) at indicated 23 °C in a N₂-filled glove box. ^b Conditions: 1,3-Diene (1.0 equiv), pinacolborane (1.05 equiv), metal complex (x mol %), ligand (x mol %) in solvent (0.1 M) at 23 °C in a N₂-filled glove box. ^c Combined isolated yield of **346** and **347**. ^d Ratio of linear : branched allylic alcohols **346** and **347**, determined by relative integration by ¹H NMR.



The preparative scale reaction of 1,3-diene **345** with Ni(cod)₂/PCy₃ (5 mol %) and HBPIn followed by an oxidative workup provided the separable allylic alcohols **346** and **347**⁹¹ in 81% combined yield in a 3.5:1 ratio (linear:branched). Doubling the catalyst loading led to a decrease in reaction time and a small improvement to 88% combined yield, supplying us with ample quantities of our compound **346**. To our knowledge, this is the first application of a regioselective metal-catalyzed 1,4-hydroboration in the context of total synthesis. Subsequent phosphorylation and regioselective Cu-catalyzed

allylic substitution^{92,93} provided the requisite *gem*-dimethyl acylcyclopentene **306** in 80% yield over two steps after acidic workup.

Scheme 3.25. Modification of Acylcyclopentene **336** and Synthesis of Silyl Dienol Ether **343**

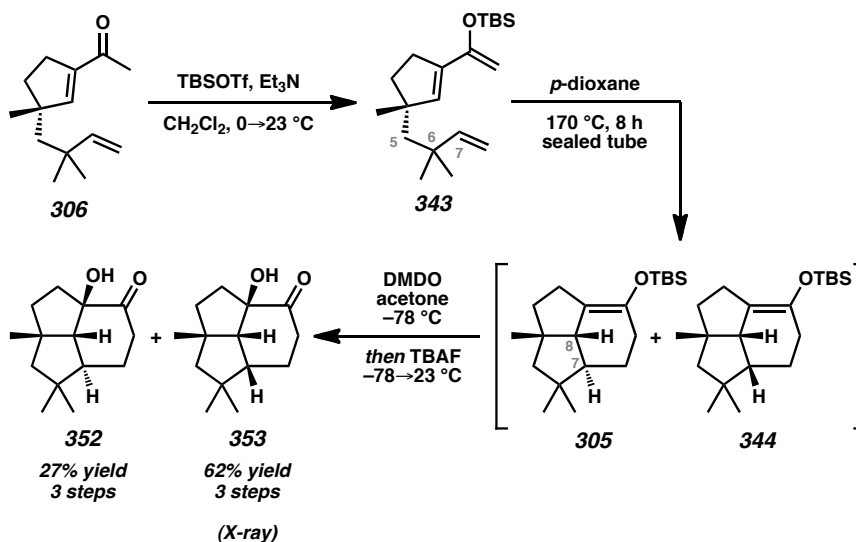


3.4.5 FURTHER INTRAMOLECULAR DIELS–ALDER STUDIES

With *gem*-dimethyl acylcyclopentene **306** in hand, silyl dienol ether formation⁹⁴ and IMDA bicyclization proceeded smoothly under thermal or microwave-assisted conditions to provide a mixture of inseparable diastereomers **305** and **344**. A highly diastereoselective Rubottom oxidation of these products with DMDO⁹⁵ followed by the addition of TBAF⁹⁶ provided α -hydroxyketones **352** and **353** in a 1:2 ratio as determined by ¹H NMR spectroscopy.^{97,98} Chromatographic separation gave **352** in 27% yield and **353** in 61% yield over three steps. The structure of tricycle **353** was confirmed by single-

crystal X-ray analysis (Figure 3.7).⁹⁹ To our surprise, although *trans-cis* α -hydroxyketone **352** was observed, the major product **353** was again derived from the more sterically congested IMDA transition state (**TS-343B**) (Scheme 3.24). The results of both IMDA reactions indicate that the desired *trans* stereochemical configuration of the desired tricyclic IMDA cycloadducts could be thermodynamically unfavorable. Optimization of the IMDA/oxidation sequence was briefly investigated.¹⁰⁰ Lower temperatures were investigated for the IMDA reaction. At temperatures as low as 90 °C, the IMDA proceeded smoothly but longer reaction times were required and lower dr was typically observed.⁸⁸ The use of *m*-CPBA as an alternative oxidant led to decreased overall yield in the Rubottom oxidation.⁸⁸

Scheme 3.26. IMDA/Rubottom Oxidation with Silyl Dienol Ether **343**



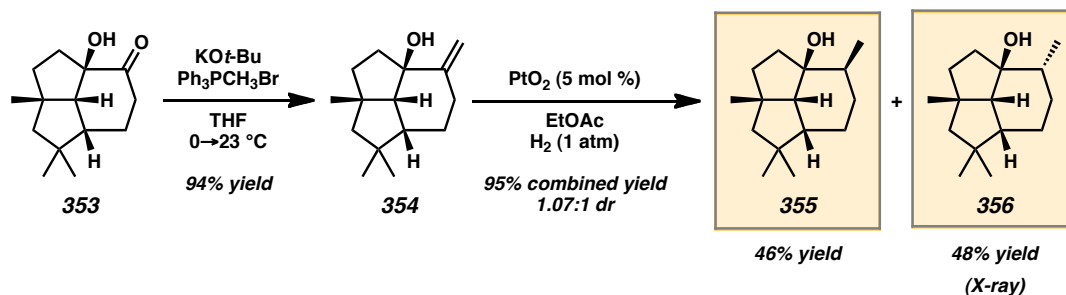
Concurrent with our thermal cyclization studies, we also tried to promote a more diastereoselective IMDA cyclization of silyl dienol ether substrate **343** using alternative

catalytic methods. The investigation of transition metal-catalyzed cycloisomerization reactions, particularly those catalyzed by Rh¹⁰¹ and Ni,¹⁰² led to no reaction. Additionally, the application of radical cation [4+2] cycloaddition protocols¹⁰³ proved unsuccessful as only desilylation could be observed, returning acylcyclopentene **306** in 60% yield.

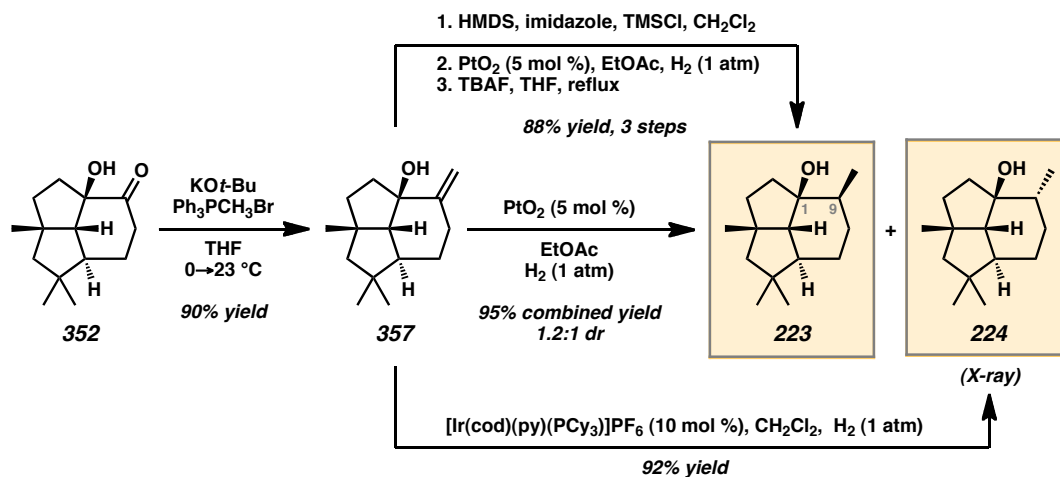
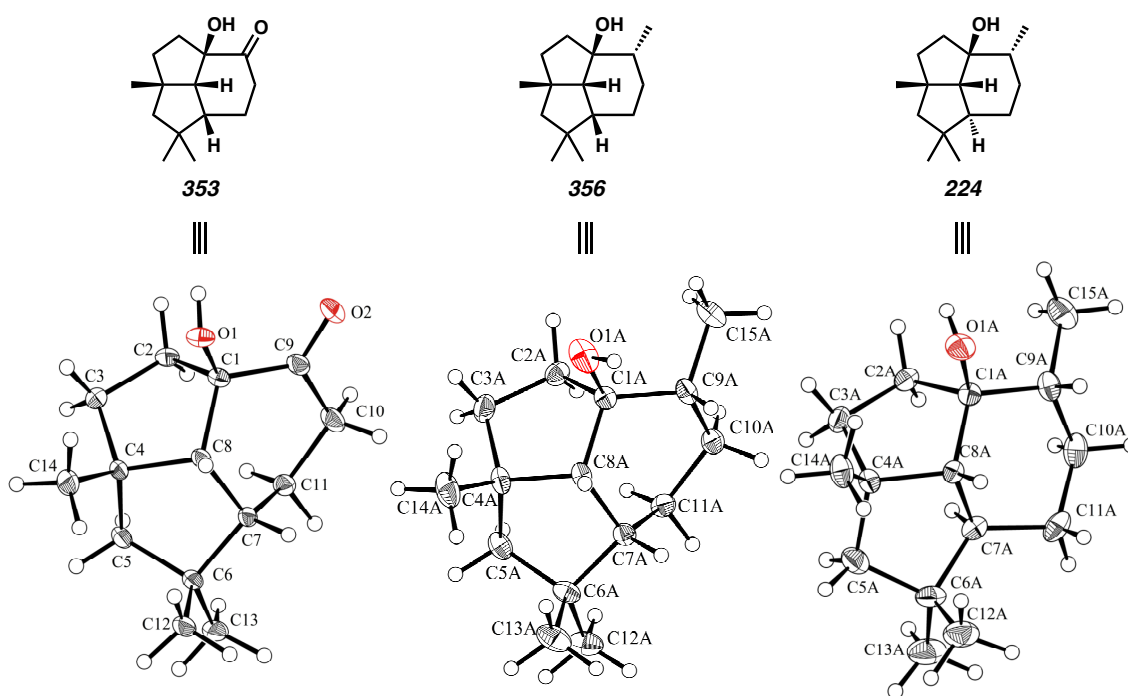
3.4.6 COMPLETION OF (–)-PRESILPHIPERFOLAN-1 β -OL AND UNNATURAL ANALOGS

After obtaining α -hydroxyketones **352** and **353**, we aimed to advance these intermediates to presilphiperfolanol natural products (Scheme 3.27). Wittig methylenation of compound **353** proceeded smoothly in 94% yield. After a brief survey of heterogeneous hydrogenation catalysts,¹⁰⁴ PtO₂ proved to be effective for the reduction of allylic alcohol **354**,¹⁰⁵ providing a mixture of diastereomers **355** and **356** in a 1.07:1 ratio. Chromatographic separation by flash column chromatography provided **355** in 46% yield and **356** in 48% yield. The structure of **356** was confirmed by single-crystal X-ray diffraction (Figure 3.7).⁹⁹

Scheme 3.27. Wittig Methylenation and Hydrogenation of α -Hydroxyketone **353**

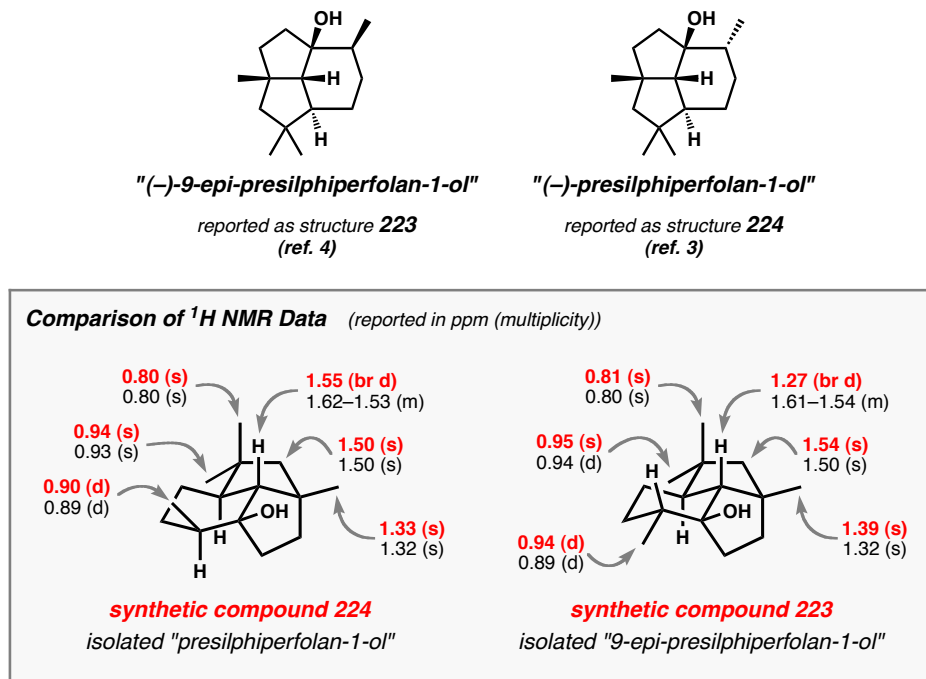
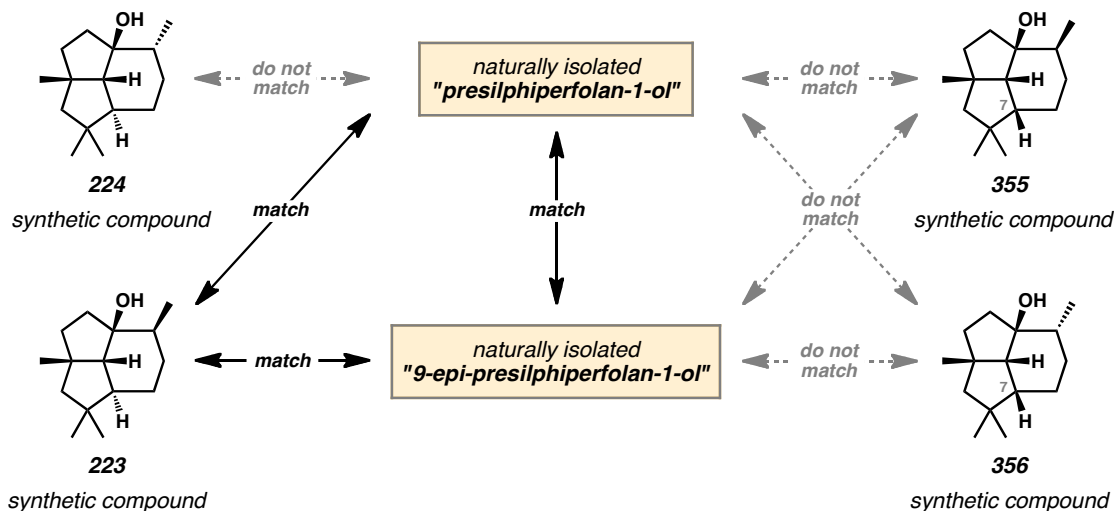


Similar transformations enabled the conversion of α -hydroxyketone **352** to presilphiperfolanol structures. Wittig methylenation proceeded efficiently to give allylic alcohol **357** in 90% yield (Scheme 3.28). While PtO_2 -catalyzed hydrogenation of olefin **357** afforded a HPLC-separable mixture of targets **223** and **224**, a diastereoselective synthesis of both target molecules could also be achieved. Tertiary alcohol-directed hydrogenation with Crabtree's catalyst^{106,107} produced 9 α -presilphiperfolan-1 β -ol **224**, the reported structure of "presilphiperfolan-1-ol,"³ in 92% yield. The structure of **224** was verified by X-ray diffraction (Figure 3.7).⁹⁹ Alternatively, efficient formation of 9 β -presilphiperfolan-1 β -ol **223**, the reported structure of "9-*epi*-presilphiperfolan-1-ol,"⁴ was accomplished in 88% yield over three steps by silylation¹⁰⁸ of tertiary allylic alcohol **223** followed by PtO_2 -catalyzed hydrogenation and desilylation with TBAF. Upon completing tricyclic alcohols **223** and **224**, we believed that had completed the total synthesis of the two reported presilphiperfolanol natural products, but careful inspection of the spectral data for the synthetic compounds provided evidence for a structural misassignment and the prompted the development of a new biosynthetic hypothesis.

Scheme 3.28. Wittig Methylenation and Hydrogenation of α -Hydroxyketone **352**Figure 3.7. X-ray Crystal Structures of Compounds **353**, **356**, and **224**

3.4.7 **STRUCTURAL REVISION AND PROPOSED BIOSYNTHESIS OF (–)-PRESILPHIPERFOLAN-1 β -OL**

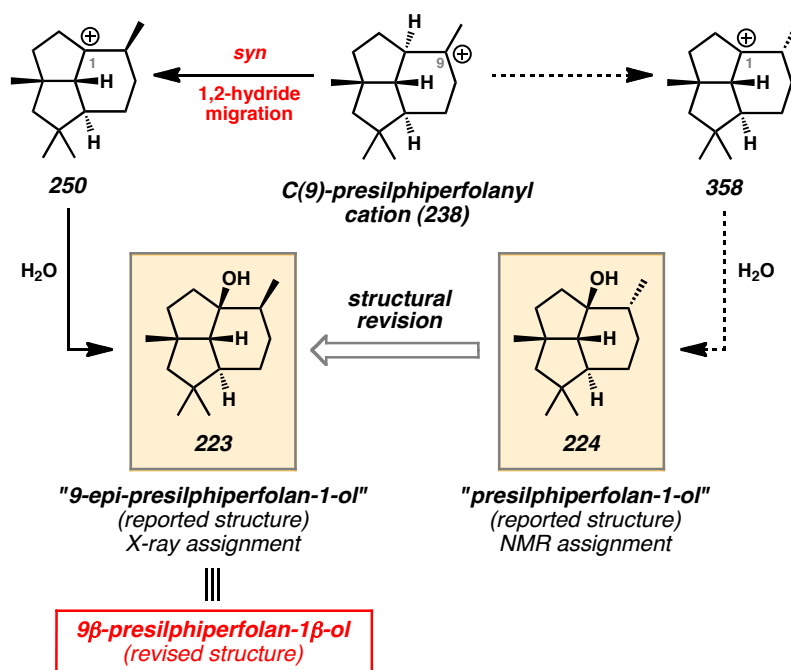
Upon completing the syntheses of **355**, **356**, **223**, and **224**, we compared our spectral data to the reported data for the naturally isolated presilphiperfolanols⁸⁸ (Figure 3.8). Natural “presilphiperfolan-1-ol”^{3,109} was assigned structure **224**¹¹⁰ based on NMR data while natural “9-*epi*-presilphiperfolan-1-ol”⁴ was assigned structure **223** based on NMR and X-ray data.^{4b} The ¹H and ¹³C NMR spectra of synthetic **223** were in excellent agreement with data for reported “9-*epi*-presilphiperfolan-1-ol” (**223**),⁴ but the spectra for synthetic **224** clearly did not match the data for isolated “presilphiperfolan-1-ol” (**224**).³ In particular, the C(15) methyl hydrogens of synthetic **224** showed a ¹H NMR resonance at 0.94 ppm compared to the corresponding resonance of reported **244**³ at 0.89 ppm. Overall, the spectral data of isolated “presilphiperfolan-1-ol” (**224**) more closely matches synthetic **223** and isolated “9-*epi*-presilphiperfolan-1-ol” **223**^{4a} than synthetic **224** (Figure 3.9). The C(7) epimers **355** and **356** did not match the spectra for either of the reported natural compounds, thereby eliminating these stereochemical configurations as candidate structures for the isolated “presilphiperfolan-1-ol” (**224**) (Figure 3.9).

Figure 3.8. Comparison of ^1H NMR Spectra of Reported and Synthetic **223** and **224**Figure 3.9. Summary of Spectral Comparisons (^1H and ^{13}C NMR)

Given the significant discrepancy between our data and König's data for compound **224**, we sought to rationalize the formation of both **223** and **224** in the context of proposed mechanisms for presilphiperfolanol biosynthesis.^{1,2,5,7,13,14,15,17,18,19} While no

proposals for the biosynthesis of **223** and **224** have been published, it is reasonable that presilphiperfolanols **221–224** are commonly derived from caryophyllenyl cation **237** (Scheme 3.1). Upon rearrangement to C(1)-presilphiperfolanyl cation **238**, a divergent pathway can be envisioned (Scheme 3.29). A simple 1,2-*syn* hydride migration to tertiary C(1)-cation **250** followed by hydration leads to “9-*epi*-presilphiperfolan-1-ol” (**223**) with 9 β -methyl (9*S*) stereochemistry without invoking the intermediacy of unfavorable secondary carbocations.² In contrast to this pathway, the formation of 9 α -methyl-oriented “presilphiperfolan-1-ol” (**224**) seems unlikely since there is no obvious pathway from C(9)-cation **238** to C(1)-cation **358** with 9 α -methyl (9*R*) stereochemistry.

Scheme 3.29. Proposed Biosynthesis of Presilphiperfolan-1 β -ol (**223**) and Structural Revision of Reported “Presilphiperfolan-1-ol” (**223**)



Based on our NMR spectral data, X-ray crystal structure for **224**, and new biosynthetic proposals, we believe the reported structure of natural “presilphiperfolan-1-ol” (**224**) is misassigned at C(9) and most likely is not a natural product. The nearly identical chemical shifts reported for **223** and **224** (Figure 3.9) suggest that the true structure of “presilphiperfolan-1-ol” (**224**) may actually be the same as “9-*epi*-presilphiperfolan-1-ol” (**223**) with the 9 β -methyl configuration (Scheme 3.29). Since the reassignment can potentially lead to confusion, we suggest that the natural product structure represented by **223** be referred to as presilphiperfolan-1 β -ol or the more descriptive names 9 β -presilphiperfolan-1 β -ol or (1*S*,4*S*,7*R*,8*R*,9*S*)-presilphiperfolan-1-ol in future discussions.

3.4.8 SUMMARY AND OUTLOOK

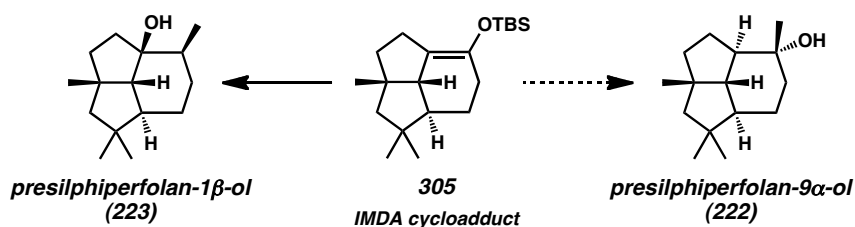
By taking advantage of the highly versatile nature of our asymmetric alkylation and ring contraction approach to versatile γ -quaternary acylcyclopentenones (**135**),⁴² the total syntheses of 9 β -presilphiperfolan-1 β -ol (**223**) and three isomeric analogs **224**, **355**, and **356** were completed. Crucial to this synthetic effort was the application of a Ni-catalyzed 1,4-hydroboration/oxidation reaction and a Cu-catalyzed allylic substitution reaction to provide acylcyclopentene **306**. A subsequent IMDA reaction and Rubottom oxidation secured the tricyclic skeleton of the presilphiperfolanol natural products. Our synthetic efforts also prompted a clarification of reported structural assignments for the naturally isolated “presilphiperfolan-1-ol” (**224**) and “9-*epi*-presilphiperfolan-1-ol” (**223**). With an

effective asymmetric synthetic route in place, we aimed to extend our strategy to access the remaining members of the presilphiperfolanol family.

3.5 PLANNED SYNTHESIS OF (–)-PRESILPHIPERFOLAN-9 α -OL

With the synthesis of 9 β -presilphiperfolan-1 β -ol (**223**) completed, we aim to extend our synthetic approach to access the remaining members of the presilphiperfolanol family. Presilphiperfolan-9 α -ol (**222**) is an attractive target given its structural similarity to presilphiperfolan-1 β -ol (**223**). By diverting IMDA cycloadduct **305** and functionalizing the tricyclic core, the synthesis of alcohol **222** could potentially be achieved in a short and concise sequence.

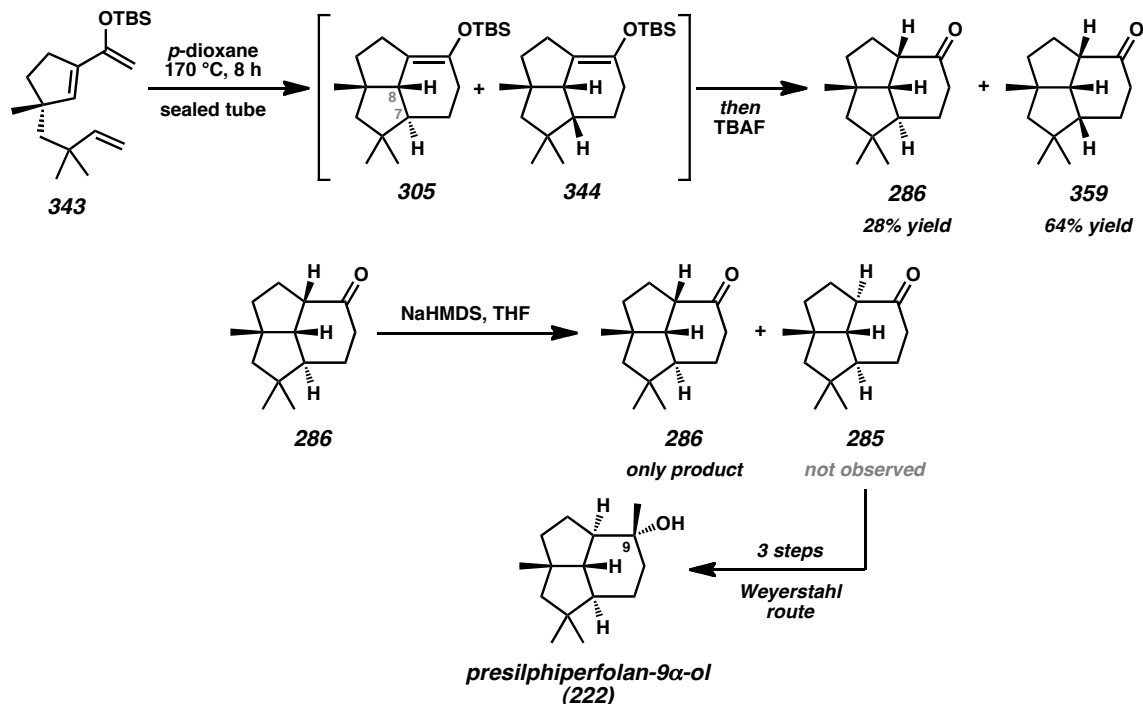
Scheme 3.30. Divergent Strategy for the Preparation of Presilphiperfolan-9 α -ol (**222**)



3.5.1 PROTONATION APPROACH

Synthetic efforts toward this end began with the IMDA cyclization of silyl dienol ether **343** as before followed by desilylation of the intermediate tricycles **305** and **344** with TBAF (Scheme 3.31). Analysis of the crude reaction mixture containing **286** and **359** by ^1H NMR spectroscopy revealed a 1:2.09 ratio of diastereomers for the IMDA

reaction. Following chromatographic separation, ketone **286** was isolated in 28% yield and ketone **359** was isolated in 64% yield. Compound **286** was identical in all respects to the racemic compounds obtained by Weyerstahl⁸ and Piers.³³ Thermodynamic equilibration of ketone **286** using NaHMDS in THF was performed according to Weyerstahl's procedure.⁸ While the desired epimer **285** was expected to be the minor component, successful epimerization would provide isomeric ketone **285** for conversion to presilphiperfolan-9 α -ol (**222**) in only three additional steps (see Section 3.2.2). Unfortunately, the reaction conditions failed to provide observable quantities of epimeric ketone **285**, but additional epimerization conditions can be evaluated. If epimerization proves unsuccessful with numerous bases, our results would be consistent with the observations of Piers³³ (see Section 3.2.3). If the ring strain of the presilphiperfolane tricyclic system disfavors stereochemical inversion at C(1), an alternative synthetic approach with a modified IMDA substrate may be needed to obtain the target compound.

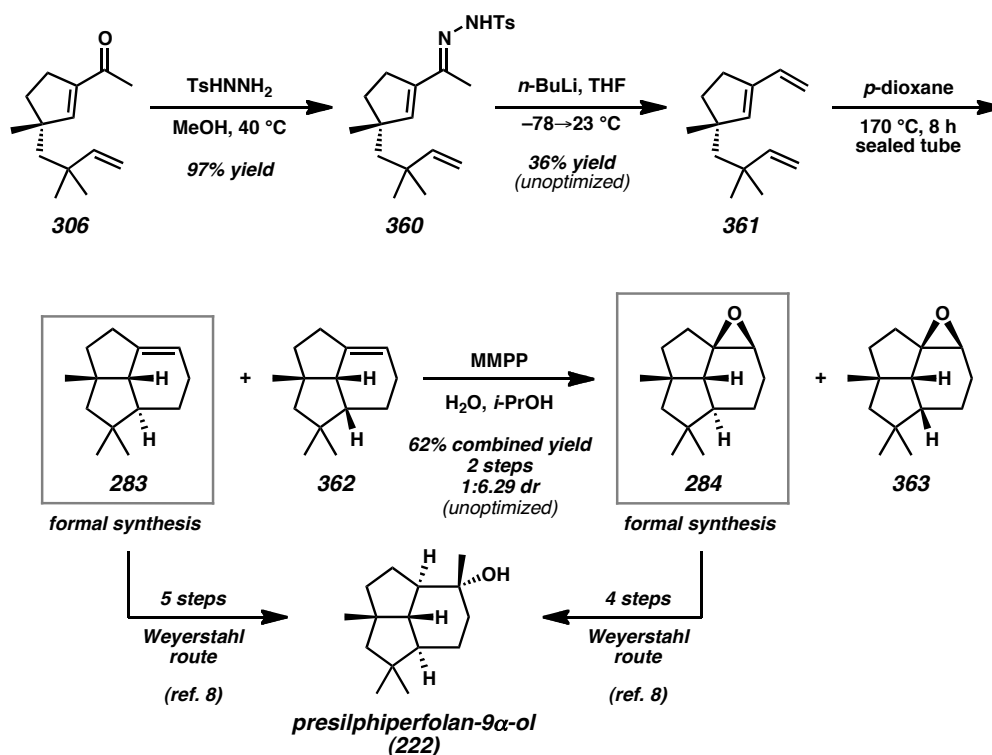
Scheme 3.31. Planned Formal Synthesis of Presilphiperfolan-9 α -ol via IMDA Substrate **343**

3.5.2 MODIFIED IMDA APPROACH

After encountering obstacles in the late-stage modification of the tricycle **305**, we considered a new approach in which the modified triene substrate **361** would be employed in the IMDA reaction (Scheme 3.32). Synthetic studies along this route have been initiated. Following a straightforward tosylhydrazone formation, the application of the Shapiro reaction¹¹¹ provided the modified IMDA cyclization substrate **361** in an unoptimized 36% yield. In future optimization efforts, Bamford–Stevens reaction conditions can also be evaluated.¹¹² Application of typical IMDA reaction conditions with *p*-dioxane as solvent and heating at 170 °C in a sealed tube afforded a mixture of inseparable olefin diastereomers **283** and **362**. Epoxidation of the mixture of olefins with MMPP provided the corresponding epoxides **284** and **363** in 62% combined yield over

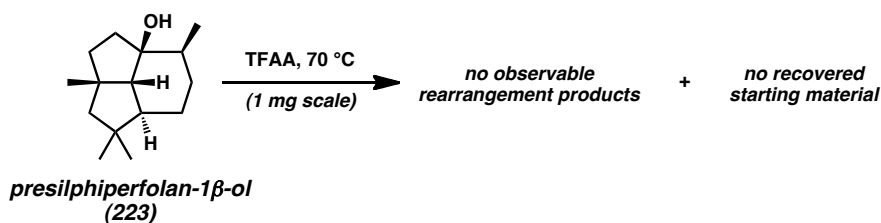
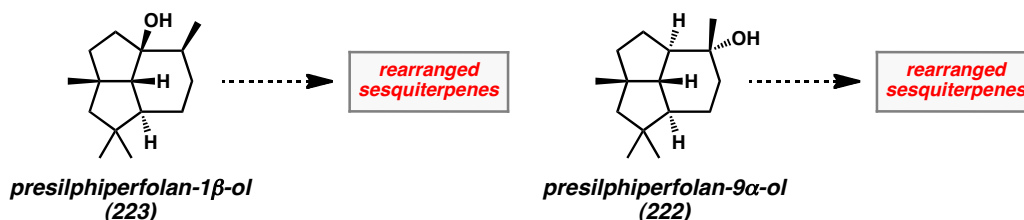
two steps and 1:6.29 dr. While optimal conditions for the synthesis and separation of **284** and **363** have not yet been identified, the ^1H NMR and ^{13}C NMR signals corresponding to epoxide **284** match those reported in the literature.⁸ In the optimization of this sequence, metal-catalyzed^{101,102} and radical cation¹⁰³ cyclization methods can also be investigated since the reported methods are suitable for triene substrates such as **361**. Once tricyclic olefin **283** or epoxide **284** is obtained as a single isomer, we can intercept Weyerstahl's racemic route (see Section 3.2.2)⁸ in a formal synthesis with only 4–5 steps remaining for the completion of an asymmetric total synthesis of presilphiperfolan-9 α -ol (**222**). Once this natural product is obtained, it can also be evaluated in biomimetic carbocationic rearrangement experiments.

Scheme 3.32. Planned Formal Synthesis of Presilphiperfolan-9 α -ol via IMDA Substrate **361**



3.6 PLANNED REARRANGEMENT OF PRESILPHIPERFOLANOLS TO OTHER SESQUITERPENE NATURAL PRODUCTS

With a completed synthesis of presilphiperfolan-1 β -ol (**223**) and promising routes for the preparation of presilphiperfol-9 α -ol (**221**), we can begin to explore biosynthetic rearrangements leading to rearranged sesquiterpene natural products (Scheme 3.33). While these types of biomimetic transformations have been studied in detail for presilphiperfolan-8 α -ol (**221**),^{5,7} little is known about the biosynthetic potential of presilphiperfolan-1 β -ol (**223**). By applying a variety of solvolytic or acidic conditions to promote carbocation formation, we can observe the evolution of the presilphiperfolane skeleton to other sesquiterpene frameworks, identifying and isolating the major rearrangement products. Preliminary rearrangement experiments have been carried out with presilphiperfolan-1 β -ol (**223**) in TFAA at 70 °C, but these conditions did not provide signs of promising rearrangement products on small scale. In future experiments, additional conditions can be evaluated and the reaction can be performed on larger scale. The anticipated rearrangement compounds will be compared to reported natural products with the aim of elucidating new sesquiterpene biosynthetic pathways stemming from presilphiperfolan-1 β -ol (**223**). In this manner, we aim to learn more about the different skeletal rearrangements of presilphiperfolanyl cations (**238**, **239**, and **250**) and contribute to a more complete understanding of the biosynthetic role of the presilphiperfolanols (Scheme 3.3).

Scheme 3.33. Planned Biomimetic Rearrangements of Synthetic Presilphiperfolanols **223** and **222****preliminary investigations:****planned biomimetic rearrangement studies:****3.7 CONCLUSION**

In summary, we have described the first asymmetric total synthesis of presilphiperfolan-1 β -ol (**223**) in 15 steps and 7.9% overall yield. Central to our approach was the further development and application of our Pd-catalyzed allylic alkylation/ring contraction methodology for the preparation of acylcyclopentenones **135** and more highly functionalized variants **306** and **308**. Successful elaboration of acylcyclopentene **306** enabled the construction of the tricyclic core of the presilphiperfolanols through an intramolecular Diels–Alder reaction. Functionalization of cycloadducts **305** and **283** completed the total synthesis of presilphiperfolan-1 β -ol (**223**), as well as unnatural presilphiperfolanol analogs **224**, **355**, and **356**. Analysis of spectral data and evaluation of presilphiperfolanol biosynthetic pathways led us to reassign the structure of reported “presilphiperfolan-1-ol” (**224**) to revised structure **223**. The synthesis of

presilphiperfolan-9 α -ol (**222**) is in progress and optimization of key steps will be necessary to complete the synthesis. The biomimetic rearrangement of the synthetic presilphiperfolanols to related sesquiterpene natural products has been initiated and will be explored in greater detail in future explorations. Our general synthetic route enables further investigation of the biosynthesis and biological activity of the presilphiperfolanols and related analogs.

3.8 EXPERIMENTAL SECTION

3.8.1 MATERIALS AND METHODS

Unless otherwise stated, reactions were performed in flame-dried glassware under an argon or nitrogen atmosphere using dry, deoxygenated solvents. Reaction progress was monitored by thin-layer chromatography (TLC). THF, Et₂O, CH₂Cl₂, toluene, benzene, CH₃CN, CyCH₃, and *p*-dioxane were dried by passage through an activated alumina column¹¹³ under argon. 1,2-DCE was distilled over CaH₂ prior to use. Triethylamine was distilled over CaH₂ prior to use. Purified water was obtained using a Barnstead NANOpure Infinity UV/UF system. Brine solutions are saturated aqueous solutions of sodium chloride. 2-Methyl-2-propen-1-ol was purchased from TCI America or Sigma-Aldrich. Zn(CH₃)₂ (1.0 M in heptanes), vinylmagnesium bromide (1.0 M in THF), and TBAF (1.0 M in THF) were purchased from Sigma-Aldrich. CDI was purchased from Sigma-Aldrich or Combi-blocks, Inc. Adam's catalyst (PtO₂-hydrate) was purchased from Strem. Anhydrous lithium hydroxide and P(NMe₂)₃ were purchased from Acros Organics. LiHMDS, KHMDS, CH₃Ph₃PBr, pinacolborane, Pd(*Pt*-Bu₃)₂, and Crabtree's catalyst ([Ir(cod)(PCy₃)(py)]PF₆)¹⁰⁶ were purchased from Sigma-Aldrich and stored in a N₂-filled glove box. Ni(cod)₂, CuCN, PCy₃, *Pt*-Bu₃, and Cy-Johnphos (CAS# [247940-06-3]) were purchased from Strem and stored in a N₂-filled glove box. NBS from Sigma-Aldrich was ground into a fine white powder with a mortar and pestle before use. NaH (60% wt. dispersion in mineral oil) from Sigma-Aldrich was purified by trituration with hexanes under a N₂ atmosphere and removal of residual solvent under vacuum. Isobutoxy-2-cyclohepten-1-one (#T271322) is commercially available from Sigma-

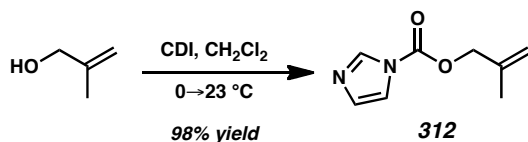
Aldrich, but was prepared by a modified procedure⁴² of Ragan.¹¹⁴ 2-Methyl-2-vinyloxirane was purchased from Sigma-Aldrich or prepared by a modification of the procedure of Isobe.⁷⁶ 2-methylene-3-buten-1-ol (isoprenol) was prepared by the procedure of Isobe.⁷⁶ Phosphinooxazoline (PHOX) ligands were prepared by methods described in our previous work.^{47a,53} Tris(4,4'-methoxydibenzylideneacetone) dipalladium(0) ($\text{Pd}_2(\text{pmdba})_3$) was prepared according to the method of Ibers^{55a} or Fairlamb.^{55b} $\text{Pd}(\text{PPh}_3)_4$ was prepared according to the procedure of Coulson.¹¹⁵ TBSOTf was prepared according to the procedure of Corey and stored under a N_2 or Ar atmosphere in a $-25\text{ }^\circ\text{C}$ freezer.¹¹⁶ $\text{FeCl}_2(\text{py-imine})$ complex **349** and [2-(N,N-dimethylaminomethyl)phenyl]lithium (**350**) were prepared according the method of Ritter and stored in a N_2 -filled glove box.^{86a} DMDO was prepared according to the procedure of Singh.⁹⁵ All other reagents were purchased from Sigma-Aldrich, Acros Organics, Strem, or Alfa Aesar and used as received unless otherwise stated. Reaction temperatures were controlled by an IKAmag temperature modulator unless otherwise indicated. Microwave-assisted reactions were performed in a Biotage Initiator 2.5 microwave reactor. Glove box manipulations were performed under a N_2 atmosphere. TLC was performed using E. Merck silica gel 60 F254 precoated glass plates (0.25 mm) and visualized by UV fluorescence quenching, *p*-anisaldehyde, or KMnO_4 staining. Silicycle SiliaFlash P60 Academic Silica gel (particle size 0.040–0.063 mm) was used for flash column chromatography. Silica gel was deactivated by pre-stirring with 1% Et_3N in hexanes for 30 min to 1 h before use for flash column chromatography. Solutions of potentially volatile reaction products were concentrated under reduced pressure (25 mm Hg) in a $0\text{ }^\circ\text{C}$ ice/water bath using a rotary evaporator. Ozonolysis reactions were

performed using an AZCO Industries HTU-500S Ozone Generator, and oxygen flow was controlled using an OzoneLab Instruments oxygen regulator with a CGA 540 fitting. ^1H NMR spectra were recorded on a Varian Inova 500 MHz spectrometer and are reported relative to residual CHCl_3 (δ 7.26 ppm), C_6H_6 (δ 7.16 ppm), or CH_2Cl_2 (δ 5.32 ppm). ^{13}C NMR spectra are recorded on a Varian Inova 500 MHz spectrometer (125 MHz) and are reported relative to CHCl_3 (δ 77.16 ppm) or C_6H_6 (δ 128.06 ppm). Data for ^1H NMR are reported as follows: chemical shift (δ ppm) (multiplicity, coupling constant (Hz), integration). Multiplicities are reported as follows: s = singlet, d = doublet, t = triplet, q = quartet, p = pentet, sept = septuplet, m = multiplet, dm = double of multiplets, br s = broad singlet, br d = broad doublet, app = apparent. Data for ^{13}C are reported in terms of chemical shifts (δ ppm). ^{19}F NMR spectra were recorded on a Varian Inova 500 (at 470 MHz) instrument and are reported in terms of chemical shift (δ ppm) without the use of a reference peak. ^{31}P NMR spectra were recorded on a Varian Inova 500 (at 202 MHz) instrument and are reported in terms of chemical shift (δ ppm) without the use of a reference peak. IR spectra were obtained using a Perkin Elmer Spectrum BXII spectrometer using thin films deposited on NaCl plates and reported in frequency of absorption (cm^{-1}). Optical rotations were measured with a Jasco P-2000 polarimeter operating on the sodium D-line (589 nm) using a 100 mm path-length cell and are reported as: $[\alpha]_{\text{D}}^{\text{T}}$ (concentration in g/100 mL, solvent, ee). Melting points were measured using a Büchi B-545 capillary melting point apparatus and the reported values are uncorrected. Preparatory HPLC was performed with an Agilent 1100 Series HPLC utilizing an Agilent ZORBAX RX-SIL 5 μm column (9.4 x 250 mm), part number 880975-201. Analytical chiral HPLC was performed with an Agilent 1100 Series HPLC

utilizing a Chiralcel AD column (4.6 mm x 25 cm) obtained from Daicel Chemical Industries Ltd. with visualization at 254 nm. Analytical UHPLC-LCMS was performed with an Agilent 1290 Infinity Series UHPLC/Agilent 6140 Quadrupole LCMS utilizing an Agilent Eclipse Plus C18 RRHD 1.8 μ m column (2.1 x 50 mm), part number 959757-902. High-resolution mass spectra (HRMS) were obtained from the Caltech Mass Spectral Facility (EI+ or FAB+) or on an Agilent 6200 Series TOF with an Agilent G1978A Multimode source in electrospray ionization (ESI+), atmospheric pressure chemical ionization (APCI+), or mixed (MM: ESI-APCI+) ionization mode.

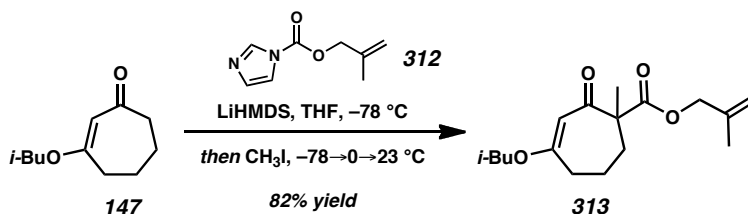
3.8.2 PREPARATIVE PROCEDURES

3.8.2.1 METHALLYL/METHYL ACYLCYCLOPENTENE ROUTE



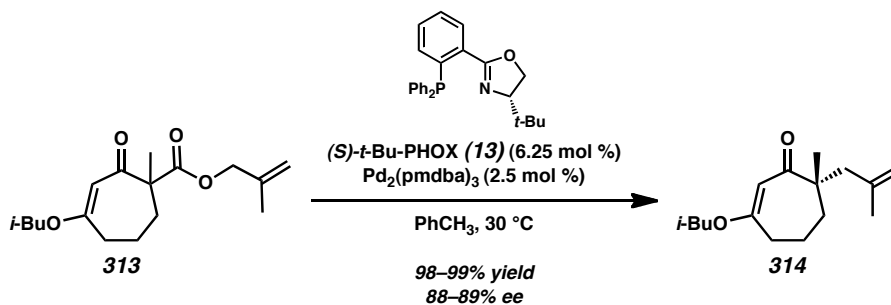
Carbamate 312. 2-methyl-2-propen-1-ol was converted to carbamate **312** using the general procedure of Sarpong.⁵⁰

To a 1 L round-bottom flask with a magnetic stir bar were added CDI (29.19 g, 180.0 mmol, 1.50 equiv) and CH_2Cl_2 (350 mL). The suspension was cooled to 0 °C and 2-methyl-2-propen-1-ol (10.1 mL, 120.0 mmol, 1.00 equiv) was added dropwise. The flask was sealed with a rubber septum, connected to a N_2 inlet, and allowed to warm to 23 °C. After 9 h of stirring, the reaction was quenched with H_2O (100 mL). The phases were separated and the organic phase was washed once more with H_2O (100 mL), dried over Na_2SO_4 , filtered, and concentrated under reduced pressure. The crude oil was purified by flash column chromatography (SiO_2 , 8 x 15 cm, 2:1→1:1 hexanes:EtOAc) to afford carbamate **312** (18.07 g, 118.0 mmol, 98% yield) as a white solid. (Note: The reagent is moisture sensitive. Storage under Ar in a sealed vial in a –25 °C freezer is recommended for maintaining reagent quality, but the reagent is typically used shortly after generation. Storage in a dessicator led to partial decomposition and slow color change to an orange solid over several months.) The spectral data match reported data.⁴⁸



β -Ketoester 313. To a 1 L round-bottom flask with a magnetic stir bar was added LiHMDS (30.18 g, 164.6 mmol, 3.00 equiv) in a N₂-filled glove box. The flask was sealed with a rubber septum and removed from the glove box, connected to a N₂ inlet, and cooled to $-78\text{ }^\circ\text{C}$ using an acetone/CO₂(s) bath. THF (390 mL) was added and the suspension was stirred vigorously for 5 min. The cooling bath was removed and the flask was allowed to warm until the solids completely dissolved. The pale orange solution was cooled to $-78\text{ }^\circ\text{C}$. A solution of vinylogous ester **147**⁴² (10.00 g, 54.87 mmol, 1.00 equiv) in THF (80 mL) in a conical 100 mL flask was added to the reaction dropwise over 1 h using positive pressure cannulation. The orange solution was stirred at $-78\text{ }^\circ\text{C}$ for 30 min. A solution of carbamate **312** (12.52 g, 82.30 mmol, 1.50 equiv) in THF (80 mL) in a conical 100 mL flask was added to the reaction dropwise over 1 h using positive pressure cannulation. The orange solution was stirred at $-78\text{ }^\circ\text{C}$ for 2 h. CH₃I (34.1 mL, 548.7 mmol, 10.00 equiv) was added dropwise. The reaction was stirred at $-78\text{ }^\circ\text{C}$ for 6 h and warmed to $0\text{ }^\circ\text{C}$ using an ice/water bath. After 11.5 h of stirring, the cooling bath was removed and the reaction was allowed to warm to $23\text{ }^\circ\text{C}$. Additional CH₃I (6.82 mL, 109.73 mmol, 2.00 equiv) was added to the reaction after 2.5 h. After an additional 9 h of stirring, the yellow solution became a yellow suspension. The reaction was quenched with 50% sat. aqueous NH₄Cl (200 mL) and Et₃N (5 mL). The biphasic mixture was stirred vigorously for 12 h. The phases were separated and the organic phase was washed with brine (2 x 100 mL). The combined aqueous phases were washed with EtOAc (2 x

150 mL). The combined organic phases were dried over Na₂SO₄, filtered, and concentrated under reduced pressure. The crude oil was purified by flash column chromatography (SiO₂, 8 x 32 cm, 3%→5%→7%→10% EtOAc in hexanes) to afford β -ketoester **313** (13.20 g, 44.80 mmol, 82% yield) as a pale yellow oil; R_f = 0.55 (4:1 hexanes:EtOAc); ¹H NMR (500 MHz, CDCl₃) δ 5.39 (s, 1H), 4.96–4.91 (m, 1H), 4.91–4.85 (m, 1H), 4.52 (d, J = 13.2 Hz, 1H), 4.47 (d, J = 13.2 Hz, 1H), 3.54–3.40 (m, 2H), 2.63–2.51 (ddd, J = 4.0, 9.9, 17.8 Hz, 1H), 2.47–2.29 (m, 2H), 2.04–1.90 (m, 2H), 1.86–1.74 (m, 1H), 1.74–1.62 (m, 1H), 1.70 (s, 3H), 1.43 (s, 3H), 0.93 (dd, J = 6.7, 1.1 Hz, 6H); ¹³C NMR (125 MHz, CDCl₃) δ 199.0, 174.0, 173.5, 139.8, 113.2, 105.2, 74.8, 68.4, 59.1, 34.4, 33.9, 27.9, 24.2, 21.4, 19.6, 19.2; IR (Neat Film NaCl) 3082, 2959, 2936, 2875, 1735, 1657, 1613, 1470, 1454, 1425, 1402, 1384, 1309, 1298, 1233, 1197, 1169, 1114, 1084, 1035, 994, 969, 957, 904, 868, 821 cm⁻¹; HRMS (MM: ESI-APCI+) m/z calc'd for C₁₇H₂₇O₄ [M+H]⁺: 295.1904; found 295.1908.



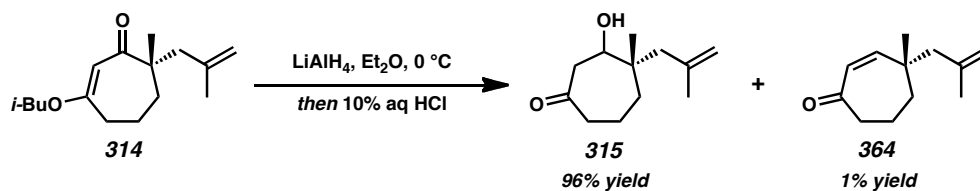
Vinylogous ester 314 (0.5 mmol scale). A 20 mL scintillation vial was loaded with β -ketoester **313** (170.3 mg, 0.58 mmol, 1.00 equiv). A separate 20 mL scintillation vial was loaded with a magnetic stir bar, Pd₂(pmdba)₃⁵⁵ (15.8 mg, 0.015 mmol, 2.5 mol %), and (S)-t-Bu-PHOX⁵³ (14.0 mg, 0.036 mmol, 6.25 mol %). The two vials and a teflon-lined hard cap were placed in a glove box antechamber, which was evacuated/backfilled

with N₂ (3 cycles, 5 min evacuation per cycle) before the items were transferred into the glove box. Toluene (5 mL) was added to the vial containing Pd₂(pmdba)₃ and (*S*)-*t*-Bu-PHOX. The vial was capped and the reaction was stirred for 30 min in a 30 °C heating block. During this time, the reaction changed from a deep purple-black suspension to a deep red-orange color. β-Ketoester **313** was dissolved in toluene (3 mL) and added to the catalyst solution dropwise, causing the solution to turn yellow. The reaction was sealed with a teflon-lined hard cap and stirred at 30 °C. After 9 h of stirring, the reaction became a deep red-orange color. The capped vial was removed from the glove box and the reaction was concentrated under reduced pressure. The crude oil was purified by flash column chromatography (SiO₂, 2 x 25 cm, 20:1→15:1 hexanes:EtOAc) to afford vinylogous ester **314** (143.9 mg, 0.58 mmol, 99% yield, 88.9% ee) as a pale yellow oil.

Vinylogous ester 314 (50 mmol scale). To a 1 L round-bottom flask with a magnetic stir bar were added Pd₂(pmdba)₃⁵⁵ (1.23 g, 1.12 mmol, 2.5 mol %), (*S*)-*t*-Bu-PHOX⁵³ (1.08 g, 2.80 mmol, 6.25 mol %), and toluene (450 mL) in a N₂-filled glove box. The flask was sealed with a rubber septum, removed from the glove box, connected to a N₂ inlet, and immersed in a 30 °C oil bath. The deep purple-black suspension gradually became a deep red-orange solution after 45 min of stirring. β-Ketoester **313** (13.20 g, 44.80 mmol, 1.00 equiv) in a 100 mL conical flask was freeze-pump-thawed using an acetone/CO₂(s) bath (3 cycles, 5 min evacuation per cycle), dissolved in toluene (50 mL), and added to the reaction dropwise using positive pressure cannulation. The solution became a deep green-brown solution. After 31.5 h of stirring, the reaction was a deep red-orange solution. The reaction was concentrated under reduced pressure and the crude

oil was purified by flash column chromatography (SiO₂, 8 x 32 cm, 3%→5%→8% EtOAc in hexanes) to afford vinylogous ester **314** (10.96 g, 43.78 mmol, 98% yield, 89.5% ee) as a pale tan oil; R_f = 0.35 (10:1 hexanes:EtOAc); ¹H NMR (500 MHz, CDCl₃) δ 5.33 (s, 1H), 4.82–4.76 (m, 1H), 4.66–4.62 (m, 1H), 3.53–3.42 (m, 2H), 2.55 (d, J = 13.3 Hz, 1H), 2.51–2.39 (m, 2H), 2.12 (d, J = 13.4, 1H), 1.97 (app. sept, J = 6.8 Hz, 1H), 1.89–1.70 (m, 3H), 1.66 (s, 3H), 1.57 (dd, J = 13.6, 8.6 Hz, 1H), 1.15 (s, 3H), 0.94 (d, J = 6.7 Hz, 6H); ¹³C NMR (125 MHz, CDCl₃) δ 206.7, 171.2, 143.0, 114.8, 105.4, 74.5, 51.2, 49.4, 36.2, 35.3, 28.0, 26.7, 24.6, 19.7, 19.3, 19.3; IR (Neat Film NaCl) 3072, 2961, 2934, 2874, 1615, 1470, 1455, 1424, 1402, 1388, 1374, 1332, 1318, 1284, 1223, 1188, 1174, 1121, 1085, 1027, 1012, 998, 969, 951, 887, 852, 745 cm⁻¹; HRMS (MM: ESI-APCI+) m/z calc'd for C₁₆H₂₇O₂ [M+H]⁺: 251.2006; found 251.2012; $[\alpha]_D^{25.0}$ –137.73 (c 1.33, CHCl₃, 88.9% ee); HPLC conditions: 0.7% IPA in hexanes, 1.0 mL/min, AD column, t_R (min): major = 8.94, minor = 8.28.

(Note: Pd₂(pmdba)₃ is preferable to Pd₂(dba)₃ in this reaction for ease of separation of pmdba from the reaction products during purification. The non-enantioselective reaction was carried out with Pd(PPh₃)₄¹¹⁵ (5 mol %) in toluene (0.1 M) at 30 °C or with Pd₂(dba)₃·CHCl₃ (2.5 mol %) and dppe (6.25 mol %) in toluene (0.1 M) at 30 °C.)

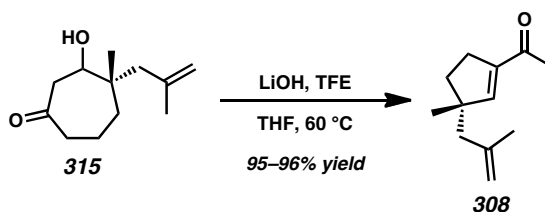


β -Hydroxyketone 315 and Cycloheptenone 364. A 500 mL round-bottom flask with a magnetic stir bar was charged with LiAlH_4 (221 mg, 5.88 mmol, 0.60 equiv) and evacuated/backfilled with N_2 (3 cycles, 5 min evacuation per cycle). Et_2O (150 mL) was added and the gray suspension was cooled to $0\text{ }^\circ\text{C}$ using an ice/water bath. A solution of vinylogous ester **314** (2.45 g, 9.80 mmol, 1.00 equiv) in Et_2O (26 mL) in a conical 100 mL flask was added to the reaction dropwise using positive pressure cannulation. The flask was washed with THF (2 x 10 mL) and washes were added to the reaction. The gray suspension was stirred at $0\text{ }^\circ\text{C}$. After 40 min of stirring, the reaction was quenched by slow dropwise addition of 10% aqueous HCl (15.2 mL). Gas evolution was observed. The reaction was allowed to warm to $23\text{ }^\circ\text{C}$ and the phases were separated. The aqueous phase was extracted with Et_2O (3 x 30 mL). Combined organic phases were dried over Na_2SO_4 , filtered, and concentrated under reduced pressure. The crude oil was purified by flash column chromatography (SiO_2 , 3 x 25 cm, 9:1 \rightarrow 3:1 hexanes: EtOAc) to afford cycloheptenone **364** (22.9 mg, 0.128 mmol, 1% yield) as a pale yellow oil and β -hydroxyketone **315** (1.85 g, 9.42 mmol, 96% yield, 1.91:1 dr) as a pale tan oil.

β -Hydroxyketone 315. $R_f = 0.17$ (4:1 hexanes: EtOAc); ^1H NMR (500 MHz, CDCl_3) mixture of two overlapping diastereomers, see Figure A5.7; ^{13}C NMR (125 MHz, CDCl_3) δ **major diastereomer**: 213.5, 143.6, 115.4, 72.7, 48.1, 46.8, 44.1, 41.7, 36.7, 25.7, 22.5, 19.2; **minor diastereomer**: 212.9, 142.7, 115.6, 73.8, 47.4, 45.7, 44.0, 41.6,

36.1, 25.8, 22.9, 18.6; IR (Neat Film NaCl) 3449, 3073, 2965, 2935, 1693, 1640, 1466, 1452, 1401, 1376, 1352, 1319, 1253, 1237, 1168, 1115, 1099, 1072, 1039, 1013, 996, 979, 963, 937, 892, 863, 809, 759, 734 cm^{-1} ; HRMS (MM: ESI-APCI+) m/z calc'd for $\text{C}_{12}\text{H}_{21}\text{O}_2$ $[\text{M}+\text{H}]^+$: 197.1536; found 197.1535; $[\alpha]_{\text{D}}^{25.0} -49.39$ (c 0.98, CHCl_3 , 88.1% ee).

Cycloheptenone 364. $R_f = 0.59$ (4:1 hexanes:EtOAc); ^1H NMR (500 MHz, CDCl_3) δ 6.11 (dd, $J = 13.0, 1.1$ Hz, 1H), 5.81 (d, $J = 13.0$ Hz, 1H), 4.91–4.86 (m, 1H), 4.72–4.67 (m, 1H), 2.68–2.46 (m, 2H), 2.19 (d, $J = 13.4$ Hz, 1H), 2.12 (d, $J = 13.3$, 1H), 1.92–1.78 (m, 3H), 1.74 (s, 3H), 1.69–1.60 (m, 1H), 1.13 (s, 3H); ^1H NMR (125 MHz, CDCl_3) δ 204.7, 153.3, 142.1, 128.1, 115.6, 51.2, 45.2, 43.1, 38.4, 28.4, 25.0, 18.5; IR (Neat Film NaCl) 3648, 3074, 2929, 2870, 1732, 1659, 1455, 1401, 1374, 1350, 1337, 1274, 1233, 1203, 1160, 1120, 1089, 1075, 1025, 977, 928, 893, 877, 862, 850, 826, 810, 771, 694, 668, 622 cm^{-1} ; HRMS (MM: ESI-APCI+) m/z calc'd for $\text{C}_{12}\text{H}_{19}\text{O}_2$ $[\text{M}+\text{H}]^+$: 179.1430; found 179.1435; $[\alpha]_{\text{D}}^{25.0} -22.90$ (c 0.24, CHCl_3 , 88.1% ee).



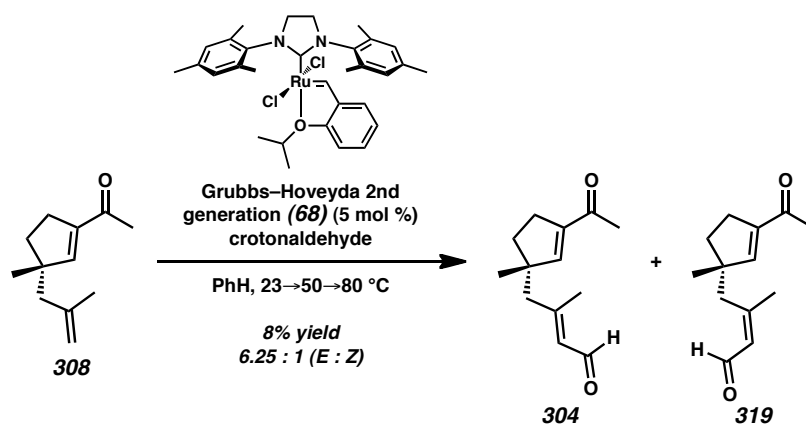
Acylcyclopentene 308 (0.5 mmol scale). β -Hydroxyketone **315** (102.4 mg, 0.522 mmol, 1.00 equiv) was dissolved in THF (5.2 mL) in a 20 mL scintillation vial with a magnetic stir bar. The solution was treated with 2,2,2-trifluoroethanol (57.1 μL , 0.783 mmol, 1.50 equiv) and anhydrous LiOH (11.5 mg, 0.783 mmol, 1.50 equiv). The headspace of the vial was purged with Ar. The vial was sealed with a teflon-lined hard cap and inserted

into a 60 °C heating block. After 14 h of stirring, the fine suspension was allowed to cool to ambient temperature, diluted with Et₂O (5 mL), dried over Na₂SO₄ with stirring for 30 min, filtered, and carefully concentrated under reduced pressure (25 mmHg) in a 0 °C ice/water bath. The crude product was purified using flash column chromatography (SiO₂, 2 x 25 cm, 15:1 hexanes:Et₂O) to afford acylcyclopentene **308** (88.0 mg, 0.494 mmol, 95% yield) as a fragrant pale tan oil.

Acylcyclopentene 308 (10 mmol scale). β-Hydroxyketone **315** (1.804 g, 9.19 mmol, 1.00 equiv) was dissolved in THF (92 mL) in a 300 mL round-bottom flask with a magnetic stir bar. The solution was treated with 2,2,2-trifluoroethanol (1.00 mL, 13.79 mmol, 1.50 equiv) and anhydrous LiOH (331 mg, 13.79 mmol, 1.50 equiv). The flask was fitted with a reflux condenser, purged with N₂, and immersed in a 60 °C oil bath. After 33 h of stirring, the fine suspension was allowed to cool to ambient temperature, diluted with Et₂O (100 mL), dried over Na₂SO₄ with stirring for 30 min, filtered, and carefully concentrated under reduced pressure (25 mmHg) in a 0 °C ice/water bath. The crude product was purified using flash column chromatography (SiO₂, 3 x 25 cm, 15:1 hexanes:Et₂O) to afford acylcyclopentene **308** (1.58 g, 8.85 mmol, 96% yield) as a fragrant pale tan oil.

Acylcyclopentene 308: R_f = 0.61 (4:1 hexanes:EtOAc); ¹H NMR (500 MHz, CDCl₃) δ 6.48 (app. t, *J* = 1.8 Hz, 1H), 4.84–4.78 (m, 1H), 4.66–4.63 (m, 1H), 2.50 (td, *J* = 7.8, 7.2, 1.5 Hz, 2H), 2.25 (s, 3H), 2.15 (dd, *J* = 3.4 Hz, 2H), 1.90 (dt, *J* = 12.8, 7.7 Hz, 1H), 1.70 (s, 3H), 1.72–1.58 (m, 1H), 1.07 (s, 3H); ¹³C NMR (125 MHz, CDCl₃) δ 197.3, 152.7,

143.1, 142.9, 114.6, 50.0, 48.7, 36.5, 29.5, 26.7, 26.0, 24.6; IR (Neat Film NaCl) 3074, 2956, 2923, 2865, 1670, 1616, 1454, 1376, 1366, 1340, 1320, 1305, 1271, 1228, 1200, 1158, 1138, 1092, 1048, 1013, 976, 934, 891, 869 cm^{-1} ; HRMS (APCI+) m/z calc'd for $\text{C}_{12}\text{H}_{19}\text{O}_2$ $[\text{M}+\text{H}]^+$: 179.1430; found 179.1430; $[\alpha]_{\text{D}}^{25.0}$ -41.19 (c 1.155, CHCl_3 , 88.1% ee).

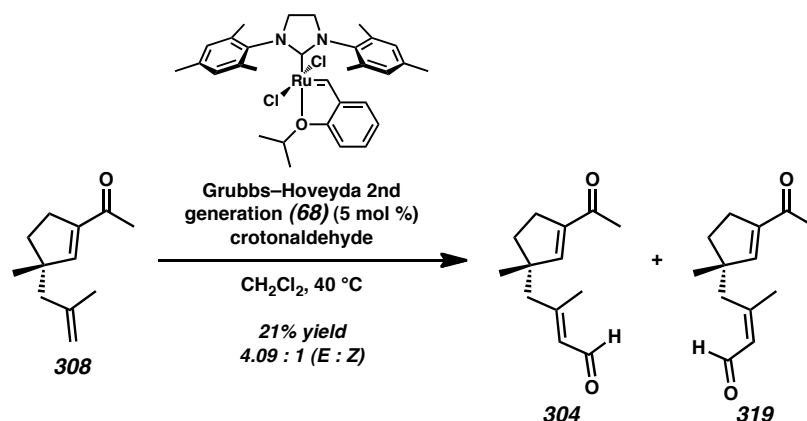


Enals 304 and 319. To a 2-neck 50 mL round-bottom flask with stir bar and attached reflux condenser connected to a N_2 -inlet was added alkene **308** (76.7 mg, 0.43 mmol, 1.00 equiv). Dry degassed benzene (5.7 mL, sparged with Ar for 1 h immediately before use) was added. Crotonaldehyde (175.7 μL , 2.15 mmol, 5.00 equiv) was added dropwise. Grubbs-Hoveyda 2nd generation catalyst (13.5 mg, 0.0215 mmol, 5 mol %) was quickly added in one portion through the side neck. The flask was sealed and the reaction was stirred at 23 $^\circ\text{C}$. After 3 h of stirring, the reaction was warmed to 50 $^\circ\text{C}$, causing a color change to dark brown. After 20.5 h of stirring, the reaction was warmed to 80 $^\circ\text{C}$. After an additional 4.5 h of stirring, ethyl vinyl ether (1 mL) was added and the reaction was diluted with hexanes and passed through a silica plug (2 x 8 cm), eluted with Et_2O , and concentrated under reduced pressure. The residue was purified by flash

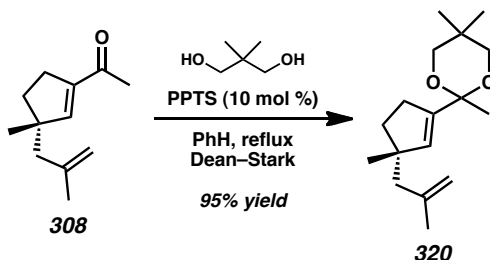
column chromatography (SiO₂, 2 x 15 cm, 15:1→10:1→1:1 hexanes:Et₂O) to afford enals **304** and **319** (7.0 mg, 0.034 mmol, 8% yield, 6.25:1 *E:Z* ratio) as a brown oil.

Enal 304 (*E* isomer): $R_f = 0.14$ (4:1 hexanes:EtOAc); ¹H NMR (500 MHz, CDCl₃) δ 9.99 (d, $J = 7.9$ Hz, 1H), 6.47 (app. t, $J = 1.8$ Hz, 1H), 5.87 (dm, $J = 8.2$ Hz, 1H), 2.66–2.49 (m, 2H), 2.38 (s, 2H), 2.31 (s, 3H), 2.20 (d, $J = 1.3$ Hz, 3H), 1.92 (ddd, $J = 13.0, 8.5, 6.6$ Hz, 1H), 1.75 (ddd, $J = 13.0, 8.3, 5.7$ Hz, 1H), 1.16 (s, 3H); ¹³C NMR (125 MHz, CDCl₃) δ 197.2, 190.9, 160.5, 150.7, 144.0, 130.8, 51.5, 50.6, 36.9, 29.7, 26.9, 26.3, 19.9; IR (Neat Film NaCl) 3317, 2956, 2927, 2856, 2773, 2726, 1710, 1668, 1624, 1453, 1405, 1379, 1367, 1340, 1304, 1269, 1197, 1135, 1113, 1048, 1022, 978, 935, 862, 836 cm⁻¹; HRMS (EI+) m/z calc'd for C₁₃H₁₈O₂ [M]⁺: 206.1307; found 206.1307; $[\alpha]_D^{25.0} -19.87$ (c 0.86, CHCl₃, 88.1% ee).

Enal 319 (*Z* isomer): $R_f = 0.13$ (4:1 hexanes:EtOAc); ¹H NMR (500 MHz, CDCl₃) δ 9.87 (d, $J = 8.0$ Hz, 1H), 6.45 (app. t, $J = 1.8$ Hz, 1H), 6.02 (dm, $J = 8.0$ Hz, 1H), 2.93 (d, $J = 13.1$ Hz, 1H), 2.66–2.52 (m, 2H), 2.61 (d, $J = 13.1$ Hz, 1H), 2.30 (s, 3H), 2.01 (d, $J = 1.3$ Hz, 3H), 1.94 (ddd, $J = 12.9, 8.5, 6.3$ Hz, 1H), 1.79 (ddd, $J = 12.9, 8.5, 5.7$ Hz, 1H), 1.20 (s, 3H); ¹³C NMR (125 MHz, CDCl₃) δ 197.1, 190.8, 160.4, 150.4, 144.3, 131.0, 50.5, 43.1, 37.3, 29.7, 27.8, 26.9, 26.5; IR (Neat Film NaCl) 3317, 2957, 2928, 2866, 2756, 1673, 1668, 1652, 1625, 1622, 1456, 1394, 1378, 1368, 1341, 1306, 1265, 1186, 1151, 1135, 1093, 1048, 1018, 978, 937, 870, 855, 802, 747 cm⁻¹; HRMS (EI+) m/z calc'd for C₁₃H₁₈O₂ [M]⁺: 206.1307; found 206.1308; $[\alpha]_D^{25.0} -63.73$ (c 0.25, CHCl₃, 88.1% ee).

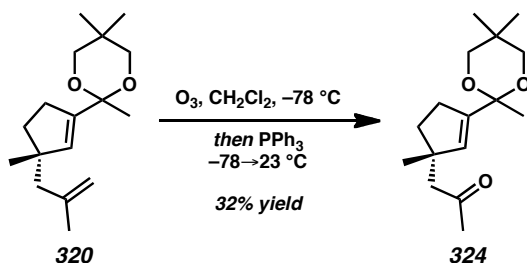


Enals 304 and 319. To a 1 dram vial with a magnetic stir bar was added Grubbs-Hoveyda 2nd generation catalyst (17.6 mg, 0.028 mmol, 5 mol %). The vial was sealed with a septum-fitted screw cap and electrical tape and covered with an inverted secondary rubber septum. The vial was evacuated/backfilled with N_2 (3 cycles, 5 min evacuation per cycle). Dry degassed CH_2Cl_2 (0.56 mL, sparged with Ar for 1 h immediately before use) was added. The sealed vial was heated at reflux for 15 min. Alkene **308** (50 mg, 0.280 mmol, 1.00 equiv) was added to the emerald green reaction and stirred at reflux for 15 min. Crotonaldehyde (34.6 μL , 0.421 mmol, 1.50 equiv) was added dropwise at reflux. After 26 h of stirring, the reaction was a deep red-brown solution. Ethyl vinyl ether (0.5 mL) was added and the reaction mixture was stirred for 30 min. The reaction was concentrated under reduced pressure and purified by flash column chromatography (SiO_2 , 2 x 20 cm, 10:1→1:1 hexanes:Et₂O) to afford enals **304** and **319** (12 mg, 0.058 mmol, 21% yield, 4.09:1 *E*:*Z* ratio) as a brown oil.



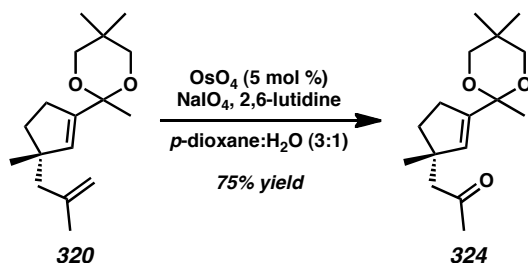
Ketal 320. To a 25 mL round-bottom flask with a magnetic stir bar were added acylcyclopentene **308** (178.3 mg, 1.00 mmol, 1.00 equiv), benzene (10 mL), neopentyl glycol (624.9 mg, 6.00 mmol, 6.00 equiv), and PPTS (25.1 mg, 0.10 mmol, 0.10 equiv). A Dean–Stark trap and reflux condenser connected to a N₂ inlet was attached and the flask was immersed in a 100 °C oil bath. The suspension gradually became a clear, colorless solution. After 4 h of stirring, the reaction was cooled to ambient temperature and poured into sat. aqueous NaHCO₃ (3 mL) and the mixture was extracted with Et₂O (3 x 10 mL). The combined organic phases were dried over Na₂SO₄, filtered, and concentrated under reduced pressure to give a white semisolid. The crude product was purified using flash column chromatography (SiO₂, 3 x 25 cm, 1%→2% EtOAc in hexanes) to afford ketal **320** (251.7 mg, 0.952 mmol, 95% yield) as a pale tan oil; *R*_f = 0.53 (10:1 hexanes:EtOAc); ¹H NMR (500 MHz, CDCl₃) δ 5.59 (t, *J* = 1.9 Hz, 1H), 4.83–4.80 (m, 1H), 4.70–4.67 (m, 1H), 3.56 (dd, *J* = 20.9, 10.9 Hz, 2H), 3.32 (dt, *J* = 10.9, 2.3 Hz, 2H), 2.38–2.23 (m, 2H), 2.15 (s, 2H), 1.94 (ddd, *J* = 12.7, 8.6, 6.7 Hz, 1H), 1.76 (s, 3H), 1.65 (ddd, *J* = 12.6, 8.2, 5.3 Hz, 1H), 1.41 (s, 3H), 1.17 (s, 3H), 1.07 (s, 3H), 0.69 (s, 3H); ¹³C NMR (125 MHz, CDCl₃) δ 144.2, 140.6, 139.1, 113.9, 98.8, 71.8, 49.4, 49.1, 37.1, 31.1, 29.8, 27.6, 27.3, 24.8, 22.9, 22.2; IR (Neat Film NaCl) 3072, 3040, 2980, 2952, 2868, 2852, 1642, 1471, 1453, 1395, 1369, 1352, 1319, 1298, 1253, 1239, 1193, 1180, 1118, 1083, 1041, 1015, 950, 911, 889, 862, 808, 793, 674 cm⁻¹; HRMS

(EI+) m/z calc'd for $C_{17}H_{28}O_2$ $[M]^{+}$: 264.2089; found 264.2086; $[\alpha]_D^{25.0}$ -5.47 (c 1.225, $CHCl_3$, 88.1% ee).

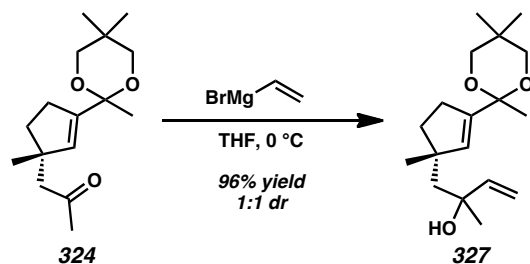


Methyl Ketone 324.¹¹⁷ To a 50 mL round-bottom flask with a magnetic stir bar was added a solution of alkene **320** (181.1 mg, 0.685 mmol, 1.00 equiv) in CH_2Cl_2 (12 mL). The flask was cooled to -78°C using an acetone/ $CO_2(s)$ bath. O_2 was bubbled through the reaction mixture for 2 min before ozone generation was turned initiated (O_2 regulator setting: $1/4\text{ L}\cdot\text{min}^{-1}$, ozonator setting: 1). Ozonation was conducted for 5 min intervals and carefully monitored until starting material was completely consumed. After 35 min of ozonation, the O_2 was bubbled through the reaction for 15 min. PPh_3 (449 mg, 1.71 mmol, 2.5 equiv) was added at -78°C , the cooling bath was removed, and the flask was allowed to warm to 23°C . The reaction was concentrated under reduced pressure and the crude product was purified using flash column chromatography (SiO_2 , $3 \times 25\text{ cm}$, $20:1 \rightarrow 15:1 \rightarrow 10:1 \rightarrow 4:1$ hexanes:EtOAc) to afford methyl ketone **324** (57.7 mg, 0.217 mmol, 32% yield) as a pale yellow oil; $R_f = 0.43$ (4:1 hexanes:EtOAc); ^1H NMR (500 MHz, $CDCl_3$) δ 5.66 (t, $J = 1.9\text{ Hz}$, 1H), 3.53 (dd, $J = 10.4, 7.7\text{ Hz}$, 2H), 3.33 (d, $J = 11.1\text{ Hz}$, 2H), 2.53 (s, 2H), 2.40–2.24 (m, 2H), 2.13 (s, 3H), 1.94 (ddd, $J = 12.9, 8.5, 6.3\text{ Hz}$, 1H), 1.77 (ddd, $J = 12.8, 8.4, 5.6\text{ Hz}$, 1H), 1.41 (s, 3H), 1.16 (s, 3H), 1.15 (s, 3H), 0.71 (s, 3H); ^{13}C NMR (125 MHz, $CDCl_3$) δ 208.3, 141.9, 137.5, 98.6, 71.8, 54.0, 47.8, 37.4,

32.1, 30.9, 29.8, 27.4, 26.7, 22.8, 22.3; IR (Neat Film NaCl) 3400, 2952, 2868, 1718, 1472, 1457, 1395, 1369, 1254, 1241, 1178, 1146, 1117, 1082, 1039, 1015, 949, 911, 862, 809, 793 cm^{-1} ; HRMS (EI+) m/z calc'd for $\text{C}_{16}\text{H}_{27}\text{O}_2$ $[\text{M}+\text{H}]^+$: 267.1955; found 267.1960; $[\alpha]_{\text{D}}^{26.0} -10.89$ (c 1.07, CHCl_3 , 88.1% ee).



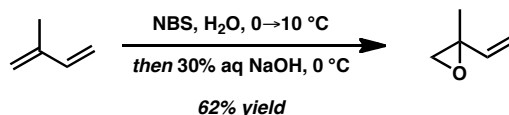
Methyl Ketone 324. To a 50 mL round-bottom flask with a magnetic stir bar was added a solution of alkene **320** (288.4 mg, 1.09 mmol, 1.00 equiv) in a mixture of *p*-dioxane:purified H_2O (3:1, 10.9 mL). The reaction was cooled to 0 °C using an ice/water bath. 2,6-Lutidine (254 μL , 2.18 mmol, 2.00 equiv) and OsO_4 (13.9 mg, 0.055 mmol, 5 mol %) were added to the reaction. The thick white suspension was stirred vigorously and the cooling bath was allowed to expire. The reaction was warmed to room temperature over several hours. After 14 h of stirring, the reaction was passed through a plug of Celite (2 x 2 cm) and eluted with EtOAc. The biphasic mixture was separated and the aqueous phase was extracted with EtOAc (3 x 20 mL). The combined organic phases were dried over Na_2SO_4 , filtered, and concentrated under reduced pressure to give a green-brown residue. The crude product was purified using flash column chromatography (SiO_2 , 3 x 25 cm, 20:1 \rightarrow 15:1 \rightarrow 10:1 hexanes:EtOAc) to afford methyl ketone **324** (217.1 mg, 0.815 mmol, 75% yield) as a pale yellow oil.



Alcohol 327. To a 50 mL round-bottom flask with a magnetic stir bar under N_2 were added THF (6 mL) and vinylmagnesium bromide solution (1.0 M in THF, 585.6 μL , 0.225 mmol, 3.00 equiv). The reaction was cooled to 0 $^{\circ}\text{C}$ using an ice/water bath. Ketone **324** (52 mg, 0.195 mmol, 1.00 equiv) in THF (2 mL) was added dropwise by positive pressure cannulation. After 30 min of stirring, the reaction was diluted with Et_2O , quenched with H_2O (2.0 mL) and sat. aqueous NH_4Cl (2.0 mL). The phases were separated and the aqueous phase was extracted with EtOAc (3 x 5 mL). The aqueous phase was acidified to pH = 1 with the addition of aqueous KCl/HCl buffer. The aqueous phase was extracted with EtOAc (3 x 5 mL). The combined organic phases were dried over Na_2SO_4 , filtered, and concentrated under reduced pressure. The crude product was purified using flash column chromatography (SiO_2 , 3.0 x 12 cm, 6:1 \rightarrow 4:1 hexanes: EtOAc) to afford alcohol **327** (55.2 mg, 0.1876 mmol, 96% yield, 1:1 dr) as a pale yellow oil. . (Note: The compound appears to be unstable to long-term storage for periods greater than 6 months.); R_f = 0.41 (4:1 hexanes: EtOAc); ^1H NMR (500 MHz, CDCl_3) mixture of two overlapping diastereomers, see Figure A5.28; ^{13}C NMR (125 MHz, CDCl_3) mixture of two overlapping diastereomers, see Figure A5.30; IR (Neat Film NaCl) 3480, 3084, 2951, 2868, 1642, 1472, 1457, 1453, 1395, 1369, 1353, 1320, 1283, 1241, 1255, 1179, 1117, 1083, 1040, 1014, 949, 912, 862, 807, 793, 758 cm^{-1} ;

HRMS (EI+) m/z calc'd for $C_{16}H_{27}O_2$ $[M+H]^+$: 295.2268; found 295.2267; $[\alpha]_D^{25.0}$ -10.14 (c 0.92, $CHCl_3$, 88.1% ee).

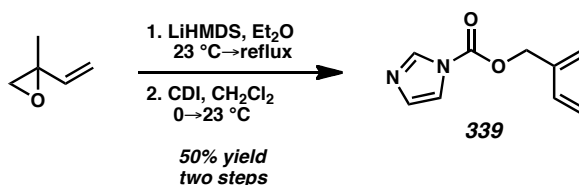
3.8.2.2 SYNTHESIS OF (–)-PRESILPHIPERFOLAN-1 β -OL AND ANALOGS



2-Methyl-2-vinyloxirane.⁷⁶ To a 3-neck 1 L round-bottom flask with mechanical stirrer was added H_2O (300 mL). The flask was cooled to 0 °C using an ice/water bath and stirred for 10 min. Isoprene (81 mL, 0.81 mol, 1.00 equiv) was added and glass stoppers were attached to the side necks. The biphasic mixture was stirred vigorously for 5 min at 0 °C. Finely powdered NBS (140.52 g, 0.790 mol, 0.975 equiv) was added portionwise through a side neck over 35 min to give a pale tan suspension. The glass stopper was reattached to the side neck and the reaction was stirred at 0 °C for 2.5 h. Subsequent warming of the reaction to 10 °C led to clarification of the reaction mixture. If stirring was halted, a clear, colorless upper aqueous phase and a clear, pale yellow lower organic phase could be observed. The reaction was cooled to 0 °C and stirred for 9 h. Chilled, ice-cold 10 M aqueous NaOH (160 mL) was added to the reaction over 15 min through an addition funnel to give a turbid white biphasic mixture. Internal temperature was maintained below 5 °C during addition. The reaction was stirred at 0 °C for 15 min. If stirring was halted, a clear, colorless organic upper phase could be observed. The phases were separated and the organic phase was washed with H_2O (2 x 15 mL) and brine (2 x 15 mL). The organic phase was transferred to a 100 mL round-bottom flask and the

crude product was distilled (80 °C, 760 mmHg) to yield the first portion of 2-methyl-2-vinyloxirane (34.66 g).

A second portion of product was isolated by extraction of the aqueous phase with Et₂O (3 x 40 mL). The combined organic phases were washed with H₂O (2 x 15 mL) and brine (2 x 15 mL), dried over MgSO₄, filtered into a 200 mL pear-shaped flask. The flask was fitted with a short-path distillation head and immersed in a 45 °C oil bath to remove Et₂O by distillation. Once Et₂O was removed, the crude product was distilled (80 °C, 760 mmHg) to yield the second portion of 2-methyl-2-vinyloxirane (7.24 g). The portions of 2-methyl-2-vinyloxirane (41.90 g, 0.498 mol, 62% yield) were combined to give a clear, colorless liquid. The spectral data match data for commercially available material.



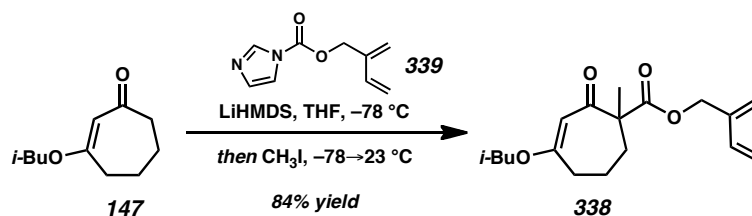
Carbamate 339. Isoprenol was prepared according to the method of Isobe⁷⁶ and converted to carbamate **339** using the general procedure of Sarpong.⁵⁰

To a 500 mL 3-neck round-bottom flask equipped with a magnetic stir bar, rubber septum, and two glass stoppers was added LiHMDS (24.09 g, 143.97 mmol, 1.20 equiv) in a N₂-filled glove box. The flask was sealed with a rubber septum and removed from the glove box. One of the glass stoppers was replaced with a reflux condenser connected to a N₂ inlet. The flask was cooled to –78 °C using an acetone/CO₂(s) bath. Et₂O (160 mL) was added and the suspension was stirred vigorously for 5 min. The cooling bath was removed and the flask was allowed to warm to 23 °C, giving a white suspension. A

solution of 2-methyl-2-vinyloxirane (10.0 g, 119.97 mmol, 1.00 equiv) in Et₂O (50 mL) in a 100 mL conical flask was added to the reaction by positive pressure cannulation, leading to the formation of a turbid pale yellow solution. The reaction was heated to reflux in a 45 °C oil bath. After 22 h of stirring, the reaction was cooled to 0 °C and stirred for 10 min. Chilled, ice-cold 2 M aqueous HCl (80 mL) was added and the reaction was stirred vigorously for 1 h. The phases were separated and the aqueous phase was extracted with Et₂O (3 x 20 mL). The combined organic phases were dried over MgSO₄, filtered, and concentrated under reduced pressure (150 mmHg) in a 0 °C ice/water bath to a volume of ca. 50 mL. The solution of volatile isoprenol was used directly in the next step.

To a 1 L round-bottom flask with a magnetic stir bar were added CDI (29.7 g, 179.96 mmol, 1.50 equiv) and CH₂Cl₂ (400 mL). An addition funnel was attached and the apparatus was connected to a N₂ inlet. The flask was cooled to 0 °C and stirred for 10 min. The solution of crude isoprenol in Et₂O (50 mL) was transferred to the addition funnel and added dropwise with vigorous stirring at 0 °C. The cooling bath was removed and the flask was allowed to warm to 23 °C. After 1 h of stirring, the reaction was quickly washed with H₂O (2 x 100 mL) and brine (2 x 100 mL). The aqueous phases were extracted with CH₂Cl₂ (3 x 50 mL). The combined organic phases were dried over MgSO₄, filtered, and concentrated under reduced pressure. The crude product was purified by flash column chromatography (SiO₂, 8 x 15 cm, 20%→30%→50% EtOAc in hexanes) to afford carbamate **339** (10.74 g, 60.26 mmol, 50% yield over two steps) as a pale yellow oil which solidifies upon storage in a –25 °C freezer. (Note: The reagent is moisture sensitive. Storage under N₂ in a sealed container in a –25 °C freezer is

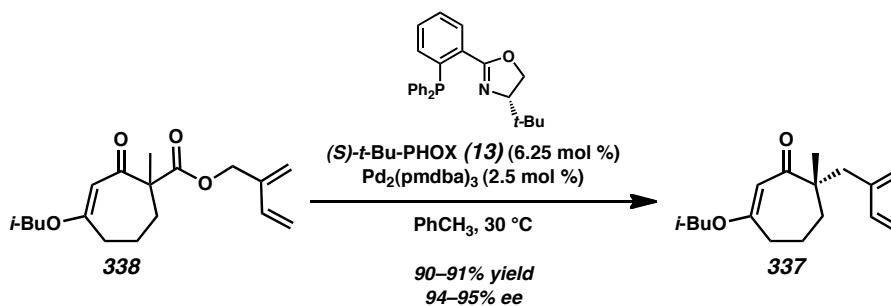
recommended for maintaining reagent quality, but the reagent is typically used shortly after generation.); $R_f = 0.15$ (4:1 hexanes:EtOAc); ^1H NMR (500 MHz, CDCl_3) δ 8.12 (s, 1H), 7.45–7.37 (m, 1H), 7.09–7.02 (m, 1H), 6.40 (dd, $J = 17.8, 11.1$ Hz, 1H), 5.38–5.34 (m, 1H), 5.34–5.31 (m, 1H), 5.30 (d, $J = 17.9$ Hz, 1H), 5.20 (d, $J = 11.2$ Hz, 1H), 5.06 (s, 2H); ^{13}C NMR (125 MHz, CDCl_3) δ 148.5, 139.2, 137.1, 135.6, 130.8, 119.9, 117.1, 115.4, 67.2; IR (Neat Film NaCl) 3132, 3091, 3010, 2952, 2929, 2855, 1763, 1599, 1526, 1472, 1403, 1390, 1318, 1290, 1281, 1240, 1172, 1095, 1058, 1007, 916, 897, 835, 768, 746 cm^{-1} ; HRMS (MM: ESI-APCI+) m/z calc'd for $\text{C}_9\text{H}_{11}\text{N}_2\text{O}_2$ $[\text{M}+\text{H}]^+$: 178.0815; found 178.0818.



β -Ketoester 338. To a 1 L round-bottom flask with a magnetic stir bar was added LiHMDS (25.83 g, 154.40 mmol, 3.00 equiv) in a N_2 -filled glove box. The flask was sealed with a rubber septum and removed from the glove box, connected to a N_2 inlet, and cooled to -78°C using an acetone/ $\text{CO}_2(\text{s})$ bath. THF (360 mL) was added and the suspension was stirred vigorously for 5 min. The cooling bath was removed and the flask was allowed to warm until the solids completely dissolved. The pale tan solution was cooled to -78°C . A solution of vinylogous ester **147**⁴² (9.38 g, 51.47 mmol, 1.00 equiv) in THF (80 mL) in a 100 mL conical flask was added to the reaction dropwise over 1 h using positive pressure cannulation. The orange solution was stirred at -78°C for 30 min. A solution of carbamate **339** (11.46 g, 64.33 mmol, 1.25 equiv) in THF (25 mL) in

a 50 mL conical flask was added to the reaction dropwise over 15 min using positive pressure cannulation. The orange solution was stirred at $-78\text{ }^{\circ}\text{C}$ for 2.5 h. CH_3I (38.4 mL, 617.58 mmol, 12.00 equiv) was added dropwise. The cooling bath was allowed to expire and the reaction warmed to $23\text{ }^{\circ}\text{C}$ over 7 h. After 13 h of stirring, the reaction was quenched with 50% sat. aqueous NH_4Cl (190 mL) and Et_3N (7.5 mL). The biphasic mixture was stirred vigorously for 12 h. The phases were separated and the organic phase was washed with brine (2 x 200 mL). The combined aqueous phases were washed with EtOAc (3 x 150 mL). The combined organic phases were dried over Na_2SO_4 , filtered, and concentrated under reduced pressure. The oil was taken up in Et_2O , leading to the precipitation of solids. The suspension was filtered through a silica gel plug (3 x 5 cm), eluting with Et_2O and concentrated under reduced pressure. The crude oil was purified by flash column chromatography (SiO_2 , 8 x 32 cm, 3%→10%→20%→40% EtOAc in hexanes) to afford β -ketoester **338** (13.22 g, 43.15 mmol, 84% yield) as a pale yellow oil; $R_f = 0.54$ (4:1 hexanes: EtOAc); ^1H NMR (500 MHz, CDCl_3) δ 6.29 (dd, $J = 17.7, 11.1\text{ Hz}$, 1H), 5.37–5.31 (m, 1H), 5.22–5.18 (m, 1H), 5.16 (d, $J = 18.2\text{ Hz}$, 1H), 5.16–5.12 (m, 1H), 5.06 (d, $J = 11.1\text{ Hz}$, 1H), 4.77 (d, $J = 13.3\text{ Hz}$, 1H), 4.69 (d, $J = 13.3\text{ Hz}$, 1H), 3.44 (dd, $J = 9.3, 6.6\text{ Hz}$, 1H), 3.42 (dd, $J = 9.3, 6.5\text{ Hz}$, 1H), 2.53 (ddd, $J = 17.8, 9.9, 3.8\text{ Hz}$, 1H), 2.43–2.28 (m, 2H), 2.00–1.87 (m, 2H), 1.81–1.68 (m, 1H), 1.65 (ddd, $J = 14.4, 7.3, 4.3\text{ Hz}$, 1H), 1.39 (s, 3H), 0.90 (d, $J = 6.7\text{ Hz}$, 6H); ^{13}C NMR (125 MHz, CDCl_3) δ 199.0, 173.9, 173.5, 140.4, 136.1, 118.4, 114.8, 105.1, 74.8, 64.3, 59.1, 34.4, 33.9, 27.9, 24.2, 21.3, 19.3; IR (Neat Film NaCl) 3090, 2859, 2935, 2874, 1735, 1653, 1649, 1613, 1471, 1456, 1424, 1401, 1384, 1309, 1275, 1233, 1197, 1169, 1114,

1084, 1032, 994, 969, 910, 869, 768 cm^{-1} ; HRMS (MM: ESI-APCI+) m/z calc'd for $\text{C}_{17}\text{H}_{27}\text{O}_2$ $[\text{M}+\text{H}]^+$: 307.1904; found 307.1899.



Vinylogous ester 337 (2 mmol scale). A 20 mL scintillation vial was loaded with β -ketoester **338** (527 mg, 1.72 mmol, 1.00 equiv). A separate 20 mL scintillation vial was loaded with a magnetic stir bar, $\text{Pd}_2(\text{pmdba})_3$ ⁵⁵ (47.2 mg, 0.043 mmol, 2.5 mol %), and (S) -*t*-Bu-PHOX⁵³ (41.7 mg, 0.108 mmol, 6.25 mol %). The two vials and a teflon-lined hard cap were placed in a glove box antechamber, which was evacuated/backfilled with N_2 (3 cycles, 5 min evacuation per cycle) before the items were transferred into the glove box. Toluene (10 mL) was added to the vial containing $\text{Pd}_2(\text{pmdba})_3$ and (S) -*t*-Bu-PHOX. The vial was capped and the reaction was stirred for 30 min in a 30 °C heating block. During this time, the reaction changed from a deep purple-black suspension to a deep red-orange color. β -Ketoester **338** was dissolved in toluene (7 mL) and added to the catalyst solution dropwise, causing the solution to turn olive green. The reaction was sealed with a teflon-lined hard cap and stirred at 30 °C. After 16.5 h of stirring, the reaction became a deep red-orange color. The capped vial was removed from the glove box and the reaction was concentrated under reduced pressure. The crude oil was purified by flash column chromatography (SiO_2 , 3 x 25 cm, 40:1→20:1→15:1

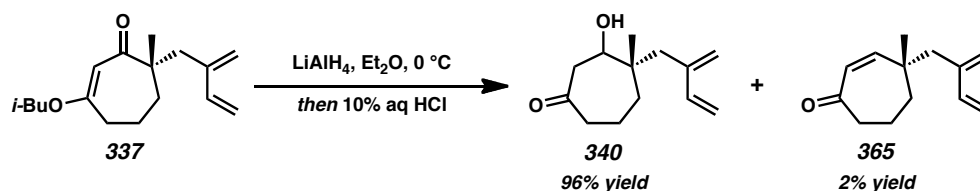
hexanes:EtOAc) to afford vinylogous ester **337** (143.9 mg, 1.57 mmol, 91% yield, 94.7% ee) as a pale yellow oil.

Vinylogous ester 337 (40 mmol scale). To a 1 L round-bottom flask with a magnetic stir bar were added $\text{Pd}_2(\text{pmdba})_3$ ⁵⁵ (1.18 g, 1.08 mmol, 2.5 mol %), (*S*)-*t*-Bu-PHOX⁵³ (1.04 g, 2.70 mmol, 6.25 mol %), and toluene (430 mL) in a N_2 -filled glove box. The flask was sealed with a rubber septum, removed from the glove box, connected to a N_2 inlet, and immersed in a 30 °C oil bath. The deep purple-black suspension gradually became a deep red-orange solution after 50 min of stirring. β -Ketoester **338** (13.22 g, 43.14 mmol, 1.00 equiv) in a 100 mL conical flask was freeze-pump-thawed using an acetone/ $\text{CO}_2(\text{s})$ bath (3 cycles, 5 min evacuation per cycle), dissolved in toluene (30 mL), and added to the reaction dropwise using positive pressure cannulation. The solution became a deep olive-green solution. After 33 h of stirring, the reaction was a deep red-orange solution. The reaction was concentrated under reduced pressure and the crude oil was purified by flash column chromatography (SiO_2 , 8 x 32 cm, 3%→5%→10% EtOAc in hexanes) to afford vinylogous ester **337** (10.20 g, 38.87 mmol, 90% yield, 95.3% ee) as a pale tan oil.

Vinylogous ester 337: R_f = 0.35 (10:1 hexanes:EtOAc); ^1H NMR (500 MHz, CDCl_3) δ 6.32 (dd, J = 17.5, 10.9 Hz, 1H), 5.29 (s, 1H), 5.25 (d, J = 17.5 Hz, 1H), 5.17–5.11 (m, 1H), 5.01 (d, J = 10.9 Hz, 1H), 4.93–4.87 (m, 1H), 3.48 (dd, J = 9.3, 6.6 Hz, 1H), 3.44 (dd, J = 9.3, 6.4 Hz, 1H), 2.56 (d, J = 13.7 Hz, 1H), 2.50–2.35 (m, 2H), 2.42 (d, J = 13.8 Hz, 1H), 1.96 (app. sept, J = 6.7 Hz, 1H), 1.88–1.74 (m, 2H), 1.74–1.61 (m, 1H), 1.54

(ddd, $J = 14.5, 8.9, 1.3$ Hz, 1H), 1.13 (s, 3H), 0.93 (d, $J = 6.7$ Hz, 6H); ^{13}C NMR (125 MHz, CDCl_3) δ 207.0, 171.0, 143.1, 140.3, 119.2, 113.9, 105.4, 74.4, 52.2, 41.1, 36.2, 35.1, 28.0, 26.3, 19.7, 19.3, 19.3; IR (Neat Film NaCl) 3085, 2959, 2934, 2873, 1811, 1722, 1699, 1614, 1470, 1464, 1455, 1423, 1402, 1387, 1373, 1317, 1260, 1212, 1187, 1174, 1110, 1083, 1019, 992, 969, 951, 898, 887, 851, 822 cm^{-1} ; HRMS (MM: ESI-APCI+) m/z calc'd for $\text{C}_{17}\text{H}_{27}\text{O}_2$ $[\text{M}+\text{H}]^+$: 263.2006; found 263.2006; $[\alpha]_{\text{D}}^{26.0} -73.44$ (c 0.92, CHCl_3 , 94.7% ee); HPLC conditions: 2.0% IPA in hexanes, 1.0 mL/min, OD-H column, t_{R} (min): major = 6.41, minor = 7.53.

(Note: $\text{Pd}_2(\text{pmdba})_3$ is preferable to $\text{Pd}_2(\text{dba})_3$ in this reaction for ease of separation of pmdba from the reaction products during purification. The non-enantioselective reaction was carried out with $\text{Pd}(\text{PPh}_3)_4$ ¹¹⁵ (5 mol %) in toluene (0.1 M) at 30 °C or with $\text{Pd}_2(\text{dba})_3 \cdot \text{CHCl}_3$ (2.5 mol %) and dppe (6.25 mol %) in toluene (0.1 M) at 30 °C.)



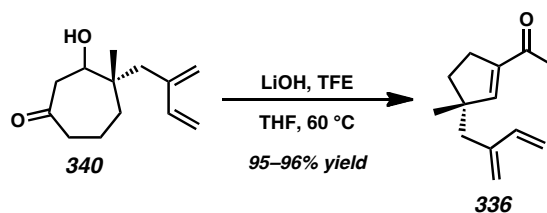
β -Hydroxyketone 340 and Cycloheptenone 365. A 1 L round-bottom flask with a magnetic stir bar was charged with LiAlH_4 (862.6 mg, 22.97 mmol, 0.60 equiv) and evacuated/backfilled with N_2 (3 cycles, 5 min evacuation per cycle). Et_2O (600 mL) was added and the gray suspension was cooled to 0 °C using an ice/water bath. A solution of vinylogous ester **337** (10.05 g, 38.28 mmol, 1.00 equiv) in Et_2O (80 mL) in a conical 100 mL flask was added to the reaction dropwise over 20 min using positive pressure

cannulation. The flask was washed with THF (2 x 10 mL) and washes were added to the reaction. The gray suspension was stirred at 0 °C. After 15 min of stirring, the reaction was quenched by slow dropwise addition of 10% aqueous HCl (59.4 mL). Gas evolution was observed. The reaction was stirred at 0 °C for 5 min and the phases were separated. The aqueous phase was extracted with Et₂O (3 x 30 mL). Combined organic phases were dried over Na₂SO₄, filtered, and concentrated under reduced pressure. The crude oil was purified by flash column chromatography (SiO₂, 3 x 25 cm, 10:1→3:1→2:1 hexanes:EtOAc) to afford cycloheptenone **365** (174.9 mg, 0.919 mmol, 2% yield) as a pale yellow oil and β-hydroxyketone **340** (7.65 g, 36.73 mmol, 96% yield, 1.26:1 dr) as a pale tan oil. (Note: Storage in a sealed container in a –25 °C freezer is recommended, but the compound is typically used shortly after generation.)

β-Hydroxyketone 340: R_f = 0.15 (4:1 hexanes:EtOAc); ¹H NMR (500 MHz, CDCl₃) mixture of two overlapping diastereomers, see Figure A5.40; ¹³C NMR (125 MHz, CDCl₃) mixture of two diastereomers: δ 214.0, 213.0, 143.4, 143.1, 140.7, 140.6, 119.5, 119.3, 113.9, 113.9, 73.5, 72.1, 47.7, 46.8, 44.1, 43.9, 41.5, 41.4, 40.7, 38.8, 36.4, 36.0, 22.1, 21.9, 19.2, 18.4; IR (Neat Film NaCl) 3447, 3084, 2966, 2933, 2873, 1810, 1696, 1628, 1590, 1465, 1457, 1400, 1351, 1321, 1252, 1166, 1113, 1064, 993, 899, 853, 802, 759, 729 cm⁻¹; HRMS (APCI+) m/z calc'd for C₁₃H₁₈O [M–OH]⁺: 191.1430; found 191.1426; $[\alpha]_D^{26.0}$ –30.27 (c 1.66, CHCl₃, 94.7% ee).

Cycloheptenone 365: R_f = 0.60 (4:1 hexanes:EtOAc); ¹H NMR (500 MHz, CDCl₃) δ 6.35 (ddd, J = 17.6, 10.9, 0.8 Hz, 1H), 6.05 (dd, J = 13.0, 1.0 Hz, 1H), 5.77 (d, J = 13.0

Hz, 1H), 5.23–5.20 (m, 1H), 5.20 (d, $J = 17.5$ Hz, 1H), 5.05 (dm, $J = 10.9$ Hz, 1H), 4.99–4.94 (m, 1H), 2.66–2.49 (m, 2H), 2.38 (d, $J = 13.6$ Hz, 1H), 2.27 (dd, $J = 13.6, 0.9$ Hz, 1H), 1.90–1.75 (m, 3H), 1.73–1.60 (m, 1H), 1.10 (s, 3H); ^{13}C NMR (125 MHz, CDCl_3) δ 204.8, 152.8, 142.3, 140.1, 128.0, 120.0, 114.3, 45.1, 43.3, 43.2, 39.0, 27.9, 18.4; IR (Neat Film NaCl) 3087, 3008, 2962, 2930, 2869, 1811, 1707, 1658, 1591, 1457, 1400, 1373, 1346, 1336, 1261, 1208, 1146, 1092, 1020, 900, 876, 801 cm^{-1} ; HRMS (MM: ESI-APCI+) m/z calc'd for $\text{C}_{13}\text{H}_{18}\text{O}$ $[\text{M}+\text{H}]^+$: 191.1430; found 191.1428; $[\alpha]_{\text{D}}^{25.0} -5.31$ (c 1.20, CHCl_3 , 94.7% ee).

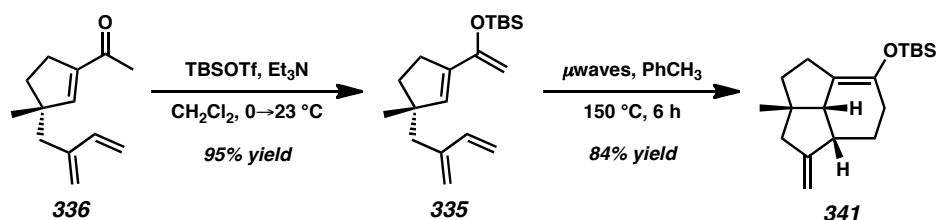


Acylcyclopentene 336 (0.4 mmol scale). β -Hydroxyketone **340** (89.3 mg, 0.428 mmol, 1.00 equiv) was dissolved in THF (4.3 mL) in a 20 mL scintillation vial with a magnetic stir bar. The solution was treated with 2,2,2-trifluoroethanol (46.9 μL , 0.643 mmol, 1.50 equiv) and anhydrous LiOH (15.4 mg, 0.643 mmol, 1.50 equiv). The headspace of the vial was purged with Ar. The vial was sealed with a teflon-lined hard cap and inserted into a 60 °C heating block. After 14 h of stirring, the fine suspension was allowed to cool to ambient temperature, diluted with Et_2O (4 mL), dried over Na_2SO_4 with stirring for 30 min, filtered, and carefully concentrated under reduced pressure (25 mmHg) in a 0 °C ice/water bath. The crude product was purified using flash column chromatography (SiO_2 , 2 x 25 cm, 15:1 hexanes: Et_2O) to afford acylcyclopentene **336** (77.1 mg, 0.405 mmol, 95% yield) as a fragrant pale tan oil.

Acylcyclopentene 336 (30 mmol scale). β -Hydroxyketone **340** (6.46 g, 31.0 mmol, 1.00 equiv) was dissolved in THF (310 mL) in a 1 L round-bottom flask with a magnetic stir bar. The solution was treated with 2,2,2-trifluoroethanol (3.39 mL, 46.5 mmol, 1.50 equiv) and anhydrous LiOH (1.116 g, 46.53 mmol, 1.50 equiv). The flask was fitted with a reflux condenser, purged with N₂, and immersed in a 60 °C oil bath. After 34 h of stirring, the fine suspension was allowed to cool to ambient temperature, diluted with Et₂O (300 mL), dried over Na₂SO₄ with stirring for 30 min, filtered, and carefully concentrated under reduced pressure (25 mmHg) in a 0 °C ice/water bath. The crude product was purified using flash column chromatography (SiO₂, 5 x 25 cm, 15:1 hexanes:Et₂O) to afford acylcyclopentene **336** (5.703 g, 29.97 mmol, 96% yield) as a fragrant pale tan oil.

R_f = 0.61 (4:1 hexanes:EtOAc); ¹H NMR (500 MHz, CDCl₃) δ 6.45 (app. t, J = 1.8 Hz, 1H), 6.35 (ddm, J = 17.6, 10.8 Hz, 1H), 5.16–5.12 (m, 1H), 5.16 (d, J = 17.8 Hz, 1H), 5.04 (dm, J = 10.9 Hz, 1H), 4.97–4.91 (m, 1H), 2.55–2.43 (m, 2H), 2.38 (d, J = 13.5 Hz, 1H), 2.32 (dd, J = 13.6, 0.9 Hz, 1H), 2.23 (s, 3H), 1.91 (ddd, J = 12.9, 7.6, 6.8 Hz, 1H), 1.65 (ddd, J = 12.9, 7.8, 6.8 Hz, 1H), 1.10 (s, 3H); ¹³C NMR (125 MHz, CDCl₃) δ 197.5, 152.7, 143.4, 142.9, 140.1, 119.3, 114.0, 50.3, 41.5, 37.0, 29.4, 26.7, 26.2; ¹H NMR (500 MHz, C₆D₆) δ 6.25 (ddd, J = 17.6, 10.8, 0.8 Hz, 1H), 6.07 (app. t, J = 1.8 Hz, 1H), 5.03 (d, J = 17.3 Hz, 1H), 5.03–4.99 (m, 1H), 4.90 (dm, J = 10.9 Hz, 1H), 4.79–4.75 (m, 1H), 2.65–2.52 (m, 2H), 2.17 (d, J = 13.5 Hz, 1H), 2.07 (dd, J = 13.5, 0.8 Hz, 1H), 1.98 (s, 3H), 1.69 (ddd, J = 12.8, 7.9, 6.8 Hz, 1H), 1.41 (ddd, J = 12.9, 7.9, 6.6 Hz, 1H), 0.90 (s,

3H); ^{13}C NMR (125 MHz, C_6D_6) δ 195.3, 150.9, 143.8, 143.4, 140.4, 119.3, 114.0, 50.2, 41.6, 37.2, 30.0, 26.4, 26.1; IR (Neat Film NaCl) 3084, 2954, 2927, 2864, 1807, 1669, 1617, 1591, 1457, 1437, 1424, 1377, 1366, 1307, 1267, 1227, 1200, 1160, 1092, 1043, 1019, 992, 934, 898, 867, 806 cm^{-1} ; HRMS (MM: ESI-APCI+) m/z calc'd for $\text{C}_{13}\text{H}_{19}\text{O}$ $[\text{M}+\text{H}]^+$: 191.1430; found 191.1427; $[\alpha]_{\text{D}}^{26.0}$ -63.18 (c 1.02, CHCl_3 , 94.7% ee).

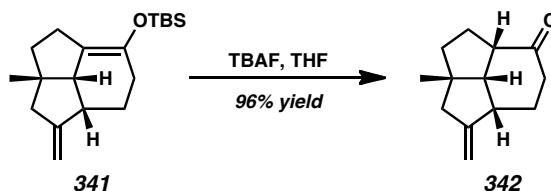
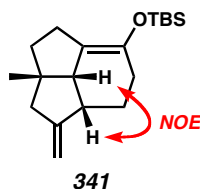


Silyl Dienol Ether 335. A 20 mL scintillation vial with a magnetic stir bar was charged with acylcyclopentene **336** (41.7 mg, 0.219 mmol, 1.00 equiv), sealed with a septum-fitted screw cap, and connected to a N_2 inlet. The headspace of the vial was gently purged with N_2 through a venting needle for 1 min. CH_2Cl_2 (2.2 mL) was added and the reaction was cooled to 0 °C using an ice/water bath. After 5 min of stirring, Et_3N (122 μL , 0.877 mmol, 4.00 equiv) was added dropwise. After 2 min of stirring, TBSOTf¹¹⁶ (101 μL , 0.438 mmol, 2.00 equiv) was added dropwise. The formation of vapor was observed. The clear, colorless solution was stirred at 0 °C for 20 min. The reaction was diluted with CH_2Cl_2 (2.2 mL) and quenched by addition of ice-cold sat. aqueous NaHCO_3 (1.5 mL) and stirred for 5 min at 0 °C. The phases were separated and the aqueous phase was extracted with CH_2Cl_2 (3 x 2 mL). The combined organic phases were dried over Na_2SO_4 , filtered, and concentrated under reduced pressure. The residue was purified by flash column chromatography with deactivated silica gel (SiO_2 , 3 x 12 cm, deactivated with 1% Et_3N in hexanes, 1% Et_3N in hexanes \rightarrow 20% Et_2O in hexanes eluent) to afford

silyl dienol ether **335** (63.1 mg, 0.207 mmol, 95% yield) as a colorless oil. (Note: Silyl dienol ether **335** appears to be sensitive to moisture. The compound was stored as a solidified benzene solution under N₂ in a –25 °C freezer.); R_f = 0.73 (10:1 hexanes:EtOAc); ¹H NMR (500 MHz, C₆D₆) δ 6.35 (ddd, J = 17.5, 10.8, 0.8 Hz, 1H), 6.06 (app. t, J = 1.8 Hz, 1H), 5.20 (dm, J = 17.5 Hz, 1H), 5.11–5.08 (m, 1H), 4.98 (dm, J = 10.9 Hz, 1H), 4.94–4.91 (m, 1H), 4.37–4.35 (m, 1H), 4.36–4.34 (m, 1H), 2.49–2.36 (m, 2H), 2.31 (d, J = 13.4 Hz, 1H), 2.24 (dd, J = 13.4, 0.9 Hz, 1H), 1.87 (ddd, J = 12.6, 8.2, 6.9 Hz, 1H), 1.59 (ddd, J = 12.6, 8.0, 5.9 Hz, 1H), 1.05 (s, 3H), 1.02 (s, 9H), 0.18 (s, 3H), 0.17 (s, 3H); ¹³C NMR (125 MHz, C₆D₆) δ 154.7, 144.5, 140.6, 139.1, 138.0, 118.8, 114.0, 92.8, 49.3, 42.4, 38.2, 31.4, 26.9, 26.1, 18.5, –4.4, –4.5; IR (Neat Film NaCl) 3119, 3084, 2956, 2928, 2857, 1802, 1631, 1589, 1472, 1462, 1389, 1373, 1361, 1315, 1284, 1256, 1225, 1210, 1164, 11121, 1092, 1063, 1016, 1005, 991, 939, 895, 865, 838, 830, 812, 779 cm^{–1}; HRMS (FAB+) m/z calc'd for C₁₉H₃₃OSi [M+H]⁺: 305.2301; found 305.2287; $[\alpha]_D^{25.0}$ –32.17 (c 1.02, CH₂Cl₂, 94.9% ee).

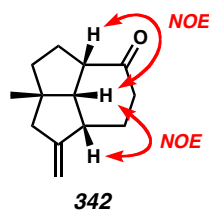
Silyl Enol Ether 341. To a 5 mL microwave vial with magnetic stir bar under N₂ were added silyl dienol ether **335** (88.3 mg, 0.290 mmol, 1.00 equiv) and toluene (4 mL). The reaction was sealed with a microwave crimp cap and subjected to microwave irradiation in a Biotage Initiator microwave reactor (temperature: 150 °C, sensitivity: low) with a gradual temperature increase over 10 min (10 °C increments). After 6 h of stirring, the vial was cooled to ambient temperature and uncapped. The reaction was concentrated under reduced pressure. The residue was purified by flash column chromatography with deactivated silica gel (SiO₂, 3 x 12 cm, deactivated with 1% Et₃N in hexanes, 1% Et₃N in

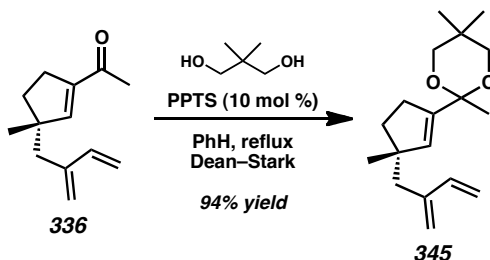
hexanes→20% Et₂O in hexanes eluent) to afford silyl enol ether **341** (74.6 mg, 0.245 mmol, 84% yield) as a colorless oil; $R_f = 0.60$ (1% Et₂O in hexanes); ¹H NMR (500 MHz, C₆D₆) δ 4.99–4.95 (m, 1H), 4.91–4.86 (m, 1H), 2.75–2.70 (m, 1H), 2.70–2.62 (m, 1H), 2.32–2.09 (m, 4H), 2.01 (dm, $J = 16.8$ Hz, 1H), 1.97–1.83 (m, 2H), 1.83–1.71 (m, 1H), 1.61 (ddd, $J = 13.1, 9.2, 3.9$ Hz, 1H), 1.48 (ddd, $J = 12.9, 11.3, 6.7$ Hz, 1H), 1.02 (s, 3H), 1.01 (s, 9H), 0.14 (s, 3H), 0.11 (s, 3H); ¹³C NMR (125 MHz, C₆D₆) δ 154.4, 143.0, 120.7, 106.1, 55.3, 47.2, 45.4, 40.3, 36.9, 26.1, 25.9, 25.9, 25.8, 24.1, 18.4, –3.5, –3.8; IR (Neat Film NaCl) 2928, 2859, 1696, 1653, 1472, 1461, 1378, 1356, 1285, 1257, 1215, 1171, 1108, 1090, 1070, 1029, 1006, 978, 990, 959, 933, 890, 874, 834, 813, 777 cm^{–1}; HRMS (EI+) m/z calc'd for C₁₉H₃₂O_{Si} [M]⁺: 304.2223; found 304.2209; $[\alpha]_D^{26.0} +114.41$ (c 1.06, CH₂Cl₂, 94.7% ee). ¹H-NOESY-2D (500 MHz, C₆D₆) spectra were obtained for **341** and selected NOE interactions are shown below.



Ketone 342. To a 20 mL scintillation vial with magnetic stir bar and silyl enol ether **341** (55.4 mg, 0.182 mmol, 1.00 equiv) was added THF (10 mL) to give a clear, colorless solution. TBAF (1.0 M in THF, 364 μ L, 0.364 mmol, 2.00 equiv) was added dropwise, leading to a pale tan solution. After 20 min of stirring, the reaction was concentrated

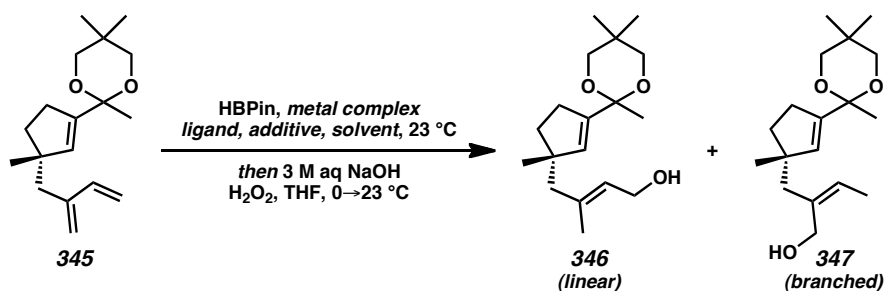
under reduced pressure (25 mmHg) in a 0 °C ice/water bath. The pale yellow residue was purified by flash column chromatography (SiO₂, 3 x 12 cm, 2%→5%→10%→20% Et₂O in hexanes) to afford ketone **342** (36.2 mg, 0.176 mmol, 96% yield) as a colorless oil; R_f = 0.30 (10:1 hexanes:EtOAc); ¹H NMR (500 MHz, CDCl₃) δ 4.93–4.89 (m, 1H), 4.80–4.76 (m, 1H), 2.89–2.79 (m, 1H), 2.70 (ddd, J = 9.8, 9.8, 8.7 Hz, 1H), 2.51 (ddd, J = 16.6, 7.8, 7.8 Hz, 1H), 2.43 (dd, J = 9.6, 9.6 Hz, 1H), 2.29 (ddd, J = 16.2, 2.9, 1.9 Hz, 1H), 2.24 (ddd, J = 16.1, 1.7, 1.7 Hz, 1H), 2.14 (ddd, J = 16.8, 5.8, 5.8 Hz, 1H), 2.06 (dd, J = 5.6, 5.6 Hz, 1H), 2.04 (dd, J = 5.6, 5.6 Hz, 1H), 1.87 (dd, J = 8.5, 8.5 Hz, 1H), 1.86 (dd, J = 8.5, 8.5 Hz, 1H), 1.63 (ddd, J = 12.6, 5.4, 5.4 Hz, 1H), 1.48 (ddd, J = 12.7, 8.5, 8.5 Hz, 1H), 1.16 (s, 3H); ¹³C NMR (125 MHz, CDCl₃) δ 215.3, 154.7, 105.2, 55.6, 52.1, 50.0, 47.8, 40.8, 40.8, 35.4, 30.5, 28.3, 24.9; IR (Neat Film NaCl) 3071, 2925, 2861, 1708, 1660, 1456, 1436, 1408, 1375, 1341, 1319, 1293, 1260, 1245, 1201, 1189, 1146, 1096, 1074, 1042, 968, 882, 802 cm⁻¹; HRMS (MM: ESI-APCI+) m/z calc'd for C₁₃H₁₉O [M+H]⁺: 191.1430; found 191.1429; $[\alpha]_D^{25.0}$ +79.03 (c 1.01, CHCl₃, 94.9% ee). ¹H-NOESY-2D (500 MHz, CDCl₃) spectra were obtained for **342** and selected NOE interactions are shown below.





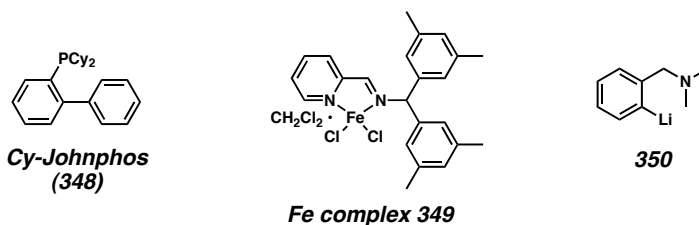
Ketal 345. To a 250 mL round-bottom flask with a magnetic stir bar were added acylcyclopentene **336** (2.08 g, 11.0 mmol, 1.00 equiv), benzene (110 mL), neopentyl glycol (6.85 g, 65.74 mmol, 6.00 equiv), and PPTS (137.7 mg, 0.548 mmol, 0.05 equiv). A Dean–Stark trap and reflux condenser connected to a N₂ inlet was attached and the flask was immersed in a 100 °C oil bath. The suspension gradually became a clear, colorless solution. After 4.5 h of stirring, the reaction was cooled to 0 °C using an ice/water bath and poured into 50% sat. aqueous NaHCO₃ (25 mL) and stirred for 5 min. The phases were separated and the organic phase was washed with brine (3 x 40 mL). The combined aqueous phases were extracted with EtOAc (3 x 50 mL). The combined organic phases were dried over Na₂SO₄, filtered, and concentrated under reduced pressure to give a white semisolid. The crude product was purified using flash column chromatography (SiO₂, 8 x 20 cm, 1%→2%→5% EtOAc in hexanes) to afford ketal **345** (2.84 g, 10.3 mmol, 94% yield) as a pale tan oil; *R_f* = 0.65 (10:1 hexanes:EtOAc); ¹H NMR (500 MHz, CDCl₃) δ 6.38 (dd, *J* = 17.4, 11.1 Hz, 1H), 5.54 (app. t, *J* = 1.9 Hz, 1H), 5.24 (d, *J* = 17.5 Hz, 1H), 5.16–5.13 (m, 1H), 5.05 (d, *J* = 10.7 Hz, 1H), 5.00–4.93 (m, 1H), 3.58 (d, *J* = 10.9 Hz, 1H), 3.50 (d, *J* = 11.0 Hz, 1H), 3.35–3.26 (m, 2H), 2.35 (d, *J* = 13.5 Hz, 1H), 2.33 (d, *J* = 13.5 Hz, 1H), 2.31–2.19 (m, 2H), 1.95 (ddd, *J* = 12.7, 8.4, 6.6 Hz, 1H), 1.65 (ddd, *J* = 12.7, 8.2, 5.6 Hz, 1H), 1.39 (s, 3H), 1.16 (s, 3H), 1.08 (s, 3H), 0.68 (s, 3H); ¹³C NMR (125 MHz, CDCl₃) δ 144.3, 140.6, 140.4, 138.7, 118.7, 113.9,

98.8, 71.8, 71.8, 49.5, 41.9, 37.2, 31.1, 29.8, 27.6, 27.6, 22.9, 22.2; IR (Neat Film NaCl) 3084, 2951, 2865, 1631, 1591, 1472, 1458, 1395, 1369, 1352, 1319, 1298, 1257, 1240, 1180, 1117, 1083, 1040, 1014, 991, 949, 895, 862, 806, 793 cm^{-1} ; HRMS (MM: ESI-APCI+) m/z calc'd for $\text{C}_{18}\text{H}_{29}\text{O}_2$ $[\text{M}+\text{H}]^+$: 277.2162; found 277.2169; $[\alpha]_{\text{D}}^{25.0}$ -6.24 (c 0.950, CHCl_3 , 94.9% ee).



entry	metal complex (mol %)	ligand or additive (mol %)	solvent	time (h)	yield (%) ^c	<i>l</i> : <i>b</i> ^d
1 ^a	Fe complex 349 (8%)	Mg powder (16%)	Et ₂ O	42	0	n.d.
2 ^a	Fe complex 349 (4%)	aryllithium 350 (8%)	Et ₂ O	10	62	1.1 : 1
3 ^b	Pd(PPh ₃) ₄ (5%)	—	PhH	41	0	n.d.
4 ^b	Pd(P ^{<i>t</i>} -Bu) ₃ (5%)	—	PhH	41	< 5	n.d.
5 ^b	Ni(cod) ₂ (5%)	PCy ₃ (5%)	PhCH ₃	52	89	3.0 : 1
6 ^b	Ni(cod) ₂ (10%)	PCy ₃ (10%)	PhCH ₃	9.5	89	3.2 : 1
7 ^b	Ni(cod) ₂ (5%)	Cy-Johnphos (348) (5%)	PhCH ₃	6.5	50	3.1 : 1
8 ^b	Ni(cod) ₂ (5%)	P(NMe ₂) ₃ (5%)	PhCH ₃	6.5	14	2.8 : 1
9 ^b	Ni(cod) ₂ (5%)	P ^{<i>t</i>} -Bu ₃ (5%)	PhCH ₃	6.5	57	8.3 : 1
10 ^b	Ni(cod) ₂ (10%)	P ^{<i>t</i>} -Bu ₃ (10%)	PhCH ₃	9.5	60	9.0 : 1

^a Conditions: 1,3-Diene (1.0 equiv), pinacolborane (1.50 equiv), metal complex (x mol %), additive (2x mol %) in solvent (0.15 M) at indicated 23 °C in a N₂-filled glove box. ^b Conditions: 1,3-Diene (1.0 equiv), pinacolborane (1.05 equiv), metal complex (x mol %), ligand (x mol %) in solvent (0.1 M) at 23 °C in a N₂-filled glove box. ^c Combined isolated yield of **346** and **347**. ^d Ratio of linear : branched allylic alcohols **346** and **347**, determined by relative integration by ¹H NMR.



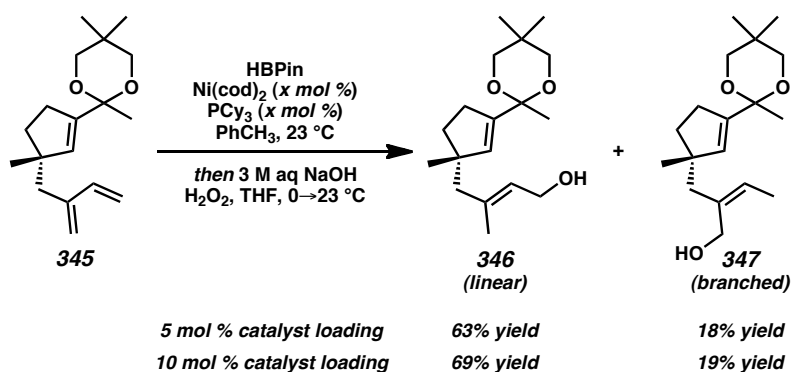
Ni- and Pd-catalyzed 1,4-Hydroboration Screening Procedure (0.1 mmol scale, Table 3.1, entries 1–8). To a 2 dram vial with magnetic stir bar were added metal source (20–100 mM solution of Ni⁸⁷ or Pd⁸⁵ source in solvent, x mol %) and ligand (20–100 mM

solution of ligand in solvent, x mol %) in a N₂-filled glove box. Additional solvent was added to bring the reaction concentration to 0.10 M relative to substrate. The reaction was stirred for 5 min at 23 °C. Pinacolborane (13.8 µL, 0.0950 mmol, 1.05 equiv) was added and the reaction was stirred for an additional 5 min. Diene substrate **345** (25.0 mg, 0.0904 mmol, 1.00 equiv) was added and the reaction was capped with a teflon-lined hard cap. Reaction progress was monitored by TLC. Once the reaction was complete, the reaction was diluted with an equal volume of THF relative to reaction solvent. The vial was capped, removed from the glove box, and cooled to 0 °C using an ice/water bath. The reaction was quenched by dropwise addition of 3 M aqueous NaOH (0.54 mL) and 30% wt. aqueous H₂O₂ (0.43 mL), stirred at 0 °C for 5 min, and then warmed to 23 °C. Once the oxidation was complete, the reaction was cooled to 0 °C, treated with sat. aqueous Na₂S₂O₃ (0.54 mL), stirred for 5 min at 0 °C, and then warmed to 23 °C. The phases were separated and the aqueous phase was extracted with EtOAc (3 x 2 mL). The combined organic phases were washed with brine, dried over Na₂SO₄, filtered, and concentrated under reduced pressure. The residue was purified by flash column chromatography (SiO₂, 2 x 25 cm, 6:1→4:1→2:1 hexanes:EtOAc) to afford branched allylic alcohol **347** and linear allylic alcohol **346**. The ratio of products was analyzed by ¹H NMR (300 or 500 MHz, C₆D₆) by comparing the relative integrations of the peaks corresponding to linear isomer **346** (δ 5.39 (t, *J* = 6.6 Hz, 1H)) and branched isomer **347** (δ 5.29 (q, *J* = 6.9 Hz, 1H)). Alternatively, the ratio of *allylborane intermediates* can be analyzed by ¹H NMR (300 or 500 MHz, C₆D₆) by comparing the relative integrations of the peaks corresponding to the linear allylborane isomer (δ 5.53 (br t, *J* = 7.4 Hz, 1H)) and the branched allylborane isomer (δ 5.32 (br q, *J* = 6.4 Hz, 1H)).

Fe-catalyzed 1,4-Hydroboration Screening Procedure (0.1 mmol scale, Table 3.1, entries 9–10). To a 2 dram vial with magnetic stir bar were added diene substrate **345** (25.0 mg, 0.0904 mmol, 1.00 equiv) and FeCl₂(py-imine) complex **349**⁸⁶ (x mol %). Et₂O (0.6 mL) was added, followed by additive (2x mol %) in a N₂-filled glove box. Finely divided Mg powder^{86a} was added as a solid and aryllithium **350**^{86b} was added as a solution in THF (1.0 M). The reaction was stirred for 5 min at 23 °C. Pinacolborane (19.7 μL, 0.136 mmol, 1.50 equiv) was added and the reaction was capped with a teflon-lined hard cap. Reaction progress was monitored by TLC. Once the reaction was complete, the reaction was diluted with an equal volume of THF relative to reaction solvent. The vial was capped, removed from the glove box, and cooled to 0 °C using an ice/water bath. The reaction was quenched by dropwise addition of 3 M aqueous NaOH (0.54 mL) and 30% wt. aqueous H₂O₂ (0.43 mL), stirred at 0 °C for 5 min, and then warmed to 23 °C. Once the oxidation was complete, the reaction was cooled to 0 °C, treated with sat. aqueous Na₂S₂O₃ (0.54 mL), stirred for 5 min at 0 °C, and then warmed to 23 °C. The phases were separated and the aqueous phase was extracted with EtOAc (3 x 2 mL). The combined organic phases were washed with brine, dried over Na₂SO₄, filtered, and concentrated under reduced pressure. The residue was purified by flash column chromatography (SiO₂, 2 x 25 cm, 6:1→4:1→2:1 hexanes:EtOAc) to afford branched allylic alcohol **347** and linear allylic alcohol **346**. The ratio of products was analyzed by ¹H NMR (300 or 500 MHz, C₆D₆) by comparing the relative integrations of the peaks corresponding to linear isomer **346** (δ 5.39 (t, *J* = 6.6 Hz, 1H)) and branched isomer **347** (δ 5.29 (q, *J* = 6.9 Hz, 1H)). Alternatively, the ratio of *allylborane intermediates* can be

analyzed by ^1H NMR (300 or 500 MHz, C_6D_6) by comparing the relative integrations of the peaks corresponding to the linear allylborane isomer (δ 5.53 (br t, J = 7.4 Hz, 1H)) and the branched allylborane isomer (δ 5.32 (br q, J = 6.4 Hz, 1H)).

(Note: Control reactions were performed with isoprene as substrate. With a $\text{Ni}(\text{cod})_2/\text{PCy}_3$ catalyst system, a 1.26:1 linear:branched ratio was observed. With a Fe complex **349** as the catalyst system, the reported 10:1 linear:branched ratio was observed.^{86a} The C(4) quaternary stereocenter is likely responsible for the differences in regioselectivity in our case.)



Linear Allylic Alcohol 346 and Branched Allylic Alcohol 347 (5 mol % catalyst loading).⁸⁷ To a 250 mL round-bottom flask with magnetic stir bar were added $\text{Ni}(\text{cod})_2$ (113.9 mg, 0.414 mmol, 5 mol %), PCy_3 (116.1 mg, 0.414 mmol, 5 mol %), and toluene (25 mL) in a N_2 -filled glove box. The pale orange solution was stirred for 5 min. Pinacolborane (1.26 mL, 8.69 mmol, 1.05 equiv) was added dropwise, causing the reaction to become a dark orange solution. Diene **345** (2.29 g, 8.28 mmol, 1.00 equiv) in toluene (8 mL) was added, causing further darkening of the reaction to a red-orange solution. The reaction was sealed with a rubber septum and stirred at 23 °C in the glove

box. After 96 h of stirring, the reaction reverted to an orange color. The reaction was diluted with toluene (33 mL) and THF (33 mL), sealed with a rubber septum, removed from the glove box, and connected to a N₂ inlet. The reaction was cooled to 0 °C using an ice/water bath and 3 M aqueous NaOH (52.2 mL) was added dropwise over 5 min. Chilled, ice cold 30% wt. aqueous H₂O₂ (39.4 mL) was added dropwise over 20 min, giving a yellow biphasic mixture. The reaction was stirred at 0 °C until the oxidation was complete by TLC (5 min). At 0 °C, sat. aqueous Na₂S₂O₃ (52.2 mL) was added dropwise over 20 min, causing the biphasic mixture to become colorless. The reaction was stirred at 0 °C for 15 min, warmed to 23 °C, and stirred for 15 min. The phases were separated and the organic phase was washed with H₂O (2 x 20 mL) and brine (2 x 20 mL). The combined aqueous phases were extracted with EtOAc (3 x 30 mL). The combined organic phases were dried over Na₂SO₄, filtered, and concentrated under reduced pressure. The residue was purified by flash column chromatography (SiO₂, 8 x 35 cm, 10:1→8:1→6:1→4:1→2:1 hexanes:EtOAc) to afford branched allylic alcohol **347** (427.2 mg, 1.45 mmol, 18% yield) as a yellow oil and linear allylic alcohol **346** (1.535 g, 5.212 mmol, 63% yield) as a yellow oil.

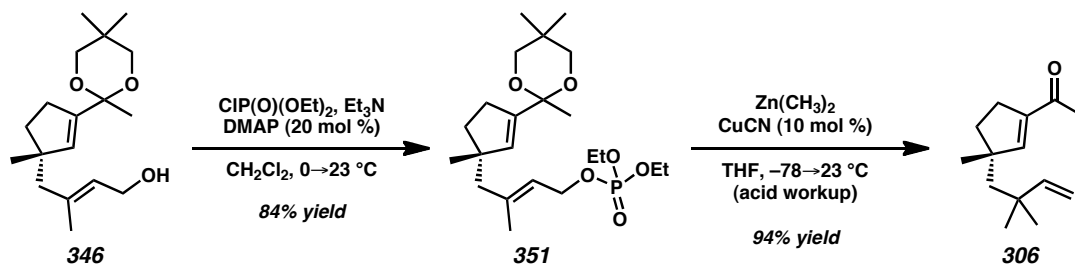
Linear Allylic Alcohol 346 and Branched Allylic Alcohol 347 (10 mol % catalyst loading).⁸⁷ To a 1 L round-bottom flask with magnetic stir bar were added Ni(cod)₂ (660 mg, 2.40 mmol, 10 mol %), PCy₃ (674 mg, 2.40 mmol, 10 mol %), and toluene (65 mL) in a N₂-filled glove box. The pale orange solution was stirred for 5 min. Pinacolborane (3.66 mL, 25.2 mmol, 1.05 equiv) was added dropwise, causing the reaction to become a dark orange solution. Diene **345** (6.64 g, 24.0 mmol, 1.00 equiv) in toluene (30 mL) was

added, causing further darkening of the reaction to a red-orange solution. The reaction was sealed with a rubber septum and stirred at 23 °C in the glove box. After 48 h of stirring, the reaction reverted to an orange color. The reaction was diluted with toluene (95 mL) and THF (95 mL), sealed with a rubber septum, removed from the glove box, and connected to a N₂ inlet. The reaction was cooled to 0 °C using an ice/water bath and 3 M aqueous NaOH (153 mL) was added dropwise over 5 min. Chilled, ice cold 30% wt. aqueous H₂O₂ (114 mL) was added dropwise over 45 min, giving a yellow biphasic mixture. The reaction was stirred at 0 °C until the oxidation was complete by TLC (5 min). At 0 °C, sat. aqueous Na₂S₂O₃ (153 mL) was added dropwise over 1 h, causing the biphasic mixture to become colorless. The reaction was stirred at 0 °C for 15 min, warmed to 23 °C, and stirred for 15 min. The phases were separated and the organic phase was washed with H₂O (2 x 50 mL) and brine (2 x 50 mL). The combined aqueous phases were extracted with EtOAc (3 x 60 mL). The combined organic phases were dried over Na₂SO₄, filtered, and concentrated under reduced pressure. The residue was purified by flash column chromatography (SiO₂, 8 x 35 cm, 10:1→8:1→6:1→4:1→2:1 hexanes:EtOAc) to afford branched allylic alcohol **347** (1.358 g, 4.6133 mmol, 19% yield) as a yellow oil and linear allylic alcohol **346** (4.876 g, 16.562 mmol, 69% yield) as a yellow oil.

Linear Allylic Alcohol 346: $R_f = 0.15$ (4:1 hexanes:EtOAc); ¹H NMR (500 MHz, C₆D₆) δ 5.63 (app. t, $J = 1.9$ Hz, 1H), 5.39 (br t, $J = 6.6$ Hz, 1H), 4.00 (d, $J = 6.6$ Hz, 2H), 3.51 (d, $J = 11.0$ Hz, 1H), 3.49 (d, $J = 11.0$ Hz, 1H), 3.30 (dd, $J = 6.9, 2.4$ Hz, 1H), 3.28 (dd, $J = 6.9, 2.4$ Hz, 1H), 2.42–2.31 (m, 2H), 2.05 (s, 2H), 1.87 (ddd, $J = 12.6, 8.1, 6.8$ Hz, 1H),

1.63–1.51 (m, 1H), 1.59 (s, 3H), 1.55 (br s, 3H), 1.16 (s, 3H), 1.01 (s, 3H), 0.50 (s, 3H); ^{13}C NMR (125 MHz, C_6D_6) δ 141.9, 138.7, 136.3, 128.7, 98.9, 71.7, 59.4, 51.2, 49.4, 37.4, 31.5, 29.7, 27.5, 22.9, 22.2, 18.6; IR (Neat Film NaCl) 3413, 3039, 2951, 2866, 2737, 2962, 1726, 1663, 1471, 1454, 1395, 1369, 1352, 1319, 1297, 1254, 1240, 1179, 1116, 1082, 1040, 1013, 950, 929, 911, 861, 808, 7793, 755 cm^{-1} ; HRMS (MM: ESI-APCI+) m/z calc'd for $\text{C}_{18}\text{H}_{29}\text{O}_3$ $[\text{M}]^{+}$: 277.2162; found 277.2155; $[\alpha]_{\text{D}}^{25.0}$ -0.82 (c 0.84, CHCl_3 , 94.9% ee).

Branched Allylic Alcohol 347: R_f = 0.21 (4:1 hexanes:EtOAc); ^1H NMR (500 MHz, C_6D_6) δ 5.71 (app. t, J = 1.9 Hz, 1H), 5.29 (br q, J = 6.9 Hz, 1H), 4.05 (s, 2H), 3.52 (d, J = 10.9 Hz, 1H), 3.49 (d, J = 10.9 Hz, 1H), 3.35–3.25 (m, 2H), 2.44–2.33 (m, 2H), 2.29 (d, J = 13.4 Hz, 1H), 2.18 (d, J = 13.3 Hz, 1H), 1.95 (ddd, J = 12.6, 7.7, 7.7 Hz, 1H), 1.64–1.56 (m, 1H), 1.58 (s, 3H), 1.55 (d, J = 6.8 Hz, 3H), 1.13 (s, 3H), 1.05 (s, 3H), 0.53 (s, 3H); ^{13}C NMR (125 MHz, C_6D_6) δ 142.1, 138.6, 138.6, 125.7, 99.0, 71.7, 60.7, 49.6, 46.5, 37.0, 31.5, 29.8, 27.6, 27.2, 22.9, 22.2, 13.4; IR (Neat Film NaCl) 3435, 3036, 2950, 2866, 2739, 2693, 1877, 1723, 1649, 1471, 1455, 1395, 1369, 1353, 1297, 1282, 1255, 1240, 1178, 1139, 1116, 1082, 1039, 1013, 950, 929, 911, 860, 808, 793, 739 cm^{-1} ; HRMS (MM: ESI-APCI+) m/z calc'd for $\text{C}_{18}\text{H}_{29}\text{O}_3$ $[\text{M}]^{+}$: 277.2162; found 277.2155; $[\alpha]_{\text{D}}^{25.0}$ -6.27 (c 1.08, CHCl_3 , 94.9% ee).



Allylic Phosphate 351.¹¹⁸ To a 300 mL round-bottom flask with a magnetic stir bar containing linear allylic alcohol **346** (1.522 g, 5.17 mmol, 1.00 equiv) in CH_2Cl_2 (103 mL) under N_2 at 0°C (ice/water bath) were added Et_3N (1.08 mL, 7.76 mmol, 1.5 equiv) and DMAP (126.3 mg, 1.03 mmol, 0.2 equiv). The pale tan solution was stirred for 5 min. Diethylchlorophosphate (1.12 mL, 7.76 mmol, 1.50 equiv) was added dropwise and the reaction was stirred for 5 min. The cooling bath was removed and the reaction was allowed to warm to 23°C . After 3 h of stirring, the reaction was quenched with sat. aqueous NH_4Cl (50 mL). The reaction was stirred for 5 min and the phases were separated. The organic phase was washed with brine (20 mL). The combined aqueous phases were extracted with CH_2Cl_2 (3 x 50 mL). The combined organic phases were dried over Na_2SO_4 , filtered, and concentrated under reduced pressure. The residue was purified by flash column chromatography (SiO_2 , 5 x 25 cm, 30% \rightarrow 40% \rightarrow 50% EtOAc in hexanes) to afford allyl phosphate **351** (1.86 g mg, 4.32 mmol, 84% yield) as a pale tan oil; $R_f = 0.20$ (2:1 hexanes:EtOAc); ^1H NMR (500 MHz, CDCl_3) δ 5.56 (app. t, $J = 1.9$ Hz, 1H), 5.40 (br t, $J = 7.0$ Hz, 1H), 4.56 (dd, $J = 7.5, 7.5$ Hz, 2H), 4.10 (dq, $J = 7.9, 7.1$ Hz, 4H), 3.52 (dd, $J = 11.1, 3.5$ Hz, 2H), 3.33 (ddd, $J = 11.1, 3.9, 2.5$ Hz, 2H), 2.38–2.21 (m, 2H), 2.17 (s, 2H), 1.90 (ddd, $J = 12.7, 8.6, 6.5$ Hz, 1H), 1.73 (br s, 3H), 1.64 (ddd, $J = 12.6, 8.4, 5.4$ Hz, 1H), 1.40 (s, 3H), 1.33 (td, $J = 7.1, 1.0$ Hz, 6H), 1.16 (s, 3H), 1.05 (s, 3H), 0.70 (s, 3H); ^{13}C NMR (125 MHz, CDCl_3) δ 141.0, 140.7, 138.7, 122.8 ($J_{\text{C-P}} = 5.7$

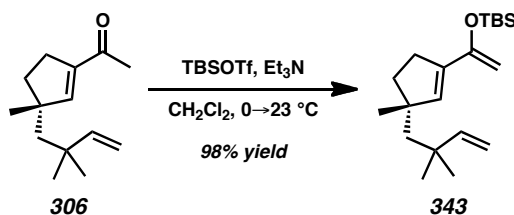
Hz), 98.7, 71.8 ($J_{\text{C-P}} = 5.3$ Hz), 64.1 ($J_{\text{C-P}} = 5.7$ Hz), 63.7 ($J_{\text{C-P}} = 5.8$ Hz), 51.0, 49.2, 37.2, 31.1, 29.8, 27.4, 27.2, 22.8, 22.3, 18.8, 16.3 ($J_{\text{C-P}} = 6.8$ Hz); IR (Neat Film NaCl) 2980, 2951, 2867, 1660, 1473, 1457, 1395, 1369, 1277, 1262, 1180, 1116, 1100, 1082, 1035, 1000, 911, 862, 807, 746 cm^{-1} ; HRMS (MM: ESI-APCI+) m/z calc'd for $\text{C}_{22}\text{H}_{39}\text{O}_6\text{PNa}$ $[\text{M}+\text{Na}]^+$: 453.2376; found 453.2385; $[\alpha]_{\text{D}}^{25.0} -3.77$ (c 0.85, CHCl_3 , 94.9% ee).

(Note: A small amount of ketal deprotection of the phosphorylated product may be observed during work-up. The resulting acylcyclopentene can also be converted to *gem*-dimethyl acylcyclopentene **306** smoothly and chemoselectively using the Cu-catalyzed allylic substitution reaction conditions below.)

Acylcyclopentene 306.⁹² To a 250 mL Schlenk flask with Kontes teflon valve and 14/20 joint with rubber septum were added a magnetic stir bar and CuCN (101 mg, 1.129 mmol, 10 mol %) in a N_2 -filled glove box. The flask was sealed and removed from the glove box. A solution of allyl phosphate **351** (4.86 g, 11.29 mmol, 1.00 equiv) in THF (120 mL) in a 100 mL conical flask was transferred to the Schlenk flask by positive pressure cannulation. Additional THF (30 mL) was added to the Schlenk flask. The reaction was a pale tan solution with insoluble pale green solids. The reaction was cooled to -78 °C using an acetone/ $\text{CO}_2(\text{s})$ bath and stirred for 15 min. $\text{Zn}(\text{CH}_3)_2$ (1.0 M in heptanes, 33.9 mL, 33.9 mmol, 3.00 equiv) was added dropwise by syringe over 15 min. The reaction became a darker tan-grey solution with insoluble pale green solids. The flask was sealed and cooling bath was allowed to slowly expire and reach 23 °C over 16 h. After an additional 48 h of stirring, the reaction was a black suspension. The reaction

was cooled to $-78\text{ }^{\circ}\text{C}$ and stirred for 10 min. The reaction was diluted with Et_2O (100 mL) and stirred for 15 min. The reaction was quenched by slow dropwise addition of 10% aqueous HCl (47 mL). The $-78\text{ }^{\circ}\text{C}$ acetone/ $\text{CO}_2(\text{s})$ cooling bath was exchanged for a $0\text{ }^{\circ}\text{C}$ ice/water bath and the reaction was stirred for 30 min. The ice/water cooling bath was removed and the reaction was allowed to warm to $23\text{ }^{\circ}\text{C}$. After 2 h of stirring, the majority of the metal salts were dissolved and TLC analysis indicated that the intermediate ketal had been converted to the corresponding acylcyclopentene. The phases were separated and the organic phase was washed with H_2O (30 mL) and sat. aqueous NaHCO_3 (30 mL). The combined aqueous phases were extracted with Et_2O (3 x 30 mL). The combined organic phases were dried over Na_2SO_4 , filtered, and concentrated under reduced pressure (25 mmHg) in a $0\text{ }^{\circ}\text{C}$ ice/water bath. The residue was purified by flash column chromatography (SiO_2 , 5 x 25 cm, 15:1 hexanes: Et_2O) to afford acylcyclopentene **306** (2.218 g, 10.750 mmol, 95% yield) as a fragrant pale tan oil; $R_f = 0.41$ (10:1 hexanes: EtOAc); ^1H NMR (500 MHz, CDCl_3) δ 6.58 (app. t, $J = 1.8\text{ Hz}$, 1H), 5.92–5.81 (m, 1H), 4.93–4.87 (m, 2H), 2.51 (dd, $J = 7.1, 1.8\text{ Hz}$, 1H), 2.49 (dd, $J = 7.1, 1.8\text{ Hz}$, 1H), 2.27 (s, 3H), 1.94 (ddd, $J = 12.9, 7.8, 7.8\text{ Hz}$, 1H), 1.67 (d, $J = 14.4\text{ Hz}$, 1H), 1.67–1.59 (m, 1H), 1.59 (d, $J = 14.4\text{ Hz}$, 1H), 1.11 (s, 3H), 1.07 (s, 3H), 1.04 (s, 3H); ^{13}C NMR (125 MHz, CDCl_3) δ 197.7, 154.1, 149.7, 142.2, 110.0, 53.5, 50.7, 38.8, 38.0, 29.7, 29.1, 28.7, 27.9, 26.8; ^1H NMR (500 MHz, C_6D_6) δ 6.16 (app. t, $J = 1.8\text{ Hz}$, 1H), 5.74–5.65 (m, 1H), 4.86–4.79 (m 2H), 2.61 (dd, $J = 7.7, 1.8\text{ Hz}$, 1H), 2.60 (dd, $J = 7.7, 1.8\text{ Hz}$, 1H), 2.02 (s, 3H), 1.72 (ddd, $J = 12.9, 7.7, 7.7\text{ Hz}$, 1H), 1.45–1.36 (m, 1H), 1.39 (d, $J = 14.4\text{ Hz}$, 1H), 1.29 (d, $J = 14.4\text{ Hz}$, 1H), 0.92 (s, 3H), 0.91 (s, 6H); ^{13}C NMR (125 MHz, C_6D_6) δ 195.0, 151.7, 149.3, 142.2, 109.5, 53.0, 50.2, 38.4, 37.5, 29.3, 29.3,

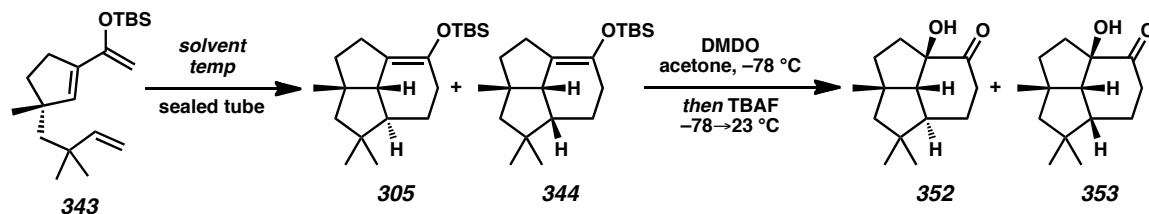
28.1, 27.3, 26.1; IR (Neat Film NaCl) 3080, 2956, 2926, 2872, 1730, 1711, 1668, 1636, 1617, 1455, 1431, 1413, 1377, 1366, 1302, 1269, 1232, 1215, 1190, 1120, 1010, 971, 934, 908, 861, 803 cm^{-1} ; HRMS (MM: ESI-APCI+) m/z calc'd for $\text{C}_{14}\text{H}_{23}\text{O}$ $[\text{M}]^{+}$: 207.1743; found 207.1753; $[\alpha]_{\text{D}}^{25.0} -10.580$ (c 1.12, CHCl_3 , 94.9% ee).



Silyl Dienol Ether 343. A 100 mL pear-shaped flask with a magnetic stir bar under N_2 was charged with acylcyclopentene **306** (400 mg, 1.93 mmol, 1.00 equiv) and CH_2Cl_2 (40 mL). The colorless solution was cooled to 0°C using an ice/water bath. After 5 min of stirring, Et_3N (1.08 mL, 7.75 mmol, 4.00 equiv) was added dropwise. After 2 min of stirring, $\text{TBSOTf}^{\text{f16}}$ (891 μL , 3.88 mmol, 2.00 equiv) was added dropwise. The formation of vapor was observed. The clear, colorless solution was stirred at 0°C for 15 min. The reaction was quenched by addition of ice-cold sat. aqueous NaHCO_3 (12 mL) and stirred for 5 min at 0°C . The phases were separated and the aqueous phase was extracted with CH_2Cl_2 (3 x 15 mL). The combined organic phases washed with brine, dried over Na_2SO_4 , filtered, and concentrated under reduced pressure. The residue was purified by flash column chromatography with deactivated silica gel (SiO_2 , 3 x 25 cm, deactivated with 1% Et_3N in hexanes, 1% Et_3N in hexanes \rightarrow 20% Et_2O in hexanes eluent) to afford silyl dienol ether **343** (607.2 mg, 1.894 mmol, 98% yield) as a colorless oil. (Note: Silyl dienol ether **343** appears to be sensitive to moisture. The compound was stored as a solidified benzene solution under N_2 in a -25°C freezer.); $R_f = 0.78$ (10:1

hexanes:EtOAc, 1% Et₃N in hexanes deactivated silica TLC plates); ¹H NMR (500 MHz, C₆D₆) δ 6.17 (app. t, *J* = 1.8 Hz, 1H), 5.89 (dd, *J* = 17.5, 10.7 Hz, 1H), 4.94 (dd, *J* = 17.5, 1.4 Hz, 1H), 4.92 (dd, *J* = 10.7, 1.4 Hz, 1H), 4.41–4.35 (m, 1H), 4.40–4.34 (m, 1H), 2.50–2.35 (m, 2H), 1.88 (ddd, *J* = 12.7, 8.7, 7.0 Hz, 1H), 1.60 (ddd, *J* = 12.7, 8.3, 5.2 Hz, 1H), 1.56 (d, *J* = 14.3 Hz, 1H), 1.47 (d, *J* = 14.3 Hz, 1H), 1.08 (s, 3H), 1.05–1.02 (m, 12H), 1.03 (s, 3H), 0.19 (s, 3H), 0.18 (s, 3H); ¹³C NMR (125 MHz, C₆D₆) δ 154.8, 150.0, 139.2, 138.3, 109.7, 92.7, 54.3, 49.8, 40.1, 38.0, 31.1, 29.9, 28.7, 28.3, 26.1, 18.5, -4.4, -4.4; IR (Neat Film NaCl) 3119, 3081, 2956, 2929, 2896, 2858, 1818, 1636, 1586, 1472, 1463, 1412, 1389, 1373, 1361, 1330, 1309, 1283, 1256, 1201, 1129, 1090, 1060, 1016, 1005, 939, 907, 838, 812, 779 cm⁻¹; HRMS (FAB+) *m/z* calc'd for C₂₀H₃₇OSi [M+H]⁺: 321.2614; found 321.2607; [α]_D^{25.0} -7.57 (*c* 0.95, CH₂Cl₂, 94.9% ee).

Table 3.2. Intramolecular Diels–Alder/Rubottom Oxidation Screening



entry ^a	temp ($^{\circ}\text{C}$)	heating method	solvent	time (h)	overall yield (%) ^b	352 : 353 ^c
1	110	oil bath	PhCH ₃	96	78	1 : 8.25
2	130	oil bath	PhCH ₃	24	83	1 : 3.58
3	150	oil bath	PhCH ₃	6	79	1 : 3.26
4	160	oil bath	PhCH ₃	2	58	1 : 2.68
5	170	sand bath	PhCH ₃	3	92	1 : 2.55
6	190	metal block	PhCH ₃	1	90	1 : 2.64
7	200	oil bath	<i>p</i> -dioxane	1	95	1 : 2.02
8	200	oil bath	CyCH ₃	1	93	1 : 2.31
9	200	microwave irradiation	PhCl	1	95	1 : 3.26
10	170	metal block	<i>p</i> -dioxane	2	91	1 : 2.03
11	170	metal block	CyCH ₃	2	93	1 : 2.07
12	170	metal block	PhCl	3	94	1 : 2.73
13	170	metal block	CH ₃ CN	2	91	1 : 2.27
14	170	metal block	1,2-DCE	2	83	0 : 1.00

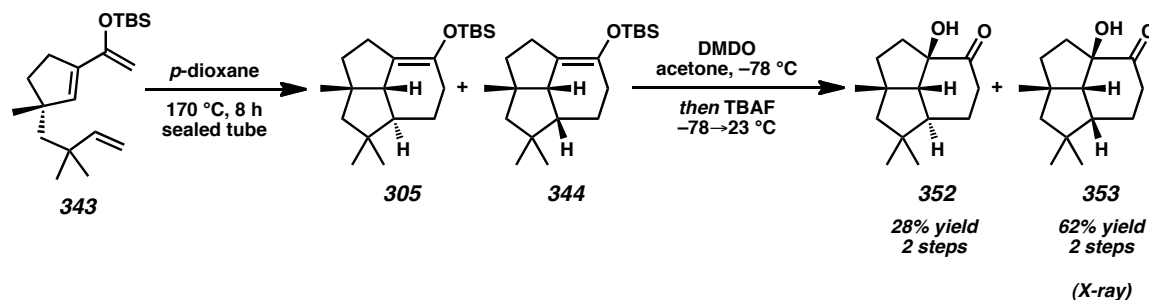
^a Conditions: silyl dienol ether **343** (1.0 equiv), solvent (0.01 M) in a sealed tube at the indicated temperature for the indicated time. ^b Combined isolated yield over two steps for **352** and **353**. ^c Ratio of *trans* : *cis* α -hydroxyketones **352** and **353**, determined by relative integration by ^1H NMR.

Intramolecular Diels–Alder/Rubottom Oxidation Screening Procedure (0.05 mmol scale, Table 3.2, entries 1–14). To a 5 mL microwave vial was added a solution of silyl dienol ether **343** in benzene (100 mg/mL, 20.0 mg, 0.0623 mmol, 1.00 equiv). The solvent was removed under reduced pressure. The vial, a magnetic stir bar, crimp cap, and crimper were placed in a glove box antechamber, which was evacuated/backfilled with N₂ (3 cycles, 5 min evacuation per cycle) before the items were transferred into the glove box. Solvent (6 mL) was added by syringe and the vial was sealed with a crimp cap. The vial was removed from the glove box and heated according to the indicated conditions for the indicated time interval. A blast shield was set up as a precaution. The vial was uncapped and the reaction was concentrated under reduced pressure. The crude

reaction mixture was analyzed by ^1H NMR to confirm the complete consumption of starting material before use in the next step.

The crude mixture of silyl enol ethers **305** and **344** was dissolved in acetone (3 mL) in a 20 mL scintillation vial with magnetic stir bar and sealed with a screw cap. The vials were cooled to $-78\text{ }^\circ\text{C}$ and stirred for 5 min. A solution of DMDO in acetone⁹⁵ (0.103 M, 607 μL , 0.0624 mmol, 1.00 equiv) was added dropwise over 5 min. The reaction was stirred for 5 min, allowed to warm to $23\text{ }^\circ\text{C}$, and concentrated under reduced pressure. The residue was purified by flash column chromatography (SiO_2 , 3 x 12 cm, 10% EtOAc in hexanes) to afford mixture of α -hydroxyketones **352** and **353** as a pale yellow solid. The ratio of products was analyzed by ^1H NMR (300 or 500 MHz, C_6D_6) by comparing the relative integrations of the peaks corresponding to *trans* isomer **352** (δ 0.64 (s, 3H)) and *cis* isomer **353** (δ 0.68 (s, 3H)).

(Note: Incomplete silyl transfer to the tertiary alcohol was observed during the Rubottom oxidation, so TBAF was added to simplify the reaction mixture. The use of anhydrous acetone solvent and dry DMDO still did not lead to clean formation of the anticipated α -silyloxyketone. Attempts to install a silyl group on the alcohol of α -hydroxyketone **352** led to a mixture of bis-, mono-, and unsilylated products. Lower overall yields were observed with *m*-CPBA as the oxidant).



α -Hydroxyketones 352 and 353. To a 20 mL microwave vial was added a solution of silyl dienol ether **343** in benzene (100 mg/mL, 98.1 mg, 0.306 mmol, 1.00 equiv). The solvent was removed under reduced pressure. The vial, a magnetic stir bar, crimp cap, and crimper were placed in a glove box antechamber, which was evacuated/backfilled with N_2 (3 cycles, 5 min evacuation per cycle) before the items were transferred into the glove box. *p*-Dioxane (12.5 mL) was added by syringe and the vial was sealed with a crimp cap. The vial was removed from the glove box and immersed in a preheated 170 $^\circ\text{C}$ heating mantle-supported sand bath regulated by a J-KEM Scientific Model 210 Temperature Controller. A blast shield was set up as a precaution. The reaction was stirred for 8 h at 170 $^\circ\text{C}$. The reaction was allowed to cool to 23 $^\circ\text{C}$ and the vial was uncapped. The reaction was diluted with hexanes (24 mL) and concentrated under reduced pressure to give a mixture of silyl enol ethers **305** and **344**.

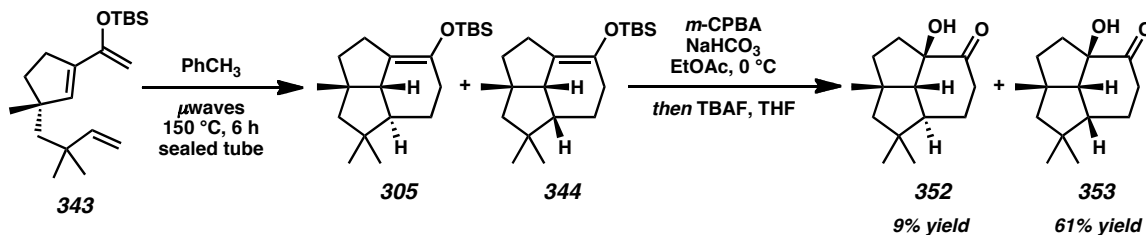
To a 50 mL round-bottom flask with magnetic stir bar was added the mixture of silyl enol ethers **352** and **353**. The flask was evacuated and backfilled with N_2 (3 cycles, 5 min evacuation per cycle). Acetone (12.5 mL) was added and the reaction was cooled to -78 $^\circ\text{C}$. After 15 min of stirring, a solution of DMDO in acetone⁹⁵ (0.0734 M, 5.0 mL, 0.367 mmol, 1.20 equiv) was added dropwise over 10 min. After an additional 5 min of stirring, TBAF (1.0 M in THF, 367 μL , 0.367 mmol, 1.20 equiv). The reaction was stirred at -78 $^\circ\text{C}$ for 5 min, the cooling bath was removed, and the reaction was allowed

to warm to 23 °C. After 15 min of stirring at 23 °C, the reaction was concentrated under reduced pressure to give a pale orange residue, which was purified by flash column chromatography (SiO₂, 5 x 30 cm, 2.5%→5%→10% EtOAc in hexanes) to afford α -hydroxyketones **352** (19.2 mg, 0.0864 mmol, 28% yield over two steps) and **353** (42.3 mg, 0.190 mmol, 62% yield over two steps) as a faint yellow solids. X-ray quality crystals of alcohol **353** (colorless to pale yellow) were grown by slow evaporation from benzene.

α -Hydroxyketone 352 (*trans*-isomer): R_f = 0.18 (10:1 hexanes:EtOAc); ¹H NMR (500 MHz, CDCl₃) δ 3.67 (br s, 1H), 2.62 (ddd, J = 16.2, 4.4, 1.8 Hz, 1H), 2.47 (ddd, J = 16.2, 12.4, 6.8 Hz, 1H), 2.43–2.35 (m, 1H), 2.03–1.97 (m, 2H), 1.86 (dddd, J = 12.0, 6.9, 1.9, 1.9 Hz, 1H), 1.86–1.74 (m, 2H), 1.77 (d, J = 13.4 Hz, 1H), 1.66 (d, J = 13.4 Hz, 1H), 1.57 (ddd, J = 12.6, 12.6, 2.3 Hz, 1H), 1.48 (dddd, J = 12.3, 12.3, 12.3, 4.4 Hz, 1H), 1.28 (s, 3H), 1.05 (s, 3H), 0.87 (s, 3H); ¹³C NMR (125 MHz, CDCl₃) δ 215.2, 87.9, 67.6, 59.8, 54.2, 47.5, 42.0, 40.2, 39.1, 38.8, 31.0, 28.8, 24.0, 22.3; ¹H NMR (500 MHz, C₆D₆) δ 3.90 (br s, 1H), 2.33 (ddd, J = 15.9, 4.4, 1.8 Hz, 1H), 2.04–1.86 (m, 3H), 1.85 (br d, J = 11.6 Hz, 1H), 1.68–1.53 (m, 2H), 1.56 (d, J = 13.2 Hz, 1H), 1.50 (d, J = 13.2 Hz, 1H), 1.38 (s, 3H), 1.25 (dddd, J = 12.1, 6.7, 2.5, 1.8 Hz, 1H), 1.15 (ddd, J = 12.6, 12.6, 2.5 Hz, 1H), 0.92 (dddd, J = 12.5, 12.5, 12.5, 4.4 Hz, 1H), 0.84 (s, 3H), 0.64 (s, 3H); ¹³C NMR (125 MHz, C₆D₆) δ 213.8, 87.7, 67.7, 59.9, 53.9, 47.5, 42.2, 40.0, 39.1, 38.5, 31.1, 28.6, 23.8, 22.2; IR (Neat Film NaCl) 3496, 2947, 2930, 2866, 1701, 1457, 1420, 1371, 1364, 1349, 1319, 1303, 1267, 1243, 1221, 1211, 1196, 1179, 1148, 1114, 1074, 1056, 1040,

1012, 986, 974, 950, 932, 909, 878, 837, 816, 751 cm^{-1} ; HRMS (EI+) m/z calc'd for $\text{C}_{14}\text{H}_{22}\text{O}_2$ $[\text{M}]^{+}$: 222.1620; found 222.1625; $[\alpha]_{\text{D}}^{25.0} +2.96$ (c 0.67, CHCl_3 , 94.9% ee).

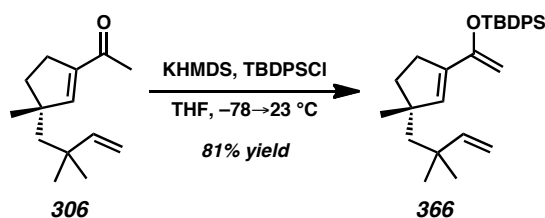
α -Hydroxyketone 353 (*cis*-isomer): $R_f = 0.14$ (10:1 hexanes:EtOAc); ^1H NMR (500 MHz, CDCl_3) δ 3.75 (br s, 1H), 2.60 (ddd, $J = 19.8, 5.0, 2.2$ Hz, 1H), 2.45 (dd, $J = 8.7, 2.0$ Hz, 1H), 2.28 (ddd, $J = 19.7, 11.6, 7.6$ Hz, 1H), 2.05 (ddd, $J = 13.3, 12.2, 8.5$ Hz, 1H), 1.88 (ddd, $J = 12.4, 12.4, 7.5$ Hz, 1H), 1.86–1.71 (m, 4H), 1.69 (d, $J = 13.1$ Hz, 1H), 1.61 (dddd, $J = 12.9, 7.1, 1.3, 1.3$ Hz, 1H), 1.52 (d, $J = 13.2$ Hz, 1H), 1.39 (s, 3H), 1.10 (s, 3H), 0.95 (s, 3H); ^{13}C NMR (125 MHz, CDCl_3) δ 215.2, 86.1, 63.9, 54.0, 52.4, 48.6, 43.9, 42.0, 40.3, 35.0, 32.1, 30.6, 25.3, 22.6; ^1H NMR (500 MHz, C_6D_6) δ 4.04 (br s, 1H), 2.34 (dd, $J = 8.8, 1.4$ Hz, 1H), 2.16–2.08 (m, 1H), 1.95 (ddd, $J = 12.0, 12.0, 1.4$ Hz, 1H), 1.95–1.82 (m, 1H), 1.68–1.58 (m, 1H), 1.55 (dd, $J = 12.0, 8.3$ Hz, 1H), 1.50–1.43 (m, 1H), 1.40 (s, 3H), 1.35 (d, $J = 13.1$ Hz, 1H), 1.33–1.22 (m, 1H), 1.26 (d, $J = 13.1$ Hz, 1H), 1.17–1.05 (m, 2H), 0.88 (s, 3H), 0.68 (s, 3H); ^{13}C NMR (125 MHz, C_6D_6) δ 213.7, 85.8, 64.0, 53.9, 52.2, 48.3, 43.6, 42.1, 40.3, 34.8, 32.1, 30.5, 25.2, 22.6; IR (Neat Film NaCl) 3415, 2970, 2948, 2866, 2759, 2717, 2658, 1708, 1485, 1467, 1456, 1443, 1399, 1384, 1368, 1363, 1331, 1304, 1254, 1242, 1223, 1211, 1180, 1167, 1153, 1137, 1114, 1071, 1054, 1017, 997, 985, 961, 949, 937, 920, 903, 874, 861, 841, 799, 788, 735 cm^{-1} ; HRMS (FAB+) m/z calc'd for $\text{C}_{14}\text{H}_{23}\text{O}_2$ $[\text{M}+\text{H}]^{+}$: 224.1698; found 224.1693; $[\alpha]_{\text{D}}^{25.0} -53.99$ (c 0.98, CHCl_3 , 94.9% ee); mp = 51–52 °C (benzene).



Silyl Enol Ethers 305 and 344. To a 20 mL microwave vial with magnetic stir bar under N_2 were added silyl dienol ether **343** (178.2 mg, 0.556 mmol, 1.00 equiv) and toluene (13 mL). The reaction was sealed with a microwave crimp cap and subjected to microwave irradiation in a Biotage Initiator microwave reactor (temperature: $150\text{ }^\circ\text{C}$, sensitivity: low) with a gradual temperature increase over 10 min ($10\text{ }^\circ\text{C}$ increments). After 2 h of stirring, the vial was uncapped and the reaction was concentrated under reduced pressure. The residue was purified by flash column chromatography (SiO_2 , 3 x 25 cm, deactivated with 1% Et_3N in hexanes, 1% Et_3N in hexanes \rightarrow 20% Et_2O in hexanes eluent) to afford a mixture of silyl enol ethers **305** and **344** (160.2 mg, 0.4997 mmol, 90% yield) as a colorless oil. The mixture of silyl enol ethers was used directly in the next step.

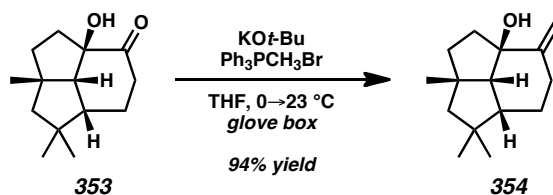
α -Hydroxyketones 352 and 353.¹¹⁹ To a 50 mL pear-shaped flask with a magnetic stir bar were added $m\text{-CPBA}$ (168.1 mg, 0.750 mmol, 1.50 equiv) and EtOAc (10 mL). The reaction was stirred until the solids dissolved. NaHCO_3 (125.9 mg, 1.499 mmol, 3.00 equiv) was added in one portion and the reaction was stirred vigorously for 1 h before the addition of H_2O (2 mL). The reaction was cooled to $0\text{ }^\circ\text{C}$ and stirred for 20 min. The mixture of silyl enol ethers **305** and **344** (160.2 mg, 0.4997 mmol, 1.00 equiv) was dissolved in EtOAc (5 mL) and cooled to $0\text{ }^\circ\text{C}$ before it was added dropwise to the biphasic mixture. After 10 min of stirring, the reaction was quenched with sat. aqueous NaHSO_4 and warmed to $23\text{ }^\circ\text{C}$. The phases were separated and the aqueous phase was

extracted with EtOAc (3 x 10 mL). The combined organic phases were dried over Na_2SO_4 , filtered, and concentrated under reduced pressure. The resulting mixture was taken up in THF (15 mL) and TBAF (1.0M in THF, 1 mL, 1.00 mmol, 2.00 equiv) was added. The reaction was concentrated under reduced pressure and purified by flash column chromatography (SiO_2 , 4 x 25 cm, 2.5%→5%→10% EtOAc in hexanes) to afford α -hydroxyketones **352** (9.0 mg, 0.043 mmol, 9% yield over two steps) as a pale yellow solid and **353** (67.5 mg, 0.304 mmol, 61% yield over two steps) as a pale yellow solid.



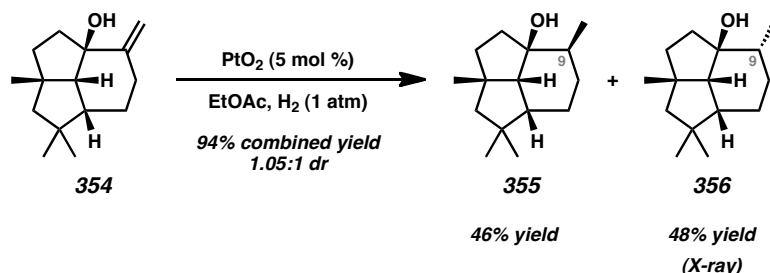
Silyl Dienol Ether 366. To a 100 mL pear-shaped flask with a magnetic stir bar was added KHMDS (154.7 mg, 0.775 mmol, 1.6 equiv) in a N_2 -filled glove box. The flask was sealed with a rubber septum and removed from the glove box and connected to a N_2 -inlet. The flask was cooled to $-78\text{ }^\circ\text{C}$ using an acetone/ $\text{CO}_2(\text{s})$ bath. After 10 min, THF (5 mL) was added and the suspension was stirred vigorously for 5 min. The cooling bath was removed and the flask was allowed to warm until the solids completely dissolved. The solution was cooled to $-78\text{ }^\circ\text{C}$. Acylcyclopentene **306** (100 mg, 0.484 mmol, 1.00 equiv) was added dropwise by syringe, leading to the formation of a pale tan-yellow mixture. The reaction was stirred at $-78\text{ }^\circ\text{C}$ for 30 min. TBDPSCI (151.2 μL , 0.581 mmol, 1.2 equiv) was added dropwise. The reaction was stirred at $-78\text{ }^\circ\text{C}$ for 5 min, the cooling bath was removed, and the reaction was allowed to warm to $23\text{ }^\circ\text{C}$ over 30 min.

The turbid tan solution was stirred at 23 °C for 1 h. The reaction was carefully concentrated under reduced pressure. The yellow residue was diluted with hexanes, passed through a Celite pipet plug, and eluted with hexanes. The filtrate was concentrated under reduced pressure and purified by flash column chromatography with deactivated silica gel (SiO₂, 3 x 12 cm, deactivated with 1% Et₃N in hexanes, 1% Et₃N in hexanes→20% Et₂O in hexanes eluent) to afford silyl dienol ether **366** (168 mg, 0.391 mmol, 81% yield) as a colorless sap. (Note: Silyl dienol ether **366** appears to be sensitive to moisture. The compound was stored as a solidified benzene solution under N₂ in a –25 °C freezer.); *R_f* = 0.63 (10:1 hexanes:EtOAc); ¹H NMR (500 MHz, C₆D₆) δ 8.65–8.54 (m, 4H), 7.99–7.86 (m, 6H), 7.16 (br s, 1H), 6.65 (dd, *J* = 17.5, 10.7 Hz, 1H), 5.69 (dd, *J* = 17.6, 1.2 Hz, 1H), 5.66 (dd, *J* = 10.7, 1.2 Hz, 1H), 4.97–4.92 (m, 1H), 4.91–4.87 (m, 1H), 3.15–3.03 (m, 2H), 2.59 (ddd, *J* = 12.7, 8.7, 6.8 Hz, 1H), 2.33 (d, *J* = 14.0 Hz, 1H), 2.31 (ddd, *J* = 12.7, 8.2, 5.4 Hz, 1H), 2.23 (d, *J* = 14.3 Hz, 1H), 1.91 (s, 9H), 1.84 (s, 3H), 1.80 (s, 3H), 1.79 (s, 3H); ¹³C NMR (125 MHz, C₆D₆) δ 154.2, 149.9, 138.9, 138.1, 135.9, 135.9, 133.4, 133.3, 130.1, 128.1, 128.1, 109.8, 94.2, 54.5, 49.8, 40.1, 38.1, 31.0, 30.0, 28.8, 28.6, 26.9, 19.8; IR (Neat Film NaCl) 3050, 3072, 2998, 2956, 2931, 2895, 2858, 1956, 1886, 1819, 1776, 1724, 1634, 1588, 1472, 1462, 1429, 1413, 1389, 1373, 1361, 1330, 1307, 1282, 1221, 1201, 1114, 1062, 1016, 939, 907, 822, 765, 742 cm^{–1}; HRMS (FAB+) *m/z* calc'd for C₃₀H₄₁OSi [M+H]⁺: 445.2927; found 445.2912; [α]_D^{25.0} +9.601 (*c* 1.29, CH₂Cl₂, 94.9% ee).



Allylic Alcohol 354.¹²⁰ To a 20 mL scintillation vial with magnetic stir bar was added Ph₃PCH₃Br (210.7 mg, 0.5898 mmol, 2.6 equiv) in a N₂-filled glove box. KOt-Bu (1.0 M in THF, 544.5 μ L, 0.5445 mmol, 2.4 equiv) was added and the bright yellow suspension was diluted with THF (3 mL). The mixture was stirred for 30 min. α -Hydroxyketone **353** (50.4 mg, 0.227 mmol, 1.00 equiv) was dissolved in THF (9 mL) and added to the reaction. The reaction was capped with a teflon-lined hard cap and stirred in the glove box. After 8.5 h, the reaction was removed from the glove box and quenched with sat. aqueous NH₄Cl (1 mL) and H₂O (1 mL). The phases were separated and the aqueous phase was extracted with Et₂O (3 x 5 mL). The combined organic phases were dried over Na₂SO₄, filtered, and concentrated under reduced pressure (25 mmHg) in a 0 $^{\circ}$ C ice/water bath. The residue was purified by flash column chromatography (SiO₂, 3 x 25 cm, 1% \rightarrow 3% \rightarrow 5% EtOAc in hexanes) to afford faintly fragrant allylic alcohol **354** (47.1 mg, 0.214 mmol, 94% yield) as a white crystalline solid; R_f = 0.34 (10:1 hexanes:EtOAc); ¹H NMR (500 MHz, CDCl₃) δ 5.31 (t, J = 2.1 Hz, 1H), 4.90 (q, J = 2.0 Hz, 1H), 2.41 (ddq, J = 17.0, 6.5, 2.0 Hz, 1H), 2.27–2.15 (m, 1H), 1.99–1.83 (m, 1H), 1.92 (td, J = 12.1, 8.0 Hz, 1H), 1.74 (td, J = 12.7, 12.1, 8.1 Hz, 1H), 1.62 (ddd, J = 13.5, 7.9, 1.8 Hz, 1H), 1.56 (dd, J = 12.4, 8.2 Hz, 1H), 1.54–1.46 (m, 1H), 1.45 (d, J = 13.1 Hz, 1H), 1.39 (s, 3H), 1.31 (d, J = 13.0 Hz, 1H), 1.29–1.20 (m, 1H), 1.08 (tddd, J = 13.6, 11.9, 6.7, 1.3 Hz, 1H), 0.97 (s, 3H), 0.80 (s, 3H); ¹³C NMR (125 MHz, CDCl₃) δ 151.2, 106.9, 84.1, 65.4, 54.6, 51.2, 49.9, 43.4, 42.3, 42.1, 33.1, 30.8, 29.1, 25.4, 22.3; IR (Neat Film NaCl)

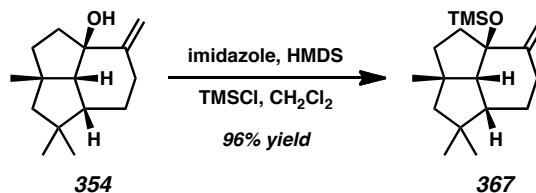
3337, 3083, 2961, 2934, 2866, 2829, 1785, 1636, 1470, 1452, 1433, 1383, 1374, 1364, 1318, 1300, 1241, 1228, 1213, 1177, 1163, 1133, 1110, 1062, 1047, 1019, 1007, 986, 960, 953, 923, 891, 867, 778, 747 cm^{-1} ; HRMS (EI+) m/z calc'd for $\text{C}_{15}\text{H}_{24}\text{O}$ $[\text{M}]^{+}$: 220.1827; found 220.1827; $[\alpha]_{\text{D}}^{25.0}$ -60.66 (c 0.45, CHCl_3 , 94.9% ee).



Alcohol 355 and Alcohol 356. To a 20 mL scintillation vial with magnetic stir bar containing allylic alcohol **354** (29.4 mg, 0.1335 mmol, 1.00 equiv) was added Adam's catalyst (PtO_2 -hydrate, 1.5 mg, 0.024 mmol, 5 mol %). The reaction was capped with a septum-fitted screw cap, evacuated for 5 min, and backfilled with an H_2 (1 atm, balloon). EtOAc (2.0 mL) was added and the reaction was stirred vigorously. After 5 min, the brown solids turned black. After 4 h of stirring, the H_2 balloon was removed. The reaction was filtered through a Celite pipet plug (0.5 x 1 cm) and eluted with EtOAc . The residue was purified by flash column chromatography (SiO_2 , 3 x 25 cm, 1%→2%→5% EtOAc in hexanes) to afford faintly fragrant alcohols **355** (13.5 mg, 0.0608 mmol, 45% yield) as a clear, colorless solid and **356** (14.2 mg, 0.0639 mmol, 48% yield) as a clear, colorless oil which solidifies upon storage in a $-25\text{ }^\circ\text{C}$ freezer. X-ray quality crystals of alcohol **356** (colorless) were grown by slow evaporation from hexanes.

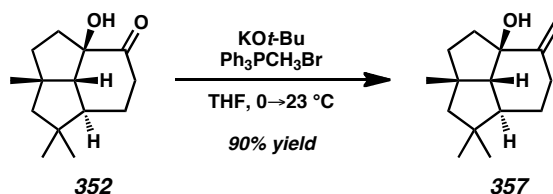
Alcohol (355) (9 β -Me isomer): $R_f = 0.22$ (10:1 hexanes:EtOAc); ^1H NMR (500 MHz, C_6D_6) δ 2.18 (d, $J = 8.9$ Hz, 1H), 1.74 (ddd, $J = 12.4, 6.5, 4.4$ Hz, 1H), 1.71–1.54 (m, 3H), 1.48–1.39 (m, 2H), 1.45 (d, $J = 12.8$ Hz, 1H), 1.39–1.28 (m, 2H), 1.31 (s, 3H), 1.25 (dd, $J = 12.8, 1.0$ Hz, 1H), 1.17–1.06 (m, 1H), 1.01 (s, 3H), 0.97 (d, $J = 6.9$ Hz, 3H), 0.86 (s, 3H), 0.84–0.70 (m, 1H); ^{13}C NMR (125 MHz, C_6D_6) δ 82.5, 62.3, 53.8, 49.8, 47.9, 45.6, 42.5, 42.0, 38.0, 32.7, 30.7, 28.6, 25.6, 25.4, 17.3; IR (Neat Film NaCl) 3453, 2928, 2867, 1722, 1463, 1383, 1364, 1375, 1310, 1285, 1236, 1204, 1217, 1181, 1163, 1155, 1137, 1067, 1048, 998, 983, 972, 963, 949, 921, 897, 888, 880, 860, 850, 840, 801, 782 cm^{-1} ; HRMS (EI +) m/z calc'd for $\text{C}_{15}\text{H}_{26}\text{O}$ $[\text{M}]^+$: 222.1984; found 222.1983; $[\alpha]_{\text{D}}^{25.0} -35.22$ (c 1.07, CHCl_3 , 94.9% ee).

Alcohol (356) (9 α -Me isomer): $R_f = 0.25$ (10:1 hexanes:EtOAc); ^1H NMR (500 MHz, C_6D_6) δ 1.94–1.82 (m, 2H), 1.72–1.44 (m, 6H), 1.50 (d, $J = 13.0$, 1H), 1.41 (s, 3H), 1.34 (dd, $J = 13.0, 0.9$ Hz, 1H), 1.31–1.20 (m, 1H), 1.14–1.00 (m, 2H), 0.98 (s, 3H), 0.94 (d, $J = 6.4$ Hz, 3H), 0.82 (s, 3H); ^{13}C NMR (125 MHz, C_6D_6) δ 85.7, 65.5, 55.5, 49.8, 48.6, 43.4, 41.9, 36.1, 34.5, 33.7, 31.1, 28.7, 25.0, 21.6, 17.0; IR (Neat Film NaCl) 3306, 2974, 2959, 2978, 2936, 2863, 1454, 1382, 1370, 1362, 1331, 1302, 1289, 1261, 1282, 1235, 1223, 1212, 1187, 1160, 1144, 1110, 1061, 1024, 1007, 999, 982, 962, 945, 926, 893, 865, 830, 797, 761 cm^{-1} ; HRMS (EI+) m/z calc'd for $\text{C}_{15}\text{H}_{26}\text{O}$ $[\text{M}]^+$: 222.1984; found 222.1982; $[\alpha]_{\text{D}}^{25.0} -6.75$ (c 1.33, CHCl_3 , 94.9% ee); mp = 108–110 $^{\circ}\text{C}$ (hexanes).



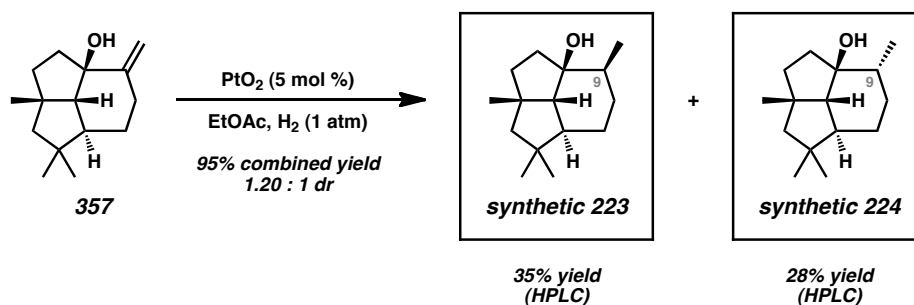
Trimethylsilyl Ether 367.¹⁰⁸ To a 20 mL scintillation vial with magnetic stir bar was added allylic alcohol **354** (10.8 mg, 0.0491 mmol, 1.00 equiv). A septum-fitted screw cap was attached and the vial was evacuated/backfilled with N₂ (3 cycles, 5 min evacuation per cycle). CH₂Cl₂ (4 mL) was added. HMDS (41.1 μL, 0.196 mmol, 4.00 equiv) and TMSCl (12 μL, 0.098 mmol, 2.0 equiv) were added dropwise, followed by imidazole (6.5 mg, 0.098 mmol, 2.0 equiv) in one portion. The clear, colorless solution turned into a turbid white solution several seconds after the addition of imidazole. After 24 h of stirring, the reaction was quenched by the addition of sat. aqueous NaHCO₃ (2 mL). The phases were separated and the aqueous phase was extracted with CH₂Cl₂ (3 x 5 mL). The combined organic phases were dried over Na₂SO₄, filtered, and concentrated under reduced pressure. The residue was purified by flash column chromatography (SiO₂, 1.5 x 25 cm, 0%→1%→2% EtOAc in hexanes) to afford trimethylsilyl ether **367** (13.8 mg, 0.0472 mmol, 96% yield) as a nearly colorless pale yellow oil; *R*_f = 0.72 (10:1 hexanes:EtOAc); ¹H NMR (500 MHz, C₆D₆) δ 5.32 (q, *J* = 1.8 Hz, 1H), 4.91 (q, *J* = 1.9 Hz, 1H), 2.45 (dd, *J* = 9.3, 1.7 Hz, 1H), 2.34 (dtd, *J* = 15.7, 3.2, 1.5 Hz, 1H), 2.20–2.08 (m, 1H), 1.96–1.87 (m, 1H), 1.89–1.73 (m, 2H), 1.65 (dddd, *J* = 13.6, 9.3, 5.6, 1.2 Hz, 1H), 1.50 (ddd, *J* = 10.4, 6.4, 2.6 Hz, 1H), 1.43 (s, 3H), 1.43 (dd, *J* = 13.1 Hz, 1H), 1.37–1.25 (m, 1H), 1.29 (dd, *J* = 13.1, 1.4 Hz, 1H), 1.05–0.92 (m, 1H), 1.00 (s, 3H), 0.81 (s, 3H), 0.25 (s, 9H); ¹³C NMR (125 MHz, C₆D₆) δ 151.8, 109.0, 86.8, 64.6, 54.3, 51.3, 50.5, 44.6, 43.5, 41.8, 32.7, 31.2, 31.2, 25.6, 23.7, 2.7; IR (Neat Film NaCl) 3083, 2952,

2868, 1731, 1638, 1459, 1383, 1373, 1364, 1315, 1300, 1259, 1249, 1214, 1187, 1162, 1120, 1069, 1058, 1027, 1011, 985, 955, 943, 926, 911, 896, 882, 838, 808, 752 cm^{-1} ; HRMS (EI+) m/z calc'd for $\text{C}_{18}\text{H}_{32}\text{OSi}$ $[\text{M}]^{+}$: 292.2223; found 292.2229; $[\alpha]_{\text{D}}^{25.0} -58.85$ (c 1.03, CH_2Cl_2 , 94.9% ee).



Allylic Alcohol 357.¹²⁰ To a 20 mL scintillation vial with magnetic stir bar was added $\text{Ph}_3\text{PCH}_3\text{Br}$ (138.8 mg, 0.3885 mmol, 2.6 equiv) in a N_2 -filled glove box. KOt-Bu (1.0 M in THF, 358.7 μL , 0.3587 mmol, 2.4 equiv) was added and the bright yellow suspension was diluted with THF (2 mL). The mixture was stirred for 30 min. α -Hydroxyketone **352** (33.2 mg, 0.149 mmol, 1.00 equiv) was dissolved in THF (6 mL) and added to the reaction. The reaction was capped with a teflon-lined hard cap and stirred in the glove box. After 8.5 h, the reaction was removed from the glove box and quenched with sat. aqueous NH_4Cl (1 mL) and H_2O (1 mL). The phases were separated and the aqueous phase was extracted with Et_2O (3 x 5 mL). The combined organic phases were dried over Na_2SO_4 , filtered, and concentrated under reduced pressure (25 mmHg) in a 0 $^{\circ}\text{C}$ ice/water bath. The residue was purified by flash column chromatography (SiO_2 , 3 x 25 cm, 1% \rightarrow 3% \rightarrow 5% EtOAc in hexanes) to afford faintly fragrant allylic alcohol **357** (29.8 mg, 0.135 mmol, 90% yield) as a colorless crystalline solid; $R_f = 0.34$ (10:1 hexanes:EtOAc); ^1H NMR (500 MHz, C_6D_6) δ 5.29–5.25 (m, 1H), 4.93–4.90 (m, 1H), 2.42 (dddd, $J = 14.5$, 4.8, 3.0, 0.8 Hz, 1H), 2.11–1.97 (m, 3H), 1.83–1.75 (m, 1H), 1.65–1.57 (m, 1H), 1.53 (d,

$J = 13.2$ Hz, 1H), 1.51 (d, $J = 13.1$ Hz, 1H), 1.41 (dddd, $J = 11.3, 5.8, 2.7, 2.7$ Hz, 1H), 1.34 (s, 3H), 1.31 (br d, $J = 12.2$ Hz, 1H), 1.04 (ddd, $J = 12.2, 12.2, 2.5$ Hz, 1H), 1.02–0.93 (m, 1H), 0.92 (s, 3H), 0.77 (s, 3H); ^{13}C NMR (125 MHz, C_6D_6) δ 153.6, 109.7, 85.0, 67.6, 60.3, 55.5, 46.5, 42.8, 40.1, 38.1, 34.8, 32.3, 28.5, 25.2, 22.2; IR (Neat Film NaCl) 3351, 2950, 2944, 2923, 2856, 1816, 1730, 1636, 1457, 1452, 1377, 1370, 1363, 1344, 1316, 1303, 1276, 1248, 1222, 1196, 1183, 1151, 1137, 1127, 1114, 1077, 1044, 1007, 987, 979, 962, 942, 931, 908, 862, 836, 815, 756, 722 cm^{-1} ; HRMS (FAB+) m/z calc'd for $\text{C}_{15}\text{H}_{25}\text{O}$ $[\text{M}+\text{H}]^+$: 221.1905; found 221.1898; $[\alpha]_{\text{D}}^{25.0} +2.96$ (c 0.67, CHCl_3 , 94.9% ee).



Alcohol 223⁴ and Alcohol 224.³ To a 20 mL scintillation vial with magnetic stir bar were added allylic alcohol **357** (6.8 mg, 0.031 mmol, 1.0 equiv), EtOAc (1.2 mL), and Adam's catalyst (PtO_2 -hydrate, 0.35 mg, 0.0015 mmol, 5 mol %). A brown suspension was obtained. The reaction was capped with a septum-fitted screw cap and the solution was sparged with H_2 (1 atm, balloon) through a long metal needle until a fine black suspension was formed. After 45 min, the needle connected to the H_2 balloon was raised above the surface of the reaction and the venting needle was removed. After 1 h of stirring, the H_2 balloon was removed and Celite (5 mg) was added. The reaction was stirred briefly, filtered through a Celite pipet plug (0.5 x 1 cm), and eluted with EtOAc.

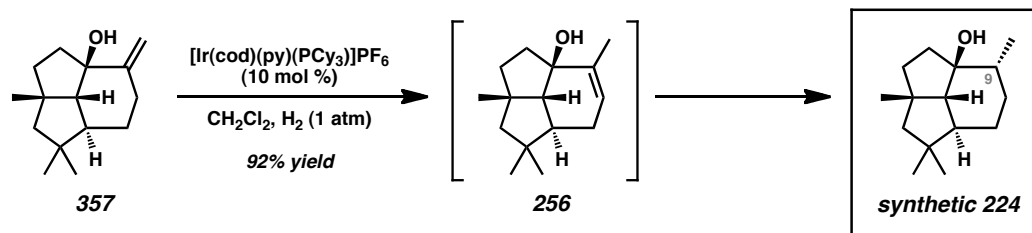
The clear filtrate was concentrated under reduced pressure (25 mmHg) in a 0 °C ice/water bath. The residue was purified by flash column chromatography (SiO₂, 3 x 12 cm, 15:1 hexanes:Et₂O) to afford a mixture of faintly fragrant alcohols **223** and **224** (6.5 mg, 0.029 mmol, 95% combined yield, 1.20:1 dr. (**223**:**224**)) as a white amorphous solid. Alcohols **223** and **224** can be separated by normal phase preparatory HPLC (SiO₂, 10%→25% Et₂O in pentane, 5.0 mL/min, ZORBAX RX-SIL column, 5 μm, 9.4 x 250 mm, manual collection every 0.2 min). The purity of fractions was analyzed by UHPLC-MS (C18, 33.5–36.0% CH₃CN in H₂O, 1.2 mL/min, Agilent Eclipse Plus C18, 1.8 μm, 2.1 x 50 mm, *t_R* (min): **223** = 7.22 (*m/z* = 205.2), **224** = 7.78 (*m/z* = 205.2). X-ray quality crystals of alcohol **224** (colorless to pale yellow) were grown by slow evaporation from hexanes.

The NMR spectra (C₆D₆) for synthetic compound **223** match spectral data for reported natural “9-*epi*-presilphiperfolan-1-ol” (assigned as **223**),⁴ but the NMR spectra (C₆D₆) for synthetic compound **224** do not match spectral data for reported “presilphiperfolan-1-ol” (assigned as **224**).³ The NMR spectra (CD₂Cl₂) for synthetic compound **224** match spectral data for reported synthetic **224**.²⁸

Alcohol 223 (9β-Me isomer): *R_f* = 0.32 (10:1 hexanes:EtOAc); ¹H NMR (500 MHz, C₆D₆) δ 1.89–1.78 (m, 2H), 1.73–1.64 (m, 1H), 1.63–1.55 (m, 2H), 1.55 (br d, *J* = 12.3 Hz, 1H), 1.50 (s, 2H), 1.48–1.38 (m, 1H), 1.36–1.25 (m, 2H), 1.33 (s, 3H), 1.19–1.05 (m, 2H), 0.94 (s, 3H), 0.90 (d, *J* = 7.0 Hz, 3H), 0.80 (s, 3H), 0.58 (br s, 1H); ¹³C NMR (125 MHz, C₆D₆) δ 84.5, 63.9, 59.4, 51.7, 46.2, 42.7, 40.5, 39.7, 36.9, 31.4, 29.9, 28.8, 22.3, 20.3, 15.8; IR (Neat Film NaCl) 3468, 2952, 2923, 2853, 1725, 1463, 1456, 1377, 1300,

1259, 1188, 1156, 1095, 1077, 104, 1008, 970, 945, 801, 720 cm^{-1} ; HRMS (EI+) m/z calc'd for $\text{C}_{15}\text{H}_{26}\text{O}$ $[\text{M}]^{+}$: 222.1984; found 222.1978; $[\alpha]_{\text{D}}^{25.0}$ -47.245 (c 0.63, CHCl_3 , 94.9% ee).

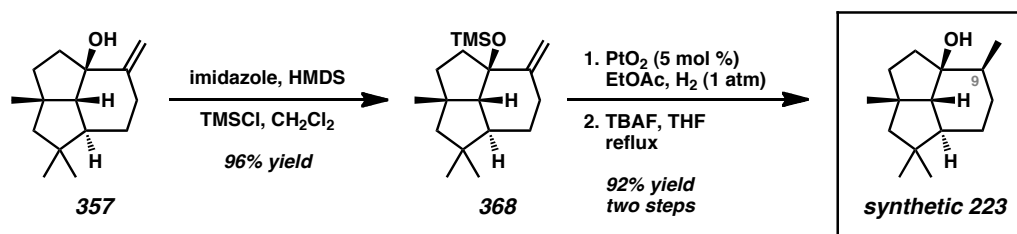
Alcohol 224 (9 α -Me isomer): R_f = 0.32 (10:1 hexanes:EtOAc); ^1H NMR (500 MHz, C_6D_6) δ 1.96 (ddd, J = 13.3, 9.1, 9.1 Hz, 1H), 1.75 (ddd, J = 13.5, 10.1, 9.0 Hz, 1H), 1.70–1.61 (m, 1H), 1.59 (ddd, J = 13.4, 10.2, 1.9 Hz, 1H), 1.53 (s, 2H), 1.52–1.34 (m, 3H), 1.39 (s, 3H), 1.27 (br d, J = 11.9 Hz, 1H), 0.95 (s, 3H), 0.94 (d, J = 7.0 Hz, 3H), 0.91–0.82 (m, 3H), 0.81 (s, 3H), 0.52 (br s, 1H); ^{13}C NMR (125 MHz, C_6D_6) δ 85.7, 66.2, 60.6, 56.2, 46.1, 42.2, 41.6, 40.4, 35.1, 32.5, 32.1, 28.7, 24.7, 22.3, 15.9; ^1H NMR (500 MHz, CD_2Cl_2) δ 1.96 (ddd, J = 13.6, 9.8, 9.8 Hz, 1H), 1.84 (ddd, J = 13.6, 9.1, 9.1 Hz, 1H), 1.82–1.76 (m, 1H), 1.65 (ddd, J = 13.5, 10.3, 1.9 Hz, 1H), 1.61–1.42 (m, 6H), 1.25 (s, 3H), 1.14–1.11 (br s, 1H), 1.08–0.96 (m, 3H), 0.95 (s, 3H), 0.93 (d, J = 6.8 Hz, 3H), 0.81 (s, 3H); IR (Neat Film NaCl) 3325, 2949, 2921, 2853, 1734, 1460, 138, 1335, 1304, 1283, 1276, 1258, 1250, 1218, 1189, 1181, 1145, 1126, 1069, 1053, 1030, 1002, 995, 974, 964, 947, 926, 907, 859, 843, 801, 778, 743 cm^{-1} ; HRMS (EI+) m/z calc'd for $\text{C}_{15}\text{H}_{26}\text{O}$ $[\text{M}]^{+}$: 222.1984; found 222.1977; $[\alpha]_{\text{D}}^{25.0}$ -3.24 (c 0.19, CHCl_3 , 94.9% ee); $[\alpha]_{\text{D}}^{22.0}$ -2.73 (c 0.68, CHCl_3 , 94.9% ee); mp = 113–116 $^{\circ}\text{C}$ (hexanes).



Alcohol 224 (9 α -Me isomer). To a 20 mL scintillation vial with magnetic stir bar were added allylic alcohol **357** (6.8 mg, 0.034 mmol, 1.0 equiv) and $[\text{Ir}(\text{cod})(\text{py})(\text{PCy}_3)]\text{PF}_6$ (2.9 mg, 0.0034 mmol, 10 mol %). A septum-fitted screw cap was attached and the vial was evacuated for 5 min and backfilled with an H_2 (1 atm, balloon). CH_2Cl_2 (8 mL) was added, giving a golden yellow-orange solution. The solution was freeze-pump-thawed using a $\text{N}_2(l)$ bath (3 cycles, 5 min evacuation per cycle), backfilling with H_2 (1 atm, balloon) for each cycle. The golden yellow-orange solution was stirred at 23 °C for 27 h. The reaction was filtered through a silica plug (0.5 x 2 cm), eluting with Et_2O . The filtrate was concentrated under reduced pressure (25 mmHg) in a 0 °C ice/water bath. The residue was purified by flash column chromatography (SiO_2 , 1.5 x 25 cm, 5% \rightarrow 10% EtOAc in hexanes) to afford faintly fragrant alcohol **224** (6.9 mg, 0.031 mmol, 92% combined yield) as a white amorphous solid.

The NMR spectra (C_6D_6) for synthetic compound **224** do not match spectral data for reported “presilhiperfolan-1-ol” (assigned as **224**).³ The NMR spectra (CD_2Cl_2) for synthetic compound **224** match spectral data for reported synthetic **224**.²⁸

(Note: Competitive olefin isomerization to a endocyclic trisubstituted alkene (**256**) is observed if the reaction is stopped at incomplete conversion, but with sufficient time, only reduced product **224** is observed.)



Trimethylsilyl Ether 368.¹⁰⁸ To a 20 mL scintillation vial with magnetic stir bar was added allylic alcohol **357** (10.8 mg, 0.049 mmol, 1.00 equiv). A septum-fitted screw cap was attached and the vial was evacuated/backfilled with N₂ (3 cycles, 5 min evacuation per cycle). CH₂Cl₂ (4 mL) was added. HMDS (41.1 μ L, 0.196 mmol, 4.00 equiv) and TMSCl (12 μ L, 0.098 mmol, 2.0 equiv) were added dropwise, followed by imidazole (6.5 mg, 0.098 mmol, 2.0 equiv) in one portion. The clear, colorless solution turned into a turbid white solution several seconds after the addition of imidazole. After 24 h of stirring, the reaction was quenched by the addition of sat. aqueous NaHCO₃ (2 mL). The phases were separated and the aqueous phase was extracted with CH₂Cl₂ (3 x 5 mL). The combined organic phases were dried over Na₂SO₄, filtered, and concentrated under reduced pressure. The residue was purified by flash column chromatography (SiO₂, 1.5 x 25 cm, 0%→1%→2% EtOAc in hexanes) to afford trimethylsilyl ether **368** (13.8 mg, 0.04717 mmol, 96% yield) as a nearly colorless pale yellow oil; R_f = 0.73 (10:1 hexanes:EtOAc); ¹H NMR (500 MHz, C₆D₆) δ 5.14–5.12 (m, 1H), 4.93–4.91 (m, 1H), 2.55–2.42 (m, 1H), 2.12–2.01 (m, 3H), 1.98–1.83 (m, 2H), 1.66–1.55 (m, 1H), 1.53 (d, J

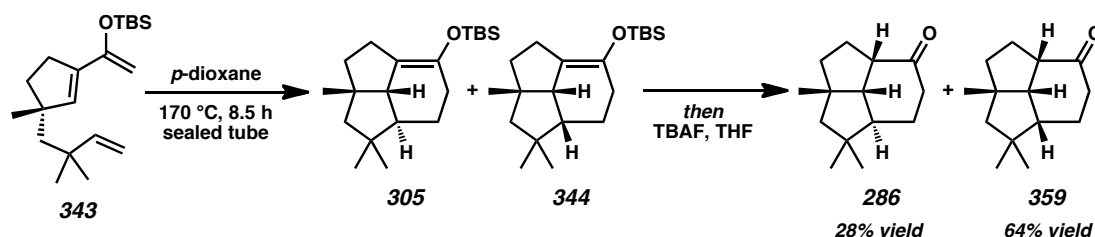
= 13.0 Hz, 1H), 1.47 (br d, J = 13.0 Hz, 1H), 1.48–1.40 (m, 1H), 1.36 (s, 3H), 1.29–1.17 (m, 1H), 0.98 (ddd, J = 12.8, 12.8, 5.7 Hz, 1H), 0.88 (s, 3H), 0.81 (s, 3H), 0.23 (s, 9H); ^{13}C NMR (125 MHz, C_6D_6) δ 153.3, 113.1, 87.9, 67.0, 59.6, 52.3, 45.8, 42.6, 40.1, 38.5, 32.0, 31.3, 28.4, 23.3, 22.2, 2.5; IR (Neat Film NaCl) 3073, 2950, 2929, 2865, 1813, 1730, 1648, 1458, 1440, 1412, 1384, 1368, 1335, 1300, 1248, 1202, 1186, 1142, 1115, 1071, 1062, 1034, 1012, 997, 976, 950, 935, 921, 906, 889, 876, 838, 812, 751 cm^{-1} ; HRMS (EI+) m/z calc'd for $\text{C}_{18}\text{H}_{32}\text{OSi}$ $[\text{M}]^+$: 292.2223; found 292.2211; $[\alpha]_{\text{D}}^{25.0}$ –94.32 (c 0.98, CH_2Cl_2 , 94.9% ee).

Alcohol 223 (9 β -Me isomer). To a 20 mL scintillation vial with magnetic stir bar containing trimethylsilyl ether **SI-8** (13.8 mg, 0.0472232 mmol, 1.00 equiv) was added Adam's catalyst (PtO_2 -hydrate, 0.54 mg, 0.0024 mmol, 5 mol %). The reaction was capped with a septum-fitted screw cap, evacuated for 5 min, and backfilled with an H_2 (1 atm, balloon). EtOAc (2.5 mL) was added and the reaction was stirred vigorously. After 10 min, the brown solids turned black. After 13.5 h of stirring, the H_2 balloon was removed. The reaction was filtered through a Celite pipet plug (0.5 x 1 cm) and eluted with EtOAc. The clear filtrate was concentrated under reduced pressure. The residue was taken up in THF (5 mL) and treated with TBAF (1.0 M in THF, 189 μL , 0.189 mmol, 4.00 equiv). The reaction was sealed with a teflon-lined hard cap and inserted into a 100 $^\circ\text{C}$ heating block. After 10.5 h of stirring, the reaction was a tan solution. The vial was cooled to 23 $^\circ\text{C}$ and an additional portion of TBAF (1.0 M in THF, 95 μL , 0.094 mmol, 2.0 equiv) was added. The vial was resealed and inserted into a 100 $^\circ\text{C}$ heating block. After an additional 16 h of stirring, the vial was cooled to 23 $^\circ\text{C}$ and concentrated

under reduced pressure (25 mmHg) in a 0 °C ice/water bath. The residue was purified by flash column chromatography (SiO₂, 2 x 20 cm, 1%→3%→5% EtOAc in hexanes) to afford faintly fragrant alcohol **223** (9.6 mg, 0.043 mmol, 92% yield) as a clear, colorless, faintly fragrant oil which solidifies upon storage in a –25 °C freezer.

The NMR spectra (C₆D₆) for synthetic compound **223** match spectral data for reported natural “9-*epi*-presilphiperfolan-1-ol” (assigned as **223**).⁴

3.8.2.3 PROGRESS TOWARD THE ASYMMETRIC SYNTHESIS OF (-)-PRESILPHIPERFOLAN-9 α -OL

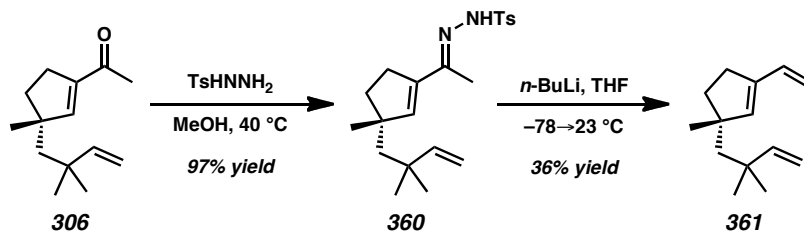


Ketone 286 and Ketone 359. To a 5 mL microwave vial was added a solution of silyl dienol ether **343** in benzene (100 mg/mL, 32.0 mg, 0.100 mmol, 1.00 equiv). The solvent was removed under reduced pressure. The vial, a magnetic stir bar, crimp cap, and crimper were placed in a glove box antechamber, which was evacuated/backfilled with N₂ (3 cycles, 5 min evacuation per cycle) before the items were transferred into the glove box. *p*-Dioxane (4.2 mL) was added by syringe and the vial was sealed with a crimp cap. The vial was removed from the glove box and immersed in a preheated 170 °C heating mantle-supported sand bath regulated by a J-KEM Scientific Model 210 Temperature Controller. A blast shield was set up as a precaution. The reaction was stirred for 8.5 h

at 170 °C. The reaction was allowed to cool to 23 °C and TBAF (1.0 M in THF, 200 μ L, 0.200 mmol, 2.00 equiv) was added dropwise, leading to a color change from a clear, colorless solution to a yellow solution. The vial was uncapped and the reaction was diluted with hexanes (5 mL) and concentrated under reduced pressure to give a crude mixture of tricyclic ketones. The mixture was passed through a silica plug (2 x 8 cm), eluted with 9:1 hexanes:EtOAc, and concentrated under reduced pressure (25 mmHg) in a 0 °C ice/water bath. Crude ^1H NMR analysis indicates a 1:2.04 dr (**305:344**) for the reaction. The mixture of tricyclic ketones was purified by flash column chromatography (SiO_2 , 3 x 25 cm, 1% \rightarrow 3% \rightarrow 5% Et_2O in hexanes) and concentrated under reduced pressure (25 mmHg) in a 0 °C ice/water bath to afford ketone **286** (5.8 mg, 0.02811 mmol, 28% yield) as a colorless oil and ketone **359** (13.2 mg, 0.06398 mmol, 64% yield) as a colorless oil.

Ketone 286 (*trans*-isomer): R_f = 0.34 (10:1 hexanes:EtOAc); ^1H NMR (500 MHz, CDCl_3) δ 2.81 (td, J = 9.0, 7.2 Hz, 1H), 2.48 (dddd, J = 16.5, 8.1, 3.3, 0.8 Hz, 1H), 2.32 (dt, J = 16.5, 8.2 Hz, 1H), 2.19 (dd, J = 12.5, 7.0 Hz, 1H), 2.08–1.95 (m, 2H), 1.79 (ddt, J = 12.1, 8.4, 3.5 Hz, 1H), 1.69 (d, J = 13.3 Hz, 1H), 1.67 (ddd, J = 13.3, 6.0 Hz, 1H), 1.59 (d, J = 13.4 Hz, 1H), 1.59–1.48 (m, 2H), 1.40 (td, J = 12.7, 3.8 Hz, 1H), 1.07 (s, 3H), 1.02 (s, 3H), 0.89 (s, 3H); ^{13}C NMR (125 MHz, CDCl_3) δ 216.5, 59.3, 58.1, 52.8, 51.0, 47.6, 42.1, 40.8, 38.5, 29.2, 29.0, 28.4, 22.8, 22.0; IR (Neat Film NaCl) 2948, 2929, 2864, 1702, 1458, 1385, 1372, 1364, 1316, 1260, 1233, 1209, 1164, 1115, 1102, 1072, 1040, 120, 952, 917, 874, 807, 746 cm^{-1} ; HRMS (EI+) m/z calc'd for $\text{C}_{14}\text{H}_{22}\text{O}$ $[\text{M}]^{+}$: 206.1671; found 206.1670; $[\alpha]_{\text{D}}^{25.0}$ -3.27 (c 0.56, CHCl_3 , 94.9% ee).

Ketone 359 (cis-isomer): $R_f = 0.28$ (10:1 hexanes:EtOAc); ^1H NMR (500 MHz, CDCl_3) δ 2.67 (dd, $J = 17.4, 9.1$ Hz, 1H), 2.64 (dd, $J = 16.8, 9.0$ Hz, 1H), 2.46 (ddd, $J = 18.0, 4.1, 2.5$ Hz, 1H), 2.05 (ddd, $J = 18.2, 14.0, 5.0$ Hz, 1H), 1.99–1.86 (m, 2H), 1.84–1.74 (m, 1H), 1.63–1.50 (m, 3H), 1.60 (d, $J = 13.2$ Hz, 1H), 1.47 (d, $J = 13.1$ Hz, 1H), 1.40 (ddd, $J = 12.7, 8.9, 7.2$ Hz, 1H), 1.24 (s, 3H), 1.13 (s, 3H), 0.97 (s, 3H); ^{13}C NMR (125 MHz, CDCl_3) δ 215.7, 54.5, 53.7, 52.7, 52.4, 49.3, 44.5, 43.5, 38.4, 33.0, 31.3, 31.1, 25.8, 23.2; IR (Neat Film NaCl) 2951, 2930, 2867, 1707, 1462, 1405, 1384, 1375, 1364, 1332, 1308, 1272, 1246, 1236, 1210, 1199, 1179, 1172, 1153, 1118, 1097, 996, 881, 892, 862, 842, 800, 784 cm^{-1} ; HRMS (EI+) m/z calc'd for $\text{C}_{14}\text{H}_{22}\text{O}$ $[\text{M}]^+$: 206.1671; found 206.1719; $[\alpha]_D^{25.0} -62.62$ (c 0.56, CHCl_3 , 94.9% ee).



Tosylhydrazone 360. A 20 mL scintillation vial with a magnetic stir bar was charged with acylcyclopentene **306** (50 mg, 0.423 mmol, 1.00 equiv) and MeOH (4 mL). TsHNNH₂ (49.6 mg, 0.2666 mmol, 1.10 equiv) in MeOH (4 mL) was added. The vial was capped with a teflon-lined hard cap and inserted into a 40 °C heating block. After 48 h of stirring, the reaction was cooled to ambient temperature. The reaction was concentrated under reduced pressure, diluted with EtOAc (5 mL) and washed with H₂O (2 x 1 mL), dried over Na₂SO₄, filtered, and concentrated under reduced pressure. The residue was purified by flash column chromatography (SiO₂, 3 x 25 cm, 3:1

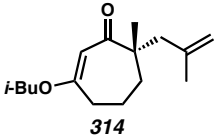
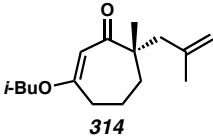
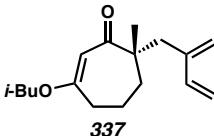
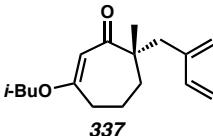
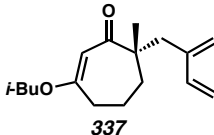
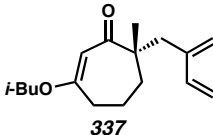
hexanes:EtOAc) to afford tosylhydrazone **360** (88.3 mg, 0.2358 mmol, 97% yield) as a pale white foam; R_f = 0.29 (4:1 hexanes:EtOAc); ^1H NMR (500 MHz, CDCl_3) δ 7.86 (d, J = 8.0 Hz, 2H), 7.30 (d, J = 7.9 Hz, 2H), 5.99 (s, 1H), 5.84 (dd, J = 17.5, 10.7 Hz, 1H), 4.91–4.79 (m, 2H), 2.49 (t, J = 7.3 Hz, 2H), 2.42 (s, 3H), 1.95–1.81 (m, 1H), 1.87 (s, 3H), 1.65–1.56 (m, 1H), 1.59 (d, J = 14.3 Hz, 1H), 1.52 (d, J = 14.3 Hz, 1H), 1.04 (s, 3H), 1.03 (s, 3H), 1.00 (s, 3H); ^{13}C NMR (125 MHz, CDCl_3) δ 150.0, 144.2, 139.7, 135.3, 129.5, 128.4, 109.6, 53.9, 50.1, 39.2, 37.9, 30.2, 29.7, 28.6, 28.1, 21.8, 12.9; IR (Neat Film NaCl) 3214, 3078, 3042, 2954, 2925, 2870, 1710, 1636, 1597, 1491, 1452, 1400, 1380, 1360, 1337, 1306, 1292, 1210, 1185, 1167, 1120, 1094, 1058, 1020, 1010, 971, 910, 872, 829, 813, 706 cm^{-1} ; HRMS (MM: ESI-APCI+) m/z calc'd for $\text{C}_{21}\text{H}_{30}\text{N}_2\text{O}_2\text{S}$ $[\text{M}+\text{H}]^+$: 375.2101; found 375.2117; $[\alpha]_D^{25.0}$ –17.83 (c 1.03, CHCl_3 , 95.3% ee).

Triene 361. To a 50 mL pear-shaped flask was added tosylhydrazone **360** (75 mg, 0.2002 mmol, 1.00 equiv). The flask was sealed with a rubber septum and evacuated/backfilled with N_2 (3 cycles, 5 min evacuation per cycle). The solids were dissolved in THF (8 mL) and cooled to $-78\text{ }^\circ\text{C}$. The solution was stirred at $-78\text{ }^\circ\text{C}$ for 20 min. A solution of $n\text{-BuLi}$ (2.47 M in hexanes, 400 μL , 0.988 mmol, 4.94 equiv) was added until a consistent orange color was obtained. During the $n\text{-BuLi}$ addition, the reaction initially became yellow but turned orange as more $n\text{-BuLi}$ was added. The solution was stirred at $-78\text{ }^\circ\text{C}$ for 5 min. The cooling bath was lowered and the reaction was allowed to warm to $23\text{ }^\circ\text{C}$ over 1 h. The solution became a deep orange color. After 2 h of stirring, the reaction was cooled to $0\text{ }^\circ\text{C}$ and quenched with 4 mL sat. aqueous NH_4Cl , warmed to $23\text{ }^\circ\text{C}$, and stirred for 5 min. Petroleum ether was added and the

phases were separated. The aqueous layer was extracted with petroleum ether (3 x 5 mL). The combined organics were dried over Na₂SO₄, filtered, and concentrated under reduced pressure (25 mmHg) in a 0 °C ice/water bath. The residue was purified by flash column chromatography (SiO₂, 2 x 25 cm, petroleum ether hexanes:EtOAc) and concentrated under reduced pressure (25 mmHg) in a 0 °C ice/water bath to afford triene **361** (13.1 mg, 0.06883 mmol, 34% yield) as a clear, colorless oil; R_f = 0.77 (hexanes); ¹H NMR (500 MHz, CDCl₃) δ 6.50 (dd, J = 17.3, 10.6 Hz, 1H), 5.90 (dd, J = 17.5, 10.7 Hz, 1H), 5.64–5.60 (m, 1H), 5.06–5.02 (m, 1H), 5.02–5.00 (m, 1H), 4.89 (dd, J = 17.5, 1.4 Hz, 1H), 4.85 (dd, J = 10.7, 1.4 Hz, 1H), 2.46–2.34 (m, 2H), 1.91 (dt, J = 12.8, 7.5 Hz, 1H), 1.64 (ddd, J = 13.1, 7.6, 6.4 Hz, 1H), 1.60 (d, J = 14.4 Hz, 1H), 1.52 (d, J = 14.3 Hz, 1H), 1.05 (s, 3H), 1.05 (s, 3H), 1.03 (s, 3H); ¹³C NMR (125 MHz, CDCl₃) δ 150.1, 141.8, 139.5, 134.2, 113.8, 109.4, 54.1, 49.5, 39.3, 38.0, 29.8, 29.5, 28.6, 28.2; IR (Neat Film NaCl) 3083, 2955, 2929, 2898, 2871, 2849, 1802, 1653, 1636, 1591, 1473, 1457, 1452, 1413, 1379, 1361, 1301, 1252, 1207, 1126, 1074, 1042, 1008, 987, 905, 898, 850 cm⁻¹; HRMS (EI+) m/z calc'd for C₁₄H₂₂ [M]⁺: 190.1721; found 190.1723; $[\alpha]_D^{25.0}$ – 15.56 (c 1.03, CHCl₃, 95.3% ee).

3.8.3 METHODS FOR DETERMINATION OF ENANTIOMERIC EXCESS

Table 3.3. Methods for the Determination of Enantiomeric Excess (Chiral HPLC)

entry	product	compound assayed	assay conditions	retention time of major isomer (min)	retention time of minor isomer (min)	% ee
1			HPLC Chiralcel OD-H 1% IPA in hexane isocratic, 1.0 mL/min	8.94	8.28	88
2			HPLC Chiralcel OD-H 2.0% IPA in hexane isocratic, 1.0 mL/min	6.41	7.53	95
3			HPLC Chiralcel AD 1.0% IPA in hexane isocratic, 1.0 mL/min	12.12	10.61	95

3.8.4 COMPARISON OF SPECTRAL DATA FOR SYNTHETIC AND REPORTED PRESILPHIPERFOLANOLS **224** AND **223**

Spectral data for synthetic “presilphiperfolan-1-ol” (assigned as **224**) and “9-*epi*-presilphiperfolan-1-ol” (assigned as **223**) (^1H NMR, ^{13}C NMR, $[\alpha]_{\text{D}}^{\text{T}}$) were compared with reported spectral data for the natural samples.^{3,4} Tables comparing compound data are shown in Table 3.4–Table 3.7. Superimposed NMR spectra are shown in Figures A5.122–A5.124. Additionally, we compared the spectra of our synthetic **224** to a reported synthetic compound prepared from isocaryophyllene.²⁸ The results are shown in Table 3.8–Table 3.9. ^1H and ^{13}C NMR spectra for naturally isolated “9-*epi*-presilphiperfolan-1-ol” (assigned as **223**)⁴ were generously provided by Prof. Suzana G. Leitão. A ^1H NMR spectrum of naturally isolated “presilphiperfolan-1-ol” (assigned as **224**) was published in a dissertation.^{3b} Unfortunately, attempts to obtain samples or spectra of naturally isolated “presilphiperfolan-1-ol” (assigned as **224**) were unsuccessful.

The NMR spectra (C_6D_6) for synthetic compound **223** match spectral data for reported natural “9-*epi*-presilphiperfolan-1-ol” (assigned as **223**),⁴ but the NMR spectra (C_6D_6) for synthetic compound **224** do not match spectral data for reported “presilphiperfolan-1-ol” (assigned as **224**).³ The NMR spectra (C_6D_6) of reported natural “presilphiperfolan-1-ol” (assigned as **224**)³ appears to match spectral data for reported natural “9-*epi*-presilphiperfolan-1-ol” (assigned as **223**).⁴ The NMR spectra (CD_2Cl_2) for synthetic compound **224** match spectral data for reported synthetic **224**.²⁸ Based on our analysis of spectral data, we believe that reported natural “presilphiperfolan-1-ol” (assigned as **224**) is misassigned at C(9) and should have the same true structure as natural “9-*epi*-presilphiperfolan-1-ol” (assigned as **223**) with a 9 β -methyl configuration.

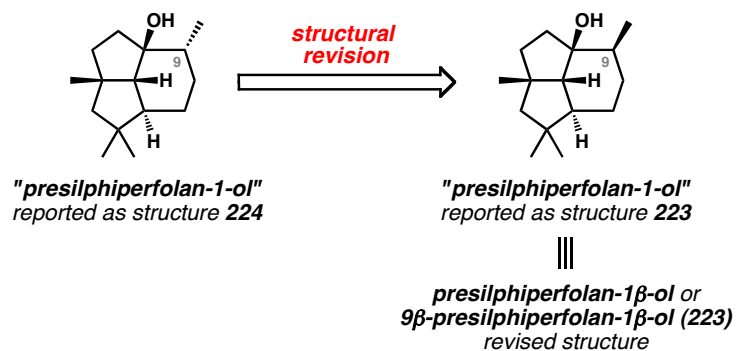
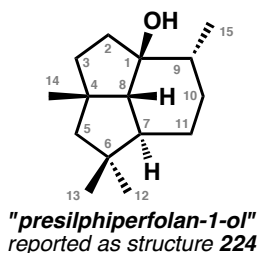


Table 3.4. Comparison of Optical Rotation Data for Synthetic and Reported Natural³ "Presilphiperfolan-1-ol" (**224**) and Reported Natural⁴ "9-*epi*-Presilphiperfolan-1-ol" (**223**)

Compound	Reported Natural Sample	Synthetic Sample
"Presilphiperfolan-1-ol" (224)	$[\alpha]_{\text{D}}^{25} = -66.0$ (<i>c</i> 0.0015)	$[\alpha]_{\text{D}}^{25} = -47.25$ (<i>c</i> 0.63, CHCl ₃ , 94.9% ee)
"9- <i>epi</i> -Presilphiperfolan-1-ol" (223)	(not reported)	$[\alpha]_{\text{D}}^{25} = -2.73$ (<i>c</i> 0.68, CHCl ₃ , 94.9% ee)

Table 3.5. Comparison of ^1H NMR Data for Synthetic and Reported Natural³ “Presilphiperfolan-1-ol” (**224**)^a

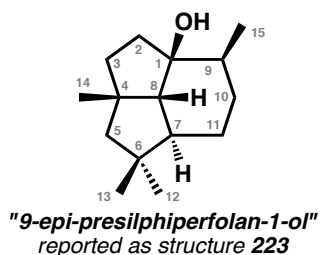
Assignment	Synthetic 224 ^b (ppm)	Multiplicity, <i>J</i> (Hz)	Natural 224 ^c (ppm)	Multiplicity, <i>J</i> (Hz)
C1	—	—	—	—
C2	1.75	ddd, 13.5, 10.1, 9.0	1.92–1.77	m
	1.52–1.34	m	1.72–1.62	m
C3	1.96	ddd, 13.3, 9.1, 9.1	1.92–1.77	m
	1.59	ddd, 13.4, 10.2, 1.9	1.62–1.53	m
C4	—	—	—	—
C5	1.53	s	1.50	s
C6	—	—	—	—
C7	0.91–0.82	m	1.17–1.08	m
C8	1.27	br d, 11.9	1.62–1.53	m
C9	1.52–1.34	m	1.62–1.53	m
C10	1.70–1.61	m	1.45–1.39	m
	0.91–0.82	m	1.33–1.20	m
C11	1.52–1.34	m	1.33–1.20	m
	0.91–0.82	m	1.17–1.08	m
C12	0.81	s	0.80	s
C13	0.95	s	0.94	s ^d
C14	1.39	s	1.32	s
C15	0.94	d, 7.0	0.89	d, 7

^a For a comparison of ^1H NMR spectra of synthetic and reported samples, see Figure A5.122.

^b ^1H NMR spectra were obtained at 500 MHz in C_6D_6 and standardized relative to residual C_6D_6 .

^c ^1H NMR spectra were obtained at 500 MHz in C_6D_6 and standardized relative to TMS.

^d Peak multiplicity was originally reported as (d, $J = 7$ Hz) in Ref. 3a, but corrected in Ref. 3b.

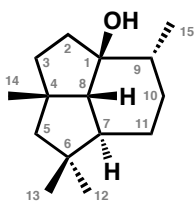
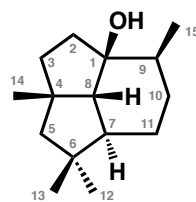
Table 3.6. Comparison of ^1H NMR Data for Synthetic and Reported Natural^d “9-*epi*-Presilphiperfolan-1-ol” (**223**)^a

Assignment	Synthetic 223 ^b (ppm)	Multiplicity, <i>J</i> (Hz)	Reported 223 ^c (ppm)	Multiplicity, <i>J</i> (Hz)
C1	—	—	—	—
C2	1.87–1.78	m	1.87–1.79	m
	1.73–1.64	m	1.72–1.61	m
C3	1.89–1.81	m	1.87–1.79	m
	1.63–1.55	m	1.61–1.54	m
C4	—	—	—	—
C5	1.50	s	1.50	s
C6	—	—	—	—
C7	1.15–1.05	m	1.16–1.09	m
C8	1.55	br d, 12.3	1.61–1.54	m
C9	1.63–1.55	m	1.61–1.54	m
C10	1.48–1.38	m	1.45–1.39	m
	1.36–1.27	m	1.34–1.24	m
C11	1.33–1.25	m	1.34–1.24	m
	1.19–1.09	m	1.16–1.09	m
C12	0.80	s	0.80	s
C13	0.94	s	0.93	s
C14	1.33	s	1.32	s
C15	0.90	d, 7.0	0.89	d, 7

^a For a comparison of ^1H NMR spectra of synthetic and reported samples, see Figure A5.124.

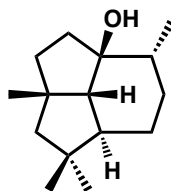
^b ^1H NMR spectra were obtained at 500 MHz in C_6D_6 and standardized relative to residual C_6D_6 .

^c ^1H NMR spectra were obtained at 400 MHz in C_6D_6 and standardized relative to TMS.

Table 3.7. Comparison of ^{13}C NMR Data for Synthetic and Reported³ Natural “Presilphiperfolan-1-ol” (**224**), Synthetic and Reported Natural⁴ “9-*epi*-Presilphiperfolan-1-ol” (**223**)^a*"presilphiperfolan-1-ol"*
reported as structure **224***"9-*epi*-presilphiperfolan-1-ol"*
reported as structure **223**

Assignment	Synthetic 224 ^b (ppm)	Reported 224 ^c (ppm)	Synthetic 223 ^b (ppm)	Reported 223 ^d (ppm)
C1	85.7	89.0	84.5	84.3
C2	32.1	39.7	39.7	39.5
C3	42.2	42.6	42.7	42.4
C4	46.1	46.2	46.2	46.0
C5	60.6	59.4	59.4	59.2
C6	40.4	41.0	40.5	40.2
C7	56.2	51.7	51.7	51.5
C8	66.2	63.9	63.9	63.7
C9	41.6	36.9	36.9	36.7
C10	35.1	29.9	29.9	29.7
C11	24.7	20.3	20.3	20.1
C12	22.3	22.3	22.3	22.1
C13	28.7	28.7	28.8	28.5
C14	32.5	31.4	31.4	31.1
C15	15.9	15.7	15.8	15.5

^a For a comparison of ^{13}C NMR spectra of synthetic and natural **223**, see Figure A5.125.^b ^{13}C NMR spectra were obtained at 125 MHz in C_6D_6 and standardized relative to residual C_6D_6 .^c ^{13}C NMR spectra were obtained at 125 MHz in C_6D_6 and standardized relative to TMS.^d ^{13}C NMR spectra were obtained at 100 MHz in C_6D_6 and standardized relative to TMS.

Table 3.8. Comparison of ^1H NMR Data for Synthetic and Reported Synthetic²⁸ **224****synthetic compound 224**

Synthetic 224 ^a (ppm)	Multiplicity, <i>J</i> (Hz)	Reported 224 ^b (ppm)	Multiplicity, <i>J</i> (Hz)
1.25	s	1.26	s
0.95	s	0.95	s
0.93	d, 6.8	0.94	d, 7
0.81	s	0.82	s

^a ^1H NMR spectra were obtained at 500 MHz in CD_2Cl_2 and standardized relative to residual CH_2Cl_2 .

^b ^1H NMR spectra were obtained at 100 or 200 MHz in CD_2Cl_2 .

Table 3.9. Comparison of ^{13}C NMR Data for Synthetic and Reported Synthetic²⁸ **224**

Synthetic 224 ^a (ppm)	Reported 224 ^b (ppm)
85.7	85.4
66.2	65.8
60.6	60.3
56.2	55.8
46.1	45.7
42.2	41.5
41.6	41.1
40.4	40.1
35.1	34.7
32.5	32.1
32.1	31.7
28.7	28.5
24.7	24.8
22.3	22.0
15.9	15.5

^a ^{13}C NMR spectra were obtained at 125 MHz in C_6D_6 and standardized relative to residual C_6D_6 .

^b ^{13}C NMR spectra were obtained at 23 or 50 MHz in $\text{C}_6\text{D}_6/\text{CCl}_4$ and standardized relative to CCl_4 .

3.9 NOTES AND REFERENCES

- (1) For the isolation of presilphiperfolan-8 α -ol (**221**), see: Bohlmann, F.; Zdero, C.; Jakupovic, J.; Robinson, H.; King, R. M. *Phytochemistry* **1981**, *20*, 2239–2244.
- (2) For the isolation of presilphiperfolan-9 α -ol (**222**), see: (a) Weyerstahl, P. in *Newer Trends in Essential Oils and Flavours* (Eds.: K. L. Dhar, R. K. Thappa, S. G. Agarwal), Tata McGraw-Hill Publishing Company Ltd., New Delhi, 1993, pp. 24–41. (b) Marco, J. A.; Sanz-Cervera, J. F.; Morante, M. D.; García-Lliso, V.; Vallès-Xirau, J.; Jakupovic, J. *Phytochemistry* **1996**, *41*, 837–844.
- (3) Presilphiperfolan-1 β -ol (**223**) was originally assigned as structure **224**. For the first records of its isolation, see: (a) Melching, S.; König, W. A. *Phytochemistry* **1999**, *51*, 517–523. (b) Melching, S. Isolierung, Strukturaufklärung und stereochemische Untersuchungen neuer sesquiterpenoider Verbindungen aus vier Chemotypen des Lebermooses *Conocephalum conicum*. Ph.D. Thesis, Universität Hamburg, April 1999.
- (4) Presilphiperfolan-1 β -ol (**223**) was subsequently isolated by another research group, but reported as a unique natural product with structure **225**. This structure was later revised to structure **223**. For these reports, see: (a) Pinto, S. C.; Leitão, G. G.; Bizzo, H. R.; Martinez, N.; Dellacassa, E.; dos Santos, Jr. F. M.; Costa, F. L. P.; de Amorim, M. B.; Leitão, S. G. *Tetrahedron Lett.* **2009**, *50*, 4785–4787. (b) Joseph-Nathan, P.; Leitão, S. G.; Pinto, S. C.; Leitão, G. G.; Bizzo, H. R.; Costa, F. L. P.; de Amorim, M. B.; Martinez, N.; Dellacassa, E.; Hernández-Barragán, A.; Pérez-Hernández, N. *Tetrahedron Lett.* **2010**, *51*, 1963–1965.
- (5) Davis, C. E.; Duffy, B. C.; Coates, R. M. *J. Org. Chem.* **2003**, *68*, 6935–6943.

- (6) Osawa, E.; Aigami, K.; Takaishi, N.; Inamoto, Y.; Fujikura, Y.; Majerski, Z.; von R. Schleyer, P.; Engler, E. M.; Farcasiu, M. *J. Am. Chem. Soc.* **1977**, *99*, 5361–5373.
- (7) Coates, R. M.; Ho, Z.; Klobus, M.; Wilson, S. R. *J. Am. Chem. Soc.* **1996**, *118*, 9249–9254.
- (8) Weyerstahl, P.; Marschall, H.; Schulze, M.; Schwöpe, I. *Liebigs Ann.* **1996**, 799–807.
- (9) Weyerstahl, P.; Marschall, H.; Seelmann, I.; Jakupovic, J. *Eur. J. Org. Chem.* **1998**, 1205–1212.
- (10) Yang, J.-L.; Liu, L.-L.; Shi, Y.-P. *Tetrahedron Lett.* **2009**, *50*, 6315–6317.
- (11) (a) Bohlmann, F.; Ziesche, J.; Gupta, R. K. *Phytochemistry* **1982**, *21*, 1331–1334. (b) Bohlmann, F.; Zdero, C. *Phytochemistry* **1982**, *21*, 2537–2541. (c) Mericli, A. H.; Mericli, F.; Jakupovic, J.; Bohlmann, F.; Dominguez, X. A.; Vega, H. S. *Phytochemistry* **1989**, *28*, 1149–1153.
- (12) Fehllhaber, H.-W.; Geipel, R.; Mercker, H.-J.; Tschesche, R.; Welmar, K.; Schönbeck, F. *Chem. Ber.* **1974**, *107*, 1720–1730.
- (13) Bohlmann, F.; Jakupovic, J. *Phytochemistry* **1980**, *19*, 259–265.
- (14) (a) Bohlmann, F.; Zdero, C. *Phytochemistry* **1981**, *20*, 2529–2534. (b) Bohlmann, F.; Zdero, C.; King, R. M.; Robinson, H. *Phytochemistry* **1981**, *20*, 2425–2427.
- (15) (a) Hanson, J. R. *Pure Appl. Chem.* **1981**, *53*, 1155–1162. (b) Bradshaw, A. P. W.; Hanson, J. R.; Nyfeler, R. *J. Chem. Soc., Perkin Trans. I* **1981**, 1469–1472.

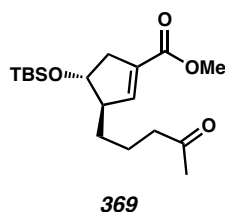
- (c) Bradshaw, A. P. W.; Hanson, J. R.; Nyfeler, R.; Sadler, I. H. *J. Chem. Soc., Chem. Commun.* **1981**, 649–650. (d) Bradshaw, A. P. W.; Hanson, J. R.; Nyfeler, R.; Sadler, I. H. *J. Chem. Soc., Perkin Trans. I* **1982**, 2187–2192.
- (16) Pinedo, C.; Wang, C.-M.; Pradier, J.-M.; Dalmais, B.; Choquer, M.; Le Pêcheur, P.; Morgant, G.; Collado, I. G.; Cane, D. E.; Viaud, M. *ACS Chem. Biol.* **2008**, *3*, 791–801.
- (17) Wang, C.-M.; Hopson, R.; Lin, X.; Cane, D. E. *J. Am. Chem. Soc.* **2009**, *131*, 8360–8361.
- (18) Wang, S. C.; Tantillo, D. J. *Org. Lett.* **2008**, *10*, 4827–4830.
- (19) Barquera-Lozada, J. E.; Cuevas, G. *J. Org. Chem.* **2011**, *76*, 1572–1577.
- (20) (a) Weyerstahl, P.; Marschall, H.; Schröder, M.; Wahlburg, H.-C.; Kaul, V. K. *Flavour Fragr. J.* **1997**, *12*, 315–325. (b) Menut, C.; Lamaty, G.; Weyerstahl, P.; Marschall, H.; Seelmann, I.; Amvam Zollo, P. H. *Flavour. Fragr. J.* **1997**, *12*, 415–421.
- (21) González-Coloma, A.; Valencia, F.; Martín, N.; Hoffmann, J. F.; Hutter, L.; Marco, J. A.; Reina, M. *J. Chem. Ecol.* **2002**, *28*, 117–129.
- (22) Pinto, S. C.; Leitão, G. G.; de Oliveira, D. R.; Bizzo, H. R.; Ramos, D. F.; Coelho, T. S.; Silva, P. E. A.; Lourenço, M. C. S.; Leitão, S. G. *Nat. Prod. Comm.* **2009**, *4*, 1675–1678.

- (23) (a) Collado, I. G.; Aleu, J.; Macías-Sánchez, A. J.; Hernández-Galán, R. *J. Chem. Ecol.* **1994**, *20*, 2631–2644. (b) Collado, I. G.; Aleu, J.; Macías-Sánchez, A. J.; Hernández-Galán, R. *J. Nat. Prod.* **1994**, *57*, 738–746.
- (24) For a review discussing the rearrangements of β -caryophyllene and isocaryophyllene, see: Collado, I. G.; Hanson, J. R.; Macías-Sánchez, A. J. *Nat. Prod. Rep.* **1998**, *15*, 187–204.
- (25) To our knowledge, the rearrangement of β -caryophyllene or β -caryophyllene derivatives in biomimetic reactions has not produced any of the presilphiperfolanol natural products. For representative studies, see the following and references therein: (a) Wallach, O.; Walker, W. *Liebigs Ann.* **1892**, *271*, 285–299. (b) Asahina, Y.; Tsukamoto, T. *J. Pharm. Soc. Jpn.* **1922**, 463–473. (c) Henderson, G. G.; McCrone, R. O. O.; Robertson, J. M. *J. Chem. Soc.* **1929**, 1368–1372. (d) Aebi, A.; Barton, D. H. R.; Burgstahler, A. W.; Lindsey, A. S. *J. Chem. Soc.* **1954**, 4659–4665. (e) Barton, D. H. R.; Nickon, A. J. *J. Chem. Soc.* **1954**, 4665–4669. (f) Parker, W.; Raphael, R. A.; Roberts, J. S. *Tetrahedron Lett.* **1965**, *6*, 2313–2316. (g) Parker, W.; Raphael, R. A.; Roberts, J. S. *J. Chem. Soc. C* **1969**, 2634–2643.
- (26) (a) Fitjer, L.; Malich, A.; Paschke, C.; Kluge, S.; Gerke, R.; Rissom, B.; Weiser, J.; Noltemeyer, M. *J. Am. Chem. Soc.* **1995**, *117*, 9180–9189. (b) Shankar, S.; Coates, R. M. *J. Org. Chem.* **1998**, *63*, 9177–9182.
- (27) (a) Gollnick, K.; Schade, G.; Cameron, A. F.; Hannaway, C.; Roberts, J. S.; Robertson, J. M. *J. Chem. Soc., Chem. Commun.* **1970**, 248–249. (b) Gollnick, K.; Schade, G.; Cameron, A. F.; Hannaway, C.; Robertson, J. M. *J. Chem. Soc.*

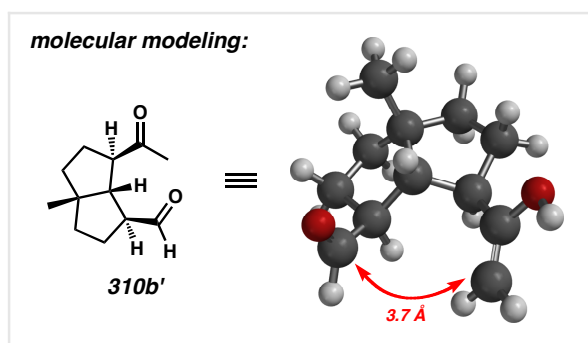
- D.*: *Chem. Commun.* **1971**, 46. (c) Cameron, A. F.; Hannaway, C.; Robertson, J. *M. J. Chem. Soc., Perkin Trans. 2* **1973**, 1938–1942.
- (28) (a) Khomenko, T. M.; Bagryanskaya, I. Y.; Gatilov, Y. V.; Korchagina, D. V.; Gatilova, V. P.; Dubovenko, Z. V.; Barkhash, V. A. *Zh. Org. Khim.* **1985**, 21, 677–678. *Russ. J. Org. Chem. (Engl. Transl.)* **1985**, 21, 614–615. (b) Khomenko, T. M.; Korchagina, D. V.; Gatilov, Y. V.; Bagryanskaya, Y. I.; Tkachev, A. V.; Vyalkov, A. I.; Kun, O. B.; Salenko, V. L.; Dubovenko, Z. V.; Barkash, V. A. *Zh. Org. Khim.* **1990**, 26, 2129–2145; *Russ. J. Org. Chem. (Engl. Transl.)* **1990**, 26, 1839–1852.
- (29) Burgess, E. M.; Penton, Jr., H. R.; Taylor, E. A. *J. Org. Chem.* **1973**, 38, 26–31.
- (30) (a) Hosomi, A.; Endo, M.; Sakurai, H. *Chem. Lett.* **1976**, 5, 941–942. (b) Hosomi, A.; Sakurai, H. *Tetrahedron Lett.* **1976**, 17, 1295–1298. (c) Sakurai, H.; Hosomi, A.; Hayashi, J. *Org. Synth.* **1984**, 62, 86–93.
- (31) For comparisons of the reactivity of MMPP and *m*-CPBA, see: Brougham, P. Cooper, M. S.; Cummeron, D. A.; Heaney, H.; Thompson, N. *Synthesis*, **1987**, 1015–1017.
- (32) For a review on radical cascade reactions, see: McCarroll, A. J.; Walton, J. C. *Angew. Chem. Int. Ed.* **2001**, 40, 2224–2248.
- (33) Gilbert, M. W. Carbocycle Construction in Terpenoid Synthesis. The Total Synthesis of (±)-Sarcodonin G and (±)-1-*Epi*-9-Norpresilphiperfolan-9-one. Ph.D. Thesis, University of British Columbia, June 2002.
- (34) Luche, J. L. *J. Am. Chem. Soc.* **1978**, 100, 2226–2227.

- (35) Wilson, S. R.; Price, M. F. *J. Org. Chem.* **1984**, *49*, 722–725.
- (36) (a) Carroll, M. F. *J. Chem. Soc.* **1940**, 704–706. (b) Carroll, M. F. *J. Chem. Soc.* **1940**, 1266–1268.
- (37) Levine, S. G. *J. Am. Chem. Soc.* **1958**, *80*, 6150–6151.
- (38) Carlsen, P. H. J.; Katsuki, T.; Martin, V. S.; Sharpless, K. B. *J. Org. Chem.* **1981**, *46*, 3936–3938.
- (39) For a general review discussing recent syntheses of terpenoid natural products, see: Maimone, T. J.; Baran, P. S. *Nature Chem. Biol.* **2007**, *3*, 396–407.
- (40) For selected reviews of the total synthesis of triquinane sesquiterpene natural products, see: (a) Mehta, G.; Srikrishna, A. *Chem. Rev.* **1997**, *97*, 671–720. (b) Singh, V.; Thomas, B. *Tetrahedron* **1998**, *54*, 3647–3692. (c) Chanon, M.; Barone, R.; Baralotto, C.; Julliard, M.; Hendrickson, J. B. *Synthesis* **1998**, 1559–1583.
- (41) For a review discussing our strategy of using natural product structures to drive the development of enantioselective catalysis, see: Mohr, J. T.; Krout, M. R.; Stoltz, B. M. *Nature* **2008**, *455*, 323–332.
- (42) (a) Hong, A. Y.; Krout, M. R.; Jensen, T.; Bennett, N. B.; Harned, A. M.; Stoltz, B. M. *Angew. Chem. Int. Ed.* **2011**, *50*, 2756–2760. (b) Hong, A. Y.; Bennett, N. B.; Krout, M. R.; Jensen, T.; Harned, A. M.; Stoltz, B. M. *Tetrahedron* **2011**, *67*, 10234–10248. (c) Bennett, N. B.; Hong, A. Y.; Harned, A. M.; Stoltz, B. M. *Org. Biomol. Chem.* **2012**, *10*, 56–59.

- (43) (a) Clive, D. L. J.; Farina, V.; Beaulieu, P. *J. Chem. Soc. Chem. Commun.* **1981**, 643–644. (b) Clive, D. L. J.; Farina, V.; Beaulieu, P. *L. J. Org. Chem.* **1982**, 47, 2572–2582.
- (44) A structurally analogous ketoester substrate **369** was evaluated in cyclization reactions during synthetic efforts toward kalmanol. See: Borrelly, S.; Paquette, L. A. *J. Am. Chem. Soc.* **1996**, 118, 727–740.



- (45) The desired tricycle could be formed through the intermediacy of ketoaldehyde **310b'**. Calculations to determine relevant bond distances were obtained by molecular modeling using Spartan '10 on an iMac computer; Wavefunction, Inc: Irvine, CA, 2006. Calculations were performed at the Molecular Mechanics (MMFF) level of theory.



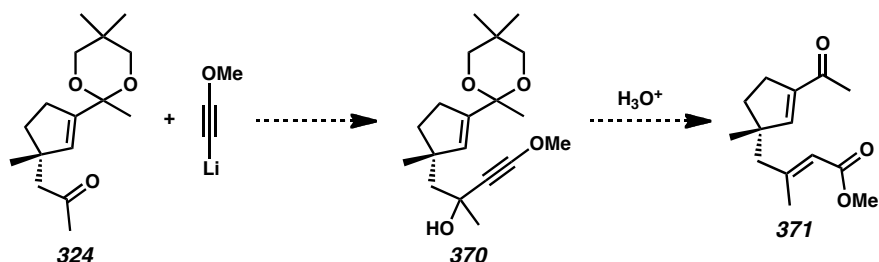
- (46) Mander, L. N.; Sethi, S. P. *Tetrahedron Lett.* **1983**, 24, 5425–5428.
- (47) For examples of asymmetric palladium-catalyzed allylic alkylation reactions of carbocyclic ketone enolates developed by our group, see: (a) Behenna, D. C.;

- Stoltz, B. M. *J. Am. Chem. Soc.* **2004**, *126*, 15044–15045. (b) Mohr, J. T.; Behenna, D. C.; Harned, A. M.; Stoltz, B. M. *Angew. Chem. Int. Ed.* **2005**, *44*, 6924–6927. (c) Behenna, D. C.; Mohr, J. T.; Sherden, N. H.; Marinescu, S. C.; Harned, A. M.; Tani, K.; Seto, M.; Ma, S.; Novák, Z.; Krout, M. R.; McFadden, R. M.; Roizen, J. L.; Enquist, Jr., J. A.; White, D. E.; Levine, S. R.; Petrova, K. V.; Iwashita, A.; Virgil, S. C.; Stoltz, B. M. *Chem. Eur. J.* **2011**, *17*, 14199–14223.
- (48) Substituted allylic carbamates have been used by others to achieve the C-acylation of enolates. For selected references, see: (a) Tanaka, T.; Okamura, N.; Bannai, K.; Hazato, A.; Sugiura, S.; Tomimori, K.; Manabe, K.; Kurozumi, S. *Tetrahedron* **1986**, *42*, 6747–6758. (b) Shone, R. L.; Deason, J. R.; Miyano, M. *J. Org. Chem.* **1986**, *51*, 268–270.
- (49) Substituted allylic carbamates have been used by Trost to achieve O-acylation of enolates under different reaction conditions. See: Trost, B. M.; Xu, J. *J. Org. Chem.* **2007**, *72*, 9372–9375.
- (50) (a) Heller, S. T.; Sarpong, R. *Org. Lett.* **2010**, *12*, 4572–4575. (b) Heller, S. T.; Sarpong, R. *Tetrahedron* **2011**, *67*, 8851–8859. (c) Heller, S. T.; Fu, T.; Sarpong, R. *Org. Lett.* **2012**, *14*, 1970–1973.
- (51) Isobutoxy-2-cyclohepten-1-one is commercially available from Sigma-Aldrich (#T271322), but was prepared on multi-decagram scale by a modified procedure based on the work of Ragan. See ref. 42a,c.
- (52) For examples of asymmetric palladium-catalyzed allylic alkylation reactions of heterocyclic ketone enolates (such as those derived from dioxanones and lactams) developed by our group, see: (a) Seto, M.; Roizen, J. L.; Stoltz, B. M. *Angew.*

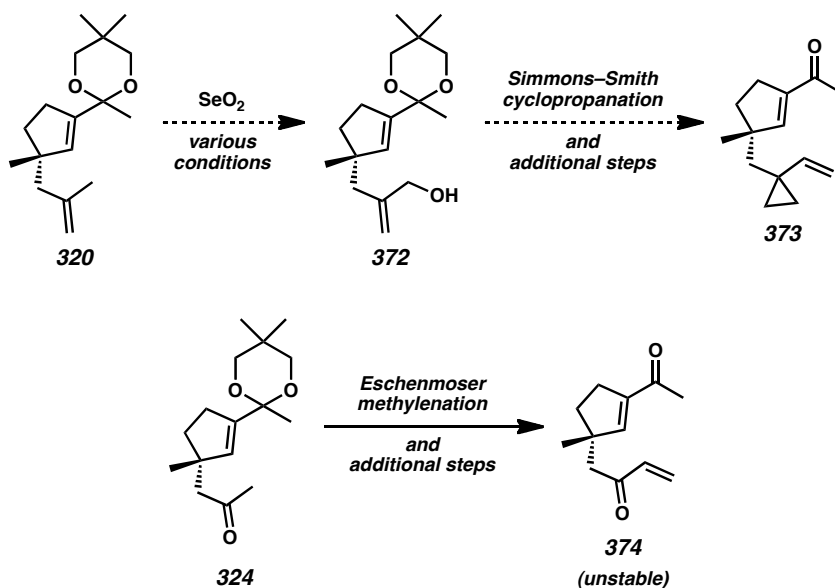
- Chem. Int. Ed.* **2008**, *47*, 6873–6876. (b) Behenna, D. C.; Liu, Y.; Yurino, T.; Kim, J.; White, D. E.; Virgil, S. C.; Stoltz, B. M. *Nature Chem.* **2012**, *4*, 130–133.
- (53) (a) Tani, K.; Behenna, D. C.; McFadden, R. M.; Stoltz, B. M. *Org. Lett.* **2007**, *9*, 2529–2531. (b) Krout, M. R.; Mohr, J. T.; Stoltz, B. M. *Org. Synth.* **2009**, *86*, 181–193.
- (54) For early reports of PHOX ligands, see: (a) von Matt, P.; Pfaltz, A. *Angew. Chem. Int. Ed. Engl.* **1993**, *32*, 566–568. (b) Sprinz, J.; Helmchen, G. *Tetrahedron Lett.* **1993**, *34*, 1769–1772. (c) Dawson, G. J.; Frost, C. G.; Williams, J. M. J.; Coote, S. J. *Tetrahedron Lett.* **1993**, *34*, 3149–3150.
- (55) (a) Ukai, T.; Kawazura, H.; Ishii, Y.; Bonnet, J. J.; Ibers, J. A. *J. Organomet. Chem.* **1974**, *65*, 253–266. (b) Fairlamb, I. J. S.; Kapdi, A. R.; Lee, A. F. *Org. Lett.* **2004**, *6*, 4435–4438.
- (56) For examples of the asymmetric alkylation of vinylogous esters or thioesters in the synthesis of natural products from our laboratory, see: (a) Elatol: White, D. E.; Stewart, I. C.; Grubbs, R. H.; Stoltz, B. M. *J. Am. Chem. Soc.* **2008**, *130*, 810–811. (b) Carissone: Levine, S. R.; Krout, M. R.; Stoltz, B. M. *Org. Lett.* **2009**, *11*, 289–292. (c) Cassiol: Petrova, K. V.; Mohr, J. T.; Stoltz, B. M. *Org. Lett.* **2009**, *11*, 293–295. (d) Elatol, Laurencenone C, α -Chamigrene, and the proposed structure of Laurencenone B: White, D. E.; Stewart, I. C.; Seashore-Ludlow, B. A.; Grubbs, R. H.; Stoltz, B. M. *Tetrahedron* **2010**, *66*, 4668–4686.
- (57) For additional formal and total syntheses completed in our group using Pd-catalyzed asymmetric allylic alkylation reactions, see: (a) Dichroanone: McFadden, R. M.; Stoltz, B. M. *J. Am. Chem. Soc.* **2006**, *128*, 7738–7739.

- (b) Cyanthiwigin F: Enquist, Jr., J. A.; Stoltz, B. M. *Nature* **2008**, *453*, 1228–1231. (c) Hamigeran B: Mukherjee, H.; McDougal, N. T.; Virgil, S. C.; Stoltz, B. M. *Org. Lett.* **2011**, *13*, 825–827. (d) Liphagal: Day, J. J.; McFadden, R. M.; Virgil, S. C.; Kolding, H.; Alleva, J. L.; Stoltz, B. M. *Angew. Chem. Int. Ed.* **2011**, *50*, 6814–6818. (e) Cyanthiwiggins B, F, and G: Enquist, Jr., J. A.; Virgil, S. C.; Stoltz, B. M. *Chem. Eur. J.* **2011**, *17*, 9957–9969.
- (58) For a related example of the asymmetric alkylation of vinylogous thioesters, see: Trost, B. M.; Bream, R. N.; Xu, J. *Angew. Chem. Int. Ed.* **2006**, *45*, 3109–3112.
- (59) For selected examples of the synthesis of trisubstituted olefins by olefin cross-metathesis, see: (a) Chatterjee, A. K.; Grubbs, R. H. *Org. Lett.* **1999**, *1*, 1751–1753. (b) Chatterjee, A. K.; Sanders, D. P.; Grubbs, R. H. *Org. Lett.* **2002**, *4*, 1939–1942. (c) Stewart, I. C.; Douglas, C. J.; Grubbs, R. H. *Org. Lett.* **2008**, *10*, 441–444. (d) Chatterjee, A. K.; Choi, T.-L.; Sanders, D. P.; Grubbs, R. H. *J. Am. Chem. Soc.* **2003**, *125*, 11360–11370.
- (60) Yu, W.; Mei, Y.; Kang, Y.; Hua, Z.; Jin, Z. *Org. Lett.* **2004**, *6*, 3217–3219.
- (61) For examples of Horner–Wadsworth–Emmons reactions on similarly hindered substrates, see: (a) Mantilli, L.; Gérard, D.; Torche, S.; Besnard, C.; Mazet, C. *Chem. Eur. J.* **2010**, *16*, 12736–12745. (b) Chakraborty, T. K.; Chattopadhyay, A. K.; Samanta, R.; Ampapathi, R. S. *Tetrahedron Lett.* **2010**, *51*, 4425–4428.
- (62) While we also planned to evaluate other organometallic additions with reagents such as lithium methoxyacetylide or the corresponding Grignard reagents, we did not have the opportunity to carry out these transformations. Following a

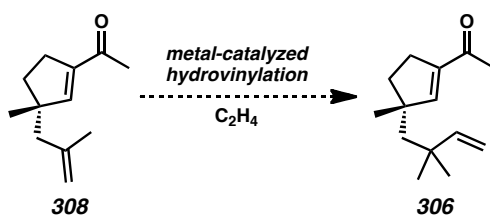
successful alkylation, an acid-promoted rearrangement could lead to enone-acrylate ester **324**.



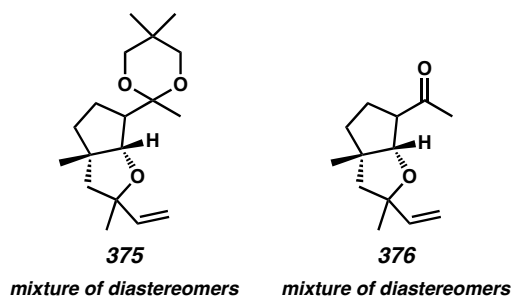
- (63) Two additional acylcyclopentenes were also targeted in alternative IMDA strategies. We envisioned that the preparation of cyclopropyl acylcyclopentene **373** could begin with the allylic oxidation of the methallyl group of ketal **320**. Numerous conditions with catalytic or stoichiometric SeO_2 were employed, but these reactions led to complex reaction mixtures. We also believed that bis-enone **374** could be productive for not only an IMDA reaction, but also an intramolecular Rauhut–Currier-type reaction. We successfully prepared small quantities of compound **374**, but it was prone to rapid decomposition.



- (64) Ni and Pd-catalyzed hydrovinylation reactions for the direct conversion of methallyl acylcyclopentene **308** to *gem*-dimethyl acyclopentene **306** were briefly investigated, but none of these transformations led to the desired product.



- (65) (a) Bellemin-Laponnaz, S.; Gisie, H.; Le Ny, J.-P.; Osborn, J. A. *Angew. Chem. Int. Ed. Engl.* **1997**, 36, 976–978. (b) Morrill, C.; Grubbs, R. H. *J. Am. Chem. Soc.* **2005**, 127, 2842–2843.
- (66) Dauben, W. G.; Michno, D. M. *J. Org. Chem.* **1977**, 42, 682–685.
- (67) Several products corresponding to tertiary alcohol conjugate addition were isolated in the reaction mixtures.

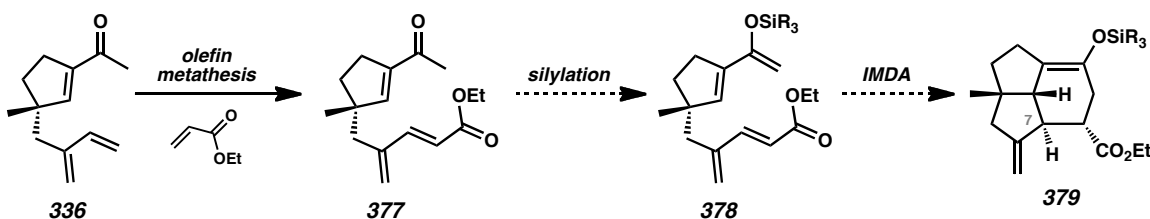


- (68) Larson, K. K.; Sarpong, R. *J. Am. Chem. Soc.* **2009**, 131, 13244–13245.
- (69) Parikh, J. R.; Doering, W. v. E. *J. Am. Chem. Soc.* **1967**, 89, 5505–5507.
- (70) Shibuya, M.; Tomizawa, M.; Iwabuchi, Y. *J. Org. Chem.* **2008**, 73, 4750–4752.

- (71) For examples of S_N2' halogenations, see: (a) Jo, H.; Lee, J.; Kim, H.; Kim, S.; Kim, D. *Tetrahedron Lett.* **2003**, *44*, 7043–7044. (b) Bakkestuen, A. K.; Gundersen, L.-L.; Petersen, D.; Utenova, B. T.; Vik, A. *Org. Biomol. Chem.* **2005**, *3*, 1025–1033. (c) Fuchter, M. J.; Levy, J.-N. *Org. Lett.* **2008**, *10*, 4919–4922. (d) Zhang, P.; Le, H.; Kyne, R. E.; Morken, J. P. *J. Am. Chem. Soc.* **2011**, *133*, 9716–9719.
- (72) For an example of S_N2' trifluoroacetoxylation, see: Ramharter, J.; Mulzer, J. *Org. Lett.* **2011**, *13*, 5310–5313.
- (73) (a) Reetz, M. T.; Westermann, J.; Steinbach, R. *Angew. Chem. Int. Ed. Engl.* **1980**, *19*, 900–901. (b) Reetz, M. T.; Westermann, J.; Kyung, S.-H. *Chem. Ber.* **1985**, *118*, 1050–1057.
- (74) Salomon, R. G.; Kochi, J. K. *J. Org. Chem.* **1973**, *38*, 3715–3718.
- (75) Our group has previously investigated 2-alkyl, 2-aryl, and 2-halo π -allyl electrophiles in Pd-catalyzed asymmetric allylic alkylation reactions (see Refs. 47, 52, and 56a,d), however, reactions with 2-vinyl π -allyl electrophiles have not been explored.
- (76) Satake, Y.; Nishikawa, T.; Hiramatsu, T.; Araki, H.; Isobe, M. *Synthesis* **2010**, 1992–1998.
- (77) Since Pd(0) is known to undergo cyclometallation with 1,3-dienes, it was believed that undesired side reactions could result from this reaction pathway.
- (78) The potentially incompatible electron-deficient olefin and diene functionalities in acylcyclopentene **336** did not appear to be a problem during the isolation and

storage of the compound. The quaternary center likely deters undesired reactivity.

- (79) For selected IMDA reviews, see: (a) Bear, B. R.; Sparks, S. M.; Shea, K. J. *Angew. Chem. Int. Ed.* **2001**, *40*, 820–849. (b) Nicolaou, K. C.; Snyder, S. A.; Montagnon, T.; Vassilikogiannakis, G. *Angew. Chem. Int. Ed.* **2002**, *41*, 1668–1698. (c) Takao, K.-i.; Munakata, R.; Tadano, K.-i. *Chem. Rev.* **2005**, *105*, 4779–4807. (d) Juhl, M.; Tanner, D. *Chem. Soc. Rev.* **2009**, *38*, 2983–2992.
- (80) Our IMDA substrate does not fit neatly into the Type I or Type II IMDA classification, making prediction of the reaction outcome less straightforward.
- (81) A related IMDA cycloaddition for the construction of an analogous tricyclic system with an activated alkyne has been reported. See: Evanno, L.; Deville, A.; Bodo, B.; Nay, B. *Tetrahedron Lett.* **2007**, *48*, 4331–4333.
- (82) Although IMDA reactions with silyl dienol ether **335** provided product **341** with the undesired C(7) stereochemistry, we believed that we could enforce an *endo* transition state for the IMDA reaction with substrate **378**. Synthesis of the precursor **377** (*E* isomer) by olefin metathesis was successful, but attempted silylation and IMDA bicyclization did not afford the desired products.

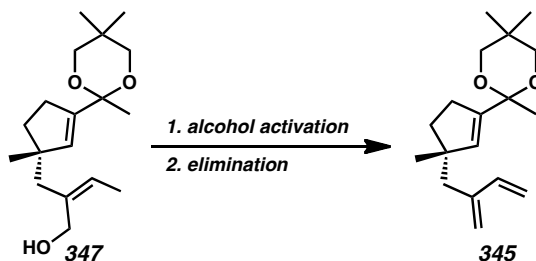


- (83) Relevant IMDA studies performed by Jung and Corey demonstrated that the diastereoselectivity of normal-demand Type I IMDA reactions can be reversed by

- substituting enone dienophiles with their corresponding sterically demanding cyclic ketal derivatives. See: (a) Jung, M. E; Halweg, K. M. *Tetrahedron Lett.* **1981**, 22, 3929–3932. (b) Corey, E. J.; Magriotis, P. A. *J. Am. Chem. Soc.* **1987**, 109, 287–289.
- (84) Krenske, E. H.; Perry, E. W.; Jerome, S. V.; Maimone, T. J.; Baran, P. S.; Houk, K. N. *Org. Lett.* **2012**, 14, 3016–3019.
- (85) Satoh, M.; Nomoto, Y.; Miyaura, N.; Suzuki, A. *Tetrahedron Lett.* **1989**, 30, 3789–3792.
- (86) (a) Wu, J. Y.; Moreau, B.; Ritter, T. *J. Am. Chem. Soc.* **2009**, 131, 12915–12917. (b) Wu, J. Y.; Stanzl, B. N.; Ritter, T. *J. Am. Chem. Soc.* **2010**, 132, 13214–13216.
- (87) (a) Ely, R. J.; Morken, J. P. *J. Am. Chem. Soc.* **2010**, 132, 2534–2535. (b) Ely, R. J.; Morken, J. P. *Org. Synth.* **2011**, 88, 342–352.
- (88) See Experimental Section for additional details, experimental procedures, reaction optimization tables, and comparisons of spectral data.
- (89) Control reactions were performed with isoprene as substrate. With a Ni(cod)₂/PCy₃ catalyst system, a 1.26:1 linear:branched ratio was observed. With Fe complex **349**, the reported 10:1 linear:branched ratio was observed. The C(4) quaternary stereocenter is likely responsible for the differences in regioselectivity in our case.
- (90) Attempts to perform the 1,4-hydroboration at an earlier stage of the synthesis were unsuccessful. Treatment of chiral vinylogous ester **337** with Ni(cod)₂, PCy₃,

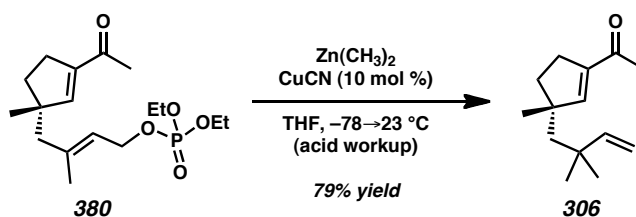
and HBpin led to a complex reaction mixture. Treatment of the same compound with Mg(0), Fe complex **349**, and HBPin also did not provide desired products.

- (91) We planned to transform undesired branched allylic alcohol **347** to 1,3-diene **345** by an elimination route, but we did not have an opportunity to sufficiently explore this recovery route.



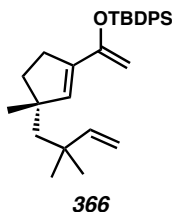
- (92) Luchaco-Cullis, C. A.; Mizutani, H.; Murphy, K. E.; Hoveyda, A. H. *Angew. Chem. Int. Ed.* **2001**, *40*, 1456–1460.

- (93) A small amount of ketal deprotection of the phosphorylated product **351** was sometimes observed in during work-up of the phosphorylation reaction. The resulting acylcyclopentene **380** can also be converted to *gem*-dimethyl acylcyclopentene **306** smoothly and chemoselectively using the Cu-catalyzed allylic substitution reaction conditions employed for ketal **351**.

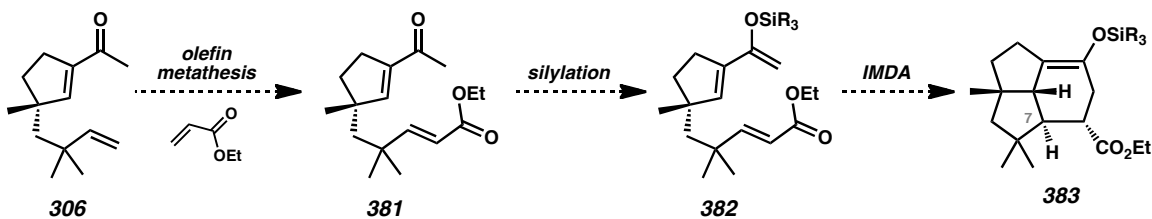


- (94) Our synthetic route makes use of TBS dienol ether **343**, but TBDPS dienol ether **366** was also investigated in the IMDA reaction. Substrate **366** provided similar

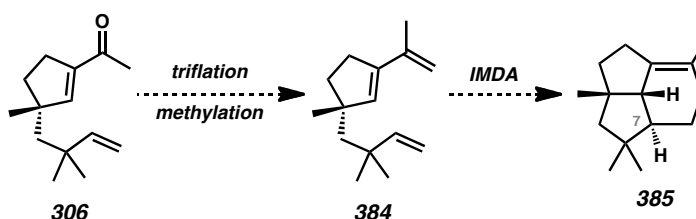
yield and dr in the thermal cyclization reaction. See Experimental Section for the preparation of this compound.



- (95) Murray, R. W.; Singh, M. *Org. Synth.* **1997**, 74, 91–96.
- (96) Incomplete silyl transfer to the tertiary alcohol was observed during the Rubottom oxidation, so TBAF was added to simplify the reaction mixture. The use of anhydrous acetone solvent and dry DMDO still did not lead to clean formation of the anticipated α -silyloxyketone. Attempts to install a silyl group on the alcohol of α -hydroxyketone **352** led to a mixture of bis-, mono-, and unsilylated products.
- (97) We planned to evaluate IMDA reactions with silyl dienol ether **382** to enforce an *endo* transition state, but attempts to construct acylcyclopentene **381** by olefin metathesis were not productive.

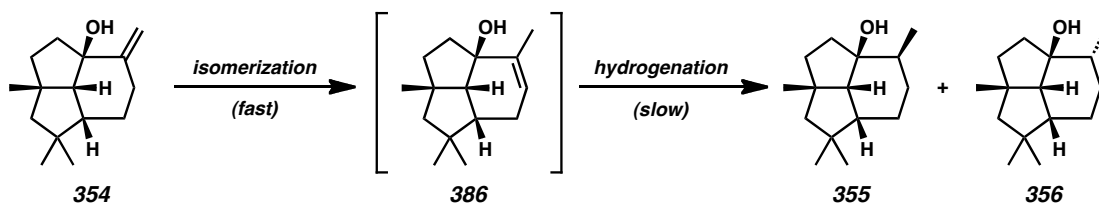


- (98) We also planned to evaluate IMDA reactions with triene **384**, but currently have not had the opportunity to explore this route.

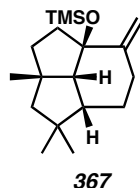


- (99) CCDC 889569 (**224**), CCDC 889570 (**353**), and CCDC 911859 (**356**) contain the supplementary crystallographic data for this chapter. These data can be obtained free of charge from The Cambridge Crystallographic Data Centre via www.ccdc.cam.ac.uk/data_request/cif.
- (100) Other temperatures were also investigated for the IMDA reaction. The reaction proceeds smoothly at temperatures as low as 90 °C, but longer reaction times are required. Lower dr was observed at lower temperatures. For a reaction screen of different solvents and temperatures, see Experimental Section for additional information (Table 3.2).
- (101) Jolly, R. S.; Luedtke, G.; Sheehan, D.; Livinghouse, T. *J. Am. Chem. Soc.* **1990**, *112*, 4965–4966.
- (102) Wender, P. A.; Jenkins, T. E. *J. Am. Chem. Soc.* **1989**, *111*, 6432–6434.
- (103) Bellville, D. J.; Wirth, D. W.; Bauld, N. L. *J. Am. Chem. Soc.* **1981**, *103*, 718–720.
- (104) Attempted hydrogenation of allylic alcohol **354** with Pd/C as catalyst in ethyl acetate at 23 °C led to rapid olefin isomerization to endocyclic olefin **386**. This compound underwent slow hydrogenation to alcohols **355** and **356**. Rapid initial olefin isomerization was also observed in reactions with Crabtree’s catalyst, but

with sufficient time, the reactions proceeded to the directed hydrogenation product **356**.

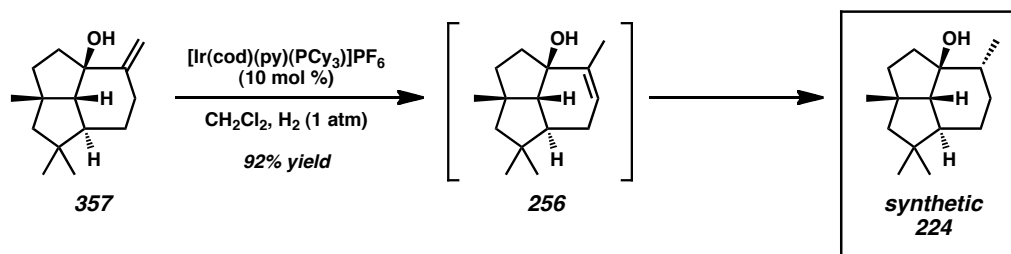


(105) The allylic alcohol **354** can be converted to trimethylsilyl ether **387**. See Experimental Section for the preparation of this compound.



(106) Crabtree, R. H.; Davis, M. W. *J. Org. Chem.* **1986**, *51*, 2655–2661.

(107) Competitive olefin isomerization of allylic alcohol **357** to the endocyclic trisubstituted alkene **256** is similarly observed if the hydrogenation reaction with Crabtree's catalyst is stopped at incomplete conversion, but if hydrogenation is allowed to go to completion, only reduced product **223** is observed.



(108) Kotoku, N.; Sumii, Y.; Kobayashi, M. *Org. Lett.* **2011**, *13*, 3514–3514.

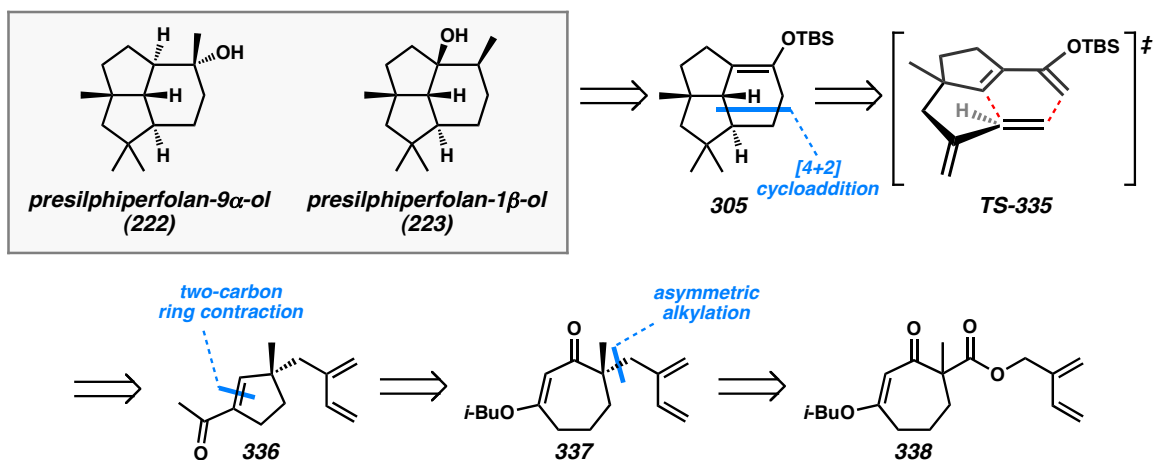
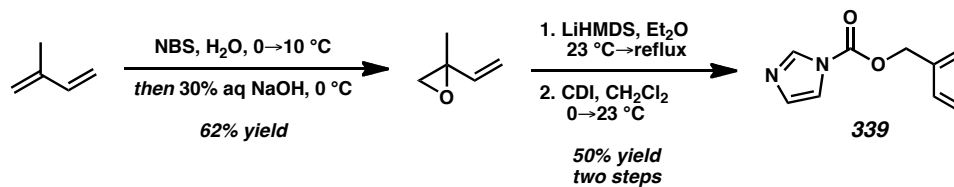
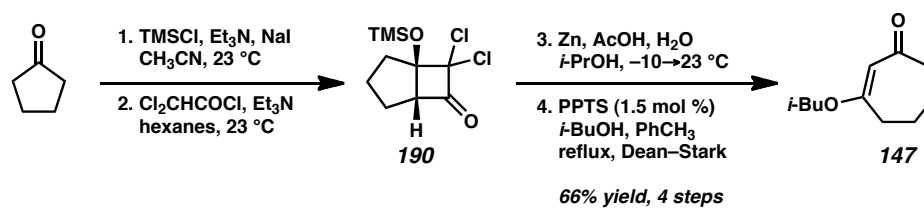
- (109) Unfortunately, attempts to obtain samples or spectra of naturally isolated “presilphiperfolan-1-ol” (**224**) were unsuccessful.
- (110) An X-ray crystal structure for a semi-synthetic compound with the same structure as our synthetic **224** (prepared from isocaryophyllene) was reported by Khomenko and co-workers (see ref. 28). The NMR data for Khomenko’s **224** and König’s **224** were acquired in different solvents. Our NMR data for synthetic **224** matches the spectral data for Khomenko’s synthetic **224** but not the spectral data for König’s natural **224**. See Experimental Section.
- (111) (a) Shapiro, R. H.; Heath, M. J. *J. Am. Chem. Soc.* **1967**, 89, 5734–5735.
(b) Kaufman, G. M.; Cook, F. B.; Shechter, H.; Bayless, J. H.; Friedman, L. J. *Am. Chem. Soc.* **1967**, 89, 5736–5737.
- (112) Bamford, W. R.; Stevens, T. S. M. *J. Chem. Soc.* **1952**, 4735–4740.
- (113) Pangborn, A. B.; Giardello, M. A.; Grubbs, R. H.; Rosen, R. K.; Timmers, F. J. *Organometallics* **1996**, 15, 1518–1520.
- (114) (a) Ragan, J. A.; Makowski, T. W.; am Ende, D. J.; Clifford, P. J.; Young, G. R.; Conrad, A. K.; Eisenbeis, S. A. *Org. Process Res. Dev.* **1998**, 2, 379–381.
(b) Ragan, J. A.; Murry, J. A.; Castaldi, M. J.; Conrad, A. K.; Jones, B. P.; Li, B.; Makowski, T. W.; McDermott, R.; Sitter, B. J.; White, T. D.; Young, G. R. *Org. Process Res. Dev.* **2001**, 5, 498–507. (c) Do, N.; McDermott, R. E.; Ragan, J. A. *Org. Synth.* **2008**, 85, 138–146.
- (115) Coulson, D. R.; Satek, L. C.; Grim, S. O. *Inorg. Synth.* **1972**, 13, 121–124.

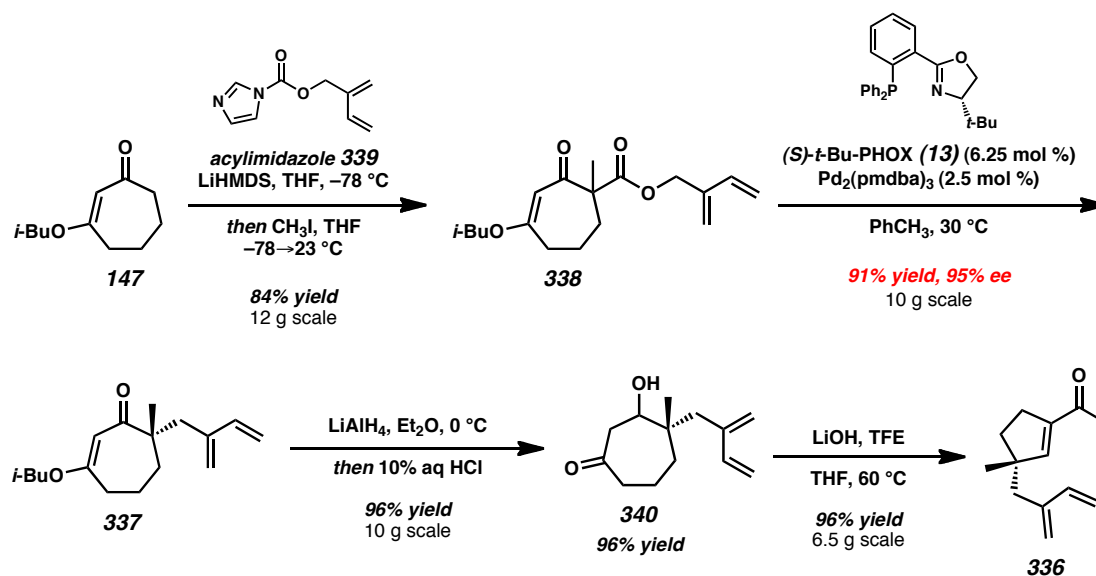
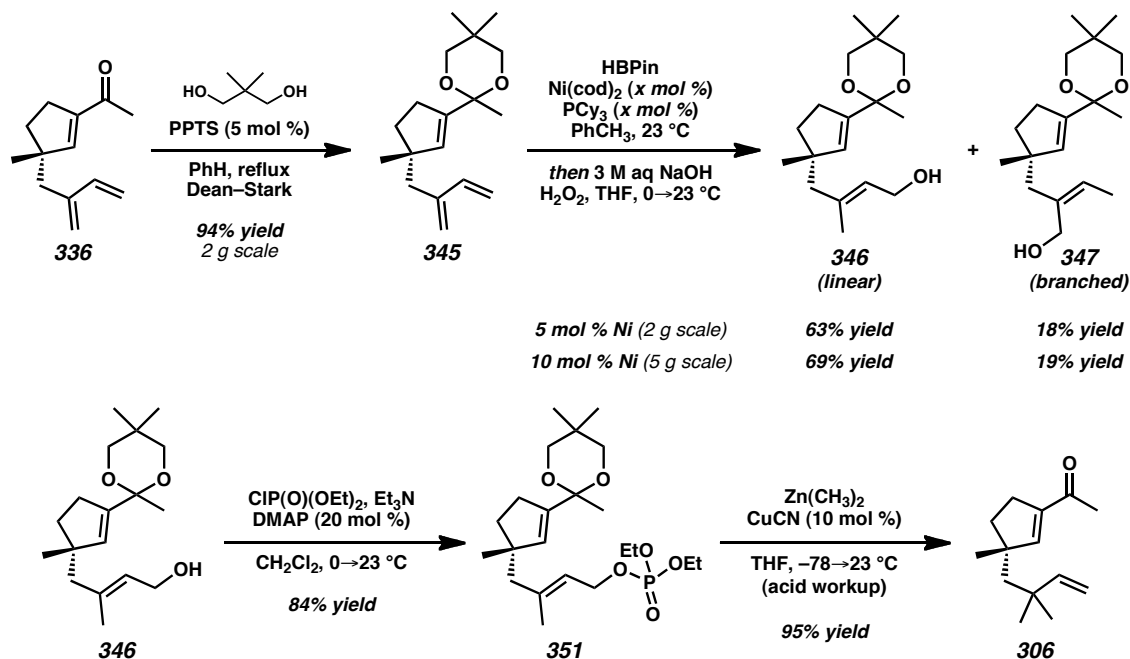
- (116) Corey, E. J.; Cho, H.; Rücker, C.; Hua, D. H. *Tetrahedron Lett.* **1981**, 22, 3455–3458.
- (117) Pappo, R.; Allen, Jr., D. S.; Lemieux, R. U.; Johnson, W. S. *J. Org. Chem.* **1956**, 21, 478–479.
- (118) Shintani, R.; Takatsu, K.; Takeda, M.; Hayashi, T. *Angew. Chem. Int. Ed.* **2011**, 50, 8656–8659.
- (119) Thompson, C. F.; Jamison, T. F.; Jacobsen, E. N. *J. Am. Chem. Soc.* **2000**, 122, 10482–10483.
- (120) Knapp, S.; Yu, Y. *Org Lett.* **2007**, 9, 1359–1362.

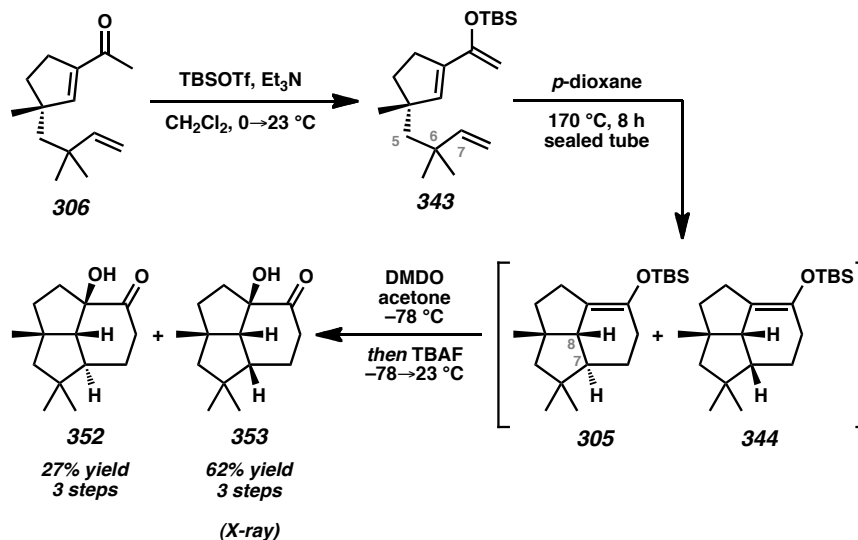
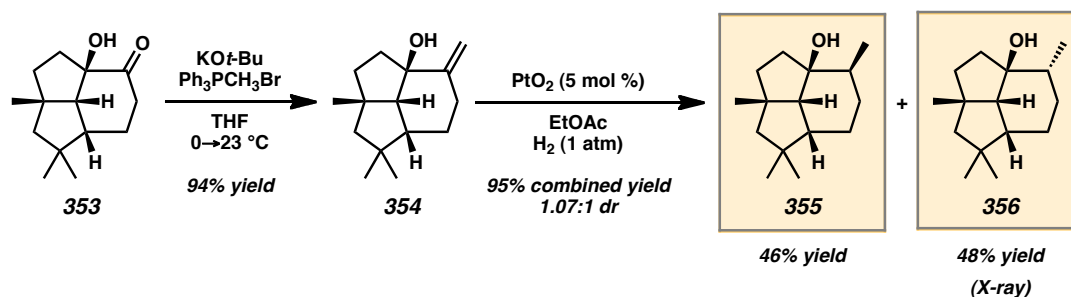
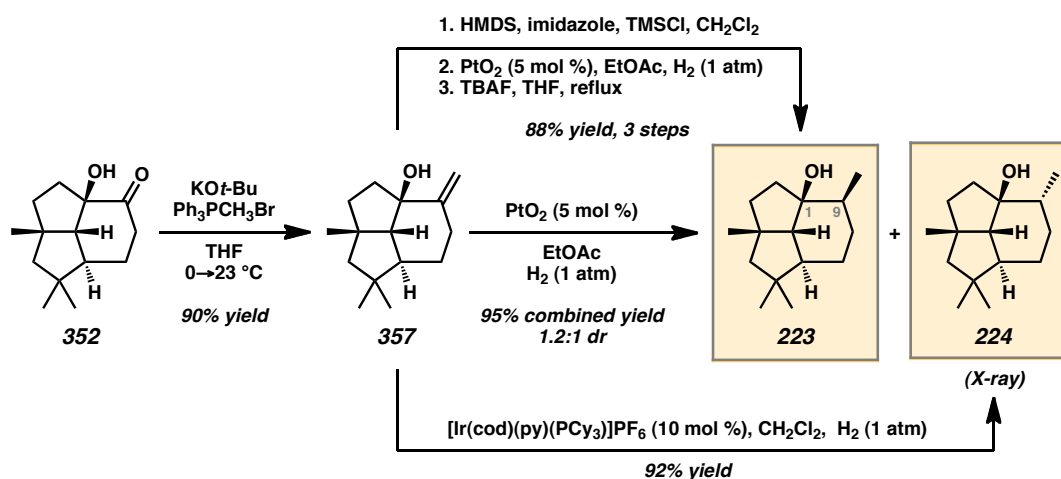
APPENDIX 4

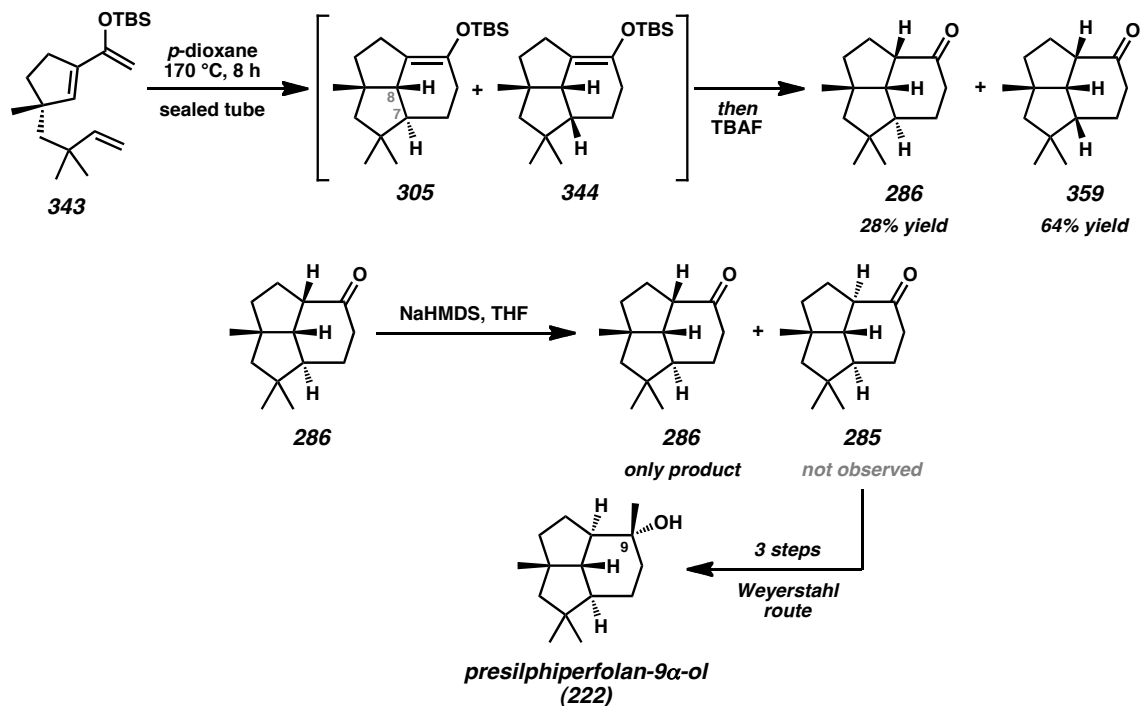
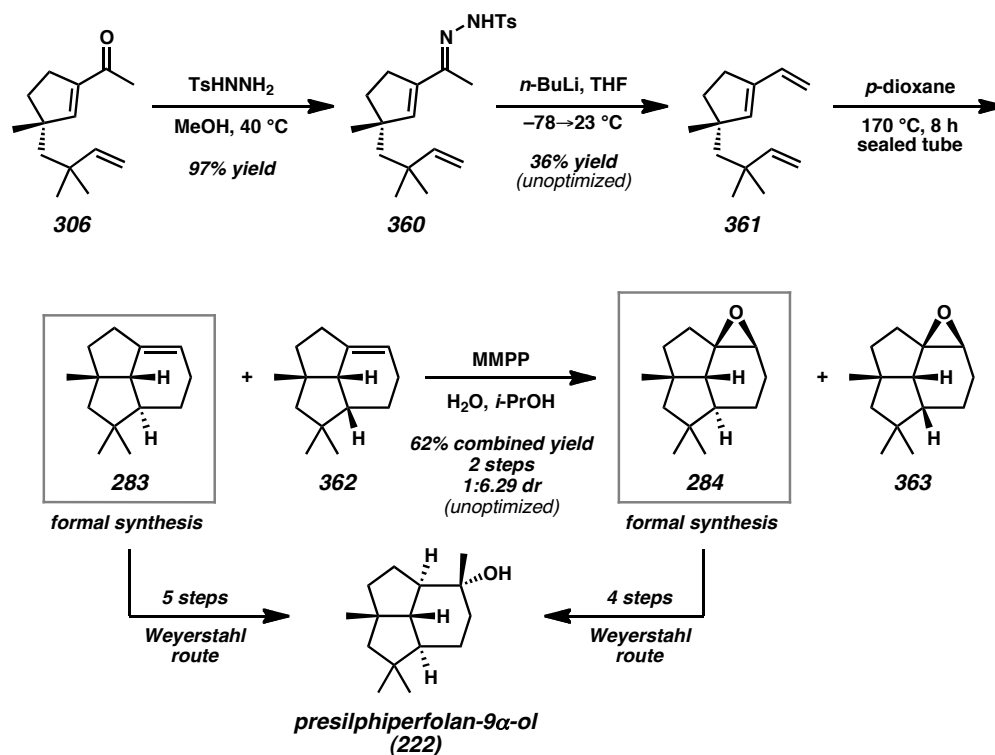
Synthetic Summary for Presilhiperfolanol Natural Products

Scheme A4.1. Retrosynthetic Analysis of Presilphiperfolanol Natural Products

Scheme A4.2. Synthesis of Isoprenyl Carbamate **339**Scheme A4.3. Synthesis of Vinylogous Ester **147**

Scheme A4.4. Asymmetric Alkylation/Ring Contraction Sequence to Methyl/Isoprenyl Acylcyclopentene **336**Scheme A4.5. Synthesis of gem-Dimethyl Acylcyclopentene **306**

Scheme A4.6. IMDA/Rubottom Sequence and Completion of Presilphiperfolan-1 β -ol (**223**)Scheme A4.7. Synthesis of Alcohols **355** and **356**Scheme A4.8. Synthesis of Presilphiperfolan-1 β -ol (**223**) and Alcohol **224**

Scheme A4.9. Planned Formal Synthesis of Presilphiperfolan-9 α -ol (**222**) via IMDA Substrate **343**Scheme A4.10. Planned Formal Synthesis of Presilphiperfolan-9 α -ol (**222**) via IMDA Substrate **361**

APPENDIX 5

Spectra Relevant to Chapter 3:

*The Catalytic Asymmetric Total Synthesis of
Presilphiperfolanol Natural Products*

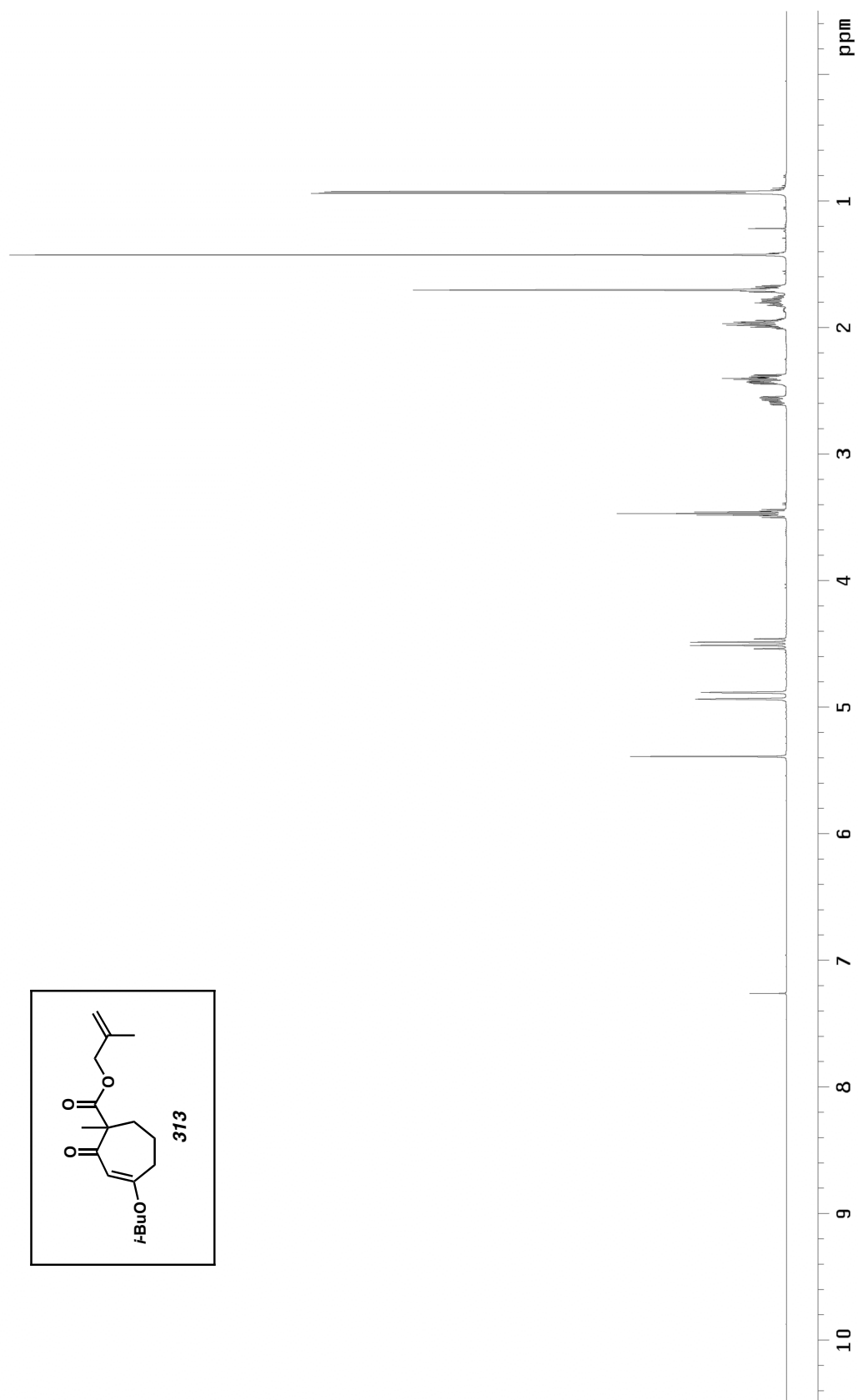


Figure A5.1. ^1H NMR (500 MHz, CDCl_3) of compound **313**.

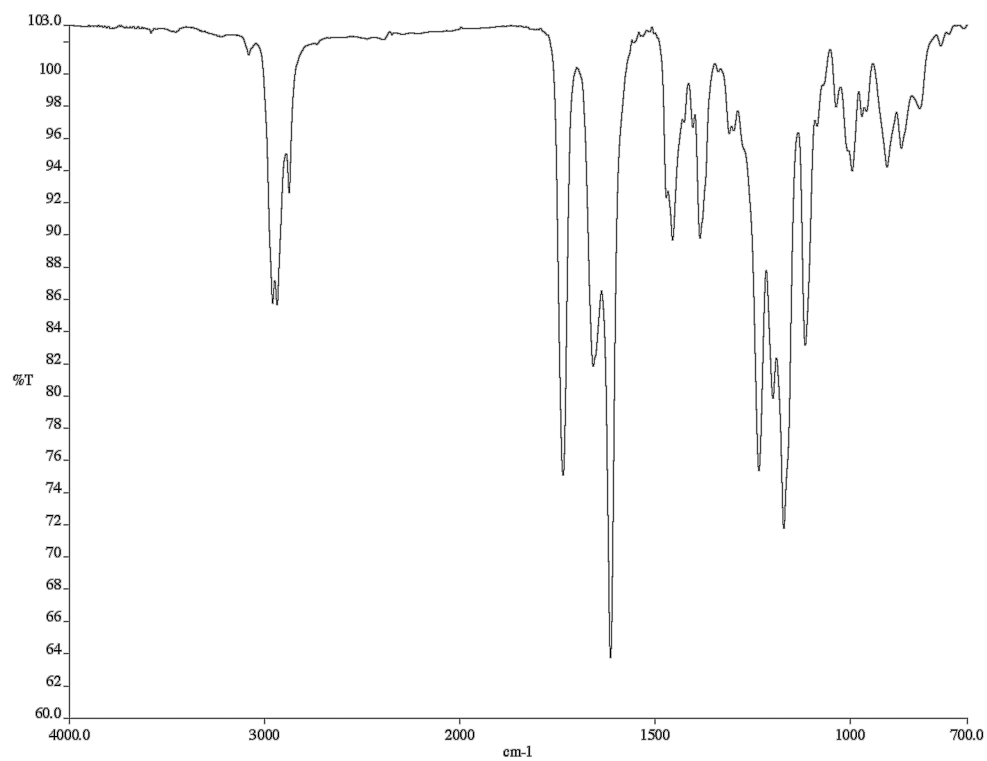


Figure A5.2. Infrared spectrum (thin film/NaCl) of compound **313**.

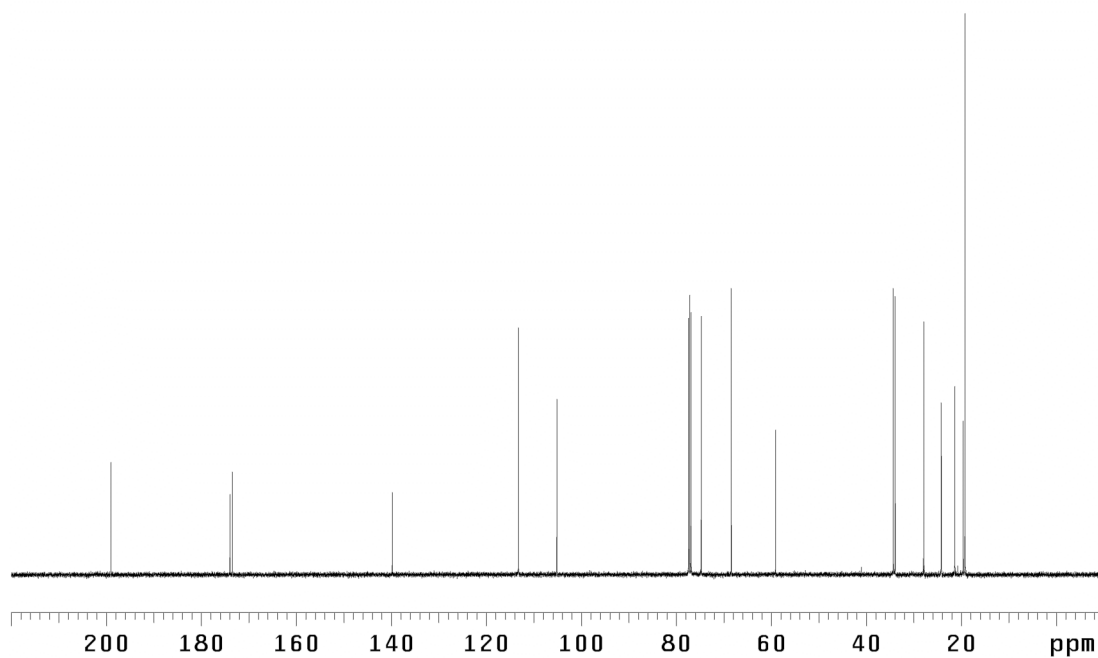
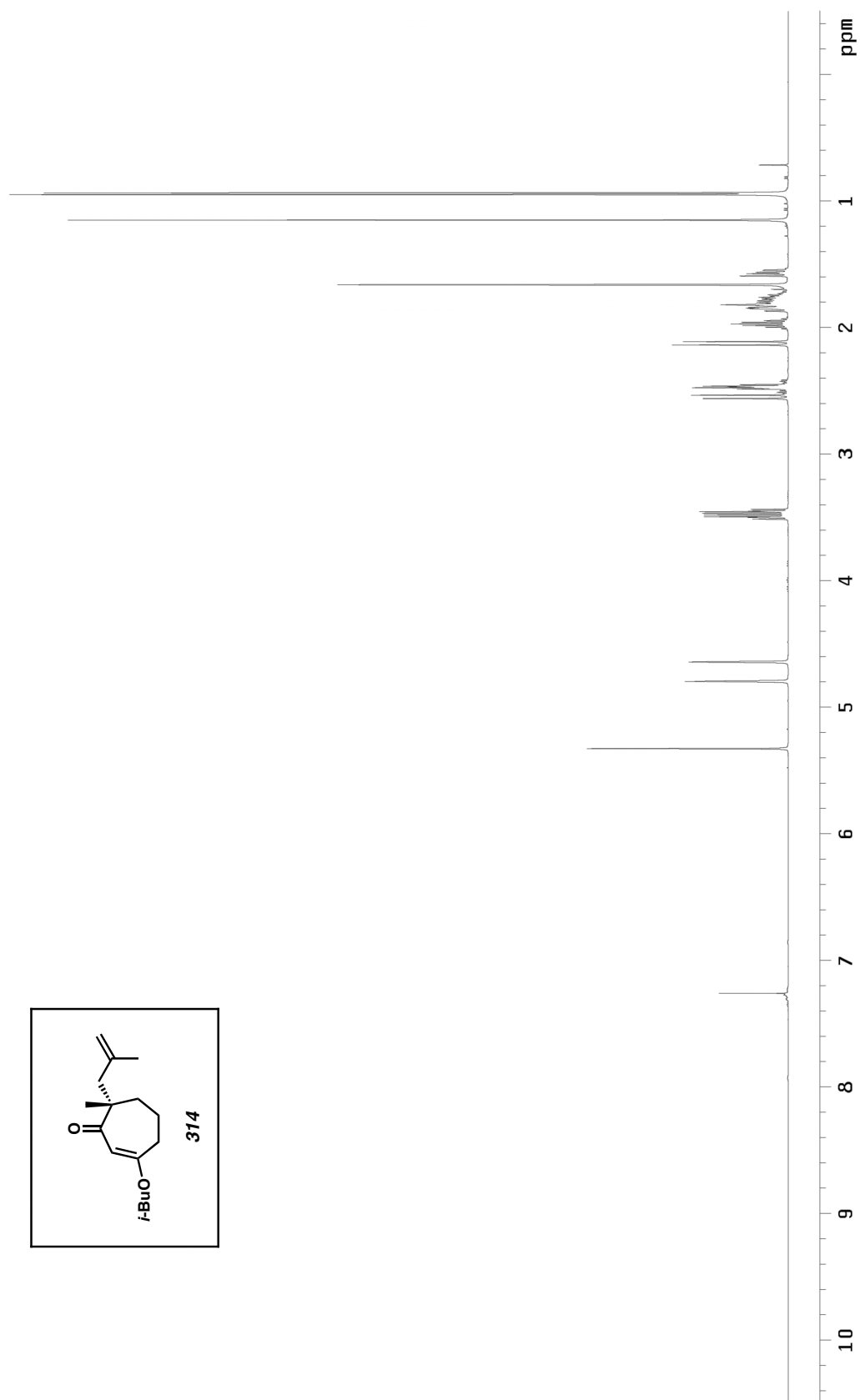


Figure A5.3. ¹³C NMR (125 MHz, CDCl₃) of compound **313**.

Figure A5.4. ¹H NMR (500 MHz, CDCl₃) of compound **314**.

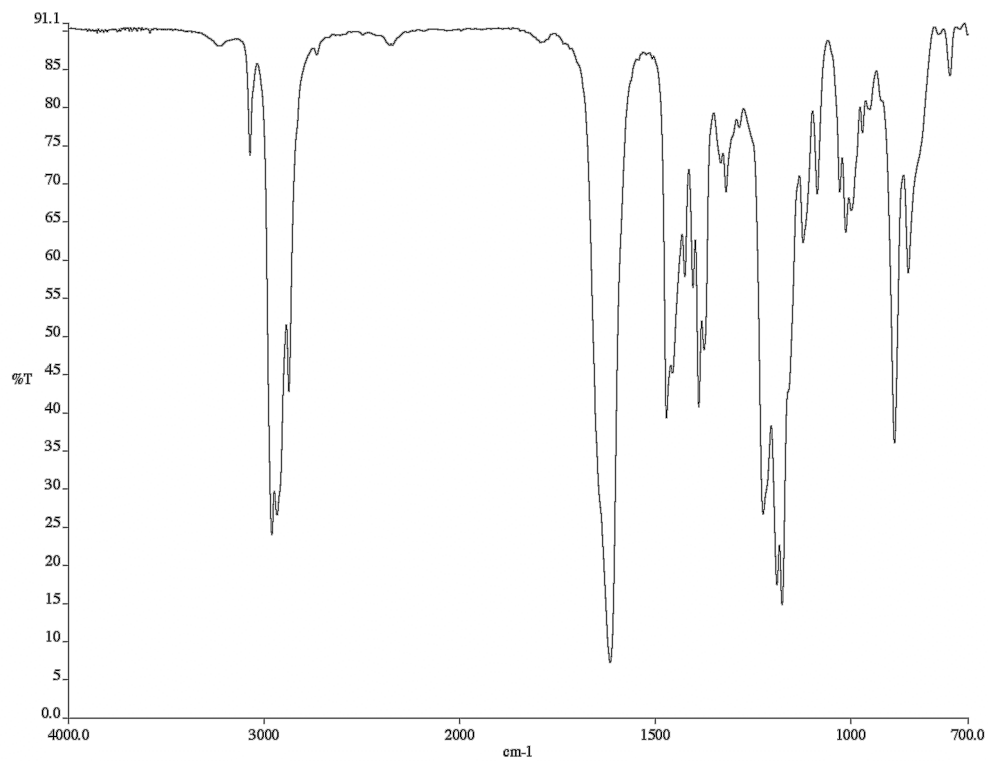


Figure A5.5. Infrared spectrum (thin film/NaCl) of compound **314**.

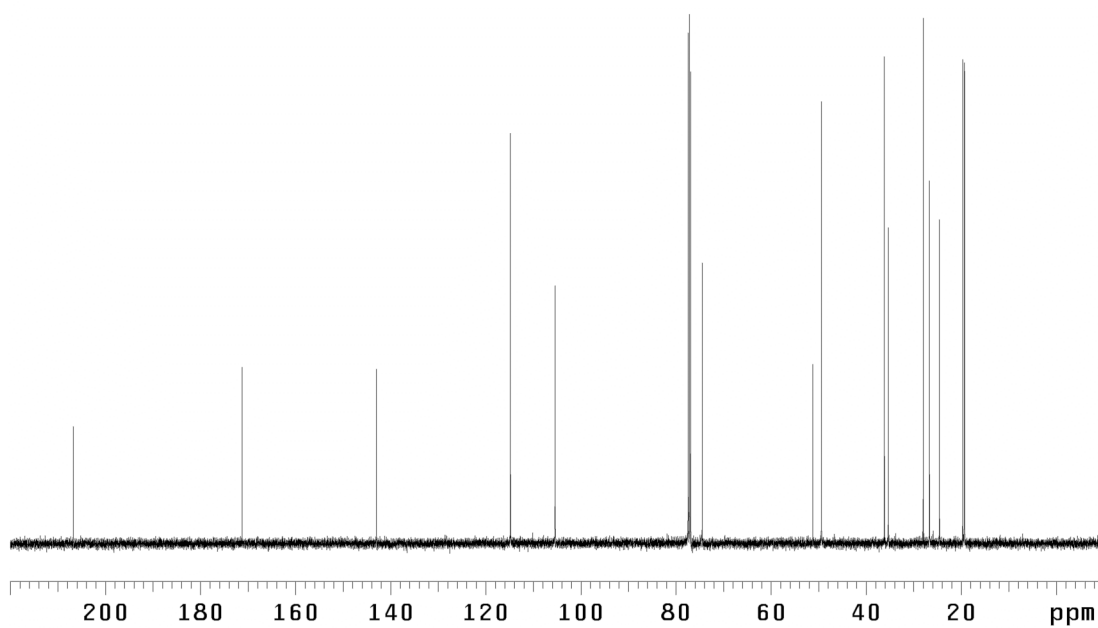


Figure A5.6. ¹³C NMR (125 MHz, CDCl₃) of compound **314**.

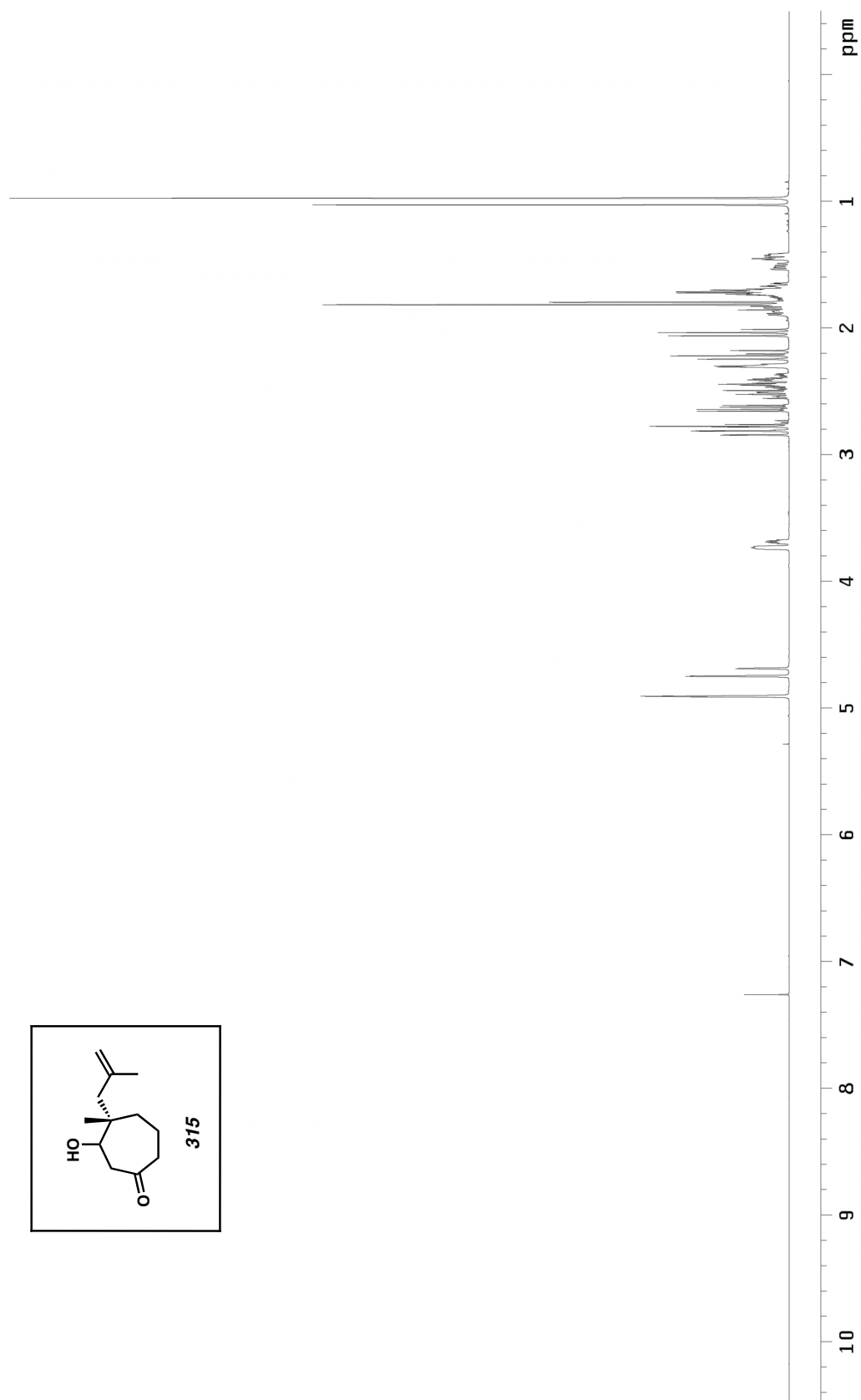


Figure A5.7. ¹H NMR (500 MHz, CDCl₃) of compound **315**.

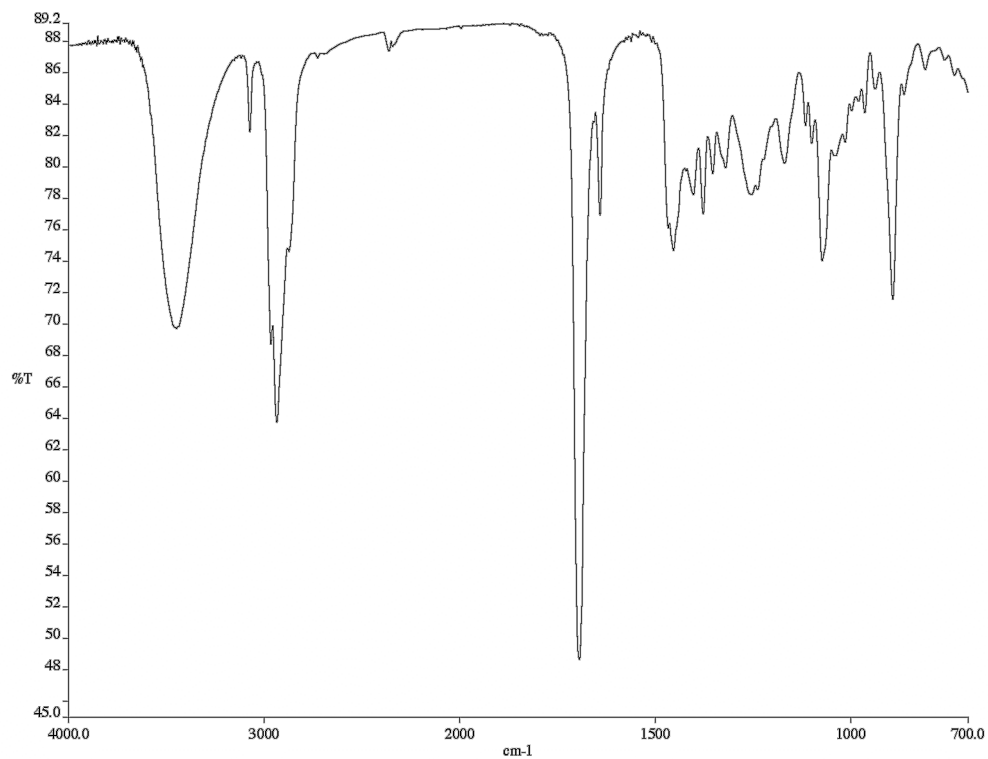


Figure A5.8. Infrared spectrum (thin film/NaCl) of compound **315**.

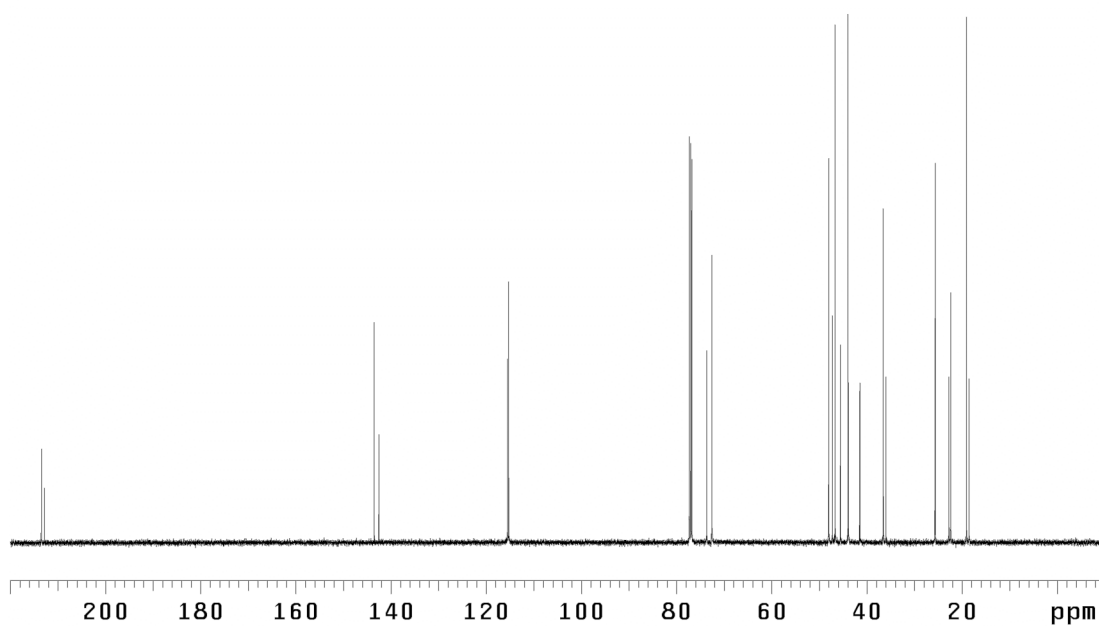


Figure A5.9. ¹³C NMR (125 MHz, CDCl₃) of compound **315**.

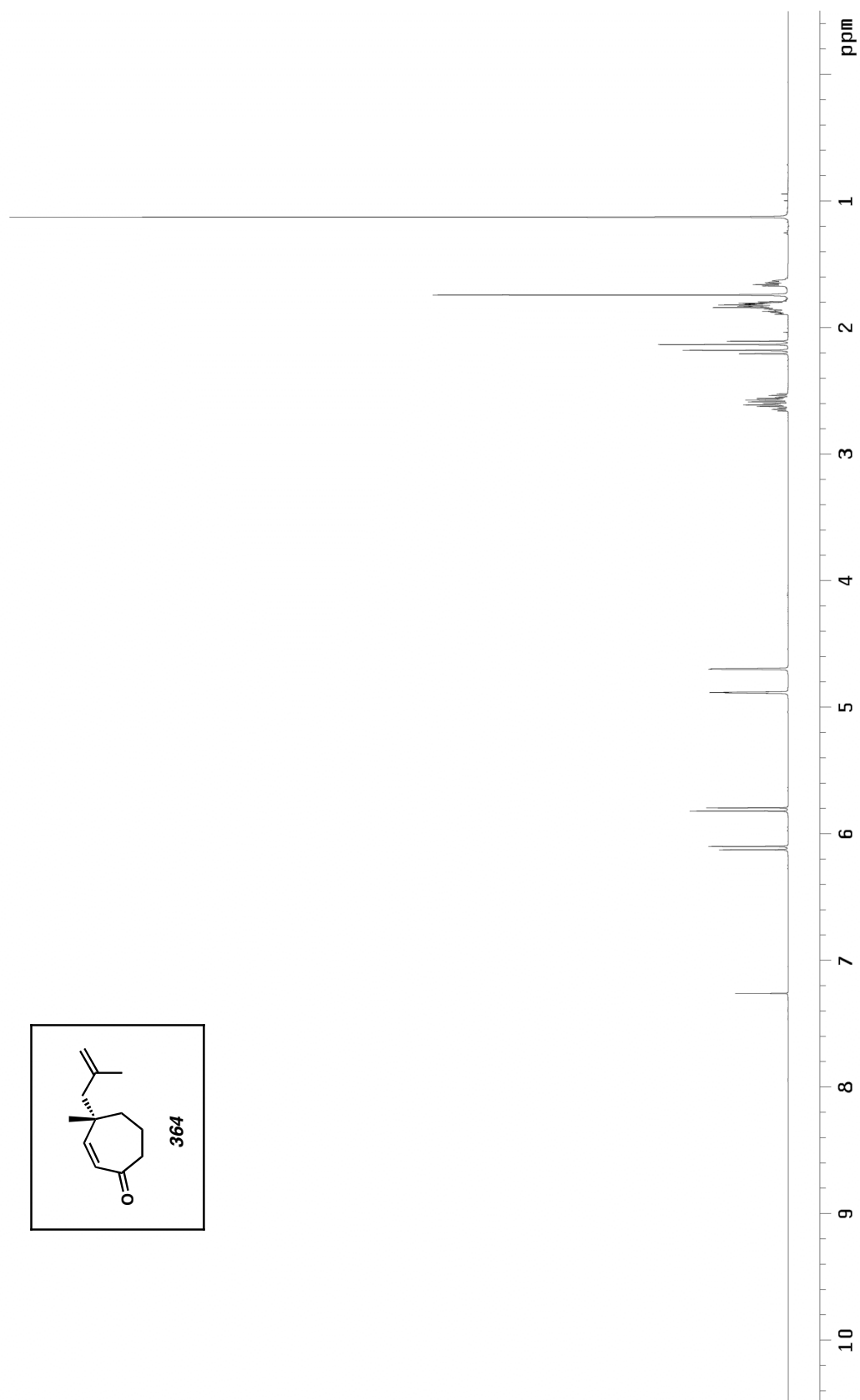


Figure A5.10. ¹H NMR (500 MHz, CDCl₃) of compound 364.

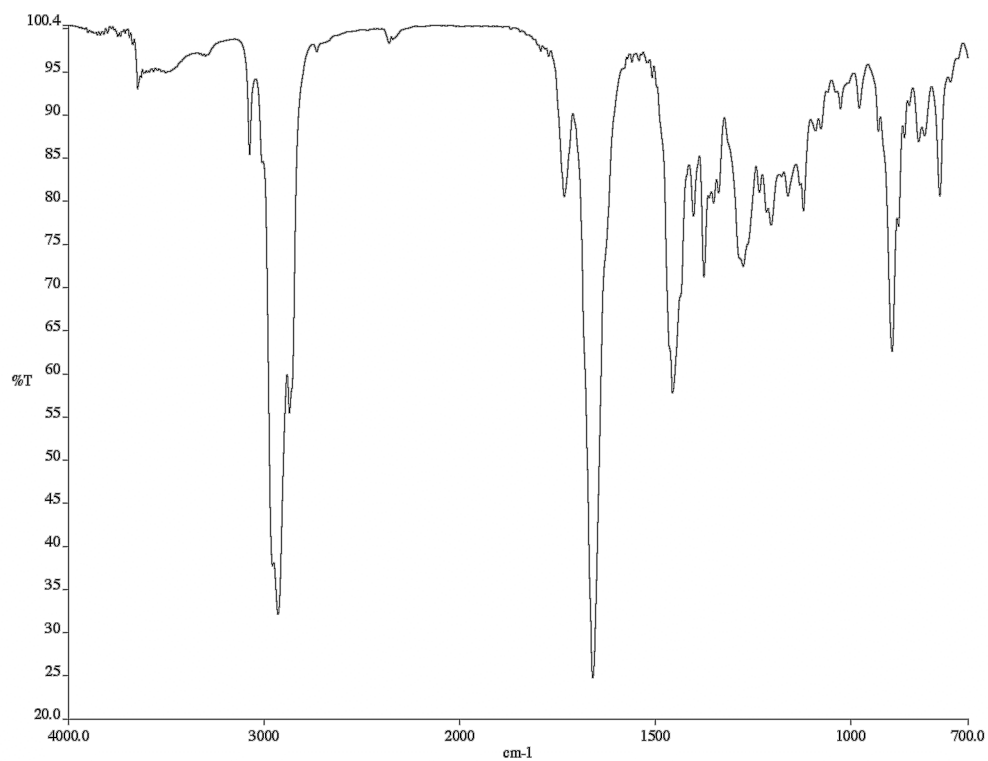


Figure A5.11. Infrared spectrum (thin film/NaCl) of compound **364**.

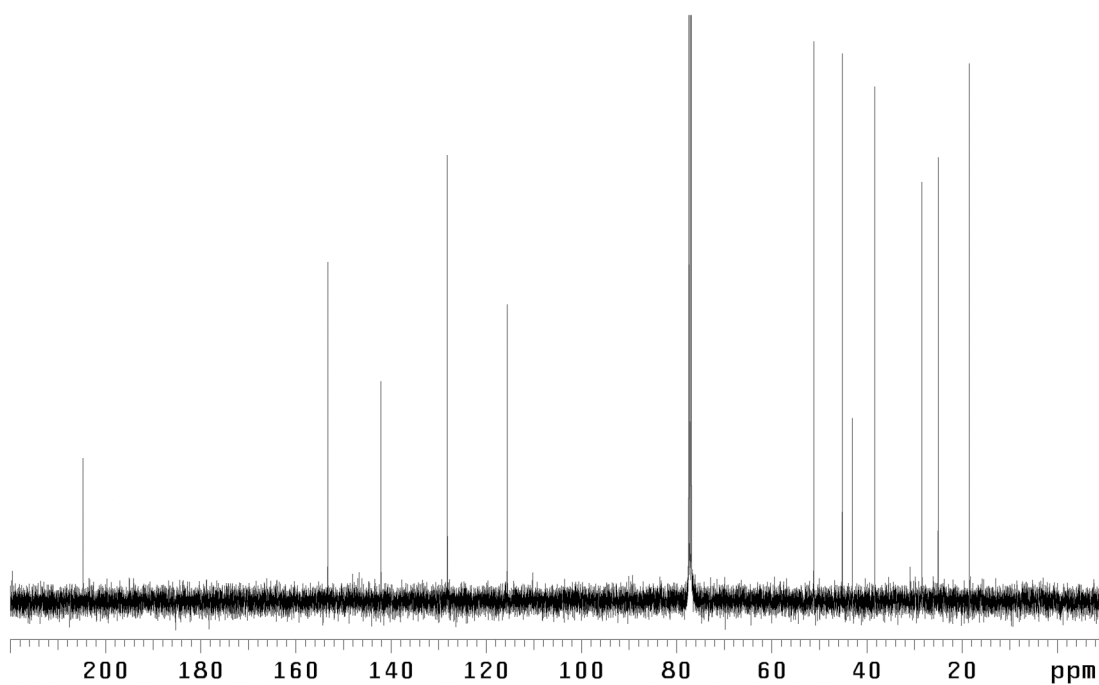
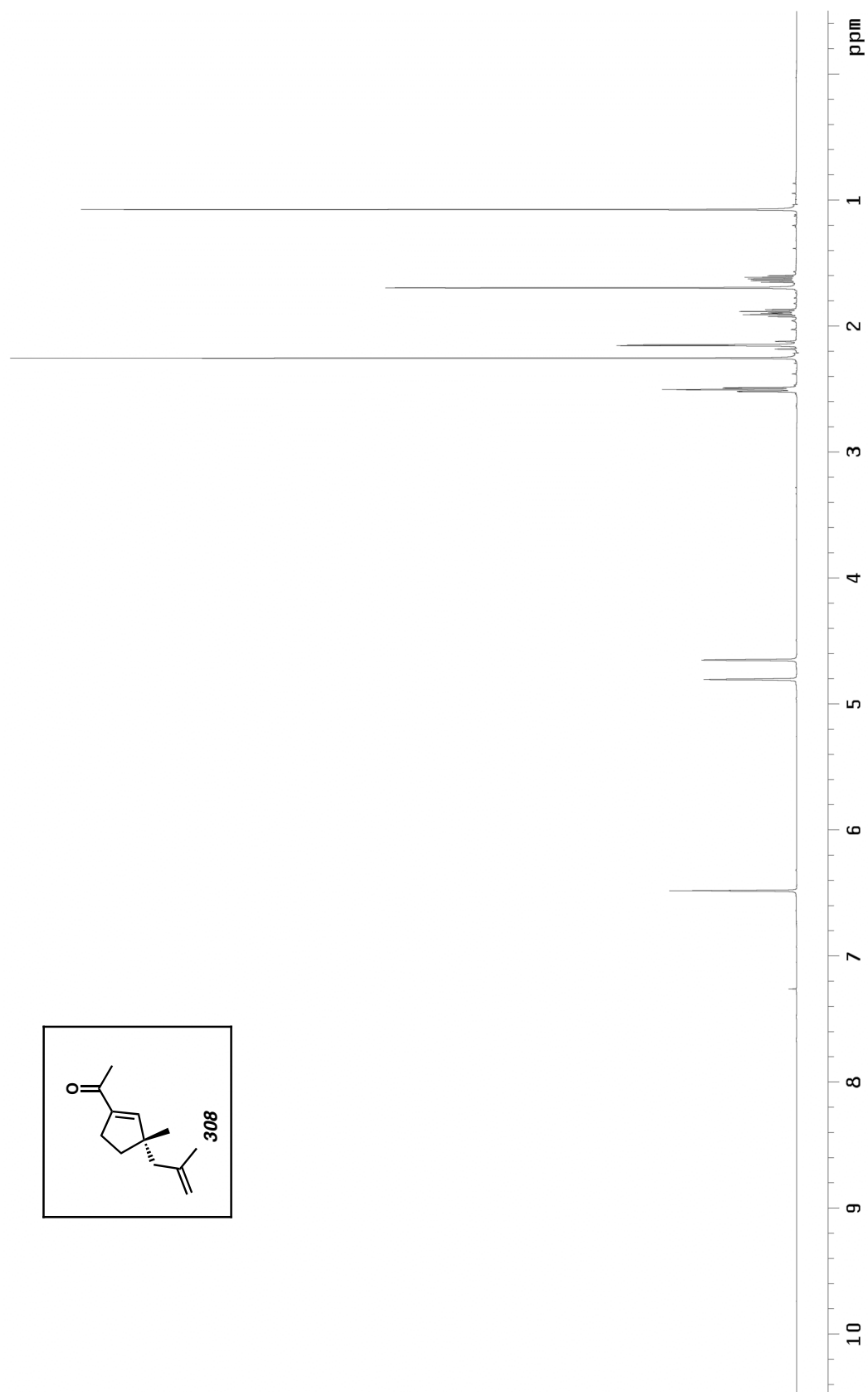


Figure A5.12. ¹³C NMR (125 MHz, CDCl₃) of compound **364**.



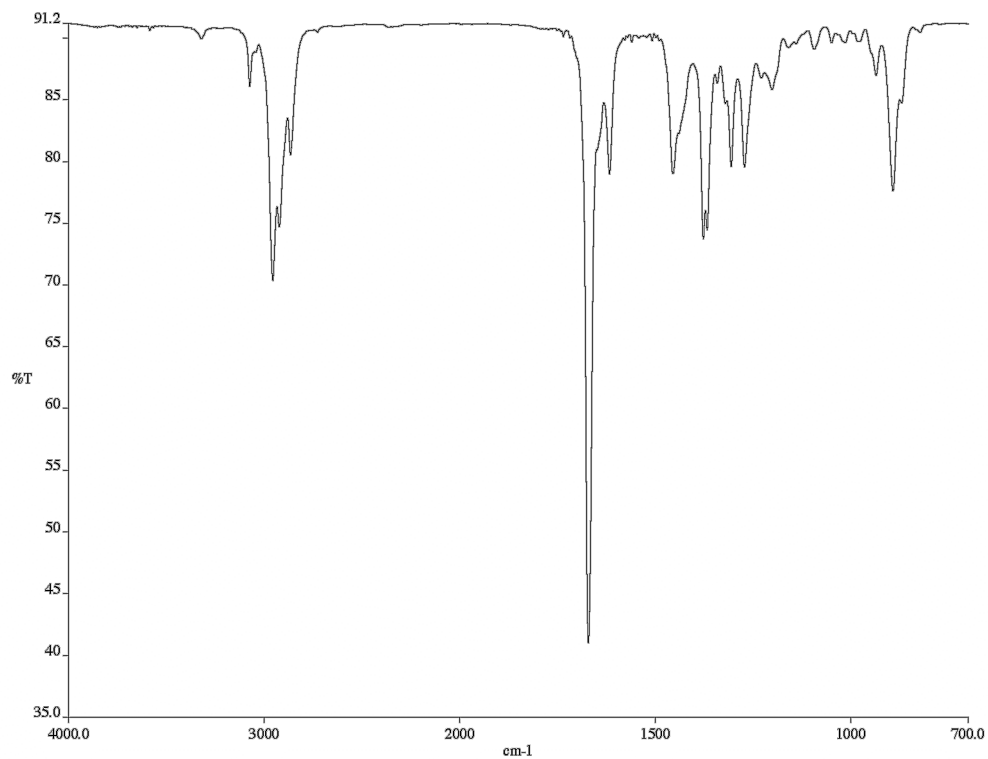


Figure A5.14. Infrared spectrum (thin film/NaCl) of compound **308**.

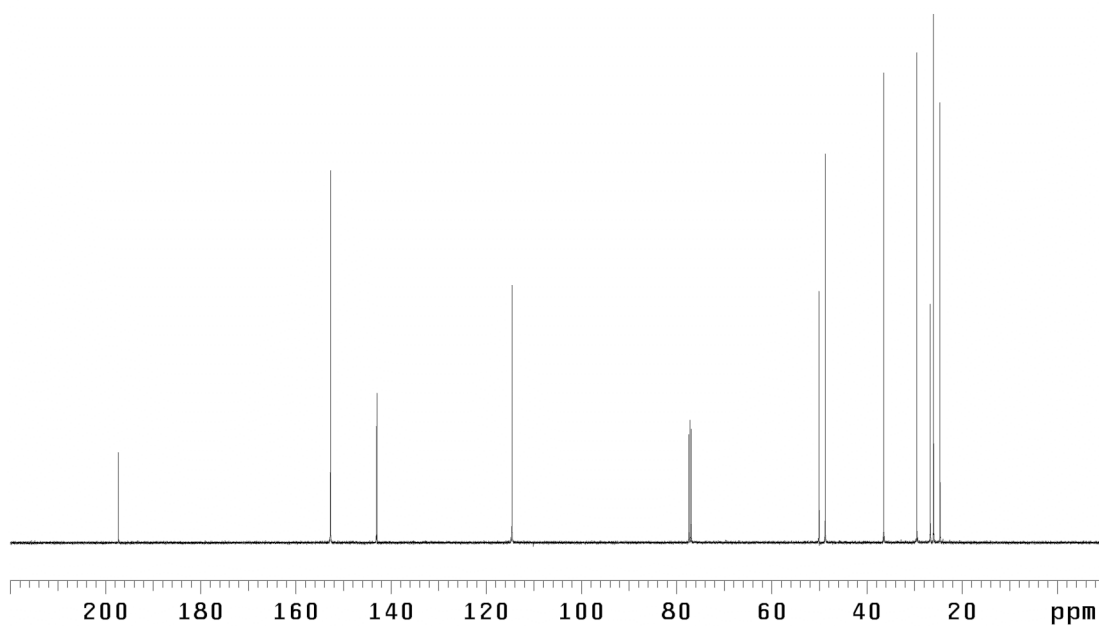
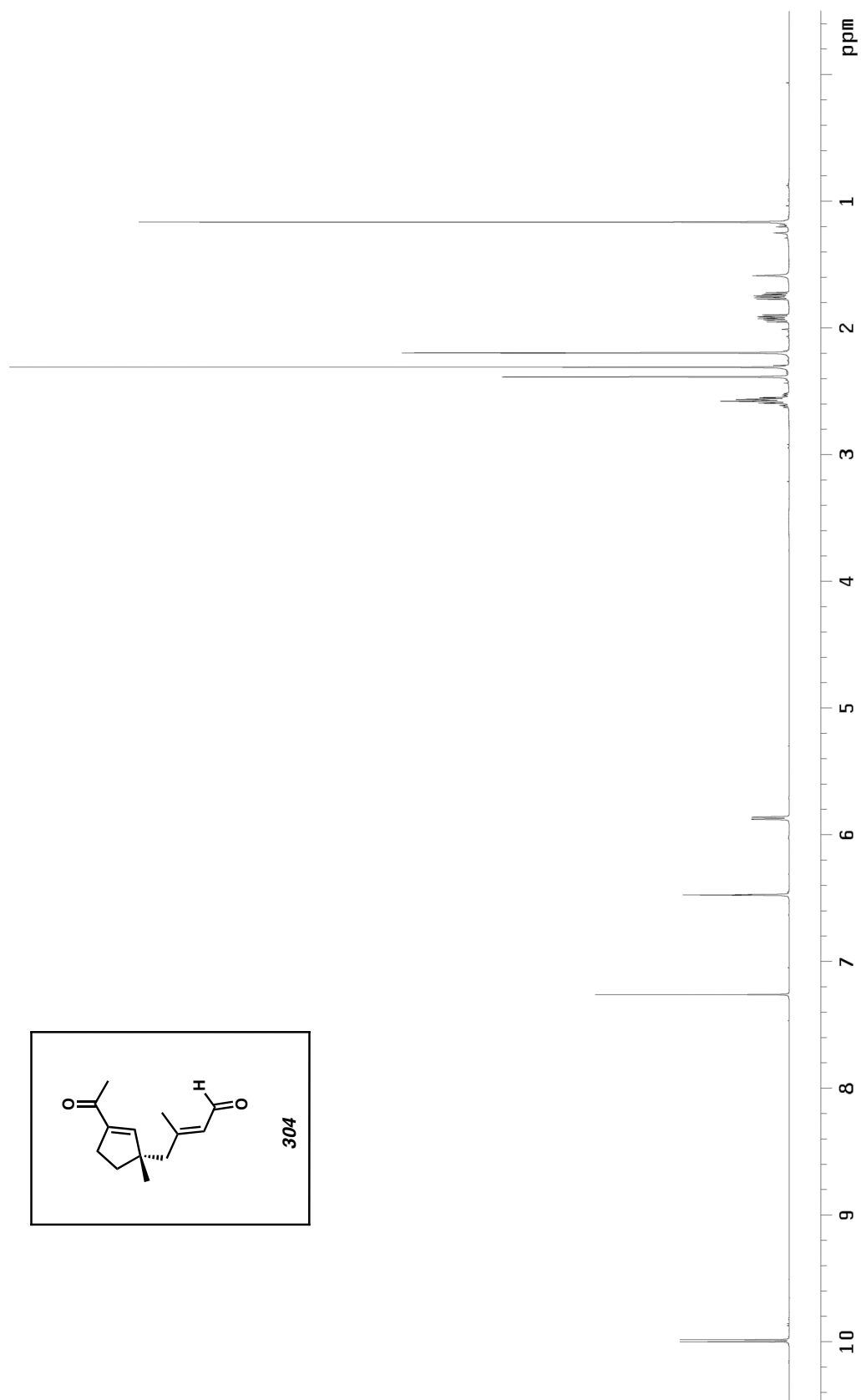


Figure A5.15. ¹³C NMR (125 MHz, CDCl₃) of compound **308**.

Figure A5.16. ^1H NMR (500 MHz, CDCl_3) of compound 304.

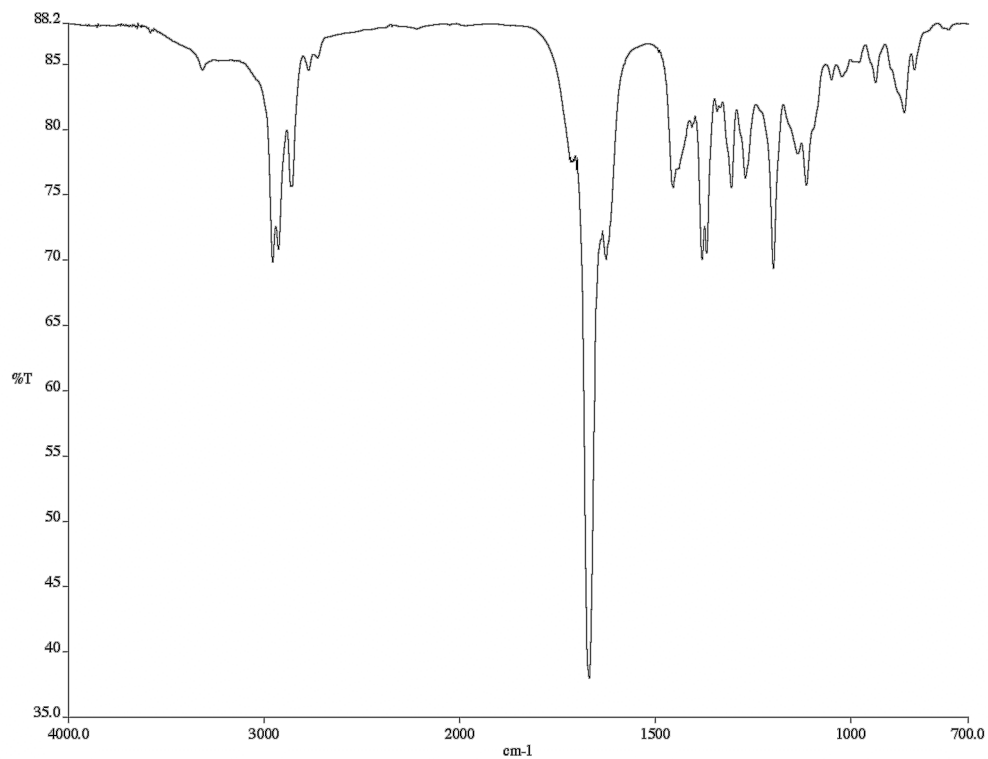


Figure A5.17. Infrared spectrum (thin film/NaCl) of compound **304**.

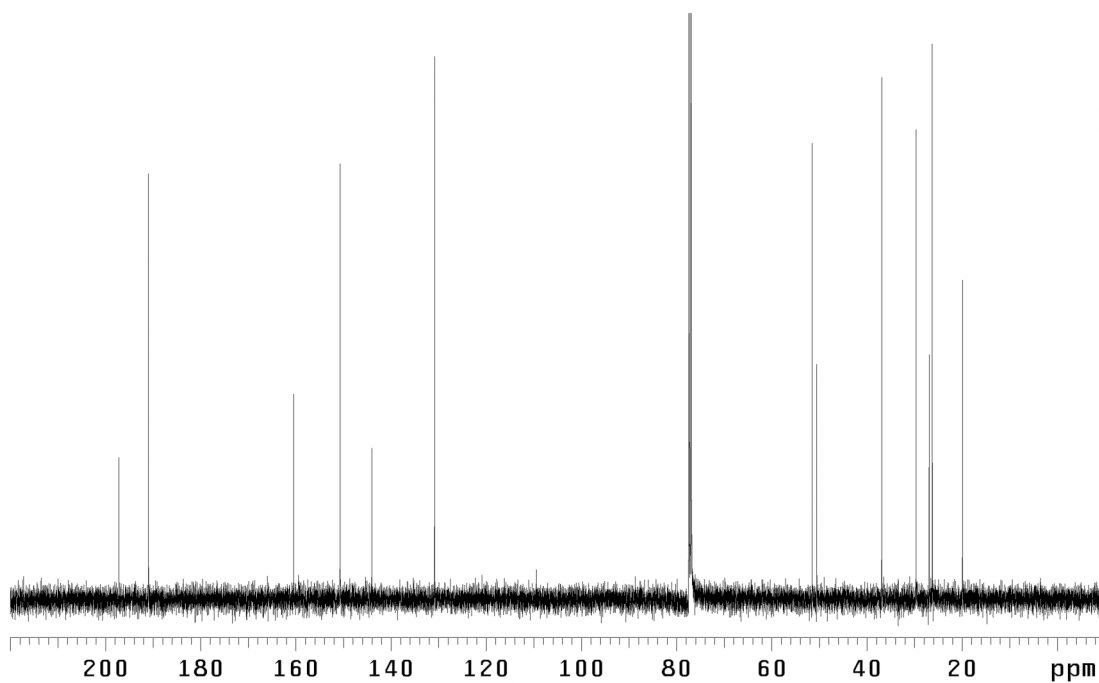


Figure A5.18. ¹³C NMR (125 MHz, CDCl₃) of compound **304**.

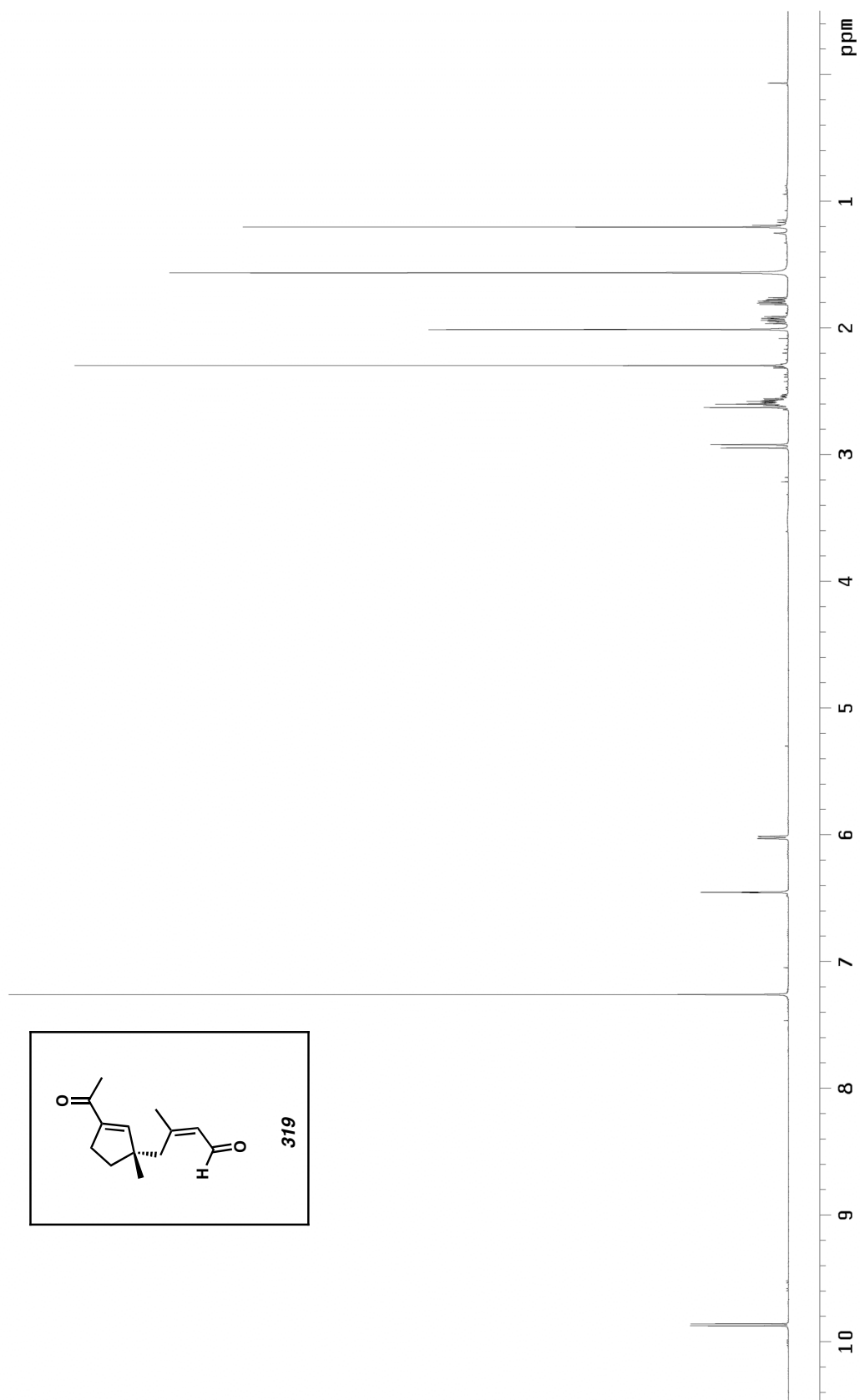


Figure A5.19. ^1H NMR (500 MHz, CDCl_3) of compound **319**.

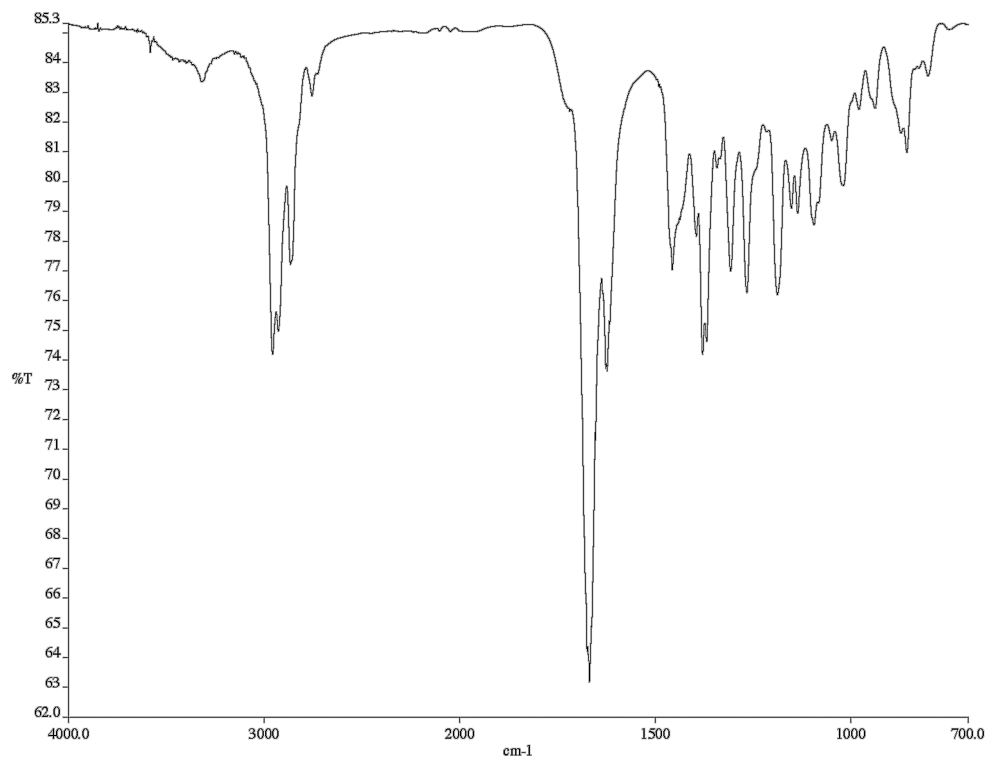


Figure A5.20. Infrared spectrum (thin film/NaCl) of compound **319**.

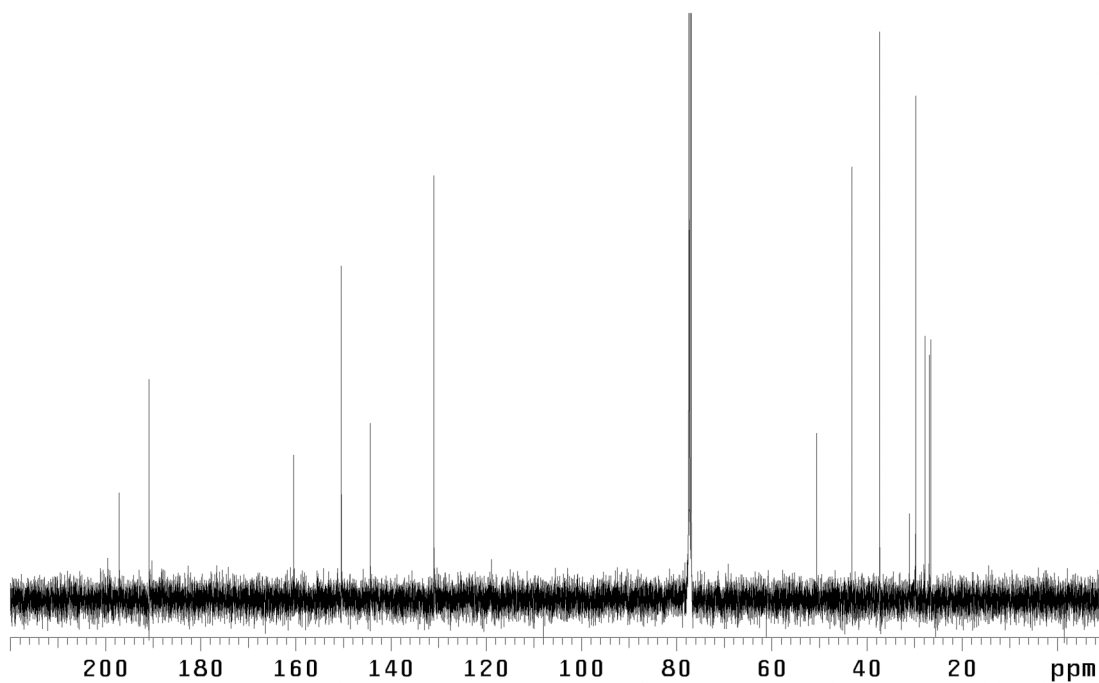
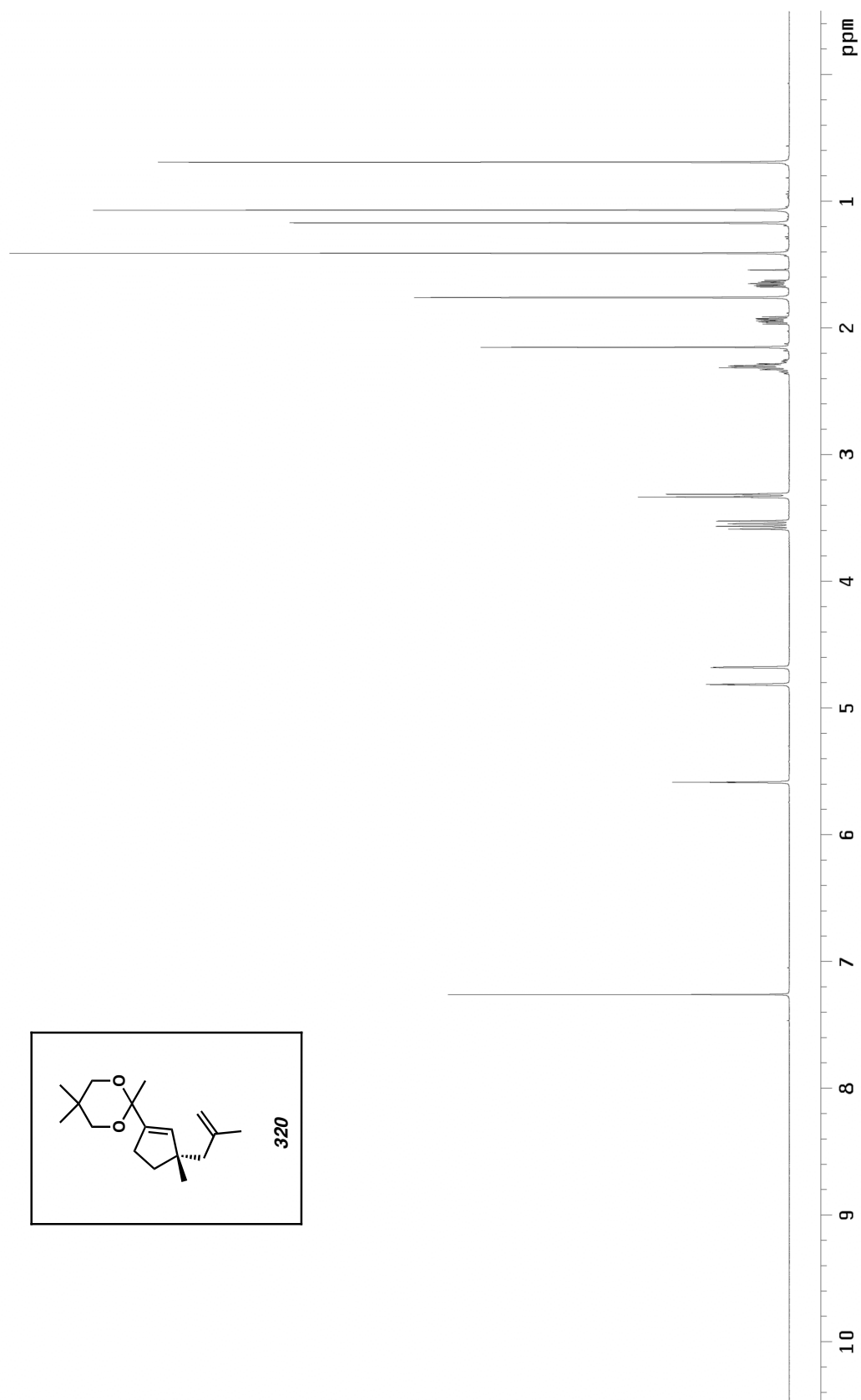


Figure A5.21. ¹³C NMR (125 MHz, CDCl₃) of compound **319**.

Figure A5.22. ¹H NMR (500 MHz, CDCl₃) of compound 320.

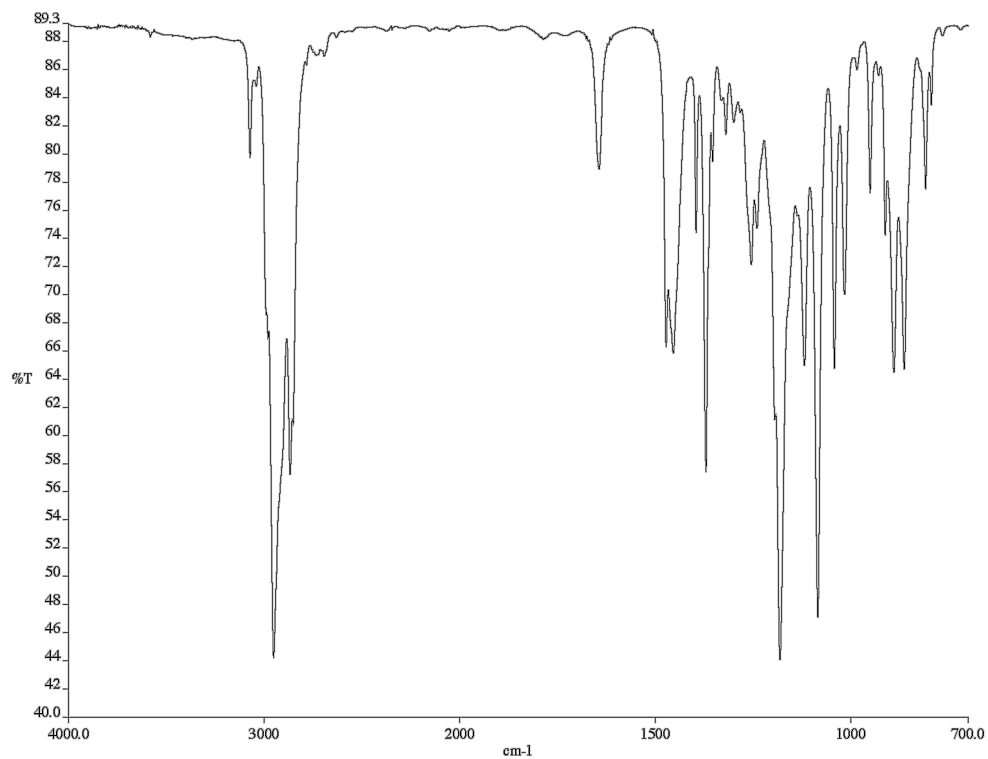


Figure A5.23. Infrared spectrum (thin film/NaCl) of compound **320**.

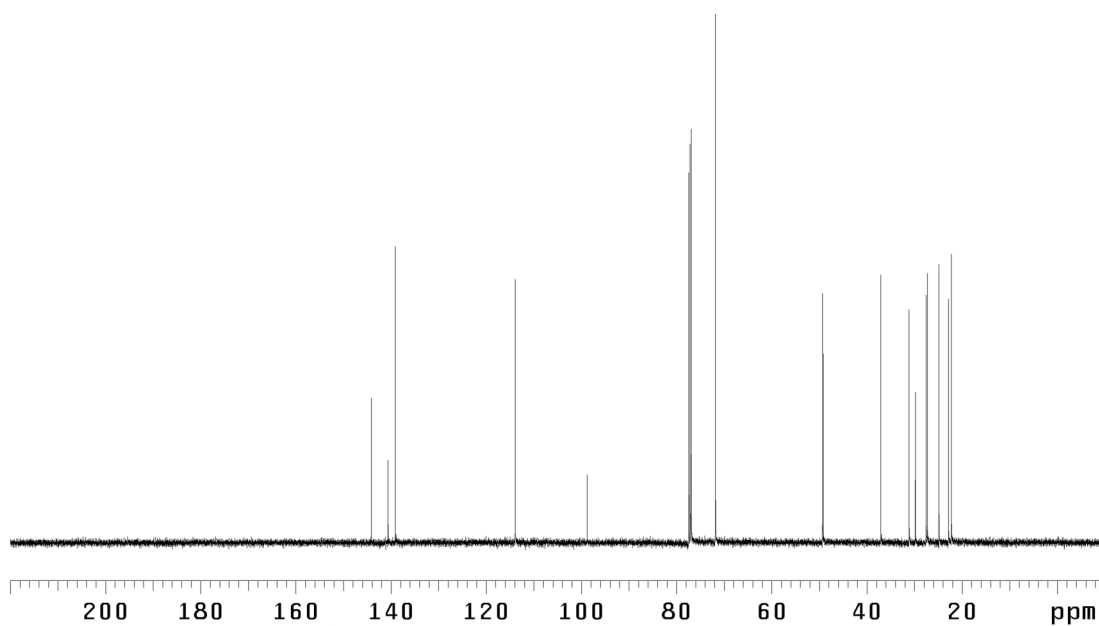


Figure A5.24. ¹³C NMR (125 MHz, CDCl₃) of compound **320**.

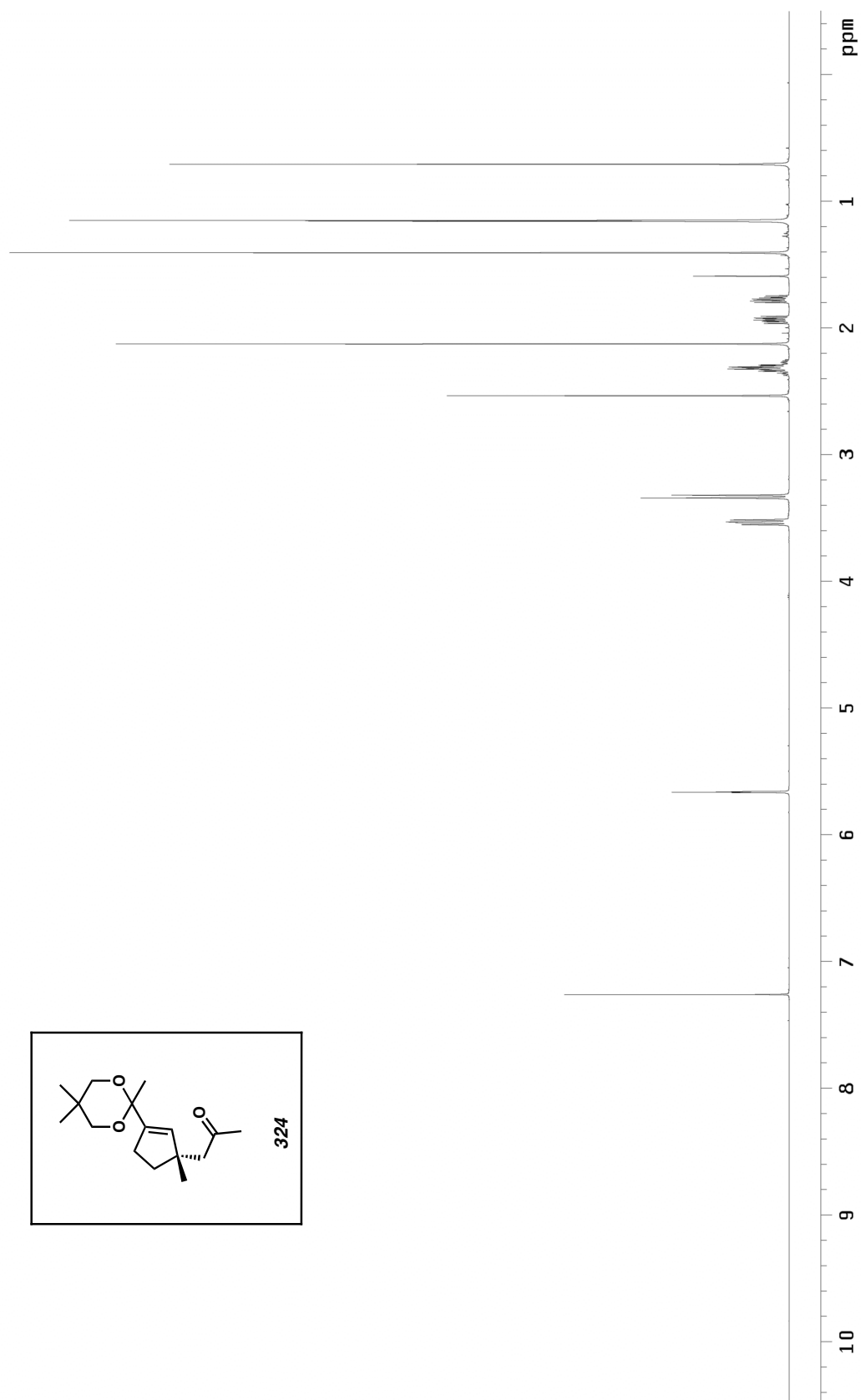


Figure A5.25. ^1H NMR (500 MHz, CDCl_3) of compound 324.

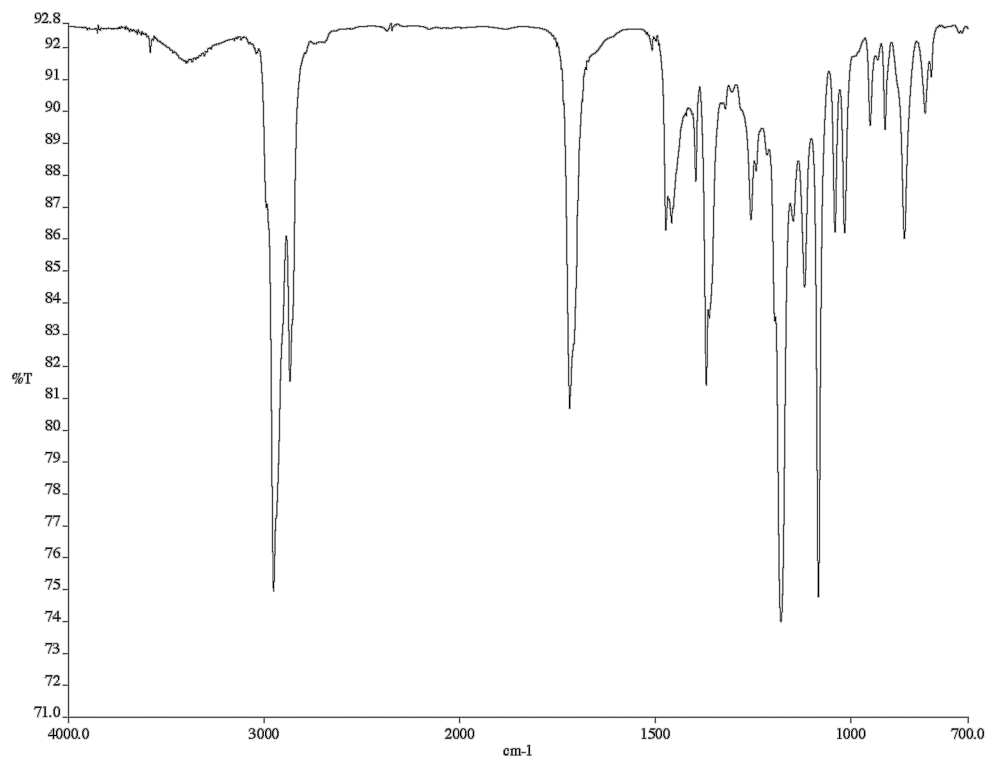


Figure A5.26. Infrared spectrum (thin film/NaCl) of compound **324**.

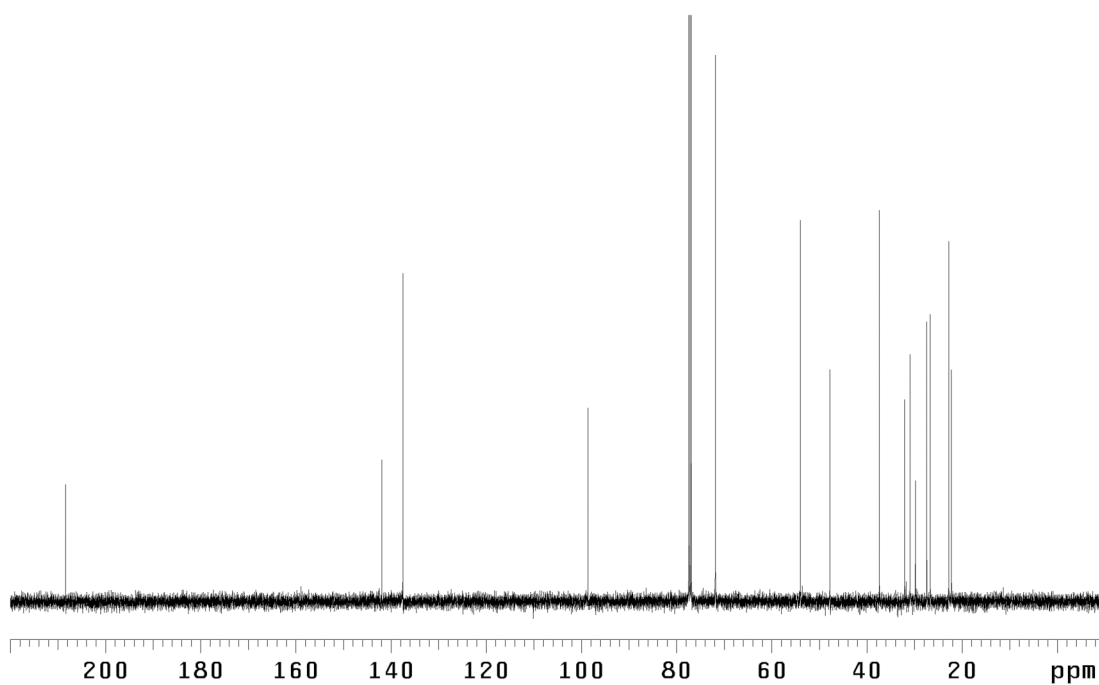
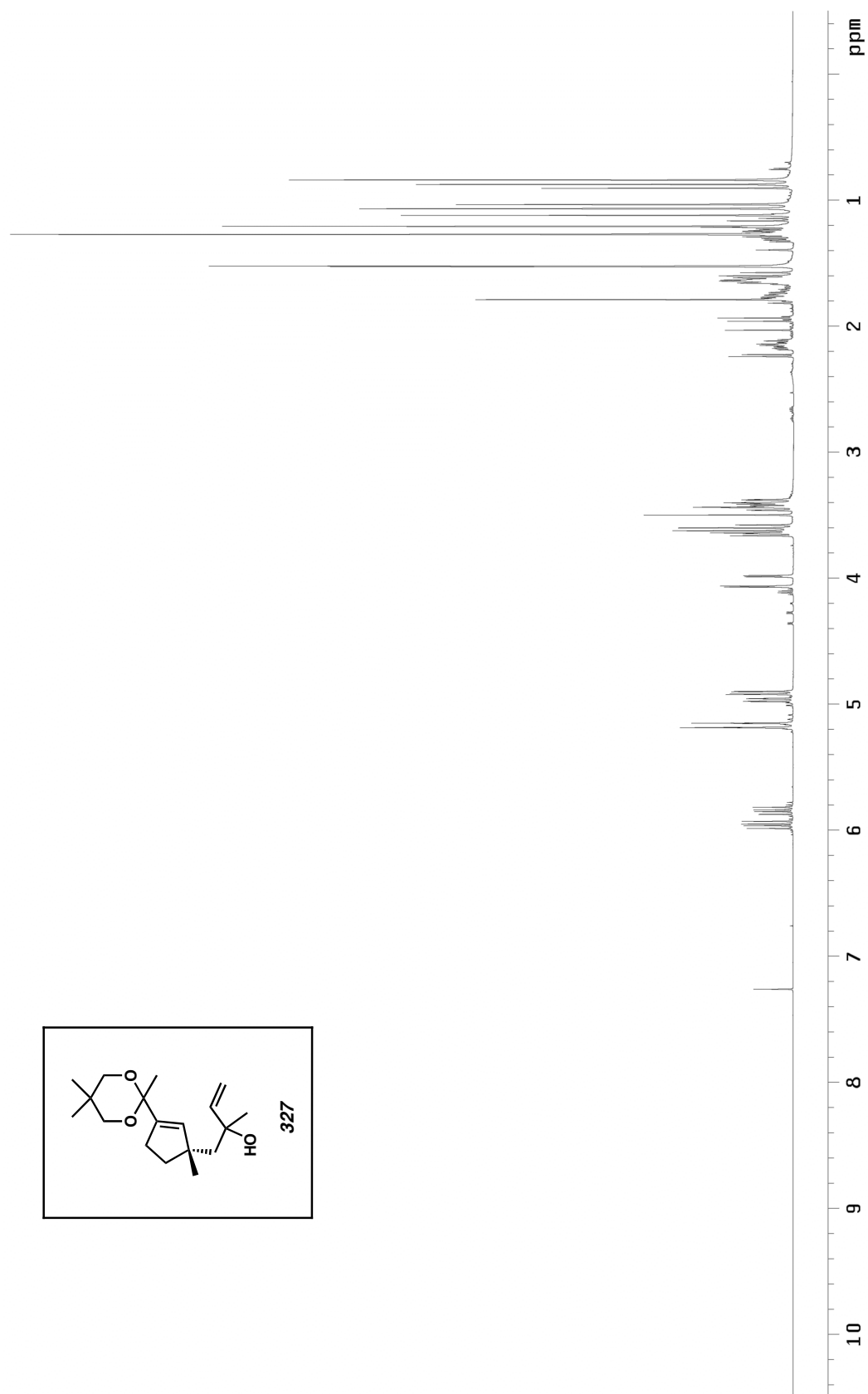


Figure A5.27. ¹³C NMR (125 MHz, CDCl₃) of compound **324**.

Figure A5.28. ^1H NMR (500 MHz, CDCl_3) of compound 327.

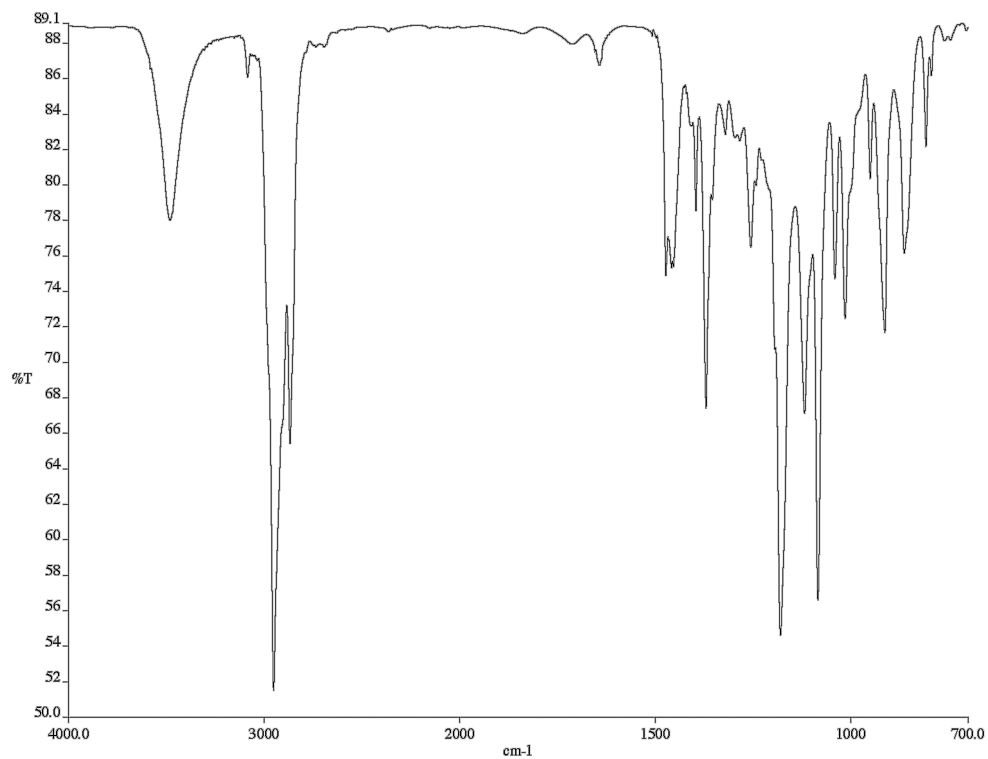


Figure A5.29. Infrared spectrum (thin film/NaCl) of compound **327**.

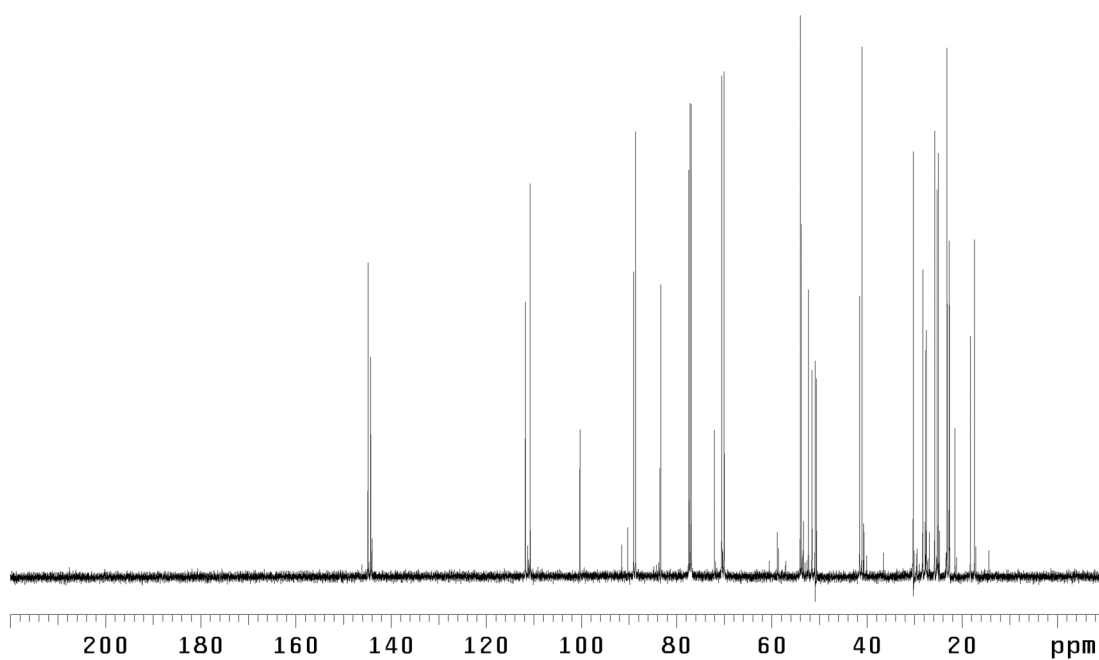
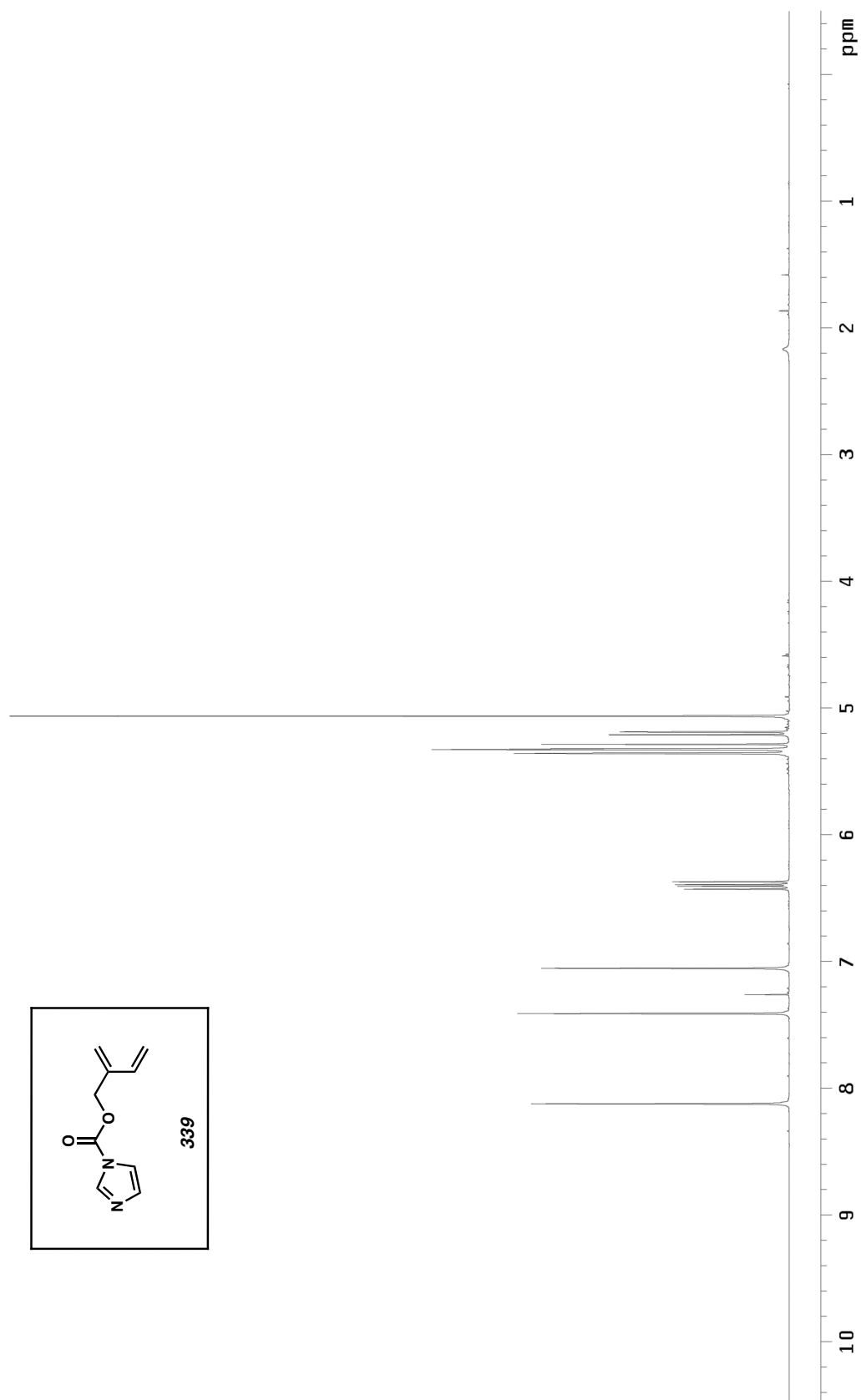


Figure A5.30. ¹³C NMR (125 MHz, CDCl₃) of compound **327**.



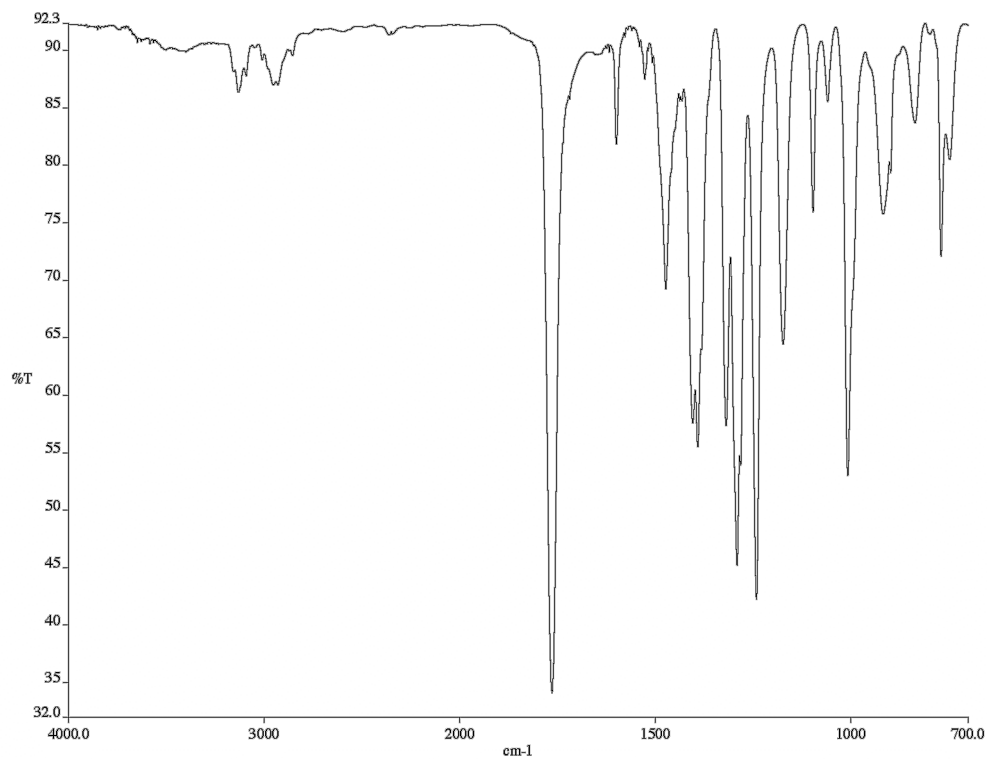


Figure A5.32. Infrared spectrum (thin film/NaCl) of compound **339**.

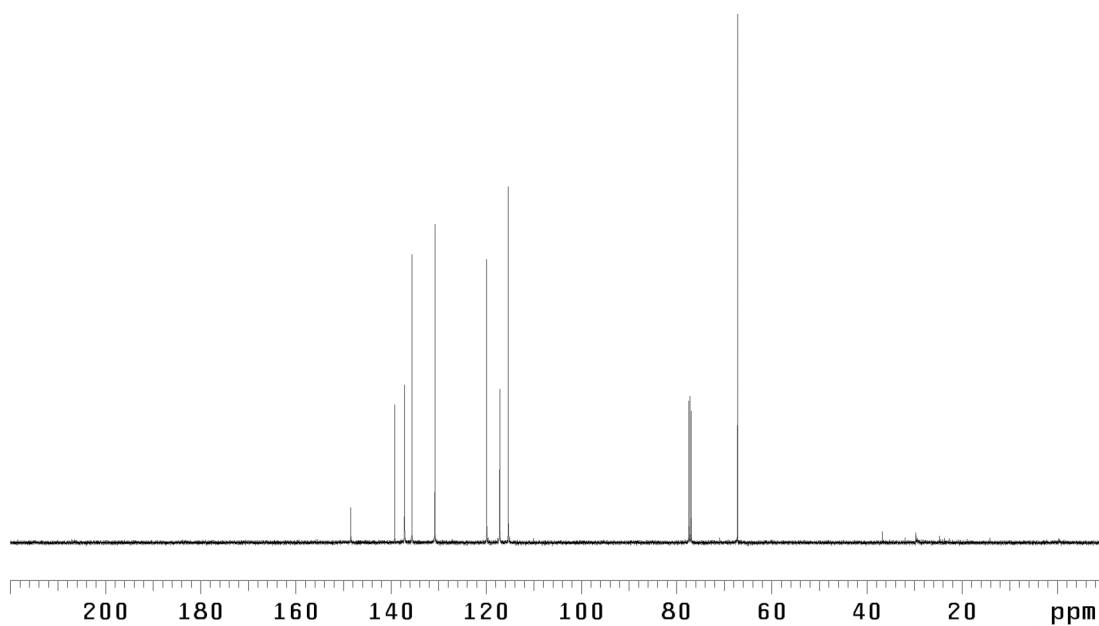
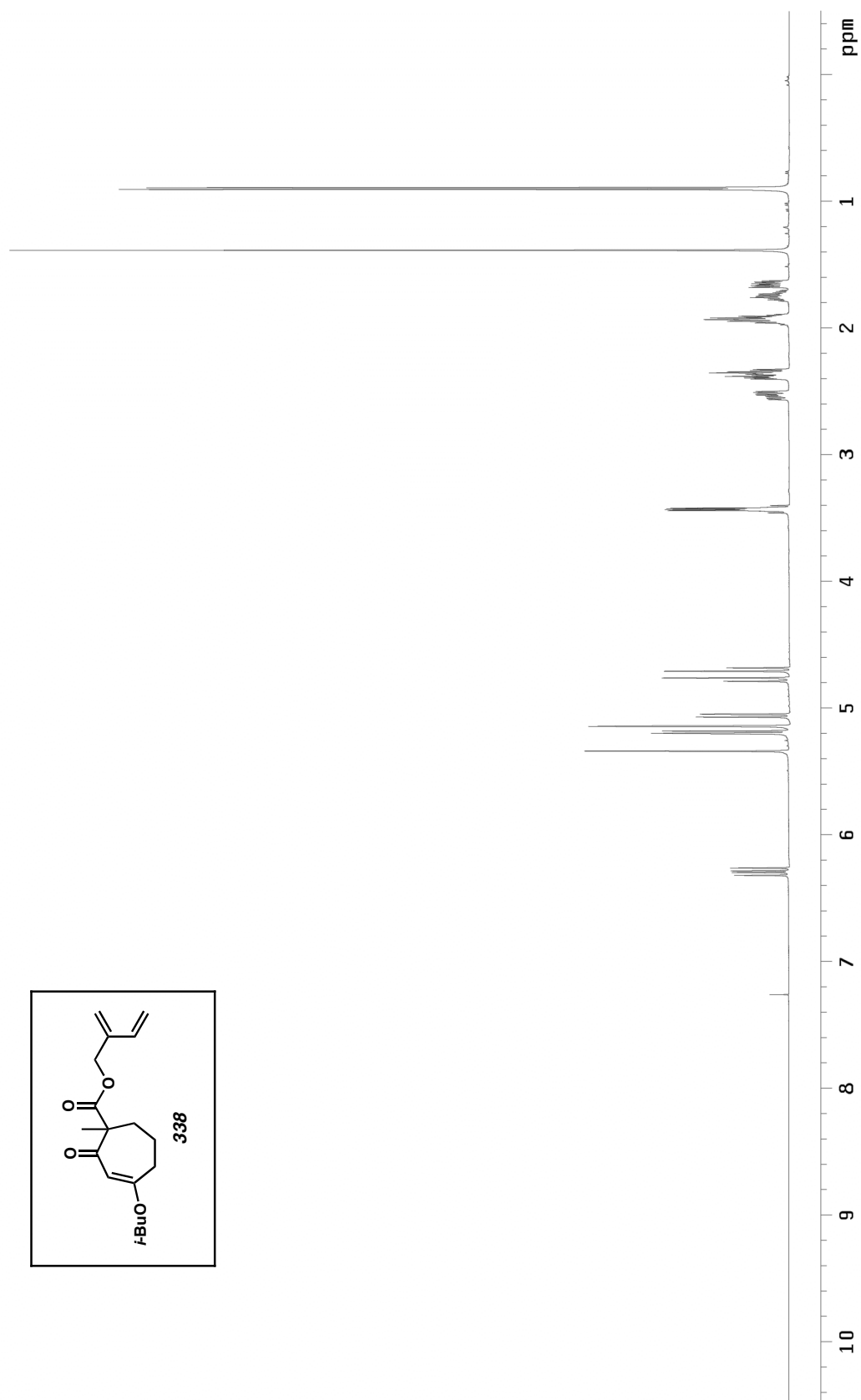


Figure A5.33. ¹³C NMR (125 MHz, CDCl₃) of compound **339**.

Figure A5.34. ^1H NMR (500 MHz, CDCl_3) of compound 338.

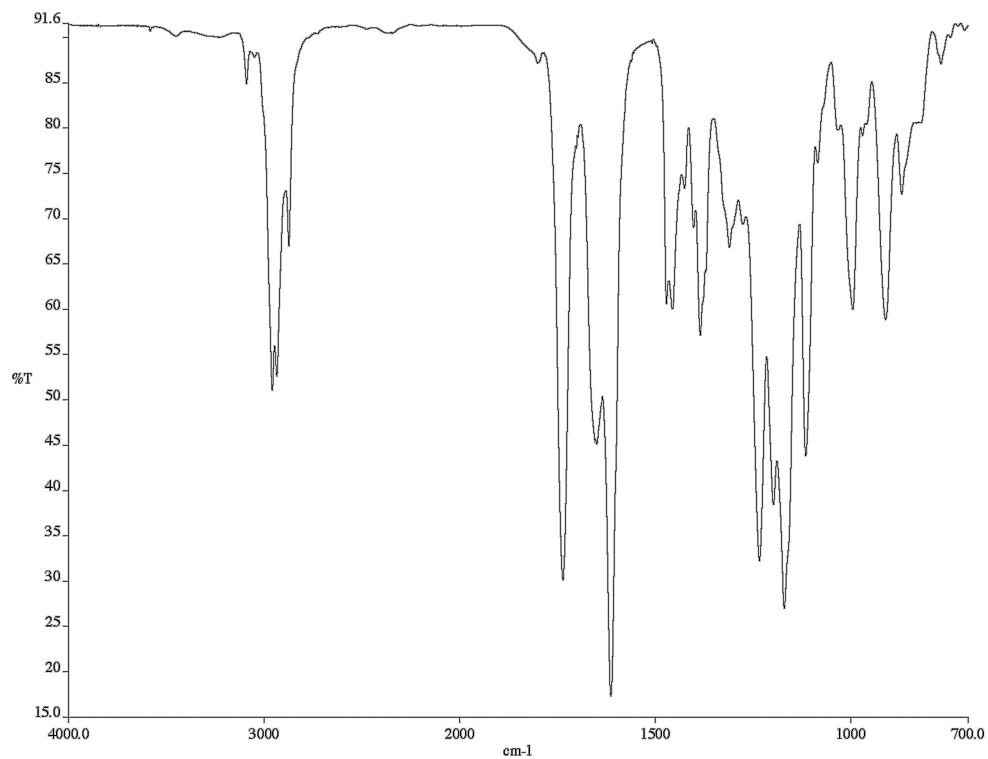


Figure A5.35. Infrared spectrum (thin film/NaCl) of compound **338**.

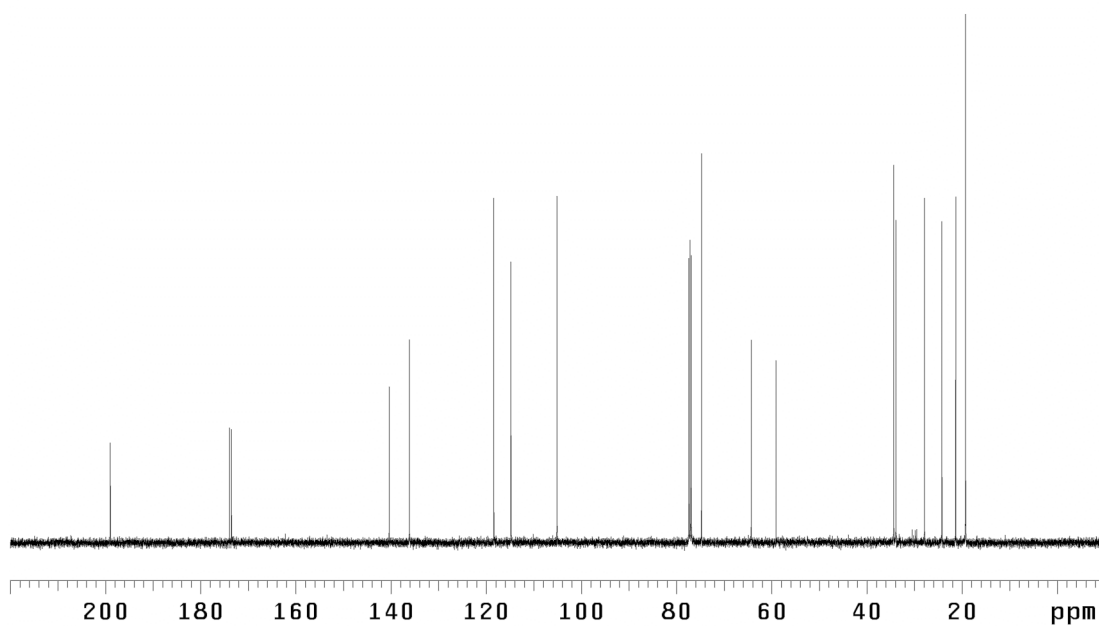
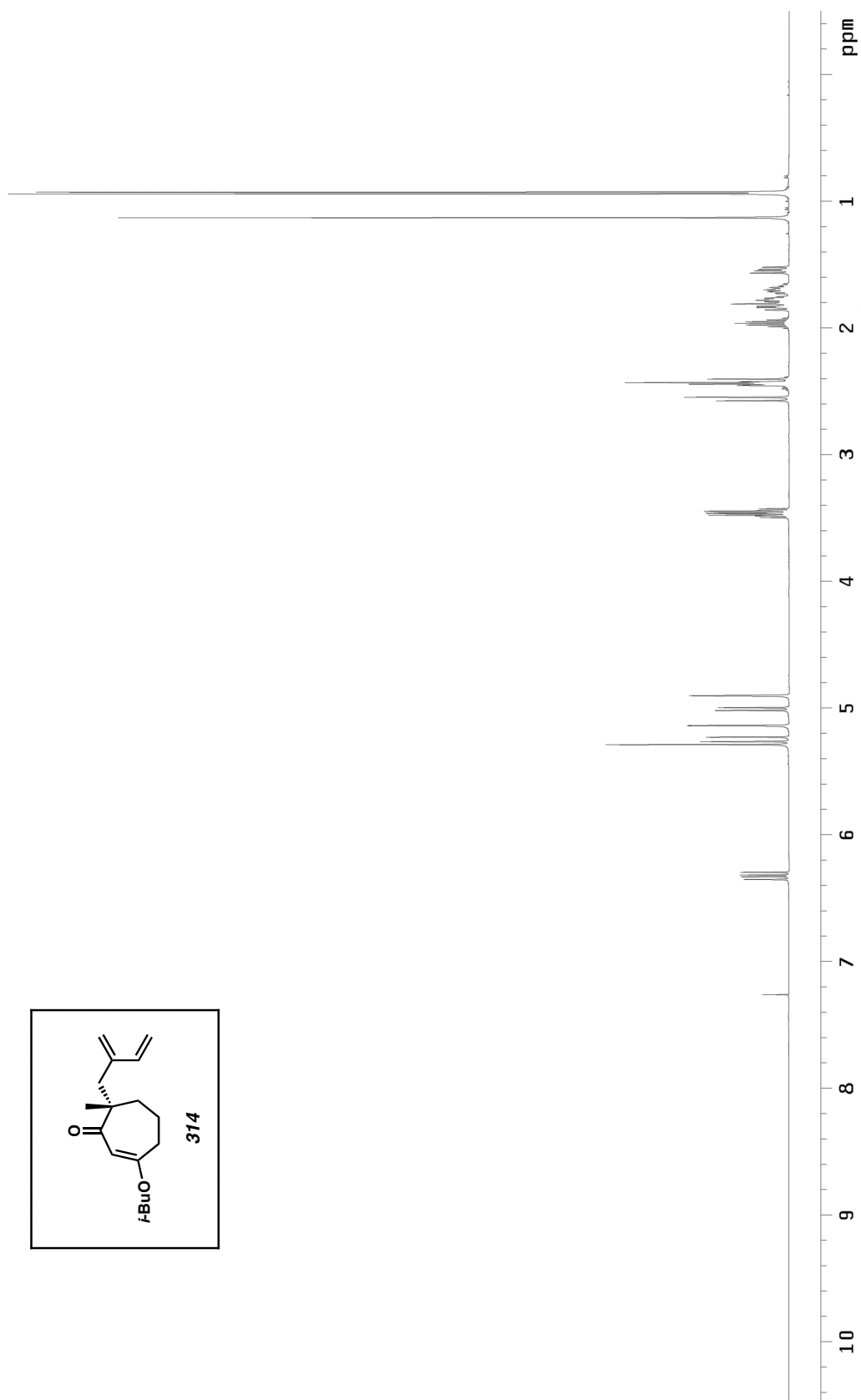


Figure A5.36. ¹³C NMR (125 MHz, CDCl₃) of compound **338**.



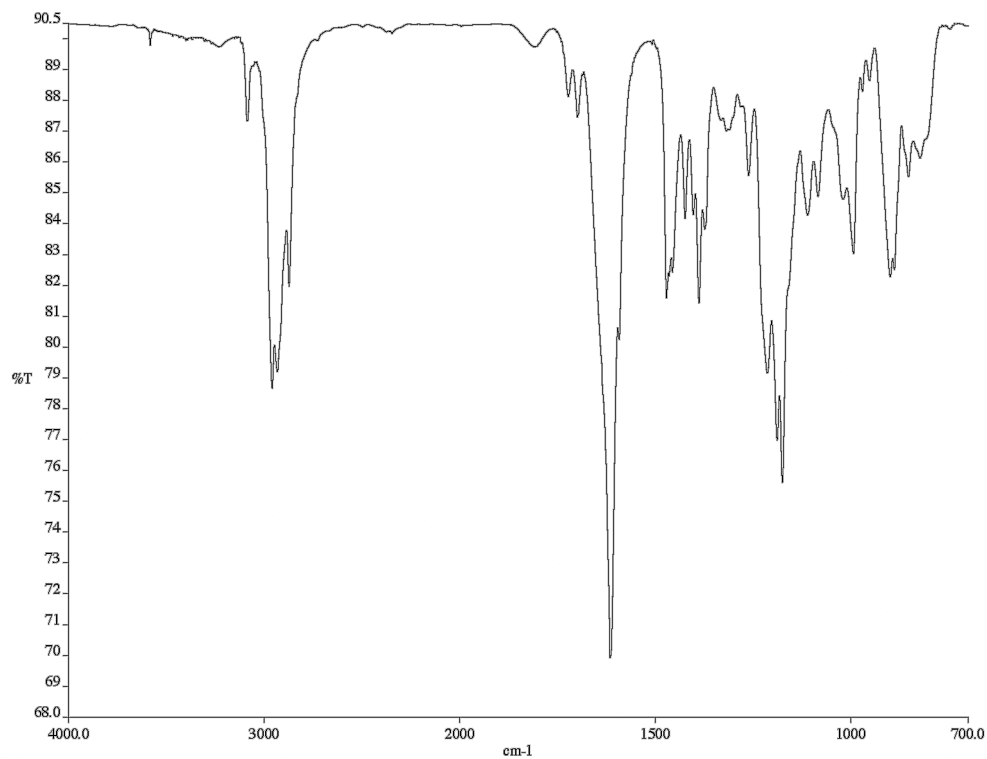


Figure A5.38. Infrared spectrum (thin film/NaCl) of compound **337**.

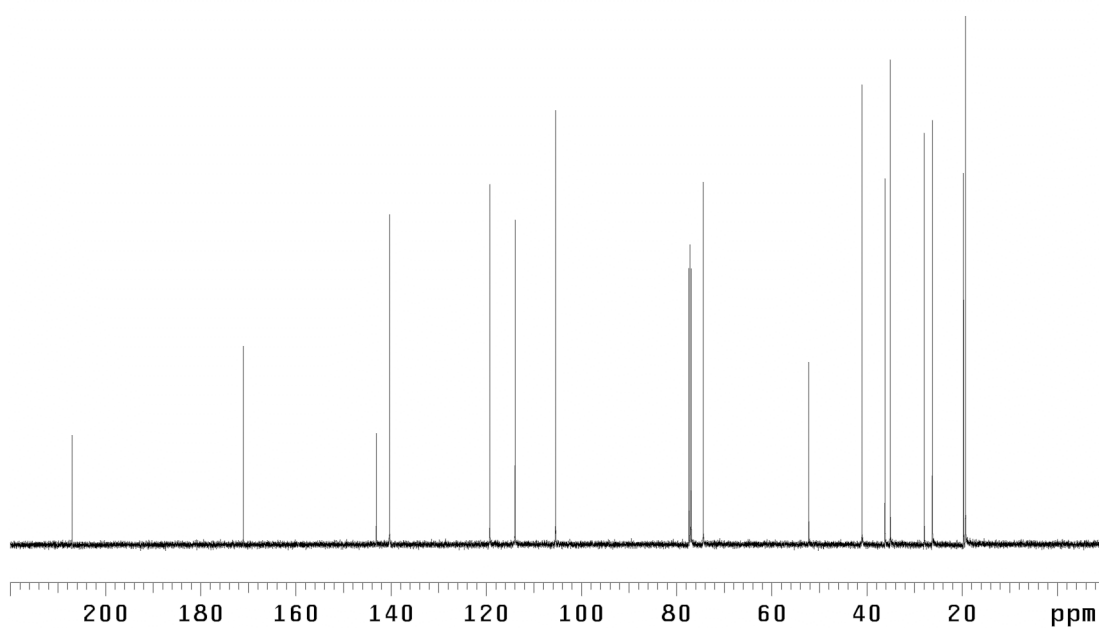


Figure A5.39. ¹³C NMR (125 MHz, CDCl₃) of compound **337**.

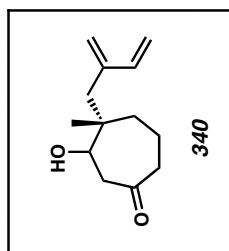
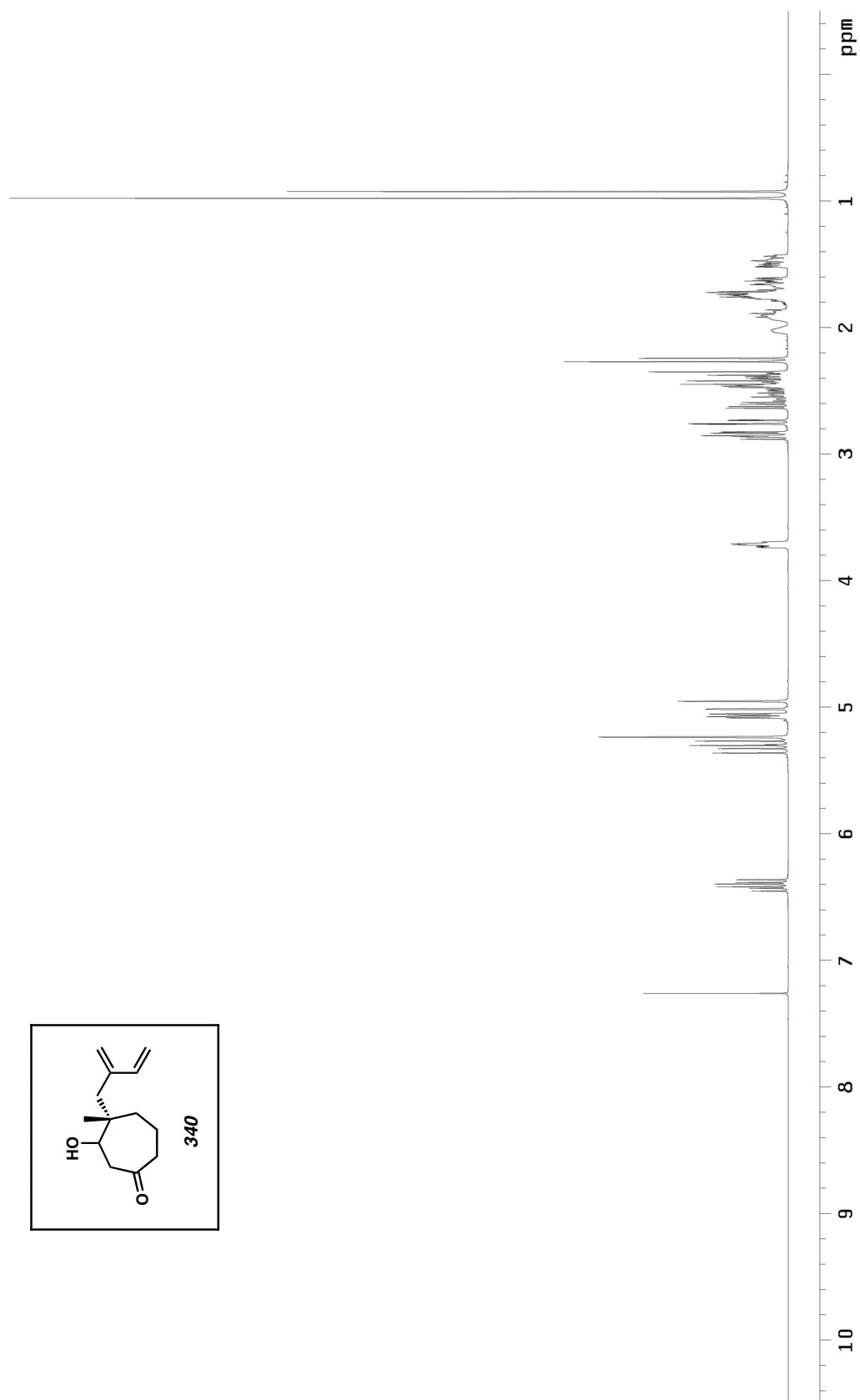


Figure A5.40. ^1H NMR (500 MHz, CDCl_3) of compound **340**.

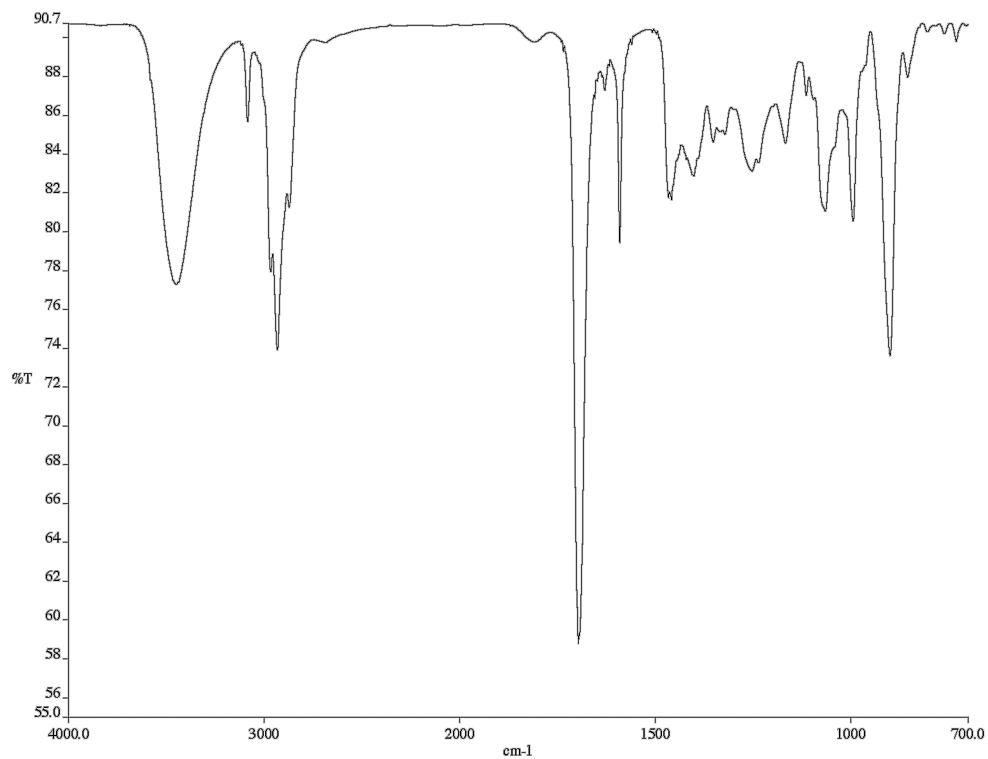


Figure A5.42. Infrared spectrum (thin film/NaCl) of compound **340**.

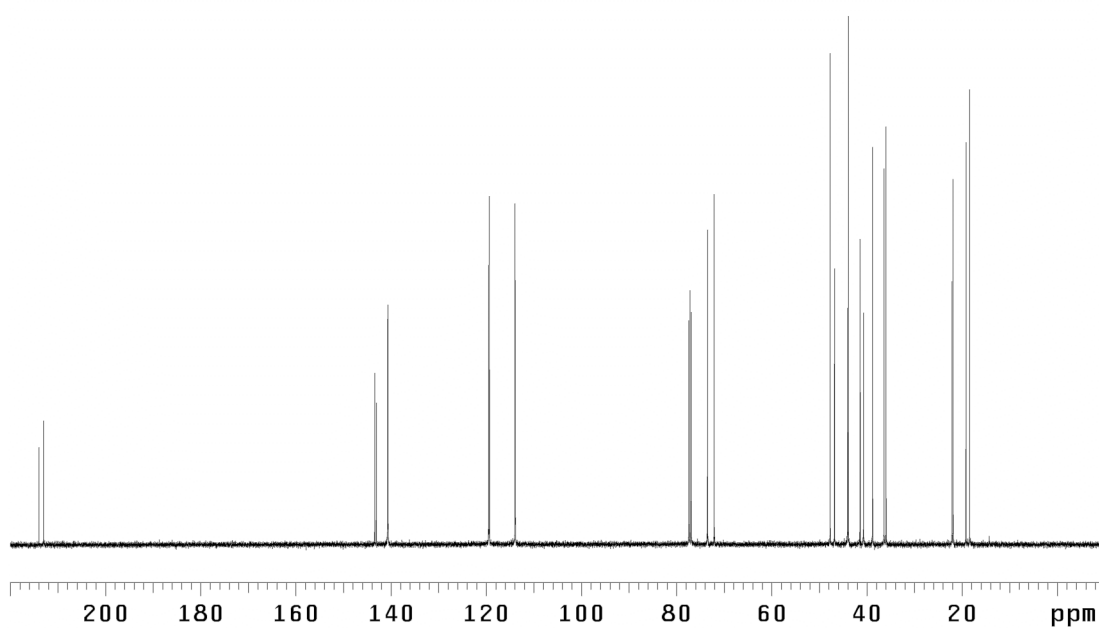


Figure A5.41. ¹³C NMR (125 MHz, CDCl₃) of compound **340**.

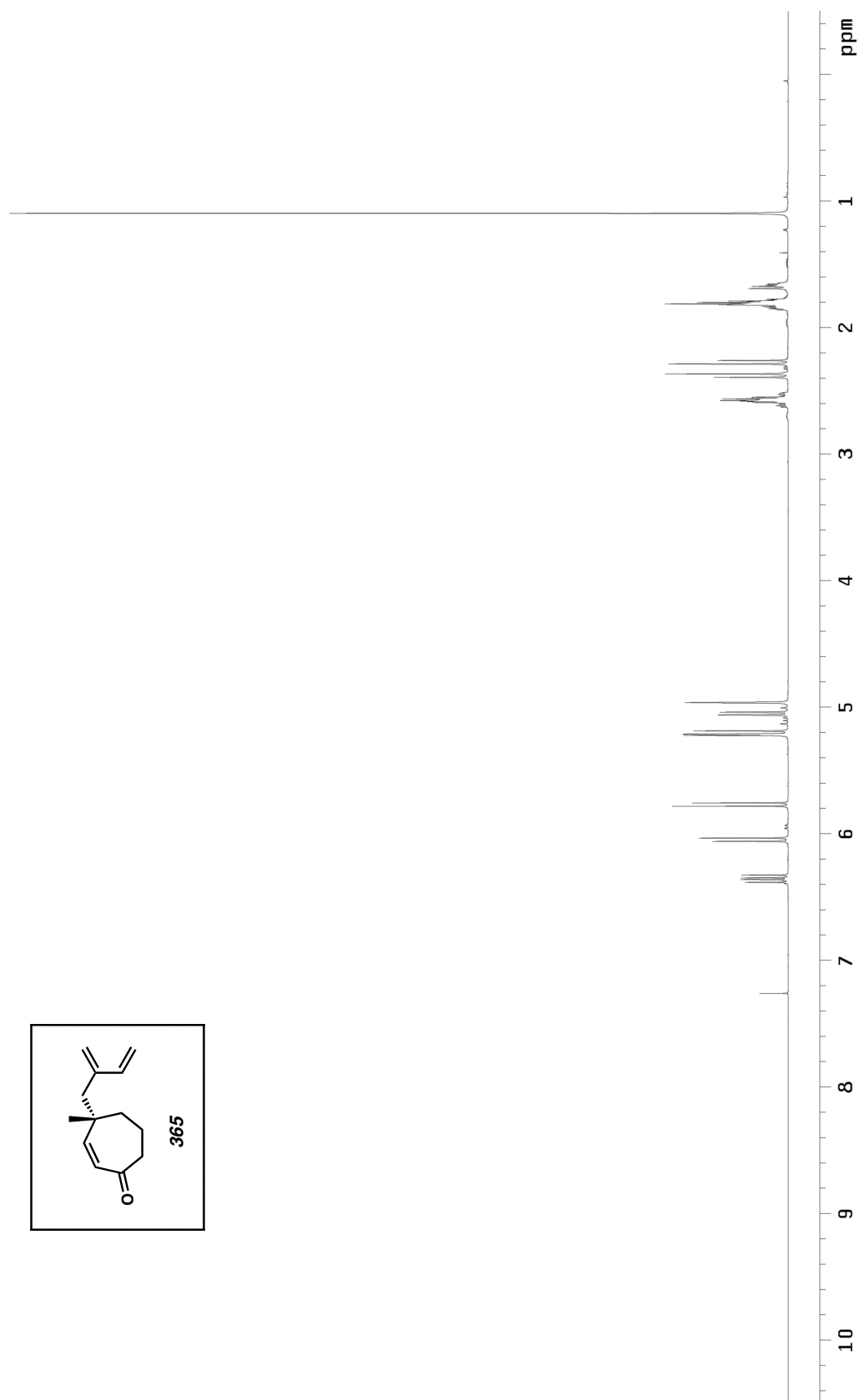


Figure A5.43. ¹H NMR (500 MHz, CDCl₃) of compound 365.

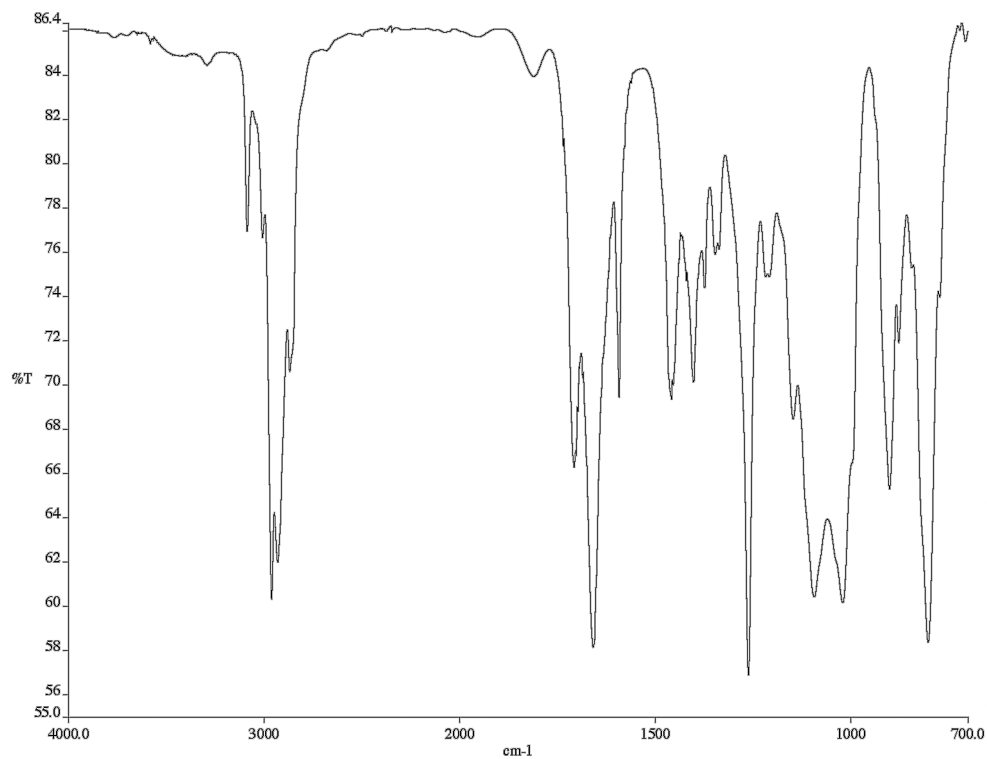


Figure A5.44. Infrared spectrum (thin film/NaCl) of compound **365**.

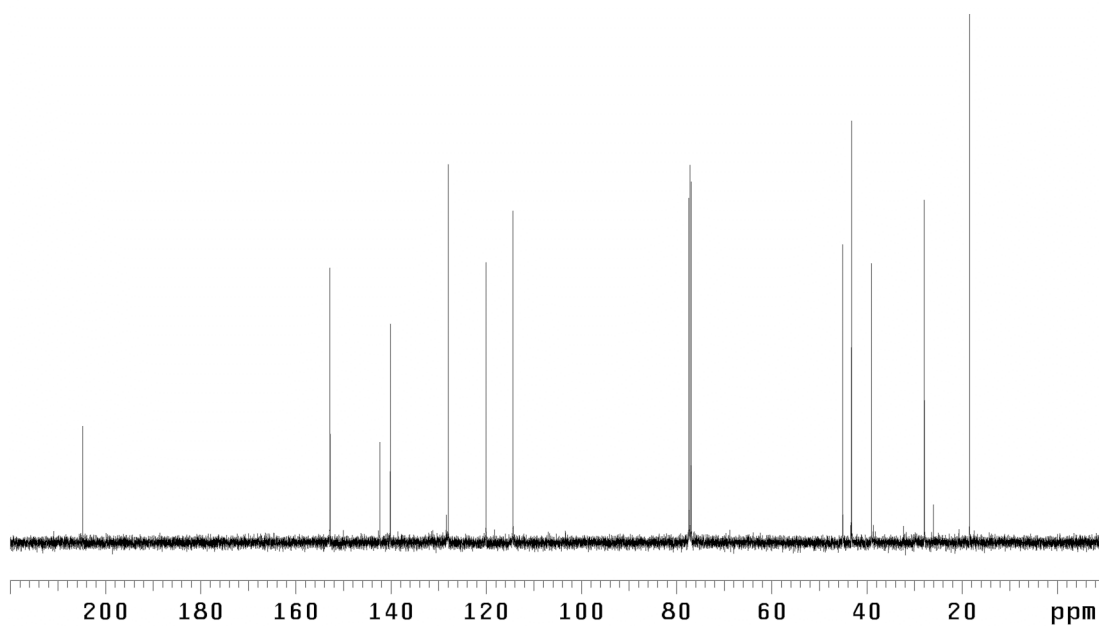
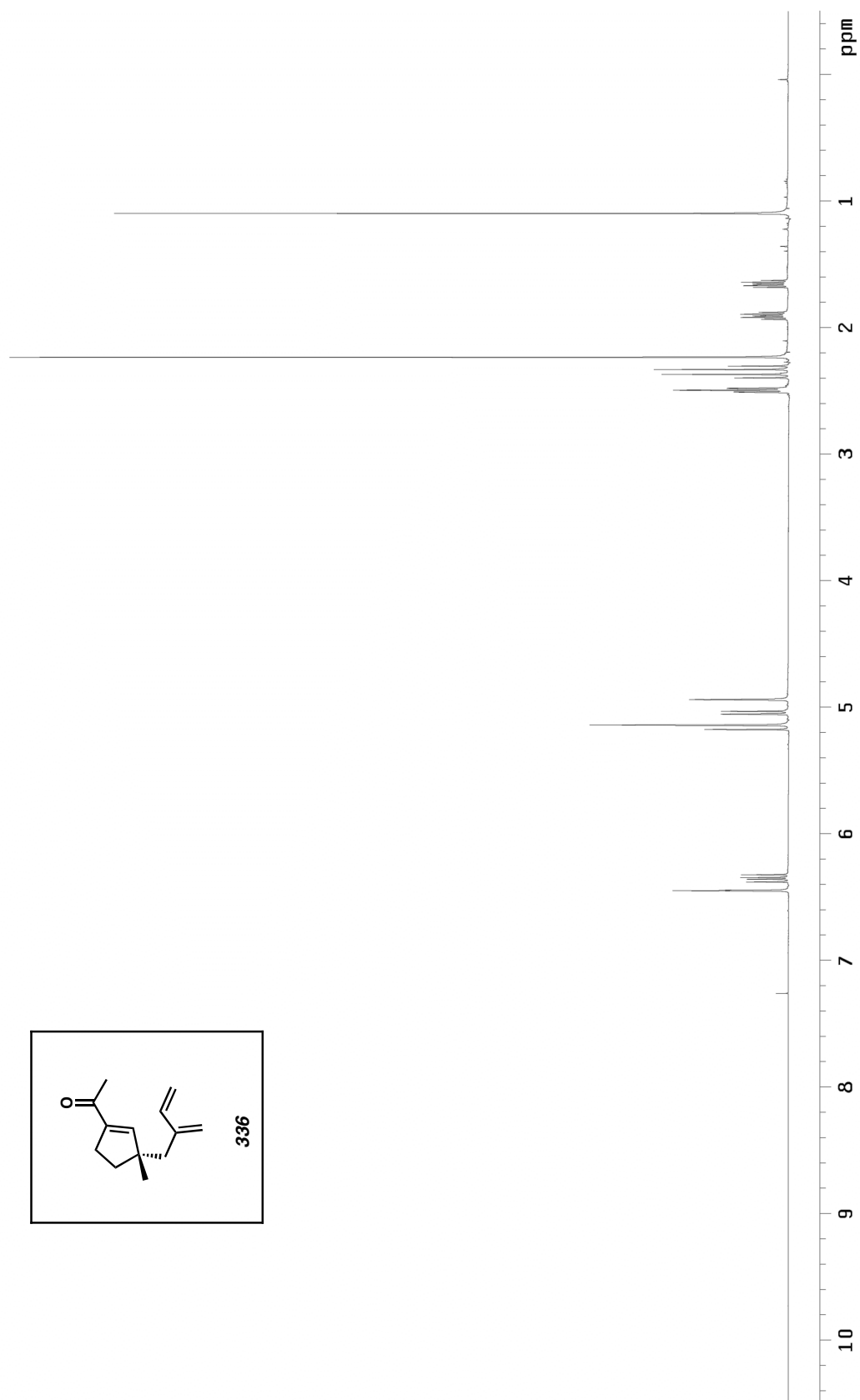


Figure A5.45. ¹³C NMR (125 MHz, CDCl₃) of compound **365**.

Figure A5.46. ¹H NMR (500 MHz, CDCl₃) of compound 336.

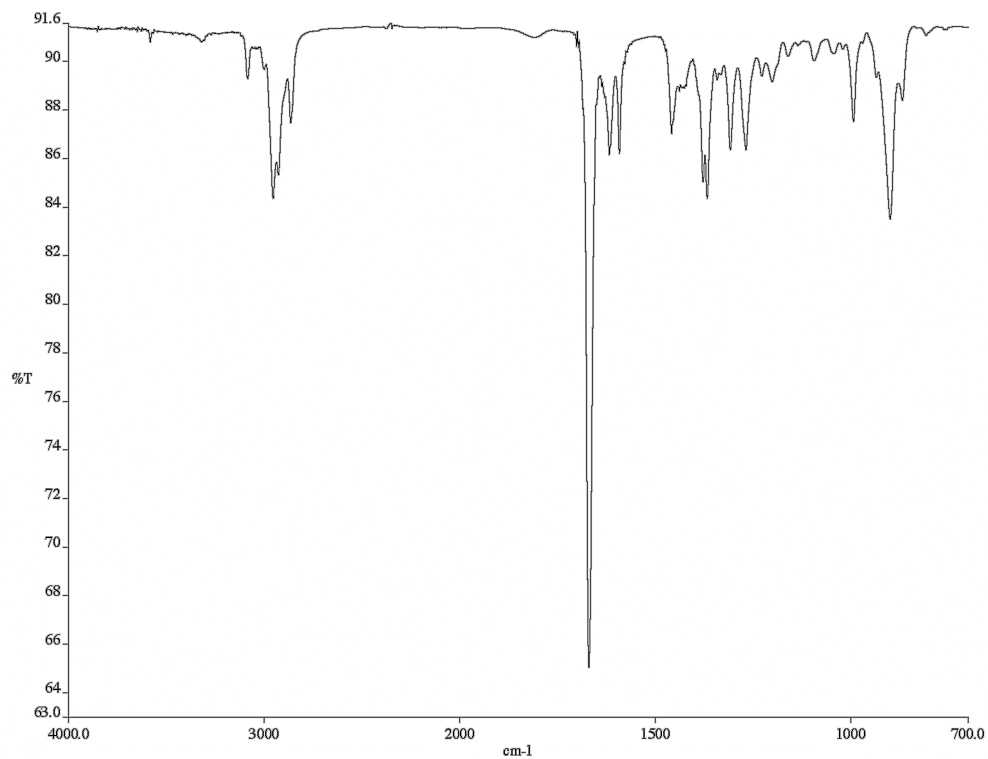


Figure A5.47. Infrared spectrum (thin film/NaCl) of compound **336**.

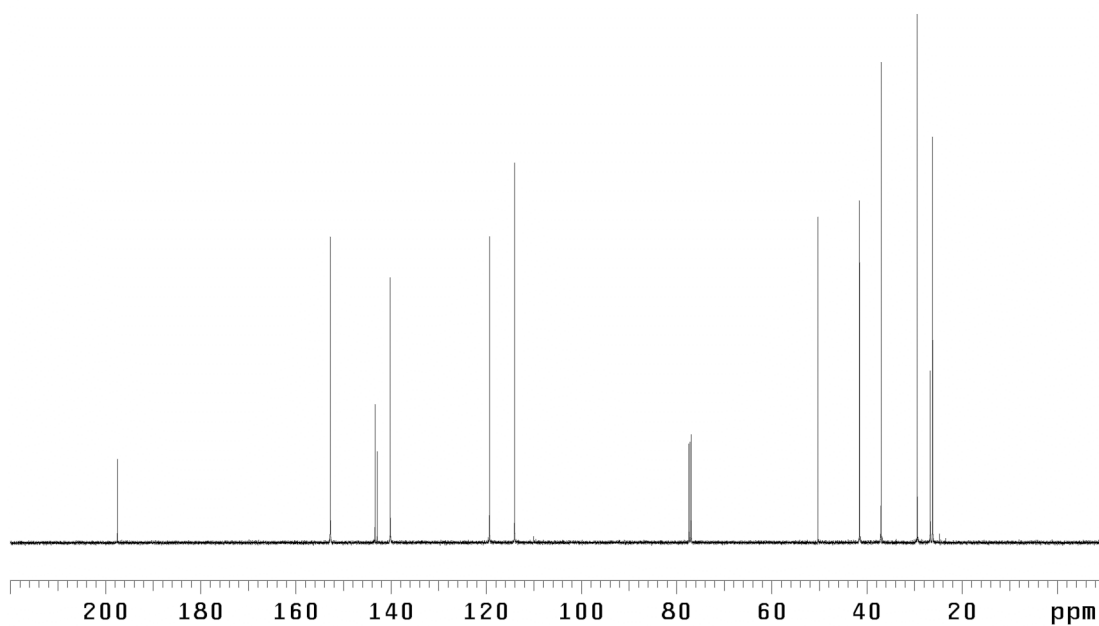


Figure A5.48. ¹³C NMR (125 MHz, CDCl₃) of compound **336**.

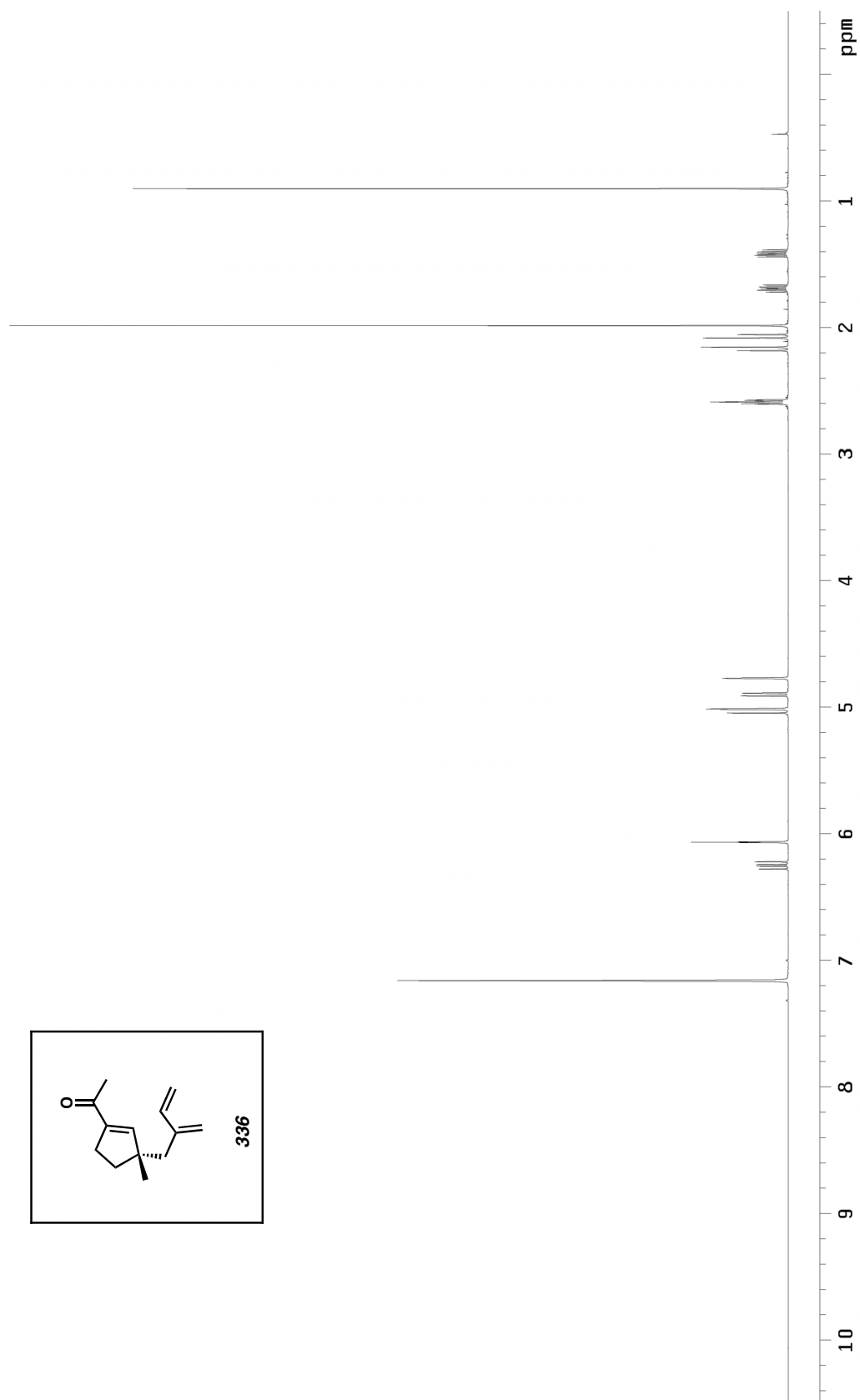


Figure A5.49. ¹H NMR (500 MHz, C₆D₆) of compound 336.

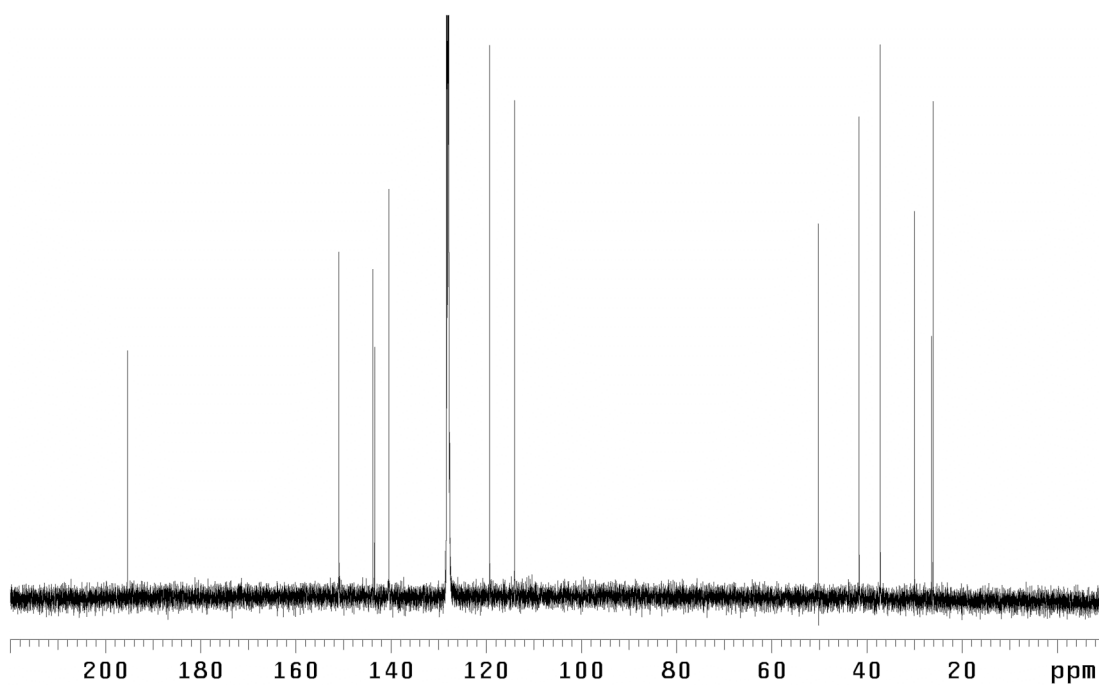


Figure A5.50. ^{13}C NMR (125 MHz, C_6D_6) of compound **336**.

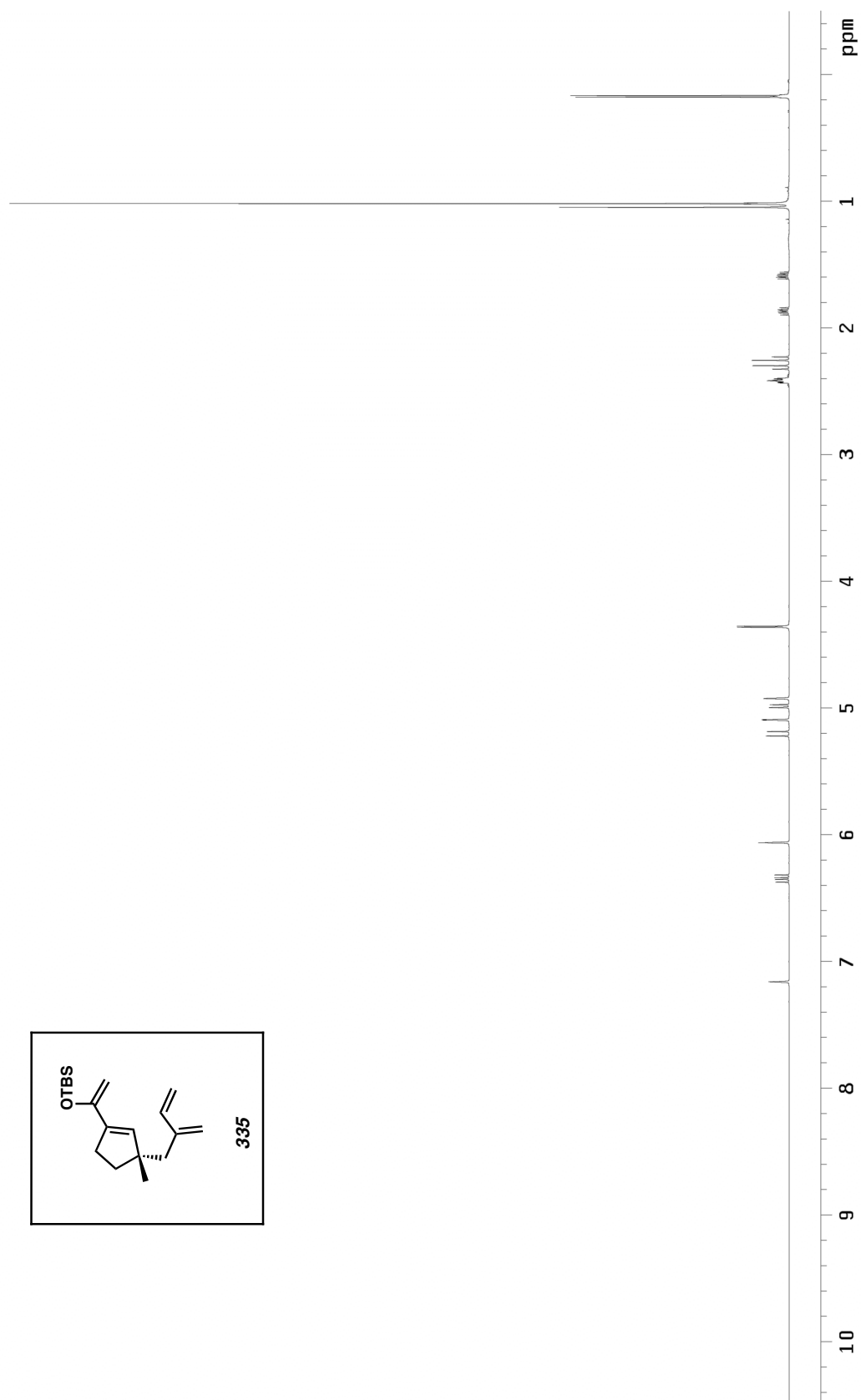


Figure A5.51. ¹H NMR (500 MHz, C₆D₆) of compound 335.

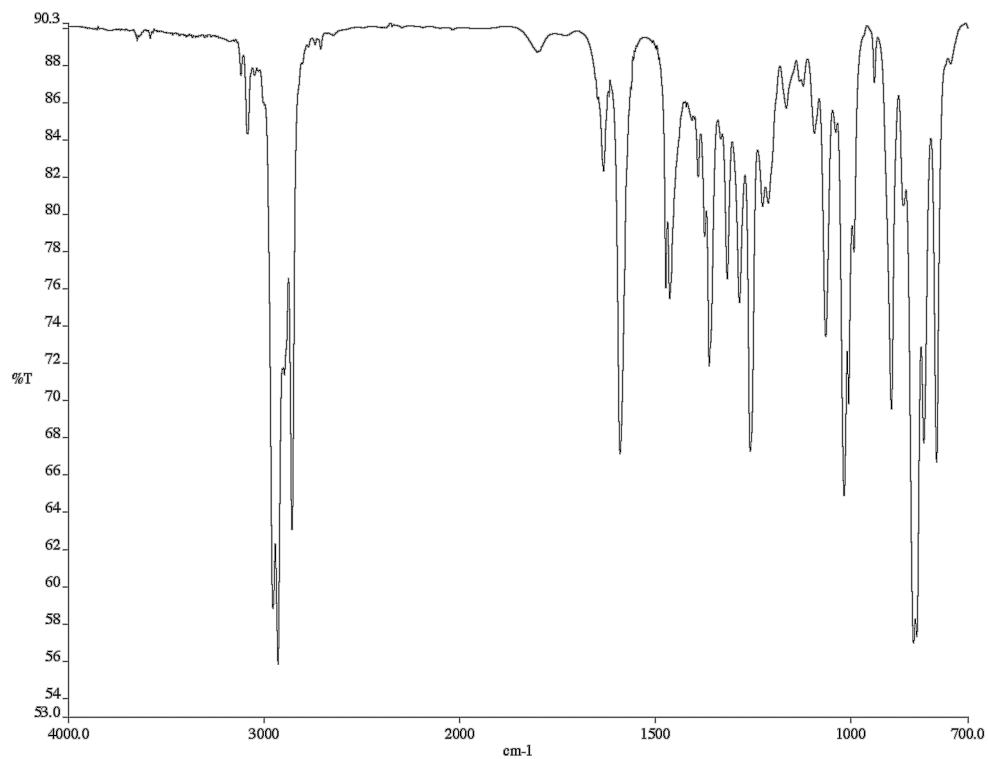


Figure A5.52. Infrared spectrum (thin film/NaCl) of compound **335**.

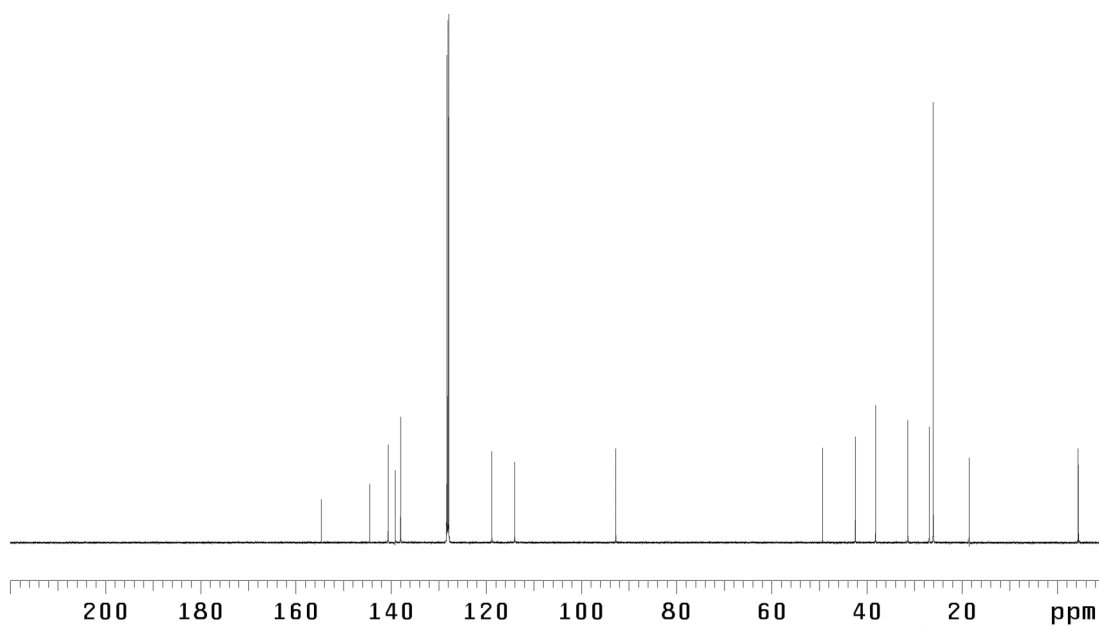


Figure A5.53. ¹³C NMR (125 MHz, C₆D₆) of compound **335**.

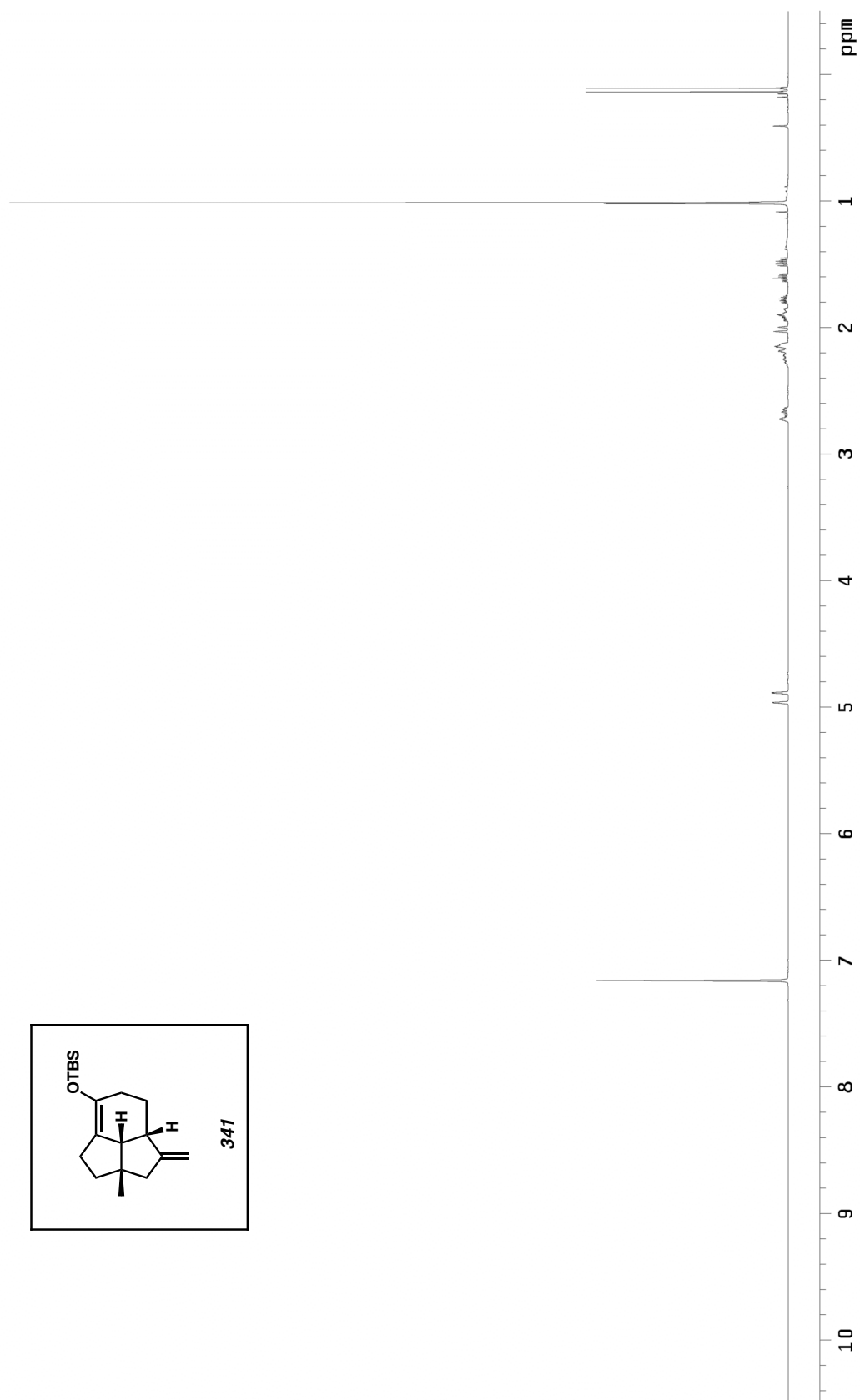


Figure A5.54. ¹H NMR (500 MHz, C₆D₆) of compound **341**.

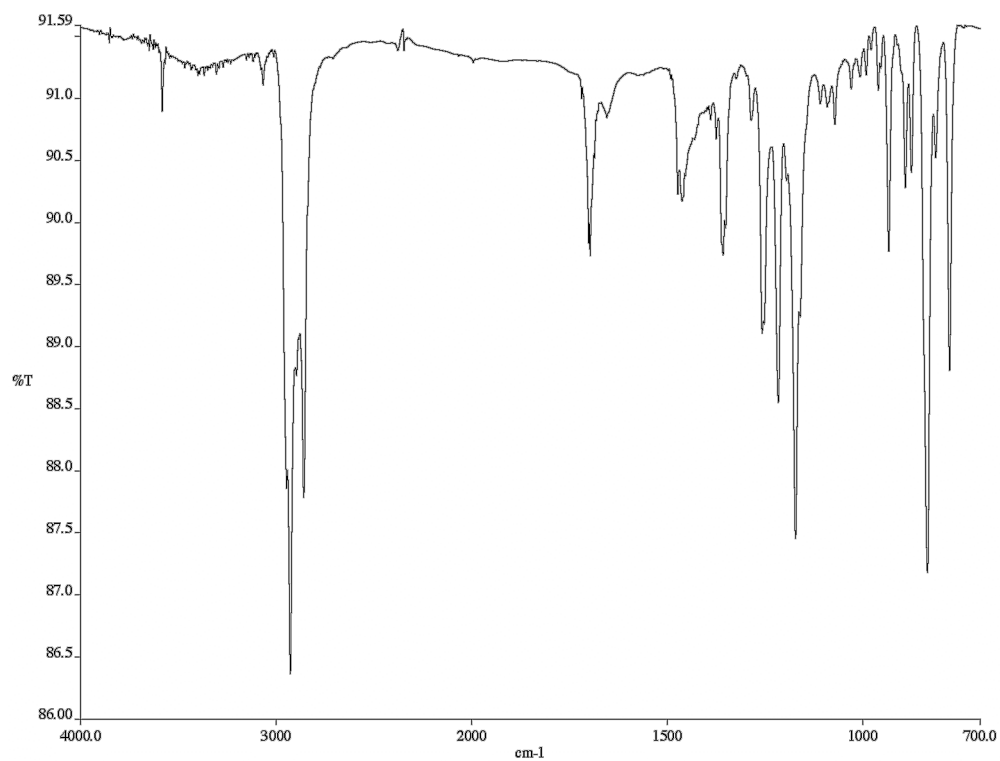


Figure A5.55. Infrared spectrum (thin film/NaCl) of compound **341**.

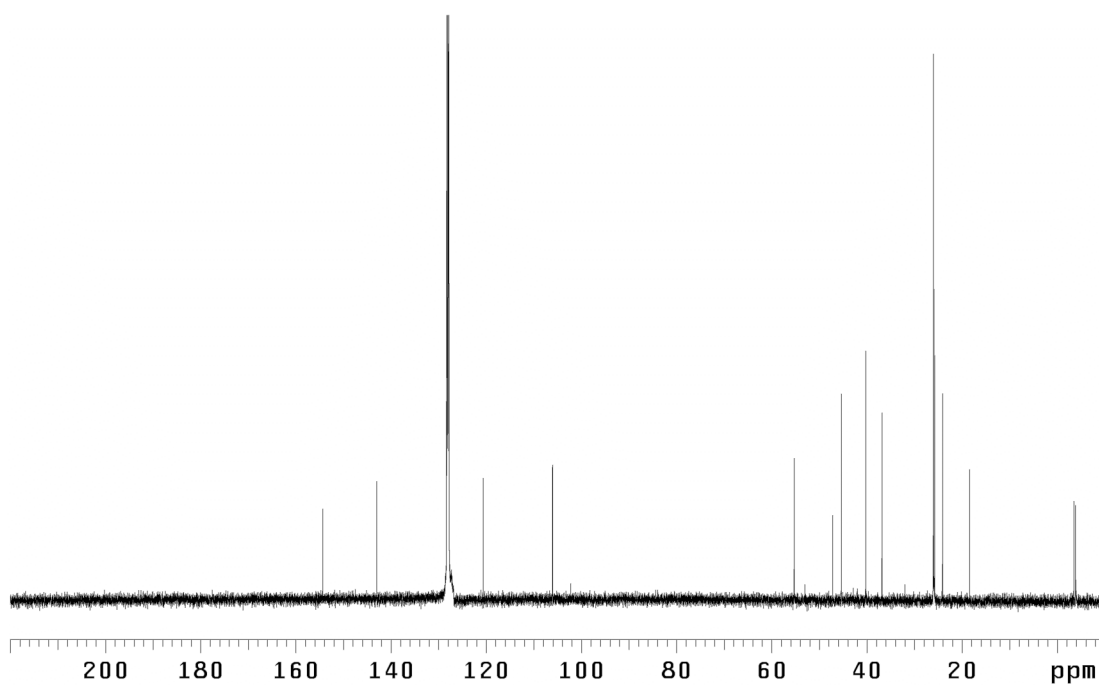


Figure A5.56. ¹³C NMR (125 MHz, C₆D₆) of compound **341**.

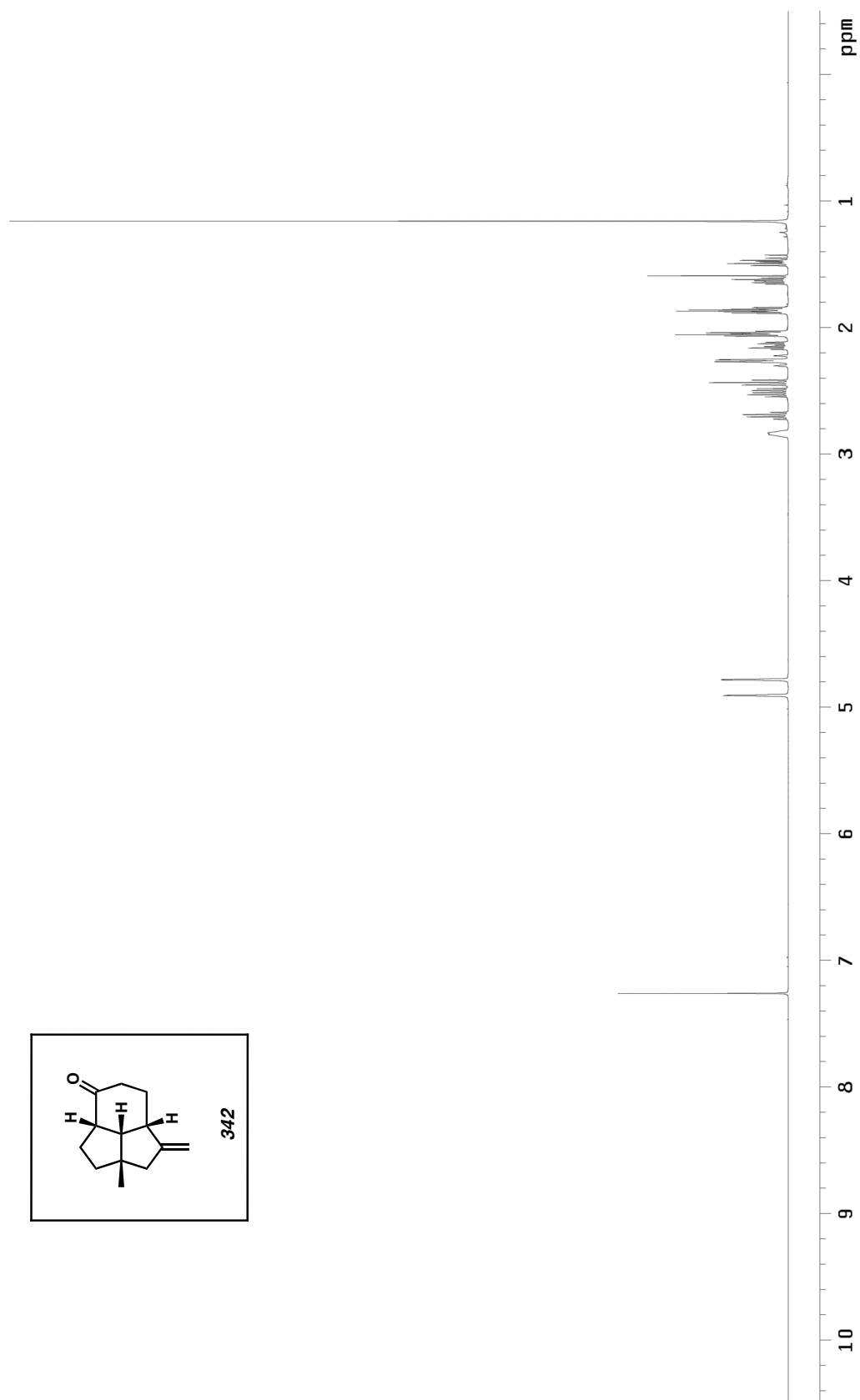


Figure A5.57. ^1H NMR (500 MHz, CDCl_3) of compound 342.

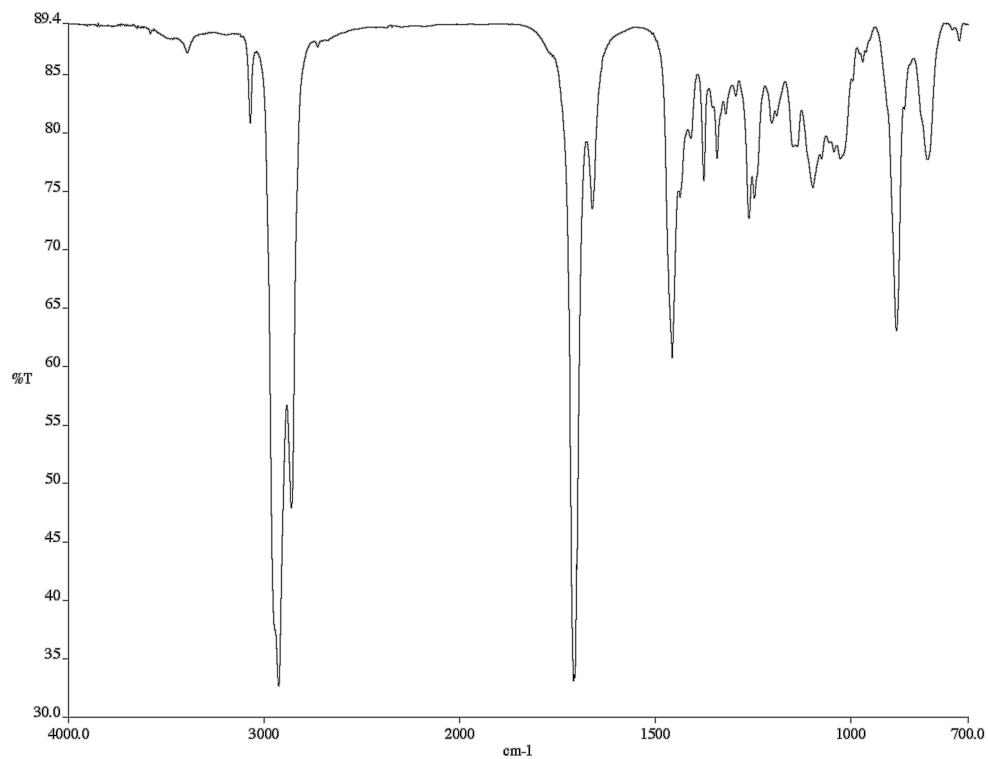


Figure A5.58. Infrared spectrum (thin film/NaCl) of compound **342**.

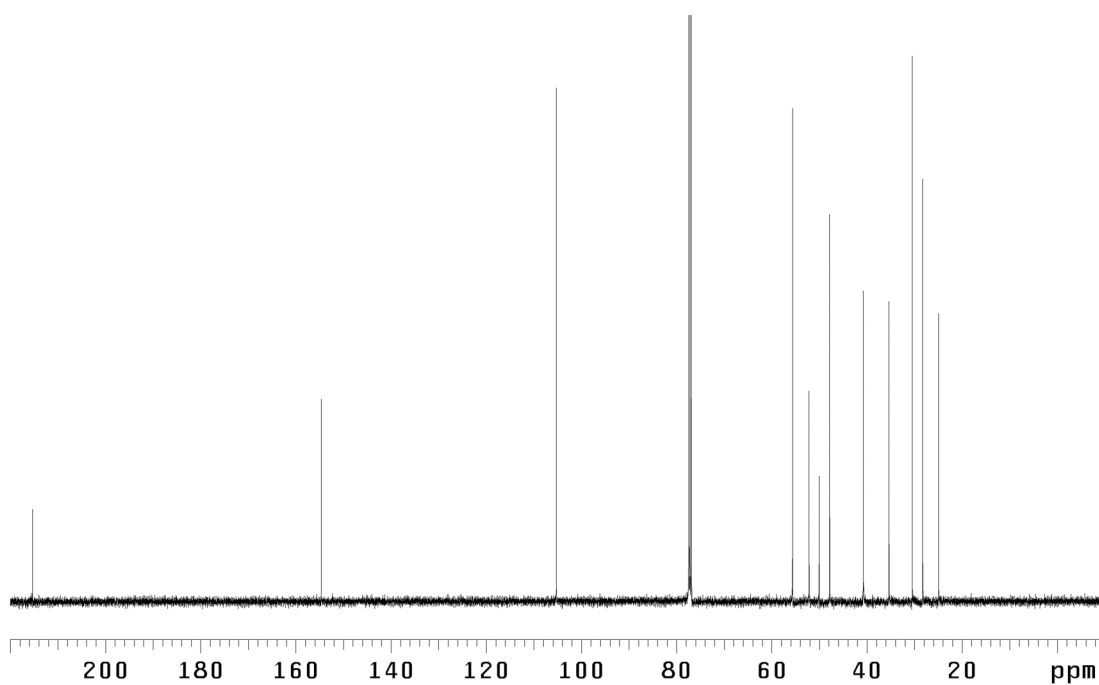
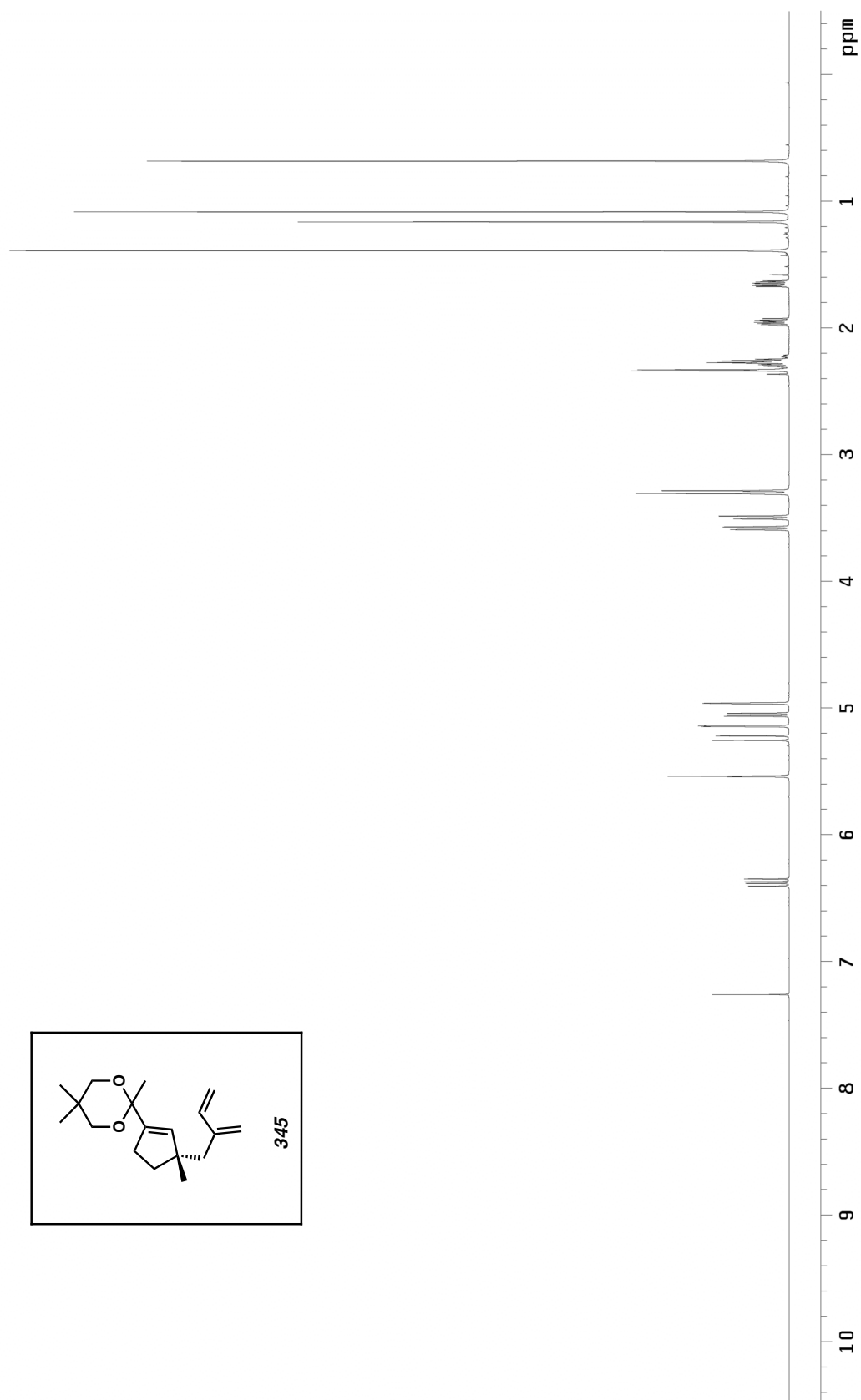


Figure A5.59. ¹³C NMR (125 MHz, CDCl₃) of compound **342**.



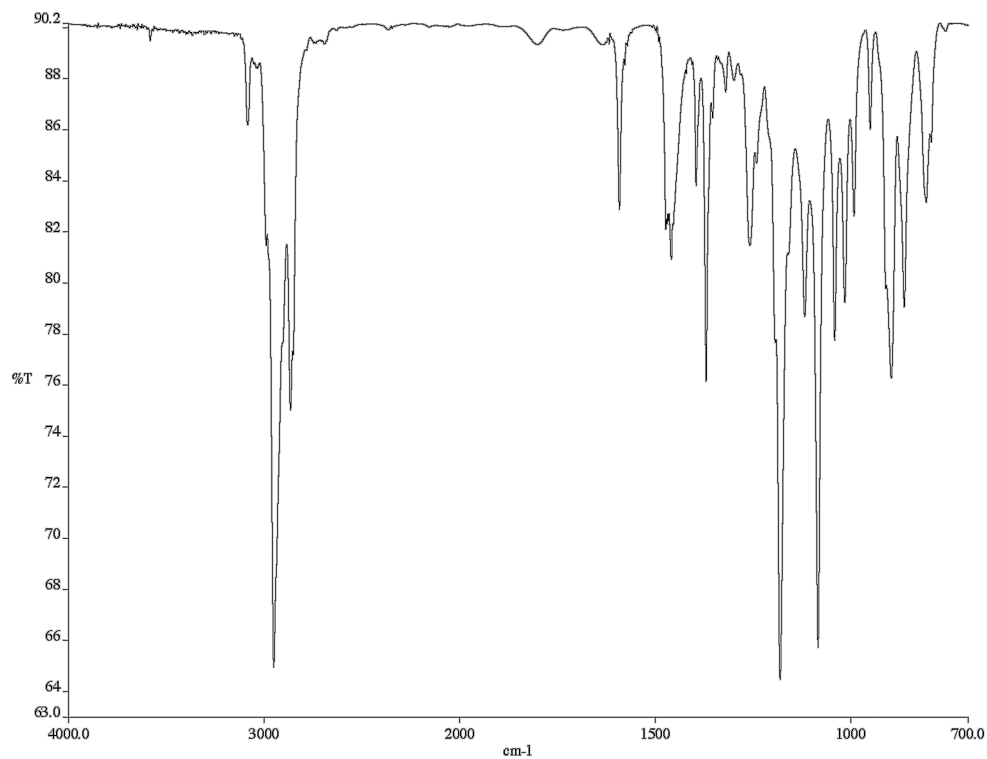


Figure A5.61. Infrared spectrum (thin film/NaCl) of compound **345**.

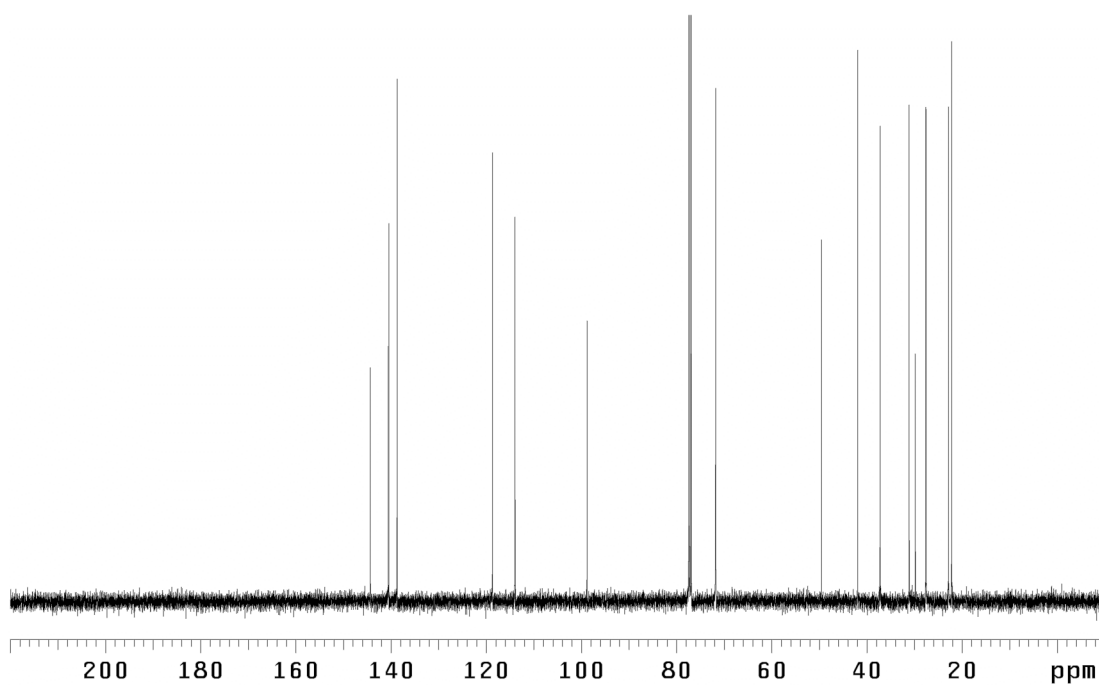


Figure A5.62. ¹³C NMR (125 MHz, CDCl₃) of compound **345**.

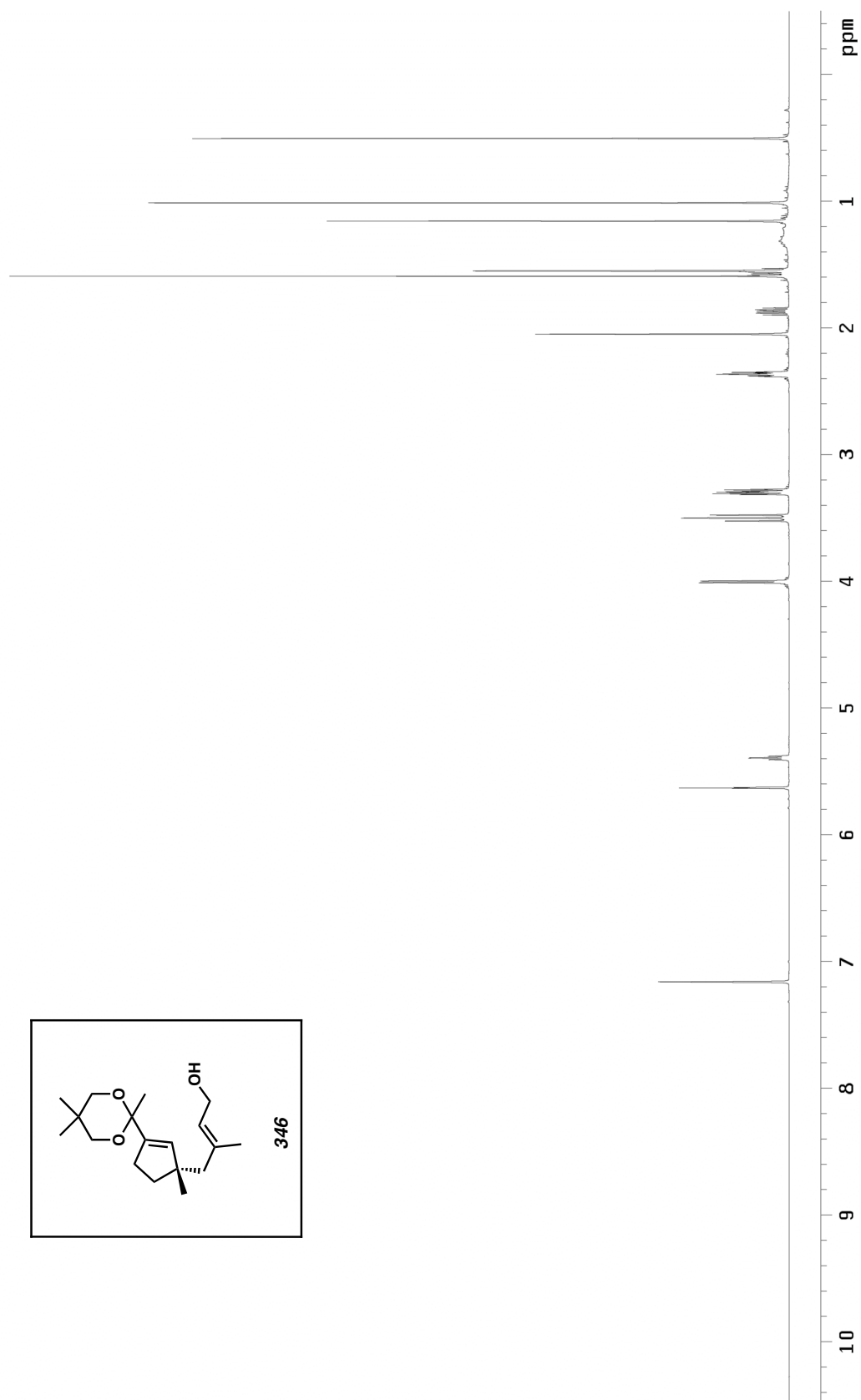


Figure A5.63. ^1H NMR (500 MHz, C_6D_6) of compound **346**.

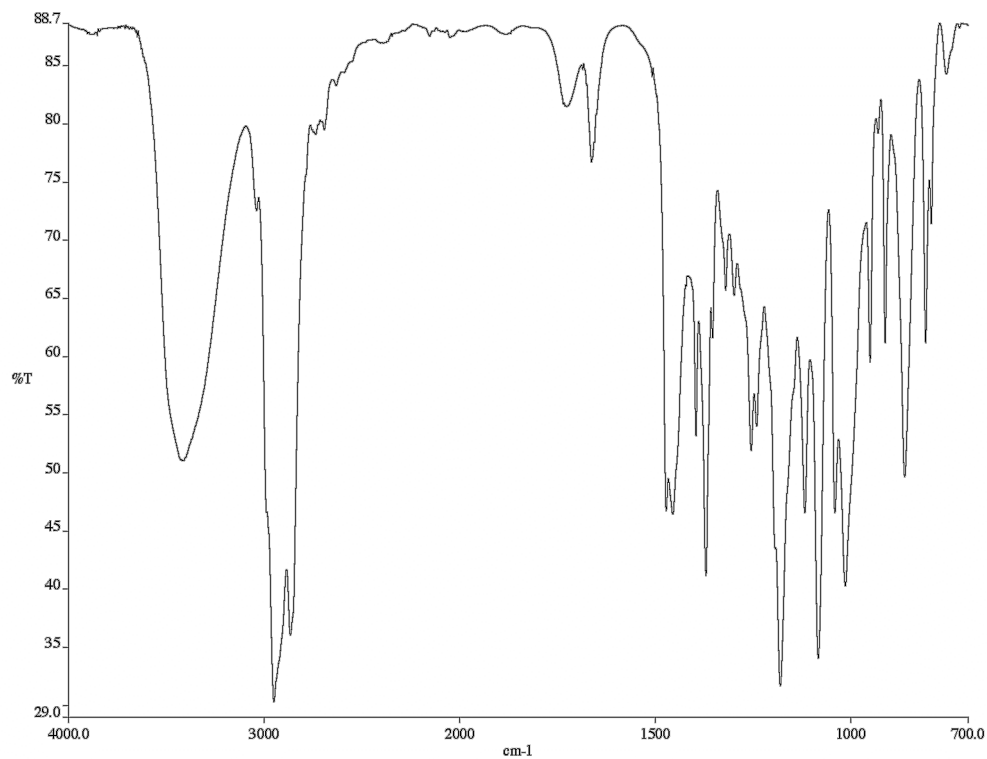


Figure A5.64. Infrared spectrum (thin film/NaCl) of compound **346**.

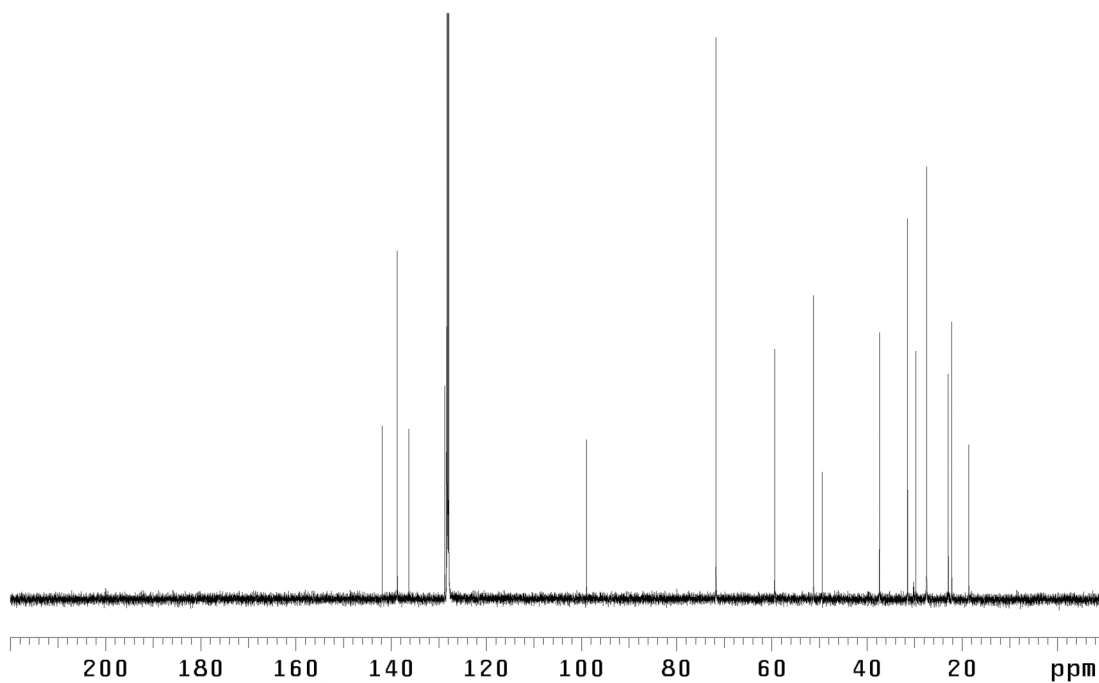
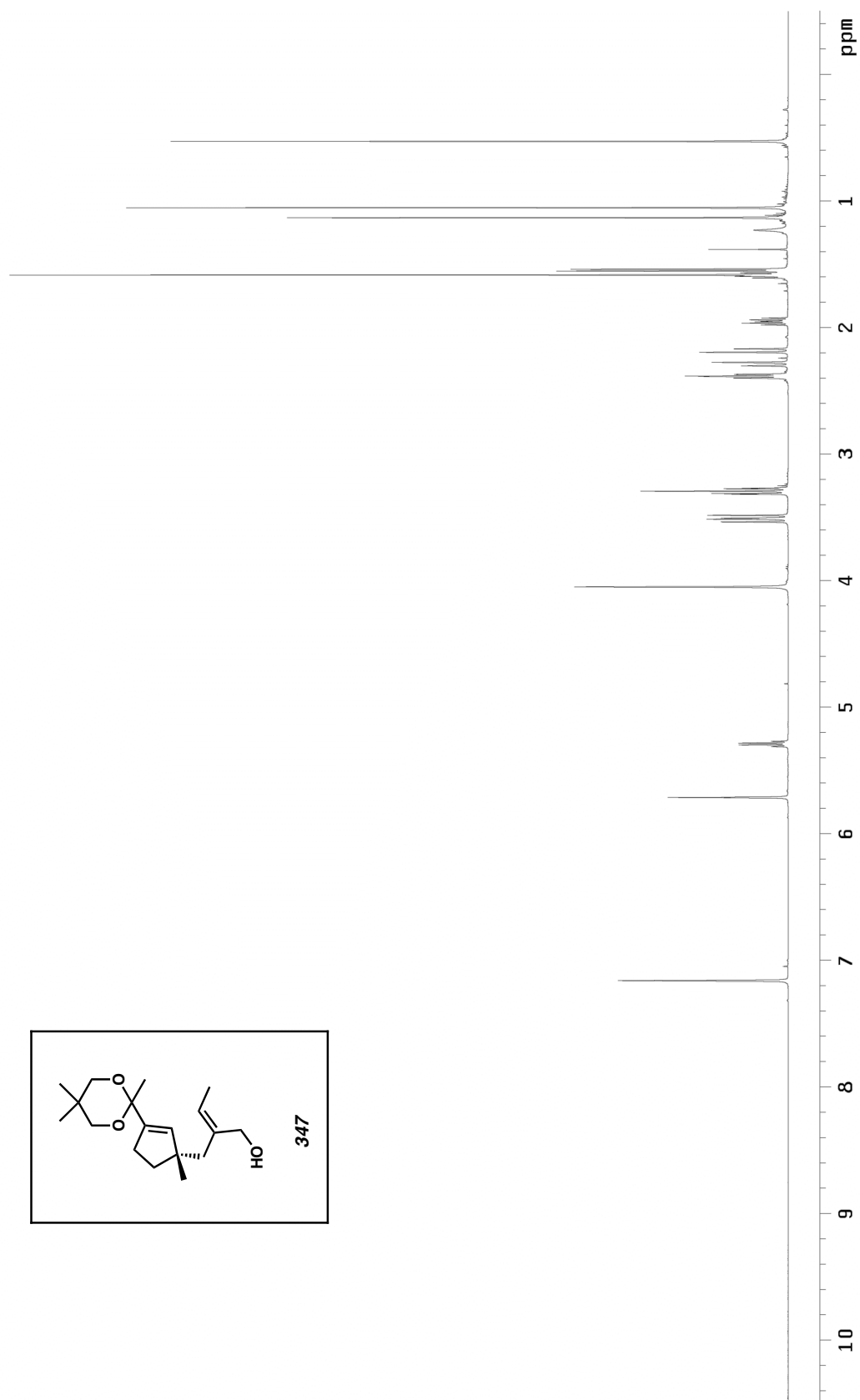


Figure A5.65. ^{13}C NMR (125 MHz, C_6D_6) of compound **346**.

Figure A5.66. ¹H NMR (500 MHz, C₆D₆) of compound 347.

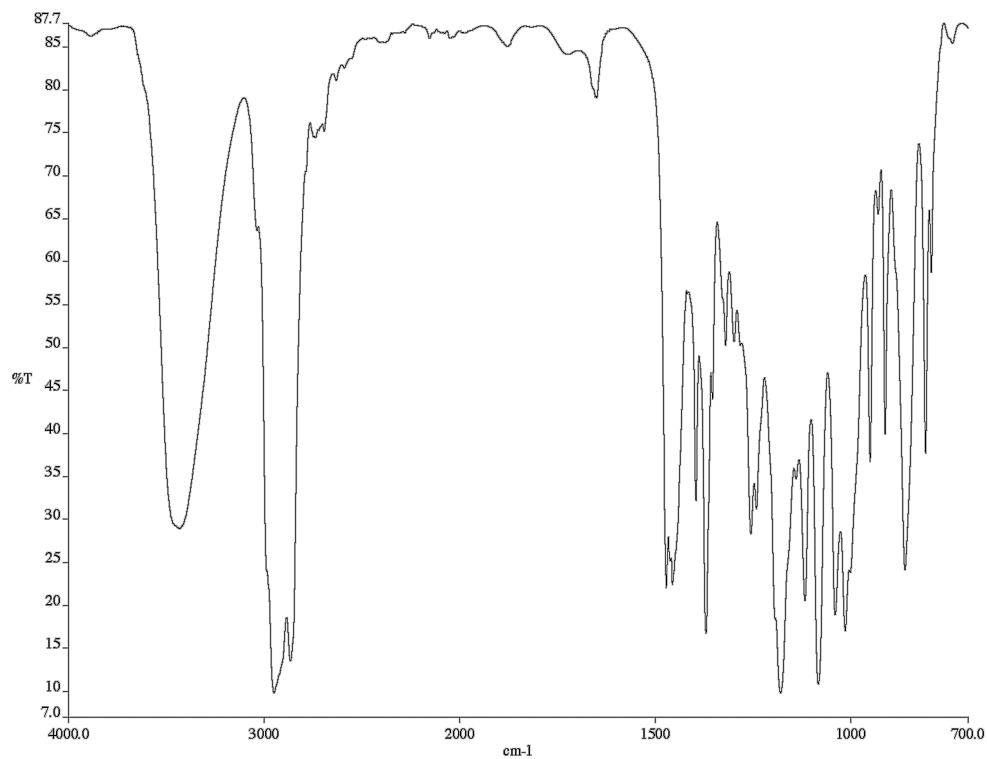


Figure A5.67. Infrared spectrum (thin film/NaCl) of compound **347**.

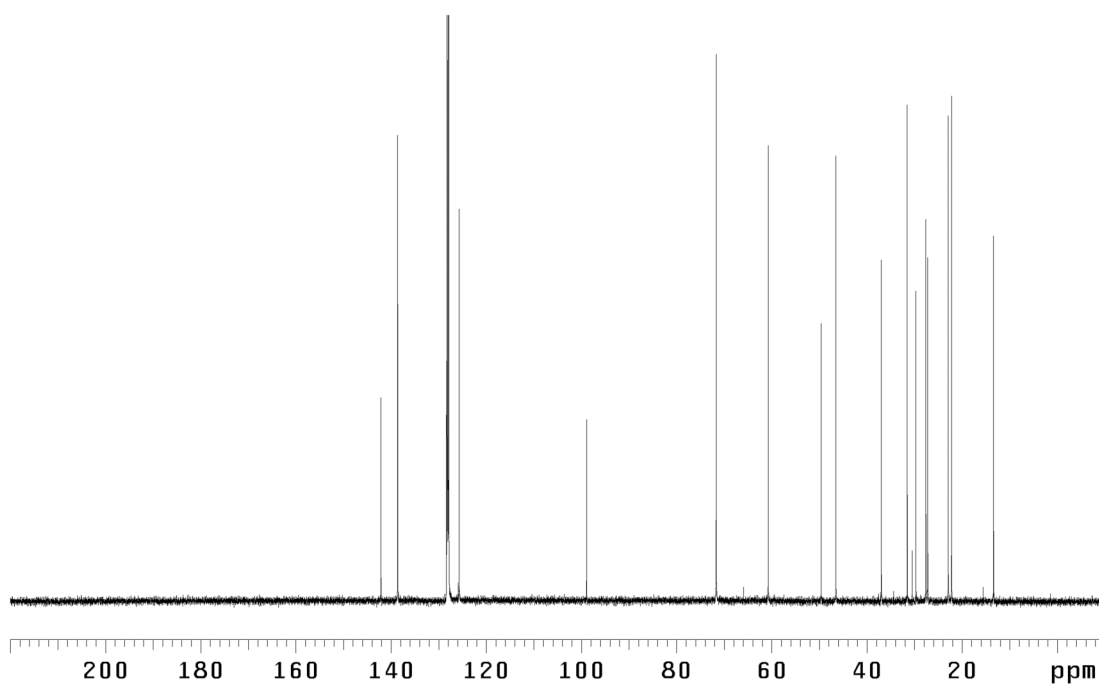


Figure A5.68. ¹³C NMR (125 MHz, C₆D₆) of compound **347**.

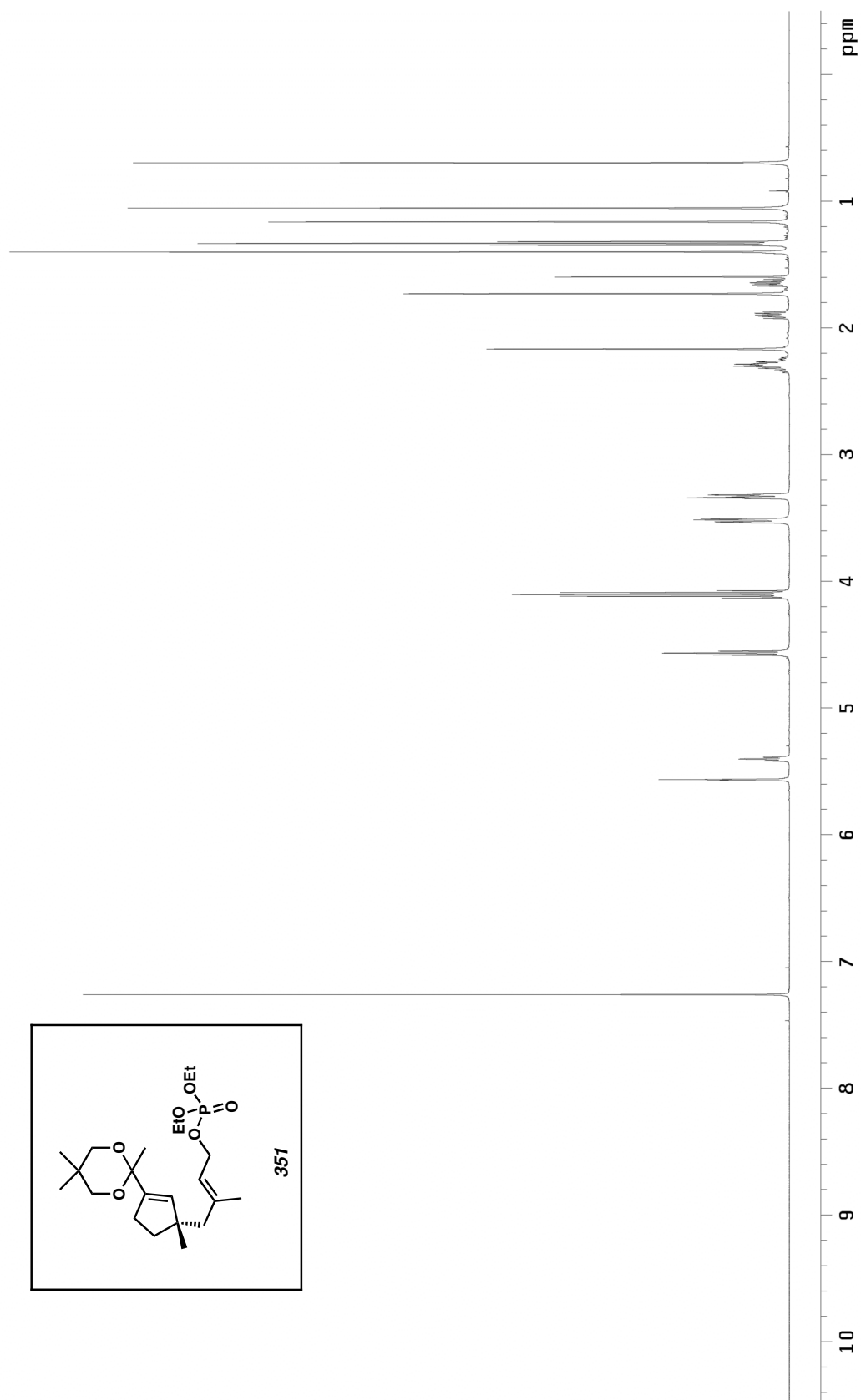


Figure A5.69. ¹H NMR (500 MHz, CDCl₃) of compound 351.

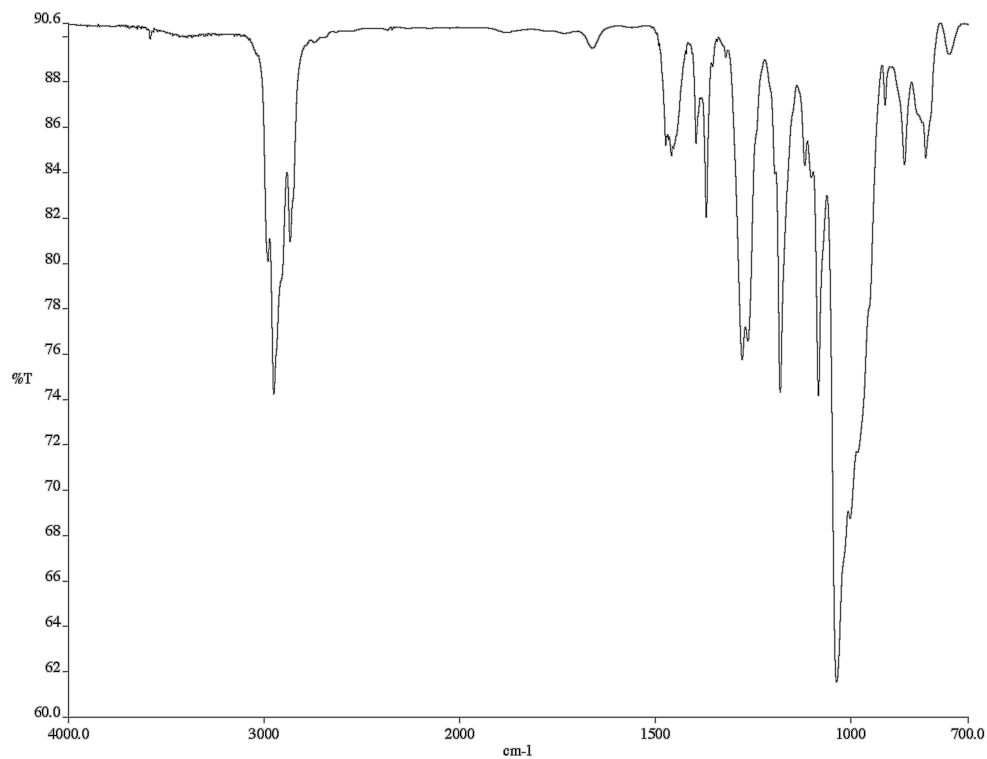


Figure A5.70. Infrared spectrum (thin film/NaCl) of compound **351**.

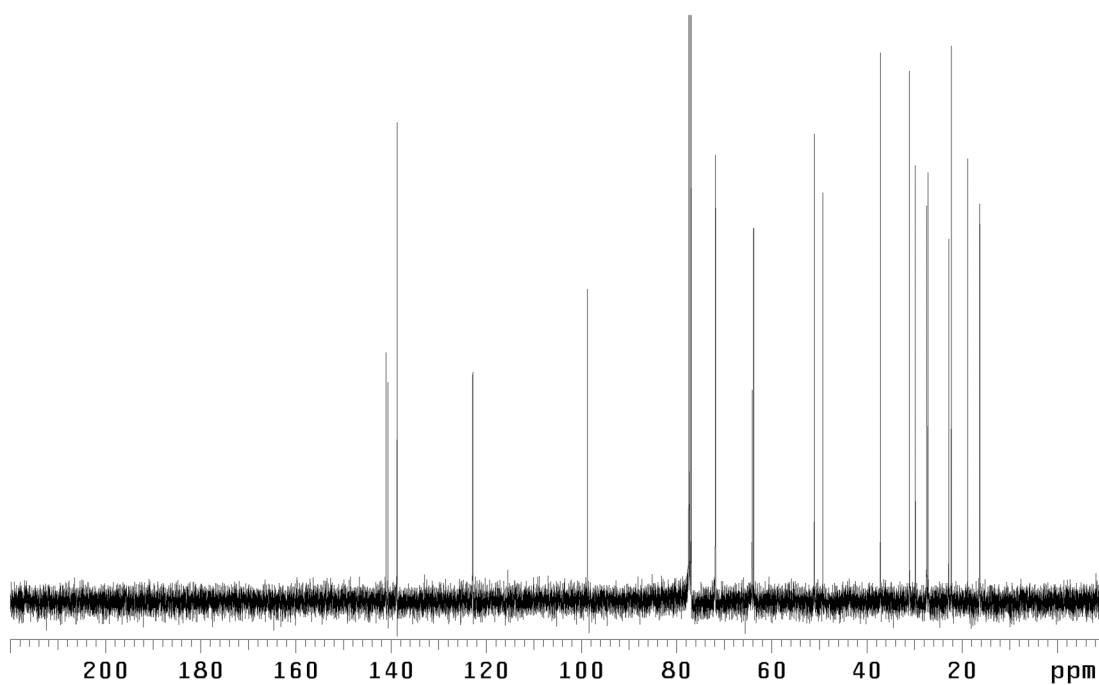


Figure A5.71. ¹³C NMR (125 MHz, CDCl₃) of compound **351**.

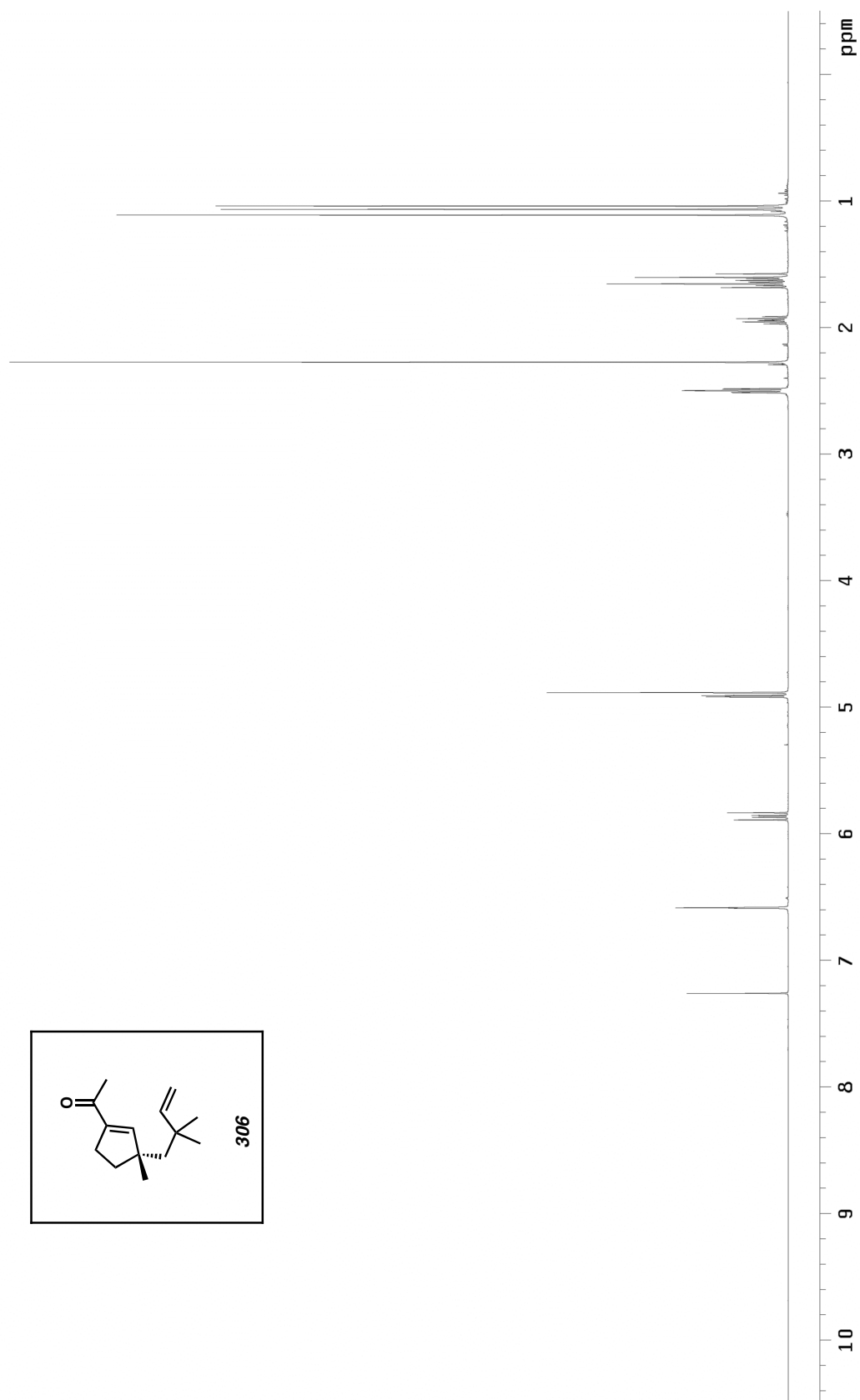


Figure A5.72. ^1H NMR (500 MHz, CDCl_3) of compound **306**.

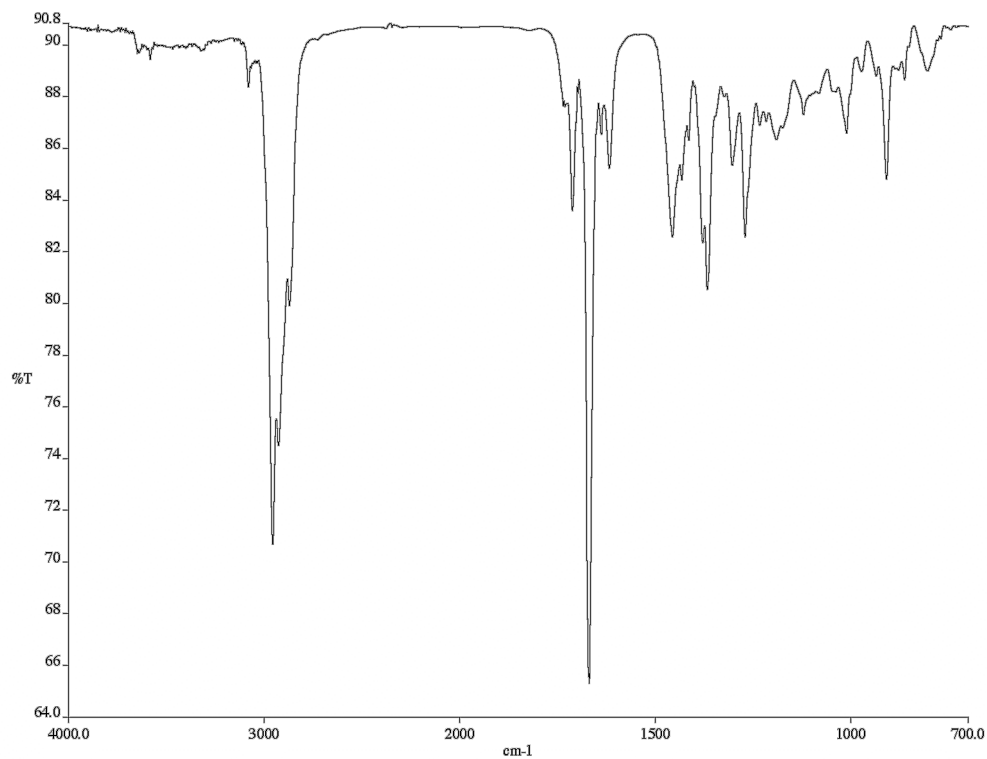


Figure A5.73. Infrared spectrum (thin film/NaCl) of compound **306**.

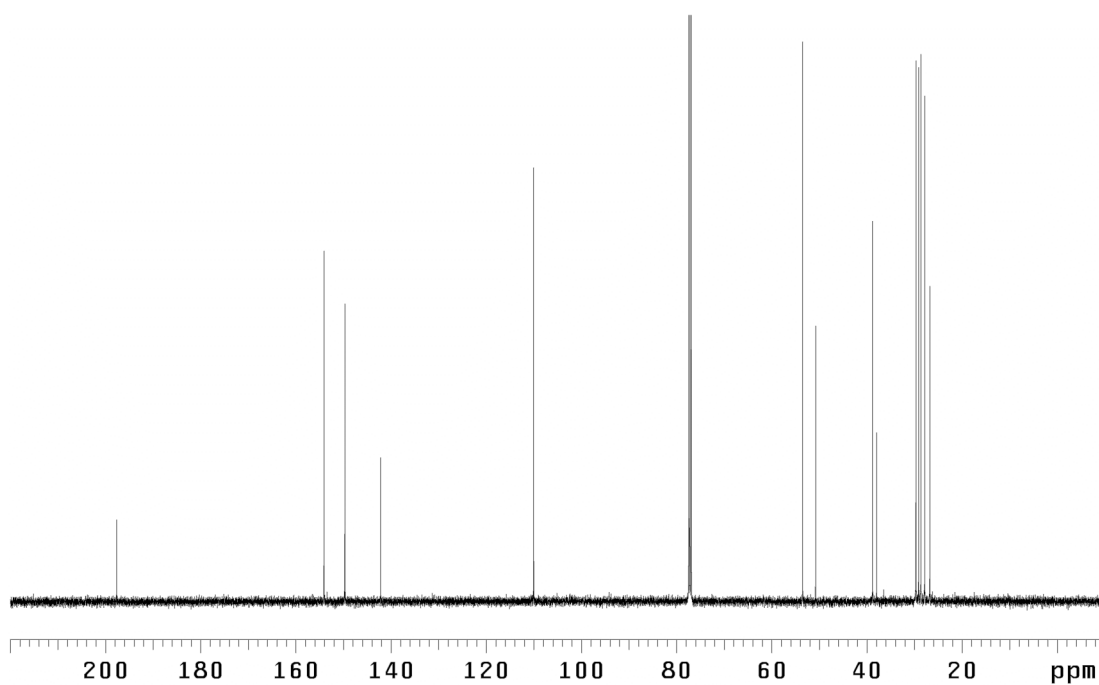


Figure A5.74. ¹³C NMR (125 MHz, CDCl₃) of compound **306**.

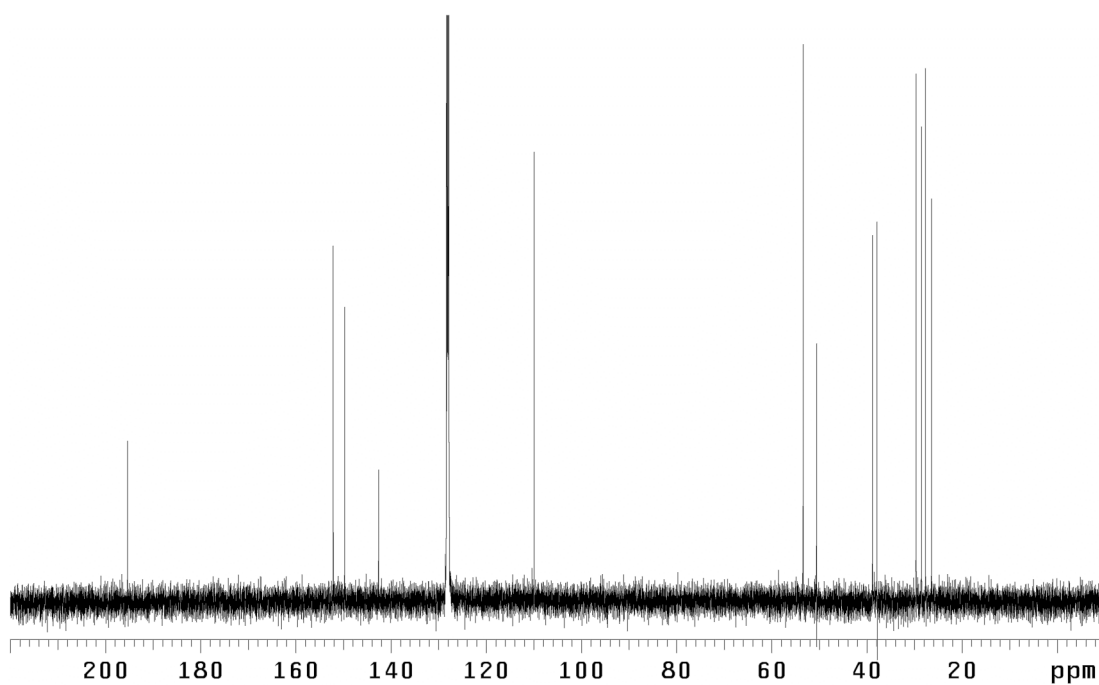


Figure A5.76. ^{13}C NMR (125 MHz, C_6D_6) of compound **306**.

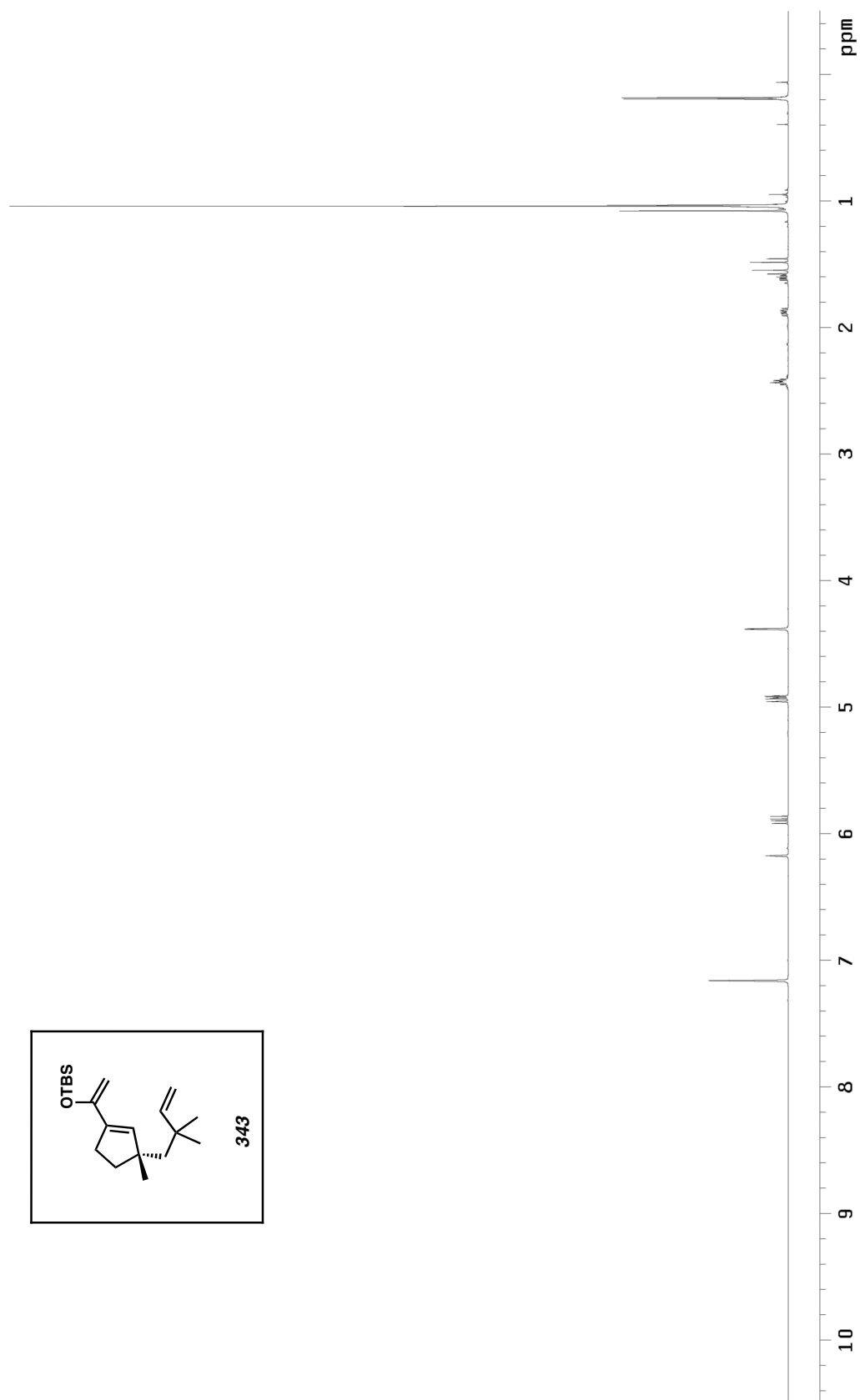


Figure A5.77. ¹H NMR (500 MHz, C₆D₆) of compound **343**.

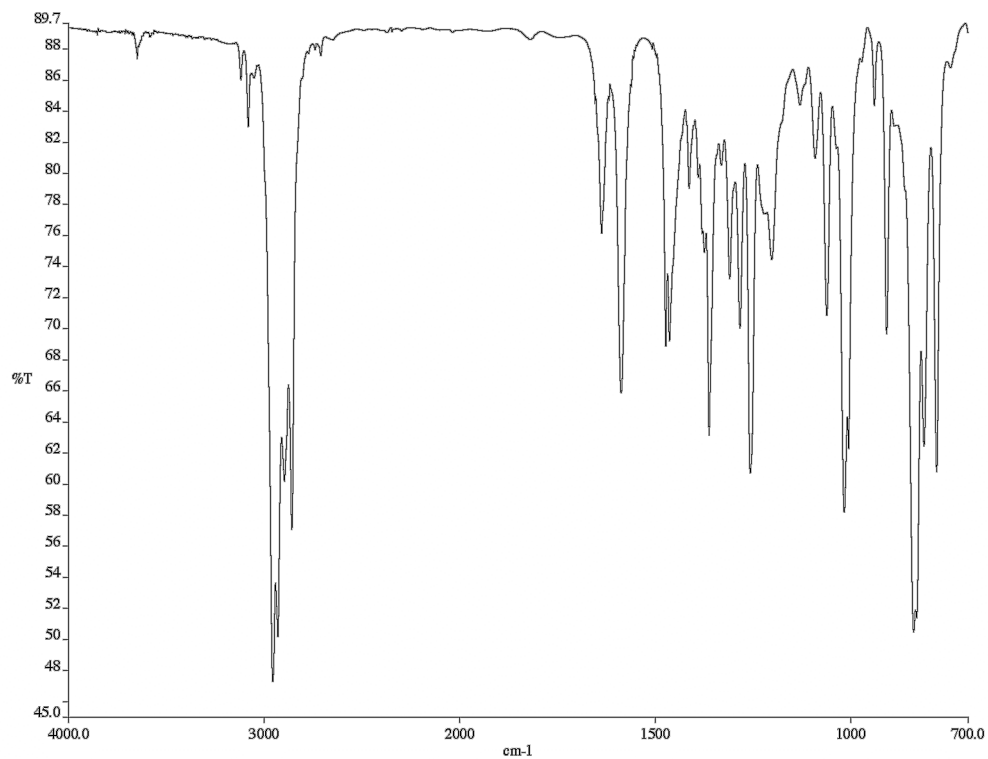


Figure A5.78. Infrared spectrum (thin film/NaCl) of compound **343**.

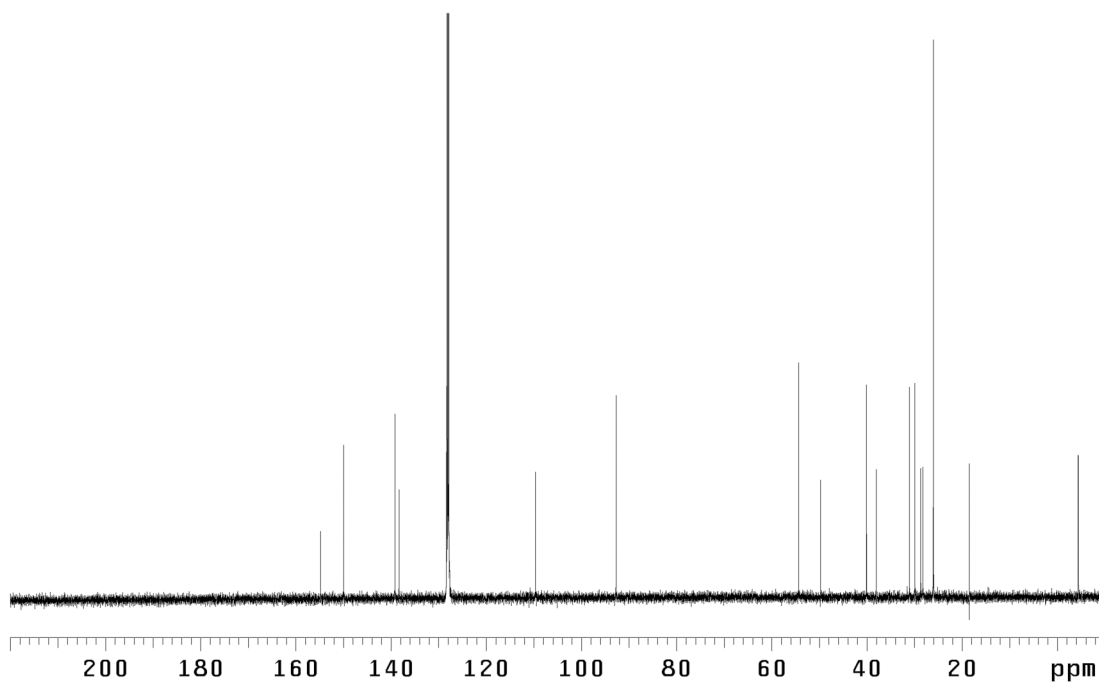


Figure A5.79. ¹³C NMR (125 MHz, C₆D₆) of compound **343**.

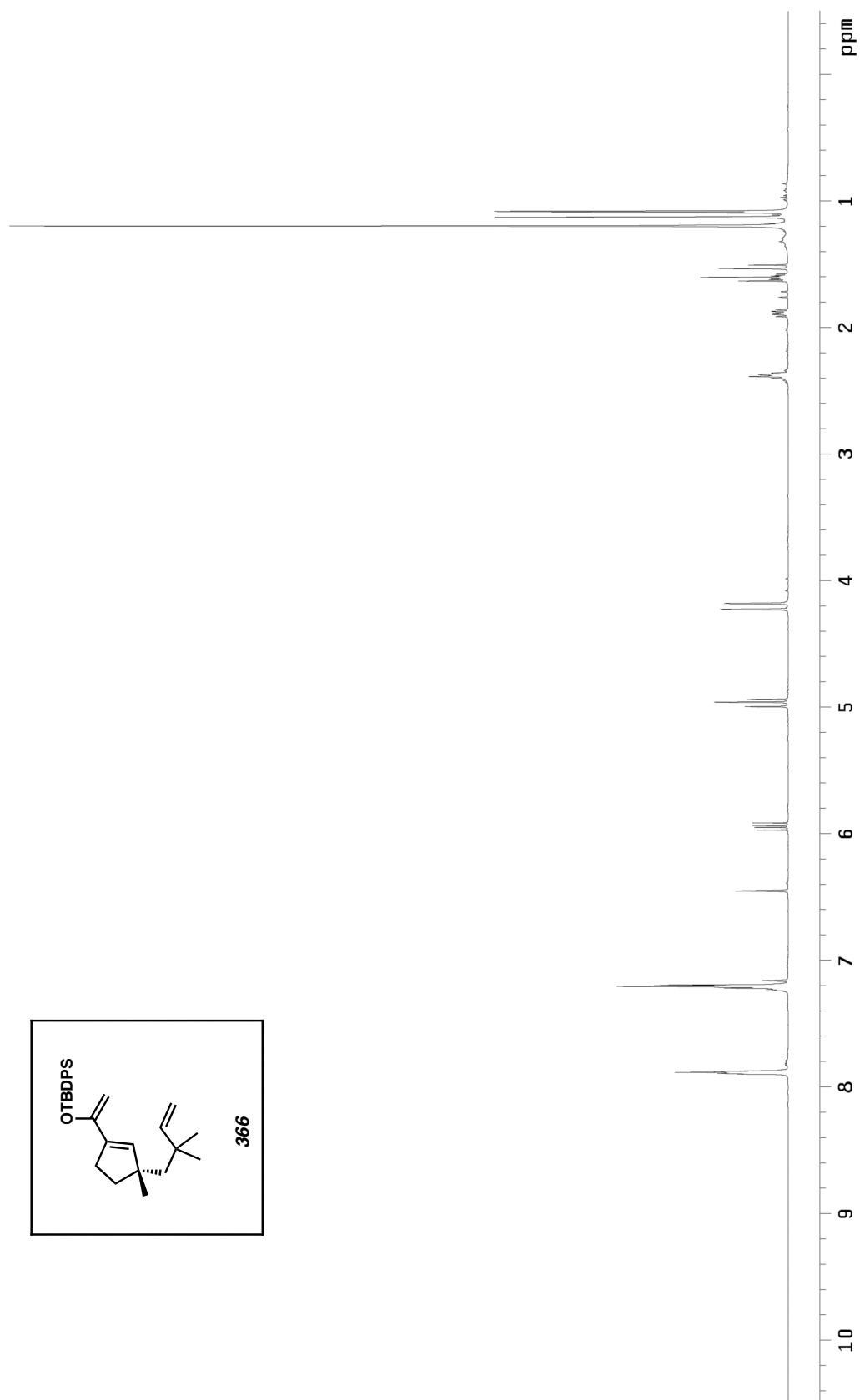


Figure A5.80. ^1H NMR (500 MHz, C_6D_6) of compound **366**.

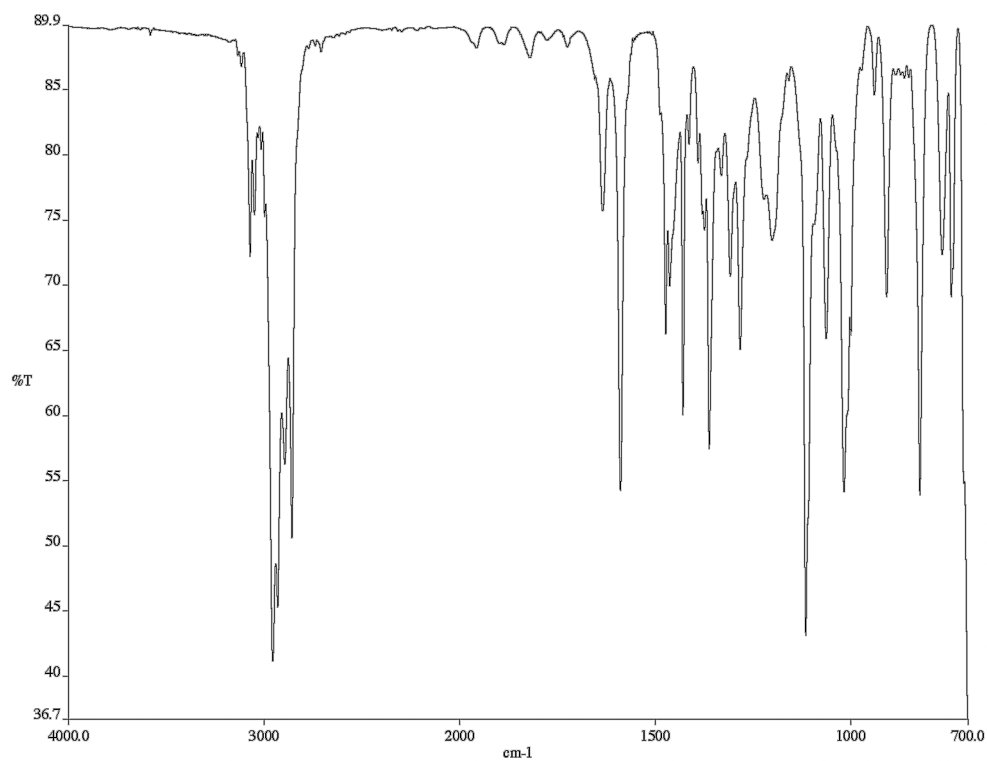


Figure A5.81. Infrared spectrum (thin film/NaCl) of compound **366**.

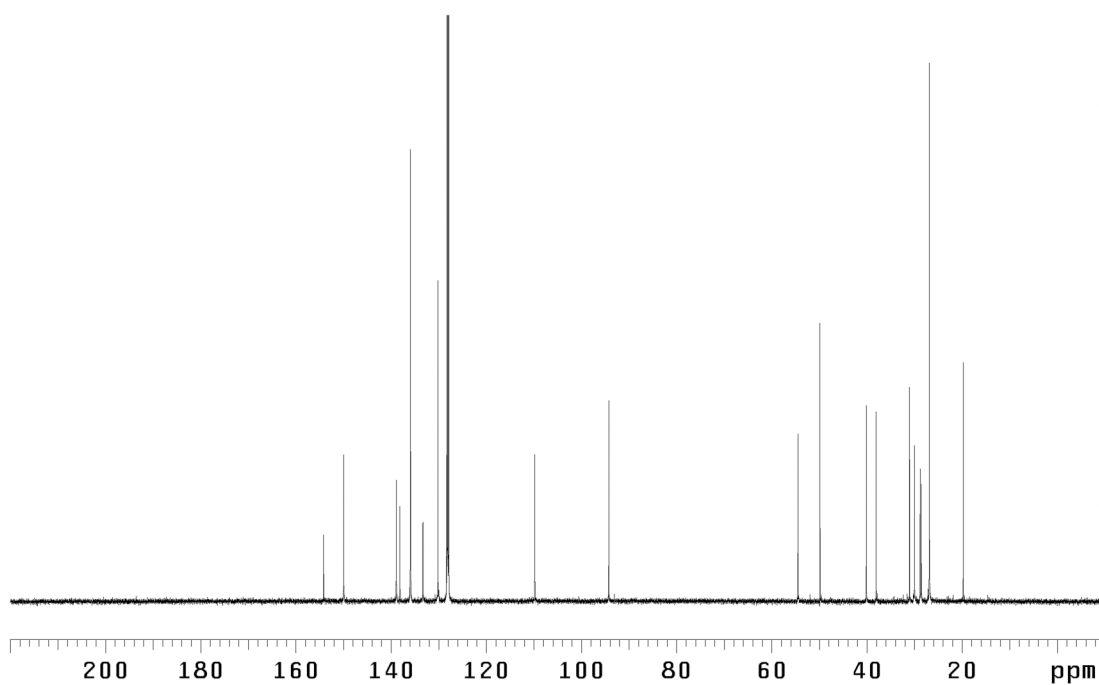


Figure A5.82. ^{13}C NMR (125 MHz, C_6D_6) of compound **366**.

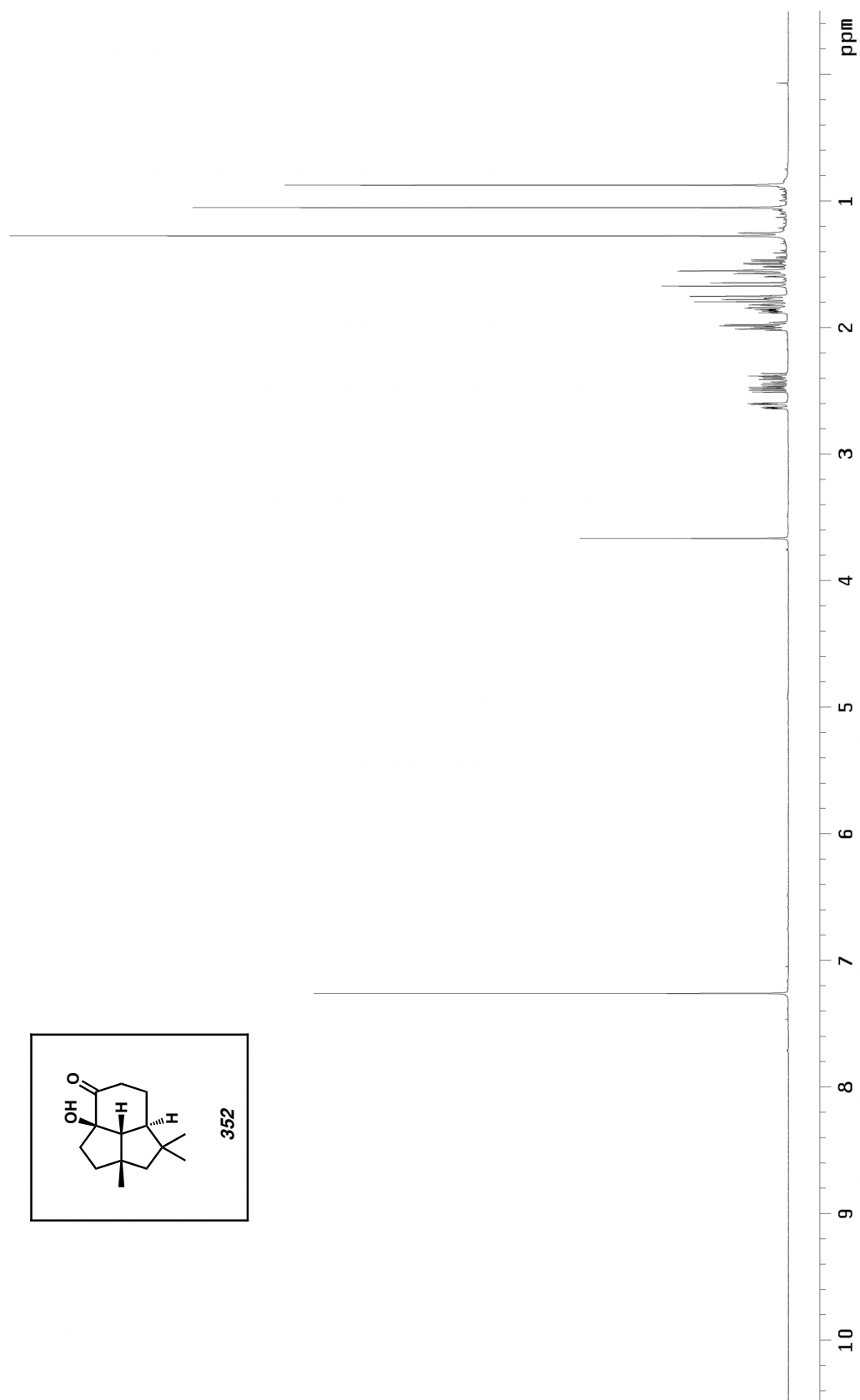


Figure A5.83. ^1H NMR (500 MHz, CDCl_3) of compound 352.

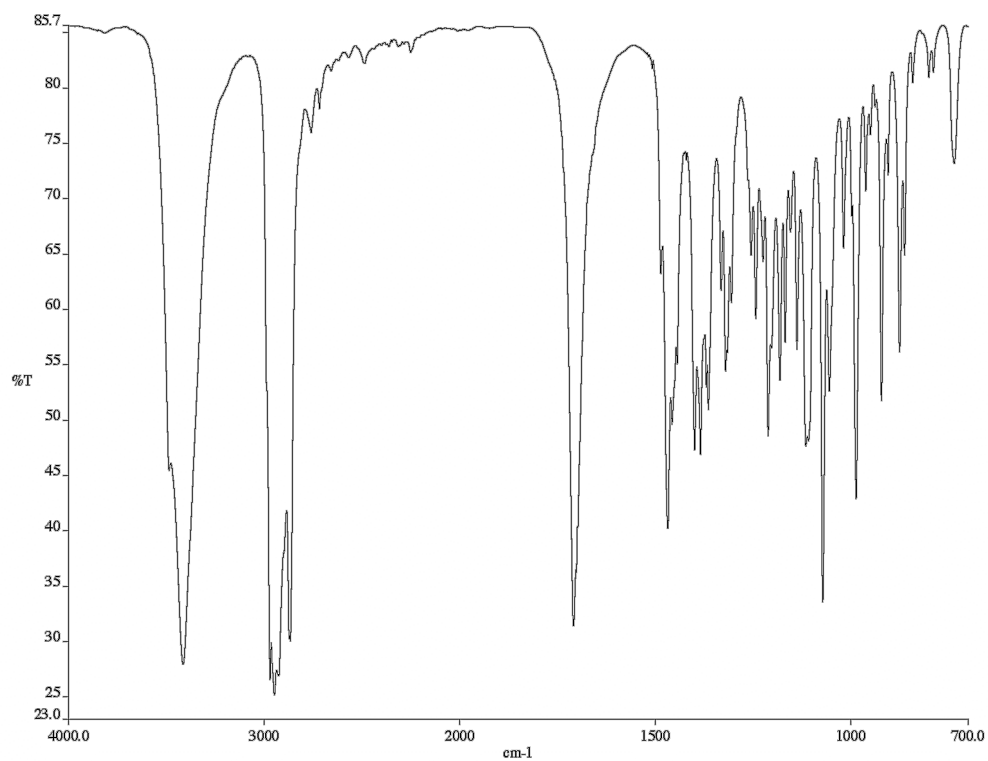


Figure A5.84. Infrared spectrum (thin film/NaCl) of compound **352**.

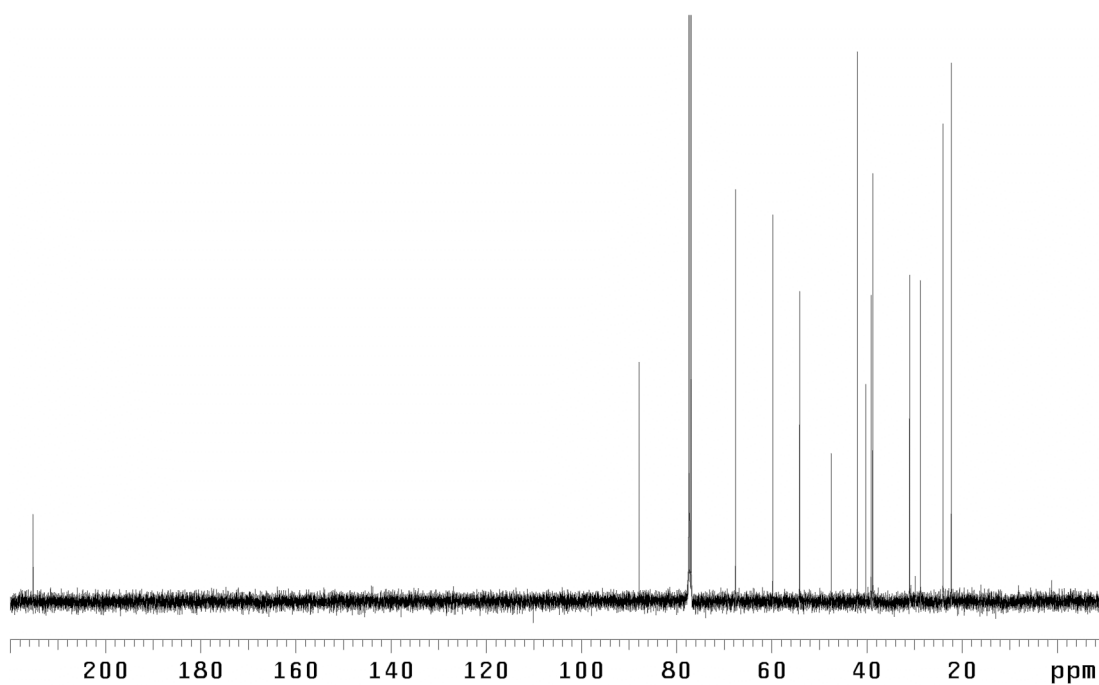


Figure A5.85. ¹³C NMR (125 MHz, CDCl₃) of compound **352**.

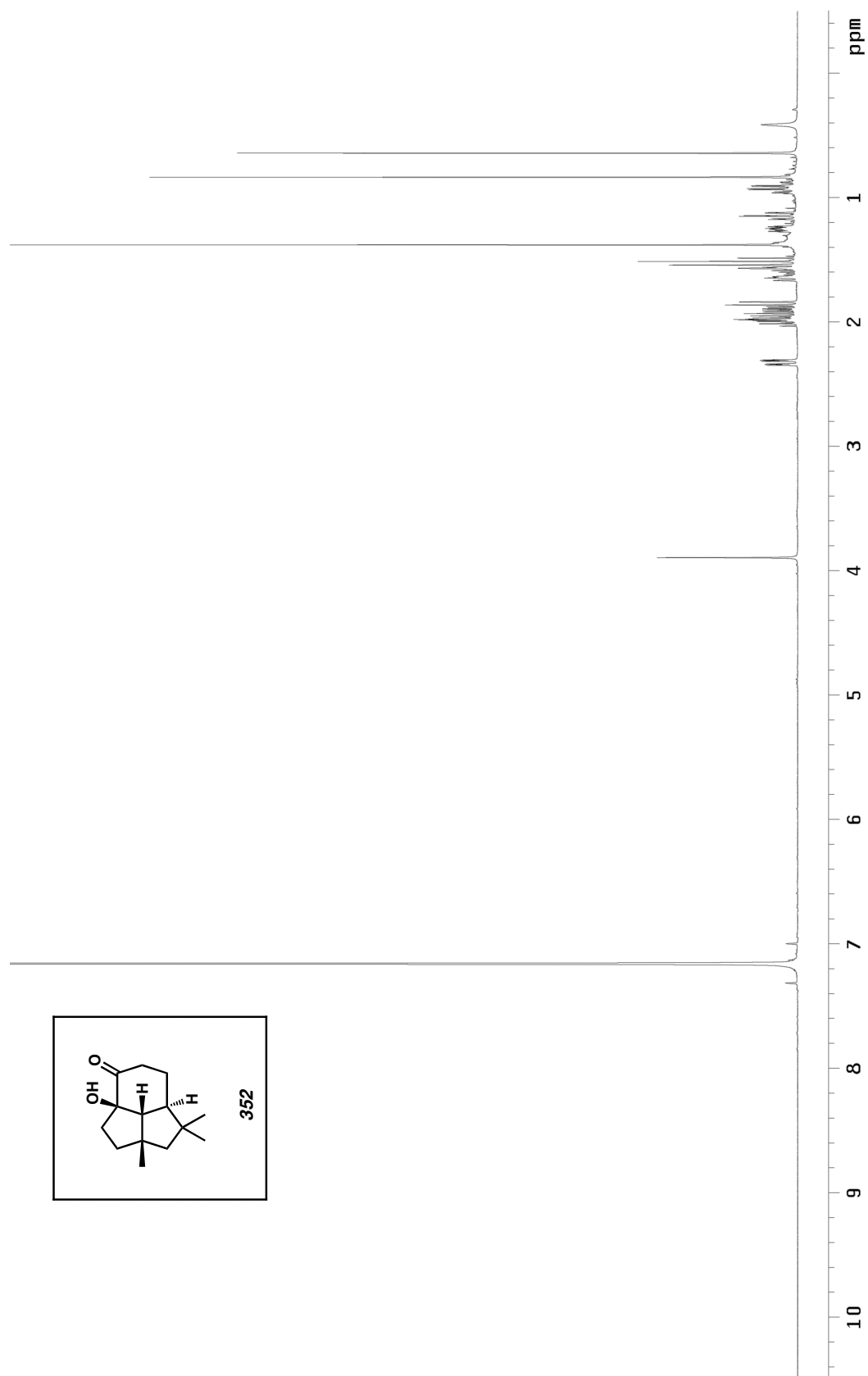


Figure A5.86. ^1H NMR (500 MHz, C_6D_6) of compound 352.

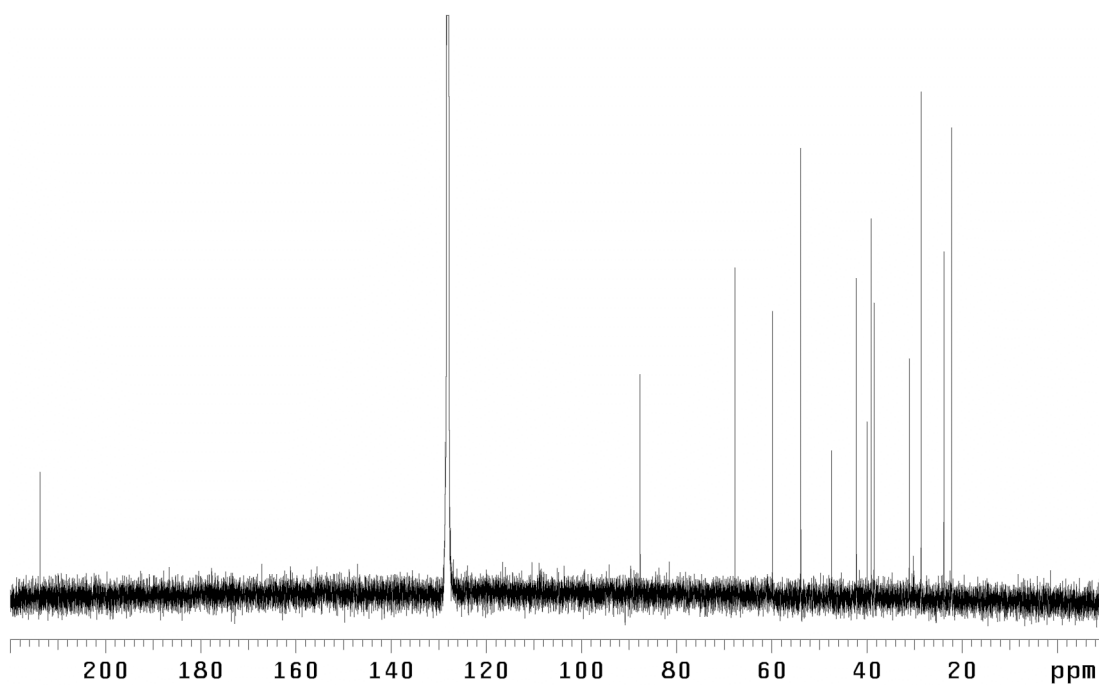


Figure A5.87. ^{13}C NMR (125 MHz, C_6D_6) of compound **352**.

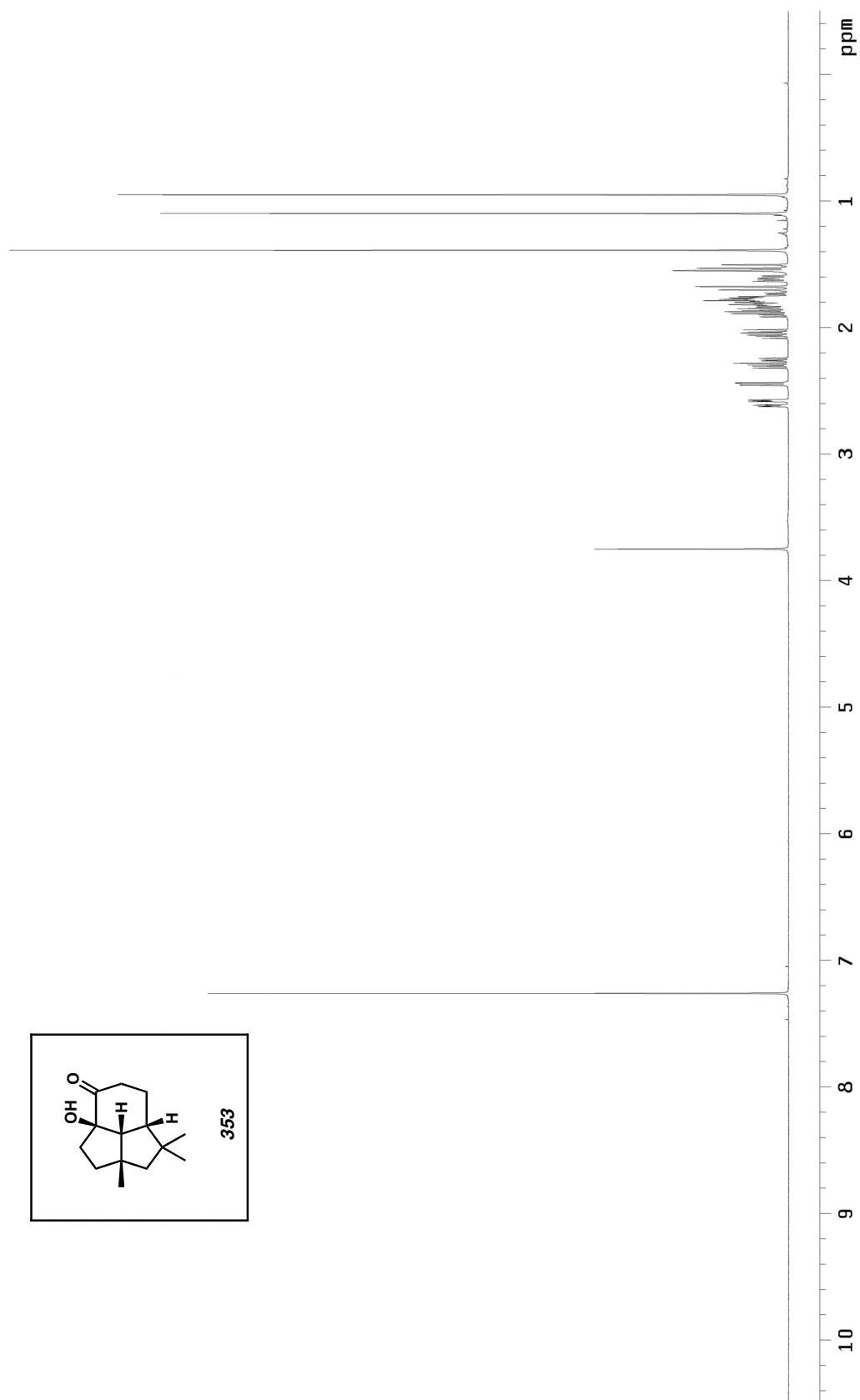


Figure A5.88. ^1H NMR (500 MHz, CDCl_3) of compound 353.

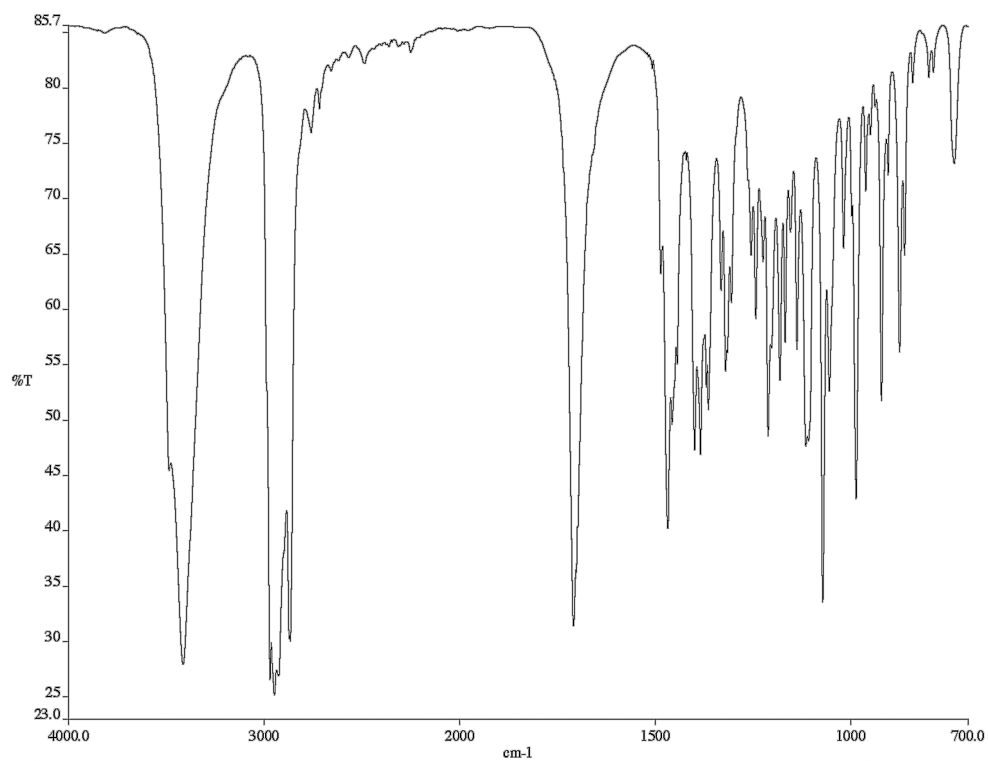


Figure A5.89. Infrared spectrum (thin film/NaCl) of compound **353**.

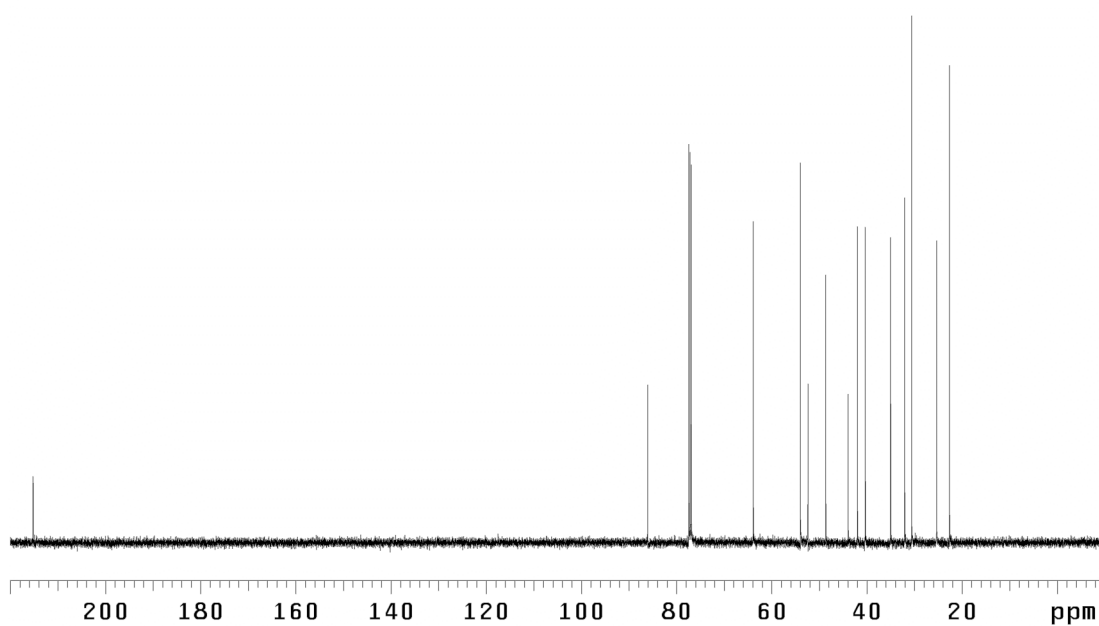


Figure A5.90. ¹³C NMR (125 MHz, CDCl₃) of compound **353**.

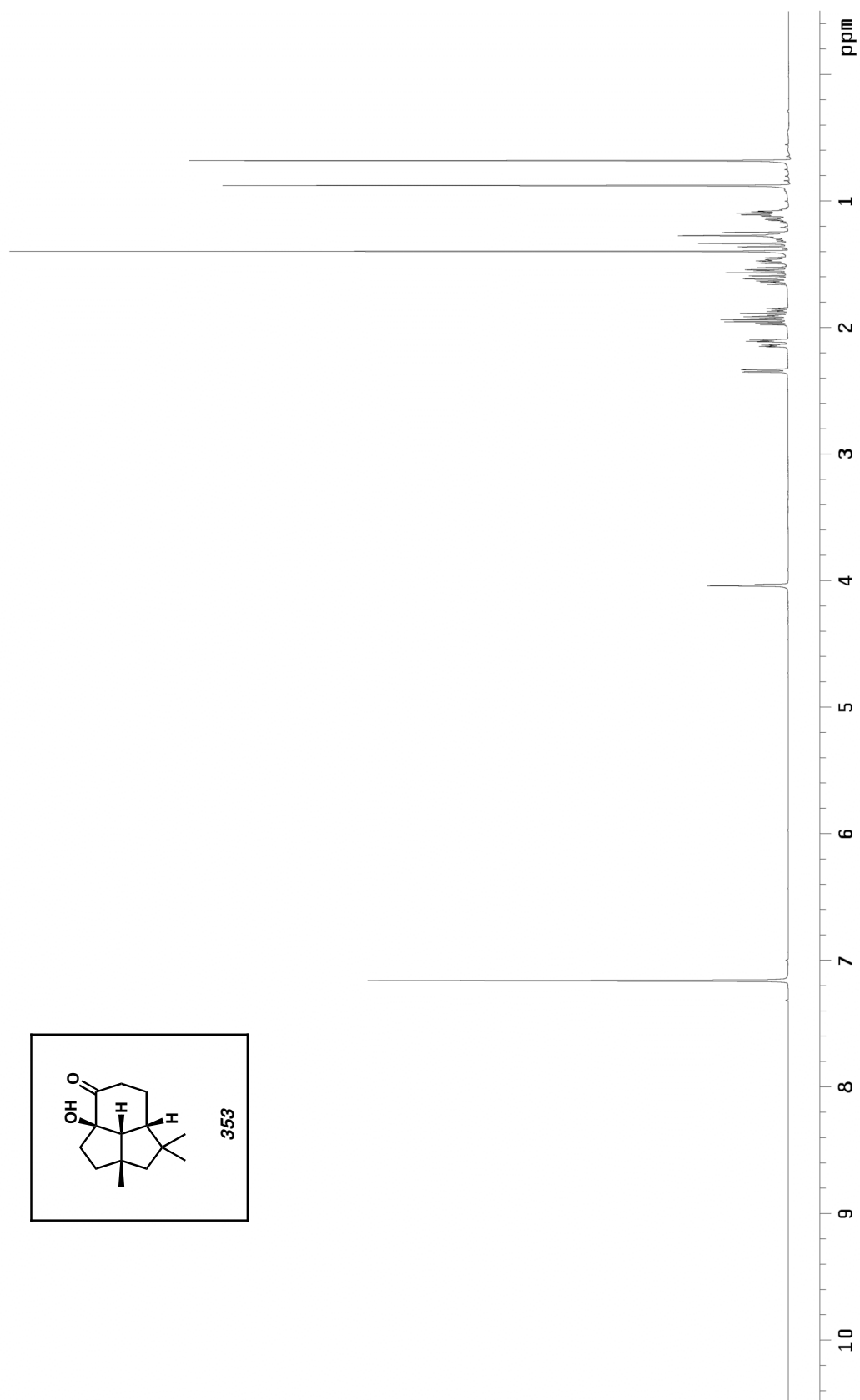


Figure A5.91. ^1H NMR (500 MHz, C_6D_6) of compound 353.

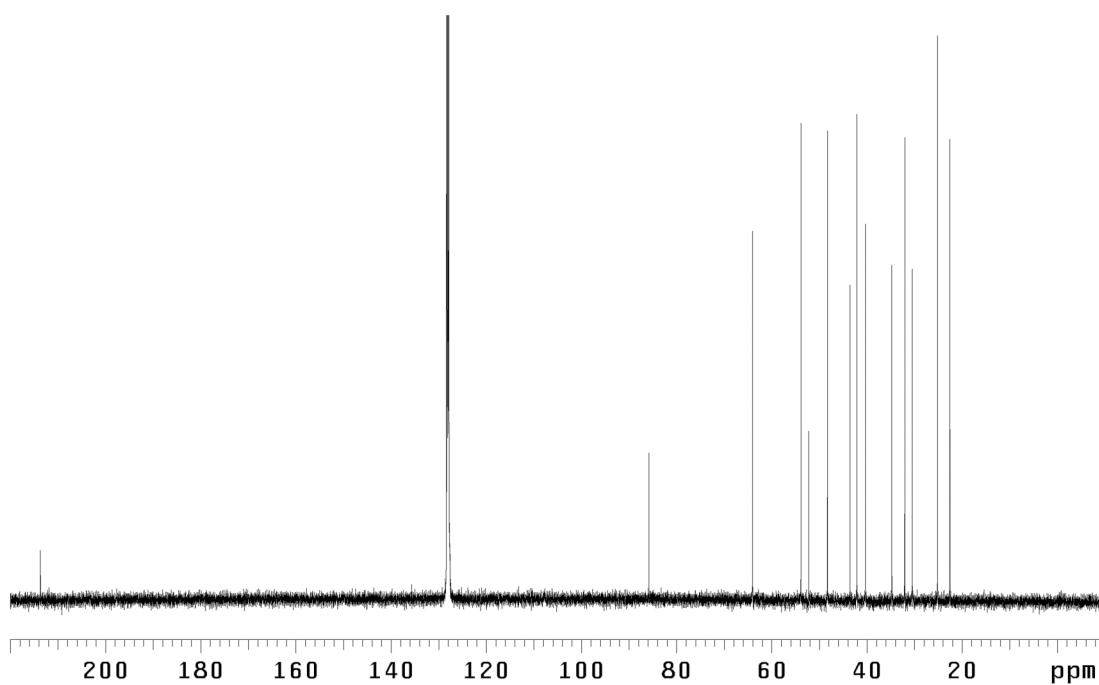


Figure A5.92. ^{13}C NMR (125 MHz, C_6D_6) of compound **353**.

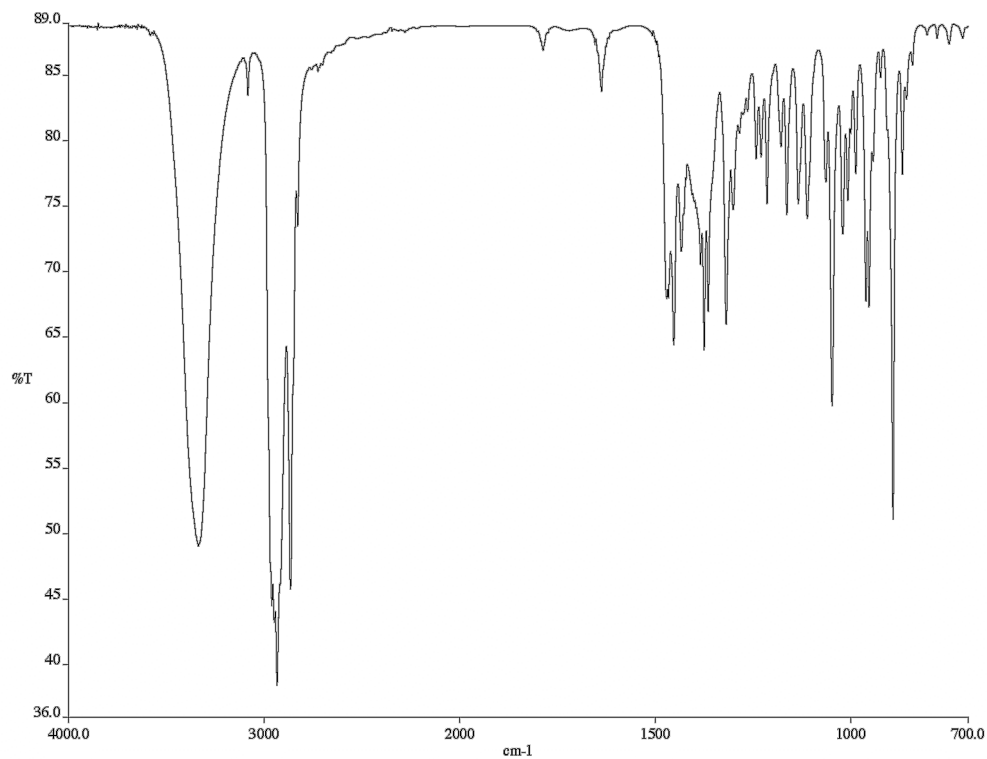


Figure A5.94. Infrared spectrum (thin film/NaCl) of compound **354**.

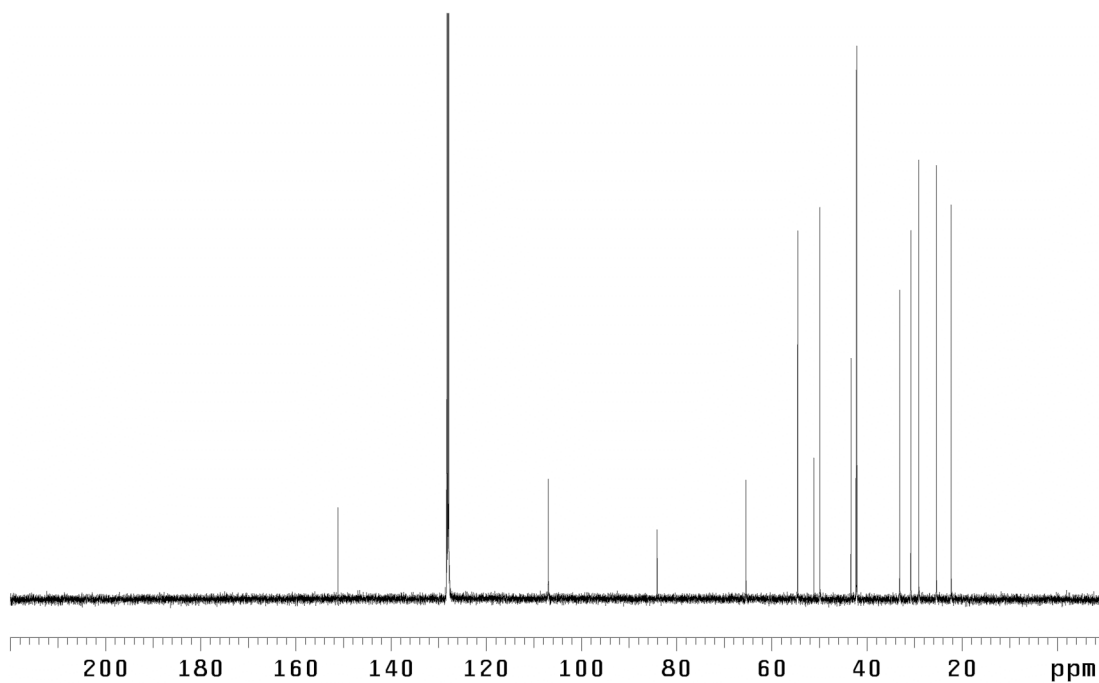


Figure A5.95. ¹³C NMR (125 MHz, C₆D₆) of compound **354**.

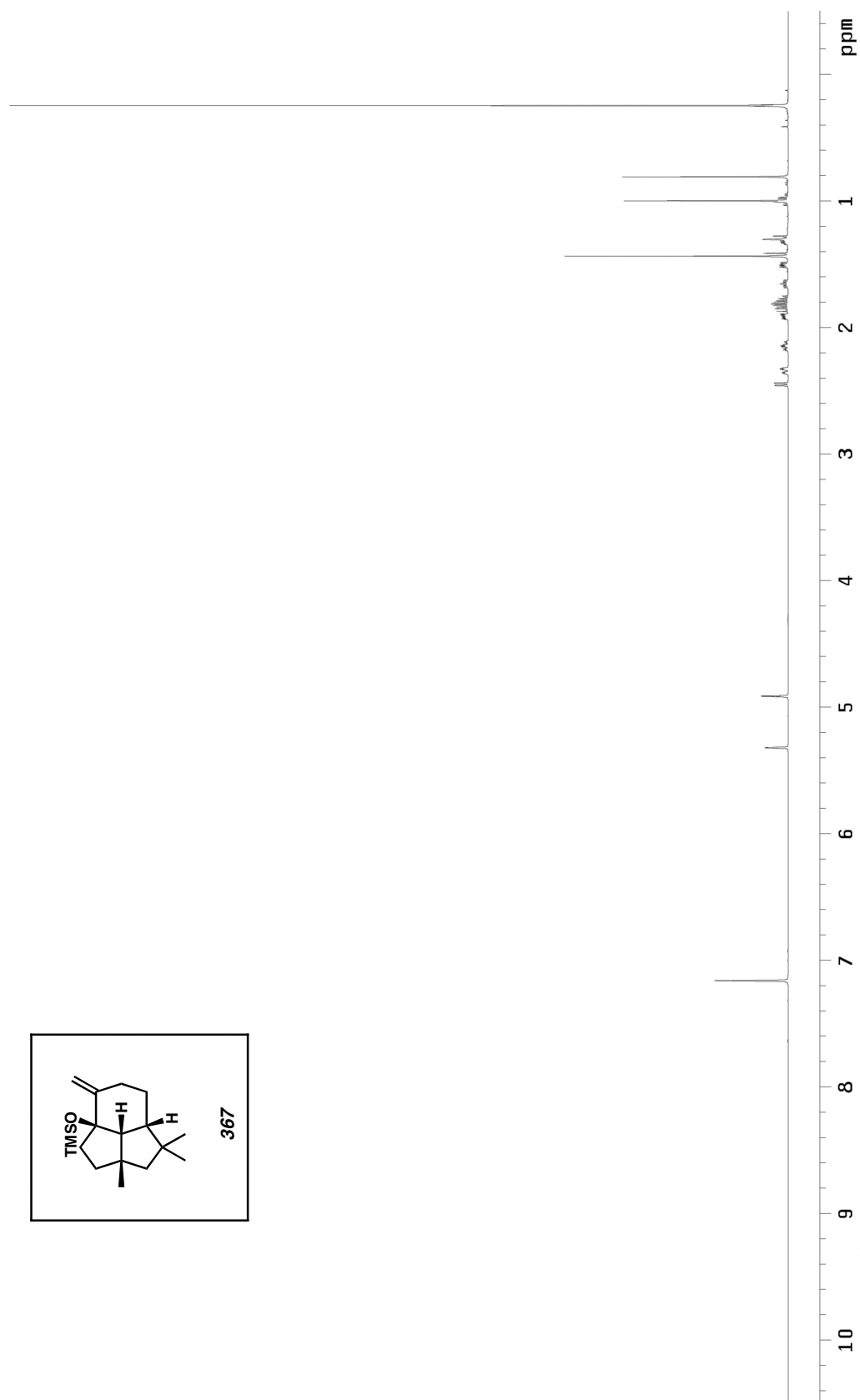


Figure A5.96. ¹H NMR (500 MHz, C₆D₆) of compound **367**.

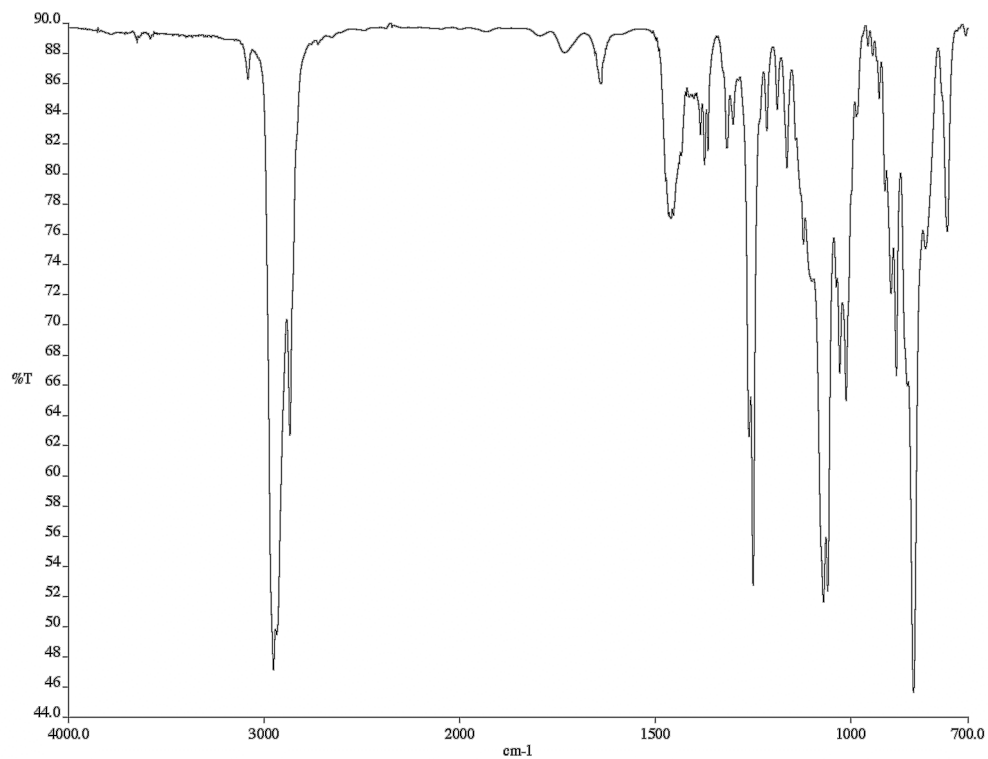


Figure A5.97. Infrared spectrum (thin film/NaCl) of compound **367**.

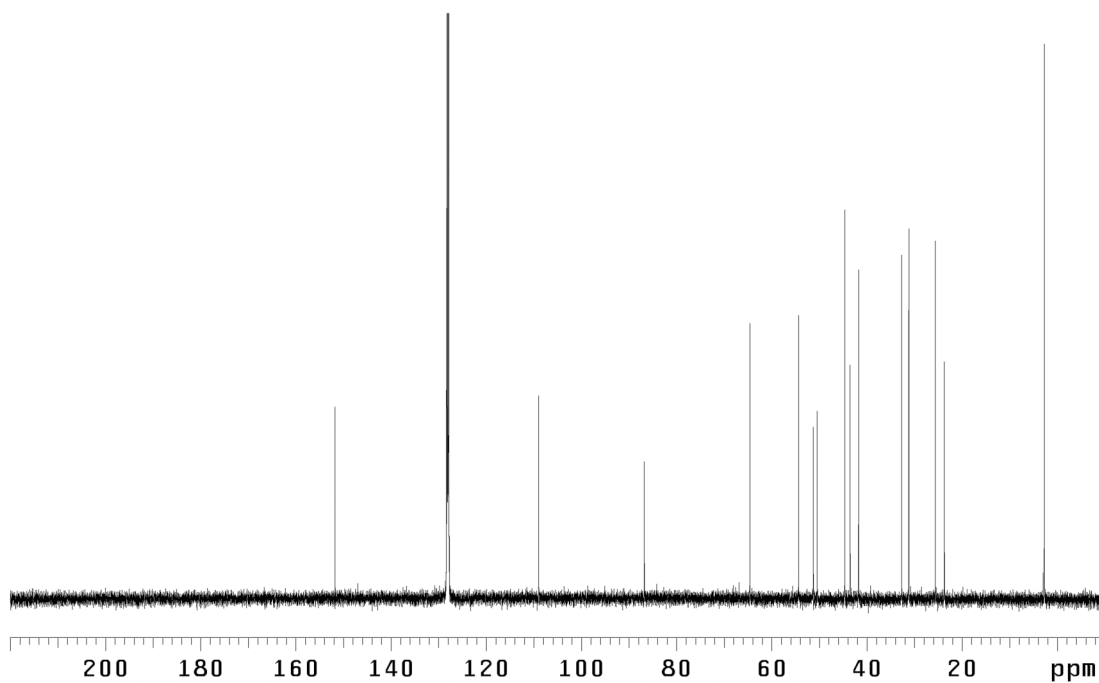
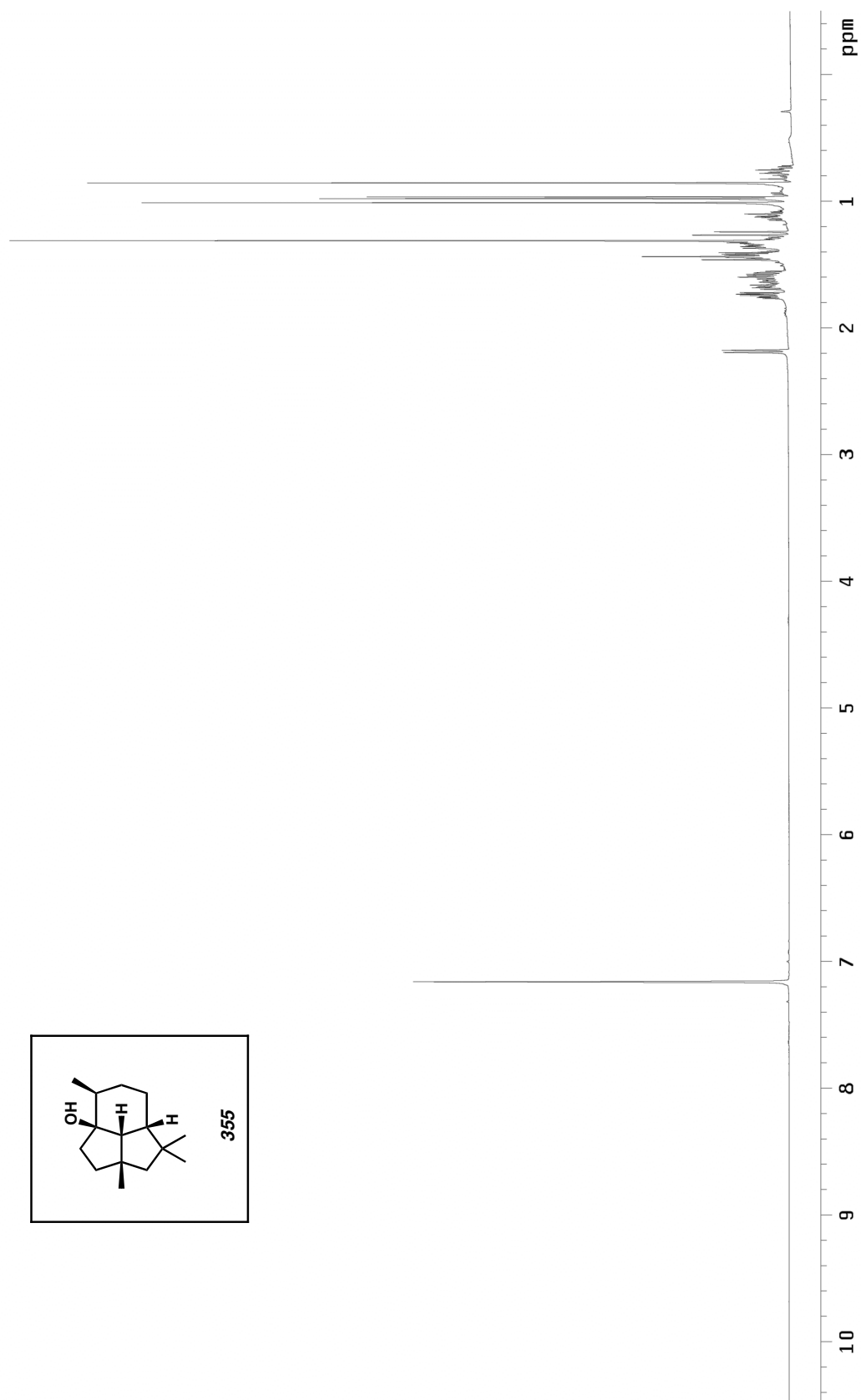


Figure A5.98. ¹³C NMR (125 MHz, C₆D₆) of compound **367**.

Figure A5.99. ^1H NMR (500 MHz, C_6D_6) of compound 355.

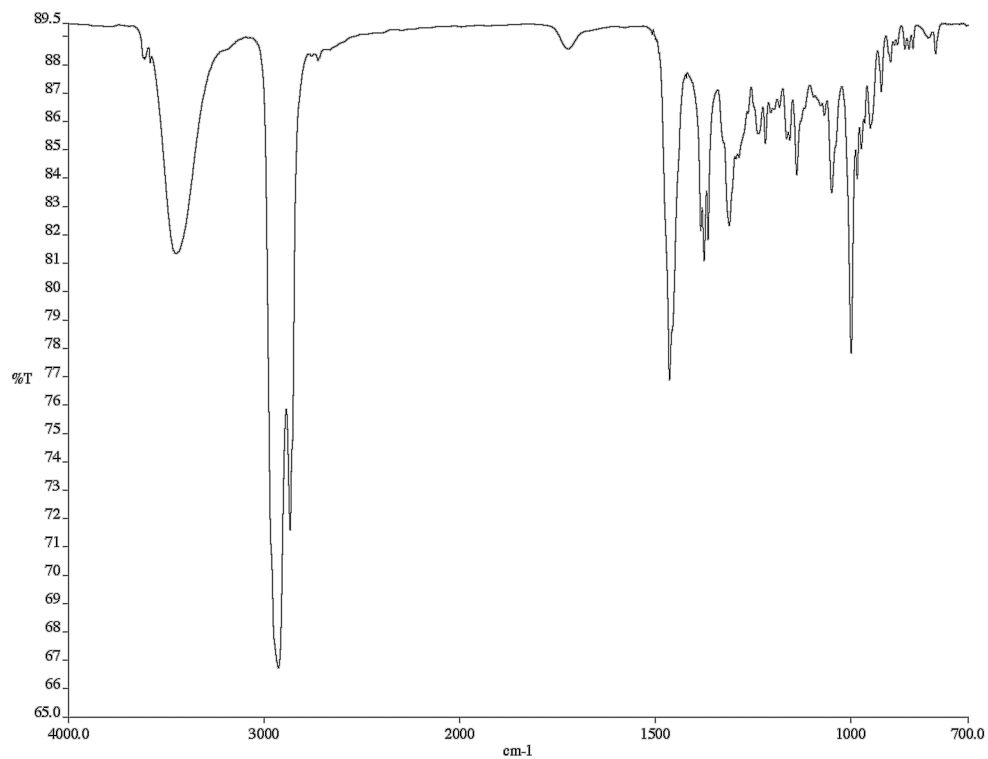


Figure A5.100. Infrared spectrum (thin film/NaCl) of compound **355**.

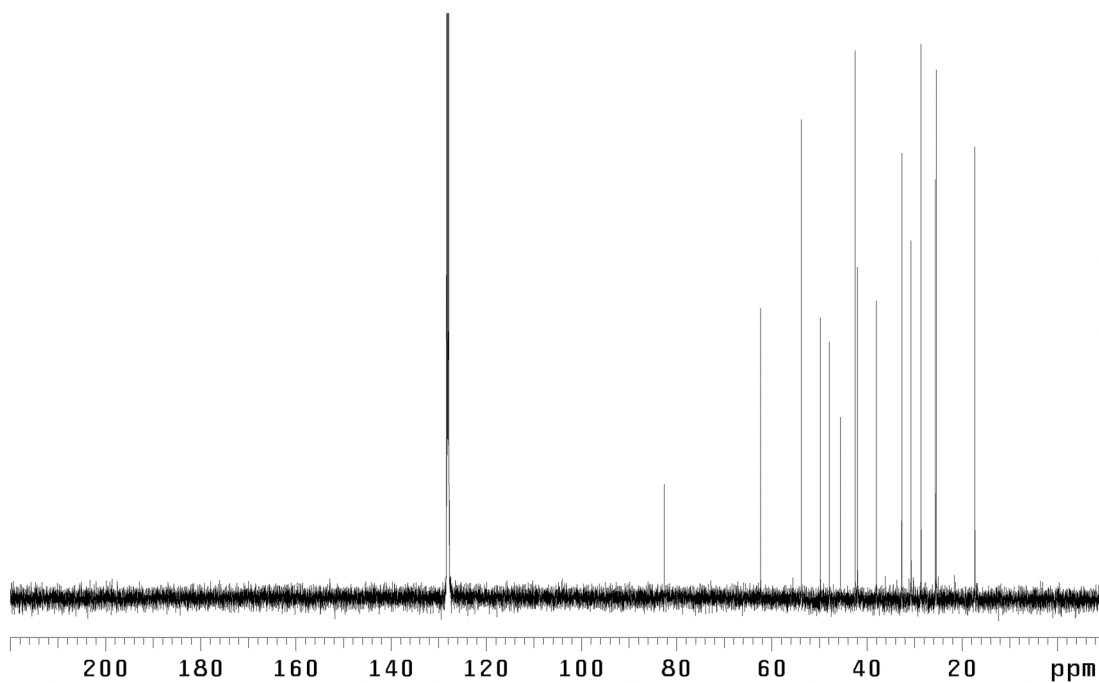


Figure A5.101. ¹³C NMR (125 MHz, C₆D₆) of compound **355**.

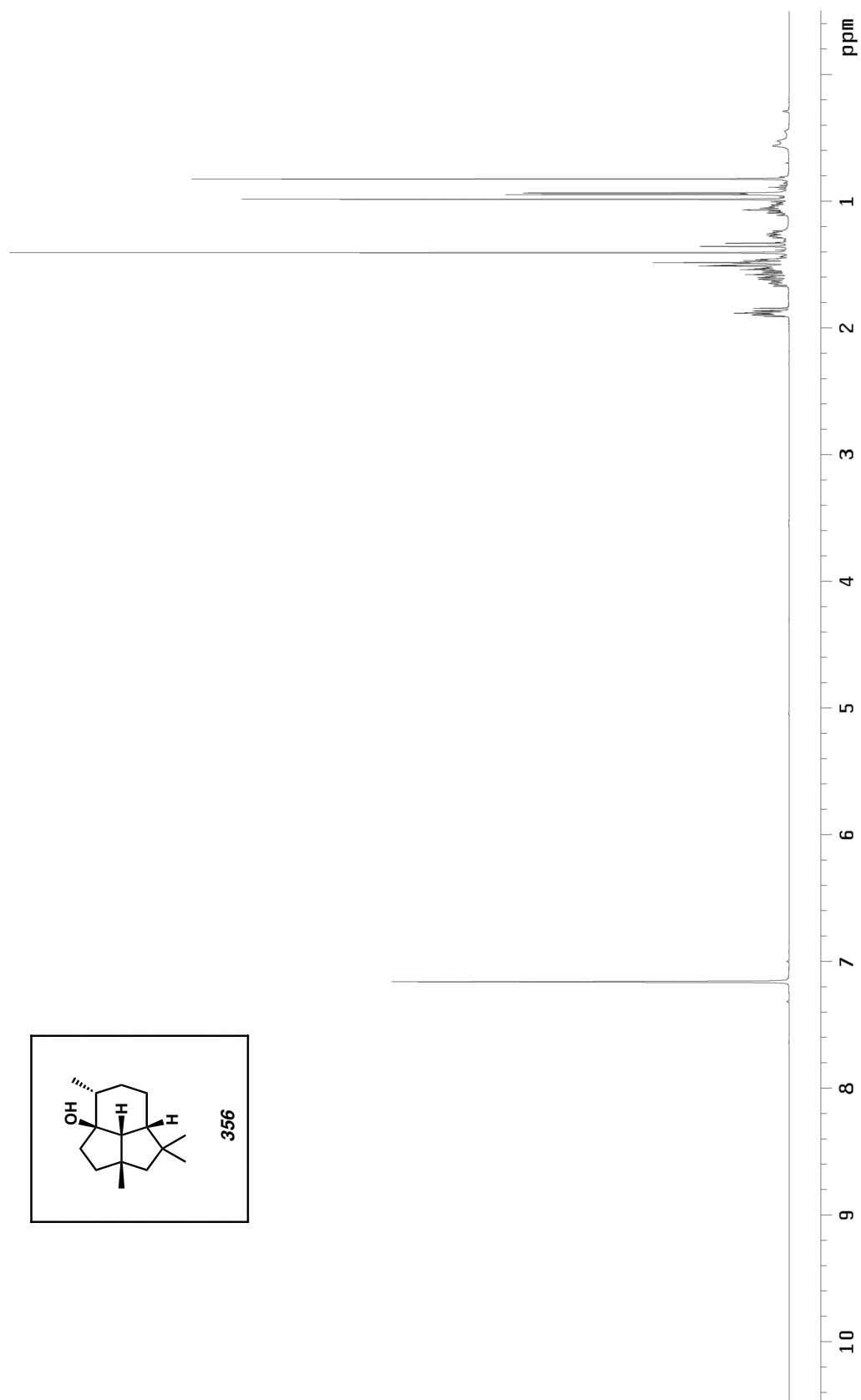


Figure A5.102. ^1H NMR (500 MHz, C_6D_6) of compound 356.

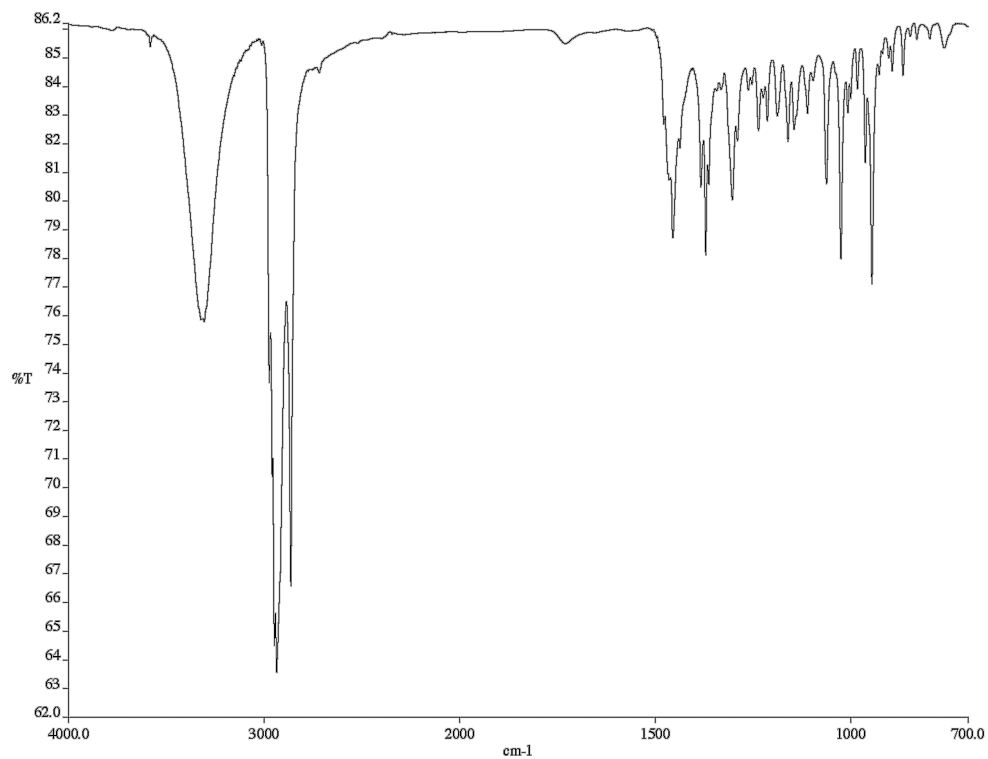


Figure A5.103. Infrared spectrum (thin film/NaCl) of compound **356**.

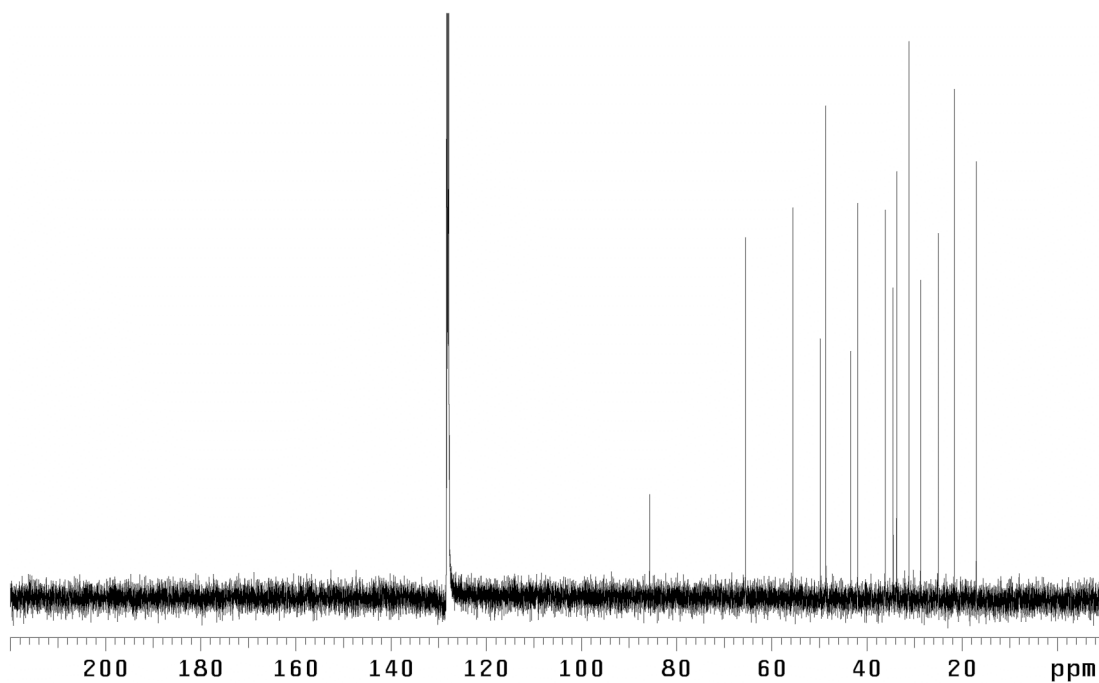


Figure A5.104. ¹³C NMR (125 MHz, C₆D₆) of compound **356**.

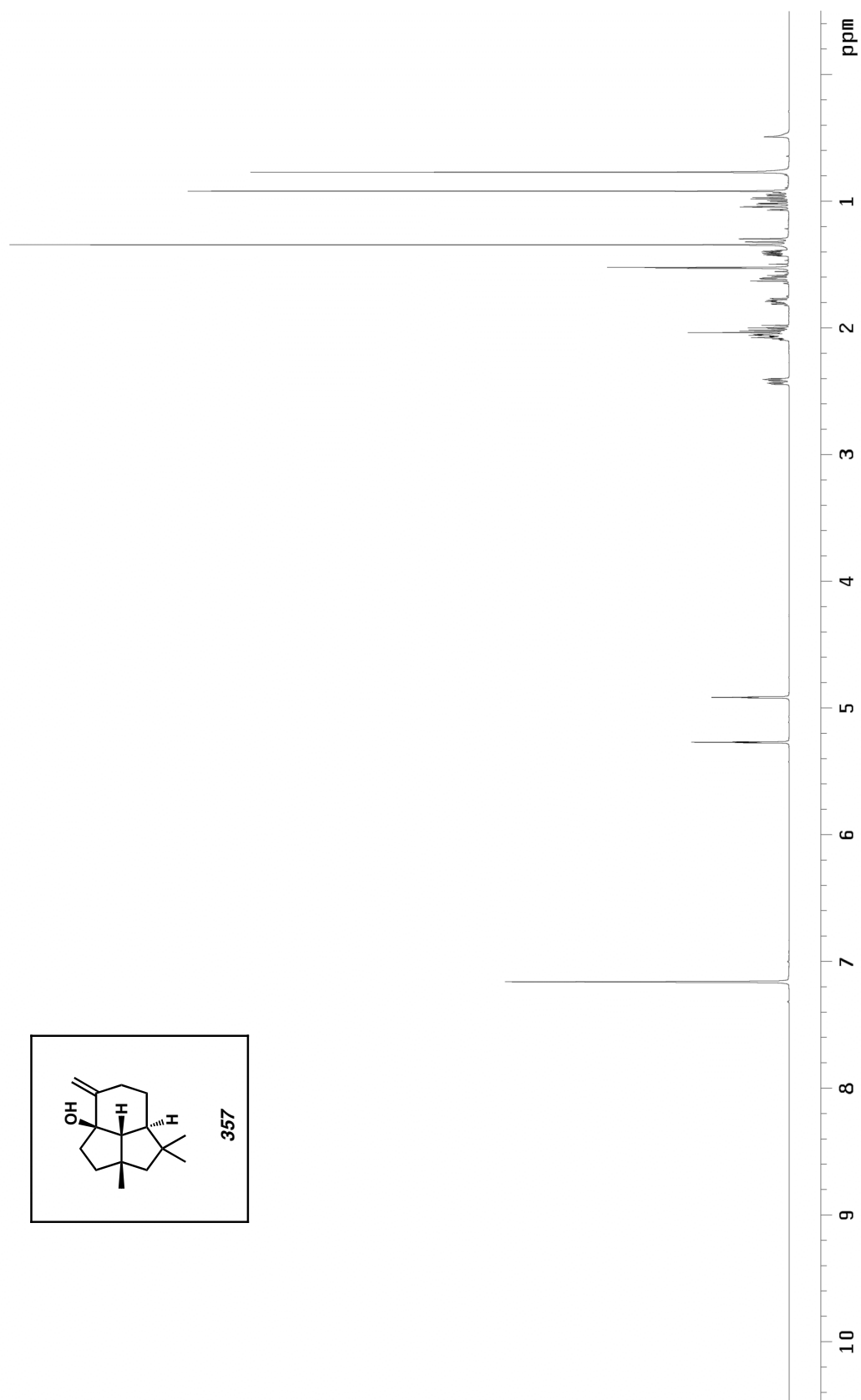


Figure A5.105. ¹H NMR (500 MHz, C₆D₆) of compound 357.

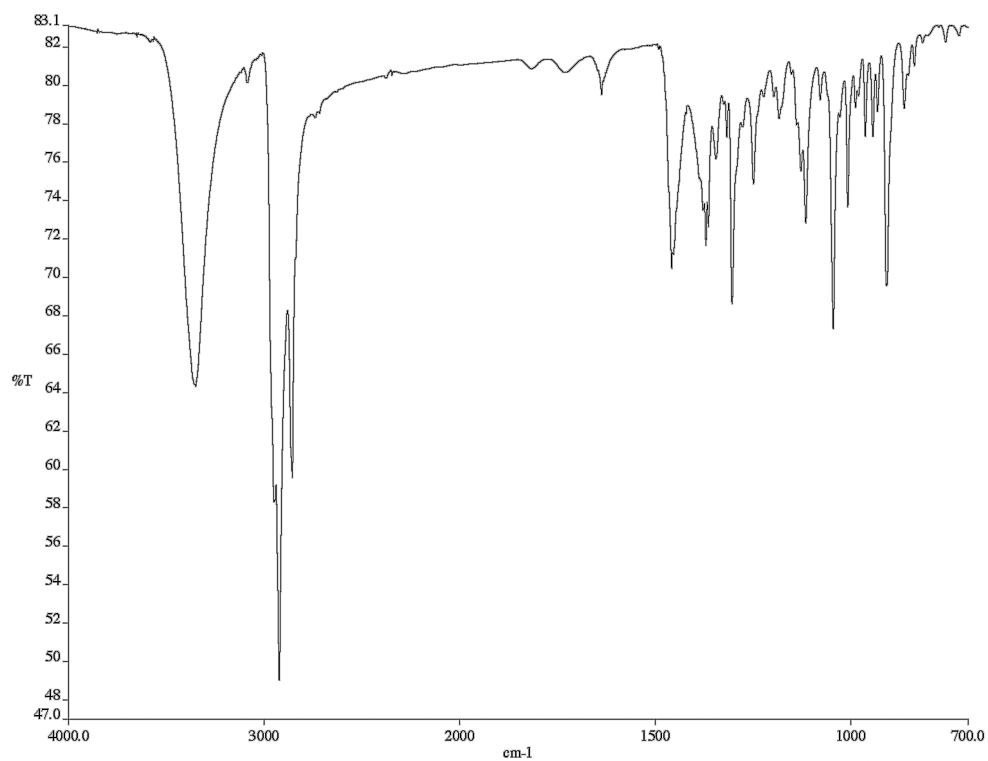


Figure A5.106. Infrared spectrum (thin film/NaCl) of compound **357**.

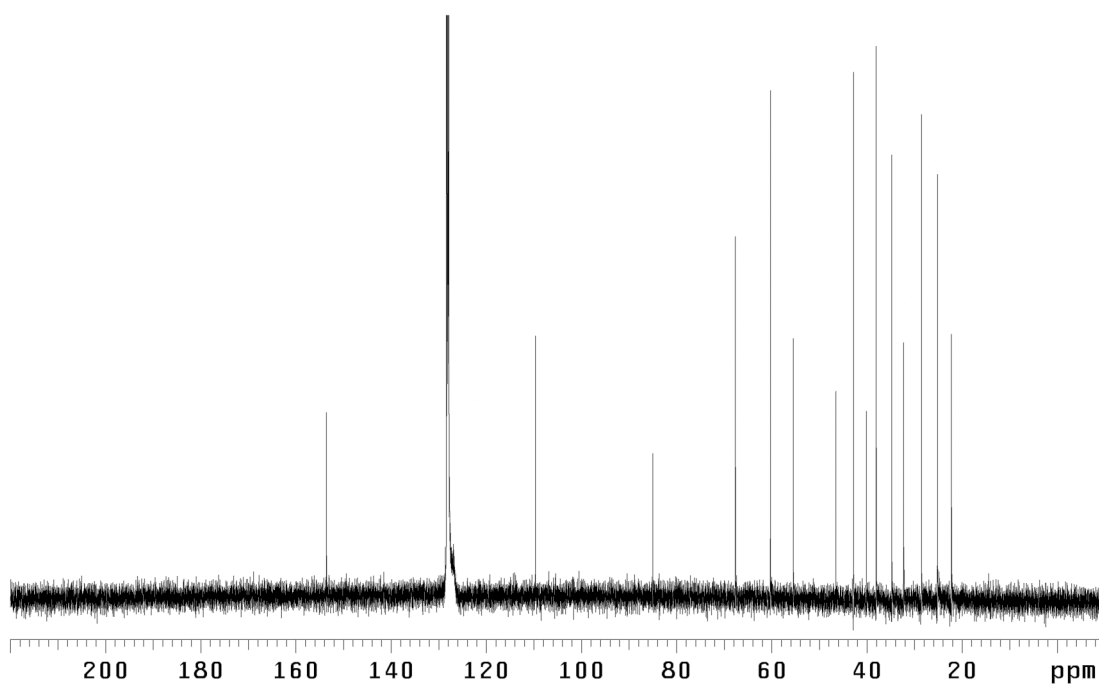


Figure A5.107. ¹³C NMR (125 MHz, C₆D₆) of compound **357**.

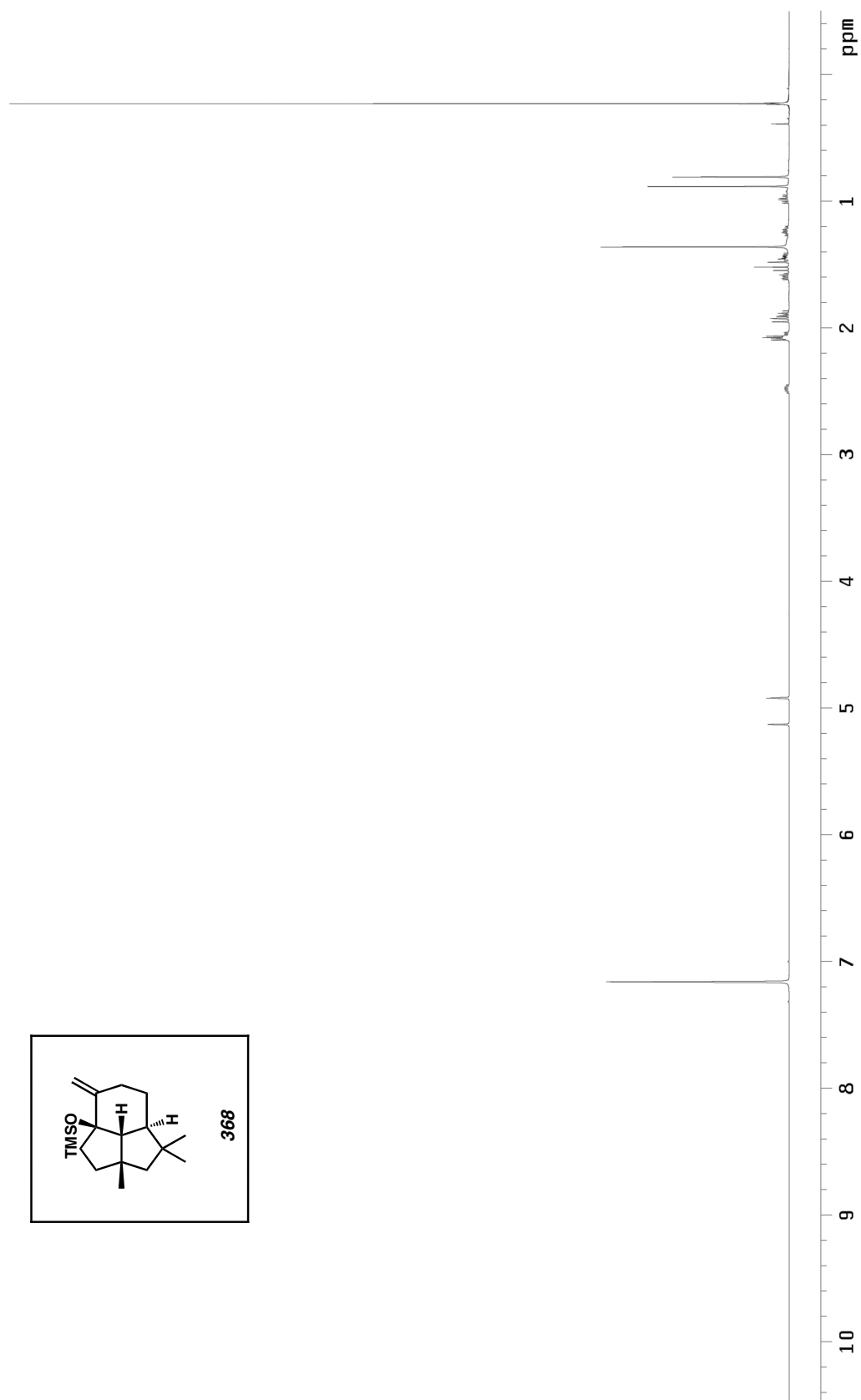


Figure A5.108. ¹H NMR (500 MHz, C₆D₆) of compound 368.

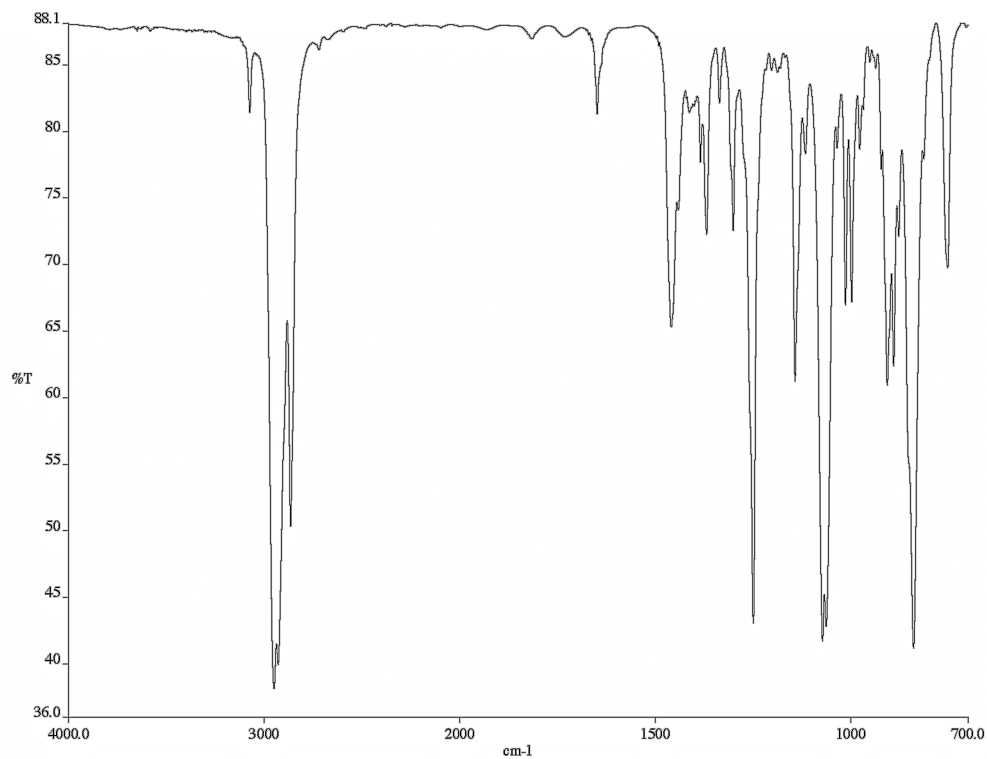


Figure A5.109. Infrared spectrum (thin film/NaCl) of compound **368**.

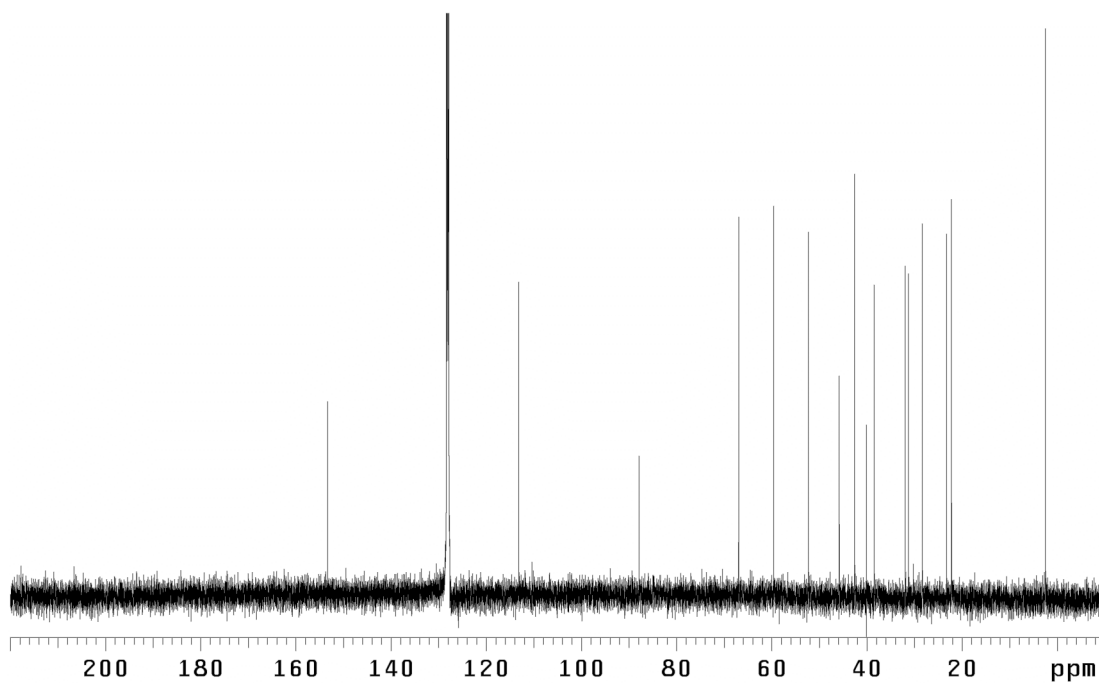


Figure A5.110. ^{13}C NMR (125 MHz, C_6D_6) of compound **368**.

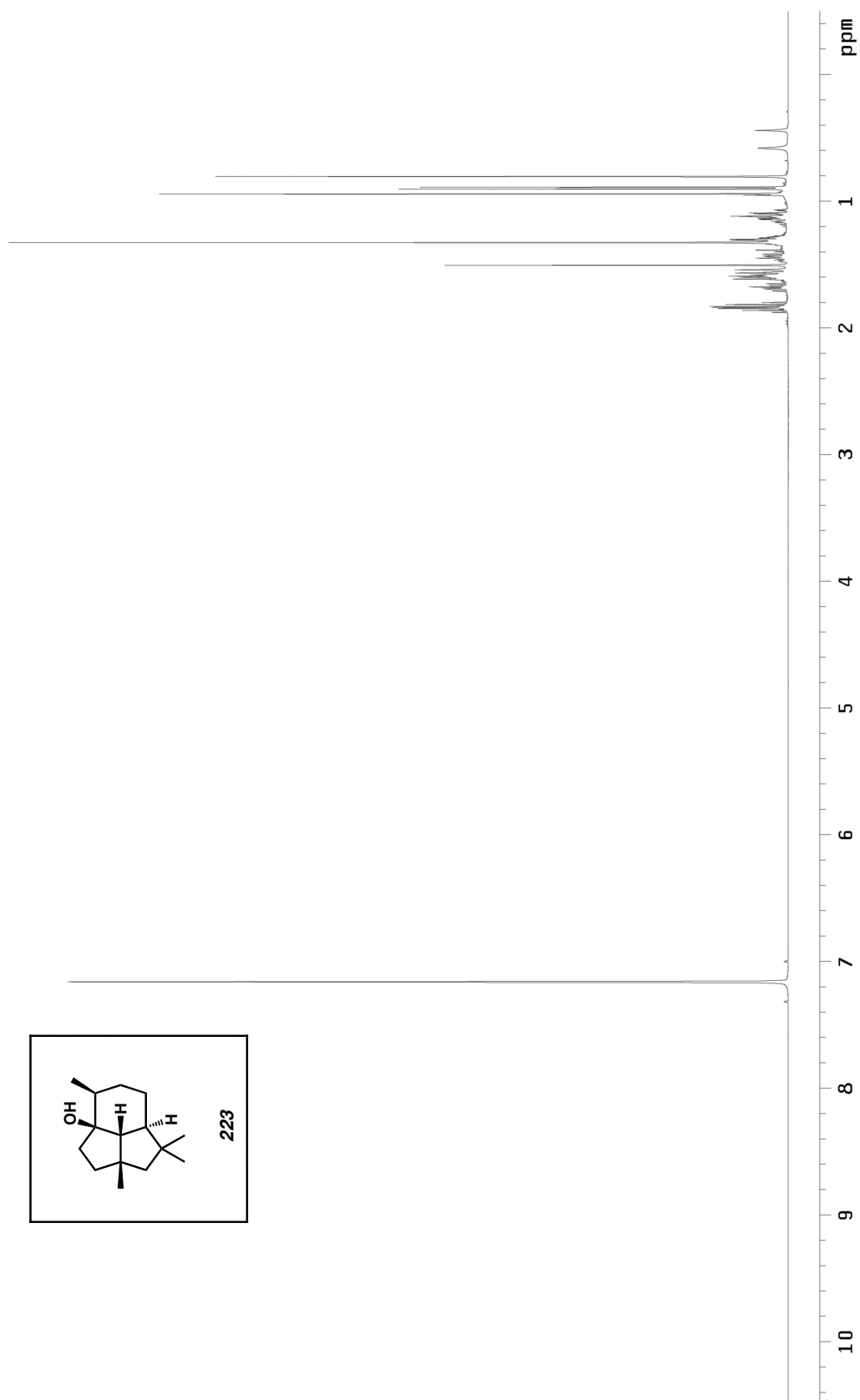


Figure A5.111. ^1H NMR (500 MHz, C_6D_6) of compound 223.

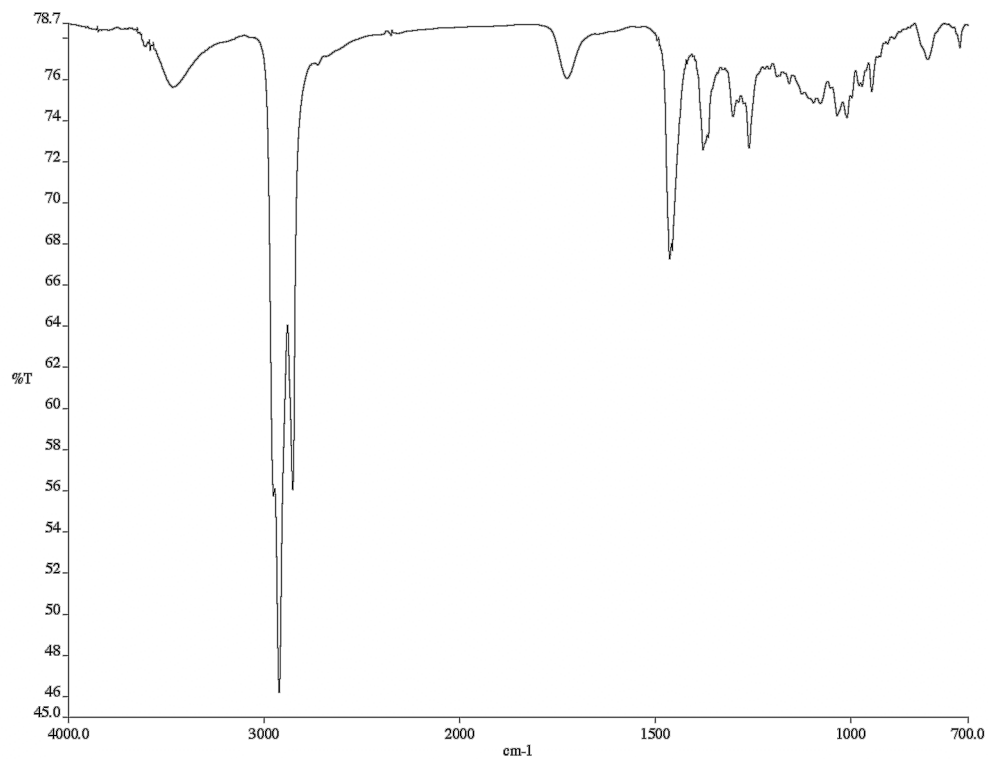


Figure A5.112. Infrared spectrum (thin film/NaCl) of compound **223**.

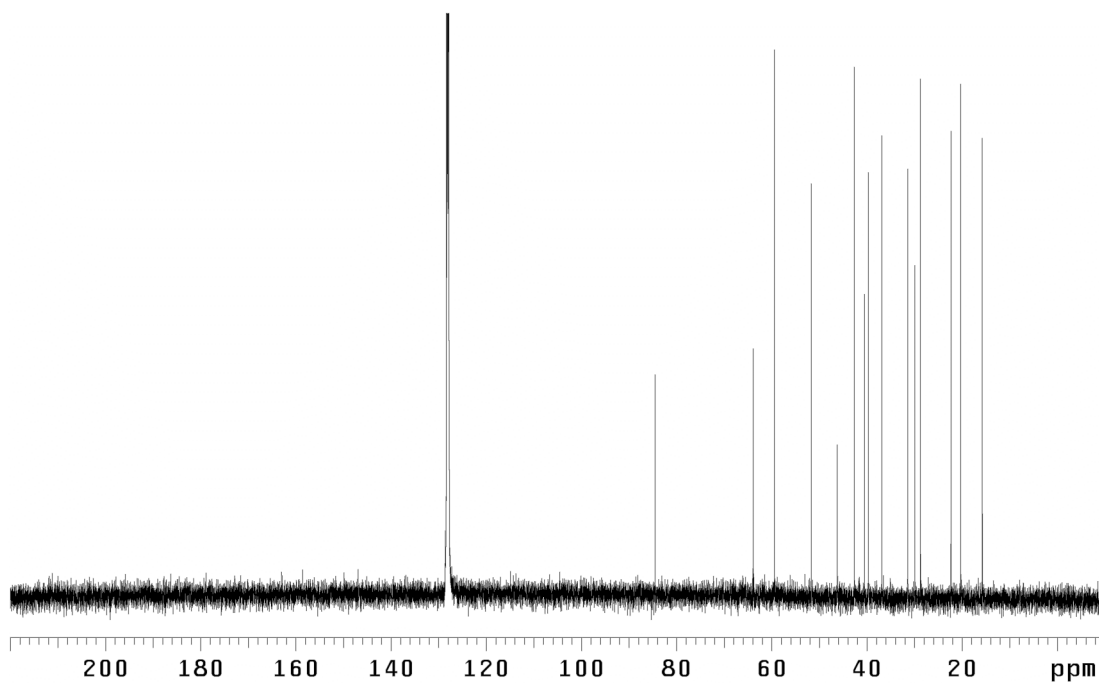


Figure A5.113. ¹³C NMR (125 MHz, C₆D₆) of compound **223**.

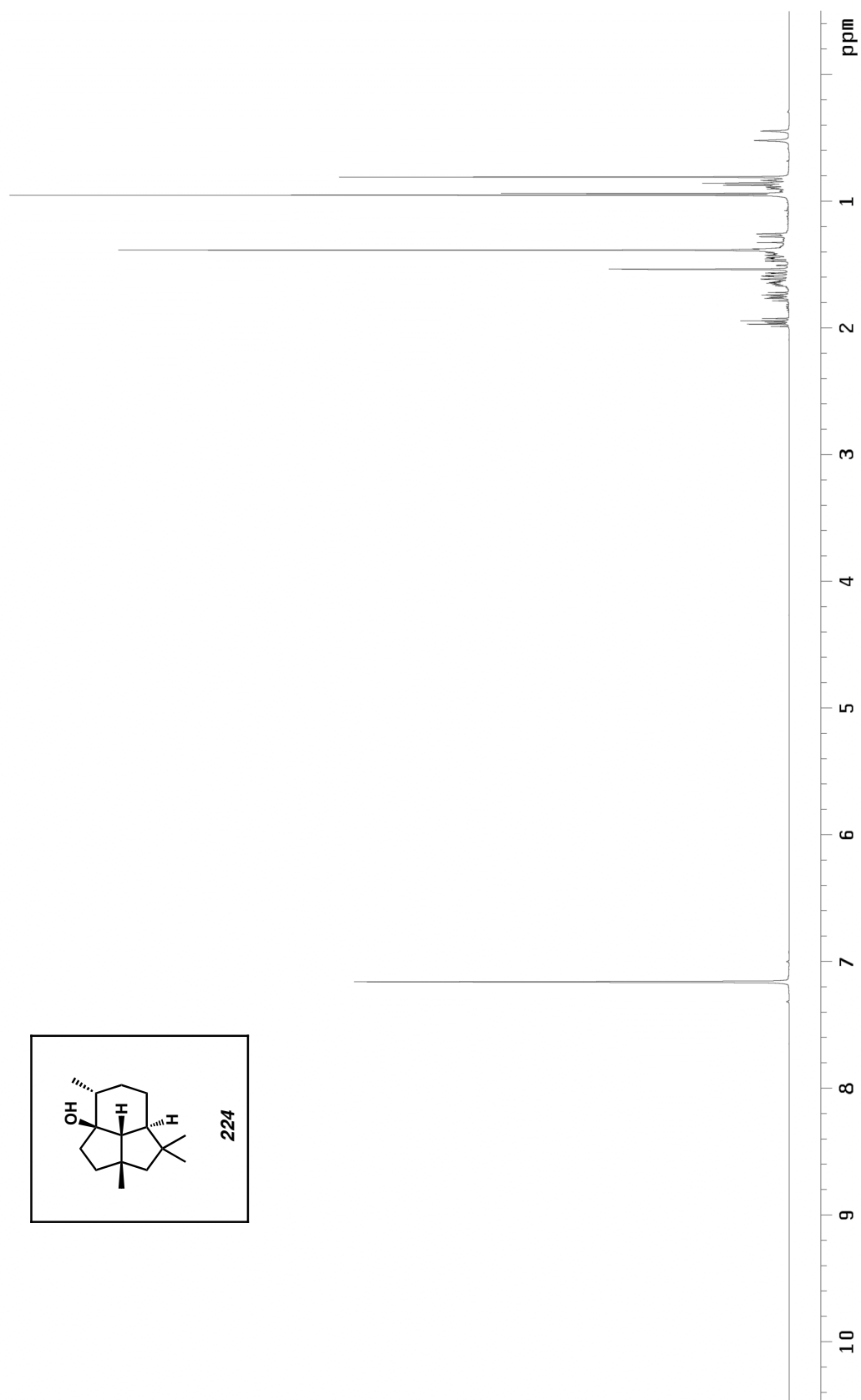


Figure A5.114. ^1H NMR (500 MHz, C_6D_6) of compound 224.

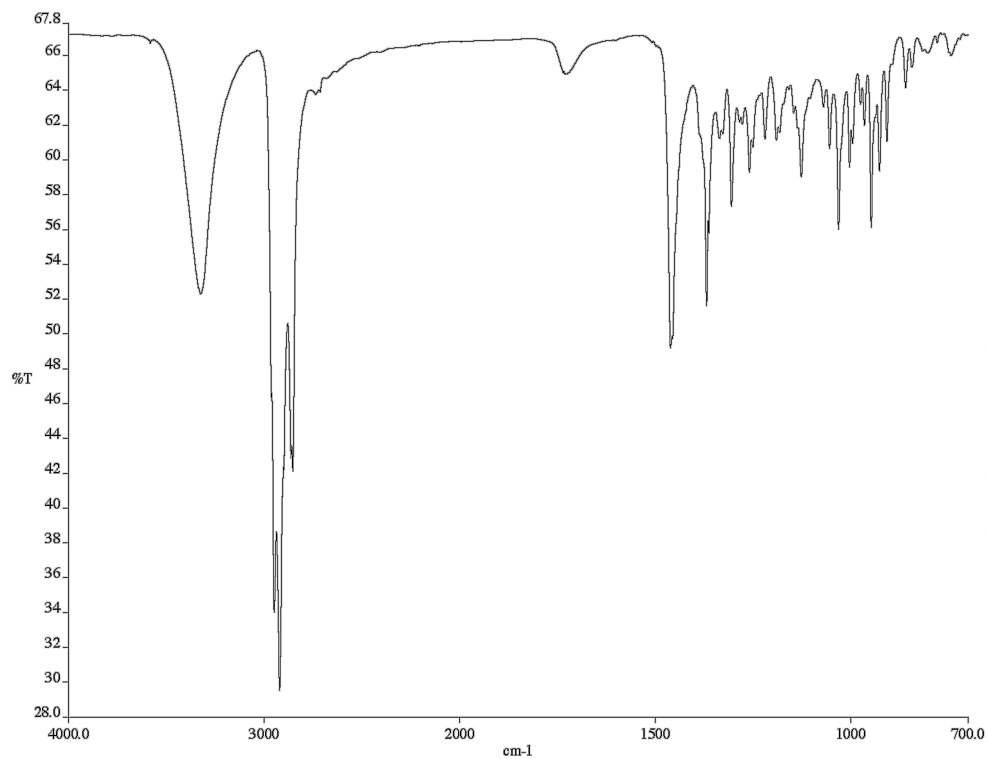


Figure A5.115. Infrared spectrum (thin film/NaCl) of compound **224**.

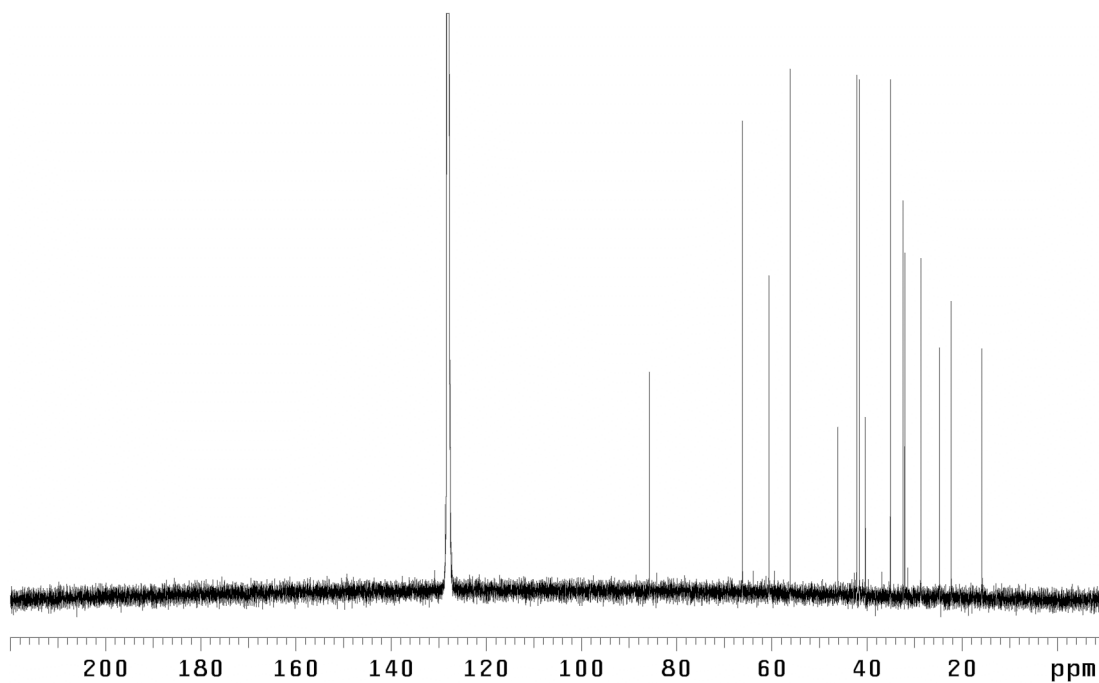


Figure A5.116. ^{13}C NMR (125 MHz, C_6D_6) of compound **224**.

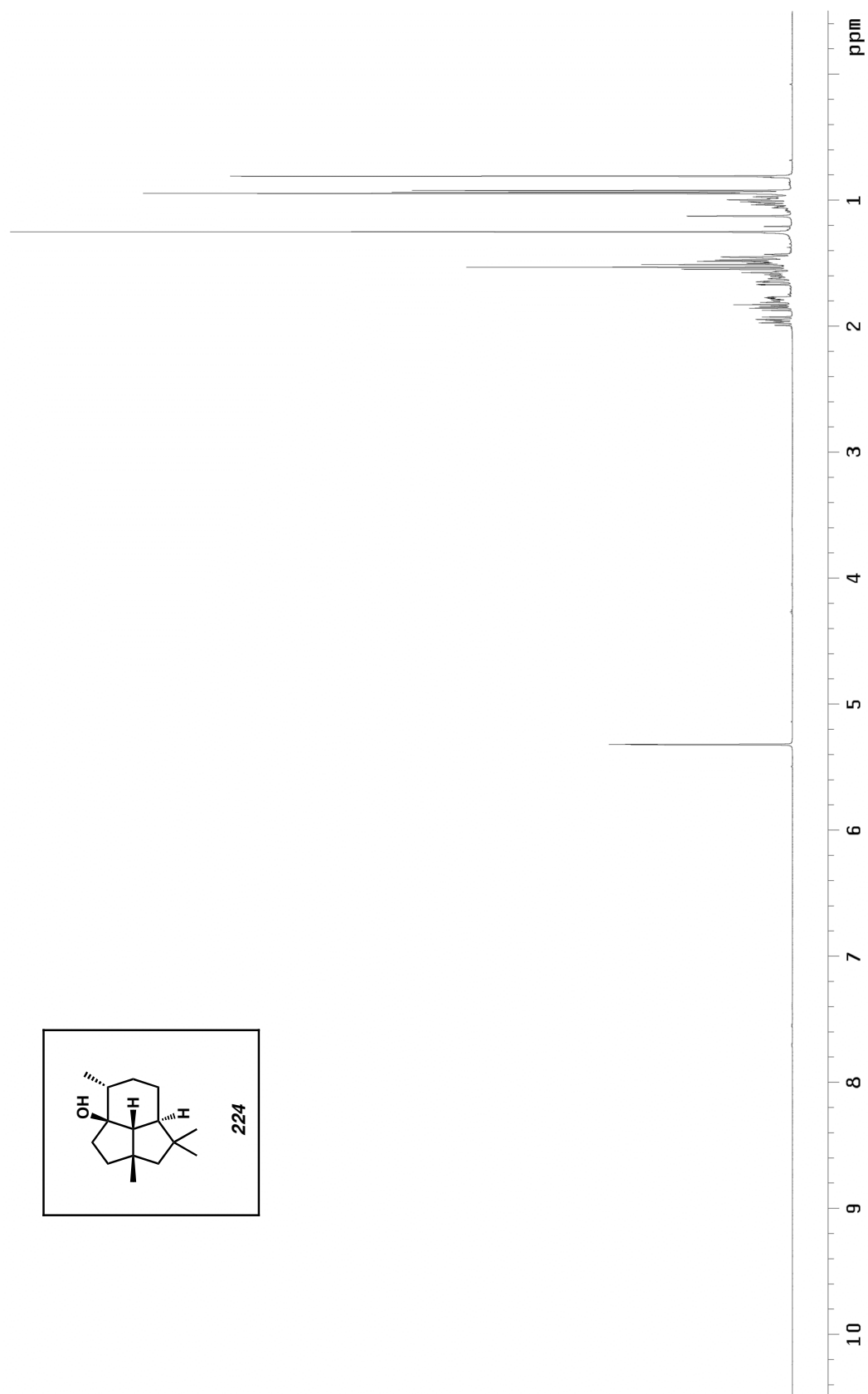


Figure A5.117. ^1H NMR (500 MHz, CD_2Cl_2) of compound **224**.

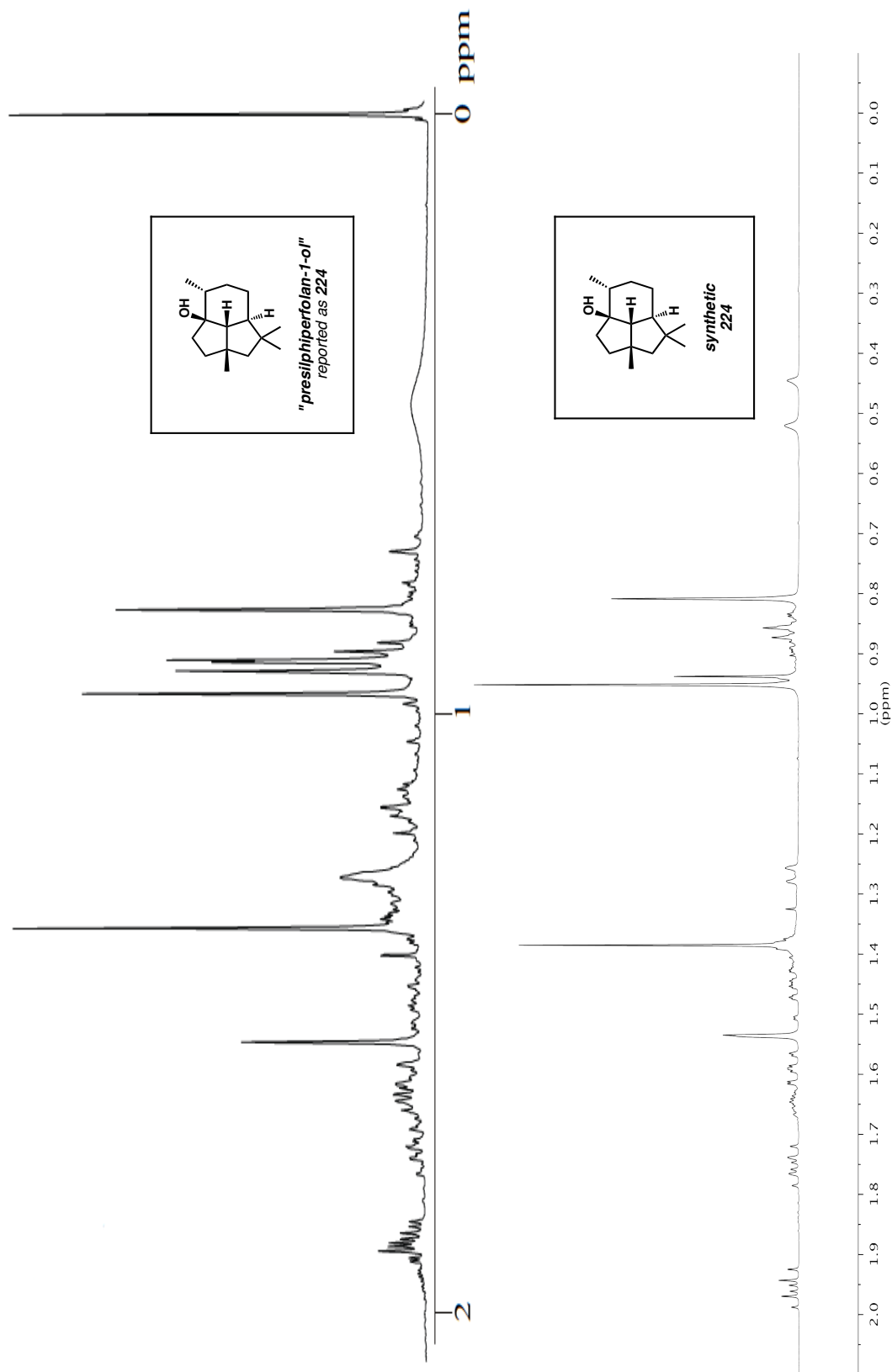


Figure A5.118. ^1H NMR comparison of reported natural compound **224** (500 MHz, C_6D_6) and synthetic compound **224** (500 MHz, C_6D_6).

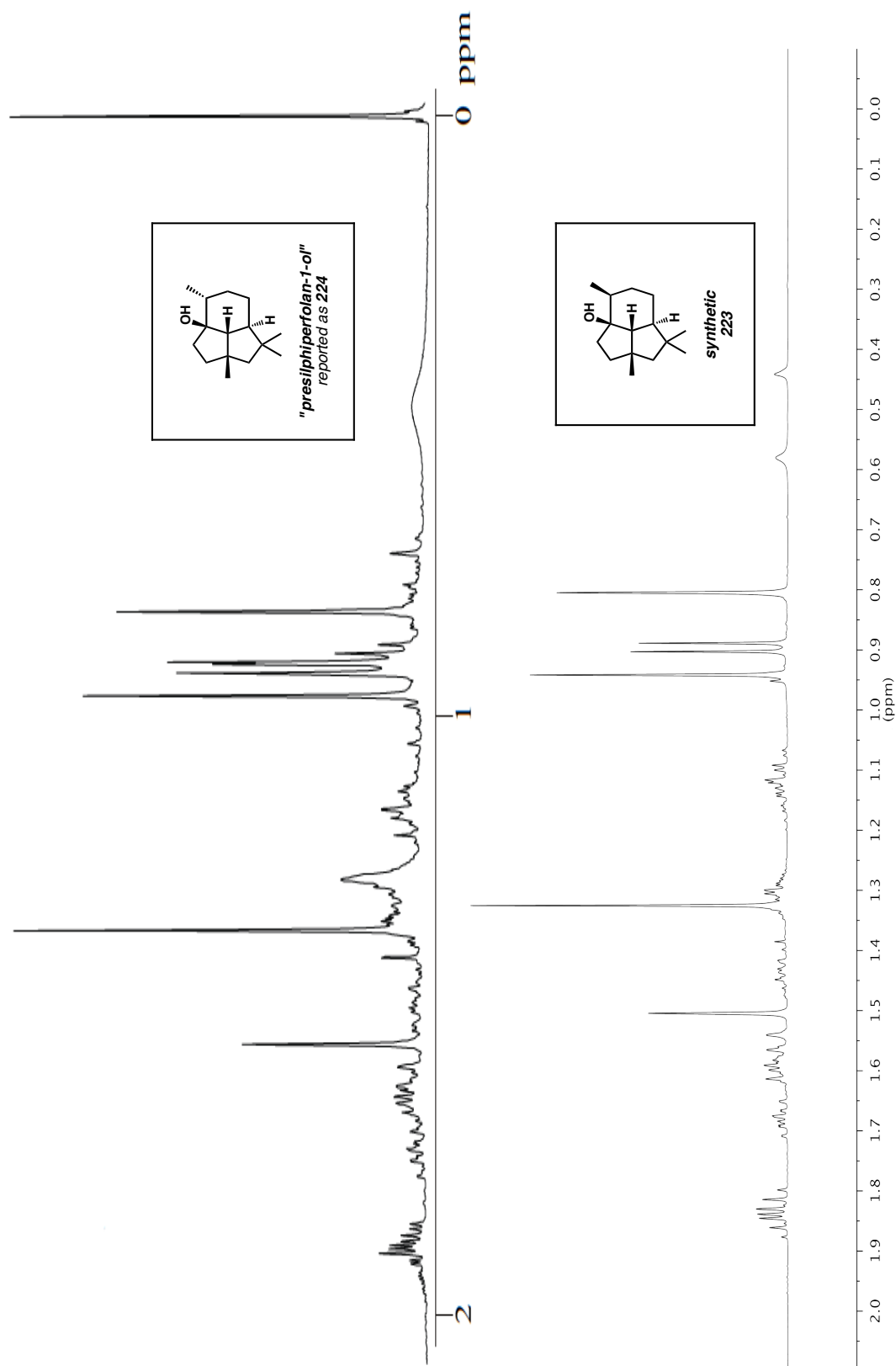


Figure A5.119. ^1H NMR comparison of reported natural compound **224** (500 MHz, C_6D_6) and synthetic compound **223** (500 MHz, C_6D_6).

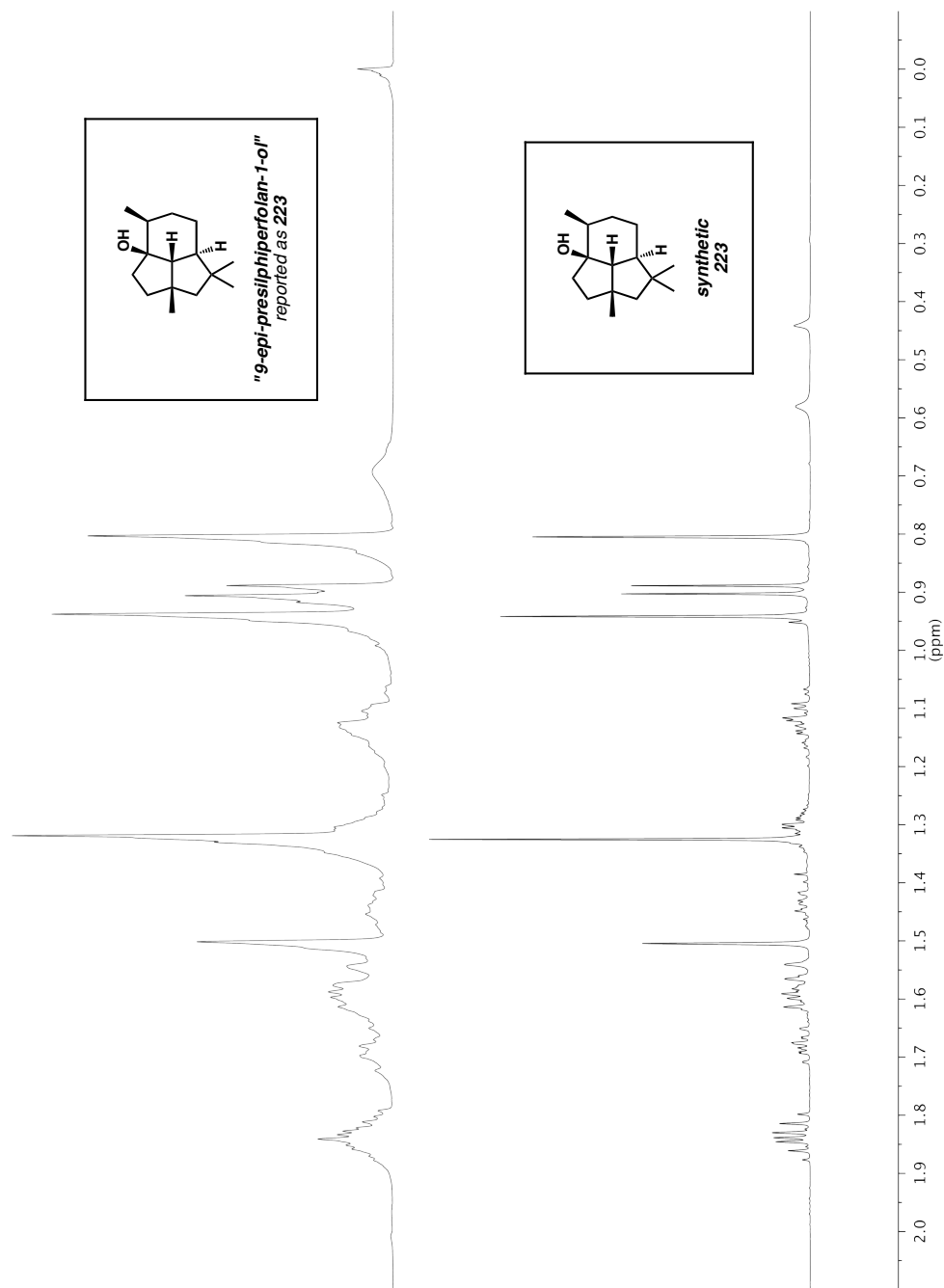


Figure A5.120. ^1H NMR comparison of reported natural compound **223** (400 MHz, C_6D_6) and synthetic compound **223** (500 MHz, C_6D_6).

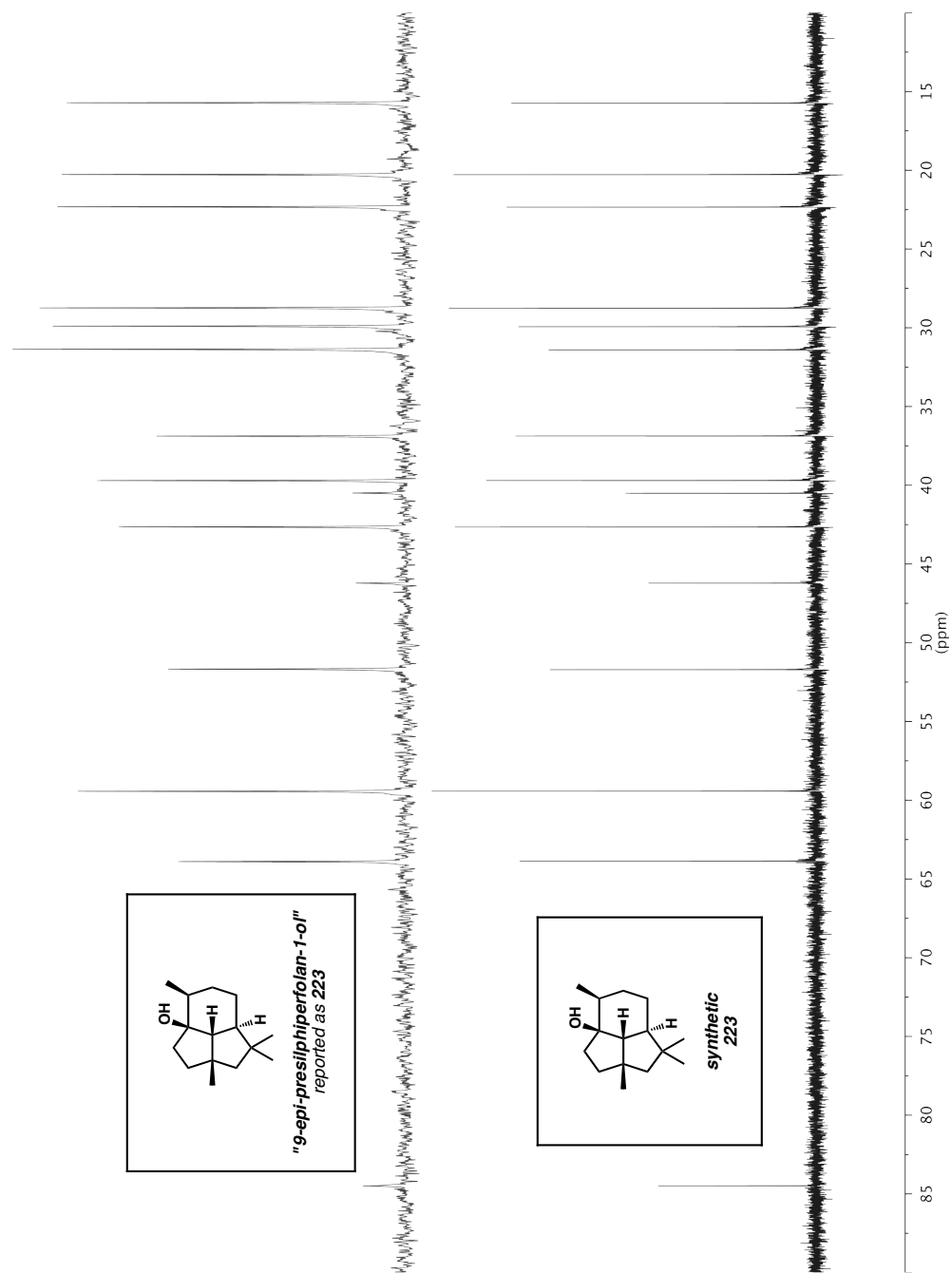


Figure A5.121. ^{13}C NMR comparison of reported natural compound **223** (100 MHz, C_6D_6) and synthetic compound **223** (125 MHz, C_6D_6).

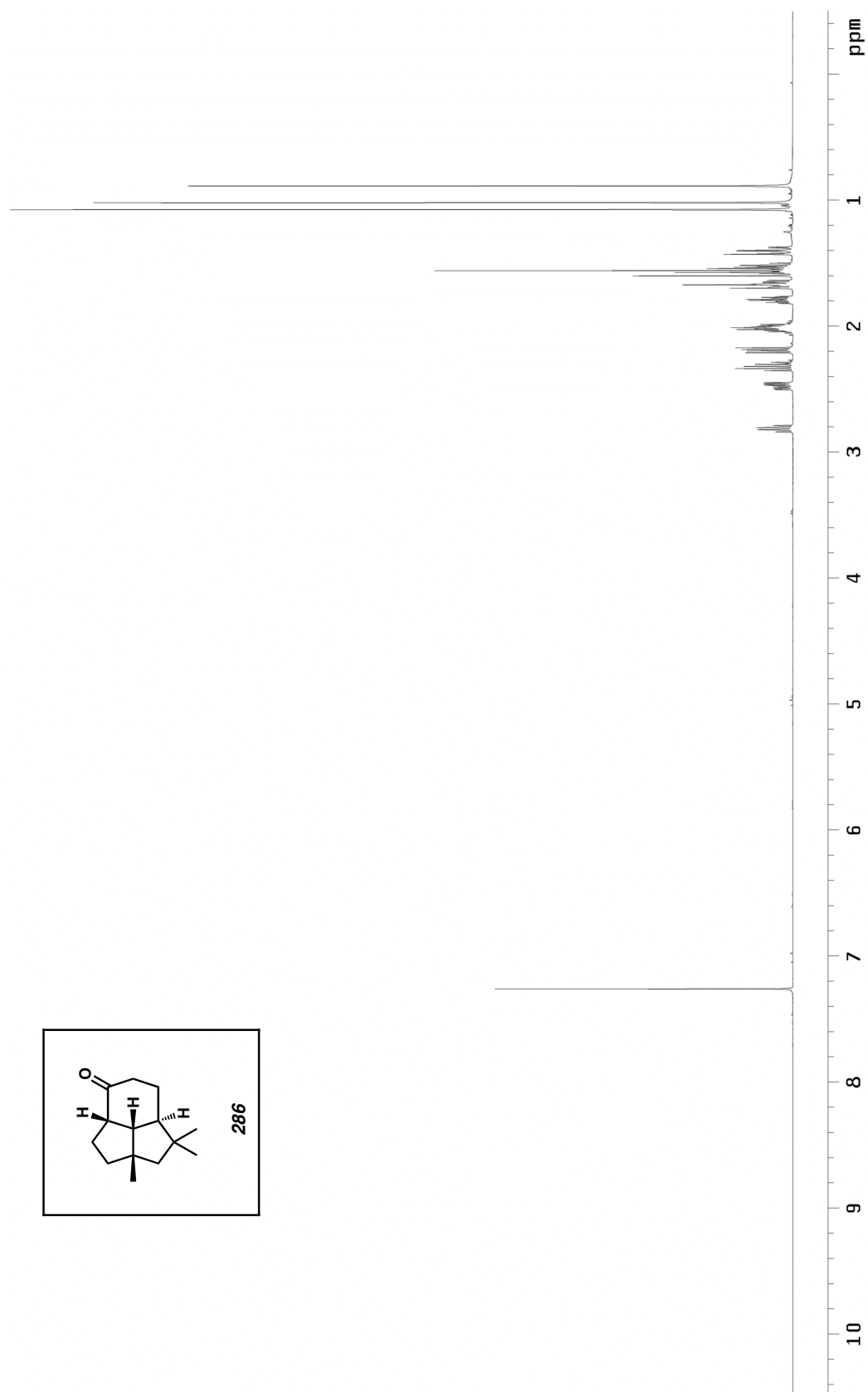


Figure A5.122. ^1H NMR (500 MHz, CDCl_3) of compound 286.

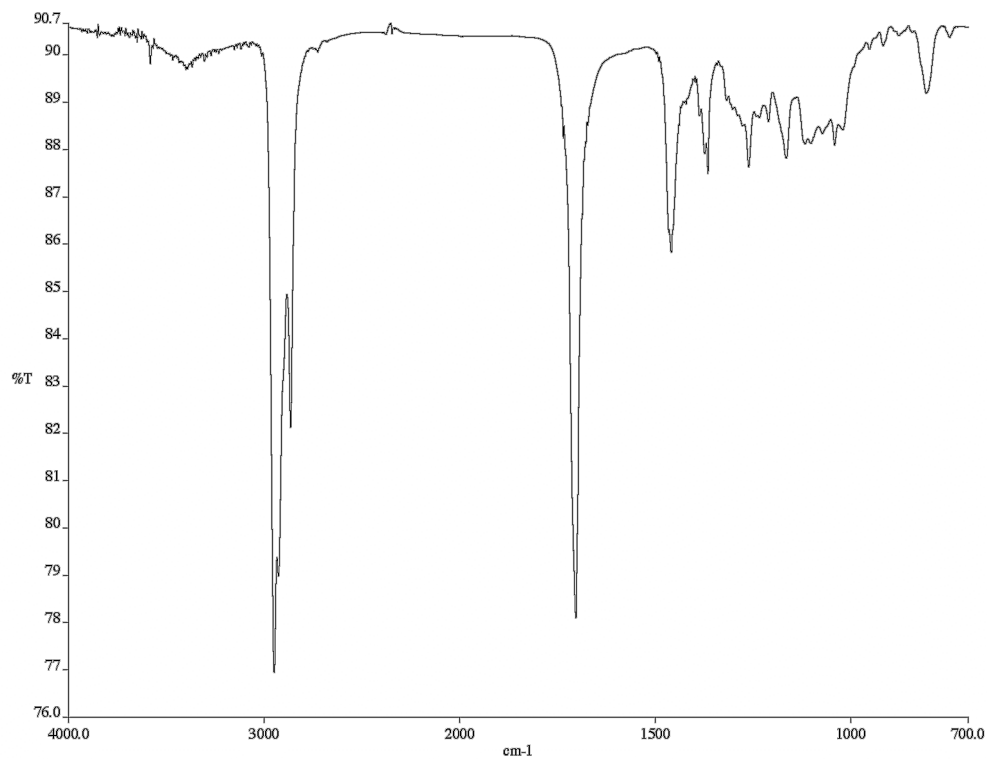


Figure A5.123. Infrared spectrum (thin film/NaCl) of compound **286**.

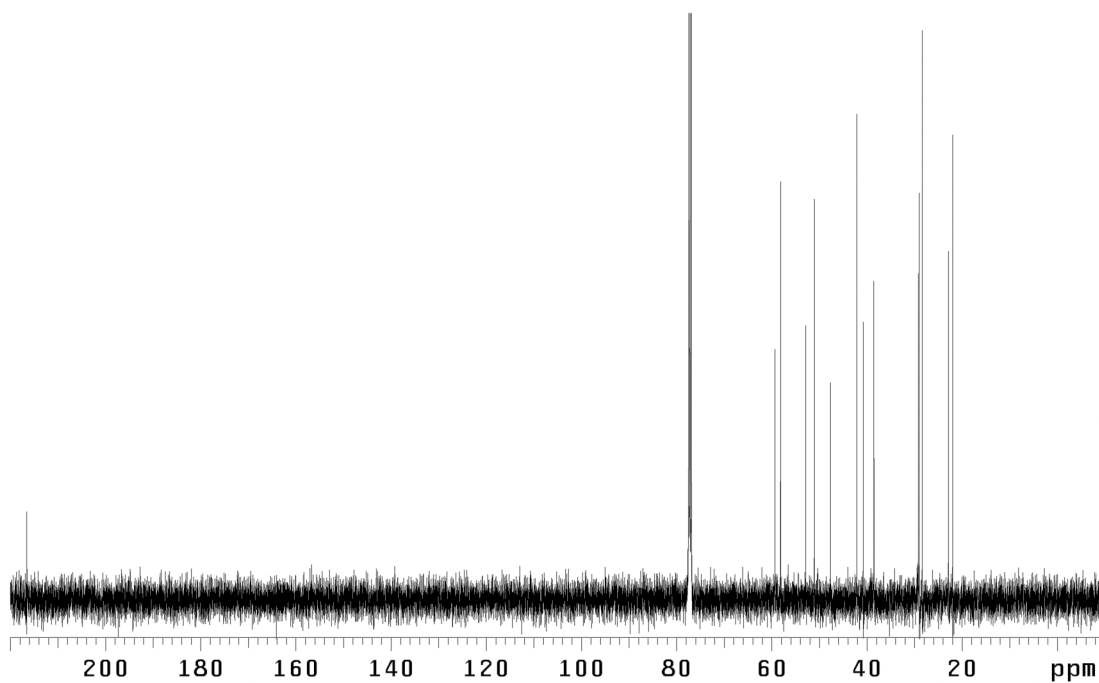


Figure A5.124. ¹³C NMR (125 MHz, CDCl₃) of compound **286**.

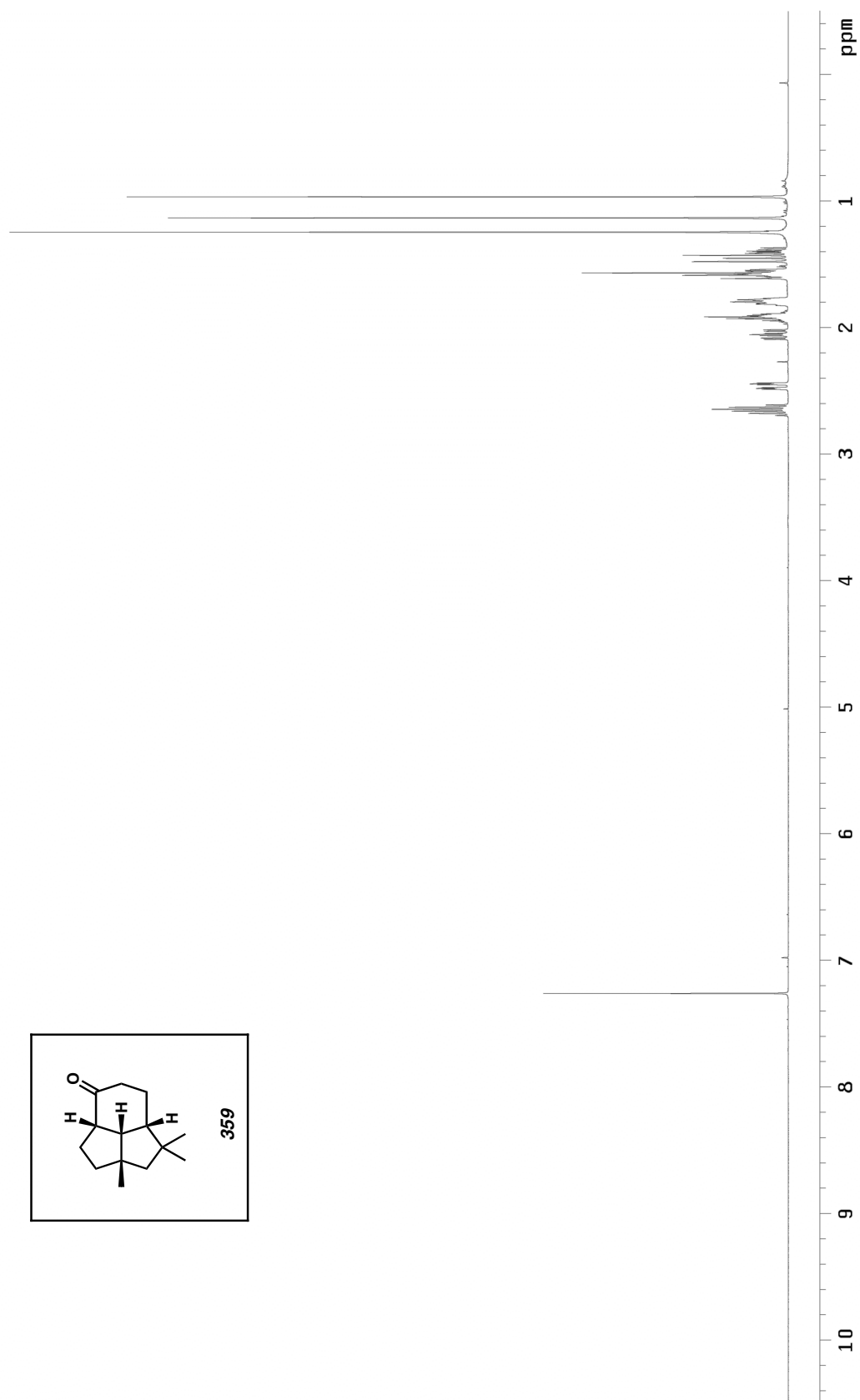


Figure A5.125. ^1H NMR (500 MHz, CDCl_3) of compound 359.

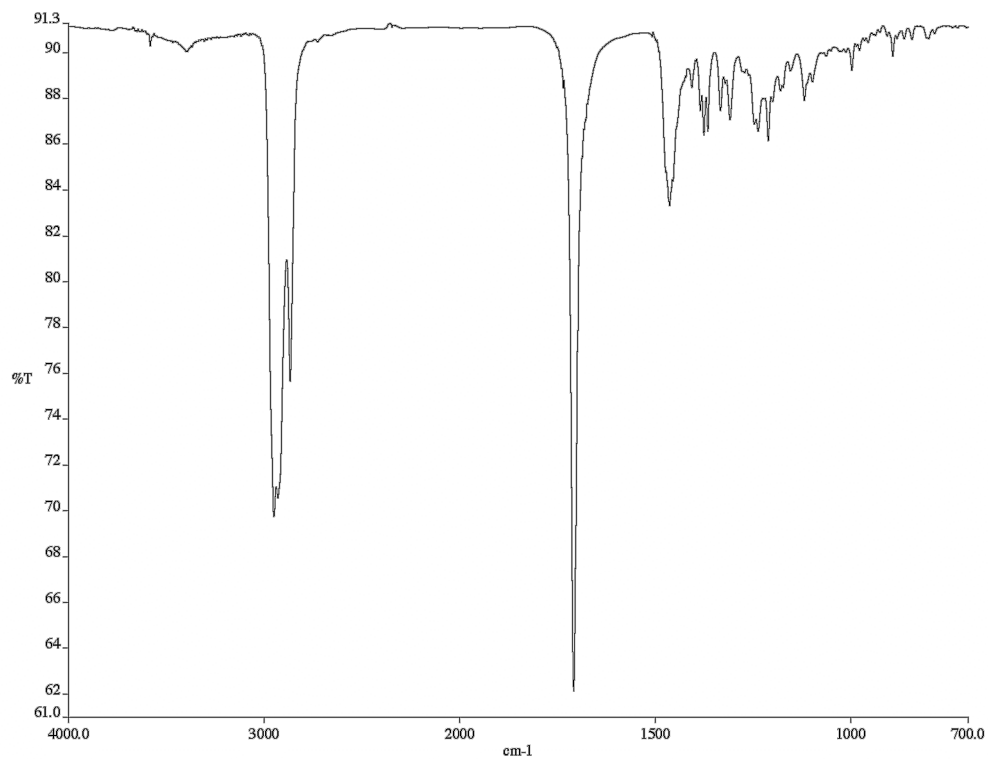


Figure A5.126. Infrared spectrum (thin film/NaCl) of compound **359**.

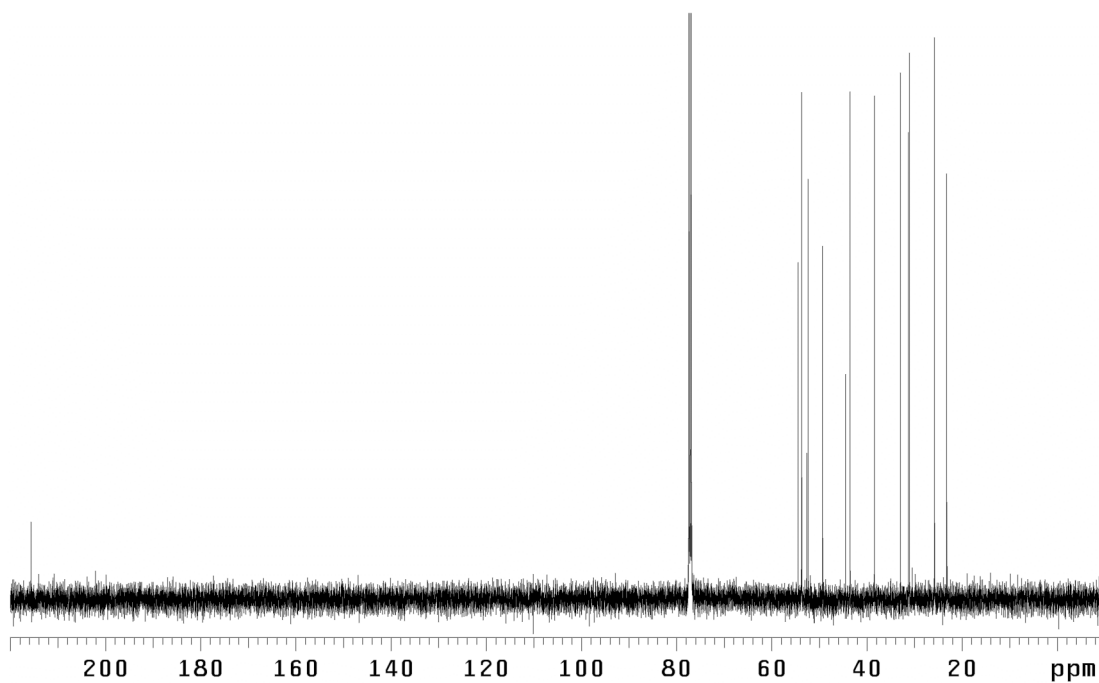
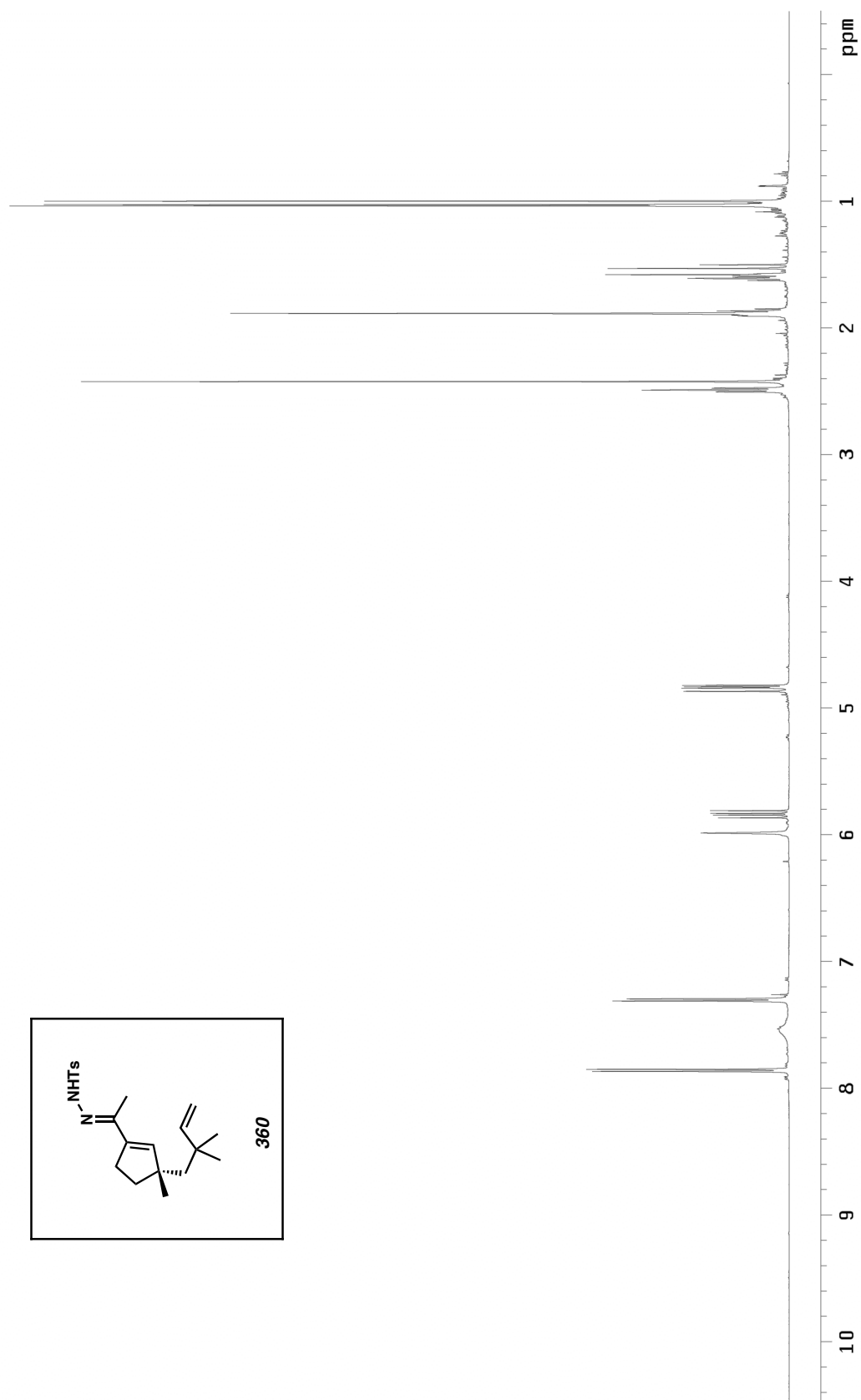


Figure A5.127. ¹³C NMR (125 MHz, CDCl₃) of compound **359**.



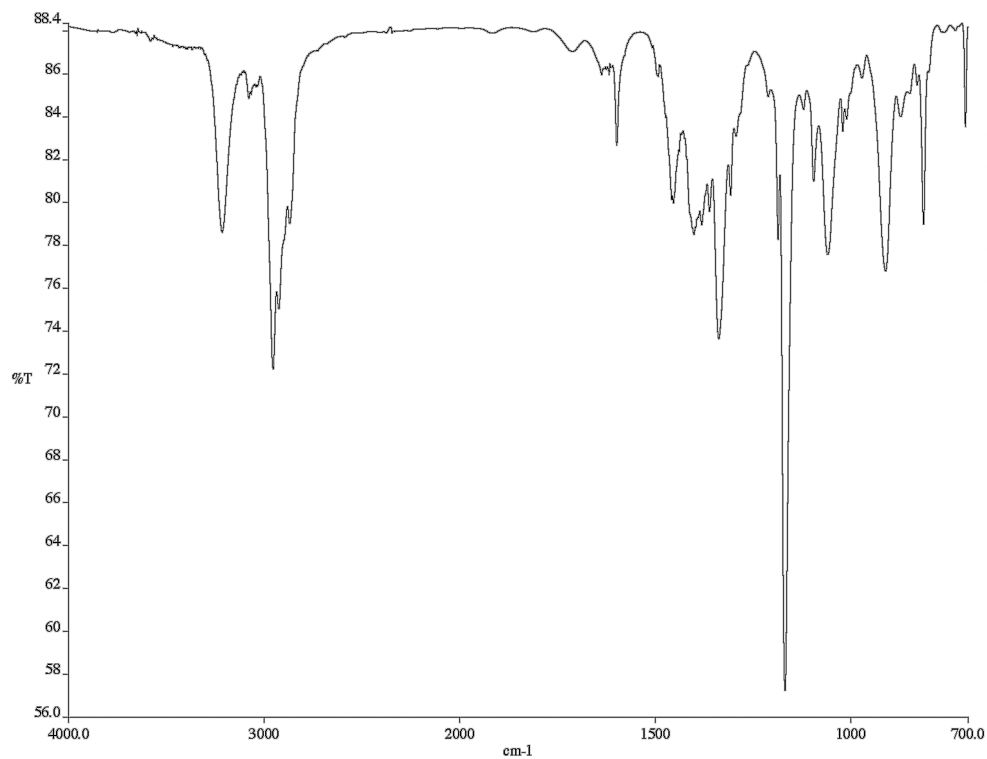


Figure A5.129. Infrared spectrum (thin film/NaCl) of compound **360**.

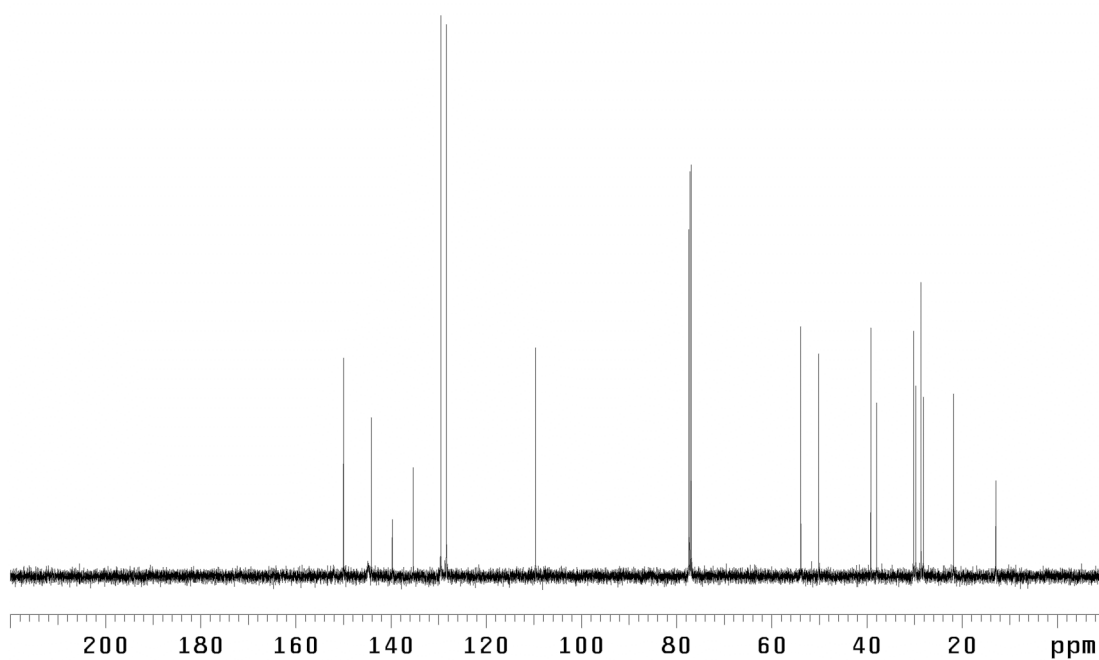


Figure A5.130. ¹³C NMR (125 MHz, CDCl₃) of compound **360**.

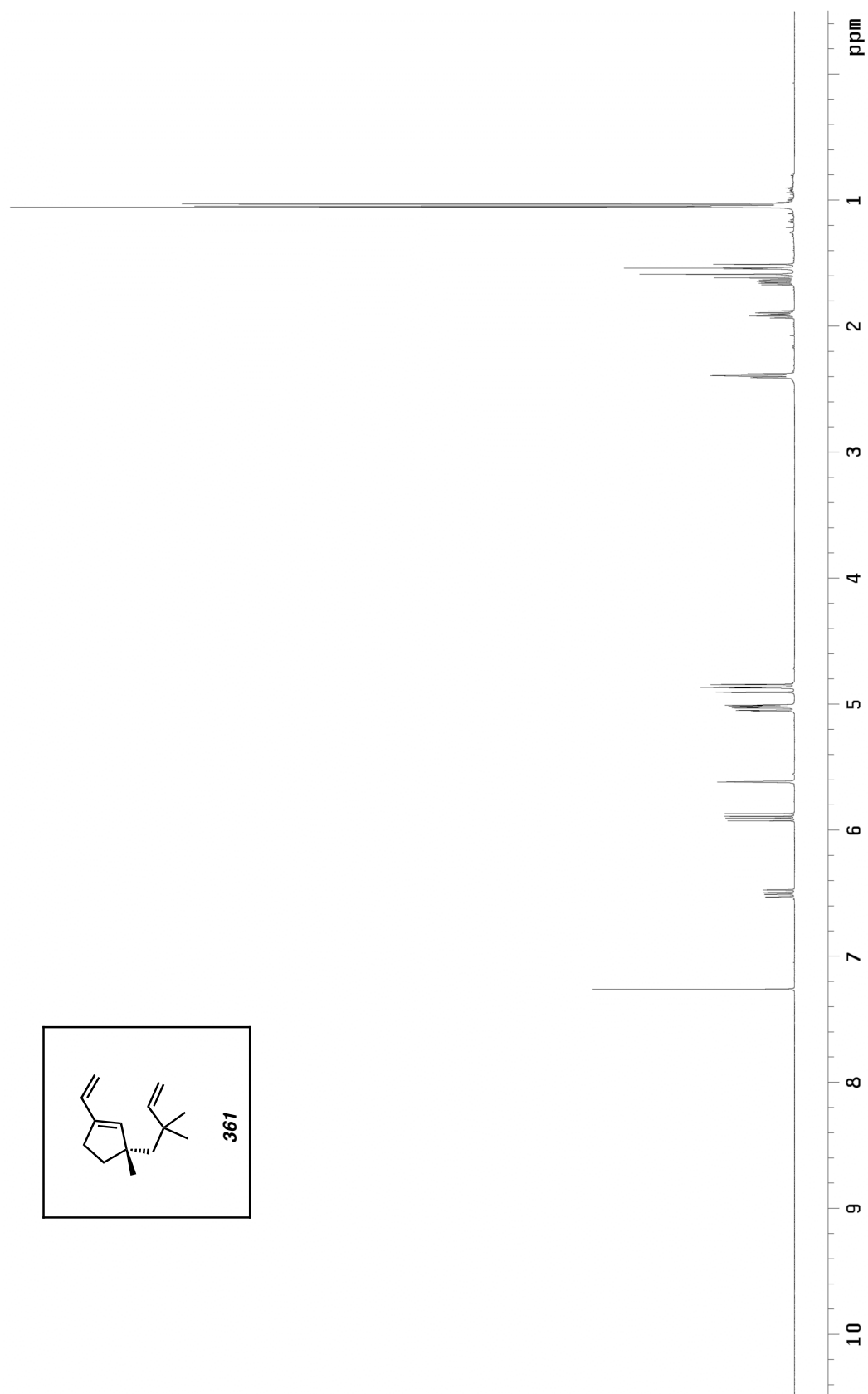


Figure A5.131. ^1H NMR (500 MHz, CDCl_3) of compound **361**.

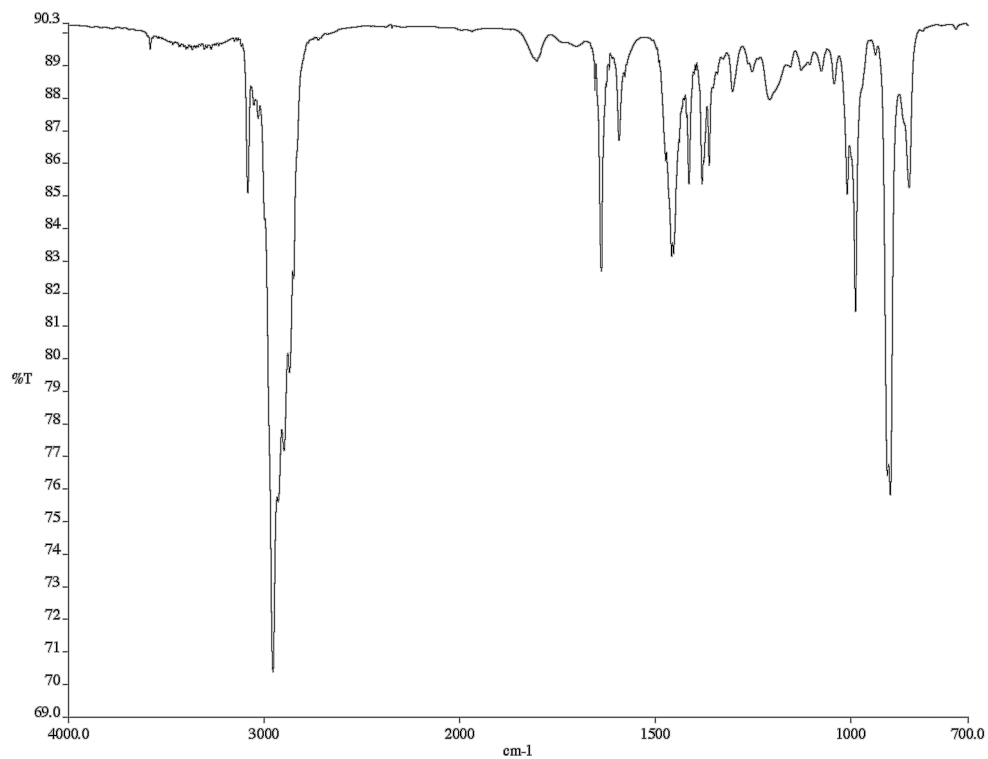


Figure A5.132. Infrared spectrum (thin film/NaCl) of compound **361**.

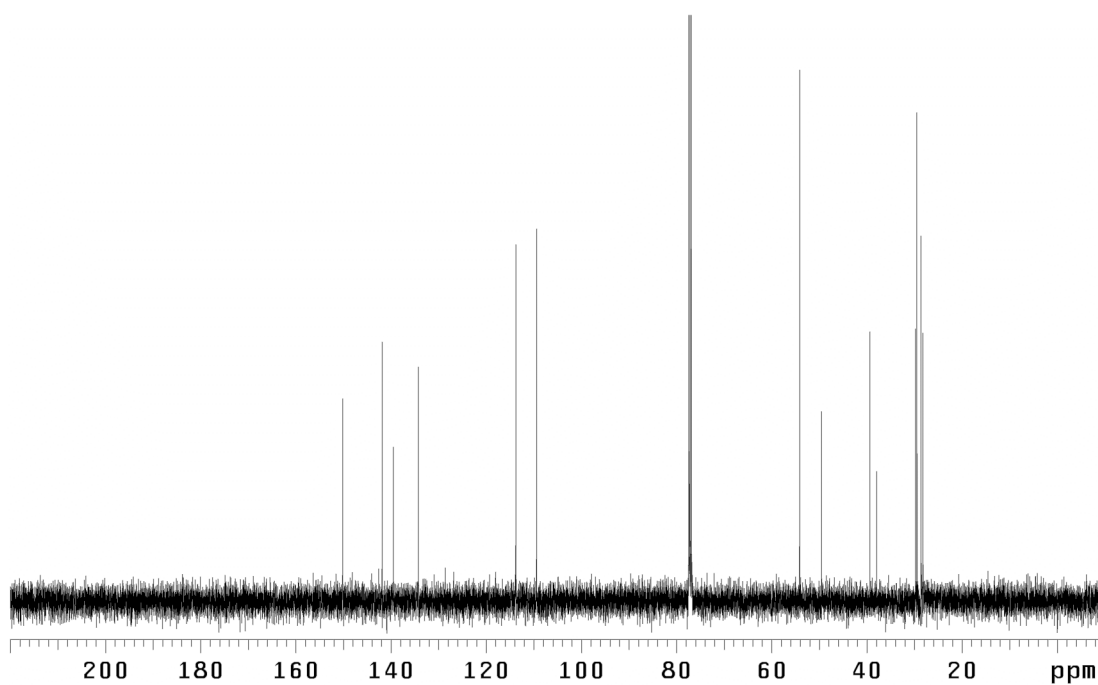


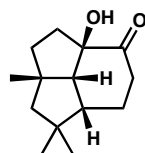
Figure A5.133. ¹³C NMR (125 MHz, CDCl₃) of compound **361**.

APPENDIX 6

X-Ray Crystallography Reports Relevant to Chapter 3:

The Catalytic Asymmetric Total Synthesis of

Presilphiperfolanol Natural Products

A6.1 CRYSTAL STRUCTURE ANALYSIS OF 353

Compound **353**
(AYH02) (CCDC 889570)

Contents

Table A6.1. Crystal data

Table A6.2. Atomic coordinates

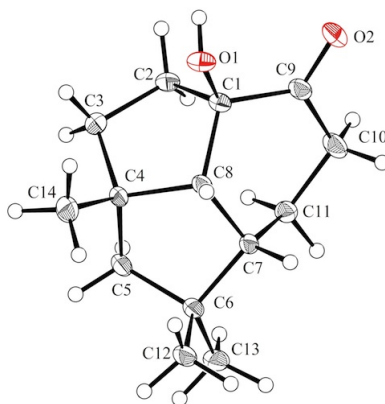
Table A6.3. Full bond distances and angles

Table A6.4. Anisotropic displacement parameters

Table A6.5. Hydrogen atomic coordinates

Table A6.6. Hydrogen bond distances and angles

Figure A6.1. α -Hydroxyketone **353** (CCDC 889570).



CCDC 889569 contains the supplementary crystallographic data for this compound. These data can be obtained free of charge from The Cambridge Crystallographic Data Centre via www.ccdc.cam.ac.uk/data_request/cif.

Table A6.1. Crystal data and structure refinement for α -hydroxyketone **353** (CCDC 889570)

Empirical formula	C ₁₄ H ₂₂ O ₂
Formula weight	222.32
Crystallization solvent	benzene, slow evaporation
Crystal shape	irregular
Crystal color	colorless
Crystal size	0.05 x 0.10 x 0.44 mm

Data Collection

Preliminary photograph(s)	rotation	
Type of diffractometer	Bruker KAPPA APEX II	
Wavelength	0.71073 Å MoK α	
Data collection temperature	100 K	
Theta range for 4413 reflections used in lattice determination	2.77 to 31.42°	
Unit cell dimensions	a = 5.8000(6) Å b = 7.3616(7) Å c = 29.454(3) Å	$\alpha = 90^\circ$ $\beta = 90^\circ$ $\gamma = 90^\circ$
Volume	1257.6(2) Å ³	
Z	4	
Crystal system	Orthorhombic	
Space group	P2(1)2(1)2(1) (# 19)	
Density (calculated)	1.174 g/cm ³	
F(000)	488	
Theta range for data collection	2.8 to 35.1°	
Completeness to theta = 25.00°	99.9%	
Index ranges	-9 ≤ h ≤ 8, -11 ≤ k ≤ 7, -46 ≤ l ≤ 46	
Data collection scan type	narrow omega and phi scans	
Reflections collected	19979	
Independent reflections	5133 [R _{int} = 0.0514]	
Reflections > 2σ(I)	4130	
Average σ(I)/(net I)	0.0579	
Absorption coefficient	0.08 mm ⁻¹	
Absorption correction	Semi-empirical from equivalents	
Max. and min. transmission	0.9962 and 0.9672	
Reflections monitored for decay	0	

Table A6.1 (cont.)

Decay of standards	0%
--------------------	----

Structure Solution and Refinement

Primary solution method	direct
Secondary solution method	difmap
Hydrogen placement	geom
Refinement method	Full-matrix least-squares on F^2
Data / restraints / parameters	5133 / 0 / 233
Treatment of hydrogen atoms	refall
Goodness-of-fit on F^2	1.56
Final R indices [$I > 2\sigma(I)$, 4130 reflections]	$R1 = 0.0515$, $wR2 = 0.0685$
R indices (all data)	$R1 = 0.0713$, $wR2 = 0.0707$
Type of weighting scheme used	calc
Weighting scheme used	calc $w = 1/[\sigma^2(F_o^2) + (0.0000P)^2 + 0.0000P]$ where $P = (F_o^2 + 2F_c^2)/3$
Max shift/error	0.000
Average shift/error	0.000
Absolute structure parameter	-0.4(8)
Largest diff. peak and hole	0.35 and -0.32 e.Å ⁻³

Programs Used

Cell refinement	SAINT V8.18C (Bruker-AXS, 2007)
Data collection	APEX2 2012.2-0 (Bruker-AXS, 2007)
Data reduction	SAINT V8.18C (Bruker-AXS, 2007)
Structure solution	SHELXS-97 (Sheldrick, 1990)
Structure refinement	SHELXL-97 (Sheldrick, 1997)
Graphics	DIAMOND 3 (Crystal Impact, 1999)

References

Special Refinement Details

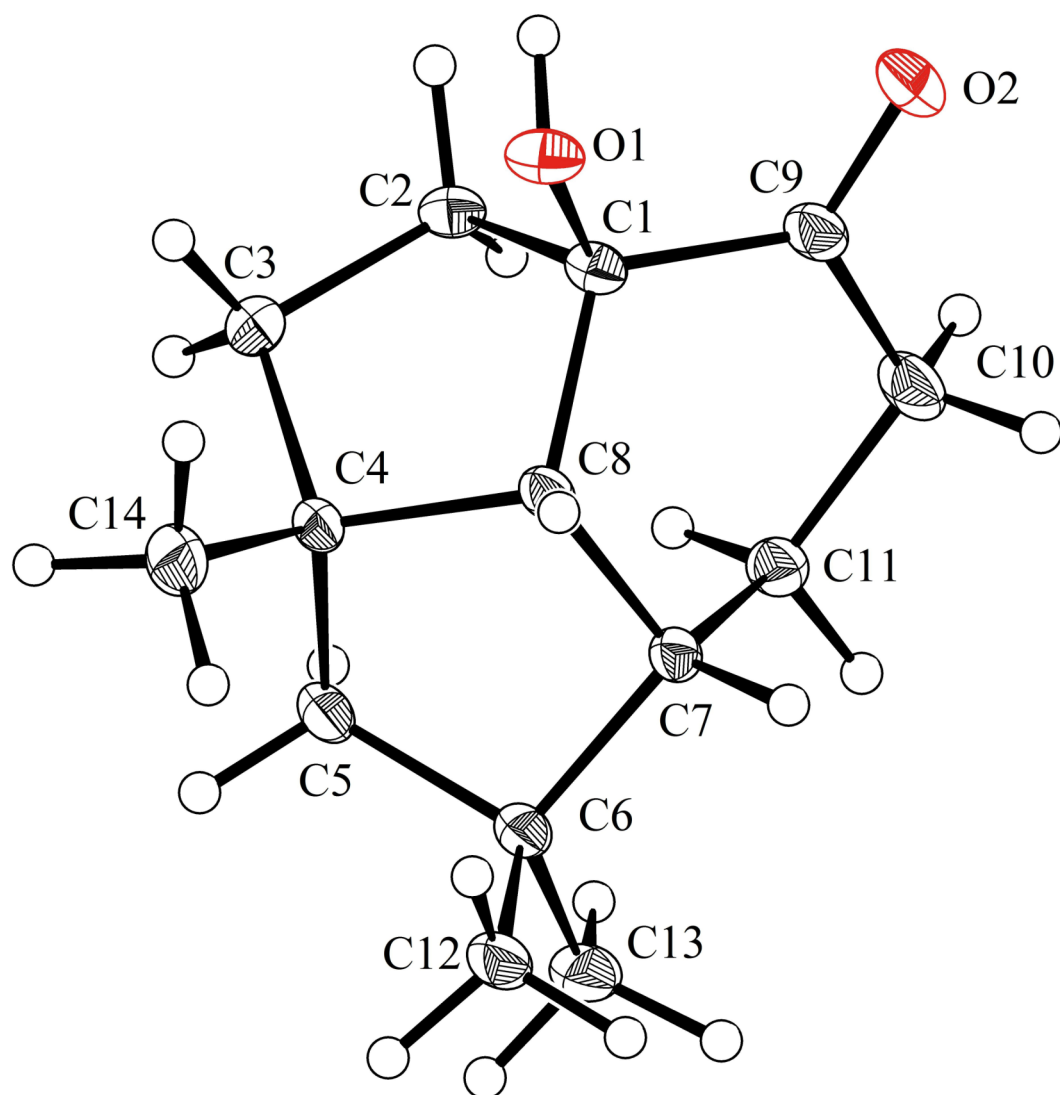
Figure A6.2. α -Hydroxyketone **353** (CCDC 889570).

Table A6.2. Atomic coordinates ($\times 10^4$) and equivalent isotropic displacement parameters ($\text{\AA}^2 \times 10^3$) for α -hydroxyketone **353** (CCDC 889570). $U(\text{eq})$ is defined as the trace of the orthogonalized U^{ij} tensor

	x	y	z	U_{eq}
C(1)	3631(2)	7788(1)	1771(1)	15(1)
C(2)	1527(2)	6527(2)	1808(1)	16(1)
C(3)	1401(2)	5619(2)	1345(1)	18(1)
C(4)	2282(2)	7021(1)	996(1)	15(1)
C(5)	339(2)	8066(2)	754(1)	18(1)
C(6)	1024(2)	10078(1)	743(1)	16(1)
C(7)	2200(2)	10316(1)	1211(1)	14(1)
C(8)	3529(2)	8518(1)	1283(1)	14(1)
C(9)	3490(2)	9258(2)	2129(1)	18(1)
C(10)	1817(2)	10785(2)	2050(1)	23(1)
C(11)	531(2)	10713(2)	1601(1)	18(1)
C(12)	2788(2)	10465(2)	368(1)	21(1)
C(13)	-1040(2)	11316(2)	665(1)	23(1)
C(14)	3888(2)	6071(2)	660(1)	23(1)
O(1)	5704(1)	6782(1)	1805(1)	20(1)
O(2)	4656(2)	9193(1)	2472(1)	28(1)

Table A6.3. Bond lengths [\AA] and angles [$^\circ$] for **353** (CCDC 889570)

C(1)-O(1)	1.4155(13)
C(1)-C(9)	1.5143(15)
C(1)-C(8)	1.5351(14)
C(1)-C(2)	1.5375(15)
C(2)-C(3)	1.5225(15)
C(2)-H(2A)	0.961(11)
C(2)-H(2B)	0.993(11)
C(3)-C(4)	1.5429(16)
C(3)-H(3A)	0.958(12)
C(3)-H(3B)	1.000(11)
C(4)-C(14)	1.5291(15)
C(4)-C(5)	1.5406(15)
C(4)-C(8)	1.5654(15)
C(5)-C(6)	1.5334(15)
C(5)-H(5A)	0.980(12)
C(5)-H(5B)	1.000(12)
C(6)-C(13)	1.5227(16)
C(6)-C(12)	1.5328(16)
C(6)-C(7)	1.5483(14)
C(7)-C(11)	1.5301(15)
C(7)-C(8)	1.5462(15)
C(7)-H(7)	0.982(10)
C(8)-H(8)	0.956(10)
C(9)-O(2)	1.2164(13)
C(9)-C(10)	1.5036(16)
C(10)-C(11)	1.5186(16)
C(10)-H(10A)	1.000(13)
C(10)-H(10B)	0.965(13)
C(11)-H(11A)	0.997(11)
C(11)-H(11B)	0.997(11)
C(12)-H(12A)	0.968(12)
C(12)-H(12B)	1.033(13)
C(12)-H(12C)	0.981(12)
C(13)-H(13A)	1.007(12)
C(13)-H(13B)	1.020(13)
C(13)-H(13C)	0.961(13)
C(14)-H(14A)	0.980(12)
C(14)-H(14B)	1.001(12)
C(14)-H(14C)	0.977(13)
O(1)-H(1)	0.804(14)
O(1)-C(1)-C(9)	111.71(9)
O(1)-C(1)-C(8)	106.39(8)
C(9)-C(1)-C(8)	113.66(9)
O(1)-C(1)-C(2)	110.67(8)
C(9)-C(1)-C(2)	109.75(9)
C(8)-C(1)-C(2)	104.39(9)
C(3)-C(2)-C(1)	103.78(9)
C(3)-C(2)-H(2A)	112.8(6)
C(1)-C(2)-H(2A)	108.1(6)

Table A6.3 (cont.)

C(3)-C(2)-H(2B)	110.7(6)
C(1)-C(2)-H(2B)	112.1(6)
H(2A)-C(2)-H(2B)	109.2(9)
C(2)-C(3)-C(4)	106.72(9)
C(2)-C(3)-H(3A)	113.5(7)
C(4)-C(3)-H(3A)	110.2(7)
C(2)-C(3)-H(3B)	108.2(6)
C(4)-C(3)-H(3B)	108.7(6)
H(3A)-C(3)-H(3B)	109.4(9)
C(14)-C(4)-C(5)	111.95(9)
C(14)-C(4)-C(3)	109.09(9)
C(5)-C(4)-C(3)	113.61(9)
C(14)-C(4)-C(8)	112.96(9)
C(5)-C(4)-C(8)	103.68(9)
C(3)-C(4)-C(8)	105.35(8)
C(6)-C(5)-C(4)	107.57(9)
C(6)-C(5)-H(5A)	114.9(7)
C(4)-C(5)-H(5A)	110.4(7)
C(6)-C(5)-H(5B)	109.9(7)
C(4)-C(5)-H(5B)	109.3(7)
H(5A)-C(5)-H(5B)	104.7(9)
C(13)-C(6)-C(12)	107.76(9)
C(13)-C(6)-C(5)	112.17(9)
C(12)-C(6)-C(5)	111.53(9)
C(13)-C(6)-C(7)	114.37(9)
C(12)-C(6)-C(7)	109.10(9)
C(5)-C(6)-C(7)	101.87(8)
C(11)-C(7)-C(8)	112.14(9)
C(11)-C(7)-C(6)	114.31(9)
C(8)-C(7)-C(6)	104.12(8)
C(11)-C(7)-H(7)	105.3(6)
C(8)-C(7)-H(7)	111.3(6)
C(6)-C(7)-H(7)	109.7(6)
C(1)-C(8)-C(7)	116.49(9)
C(1)-C(8)-C(4)	106.06(8)
C(7)-C(8)-C(4)	107.38(9)
C(1)-C(8)-H(8)	107.7(6)
C(7)-C(8)-H(8)	110.1(6)
C(4)-C(8)-H(8)	108.9(6)
O(2)-C(9)-C(10)	121.13(10)
O(2)-C(9)-C(1)	121.44(10)
C(10)-C(9)-C(1)	117.42(9)
C(9)-C(10)-C(11)	115.22(10)
C(9)-C(10)-H(10A)	106.4(7)
C(11)-C(10)-H(10A)	110.9(7)
C(9)-C(10)-H(10B)	108.4(8)
C(11)-C(10)-H(10B)	111.5(8)
H(10A)-C(10)-H(10B)	103.6(10)
C(10)-C(11)-C(7)	110.44(9)
C(10)-C(11)-H(11A)	109.4(6)
C(7)-C(11)-H(11A)	110.6(6)

Table A6.3 (cont.)

C(10)-C(11)-H(11B)	111.1(6)
C(7)-C(11)-H(11B)	110.9(6)
H(11A)-C(11)-H(11B)	104.4(9)
C(6)-C(12)-H(12A)	112.4(7)
C(6)-C(12)-H(12B)	114.1(7)
H(12A)-C(12)-H(12B)	105.9(9)
C(6)-C(12)-H(12C)	110.5(7)
H(12A)-C(12)-H(12C)	108.0(10)
H(12B)-C(12)-H(12C)	105.5(10)
C(6)-C(13)-H(13A)	112.8(7)
C(6)-C(13)-H(13B)	113.7(7)
H(13A)-C(13)-H(13B)	107.3(10)
C(6)-C(13)-H(13C)	110.8(7)
H(13A)-C(13)-H(13C)	107.9(9)
H(13B)-C(13)-H(13C)	103.7(10)
C(4)-C(14)-H(14A)	109.7(7)
C(4)-C(14)-H(14B)	110.7(7)
H(14A)-C(14)-H(14B)	105.5(9)
C(4)-C(14)-H(14C)	113.0(7)
H(14A)-C(14)-H(14C)	109.2(10)
H(14B)-C(14)-H(14C)	108.4(10)
C(1)-O(1)-H(1)	110.1(10)

Symmetry transformations used to generate equivalent atoms:

Table A6.4. Anisotropic displacement parameters ($\text{\AA}^2 \times 10^4$) for α -hydroxyketone **353** (CCDC 889570). The anisotropic displacement factor exponent takes the form: $-2\pi^2 [h^2 a^{*2} U^{11} + \dots + 2 h k a^* b^* U^{12}]$

	U^{11}	U^{22}	U^{33}	U^{23}	U^{13}	U^{12}
C(1)	143(5)	177(5)	124(5)	12(4)	-11(4)	17(5)
C(2)	186(5)	177(5)	132(5)	40(5)	16(5)	-4(5)
C(3)	231(6)	148(5)	171(6)	12(4)	-4(5)	-26(5)
C(4)	209(5)	144(5)	103(5)	-11(4)	0(4)	-24(5)
C(5)	225(6)	196(6)	124(5)	-16(5)	-29(5)	-36(5)
C(6)	188(6)	170(5)	131(5)	7(4)	-34(4)	-30(4)
C(7)	146(5)	138(5)	127(5)	0(4)	-11(4)	-28(4)
C(8)	156(5)	163(5)	99(5)	0(4)	13(4)	-19(5)
C(9)	219(5)	209(6)	112(5)	12(4)	15(4)	-39(5)
C(10)	296(7)	266(7)	128(6)	-55(5)	0(5)	73(6)
C(11)	204(5)	174(6)	148(5)	-3(5)	6(4)	27(5)
C(12)	296(6)	218(6)	121(6)	25(5)	-11(5)	-72(6)
C(13)	254(7)	228(6)	198(6)	43(5)	-84(5)	-21(5)
C(14)	313(7)	207(6)	170(6)	-39(5)	32(5)	0(6)
O(1)	186(4)	245(4)	176(4)	57(4)	-14(3)	43(4)
O(2)	389(5)	279(5)	174(4)	-32(4)	-114(4)	21(4)

Table A6.5. Hydrogen coordinates ($\times 10^3$) and isotropic displacement parameters ($\text{\AA}^2 \times 10^3$) for α -hydroxyketone **353** (CCDC 889570)

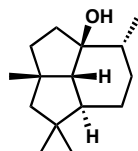
	x	y	z	U _{iso}
H(2A)	181(2)	568(1)	205(1)	11(3)
H(2B)	8(2)	721(1)	187(1)	9(3)
H(3A)	-12(2)	522(2)	126(1)	17(3)
H(3B)	247(2)	456(2)	134(1)	13(3)
H(5A)	3(2)	753(2)	46(1)	24(3)
H(5B)	-113(2)	791(2)	93(1)	24(3)
H(7)	325(2)	1136(1)	120(1)	4(2)
H(8)	508(2)	864(1)	118(1)	7(3)
H(10A)	272(2)	1194(2)	208(1)	39(4)
H(10B)	77(2)	1084(2)	230(1)	40(4)
H(11A)	-28(2)	1189(2)	155(1)	15(3)
H(11B)	-73(2)	979(2)	161(1)	17(3)
H(12A)	223(2)	1013(2)	7(1)	30(4)
H(12B)	434(2)	979(2)	41(1)	27(3)
H(12C)	318(2)	1176(2)	36(1)	32(4)
H(13A)	-63(2)	1264(2)	69(1)	25(3)
H(13B)	-237(2)	1109(2)	88(1)	30(4)
H(13C)	-171(2)	1110(2)	37(1)	30(3)
H(14A)	307(2)	507(2)	51(1)	25(3)
H(14B)	522(2)	550(2)	82(1)	26(3)
H(14C)	450(2)	689(2)	43(1)	31(3)
H(1)	568(2)	615(2)	203(1)	37(4)

Table A6.6. Hydrogen bonds for α -hydroxyketone **353** (CCDC 889570) [\AA and $^\circ$]

D-H...A	d(D-H)	d(H...A)	d(D...A)	<(DHA)
O(1)-H(1)...O(2)#1	0.804(14)	2.071(15)	2.8653(12)	169.7(13)

Symmetry transformations used to generate equivalent atoms:

#1 $-x+1, y-1/2, -z+1/2$

A6.2 CRYSTAL STRUCTURE ANALYSIS OF 224Compound **224**

(AYH01) (CCDC 889569)

Contents

Table A6.7. Crystal data

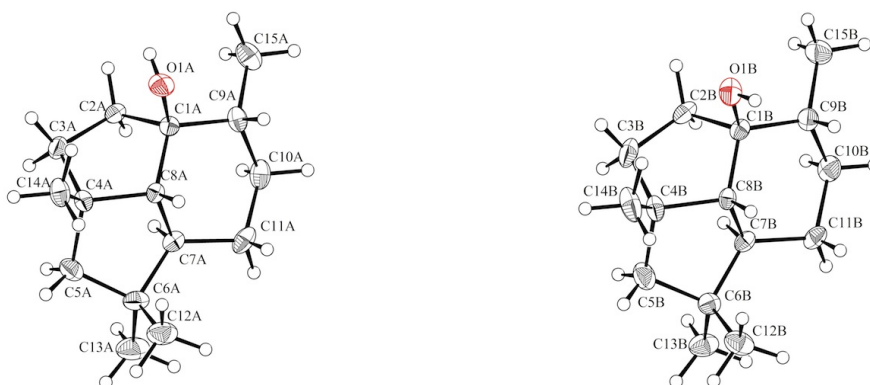
Table A6.8. Atomic coordinates

Table A6.9. Full bond distances and angles

Table A6.10. Anisotropic displacement parameters

Table A6.11. Hydrogen atomic coordinates

Table A6.12. Hydrogen bond distances and angles

*Figure A6.3. Tertiary alcohol **224** (CCDC 889569).*

CCDC 889569 contains the supplementary crystallographic data for this compound. These data can be obtained free of charge from The Cambridge Crystallographic Data Centre via www.ccdc.cam.ac.uk/data_request/cif.

Table A6.7. Crystal data and structure refinement for tertiary alcohol **224** (CCDC 889569)

Empirical formula	C ₁₅ H ₂₆ O
Formula weight	222.36
Crystallization solvent	hexanes, slow evaporation
Crystal shape	block
Crystal color	colorless
Crystal size	0.20 x 0.42 x 0.44 mm

Data Collection

Preliminary photograph(s)	rotation	
Type of diffractometer	Bruker KAPPA APEX II	
Wavelength	0.71073 Å MoK α	
Data collection temperature	100 K	
Theta range for 9919 reflections used in lattice determination	2.35 to 33.56°	
Unit cell dimensions	a = 17.8200(13) Å b = 9.0182(4) Å c = 18.7656(9) Å	$\alpha = 90^\circ$ $\beta = 112.479(2)^\circ$ $\gamma = 90^\circ$
Volume	2786.6(3) Å ³	
Z	8	
Crystal system	Monoclinic	
Space group	I2 (# 5)	
Density (calculated)	1.060 g/cm ³	
F(000)	992	
Theta range for data collection	2.3 to 41.1°	
Completeness to theta = 25.00°	99.8%	
Index ranges	-30 ≤ h ≤ 32, -16 ≤ k ≤ 16, -30 ≤ l ≤ 34	
Data collection scan type	narrow omega and phi scans	
Reflections collected	66426	
Independent reflections	17149 [R _{int} = 0.0390]	
Reflections > 2 s(I)	11947	
Average s(I)/(net I)	0.0568	
Absorption coefficient	0.06 mm ⁻¹	
Absorption correction	Semi-empirical from equivalents	
Max. and min. transmission	0.9874 and 0.9726	
Reflections monitored for decay	0	

Table A6.7 (cont.)

Decay of standards	0%
--------------------	----

Structure Solution and Refinement

Primary solution method	direct
Secondary solution method	difmap
Hydrogen placement	geom
Refinement method	Full-matrix least-squares on F ²
Data / restraints / parameters	17149 / 1 / 498
Treatment of hydrogen atoms	refall
Goodness-of-fit on F ²	2.14
Final R indices [I>2σ (I), 11947 reflections]	R1 = 0.0566, wR2 = 0.0604
R indices (all data)	R1 = 0.0987, wR2 = 0.0618
Type of weighting scheme used	calc
Weighting scheme used	calc $w=1/[\sigma^2(F_o^2)+(0.0000P)^2+0.0000P]$ where $P=(F_o^2+2F_c^2)/3$
Max shift/error	0.001
Average shift/error	0.000
Absolute structure parameter	-0.4(5)
Extinction coefficient	0.00083(11)
Largest diff. peak and hole	0.62 and -0.30 e.Å ⁻³

Programs Used

Cell refinement	SAINT V8.18C (Bruker-AXS, 2007)
Data collection	APEX2 2012.2-0 (Bruker-AXS, 2007)
Data reduction	SAINT V8.18C (Bruker-AXS, 2007)
Structure solution	SHELXS-97 (Sheldrick, 1990)
Structure refinement	SHELXL-97 (Sheldrick, 1997)
Graphics	DIAMOND 3 (Crystal Impact, 1999)

References

Special Refinement Details

Figure A6.4. Tertiary alcohol **224**, crystal form A (CCDC 889569).

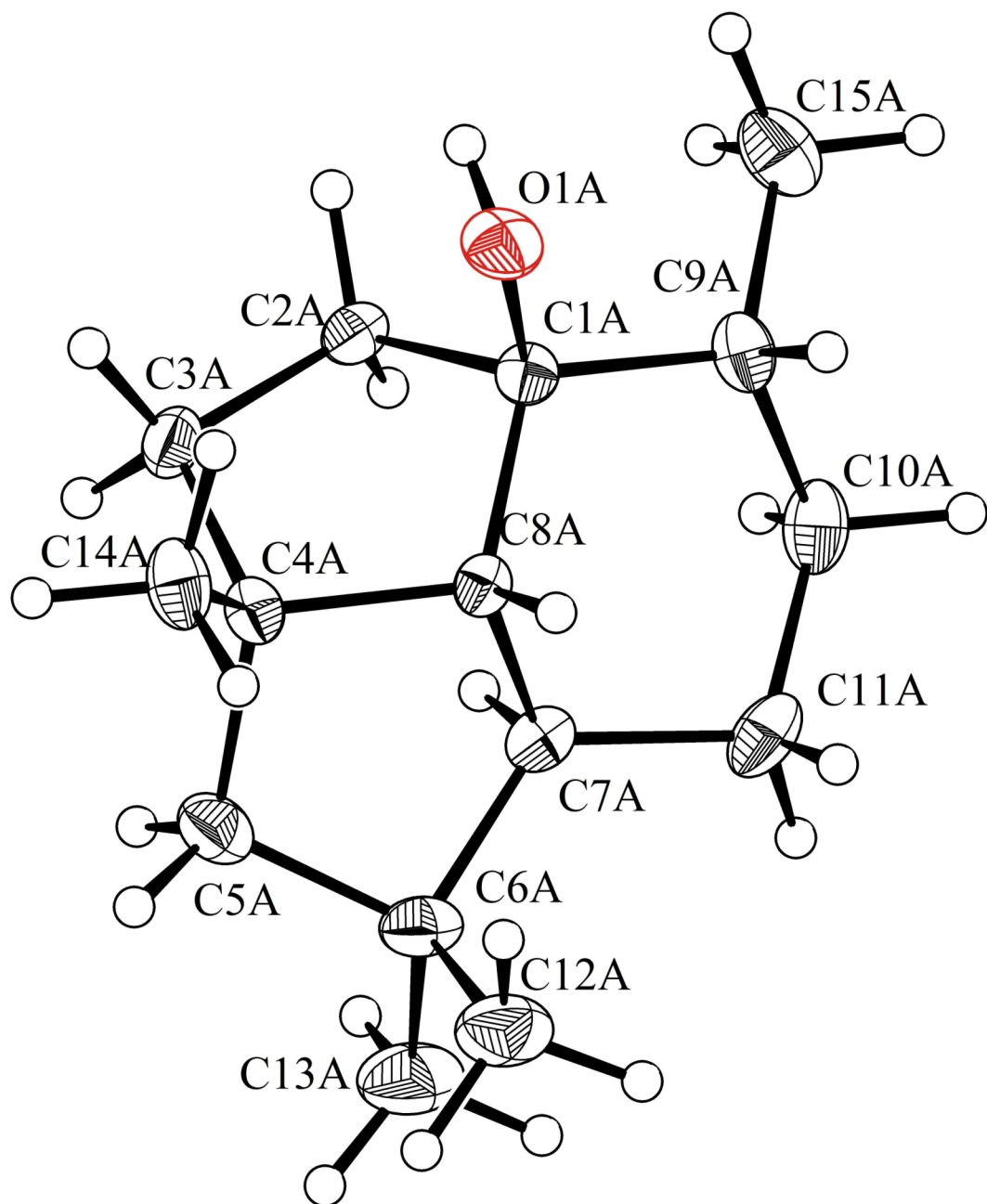


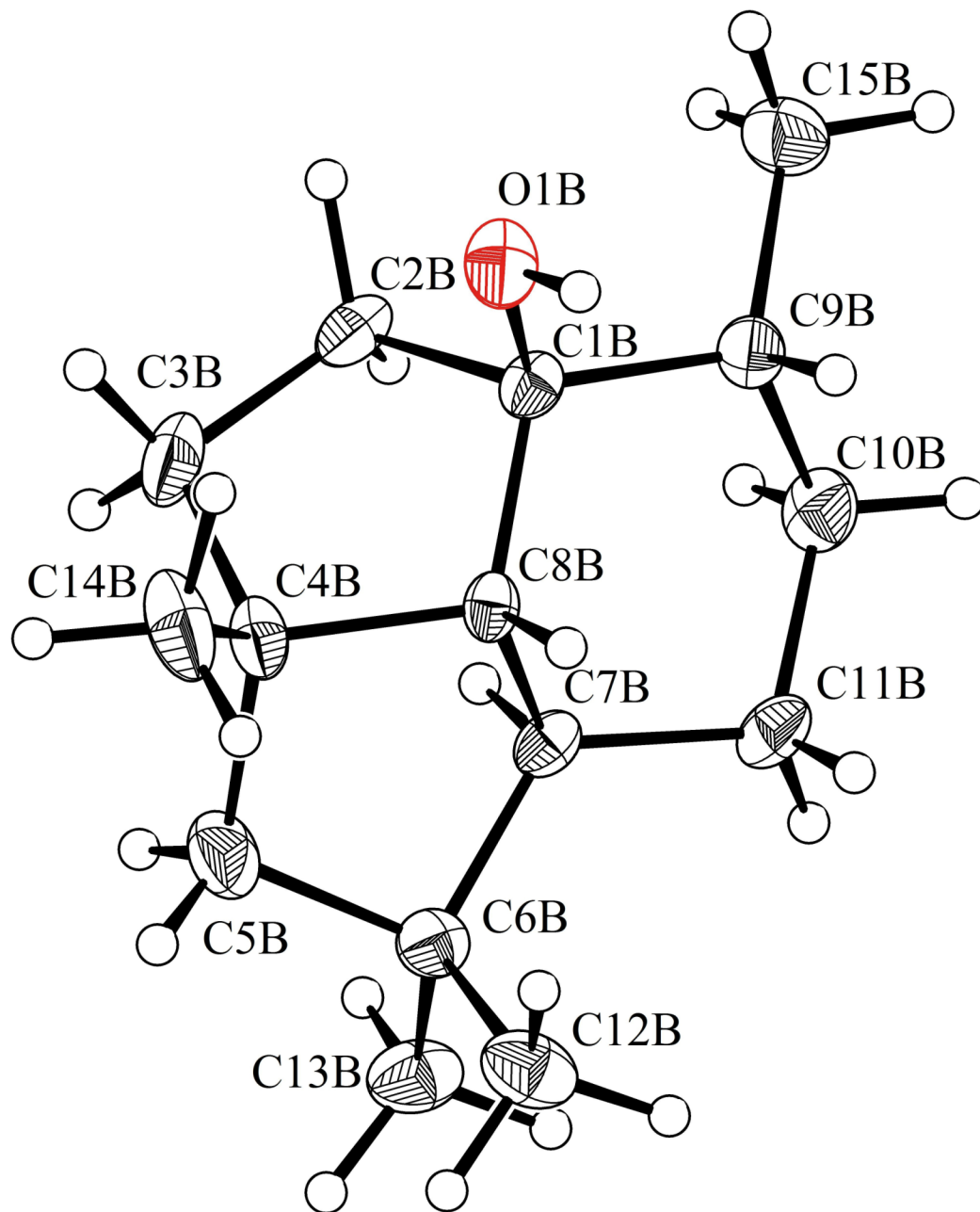
Figure A6.5. Tertiary alcohol **224**, crystal form B (CCDC 889569).

Table A6.8. Atomic coordinates ($\times 10^4$) and equivalent isotropic displacement parameters ($\text{\AA}^2 \times 10^3$) for tertiary alcohol **224** (CCDC 889569). $U(\text{eq})$ is defined as the trace of the orthogonalized U^{ij} tensor

	x	y	z	U_{eq}
O(1A)	3956(1)	967(1)	101(1)	27(1)
C(1A)	3287(1)	100(1)	135(1)	17(1)
C(2A)	2590(1)	164(1)	-659(1)	20(1)
C(3A)	2207(1)	1716(1)	-689(1)	22(1)
C(4A)	2422(1)	2238(1)	158(1)	19(1)
C(5A)	1685(1)	2307(1)	413(1)	26(1)
C(6A)	1833(1)	1161(1)	1065(1)	25(1)
C(7A)	2330(1)	16(1)	827(1)	19(1)
C(8A)	2938(1)	944(1)	632(1)	16(1)
C(9A)	3615(1)	-1426(1)	480(1)	22(1)
C(10A)	3068(1)	-2264(1)	806(1)	27(1)
C(11A)	2742(1)	-1325(1)	1303(1)	28(1)
C(12A)	2309(1)	1842(1)	1857(1)	37(1)
C(13A)	1044(1)	514(1)	1063(1)	40(1)
C(14A)	2882(1)	3712(1)	315(1)	27(1)
C(15A)	3827(1)	-2400(1)	-80(1)	34(1)
O(1B)	5561(1)	934(1)	1119(1)	28(1)
C(1B)	5724(1)	1902(1)	1778(1)	18(1)
C(2B)	6641(1)	1788(1)	2244(1)	24(1)
C(3B)	6751(1)	344(1)	2714(1)	31(1)
C(4B)	5919(1)	-77(1)	2750(1)	23(1)
C(5B)	5896(1)	-2(1)	3573(1)	32(1)
C(6B)	5334(1)	1292(1)	3590(1)	22(1)
C(7B)	5432(1)	2293(1)	2970(1)	18(1)
C(8B)	5373(1)	1228(1)	2320(1)	17(1)
C(9B)	5359(1)	3445(1)	1494(1)	22(1)
C(10B)	5299(1)	4442(1)	2131(1)	28(1)
C(11B)	4935(1)	3678(1)	2654(1)	25(1)
C(12B)	4460(1)	773(1)	3385(1)	33(1)
C(13B)	5631(1)	2046(1)	4378(1)	32(1)
C(14B)	5634(1)	-1585(1)	2379(1)	36(1)
C(15B)	5790(1)	4240(1)	1045(1)	32(1)

Table A6.9. Bond lengths [\AA] and angles [$^\circ$] for tertiary alcohol **224** (CCDC 889569)

O(1A)-C(1A)	1.4471(9)
O(1A)-H(1A)	0.734(10)
C(1A)-C(8A)	1.5110(10)
C(1A)-C(2A)	1.5328(10)
C(1A)-C(9A)	1.5385(11)
C(2A)-C(3A)	1.5483(11)
C(2A)-H(2A)	0.968(8)
C(2A)-H(2B)	0.969(8)
C(3A)-C(4A)	1.5590(11)
C(3A)-H(3A)	0.999(8)
C(3A)-H(3B)	0.996(8)
C(4A)-C(14A)	1.5305(11)
C(4A)-C(8A)	1.5400(11)
C(4A)-C(5A)	1.5601(11)
C(5A)-C(6A)	1.5450(12)
C(5A)-H(5A)	1.001(8)
C(5A)-H(5B)	0.974(9)
C(6A)-C(13A)	1.5221(12)
C(6A)-C(12A)	1.5305(12)
C(6A)-C(7A)	1.5333(11)
C(7A)-C(11A)	1.5158(12)
C(7A)-C(8A)	1.5198(10)
C(7A)-H(7A)	0.998(7)
C(8A)-H(8A)	0.951(7)
C(9A)-C(15A)	1.5236(12)
C(9A)-C(10A)	1.5335(12)
C(9A)-H(9A)	0.977(8)
C(10A)-C(11A)	1.5288(13)
C(10A)-H(10A)	0.998(8)
C(10A)-H(10B)	1.018(9)
C(11A)-H(11A)	0.972(9)
C(11A)-H(11B)	0.999(9)
C(12A)-H(12A)	0.995(10)
C(12A)-H(12B)	0.992(9)
C(12A)-H(12C)	0.999(10)
C(13A)-H(13A)	0.977(11)
C(13A)-H(13B)	0.970(10)
C(13A)-H(13C)	0.942(11)
C(14A)-H(14A)	0.976(9)
C(14A)-H(14B)	0.983(9)
C(14A)-H(14C)	0.989(9)
C(15A)-H(15A)	0.979(10)
C(15A)-H(15B)	1.024(10)
C(15A)-H(15C)	0.987(10)
O(1B)-C(1B)	1.4494(10)
O(1B)-H(1B)	0.748(11)
C(1B)-C(8B)	1.5103(10)
C(1B)-C(2B)	1.5338(11)
C(1B)-C(9B)	1.5419(11)
C(2B)-C(3B)	1.5428(13)

Table A6.9 (cont.)

C(2B)-H(2C)	0.977(8)
C(2B)-H(2D)	1.005(9)
C(3B)-C(4B)	1.5564(13)
C(3B)-H(3C)	0.977(10)
C(3B)-H(3D)	0.998(9)
C(4B)-C(14B)	1.5232(12)
C(4B)-C(8B)	1.5430(11)
C(4B)-C(5B)	1.5621(12)
C(5B)-C(6B)	1.5472(12)
C(5B)-H(5C)	0.959(10)
C(5B)-H(5D)	0.961(10)
C(6B)-C(13B)	1.5264(11)
C(6B)-C(12B)	1.5283(12)
C(6B)-C(7B)	1.5340(11)
C(7B)-C(11B)	1.5145(11)
C(7B)-C(8B)	1.5238(10)
C(7B)-H(7B)	0.984(7)
C(8B)-H(8B)	0.984(8)
C(9B)-C(15B)	1.5198(12)
C(9B)-C(10B)	1.5316(12)
C(9B)-H(9B)	0.967(7)
C(10B)-C(11B)	1.5329(12)
C(10B)-H(10C)	1.011(9)
C(10B)-H(10D)	0.966(10)
C(11B)-H(11C)	0.956(8)
C(11B)-H(11D)	0.967(8)
C(12B)-H(12D)	0.980(9)
C(12B)-H(12E)	0.968(9)
C(12B)-H(12F)	0.998(9)
C(13B)-H(13D)	0.994(10)
C(13B)-H(13E)	0.987(10)
C(13B)-H(13F)	0.976(9)
C(14B)-H(14D)	0.995(10)
C(14B)-H(14E)	0.964(10)
C(14B)-H(14F)	0.991(10)
C(15B)-H(15D)	1.014(11)
C(15B)-H(15E)	0.984(10)
C(15B)-H(15F)	0.962(10)
C(1A)-O(1A)-H(1A)	110.4(9)
O(1A)-C(1A)-C(8A)	107.21(6)
O(1A)-C(1A)-C(2A)	108.20(6)
C(8A)-C(1A)-C(2A)	102.06(6)
O(1A)-C(1A)-C(9A)	108.36(6)
C(8A)-C(1A)-C(9A)	111.76(6)
C(2A)-C(1A)-C(9A)	118.63(6)
C(1A)-C(2A)-C(3A)	104.58(6)
C(1A)-C(2A)-H(2A)	109.6(5)
C(3A)-C(2A)-H(2A)	111.5(5)
C(1A)-C(2A)-H(2B)	110.0(5)
C(3A)-C(2A)-H(2B)	111.5(5)

Table A6.9 (cont.)

H(2A)-C(2A)-H(2B)	109.5(6)
C(2A)-C(3A)-C(4A)	107.62(6)
C(2A)-C(3A)-H(3A)	111.5(5)
C(4A)-C(3A)-H(3A)	111.5(4)
C(2A)-C(3A)-H(3B)	111.2(5)
C(4A)-C(3A)-H(3B)	109.2(5)
H(3A)-C(3A)-H(3B)	105.9(7)
C(14A)-C(4A)-C(8A)	112.91(6)
C(14A)-C(4A)-C(3A)	111.26(7)
C(8A)-C(4A)-C(3A)	102.70(6)
C(14A)-C(4A)-C(5A)	110.99(7)
C(8A)-C(4A)-C(5A)	103.88(6)
C(3A)-C(4A)-C(5A)	114.65(7)
C(6A)-C(5A)-C(4A)	107.85(6)
C(6A)-C(5A)-H(5A)	112.3(5)
C(4A)-C(5A)-H(5A)	111.2(5)
C(6A)-C(5A)-H(5B)	109.3(5)
C(4A)-C(5A)-H(5B)	110.6(5)
H(5A)-C(5A)-H(5B)	105.5(7)
C(13A)-C(6A)-C(12A)	108.90(8)
C(13A)-C(6A)-C(7A)	112.14(8)
C(12A)-C(6A)-C(7A)	112.71(7)
C(13A)-C(6A)-C(5A)	112.13(8)
C(12A)-C(6A)-C(5A)	111.38(8)
C(7A)-C(6A)-C(5A)	99.39(6)
C(11A)-C(7A)-C(8A)	110.62(7)
C(11A)-C(7A)-C(6A)	124.72(7)
C(8A)-C(7A)-C(6A)	104.02(6)
C(11A)-C(7A)-H(7A)	105.1(4)
C(8A)-C(7A)-H(7A)	105.6(4)
C(6A)-C(7A)-H(7A)	105.3(4)
C(1A)-C(8A)-C(7A)	111.77(6)
C(1A)-C(8A)-C(4A)	108.72(6)
C(7A)-C(8A)-C(4A)	103.50(6)
C(1A)-C(8A)-H(8A)	109.4(4)
C(7A)-C(8A)-H(8A)	108.5(4)
C(4A)-C(8A)-H(8A)	114.8(4)
C(15A)-C(9A)-C(10A)	110.76(7)
C(15A)-C(9A)-C(1A)	112.32(7)
C(10A)-C(9A)-C(1A)	114.30(7)
C(15A)-C(9A)-H(9A)	106.5(4)
C(10A)-C(9A)-H(9A)	107.2(4)
C(1A)-C(9A)-H(9A)	105.1(5)
C(11A)-C(10A)-C(9A)	114.74(7)
C(11A)-C(10A)-H(10A)	108.7(5)
C(9A)-C(10A)-H(10A)	110.0(5)
C(11A)-C(10A)-H(10B)	110.1(5)
C(9A)-C(10A)-H(10B)	108.3(5)
H(10A)-C(10A)-H(10B)	104.6(7)
C(7A)-C(11A)-C(10A)	107.07(7)
C(7A)-C(11A)-H(11A)	108.1(5)

Table A6.9 (cont.)

C(10A)-C(11A)-H(11A)	110.8(5)
C(7A)-C(11A)-H(11B)	109.7(5)
C(10A)-C(11A)-H(11B)	111.6(5)
H(11A)-C(11A)-H(11B)	109.4(7)
C(6A)-C(12A)-H(12A)	109.7(6)
C(6A)-C(12A)-H(12B)	111.9(5)
H(12A)-C(12A)-H(12B)	108.4(8)
C(6A)-C(12A)-H(12C)	109.7(6)
H(12A)-C(12A)-H(12C)	106.1(7)
H(12B)-C(12A)-H(12C)	110.9(8)
C(6A)-C(13A)-H(13A)	111.6(6)
C(6A)-C(13A)-H(13B)	110.7(6)
H(13A)-C(13A)-H(13B)	107.8(8)
C(6A)-C(13A)-H(13C)	110.6(7)
H(13A)-C(13A)-H(13C)	107.4(8)
H(13B)-C(13A)-H(13C)	108.6(9)
C(4A)-C(14A)-H(14A)	109.6(5)
C(4A)-C(14A)-H(14B)	110.9(5)
H(14A)-C(14A)-H(14B)	108.3(7)
C(4A)-C(14A)-H(14C)	111.3(5)
H(14A)-C(14A)-H(14C)	108.5(7)
H(14B)-C(14A)-H(14C)	108.1(7)
C(9A)-C(15A)-H(15A)	109.1(5)
C(9A)-C(15A)-H(15B)	112.0(5)
H(15A)-C(15A)-H(15B)	108.4(8)
C(9A)-C(15A)-H(15C)	110.9(6)
H(15A)-C(15A)-H(15C)	110.3(8)
H(15B)-C(15A)-H(15C)	106.0(8)
C(1B)-O(1B)-H(1B)	109.6(8)
O(1B)-C(1B)-C(8B)	109.42(6)
O(1B)-C(1B)-C(2B)	105.54(6)
C(8B)-C(1B)-C(2B)	102.40(6)
O(1B)-C(1B)-C(9B)	109.12(6)
C(8B)-C(1B)-C(9B)	111.58(6)
C(2B)-C(1B)-C(9B)	118.31(7)
C(1B)-C(2B)-C(3B)	104.90(7)
C(1B)-C(2B)-H(2C)	110.2(5)
C(3B)-C(2B)-H(2C)	112.0(5)
C(1B)-C(2B)-H(2D)	109.8(5)
C(3B)-C(2B)-H(2D)	112.7(5)
H(2C)-C(2B)-H(2D)	107.3(7)
C(2B)-C(3B)-C(4B)	108.38(6)
C(2B)-C(3B)-H(3C)	111.3(5)
C(4B)-C(3B)-H(3C)	111.5(5)
C(2B)-C(3B)-H(3D)	108.0(5)
C(4B)-C(3B)-H(3D)	109.9(5)
H(3C)-C(3B)-H(3D)	107.7(7)
C(14B)-C(4B)-C(8B)	114.15(7)
C(14B)-C(4B)-C(3B)	110.72(8)
C(8B)-C(4B)-C(3B)	102.28(7)
C(14B)-C(4B)-C(5B)	111.10(8)

Table A6.9 (cont.)

C(8B)-C(4B)-C(5B)	103.54(7)
C(3B)-C(4B)-C(5B)	114.67(7)
C(6B)-C(5B)-C(4B)	108.32(7)
C(6B)-C(5B)-H(5C)	110.3(6)
C(4B)-C(5B)-H(5C)	112.0(6)
C(6B)-C(5B)-H(5D)	107.5(6)
C(4B)-C(5B)-H(5D)	111.5(6)
H(5C)-C(5B)-H(5D)	107.2(8)
C(13B)-C(6B)-C(12B)	108.80(7)
C(13B)-C(6B)-C(7B)	112.00(7)
C(12B)-C(6B)-C(7B)	113.00(7)
C(13B)-C(6B)-C(5B)	111.61(7)
C(12B)-C(6B)-C(5B)	111.70(8)
C(7B)-C(6B)-C(5B)	99.55(6)
C(11B)-C(7B)-C(8B)	110.85(7)
C(11B)-C(7B)-C(6B)	124.21(7)
C(8B)-C(7B)-C(6B)	104.03(6)
C(11B)-C(7B)-H(7B)	105.4(4)
C(8B)-C(7B)-H(7B)	105.6(4)
C(6B)-C(7B)-H(7B)	105.3(4)
C(1B)-C(8B)-C(7B)	111.41(6)
C(1B)-C(8B)-C(4B)	108.52(6)
C(7B)-C(8B)-C(4B)	103.07(6)
C(1B)-C(8B)-H(8B)	110.3(4)
C(7B)-C(8B)-H(8B)	110.5(4)
C(4B)-C(8B)-H(8B)	112.9(4)
C(15B)-C(9B)-C(10B)	110.84(7)
C(15B)-C(9B)-C(1B)	112.46(7)
C(10B)-C(9B)-C(1B)	113.92(7)
C(15B)-C(9B)-H(9B)	109.4(4)
C(10B)-C(9B)-H(9B)	105.7(4)
C(1B)-C(9B)-H(9B)	104.0(4)
C(9B)-C(10B)-C(11B)	114.14(7)
C(9B)-C(10B)-H(10C)	108.9(5)
C(11B)-C(10B)-H(10C)	106.1(5)
C(9B)-C(10B)-H(10D)	110.2(5)
C(11B)-C(10B)-H(10D)	108.0(5)
H(10C)-C(10B)-H(10D)	109.3(7)
C(7B)-C(11B)-C(10B)	107.05(7)
C(7B)-C(11B)-H(11C)	110.3(5)
C(10B)-C(11B)-H(11C)	110.8(5)
C(7B)-C(11B)-H(11D)	111.4(5)
C(10B)-C(11B)-H(11D)	111.1(5)
H(11C)-C(11B)-H(11D)	106.2(6)
C(6B)-C(12B)-H(12D)	110.6(5)
C(6B)-C(12B)-H(12E)	111.3(5)
H(12D)-C(12B)-H(12E)	107.6(7)
C(6B)-C(12B)-H(12F)	111.6(5)
H(12D)-C(12B)-H(12F)	107.9(7)
H(12E)-C(12B)-H(12F)	107.7(8)
C(6B)-C(13B)-H(13D)	110.8(6)

Table A6.9 (cont.)

C(6B)-C(13B)-H(13E)	111.4(5)
H(13D)-C(13B)-H(13E)	106.1(7)
C(6B)-C(13B)-H(13F)	109.9(5)
H(13D)-C(13B)-H(13F)	108.5(7)
H(13E)-C(13B)-H(13F)	110.2(8)
C(4B)-C(14B)-H(14D)	110.1(6)
C(4B)-C(14B)-H(14E)	108.0(5)
H(14D)-C(14B)-H(14E)	110.4(8)
C(4B)-C(14B)-H(14F)	111.5(6)
H(14D)-C(14B)-H(14F)	108.0(8)
H(14E)-C(14B)-H(14F)	108.9(8)
C(9B)-C(15B)-H(15D)	112.1(6)
C(9B)-C(15B)-H(15E)	112.4(6)
H(15D)-C(15B)-H(15E)	106.9(8)
C(9B)-C(15B)-H(15F)	111.9(5)
H(15D)-C(15B)-H(15F)	105.2(8)
H(15E)-C(15B)-H(15F)	107.9(8)

Symmetry transformations used to generate equivalent atoms:

Table A6.10. Anisotropic displacement parameters ($\text{\AA}^2 \times 10^4$) for tertiary alcohol **224** (CCDC 889569). The anisotropic displacement factor exponent takes the form: $-2\pi^2 [h^2 a^{*2} U^{11} + \dots + 2 h k a^* b^* U^{12}]$

	U^{11}	U^{22}	U^{33}	U^{23}	U^{13}	U^{12}
O(1A)	202(3)	283(3)	360(4)	20(3)	153(3)	-34(3)
C(1A)	139(3)	171(4)	191(3)	2(3)	62(3)	-36(3)
C(2A)	199(4)	235(4)	165(4)	12(3)	77(3)	-21(3)
C(3A)	218(4)	256(4)	177(4)	52(3)	56(3)	15(3)
C(4A)	163(3)	173(4)	208(4)	8(3)	55(3)	9(3)
C(5A)	192(4)	306(5)	278(5)	-26(4)	82(4)	40(4)
C(6A)	211(4)	343(5)	223(4)	-36(4)	115(3)	-30(4)
C(7A)	185(4)	224(4)	164(3)	-10(3)	58(3)	-53(3)
C(8A)	142(3)	168(4)	149(3)	2(3)	34(3)	-23(3)
C(9A)	190(4)	185(4)	248(4)	1(3)	34(3)	4(3)
C(10A)	286(5)	176(4)	292(5)	35(4)	40(4)	-28(4)
C(11A)	307(5)	284(5)	227(4)	71(4)	90(4)	-87(4)
C(12A)	356(5)	512(7)	248(5)	-87(5)	135(4)	16(5)
C(13A)	317(5)	561(7)	409(6)	-19(6)	231(5)	-58(5)
C(14A)	245(4)	167(4)	329(5)	26(4)	49(4)	1(3)
C(15A)	344(5)	260(5)	414(6)	-46(5)	137(5)	61(4)
O(1B)	319(4)	286(3)	183(3)	-61(3)	28(3)	61(3)
C(1B)	170(3)	198(4)	173(3)	-45(3)	54(3)	7(3)
C(2B)	166(4)	341(5)	223(4)	-81(4)	78(3)	20(3)
C(3B)	218(4)	365(5)	289(5)	-25(4)	35(4)	131(4)
C(4B)	268(4)	190(4)	170(4)	-6(3)	19(3)	64(3)
C(5B)	371(5)	351(5)	194(4)	42(4)	51(4)	98(5)
C(6B)	198(4)	276(4)	170(4)	-19(3)	49(3)	-12(3)
C(7B)	142(3)	206(4)	204(4)	-53(3)	64(3)	-15(3)
C(8B)	141(3)	165(4)	170(3)	-17(3)	21(3)	11(3)
C(9B)	194(4)	193(4)	254(4)	12(3)	81(3)	-12(3)
C(10B)	313(5)	171(4)	367(5)	-11(4)	151(4)	4(4)
C(11B)	256(4)	217(4)	316(5)	-56(4)	158(4)	29(3)
C(12B)	299(5)	406(6)	256(5)	24(5)	86(4)	-101(4)
C(13B)	270(5)	468(6)	212(4)	-72(4)	94(4)	-45(5)
C(14B)	500(6)	207(5)	255(5)	4(4)	1(4)	88(4)
C(15B)	330(5)	310(5)	345(6)	45(5)	160(4)	-32(4)

Table A6.11. Hydrogen coordinates ($\times 10^3$) and isotropic displacement parameters ($\text{\AA}^2 \times 10^3$) for tertiary alcohol **224** (CCDC 889569)

	x	y	z	U _{iso}
H(1A)	399(1)	87(1)	-27(1)	38(4)
H(2A)	220(1)	-62(1)	-70(1)	16(2)
H(2B)	280(1)	5(1)	-106(1)	19(2)
H(3A)	161(1)	170(1)	-98(1)	21(2)
H(3B)	243(1)	244(1)	-96(1)	21(2)
H(5A)	161(1)	333(1)	57(1)	21(2)
H(5B)	118(1)	206(1)	-2(1)	29(2)
H(7A)	195(1)	-40(1)	33(1)	14(2)
H(8A)	336(1)	123(1)	110(1)	9(2)
H(9A)	413(1)	-122(1)	91(1)	15(2)
H(10A)	260(1)	-271(1)	38(1)	22(2)
H(10B)	338(1)	-315(1)	112(1)	28(2)
H(11A)	234(1)	-187(1)	143(1)	31(2)
H(11B)	319(1)	-100(1)	179(1)	30(2)
H(12A)	196(1)	258(1)	198(1)	45(3)
H(12B)	281(1)	235(1)	187(1)	34(3)
H(12C)	244(1)	106(1)	226(1)	42(3)
H(13A)	114(1)	-24(1)	146(1)	52(3)
H(13B)	73(1)	6(1)	57(1)	45(3)
H(13C)	72(1)	126(1)	116(1)	51(3)
H(14A)	304(1)	398(1)	86(1)	29(2)
H(14B)	254(1)	451(1)	0(1)	32(2)
H(14C)	338(1)	364(1)	20(1)	29(2)
H(15A)	412(1)	-328(1)	19(1)	37(3)
H(15B)	418(1)	-186(1)	-31(1)	46(3)
H(15C)	333(1)	-270(1)	-52(1)	43(3)
H(1B)	511(1)	90(1)	89(1)	44(3)
H(2C)	683(1)	266(1)	258(1)	18(2)
H(2D)	694(1)	177(1)	188(1)	30(2)
H(3C)	717(1)	45(1)	323(1)	36(3)
H(3D)	693(1)	-45(1)	244(1)	35(3)
H(5C)	571(1)	-91(1)	371(1)	41(3)
H(5D)	642(1)	20(1)	396(1)	40(3)
H(7B)	600(1)	263(1)	319(1)	9(2)
H(8B)	480(1)	93(1)	203(1)	15(2)
H(9B)	480(1)	324(1)	116(1)	8(2)
H(10C)	586(1)	476(1)	248(1)	26(2)
H(10D)	497(1)	531(1)	191(1)	34(3)
H(11C)	495(1)	432(1)	307(1)	22(2)
H(11D)	437(1)	344(1)	237(1)	19(2)
H(12D)	443(1)	9(1)	378(1)	33(3)
H(12E)	426(1)	26(1)	289(1)	33(3)
H(12F)	409(1)	162(1)	335(1)	39(3)
H(13D)	527(1)	289(1)	438(1)	41(3)

Table A6.11 (cont.)

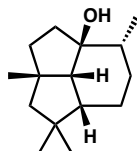
H(13E)	618(1)	246(1)	451(1)	39(3)
H(13F)	563(1)	134(1)	477(1)	31(3)
H(14D)	509(1)	-182(1)	238(1)	47(3)
H(14E)	603(1)	-231(1)	267(1)	40(3)
H(14F)	559(1)	-160(1)	184(1)	43(3)
H(15D)	552(1)	521(1)	82(1)	57(3)
H(15E)	581(1)	364(1)	61(1)	44(3)
H(15F)	634(1)	450(1)	137(1)	40(3)

Table A6.12. Hydrogen bonds for tertiary alcohol **224** (CCDC 889569) [\AA and $^\circ$]

D-H...A	d(D-H)	d(H...A)	d(D...A)	<(DHA)
O(1A)-H(1A)...O(1B)#1	0.734(10)	2.033(10)	2.7380(9)	161.1(11)
O(1B)-H(1B)...O(1A)	0.748(11)	2.028(11)	2.7658(9)	168.8(11)

Symmetry transformations used to generate equivalent atoms:

#1 -x+1,y,-z

A6.3 CRYSTAL STRUCTURE ANALYSIS OF 356Compound **356**

(AYH03) (CCDC 911859)

Contents

Table A6.13. Crystal data

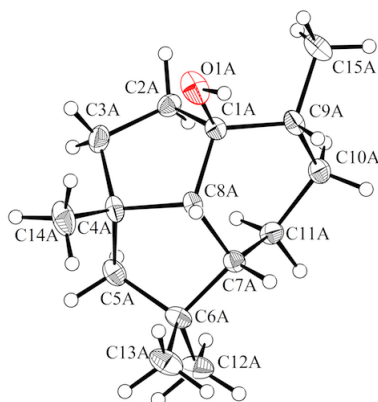
Table A6.14. Atomic coordinates

Table A6.15. Full bond distances and angles

Table A6.16. Anisotropic displacement parameters

Table A6.17. Hydrogen atomic coordinates

Table A6.18. Hydrogen bond distances and angles

*Figure A6.6. Tertiary Alcohol **356** (CCDC 911859).*

CCDC 911859 contains the supplementary crystallographic data for this compound. These data can be obtained free of charge from The Cambridge Crystallographic Data Centre via www.ccdc.cam.ac.uk/data_request/cif.

Table A6.13. Crystal data and structure refinement for tertiary alcohol **356** (CCDC 911859)

Empirical formula	C ₁₅ H ₂₆ O
Formula weight	222.36
Crystallization solvent	hexanes, slow evaporation
Crystal shape	block
Crystal color	colorless
Crystal size	0.11 x 0.2 x 0.43 mm

Data Collection

Preliminary photograph(s)	rotation	
Type of diffractometer	Bruker APEX-II CCD	
Wavelength	0.71073 Å MoK α	
Data collection temperature	100 K	
Theta range for 9851 reflections used in lattice determination	2.25 to 35.10°	
Unit cell dimensions	a = 20.8725(14) Å b = 9.2598(6) Å c = 16.2667(11) Å	$\alpha = 90^\circ$ $\beta = 119.717(3)^\circ$ $\gamma = 90^\circ$
Volume	2730.5(3) Å ³	
Z	8	
Crystal system	monoclinic	
Space group	C 1 2 1 (# 5)	
Density (calculated)	1.082 g/cm ³	
F(000)	992	
Theta range for data collection	2.2 to 38.1°	
Completeness to theta = 25.00°	99.9%	
Index ranges	-35 ≤ h ≤ 35, -16 ≤ k ≤ 15, -27 ≤ l ≤ 27	
Data collection scan type	and scans	
Reflections collected	78345	
Independent reflections	13415 [R _{int} = 0.0435]	
Reflections > 2 s(I)	11403	
Average s(I)/(net I)	0.0343	
Absorption coefficient	0.06 mm ⁻¹	
Absorption correction	Semi-empirical from equivalents	
Max. and min. transmission	1.0000 and 0.9268	

Table A6.13 (cont.)

Structure Solution and Refinement

Primary solution method	dual
Secondary solution method	?
Hydrogen placement	geom
Refinement method	Full-matrix least-squares on F^2
Data / restraints / parameters	13415 / 1 / 299
Treatment of hydrogen atoms	constr
Goodness-of-fit on F^2	1.51
Final R indices [$I > 2\sigma(I)$, 11403 reflections]	$R1 = 0.0453$, $wR2 = 0.1039$
R indices (all data)	$R1 = 0.0591$, $wR2 = 0.1084$
Type of weighting scheme used	calc
Weighting scheme used	
Max shift/error	0.001
Average shift/error	0.000
Absolute structure parameter	0.5(3)
Extinction coefficient	0.00083(11)
Largest diff. peak and hole	0.39 and -0.26 e. \AA^{-3}

Programs Used

Cell refinement	SAINT V8.27B (Bruker-AXS, 2007)
Data collection	APEX2 2012.4-3 (Bruker-AXS, 2007)
Data reduction	SAINT V8.27B (Bruker-AXS, 2007)
Structure solution	SHELXT (Sheldrick, 2012)
Structure refinement	SHELXL-2012/6 (Sheldrick, 2012)
Graphics	DIAMOND 3 (Crystal Impact, 1999)

References**Special Refinement Details**

Figure A6.7. Tertiary alcohol **356**, crystal form A (CCDC 889569).

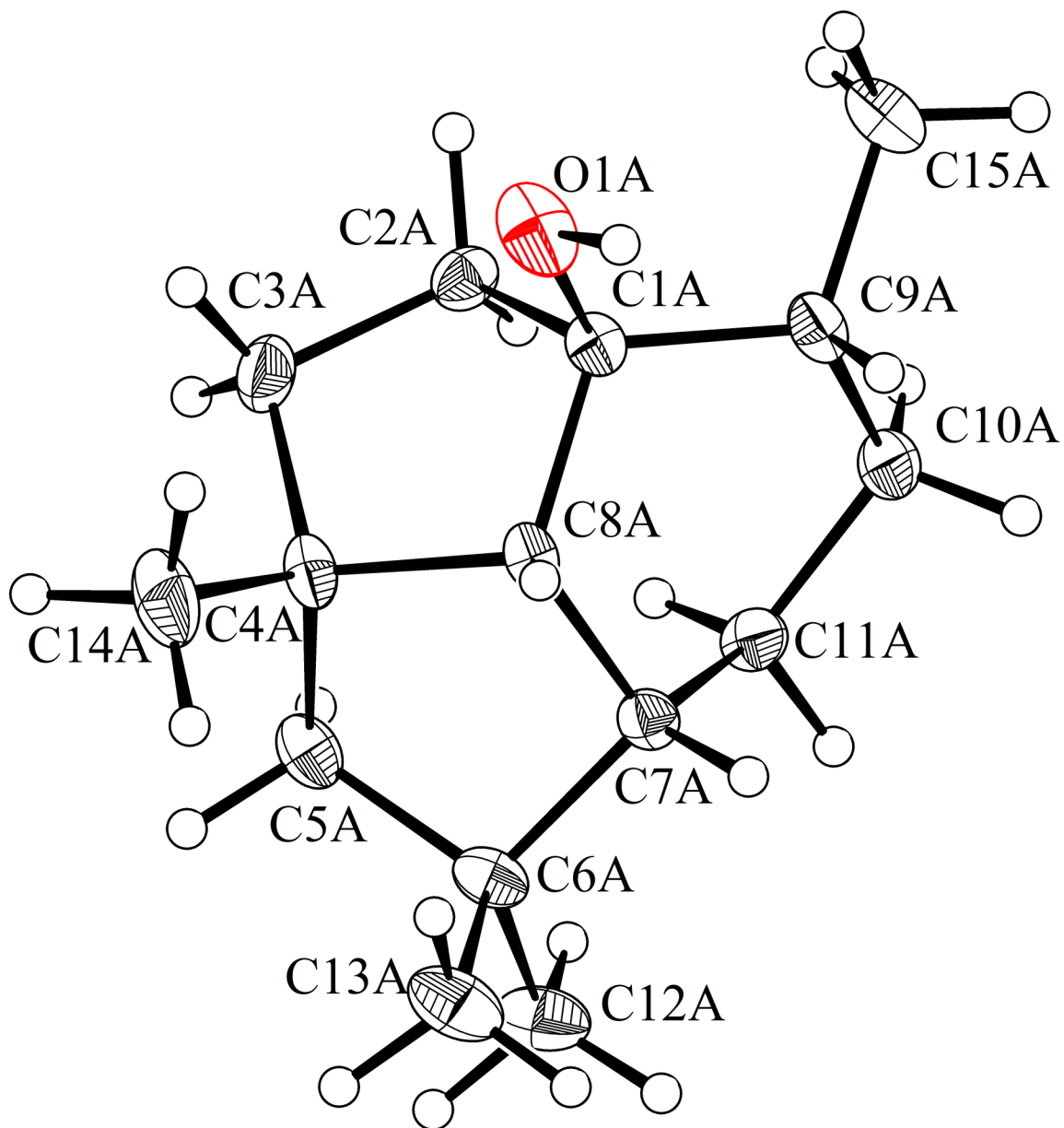


Table A6.14. Atomic coordinates ($\times 10^4$) and equivalent isotropic displacement parameters ($\text{\AA}^2 \times 10^3$) for tertiary alcohol **356** (CCDC 911859). $U(\text{eq})$ is defined as the trace of the orthogonalized U^{ij} tensor

	x	y	z	U_{eq}
O(1A)	6050(1)	724(1)	5532(1)	33(1)
C(1A)	6702(1)	1621(1)	5956(1)	17(1)
C(2A)	7062(1)	1474(1)	5338(1)	20(1)
C(3A)	7417(1)	-19(2)	5586(1)	26(1)
C(4A)	7663(1)	-279(1)	6640(1)	20(1)
C(5A)	8483(1)	78(1)	7322(1)	23(1)
C(6A)	8522(1)	929(1)	8156(1)	21(1)
C(7A)	7823(1)	1887(1)	7662(1)	18(1)
C(8A)	7242(1)	881(1)	6892(1)	16(1)
C(9A)	6511(1)	3156(1)	6104(1)	20(1)
C(10A)	7205(1)	4104(1)	6645(1)	24(1)
C(11A)	7929(1)	3280(1)	7243(1)	20(1)
C(12A)	9249(1)	1761(2)	8692(1)	31(1)
C(13A)	8463(1)	-68(2)	8869(1)	33(1)
C(14A)	7478(1)	-1839(1)	6763(1)	34(1)
C(15A)	5955(1)	3889(2)	5180(1)	28(1)
O(1B)	4896(1)	726(1)	3769(1)	34(1)
C(1B)	4743(1)	-64(1)	2928(1)	17(1)
C(2B)	5437(1)	42(1)	2837(1)	20(1)
C(3B)	5417(1)	1576(1)	2484(1)	23(1)
C(4B)	4592(1)	1972(1)	1854(1)	19(1)
C(5B)	4301(1)	1758(1)	787(1)	24(1)
C(6B)	3549(1)	996(1)	372(1)	25(1)
C(7B)	3672(1)	-62(1)	1173(1)	20(1)
C(8B)	4161(1)	815(1)	2089(1)	16(1)
C(9B)	4481(1)	-1590(1)	2961(1)	23(1)
C(10B)	4232(1)	-2424(1)	2031(1)	27(1)
C(11B)	4026(1)	-1488(1)	1156(1)	23(1)
C(12B)	3338(1)	275(2)	-573(1)	40(1)
C(13B)	2927(1)	2037(2)	204(1)	35(1)
C(14B)	4463(1)	3519(1)	2076(1)	32(1)
C(15B)	5051(1)	-2467(2)	3800(1)	39(1)

Table A6.15. Bond lengths [\AA] and angles [$^\circ$] for tertiary alcohol **356** (CCDC 911859)

O(1A)-H(1A)	0.8400
O(1A)-C(1A)	1.4453(13)
C(1A)-C(2A)	1.5308(14)
C(1A)-C(8A)	1.5346(14)
C(1A)-C(9A)	1.5270(15)
C(2A)-H(2A1)	0.9900
C(2A)-H(2A2)	0.9900
C(2A)-C(3A)	1.5250(18)
C(3A)-H(3A1)	0.9900
C(3A)-H(3A2)	0.9900
C(3A)-C(4A)	1.5463(17)
C(4A)-C(5A)	1.5448(16)
C(4A)-C(8A)	1.5658(14)
C(4A)-C(14A)	1.5334(17)
C(5A)-H(5A1)	0.9900
C(5A)-H(5A2)	0.9900
C(5A)-C(6A)	1.5364(17)
C(6A)-C(7A)	1.5478(15)
C(6A)-C(12A)	1.5318(17)
C(6A)-C(13A)	1.5343(16)
C(7A)-H(7A)	1.0000
C(7A)-C(8A)	1.5493(15)
C(7A)-C(11A)	1.5247(15)
C(8A)-H(8A)	1.0000
C(9A)-H(9A)	1.0000
C(9A)-C(10A)	1.5426(17)
C(9A)-C(15A)	1.5294(16)
C(10A)-H(10A)	0.9900
C(10A)-H(10B)	0.9900
C(10A)-C(11A)	1.5338(16)
C(11A)-H(11A)	0.9900
C(11A)-H(11B)	0.9900
C(12A)-H(12A)	0.9800
C(12A)-H(12B)	0.9800
C(12A)-H(12C)	0.9800
C(13A)-H(13A)	0.9800
C(13A)-H(13B)	0.9800
C(13A)-H(13C)	0.9800
C(14A)-H(14A)	0.9800
C(14A)-H(14B)	0.9800
C(14A)-H(14C)	0.9800
C(15A)-H(15A)	0.9800
C(15A)-H(15B)	0.9800
C(15A)-H(15C)	0.9800
O(1B)-H(1B)	0.8400
O(1B)-C(1B)	1.4410(13)
C(1B)-C(2B)	1.5298(14)
C(1B)-C(8B)	1.5350(14)
C(1B)-C(9B)	1.5261(16)
C(2B)-H(2B1)	0.9900

Table A6.15 (cont.)

C(2B)-H(2B2)	0.9900
C(2B)-C(3B)	1.5243(17)
C(3B)-H(3B1)	0.9900
C(3B)-H(3B2)	0.9900
C(3B)-C(4B)	1.5495(16)
C(4B)-C(5B)	1.5417(16)
C(4B)-C(8B)	1.5638(14)
C(4B)-C(14B)	1.5336(17)
C(5B)-H(5B1)	0.9900
C(5B)-H(5B2)	0.9900
C(5B)-C(6B)	1.5387(17)
C(6B)-C(7B)	1.5469(16)
C(6B)-C(12B)	1.5270(19)
C(6B)-C(13B)	1.5282(18)
C(7B)-H(7B)	1.0000
C(7B)-C(8B)	1.5533(15)
C(7B)-C(11B)	1.5211(16)
C(8B)-H(8B)	1.0000
C(9B)-H(9B)	1.0000
C(9B)-C(10B)	1.5414(18)
C(9B)-C(15B)	1.5258(18)
C(10B)-H(10C)	0.9900
C(10B)-H(10D)	0.9900
C(10B)-C(11B)	1.5349(18)
C(11B)-H(11C)	0.9900
C(11B)-H(11D)	0.9900
C(12B)-H(12D)	0.9800
C(12B)-H(12E)	0.9800
C(12B)-H(12F)	0.9800
C(13B)-H(13D)	0.9800
C(13B)-H(13E)	0.9800
C(13B)-H(13F)	0.9800
C(14B)-H(14D)	0.9800
C(14B)-H(14E)	0.9800
C(14B)-H(14F)	0.9800
C(15B)-H(15D)	0.9800
C(15B)-H(15E)	0.9800
C(15B)-H(15F)	0.9800
C(1A)-O(1A)-H(1A)	109.5
O(1A)-C(1A)-C(2A)	106.76(9)
O(1A)-C(1A)-C(8A)	105.75(9)
O(1A)-C(1A)-C(9A)	110.62(8)
C(2A)-C(1A)-C(8A)	104.70(8)
C(9A)-C(1A)-C(2A)	115.98(9)
C(9A)-C(1A)-C(8A)	112.33(9)
C(1A)-C(2A)-H(2A1)	111.0
C(1A)-C(2A)-H(2A2)	111.0
H(2A1)-C(2A)-H(2A2)	109.0
C(3A)-C(2A)-C(1A)	103.86(9)
C(3A)-C(2A)-H(2A1)	111.0

Table A6.15 (cont.)

C(3A)-C(2A)-H(2A2)	111.0
C(2A)-C(3A)-H(3A1)	110.4
C(2A)-C(3A)-H(3A2)	110.4
C(2A)-C(3A)-C(4A)	106.57(9)
H(3A1)-C(3A)-H(3A2)	108.6
C(4A)-C(3A)-H(3A1)	110.4
C(4A)-C(3A)-H(3A2)	110.4
C(3A)-C(4A)-C(8A)	105.20(9)
C(5A)-C(4A)-C(3A)	113.75(9)
C(5A)-C(4A)-C(8A)	103.39(9)
C(14A)-C(4A)-C(3A)	108.95(10)
C(14A)-C(4A)-C(5A)	111.67(10)
C(14A)-C(4A)-C(8A)	113.71(9)
C(4A)-C(5A)-H(5A1)	110.3
C(4A)-C(5A)-H(5A2)	110.3
H(5A1)-C(5A)-H(5A2)	108.5
C(6A)-C(5A)-C(4A)	107.31(8)
C(6A)-C(5A)-H(5A1)	110.3
C(6A)-C(5A)-H(5A2)	110.3
C(5A)-C(6A)-C(7A)	102.26(8)
C(12A)-C(6A)-C(5A)	111.37(9)
C(12A)-C(6A)-C(7A)	114.86(11)
C(12A)-C(6A)-C(13A)	107.42(10)
C(13A)-C(6A)-C(5A)	111.73(11)
C(13A)-C(6A)-C(7A)	109.24(9)
C(6A)-C(7A)-H(7A)	109.0
C(6A)-C(7A)-C(8A)	103.52(9)
C(8A)-C(7A)-H(7A)	109.0
C(11A)-C(7A)-C(6A)	114.14(8)
C(11A)-C(7A)-H(7A)	109.0
C(11A)-C(7A)-C(8A)	112.09(8)
C(1A)-C(8A)-C(4A)	106.16(8)
C(1A)-C(8A)-C(7A)	115.40(9)
C(1A)-C(8A)-H(8A)	109.1
C(4A)-C(8A)-H(8A)	109.1
C(7A)-C(8A)-C(4A)	107.92(8)
C(7A)-C(8A)-H(8A)	109.1
C(1A)-C(9A)-H(9A)	107.0
C(1A)-C(9A)-C(10A)	112.03(8)
C(1A)-C(9A)-C(15A)	112.89(10)
C(10A)-C(9A)-H(9A)	107.0
C(15A)-C(9A)-H(9A)	107.0
C(15A)-C(9A)-C(10A)	110.44(10)
C(9A)-C(10A)-H(10A)	108.4
C(9A)-C(10A)-H(10B)	108.4
H(10A)-C(10A)-H(10B)	107.5
C(11A)-C(10A)-C(9A)	115.42(9)
C(11A)-C(10A)-H(10A)	108.4
C(11A)-C(10A)-H(10B)	108.4
C(7A)-C(11A)-C(10A)	112.92(9)
C(7A)-C(11A)-H(11A)	109.0

Table A6.15 (cont.)

C(7A)-C(11A)-H(11B)	109.0
C(10A)-C(11A)-H(11A)	109.0
C(10A)-C(11A)-H(11B)	109.0
H(11A)-C(11A)-H(11B)	107.8
C(6A)-C(12A)-H(12A)	109.5
C(6A)-C(12A)-H(12B)	109.5
C(6A)-C(12A)-H(12C)	109.5
H(12A)-C(12A)-H(12B)	109.5
H(12A)-C(12A)-H(12C)	109.5
H(12B)-C(12A)-H(12C)	109.5
C(6A)-C(13A)-H(13A)	109.5
C(6A)-C(13A)-H(13B)	109.5
C(6A)-C(13A)-H(13C)	109.5
H(13A)-C(13A)-H(13B)	109.5
H(13A)-C(13A)-H(13C)	109.5
H(13B)-C(13A)-H(13C)	109.5
C(4A)-C(14A)-H(14A)	109.5
C(4A)-C(14A)-H(14B)	109.5
C(4A)-C(14A)-H(14C)	109.5
H(14A)-C(14A)-H(14B)	109.5
H(14A)-C(14A)-H(14C)	109.5
H(14B)-C(14A)-H(14C)	109.5
C(9A)-C(15A)-H(15A)	109.5
C(9A)-C(15A)-H(15B)	109.5
C(9A)-C(15A)-H(15C)	109.5
H(15A)-C(15A)-H(15B)	109.5
H(15A)-C(15A)-H(15C)	109.5
H(15B)-C(15A)-H(15C)	109.5
C(1B)-O(1B)-H(1B)	109.5
O(1B)-C(1B)-C(2B)	106.56(9)
O(1B)-C(1B)-C(8B)	106.27(9)
O(1B)-C(1B)-C(9B)	110.55(8)
C(2B)-C(1B)-C(8B)	104.50(8)
C(9B)-C(1B)-C(2B)	115.84(9)
C(9B)-C(1B)-C(8B)	112.46(9)
C(1B)-C(2B)-H(2B1)	110.9
C(1B)-C(2B)-H(2B2)	110.9
H(2B1)-C(2B)-H(2B2)	108.9
C(3B)-C(2B)-C(1B)	104.21(9)
C(3B)-C(2B)-H(2B1)	110.9
C(3B)-C(2B)-H(2B2)	110.9
C(2B)-C(3B)-H(3B1)	110.4
C(2B)-C(3B)-H(3B2)	110.4
C(2B)-C(3B)-C(4B)	106.49(8)
H(3B1)-C(3B)-H(3B2)	108.6
C(4B)-C(3B)-H(3B1)	110.4
C(4B)-C(3B)-H(3B2)	110.4
C(3B)-C(4B)-C(8B)	105.14(8)
C(5B)-C(4B)-C(3B)	113.77(9)
C(5B)-C(4B)-C(8B)	103.52(9)
C(14B)-C(4B)-C(3B)	109.44(10)

Table A6.15 (cont.)

C(14B)-C(4B)-C(5B)	111.62(10)
C(14B)-C(4B)-C(8B)	113.13(9)
C(4B)-C(5B)-H(5B1)	110.2
C(4B)-C(5B)-H(5B2)	110.2
H(5B1)-C(5B)-H(5B2)	108.5
C(6B)-C(5B)-C(4B)	107.47(8)
C(6B)-C(5B)-H(5B1)	110.2
C(6B)-C(5B)-H(5B2)	110.2
C(5B)-C(6B)-C(7B)	102.34(8)
C(12B)-C(6B)-C(5B)	111.34(11)
C(12B)-C(6B)-C(7B)	114.63(12)
C(12B)-C(6B)-C(13B)	107.50(11)
C(13B)-C(6B)-C(5B)	112.33(11)
C(13B)-C(6B)-C(7B)	108.75(10)
C(6B)-C(7B)-H(7B)	108.9
C(6B)-C(7B)-C(8B)	103.49(9)
C(8B)-C(7B)-H(7B)	108.9
C(11B)-C(7B)-C(6B)	114.39(9)
C(11B)-C(7B)-H(7B)	108.9
C(11B)-C(7B)-C(8B)	112.13(9)
C(1B)-C(8B)-C(4B)	106.41(8)
C(1B)-C(8B)-C(7B)	115.49(9)
C(1B)-C(8B)-H(8B)	108.9
C(4B)-C(8B)-H(8B)	108.9
C(7B)-C(8B)-C(4B)	107.94(8)
C(7B)-C(8B)-H(8B)	108.9
C(1B)-C(9B)-H(9B)	106.9
C(1B)-C(9B)-C(10B)	112.45(9)
C(10B)-C(9B)-H(9B)	106.9
C(15B)-C(9B)-C(1B)	112.98(11)
C(15B)-C(9B)-H(9B)	106.9
C(15B)-C(9B)-C(10B)	110.18(11)
C(9B)-C(10B)-H(10C)	108.4
C(9B)-C(10B)-H(10D)	108.4
H(10C)-C(10B)-H(10D)	107.5
C(11B)-C(10B)-C(9B)	115.49(10)
C(11B)-C(10B)-H(10C)	108.4
C(11B)-C(10B)-H(10D)	108.4
C(7B)-C(11B)-C(10B)	112.84(10)
C(7B)-C(11B)-H(11C)	109.0
C(7B)-C(11B)-H(11D)	109.0
C(10B)-C(11B)-H(11C)	109.0
C(10B)-C(11B)-H(11D)	109.0
H(11C)-C(11B)-H(11D)	107.8
C(6B)-C(12B)-H(12D)	109.5
C(6B)-C(12B)-H(12E)	109.5
C(6B)-C(12B)-H(12F)	109.5
H(12D)-C(12B)-H(12E)	109.5
H(12D)-C(12B)-H(12F)	109.5
H(12E)-C(12B)-H(12F)	109.5
C(6B)-C(13B)-H(13D)	109.5

Table A6.15 (cont.)

C(6B)-C(13B)-H(13E)	109.5
C(6B)-C(13B)-H(13F)	109.5
H(13D)-C(13B)-H(13E)	109.5
H(13D)-C(13B)-H(13F)	109.5
H(13E)-C(13B)-H(13F)	109.5
C(4B)-C(14B)-H(14D)	109.5
C(4B)-C(14B)-H(14E)	109.5
C(4B)-C(14B)-H(14F)	109.5
H(14D)-C(14B)-H(14E)	109.5
H(14D)-C(14B)-H(14F)	109.5
H(14E)-C(14B)-H(14F)	109.5
C(9B)-C(15B)-H(15D)	109.5
C(9B)-C(15B)-H(15E)	109.5
C(9B)-C(15B)-H(15F)	109.5
H(15D)-C(15B)-H(15E)	109.5
H(15D)-C(15B)-H(15F)	109.5
H(15E)-C(15B)-H(15F)	109.5

Symmetry transformations used to generate equivalent atoms:

Table A6.16. Anisotropic displacement parameters ($\text{\AA}^2 \times 10^4$) for tertiary alcohol **356** (CCDC 911859). The anisotropic displacement factor exponent takes the form: $-2\pi^2 [h^2 a^{*2} U^{11} + \dots + 2 h k a^* b^* U^{12}]$

	U^{11}	U^{22}	U^{33}	U^{23}	U^{13}	U^{12}
O(1A)	149(3)	246(4)	534(6)	-12(4)	133(4)	-50(3)
C(1A)	134(4)	166(4)	209(4)	7(3)	94(3)	-15(3)
C(2A)	187(4)	248(5)	187(4)	-31(4)	102(3)	-19(4)
C(3A)	252(5)	263(6)	274(5)	-77(5)	146(4)	26(4)
C(4A)	187(4)	148(5)	295(5)	-10(4)	136(4)	20(3)
C(5A)	175(4)	233(5)	300(5)	31(4)	132(4)	43(4)
C(6A)	186(4)	228(5)	204(4)	71(4)	84(4)	14(4)
C(7A)	202(4)	176(4)	170(4)	30(3)	106(3)	14(4)
C(8A)	163(4)	135(4)	228(4)	25(3)	129(3)	5(3)
C(9A)	225(4)	179(5)	240(5)	52(4)	144(4)	54(4)
C(10A)	310(5)	140(5)	235(5)	20(4)	117(4)	13(4)
C(11A)	243(5)	158(5)	183(4)	3(4)	88(4)	-38(4)
C(12A)	203(5)	375(7)	259(5)	52(5)	39(4)	-22(5)
C(13A)	329(6)	355(7)	302(6)	179(5)	154(5)	67(5)
C(14A)	324(6)	150(5)	531(8)	-3(5)	204(6)	4(5)
C(15A)	216(5)	275(6)	324(6)	102(5)	120(4)	66(4)
O(1B)	552(6)	301(5)	200(4)	-41(4)	224(4)	19(4)
C(1B)	205(4)	163(4)	163(4)	-4(3)	108(3)	12(4)
C(2B)	174(4)	214(5)	197(4)	-20(4)	88(3)	5(4)
C(3B)	212(4)	218(5)	266(5)	-36(4)	122(4)	-66(4)
C(4B)	236(4)	133(4)	246(4)	6(4)	151(4)	-7(4)
C(5B)	270(5)	246(5)	232(5)	76(4)	157(4)	36(4)
C(6B)	240(5)	275(6)	187(4)	51(4)	77(4)	45(4)
C(7B)	178(4)	184(5)	208(4)	10(4)	82(3)	-7(4)
C(8B)	183(4)	128(4)	191(4)	10(3)	113(3)	12(3)
C(9B)	284(5)	184(5)	283(5)	83(4)	184(4)	46(4)
C(10B)	312(6)	133(5)	351(6)	5(4)	159(5)	-20(4)
C(11B)	234(5)	176(5)	242(5)	-55(4)	89(4)	-30(4)
C(12B)	425(7)	498(9)	184(5)	16(6)	78(5)	39(7)
C(13B)	256(5)	395(8)	358(6)	163(6)	124(5)	110(5)
C(14B)	430(7)	135(5)	495(8)	-21(5)	294(6)	-18(5)
C(15B)	546(9)	309(7)	331(7)	166(6)	231(7)	141(6)

Table A6.17. Hydrogen coordinates ($\times 10^3$) and isotropic displacement parameters ($\text{\AA}^2 \times 10^3$) for tertiary alcohol **356** (CCDC 911859)

	x	y	z	U_{iso}
H(1A)	579	90	579	49
H(2A1)	669	154	466	24
H(2A2)	744	223	549	24
H(3A1)	785	-6	548	31
H(3A2)	706	-76	518	31
H(5A1)	878	-82	755	28
H(5A2)	868	66	699	28
H(7A)	766	213	813	21
H(8A)	696	38	715	19
H(9A)	628	308	651	24
H(10A)	726	471	618	28
H(10B)	713	476	707	28
H(11A)	815	305	684	24
H(11B)	828	391	776	24
H(12A)	925	232	920	47
H(12B)	930	242	826	47
H(12C)	966	108	896	47
H(13A)	886	-80	909	50
H(13B)	798	-55	856	50
H(13C)	852	50	941	50
H(14A)	772	-251	654	51
H(14B)	694	-198	640	51
H(14C)	765	-202	743	51
H(15A)	617	400	477	42
H(15B)	582	484	532	42
H(15C)	551	329	486	42
H(1B)	529	43	423	50
H(2B1)	589	-12	346	24
H(2B2)	542	-68	238	24
H(3B1)	568	162	211	28
H(3B2)	566	225	302	28
H(5B1)	424	270	47	28
H(5B2)	465	116	69	28
H(7B)	319	-26	113	24
H(8B)	384	132	229	19
H(9B)	404	-149	304	28
H(10C)	463	-309	212	32
H(10D)	380	-302	190	32
H(11C)	448	-129	112	28
H(11D)	368	-203	58	28
H(12D)	288	-26	-80	60
H(12E)	373	-40	-49	60
H(12F)	328	102	-104	60
H(13D)	290	282	-22	52
H(13E)	302	244	81	52
H(13F)	246	152	-9	52

Table A6.17 (cont.)

H(14D)	476	419	193	49
H(14E)	461	359	275	49
H(14F)	394	376	169	49
H(15D)	548	-266	372	58
H(15E)	483	-338	383	58
H(15F)	521	-192	439	58

Table A6.18. Hydrogen bonds for tertiary alcohol **356** (CCDC 911859) [\AA and $^\circ$]

D-H...A	d(D-H)	d(H...A)	d(D...A)	<(DHA)
O(1A)-H(1A)...O(1B)#1	0.84	1.91	2.7228(13)	162.5
O(1B)-H(1B)...O(1A)	0.84	1.94	2.6796(14)	146.9

Symmetry transformations used to generate equivalent atoms:

#1 +1

APPENDIX 7

Theoretical Investigation of the Relative Free Energies of Presilphiperfolanol Natural Products and Synthetic Intermediates[†]

A7.1 INTRODUCTION AND BACKGROUND

Our group recently completed the asymmetric total synthesis of presilphiperfolan-1 β -ol (**223**) (Chapter 3, Section 4) and is pursuing the synthesis of presilphiperfolan-9 α -ol (**222**) (Chapter 3, Section 5). Central to the synthetic route to these compounds is the IMDA reaction of an acylcyclopentene-derived silyl dienol ether or 1,3-diene containing a pendent olefin.

A7.2 QUANTUM CALCULATIONS

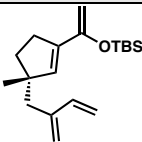
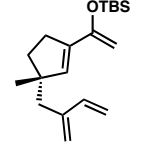
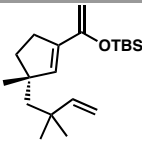
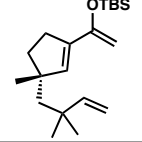
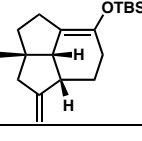
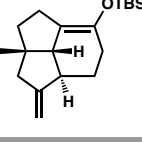
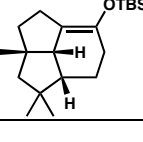
A theoretical study was undertaken to compare the relative free energies ($\Delta\Delta G$) of IMDA cycloadducts as well as the possible protonation and Rubottom oxidation products. Additionally, we sought a direct comparison of the relative free energies of

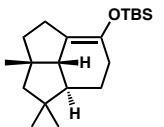
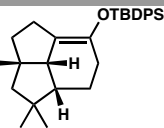
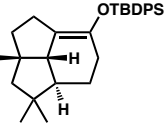
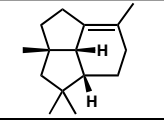
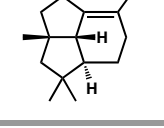
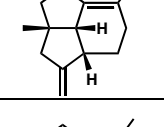
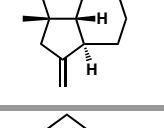
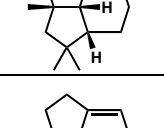
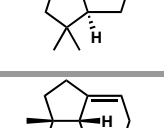
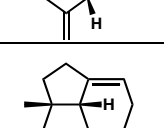
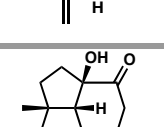
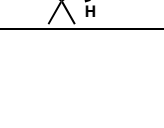
[†] The computational results described in this appendix are unpublished preliminary findings.

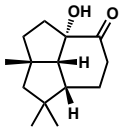
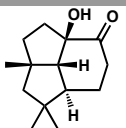
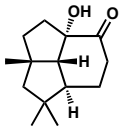
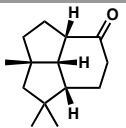
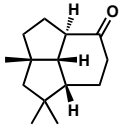
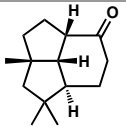
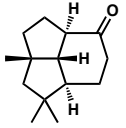
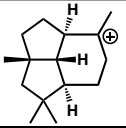
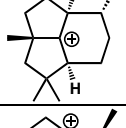
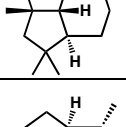
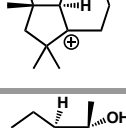
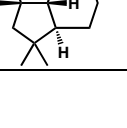
various presilphiperfolanyl cations and their corresponding hydration products to better understand which stereochemical configurations have greater ring strain.

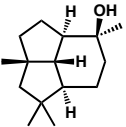
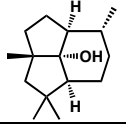
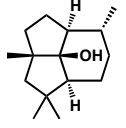
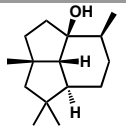
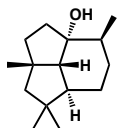
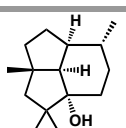
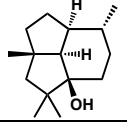
All calculations were performed with Mac Spartan '10 on an iMac computer; Wavefunction, Inc: Irvine, CA, 2006. All structures were optimized using the B3LYP 6–31G** method. Relative energies of optimized structures are shown for different sets of isomeric presilphiperfolane compounds.

Table A7.1. Relative Free Energies of Various Presilphiperfolane Structures

entry	structure	ΔG (hartrees)	ΔG (kJ/mol)	ΔG (kcal/mol)	$\Delta\Delta G$ (kcal/mol)
1		-1108.063437	-2909220.775456	-695320.4530249	0
2		-1108.059503	-2909210.462491	-695317.9881672	+2.4648577
3		-1148.599679	-3015648.686934	-720757.3343534	0
4		-1148.595616	-3015638.019527	-720754.7847818	+2.5495716
5		-1108.1077728	-2909337.179108	-695348.27416538	0
6		-1108.0969727	-2909308.82344324	-695341.496998863	+6.777166517
7		-1148.6525122	-3015787.4005116	-720790.48769398	0

8		-1148.6474175	-3015774.0243757	-720787.29072078	+3.1969732
9		-1532.1234551	-4022590.4377897	-961422.18876428	0
10		-1532.1161113	-4022571.1566414	-961417.58045922	+4.60830506
11		-586.0843565	-1538764.595208	-367773.5648202	0
12		-586.0790022	-1538750.537492	-367770.2049455	+3.3598747
13		-545.5404505	-1432316.561896	-342331.8742581	0
14		-545.5288976	-1432286.2297546	-342324.62470234	+7.24955576
15		-546.7635317	-1435527.761831	-343099.3694625	0
16		-546.7581178	-1435513.547636	-343095.9721882	+3.3972743
17		-506.2188618	-1329077.7229	-317657.1995458	0
18		-506.2079823	-1329049.15877	-317650.372555	+6.8269908
19		-697.2133531	-1830533.798007	-437508.0779175	0

20		-697.2095231	-1830523.742341	-437505.6745557	+2.4033618
21		-697.2237546	-1830561.1071471	-437514.60495866	0
22		-697.1990379	-1830496.213446	-437499.0949919	+15.50996676
23		-621.9996253	-1633060.1406251	-390310.74106718	0
24		-621.9970009	-1633053.250262	-390309.094231	+1.64683618
25		-622.0012267	-1633064.345101	-390311.7459611	0
26		-621.9866554	-1633026.08815	-390302.6023303	+9.1436308
27		-586.4187974	-1539642.669857	-367983.4296982	+9.8688437
28		-586.4149622	-1539632.600539	-367981.0230734	+12.2754685
29		-586.4345244	-1539683.961099	-367993.2985419	0
30		-586.4145264	-1539631.456346	-367980.7496047	+12.5489372
31		-662.4990605	-1739391.415843	-415724.525775	+7.2459789

32		-662.5106077	-1739421.733018	-415731.7717539	0
33		-662.4872954	-1739360.52657	-415717.1430617	+11.8576098
34		-662.5061917	-1739410.13881	-415729.0006715	0
35		-662.5238275	-1739456.441606	-415740.0673055	0
36		-662.5049548	-1739406.891328	-415728.2245049	+11.8428006
37		-662.4881093	-1739362.663465	-415717.6537918	0
38		-662.4821849	-1739347.108951	-415713.9361738	+3.717618

APPENDIX 8

Theoretical Investigation of the Terpene Cyclization Pathways

Relevant to Presilphiperfolanol Natural Products[†]

A8.1 INTRODUCTION AND BACKGROUND

Our group recently completed the asymmetric total synthesis of presilphiperfolan-1 β -ol (**223**) and an C(9)-epimeric analog (**224**) (see Chapter 3, Section 4). We plan to investigate the rearrangement of these compounds to biosynthetically related sesquiterpene natural products.

A8.2 QUANTUM CALCULATIONS

A theoretical study was undertaken to identify carbocation rearrangement pathways relevant to the presilphiperfolanol natural products. We sought to provide additional

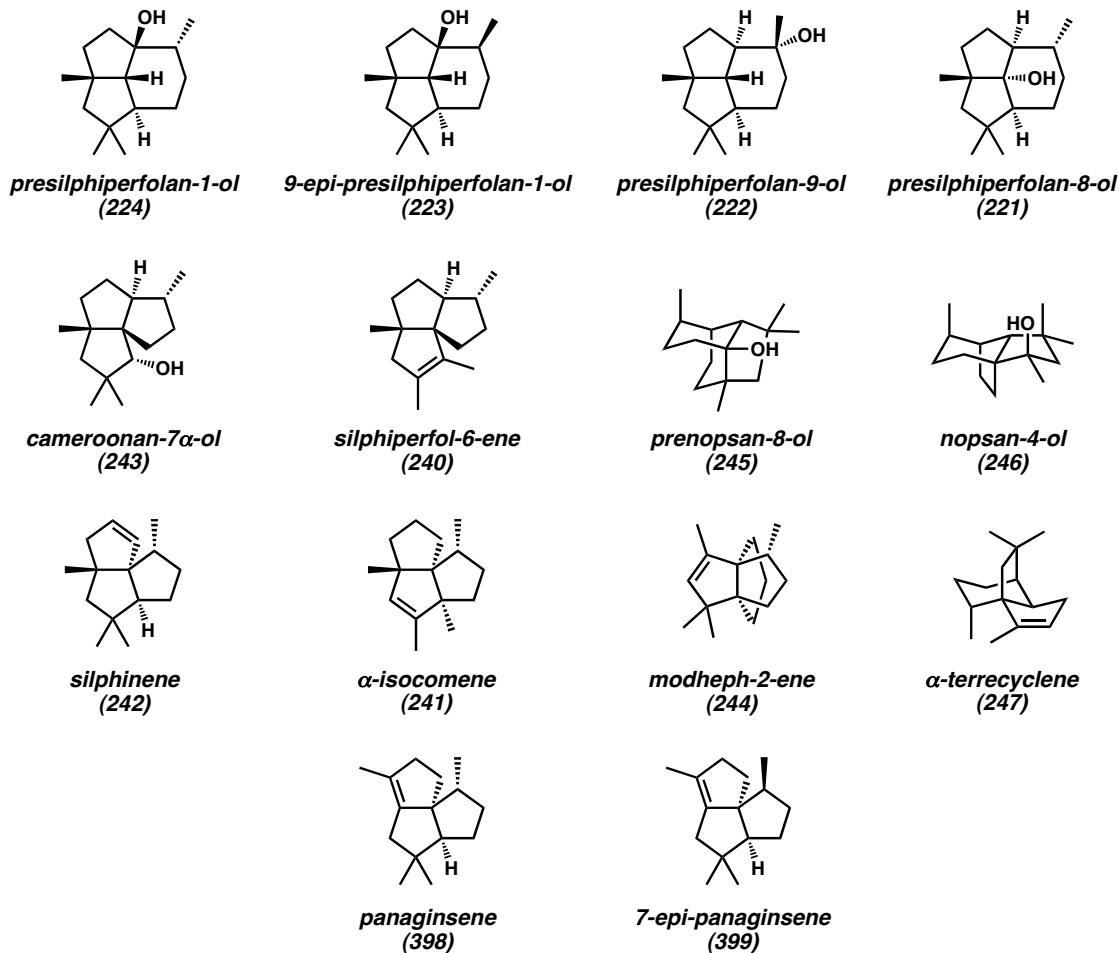
[†] This work was performed in collaboration with Dr. Young J. Hong and Prof. Dean J. Tantillo at UC Davis. Calculations were conducted by Dr. Young J. Hong. The computational results described in this appendix are unpublished preliminary findings.

evidence for our proposed mechanism for the biosynthesis of presilphiperfolan-1 β -ol (**223**) and predict sesquiterpene compounds that may be formed in rearrangement studies.

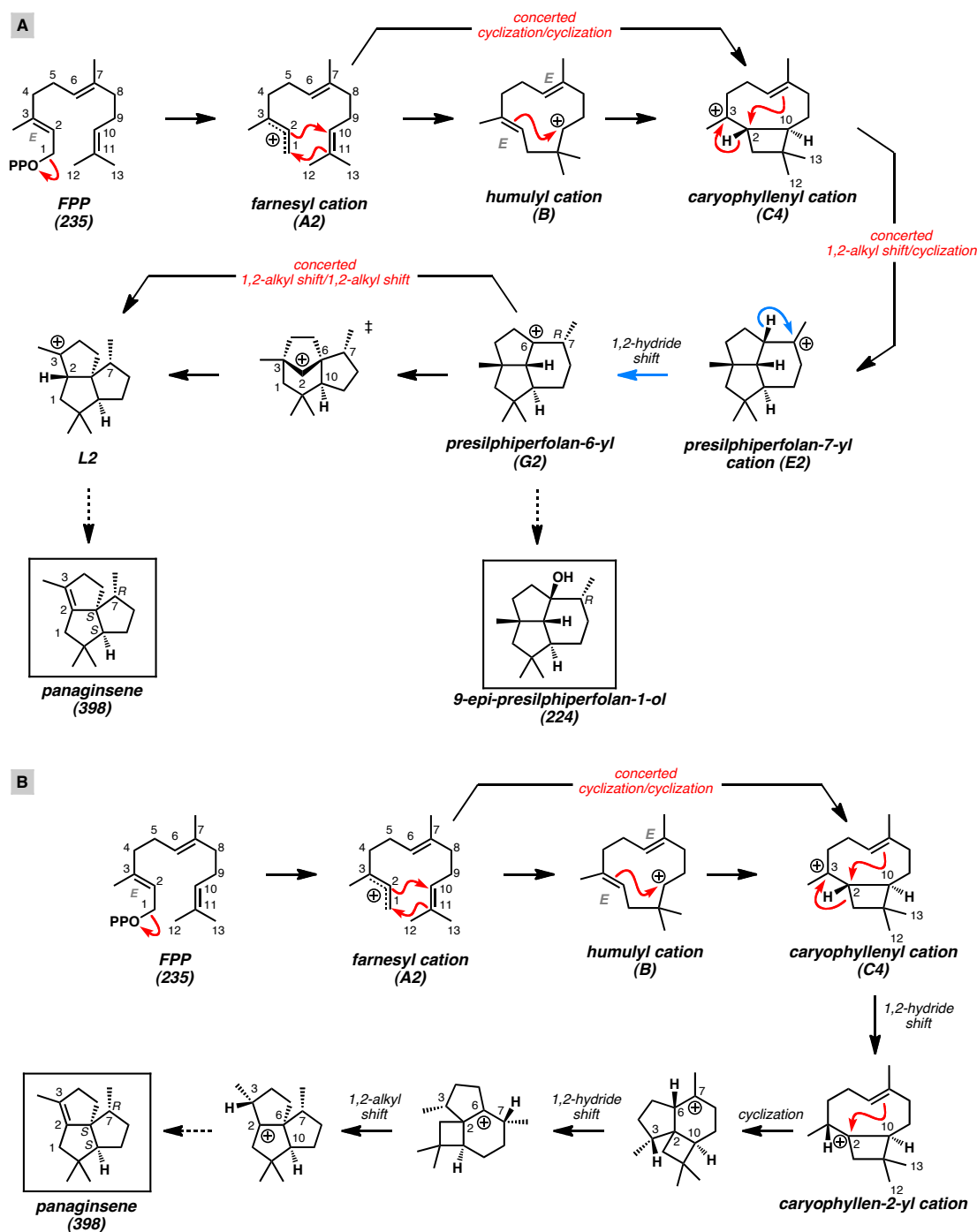
All calculations were performed with GAUSSIAN03 and GAUSSIAN09. All structures were optimized using the B3LYP/6-31+G(d,p) method. We report a set of energies, B3LYP/6-31+G(d,p)//B3LYP/6-31+G(d,p), mPW1PW91/6-31+G(d,p)//B3LYP/6-31+G(d,p) and mPWB1K/6-31+G(d,p)//B3LYP/6-31+G(d,p) to account for known shortcomings of B3LYP (in terms of relative energies). Our discussions are based on mPW1PW91/6-31+G(d,p)//B3LYP/6-31+G(d,p) energies unless noted otherwise. All stationary points were characterized by frequency calculations and reported energies include zero-point energy corrections (unscaled) from the method used for geometry optimization. Intrinsic reaction coordinate (IRC) calculations were used for further characterization of all transition state structures. Atom numbering in this appendix adopts the system for farnesyl diphosphate (FPP, Scheme A8.1) to facilitate to probe into skeletal rearrangements, which differs from those of natural products.

Structures of relevant terpenes and terpene alcohols are listed in Figure A8.1. Potential rearrangement pathways are illustrated in Scheme A8.1 and Scheme A8.2. The results of quantum calculations are summarized in Figure A8.2–Figure A8.5. Reaction energy profiles are shown in Figure A8.6 and Figure A8.7.

Figure A8.1. Structures of terpenes and terpene alcohols of interest.



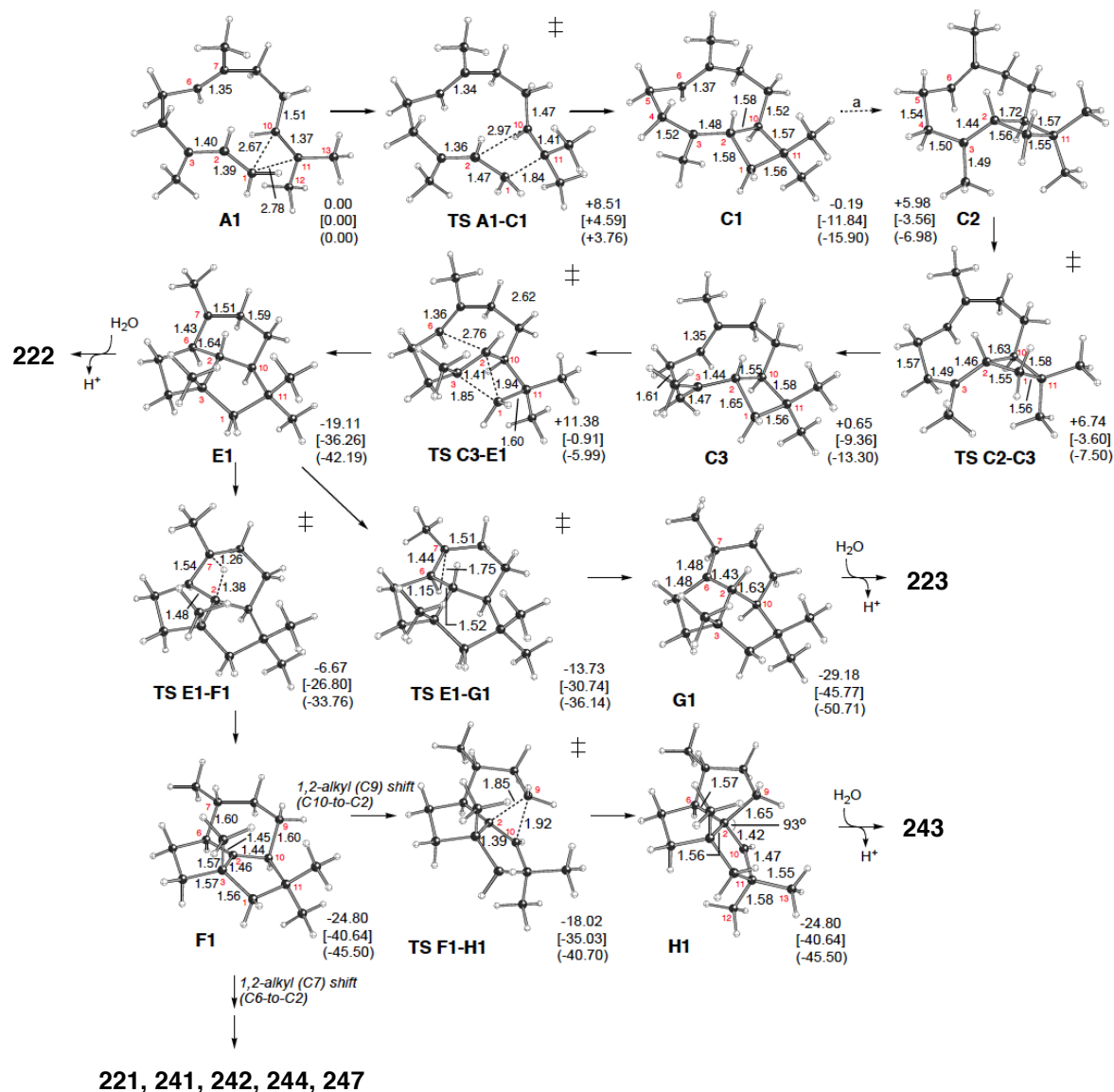
Scheme A8.2. Carbocation rearrangements leading to the epimer presilphiperfolanol **398** and terpene **224**.



(a) Proposed alternative pathway to lead to form **398**.

(b) Different configuration of C6=C7 π -bond in **A2** (Figure A8.3) from that in **A1** (Figure A8.2) leads to **E2** (Figure A8.3) which is 6-epimer of presilphiperfolan-7-yl cation of **E1** (Figure A8.2).

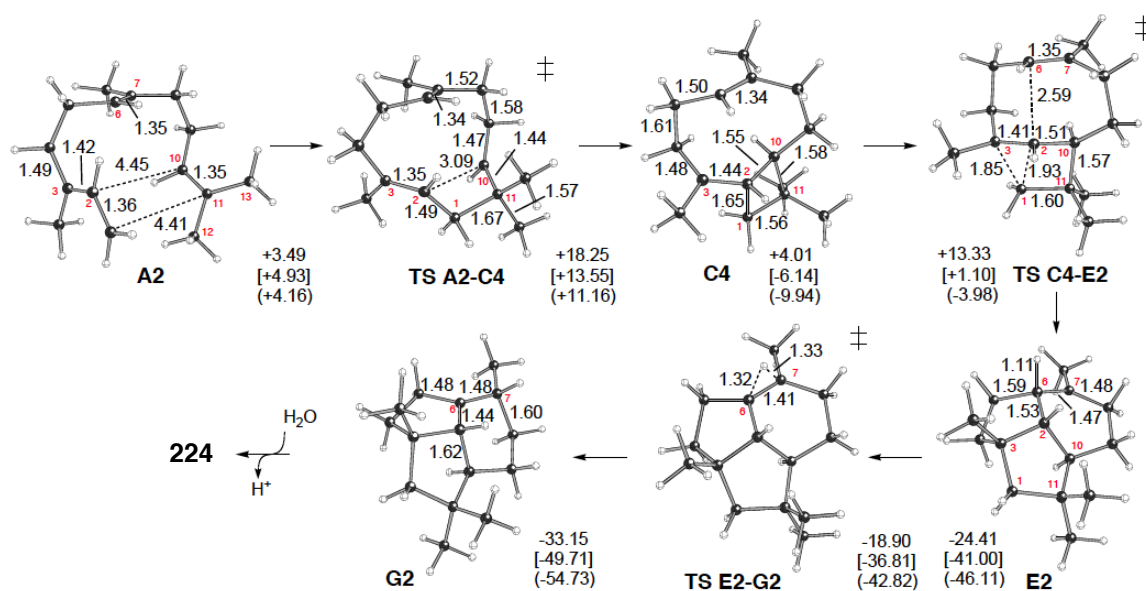
Figure A8.2. Possible reaction pathway to the cations that proceed to alcohols **2**, **5** and closely related terpenes and terpene alcohol(s).



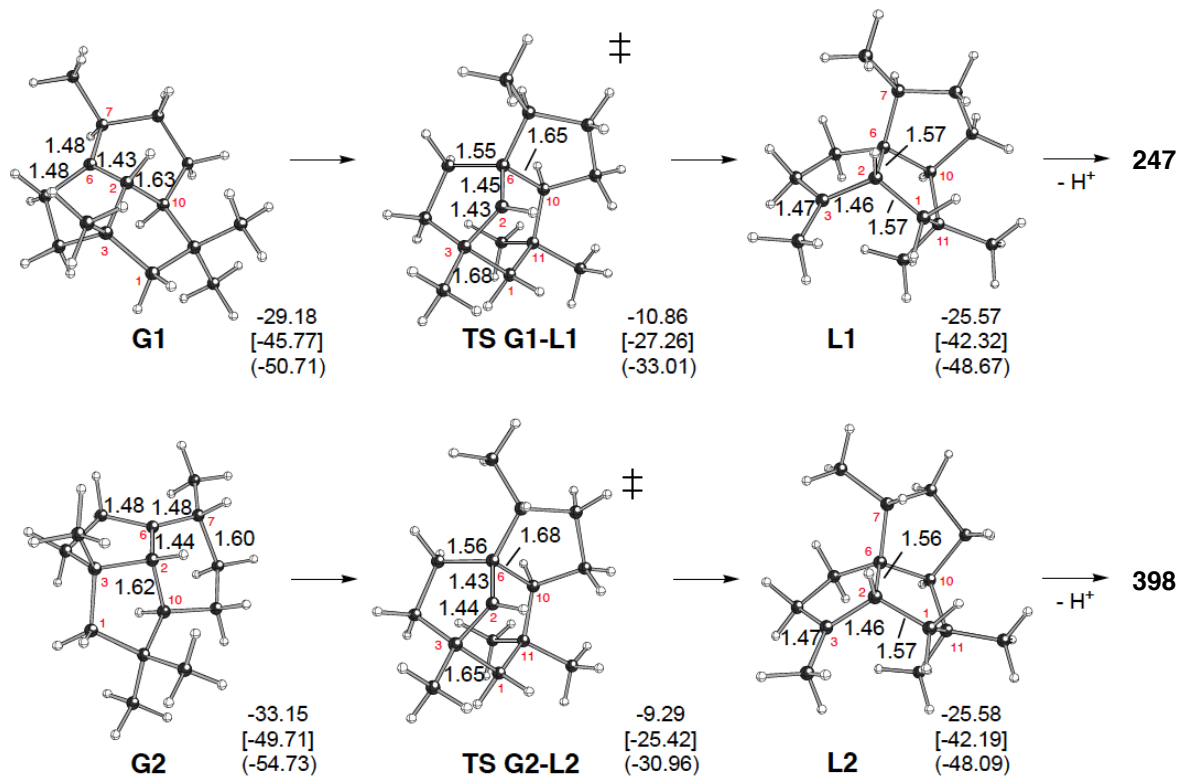
Computed structures (distances in Å) and energies (in kcal/mol) of carbocations and transition state structures are shown; B3LYP/6-31+G(d,p)//B3LYP/6-31+G(d,p) in normal text, mPW1PW91/6-31+G(d,p)//B3LYP/6-31+G(d,p) in brackets and MPWB1K/6-31+G(d,p)//B3LYP/6-31+G(d,p) in parentheses.

(a) We were unable to locate the transition state structure for the conformation change of **C1** and **C2**. We examined previously the formation of **221–222**, **241–242**, **244**, **247**.

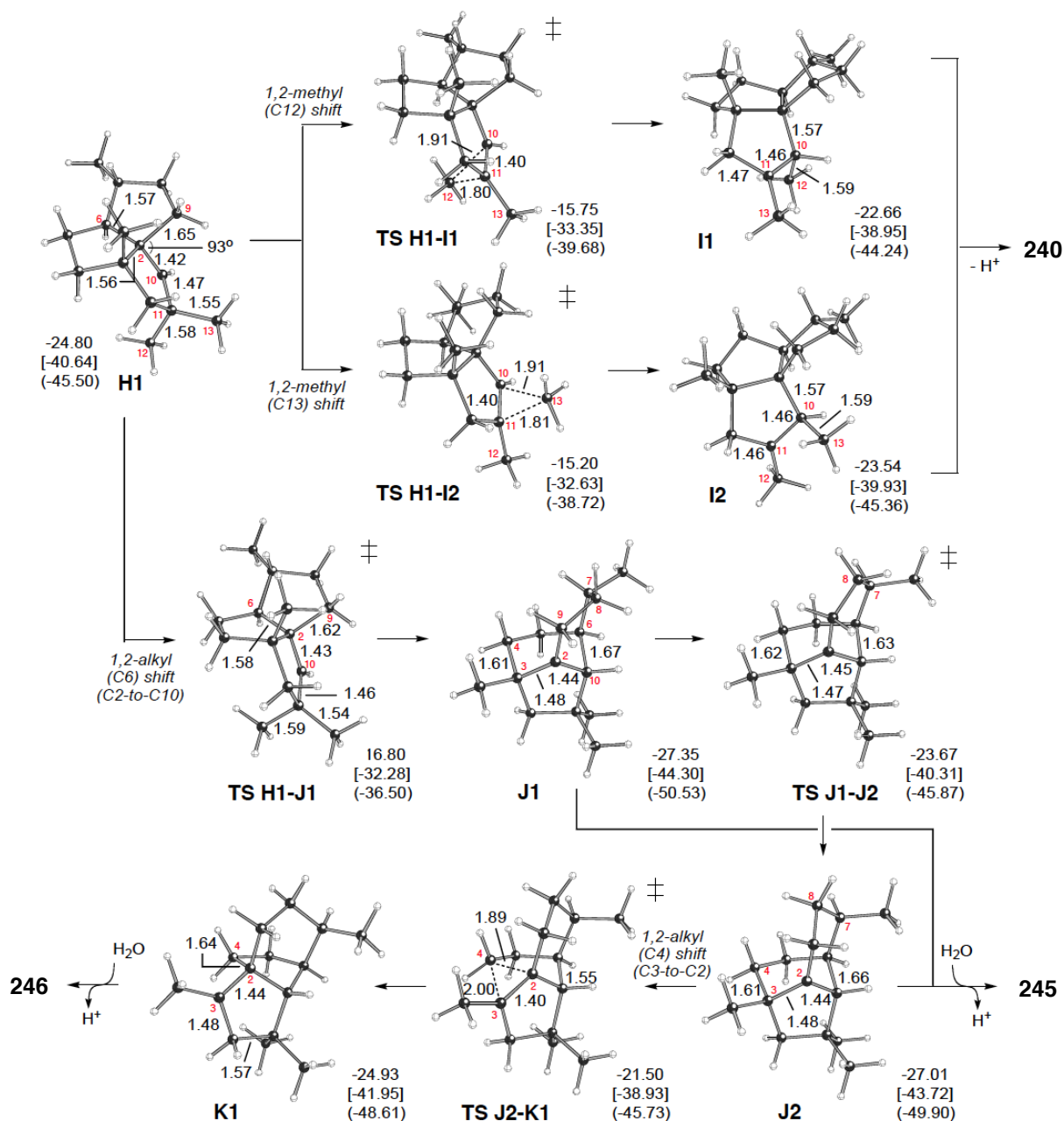
Figure A8.3. Possible reaction pathway to the cation that proceeds to the epimer **224**.



Computed structures (distances in Å) and energies (in kcal/mol) of carbocations and transition state structures are shown; B3LYP/6-31+G(d,p)//B3LYP/6-31+G(d,p) in normal text, mPW1PW91/6-31+G(d,p)//B3LYP/6-31+G(d,p) in brackets and MPWB1K/6-31+G(d,p)//B3LYP/6-31+G(d,p) in parentheses. Note C6–C7 configuration in **A2** differs from that in **A1**.

Figure A8.4. Possible reaction pathway to the cation that proceeds to the epimer **224**.

Possible rearrangements of **G1** and **G2**. Computed structures (distances in Å) and energies (in kcal/mol) of carbocations and transition state structures are shown; B3LYP/6-31+G(d,p)//B3LYP/6-31+G(d,p) in normal text, mPW1PW91/6-31+G(d,p)//B3LYP/6-31+G(d,p) in brackets and MPWB1K/6-31+G(d,p)//B3LYP/6-31+G(d,p) in parentheses. Panaginsene (**398**) also forms from a different reaction pathway (Scheme A8.1).

Figure A8.5. Possible reaction pathway to the cations that proceed to **240**, **245**, **246**.

conformation change, which appears to allow to align C2–C6 bond (slight elongation to 1.58 Å vs shorten of C2–C9 bond to 1.62 Å) and cationic center (C10). IRC calculations for **TS H1-I1** indicate 1,2-alkyl shift is accompanied with conformation change.

Figure A8.6. Reaction energy profiles (kcal/mol) for formation of **221–223**, **240–247** computed with *mPW1PW91/6-31+G(d,p)//B3LYP/6-31+G(d,p)*.

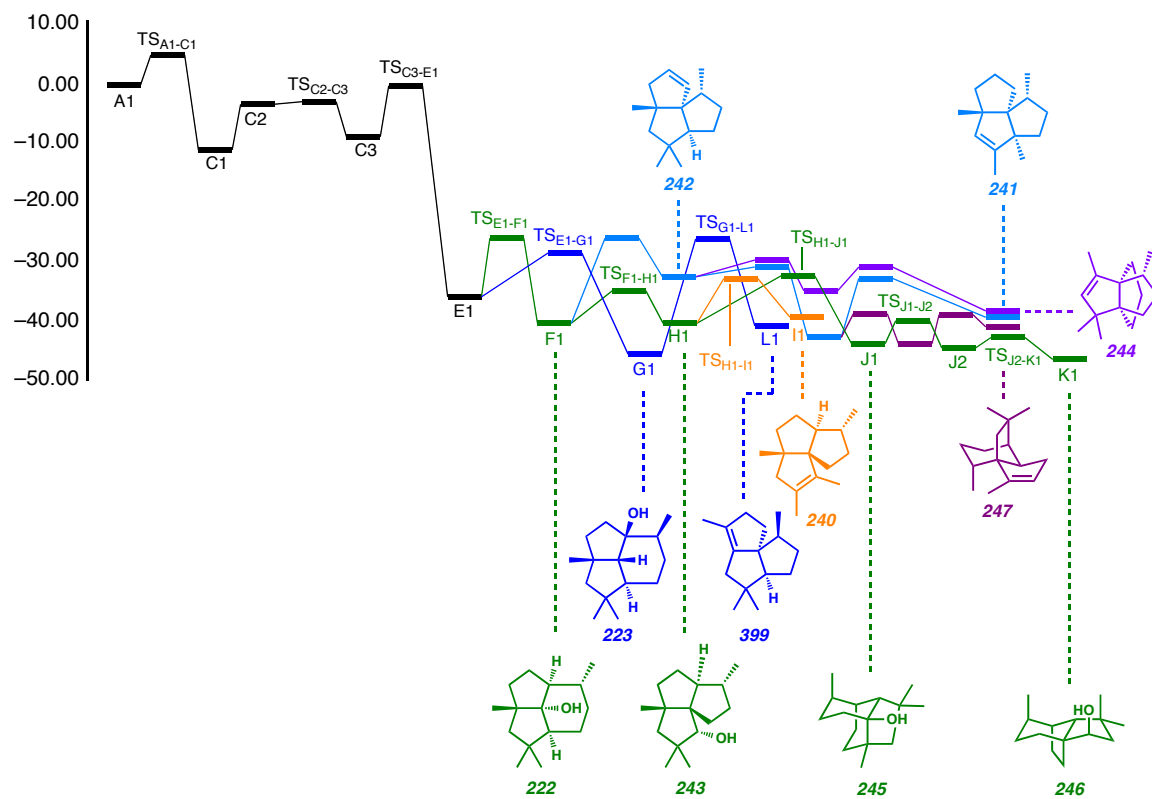
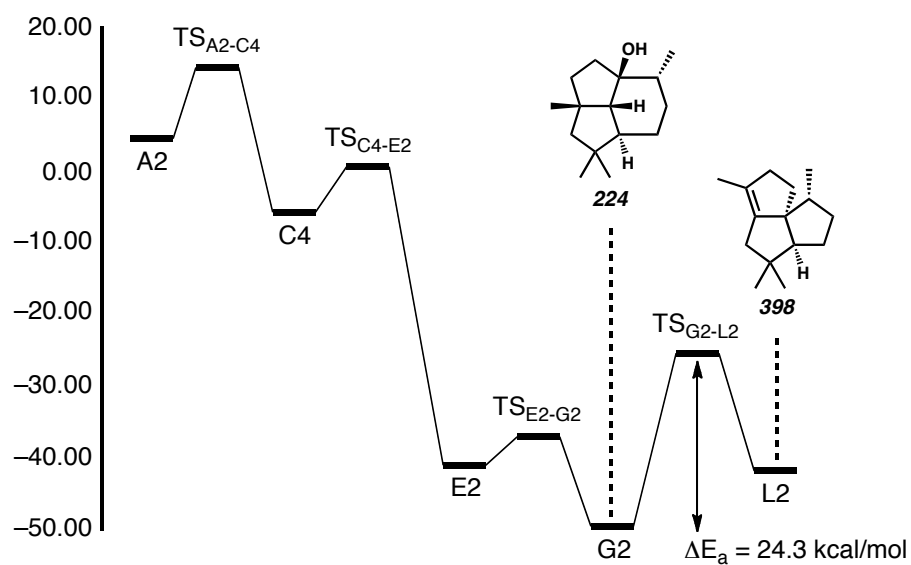


Figure A8.7. Reaction energy profile (kcal/mol) for formation of **224** and **398** computed with *mPW1PW91/6-31+G(d,p)//B3LYP/6-31+G(d,p)*.



APPENDIX 9

Enantioselective Protonations[†]

A9.1 INTRODUCTION AND BACKGROUND

Enantioselective protonation is a common process in biosynthetic sequences. The decarboxylase and esterase enzymes that effect this valuable transformation are able to control both the steric environment around the proton acceptor (typically an enolate) and the proton donor (typically a thiol). Recently, several chemical methods to achieve enantioselective protonation have been developed by exploiting various means of enantiocontrol in different mechanisms. These laboratory transformations have proven useful for the preparation of a number of valuable organic compounds.

A fundamental method to generate a tertiary carbon stereocenter is to deliver a proton to a carbanion intermediate. However, enantioselective transfer of a proton presents unusual challenges, specifically, manipulating a very small atom and avoiding product

[†] This review was written in collaboration with J. T. Mohr. A similar version has been published. See: Mohr, J. T.; Hong, A. Y.; Stoltz, B. M. *Nature Chem.* **2009**, *1*, 359–369.

racemization at a particularly labile stereocenter. As a result, the conditions for a successful enantioselective protonation protocol may be very specific to a certain substrate class. Tertiary carbon stereocenters are extremely common in valuable biologically active natural products, and thus the need for synthetically useful enantioselective methods to form these stereocenters is vital.¹

In this chapter, several strategic approaches to enantioselective protonation are presented. Emphasis has been placed on recently developed methods and their accompanying mechanisms in order to update the most recent prior reviews on this topic.² Each method relies on particular stereochemical control elements based on the mechanism of the protonation transformation. Appreciation of these controlling elements may lead to improved methods for preparing valuable chiral materials for a variety of synthetic applications.

A9.2 IMPORTANT FACTORS IN ACHIEVING ENANTIOSELECTIVE PROTONATION

Several of the most important practical features of enantioselective protonation were enumerated in Fehr's 1996 review.² Principal among these is the fact that enantioselective protonations are necessarily kinetic processes since under thermodynamic control racemate would be formed. Accordingly, it is often necessary to match the pK_a of the proton donor and the product to prevent racemization before product isolation. It is unfortunate that the same anion stabilizing groups (e.g., ketones) that make protonations relatively easy to achieve also impart a degree of instability in the

product. This has led some researchers to explore hydrogen atom transfer reactions in lieu of Brønsted acid-mediated protonations (see Section A9.4.4).

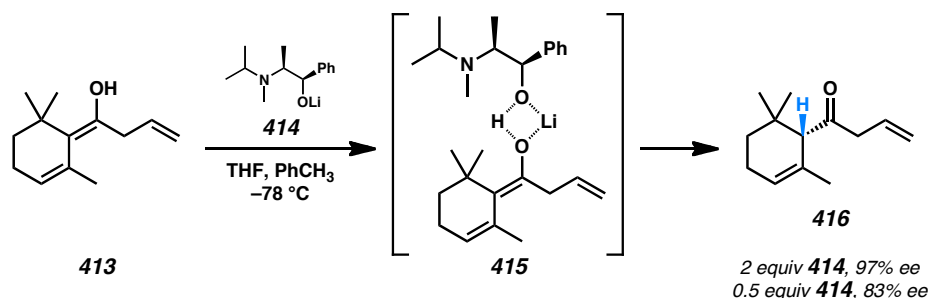
In addition to the obvious challenges of product stability under the reaction conditions, the rapid rate of proton exchange in solution often leads to significant levels of background reaction without the intercession of the chiral control element. As a result, typical proton donors are relatively weak acids that react with the proton acceptor in a slower and more controlled fashion.

Since substrates for enantioselective protonation generally involve a prochiral sp^2 -hybridized atom, the stereochemistry of the substrate is a concern. In some cases, the ability to generate stereodefined proton acceptors (e.g., a pure *E*- or *Z*-enolate) is critical to the success of a protonation method. In other cases, however, the two stereoisomers of enolate may in fact lead to the same enantiomer of product.^{2d} To obviate this concern many researchers choose to investigate cyclic substrates; in turn, this may lead to a limited substrate scope for a particular system. The method to access the reactive proton acceptor is among the most important facets of each protonation system, and many strategies have been explored (e.g., conjugate addition, addition to ketenes, and decarboxylation from β -ketoesters).

Finally, the fine mechanistic details of enantioselective protonations are often not well understood. Since typical proton acceptors are stabilized anions, there are multiple Lewis basic sites available for protonation. It is likely that these sites protonate at kinetically different rates dependent on the specific reaction conditions. Potentially, enantioselective protonations may be achieved either by direct protonation to generate the desired stereocenter, or by protonation at a different site followed by enantioselective

tautomerization. In an important recent report, Fehr³ demonstrated that isolated enol **413** (Scheme A9.1) could be transformed enantioselectively into ketone **416** (an immediate precursor to the rose-smelling fragrance compound (*S*)-(α)-damascone) via the proposed aggregate complex **415**, and this mechanistic course seemed to be operative in the analogous protonation of a lithium enolate with the conjugate acid of alkoxide **414**. Based on these findings, perhaps some protonation protocols are more accurately described as enantioselective *tautomerization* reactions. Although ultimately inconsequential in terms of the products obtained, insights into the specific mechanistic course of the reaction are important in order to improve these systems. However, only rarely have these levels of mechanistic understanding been realized.

Scheme A9.1. Enantioselective Tautomerization of an Isolated Enol



A9.3 ENANTIOSELECTIVE PROTONATION IN ENZYMATIC SYSTEMS

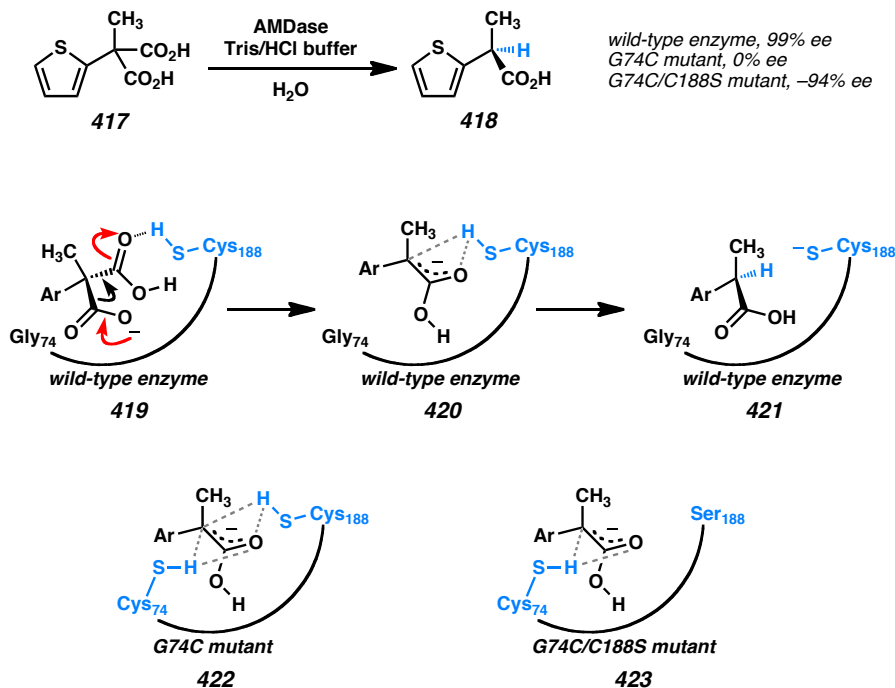
A9.3.1 DECARBOXYLASE ENZYMES

Nature has evolved several efficient enzymes that catalyze enantioselective protonation reactions on useful organic building blocks. In recent reports,

decarboxylases and esterases have proven to be two popular classes of natural enzymes for the construction of α -stereocenters adjacent to ketones. Esterases release latent enolates from prochiral substrates while decarboxylases generate enolates in situ from malonic acid derivatives (Scheme A9.2–Scheme A9.4).

Ohta and co-workers⁴ isolated arylmalonate decarboxylase (AMDase) from Gram-negative bacterium *Alcaligenes bronchisepticus* and found that it catalyzes the decarboxylative enantioselective protonation of α -aryl- α -methyl-malonates through the proposed mechanism in Scheme A9.2. Yields and enantiomeric excesses were excellent for substrates with various α -aryl substituents (up to 99% yield and 99% ee). Experiments have shown that the Cys188 residue is essential for activity, and this site is the putative proton donor that stabilizes the enolate intermediate. A Hammett study⁵ of the reaction found a ρ value of +1.19, which is consistent with a negatively charged transition state.⁴ Recently, preliminary X-ray diffraction experiments and an X-ray crystal structure of AMDase were reported.⁶

Scheme A9.2. Enzymatic Decarboxylative Protonation with Wild-Type and Mutant Decarboxylases

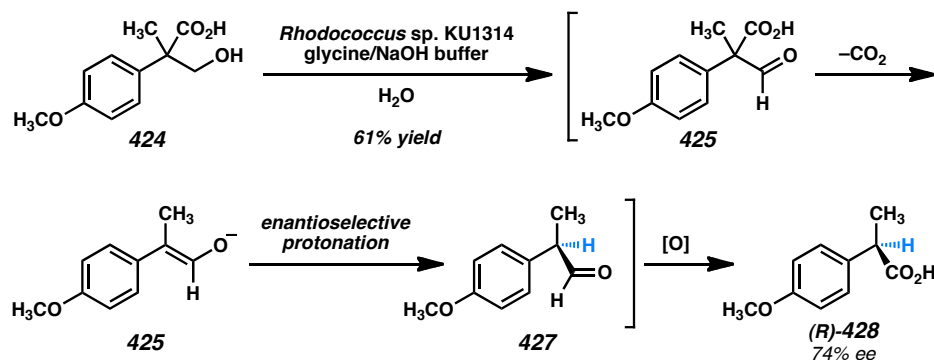


Accessing the opposite enantiomeric series of products required additional investigation.⁷ Analysis of the enzyme amino acid sequence was carried out to check for homology with known enzymes. The Cys188 residue is conserved in several racemase enzymes from other microorganisms. Glutamate racemase, found in the bacterium *Lactobacillus fermenti*, contains an active site similar to that of AMDase, but with cysteine residues (Cys188 and Cys74) on both sides of the substrate. Presumably, one of the cysteine residues acts as a base and generates an enolate intermediate, which can then be protonated non-selectively from either cysteine residue to give rise to a racemic mixture. When Ohta and co-workers prepared a G74C mutant of AMDase to mimic these racemase enzymes, they found that racemic α -thienylpropionic acid (**418**, Scheme A9.2) was formed in 37% yield from the malonic acid substrate (**417**). Further explorations based on this homology hypothesis led to the preparation of a double mutant

of AMDase (G74C/C188S) that removed the native cysteine residue while maintaining the mutant residue on the opposite face of the substrate. The opposite enantiomer of product was indeed obtained with this new enzyme in 94% enantiomeric excess, although yields decreased to 60% and the activity of this mutant was several orders of magnitude lower than the wild-type. Some activity was rescued by performing random mutagenesis and identifying more active triple mutants.⁸

Decarboxylase-type activity was also observed in the conversion of β -hydroxyacid **424** to optically active α -arylpropionic acid (*R*)-**428** by Gram-positive bacteria *Rhodococcus sp.* KU1314 (Scheme A9.3).⁹ In the proposed metabolic pathway, enzymes in the microorganism non-selectively oxidize hydroxyacid substrate **424** to aldehyde **425** and then decarboxylate the corresponding acid to form enolate **425** that undergoes enantioselective protonation to generate aldehyde **427**. Subsequent non-selective oxidation affords enantioenriched α -arylpropionic acid **428**. Mechanistic experiments were consistent with this proposed enantioselective protonation mechanism rather than alternative possibilities such as enantioselective oxidation steps. Enantioselectivity and yield varied considerably depending on the aryl and alkyl groups at the α -position in the substrate, but enantiomeric excesses up to 85% could be achieved. Employing an electron poor aryl group appeared to give poor enantioselectivity due to increased acidity of the proton in the presumed aldehyde intermediate. When the alkyl group was changed from methyl to ethyl, the reaction yield dropped, suggesting that the enzyme is sensitive to sterics.

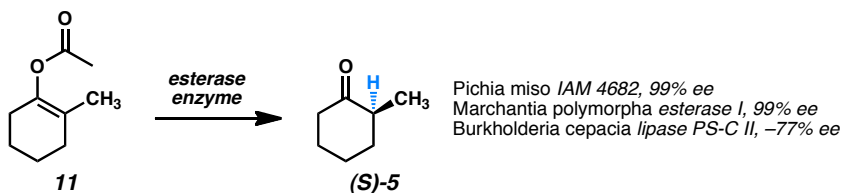
Scheme A9.3. Enzymatic Oxidation/Decarboxylation/Protonation/Oxidation Cascade



A9.3.2 ESTERASE ENZYMES

Several researchers have employed esterases to obtain enantioenriched protonation products. In 1990, Ohta and co-workers¹⁰ reported that live *Pichia miso* IAM 4682 yeast cells catalyze the conversion of enol acetates to enantioenriched ketones (e.g., **11** \rightarrow **5**, Scheme A9.4). High levels of enantiomeric excess were attained with a variety of enol esters. For larger ring systems, the reaction yield and absolute configuration varied unpredictably with ring size. In an impressive application, this yeast-mediated reaction was used to generate an α -stereocenter in a 12-membered ring with 96% ee.

Scheme A9.4. Enzymatic Hydrolysis of Enol Acetates



Hirata and co-workers¹¹ reported that liverwort *Marchantia polymorpha* esterase I also catalyzes the same reaction on a variety of substrates with differing alkyl side chains, but the facial preference for proton delivery varied for different enolate substitutions. For example, the enzyme delivered (*S*)-2-methylcyclohexanone (**5**) and (*R*)-2-*n*-propylcyclohexanone from their respective enol acetates in 99% conversion and 99% ee. Lipase PS-C II, originating from Gram-negative bacteria *Burkholderia cepacia*, may also be used for the hydrolysis of 1-acetoxy-2-methylcyclohexene (**11**). Sakai and co-workers¹² discovered that the enantiomeric excess of the product ((*R*)-**5**) was largely dependent on the temperature and the proton source. The best results were obtained by running the reaction at 0 °C with solid-supported enzyme PS-C II and ethanol as proton source (82% conversion, 77% ee).

Among these enzymatic approaches, a general problem appears to be the difficulty of enzyme modification to give the unnatural antipode of product. Another limitation is the need for buffers to help stabilize enzymes or cells. Substrate scope is also limited due to the specificity of substrate recognition. For these reasons, enzymatic reactions do not provide a general solution to the synthesis of enantioenriched protonation products. Laboratory means for enantioselective protonation may enable a more universal protocol due to the ability to tune the structural and electronic features of the catalyst. These natural systems do, however, demonstrate many of the key controlling elements necessary for successful enantioselective protonation.

A9.4 STRATEGIC APPROACHES TO NONENZYMATIC ENANTIOSELECTIVE PROTONATION

A9.4.1 GENERAL CONSIDERATIONS

Using enzymatic systems as a guide to the important factors in achieving enantioselective protonation, two distinct factors have been envisioned as opportunities for asymmetric induction: the use of a chiral Brønsted acid (see Section A9.4.2) and generation of a chiral proton acceptor intermediate (see Section A9.4.3). Whereas the enzymatic systems exploit both of these control elements, many laboratory methods have sought to use only a single control element not only to minimize the amount of enantiopure material required for the transformation, but also to eliminate complicating diastereomeric interactions possible in systems with multiple chiral additives. In practice, some of these systems seem to involve protonation through an aggregate complex of both proton acceptor and proton donor, typically in a metal complex (e.g., Fehr's tautomerization depicted in Scheme A9.1).

An additional factor important in improving efficiency of enantioselective protonation systems is achieving catalysis. For example, catalytic generation of a chiral metal/enolate complex *in situ* minimizes the amount of chiral controller required. Alternatively, coupling of a catalytic chiral proton donor to a stoichiometric achiral proton source achieves a similarly efficient use of chiral information. In the latter case, however, a specific order of *thermodynamic* acidity of the reaction components must be employed (necessarily in this order of decreasing Brønsted acidity: stoichiometric proton source, catalytic chiral protonating agent, and product). An accompanying balance of

kinetic rates of proton transfer between all of these components must also be achieved to allow a reasonable rate of protonation through the catalyzed pathway while avoiding undesired background reaction between the prochiral proton acceptor and the stoichiometric achiral proton donor. Vedejs and co-workers have disclosed a study of these factors that is representative of these important issues.¹³

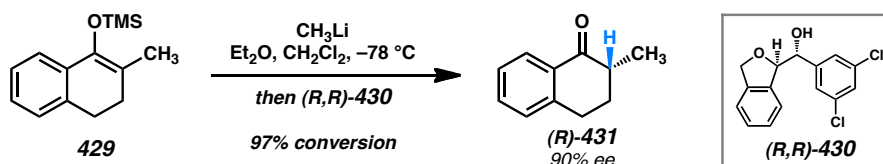
A9.4.2 ENANTIOSELECTIVE PROTONATION BY MEANS OF CHIRAL PROTON DONOR

Perhaps the most fundamental means of achieving an enantioselective protonation is to employ a chiral proton donor. The acidic proton often comes from an oxygen, nitrogen, or carbon atom in the proton donor. Indeed, the earliest enantioselective protonation protocols employed this technique.

Among the most popular substrates for enantioselective protonation are lithium enolates, which are often generated from ketones, enol acetates, or silyl enol ethers at low temperatures. This method most closely resembles an esterase approach taken by Nature. Kim and co-workers¹⁴ have synthesized a family of hydroxyethers as chiral proton sources (e.g., **430**, Scheme A9.5) capable of protonating lithium enolates of tetralones and indanones (prepared in situ from silyl enol ethers such as **429**) in up to 97% yield and 90% ee. The acidity of the Brønsted acids had a strong correlation to enantioselectivity and salt-free conditions were important to selectivity. A π - π -stacking interaction between the substrate and rigid proton source was proposed as the chiral controlling interaction during the protonation event. Since cyclohexanone-derived enolates lack an

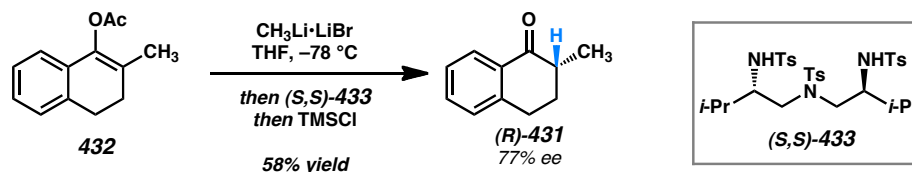
aryl group to participate in the stacking interaction, poor ee was observed for these substrates.

Scheme A9.5. Kim's Enolate Protonation



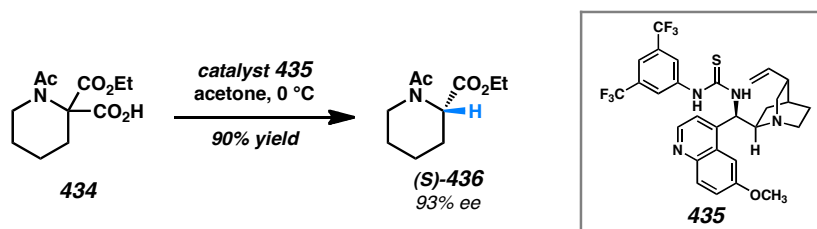
Eames and co-workers¹⁵ have developed several strategies for the asymmetric protonation of prochiral tetralone enolates based on structurally different chiral proton sources. In one example, tris(sulfonamide) protonating agents with chiral backbones (e.g., **433**, Scheme A9.6) provided yields of ketone products (e.g., **431**) up to 70% and enantiomeric excesses of up to 77%.^{15c} In these systems, it is believed that the enolates and proton sources can form an organized transition state that is guided by lithium chelation and perhaps more closely resembles a chiral aggregate intermediate than a direct enolate protonation. In some cases it was possible to access the opposite antipode of the product ketone by employing an external quench strategy.¹⁵

Scheme A9.6. Eames's Enolate Protonation



Enolate intermediates can also be accessed through decarboxylation. Proton donors derived from *Cinchona* alkaloids (e.g., **435**, Scheme A9.7) have proven to be especially useful reagents for this enantioselective protonation strategy. Rouden and co-workers¹⁶ have shown that cyclic and acyclic α -aminomalonate hemiester substrates (e.g., **434**) can be protonated with high levels of enantioselectivity. Enantiomeric excesses of product esters (e.g., **436**) up to 93% could be achieved in cyclic cases and 89% in acyclic cases. Products in the opposite enantiomeric series could be generated in comparable ee using catalysts prepared from naturally occurring diastereomeric alkaloids. The alkaloid derivatives are believed to serve as dual-purpose reagents: they deprotonate malonate hemiester substrates and promote a decarboxylation event. The intermediate enolate can be protonated by the tertiary ammonium salt to give enantioenriched products. This approach is biomimetic and resembles decarboxylase enzymes in Nature.

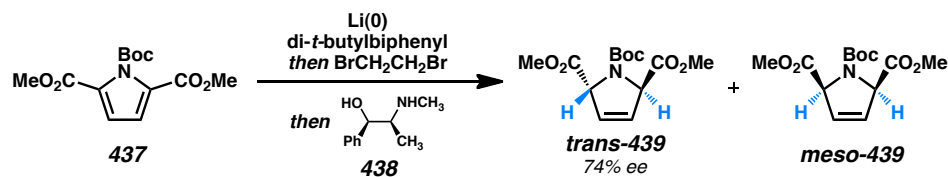
Scheme A9.7. Rouden's Decarboxylative Protonation



Work done by Donohoe and co-workers¹⁷ has shown that it is possible to perform dissolving metal reductions of pyrrole esters and quench the resulting enolate intermediates with a chiral proton source. Reduction of 2,5-disubstituted pyrroles (e.g., **434**, Scheme A9.8) led to a separable 1:1 mixture of *trans*- and *meso*-diasastereomers of

ester **439**, but the asymmetric induction in the chiral *trans*-product was good when (–)-ephedrine (**438**) was used as the chiral proton source. Based on enantioselectivities of reactions with substituted ephedrine derivatives, it was proposed that the hydroxyl group provides the proton and that the ephedrine molecule needs to interact with the lithium cation in a bidentate fashion for optimal asymmetric induction. Considering this proposal, this transformation may be more accurately described as protonation through a chiral aggregate of Brønsted acid and base. A related transformation of pyrrole monoesters with oxazolidinone proton donors yielded reduced products in up to 68% ee and 58% yield. These partially reduced pyrroles could be elaborated to form uncommon dihydroxylated amino acids found in the marine mussel *Mytilus edulis*.¹⁷

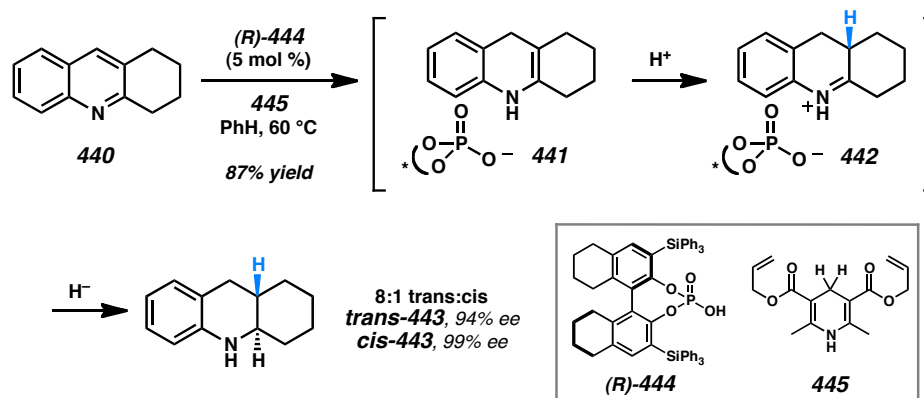
Scheme A9.8. Donohoe's Partial Pyrrole Reduction



It is often possible to employ catalytic amounts of chiral protonating agents, provided that an appropriate stoichiometric proton source can be identified. For this purpose, a number of chiral organic catalysts have been employed in various transformations. In order to achieve a heterocycle reduction/protonation strategy analogous to that used by Donohoe and co-workers (Scheme A9.8), Rueping and co-workers¹⁸ were able to reduce substituted quinolines enantioselectively (Scheme A9.9). Initial hydride reduction of annulated quinoline **440** by a Hantzsch dihydropyridine (**445**) to form enamine **441** was

followed by enantioselective protonation with a catalytic chiral BINOL-phosphoric acid (**444**). Terminal hydride reduction of iminium ion **442** yielded optically active tetrahydroquinoline **443** as an 8:1 mixture of *trans*- and *cis*-diastereomers with the diastereomers formed in 94% and 99% enantiomeric excess, respectively. Up to 84% yield and 85% enantiomeric excess could be obtained for *mono*-substituted quinolines using the optimal reaction conditions.

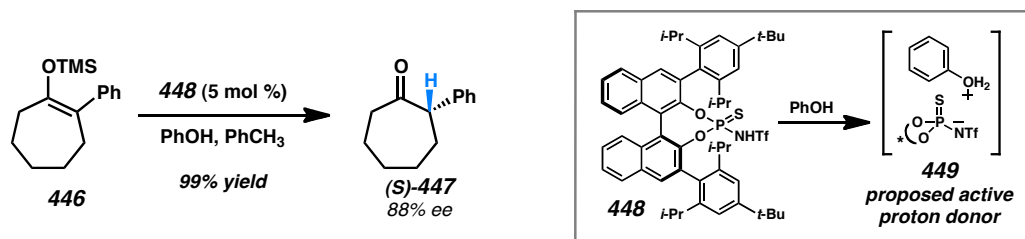
Scheme A9.9. Rueping's Quinoline Reduction/Protonation



In a mechanistically different approach, Cheon and Yamamoto¹⁹ used a related BINOL *N*-triflyl thiophosphoramidate catalyst (**448**) to directly protonate cyclic silyl enol ethers (e.g., **446** → **447**, Scheme A9.10). Regeneration of the chiral proton source was made possible by using phenol as the achiral proton source. With this system, yields up to 99% and enantiomeric excesses up to 90% were achieved. The highest levels of enantioselectivity were obtained with substrates bearing an aryl substituent at the α -position and 7-membered rings performed somewhat better than 6-membered rings. Comparable selectivity and yield could be obtained with catalyst loadings as low as 0.05

mol %. In control experiments, the protonation reaction did not proceed without an achiral proton source, even with stoichiometric chiral Brønsted acid. This observation led to a proposed mechanism that involves pre-association of the chiral and achiral proton sources to form an oxonium ion pair (**449**) that then protonates the silyl enol ether substrate.

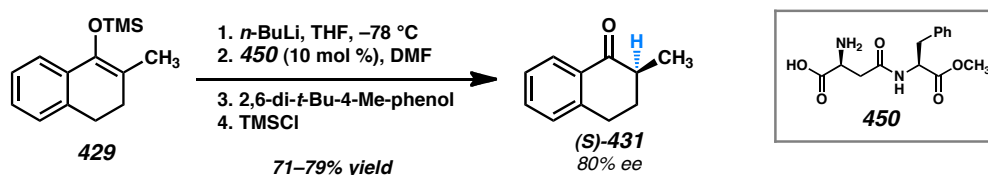
Scheme A9.10. Yamamoto's Enol Silane Protonation



A common approach to enantioselective protonation employs a lithium enolate, catalytic chiral proton source, and stoichiometric achiral proton source. These lithium enolates are often prepared from the corresponding enol silanes. Reports of amino acids as catalytic proton sources have appeared in recent literature. Yanagisawa and co-workers²⁰ employed commercially available dipeptide **450** (Scheme A9.11) for the protonation of lithium enolates of tetralones and cyclohexanones. The catalytic proton source is regenerated through proton transfer from 2,6-di-*t*-butyl-4-methylphenol (BHT). The steric bulk of the phenol is important to suppressing background enolate protonation through a non-selective pathway. The structure of the chiral proton donor is very specific to the success of the reaction because isomeric dipeptide aspartame afforded racemic product. Enolates generated from deprotonation of racemic ketone **431** with lithium

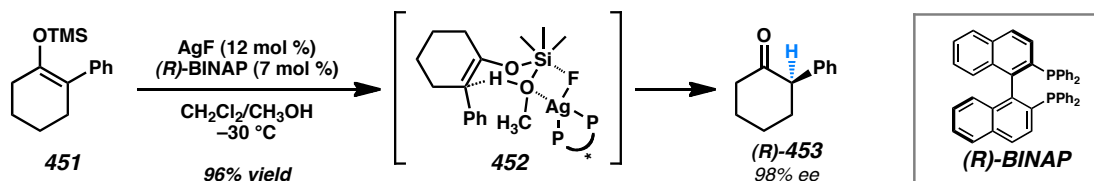
diisopropylamide could also be protonated with comparable yield and enantioselectivity using this system.

Scheme A9.11. Yanagisawa's Lithium Enolate Protonation



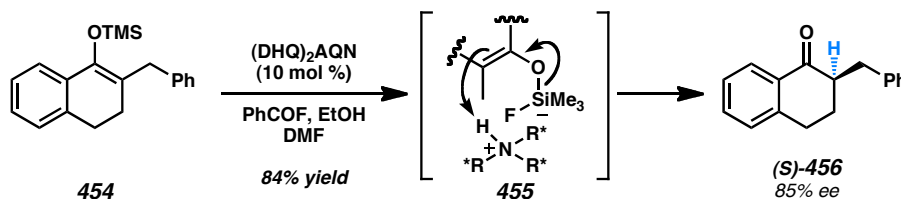
In separate work from Yanagisawa and co-workers,²¹ enol silanes were found to react to form ketones in the presence of the complex of AgF and BINAP (Scheme A9.12) with methanol as a proton donor. Excellent enantiomeric excesses were reported for a variety of cyclic ketones. Cyclohexanone-derived enol silanes yielded significantly higher ee products than tetralone-derived enol ethers. The highest levels of ee (up to 99%) were found for α -arylcyclohexanones. Although the fine mechanistic details have not been elucidated, one possibility is that the chiral Lewis acidic Ag•BINAP complex binds methanol to generate a potent chiral Brønsted acid capable of protonating the latent enolate. Taking the fluoride activation component into account, aggregate complex **452** was proposed as a potential intermediate leading to the observed enantiomer of product ketone.

Scheme A9.12. Yanagisawa's Enol Silane Protonation



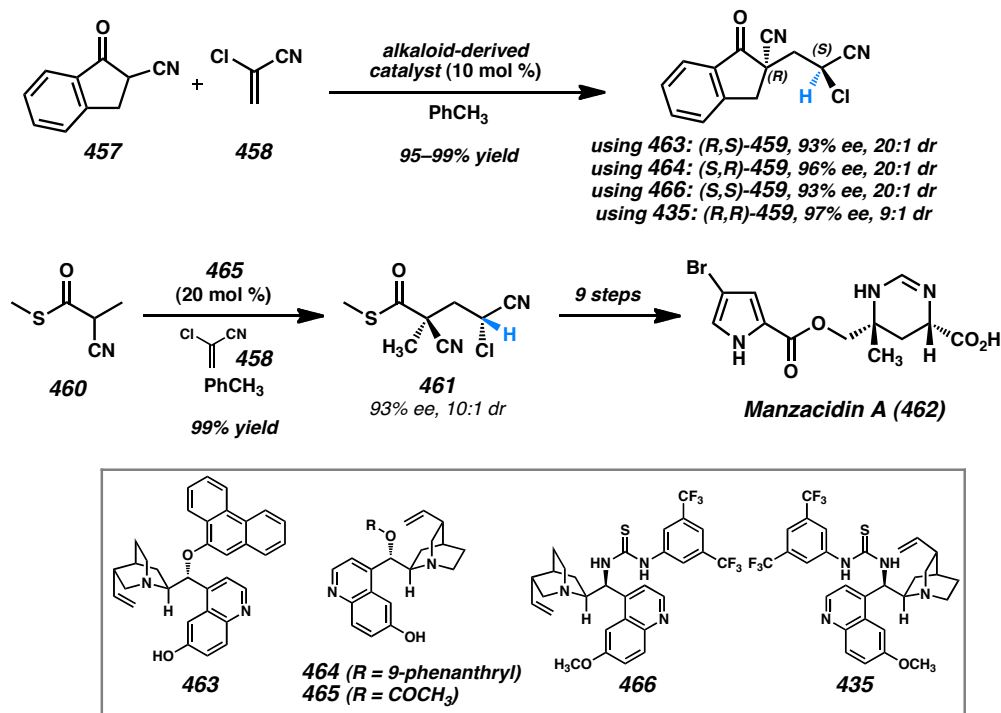
Levacher and co-workers²² have reported that catalytic amounts of *Cinchona* alkaloid derivatives can be coupled to latent hydrogen fluoride sources to achieve enantioselective protonation of silyl enol ethers of 1-indanones and 1-tetralones (e.g., **454** \rightarrow **456**, Scheme A9.13). The hydrogen fluoride, generated in situ from benzoyl fluoride and ethanol, is presumed to interact with the alkaloid-derived catalyst to form a cinchonium fluoride. The fluoride anion of this active catalyst then activates the silyl group to facilitate proton delivery from the ammonium cation (e.g., **455**) through a proposed transition state reminiscent of the $\text{Ag}\cdot\text{BINAP}$ protonation protocol described above. The optimal alkaloid catalyst was $(\text{DHQ})_2(\text{AQN})$, a common ligand for Sharpless' enantioselective dihydroxylation reactions.²³ Yields up to 86% and enantiomeric excesses up to 92% were reported. Protonation of cyclohexanone-derived enol silanes gave moderate enantiomeric excess. Later work revealed that carboxylic acids (e.g., citric acid) could be used directly with the alkaloid-derived catalysts to carry out the enol silane protonation.²⁴ Enantioselectivity for this variant of the reaction was moderately diminished, however (ee up to 75%). The use of chiral carboxylic acids revealed a moderate, but measureable, influence of both the proton donor and the catalyst on enantioselection, with the catalyst influence apparently dominating.

Scheme A9.13. Levacher's Enol Silane Protonation



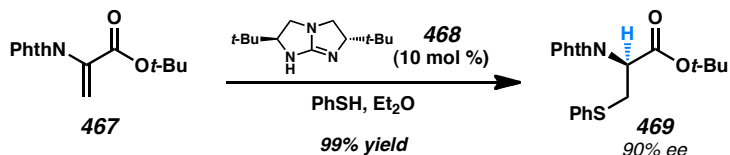
In a series of reports by Deng and co-workers,²⁵ bifunctional *Cinchona* alkaloid-derivatives (e.g., **435**, **463–466**, Scheme A9.14) were reported to catalyze tandem asymmetric conjugate addition/protonation reactions of cyclic and acyclic α -cyanoketone nucleophiles (e.g., **457** and **460**) to 2-chloroacrylonitrile (**458**). The *Cinchona* alkaloid derivative is proposed to serve two functions: activating the Michael acceptor for addition and serving as the chiral Brønsted acid for the protonation of the nitrile-stabilized carbanion intermediate. The postulated stereochemical model involves a network of hydrogen bonding interactions, and it was found that modification of this network by masking the phenolic hydroxyl group and introducing a thiourea moiety led to preferential formation of the diastereomeric products in excellent ee. By virtue of this discovery, all four stereoisomeric products of **459** could be prepared with high degrees of diastereo- and enantioselectivity. This method was applied to an enantioselective formal synthesis of (–)-manzacidin A (**462**) via the intermediate thioester **461**, prepared in 93% ee from α -cyanothioester **460** and 2-chloroacrylonitrile (**458**). A very similar transformation was reported by Wu and co-workers²⁶ for the conjugate addition of thiophenol to an α -substituted acrylamide with subsequent enantioselective protonation in up to 60% ee.

Scheme A9.14. Deng's Conjugate Addition/Protonation



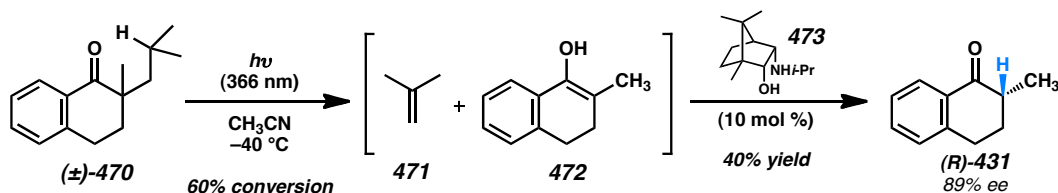
Organic catalysts other than *Cinchona* alkaloids have shown promise for catalytic asymmetric protonation as well. Tan and co-workers²⁷ used thiols and phosphine oxides as nucleophiles for 1,4-addition into various phthalimidoacrylates and itaconimides (e.g., **467** → **469** Scheme A9.15). Subsequent protonation of the intermediate enolates by the conjugate acid of chiral bicyclic guanidine catalyst **468** gave up to 99% yield and 94% enantiomeric excess. Interestingly, the presence of water and relatively acidic thiophenols did not lead to appreciable amounts of non-selective enolate quenching. Kinetic isotope effects were explored with D₂O and a primary kinetic isotope effect of 1.5 was found, consistent with cleavage or formation of a bond containing H or D in the rate-determining step.

Scheme A9.15. Tan's Conjugate Addition/Protonation



An unusual technique to generate an enol in situ was reported by Hénin, Muzart and co-workers.²⁸ In this work, a racemic α -quaternary ketone (e.g., **470**, Scheme A9.16) was exposed to laser photolysis at 366 nm. This irradiation caused a Norrish type II fragmentation (**470** \rightarrow **472**) to occur with concomitant loss of isobutylene. The enol (**472**) then undergoes enantioselective transformation to the corresponding ketone (**431**) in the presence of amino alcohol **473**. Although high ee was realized for this dealkylative protonation in some cases, yields were low largely due to undesired fragmentation reactions initiated by the photochemical irradiation and decomposition of the resulting radical intermediates. This method represents one of the few enantioselective stereoablative transformations²⁹ involving destruction of a quaternary stereocenter.

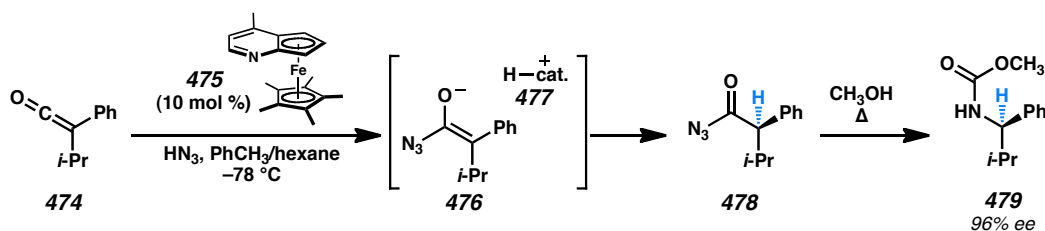
Scheme A9.16. Hénin/Muzart Norrish Type II Fragmentation/Protonation



A variety of transformations catalyzed by planar-chiral heterocycles involve protonation as the enantiodetermining step. In one recent example from Fu and co-

workers,³⁰ catalyst **478** (Scheme A9.17) was found to promote the addition of HN_3 to ketenes (e.g., **474**). The resulting acyl azides (e.g., **476**) then underwent Curtius rearrangement at elevated temperatures. The carbamate products (e.g., **479**) were isolated with up to 97% ee, presumably from enantioselective protonation of the amide enolate intermediate (**476**). Sterically large ketenes performed best since less encumbered ketenes suffered from rapid uncatalyzed background reaction even at cryogenic temperatures. In control experiments, hydrazoic acid was found to be readily deprotonated by planar-chiral heterocycle catalyst **575**. Since the reaction also proceeded with higher selectivity at low substrate concentration, a mechanism involving an ion pair **476** + **477** was proposed. This behavior of the catalyst as a chiral Brønsted acid (i.e., **477**) rather than the more typical role of these catalysts as Lewis bases³¹ is somewhat unusual, but also serves as a testament to the privileged nature of these catalysts.³²

Scheme A9.17. Fu's Addition of Hydrazoic Acid to Ketenes Followed by Curtius Rearrangement



Although the particular example in Scheme A9.17 is thought to occur through a protonated catalyst molecule as the proton donor, other similar transformations may proceed through a different mechanism (see section A9.4.3), however in both examples the lack of a nonlinear relationship³³ between catalyst ee and product ee suggests that only one catalyst molecule is involved in the enantioselective step and therefore a hybrid

mechanism is unlikely. Regardless of which of these two mechanistic hypotheses is operative, the transformation remains an enantioselective protonation process. An understanding of the mechanistic details, however, is helpful in order to understand the stereochemical control elements important to the success of the transformation.

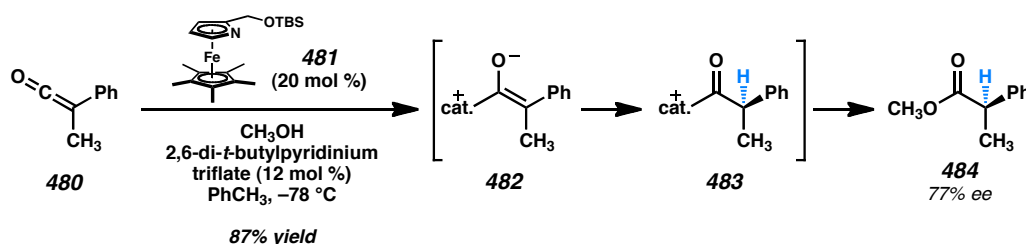
A9.4.3 ENANTIOSELECTIVE PROTONATION BY MEANS OF CHIRAL BRØNSTED BASE

The most common form of chiral Brønsted base employed in enantioselective protonations has been chiral metal enolates. To circumvent the challenge of stereoselective generation of acyclic enolates, the majority of methods have focused on cyclic enolate precursors. A variety of techniques for enolate generation have been employed including simple deprotonations, pericyclic reactions, decarboxylations, and dehalogenations. The synthesis of the specific enolate precursor required for a protonation protocol (e.g., enol silane, acrylate, or β -ketoester) may determine how useful the method is for the preparation of specific target molecules. Although several successful chiral Brønsted base protonation protocols have been developed, substrate scope remains a significant problem. Especially lacking are general methods capable of protonation of acyclic enolates with high selectivity.

Planar-chiral heterocycle catalysts have also been employed in the generation of chiral Brønsted base intermediates for enantioselective protonation. Fu and co-workers³⁴ employed azaferrocene catalyst **481** (Scheme A9.18). In the proposed reaction mechanism the heterocycle catalyst reacts with a ketene (e.g., **480**) to form a zwitterionic chiral enolate intermediate (**482**). Subsequent protonation of the enolate by methanol or

an achiral pyridinium cocatalyst then forms an acylferrocenium ion (e.g., **483**) that goes on to form an enantioenriched ester (e.g., **484**). Evidence for this distinct reaction mechanism included the fact that catalyst **481** did not appreciably deprotonate methanol in solution.³⁵ However, in the case above (Scheme A9.17) the catalyst **475** does readily deprotonate hydrazoic acid. The remarkable ability of these Lewis base catalysts to achieve enantioselective protonation through two different mechanisms highlights the importance of understanding the details of the reaction pathways. The preliminary mechanistic evidence does not always provide sufficient information to determine the operative mechanism, however.³⁶

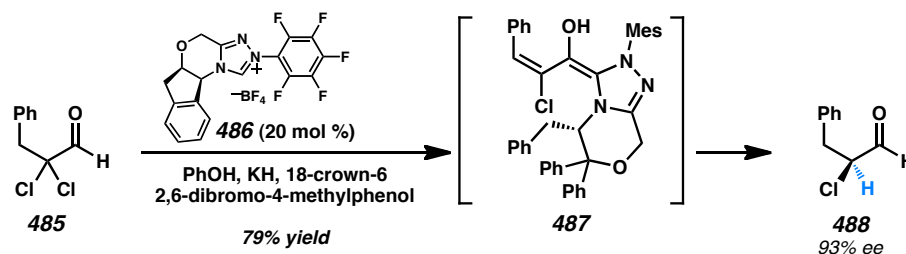
Scheme A9.18. Fu's Addition of Alcohols to Ketenes



Other organic molecules have been employed for the generation of chiral enolates as well. For example, Rovis and co-workers³⁷ found that treatment of α,α -dichloroaldehydes such as **485** (Scheme A9.19) with enantiopure triazolium salt catalyst **486** in the presence of a stoichiometric phenoxide base and phenol led to α -chloroaldehydes with high enantiomeric excess. The proposed path of the reaction involves addition of the carbene conjugate base of catalyst **486** to the aldehyde substrate. Subsequent elimination of HCl then generates a zwitterionic enolate intermediate (**487**)

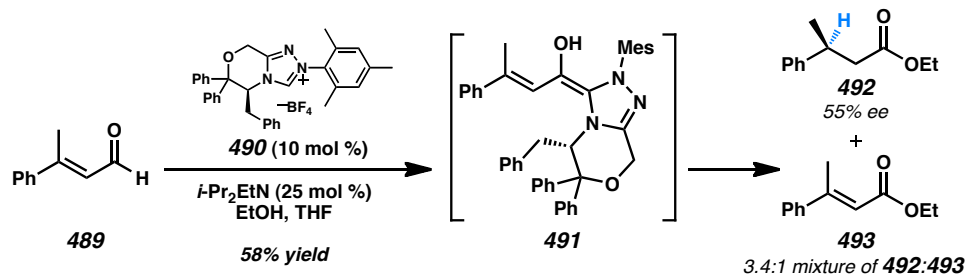
that is subject to protonation to form enantioenriched aldehyde **488**. The precise structure of the putative enolate is a matter of conjecture since a number of different strain elements are likely in competition in this intermediate. Nonetheless, this method represents a very valuable technique for the preparation of useful, but synthetically challenging, chiral synthons.

Scheme A9.19. Rovis' Protonation of Chloroenolates



In a separate application of carbene catalysis, Scheidt and co-workers³⁸ found that homoenolate equivalents (e.g., **491**, Scheme A9.20), generated in situ from enals such as **489**, could undergo enantioselective protonation when chiral triazolium catalyst **490** was employed. Ester products (e.g., **482**) were obtained in up to 58% yield and up to 59% ee, although competitive formation of overoxidized enoate byproduct **493** complicated the reaction. Although the degree of enantioselectivity observed for this transformation was modest, this represents a significant advance in the type of proton acceptor that can be used for enantioselective protonation reactions since the site of protonation is relatively distant from the chiral control element.

Scheme A9.20. Scheidt's Protonation of Homoenolate Equivalents

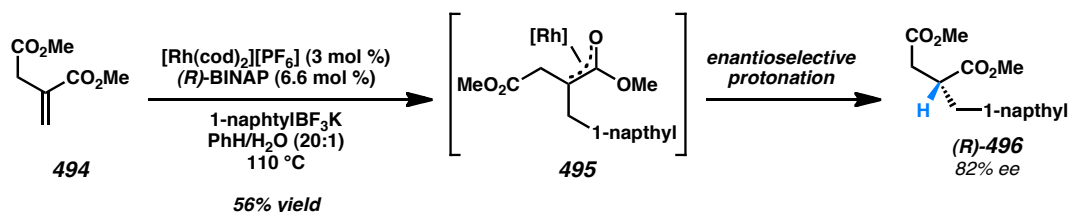


Metal-catalyzed 1,4-additions of organoboranes or organosilanes to enone systems have proven to be a popular strategy for generating chiral enolates for asymmetric protonation. These reactions can employ neutral or cationic rhodium complexes. Arylboron, arylstannane, arylsilicon, or arylzinc (and in some cases, vinylboron) reagents can be used for coupling, but yields and enantioselectivities can depend on the type of organometallic reagent chosen. Atropisomeric bis(phosphine) ligands such as BINAP and its analogues give excellent enantioselectivities for simple β -unsubstituted enone substrates. Diverse proton sources have been used to enable the formation of α -stereocenters. The optimal proton source varies from system to system, but phenols and other low- pK_a proton sources are common. Recent examples have mainly explored simple β -unsubstituted systems, so issues of diastereoselectivity in the generation of multiple stereocenters have not been fully addressed.

Frost and co-workers³⁹ explored Rh-catalyzed additions of organotrifluoroborate salts to itaconate substrates with water as the stoichiometric proton donor (e.g., **494** \rightarrow **495** \rightarrow **496**, Scheme A9.21). The metal-to-ligand ratio was found to be important in the selectivity of the reaction. Equimolar amounts of metal and ligand gave racemic product in high yield, but 2.2 equivalents of ligand relative to metal gave product in 82% ee and

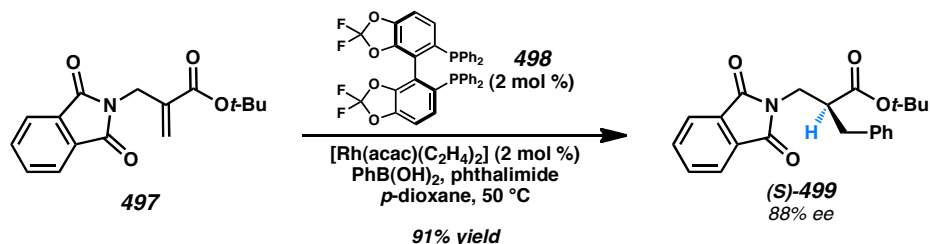
56% yield. Interestingly, high reaction temperature was found to be an important factor in this reaction; racemic product was obtained when the reaction was carried out at 60 or 80 °C instead of 110 °C. In related work, Frost showed that organosiloxanes are also viable nucleophilic components for 1,4-addition, but such systems give poor yields and low enantioselectivity.⁴⁰ In a separate system involving aryl boronic acid organometallic components in microwave reactors, Frost and co-workers⁴¹ examined whether a chiral proton source affected the stereochemical outcome of the reaction. When (*R*)-, (*S*)-, or racemic-BINOL was used with a Rh•BINAP catalyst, the yields and enantioselectivities were comparable in each of the three scenarios. This suggests that the chirality of the bis(phosphine) ligand is the dominant stereodetermining factor.

Scheme A9.21. Frost's Rh-Catalyzed Conjugate Addition/Protonation



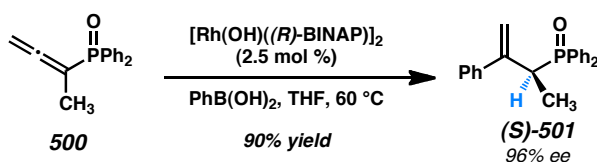
Sibi and co-workers⁴² also investigated rhodium-catalyzed conjugate addition-protonation as a method for accessing β^2 -amino esters from enoates (e.g., **497** \rightarrow **499**, Scheme A9.22). Reaction screening revealed that (*S*)-DifluorPhos ligand (**498**) and phthalimide proton donor provided the best enantioselectivity. The best substrate provided 95% yield and 91% ee. Notably, lower temperatures could be used to increase product ee.

Scheme A9.22. Sibi's Rh-Catalyzed Conjugate Addition/Protonation



Hayashi and co-workers⁴³ reported a related conjugate addition/protonation sequence for an analogous diphenylphosphinylallene (e.g., **500**) system with a cationic dimeric rhodium μ_2 -hydroxide catalyst (Scheme A9.23). Temperature did not appear to have an effect on enantioselectivities, but the choice of THF as solvent instead of dioxane improved product ee by more than 20%. Minimal isomerization of the β,γ -unsaturated products (e.g., **501**) was observed under the reaction conditions, and excellent yields (up to 97%) and enantiomeric excesses (up to 98%) were obtained. In this case, the arylboronic acid appears to be acting as the proton source based on an NMR experiment.

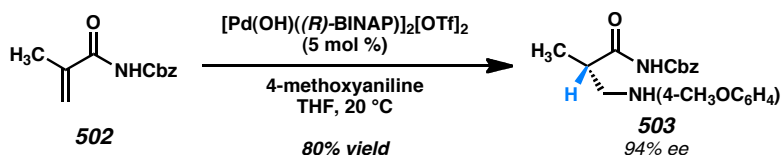
Scheme A9.23. Hayashi's Rh-Catalyzed Conjugate Addition/Protonation



Sodeoka and co-workers⁴⁴ found that this conjugate addition/protonation sequence is viable with palladium complexes and heteroatom nucleophiles as well (**502** \rightarrow **503**, Scheme A9.24). A bimetallic palladium μ_2 -hydroxide complex effected the conjugate addition of aniline derivatives to acrylamides. With BINAP as ligand, the enolate

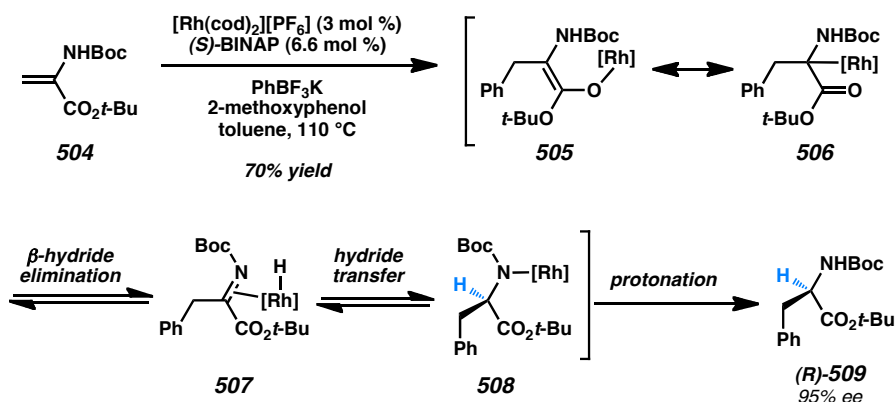
intermediate was protonated enantioselectively to give product **502** in 80% yield and 94% ee. Although this is a promising result, the substrate scope has not been fully investigated.

Scheme A9.24. Conjugate Addition/Protonation with a Nitrogen Nucleophile Catalyzed by Palladium



Genet, Darses, and co-workers⁴⁵ sought to make α -amino esters using a similar conjugate addition/protonation strategy (e.g., **504** \rightarrow **509**, Scheme A9.25). In this system, boronic esters, boronic acids, and organosilanes did not provide adequate conversion or enantioselectivity. Organostannanes, however, were reactive under these conditions. In the screening of various proton sources, phenol derivatives appeared to provide the best enantioselectivity. Guaiacol (2-methoxyphenol) was determined to be the best proton donor, giving products with up to 91% yield and 88% ee. Higher temperatures and optimized solvents (such as toluene or *p*-dioxane) increased conversion and enantioselectivity. As in Frost's work, the ratio of metal to ligand did have a notable effect on the enantioselectivity of the reaction, with 2.2 equivalents of chiral ligand relative to metal being optimal. Chiral proton sources were also added to see if the chiral ligand or chiral proton source was the dominant selectivity factor. Studies with (*R*)-BINAP and both enantiomers of BINOL provided identical enantiomeric excesses, implying that the chirality of the enolate is dominant, as in the reports by Frost.

Scheme A9.25. Divergent Pathway Consisting of β -Hydride Elimination, Hydride Transfer, and Protonation

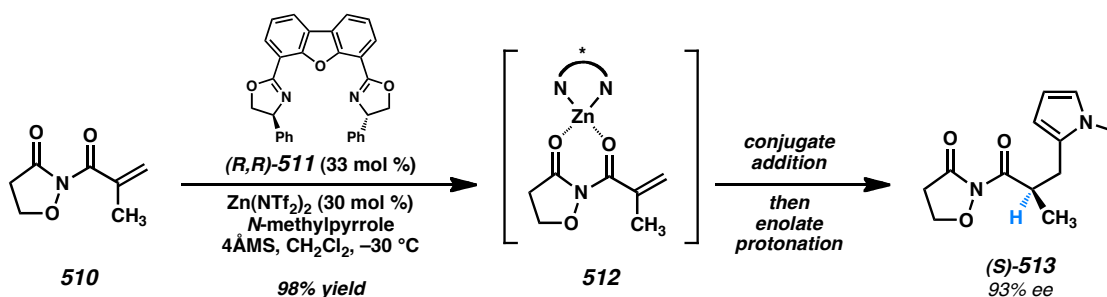


Mechanistic studies showed that the hydrogen on the enamide was essential for reactivity. Deuterium labeling studies showed that the reaction did not proceed via a direct protonation of the rhodium enolate (**505**); in a substrate with a labeled carbamate proton, deuterium incorporation at the α -carbon was high (41%). Based on this observation, a mechanism involving sequential conjugate addition, β -hydride elimination from the carbamate (**506** \rightarrow **507**), and intramolecular hydride transfer to the α -carbon (**507** \rightarrow **508**) was proposed. This proposed reaction pathway was supported by DFT calculations with the B3LYP/BII level of theory.^{45b} In light of these mechanistic insights, a more electron-poor bis(phophine) ligand was chosen to facilitate the postulated β -hydride elimination step, and DifluorPhos (**498**) was experimentally shown to give higher enantiomeric excesses.

A related conjugate addition/enantioselective protonation strategy consisted of a Friedel–Crafts-type addition of pyrroles to α -substituted acrylates (e.g., **510** \rightarrow **513**,

Scheme A9.26).⁴⁶ Sibi and co-workers employed $\text{Zn}(\text{NTf}_2)_2$ complexed with chiral dbfox ligand **511** as a Lewis acid catalyst to achieve up to 98% yield and up to 98% ee. The enolate intermediate (**512**) generated from the Friedel–Crafts reaction can be quenched by a proton from the pyrrole fragment to give a chiral product. The isoxazolidinone auxiliary is believed to be critical for improving reactivity and providing greater enolate control during the course of the reaction.

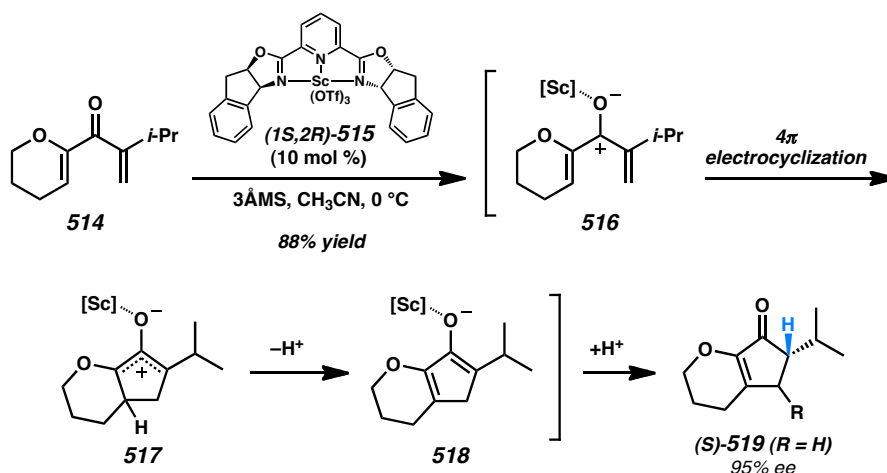
Scheme A9.26. Friedel–Crafts-Type Conjugate Addition Followed by Enantioselective Protonation



A distinct method of accessing a chiral metal enolate is the use of a pericyclic reaction. In the case of the Nazarov cyclization, the enantioselective reaction would not only generate a new stereocenter, but also a new five-membered ring. However, until recently enantioselective variants of this classical reaction were unknown. In studies directed toward the development of a general enantioselective Nazarov cyclization, Trauner and co-workers⁴⁷ discovered that high ee cyclopentenone products could be synthesized from electronically activated substrates such as dienone **514** in the presence of $\text{Sc}\cdot\text{PYBOX}$ complex **515** (Scheme A9.27). Interestingly, this enantioselective protonation protocol requires no external proton source. Unfortunately, in cases where a second stereocenter would be generated at the β -carbon (i.e., **519** where $\text{R} \neq \text{H}$), low

diastereoselectivity was observed. This was interpreted as a result of low stereoselectivity in the electrocyclization step (**518** → **517**) followed by high selectivity in the protonation step (**518** → **519**).

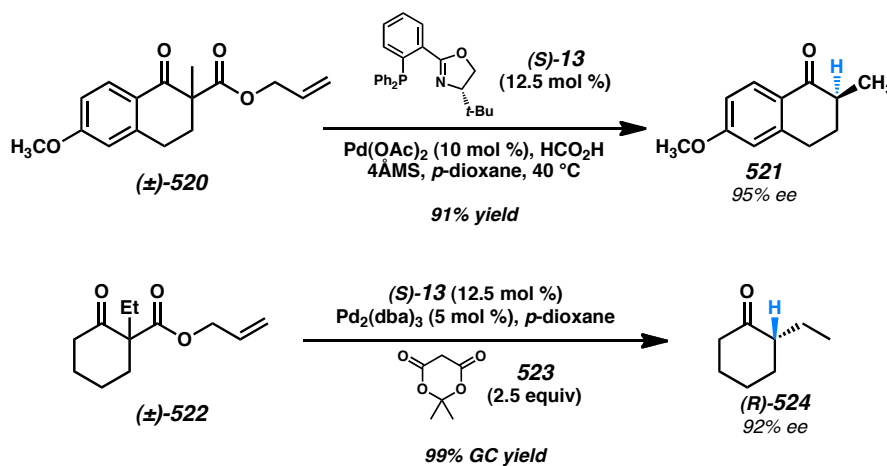
Scheme A9.27. Trauner's Nazarov Cyclization/Enantioselective Protonation



A different strategy for accessing chiral metal enolates is decarboxylation of β -ketoesters. The nature of the ester is typically important to enable enolate formation. In the case of palladium-catalyzed protonation reactions, benzyl and allyl esters have been the most common enolate precursors. The first examples of these reactions, developed extensively by Hénin, Muzart, and co-workers,⁴⁸ employed an initiation step such as Pd-mediated hydrogenolysis to generate an achiral enol (or enolate)⁴⁹ intermediate that was subsequently protonated with a chiral Brønsted acid (typically an amino alcohol). The results of these studies showed a strong dependence on the specific reaction conditions (e.g., temperature and source of palladium on carbon).

More recently, this strategy has been refined to instead generate a chiral Pd-enolate intermediate from allyl β -ketoester substrates (e.g., **520** and **522**, Scheme A9.28) in the hopes that chirality at the metal might impart improved stereocontrol in the protonation step and obviate the need for heterogeneous Pd catalysts. Stoltz and co-workers⁵⁰ found that the catalyst derived from Pd(OAc)₂ and phosphinooxazoline (PHOX) ligand **13** was capable of achieving enantioselective protonation in the presence of formic acid and molecular sieves (MS). High enantiomeric excesses were obtained for a range of cyclic ketone products including tetralone- and cyclohexanone-derived ketones (e.g., **520** and **522**). Attempts to track the source of the proton incorporated in the product with isomeric *mono*-deuterated formic acids (DCO₂H and HCO₂D) led to inconclusive results: with DCO₂H the formyl deuterium was not incorporated into the product, but with HCO₂D only 35% D incorporation was observed in the product, suggesting that another unidentified proton donor is also participating in the reaction.

Scheme A9.28. Stoltz' Palladium-Catalyzed Decarboxylative Protonation Reactions

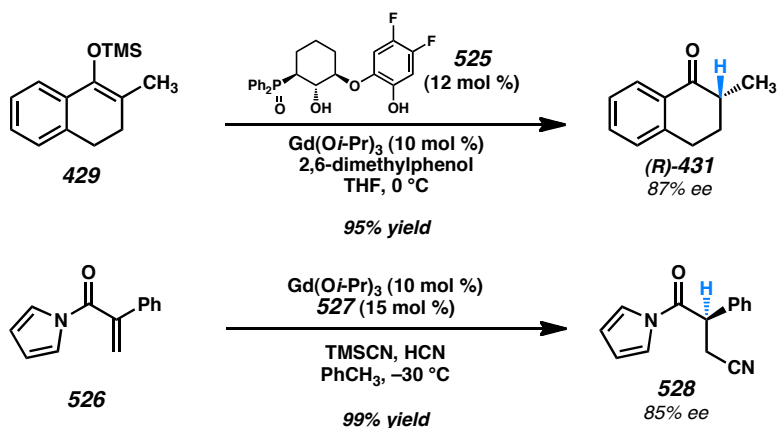


The heterogeneous additive (MS) in the reaction is important to the selectivity for protonation in preference to the competitive allylation reaction also catalyzed by the Pd•PHOX complex,⁵¹ and the specific amount required varied somewhat depending on the substrate. To address this issue, a related *homogeneous* protonation system was developed by Stoltz and co-workers⁵² employing Meldrum's acid (**523**, Scheme A9.28) as the achiral proton donor and a Pd•PHOX catalyst. Similar substrate scope and enantioselectivity was observed with this system, but without the need to optimize the amounts of additives to achieve optimal results. Initial mechanistic studies found zero-order kinetic dependence in substrate, which suggests a fast initial reaction between catalyst and substrate and a slow subsequent step, presumably either decarboxylation or protonation of the putative enolate intermediate common to both the protonation and allylic alkylation reactions with this catalyst system.⁵³ However, in the protonation reaction opposite enolate facial preference was observed for tetralone- and cyclohexanone-derived enolates, whereas in the alkylation reaction consistent enantiofacial selectivity was observed.⁵¹ This unexpected result suggests a substantial difference in the bond-forming portion of the mechanism.

Kanai, Shibasaki, and co-workers⁵⁴ recently reported the use of a chiral gadolinium complex for the enantioselective protonation of Gd-enolates generated in situ (Scheme A9.29). The Gd-enolates were accessed by two means: transmetallation from enol silane (e.g., **429**) or conjugate addition of cyanide to *N*-acryloyl pyrroles (e.g., **526**). Based on optimization studies, a polymetallic enolate intermediate was proposed. The optimal ligand-to-metal ratio is consistent with a 5:6 complex. The lack of reactivity in the absence of ligand **525** was also interpreted as the necessity of polynuclear Gd complexes

for the success of the reaction. Kinetic studies also suggested that the reaction proceeds via transmetallation from Si to Gd, and that this step is rate-limiting. 2,6-Dimethylphenol was the preferred proton source, providing indanone and tetralone products in up to 99% yield and up to 88% ee. The same Gd•**525** complex was also effective for the conjugate addition/protonation of cyanide to *N*-acryloyl pyrroles (e.g., **526** → **528**). In this case, hydrogen cyanide was the preferred proton source. This transformation was capable of producing *N*-acyl pyrroles in up to 99% yield and up to 91% ee. In the case of product **528**, recrystallization could be carried out to provide a 74% yield of material with >99% ee. The versatility of this polynuclear Gd catalyst to effect protonation of considerably different enolate intermediates is important to the prospect of a general system for enolate protonation.

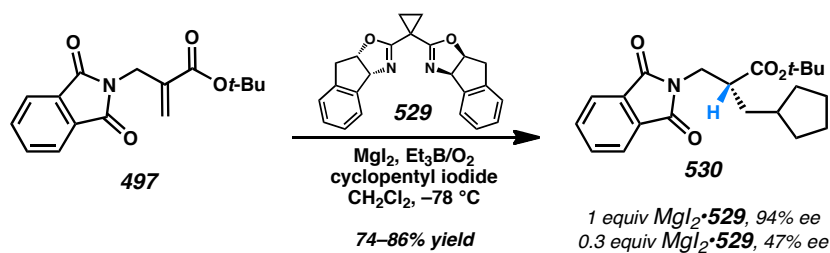
Scheme A9.29. Kanai and Shibasaki's Gadolinium-Catalyzed Protonation Reactions



A9.4.4 ENANTIOSELECTIVE HYDROGEN ATOM TRANSFER

An analogous strategy for arriving at protonation products is to exploit radical chemistry with a terminal H-atom abstraction step. Although not explicitly an enantioselective protonation reaction, many of the same challenges apply when manipulating a hydrogen atom. A recent example of this tactic by Sibi and co-workers^{55,56} has led to new methods for synthesizing β -amino acid derivatives (Scheme A9.30). By employing a Lewis acid complex formed from MgI_2 and bis(oxazoline) ligand **530**, tributyltin hydride, and triethylborane/ O_2 , alkyl radicals (from alkyl halides) can undergo radical conjugate addition followed by enantioselective hydrogen atom transfer to afford optically active products (e.g., **529**) in up to 95% yield and up to 98% ee. The reaction is believed to proceed through a bidentate chelate of the substrate to the chiral magnesium complex. The process can be made catalytic in Lewis acid without a significant effect on yield, but product ee suffered greatly in some cases due to a rapid uncatalyzed background reaction. These reactions have the benefit of being essentially neutral as opposed to the acidic or basic conditions required for the transformations described above.

Scheme A9.30. Radical Conjugate Addition Followed by Enantioselective H-Atom Transfer



A9.5 CONCLUSION

From the enantioselective enzymatic protonation reactions of nature to the variety of techniques for achieving enantioselective protonation in laboratories, a great deal of energy has been dedicated to understanding this deceptively simple transformation. Despite the many systems reported to date, the search for a highly efficient system with a broad scope continues. Moreover, although many of the key parameters needed to create a successful system have been enumerated here and elsewhere, the current level of mechanistic understanding in nearly all of the enantioselective protonation reactions reported to date remains relatively immature. Nonetheless, these useful transformations allow the synthesis of valuable chiral materials including natural products like α - and β -amino acids. Given these preliminary successes and improved understanding of the underlying mechanisms, enantioselective protonation reactions should continue to rise to prominence as an important tool for synthetic organic chemistry.

A9.6 NOTES AND REFERENCES

- (1) Mohr, J. T.; Krout, M. R.; Stoltz, B. M. *Nature* **2008**, *455*, 323–332.
- (2) (a) Fehr, C. *Angew. Chem., Int. Ed. Engl.* **1996**, *35*, 2566–2587. (b) Yanagisawa, A.; Ishihara, K.; Yamamoto, H. *Synlett* **1997**, 411–420. (c) Eames, J.; Weerasooriya, N. *Tetrahedron: Asymmetry* **2001**, *12*, 1–24. (d) Duhamel, L.; Duhamel, P.; Plaquevent, J.-C. *Tetrahedron: Asymmetry* **2004**, *15*, 3653–3691. (e) Yanagisawa, A.; Yamamoto, H. in *Comprehensive Asymmetric Catalysis, Vol. III* (eds Jacobsen, E. N., Pfaltz, A. & Yamamoto, H.) 1295–1306 (Springer, 1999). (f) Yanagisawa, A.; Yamamoto, H. in *Comprehensive Asymmetric Catalysis, Suppl. 2* (eds Jacobsen, E. N., Pfaltz, A. & Yamamoto, H.) 125–132 (Springer, 2004). (g) Blanchet, J.; Baudoux, J.; Amere, M.; Lasne, M.-C.; Rouden, J. *Eur. J. Org. Chem.* **2008**, 5493–5506.
- (3) Fehr, C. *Angew. Chem., Int. Ed.* **2007**, *46*, 7119–7121.
- (4) (a) Miyamoto, K.; Ohta, H. *Eur. J. Biochem.* **1992**, *210*, 475–481. (b) Matoishi, K.; Ueda, M.; Miyamoto, K.; Ohta, H. *J. Mol. Catal. B: Enzym.* **2004**, *27*, 161–168.
- (5) Hansch, C.; Leo, A.; Taft, R. W. *Chem. Rev.* **1991**, *91*, 165–195 and references therein.
- (6) (a) Nakasako, M.; Obata, R.; Okubo, R.; Nakayama, S.; Miyamoto, K.; Ohta, H. *Acta Crystallogr. Sect. F*, **2008**, *64*, 610–613. (b) Kuettner, E. B.; Keim, A.; Kircher, M.; Rosmus, S.; Strater, N. *J. Mol. Biol.* **2008**, *377*, 386–394.

- (7) (a) Terao, Y.; Ijima, Y.; Miyamoto, K.; Ohta, H. *J. Mol. Catal. B: Enzym.* **2007**, *45*, 15–20. (b) Ijima, Y.; Matoishi, K.; Terao, Y.; Doi, N.; Yanagawa, H.; Ohta, H. *Chem. Commun.* **2005**, 877–879.
- (8) Terao, Y.; Miyamomoto, K.; Ohta, H. *Appl. Microbiol. Biotechnol.* **2006**, *73*, 647–653.
- (9) Miyamoto, K.; Hirokawa, S.; Ohta, H. *J. Mol. Catal. B: Enzym.* **2007**, *46*, 14–19.
- (10) Matsumoto, K.; Tsutsumi, S.; Ihori, T.; Ohta, H. *J. Am. Chem. Soc.* **1990**, *112*, 9614–9619.
- (11) Hirata, T.; Shimoda, K.; Kawano, T. *Tetrahedron: Asymmetry* **2000**, *11*, 1063–1066.
- (12) Sakai, T.; Matsuda, A.; Tanaka, Y.; Korenaga, T.; Ema, T. *Tetrahedron: Asymmetry* **2004**, *15*, 1929–1932.
- (13) Vedejs, E.; Kruger, A. W.; Suna, E. *J. Org. Chem.* **1999**, *64*, 7863–7870.
- (14) Kim, B. M.; Kim, H.; Kim, W.; Im, K. Y.; Park, J. K. *J. Org. Chem.* **2004**, *69*, 5104–5107.
- (15) (a) Boyd, E.; Coumbarides, G. S.; Eames, J.; Hay, A.; Jones, R. V. H.; Stenson, R. A.; Suggate, M. J. *Tetrahedron Lett.* **2004**, *45*, 9465–9468. (b) Coumbarides, G. S.; Eames, J.; Ghilagaber, S.; Suggate, M. J. *Tetrahedron Lett.* **2004**, *45*, 9469–9474. (c) Coumbarides, G. S.; Eames, J.; Scheuermann, J. E. W.; Sibbons, K. F.; Suggate, M. J.; Watkinson, M. *Bull. Chem. Soc Jpn.* **2005**, *78*, 906–909.

- (16) (a) Amere, M.; Lasne, M.-C.; Rouden, J. *Org. Lett.* **2007**, 9, 2621–2624.
(b) Seitz, T.; Baudoux, J.; Bekolo, H.; Cahard, D.; Plaquevent, J.-C.; Lasne, M.-C.; Rouden, J. *Tetrahedron* **2006**, 62, 6155–6165.
- (17) (a) Carbery, D. R.; Donohoe, T. J. *Chem. Commun.* **2004**, 722–723. (b) Donohoe, T. J.; Freestone, G. C.; Headley, C. E.; Rigby, C. L.; Cousins, R. P. C.; Bhalay, G. *Org. Lett.* **2004**, 6, 3055–3058.
- (18) Rueping, M.; Theissmann, T.; Raja, S.; Bats, J. W. *Adv. Synth. Catal.* **2008**, 350, 1001–1006.
- (19) Cheon, C. H.; Yamamoto, H. *J. Am. Chem. Soc.* **2008**, 130, 9246–9247.
- (20) Mitsuhashi, K.; Ito, R.; Arai, T.; Yanagisawa, A. *Org. Lett.* **2006**, 8, 1721–1724.
- (21) (a) Yanagisawa, A.; Touge, T.; Arai, T. *Angew. Chem., Int. Ed.* **2005**, 44, 1546–1548. (b) Yanagisawa, A.; Touge, T.; Arai, T. *Pure Appl. Chem.* **2006**, 78, 519–523.
- (22) Poisson, T.; Dalla, V.; Marsais, F.; Dupas, G.; Oudeyer, S.; Levacher, V. *Angew. Chem., Int. Ed.* **2007**, 46, 7090–7093.
- (23) Becker, H.; Sharpless, K. B. *Angew. Chem., Int. Ed. Engl.* **1996**, 35, 448–451.
- (24) Poisson, T.; Oudeyer, S.; Dalla, V.; Marsais, F.; Levacher, V. *Synlett* **2008**, 16, 2447–2450.
- (25) (a) Wang, Y.; Liu, X.; Deng, L. *J. Am. Chem. Soc.* **2006**, 128, 3928–3930.
(b) Wang, B.; Wu, F.; Wang, Y.; Liu, X.; Deng, L. *J. Am. Chem. Soc.* **2007**, 129, 768–769.

- (26) Li, B.-J.; Jiang, L.; Liu, M.; Chen, Y.-C.; Ding, L.-S.; Wu, Y. *Synlett* **2005**, 603–606.
- (27) Leow, D.; Lin, S.; Chittimalla, S. K.; Fu, X.; Tan, C.-H. *Angew. Chem. Int. Ed.* **2008**, *47*, 5641–5645.
- (28) (a) Hénin, F.; Muzart, J.; Pete, J.-P.; M'boungou-M'passi, A.; Rau, H. *Angew. Chem., Int. Ed. Engl.* **1991**, *30*, 416–418. (b) Hénin, F.; M'boungou-M'passi, A.; Muzart, J.; Pete, J.-P. *Tetrahedron* **1994**, *50*, 2849–2864.
- (29) Mohr, J. T.; Ebner, D. C.; Stoltz, B. M. *Org. Biomol. Chem.* **2007**, *5*, 3571–3576.
- (30) Dai, X.; Nakai, T.; Romero, J. A. C.; Fu, G. C. *Angew. Chem., Int. Ed.* **2007**, *46*, 4367–4369.
- (31) Denmark, S. E.; Beutner, G. L. *Angew. Chem., Int. Ed.* **2008**, *47*, 1560–1638.
- (32) Hodous, B. L.; Fu, G. C. *J. Am. Chem. Soc.* **2002**, *124*, 10006–10007.
- (33) Girard, C.; Kagan, H. B. *Angew. Chem., Int. Ed.* **1998**, *37*, 2922–2959.
- (34) Hodous, B. L.; Ruble, J. C.; Fu, G. C. *J. Am. Chem. Soc.* **1999**, *121*, 2637–2638.
- (35) Wiskur, S. L.; Fu, G. C. *J. Am. Chem. Soc.* **2005**, *127*, 6176–6177.
- (36) Schaefer, C.; Fu, G. C. *Angew. Chem., Int. Ed.* **2005**, *44*, 4606–4608.
- (37) Reynolds, N. T.; Rovis, T. *J. Am. Chem. Soc.* **2005**, *127*, 16406–16407.
- (38) Maki, B. E.; Chan, A.; Scheidt, K. A. *Synthesis* **2008**, 1306–1315.

- (39) Moss, R. J.; Wadsworth, K. J.; Chapman, C. J.; Frost, C. G. *Chem. Commun.* **2004**, 1984–1985.
- (40) Hargrave, J. D.; Herbert, J.; Bish, G.; Frost, C. G. *Org. Biomol. Chem.* **2006**, *4*, 3235–3241.
- (41) Frost, C. G.; Penrose, S. D.; Lambshead, K.; Raithby, P. R.; Warren, J. E.; Gleave, R. *Org. Lett.* **2007**, *9*, 2119–2122.
- (42) Sibi, M. P.; Tatamidani, H.; Patil, K. *Org. Lett.* **2005**, *7*, 2571–2573.
- (43) Nishimura, T.; Hirabayashi, S.; Yasuhara, Y.; Hayashi, T. *J. Am. Chem. Soc.* **2006**, *128*, 2556–2557.
- (44) Hamashima, Y.; Somei, H.; Shimura, Y.; Tamura, T.; Sodeoka, M. *Org. Lett.* **2004**, *6*, 1861–1864.
- (45) (a) Navarre, L.; Darses, S.; Genet, J.-P. *Angew. Chem., Int. Ed.* **2004**, *43*, 719–723. (b) Navarre, L.; Martinez, R.; Genet, J.-P.; Darses, S. *J. Am. Chem. Soc.* **2008**, *130*, 6159–6169.
- (46) Sibi, M. P.; Coulomb, J.; Stanley, L. M. *Angew. Chem., Int. Ed.* **2008**, *47*, 9913–9915.
- (47) Liang, G.; Trauner, D. *J. Am. Chem. Soc.* **2004**, *126*, 9544–9545.
- (48) Aboulhoda, S. J.; Hénin, F.; Muzart, J.; Thorey, C.; Behnen, W.; Martens, J.; Mehler, T. *Tetrahedron: Asymmetry* **1994**, *5*, 1321–1326.

- (49) (a) Detalle, J.-F.; Riahi, A.; Steinmetz, V.; Hénin, F.; Muzart, J. *J. Org. Chem.* **2004**, *69*, 6528–6532. (b) Kukula, P.; Matousek, V.; Mallat, T.; Baiker, A. *Tetrahedron: Asymmetry* **2007**, *18*, 2859–2868. (c) Kukula, P.; Matousek, V.; Mallat, T.; Baiker, A. *Chem.–Eur. J.* **2008**, *14*, 2699–2708.
- (50) Mohr, J. T.; Nishimata, T.; Behenna, D. C.; Stoltz, B. M. *J. Am. Chem. Soc.* **2006**, *128*, 11348–11349.
- (51) (a) Behenna, D. C.; Stoltz, B. M. *J. Am. Chem. Soc.* **2004**, *126*, 15044–15045. (b) Mohr, J. T.; Behenna, D. C.; Harned, A. M.; Stoltz, B. M. *Angew. Chem., Int. Ed.* **2005**, *44*, 6924–6927. (c) Seto, M.; Roizen, J. L.; Stoltz, B. M. *Angew. Chem., Int. Ed.* **2008**, *47*, 6873–6876. (d) For a review, see: Mohr, J. T.; Stoltz, B. M. *Chem.–Asian J.* **2007**, *2*, 1476–1491.
- (52) Marinescu, S. C.; Nishimata, T.; Mohr, J. T.; Stoltz, B. M. *Org. Lett.* **2008**, *10*, 1039–1042.
- (53) Keith, J. A.; Behenna, D. C.; Mohr, J. T.; Ma, S.; Marinescu, S. C.; Oxgaard, J.; Stoltz, B. M.; Goddard, III, W. A. *J. Am. Chem. Soc.* **2007**, *129*, 11876–11877.
- (54) Morita, M.; Drouin, L.; Motoki, R.; Kimura, Y.; Fujimori, I.; Kanai, M.; Shibasaki, M. *J. Am. Chem. Soc.* **2009**, *131*, 3858–3859.
- (55) Sibi, M. P.; Asano, Y.; Sausker, J. B. *Angew. Chem., Int. Ed.* **2001**, *40*, 1293–1296.
- (56) Sibi, M. P.; Patil, K. *Angew. Chem., Int. Ed.* **2004**, *43*, 1235–1238.

APPENDIX 10

Pd-Catalyzed Asymmetric Allylic Alkylation of α -Oxygenated Enolates: Synthetic Studies and Preliminary Mechanistic Hypotheses[†]

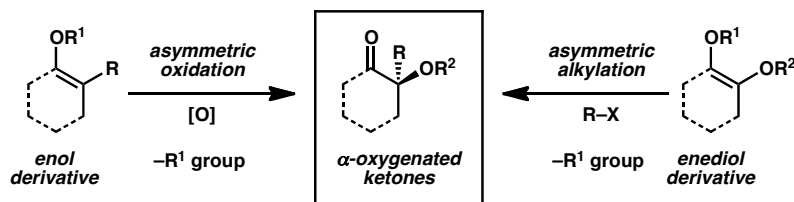
A10.1 INTRODUCTION AND BACKGROUND

The asymmetric synthesis of α -oxygenated ketone motifs represents an important problem in catalysis because methods would provide access to enantioenriched oxidized building blocks for the total synthesis of diverse natural products. One strategy for constructing these units is the enantioselective oxidation of substituted enol derivatives (Scheme A10.1). Several chiral reagents such as Shi's catalyst¹ can effect this transformation in an asymmetric manner. While numerous groups have pursued this approach, a key challenge is the suppression of undesired oxidation of other functional groups in the substrate. Another method for obtaining α -oxygenated ketones is the

[†] Portions of this work concerning α -benzoyloxy β -ketoesters were reported in Hong, A. Y.; Bennett, N. B.; Krout, M. R.; Jensen, T.; Harned, A. M.; Stoltz, B. M. *Tetrahedron* **2011**, 67, 10234–10248. Early investigations of α -alkoxy silyl enol ethers and enol carbonates were performed by Dr. Douglas C. Behenna and Dr. Jennifer L. Roizen. Dr. Nolan T. McDougal conducted investigations of β -ester enol carbonate substrates. Related experiments on other chelating substrates are the subject of current synthetic and computational investigations by Douglas C. Duquette, Nathan B. Bennett, Dr. Jimin Kim, and Dr. Douglas C. Behenna. The results in Section A10.2.2 are unpublished.

asymmetric alkylation of 1,2-enediol derivatives (Scheme A10.1). The formation of stereocenters through this strategy can be difficult due to the lack of differentiation between the two nucleophilic sites. Despite the inherent challenge of chemoselectivity, this method may be more synthetically versatile, since asymmetric induction can potentially be achieved under milder conditions and enable the convergent assembly of α -oxygenated chiral ketone motifs.

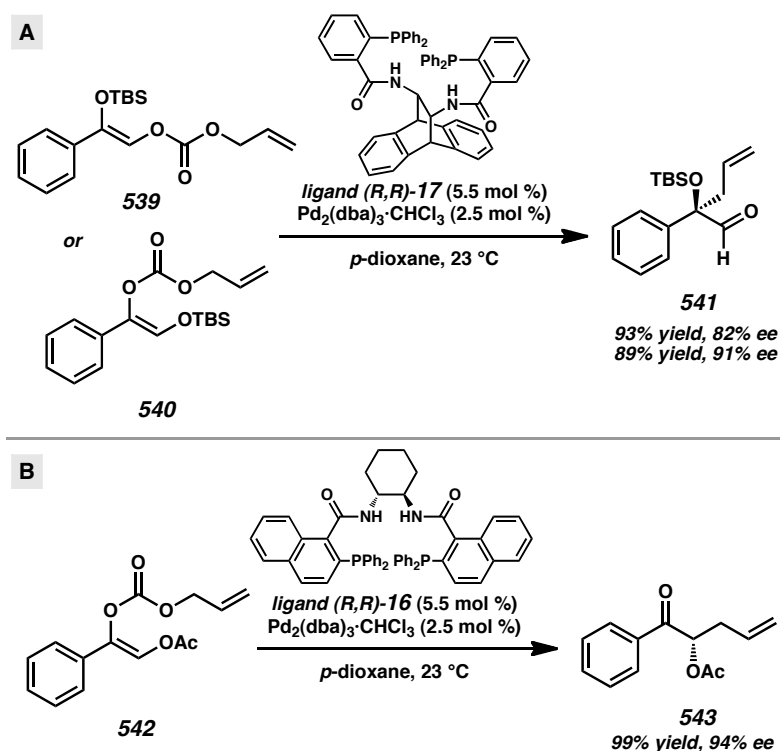
Scheme A10.1. Strategies for the Formation of Tertiary α -Oxygenated Ketone Motifs

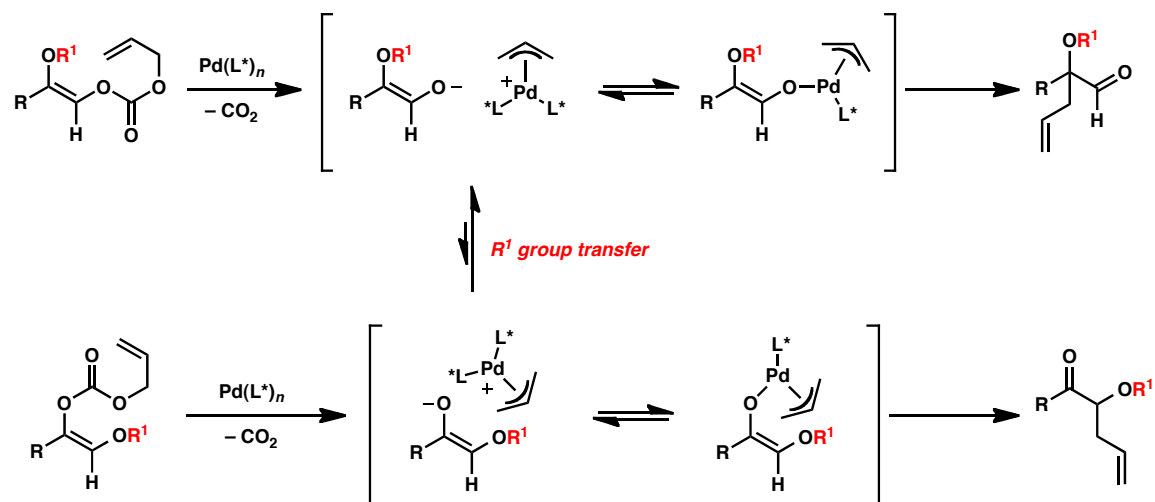


Asymmetric palladium-catalyzed Tsuji allylation reactions of non-shielded, unstabilized enolates were first reported by our group^{2,3,4} and subsequently by Trost.⁵ While both catalyst systems typically make use of $\text{Pd}(0)$ precursors, our conditions employ P,N -chelating PHOX ligands⁶ while Trost's conditions employ P,P -chelating ligands.⁷ Based on these early developments, the extension of the methodology to 1,2-enediol derivatives emerged as a particularly promising strategy for obtaining chiral α -oxygenated ketone products. Trost was the first to successfully achieve the enantioselective alkylation of 1,2-enediol derivatives^{8a} (Scheme A10.2A), with the initial report demonstrating that a variety of acyclic α -silyloxy enol carbonates could be converted to α -silyloxy ketone or aldehyde products by selective alkylation of benzylic enolates. Notably, isomeric substrates **539** and **540** yielded the same product **541** under

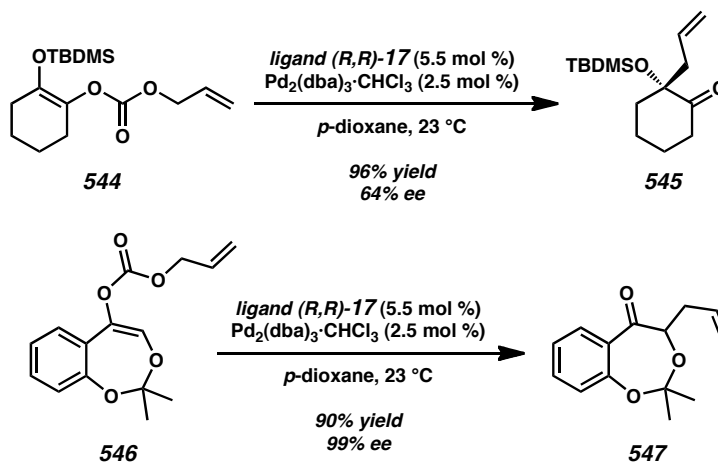
the optimized reaction conditions. A subsequent communication showed that α -acyloxy enol carbonates, such as **542**, could be converted to their corresponding chiral ketones by selective alkylation at the carbon bearing the acyloxy group (Scheme A10.2B).^{8b} Crucial to the success of these transformations were the substituent on the α -oxygen and the choice of bis-phosphine ligand (**16** or **17**). These two key variables influence the mechanistic pathway for the enantioselective and regioselective alkylation of mono-protected 1,2-enediols (Scheme A10.3).

Scheme A10.2. Asymmetric Alkylation of Linear α -Oxygenated Substrates by Trost

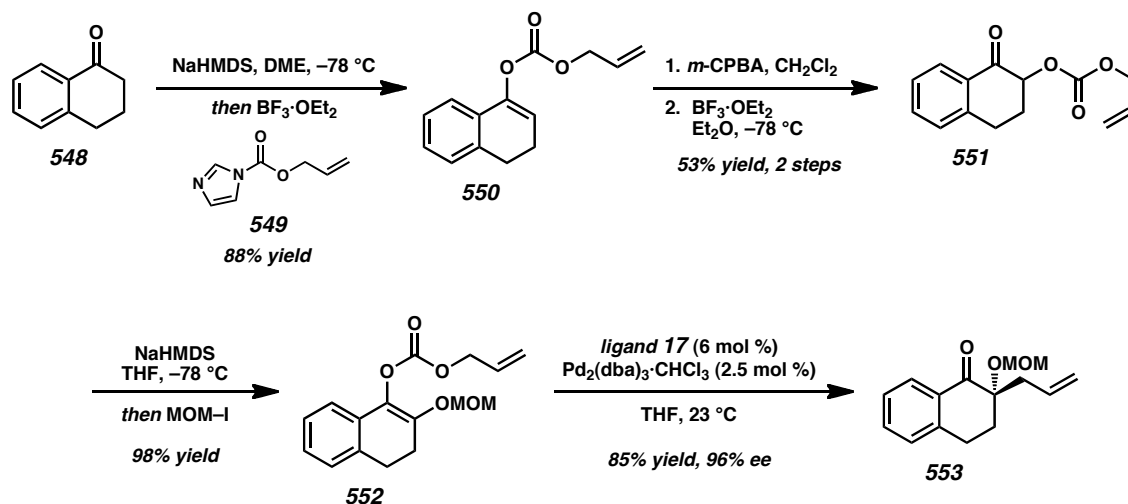


Scheme A10.3. Mechanistic Pathways for the Asymmetric Alkylation of α -Oxygenated Substrates

While the asymmetric alkylation of a variety of acyclic compounds proved successful, generalization to cyclic substrates poses new challenges and requires further reaction development. In Trost's early communications, only two examples of cyclic substrates were reported^{9a} (Scheme A10.4). In the case of exocyclic α -oxygenated **544**, asymmetric induction was much lower than the corresponding acyclic substrates. On the other hand, asymmetric alkylation with endocyclic α -oxygenated **546**, which is unable to undergo group transfer reactions, proved to be more fruitful. Even among acyclic substrates, deviation from styrenyl 1,2-dienol derivatives typically led to lower reaction yields. The lack of broadly effective asymmetric transformations for cyclic substrates and some acyclic substrates suggests that these difficult problems require a more general solution.

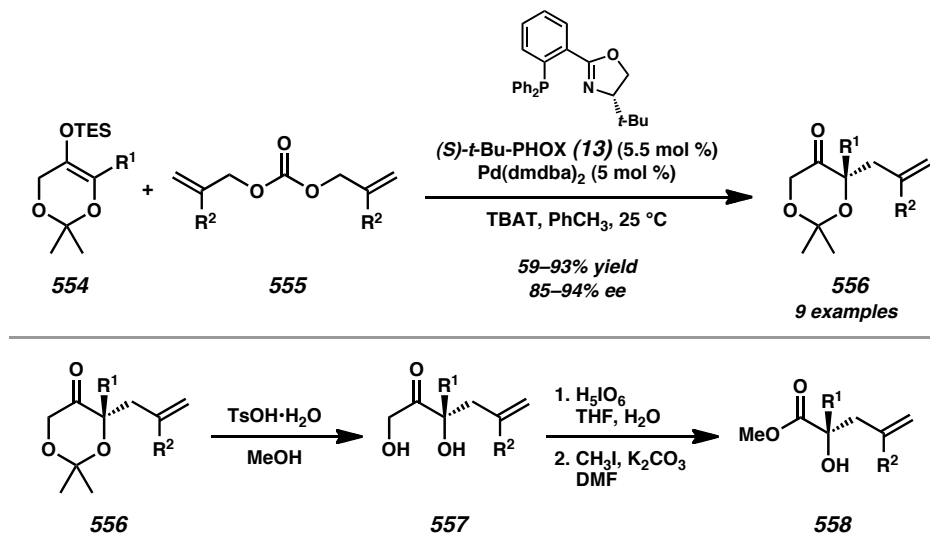
Scheme A10.4. Asymmetric Alkylation of Cyclic α -Oxygenated Substrates by Trost

A recent report from the Trost group has outlined a strategy for the synthesis of protected tertiary α -hydroxy ketones from α -tetralone or 1-benzosuberone substrates (Scheme A10.5).⁹ Initial enol carbonate formation followed by *m*-CPBA oxidation provides an intermediate epoxide, which undergoes fragmentation and acyl transfer to yield a keto carbonate such as **551**. Deprotonation leads to a second acyl transfer and the acyloxy enolate can be trapped with MOMI or BOMI to give decarboxylative alkylation substrates such as **552**. Using standard asymmetric alkylation conditions with $\text{Pd}_2(\text{dba})_3 \cdot \text{CHCl}_3$ and bis-phosphine ligand **17**, the protected tertiary α -hydroxy ketones **553** can be obtained. This method has enabled the incorporation of numerous substituted allylic fragments, but the evaluations of the substrate scope have focused on benzannulated five- and six-membered rings.

Scheme A10.5. Asymmetric Alkylation of Additional Cyclic α -Oxygenated Substrates by Trost

Concurrent with these investigations, our group sought to develop asymmetric alkylation methodology for a broad range of carbocyclic and heterocyclic ketone substrates. Toward this overall goal, we initially pursued dioxanone-derived substrates (Scheme A10.6).¹⁰ Using modified asymmetric alkylation conditions, silyl enol ethers **554** were converted to a variety of α -tetrasubstituted dioxanone products **556**, which could be advanced to acyclic α -hydroxy acid derivatives. While we were encouraged by our ability to make a variety of useful acyclic α -oxygenated compounds, we turned our attention to the asymmetric alkylation of exocyclic α -oxygenated compounds to develop a more general synthetic method.

Scheme A10.6. Asymmetric Alkylation of Dioxanone Derivatives and Further Manipulations



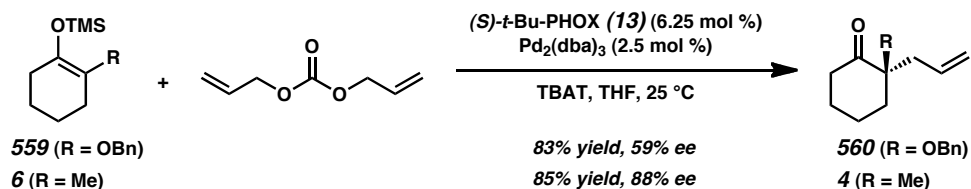
A10.2 Pd-CATALYZED ASYMMETRIC ALKYLATION OF CYCLIC α -OXYGENATED SUBSTRATES

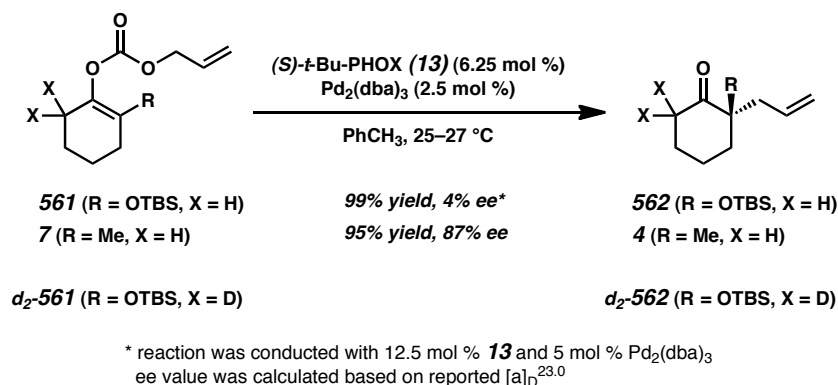
In our efforts to expand the substrate scope of our asymmetric alkylation methodology, we investigated α -oxygenated silyl enol ethers, enol carbonates, and β -ketoesters to obtain synthetically useful oxidized chiral ketone building blocks. The versatility of our Pd-catalyzed asymmetric alkylation methodology^{2,3,4} allows us to investigate all three substrate classes to identify promising substrates for our desired transformation.

A10.2.1 PREVIOUS EVALUATION SILYL ENOL ETHER AND ENOL CARBONATE SUBSTRATES

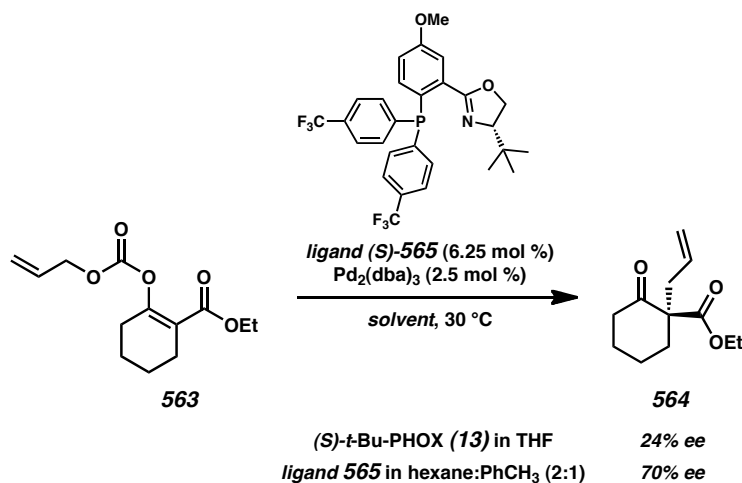
With simple modifications of our standard synthetic routes, α -benzyloxy silyl enol ether **559** and α -OTBS enol carbonate **561** were prepared (Scheme A10.7 and Scheme A10.8). Using our standard Pd-catalyzed asymmetric alkylation conditions with $\text{Pd}(\text{dba})_2$ and a (*S*)-*t*-Bu-PHOX (**13**),^{2,3,4} the silyl enol ether and enol carbonate substrates were efficiently converted to the corresponding allylation products. In the presence of TBAT and diallyl carbonate, α -benzyloxy silyl enol ether **6** afforded cyclohexanone **6** in 83% yield (Scheme A10.7). The transformation of α -OTBS enol carbonate **561** to cyclohexanone **562** by decarboxylative alkylation also proceeded smoothly in 99% yield (Scheme A10.8). However, to our surprise, the enantioselectivity of both reactions were quite low compared to more typical substrates with α -alkyl substituents (Scheme A10.7 and Scheme A10.8). While benzyl migration is unlikely in the case of substrate **559**, silyl migration upon enolate formation could be responsible for the low asymmetric induction with substrate **561**. So far, our attempts to probe the extent of silyl migration in the latter reaction using α' -deuterated substrate d_2 -**561** have been inconclusive.

Scheme A10.7. Asymmetric Alkylation of α -Oxygenated Silyl Enol Ether Substrates



Scheme A10.8. Asymmetric Alkylation of α -Oxygenated Enol Carbonate Substrates

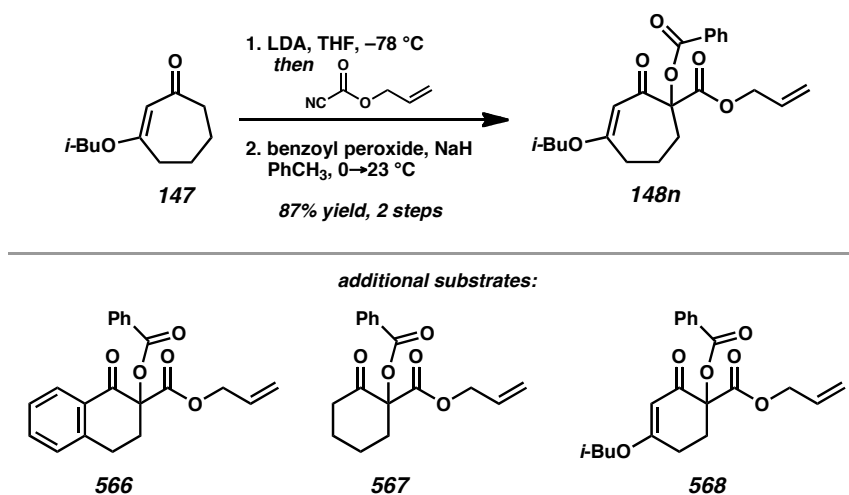
In addition to these experiments with α -oxygenated substrates, β -ester enol carbonate substrates were also investigated in our group (Scheme A10.9). With ester-containing enol carbonate **563**, we were able to obtain β -ketoester **564** in only 24% ee.^{16d} Using Symyx high-throughput screening technology,¹¹ we were able to optimize ligand and solvent combinations to improve our results to 70% ee. In this case, the use of electron-deficient PHOX ligand **565** and a mixture of hexane:toluene (2:1) proved to be optimal.

Scheme A10.9. Asymmetric Alkylation of a β -Ester Enol Carbonate Substrate

A10.2.2 EVALUATION OF α -OXYGENATED β -KETOESTER SUBSTRATES

After investigating α -oxygenated silyl enol ether and enol carbonate substrates, we turned our attention to β -ketoester substrates.³ During the development of our asymmetric alkylation/ring contraction methodology,¹² we were particularly interested in evaluating cyclic substrates with α -heteroatom-substituted tertiary centers. Beginning from simple cyclic ketones such as **147**, treatment with LDA and allyl cyanofornate followed by oxidation with NaH and benzoyl peroxide enabled efficient access to α -benzoyloxy **148n** in 87% yield over two steps^{12b} (Scheme A10.10). This procedure proved to be reasonably general, providing access to gram-quantities of tetralone **566**, cyclohexanone **567**, and vinylogous ester **568** in good yields in a short, concise reaction sequence.

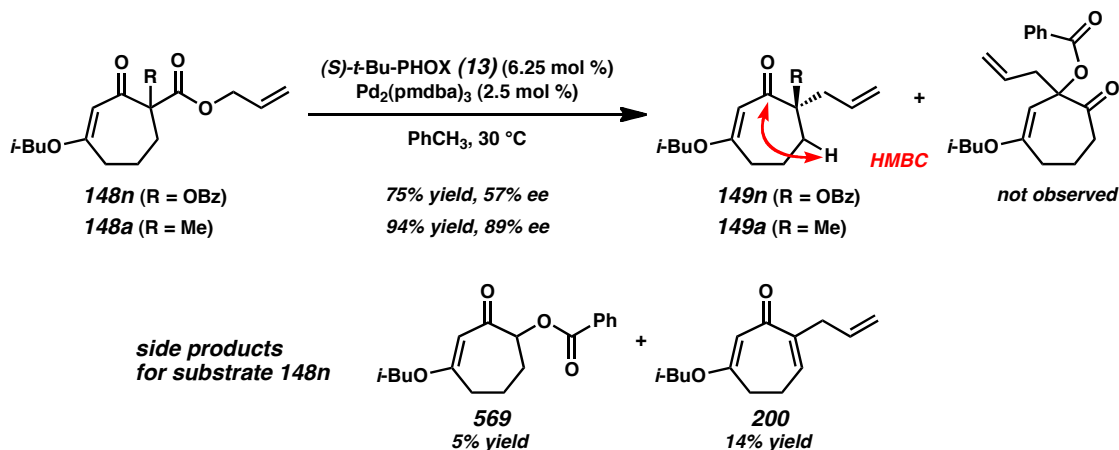
Scheme A10.10. Synthesis of α -Acyloxy β -Ketoester Substrates



With these substrates in hand, we were poised to evaluate the asymmetric alkylation reaction (Scheme A10.11). Using our standard β -ketoester conditions with catalytic (*S*)-

t-Bu-PHOX (**13**)¹³ and Pd₂(pmdba)₃ in toluene, we found that with β -ketoester **148n** was converted to α -benzoyloxy product **149n** in 75% yield and 57% ee.^{12b} These results continue the trend of reduced asymmetric induction compared to the corresponding α -alkyl substrates. The lack of benzoyl migration was verified by HMBC and HSQC experiments and is consistent with our proposed inner-sphere extended reductive elimination mechanism for C–C bond formation with the PHOX ligand system with unstabilized enolates.^{4,14,15} The remainder of the mass balance in the reaction for substrate **148n** consisted of protonation product **569** and elimination product **200**.

Scheme A10.11. Asymmetric Alkylation of a Vinylogous Ester-Derived β -Ketoester Substrate



Screening of alternative solvents and ligands provided unexpected results. Investigation of THF and pentane:toluene (2:1) as the reaction medium did not show a clear solvent effect on the enantioselectivity of the reaction (Table A10.1). Investigation of different ligands showed a more meaningful pattern. Employing electron-deficient PHOX ligand **14**¹⁶ provided product in 82% yield but only 29% ee. This result is

especially surprising in that ligand **14** usually has a beneficial effect on many of our asymmetric alkylation reactions.^{16,17} Investigation of the electron-rich ligand **570**^{13b} provided product **149n** in a much lower 28% yield and 50% ee. At this time, the investigation of other α -benzoyloxy substrates such as the ones depicted in Scheme A10.10 has not been conducted.

Table A10.1. Solvent and Ligand Effects on the Asymmetric Alkylation of a Vinylogous Ester-Derived β -Ketoester Substrate

entry	ligand	solvent	yield (%)	ee (%)
1	(S)- 13	PhCH ₃	75	57
2	(S)- 14	PhCH ₃	82	29
3	(S)- 13	THF	58	50
4	(S)- 13	pentane:PhCH ₃ (2:1)	83	45
5	(S)- 570	PhCH ₃	28	50

ligands:

(S)-*t*-Bu-PHOX
(**13**)

(S)-(*CF*₃)₃-*t*-Bu-PHOX
(**14**)

(S)-Cy₂-*t*-Bu-PHOX
(**570**)

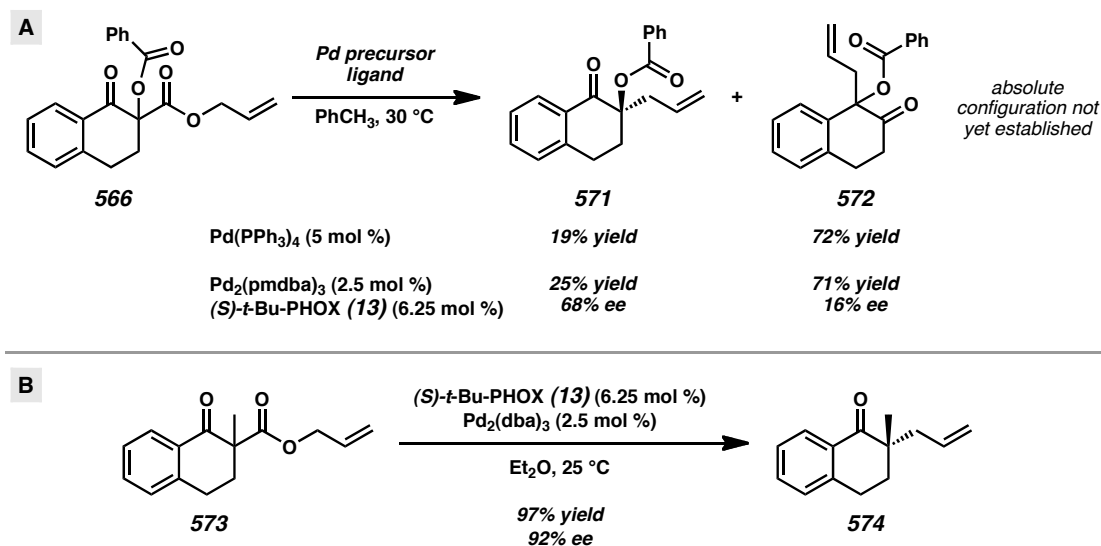
Currently, the precise nature of the observed secondary effects arising from α -oxygenated substrates is unclear. One possible interpretation for the correlation between ligand electronics and asymmetric induction is an electrostatic pairing or chelation

interaction between the substrate and the palladium center. With PHOX as ligand, the intermediate Pd(II) species formed after oxidative addition and decarboxylation may have an affinity for the ester moiety of the substrate, interacting with it in an apical fashion above the square plane. This perturbed configuration induced by the substrate would lead to the opposite enantiomer of the product. Additionally, it may be possible that the diminished ee values could be the result of substrate-induced steric interactions with the palladium center. While these interactions are not enough to reverse the absolute configuration of the product **149n**, the contribution of this pathway manifests itself in a significantly reduced ee value. Rendering the Pd(II) center more electron-poor, accomplished by using ligand **14**, presumably increased the contribution of this secondary interaction and led to even lower asymmetric induction. The use of an electron-rich ligand such as **570** would be expected to reduce the tendency for secondary interaction, but asymmetric induction with this ligand did not follow a clear pattern. It is unknown whether this ligand changes other aspects of the overall reaction mechanism.

While the ligand effects on the asymmetric alkylation of seven-membered substrate **148n** were surprising, we wondered whether the observed reduction in ee would prove general for β -ketoesters with different ring sizes. To this end, we investigated tetralone substrate **566** (Scheme A10.12A). When we applied our standard conditions, we observed a mixture of α -tetralone **571** (25% yield) and β -tetralone **572** (71% yield). If Pd(PPh₃)₄ is employed as the catalyst, a similar product distribution is observed. When compared to the case of vinylogous ester substrate **148n**, which showed no acyl transfer in isolated product **149n** (Scheme A10.11), the propensity for benzoyl migration appears to be substrate-dependent. The greater stability of a styrenyl enolate generated from

substrate **566** may facilitate benzoyl migration and allylation at the benzylic position. The ee for both allylation products was quite low compared to related α -alkyl substrates such as **573** (Scheme A10.12B), again supporting the trend of a detrimental effect of α -acyloxy groups on Pd-catalyzed asymmetric alkylation reactions with the PHOX ligand system.

Scheme A10.12. Asymmetric Allylation of a Tetralone-Derived β -Ketoester Substrate

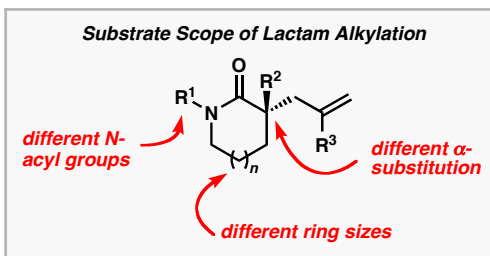
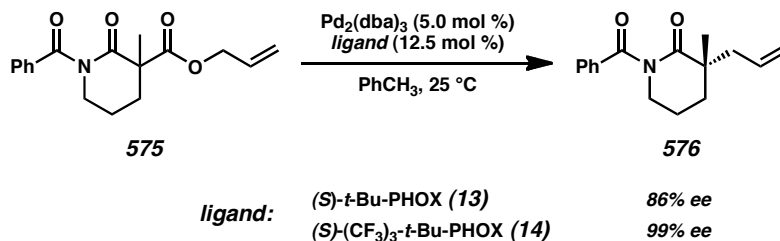


A10.2.3 RECENT INVESTIGATION OF *N*-ACYL LACTAM SUBSTRATES

Our group recently extended the asymmetric alkylation technology to *N*-heterocycles.¹⁸ By taking advantage of Symyx high-throughput screening technology, we were able to find the optimal conditions for the conversion of lactam-derived substrates such as **575** to their corresponding alkylation products in an efficient manner. This transformation is quite general for different α -substitution patterns, ring sizes, and substituted *N*-benzoyl groups (Scheme A10.13).

One of the key findings of our study was the importance of (*S*)-(CF₃)₃-*t*-Bu-PHOX (**14**) for achieving consistently high enantioselectivities. With (*S*)-*t*-Bu-PHOX (**13**), the reaction on the standard substrate shows only 86% ee, while the use of (*S*)-(CF₃)₃-*t*-Bu-PHOX (**14**) gives product in 99% ee. This trend is consistent across different substrates and solvents. If the *N*-benzoyl group is replaced with an alkyl group or hydrogen atom, the yields and conversions for the reactions typically suffer.

One possible interpretation of the ligand effect on ee and the importance of the benzoyloxy group is the intermediacy of an electrostatically-paired, chelated, or sterically perturbed palladium intermediate in the catalytic cycle. It is possible that the use of a benzoyl group provides a handle for these effects and the use of an electron-deficient PHOX ligand helps increase this secondary interaction. High enantioselectivities were generally conserved when a variety of acyl derivatives were evaluated as *N*-protecting groups. When compared to the α -oxygenated substrates, the *N*-acyl group in the lactam substrates is formally situated at the α' -position compared to α -oxygenated substrates. Current efforts by other members of the group are focused on the rational design of substrates to take advantage of this secondary interaction hypothesis and render other challenging substrate classes amenable to effective asymmetric induction. Computational investigations are also being initiated to help elucidate the precise nature of the observed increase in ee relative to cycloalkanone-type substrates.

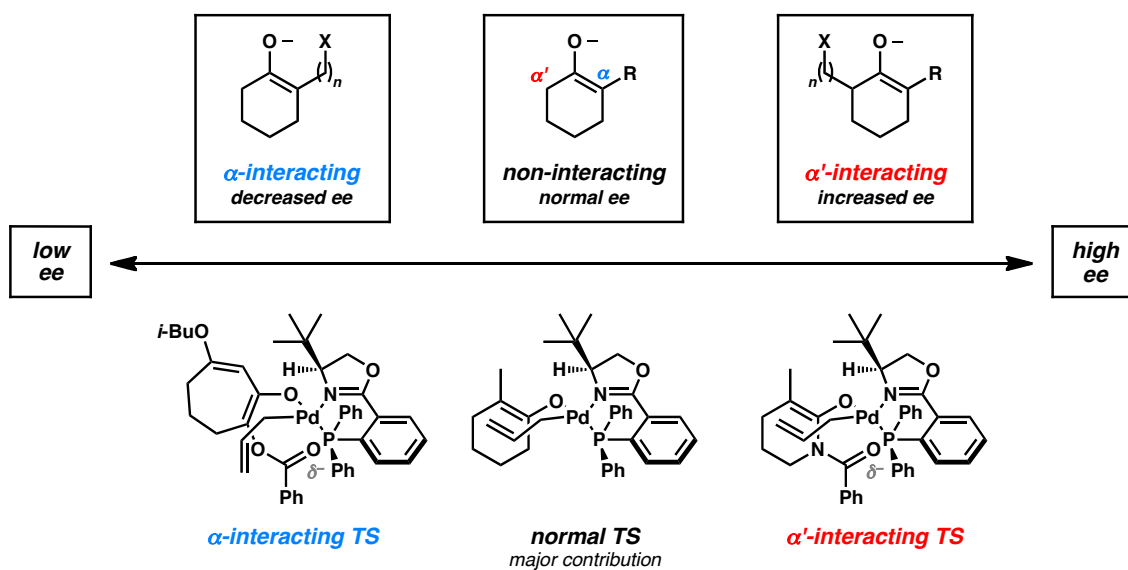
Scheme A10.13. Asymmetric Alkylation of *N*-Acyl Lactams

A10.2.4 POSSIBLE MECHANISTIC IMPLICATIONS OF α - AND α' -INTERACTING ASYMMETRIC ALKYLATION SUBSTRATES

Based on the experimental data gathered to date, we can divide asymmetric alkylation substrates into several general classes based on substitution pattern: non-interacting, α -interacting, and α' -interacting (Scheme A10.14). Non-interacting substrates give standard enantioselectivities for the PHOX ligand system within the usual range of 85–92% ee. Substrates in the α' -interacting class tend to provide higher enantioselectivities due to an electrostatic, chelating, or steric interaction which enforces the desired transition state. This interaction is enhanced with electron-deficient ligands such as **14**. Such ligands may render palladium more electrophilic and more susceptible to secondary interactions beyond the square planar ligands. In these cases, products with greater than 95% ee are common. On the other hand, α -donating substrates can help favor an alternate transition state that leads to the undesired enantiomeric product by an analogous

electrostatic or chelation interaction. The use of electron-deficient ligands such as **14** can again increase the contribution of the electrostatic or chelation transition state, but in this case, lower enantioselectivities are typically observed. The experiments performed on the α -benzoyloxy substrates and the *N*-benzoyl lactam substrates may demonstrate two important and opposing perturbations of the standard transition state for the asymmetric Tsuji allylation with the PHOX ligand system. Taken together, this preliminary model provides useful guidelines for planning asymmetric palladium-catalyzed alkylation reactions with vicinal heteroatoms that are capable of interaction. Future experiments and computational studies will seek to clarify the nature of this unexpected interaction.

Scheme A10.14. Interacting Substrate Types and Possible Transition States



A10.3 CONCLUSION

Recent efforts toward the development of a palladium-catalyzed asymmetric alkylation reaction for α -oxygenated cyclic ketone substrates with the PHOX ligand system has implicated a secondary interaction which appears to be detrimental to asymmetric induction. Employing more electron-deficient ligands leads to even poorer enantioselectivities. This trend held across several substrates examined. Exploration of other cyclic frameworks and *N*-donating groups is underway.

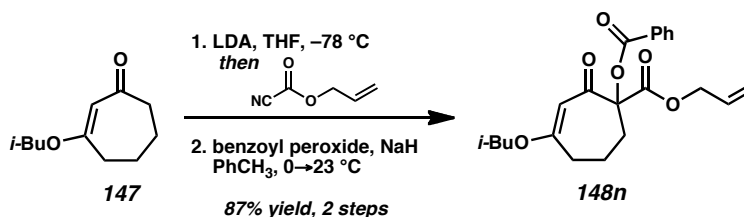
These results are more meaningful when considered in conjunction with the findings from palladium-catalyzed enantioselective alkylation reactions on lactam substrates bearing an *N*-benzoyl group, which suggest that a similar secondary interaction from a different position in the substrate facilitates high asymmetric induction. Overall, these experiments help form a preliminary model that can assist in the planning of reactions with substrates containing functionality that can interact with our Pd(II)·PHOX catalyst system. Understanding this unexpected interaction will be essential in our efforts to develop a method for the asymmetric alkylation of 1,2-enediol-type substrates to obtain valuable chiral α -oxygenated ketone products.

A10.4 EXPERIMENTAL SECTION

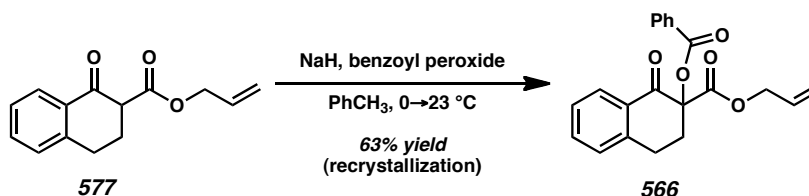
A10.4.1 MATERIALS AND METHODS

Unless otherwise stated, reactions were performed in flame-dried glassware under an argon or nitrogen atmosphere using dry, deoxygenated solvents. Reaction progress was monitored by thin-layer chromatography (TLC). Solvents were dried by passage through an activated alumina column¹⁹ under argon. Diisopropylamine was distilled over CaH_2 prior to use. NaH (60% wt. dispersion in mineral oil) from Sigma-Aldrich was purified by trituration with hexanes under a N_2 atmosphere and removal of residual solvent under vacuum. α -Tetralone was distilled before use. Brine solutions are saturated aqueous solutions of sodium chloride. Benzoyl peroxide (reagent grade, $\geq 98\%$, Luperox A98, catalog #179881) was purchased from Sigma-Aldrich. All other reagents were purchased from Sigma-Aldrich and used as received unless otherwise stated. Allyl cyanofornate was prepared according to the method of Mander^{20a} or Rattigan.^{20b} Phosphinooxazoline (PHOX) ligands **13** ((*S*)-*t*-Bu-PHOX),¹³ **14** ((*S*)-*p*-(CF_3)₃-*t*-Bu-PHOX),¹⁶ and **570** ((*S*)-PCy₂-*t*-Bu-PHOX)^{13b} were prepared by methods described in our previous work. Tris(4,4'-methoxydibenzylideneacetone)dipalladium(0) ($\text{Pd}_2(\text{pmdba})_3$) was prepared according to the method of Ibers^{21a} or Fairlamb.^{21b} Reaction temperatures were controlled by an IKAmag temperature modulator. Glove box manipulations were performed under a N_2 atmosphere. TLC was performed using E. Merck silica gel 60 F254 precoated glass plates (0.25 mm) and visualized by UV fluorescence quenching, *p*-anisaldehyde or KMnO_4 staining. Silicycle SiliaFlash P60 Academic Silica gel (particle size 0.040–0.063 mm) was used for flash chromatography. Automated flash column chromatography was

performed on a Teledyne Isco CombiFlash R_f system. ^1H NMR spectra were recorded on a Varian Mercury 300 MHz spectrometer (at 300 MHz) and are reported relative to residual CHCl_3 (δ 7.26 ppm). ^{13}C spectra were recorded on a Varian Mercury 300 MHz (at 75 MHz) and are reported relative to CHCl_3 (δ 77.16 ppm). Data for ^1H NMR are reported as follows: chemical shift (δ ppm) (multiplicity, coupling constant (Hz), integration). Multiplicities are reported as follows: s = singlet, d = doublet, t = triplet, q = quartet, m = multiplet, br s = broad singlet, app = apparent. Data for ^{13}C NMR are reported in terms of chemical shifts (δ ppm). IR spectra were obtained by use of a Perkin Elmer Spectrum BXII spectrometer using thin films deposited on NaCl plates and reported in frequency of absorption (cm^{-1}). High-resolution mass spectra (HRMS) were obtained from the Caltech Mass Spectral Facility or on an Agilent 6200 Series TOF with an Agilent G1978A Multimode source in electrospray ionization (ESI+), atmospheric pressure chemical ionization (APCI+), or mixed (MM: ESI-APCI+) ionization mode.

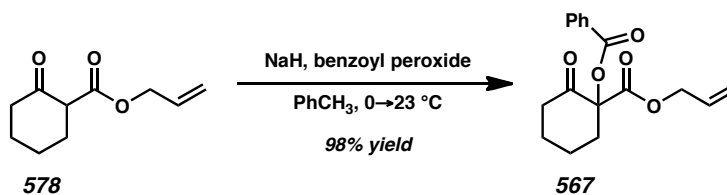
A10.4.2 PREPARATIVE PROCEDURES**A10.4.2.1 α -BENZOYLOXY β -KETOESTER SUBSTRATE SYNTHESIS**

α -Benzoyloxy β -Ketoester 148n. Compound was prepared according to previously described procedures in Chapter 2.^{12b} For experimental procedure and characterization data, see Chapter 2.



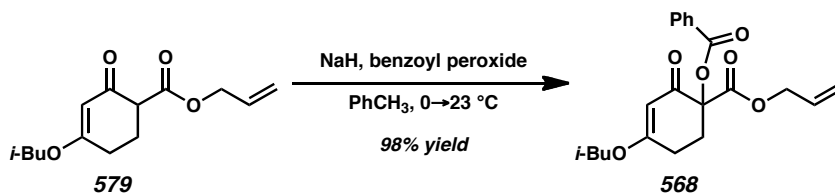
α -Benzoyloxy β -Ketoester 566. β -Ketoester **577**³ (4.0 g, 17.36 mmol, 1.00 equiv) in a 250 mL round-bottom flask under N_2 was dissolved in toluene (96 mL) and cooled to $0\text{ }^{\circ}\text{C}$ using an ice/water bath. NaH (624 mg, 26.04 mmol, 1.50 equiv) was added slowly and the reaction progressed to a pale yellow slurry. After 10 min of stirring at $0\text{ }^{\circ}\text{C}$, benzoyl peroxide (4.64 g, 19.10 mmol, 1.10 equiv) was added portionwise, giving the reaction a deeper yellow color. The reaction was stirred allowed to warm to ambient temperature slowly as the cooling bath expired. After 10 h of stirring, the reaction was quenched with H_2O (30 mL) and the layers were separated. The organic layer was washed with brine (2 x 20 mL). The combined aqueous layers were extracted with EtOAc (2 x 50 mL). The combined organics were dried over Na_2SO_4 , filtered, and

concentrated under reduced pressure. The residue was purified by automated flash column chromatography using Teledyne Isco CombiFlash R_f (SiO₂, 32 g loading cartridge, 330 g column, multi-step gradient, hold 0% [1 min]→ramp to 10% [9 min]→hold 10% [12 min]→ramp to 20% [1 min]→hold 100% EtOAc in hexanes [12 min]). The sample was further purified by recrystallization from refluxing Et₂O. β -Ketoester **566** (3.82 g, 10.90 mmol, 63% yield) was obtained as white needles; R_f = 0.17 (10:1 hexanes:EtOAc); ¹H NMR (300 MHz, CDCl₃) δ 8.13–8.01 (m, 3H), 7.63–7.48 (m, 2H), 7.48–7.40 (m, 2H), 7.37 (br t, *J* = 7.6, 1H), 7.26 (d, *J* = 7.4, 1H), 5.82 (dddd, *J* = 17.4, 10.2, 5.6, 5.6 Hz, 1H), 5.21–5.09 (m, 2H), 4.76 (dddd, *J* = 13.3, 5.6, 1.5, 1.5 Hz, 1H), 4.68 (dddd, *J* = 13.4, 5.6, 1.5, 1.5 Hz, 1H), 3.16–3.05 (m, 2H), 2.97–2.85 (m, 1H), 2.85–2.74 (m, 1H); ¹³C NMR (75 MHz, CDCl₃) δ 189.5, 167.8, 165.3, 142.4, 134.0, 133.6, 132.0, 131.2, 130.2, 129.3, 128.7, 128.6, 128.5, 128.5, 127.3, 118.7, 83.3, 66.6, 31.9, 25.8; IR (Neat Film NaCl) 3068, 2931, 1736, 1702, 1602, 1485, 1452, 1352, 1335, 1304, 1279, 1224, 1179, 1160, 1122, 1104, 1082, 1025, 995, 972, 944, 917, 848, 803, 767, 734, 710 cm⁻¹; HRMS (MM: ESI-APCI+) *m/z* calc'd for C₂₁H₁₈O₅ [M+H]⁺: 351.1227; found 351.1227.



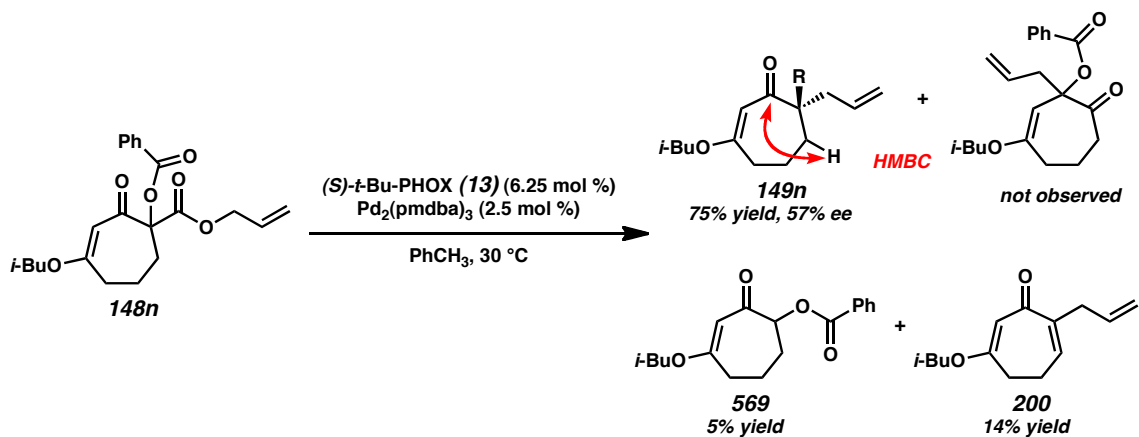
α -Benzoyloxy β -Ketoester 567. β -Ketoester **578**³ (1.00 g, 5.49 mmol, 1.00 equiv) in a 250 mL round-bottom flask under N₂ was dissolved in toluene (55 mL) and cooled to 0 °C using an ice/water bath and stirred for 10 min. NaH (198 mg, 8.23 mmol, 1.50 equiv)

was added and the reaction stirred at 0 °C for 10 min. Benzoyl peroxide (1.46 g, 6.04 mmol, 1.10 equiv) was added slowly portionwise. After 5 min of stirring, the reaction was quenched with H₂O (25 mL) and the layers were separated. The organic layer was washed with brine (15 mL). The combined aqueous layers were extracted with EtOAc (3 x 25 mL). The combined organics were dried over Na₂SO₄, filtered, and concentrated under reduced pressure. The crude product was purified by flash column chromatography (SiO₂, 5 x 25 cm, 10:1→4:1 hexanes:EtOAc) to afford α -benzoyloxy vinylogous ester **567** (1.47 g, 4.87 mmol, 89% yield) as a pale yellow oil; R_f = 0.43 (4:1 hexanes:EtOAc); ¹H NMR (300 MHz, CDCl₃) δ 8.12–8.02 (m, 2H), 7.64–7.54 (m, 1H), 7.50–7.40 (m, 2H), 5.90 (ddt, J = 17.2, 10.4, 5.8, 5.8 Hz, 1H), 5.32 (app dq, J = 17.2, 1.5 Hz, 1H), 5.22 (app dq, J = 10.4, 1.3 Hz, 1H), 4.72 (dt, J = 5.8, 1.4 Hz, 2H), 3.06–2.88 (m, 1H), 2.78–2.64 (m, 1H), 2.64–2.50 (m, 1H), 2.43–2.30 (m, 1H), 2.12–1.67 (m, 4H); ¹³C NMR (75 MHz, CDCl₃) δ 201.4, 167.8, 165.1, 133.6, 131.5, 130.1, 129.2, 128.5, 119.0, 85.91, 66.6, 40.4, 36.5, 27.5, 21.1; IR (Neat Film NaCl) 3067, 2946, 2868, 1730, 1724, 1601, 1451, 1426, 1314, 1278, 1248, 1221, 1178, 1145, 1110, 1096, 1071, 1052, 1025, 988, 957, 939, 911, 861, 842, 802, 780, 746, 710 cm⁻¹; HRMS (MM: ESI-APCI+) m/z calc'd for C₁₇H₁₉O₅ [M+H]⁺: 303.1227; found 303.1221.

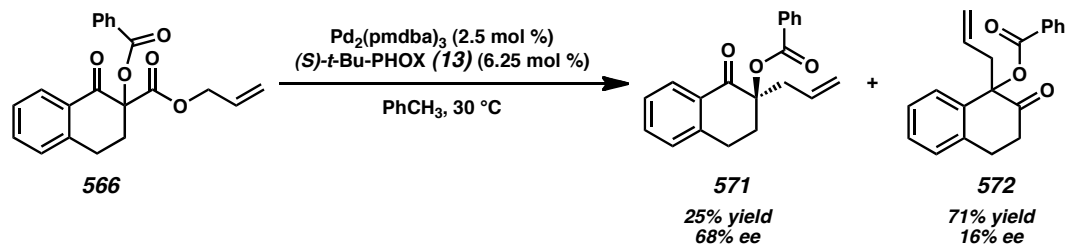


α -Benzoyloxy β -Ketoester 568. β -Ketoester **579**^{12a} (346 mg, 1.37 mmol, 1.00 equiv) in a 20 mL scintillation vial under Ar was dissolved in toluene (7 mL) and cooled to 0 °C

using an ice/water bath. NaH (49 mg, 2.06 mmol, 1.50 equiv) was added and the reaction stirred at 0 °C for 10 min. Benzoyl peroxide (365 mg, 1.51 mmol, 1.10 equiv) was added slowly portionwise. The mixture became thick and difficult to stir. Additional toluene (2 mL) was added and the reaction was shaken until homogeneous and allowed to warm to ambient temperature. The reaction became a yellow-orange slurry. After 10 min of stirring, the reaction was quenched with H₂O (5 mL) and the layers were separated. The organic layer was washed with brine (5 mL). The combined aqueous layers were extracted with EtOAc (3 x 10 mL). The combined organics were dried over Na₂SO₄, filtered, and concentrated under reduced pressure. The crude product was purified by flash column chromatography (SiO₂, 5 x 20 cm, 10:1→4:1→2:1 hexanes:EtOAc) to afford α -benzoyloxy vinylogous ester **568** (501 mg, 1.34 mmol, 98% yield) as a pale yellow oil; R_f = 0.31 (4:1 hexanes:EtOAc); ¹H NMR (300 MHz, CDCl₃) δ 8.11–8.01 (m, 2H), 7.64–7.50 (m, 1H), 7.48–7.38 (m, 2H), 5.89 (dddd, J = 17.2, 10.4, 5.6, 5.6 Hz, 1H), 5.49 (s, 1H), 5.31 (app dq, J = 17.2, 1.5 Hz, 1H), 5.21 (app dq, J = 10.5, 1.3 Hz, 1H), 4.72 (br dt, J = 5.6, 1.5 Hz, 2H), 3.65 (d, J = 6.5 Hz, 2H), 2.86–2.66 (m, 2H), 2.63–2.42 (m, 1H), 2.03 (sept, J = 6.7 Hz, 1H), 0.98 (d, J = 6.7 Hz, 7H); ¹³C NMR (75 MHz, CDCl₃) δ 188.9, 177.5, 167.6, 165.3, 133.6, 131.5, 130.2, 129.5, 128.5, 118.8, 101.2, 82.1, 75.5, 66.6, 28.8, 27.8, 26.5, 19.1; IR (Neat Film NaCl) 3072, 2961, 2932, 2875, 1742, 1738, 1732, 1677, 1674, 1605, 1471, 1451, 1425, 1408, 1386, 1370, 1345, 1316, 1283, 1253, 1199, 1178, 1114, 1073, 1025, 1017, 986, 925, 827, 803, 784, 762, 710 cm⁻¹; HRMS (MM: ESI-APCI+) m/z calc'd for C₂₁H₂₅O₆ [M+H]⁺: 373.1646; found 373.1644.

A10.4.2.2 Pd-CATALYZED DECARBOXYLATIVE ALKYLATION REACTIONS

α -Benzoyloxymethyl Ketone 149n. Reactions with alternative solvents or ligands were conducted in an analogous manner. $\text{Pd}_2(\text{pmdba})_3$ (62.8 mg, 0.057 mmol, 2.5 mol %) and (S) -*t*-Bu-PHOX (**13**) (55.5 mg, 0.143 mmol, 6.25 mol %) were placed in a 250 mL round-bottom flask. The flask was evacuated/backfilled with N_2 (3 cycles, 10 min evacuation per cycle). Toluene (18 mL, sparged with N_2 for 1 h immediately before use) was added and the deep maroon suspension was immersed in an oil bath preheated to 30 °C. After 30 min of stirring, β -ketoester **148n** (885 mg, 2.29 mmol, 1.00 equiv) was added as a solution in toluene (4.9 mL, sparged with N_2 immediately before use) using positive pressure cannulation. The dark orange catalyst solution turned olive green immediately upon addition of β -ketoester **148n**. The reaction was stirred at 30 °C for 19.5 h, allowed to cool to ambient temperature, concentrated under reduced pressure. The crude oil was purified by flash column chromatography (SiO_2 , 5 x 13 cm, 20:1 \rightarrow 15:1 \rightarrow 10:1 \rightarrow 6:1 hexanes:EtOAc) to afford vinylogous ester **149n** (589.8 mg, 1.72 mmol, 75% yield) as a pale yellow oil. For characterization data, see Chapter 2.



α -Benzoyloxy Ketone 571 and α -Benzoyloxy Ketone 572. A 20 mL scintillation vial was loaded with β -ketoester **566** (61.2 mg, 0.175 mmol, 1.00 equiv). A separate 20 mL scintillation vial was loaded with $\text{Pd}_2(\text{pmdba})_3$ (4.7 mg, 0.044 mmol, 2.5 mol %), (S) -*t*-Bu-PHOX (**13**) (4.3 mg, 0.011 mmol, 6.25 mol %), and magnetic stir bar. The two vials and a teflon-lined hard cap were evacuated/backfilled with N_2 in a glove box antechamber (3 cycles, 5 min evacuation per cycle) before being transferred into the glove box. Toluene (1 mL) was added to the vial containing $\text{Pd}_2(\text{pmdba})_3$ and (S) -*t*-Bu-PHOX (**13**). The vial was capped and heated to 30 °C for 30 min. During this time, the mixture developed a dark orange color. β -Ketoester **566** was dissolved in toluene (1 mL) and added to the catalyst solution dropwise, causing the solution to turn olive green. The solution was stirred at 30 °C in a heating block. The capped vial was removed from the glove box after 18.5 h of stirring. The reaction was concentrated under reduced pressure and purified by flash column chromatography (SiO_2 , 2 x 25 cm, 10:1 \rightarrow 4:1 hexanes: Et_2OAc) to afford α -benzoyloxy ketone **571** (13.6 mg, 0.796 mmol, 25% yield) as a clear oil and α -benzoyloxy ketone **572** (38.3 mg, 0.125 mmol, 71% yield) as a white solid.

α -Benzoyloxy Ketone 571: R_f = 0.53 (4:1 hexanes: Et_2O); ^1H NMR (300 MHz, CDCl_3) δ 8.14 (dd, J = 7.9, 1.5 Hz, 1H), 8.08–7.99 (m, 2H), 7.61–7.48 (m, 2H), 7.47–7.40 (m,

2H), 7.36 (br t, $J = 7.6$ Hz, 1H), 7.26 (d, $J = 7.7$ Hz, 1H), 6.23–5.99 (m, 1H), 5.34–5.21 (m, 2H), 3.23–2.95 (m, 3H), 2.85–2.65 (m, 2H), 2.39–2.23 (m, 1H); ^{13}C NMR (75 MHz, CDCl_3) δ 194.1, 165.1, 142.3, 133.9, 133.2, 132.0, 131.5, 130.4, 130.0, 128.8, 128.7, 128.5, 127.2, 119.8, 83.0, 38.7, 30.0, 26.6; IR (Neat Film NaCl) 3068, 2929, 1718, 1692, 1602, 1584, 1450, 1328, 1314, 1285, 1261, 1239, 1221, 1208, 1176, 1157, 1112, 1070, 1026, 992, 935, 918, 866, 841, 785, 739, 710 cm^{-1} ; HRMS (MM: ESI-APCI+) m/z calc'd for $\text{C}_{21}\text{H}_{18}\text{O}_3$ $[\text{M}+\text{H}]^+$: 307.1329; found 307.1332; $[\alpha]_{\text{D}}^{25.0} +10.83$ (c 1.32, CHCl_3 , 68.1% ee); HPLC conditions: 2.0% EtOH in hexanes, 1.0 mL/min, OD-H column, t_{R} (min): major = 9.35, minor = 10.49.

α -Benzoyloxy Ketone 572: $R_{\text{f}} = 0.43$ (4:1 hexanes:Et₂O); ^1H NMR (300 MHz, CDCl_3) δ 8.09–8.00 (m, 2H), 7.63–7.52 (m, 1H), 7.49–7.39 (m, 2H), 7.32 (br dt, $J = 6.5, 1.6$ Hz, 1H), 7.28–7.15 (m, 3H), 5.67 (dddd, $J = 16.6, 10.6, 7.3, 7.3$ Hz, 1H), 5.18–5.04 (m, 2H), 3.34–3.09 (m, 2H), 3.05–2.92 (m, 1H), 2.87 (dt, $J = 7.3, 1.2$ Hz, 2H), 2.79 (ddd, $J = 16.2, 6.7, 5.8$ Hz, 1H); ^{13}C NMR (75 MHz, CDCl_3) δ 206.6, 164.9, 137.5, 135.7, 133.5, 130.9, 130.0, 129.7, 128.5, 128.2, 128.1, 127.2, 125.3, 120.2, 82.0, 44.3, 37.7, 28.0; IR (Neat Film NaCl) 3078, 2915, 1717, 1641, 1601, 1584, 1490, 1451, 1349, 1316, 1278, 1175, 1107, 1096, 1070, 1026, 989, 975, 923, 869, 764, 744, 711 cm^{-1} ; HRMS (EI+) m/z calc'd for $\text{C}_{20}\text{H}_{18}\text{O}_3$ $[\text{M}]^+$: 306.1256; found 306.1243; $[\alpha]_{\text{D}}^{25.0} +15.68$ (c 0.44, CHCl_3 , 15.5% ee); HPLC conditions: 1.0% EtOH in hexanes, 1.0 mL/min, OD-H column, t_{R} (min): major = 12.42, minor = 14.53.

A10.5 NOTES AND REFERENCES

- (1) (a) Wang, Z.-X.; Tu, Y.; Frohn, M.; Zhang, J.-R.; Shi, Y. *J. Am. Chem. Soc.* **1997**, *119*, 11224–11235. (b) Zhu, Y.; Tu, Y.; Yu, H.; Shi, Y. *Tetrahedron Lett.* **1998**, *39*, 7819–7822. (c) Zhu, Y.; Manske, K. J.; Shi, Y. *J. Am. Chem. Soc.* **1999**, *121*, 4080–4081.
- (2) Silyl enol ether and enol carbonate substrates: Behenna, D. C.; Stoltz, B. M. *J. Am. Chem. Soc.* **2004**, *126*, 15044–15045.
- (3) β -Ketoester substrates: Mohr, J. T.; Behenna, D. C.; Harned, A. M.; Stoltz, B. M. *Angew. Chem. Int. Ed.* **2005**, *44*, 6924–6927.
- (4) Full paper: Behenna, D. C.; Mohr, J. T.; Sherden, N. H.; Marinescu, S. C.; Harned, A. M.; Tani, K.; Seto, M.; Ma, S.; Novák, Z.; Krout, M. R.; McFadden, R. M.; Roizen, J. L.; Enquist, Jr., J. A.; White, D. E.; Levine, S. R.; Petrova, K. V.; Iwashita, A.; Virgil, S. C.; Stoltz, B. M. *Chem. Eur. J.* **2011**, *17*, 14199–14223.
- (5) (a) Trost, B. M.; Xu, J. *J. Am. Chem. Soc.* **2005**, *127*, 17180–17181. (b) Trost, B. M.; Xu, J. *J. Am. Chem. Soc.* **2005**, *127*, 2846–2847. (c) Trost, B. M.; Xu, J.; Schmidt, T. *J. Am. Chem. Soc.* **2009**, *131*, 18343–18357.
- (6) For early reports of chiral phosphinooxazoline (PHOX) ligands, see: (a) von Matt, P.; Pfaltz, A. *Angew. Chem. Int. Ed. Engl.* **1993**, *32*, 566–568. (b) Sprinz, J.; Helmchen, G. *Tetrahedron Lett.* **1993**, *34*, 1769–1772. (c) Dawson, G. J.; Frost, C. G.; Williams, J. M. J.; Coote, S. J. *Tetrahedron Lett.* **1993**, *34*, 3149–3150.

- (7) For an early report of Trost ligands in Pd-catalyzed asymmetric alkylation reactions, see: Trost, B. M.; Van Vranken, D. L.; Bingel, C. *J. Am. Chem. Soc.* **1992**, *114*, 9327–9343.
- (8) (a) Trost, B. M.; Xu, J. Reichle, M. *J. Am. Chem. Soc.* **2008**, *129*, 282–283.
(b) Trost, B. M.; Xu, J. *J. Am. Chem. Soc.* **2008**, *130*, 11852–11853.
- (9) Trost, B. M.; Koller, R.; Schöffner, B. *Angew. Chem. Int. Ed.* **2012**, *51*, 8290–8293.
- (10) Dioxanone substrates: Seto, M.; Roizen, J. L.; Stoltz, B. M. *Angew. Chem. Int. Ed.* **2008**, *47*, 6873–6876.
- (11) For an example of the use of the Symyx Core Module in reaction optimization in our research, see: McDougal, N. T.; Virgil, S. C.; Stoltz, B. M. *Synlett* **2010**, 1712–1716.
- (12) (a) Hong, A. Y.; Krout, M. R.; Jensen, T.; Bennett, N. B.; Harned, A. M.; Stoltz, B. M. *Angew. Chem. Int. Ed.* **2011**, *50*, 2756–2760. (b) Hong, A. Y.; Bennett, N. B.; Krout, M. R.; Jensen, T.; Harned, A. M.; Stoltz, B. M. *Tetrahedron* **2011**, *67*, 10234–10248. (c) Bennett, N. B.; Hong, A. Y.; Harned, A. M.; Stoltz, B. M. *Org. Biomol. Chem.* **2012**, *10*, 56–59.
- (13) For the preparation of (*S*)-*t*-Bu-PHOX (**13**), see: (a) Behenna, D. C.; Stoltz, B. M. *J. Am. Chem. Soc.* **2004**, *126*, 15044–15045. (b) Tani, K.; Behenna, D. C.; McFadden, R. M.; Stoltz, B. M. *Org. Lett.* **2007**, *9*, 2529–2531. (c) Krout, M. R.; Mohr, J. T.; Stoltz, B. M. *Org. Synth.* **2009**, *86*, 181–193.

- (14) For computational studies on our Pd-catalyzed asymmetric alkylation reactions using the PHOX ligand system, see: (a) Keith, J. A.; Behenna, D. C.; Mohr, J. T.; Ma, S.; Marinescu, S. C.; Oxgaard, J.; Stoltz, B. M.; Goddard, III, W. A. *J. Am. Chem. Soc.* **2007**, *129*, 11876–11877. (b) Keith, J. A.; Behenna, D. C.; Sherden, N.; Mohr, J. T.; Ma, S.; Marinescu, S. C.; Nielsen, R. J.; Oxgaard, J.; Stoltz, B. M.; Goddard, III, W. A. *J. Am. Chem. Soc.* **2012**, *134*, 19050–19060.
- (15) Sherden, N. H.; Behenna, D. C.; Virgil, S. C.; Stoltz, B. M. *Angew. Chem. Int. Ed.* **2009**, *48*, 6840–6843.
- (16) For the preparation of electron-deficient PHOX ligand (*S*)-(CF₃)₃-*t*-Bu-PHOX (**14**), see: (a) White, D. E.; Stewart, I. C.; Grubbs, R. H.; Stoltz, B. M. *J. Am. Chem. Soc.* **2008**, *130*, 810–811. (b) McDougal, N. T.; Streuff, J.; Mukherjee, H.; Virgil, S. C.; Stoltz, B. M. *Tetrahedron Lett.* **2010**, *51*, 5550–5554.
- (17) For reported examples of reactions in which electron-deficient PHOX ligand **14** provides increased yield and enantioselectivity, see: (a) Streuff, J.; White, D. E.; Virgil, S. C.; Stoltz, B. M. *Nature Chem.* **2010**, *2*, 192–196. (b) White, D. E.; Stewart, I. C.; Seashore-Ludlow, B. A.; Grubbs, R. H.; Stoltz, B. M. *Tetrahedron* **2010**, *66*, 4668–4686. (c) McDougal, N. T.; Virgil, S. C.; Stoltz, B. M. *Synlett* **2010**, 1712–1716. (d) Mukherjee, H.; McDougal, N. T.; Virgil, S. C.; Stoltz, B. M. *Org. Lett.* **2011**, *13*, 825–827.
- (18) Lactam substrates: Behenna, D. C.; Liu, Y.; Yurino, T.; Kim, J.; White, D. E.; Virgil, S. C.; Stoltz, B. M. *Nature Chem.* **2012**, *4*, 130–133.
- (19) Pangborn, A. B.; Giardello, M. A.; Grubbs, R. H.; Rosen, R. K.; Timmers, F. J. *Organometallics* **1996**, *15*, 1518–1520.

- (20) (a) Mander, L. N.; Sethi, S. P. *Tetrahedron Lett.* **1983**, 24, 5425–5428.
(b) Donnelly, D. M.; Finet, J. P.; Rattigan, B. A. *J. Chem. Soc. Perkin Trans. 1* **1993**, 1729–1735.
- (21) (a) Ukai, T.; Kawazura, H.; Ishii, Y.; Bonnet, J. J.; Ibers, J. A. *J. Organomet. Chem.* **1974**, 65, 253–266. (b) Fairlamb, I. J. S.; Kapdi, A. R.; Lee, A. F. *Org. Lett.* **2004**, 6, 4435–4438.

APPENDIX 11

Pd-Catalyzed Asymmetric Allylic Alkylation of Dienolates:

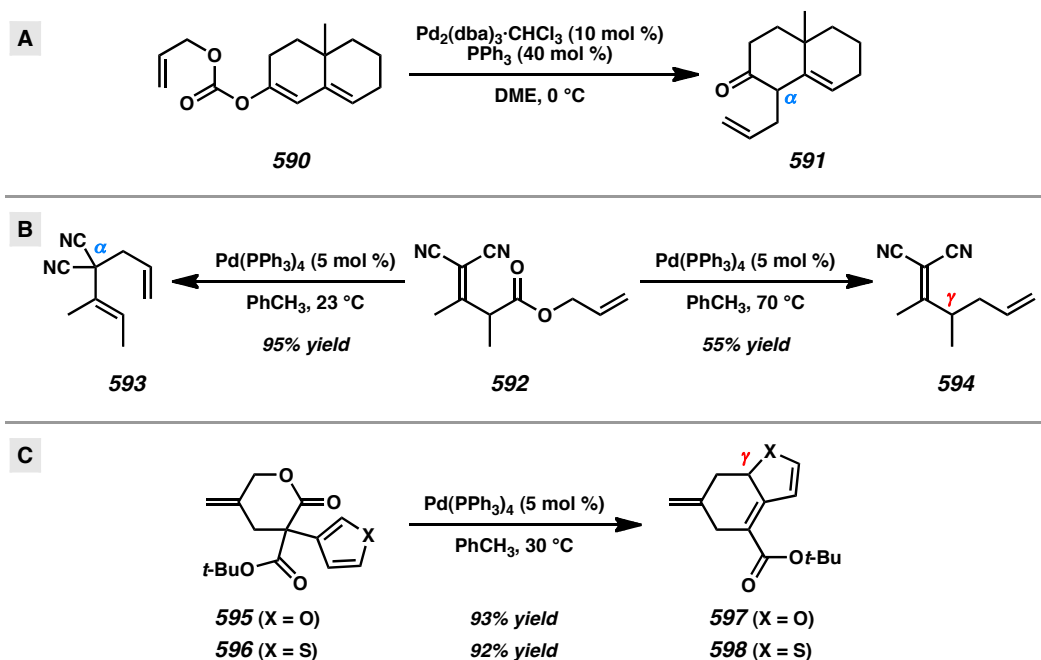
The Synthesis of α - and γ -Quaternary Cyclohexenones[†]

A11.1 INTRODUCTION AND BACKGROUND

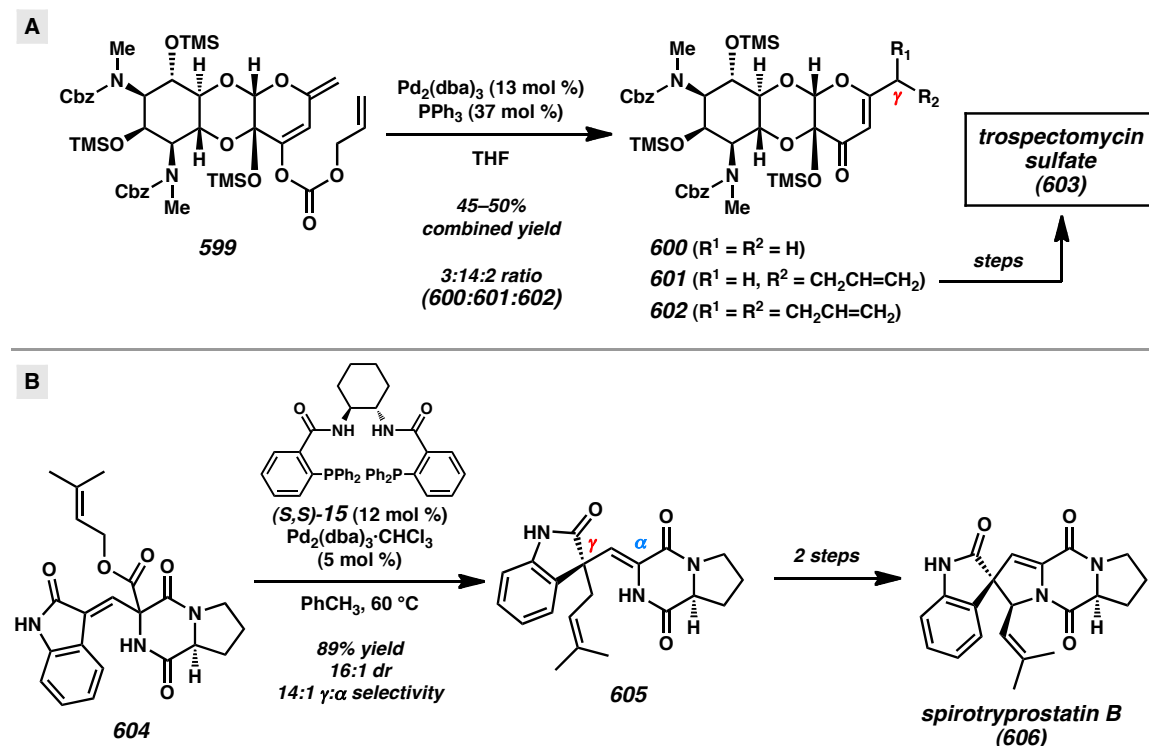
The construction of highly substituted stereocenters that are remote from reactive functional groups is a challenging problem in asymmetric catalysis. Within this context, many research groups have investigated methods for the remote functionalization of dienolates. These intermediates, which possess nucleophilic sites at oxygen, the α -carbon, and the γ -carbon, can be susceptible to numerous reaction pathways. To harness the reactivity of dienolates for useful asymmetric reactions, the dual challenges of regioselectivity and enantioselectivity must be solved. Considering the relatively mild conditions of Pd-catalyzed allylic alkylation reactions,¹ numerous groups have sought to develop regioselective asymmetric reactions for the synthesis of remote stereocenters.

[†] This work was performed in collaboration with Dr. Kristy Tran, a postdoctoral scholar in the Stoltz Group, and Dr. Scott Virgil, the Manager of the Caltech Center for Catalysis and Chemical Synthesis (3CS). Dr. Kristy Tran studied asymmetric alkylation reactions on przewalskin B and nootkastatin 1 synthetic intermediates and contributed to reaction screening efforts. The results in this appendix are unpublished.

In the past few decades, the Pd-catalyzed allylic alkylation of dienolates has been explored with increasing interest. Several studies have provided insight into the preferred reactivity of Pd dienolates (Scheme A11.1). Early studies by Tsuji showed that bicyclic dienol carbonate **590** undergoes selective α -alkylation to non-conjugated enone **591**.² Tunge also observed selective α -alkylation of substrate **592** to give product **593** at ambient temperature, but heating of the reaction mixture led to selective formation of the γ -alkylation product **594** through a Cope rearrangement mechanism.³ While α -alkylation often appears to be kinetically favored, the selective γ -alkylation of Pd dienolates has been observed in some cases. For instance, Hayashi and co-workers have shown that allylic lactones **595** and **596** undergo decarboxylative γ -alkylation by enolate-assisted dearomatization of a furan or thiophene.⁴

Scheme A11.1. Pd-Catalyzed α -Selective and γ -Selective Alkylation of Dienolates

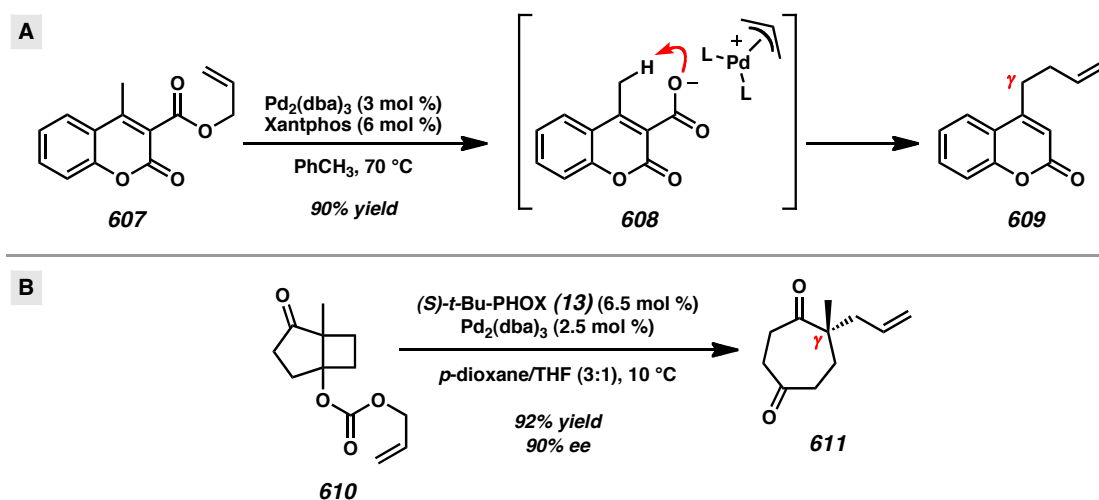
The issue of α -alkylation versus γ -alkylation can arise during the synthesis of complex molecules (Scheme A11.2). In synthetic studies toward the antibiotic trospectomycin sulfate (**603**), Herrinton and co-workers from Upjohn Company showed that γ -alkylation was preferred when allyl enol carbonate **599** was subjected to Tsuji's allylic alkylation conditions.⁵ Under these reaction conditions, no α -alkylation was observed. Aside from the major γ -alkylation product **601**, only protonation product **600** and double alkylation product **602** could be detected. Trost also observed that γ -alkylation was dominant in the diastereoselective prenylation of intermediate **604**.⁶ When chiral ligand **15** was employed, a 14:1 ratio of γ -alkylation: α -alkylation was observed along with excellent dr. These results suggest that the alkylation of an oxindole-derived enolate was preferred over a diketopiperazine-derived enolate. From prenylated oxindole **605**, the total synthesis of the alkaloid spirotryprostatin B (**606**) was completed in two additional steps.

Scheme A11.2. Pd-Catalyzed γ -Selective Alkylation of Dienolates in Total Synthesis

While Pd-catalyzed γ -alkylation reactions have been explored numerous contexts, it is possible to achieve remote functionalization without the intermediacy of Pd-dienolates (Scheme A11.3). To complement palladium dienolate-based reactivity, several research groups have taken advantage of unconventional reactions to achieve efficient γ -alkylation reactions. Tunge has observed unusual reactivity in the allylation of 4-methyl coumarins such as **607**.⁷ The reaction is believed to proceed via initial oxidative addition, carboxylate deprotonation of the vicinal methyl group, and C-alkylation to give the observed product **609**. This reaction proved general for various 4-methyl coumarins. Additionally, Blechert has shown that bicyclic ring systems containing masked cyclobutoxides such as **610** can undergo C–C bond cleavage and asymmetric enolate

alkylation in the presence of catalytic $\text{Pd}_2(\text{dba})_3$ and (*S*)-*t*-Bu-PHOX (**13**).⁸ This reaction leads to chiral 1,4-cycloheptanedione products with quaternary stereocenters.

Scheme A11.3. Pd-Catalyzed γ -Alkylation Reactions



While most of the studies above have focused on the regioselectivity of Pd dienolate alkylation, less attention has been given to enantioselective variants. To our knowledge, a general and broadly applicable method for the enantioselective γ -alkylation of dienolates has not been developed. The Pd-catalyzed decarboxylative asymmetric allylic alkylation reactions pioneered by our group^{9,10,11} and subsequently by the Trost group¹² could provide a suitable starting point for the proposed reaction methodology. While past work in our group has primarily focused on the enantioselective alkylation of carbocyclic^{9,10,11} or heterocyclic enolates^{13,14} as well as asymmetric protonation¹⁵ and enolate alkylation cascade processes,¹⁶ reactions of extended enolates have not been studied in much detail. Thus, we aimed to apply our Pd-PHOX catalyst system to masked dienolate substrates to develop a highly regioselective and enantioselective reaction.

A11.2 ASYMMETRIC Pd-CATALYZED DECARBOXYLATIVE ALKYLATION OF CYCLIC α,β -UNSATURATED δ -KETOESTER SUBSTRATES

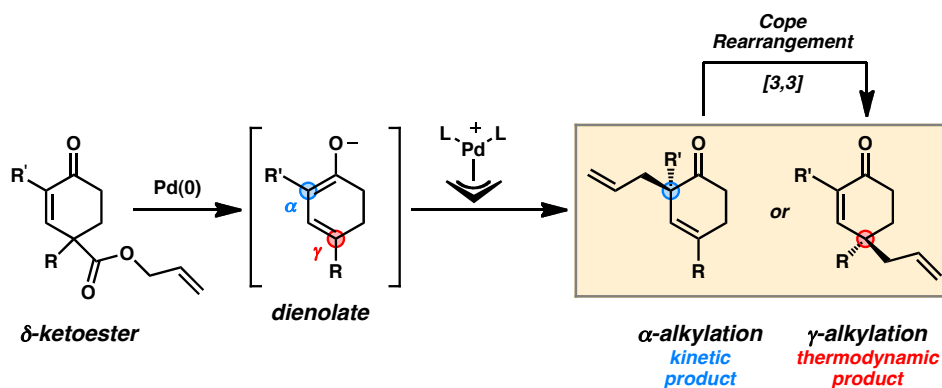
In our efforts to expand the substrate scope of our asymmetric alkylation methodology,^{9,10,11} we became interested in α,β -unsaturated δ -ketoester substrates to see if we could construct chiral ketone building blocks containing remote stereocenters. The development of a new method for this class of masked dienolate substrates would enable divergent access to α - and γ -quaternary ketone products, which could serve as valuable precursors for the synthesis of structurally complex molecules.

A11.2.1 REACTION DESIGN

In the ongoing effort to develop novel strategies for the formation of γ -quaternary stereocenters in cyclic ketone frameworks, we reasoned that δ -ketoesters with a single unit of unsaturation between the ketone and ester moieties could give rise to a dienolate intermediate in the presence of a Pd(0) catalyst after oxidative addition and decarboxylation (Scheme A11.4). The resulting palladium-bound dienolate could undergo asymmetric alkylation at either the α -position or γ -position upon reaction with the chiral Pd π -allyl complex. The γ -alkylated product likely would be the thermodynamic product due to the favorable conjugation of the enone functionality while the α -quaternary ketone likely would be the kinetic product. In the event that α -alkylation is favored by a particular catalyst system, a suprafacial Cope rearrangement could enable conversion of the resulting kinetic product to its thermodynamically favored

γ -quaternary isomer with retention of chiral information. Notably, this pathway would enable divergent access to α - and γ -quaternary cyclic enone products. In the event that γ -alkylation is preferred, the reaction would provide a rare example of the direct γ -alkylation of palladium dienolates. Both outcomes would be desirable and synthetically useful, so we were interested in exploring this reaction with several different types of substrates to achieve high regioselectivity and enantioselectivity.

Scheme A11.4. Asymmetric Alkylation of Dienolates

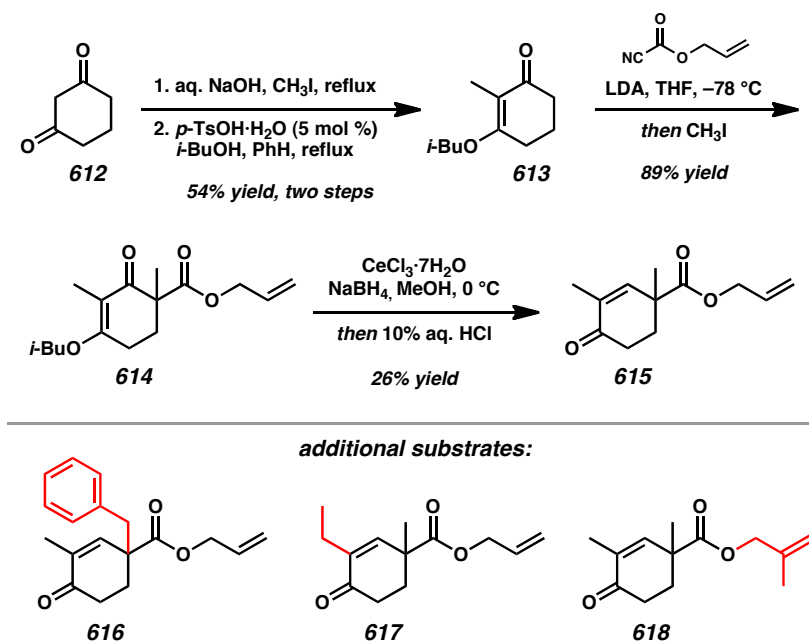


A11.2.2 SYNTHESIS OF α,β -UNSATURATED δ -KETOESTER SUBSTRATES

In order to test our proposed reaction, we targeted a number of δ -ketoester substrates with different substitution patterns. A number of monocyclic substrates were prepared in a short sequence from 1,3-cyclohexanedione (Scheme A11.5). Dione α -alkylation followed by vinylogous ester formation enables the installation of the first substituent. Subsequent acylation with allyl cyanoformate,¹⁷ a second alkylation, and Stork–Danheiser ketone transposition¹⁸ completes the substrate synthesis and provides a second point of substitution. While the ketone transposition step is currently low yielding,

further optimization can improve the efficiency of the transformation. Using this synthetic route, substitution at the α - and γ -positions as well as the allyl group of the δ -ketoester substrates could be modified to give a variety of different substrates. Currently, substrates **615** and **616** have been prepared, but the synthesis of **617** and **618** are ongoing.

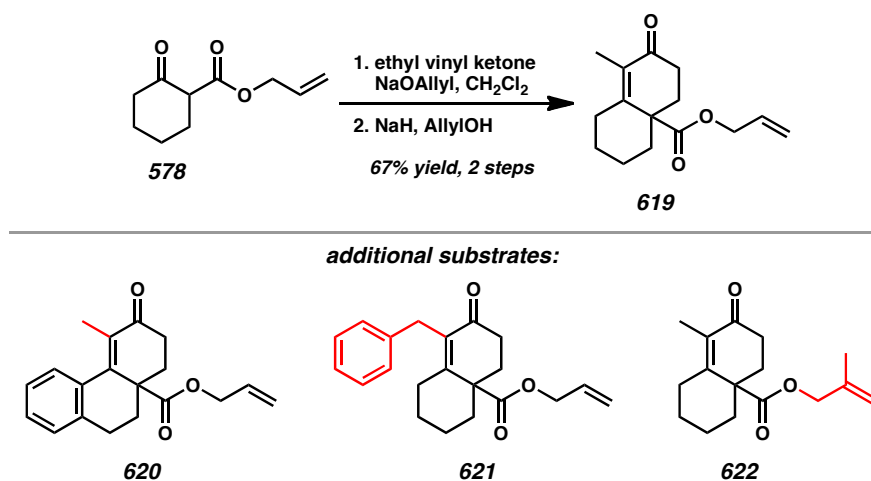
Scheme A11.5. Unoptimized Synthetic Route Toward Monocyclic Substrates



The synthesis of bicyclic substrates proceeded in a straightforward manner from known compounds (Scheme A11.6). Subjection of β -ketoester **578**¹⁰ to a stepwise Robinson annulation with ethyl vinyl ketone enabled the formation of δ -ketoester **619**. Alkylation and cyclization with different alkyl vinyl ketones would enable the synthesis of additional substrates in the bicyclic series. In this manner, substitution at the α -position of the enone and the allyl fragment could be manipulated to give a variety of substitution patterns. The synthesis of substrates **620**, **621**, and **622** is currently in

progress. With a diverse collection of monocyclic and polycyclic substrates, it will be possible to evaluate substrate-based reactivity trends.

Scheme A11.6. Unoptimized Synthetic Route Toward Bicyclic Substrates

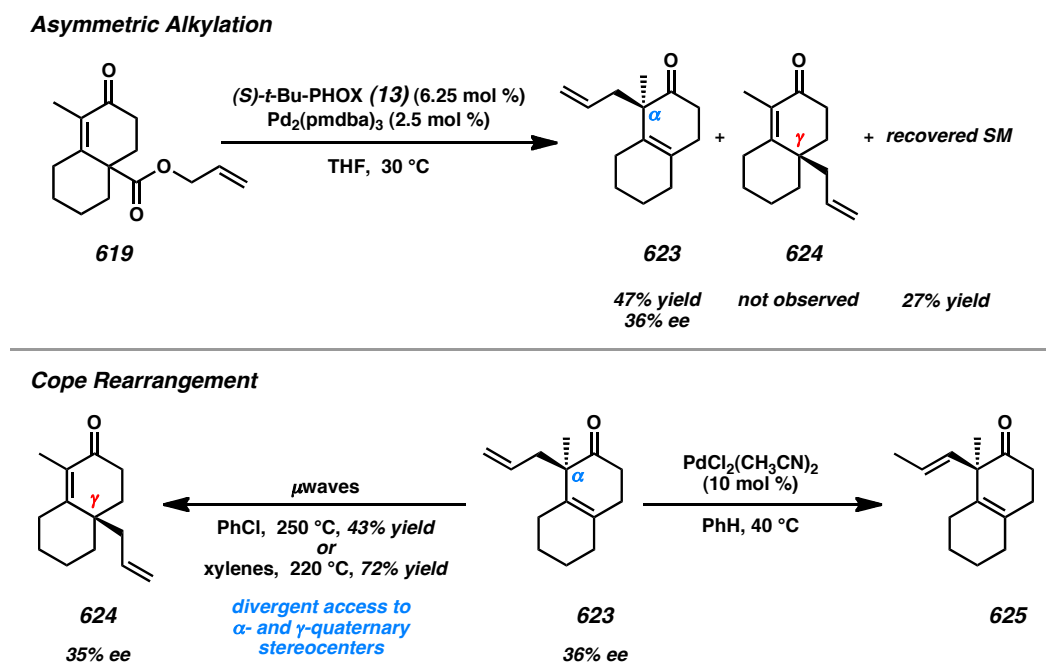


A11.2.3 PRELIMINARY STUDIES AND PROOF OF CONCEPT

With a synthetic route to numerous substrates, we were poised to evaluate asymmetric alkylations with this new α,β -unsaturated δ -ketoester substrate class. For our initial investigations, bicyclic substrate **619** was subjected to our standard reaction conditions^{9,10,11} with catalytic (*S*)-*t*-Bu-PHOX (**13**)¹⁹ and Pd₂(pmdba)₃ in THF at 30 °C (Scheme A11.7). Although the reaction was sluggish, α -alkylation product **623** was isolated in 47% yield and 36% ee along with recovered starting material in 27% yield. While none of the γ -alkylated product was formed in the Pd-catalyzed asymmetric alkylation reaction, microwave irradiation of the α -alkylated bicycle **623** enabled its conversion to the γ -alkylated isomer **624** with retention of enantiomeric excess. So far, attempts to effect the same rearrangement with Pd(II) catalysts such as PdCl₂(NPh)₂

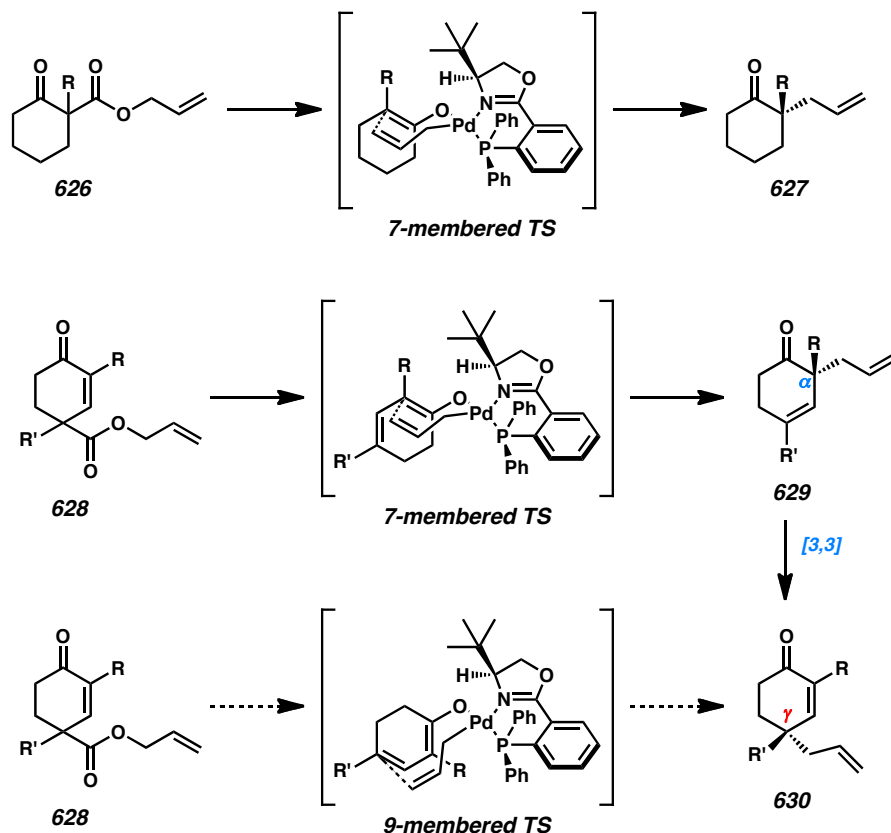
only led to olefin isomerization, but other conditions can be evaluated.²⁰ Taken together, these results provided a promising starting point for further reaction development.

Scheme A11.7. Early Investigation of δ -Ketoester Substrates



In order to rationalize the preference for α -alkylation, we consulted our inner-sphere mechanistic model for our Pd-PHOX ligand system (Scheme A11.8).^{11,21,22} A seven-membered transition state for extended reductive elimination should favor the formation of α -alkylation product by analogy to our typical cyclic ketone enolate-derived substrates. In order to directly access γ -alkylation products through an inner-sphere mechanism, a nine-membered transition state would be required. Since this is highly unlikely, it seems possible that γ -alkylation could alternatively arise by either an initial α -alkylation of a dienolate followed by a thermal or metal-catalyzed Cope-type rearrangement²⁰ or direct γ -alkylation through an outer-sphere mechanism.

Scheme A11.8. Possible Inner-Sphere Transition States for Asymmetric Dienolate Alkylation



With our successful demonstration of the desired reaction design elements, we turned our attention to the optimization of the reaction conditions to improve the yield and enantioselectivity of the unoptimized transformation (Table A11.1, entry 1). Previous optimization efforts on other substrate types have shown that solvent and ligand choice can improve the efficiency and selectivity of asymmetric alkylation reactions. In particular, nonpolar solvents have proven to be effective reaction media. When we performed the Pd-catalyzed asymmetric dienolate alkylation reaction in toluene at elevated temperatures with catalytic (*S*)-*t*-Bu-PHOX (**13**) and $\text{Pd}_2(\text{pmdba})_3$, we observed

complete consumption of starting material. α -Alkylated bicycle **623** was isolated in an improved 82% yield and 66% ee (entry 2).

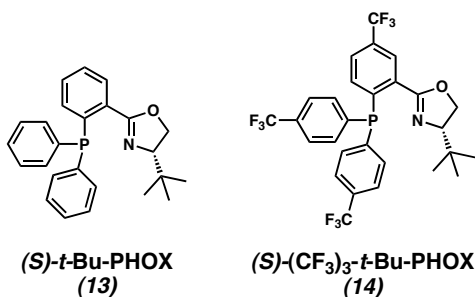
We aimed to improve the reaction further and obtain higher asymmetric induction (Table A11.1). To do this, we sought to employ electron-deficient PHOX ligand **14**,²³ which proved vital for the enantioselective alkylation of challenging substrates.²⁴ Treatment of substrate **619** with electron-deficient PHOX ligand **14** and Pd₂(pmdba)₃ in toluene or a mixture of hexane:toluene (2:1) led to a slight improvement to 74–75% ee, but a decrease in yield was observed (entries 3–4). The reaction did not proceed to full conversion even with prolonged reaction times. Despite this disappointing finding, γ -alkylated product **624** was isolated for the first time in 9–13% yield and 13–14% ee.

Currently, it is unclear whether γ -disubstituted **624** is formed through an inner-sphere or outer-sphere mechanism, but the difference in ee between the α -alkylation product **623** and γ -alkylation product **624** has possible mechanistic implications. Potential Cope-type reactions that may be operative under the reaction conditions are most likely stereospecific. Since the reaction temperatures in these studies (50–65 °C) are significantly lower than the temperatures employed for a thermal rearrangement (220–250 °C) (Scheme A11.7), this pathway is likely not operative. However, metal-catalyzed sigmatropic rearrangements cannot be ruled out at this time. Based on this reasoning, it seems likely that the mechanistic pathways leading to the two alkylation products do not overlap for the key C–C bond-forming event catalyzed by palladium and this fact is reflected in the non-equivalent ee values.

Table A11.1. Further Optimization of Pd-Catalyzed Asymmetric Dienolate Alkylation

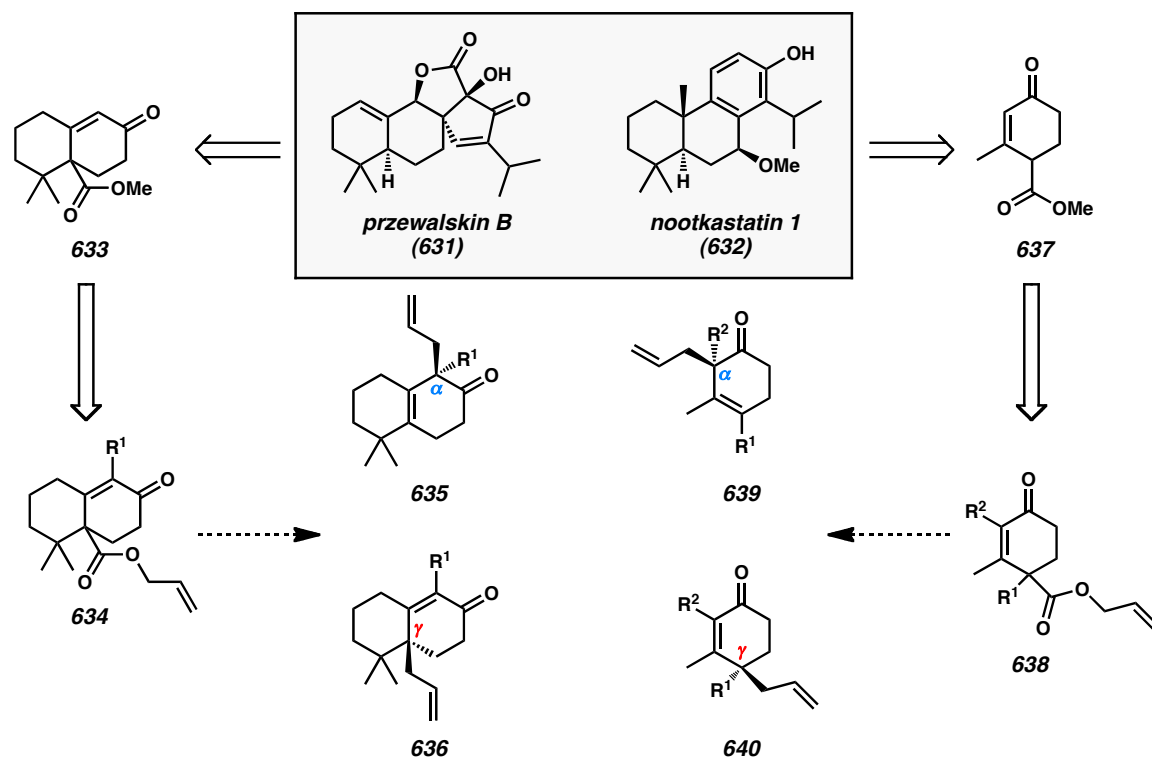
619 $\xrightarrow[\text{solvent, temp}]{\text{ligand (6.25 mol \%)} \quad \text{Pd}_2(\text{pmdba})_3 \text{ (2.5 mol \%)}} 623 + 624 + \text{recovered SM}$

entry	ligand	solvent	temperature	time	α-alkylation	γ-alkylation	recovered 619
1	13	THF	30 °C	80 h	47% yield 36% ee	not observed	27% yield
2	13	PhCH ₃	50→65 °C	50 h	82% yield 66% ee	trace	trace
3	14	PhCH ₃	60 °C	100 h	57% yield 75% ee	9% yield 13% ee	8% yield
4	14	hexane:PhCH ₃ (2:1)	50→65 °C	100 h	49% yield 74% ee	12% yield 14% ee	26% yield



A11.2.4 CONCURRENT INVESTIGATION OF SUBSTRATES INSPIRED BY SYNTHETIC EFFORTS TOWARD PRZEWALSKIN B

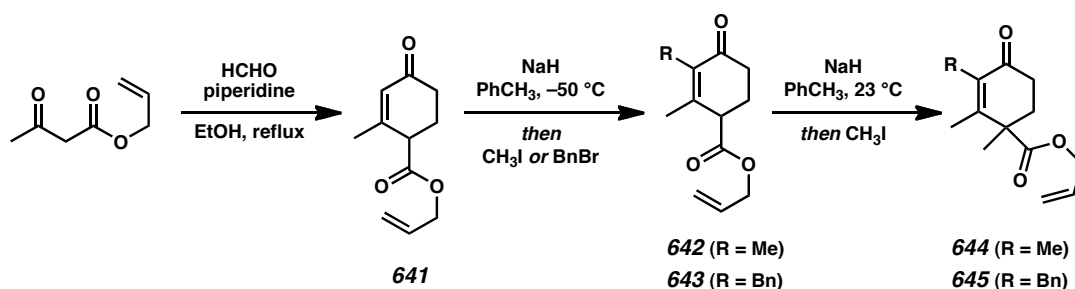
During a synthetic campaign toward the biologically active natural products przewalskin B²⁵ and nootkastatin 1²⁶ by members of our research group, several monocyclic and bicyclic intermediates in the synthetic route prompted evaluation of allyl-containing analogs as Pd-catalyzed asymmetric dienolate alkylation substrates (Scheme A11.9). To this end, we aimed to prepare monocyclic δ-ketoester **638** and bicyclic δ-ketoester **634** by straightforward modification of existing synthetic routes.

Scheme A11.9. δ -Ketoester Substrates Inspired by Przewalskin B and Nootkastatin 1

One synthetic route toward these natural products strategically employed a methyl ester derivative of Hagemann's ester²⁷ (Scheme A11.9). By adapting reported synthetic procedures, allyl acetoacetate could be converted to an allyl-containing analog **641** in the presence of formaldehyde, piperidine, and ethanol under refluxing conditions (Scheme A11.10). In the subsequent regioselective alkylation of the Hagemann's ester derivative **641**, the choice of reaction temperature was essential. When alkylation reactions were initiated at ambient temperature and subsequently heated to reflux, complex mixtures of *C*-alkylation and *O*-alkylation products were observed, but when the reaction was conducted at $-50\text{ }^{\circ}\text{C}$, reactions smoothly proceeded to desired products **642** and **643**.²⁸ A

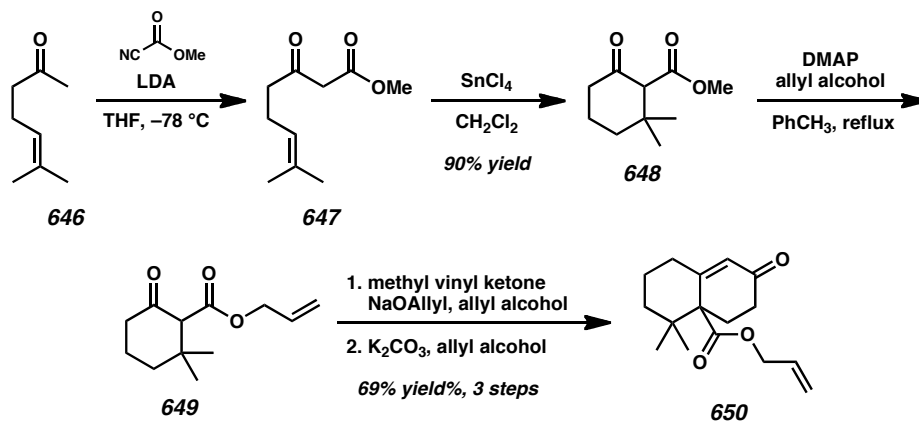
second alkylation, which proceeded at ambient temperature, enabled the formation of α,γ -quaternary substrates **644** and **645**. These sequential alkylations should enable the installation of many combinations of substituents.

Scheme A11.10. Synthesis of Monocyclic Substrates

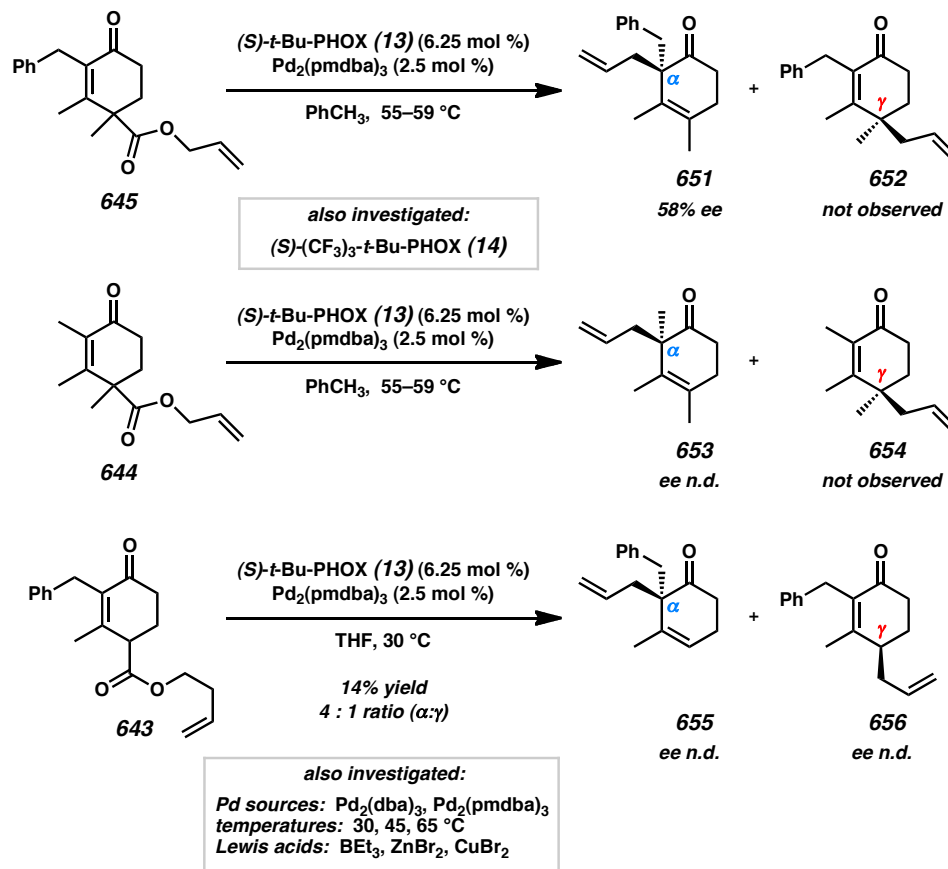


A second synthetic route toward przewalskin B (**631**) and nootkastatin 1 (**632**) targeted bicyclic enone **633** as a key intermediate (Scheme A11.9). The synthesis of allyl derivative **650** proceeded with the acylation of ketone **646** and Sn -mediated cyclization of the resulting β -ketoester **647** (Scheme A11.11). Cyclic β -ketoester **648** could be converted to bicyclic enone **650** through a three-step sequence involving transesterification, conjugate addition, and aldol condensation. By varying the conjugate acceptor, it may be possible to synthesize α -functionalized derivatives of **650**.

Scheme A11.11. Synthesis of Bicyclic Substrates



The δ -ketoester substrates **643**, **644**, and **645** were subjected to our Pd-catalyzed allylic alkylation reaction conditions^{9,10,11} with (*S*)-*t*-Bu-PHOX (**13**) and $\text{Pd}_2(\text{pmdba})_3$ (Scheme A11.12). In contrast to simple β -ketoester substrates, heating was required to promote the reaction. Monocyclic δ -ketoester substrates **645** and **644** containing α -quaternary centers underwent selective α -alkylation of the intermediate dienolate. In contrast, δ -tertiary substrate **643** led to a 4:1 mixture of α -alkylation: δ -alkylation in 14% combined yield along with δ -protonation product. These results indicate the potential importance of nucleophile steric effects on the regioselectivity of the alkylation event. With this substrate, the effect of different Pd sources, temperatures, and Lewis acids were also investigated, but these factors did not significantly perturb the selectivity of the reaction. At this time, alkylation reactions have not been performed on bicyclic substrate **650**.

Scheme A11.12. Asymmetric Alkylation of Additional δ -Ketoester Substrates

While further studies are certainly necessary to render these asymmetric alkylation reactions more efficient and enantioselective, initial studies with these substrates complements the studies performed with simple monocyclic and bicyclic substrates (Section A11.2.3) and these experiments provide the foundation for future investigations. Our preliminary studies have identified a number of variables that can be further tuned to identify improved reaction conditions for the asymmetric alkylation of dienolates. In order to more efficiently evaluate and compare the impact of changing these variables, we turned our attention to a high-throughput screening approach.

A11.3 SYMYX HIGH-THROUGHPUT REACTION SCREENING

Having identified the key variables as solvent, ligand, and temperature, we sought to identify the optimal combination of these reaction components. High-throughput reaction optimization became a key component of our screening efforts and we anticipated that we could quickly identify efficient reaction conditions using the Symyx Core Module at the Caltech Center for Catalysis and Chemical Synthesis (3CS). This approach has previously enabled us to optimize Pd-catalyzed asymmetric alkylation reactions for a number of challenging substrates.^{14,24c}

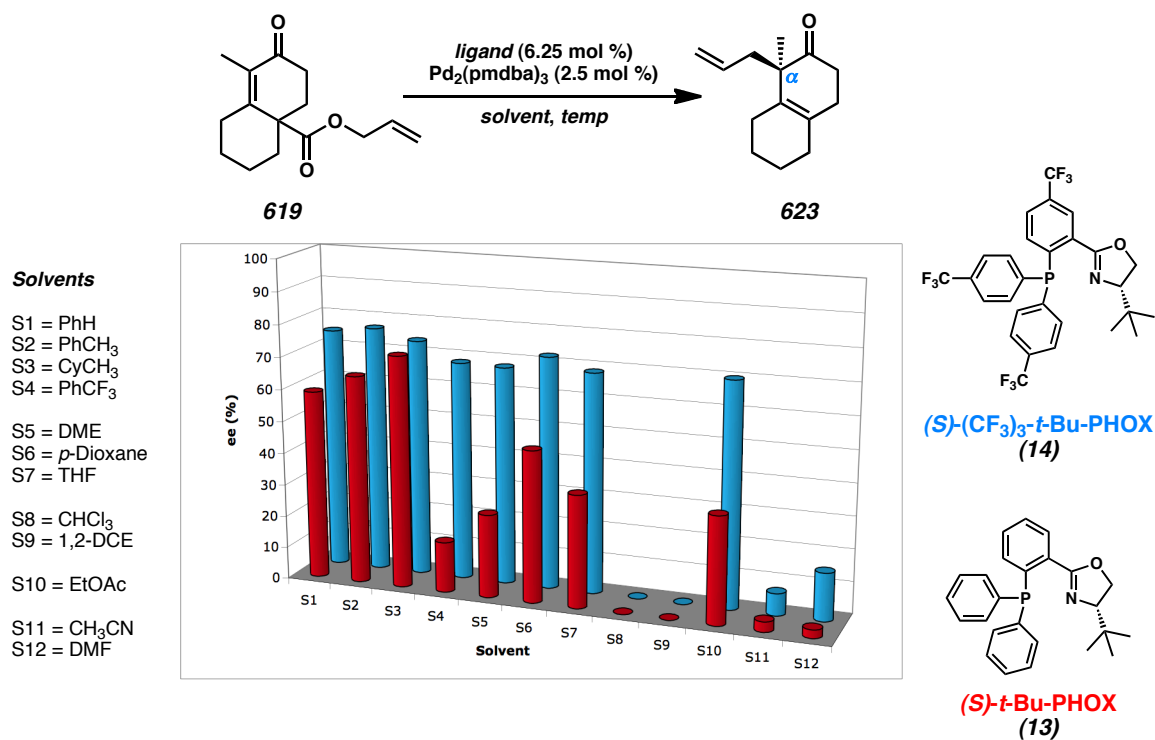
In the design of our initial reaction screen, we investigated two ligands and twelve solvents for the asymmetric alkylation of δ -ketoester **619** (Figure A11.1), we chose a reaction temperature of 60 °C and reaction time of 48 h to allow sufficient time for conversion to product. Our screen allowed us to identify trends for solvent and ligand effects that will guide the design of further reaction screens.

A consistent solvent trend emerged from our reaction screen. Halogenated solvents such as chloroform, 1,2-dichloroethane, and α,α,α -trifluorotoluene resulted in no conversion to product. Polar aprotic solvents such as acetonitrile and DMF provided bicycle **623** with very low asymmetric induction. Etheral solvents such as DME, *p*-dioxane, and THF generally provided product in significantly lower ee. Ester solvents such as ethyl acetate performed similarly. The highest selectivities were observed with aromatic or alkane solvents. In general, the ee of product **623** from asymmetric alkylation reactions with (*S*)-*t*-Bu-PHOX (**13**) appeared to be quite solvent dependent.

The relative performance of (*S*)-*t*-Bu-PHOX (**13**) and its electron-deficient analog **14** became clearer in our reaction screen. Unlike (*S*)-*t*-Bu-PHOX (**13**), asymmetric

alkylation reactions with ligand **14** consistently provided results in the 70–80% ee range for a variety of different solvents. While reactions in polar aprotic solvents and halogenated solvents remained poor, reactions in other solvents performed with consistently good asymmetric induction. Taken together, it appears that the investigation of future reactions should focus on aromatic or alkane solvents and employ electron-deficient PHOX ligands.

Figure A11.1. Symyx Reaction Screening of an Asymmetric Dienolate Alkylation Reaction

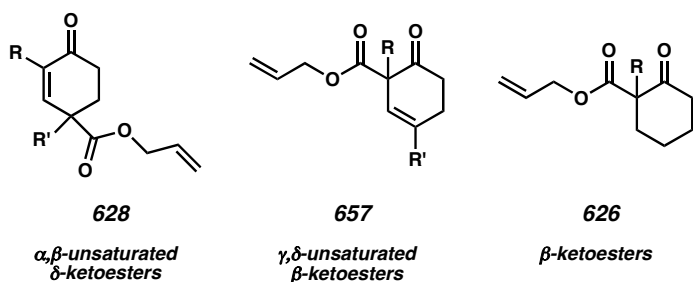


A11.4 FUTURE DIRECTIONS

In future studies, it will be important to investigate a new class of substrates to probe the importance of functional group configuration (Scheme A11.13). The α,β -unsaturated

δ -ketoester substrates investigated previously, such as **628**, have the ester substituent positioned far away from the ketone moiety such that a transition metal is incapable coordinating to both groups at the same time. These substrates react very slowly and only proceed to full conversion with heating. This observation may suggest that pre-chelation of Pd to the substrate, as in the case of simple β -ketoesters **626**, can help direct the initial oxidative addition event. By investigating substrates such as γ,δ -unsaturated β -ketoesters **657** with ketone and ester moieties in close proximity for initial chelation, the importance of this effect on reaction initiation can be evaluated. These studies will help identify the optimal substrate configuration for our desired transformations.

Scheme A11.13. Comparison of Asymmetric Alkylation Substrates



To improve the efficiency of our reaction, it may be possible to effect γ -alkylation in a single reaction by performing the initial Pd-catalyzed alkylation at low temperature and heating the reaction to promote a [3,3]-sigmatropic rearrangement to form the thermodynamic product. Notably, this approach could potentially enable access to both α -quaternary and γ -quaternary stereocenters through the Pd-catalyzed asymmetric alkylation of dienolates.

Furthermore, we plan to conduct further optimizations with regard to ligand, solvent, and temperature for improving the α -alkylation reaction of dienolates. High-throughput reaction screening technology provided by the Caltech Center for Catalysis and Chemical Synthesis (3CS) will be essential in this effort. While our initial screen identified several promising solvents, we have yet to thoroughly evaluate sterically and electronically differentiated ligand sets and different reaction temperatures. It may be advantageous to look beyond PHOX ligands if ee values reach an upper limit. For this purpose, chiral bis-phosphine Trost ligands²⁹ can be evaluated in expanded multivariable reaction screens.

In parallel with these efforts, we also hope to identify milder conditions for the Cope rearrangement to facilitate a stereocontrolled transfer of chiral information from the α -carbon to the γ -carbon of the enone system of our substrates. To achieve this goal, we plan to further investigate metal or Lewis acid catalysts that are capable of promoting the sigmatropic rearrangement to enable access to γ -quaternary ketones.

Additionally, we aim to identify conditions that promote direct γ -alkylation, and we expect that the capabilities of 3CS will be indispensable for this campaign. Our initial experiments with electron-deficient PHOX ligands show that it is possible to increase the contribution of this mechanistic pathway (Table A11.1), but significant work remains for improving both the yield and ee of the transformation.

A11.5 CONCLUSION

In summary, we have conducted preliminary investigations into the Pd-catalyzed decarboxylative asymmetric alkylation of dienolates to access either α - or γ -alkylation products. Our studies have shown that the α -alkylation product is favored, but can be

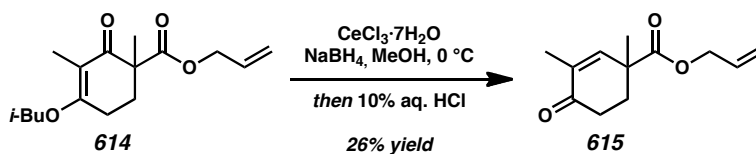
converted to the γ -alkylation product through a Cope rearrangement with retention of stereochemical information. Further modification of the Pd-catalyzed asymmetric alkylation reaction has enabled the identification of conditions that appear to provide minor amounts of γ -alkylation product. High-throughput reaction screening has enabled optimization of the dienolate alkylation reaction to increase yield and ee for the favored α -alkylation product. Further investigation of solvents, ligands, and reaction temperatures, as well as new substrates, will be conducted in the future.

A11.6 EXPERIMENTAL SECTION

A11.6.1 MATERIALS AND METHODS

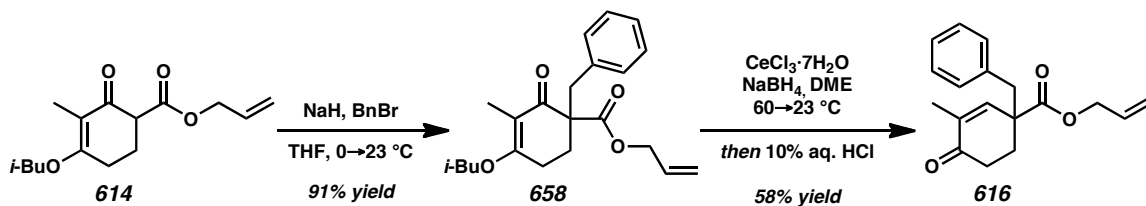
Unless otherwise stated, reactions were performed in flame-dried glassware under an argon or nitrogen atmosphere using dry, deoxygenated solvents. Reaction progress was monitored by thin-layer chromatography (TLC). Solvents were dried by passage through an activated alumina column³⁰ under argon. Diisopropylamine was distilled over CaH₂ prior to use. NaH (60% wt. dispersion in mineral oil) from Sigma-Aldrich was purified by trituration with hexanes under a N₂ atmosphere and removal of residual solvent under vacuum. Brine solutions are saturated aqueous solutions of sodium chloride. All other reagents were purchased from Sigma-Aldrich and used as received unless otherwise stated. Allyl cyanoformate was prepared according to the method of Mander or Rattigan.¹⁷ Phosphinooxazoline (PHOX) ligands **13** ((*S*)-*t*-Bu-PHOX),¹⁹ **14** ((*S*)-*p*-(CF₃)₃-*t*-Bu-PHOX)²³ were prepared by methods described in our previous work. Tris(4,4'-methoxydibenzylideneacetone)dipalladium(0) (Pd₂(pmdba)₃) was prepared according to the method of Ibers^{31a} or Fairlamb.^{31b} Reaction temperatures were controlled by an IKAmag temperature modulator. Microwave-assisted experiments were carried out in sealed reaction vials in a Biotage Initiator 2.5 microwave reactor. Glove box manipulations were performed under a N₂ atmosphere. A customized glove box containing a Symyx Core Module equipped with programmable automated liquid handling, stirring, heating, and cooling capabilities was employed in high-throughput reaction screening. Concentration of liquid samples in multi-well plates was achieved using a Thermo Scientific SPD121P SpeedVac inside a glove box. TLC was performed

using E. Merck silica gel 60 F254 precoated glass plates (0.25 mm) and visualized by UV fluorescence quenching, *p*-anisaldehyde or KMnO₄ staining. Silicycle SiliaFlash P60 Academic Silica gel (particle size 0.040–0.063 mm) was used for flash chromatography. ¹H NMR spectra were recorded on a Varian Mercury 300 MHz or a Varian Inova 500 MHz spectrometer (at 300 MHz) and are reported relative to residual CHCl₃ (δ 7.26 ppm). ¹³C spectra were recorded on a Varian Mercury 300 MHz (at 75 MHz) and are reported relative to CHCl₃ (δ 77.16 ppm). Data for ¹H NMR are reported as follows: chemical shift (δ ppm) (multiplicity, coupling constant (Hz), integration). Multiplicities are reported as follows: s = singlet, d = doublet, t = triplet, q = quartet, m = multiplet, br s = broad singlet, app = apparent. Data for ¹³C NMR are reported in terms of chemical shifts (δ ppm). IR spectra were obtained by use of a Perkin Elmer Spectrum BXII spectrometer using thin films deposited on NaCl plates and reported in frequency of absorption (cm⁻¹). Analytical chiral GC was performed with an Agilent 6850 GC utilizing a G-TA (30 m x 0.25 mm) column (1.0 mL/min carrier gas flow). Optical rotations were measured with a Jasco P-2000 polarimeter operating on the sodium D-line (589 nm) using a 100 mm path length cell and are reported as: [α]_D^T (concentration in g/100 mL, solvent, ee). High-resolution mass spectra (HRMS) were obtained from the Caltech Mass Spectral Facility or on an Agilent 6200 Series TOF with an Agilent G1978A Multimode source in electrospray ionization (ESI+), atmospheric pressure chemical ionization (APCI+), or mixed (MM: ESI-APCI+) ionization mode.

A11.6.2 PREPARATIVE PROCEDURES**A11.6.2.1 δ -KETOESTER SUBSTRATE SYNTHESIS**

δ -Ketoester 615. Compound **614** was prepared according to previously reported procedures.³²

To a 100 mL round-bottom flask with a magnetic stir bar was added MeOH (12 mL) and $\text{CeCl}_3 \cdot 7\text{H}_2\text{O}$ (1.81 g, 4.87 mmol, 1.00 equiv). The clear solution was cooled to 0 °C with an ice/water bath. A solution of β -ketoester (1.37 g, 4.87 mmol, 1.00 equiv) in MeOH (7 mL) was added to the reaction. NaBH_4 (553 mg, 14.61 mmol, 3.00 equiv) was added slowly portionwise, leading to gas evolution. The reaction became an opaque white suspension with a pale yellow tint. After 30 min of stirring at 0 °C, additional $\text{CeCl}_3 \cdot 7\text{H}_2\text{O}$ (0.905 g, 2.435 mmol, 0.5 equiv) and NaBH_4 (277 mg, 7.31 mmol, 1.5 equiv) were added. After an additional 30 min of stirring 0 °C, 10% aqueous HCl (8.31 mL) was added dropwise. The reaction was diluted with CH_2Cl_2 (50 mL). The layers were separated and the organic layer was washed with brine (10 mL). The aqueous layer was extracted with CH_2Cl_2 (3 x 20 mL). The combined organic layers were dried over MgSO_4 , filtered, and concentrated under reduced pressure. The residue was purified by flash column chromatography (SiO_2 , 3 x 25 cm, 4:1 \rightarrow 2:1 \rightarrow 1:1 hexanes:EtOAc) to afford δ -ketoester **615** (291 mg, 1.397 mmol, 29% yield).



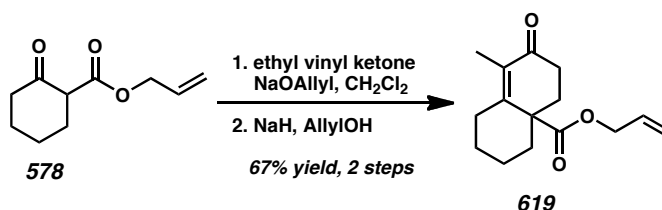
β-Ketoester 658. Compound **614** was prepared according to previously reported procedures.³²

To a 250 mL round-bottom flask with magnetic stir bar was added NaH (181 mg, 7.56 mmol, 1.10 equiv). The flask was evacuated and backfilled with N₂ (3 cycles, 5 min evacuation per cycle). THF (60 mL) was added. The reaction was cooled to 0 °C to give a pale gray suspension. β-Ketoester (1.83 g, 6.87 mmol, 1.00 equiv) in THF (9 mL) was added dropwise, giving a yellow suspension. The reaction was stirred at 0 °C for 30 min and benzyl bromide (898 μL, 7.56 mmol, 1.10 equiv) was added dropwise. After 1.5 h of stirring, the cooling bath was removed and the reaction was allowed to warm to 23 °C. After an additional 1.5 h of stirring, the reaction was quenched with 50% sat. aqueous NH₄Cl (14 mL). The reaction was extracted with Et₂O (3 x 100 mL). The combined organics were dried over MgSO₄, filtered, and concentrated under reduced pressure. The residue was purified by flash column chromatography (SiO₂, 3 x 25 cm, 20:1→10:1→6:1 hexanes:EtOAc) to afford β-ketoester **658** (291 mg, 1.397 mmol, 91% yield) as a clear, colorless oil; *R*_f = 0.50 (10:1 hexanes:EtOAc); ¹H NMR (300 MHz, CDCl₃) δ 7.26–7.17 (m, 3H), 7.17–7.13 (m, 2H), 5.86 (ddt, *J* = 17.2, 10.7, 5.5 Hz, 1H), 5.26 (dq, *J* = 17.2, 1.6 Hz, 1H), 5.20 (dq, *J* = 10.5, 1.3 Hz, 1H), 4.62 (ddt, *J* = 13.5, 5.4, 1.5 Hz, 1H), 4.56 (ddt, *J* = 13.5, 5.5, 1.5 Hz, 1H), 3.73–3.66 (m, 2H), 3.34 (d, *J* = 13.7 Hz, 1H), 3.22 (d, *J* = 13.7 Hz, 1H), 2.74–2.65 (m, 1H), 2.48–2.41 (m, 1H), 2.35 (ddd, *J* = 13.6, 5.4, 3.4 Hz, 1H), 1.95 (app sept, *J* = 6.6 Hz, 1H), 1.81–1.72 (m, 2H), 0.96 (d, *J* = 2.1 Hz, 3H), 0.95 (d, *J* =

2.1 Hz, 3H); ^{13}C NMR (125 MHz, CDCl_3) δ 192.1, 175.9, 168.0, 165.1, 133.6, 131.7, 130.0, 129.6, 128.6, 118.7, 102.2, 88.8, 75.2, 66.6, 33.8, 31.2, 27.9, 21.2, 19.2, 19.2; IR (Neat Film NaCl) 3085, 3063, 3028, 2960, 2931 2875, 2342, 2360, 1729, 1653, 1618, 1596, 1471, 1454, 1424, 1382, 1354, 1327, 1268, 1230, 1210, 1179, 1137, 1096, 1066, 1031, 1005, 981, 934, 872, 818, 785, 744 cm^{-1} ; HRMS (MM: ESI-APCI+) m/z calc'd for $\text{C}_{22}\text{H}_{29}\text{O}_4$ $[\text{M}+\text{H}]^+$: 257.2060; found 257.2047.

δ -Ketoester 616. To a 20 mL scintillation vial with magnetic stir bar was added β -ketoester **658** (60 mg, 0.168 mmol, 1.00 equiv), $\text{CeCl}_3 \cdot 7\text{H}_2\text{O}$ (62.7 mg, 0.168 mmol, 1.00 equiv), and dimethoxyethane (3 mL). The reaction was capped with a teflon-lined hard cap, immersed in a 60 °C heating block, and stirred for 40 min. The finely dispersed suspension was cooled to 23 °C and NaBH_4 (19.0 mg, 0.504 mmol, 3.00 equiv) was added portionwise. The reaction developed a pale yellow tint. After 40 min, the reaction was quenched with 10% aqueous HCl (1 mL). The reaction faded to a clear, colorless biphasic mixture. The reaction was vigorously stirred for 15 min. The mixture was extracted with Et_2O (3 x 10 mL). The combined organics were dried over Na_2SO_4 , filtered, and concentrated under reduced pressure. The residue was purified by flash column chromatography (SiO_2 , 1.5 x 25 cm, 10:1→5:1 hexanes:EtOAc) to afford δ -ketoester **616** (27.6 mg, 0.097 mmol, 58% yield); R_f = 0.51 (4:1 hexanes:EtOAc); ^1H NMR (500 MHz, CDCl_3) δ 7.34–7.22 (m, 3H), 7.15–7.06 (m, 2H), 6.74 (t, J = 1.4 Hz, 1H), 5.86 (ddt, J = 17.2, 10.4, 5.8 Hz, 1H), 5.32–5.22 (m, 2H), 4.59 (q, J = 1.3 Hz, 1H), 4.58 (q, J = 1.3 Hz, 1H), 3.11 (d, J = 13.4 Hz, 1H), 3.05 (d, J = 13.3 Hz, 1H), 2.57–2.42 (m, 2H), 2.37 (dddd, J = 13.1, 6.5, 5.3, 1.3 Hz, 1H), 2.03 (ddd, J = 13.5, 9.9, 5.3 Hz, 1H),

1.82 (d, $J = 1.4$ Hz, 3H); ^{13}C NMR (125 MHz, CDCl_3) δ 198.8, 173.0, 145.6, 135.9, 135.7, 131.7, 130.0, 128.5, 127.3, 118.9, 66.0, 49.4, 45.0, 34.8, 30.7, 16.3; IR (Neat Film NaCl) 3435, 3339, 3087, 3063, 3029, 2953, 2923, 2882, 1730, 1676, 1648, 1604, 1584, 1496, 1448, 1420, 1379, 1364, 1330, 1274, 1260, 1226, 1182, 1157, 1112, 1084, 1064, 1044, 1031, 983, 935, 889, 799, 774, 744, 725, 702 cm^{-1} ; HRMS (FAB+) m/z calc'd for $\text{C}_{18}\text{H}_{21}\text{O}_3$ $[\text{M}+\text{H}]^+$: 285.1491; found 285.1499.



δ -Ketoester 619. Compound **578** was prepared according to previously reported procedures.¹⁰

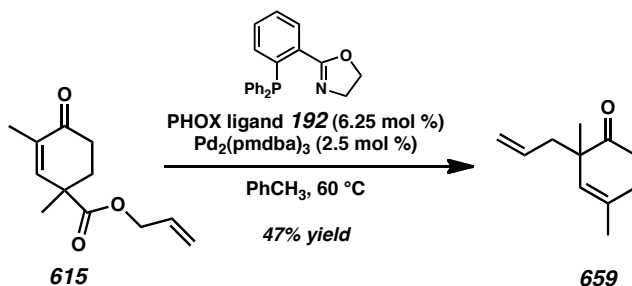
To a 250 mL round-bottom flask with magnetic stir bar was added β -ketoester (2.0 g, 10.98 mmol, 1.00 equiv), CH_2Cl_2 (75 mL), and sodium allyloxide (15 mg, 0.188 mmol, 2.5 mol %). The suspension was stirred vigorously as ethyl vinyl ketone (750 mL, 0.68 mmol, 0.68 equiv) in CH_2Cl_2 (7 mL) was added. The reaction became increasingly turbid as the reaction progressed. After 4.5 h of stirring, the reaction was treated with an additional portion of ethyl vinyl ketone (750 mL, 0.68 mmol, 0.68 equiv). After an additional 13.5 h of stirring, another portion of sodium allyloxide (15 mg, 0.188 mmol, 2.5 mol %) was added. After an additional 5 h of stirring, the reaction was quenched with sat. aqueous NH_4Cl (5 mL) and H_2O (5 mL). The layers were separated and the aqueous layer was extracted with CH_2Cl_2 (2 x 10 mL). The organic layers were dried

over Na₂SO₄, filtered, and concentrated under reduced pressure to give a pale tan oil, which was used directly in the next step.

A 250 mL round-bottom flask under N₂ was charged with allyl alcohol (40 mL) and cooled to 0 °C. NaH (60% wt. dispersion, 2.20 g, 54.90 mmol, 5.0 equiv) was added slowly to minimize gas evolution. The flask was equipped with an addition funnel containing the crude diketoester in Et₂O (10 mL). The solution was added dropwise, leading to the clarification of the reaction mixture. Upon complete addition, the reaction was a turbid yellow solution. After 6.5 min of stirring, the reaction was quenched with sat. aqueous NH₄Cl (5 mL) and H₂O (5 mL). The reaction was concentrated under reduced pressure to remove the majority of the allyl alcohol. The yellow mixture was extracted with Et₂O (3 x 20 mL). The combined organics were dried over MgSO₄, filtered, and concentrated under reduced pressure. The residue was purified by flash column chromatography (SiO₂, 5 x 10 cm, 20:1→15:1→10:1→6:1→4:1→2:1→1:1→1:1 hexanes:EtOAc) to afford δ -ketoester **619** (1.8415 g, 7.31 mmol, 67% yield over two steps); *R*_f = 0.49 (4:1 hexanes:EtOAc); ¹H NMR (500 MHz, CDCl₃) δ 5.90 (ddt, *J* = 17.2, 10.4, 5.8 Hz, 1H), 5.31 (dq, *J* = 17.2, 1.5 Hz, 1H), 5.25 (dq, *J* = 10.4, 1.2 Hz, 1H), 4.63 (dt, *J* = 5.6, 1.3 Hz, 2H), 2.85 (ddt, *J* = 15.1, 4.4, 2.1 Hz, 1H), 2.46–2.34 (m, 3H), 2.30–2.23 (m, 1H), 2.16–2.07 (m, 1H), 1.95–1.85 (m, 2H), 1.84 (d, *J* = 1.4 Hz, 3H), 1.76–1.68 (m, 1H), 1.49–1.29 (m, 3H); ¹³C NMR (125 MHz, CDCl₃) δ 198.5, 174.0, 155.8, 131.9, 131.3, 119.0, 65.9, 49.8, 39.0, 34.7, 34.5, 29.8, 26.3, 23.1, 11.2; IR (Neat Film NaCl) 3435, 3319, 3084, 2934, 2861, 1724, 1670, 1666, 1617, 1452, 1375, 1360, 1342, 1314, 1295, 1265, 1251, 1225, 1175, 1155, 1136, 1095, 1081, 1064, 1014, 1000,

974, 931, 897, 864, 833, 816, 785, 758, 708 cm^{-1} ; HRMS (EI+) m/z calc'd for $\text{C}_{15}\text{H}_{20}\text{O}_3$ [M] $^{+}$: 248.1412; found 248.1422.

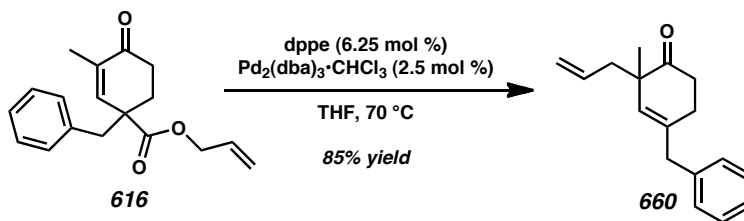
A11.6.2.2 Pd-CATALYZED DECARBOXYLATIVE ALKYLATION REACTIONS



β,γ -Unsaturated Ketone 659. A 1 dram vial containing δ -ketoester **615** (290.9 mg, 1.397 mmol, 1.00 equiv) was evacuated/backfilled with N_2 in a glove box antechamber (3 cycles, 5 min evacuation per cycle) before being transferred into an N_2 glove box. A 20 mL scintillation vial with magnetic stir bar was loaded with $\text{Pd}_2(\text{pmdba})_3$ (38.3 mg, 0.0349 mmol, 2.5 mol %) and achiral PHOX ligand **192** (28.9 mg, 0.0873 mmol, 6.25 mol %) in the glove box. Toluene (10 mL) was added and the vial was capped with a teflon-lined hard cap. The vial was inserted into a 30 $^\circ\text{C}$ heating block and stirred for 30 min. During this time, the mixture developed a dark orange color. β -Ketoester **65** was dissolved in toluene (4 mL) and added to the catalyst solution dropwise, causing the solution to turn olive green. The vial was capped with a teflon-lined hard cap and removed from the glove box. The vial was inserted into a 60 $^\circ\text{C}$ heating block and stirred for 57 h. The yellow-brown solution was heated to 70 $^\circ\text{C}$ and stirred for 13 h. The reaction became a yellow-brown solution. The reaction was concentrated under reduced

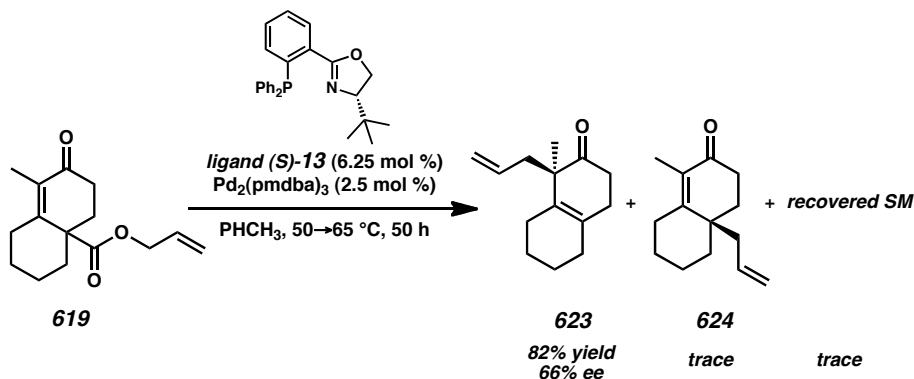
pressure and purified by flash column chromatography (SiO₂, 3 x 25 cm, 1%→2.5% Et₂O in hexanes) to afford β,γ -unsaturated ketone **659** (108 mg, 0.658 mmol, 47% yield);

R_f = 0.67 (4:1 hexanes:EtOAc); ¹H NMR (500 MHz, CDCl₃) δ 5.70–5.60 (m, 1H), 5.23 (q, J = 1.4 Hz, 1H), 5.02–4.96 (m, 2H), 2.55–2.42 (m, 2H), 2.38 (ddt, J = 13.8, 7.7, 1.1 Hz, 1H), 2.32 (t, J = 7.2 Hz, 1H), 2.11 (ddt, J = 13.6, 7.0, 1.3 Hz, 1H), 1.76 (d, J = 0.9 Hz, 3H), 1.09 (s, 3H); ¹³C NMR (125 MHz, CDCl₃) δ 214.9, 134.3, 133.5, 129.1, 117.8, 48.2, 44.6, 37.1, 30.3, 25.1, 23.3; IR (Neat Film NaCl) 3045, 2969, 2928, 2848, 2730, 1714, 1678, 1640, 1447, 1372, 1338, 1291, 1248, 1180, 1152, 1106, 1090, 1017, 996, 916, 888, 844, 785 cm⁻¹; HRMS (MM: ESI-APCI+) m/z calc'd for C₁₁H₁₆O [M+H]⁺: 165.1274; found 165.1273; GC conditions: 90 °C isothermal, G-TA column, t_R (min): major = 21.03, minor = 22.51.



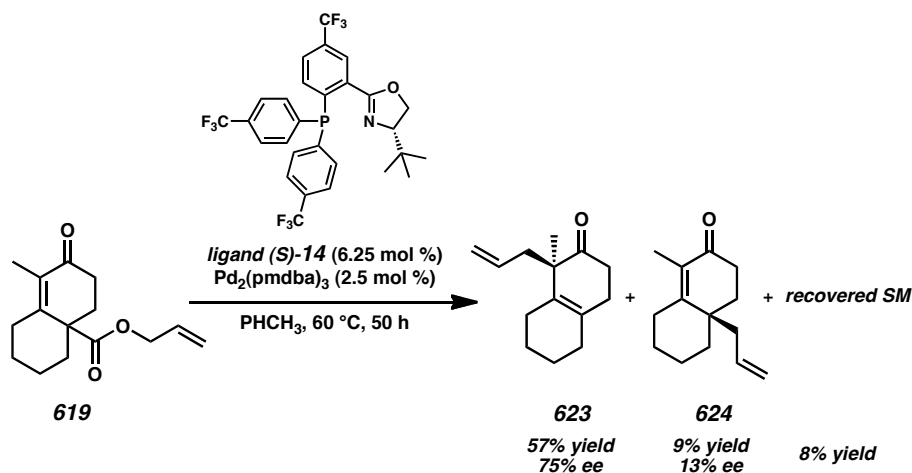
β,γ -Unsaturated Ketone 660. To a 20 mL scintillation vial with magnetic stir bar was added dppe (40.9 mg, 0.103 mmol, 6.25 mol %) and Pd₂(dba)₃·CHCl₃ (42.5 mg, 0.041 mmol, 2.5 mol %). The vial was sealed with a septum-fitted screw cap and evacuated/backfilled with N₂ (3 cycles, 5 min evacuation per cycle). THF (8 mL) was added. The reaction was immersed in a 70 °C heating block for 15 min. The vial was cooled to 23 °C and a solution of δ -ketoester **616** (466.7 mg, 1.64 mmol, 1.00 equiv) in THF (8.4 mL) was cannulated into the reaction, leading to the formation of a yellow solution. After 8 h of stirring, the reaction was yellow-orange in color. The reaction was

concentrated under reduced pressure, and the residue was and purified by flash column chromatography (SiO₂, 3 x 25 cm, 1%→2%→3% Et₂O in hexanes) to afford β,γ -unsaturated ketone **660** (333.9 mg, 1.389 mmol, 85% yield); R_f = 0.51 (4:1 hexanes:EtOAc); ¹H NMR (500 MHz, CDCl₃) δ 7.33–7.27 (m, 2H), 7.25–7.16 (m, 3H), 5.74–5.60 (m, 1H), 5.36 (t, J = 1.3 Hz, 1H), 5.06–4.99 (m, 2H), 3.39 (d, J = 14.8 Hz, 1H), 3.35 (d, J = 14.8 Hz, 1H), 2.54–2.36 (m, 3H), 2.28–2.23 (m, 2H), 2.14 (ddt, J = 13.5, 7.1, 1.3 Hz, 1H), 1.15 (s, 3H); ¹³C NMR (125 MHz, CDCl₃) δ 214.7, 139.3, 136.7, 134.2, 130.7, 128.9, 128.5, 126.4, 118.0, 48.4, 44.5, 43.8, 37.3, 28.1, 25.3; IR (Neat Film NaCl) 3405, 3076, 3062, 3026, 3003, 2966, 2926, 2907, 2846, 1712, 1673, 1640, 1602, 1584, 1494, 1453, 1436, 1417, 1376, 1340, 1294, 1272, 1239, 1178, 1102, 1075, 1030, 996, 917, 872, 796, 7533, 729, 700, 610 cm⁻¹; HRMS (MM: ESI-APCI+) m/z calc'd for C₁₇H₂₁O [M+H]⁺: 241.1587; found 241.1581.



β,γ -Unsaturated Ketone 623. A 1 dram vial containing δ -ketoester **619** (150 mg, 0.604 mmol, 1.00 equiv) was evacuated/backfilled with N₂ in a glove box antechamber (3 cycles, 5 min evacuation per cycle) before being transferred into an N₂ glove box. A 20 mL scintillation vial with magnetic stir bar was loaded with Pd₂(pmdba)₃ (16.6 mg,

0.0151 mmol, 2.5 mol %) and (*S*)-*t*-Bu-PHOX (**13**) (14.7 mg, 0.03775 mmol, 6.25 mol %) in the glove box. Toluene (6 mL) was added and the vial was capped with a teflon-lined hard cap. The vial was inserted into a 30 °C heating block and stirred for 30 min. During this time, the mixture developed a dark orange color. δ -Ketoester **619** was dissolved in toluene (4 mL) and added to the catalyst solution dropwise, causing the solution to turn olive green. The vial was capped with a teflon-lined hard cap and removed from the glove box. The vial was inserted into a 50 °C heating block and stirred for 44 h. The olive green solution was heated to 65 °C and stirred for 6 h. The reaction became a brown-orange solution. The reaction was concentrated under reduced pressure and purified by flash column chromatography (SiO₂, 2 x 25 cm, 1%→2%→2.5% Et₂O in hexanes) to afford β,γ -unsaturated ketone **624** (100 mg, 0.493 mmol, 82% yield).

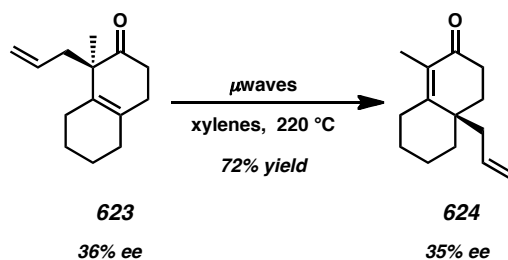


β,γ -Unsaturated Ketone 623 and α,β -Unsaturated Ketone 624. A 1 dram vial containing δ -ketoester **619** (126.2 mg, 0.50 mmol, 1.00 equiv) was evacuated/backfilled with N₂ in a glove box antechamber (3 cycles, 5 min evacuation per cycle) before being transferred into an N₂ glove box. A 20 mL scintillation vial with magnetic stir bar was

loaded with $\text{Pd}_2(\text{pmdba})_3$ (13.7 mg, 0.0125 mmol, 2.5 mol %) and (*S*)-(CF₃)₃-*t*-Bu-PHOX²⁰ (**13**) (18.5 mg, 0.03125 mmol, 6.25 mol %) in the glove box. Toluene (3 mL) was added and the vial was capped with a teflon-lined hard cap. The vial was inserted into a 30 °C heating block and stirred for 30 min. During this time, the mixture developed a dark orange color. δ -Ketoester **619** was dissolved in toluene (2 mL) and added to the catalyst solution dropwise, causing the solution to turn olive green. The vial was capped with a teflon-lined hard cap and removed from the glove box. The vial was inserted into a 60 °C heating block and stirred for 133 h. The reaction was concentrated under reduced pressure and purified by flash column chromatography (SiO₂, 2 x 25 cm, 3%→5%→10% Et₂O in hexanes) to afford β,γ -unsaturated ketone **623** (58.0 mg, 0.2839 mmol, 57% yield, 75.1% ee), α,β -unsaturated ketone **624** (9.6 mg, 0.04699 mmol, 9% yield, 13.1% ee), and recovered δ -ketoester **619** (10.3 mg, 0.0415 mmol, 8% yield).

β,γ -Unsaturated Ketone 623: R_f = 0.73 (4:1 hexanes:EtOAc); ¹H NMR (500 MHz, CDCl₃) δ 5.51 (ddt, J = 17.3, 10.1, 7.2 Hz, 1H), 4.99–4.90 (m, 2H), 2.59–2.47 (m, 2H), 2.41 (dt, J = 14.0, 6.6 Hz, 1H), 2.31–2.14 (m, 3H), 2.07–1.91 (m, 4H), 1.65–1.54 (m, 4H), 1.13 (s, 3H); ¹³C NMR (125 MHz, CDCl₃) δ 215.2, 134.8, 132.2, 129.9, 117.1, 51.5, 41.5, 37.5, 30.8, 30.4, 24.4, 23.6, 23.1, 22.9; IR (Neat Film NaCl) 3076, 2966, 2928, 2857, 2841, 1713, 1639, 1448, 1369, 1335, 1293, 1275, 1202, 1156, 1130, 1094, 1068, 1020, 994, 912, 871, 856, 827, 803, 754 cm⁻¹; HRMS (MM: ESI-APCI+) m/z calc'd for C₁₄H₂₁O [M+H]⁺: 205.1587; found 205.1588; $[\alpha]_D^{25.0}$ +4.34 (*c* 0.99, CHCl₃, 75.1% ee); GC conditions: 105 °C isothermal, G-TA column, t_R (min): major = 78.92, minor = 77.23.

α,β -Unsaturated Ketone 624: $R_f = 0.63$ (4:1 hexanes:EtOAc); ^1H NMR (500 MHz, CDCl_3) δ 5.80–5.69 (m, 1H), 5.14–5.07 (m, 2H), 2.72 (dddd, $J = 15.1, 4.3, 2.6, 1.6$ Hz, 1H), 2.52–2.40 (m, 2H), 2.37–2.29 (m, 2H), 2.12 (dddd, $J = 15.1, 13.7, 5.3, 1.4$ Hz, 1H), 1.96–1.88 (m, 2H), 1.81–1.75 (m, 1H), 1.77 (d, $J = 1.4$ Hz, 3H), 1.69–1.54 (m, 3H), 1.36 (dt, $J = 13.7, 12.8, 4.4$ Hz, 1H), 1.22 (tdd, $J = 13.1, 4.3, 1.1$ Hz, 1H); ^{13}C NMR (500 MHz, CDCl_3) δ 199.2, 162.7, 134.0, 129.3, 118.3, 39.4, 38.0, 37.7, 33.7, 33.4, 27.7, 26.8, 21.1, 11.1; IR (Neat Film NaCl) 3014, 2929, 2860, 1664, 1637, 1607, 1456, 1374, 1361, 1334, 1324, 1296, 1248, 1206, 1189, 1150, 1128, 1087, 1058, 994, 963, 914, 876, 796, 758 cm^{-1} ; HRMS (MM: ESI-APCI+) m/z calc'd for $\text{C}_{14}\text{H}_{21}\text{O}$ $[\text{M}+\text{H}]^+$: 205.1587; found 205.1594; $[\alpha]_D^{25.0} +14.49$ (c 0.88, CHCl_3 , 13.1% ee); GC conditions: 130 °C isothermal, G-TA column, t_R (min): major = 48.46, minor = 45.91.

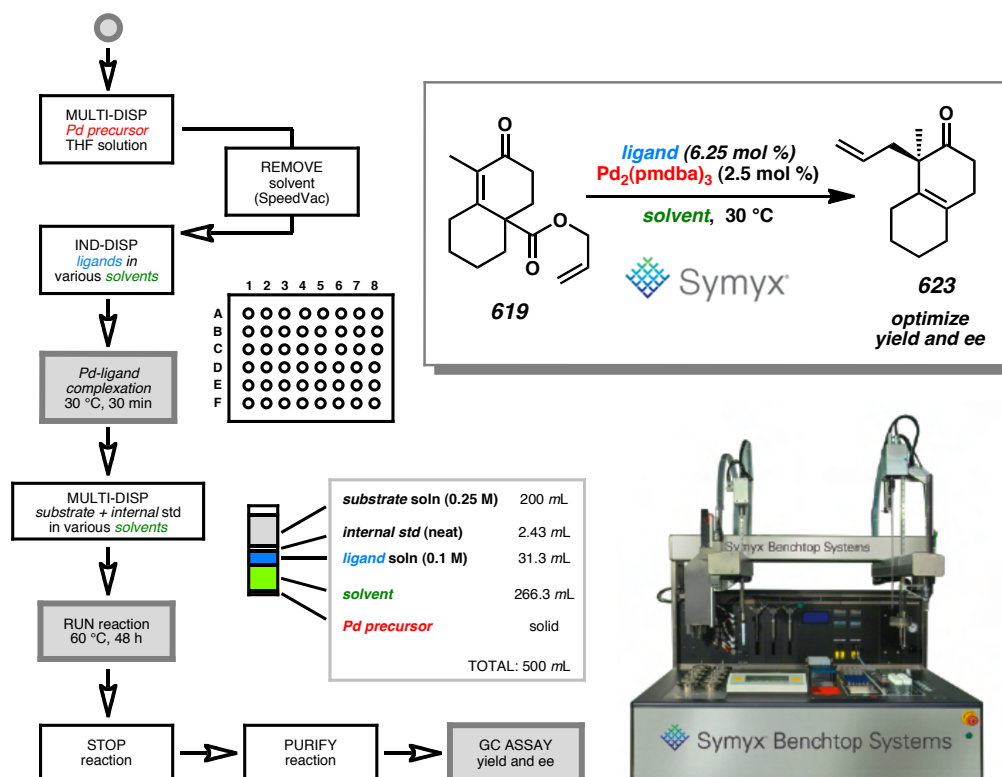


α,β -Unsaturated Ketone 624. To a 5 mL microwave vial with magnetic stir bar was added β,γ -unsaturated enone **623** (88.3 mg, 0.290 mmol, 1.00 equiv) and xylenes (3.5 mL). The reaction was sealed with a microwave crimp cap and subjected to microwave irradiation in a Biotage Initiator microwave reactor (temperature: 220 °C, sensitivity: low). After 24 h of stirring, the vial was uncapped and the reaction was concentrated under reduced pressure. The residue was purified by flash column chromatography (SiO_2 , 2 x 20 cm, 3%→6% Et_2O in hexanes) to give recovered α,β -unsaturated ketone

623 (3.9 mg, 0.0191 mmol, 13% yield) and β,γ -unsaturated ketone **624** (22 mg, 0.108 mmol, 72% yield, 35% ee).

A11.6.2.3 HIGH-THROUGHPUT REACTION SCREENING

Figure A11.2. Symyx Workflow for Asymmetric Alkylation Reactions with Substrate **619**



Symyx High-Throughput Reaction Screening Procedure. A chiral GC calibration curve with 7 data points was determined for β,γ -unsaturated ketone **623** over the concentration range of 0.1 mM–0.2 M using tetradecane as the internal standard. A linear plot provided the formula $\text{mmol}_{623} = K[\text{mmol}_{\text{std}}][A_{623}/A_{\text{std}}]$, where $K = 1.1009248426$ and std = internal tetradecane standard.

The reaction screen was set up using 48-well plates (R= rows, C = columns) in a N₂-filled customized glove box equipped with a Symyx Core Module as depicted in Figure A11.2. Stock solutions of Pd₂(pmbda)₃ in THF (40 mg in 20 mL, 2 mg/mL), (*S*)-*t*-Bu-PHOX (**13**) in THF (35 mg in 5 mL, 7 mg/mL), and (*S*)-(CF₃)₃-*t*-Bu-PHOX (**14**) in THF (50 mg in 5 mL, 10 mg/mL) were prepared. A stock solution of substrate **619** in THF (372.5 mg in 6 mL, 0.25 M) was prepared in a 20 mL scintillation vial. Tetradecane was added to a 20 mL scintillation vial.

The stock solution of Pd₂(pmbda)₃ in THF (700 µL) was dispensed into 2 mL vials using the Multi-Dispense (**D-M**) command (24 vials, 3R x 8C array, 1 plate). The vials were redistributed between two plates (24 vials, 1R x 12C array, 2 plates) and the solutions were concentrated using a Thermo Scientific SPD121P SpeedVac over 1 h.

During this time, the two ligand solutions ((*S*)-*t*-Bu-PHOX (**13**) solution, 173 µL, (*S*)-(CF₃)₃-*t*-Bu-PHOX (**14**) solution, 185 µL) were dispensed into the 1.2 mL vials using the Multi-Dispense (**D-M**) command (12 vials, 1R x 12C array for each ligand, 2 plates total). The solutions were concentrated using the SpeedVac over 45 min.

The plates containing the 2 mL vials with Pd₂(pmbda)₃ were loaded with stir bars. The vials were redistributed between two plates (24 vials, 2R x 12C array, 2 plates). 12 Solvents (8 mL) were poured into 20 mL scintillation vials and arranged in two plates (12 vials, 2R x 6C array, 2 plates).

The 1.2 mL vials in the plate with (*S*)-*t*-Bu-PHOX (**13**) were filled with the various solvents (200 µL) using the Individual-Dispense (**D-I**) command. These resulting solutions of ligand in various solvents (200 + 50 µL solvent chase) were added to first row of the plate with vials containing Pd₂(pmbda)₃ using the Individual Dispense +

Solvent Flush (**D-IS**) command. Solutions that were not successfully transferred were pipetted manually (12 vials, 1R x 12C array, 1 plates).

As above, the 1.2 mL vials in the plate with (*S*)-(CF₃)₃-*t*-Bu-PHOX (**14**) were filled with the various solvents (200 µL) using the Individual-Dispense (**D-I**) command. These solutions of ligand in various solvents (200 + 50 µL chase) were added to second row of the plate with vials containing Pd₂(pmbda)₃ using the Individual Dispense + Solvent Flush (**D-IS**) command. Solutions that were not successfully transferred were pipetted manually (12 vials, 1R x 12C array, 1 plates). Complexation was carried out in Positions 4/5/6 with the stir rate set to 600 rpm and temperature set to 30 °C for 1 h. Color changes were observable.

During this time, substrate **619** solution (200 µL) was dispensed into 1.2 mL vials using the Multi-Dispense (**D-M**) command (12 vials, 1R x 12C array for each ligand, 2 plates total). The solutions were concentrated using the SpeedVac over 45 min.

The plate containing vials with substrate **619** was filled with the various solvents (200 µL) using the Individual-Dispense (**D-I**) command. These vials with substrate in various solvents (200 + 50 µL chase) were added to both rows of the plate with vials containing Pd₂(pmbda)₃ and ligand using the Individual Dispense + Solvent Flush (**D-IS**) command. Solutions that were not successfully transferred were pipetted manually (24 vials, 2R x 12C array, 2 plates).

Tetradecane with solvent flush (2 + 10 µL) was dispensed into reaction vials using the Individual Dispense + Solvent Flush (**D-IS**) command (24 vials, 2R x 12C, 1 plate). Vials were consolidated onto one plate (A1–8, B1–8, D1–4, E1–4), teflon-lined hard caps

were attached, and reaction was initiated in Positions 4/5/6 with the stir rate set to 600 rpm and temperature set to 30 °C for 48 h. Color changes were observable.

The heating was turned off and stir bars were removed in the glove box using a stir bar retriever. The plates were removed from the glove box. Reaction mixtures were passed through a silica pipet plug (0.5 x 1.0 mm) into 1 dram vials, eluting with Et₂O until a total volume of 4 mL was obtained. An aliquot of this solution (600 µL) was pipetted into a 1 mL analysis vial. Et₂O (300 µL) was added to dilute the sample. Typically, a pale yellow solution was obtained. Samples were analyzed on a chiral GC with an autosampler (GC conditions: 105 °C isothermal, G-TA column) to determine yield and ee using the calibration curve.

A11.7 NOTES AND REFERENCES

- (1) Weaver, J. D.; Recio, A., III; Grenning, A. J.; Tunge, J. A. *Chem. Rev.* **2011**, *111*, 1846–1913.
- (2) Tsuji, J.; Minami, I.; Shimizu, I. *Tetrahedron Lett.* **1983**, *24*, 1793–1796.
- (3) Waetzig, S. R.; Rayabarapu, D. K.; Weaver, J. D.; Tunge, J. A. *Angew. Chem. Int. Ed.* **2006**, *45*, 4977–4980.
- (4) Shintani, R.; Tsuji, T.; Park, S.; Hayashi, T. *Chem. Commun.* **2010**, *46*, 1697–1699.
- (5) Herrinton, P. M.; Klotz, K. L.; Hartley, W. M. *J. Org. Chem.* **1993**, *58*, 678–682.
- (6) Trost, B. M.; Stiles, D. T. *Org. Lett.* **2007**, *9*, 2763–2766.
- (7) Jana, R.; Partridge, J. J.; Tunge, J. A. *Angew. Chem. Int. Ed.* **2011**, *50*, 5157–5161.
- (8) Schulz, S. R.; Blechert, S. *Angew. Chem. Int. Ed.* **2007**, *46*, 3966–3970.
- (9) Silyl enol ether and enol carbonate substrates: Behenna, D. C.; Stoltz, B. M. *J. Am. Chem. Soc.* **2004**, *126*, 15044–15045.
- (10) β -Ketoester substrates: Mohr, J. T.; Behenna, D. C.; Harned, A. M.; Stoltz, B. M. *Angew. Chem. Int. Ed.* **2005**, *44*, 6924–6927.
- (11) Full paper: Behenna, D. C.; Mohr, J. T.; Sherden, N. H.; Marinescu, S. C.; Harned, A. M.; Tani, K.; Seto, M.; Ma, S.; Novák, Z.; Krout, M. R.; McFadden, R. M.; Roizen, J. L.; Enquist, Jr., J. A.; White, D. E.; Levine, S. R.; Petrova, K.

- V.; Iwashita, A.; Virgil, S. C.; Stoltz, B. M. *Chem. Eur. J.* **2011**, *17*, 14199–14223.
- (12) (a) Trost, B. M.; Xu, J. *J. Am. Chem. Soc.* **2005**, *127*, 17180–17181. (b) Trost, B. M.; Xu, J. *J. Am. Chem. Soc.* **2005**, *127*, 2846–2847. (c) Trost, B. M.; Xu, J.; Schmidt, T. *J. Am. Chem. Soc.* **2009**, *131*, 18343–18357.
- (13) Dioxanone substrates: Seto, M.; Roizen, J. L.; Stoltz, B. M. *Angew. Chem. Int. Ed.* **2008**, *47*, 6873–6876.
- (14) Lactam substrates: Behenna, D. C.; Liu, Y.; Yurino, T.; Kim, J.; White, D. E.; Virgil, S. C.; Stoltz, B. M. *Nature Chem.* **2012**, *4*, 130–133.
- (15) Enantioselective protonation: (a) Mohr, J. T.; Nishimata, T.; Behenna, D. C.; Stoltz, B. M. *J. Am. Chem. Soc.* **2006**, *128*, 11348–11349. (b) Marinescu, S. C.; Nishimata, T.; Mohr, J. T.; Stoltz, B. M. *Org. Lett.* **2008**, *10*, 1039–1042.
- (16) Conjugate Addition/Allylation Cascade: Streuff, J.; White, D. E.; Virgil, S. C.; Stoltz, B. M. *Nature Chem.* **2010**, *2*, 192–196.
- (17) (a) Mander, L. N.; Sethi, S. P. *Tetrahedron Lett.* **1983**, *24*, 5425–5428. (b) Donnelly, D. M. X.; Finet, J.-P.; Rattigan, B. A. *J. Chem. Soc. Perkin Trans. I* **1993**, 1729–1735.
- (18) Stork, G.; Danheiser, R. L. *J. Org. Chem.* **1973**, *38*, 1775–1776.
- (19) For a preparation of (*S*)-*t*-Bu-PHOX (**13**), see: (a) Behenna, D. C.; Stoltz, B. M. *J. Am. Chem. Soc.* **2004**, *126*, 15044–15045. (b) Tani, K.; Behenna, D. C.;

- McFadden, R. M.; Stoltz, B. M. *Org. Lett.* **2007**, *9*, 2529–2531. (c) Krout, M. R.; Mohr, J. T.; Stoltz, B. M. *Org. Synth.* **2009**, *86*, 181–193.
- (20) (a) Overman, L. E.; Knoll, F. M. *J. Am. Chem. Soc.* **1980**, *102*, 865–867.
(b) Overman, L. E.; Jacobsen, E. J. *J. Am. Chem. Soc.* **1982**, *104*, 7225–7231.
(c) Overman, L. E.; Renaldo, A. F. *Tetrahedron Lett.* **1983**, *24*, 3757–3760.
(d) Overman, L. E.; Renaldo, A. F. *J. Am. Chem. Soc.* **1990**, *112*, 3945–3949.
- (21) (a) Keith, J. A.; Behenna, D. C.; Mohr, J. T.; Ma, S.; Marinescu, S. C.; Oxgaard, J.; Stoltz, B. M.; Goddard, III, W. A. *J. Am. Chem. Soc.* **2007**, *129*, 11876–11877.
(b) Keith, J. A.; Behenna, D. C.; Sherden, N.; Mohr, J. T.; Ma, S.; Marinescu, S. C.; Nielsen, R. J.; Oxgaard, J.; Stoltz, B. M.; Goddard, III, W. A. *J. Am. Chem. Soc.* **2012**, *134*, 19050–19060.
- (22) Sherden, N. H.; Behenna, D. C.; Virgil, S. C.; Stoltz, B. M. *Angew. Chem. Int. Ed.* **2009**, *48*, 6840–6843.
- (23) For a preparation of electron-deficient PHOX ligand **14** ((*S*)-(CF₃)₃-*t*-Bu-PHOX), see: (a) White, D. E.; Stewart, I. C.; Grubbs, R. H.; Stoltz, B. M. *J. Am. Chem. Soc.* **2008**, *130*, 810–811. (b) McDougal, N. T.; Streuff, J.; Mukherjee, H.; Virgil, S. C.; Stoltz, B. M. *Tetrahedron Lett.* **2010**, *51*, 5550–5554.
- (24) For reported examples of reactions in which electron-deficient PHOX ligand **14** provides increased yield and enantioselectivity, see: (a) Streuff, J.; White, D. E.; Virgil, S. C.; Stoltz, B. M. *Nature Chem.* **2010**, *2*, 192–196. (b) White, D. E.; Stewart, I. C.; Seashore-Ludlow, B. A.; Grubbs, R. H.; Stoltz, B. M. *Tetrahedron* **2010**, *66*, 4668–4686. (c) McDougal, N. T.; Virgil, S. C.; Stoltz, B. M. *Synlett*

- 2010**, 1712–1716. (d) Mukherjee, H.; McDougal, N. T.; Virgil, S. C.; Stoltz, B. M. *Org. Lett.* **2011**, *13*, 825–827.
- (25) Xu, G.; Hou, A.-J.; Zheng, Y.-T.; Zhao, Y.; Li, X.-L.; Peng, L.-Y.; Zhao, Q.-S. *Org. Lett.* **2007**, *9*, 291–293.
- (26) Pettit, G. R.; Tan, R.; Northen, J. S.; Herald, D. L.; Chapuis, J.-C.; Pettit, R. K. *J. Nat. Prod.* **2004**, *67*, 1476–1482.
- (27) For a review of the uses of Hagemann's ester, see: Pollini, G. P.; Benetti, S.; De Risi, C.; Zanirato, V. *Tetrahedron* **2010**, *66*, 2775–2802.
- (28) Prolonged storage of δ -ketoesters **642** and **643** at ambient temperature or in a -25°C freezer led to facile aromatization.
- (29) For an early report of Trost ligands in Pd-catalyzed asymmetric alkylation reactions, see: Trost, B. M.; Van Vranken, D. L.; Bingel, C. *J. Am. Chem. Soc.* **1992**, *114*, 9327–9343.
- (30) Pangborn, A. B.; Giardello, M. A.; Grubbs, R. H.; Rosen, R. K.; Timmers, F. J. *Organometallics* **1996**, *15*, 1518–1520.
- (31) (a) Ukai, T.; Kawazura, H.; Ishii, Y.; Bonnet, J. J.; Ibers, J. A. *J. Organomet. Chem.* **1974**, *65*, 253–266. (b) Fairlamb, I. J. S.; Kapdi, A. R.; Lee, A. F. *Org. Lett.* **2004**, *6*, 4435–4438.
- (32) Levine, S. R.; Krout, M. R.; Stoltz, B. M. *Org. Lett.* **2009**, *11*, 289–292.

APPENDIX 12

Progress Toward the Total Synthesis of Crinine

and Related Amaryllidaceae Alkaloids[†]

A12.1 INTRODUCTION AND BACKGROUND

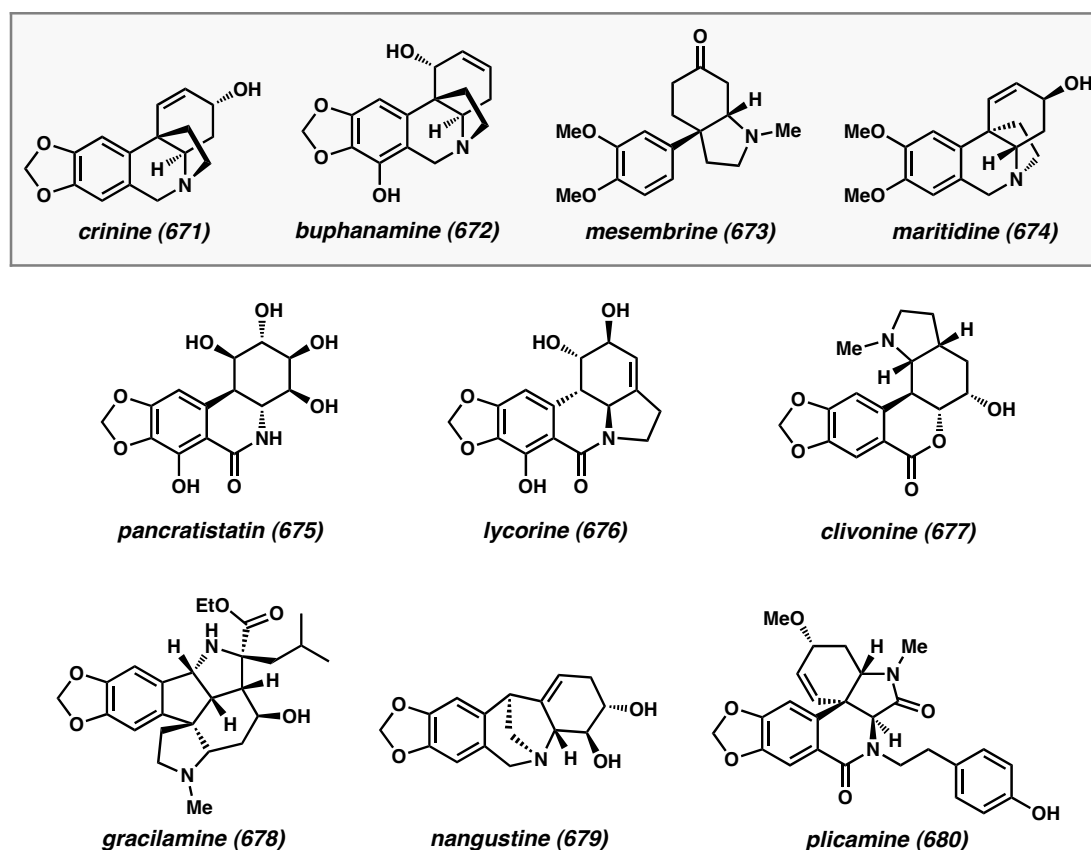
The complex polyheterocyclic *Amaryllidaceae* alkaloids have generated much scientific interest because of their wide range of biological activity. Hundreds of natural products have been isolated from a variety of plants across the globe and some of these have displayed anticancer, antimalarial, antiviral, and anti-inflammatory activity (Scheme A12.1). Additionally, several compounds inhibit acetylcholinesterase or stimulate the human immune system. Crinine (**671**) in particular has shown the ability to block serotonin transport proteins.¹ The broad range of biological activity of these compounds has inspired many novel total syntheses.²

Our research group became interested in the *Amaryllidaceae* alkaloids because of the synthetic challenges posed by their unique chemical structures with their wide range of

[†] The results in this appendix are unpublished.

polycyclic architectures and substitution patterns. We were particularly interested in natural products such as crinine (**671**), buphanamine (**672**), mesembrine (**673**), and maritidine (**674**), which feature an aryl-substituted all-carbon quaternary stereocenter situated at the junction of three different rings. The high degree of oxidation of both aromatic and aliphatic rings poses additional synthetic challenges. Overall, we saw the total synthesis of these molecules as a testing ground for synthetic methods developed by our group as well as a motivation for the development of novel transformations. The reaction development and total synthesis efforts described herein have been directed toward the natural product crinine and related alkaloids.

Scheme A12.1. Representative Amaryllidaceae Alkaloids



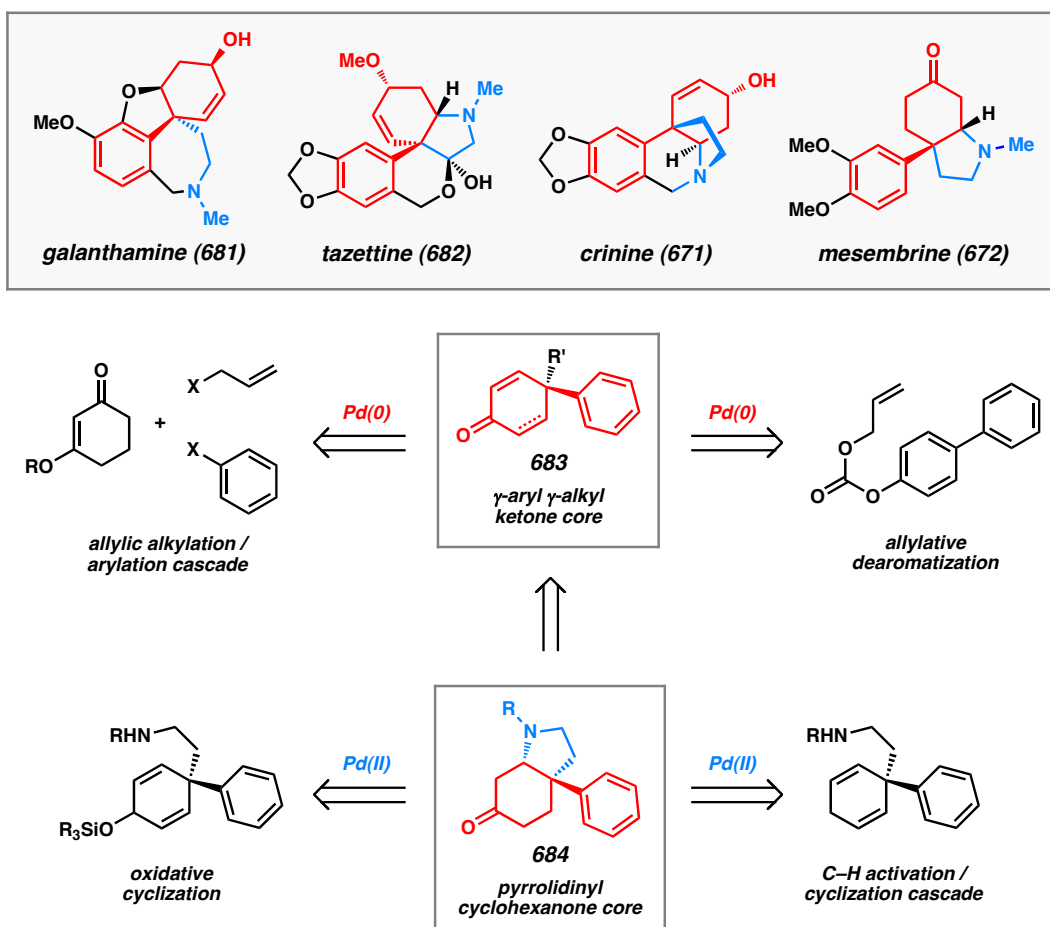
A12.2 SYNTHETIC STRATEGIES TOWARD CRININE-TYPE ALKALOIDS

Intrigued by the stereochemically dense polyheterocyclic skeletons and unique biological activity of the *Amaryllidaceae* alkaloids, we sought to devise new transition metal-catalyzed synthetic strategies for the preparation of the common γ -aryl γ -alkyl cyclohexanoid core **683** (Scheme A12.2). As a particularly versatile transition metal, palladium can catalyze allylic alkylation and arylation reactions from the Pd(0) oxidation state, as well as Wacker-type heterocyclizations or C–H activation reactions from the Pd(II) oxidation state. In our synthetic approaches, we aimed to take advantage of these powerful reactions to efficiently assemble the conserved core structures that can be advanced to numerous structurally diverse alkaloid natural products.

In order to access the common γ -aryl γ -alkyl cyclohexanoid core **683** of the target alkaloids such as crinine, Pd(0)-catalyzed transformations appeared to be particularly promising for the construction of the key quaternary center (Scheme A12.2). The asymmetric α -arylation/ α -allylation of a suitable vinylogous ester coupled with a Stork–Danheiser ketone transposition would efficiently forge the desired ring system. While arylative modifications of our group's Pd-catalyzed asymmetric alkylation chemistry have not been explored in detail, the development of such reactions would streamline the total synthesis of alkaloids as well as many other natural products. Another strategy for the synthesis of the γ -aryl γ -alkyl cyclohexanoid core **683** could be based on the metal-catalyzed allylative dearomatization of a 4-aryl phenol precursor followed by a dienone desymmetrization. This strategy would provide a powerful new C–C bond-forming

reaction for converting simple phenolic compounds to highly functionalized ring systems in a short sequence.

Scheme A12.2. Pd-Catalysis Strategies Toward Crinine and Related Amaryllidaceae Alkaloids



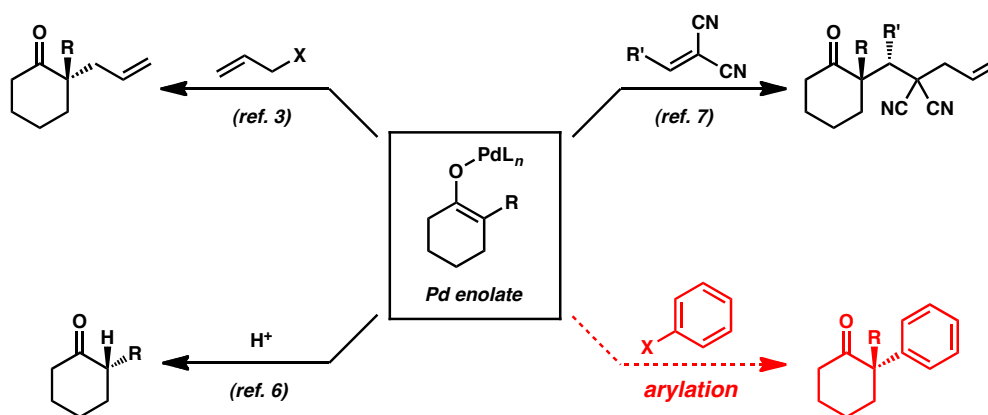
Alternatively, the pursuit of the more highly functionalized pyrrolidinyl cyclohexanoid core **284** of the target alkaloids could provide additional synthetic approaches (Scheme A12.2). $Pd(II)$ -catalyzed oxidative cyclization or C–H activation reactions can enable construction of the key pyrrolidine ring of many alkaloids in the family. A distinct advantage of the oxidative cyclization strategy is that air or oxygen

can be used as an abundant, inexpensive terminal oxidant for C–N bond formation. The C–H activation/allylic amination strategy would provide an efficient and novel method for the generation of allyl electrophiles for polycyclic alkaloid synthesis.

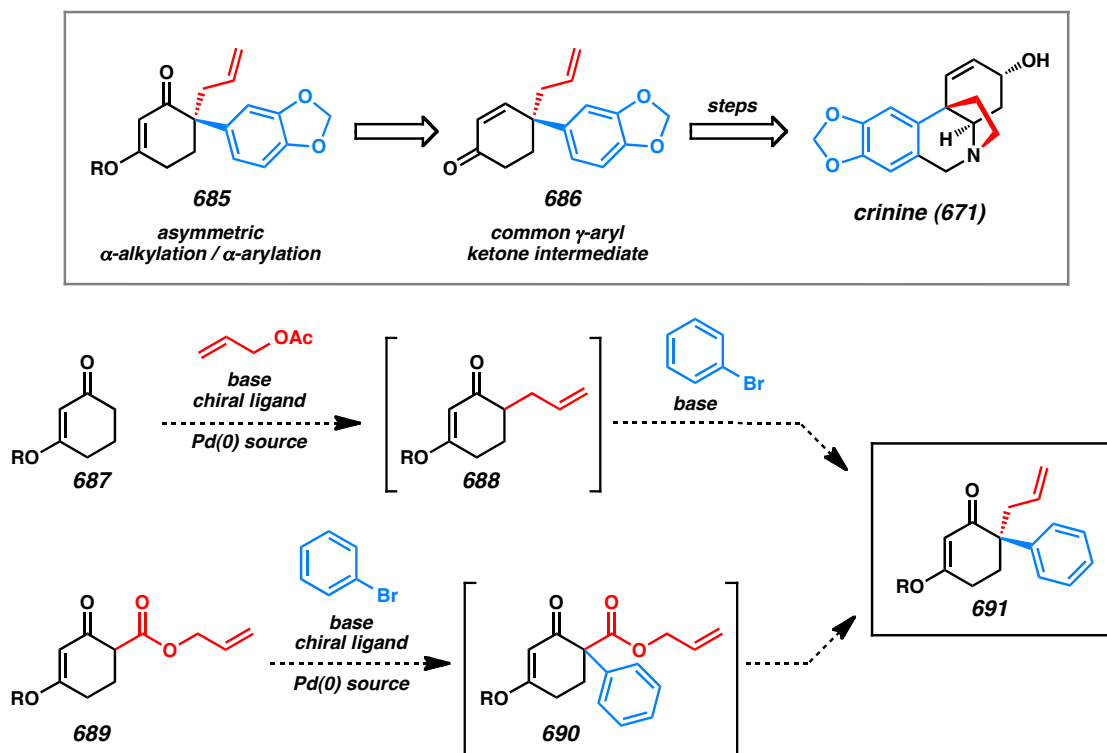
A12.2.1 α -ARYLATION/ α -ALKYLATION CASCADE STRATEGY

The catalytic enantioselective decarboxylative alkylation reactions developed in our group^{3,4} have enabled the efficient total syntheses of a number of diverse natural products.⁵ Significant advances in reaction development would enable access to other classes of natural products with unique structural challenges. In our research program, we have explored the interception of palladium enolates with different electrophiles in an effort to discover new asymmetric reactions (Scheme A12.3). In this manner, we have discovered novel asymmetric protonation⁶ and conjugate addition cascade reactions.⁷

Scheme A12.3. Development of Novel Asymmetric Reactions by Interception of Pd Enolates



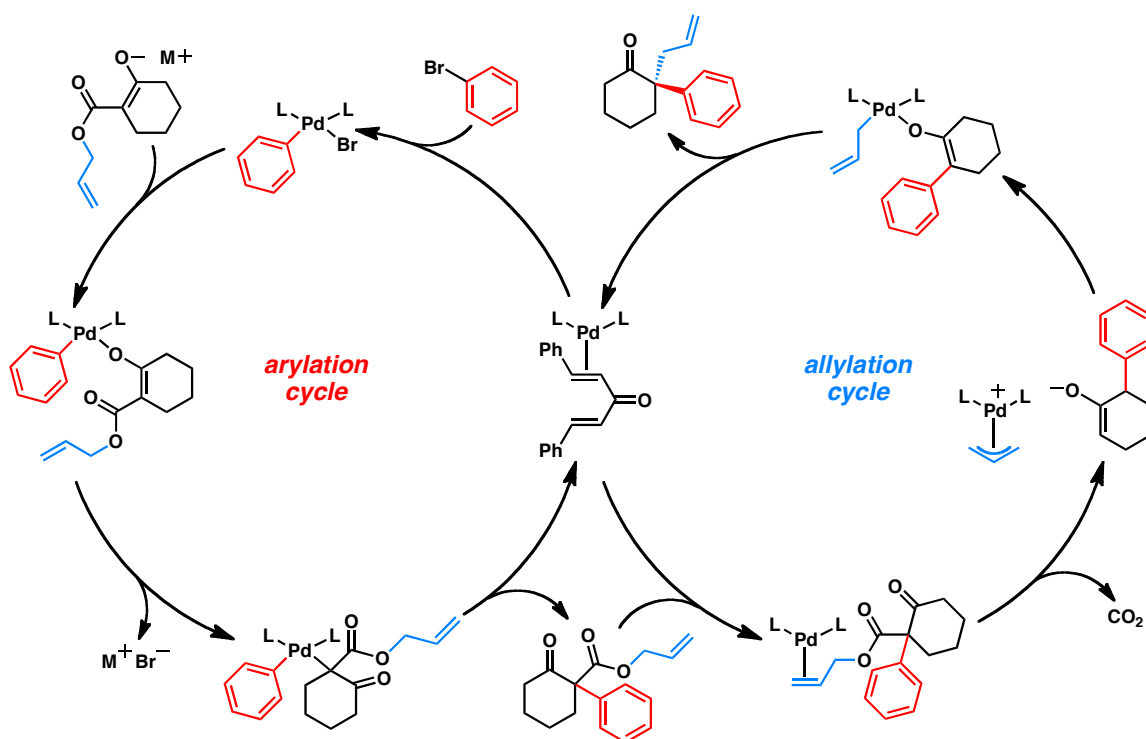
While much of our group's past work has focused on the total synthesis of terpenoid natural products,⁵ we aim to extend our reaction methodology to enable access to diverse alkaloid structures. In particular, crinine and related *Amaryllidaceae* alkaloids possess complex heterocyclic architectures with aryl-substituted quaternary centers. Upon analysis of the γ -aryl cyclohexenone core of these molecules, the opportunity for the development of an asymmetric α -arylation/ α -allylation reaction became apparent. Once this reaction is reduced to practice, the functionalized products **685** can be converted to γ -aryl γ -allyl cyclohexenones **686** using a Stork–Danheiser ketone transposition reaction (Scheme A12.4).⁸ Further synthetic manipulations could deliver the desired polycyclic ring system of crinine (**671**) and related alkaloids. With this overall strategy in mind, we sought to develop a general, robust reaction that would be amenable to our planned synthesis.

Scheme A12.4. α -Arylation/ α -Allylation Approach to Crinine

To access α -aryl α -allyl vinylogous esters in an efficient and catalytic manner, we envisioned that two distinct palladium-catalyzed carbon-carbon bond forming reactions could forge the α -quaternary stereocenter in an asymmetric fashion. Since Pd(0) complexes are known to catalyze both enantioselective allylation^{3,9} and arylation reactions,¹⁰ we reasoned that both transformations could occur in the same reaction flask using a single palladium catalyst (Scheme A12.4). Mechanistically, the reaction could proceed with an initial α -allylation of the enolate of cyclic vinylogous ester **687** followed by α -arylation, giving α,α -disubstituted vinylogous ester **691**. Conversely, the use of an allyl β -ketoester such as **689** could provide the same product through initial α -arylation followed by decarboxylative allylation. Numerous reaction pathways are possible and

the two described are representative examples. A plausible mechanism for the second reaction type is outlined in Scheme A12.5.

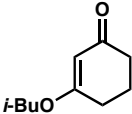
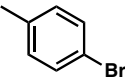
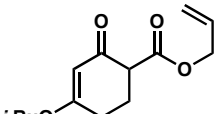
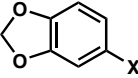
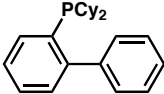
Scheme A12.5. A Possible Mechanistic Pathway for α -Arylation/ α -Allylation Reaction



In order to develop our desired reaction, we first sought to demonstrate proof of principle with a suitable achiral transformation and scrutinized numerous reaction variables. Different substrates, allyl sources, aryl halides, bases, palladium precursors, chiral ligands, solvents, and temperatures were investigated. The use of different substrates, allyl sources, and aryl sources provided the means for probing the different reaction pathways. Employing various bases enabled careful tuning of the deprotonation event for each particular substrate. Of the many variables, much effort was invested in the identification of the best combination of commercial Pd sources and ligands for our

desired transformation. We primarily considered Pd(0) complexes with mono- or bidentate phosphines. Our ligands of choice were electron-rich, bulky alkyl phosphines, which would promote C–C bond-forming reductive elimination. After considerable experimentation, we found that many reactions led to complex mixtures with only traces of observable desired product (Table A12.1). While we maintained our interest in this reaction for its potential to streamline the synthesis of our crinine and other alkaloids, we shifted our attention to explore other promising synthetic approaches.

Table A12.1. Summary of α -Arylation/ α -Allylation Screening Efforts

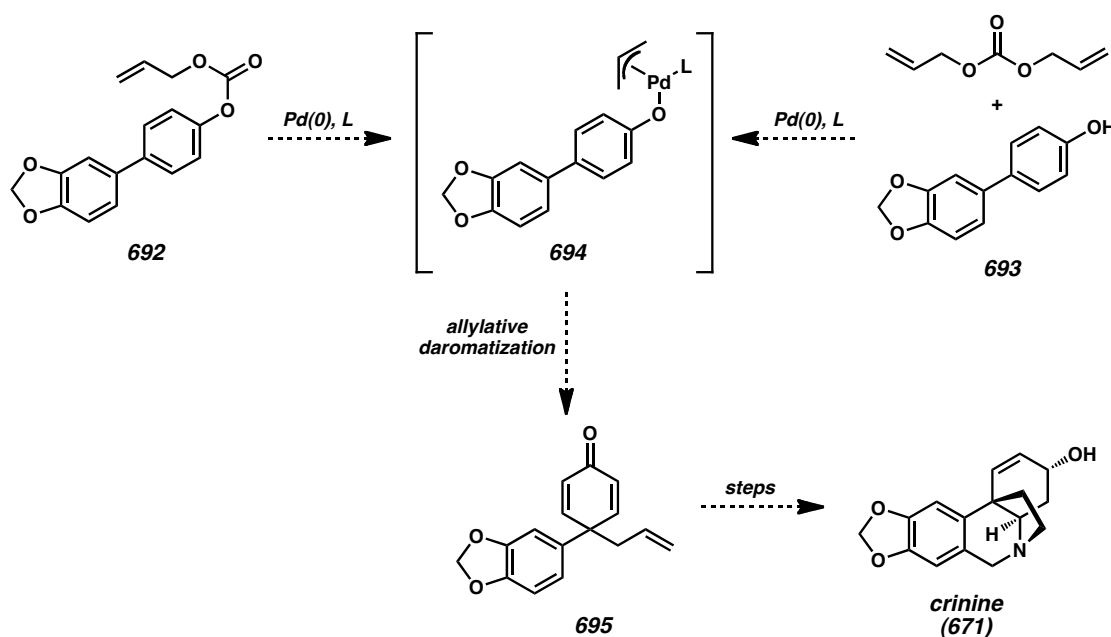
Substrates	Aryl Fragments	Bases	Pd sources	Ligands
 70		K_2CO_3 $NaOt-Bu$ NaH	$Pd(dba)_2$ $Pd(PPh_3)_4$ $Pd(OAc)_2$	BINAP $P(t-Bu)_3$
 579	 $X = Br, OTf$	$LiHMDS$ $KHMDS$ LDA	$PdCl_2(dppf)$ $[PdBr(t-Bu_3P)]_2$	

A12.2.2 ALLYLATIVE DEAROMATIZATION STRATEGY

By taking advantage of Pd(0) catalysis, it may be possible to achieve the allylative dearomatization of substituted 4-substituted phenols to form γ -quaternary cyclohexadienones resembling core structure **683** (Scheme A12.2). The feasibility of this transformation was demonstrated by Miura in his studies on the Pd-catalyzed *O*-allylation of phenols.¹¹ Danishefsky subsequently adapted the reaction conditions for the total

synthesis of garsubellin A.¹² The related Pd-catalyzed dearomatization of *p*-substituted benzyl chlorides has been investigated experimentally by Yamamoto¹³ and computationally by Lin.¹⁴ Taking these reports into account, we designed a dearomatization reaction that could provide the targeted γ -aryl γ -allyl cyclohexanone core for the synthesis of crinine (**671**) and related alkaloids (Scheme A12.6). The dearomatization reaction may proceed in an intra- or intermolecular manner, giving an intermediate Pd π -allyl phenoxide which can undergo allylation to effect the quaternization of the *para* position. With additional manipulations, it should be possible to advance the key tricycle **695** to crinine (**671**).

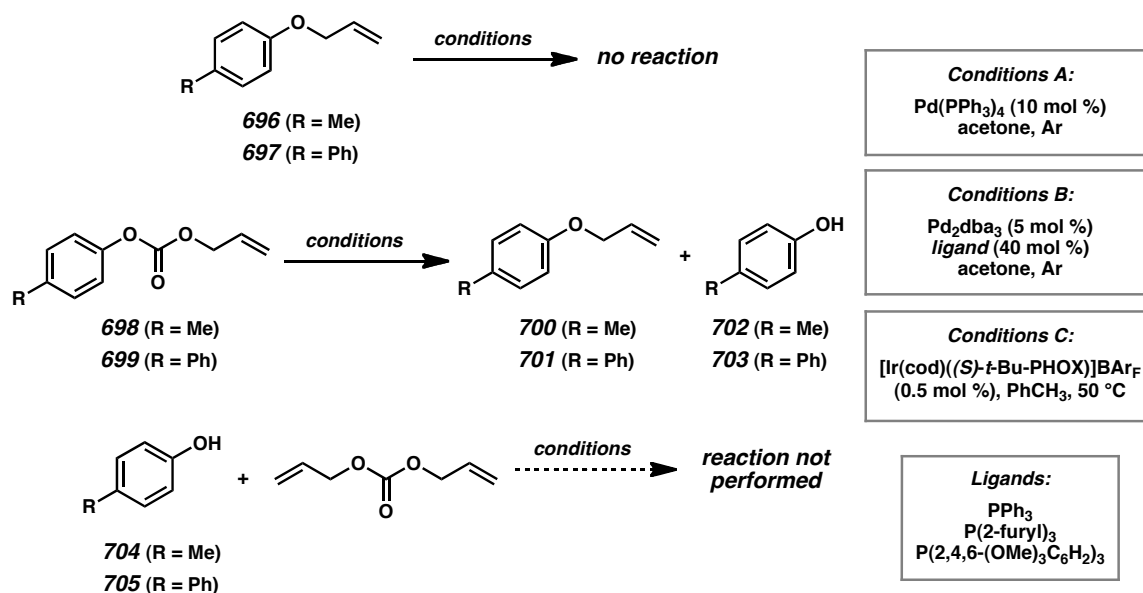
Scheme A12.6. Allylative Dearomatization Approach to Crinine



To test the viability of this approach, we opted to investigate simple model systems using *p*-cresol or 4-phenylphenol derivatives as substrates (Scheme A12.7). To test

intramolecular allylation reactions, we employed aryl allyl ethers **696** and **696** and aryl allyl carbonates **698** and **699**. To test intermolecular allylations, we planned to study reactions of the parent phenols with diallyl carbonate. Different palladium sources were evaluated with electron-rich, neutral, and electron-deficient phosphine ligands. Iridium(I) complexes, which are also known to promote allylation reactions, were also tested with the aryl allyl ether and aryl allyl carbonate starting materials. So far, the reaction conditions explored have either showed no reaction or led to a mixture of aryl allyl ethers and phenols. While the conditions evaluated are by no means exhaustive, these initial results prompted us to evaluate alternative strategies employing Pd(II) catalysis.

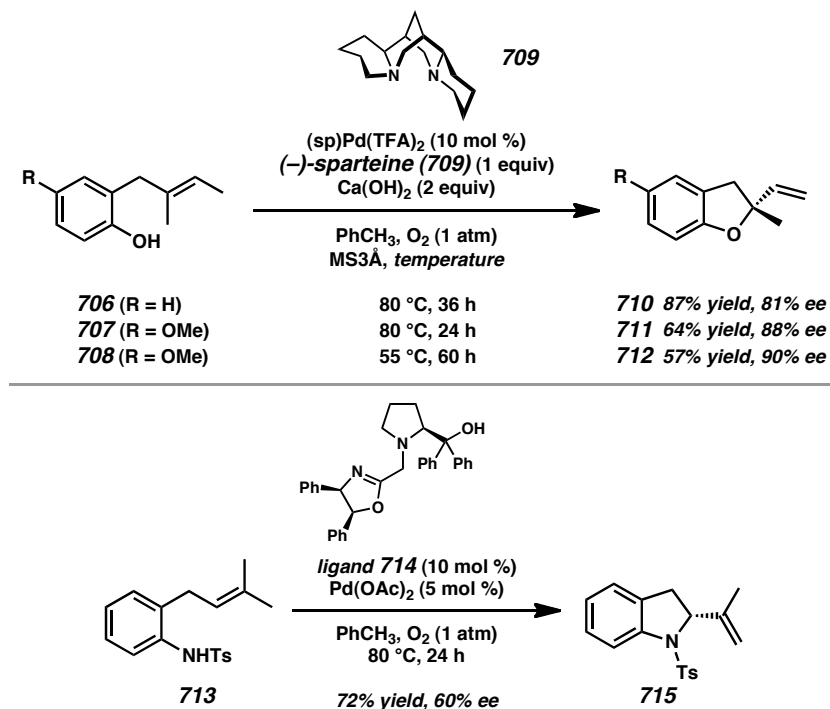
Scheme A12.7. Summary of Allylative Dearomatization Screening Efforts



A12.2.3 OXIDATIVE CYCLIZATION APPROACH

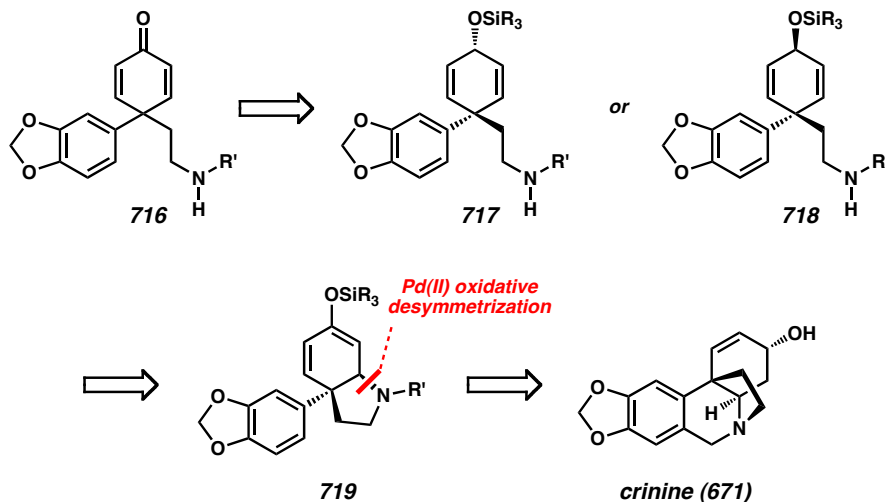
While the application of Pd(0)-catalyzed asymmetric allylic alkylation approaches to the synthesis of crinine (**671**) and related alkaloids is particularly attractive given our group's interest in methodology-driven total synthesis, other metal-catalyzed transformations developed by our group can allow us to accomplish the same synthetic goal. Our group has developed several enantioselective Pd(II)-catalyzed Wacker-type oxidative cyclization reactions that employ air or oxygen as the terminal oxidant¹⁵ (Scheme A12.8). With phenol^{15d} and aniline¹⁶ substrates, good to excellent asymmetric induction can be achieved in the cyclization reaction, giving chiral dihydrobenzofurans and indolines. Additionally, the aerobic oxidative cyclization technology has been applied to the total synthesis of numerous of natural products.¹⁷ Within this context, the total synthesis of the crinine-type alkaloids provides an excellent means for advancing our reaction methodology, particularly in the area of asymmetric catalysis.

Scheme A12.8. Asymmetric Aerobic Pd(II)-Catalyzed Wacker-Type Heterocyclizations



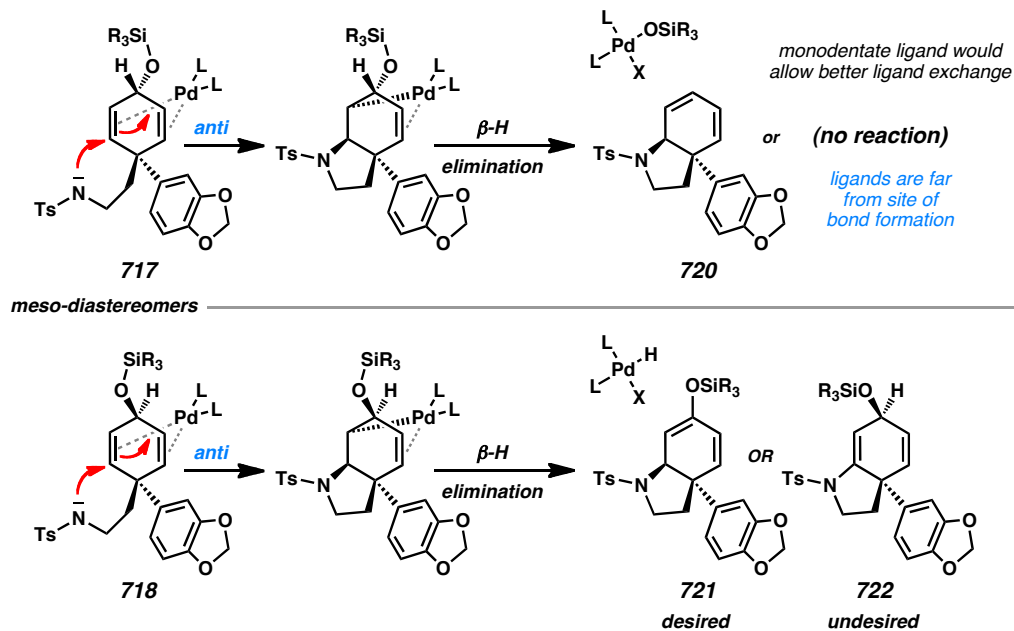
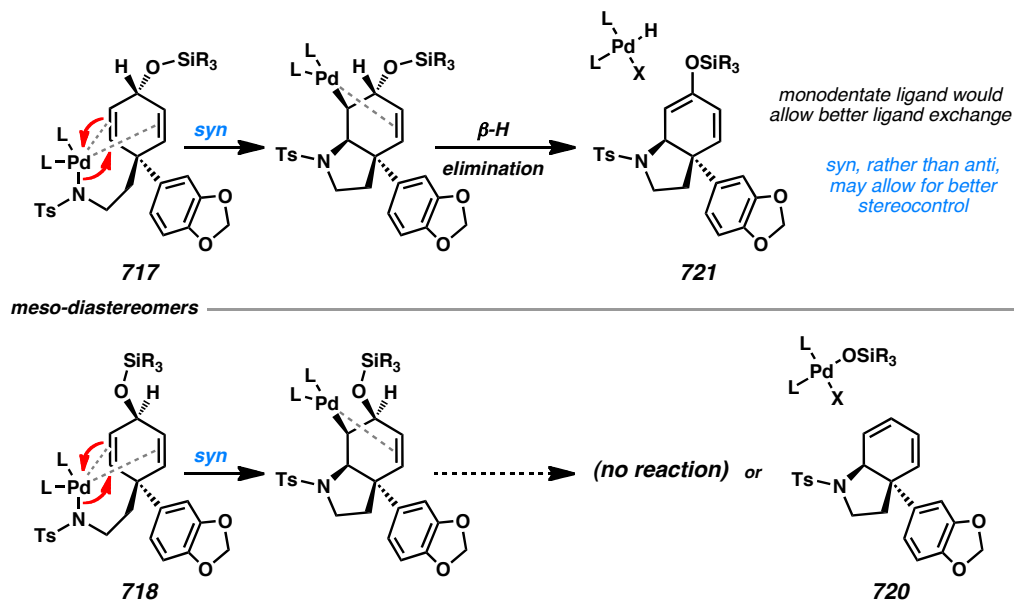
Our oxidative cyclization approach targets pyrrolidiny cyclohexanone **719**, which is based on core structure **684** (Scheme A12.2). A precursor cyclohexanedione **716** can be advanced to 3-substituted 1,4-diene **717** or **718**. These key substrates could lead to the advanced tetracyclic pyrrolidine **719** following a Wacker-type aminocyclization reaction (Scheme A12.9). In contrast to previous oxidative cyclization reactions that have been studied in our group, the primary challenge in this case is the development of a catalyst system that is capable of desymmetrization of C_s symmetric *meso*-substrate **717** or **718**.

Scheme A12.9. Oxidative Cyclization Approach to Crinine



In designing a suitable oxidative cyclization reaction for the total synthesis of crinine and related alkaloids, it will be important to understand stereochemical implications of *syn*- or *anti*-aminopalladation mechanisms. Past studies in our group have shown that cyclizations with alcohols typically proceed through a *syn*-nucleopalladation mechanism, while cyclizations with carboxylates typically proceed through an *anti*-nucleopalladation mechanism.^{15d} Amine nucleophiles, on the other hand, can undergo cyclization through both pathways,¹⁸ making it difficult to predict the stereochemical outcome.

The precise mechanistic pathway is expected to have a significant impact on the stereochemical outcome of the oxidative cyclization reaction with silyloxydiene substrate **717** or **718**, which are *meso*-diastereomers. Depending on the α - or β -orientation of the silyloxy group and the *syn*- or *anti*-aminopalladation mechanism, β -hydride elimination may not be possible in some cases, and both pathways can produce undesired reaction products (Scheme A12.10 and Scheme A12.11).

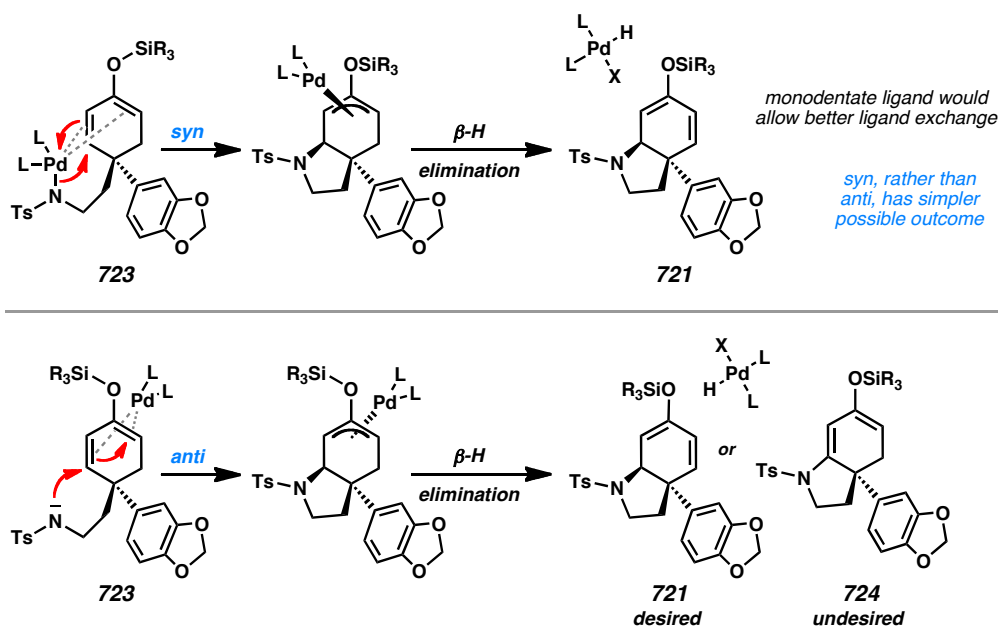
Scheme A12.10. Stereochemical Outcomes of Anti-Aminopalladation with Substrates **717** and **718**Scheme A12.11. Stereochemical Outcomes of Syn-Aminopalladation with Substrates **717** and **718**

An alternative oxidative cyclization substrate is possible if silyl dienol ether **723** is employed as the reaction substrate (Scheme A12.12). In this case, the substrate is a

racemate. From the analysis of the reaction mechanism, it appears that a simpler reaction outcome for this substrate can be expected from a *syn*-aminopalladation pathway as opposed to an *anti*-aminopalladation pathway.

With multiple possible outcomes for each different substrate and mechanism, initial cyclization experiments will provide clues for the dominant pathway. Once a suitable oxidative cyclization reaction is identified for the formation of desired silyl dienol ether **721**, protonation and allylic alcohol formation followed by a Pictet–Spengler cyclization can lead to crinine (**671**) and other target alkaloids.

Scheme A12.12. Stereochemical Outcomes of *Syn* and *Anti*-Aminopalladation with Substrate **723**

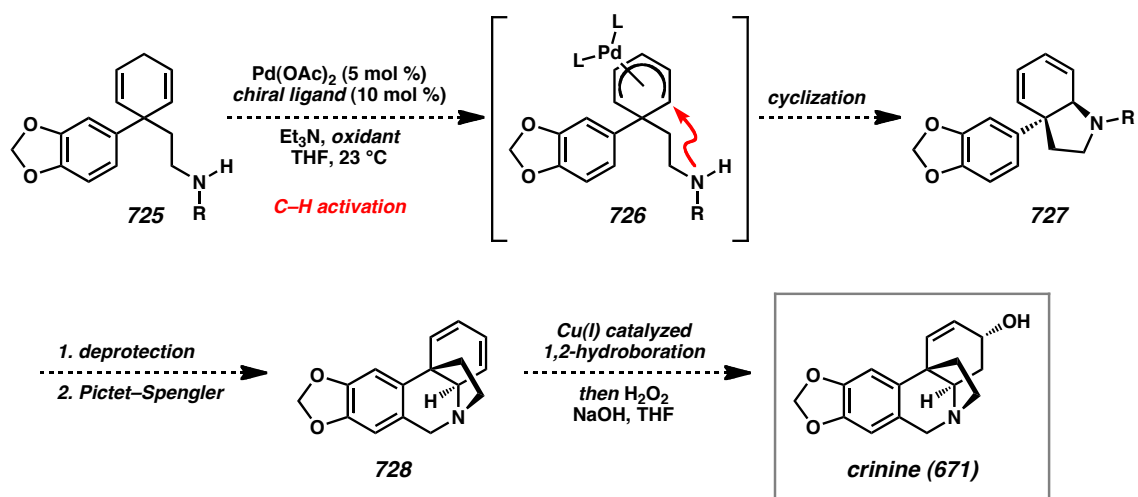


A12.2.4 C–H ACTIVATION/INTRAMOLECULAR AMINATION STRATEGY

As an alternative Pd(II)-catalyzed approach, a C–H activation/*N*-allylation strategy can be employed to construct the desired pyrrolidinyll cyclohexanoid core **684** (Scheme

A12.13). Recently, Trost reported a strategy for the C–H activation of 1,4-dienes followed by nucleophilic attack of the resulting Pd π -allyl species with a carbon nucleophile.¹⁹ Based on this precedent, we reasoned it should be possible to trap allyl electrophile intermediates with pendent amines to form the key pyrrolidine ring as in the oxidative cyclization reactions discussed previously (Section A12.2.3). However, one key difference is that the reaction can be rendered enantioselective under the influence of a suitable chiral ligand. After allylic alkylation by the pendent amine nucleophile, tetracyclic diene **727** can be obtained. After deprotection and Pictet–Spengler cyclization, it should be possible to obtain the core of crinine. In order to advance pentacycle **728** to the natural product, a Cu(I)-catalyzed 1,2-hydroboration of 1,3-dienes can be employed to install the necessary oxidation.²⁰ Following a mild oxidation, it should be possible to obtain crinine in a short sequence of transformations.

Scheme A12.13. C–H Activation/Intramolecular Cyclization Approach to Crinine

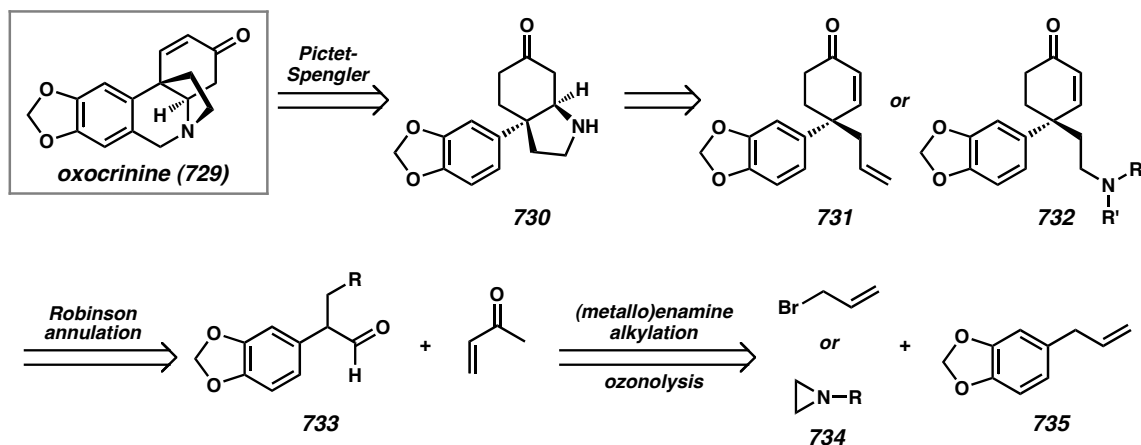


A12.3 PROGRESS TOWARD THE SYNTHESIS OF (±)-OXOCRININE

During our investigations of catalytic enantioselective strategies, we simultaneously sought to develop an efficient route for converting the target α -aryl vinylogous esters to *Amaryllidaceae* alkaloid targets. We chose to pursue oxocrinine²¹ (**729**) because it can be elaborated to numerous crinine derivatives (Scheme A12.1). Initial retrosynthetic disconnection of the target suggested that a late stage Pictet–Spengler reaction could complete the tetrahydroisoquinoline ring. Simplification of the pyrrolidine ring of **730** revealed a γ -aryl cyclohexenone, which can be assembled using a Robinson annulation. Further analysis led to simple aromatic precursors, which can be obtained from readily available commercial compounds.

To lay the foundation for a route toward oxocrinine, we sought to convert intermediate cyclohexenone **731** or the more functionalized amine **732** to the natural product in an efficient manner from simple starting materials. Our synthetic efforts toward both of these intermediates proceeded from inexpensive and commercial safrole (**735**). Notably, this synthetic route can be adapted for the synthesis of maritidine and mesembrine if methyl eugenol (**737**) is used as the aromatic starting material (Scheme A12.1).

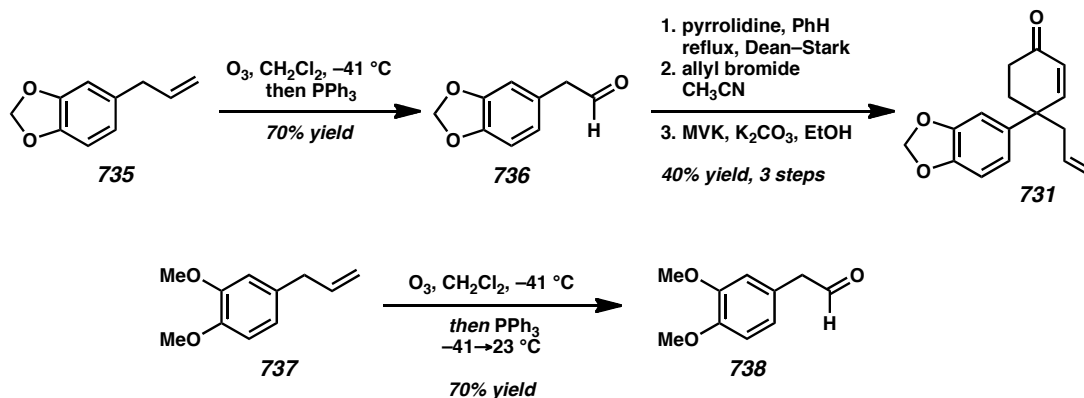
Scheme A12.14. Retrosynthetic Analysis of Oxocrinine



A12.3.1 STORK ENAMINE ALKYLATION ROUTE

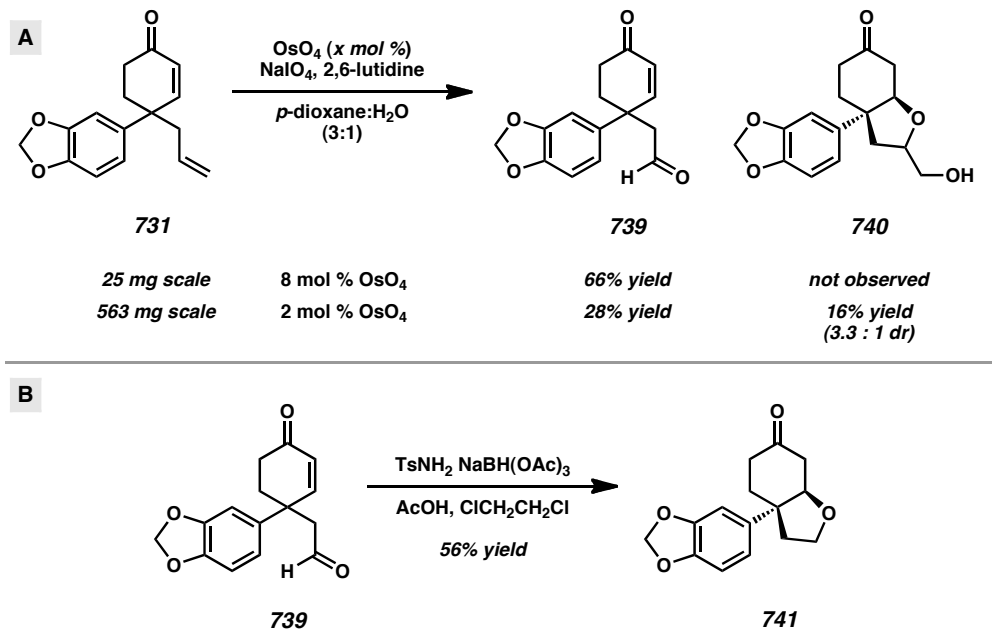
Beginning from safrole (**735**), ozonolysis of the terminal olefin provided aldehyde **736** in 70% yield after distillation (Scheme A12.15). The related ozonolysis of methyl eugenol (**737**) also proceeded efficiently under the same conditions in 70% yield, providing an analogous starting point for the synthesis of maritidine (**674**) and mesembrine (**673**) (Scheme A12.15). Subsequent Stork enamine alkylation and Robinson annulation enabled rapid access to tricyclic enone **731** bearing a γ -quaternary center in 40% yield after three steps. The successful development of an asymmetric α -arylation/ α -allylation reaction would provide material that could enter the synthetic route at this stage of the synthesis (Section A12.2.1).

Scheme A12.15. Stork Enamine Alkylation and Robinson Annulation



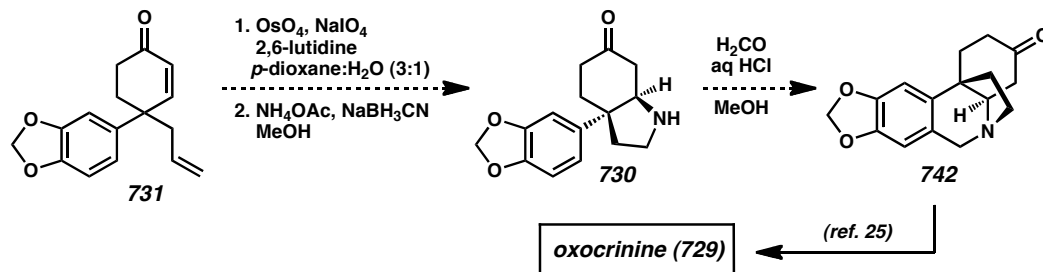
From cyclohexenone **731**, allyl functionalization to a diethylamino side chain was attempted. Using modified Lemieux–Johnson conditions for Os-catalyzed oxidative olefin cleavage,²² we observed different results depending on the scale of the reaction and the catalyst loading (Scheme A12.16A). On a smaller reaction scale with 8 mol % catalyst loading, aldehyde **739** was observed as the sole product in 66% yield. However, when more substrate was used in the presence of 2 mol % OsO₄, the formation of hydroxy tetrahydrofuran **740** was observed in addition to aldehyde **739**. Further optimization will be necessary to both increase the yield of the desired aldehyde **739** while also suppressing the formation of undesired hydroxy tetrahydrofuran **740**. Attempts to perform reductive amination reactions on aldehyde **739** proved unsuccessful as only tetrahydrofuran **741** was observed under several reaction conditions (Scheme A12.16B). The in situ generation of alcohol nucleophiles leads to spontaneous cyclization to form tetrahydrofuran products, as evidenced by the formation of **740** and **741**.

Scheme A12.16. Attempted Allyl Functionalization



While further optimization remains, the allyl group in intermediate **731** can be functionalized to form an aminoethyl side chain and elaborated to pyrrolidinyll cyclohexanone **730** using known transformations of analogous synthetic intermediates in the reported syntheses of mesembrine^{23,24} (Scheme A12.17). The completion of the synthesis can be achieved using a Pictet–Spengler reaction to form the remaining tetrahydroisoquinoline ring system in pentacycle **742**. By employing a known two-step procedure for the desaturation of the cyclohexanone moiety to a cyclohexenone,²⁵ the total synthesis of oxocrinine (**729**) can be completed.

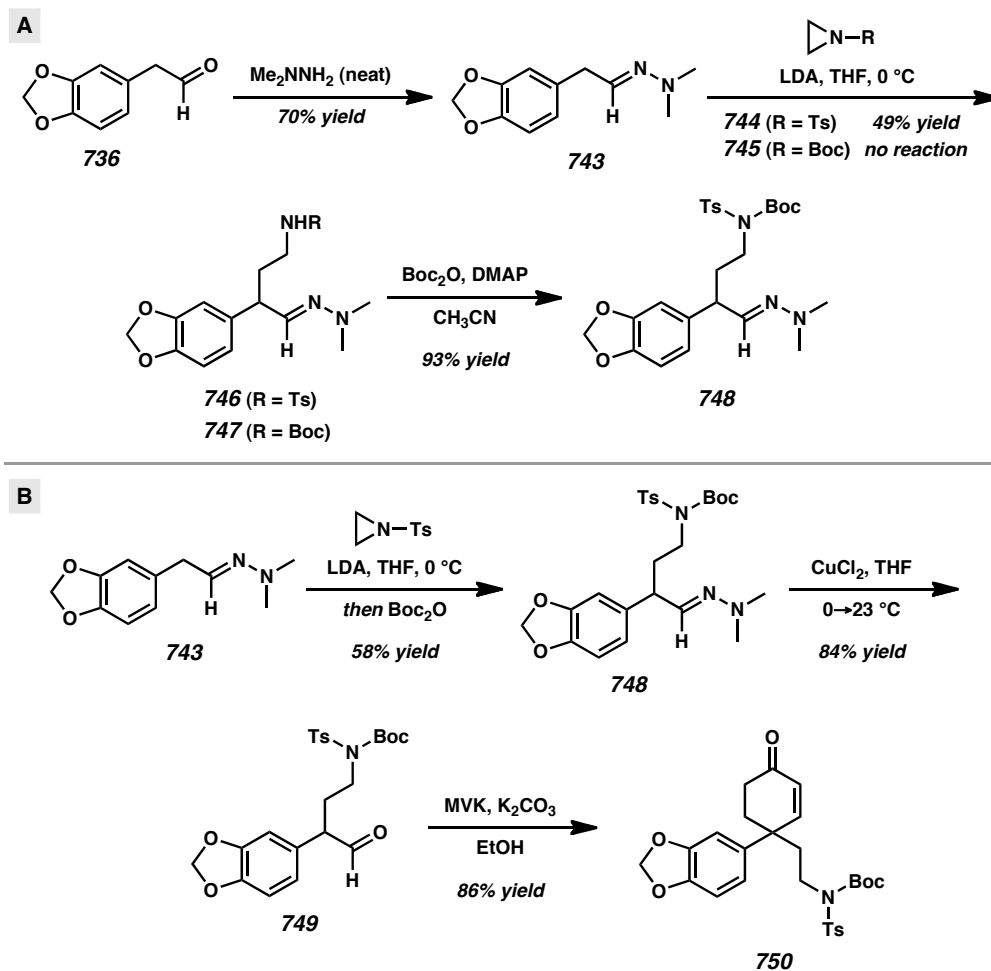
Scheme A12.17. Proposed Completion of (±)-Oxocrinine by Allyl Functionalization



A12.3.2 METALLOENAMINE-MEDIATED AZIRIDINE OPENING ROUTE

An alternative route to oxocrinine was designed to strategically install the ethyl side chain in a higher oxidation state to enable a more convergent synthetic route (Scheme A12.18A). Condensation of aldehyde **736** with *N,N*-dimethylhydrazine enabled formation of hydrazone **743** in 70% yield. Subsequent metalloenamine alkylation with *p*-tosylaziridine²⁶ enabled the formation of tosylamide **746** in 49% yield. Attempts to effect the same reaction with *N*-Boc aziridine (**745**) were unsuccessful. A facile carbamoylation provided doubly-protected amine **748** in 93% yield. To improve the overall efficiency of the reaction sequence, we envisioned that the addition of Boc_2O after metalloenamine alkylation could form *N,N*-Boc-Ts-amine **748** in a single reaction flask (Scheme A12.18B). We were pleased to observe that this was, indeed, the case and we were able to obtain Boc-Ts-amine **748** in 58% yield. A facile hydrolysis of the hydrazone functionality was facilitated by CuCl_2 , giving aldehyde **749** in 84% yield. With aldehyde **749**, Robinson annulation as before (**736**→**731**, Scheme A12.15) smoothly provided cyclohexenone **750** in 86% yield.

Scheme A12.18. Metalloenamine Alkylation Using Aziridines and Amine Carbamoylation



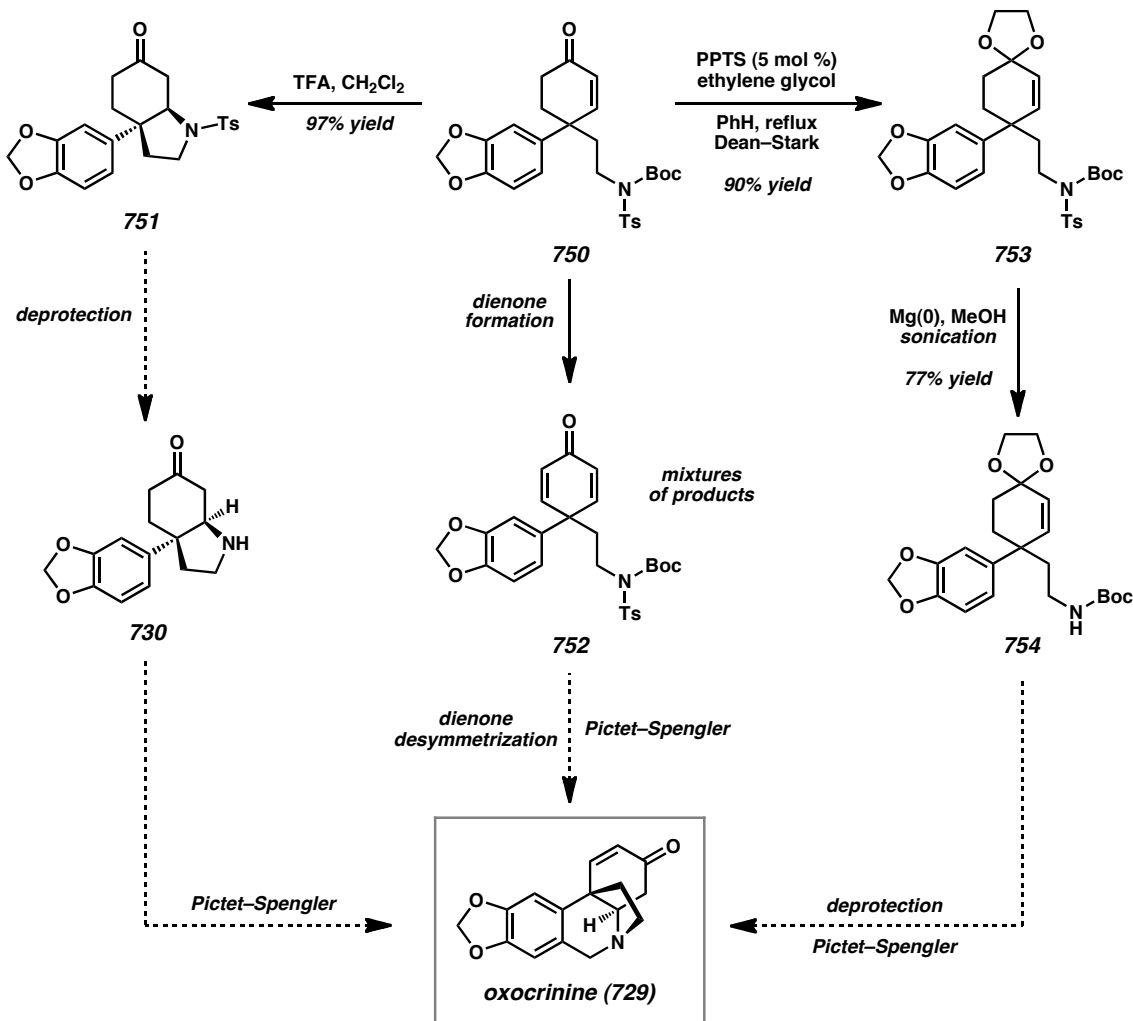
From highly functionalized cyclohexenone **750**, numerous manipulations can provide compounds that can serve as substrates for oxidative cyclization reactions or enable the completion of a synthesis of oxocrinine (Scheme A12.19). Treatment with TFA leads to Boc group removal followed by spontaneous cyclization to *N*-tosylpyrrolidine **751** in 97% yield. Notably, tosylpyrrolidine **751** resembles the tricyclic structure of mesembrine (Scheme A12.1) and possesses 15 of the 16 carbons present in oxocrinine. Attempts to effect tosyl group removal with SmI_2 or lithium naphthalenide have proven unsuccessful so far, but additional conditions can be investigated. To circumvent the deprotection

issues, it may be possible to prepare *o*-nitrophenyl aziridine²⁷ as a more easily deprotected substitute for *p*-tosylaziridine. Once suitable cyclization conditions are found, a precedented Pictet–Spengler reaction can be conducted to complete the pentacyclic core of oxocrinine (**729**).

If manipulations on *N*-tosylpyrrolidine **751** prove challenging, it may be possible to arrive at oxocrinine (**729**) through an alternative reaction sequence. Formation of ketal **753** proceeded smoothly in 90% yield. While Mg(0)-mediated reductive tosyl removal proved unsuccessful for *N*-tosylpyrrolidine **751**, we found that it proceeded smoothly for *N,N*-Boc-Ts-amine **753** in 77% yield. Following a global deprotection and Pictet–Spengler reaction, oxocrinine (**729**) can be obtained. It may even be possible to achieve this transformation in a single reaction flask for maximum efficiency.

A third synthetic route proceeding through the desymmetrization of dienone **752** by an amine nucleophile was also envisioned. The application of Saegusa–Ito reaction conditions to cyclohexenone **750** led to an inseparable mixture of cyclohexadienone **752** and starting material, although this reaction has not been fully optimized.²⁸ An α -bromination/elimination route was also evaluated with trimethylphenylammonium tribromide (PTAB) and DBU, but over-bromination product contaminated the cyclohexadienone **752** that was formed in this manner. Oxidation attempts with IBX and related hypervalent iodine reagents proved unsuccessful. Once a cyclohexanedione such as **752** is obtained and one of the protecting groups is removed, it should be possible to induce an amine conjugate addition/desymmetrization process with a chiral organocatalyst to give the pyrrolidinyl cyclohexanoid core structure **684** (Scheme A12.2).

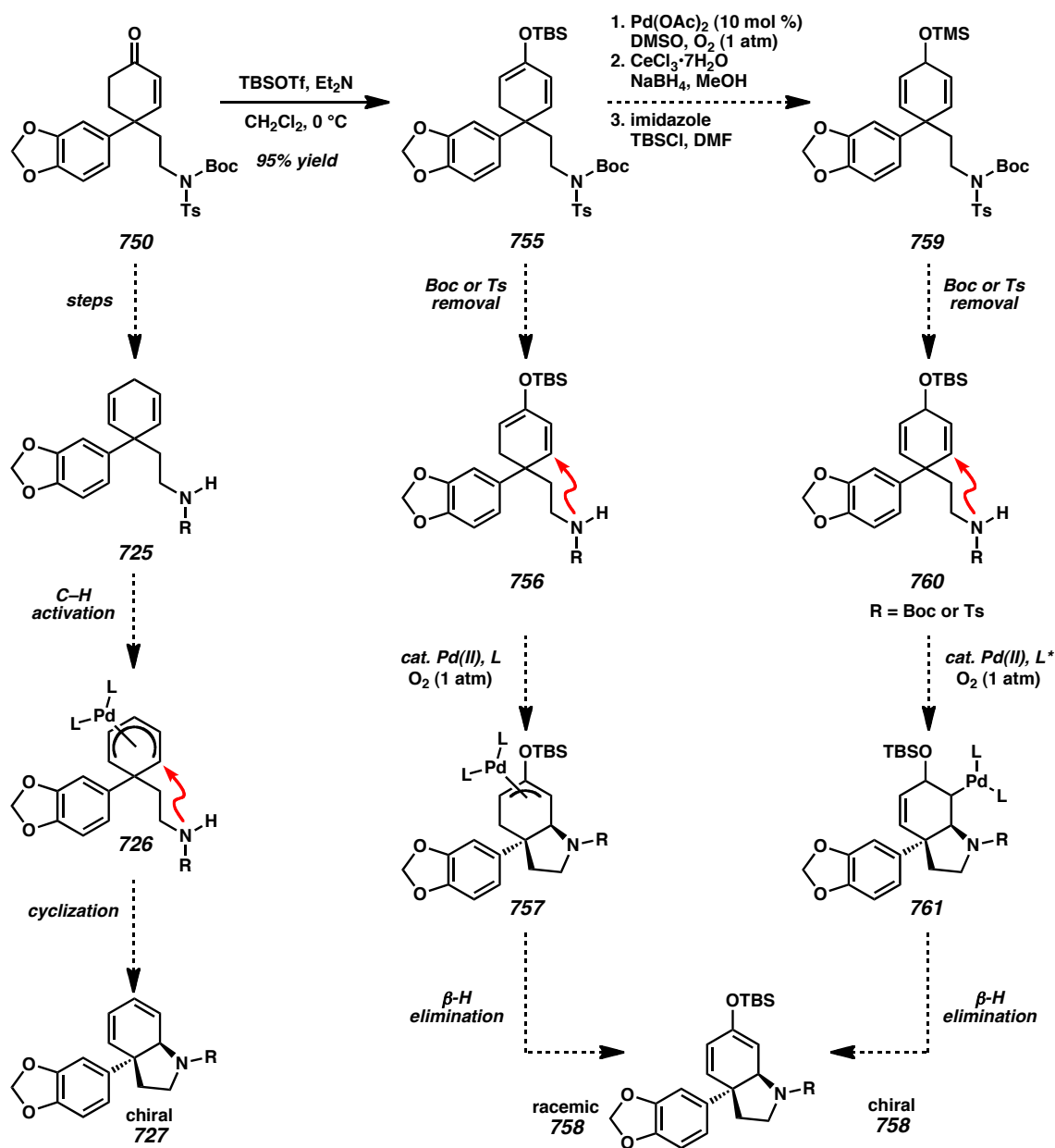
Scheme A12.19. Planned Completion of (±)-Oxocrinine by Pyrrolidine Formation



Additional manipulations of versatile cyclohexenone **750** can enable the synthesis of substrates for stereoselective cyclization reactions (Scheme A12.20). Elaboration to a silyl dienol ether such as **755** can enable the investigation of achiral Pd-catalyzed aerobic oxidative cyclizations (Section A12.2.3). Additionally, Saegusa–Ito oxidation, Luche reduction, and silylation can enable conversion to 3-siloxy-1,4-diene **759**, which can be investigated in oxidative cyclization reactions. Upon formation of pyrrolidinyl cyclohexanone **758**, the remaining ring can be formed in a Pictet–Spengler cyclization.

Another point of entry for an asymmetric synthesis of oxocrinine can be achieved using 1,4-diene **725** (Section A12.2.4). This compound would serve as a C–H activation substrate that would lead to alternative pyrrolidine **727**. Further elaboration of this core can enable the synthesis of oxocrinine in an enantioselective manner.

Scheme A12.20. Synthesis of Oxidative Cyclization and C-H Activation Substrates

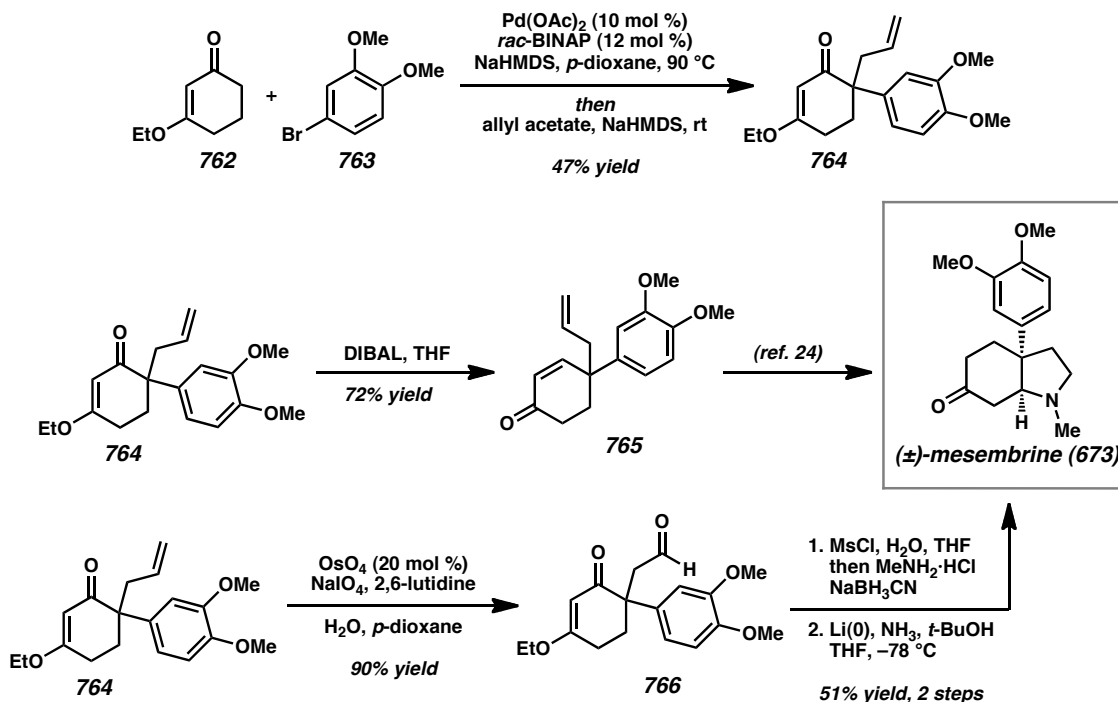


A12.4 RECENT DEVELOPMENTS IN THE TOTAL SYNTHESIS OF CRININE-TYPE AND RELATED AMARYLLIDACEAE ALKALOIDS

During the course of our synthetic investigations, a number of reports in the literature successfully developed new reaction methodology relevant to the key concepts described in our work. Several of the relevant communications are summarized below.

A12.4.1 ZHANG'S Pd-CATALYZED α -ALKYLATION/ α -ARYLATION STRATEGY IN THE TOTAL SYNTHESIS OF (\pm)-MESEMBRINE

After conducting considerable experimentation on our planned α -arylation/ α -allylation reaction, a similar transformation was reported by Zhang and co-workers (Scheme A12.21).²³ As in our strategy (Section A12.2.1), the arylation and allylation transformations were accomplished with a single palladium catalyst to provide cyclic vinylogous esters with α -aryl quaternary centers in yields ranging from 14–72%. Although chiral ligands such as (*R*)-BINAP were screened, ee values greater than 13% could not be achieved. The authors were able to demonstrate the synthetic utility of the method by performing a Stork–Danheiser ketone transposition on the α -aryl vinylogous ester to provide γ -quaternary cyclohexenone **765** that is a known mesembrine synthetic precursor.²⁴ Alternatively, they were able to convert the α -aryl vinylogous ester **764** to mesembrine (**673**) to achieve a five step total synthesis in 22% overall yield. This work demonstrates that concise syntheses of these alkaloids can be accomplished using this α -arylation/ α -allylation approach.

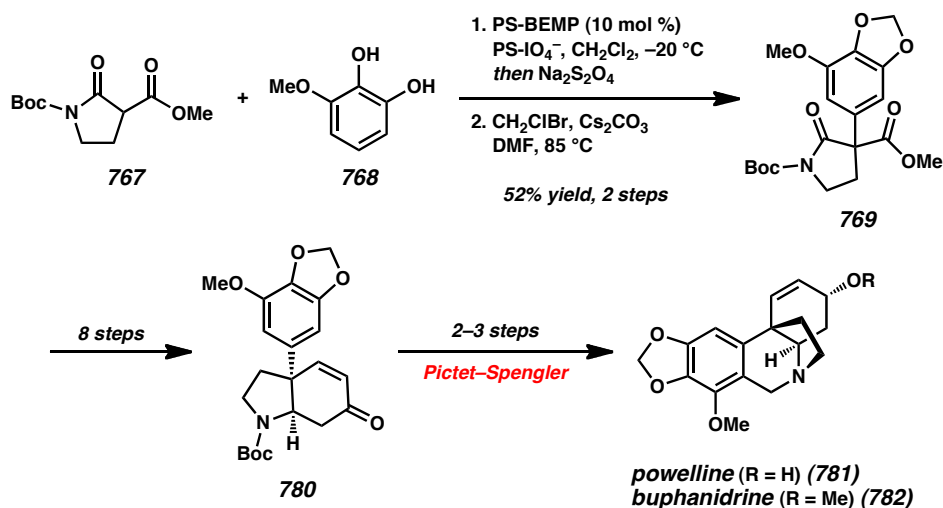
Scheme A12.21. Reported Pd-Catalyzed α -Arylation/ α -Allylation of Vinylogous Esters

Despite this promising recent advance, the development of an efficient enantioselective catalyst system remains a formidable challenge due to the complex, multicomponent nature of the reaction. Future work will seek to identify the optimal palladium precursors and ligands for the desired transformation. Instrumentation for high-throughput reaction screening in the Caltech Center for Catalysis and Chemical Synthesis (3CS) has already enabled the optimization of challenging asymmetric palladium-catalyzed reactions^{4b,29} so we believe that the Symyx Core Module will greatly facilitate the development of a highly enantioselective α -arylation/ α -allylation reaction for the total synthesis of crinine (**671**) and related *Amaryllidaceae* alkaloids.

A12.4.2 DIXON'S SYNTHESSES OF (±)-BUPHANIDRINE AND (±)-POWELLINE BY β -KETOESTER α -ARYLATION

Dixon and co-workers recently developed a synthetic route for the preparation of powelline (**781**) and buphanidrine (**782**), which are crinine derivatives with further aromatic oxidation³⁰ (Scheme A12.22). The key transformation is the organocatalytic oxidative coupling of β -ester lactams and electron-rich arenes to forge the key all-carbon quaternary stereocenter. Polymer-supported phosphazene superbase (PS-BEMP) and iodate are employed in the arylation reaction. Further manipulation leads to pyrrolidinyll cyclohexenone **780**, which resembles our synthetic intermediate **751**. A late-stage Pictet–Spengler provides the target crinine-type alkaloids.

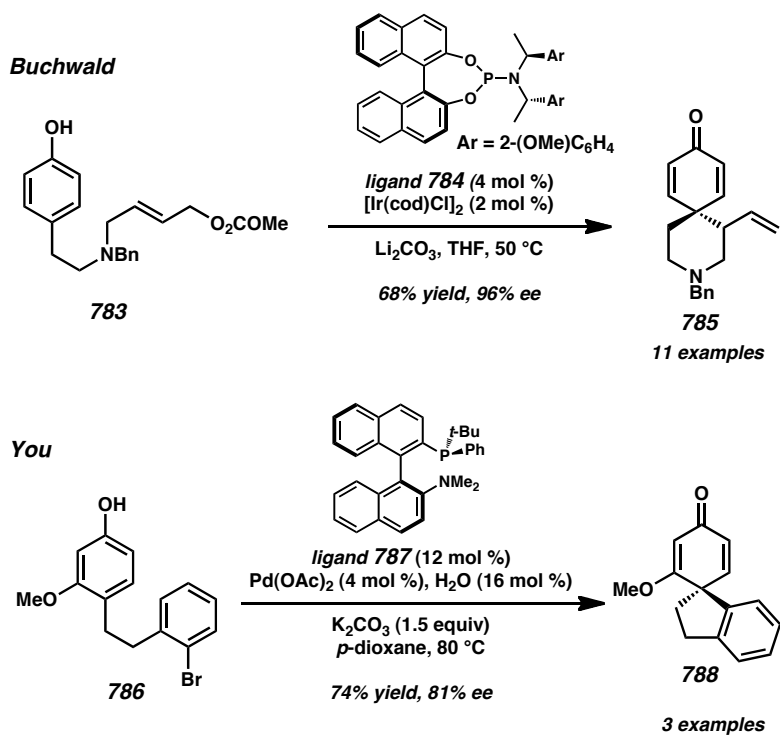
Scheme A12.22. Reported Pd-Catalyzed α -Arylation of β -Ester Lactams



A12.4.3 ENANTIOSELECTIVE ALLYLATIVE DEAROMATIZATION REACTIONS CATALYZED BY PALLADIUM(0) AND IRIIDIUM (I)

Shortly after our preliminary investigations of allylative dearomatization reactions (Section A12.2.2), intramolecular variants were reported independently by Buchwald³¹ and You³² (Scheme A12.23). While the Buchwald group made use of catalytic Pd(0) and an chiral aminophosphine ligand to achieve the dearomatization reaction, the You group employed catalytic Ir(I) and a chiral phosphoramidite to perform the analogous C–C bond formation. Both reports provide multiple examples of successful asymmetric dearomatization reactions.

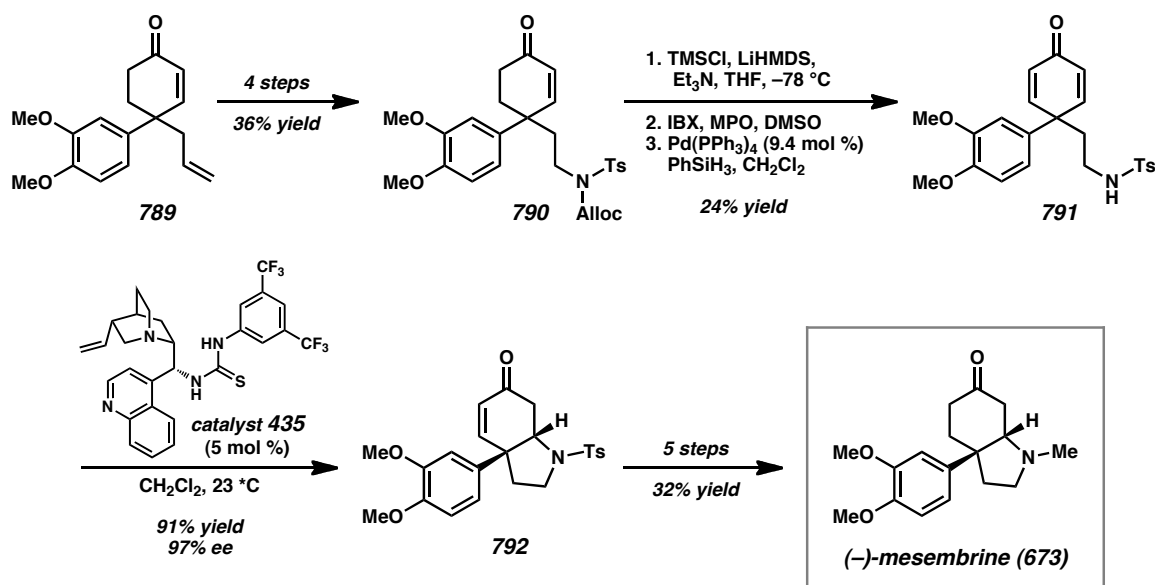
Scheme A12.23. Reported Pd(0) and Ir(I)-Catalyzed Allylative Dearomatization Reactions



A12.4.4 YOU'S ENANTIOSELECTIVE DIENONE DESYMMETRIZATION

A new method for the catalytic, asymmetric desymmetrization of γ -quaternary cyclohexadienones with sulfonamide nucleophiles using *Cinchona* alkaloid catalyst **435** was recently reported by You³³ (Scheme A12.24). The reaction, which displays a wide substrate scope, was successfully applied to the total synthesis of (–)-mesembrine (**673**). Many of the synthetic intermediates, such as γ -allyl γ -aryl cyclohexenone **789**, γ -allyl γ -ethylamino cyclohexenone **790**, and cyclohexadienone **791**, strongly resemble the synthetic intermediates in our synthetic route toward oxocrinine (Section A12.3, c.f. **731**, **750**, and **752**). Cyclohexadienone **789** should be accessible by Stork enamine alkylation and Robinson annulation of aldehyde **738** (Scheme A12.15).

Scheme A12.24. Reported Cyclohexadienone Desymmetrization with Sulfonamide Nucleophiles



A12.5 CONCLUSION

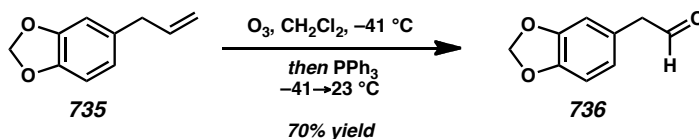
In summary, we have investigated several synthetic strategies employing Pd(0) and Pd(II)-catalysis to prepare of the γ -aryl γ -alkyl cyclohexanone core of crinine (**671**). In particular, we have explored an α -arylation/ α -allylation reaction as well as an allylative dearomatization reaction. For Pd(II)-catalyzed transformations, we have proposed oxidative cyclization and C–H activation routes to access advanced tetracyclic intermediates. While efforts to identify an effective asymmetric transformation is ongoing, we plan to incorporate high-throughput reaction screening into our research efforts to help us identify promising reactions. During our reaction development campaign, we have devised reaction sequences for advancing the anticipated products to the target alkaloids while also pursuing completing the synthesis of (\pm)-oxocrinine (**729**). Current synthetic routes have enabled formation of a substantial portion of the heterocyclic skeleton of crinine (**671**) and related alkaloids from simple, readily available precursors. During our synthetic investigations on these two fronts, recent reports of catalytic transformations have demonstrated the viability of our target-inspired synthetic methods.

A12.6 EXPERIMENTAL SECTION

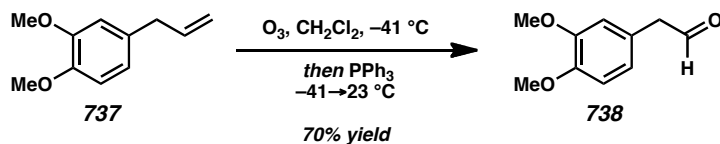
A12.6.1 MATERIALS AND METHODS

Unless otherwise stated, reactions were performed in flame-dried glassware under an argon or nitrogen atmosphere using dry, deoxygenated solvents. Reaction progress was monitored by thin-layer chromatography (TLC). Solvents were dried by passage through an activated alumina column³⁴ under argon. MeOH distilled over Mg(OMe)₂ prior to use. Diisopropylamine was distilled over CaH₂ prior to use. Safrole (**735**) and methyl eugenol (**737**) were purchased from Sigma-Aldrich. Methyl vinyl ketone was distilled prior to use. NaH (60% wt. dispersion in mineral oil) from Sigma-Aldrich was purified by trituration with hexanes under a N₂ atmosphere and removal of residual solvent under vacuum. TBSOTf was prepared according to the procedure of Corey.³⁵ *p*-Tosylaziridine was prepared according to the procedure of Gibson.²⁶ Brine solutions are saturated aqueous solutions of sodium chloride. All other reagents were purchased from Sigma-Aldrich and used as received unless otherwise stated. Sonication was performed using a VWR International Aquasonic Model 75D ultrasonic cleaner. Ozonolysis reactions were performed using an OzoneLab OL80 Desktop Ozone Generator, and oxygen flow was controlled using an OzoneLab Instruments oxygen regulator with a CGA 540 fitting. Reaction temperatures were controlled by an IKAmag temperature modulator. TLC was performed using E. Merck silica gel 60 F254 precoated glass plates (0.25 mm) and visualized by UV fluorescence quenching, *p*-anisaldehyde or KMnO₄ staining. Silicycle SiliaFlash P60 Academic Silica gel (particle size 0.040-0.063 mm) was used for flash chromatography. Automated flash column chromatography was performed on a

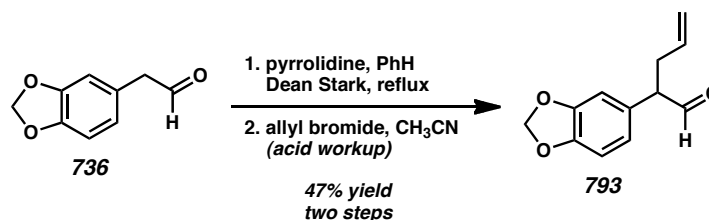
Teledyne Isco CombiFlash R_f system. ^1H NMR spectra were recorded on a Varian Mercury 300 MHz spectrometer (at 300 MHz) and are reported relative to residual CHCl_3 (δ 7.26 ppm). ^{13}C spectra were recorded on a Varian Mercury 300 MHz (at 75 MHz) and are reported relative to CHCl_3 (δ 77.16 ppm). Data for ^1H NMR are reported as follows: chemical shift (δ ppm) (multiplicity, coupling constant (Hz), integration). Multiplicities are reported as follows: s = singlet, d = doublet, t = triplet, q = quartet, m = multiplet, br s = broad singlet, app = apparent. Data for ^{13}C NMR are reported in terms of chemical shifts (δ ppm). IR spectra were obtained by use of a Perkin Elmer Spectrum BXII spectrometer using thin films deposited on NaCl plates and reported in frequency of absorption (cm^{-1}). High-resolution mass spectra (HRMS) were obtained from the Caltech Mass Spectral Facility or on an Agilent 6200 Series TOF with an Agilent G1978A Multimode source in electrospray ionization (ESI+), atmospheric pressure chemical ionization (APCI+), or mixed (MM: ESI-APCI+) ionization mode.

A12.6.2 PREPARATIVE PROCEDURES**A12.6.2.1 SYNTHESIS OF γ -ARYL γ -ALLYL CYCLOHEXENONE 731**

Aldehyde 736. To a 500 mL round bottom flask with magnetic stir bar was added safrole (**737**) (11.84 mL, 80.00 mmol, 1.00 equiv) and CH_2Cl_2 (300 mL). The clear solution was cooled to $-41\text{ }^\circ\text{C}$ using a $\text{CH}_3\text{CN}/\text{CO}_2(\text{s})$ bath. O_2 was bubbled through the reaction mixture for 2 min before ozone generation was turned on (O_2 regulator setting: $1/2\text{ L}\cdot\text{min}^{-1}$, ozonator setting: 10). After 2.5 h min of ozonation, the O_2 was bubbled through the reaction for 30 min. The reaction was quenched with PPh_3 (20.98 g, 80.00 mmol, 1.00 equiv) at $-78\text{ }^\circ\text{C}$. The cooling bath was removed and the flask was allowed to warm to $23\text{ }^\circ\text{C}$ and stir for 1 h. The turbid orange-brown reaction was concentrated under reduced pressure, swirled in 1:1 hexanes: Et_2O , and filtered to remove solids. The filter cake was washed with Et_2O until the filtrate no longer showed product by TLC. The combined filtrate was concentrated under reduced pressure and the filtration process was repeated. The crude material was distilled using a short-path distillation apparatus $130\text{ }^\circ\text{C}$ oil bath ($85\text{ }^\circ\text{C}$, 0.5 mmHg) to give aldehyde **736** (9.16 g, 55.80 mmol, 70% yield) as a pale yellow sap. Data for the compound matches reported data.³⁶

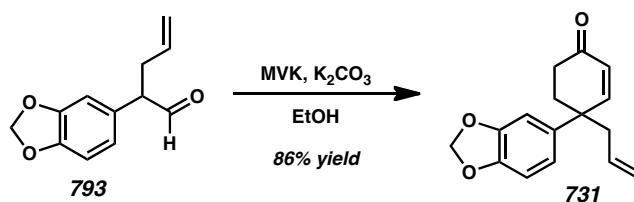


Aldehyde 738. To a 500 mL round bottom flask with magnetic stir bar was added methyl eugenol (**737**) (27.53 mL, 160.00 mmol, 1.00 equiv) and CH_2Cl_2 (300 mL). The clear solution was cooled to $-41\text{ }^\circ\text{C}$ using a $\text{CH}_3\text{CN}/\text{CO}_2(\text{s})$ bath. O_2 was bubbled through the reaction mixture for 2 min before ozone generation was turned on (O_2 regulator setting: $1/2\text{ L}\cdot\text{min}^{-1}$, ozonator setting: 10). After 16 h min of ozonation, the O_2 was bubbled through the reaction for 30 min. Me_2S (11.75 mL, 160.00 mmol, 1.00 equiv) was added at $-78\text{ }^\circ\text{C}$. The cooling bath was removed and the flask was allowed to warm to $23\text{ }^\circ\text{C}$ and stir for 18 h, but incomplete conversion of ozonide was observed. The reaction was quenched with PPh_3 (41.96 g, 160.00 mmol, 1.00 equiv). The turbid orange-brown reaction was concentrated under reduced pressure and partitioned between H_2O and EtOAc . The combined organic phases were dried over Na_2SO_4 , filtered, and concentrated under reduced pressure. The crude residue was purified by flash column chromatography (SiO_2 , $5 \times 25\text{ cm}$, $2\% \rightarrow 10\% \rightarrow 20\% \rightarrow 30\% \rightarrow 50\%$ Et_2O in hexanes). The material was further purified by distillation using a short-path distillation apparatus $140\text{ }^\circ\text{C}$ oil bath ($100\text{ }^\circ\text{C}$, 0.5 mmHg) to give aldehyde **738** (8.974 g, 49.80 mmol, 731% yield) as a pale yellow sap. Data for the compound matches reported data.³⁷

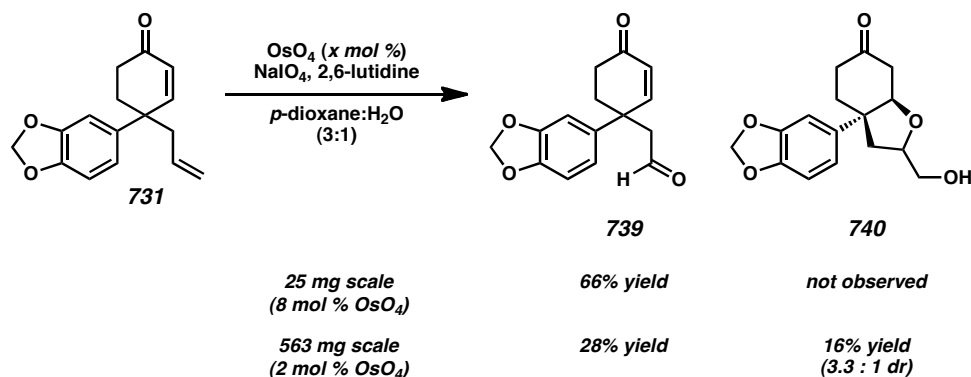


α -Allyl Aldehyde 793. To a 50 mL round-bottom flask with magnetic stir bar was added aldehyde **736** (164 mg, 1.00 mmol, 1.00 equiv), pyrrolidine (167 μ L, 2.00 mmol, 2.00 equiv), and benzene (5 mL). A Dean–Stark trap and reflux condenser connected to a N₂ inlet was attached and the flask was immersed in a 100 °C oil bath. After 5 h of stirring, the reaction was cooled to 23 °C and the Dean–Stark trap was replaced with a septum, minimizing exposure to air and moisture. The reaction was concentrated under reduced pressure (ca. 15 mmHg) in a 50 °C oil bath. The resulting yellow-orange solid was redissolved in anhydrous CH₃CN (5 mL) and concentrated under reduced pressure (ca. 15 mmHg) in a 50 °C oil bath (3 x). The reaction was cooled to 23 °C and CH₃CN (10 mL) was added. Allyl bromide was slowly added dropwise, giving a brown mixture. After 15 h of stirring, the reaction was concentrated under reduced pressure and taken up in H₂O. The aqueous mixture was extracted with EtOAc (3 x 5 mL). The aqueous layer was acidified to pH = 4 with 1 M aqueous AcOH. The acidified aqueous phase was extracted with EtOAc (3 x 5 mL). The combined organic phases were dried over Na₂SO₄, filtered, and concentrated under reduced pressure. The brown residue was purified by automated flash column chromatography using a Teledyne Isco CombiFlash R_f (SiO₂, 5 g loading cartridge, 24 g column, 0%→10%→20% EtOAc in hexanes) to afford α -allyl aldehyde **793** (95.4 mg, 0.47 mmol, 47% yield over two steps); ¹H NMR (300 MHz, CDCl₃) δ 9.64 (d, *J* = 1.7 Hz, 1H), 6.89–6.76 (m, 1H), 6.70–6.60 (m, 2H), 5.97 (s, 2H), 5.71 (ddt, *J*

= 17.1, 10.3, 6.9 Hz, 1H), 5.12–4.95 (m, 2H), 3.52 (ddd, J = 8.3, 6.7, 1.7 Hz, 1H), 2.79 (dt, J = 14.8, 6.8, 1.3 Hz, 1H), 2.44 (dddt, J = 14.7, 8.1, 6.8, 1.3 Hz, 1H).



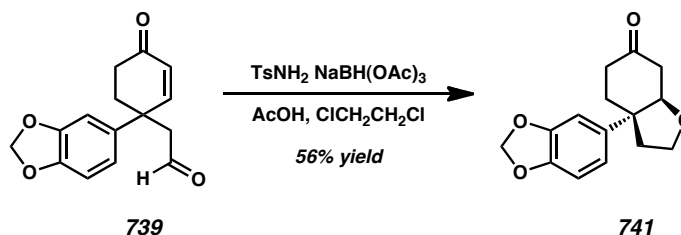
γ -Aryl γ -Allyl Cyclohexenone **731.** To a 100 mL round bottom flask with magnetic stir bar was added α -allyl aldehyde **793** (520 mg, 2.55 mmol, 1.00 equiv) and EtOH (50 mL). The reaction was cooled to 0 °C using an ice/water bath. Methyl vinyl ketone (507 μ L, 5.09 mmol, 2.00 equiv) was added dropwise, followed by portionwise addition of K_2CO_3 (3.52 g, 25.46 mmol, 10.00 equiv). The reaction was allowed to warm to 23 °C and stirred for 4.5 h. The reaction was passed through a plug of Celite and concentrated under reduced pressure. The brown residue was purified by automated flash column chromatography using a Teledyne Isco CombiFlash R_f (SiO_2 , 12 g loading cartridge, 120 g column, 0% \rightarrow 10% \rightarrow 20% EtOAc in hexanes) to give γ -aryl γ -allyl cyclohexenone **731** (563 mg, 2.20 mmol, 86% yield); 1H NMR (300 MHz, $CDCl_3$) δ 7.03 (dd, J = 10.3, 1.2 Hz, 1H), 6.87–6.62 (m, 3H), 6.15 (d, J = 10.3 Hz, 1H), 5.96 (s, 2H), 5.56 (dddd, J = 16.4, 10.3, 8.4, 5.9 Hz, 1H), 5.13–5.03 (m, 2H), 2.66 (ddt, J = 14.1, 5.8, 1.5 Hz, 1H), 2.45 (dd, J = 14.1, 8.5 Hz, 1H), 2.39–2.11 (m, 4H).



Aldehyde 739 (25 mg scale, 8 mol % OsO₄).²² To a 1 dram vial with magnetic stir bar was added γ -aryl γ -allyl cyclohexenone **731** (25.2 mg, 0.098 mmol, 1.00 equiv), *p*-dioxane (0.75 mL), and H₂O (0.25 mL). The reaction was cooled to 0 °C with an ice/water bath. 2,6-Lutidine (22.9 μ L, 0.1966 mmol, 2.00 equiv) was added and the reaction was stirred for 10 min. NaIO₄ (84 mg, 0.3933 mmol, 4.00 equiv) was added, followed by OsO₄ (2.0 mg, 0.0079 mmol, 8 mol %). The reaction mixture was stirred at 0 °C. After 20 min of stirring, the reaction became a thick white slurry. After 5 h of stirring, the reaction was diluted with H₂O (2 mL) and passed through a plug of silica gel, eluting with EtOAc. The biphasic mixture was separated and the aqueous layer was extracted with EtOAc (3 x 5 mL). The combined organic phases were dried over Na₂SO₄, filtered, and concentrated under reduced pressure. The residue was purified by flash column chromatography (SiO₂, 1 x 20 cm, 4:1→3:1→2:1→1:1 EtOAc in hexanes) to give aldehyde **739** (16.7 mg, 0.067 mmol, 66% yield).

Aldehyde 739 (25 mg scale, 2 mol % OsO₄).²² To a 100 mL round-bottom flask with magnetic stir bar was added γ -aryl γ -allyl cyclohexenone **731** (563 mg, 2.20 mmol, 1.00 equiv), *p*-dioxane (16.5 mL), and H₂O (5.5 mL). The reaction was cooled to 0 °C with an ice/water bath. 2,6-Lutidine (471 μ L, 471 mmol, 2.00 equiv) was added and the reaction

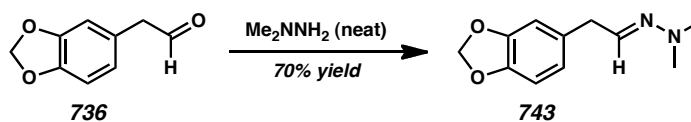
was stirred for 10 min. NaIO₄ (1.88 g, 8.80 mmol, 4.00 equiv) was added, followed by OsO₄ (11.18 mg, 0.044 mmol, 2 mol %). The reaction mixture was stirred at 0 °C. After 20 min of stirring, the reaction became a thick white slurry. After 5 h of stirring, the reaction was diluted with H₂O (2 mL) and passed through a plug of Celite, eluting with EtOAc. The biphasic mixture was separated and the aqueous layer was extracted with EtOAc. The biphasic mixture was separated and the aqueous layer was extracted with EtOAc (3 x 10 mL). The combined organic phases were dried over Na₂SO₄, filtered, and concentrated under reduced pressure. The residue was purified by automated flash column chromatography using a Teledyne Isco CombiFlash R_f (SiO₂, 5 g loading cartridge, 40 g column, 0%→30%→60%→80% EtOAc in hexanes) to give aldehyde **739** (160 mg, 0.622 mmol, 28% yield) and alcohol **740** (101.4 mg, 0.349 mmol, 16% yield, 3.3:1 dr); ¹H NMR (300 MHz, CDCl₃) δ 9.64 (t, *J* = 2.4 Hz, 1H), 7.14 (dd, *J* = 10.3, 1.1 Hz, 1H), 6.91–6.71 (m, 3H), 6.20 (d, *J* = 10.2 Hz, 1H), 5.96 (s, 2H), 3.00 (dd, *J* = 16.0, 2.1 Hz, 1H), 2.82 (dd, *J* = 16.0, 2.6 Hz, 1H), 2.54–2.16 (m, 4H).



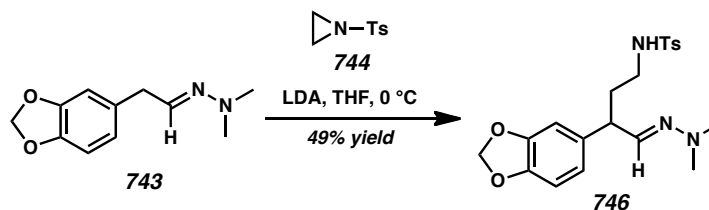
Tetrahydrofuran 741. To a 1 dram vial with magnetic stir bar was added aldehyde **739** (8.3 mg, 0.03 mmol, 1.00 equiv), tosylamide (5.14 mg, 0.03 mmol, 1.00 equiv) and 1,2-dichloroethane (0.5 mL). AcOH (5.2 μL, 0.09 mmol, 3.00 equiv), NaBH(OAc)₃ (12.7 mg, 0.06 mmol, 2.00 equiv), and additional 1,2-dichloroethane (0.5 mL) were added. After 40 h of stirring, the reaction was quenched with sat. aqueous NaHCO₃ and extracted with CH₂Cl₂ (3 x 2 mL). The combined organic phases were dried over

Na₂SO₄, filtered, and concentrated under reduced pressure. The residue was purified by preparatory TLC (SiO₂, 3:1 hexanes:EtOAc) to give tetrahydrofuran **741** (4.4 mg, 0.0169 mmol, 56% yield); ¹H NMR (300 MHz, CDCl₃) δ 6.87 (t, *J* = 1.2 Hz, 1H), 6.85–6.75 (m, *J* = 1.2 Hz, 2H), 5.97 (s, 2H), 4.49 (ddd, *J* = 3.9, 2.8, 1.0 Hz, 1H), 4.03 (dt, *J* = 8.8, 7.4 Hz, 1H), 3.92–3.81 (m, 1H), 2.83–2.72 (m, 1H), 2.66 (dd, *J* = 16.6, 4.1 Hz, 1H), 2.40–2.09 (m, 6H).

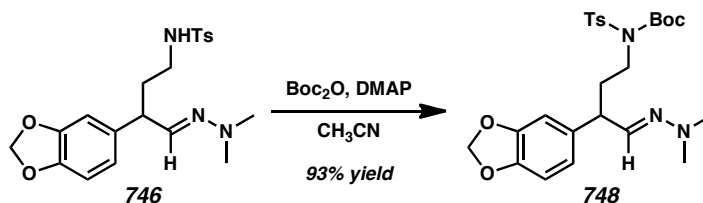
A12.6.2.2 SYNTHESIS OF γ -ARYL γ -ETHYLAMINO CYCLOHEXENONE **750**



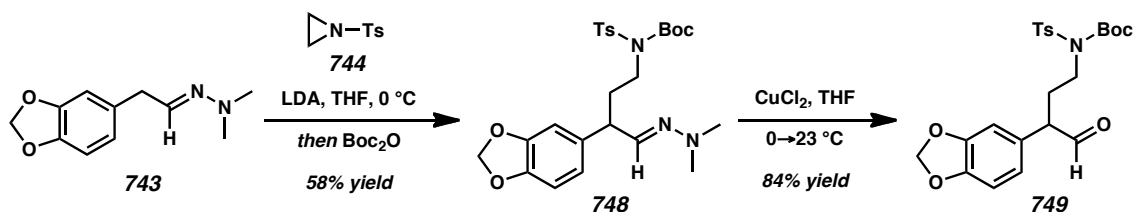
Hydrazone 743. To a 25 mL round-bottom flask with magnetic stir bar was added *N,N*-dimethylhydrazine (1.39 mL, 18.27 mmol, 3.00 equiv) and aldehyde **736** (1.0 g, 6.09 mmol, 1.00 equiv). A reflux condenser was attached and the reaction was heated to reflux. The orange solution was stirred for 6.5 h. H₂O (5 mL) was added and the mixture was extracted with Et₂O (4 x 10 mL). The combined organic phases were dried over MgSO₄, filtered, and concentrated under reduced pressure. The residue was purified by flash column chromatography (SiO₂, 2 x 25 cm, 6:1→4:1→2:1 EtOAc in hexanes) to give hydrazone **743** (0.874 g, 4.24 mmol, 70% yield) as a yellow liquid. Data for the compound matches reported data.³⁸



Sulfonamide 746. A solution of LDA in THF (0.5 M) was prepared and kept at 0 °C under N₂. A portion of this solution (3.4 mL, 1.70 mmol, 1.50 equiv) was added to a 50 mL round-bottom flask with magnetic stir bar at 0 °C under N₂. Hydrazone **743** (334 mg, 1.62 mmol, 1.00 equiv) was added to the LDA solution dropwise at 0 °C and stirred for 1 h to give a red-brown solution. *p*-Tosylaziridine²⁶ (320 mg, 1.62 mmol, 1.00 equiv) in a THF (1 mL) in a 1 dram vial under N₂ was drawn up in a syringe and added to the reaction dropwise. The reaction was stirred at 0 °C. After 2 h of stirring, the reaction was warmed to 23 °C and stirred for an additional 2 h. The reaction was quenched with NH₄Cl and extracted with CH₂Cl₂ (3 x 10 mL). The combined organic phases were dried over Na₂SO₄, filtered, and concentrated under reduced pressure. The residue was purified by flash column chromatography (deactivated SiO₂, 2 x 25 cm, 1:2 pentane:Et₂O with 5% Et₃N→1:3 pentane:Et₂O with 5% Et₃N→1:4 pentane:Et₂O with 5% Et₃N) to give sulfonamide **746** (323 mg, 0.80 mmol, 49% yield) as a brown gel; ¹H NMR (300 MHz, CDCl₃) δ 7.70 (d, *J* = 8.3 Hz, 2H), 7.28 (d, *J* = 7.9 Hz, 2H), 6.69 (d, *J* = 7.8 Hz, 1H), 6.62–6.44 (m, 3H), 5.92 (s, 2H), 5.27 (t, *J* = 5.9 Hz, 1H), 3.41 (dt, *J* = 8.1, 5.8 Hz, 1H), 2.94 (qd, *J* = 6.3, 3.3 Hz, 2H), 2.73 (s, 6H), 2.42 (s, 3H), 2.00 (ddt, *J* = 14.5, 8.2, 6.3 Hz, 1H), 1.85 (dq, *J* = 13.4, 6.5 Hz, 1H).



***N*-Boc Sulfonamide 748.** To a 25 mL round-bottom flask with magnetic stir bar was added hydrazone **746** (10 mg, 0.025 mmol, 1.00 equiv), CH₃CN (1 mL), and DMAP (1.22 mg, 0.005 mmol, 0.40 equiv). The reaction was stirred for 13 h and additional DMAP (1.22 mg, 0.005 mmol, 0.40 equiv) was added. After 10 min of stirring, the reaction was concentrated under reduced pressure, quenched with sat. aqueous NaHCO₃ and extracted with EtOAc (3 x 2 mL). The combined organic phases were dried over Na₂SO₄, filtered, and concentrated under reduced pressure. The residue was purified by flash column chromatography (SiO₂, 1 x 20 cm, 4:1 hexanes:EtOAc) to give *N*-Boc sulfonamide **748** (11.7 mg, 0.23 mmol, 93% yield); ¹H NMR (300 MHz, CDCl₃) δ 7.75 (d, *J* = 8.4 Hz, 2H), 7.27 (d, *J* = 8.4 Hz, 2H), 6.79–6.67 (m, 3H), 6.59 (d, *J* = 6.0 Hz, 1H), 5.92 (s, 2H), 3.86 (ddd, *J* = 14.2, 10.9, 5.0 Hz, 1H), 3.71 (ddd, *J* = 14.3, 10.7, 5.4 Hz, 1H), 3.47 (td, *J* = 7.5, 5.9 Hz, 1H), 2.75 (s, 6H), 2.42 (s, 3H), 2.39–2.04 (m, 2H), 1.31 (s, 9H); ¹³C NMR (75 MHz, CDCl₃) δ 150.9, 148.0, 146.4, 144.1, 139.0, 137.6, 136.1, 129.3, 127.9, 120.9, 108.5, 108.2, 101.0, 84.1, 46.7, 45.9, 43.3, 34.4, 28.0, 21.7.

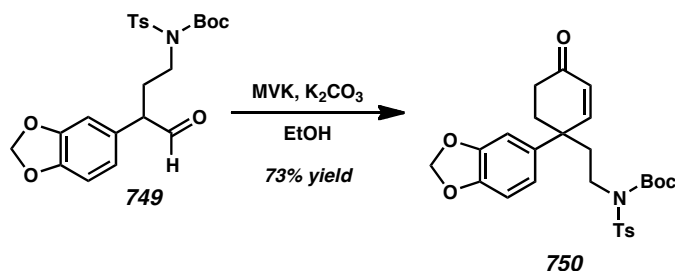


Hydrazone 748. To a 100 mL round-bottom flask with magnetic stir bar under N₂ was added THF (12 mL). The flask was cooled to 0 °C using an ice/water bath and *N,N*-

diisopropylamine (284 μL , 2.74 mmol, 1.05 equiv) was added, followed by dropwise addition of *n*-BuLi solution in hexanes (2.51 M, 1.04 mL, 2.01 mmol, 1.00 equiv). The mixture was stirred at 0 °C for 15 min. Hydrazone **746** (539 mg, 2.61 mmol, 1.00 equiv) in THF (4 mL) in a 10 mL conical flask was added to the reaction dropwise by positive pressure cannulation. The reaction was stirred at 0 °C for 1 h. *p*-Tosylaziridine²⁶ (515 mg, 2.61 mmol, 1.00 equiv) in THF (4 mL) in a 10 mL conical flask was added to the reaction dropwise by positive pressure cannulation. The reaction was stirred at 0 °C for 2 h. Boc₂O (1.71 mg, 7.83 mmol, 3.00 equiv) in THF (6 mL) in a 25 mL conical flask was added to the reaction dropwise by positive pressure cannulation. The reaction was stirred at 0 °C for 30 min. The reaction was quenched with brine (10 mL) and extracted with Et₂O (3 x 25 mL). The combined organic phases were dried over Na₂SO₄, filtered, and concentrated under reduced pressure. The residue was purified by flash column chromatography (SiO₂, 3 x 22 cm, 5:1→3:1→1:1 hexanes:Et₂O) to give hydrazone **748** (760 mg, 1.51 mmol, 58% yield).

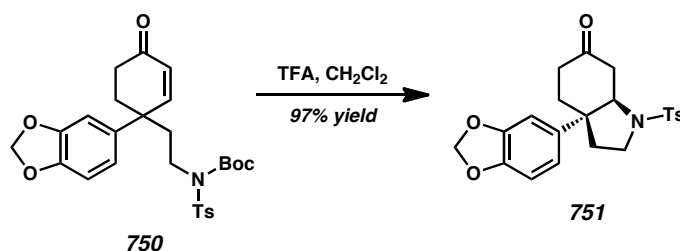
Aldehyde 749. To a 50 mL round-bottom flask with magnetic stir bar was added *N,N*-Boc-Ts hydrazone **748** (760 mg, 1.51 mmol, 1.00 equiv) and THF (15 mL). The yellow solution was cooled to 0 °C. CuCl₂ (244 mg, 1.81 mmol, 1.20 equiv) was dissolved in H₂O (1.81 mL) and added to the hydrazone solution dropwise. After 7 h, the reaction was diluted with Et₂O and treated with NH₄OH until the aqueous layer became dark blue. The mixture was extracted with Et₂O (3 x 25 mL). The combined organic phases were dried over Na₂SO₄, filtered, and concentrated under reduced pressure. The residue was taken up in Et₂O and passed through a short plug of silica gel, eluting with Et₂O. The

filtrate was concentrated under reduced pressure and the residue was purified by flash column chromatography (SiO₂, 2 x 25 cm, 4:1 hexanes:EtOAc) to give aldehyde **749** (586 mg, 1.27 mmol, 84% yield); ¹H NMR (300 MHz, CDCl₃) δ 9.63 (d, *J* = 1.3 Hz, 1H), 7.75 (d, *J* = 8.4 Hz, 2H), 7.29 (dd, *J* = 8.7, 0.7 Hz, 2H), 6.82 (d, *J* = 8.4 Hz, 1H), 6.72–6.65 (m, 2H), 5.97 (s, 2H), 3.96–3.65 (m, 2H), 3.64–3.51 (m, 1H), 2.59–2.36 (m, 1H), 2.44 (s, 3H), 2.23–1.99 (m, 1H), 1.32 (s, 9H); ¹³C NMR (75 MHz, CDCl₃) δ 199.2, 151.0, 148.6, 147.5, 144.4, 137.3, 129.4, 128.7, 127.9, 122.5, 109.1, 109.0, 101.4, 84.6, 56.2, 45.4, 29.9, 28.0, 21.8.



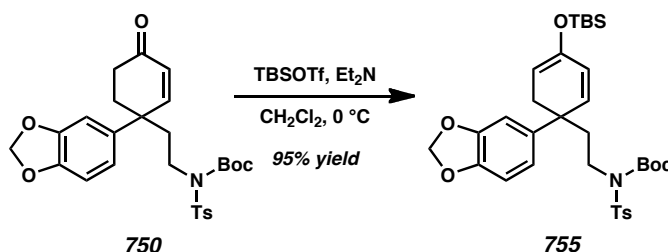
γ -Aryl γ -Ethylamino Cyclohexenone 750. To a 50 mL round bottom flask with magnetic stir bar was added α -allyl aldehyde **749** (252 mg, 0.546 mmol, 1.00 equiv) and EtOH (6 mL). The reaction was cooled to 0 °C using an ice/water bath. Methyl vinyl ketone (109 μ L, 1.093 mmol, 2.00 equiv) was added dropwise, followed by portionwise addition of K₂CO₃ (755 mg, 5.46 mmol, 10.00 equiv). The reaction was allowed to warm to 23 °C and stirred for 10.5 h. The reaction was diluted with EtOAc (6 mL) and passed through a plug of Celite, eluting with EtOAc. The filtrate was concentrated under reduced pressure. The residue was purified by flash column chromatography (SiO₂, 2.5 x 25 cm, 1:0→2:1→1:1 hexanes:Et₂O) to give γ -aryl γ -ethylamino cyclohexenone **750** (204 mg, 0.398 mmol, 73% yield) as a white foam; ¹H NMR (300 MHz, CDCl₃) δ 7.71 (d, *J* =

8.4 Hz, 2H), 7.27 (d, $J = 8.9$ Hz, 2H), 7.17 (dd, $J = 10.3, 1.3$ Hz, 1H), 6.87 (t, $J = 1.2$ Hz, 1H), 6.78 (d, $J = 1.1$ Hz, 2H), 6.20 (d, $J = 10.2$ Hz, 1H), 5.96 (s, 2H), 3.76 (ddd, $J = 14.2, 11.9, 4.5$ Hz, 1H), 3.63 (ddd, $J = 14.2, 11.3, 5.4$ Hz, 1H), 2.42 (s, 3H), 2.40–2.12 (m, 6H), 1.41–1.24 (m, 9H); ^{13}C NMR (75 MHz, CDCl_3) δ 199.3, 154.1, 150.8, 148.4, 146.7, 144.4, 137.3, 136.0, 130.1, 129.4, 127.8, 120.2, 108.3, 107.3, 101.3, 84.6, 43.6, 43.0, 41.2, 36.5, 34.4, 28.0, 21.7; IR (Neat Film NaCl) 3369, 2979, 2930, 1726, 683, 1598, 1505, 1487, 1456, 1435, 1394, 1352, 1281, 1243, 1186, 1157, 1141, 1088, 1039, 990, 936, 919, 864, 850, 813, 772, 728, 720 cm^{-1} .



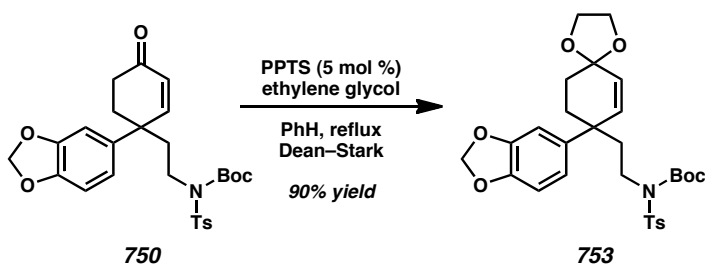
Tosylpyrrolidine 751. To a 20 mL scintillation vial with magnetic stir bar was added γ -aryl γ -ethylamino cyclohexenone **750** (60 mg, 0.117 mmol, 1.00 equiv), CH_2Cl_2 (1.2 mL) and trifluoroacetic acid (120 μL). The reaction turned orange upon addition of acid. After 24 h of stirring, additional trifluoroacetic acid (360 μL) was added. After an addition 10 min of stirring, the reaction was concentrated under reduced pressure. The material was purified by flash column chromatography (SiO_2 , 2 x 25 cm, 2:1 \rightarrow 1:1 hexanes:EtOAc) to give tosylpyrrolidine **751** (47.1 mg, 0.1139 mmol, 97% yield) as a white solid; ^1H NMR (300 MHz, CDCl_3) δ 7.64 (d, $J = 8.3$ Hz, 2H), 7.25 (d, $J = 7.4$ Hz, 2H), 6.58 (d, $J = 8.2$ Hz, 1H), 6.52 (d, $J = 2.0$ Hz, 1H), 6.46 (dd, $J = 8.2, 2.1$ Hz, 1H), 5.93 (d, $J = 1.4$ Hz, 1H), 5.92 (d, $J = 1.4$ Hz, 1H), 4.20 (t, $J = 6.4$ Hz, 1H), 3.57 (ddd, $J =$

10.2, 7.1, 5.9 Hz, 1H), 3.28 (dt, $J = 10.2, 7.3$ Hz, 1H), 2.94 (dd, $J = 6.4, 2.0$ Hz, 2H), 2.42 (s, 3H), 2.37–2.24 (m, 1H), 2.23–2.07 (m, 4H), 1.99 (ddd, $J = 13.1, 7.6, 5.9$ Hz, 1H); ^{13}C NMR (75 MHz, CDCl_3) δ 209.6, 148.3, 146.4, 143.9, 137.8, 134.3, 129.8, 127.6, 118.8, 108.2, 106.6, 101.3, 63.2, 49.2, 47.1, 44.9, 37.6, 36.3, 33.5, 21.7; IR (Neat Film NaCl) 3412, 2952, 2896, 2327, 1717, 1679, 1598, 1507, 1490, 1468, 1434, 1341, 1234, 1305, 1234, 1162, 1090, 1037, 934, 814, 771, 737, 709 cm^{-1} .



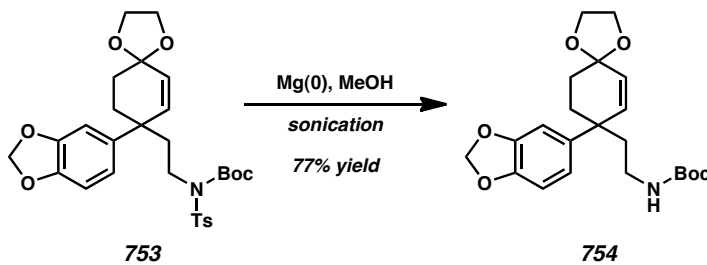
Silyl Dienol Ether 755. To a 1/2 dram vial with magnetic stir bar was added γ -aryl γ -ethylamino cyclohexenone **750** (20 mg, 0.0389 mmol, 1.00 equiv) and CH_2Cl_2 (120 μL). The vial was cooled to 0 $^\circ\text{C}$ and Et_3N (21.7 μL , 0.1558 mmol, 4.00 equiv) was added, followed by TBSOTf (17.9 μL , 0.0779 mmol, 2.00 equiv). The reaction became a yellow solution. After 15 min of stirring, the reaction was quenched with sat. aqueous NaHCO_3 (0.15 mL). The reaction was warmed to 23 $^\circ\text{C}$, diluted with EtOAc, and dried over Na_2SO_4 , filtered, and concentrated under reduced pressure. The residue was purified by automated flash column chromatography (SiO_2 , 1 x 20 cm, 10:1 \rightarrow 6:1 hexanes:EtOAc) to give silyl dienol ether **755** (22.7 mg, 0.03698 mmol, 95% yield); ^1H NMR (300 MHz, CDCl_3) δ 7.73 (d, $J = 8.3$ Hz, 2H), 7.27 (d, $J = 7.5$ Hz, 2H), 6.94 (d, $J = 1.8$ Hz, 1H), 6.89 (dd, $J = 8.1, 1.9$ Hz, 1H), 6.76 (d, $J = 8.1$ Hz, 1H), 5.98 (dd, $J = 10.0, 0.8$ Hz, 1H), 5.93 (s, 2H), 5.87 (dd, $J = 10.0, 2.1$ Hz, 1H), 4.81 (ddd, $J = 5.0, 4.1, 1.9$ Hz, 1H), 3.68 (ddd, J

= 8.9, 6.3, 1.6 Hz, 2H), 2.54 (t, J = 4.4 Hz, 2H), 2.42 (s, 3H), 2.30 (ddd, J = 12.7, 9.6, 6.9 Hz, 1H), 2.19 (ddd, J = 12.8, 10.0, 7.1 Hz, 1H), 1.32 (s, 9H), 0.90 (s, 9H), 0.10 (s, 3H), 0.08 (s, 3H); ^{13}C NMR (75 MHz, CDCl_3) δ 150.9, 147.8, 147.7, 145.9, 144.1, 140.0, 137.5, 134.9, 129.3, 127.9, 126.8, 119.6, 108.0, 107.4, 101.5, 101.0, 84.2, 44.1, 41.0, 40.1, 36.7, 28.1, 25.8, 21.8, 18.2, -4.3, -4.4.



Ketal 753. To a 50 mL round-bottom flask with magnetic stir bar was added γ -aryl γ -ethylamino cyclohexenone **750** (46 mg, 0.0896 mmol, 1.00 equiv) and benzene (18 mL). PPTS (1.12 mg, 0.0045 mmol, 5 mol %) was added, followed by ethylene glycol (55 μL , 0.99 mmol, 11.0 equiv). A Dean–Stark trap and reflux condenser connected to a N_2 inlet was attached and the flask was immersed in a 95 $^\circ\text{C}$ oil bath. After 48 h of stirring, the reaction was cooled to 23 $^\circ\text{C}$ and quenched with sat. aqueous NaHCO_3 (5 mL). The mixture was extracted with EtOAc (3 x 5 mL). The combined organic phases were dried over Na_2SO_4 , filtered, and concentrated under reduced pressure. The residue was purified by automated flash column chromatography (SiO_2 , 2 x 20 cm, 4:1 \rightarrow 3:1 \rightarrow 2:1 hexanes:EtOAc) to give ketal **753** (45.2 mg, 0.081 mmol, 90% yield); ^1H NMR (300 MHz, CDCl_3) δ 7.73 (d, J = 8.4 Hz, 2H), 7.27 (d, J = 8.1 Hz, 2H), 6.88 (d, J = 1.8 Hz, 1H), 6.81 (dd, J = 8.1, 1.8 Hz, 1H), 6.74 (d, J = 8.2 Hz, 1H), 6.12 (dd, J = 10.2, 1.5 Hz, 1H), 5.93 (s, 2H), 5.83 (dd, J = 10.2, 1.2 Hz, 1H), 4.07–3.94 (m, 3H), 3.96–3.84 (m, 1H),

3.76 (ddd, $J = 14.1, 12.0, 4.6$ Hz, 1H), 3.62 (ddd, $J = 14.2, 11.6, 5.2$ Hz, 1H), 2.42 (s, 3H), 2.34–2.19 (m, 1H), 2.18–2.00 (m, 2H), 1.91 (dddd, $J = 13.1, 4.8, 3.2, 1.4$ Hz, 1H), 1.82–1.55 (m, 2H), 1.32 (s, 9H); ^{13}C NMR (75 MHz, CDCl_3) δ 150.8, 147.9, 146.1, 144.2, 138.5, 137.5, 136.9, 129.3, 128.9, 127.9, 120.3, 108.0, 107.6, 105.5, 101.1, 84.3, 64.8, 64.5, 43.9, 42.3, 41.3, 35.1, 30.0, 28.0, 21.7 cm^{-1} ; IR (Neat Film NaCl) 2978, 2954, 2932, 2884, 2254, 1727, 1598, 1504, 1487, 1455, 1324, 1395, 1354, 1283, 1243, 1147, 1141, 1088, 1039, 992, 938, 906, 850, 812, 771, 733 cm^{-1} .



N-Boc Amine 754. To a 20 mL scintillation vial was added ketal **753** (26.1 mg, 0.047 mmol, 1.00 equiv) and Mg turnings (2.4 mg, 0.108 mmol, 10.00 equiv). The vial was sealed with a septum-fitted screw cap and evacuated/backfilled with N_2 (3 x 5 min cycles). Anhydrous MeOH (1 mL) was added and the vial was sealed with tape. The vial was sonicated for 3 h. The turbid white suspension was diluted with H_2O (1 mL) and extracted with Et_2O (3 x 5 mL). The combined organic phases were dried over Na_2SO_4 , filtered, and concentrated under reduced pressure. The residue was purified by automated flash column chromatography (SiO_2 , 1 x 20 cm, 4:1→2:1→1:1 hexanes:EtOAc) to give ketal **754** (14.6 mg, 0.036 mmol, 77% yield); ^1H NMR (300 MHz, CDCl_3) δ 6.82–6.76 (m, 1H), 6.71 (d, $J = 1.6$ Hz, 2H), 6.08–5.97 (m, 1H), 5.90 (s, 2H), 5.75 (dd, $J = 10.2, 1.1$ Hz, 1H), 4.43 (t, $J = 5.8$ Hz, 1H), 4.09–3.79 (m, 4H), 3.15–

2.79 (m, 2H), 2.04–1.76 (m, 4H), 1.76–1.52 (m, 2H), 1.39 (s, 9H); ^{13}C NMR (75 MHz, CDCl_3) δ 155.8, 147.9, 145.9, 138.9, 137.1, 128.5, 120.1, 108.0, 107.3, 105.4, 101.0, 79.1, 64.7, 64.5, 42.1, 41.8, 36.8, 35.2, 30.1, 28.5 cm^{-1} ; IR (Neat Film NaCl) 3360, 2974, 2933, 2885, 2779, 1708, 1611, 1505, 1488, 1455, 1434, 1393, 1366, 1349, 1300, 1242, 1172, 1142, 1122, 1064, 1039, 982, 936, 904, 868, 813, 777, 731 cm^{-1} .

A12.7 NOTES AND REFERENCES

- (1) For reports describing the isolation of crinine (**671**), see: (a) Boit, H.-G. *Chem Ber.* **1954**, 87, 1704–1707. (b) Mason, L. H.; Puschett, E. R.; Wildman, W. C. *J. Am. Chem. Soc.* **1955**, 77, 1253–1256.
- (2) For reviews describing the total synthesis of *Amaryllidaceae* alkaloids, see: (a) Jin, Z. *Nat. Prod. Rep.* **2003**, 20, 606–614. (b) Rinner, U.; Hudlicky, R. *Synlett* **2005**, 365–387. (c) Hudlicky, T.; Reed, J. W. *The Way of Synthesis: Evolution of Design and Methods for Natural Products*; Wiley-VCH: Weinheim, Germany, 2007; pp 689–726.
- (3) Carbocyclic substrates: (a) Behenna, D. C.; Stoltz, B. M. *J. Am. Chem. Soc.* **2004**, 126, 15044–15045. (b) Mohr, J. T.; Behenna, D. C.; Harned, A. M.; Stoltz, B. M. *Angew. Chem. Int. Ed.* **2005**, 44, 6924–6927. (c) Behenna, D. C.; Mohr, J. T.; Sherden, N. H.; Marinescu, S. C.; Harned, A. M.; Tani, K.; Seto, M.; Ma, S.; Novák, Z.; Krout, M. R.; McFadden, R. M.; Roizen, J. L.; Enquist, Jr., J. A.; White, D. E.; Levine, S. R.; Petrova, K. V.; Iwashita, A.; Virgil, S. C.; Stoltz, B. M. *Chem. Eur. J.* **2011**, 17, 14199–14223.
- (4) Heterocyclic substrates: (a) Seto, M.; Roizen, J. L.; Stoltz, B. M. *Angew. Chem. Int. Ed.* **2008**, 47, 6873–6876. (b) Behenna, D. C.; Liu, Y.; Yurino, T.; Kim, J.; White, D. E.; Virgil, S. C.; Stoltz, B. M. *Nature Chem.* **2012**, 4, 130–133.
- (5) For formal and total syntheses completed in our group using Pd-catalyzed asymmetric allylic alkylation reactions, see: (a) Dichroanone: McFadden, R. M.; Stoltz, B. M. *J. Am. Chem. Soc.* **2006**, 128, 7738–7739. (b) Elatol: White, D. E.; Stewart, I. C.; Grubbs, R. H.; Stoltz, B. M. *J. Am. Chem. Soc.* **2008**, 130, 810–811. (c) Cyanthiwigin F: Enquist, Jr., J. A.; Stoltz, B. M. *Nature* **2008**, 453,

- 1228–1231. (d) Carissone: Levine, S. R.; Krout, M. R.; Stoltz, B. M. *Org. Lett.* **2009**, *11*, 289–292. (e) Cassiol: Petrova, K. V.; Mohr, J. T.; Stoltz, B. M. *Org. Lett.* **2009**, *11*, 293–295. (f) Elatol, Laurencenone C, α -Chamigrene, and the proposed Structure of Laurencenone B: White, D. E.; Stewart, I. C.; Seashore-Ludlow, B. A.; Grubbs, R. H.; Stoltz, B. M. *Tetrahedron* **2010**, *66*, 4668–4686. (g) Hamigeran B: Mukherjee, H.; McDougal, N. T.; Virgil, S. C.; Stoltz, B. M. *Org. Lett.* **2011**, *13*, 825–827. (h) Liphagal: Day, J. J.; McFadden, R. M.; Virgil, S. C.; Kolding, H.; Alleva, J. L.; Stoltz, B. M. *Angew. Chem. Int. Ed.* **2011**, *50*, 6814–6818. (i) Cyanthiwiggins B, F, and G: Enquist, Jr., J. A.; Virgil, S. C.; Stoltz, B. M. *Chem. Eur. J.* **2011**, *17*, 9957–9969. (j) Presilphiperfolan-1-ol and the Proposed Structure of Presilphiperfolan-1-ol: Hong, A. Y.; Stoltz, B. M. *Angew. Chem. Int. Ed.* **2012**, *51*, 9674–9678.
- (6) (a) Mohr, J. T.; Nishimata, T.; Behenna, D. C.; Stoltz, B. M. *J. Am. Chem. Soc.* **2006**, *128*, 11348–11349. (b) Marinescu, S. C.; Nishimata, T.; Mohr, J. T.; Stoltz, B. M. *Org. Lett.* **2008**, *10*, 1039–1042.
- (7) Streuff, J.; White, D. E.; Virgil, S. C.; Stoltz, B. M. *Nature Chem.* **2010**, *2*, 192–196.
- (8) Stork, G.; Danheiser, R. L. *J. Org. Chem.* **1973**, *38*, 1775–1776.
- (9) Trost, B. M.; Xu, J. *J. Am. Chem. Soc.* **2005**, *127*, 2846–2847.
- (10) (a) Lee, S.; Hartwig, J. F. *J. Org. Chem.* **2001**, *66*, 3402–3415. (b) Åhman, J.; Wolfe, J. P.; Troutman, M. V.; Palucki, M.; Buchwald, S. L. *J. Am. Chem. Soc.* **1998**, *120*, 1918–1919.

- (11) Satoh, T.; Ikeda, M.; Miura, M.; Nomura, M. *J. Org. Chem.* **1997**, *62*, 4877–4879.
- (12) Siegel, D. R.; Danishfsky, S. J. *J. Am. Chem. Soc.* **2001**, *123*, 1048–1049.
- (13) (a) Bao, M.; Nakamura, H.; Yamamoto, Y. *J. Am. Chem. Soc.* **2001**, *123*, 759–760. (b) Lu, S.; Xu, Z.; Bao, M.; Yamamoto, Y. *Angew. Chem. Int. Ed.* **2008**, *47*, 4366–4369.
- (14) Ariaifard, A.; Lin, Z. *J. Am. Chem. Soc.* **2006**, *128*, 13010–13016.
- (15) For reports describing Pd-catalyzed Wacker-type oxidative cyclization reactions, see: (a) Trend, R. M.; Ramtohul, Y. K.; Ferreira, E. M.; Stoltz, B. M. *Angew. Chem. Int. Ed.* **2003**, *42*, 2892–2895. (b) Ferreira, E. M.; Stoltz, B. M. *J. Am. Chem. Soc.* **2003**, *125*, 9578–9579. (c) Zhang, H.; Ferreira, E. M.; Stoltz, B. M. *Angew. Chem. Int. Ed.* **2004**, *43*, 6144–6148. (d) Trend, R. M.; Ramtohul, Y. K.; Stoltz, B. M. *J. Am. Chem. Soc.* **2005**, *127*, 17778–17788. (e) Ebner, D. C.; Novák, Z.; B. M. *Synlett* **2006**, *20*, 3533–3539. (f) Ferreira, E. M.; Zhang, H.; Stoltz, B. M. *Tetrahedron* **2008**, *64*, 5987–6001.
- (16) (a) Ferreira, E. M. The Design and Development of Palladium-Catalyzed Aerobic Oxidative Transformations. Ph.D. Thesis. California Institute of Technology, Pasadena, CA, 2005. (b) Ferreira, E. M.; Chiba, J.; O'Connor, N. R.; Stoltz, B. M. unpublished results.
- (17) For the application of Pd-catalyzed Wacker-type oxidative cyclization reactions to total synthesis, see: (a) Garg, N. K.; Caspi, D. D.; Stoltz, B. M. *J. Am. Chem. Soc.* **2004**, *126*, 9552–9553. (b) Garg, N. K.; Caspi, D. D.; Stoltz, B. M. *J. Am. Chem. Soc.* **2005**, *127*, 5970–5978. (c) Garg, N. K.; Caspi, D. D.; Stoltz, B. M.

- Synlett* **2006**, 3081–3087. (d) Liu, Q.; Ferreira, E. M.; Stoltz, B. M. *J. Org. Chem.* **2007**, 72, 7352–7358. (e) Tadross, P. M.; Bugga, P.; Stoltz, B. M. *Org. Biomol. Chem.* **2011**, 9, 5354–5357.
- (18) (a) Liu, G.; Stahl, S. S. *J. Am. Chem. Soc.* **2007**, 129, 6328–6335. (b) Weinstein, A. B.; Stahl, S. S. *Angew. Chem. Int. Ed.* **2012**, 51, 11505–11509.
- (19) (a) Trost, B. M.; Hansmann, M. M.; Thaisrivongs, D. A. *Angew. Chem. Int. Ed.* **2012**, 51, 4950–4953. (b) Trost, B. M.; Thaisrivongs, D. A.; Hansmann, M. M. *Angew. Chem. Int. Ed.* **2012**, 51, 11522–11526.
- (20) Sasaki, Y.; Zhong, C.; Sawamura, M.; Ito, M. *J. Am. Chem. Soc.* **2010**, 132, 1226–1227.
- (21) For a report describing the isolation of oxocrinine (**729**), see: Ali, A. A.; El Sayed, H. M.; Abdallah, O. M.; Steglich, W. *Phytochem.* **1986**, 25, 2399–2401.
- (22) Yu, W.; Mei, Y.; Kang, Y.; Hua, Z.; Jin, Z. *Org. Lett.* **2004**, 6, 3217–3219.
- (23) Zhao, Y.; Zhou, Y.; Liang, L.; Yang, X.; Du, F.; Li, L.; Zhang, H. *Org. Lett.* **2009**, 11, 555–558.
- (24) Taber, D. F.; He, Y. *J. Org. Chem.* **2005**, 70, 7711–7714.
- (25) Sanchez, I. H.; Lopez, F. J.; Soria, J. J.; Larraza, M. I.; Flores, H. J. *J. Am. Chem. Soc.* **1983**, 105, 7640–7643.
- (26) Stones, G.; Tripoli, R.; McDavid, C. L.; Roux-Duplâtre, K.; Kennedy, A. R.; Sherrington, D. C.; Gibson, C. L. *Org. Biomol. Chem.* **2008**, 6, 374–384.

- (27) Skerlj, R. T.; Nan, S.; Zhou, Y.; Bridger, G. J. *Tetrahedron Lett.* **2002**, *43*, 7569–7571.
- (28) Mild and practical conditions for the direct Saegusa–Ito oxidation of ketones were recently developed by Stahl. These conditions may be useful in the synthetic route. See: (a) Diao, T.; Stahl, S. S. *J. Am. Chem. Soc.* **2011**, *133*, 14566–14569. (b) Diao, T.; Wadzinski, T. J.; Stahl, S. S. *Chem. Sci.* **2012**, *3*, 887–891.
- (29) For an example of the use of the Symyx Core Module in reaction optimization in our research, see: McDougal, N. T.; Virgil, S. C.; Stoltz, B. M. *Synlett* **2010**, 1712–1716.
- (30) Bogle, K. M.; Hirst, D. J.; Dixon, D. J. *Org. Lett.* **2010**, *12*, 1252–1254.
- (31) Rousseaux, S.; García-Fortanet, J.; Sanchez, M. A. D. A.; Buchwald, S. L. *J. Am. Chem. Soc.* **2011**, *133*, 9282–9285.
- (32) Wu, Q.-F.; Liu, W.-B.; Zhuo, C.-X.; Rong, Z.-Q.; Ye, K.-Y.; You, S.-L. *Angew. Chem. Int. Ed.* **2011**, *50*, 4455–4458.
- (33) Gu, Q.; You, S.-L. *Chem. Sci.* **2011**, *2*, 1519–1522.
- (34) Pangborn, A. B.; Giardello, M. A.; Grubbs, R. H.; Rosen, R. K.; Timmers, F. J. *Organometallics* **1996**, *15*, 1518–1520.
- (35) Corey, E. J.; Cho, H.; Rücker, C.; Hua, D. H. *Tetrahedron Lett.* **1981**, *22*, 3455–3458.
- (36) Boehm, J. C.; Gleason, J. G.; Pendrak, I.; Sarau, H. M.; Schmidt, D. B.; Foley, J. J.; Kingsbury, W. D. *J. Med. Chem.* **1993**, *36*, 3333–3340.

- (37) Dragoli, D. R.; Burdett, M. T.; Ellman, J. A. *J. Am. Chem. Soc.* **2001**, *123*, 10127–10128.
- (38) Enders, D.; Lenzen, A.; Backes, M.; Janeck, C.; Catlin, K.; Lannou, M.-L.; Runsink, J.; Raabe, G. *J. Org. Chem.* **2005**, *70*, 10538–10551.

APPENDIX 13

Modular Synthesis of Olefin-Oxazoline (OlefOX) Ligands and Applications in Asymmetric Transition Metal-Catalyzed Reactions[†]

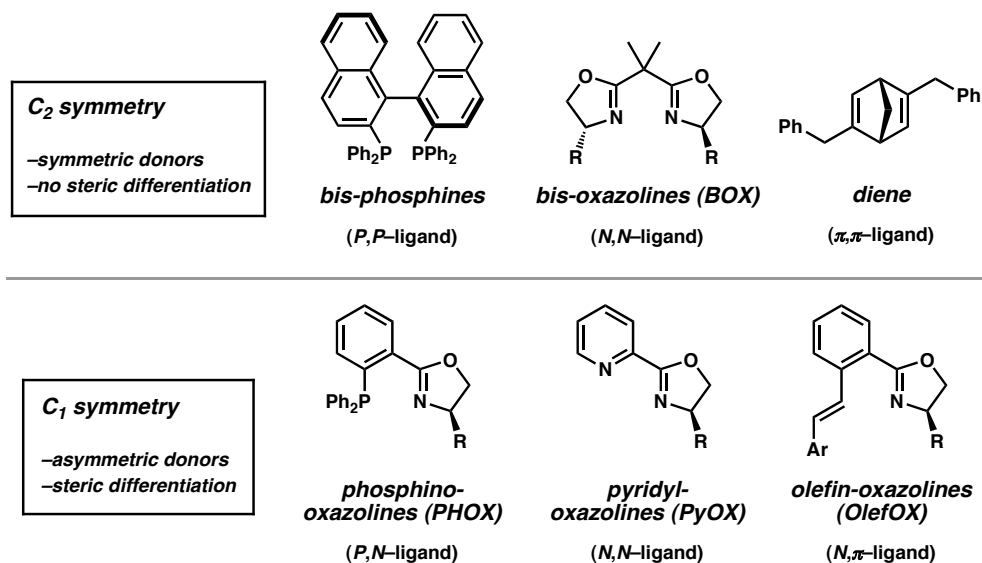
A13.1 INTRODUCTION AND BACKGROUND

The rational design of new classes of chiral ligands with unique structural and electronic properties can greatly impact the development of asymmetric transition metal-catalyzed transformations. A number of privileged ligand scaffolds based on C_2 -symmetric chiral bis-phosphines,¹ bis-oxazolines (BOX),^{2,3} and more recently, chiral dienes,^{4,5} have proven to be important tools for chemists seeking to develop new organometallic reaction methodologies (Figure A13.1). A less common but nevertheless powerful strategy for achieving structural and electronic variation of transition metal complexes relies on the use of C_1 -symmetric chiral bidentate ligands. Within this class of ligands, phosphinooxazoline (PHOX) ligands^{6,7,8} have proven to be particularly successful

[†] This work was primarily performed in collaboration with Annie F. Chin, a William N. Lacey Summer Undergraduate Research Fellow in the Caltech SURF Program. Maria J. Cano, a visiting graduate scholar from the University of Granada (Spain), conducted research on related *spiro*-ketimine-olefin ligands. Portions of this work were submitted in a final report and presented during a public seminar by Annie F. Chin for the Caltech SURF program. The results in this appendix are unpublished.

in the development of enantioselective hydrogenation,⁹ transfer hydrogenation,¹⁰ hydrosilylation,¹¹ cross-coupling,¹² and allylic alkylation¹³ reactions. Pyridine-oxazoline (PyOX) ligands have shown remarkable potential for asymmetric induction in asymmetric oxidative cyclization,¹⁴ conjugate addition,¹⁵ and α -halogenation¹⁶ reactions. Chiral C_1 -symmetric bidentate ligands such as these are potentially powerful ligands because they provide opportunities for independent tuning of the steric and electronic properties of the two donor ligands. The nonequivalent donor atoms of the bidentate ligand can translate into differentiation of the remaining binding sites at the metal center and promote novel reactivity. For these reasons, the development of new, useful C_1 -symmetric bidentate ligands would be valuable for asymmetric catalysis.

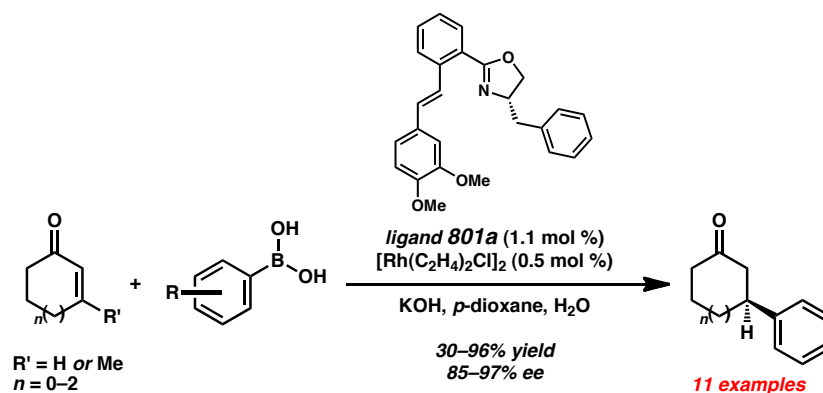
Figure A13.1. Chiral C_2 -Symmetric and C_1 -Symmetric Bidentate Ligand Scaffolds



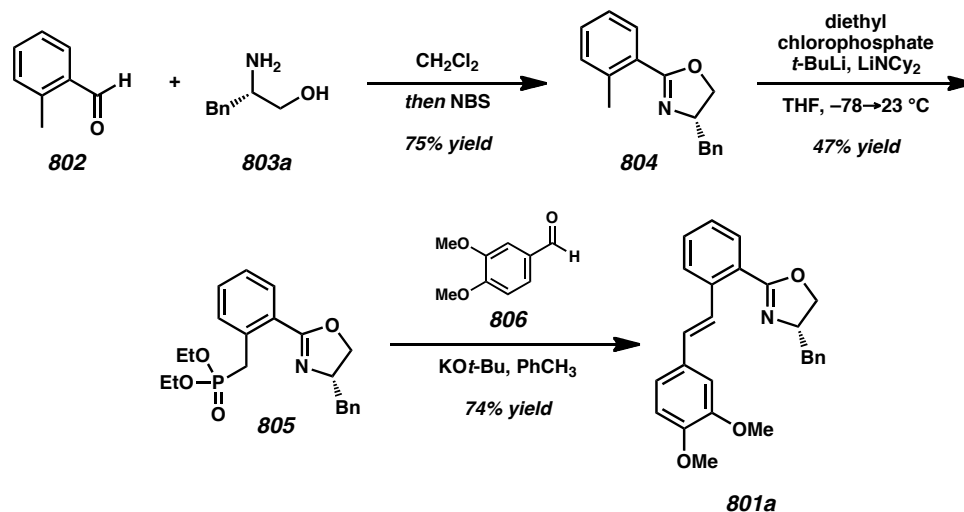
In seeking to develop unique C_1 -symmetric hybrid ligands, Glorius recently drew inspiration from bis-oxazoline ligands and diene ligands to pioneer a new type of chiral

ligand **800** based on an olefin-oxazoline (OlefOX) framework.¹⁷ These ligands proved to be effective in enantioselective rhodium-catalyzed conjugate additions of arylboronic acids to cyclic enone substrates (Scheme A13.1).

Scheme A13.1. Glorius' Application of OlefOX Ligands (**801**) to Rh-Catalyzed Conjugate Additions.



The synthetic strategy for the preparation of these ligands relies on the coupling of an amino alcohol with an aromatic aldehyde to form the oxazoline ring and a Horner–Wadsworth–Emmons reaction to form the stilbene olefin. The sequence provides the optimized ligand **801a** in 26% overall yield over three steps (Scheme A13.2). Using this synthetic route, a variety of different OlefOX ligands were prepared.

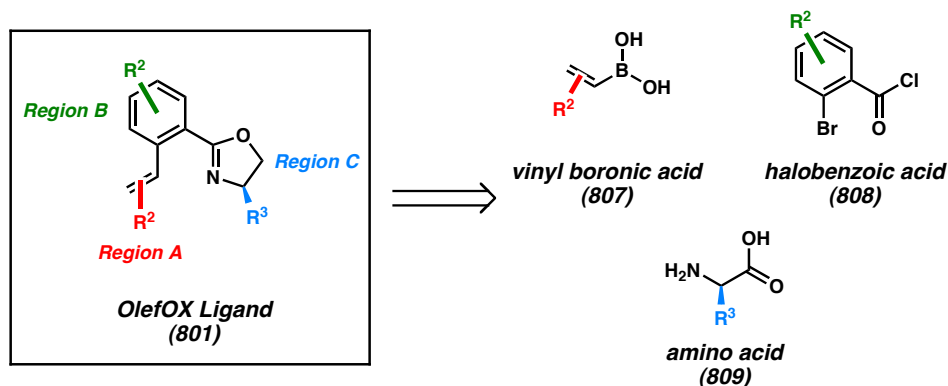
Scheme A13.2. Glorius' Synthesis of OlefOX Ligands **801**

While the early work of Glorius provides synthetic access to a promising new ligand scaffold, the reported route contains several limitations. Access to differentially substituted 2-methyl benzaldehydes stands as one major challenge to the backbone modification of these ligands. Additionally, the reported synthetic route requires the use of stoichiometric quantities of pyrophoric strong bases to prepare the requisite phosphonates for the Horner–Wadsworth–Emmons reaction. Some substitution patterns, such as highly substituted olefins, may be difficult to prepare using the outlined route. The preparation of OlefOX ligands (**801**) can be improved by designing new synthetic routes to increase overall yield and achieve steric and electronic diversity. Additionally, further application of this ligand class to other enantioselective organometallic transformations should be explored.

A13.2 SYNTHESIS OF OLEFIN-OXAZOLINE (OLEFOX) LIGANDS

In our general program for the discovery of novel asymmetric transition metal-catalyzed transformations, a premium is placed on fundamental new concepts for catalyst and ligand design. We envisioned that an improved and more general synthetic route for the synthesis of olefin-oxazoline (OlefOX) ligands (**801**) could provide new opportunities for steric and electronic diversification. To enable a more efficient and scalable synthesis of diverse OlefOX ligands, we envisioned that alternative retrosynthetic disconnections could point to commercially available vinyl boronic acids (**807**), halobenzoic acids (**808**), and amino acids (**809**) as readily-available starting materials (Scheme A13.3). Additionally, we believed that this design platform could be extended to the synthesis of novel classes of higher hapticity chiral oxazoline-based ligands.

Scheme A13.3. Retrosynthetic Analysis of OlefOX Ligands

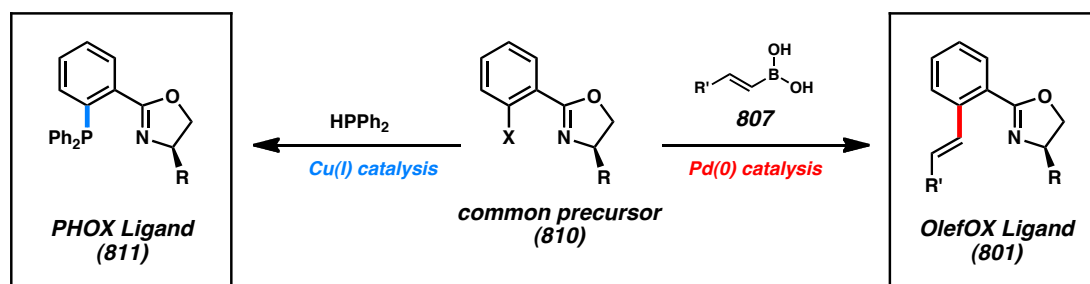


A13.2.1 DEVELOPMENT OF AN IMPROVED OLEFOX LIGAND SYNTHESIS

In our efforts to design a new synthetic route toward OlefOX ligands (**801**), we recognized that the key C–C bond connecting the aromatic backbone to the coordinating

alkene unit could be forged by a palladium-catalyzed cross-coupling reaction (Scheme A13.3). The main advantage of this strategy is different olefin geometries and degrees of olefin substitution can be incorporated into the final ligand structure by simply choosing the appropriate vinyl boronic acid. A significant benefit is the fact that many vinyl boronic acids are commercially available¹⁸ or readily prepared, thus making broad ligand diversification simple and straightforward. The common halooxazoline precursor **810** can be made on large scale, thereby facilitating access to these ligands.

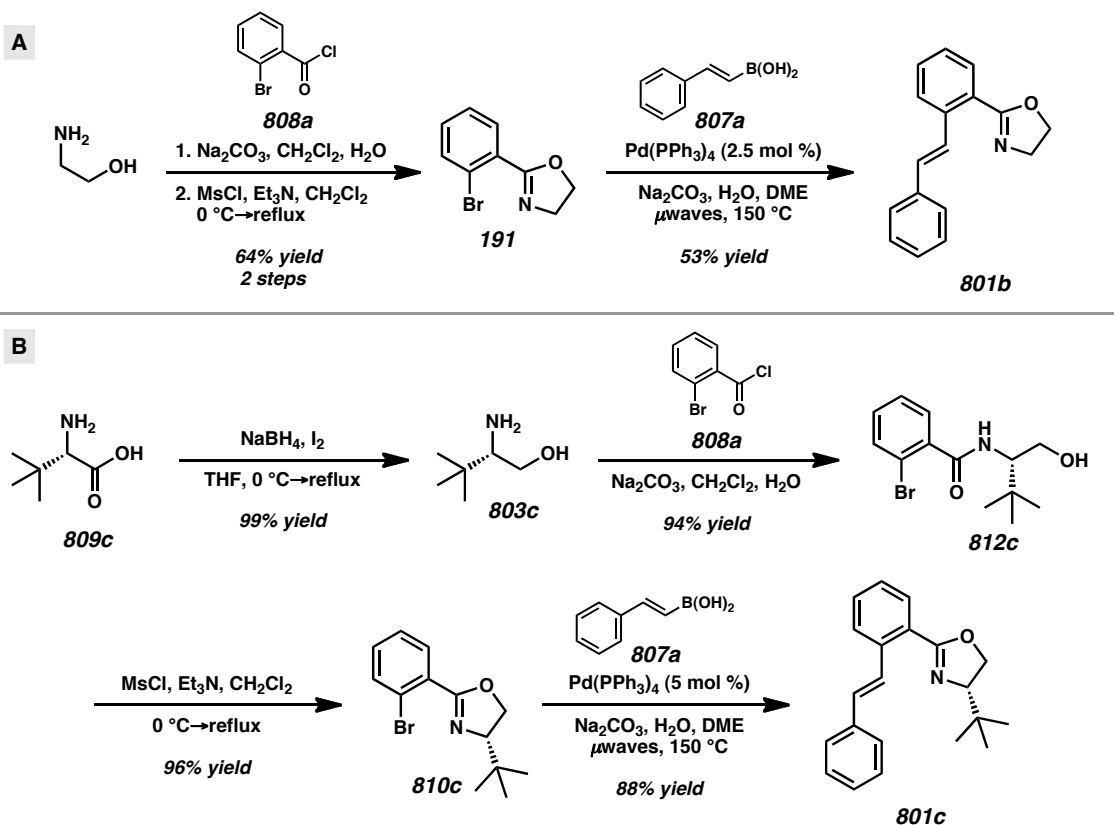
Scheme A13.4. Divergent Synthesis of PHOX and OlefOX Ligands from Bromoaryl Oxazolines



By modifying our reported route for the synthesis of PHOX ligands (**811**),^{8,13a} we were able to quickly evaluate this cross-coupling strategy for the divergent preparation of OlefOX ligands (**801**) (Scheme A13.5A). With ethanolamine as the precursor to an achiral ligand, we were able to perform an initial amidation followed by cyclization to afford bromoaryl oxazoline **191** in 64% yield over two steps. After briefly screening several reaction conditions, we found that the Suzuki coupling of vinyl boronic acid **807a** and bromoaryl oxazoline **191** could be achieved in the presence of $\text{Pd(PPh}_3)_4$ (5 mol %) and Na_2CO_3 in a mixture of H_2O and dimethoxyethane at 150 °C with microwave

irradiation. The desired achiral olefin-oxazoline ligand **801b** was successfully obtained in 53% yield.

Scheme A13.5. A General Synthesis of OlefOX Ligands by Pd Catalyzed Cross-Coupling



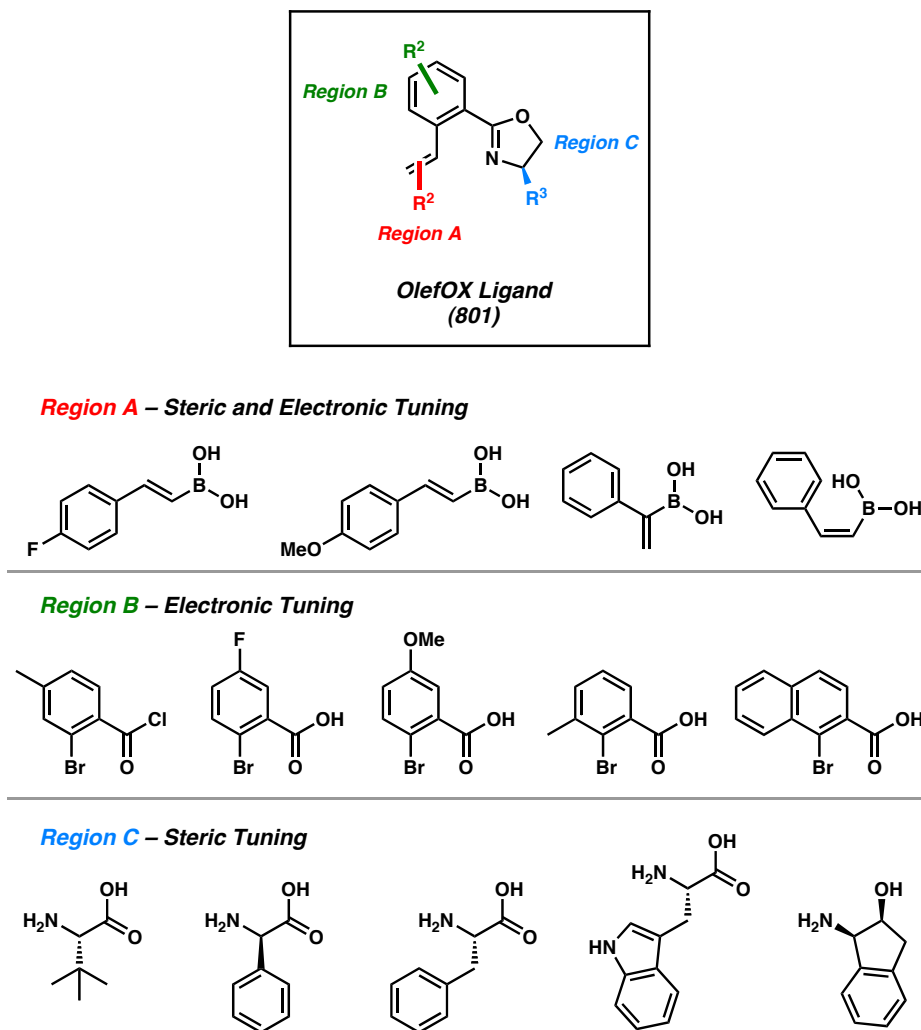
After demonstrating the viability of our synthetic approach, we turned our attention to the synthesis of chiral olefin-oxazoline (OlefOX) ligands (Scheme A13.5B). Beginning from a commercially available amino acid such as (*S*)-*tert*-leucine (**809c**), we were able to effect a borane-mediated reduction to the corresponding amino alcohol **803c** in 99% yield. Subsequent coupling with commercially available 2-bromobenzoyl chloride (**808a**) enabled access to hydroxyamide **812c** in 94% yield. Bromoaryl oxazoline formation proceeded smoothly in 96% yield, providing multi-gram quantities for the

synthesis of chiral OlefOX ligands. Suzuki coupling as described previously provided ligand **801c** in 88% yield. While these conditions have not been optimized, the cross-coupling strategy has enabled efficient formation of chiral OlefOX ligand **801c** in 79% overall yield over four steps. This synthetic route marks a significant improvement over the slightly shorter, but less efficient and less flexible preparation reported by Glorius.¹⁷

A13.2.2 STERIC/ELECTRONIC MODIFICATION OF OLEFOX LIGANDS

With a general synthetic route in place, we turned our attention to the steric and electronic modification of OlefOX ligands. A brief survey of commercially available starting materials revealed that a number of unique substituted vinyl boronic acids,¹⁸ 2-bromobenzoic acid derivatives,¹⁹ and amino acids could be readily obtained (Figure A13.2). We recognized that the electronic properties of the olefinic **Region A** can be modified by selecting vinyl boronic acid starting materials with electron-donating or electronic-withdrawing groups. Additionally, opportunities for incorporating 1,1-disubstituted and alkyl-substituted vinyl boronic acids are possible using our approach. **Region B** electronic modification is greatly enabled by the commercial availability of numerous 2-halobenzoic acids or acid chlorides with variable aromatic substitution. Lastly, **Region C** modification with natural and unnatural amino acids or amino alcohols can allow for even greater steric diversity of synthetic OlefOX ligands.

Figure A13.2. Steric and Electronic Modification of the OlefOX Ligand Scaffold



We began our derivatization studies by focusing on modification of the **Region C** (Table A13.1). From a variety of amino alcohols (**803**), which can be purchased or obtained by borane reduction of amino acids (**809**) (Scheme A13.5), amidation generally proceeded smoothly in 91–97% yield. The exception to this trend was the hydroxyamide formation reaction for (*S*)-tryptophanol (**803h**), which proceeded in 51% yield. Subsequent cyclization of hydroxyamides proceeded in good to moderate yields ranging from 60–87% yield. With a variety of differentially functionalized bromoaryl oxazolines

in hand, we were poised to prepare numerous OlefOX ligands using Suzuki cross-coupling. To our delight, the reactions to prepare these ligands proceeded smoothly in good yields ranging from 69–88% yield. At this time, the final cross coupling reaction to form tryptophan-derived ligand **801h** has not been performed.

Having achieved a variety of OlefOX ligands with different substitution patterns at the **Region C**, we turned our attention to the derivatization of **Region A** by employing our key Suzuki cross-coupling strategy to incorporate a number of differentially-substituted vinyl boronic acids (Table A13.2). Using the phenylalanine-derived 2-bromoaryl oxazoline **810f** as the common starting material, we were able to prepare several OlefOX derivatives with differing alkene and aromatic substitution and geometry. In general, it appeared that electron-neutral or electron-rich vinyl boronic acids such as the 2-phenyl vinyl, 2-(4-methoxy)phenyl vinyl, and 2-cyclohexyl vinyl boronic acids underwent the cross-coupling in to give ligands **801f**, **801i**, **807j** and in good yields (76–81% yield). Electron-deficient or sterically-demanding boronic acids were considerably less efficient, as 2-(4-fluoro)phenyl and 1-phenyl vinyl boronic acid gave products **801k** and **801l** in 22–44% yield. In addition to the synthesized ligands depicted in Table A13.2, we planned to prepare several more ligands (**801o–q**) using the same Suzuki reaction using other commercial vinyl boronic acids, but we have not completed them at this time.

Table A13.1. Region C Modification of OlefOX Ligands

synthetic sequence

amino alcohol (803)

hydroxyamide (812)

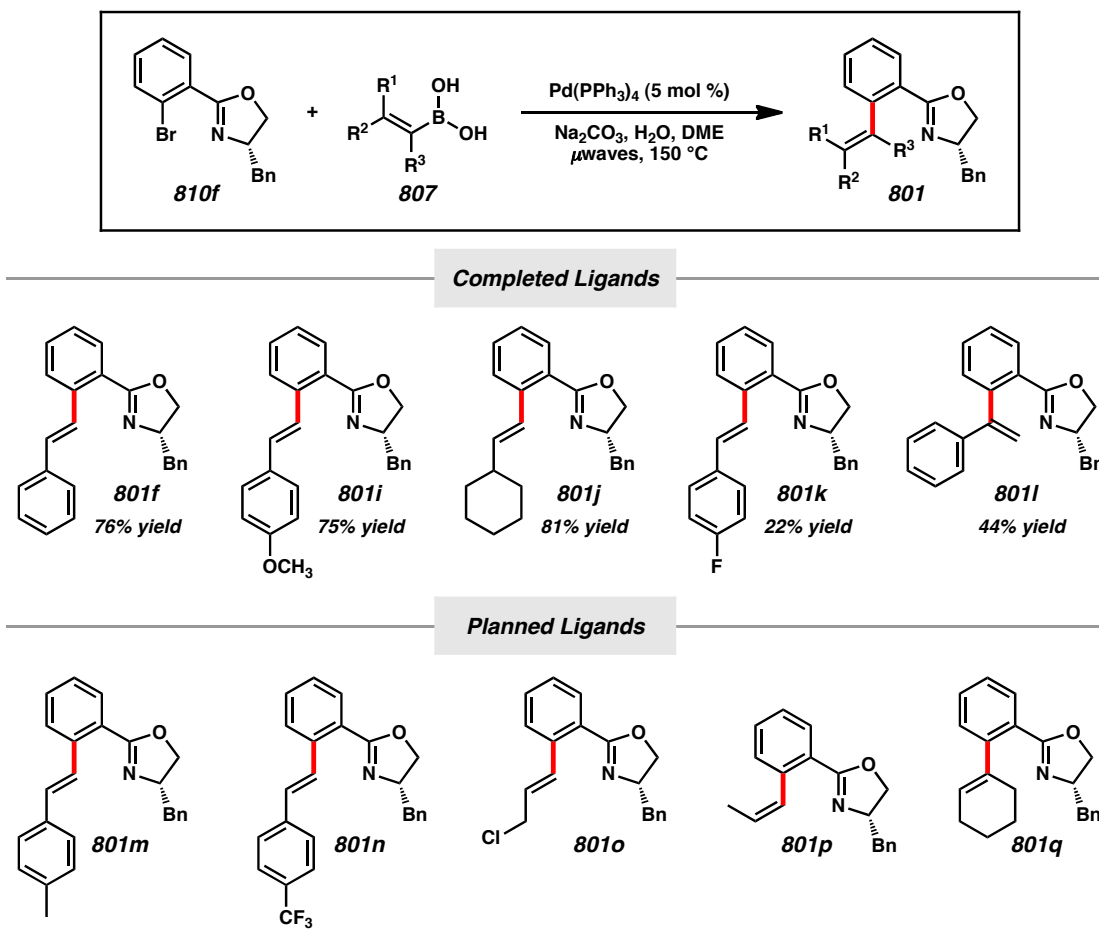
oxazoline (810)

OlefOX ligand (801)

entry	803	812	yield (%) ^d	810	yield (%) ^d	801	yield (%) ^d
1	<div>803c</div>	812c	94	810c	96	801c	88
2	<div>803d</div>	812d	91	810d	61	801d	69
3	<div>803e</div>	812e	97	810e	60	801e	84
4	<div>803a</div>	812f	97	810f	68	801f	76
5	<div>803g</div>	812g	94	810g	87	801g	80
6	<div>803h</div>	812h	51	810h	64	801h	—

^a Conditions A: amino alcohol **803** (1.00 equiv), 2-bromobenzoyl chloride (1.15 equiv), 1.19 M aq. Na₂CO₃ in H₂O (3.00 equiv) in CH₂Cl₂ (0.3 M) 23 °C. ^b Conditions B: hydroxyamide **812** (1.00 equiv), 2-bromobenzoyl chloride (1.15 equiv), 1.19 M aq. Na₂CO₃ in H₂O (3.00 equiv) in CH₂Cl₂ (0.3 M) 23 °C. ^c Conditions C: bromoaryl oxazoline **810** (1.00 equiv), vinylboronic acid **807a** (1.00 equiv), Pd(PPh₃)₄ (5 mol %), 2 M aq. Na₂CO₃ (2.60 equiv) in *p*-dioxane (0.1 M) at 150 °C with microwave irradiation. ^d Isolated yield.

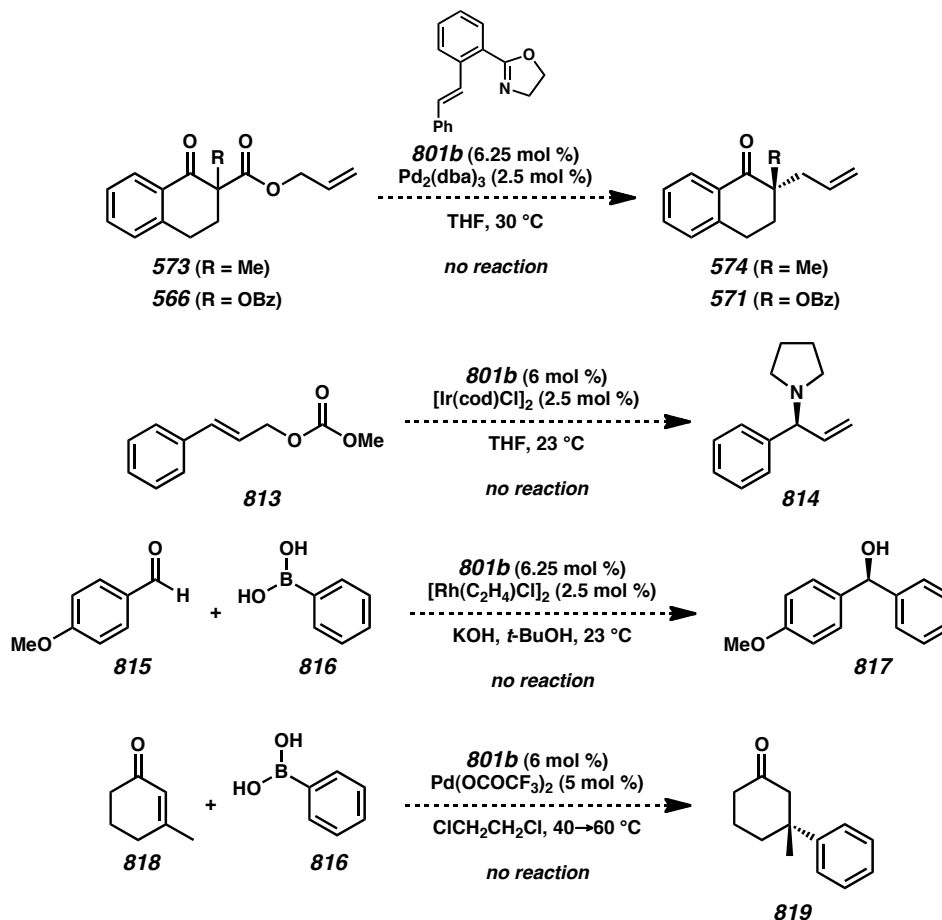
Table A13.2. Region A Modification of OlefOX Ligands



While we were able to achieve successful **Region A** and **Region C** modification by the appropriate selection of amino acid and vinyl boronic acid starting materials, we have yet to prepare OlefOX derivatives bearing a substituted **Region B**. This can be accomplished by employing a variety of commercially available 2-bromobenzoic acids, benzonitriles, benzaldehydes, and benzoyl chlorides.¹⁹ Since many analogous PHOX ligands have been prepared in this manner, this should be a straightforward operation.^{8b} Once these studies are completed, we will be able to show that all of the key regions of OlefOX ligand scaffold can be modified using our modular synthetic approach.

A13.2.3 APPLICATION OF OLEFOX LIGANDS TO ASYMMETRIC TRANSITION METAL CATALYZED REACTIONS

With a collection of OlefOX derivatives at our disposal, asymmetric transition metal-catalyzed transformations were investigated with these chiral ligands. While efforts to apply these ligands to palladium¹³ and iridium-catalyzed²⁰ allylic alkylation reactions, palladium-catalyzed 1,4-conjugate addition reactions,¹⁵ rhodium-catalyzed 1,2-addition reactions,²¹ have not been successful so far (Scheme A13.6), investigations are preliminary and many reaction types with rhodium, iridium, palladium, platinum, and copper as catalysts have yet to be investigated. Once a suitable reaction is found, high-throughput reaction screening at the Caltech Center for Catalysis and Chemical Synthesis (3CS) can enable the simultaneous investigation of numerous reaction variables and facilitate rapid reaction optimization.²²

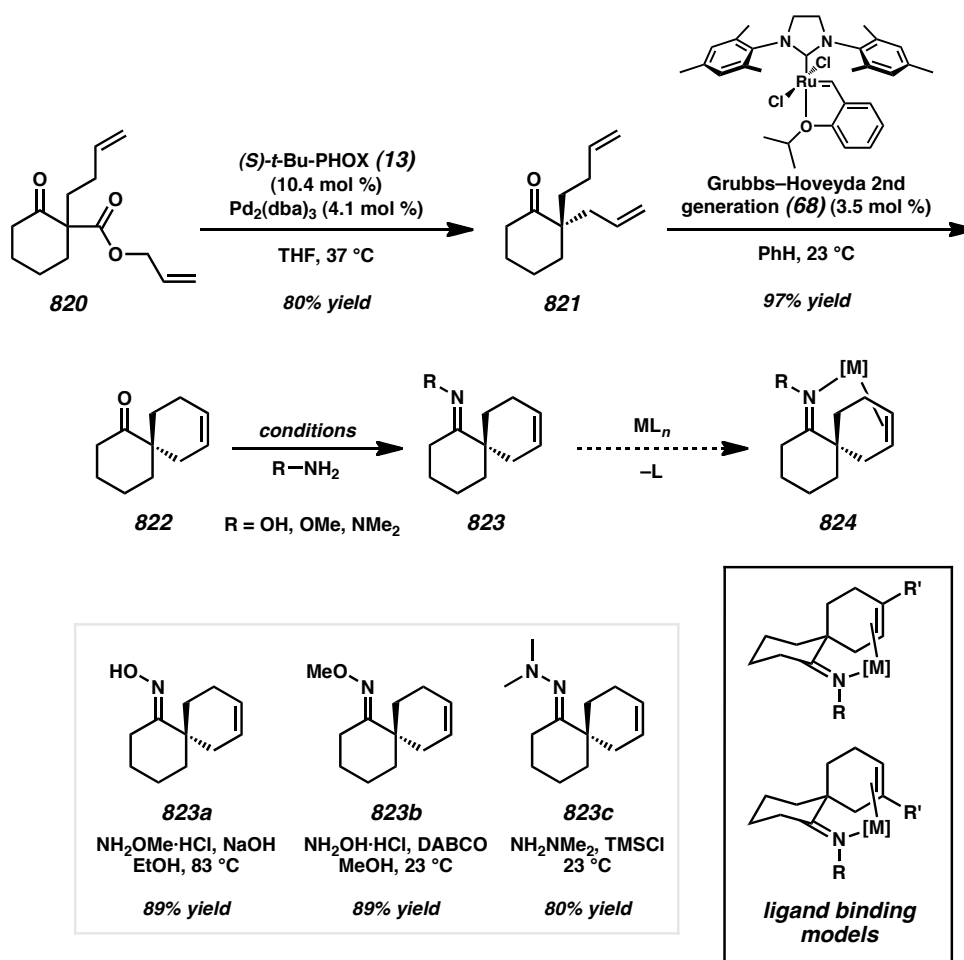
Scheme A13.6. Attempted Transition-Metal Catalyzed Reactions with Achiral OlefOX Ligand **801b**

A13.3 SYNTHESIS OF RELATED *SPIRO*-KETIMINE-OLEFIN LIGANDS

While most of our effort has focused on the synthesis of OlefOX ligands, the synthesis of related chiral *N*, π -bidentate *spiro*-ketimine-olefin ligands have been pursued by others in our group (Scheme A13.7). Following standard functionalizations of cyclohexanone, β -ketoester **820** can enable a subsequent Pd-catalyzed asymmetric allylic alkylation¹³ to give α -quaternary ketone **821**. Ring-closing metathesis with Grubbs–Hoveyda 2nd generation catalyst (**68**) provides spirocyclic product **822**. Condensation with various amines such as can afford a variety of *spiro*-ketimine-olefin ligands such as

823a, **823b**, and **823c**. Complexation of these ligands with late transition metals can provide complexes with the general structure **824**.

Scheme A13.7. Synthesis of Spiro-Ketimine-Olefin Ligands

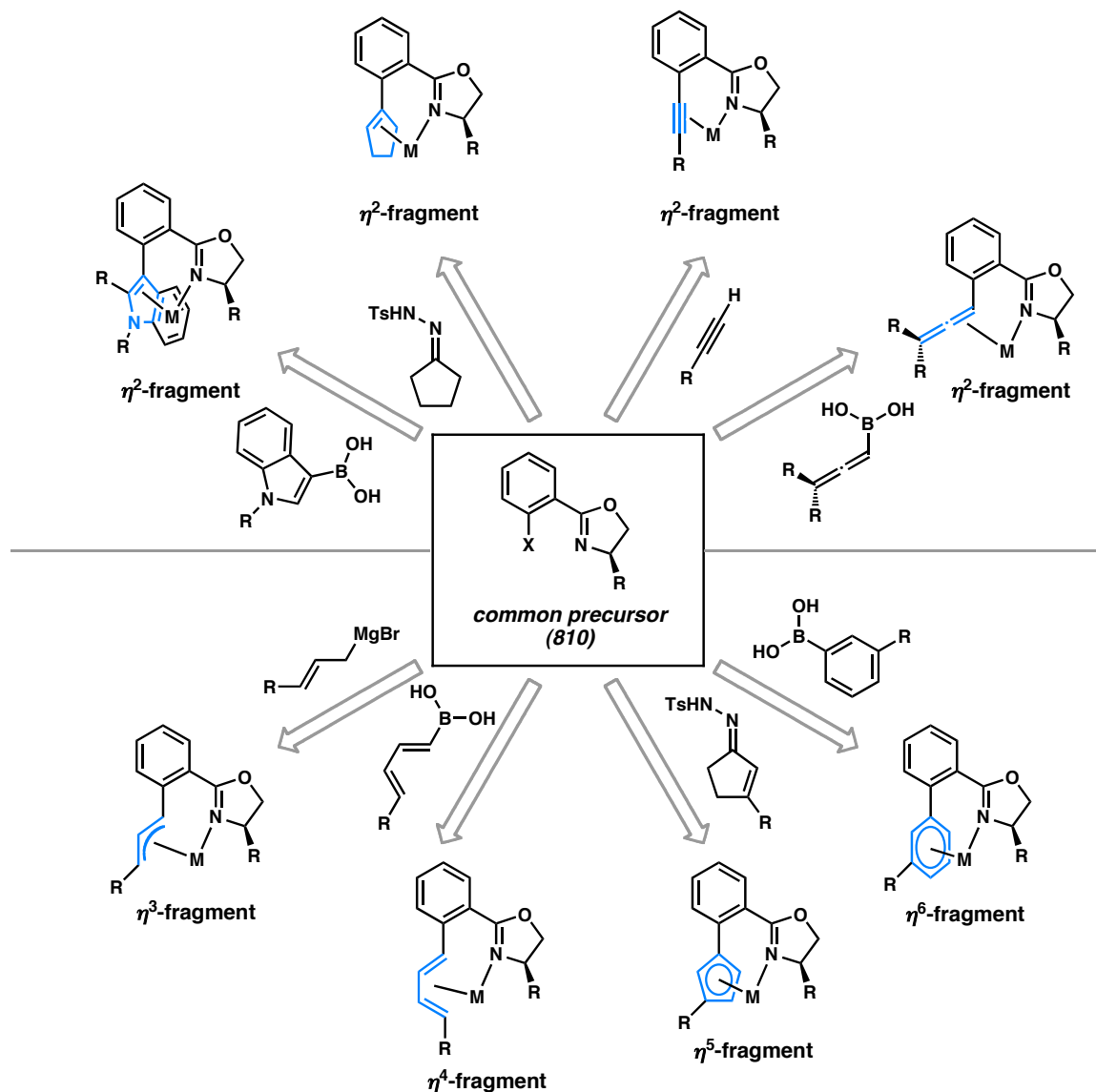


In future studies, modification of the ketimine moiety can be achieved by using simple amines such as benzylamine or even chiral amines such as α -phenethylamine to provide additional chiral information. Modification of the olefin substitution pattern can be achieved by varying the allyl fragment or α -substituent prior to the asymmetric alkylation and metathesis steps. Additionally, the size of both rings can be varied to

influence the bite angle of the bidentate ligand. Overall, these related ligands should provide different electronic and steric properties compared to OlefOX ligands.

A13.4 FUTURE DIRECTIONS

While the work summarized is preliminary and unoptimized, the synthesis of OlefOX ligands using a cross-coupling strategy has been successfully demonstrated. **Regions A, B, and C** can be varied in our modular synthetic approach to give a diverse collection of chiral ligands. To extend the key cross-coupling concept, it may be possible to unite the common bromoaryl oxazoline precursor **810** with other coupling partners to form novel ligand types, enabling the evaluation of these ligands in asymmetric transition metal-catalyzed transformations. Additional novel ligand types can be prepared using this approach (Scheme A13.8). If we consider other η^2 -coordinating carbon-based ligands, we can imagine that cyclic alkenes, heteroaromatics, alkynes, and allenes can serve as useful components of new chiral ligands. These compounds can be formed from Suzuki, Sonagashira, or Barluenga cross-coupling reactions. By broadening the scope to η^3 -, η^3 -, η^3 -, or η^6 -coordinating carbon-based ligands, we can introduce π -allyl, dienyl, cyclopentadienyl, or arene fragments for new ligands using Kumada, Suzuki, or Barluenga cross-coupling reactions. The unifying feature is that all of these ligands are potentially accessible from a parent halo oxazoline through a cross-coupling reaction.

Scheme A13.8. Synthesis of Novel η^2 - η^6 Chiral C,N-Ligands from a Common Precursor

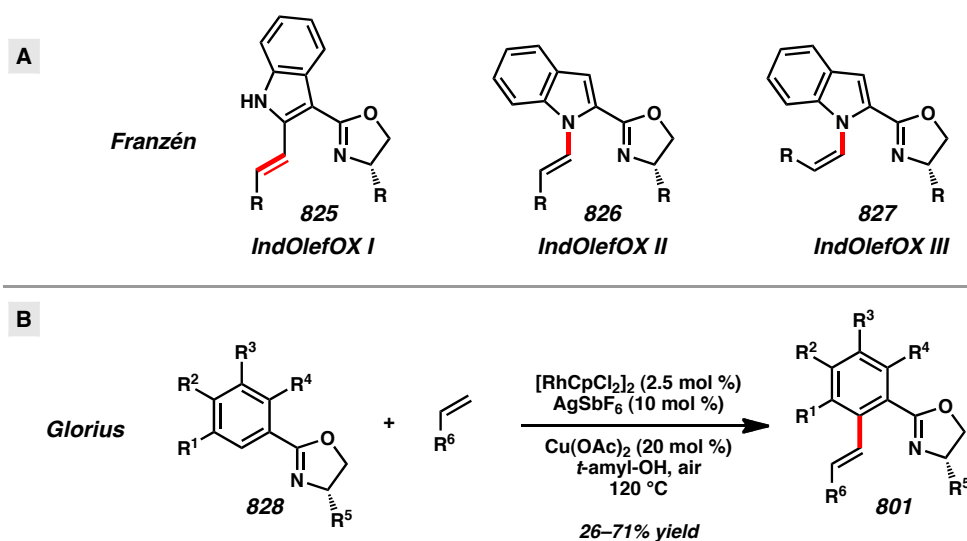
A13.5 RECENT DEVELOPMENTS IN C_1 -SYMMETRIC LIGAND DESIGN

During the course of our synthetic investigations, several reports pertaining to OlefOX ligands and our general ligand design platform have appeared in the past two years (Scheme A13.9A). Franzén and co-workers were able to prepare OlefOX derivatives with the phenyl backbone substituted for an indole ring (IndOlefOX).²³ One

type of ligand has the olefin moiety bound to the C(2) position of the indole (**825**), while the second and third types have the olefin moiety directly bound to the indole nitrogen (**826** and **827**). These classes of ligands have proved successful in rhodium-catalyzed conjugate addition reactions with various arylboron compounds.

Glorius recently employed a C–H activation strategy analogous to our cross-coupling approach for the synthesis of OlefOX ligands (**801**) (Scheme A13.9B).²⁴ His work employed rhodium-catalyzed oxidative Heck reactions to couple aryl-oxazolines with styrenes to obtain OlefOX ligands in good to modest yields (26–71% yield). This alternative synthesis affords ligands in higher yields compared to their earlier report.¹⁷

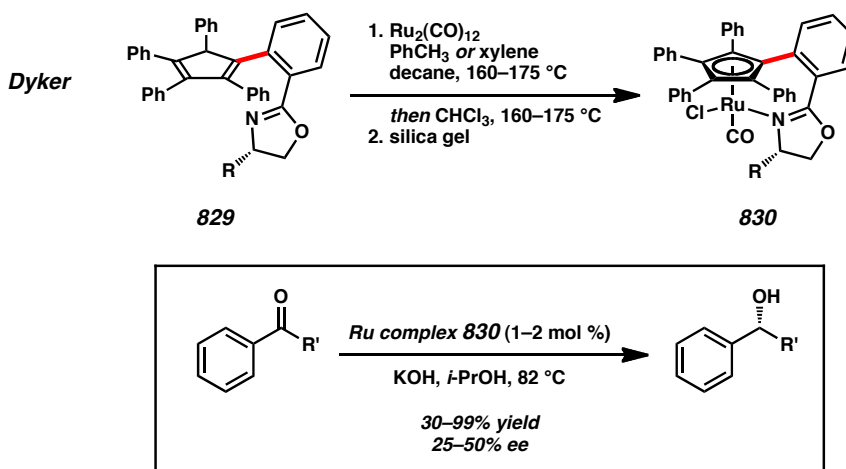
Scheme A13.9. Recent Developments in OlefOX Ligand Synthesis



By targeting chiral oxazoline-based ligands in a manner resembling our proposed ligand design platform (Section A13.4A), Dyker was able to prepare cyclopentadienyl-oxazoline ligands such as **829** and employ them in ruthenium-catalyzed transfer

hydrogenation reactions (Scheme A13.10).²⁵ With acetophenone derivatives as substrates, good yields can be achieved, but asymmetric induction is low to moderate with the ligands investigated.

Scheme A13.10. Recent Developments in the Design of Novel Chiral C_1 -Symmetric Ligands



A13.6 CONCLUSION

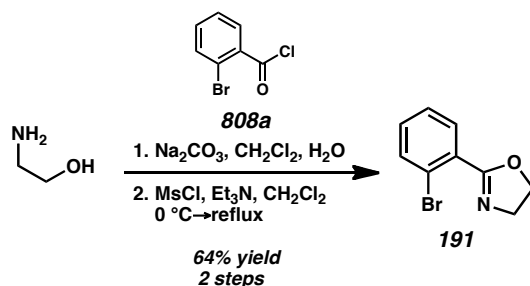
In summary, we have developed a novel synthetic route for the preparation of diverse olefin-oxazoline (OlefOX) ligands from commercial and readily available amino acid, vinyl boronic acid, and 2-halobenzoic acid derivatives. To date, we have prepared 11 unique ligands. The synthetic route is amenable to steric and electronic modifications of the three distinct structural regions of the ligand scaffold. Preliminary investigations of these ligands in transition metal-catalyzed reactions have been conducted. A related series of *spiro*-ketimine-olefin ligands has also been prepared. Our cross-coupling route to PHOX and OlefOX ligands from common bromoaryl oxazolines can potentially be generalized to new, undeveloped classes of chiral oxazoline-based ligands.

A13.7 EXPERIMENTAL SECTION

A13.7.1 MATERIALS AND METHODS

Unless otherwise stated, reactions were performed in flame-dried glassware under an argon or nitrogen atmosphere using dry, deoxygenated solvents. Reaction progress was monitored by thin-layer chromatography (TLC). Solvents were dried by passage through an activated alumina column²⁶ under argon. Triethylamine was distilled over CaH₂ prior to use. Vinyl boronic acids were purchased from Sigma-Aldrich. Pd(PPh₃)₄ was prepared according to the procedure of Coulson.²⁷ Purified water was obtained using a Barnstead NANOpure Infinity UV/UF system. Brine solutions are saturated aqueous solutions of sodium chloride. Starting materials were purchased from Aldrich, Strem, or Alfa Aesar and used as received unless otherwise stated. Reaction temperatures were controlled by an IKAmag temperature modulator. Microwave-assisted experiments were carried out in sealed reaction vials in a Biotage Initiator 2.5 microwave reactor. Glove box manipulations were performed under a N₂ atmosphere. TLC was performed using E. Merck silica gel 60 F254 precoated glass plates (0.25 mm) and visualized by UV fluorescence quenching, *p*-anisaldehyde or KMnO₄ staining. Silicycle SiliaFlash P60 Academic Silica gel (particle size 0.040-0.063 mm) was used for flash chromatography. Automated flash column chromatography was performed on a Teledyne Isco CombiFlash R_f system. ¹H NMR spectra were recorded on a Varian Mercury 300 MHz or a Varian Inova 500 MHz spectrometer (at 300 MHz and 500 MHz respectively) and are reported relative to residual CHCl₃ (δ 7.26 ppm) or acetone (δ 2.05 ppm). ¹³C spectra were recorded on a Varian Mercury 300 MHz or a Varian Inova 500 MHz spectrometer (at 75

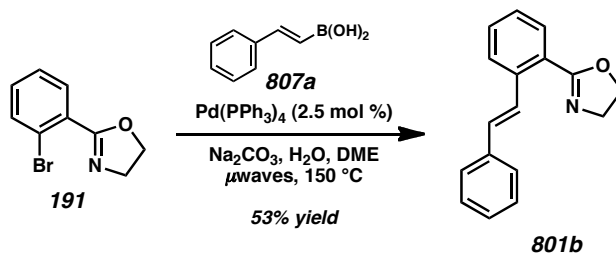
MHz and 125 MHz respectively) and are reported relative to CHCl_3 (δ 77.16 ppm) or acetone (δ 29.84 or 206.25 ppm). ^{19}F spectra were recorded on a Varian Mercury 300 MHz (at 282 MHz) are reported in terms of chemical shift (δ ppm) without the use of a reference peak. Data for ^1H NMR are reported as follows: chemical shift (δ ppm) (multiplicity, coupling constant (Hz), integration). Multiplicities are reported as follows: s = singlet, d = doublet, t = triplet, q = quartet, m = multiplet, br s = broad singlet, app = apparent. Data for ^{13}C and ^{19}F NMR are reported in terms of chemical shift (δ ppm). IR spectra were obtained by use of a Perkin Elmer Spectrum BXII spectrometer using thin films deposited on NaCl plates and reported in frequency of absorption (cm^{-1}). High-resolution mass spectra (HRMS) were obtained from the Caltech Mass Spectral Facility.

A13.7.2 PREPARATIVE PROCEDURES**A13.7.2.1 SYNTHESIS OF ACHIRAL OLEFOX LIGAND 801b**

Bromoaryl oxazoline 191.²⁸ To a solution of ethanolamine (1.32 mL, 21.9 mmol, 1.20 equiv) in CH₂Cl₂ (60 mL) in a 250 mL round-bottom flask was added a solution of Na₂CO₃ (5.80 g, 54.7 mmol, 3.00 equiv) in H₂O (45 mL). Neat 2-bromobenzoyl chloride (4.00 g, 2.38 mL, 18.2 mmol, 1.00 equiv) was added dropwise via syringe to the vigorously stirred biphasic system. The reaction flask was capped with a yellow plastic stopper and stirred for 7.5 h at 23 °C. The layers were separated and the aqueous phase was extracted with CH₂Cl₂ (2 x 25 mL). The combined organics were dried over Na₂SO₄, filtered, and concentrated under reduced pressure to afford a white solid. The crude product was dissolved in CH₂Cl₂ (50 mL) and hexanes (10 mL) was added. The solution was concentrated to ca. 25 mL under reduced pressure resulting in precipitation of the intermediate amide (4.02 g, 16.4 mmol, 90% yield) as a white solid.

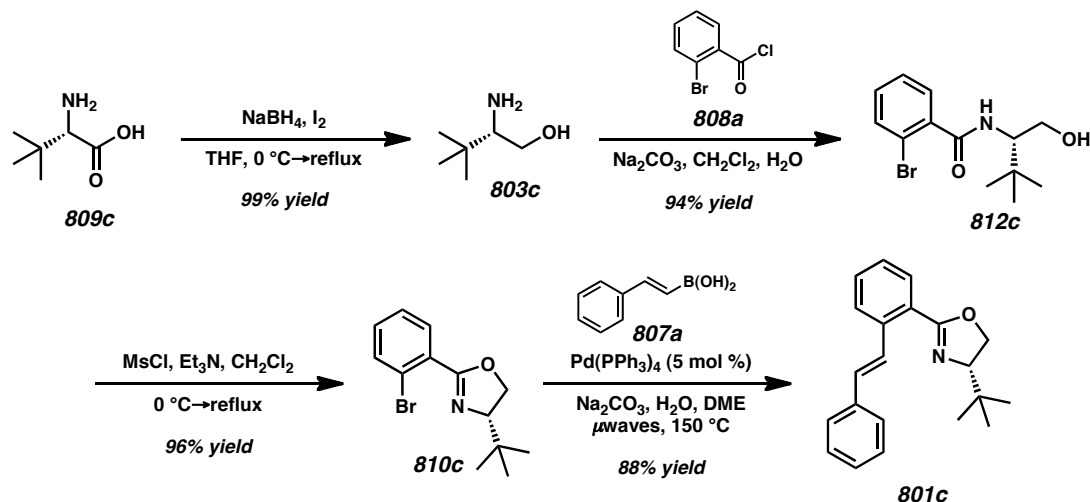
The intermediate amide (2.0 g, 8.2 mmol, 1.00 equiv) was dissolved in CH₂Cl₂ (62 mL) in a 100 mL round-bottom flask equipped with a reflux condenser. Et₃N (3.43 mL, 24.5 mmol, 3.00 equiv) was added and the solution was cooled to 0 °C by use of an ice/water bath. Methanesulfonyl chloride (952 µL, 12.3 mmol, 1.50 equiv) was added dropwise. The reaction mixture was stirred at 0 °C for 30 min and heated to 40 °C in an

oil bath. After 5 h of stirring, the resulting yellow solution was allowed to cool to ambient temperature, diluted with CH₂Cl₂ (25 mL), and washed with H₂O (2 x 25 mL) and brine (25 mL). The organic layer was dried over Na₂SO₄, filtered, and concentrated under reduced pressure to afford a thick, pale yellow oil. The crude oil was purified by flash chromatography (SiO₂, 5 x 10 cm, 6:2:2 hexanes:EtOAc:toluene) to afford 2-(2-bromo-phenyl)-4,5-dihydrooxazole **191** (1.31 g, 5.79 mmol, 71% yield); *R*_f = 0.45 (9:1 CHCl₃:MeOH); ¹H NMR (500 MHz, CDCl₃) δ 7.72 (dd, *J* = 7.8, 2.0 Hz, 1H), 7.65 (dd, *J* = 8.1, 1.0 Hz, 1H), 7.35 (app dt, *J* = 7.6, 1.2 Hz, 1H), 7.29 (app dt, *J* = 7.6, 1.7 Hz, 1H), 4.46 (t, *J* = 9.6 Hz, 2H), 4.12 (t, *J* = 9.6 Hz, 2H); ¹³C NMR (125 MHz, CDCl₃) δ 164.0, 134.1, 131.8, 131.5, 129.8, 127.2, 122.0, 67.8, 55.5; IR (Neat Film NaCl) 3390, 3070, 2966, 2904, 2868, 1729, 1646, 1589, 1432, 1362, 1328, 1272, 1243, 1093, 1026, 938 cm⁻¹; HRMS (EI+) *m/z* calc'd for C₉H₈BrNO [M]⁺: 224.9789; found 224.9779.



Olefin-Oxazoline Ligand 801b. A 20 mL microwave vial with a magnetic stir bar was flame-dried under vacuum and cooled under N₂. *Trans*-2-phenylvinyl boronic acid (452 mg, 3.05 mmol, 1.50 equiv), and Pd(PPh₃)₄ (59 mg, 0.051 mmol, 0.025 equiv) were added before the vial was sealed with a microwave crimp cap. The contents were evacuated and backfilled with N₂ (3 cycles, 5 min evacuation per cycle). Bromoaryl oxazoline **191** (460 mg, 2.03 mmol, 1.00 equiv) in DME (1 mL) was added to the

syringe, followed by aqueous Na_2CO_3 (561 mg, 2 M, 2.60 equiv). The mixture was stirred for 5 min. The reaction was subjected to microwave irradiation in a Biotage Initiator microwave reactor (temperature: 150 °C, sensitivity: very high) until no further changes could be observed by TLC. After 2.5 h of irradiation, the layers were separated and the aqueous layer was extracted with diethyl ether (3 x 15 mL). The organics were dried with Na_2SO_4 , filtered, and concentrated under reduced pressure to afford an oil. The crude material was purified by automated flash column chromatography using a Teledyne Isco CombiFlash R_f system (SiO_2 , 12 g loading cartridge, 80 g column, 0→10→30→60% EtOAc in hexanes) to give olefin-oxazoline **801b** as a slowly crystallizing yellow sap (268.4 mg, 1.08 mmol, 53% yield); R_f = 0.51 (2:1 hexanes:EtOAc); ^1H NMR (300 MHz, CDCl_3) δ 8.07 (d, J = 16.3 Hz, 1H), 7.84 (dd, J = 7.8, 1.5 Hz, 1H), 7.73 (dm, J = 7.8 Hz, 1H), 7.60–7.49 (m, 2H), 7.50–7.40 (m, 1H), 7.42–7.20 (m, 4H), 7.03 (d, J = 16.3 Hz, 1H), 4.43 (td, J = 9.5, 1.0 Hz, 2H), 4.14 (td, J = 9.5, 1.0 Hz, 2H).

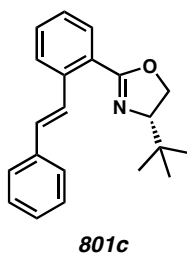
A13.7.2.2 GENERAL OLEFOX LIGAND SYNTHESIS PROCEDURES**General Procedures A–C: Amino Acid Reduction, Amide Formation, and Oxazoline**

Construction. General, scalable procedures for the preparation of amino alcohol (**809**), hydroxy amide (**812**), and bromoaryl oxazoline (**810**) intermediates can be found in ref. 8b.

General Procedure D: Suzuki Coupling. A 20 mL microwave vial with a magnetic stir bar under N_2 was charged with bromoaryl oxazoline **810c** (120 mg, 0.424 mmol, 1.00 equiv), *trans*-2-phenylvinyl boronic acid (75.3 mg, 0.509 mmol, 1.00 equiv), and $\text{Pd}(\text{PPh}_3)_4$ (25.4 mg, 0.022 mmol, 0.05 equiv) and capped with a microwave crimp cap. DME (5 mL) and aqueous Na_2CO_3 (0.552 mL, 2 M, 2.60 equiv) were added to the vial and additional DME was added to the total volume to 10 mL. The mixture was stirred for 5 min and subjected to microwave irradiation in a Biotage Initiator microwave reactor (temperature: 150 °C, sensitivity: high) until no further changes could be observed by TLC. After 30 min of irradiation, the layers were separated and the aqueous layer was extracted with diethyl ether (3 x 15 mL). The organics were dried with Na_2SO_4 , filtered,

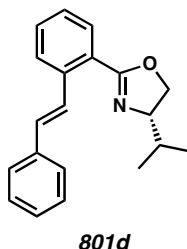
and concentrated under reduced pressure to afford an oil. The crude material was purified by flash column chromatography (SiO₂, 3.0 x 25 cm, 15:1:1→10:1:1 hexanes:EtOAc:acetone) to give olefin-oxazoline ligand **801c** as a white solid (113.7 mg, 0.37 mmol, 87.8% yield).

A13.7.2.3 CHARACTERIZATION DATA FOR OLEFOX LIGANDS 801

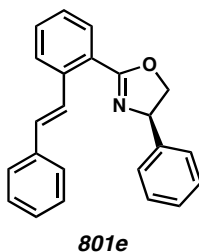


Olefin-Oxazoline Ligand (801). Prepared using General Procedure D. Bromoaryl oxazoline **810c** (120 mg, 0.424 mmol, 1.00 equiv), *trans*-2-phenylvinyl boronic acid (75.3 mg, 0.509 mmol, 1.20 equiv), Pd(PPh₃)₄ (25.4 mg, 0.022 mmol, 0.05 equiv), 2 M Na₂CO₃ (0.552 mL, 1.104 mmol, 2.60 equiv). 113.7 mg, 0.37 mmol, 87.8% yield. Flash column chromatography (SiO₂, 3.0 x 25 cm, 15:1 hexanes:EtOAc). *R_f* = 0.63 (9:1 hexanes: EtOAc). ¹H NMR (300 MHz, CDCl₃) δ 8.24 (d, *J* = 16.3 Hz, 1H), 7.85 (dd, *J* = 7.8, 1.3 Hz, 1H), 7.82–7.72 (dm, *J* = 7.8 Hz, 1H), 7.62–7.53 (m, 2H), 7.46 (dddd, *J* = 7.9, 7.9, 1.5, 0.6 Hz, 1H), 7.43–7.23 (m, 4H), 7.06 (d, *J* = 16.3 Hz, 1H), 4.37 (dd, *J* = 9.5, 7.7 Hz, 1H), 4.28–4.12 (m, 2H), 1.04 (s, 9H); ¹³C NMR (75 MHz, CDCl₃) δ 163.3, 138.1, 137.8, 130.7, 130.5, 130.1, 128.7, 128.1, 127.7, 127.2, 126.9, 126.5, 126.3, 77.2, 68.2, 34.1, 26.1; IR (Neat Film NaCl) 3584, 3401, 3081, 3062, 3026, 2960, 2897, 2868, 1638, 1598, 1494, 1482, 1448, 1353, 1333, 1304, 1290, 1241, 1224, 1209, 1164, 1122, 1048,

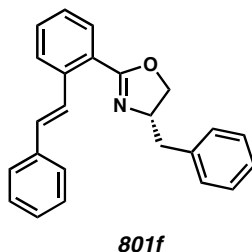
1040, 1026, 987, 973, 904, 761 cm^{-1} ; HRMS (FAB+) m/z calc'd for $\text{C}_{21}\text{H}_{24}\text{ON}$ $[\text{M}+\text{H}]^+$: 306.1858, found 306.1863.



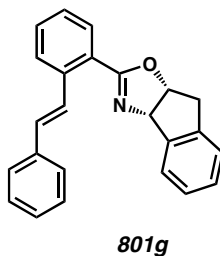
Olefin-Oxazoline Ligand (801d). Prepared using General Procedure D. Bromoaryl oxazoline **810d** (240 mg, 0.895 mmol, 1.00 equiv), *trans*-2-phenylvinyl boronic acid (159 mg, 1.074 mmol, 1.20 equiv), $\text{Pd}(\text{PPh}_3)_4$ (52.0 mg, 0.045 mmol, 0.05 equiv), 2 M Na_2CO_3 (1.16 mL, 2.32 mmol, 2.60 equiv). 179.8 mg, 0.62 mmol, 68.9% yield. Flash column chromatography (SiO_2 , 3.0 x 25 cm, 15:1→12:1 hexanes:EtOAc). R_f = 0.73 (4:1 hexanes:EtOAc); ^1H NMR (300 MHz, CDCl_3) δ 8.28 (d, J = 16.3 Hz, 1H), 7.90 (dd, J = 7.8, 1.5 Hz, 1H), 7.79 (d, J = 8.1 Hz, 1H), 7.68–7.56 (m, 2H), 7.55–7.24 (m, 5H), 7.10 (d, J = 16.3 Hz, 1H), 4.43 (dd, J = 9.1, 7.6 Hz, 1H), 4.30–4.06 (m, 2H), 1.93 (dq, J = 13.3, 6.7 Hz, 1H), 1.15 (d, J = 6.7 Hz, 3H), 1.05 (d, J = 6.7 Hz, 3H); ^{13}C NMR (75 MHz, CDCl_3) δ 163.2, 137.9, 137.7, 130.6, 130.3, 130.0, 128.6, 127.9, 127.6, 127.1, 126.8, 126.3, 126.2, 73.4, 69.8, 33.1, 18.9, 18.6; IR (Neat Film NaCl) 3583, 3400, 3060, 3023, 2958, 2928 2896, 2872, 1642, 1599, 1578, 1495, 1484, 1467, 1448, 1382, 1348, 1306, 1278, 1218, 1242, 1118, 1043, 965, 903, 760, 737 cm^{-1} ; HRMS (FAB+) m/z calc'd for $\text{C}_{20}\text{H}_{22}\text{ON}$ $[\text{M}+\text{H}]^+$: 292.1701, found 292.1691.



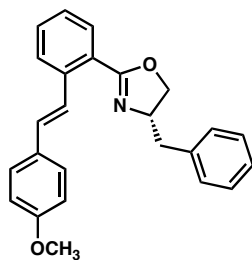
Olefin-Oxazoline Ligand (801e). Prepared using General Procedure D. Bromoaryl oxazoline **810e** (240 mg, 0.738 mmol, 1.00 equiv), *trans*-2-phenylvinyl boronic acid (130.0 mg, 0.886 mmol, 1.2 equiv), Pd(PPh₃)₄ (41.6 mg, 0.037 mmol, 0.05 equiv), 2 M Na₂CO₃ (1.0 mL, 1.92 mmol, 2.6 equiv). 200.6 mg, 0.62 mmol, 83.5% yield. Flash column chromatography (SiO₂, 3.0 x 25 cm, 12:1 hexanes:EtOAc). R_f = 0.68 (4:1 hexanes: EtOAc). ¹H NMR (300 MHz, CDCl₃) δ 8.07 (d, J = 16.3 Hz, 1H), 7.79 (dd, J = 7.8, 1.5 Hz, 1H), 7.65 (d, J = 7.8 Hz, 1H), 7.43–7.07 (m, 12H), 6.93 (d, J = 16.3 Hz, 1H), 5.36 (dd, J = 10.2, 8.1 Hz, 1H), 4.66 (dd, J = 10.2, 8.4 Hz, 1H), 4.16 (dd, J = 8.2, 8.2 Hz, 1H); ¹³C NMR (75 MHz, CDCl₃) δ 164.8, 142.6, 138.1, 137.6, 131.0, 130.7, 130.2, 128.8, 128.7, 127.7, 127.6, 127.2, 126.9, 126.7, 126.4, 126.1, 74.2, 70.7; IR (Neat Film NaCl) 3060, 3025, 2954, 2923, 2853, 1640, 1598, 1577, 1566, 1494, 1484, 1449, 1352, 1309, 1275, 1258, 1240, 1217, 1120, 1055, 1035, 953, 896, 760, 738 cm⁻¹; HRMS (FAB+) m/z calc'd for C₂₃H₂₀ON [M+H]⁺: 326.1545, found 326.1536.



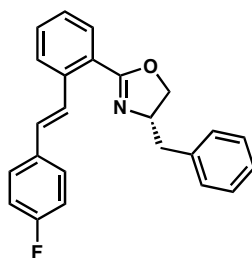
Olefin-Oxazoline Ligand (801f). Prepared using General Procedure D. Bromoaryl oxazoline **810f** (240 mg, 0.759 mg, 1.00 equiv), *trans*-2-phenylvinyl boronic acid (134.0 mg, 0.911 mmol, 1.20 equiv), Pd(PPh₃)₄ (42.0 mg, 0.038 mmol, 0.05 equiv), 2 M Na₂CO₃ (1.0 mL, 1.97 mmol, 2.60 equiv). 195.8 mg, 0.58 mmol, 76.0% yield. Flash column chromatography (SiO₂, 3.0 x 25 cm, 12:1→9:1 hexanes:EtOAc). *R_f* = 0.21 (4:1 hexanes:EtOAc). ¹H NMR (300 MHz, CDCl₃) δ 8.01 (d, *J* = 16.3 Hz, 1H), 7.71 (dd, *J* = 7.9, 1.5 Hz, 1H), 7.57 (d, *J* = 7.5 Hz, 1H), 7.38–7.31 (m, 2H), 7.32–6.99 (m, 10H), 6.87 (d, *J* = 16.3 Hz, 1H), 4.49 (dtd, *J* = 9.4, 7.4, 6.2 Hz, 1H), 4.17 (dd, *J* = 9.4, 8.4 Hz, 1H), 3.93 (dd, *J* = 8.4, 7.5 Hz, 1H), 3.02 (dd, *J* = 13.8, 6.2 Hz, 1H), 2.67 (dd, *J* = 13.8, 7.5 Hz, 1H); ¹³C NMR (75 MHz, CDCl₃) δ 163.7, 138.1, 137.6, 130.8, 130.6, 130.1, 129.3, 128.6, 128.5, 128.0, 127.6, 127.1, 126.9, 126.4, 126.4, 126.0, 71.2, 68.4, 41.9; IR (Neat Film NaCl) 3635, 3401, 3060, 3025, 2918, 1638, 1599, 1577, 1566, 1495, 1484, 1450, 1352, 1310, 1275, 1244, 1217, 1120, 1072, 1049, 1030, 967, 926, 860, 760, 738 cm⁻¹; HRMS (FAB+) *m/z* calc'd for C₂₄H₂₂NO [M+H]⁺: 340.1701, found 340.1686.



Olefin-Oxazoline Ligand (801g). Prepared using General Procedure D. Bromoaryl oxazoline **310g** (240 mg, 0.764 mmol, 1.00 equiv), *trans*-2-phenylvinyl boronic acid (135.7 mg, 0.917 mmol, 1.20 equiv), Pd(PPh₃)₄ (43.91 mg, 0.038 mmol, 0.05 equiv), 2 M Na₂CO₃ (0.99 mL, 1.99 mmol, 2.60 equiv). 205.5 mg, 0.61 mmol, 79.7% yield. Flash column chromatography (SiO₂, 3.0 x 25 cm, 12:1→6:1 hexanes:EtOAc. *R_f* = 0.55 (4:1 hexanes:EtOAc). ¹H NMR (300 MHz, CDCl₃) δ 7.91 (d, *J* = 16.3 Hz, 1H), 7.84 (dd, *J* = 7.8, 1.5 Hz, 1H), 7.79–7.66 (m, 2H), 7.51–7.28 (m, 10H), 7.04 (d, *J* = 16.3 Hz, 1H), 5.86 (d, *J* = 7.8 Hz, 1H), 5.48 (ddd, *J* = 8.0, 6.3, 1.8 Hz, 1H), 3.53 (dd, *J* = 18.0, 6.3 Hz, 1H), 3.42 (d, *J* = 16.8 Hz, 1H); ¹³C NMR (75 MHz, CDCl₃) δ 163.8, 142.3, 139.6, 137.5, 137.5, 130.6, 130.0, 129.8, 128.5, 128.4, 127.5, 127.4, 127.4, 127.0, 126.7, 126.4, 125.9, 125.5, 125.4, 82.7, 77.4, 39.8; IR (Neat Film NaCl) 3583, 3392, 3061, 3024, 2921, 2361, 1949, 1632, 1598, 1496, 1481, 1460, 1449, 1347, 1316, 1283, 1258, 1234, 1214, 1167, 1119, 1044, 992, 962, 926, 898, 859, 760, 750, 715 cm⁻¹; HRMS (FAB+) *m/z* calc'd for C₂₄H₂₀NO [M+H]⁺: 338.1545, found 338.1537.

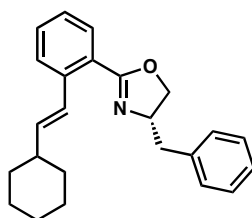
**801f**

Olefin-Oxazoline Ligand (301). Prepared using General Procedure D. Bromoaryl oxazoline **310f** (240 mg, 0.759 mmol, 1.00 equiv), *trans*-2-(4-methylphenyl)vinyl boronic acid (148.6 mg, 0.835 mmol, 1.10 equiv), Pd(PPh₃)₄ (43.9 mg, 0.038 mmol, 0.05 equiv), 2 M Na₂CO₃ (0.986 mL, 1.97 mmol, 2.60 equiv). 210 mg, 0.57 mmol, 74.9% yield. Flash column chromatography (SiO₂, 3.0 x 25 cm, 10:1:1 hexanes:EtOAc:acetone). *R_f* = 0.42 (10:1:1 hexanes:EtOAc:acetone); HRMS (FAB+) *m/z* calc'd for C₂₅H₂₃NO₂ [M+H]⁺: 369.1729, found 369.1710.

**801k**

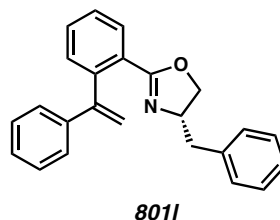
Olefin-Oxazoline Ligand (301k). Prepared using General Procedure D. Bromoaryl oxazoline **310k** (240 mg, 0.759 mmol, 1.00 equiv), *trans*-2-(4-fluorophenyl)vinylboronic acid (151 mg, 0.911 mmol, 1.20 equiv), Pd(PPh₃)₄ (43.9 mg, 0.038 mmol, 0.05 equiv), 2 M Na₂CO₃ (0.986 mL). 59.6 mg, 0.17 mmol, 22.0% yield. Flash column chromatography (SiO₂, 3.0 x 25 cm, 10:1:1 hexanes:EtOAc:acetone). *R_f* = 0.49 (10:1:1 hexanes:acetone:EtOAc). ¹H NMR (300 MHz, CDCl₃) δ 7.94 (d, *J* = 16.3 Hz, 1H), 7.76

(dd, $J = 7.8, 1.4$ Hz, 1H), 7.63 (dd, $J = 8.1, 1.3$ Hz, 1H), 7.45–7.30 (m, 2H), 7.31–7.12 (m, 5H), 7.02–6.81 (m, 2H), 4.69–4.51 (m, 1H), 4.31 (dd, $J = 9.4, 8.4$ Hz, 1H), 4.05 (dd, $J = 8.4, 7.4$ Hz, 1H), 3.11 (dd, $J = 13.8, 6.3$ Hz, 1H), 2.78 (dd, $J = 13.8, 7.5$ Hz, 1H); ^{13}C NMR (75 MHz, CDCl_3) δ 164.0 ($J_{\text{CF}} = 13.3$ Hz), 138.1 ($J_{\text{CF}} = 9.2$ Hz), 134.0 ($J_{\text{CF}} = 3.3$ Hz), 131.0, 130.3, 129.5, 129.4, 128.6, 128.5, 128.4, 127.9 ($J_{\text{CF}} = 2.6$ Hz), 127.3, 126.6, 126.4, 126.1, 115.8, 115.5, 71.4, 68.6, 42.1; ^{19}F NMR (282 MHz, CDCl_3) δ -114.26 (tt, $J = 8.6, 5.4$ Hz); HRMS (EI+) m/z calc'd for $\text{C}_{24}\text{H}_{19}\text{FNO}$ $[\text{M}]^{+}$: 356.1451, found 356.1455.

**801j**

Olefin-Oxazoline Ligand (801j). Prepared using General Procedure D. Bromoaryl oxazoline **310f** (240 mg, 0.759 mmol, 1.00 equiv), *trans*-2-cyclohexylvinyl boronic acid (134.8 mg, 0.911 mmol, 1.20 equiv), $\text{Pd}(\text{PPh}_3)_4$ (43.9 mg, 0.038 mmol, 0.05 equiv), 2 M Na_2CO_3 (0.986 mL, 1.97 mmol, 2.60 equiv). 212 mg, 0.61 mmol, 80.8% yield. Flash column chromatography (SiO_2 , 3.0 x 25 cm, 15:2:2 hexanes:EtOAc:acetone). $R_f = 0.31$ (15:1:1 hexanes:EtOAc:acetone). ^1H NMR (300 MHz, CDCl_3) δ 7.82 (dd, $J = 7.7, 1.5$ Hz, 1H), 7.63 (dd, $J = 8.0, 1.3$ Hz, 1H), 7.46–7.21 (m, 9H), 6.19 (dd, $J = 15.9, 6.8$ Hz, 1H), 4.79–4.60 (m, 1H), 4.38 (dd, $J = 9.5, 8.4$ Hz, 1H), 4.15 (dd, $J = 8.4, 7.4$ Hz, 1H), 3.25 (dd, $J = 13.8, 5.9$ Hz, 1H), 2.88 (dd, $J = 13.8, 7.7$ Hz, 1H), 2.35–2.14 (m, 1H), 1.98–1.69 (m, 3H), 1.55–1.15 (m, 6H); ^{13}C NMR (75 MHz, CDCl_3) δ 164.1, 138.6, 138.5, 138.1, 130.5, 129.8, 129.3, 128.4, 126.4, 126.3, 126.3, 126.2, 125.6, 71.2, 68.3, 41.8,

41.2, 32.8, 26.2, 26.1; IR (Neat Film NaCl); HRMS (EI+) m/z calc'd for $C_{24}H_{27}NO$ $[M+H]^+$: 345.2093, found 345.2090.



Olefin-Oxazoline Ligand (801I). Prepared using General Procedure D. Bromoaryl oxazoline **310f** (240 mg, 0.759 mmol, 1.00 equiv), 1-phenylvinyl boronic acid (123.5 mg, 0.835 mmol, 1.10 equiv), $Pd(PPh_3)_4$ (43.9 mg, 0.038 mmol, 0.05 equiv), 2 M Na_2CO_3 (0.986 mL, 1.97 mmol, 2.60 equiv). 112.4 mg, 0.33 mmol, 74.9% yield. Flash column chromatography (SiO_2 , 2.0 x 25 cm, 10:1:1 hexanes:EtOAc:acetone). R_f = 0.52 (10:1:1 hexanes:EtOAc:acetone).

A13.8 NOTES AND REFERENCES

- (1) For reviews of chiral bis-phosphine ligands, see: (a) Tang, W.; Zhang, X. *Chem. Rev.* **2003**, *103*, 3029–3070. (b) Shimizu, H.; Nagasaki, I.; Saito, T. *Tetrahedron* **2005**, *61*, 5405–5432. (c) Li, Y.-M.; Kwong, F.-Y.; Yu, W.-Y.; Chang, A. S. C. *Coord. Chem. Rev.* **2007**, *251*, 2119–2144.
- (2) For reviews of chiral bis-oxazoline (BOX) ligands, see: (a) Pfaltz, A. *Acc. Chem. Res.* **1993**, *26*, 339–345. (b) Ghosh, A. K.; Mathivanan, P.; Cappiello, J. *Tetrahedron: Asymmetry* **1998**, *9*, 1–45. (c) McManus, H. A.; Guiry, P. J. *Chem. Rev.* **2004**, *104*, 4151–4202.
- (3) For early reports of chiral bis-oxazoline (BOX) ligands, see: (a) Lowenthal, R. E.; Abiko, A.; Masamune, S. *Tetrahedron Lett.* **1990**, *31*, 6005–6008. (b) Evans, D. A.; Woerpel, K. A.; Hinman, M. M.; Faul, M. M. *J. Am. Chem. Soc.* **1991**, *113*, 726–728.
- (4) For reviews of chiral diene ligands, see: (a) Glorius, F. *Angew. Chem. Int. Ed.* **2004**, *43*, 3364–3366. (b) Defieber, C.; Grützmacher, H.; Carreira, E. M. *Angew. Chem. Int. Ed.* **2008**, *47*, 4482–4502. (c) Johnson, J. B.; Rovis, T. *Angew. Chem. Int. Ed.* **2008**, *47*, 840–871.
- (5) For early reports of chiral diene ligands, see: (a) Hayashi, T.; Ueyama, K.; Tokunaga, N.; Yoshida, K. *J. Am. Chem. Soc.* **2003**, *125*, 11508–11509. (b) Fischer, C.; Defieber, C.; Suzuki, T.; Carreira, E. M. *J. Am. Chem. Soc.* **2004**, *126*, 1628–1269.

- (6) For reviews of chiral phosphinooxazoline (PHOX) ligands, see: (a) Helmchen, G.; Pfaltz, A. *Acc. Chem. Res.* **2000**, *33*, 336–345. (b) McManus, H. A.; Guiry, P. *J. Chem. Rev.* **2004**, *104*, 4151–4202.
- (7) For early reports of chiral phosphinooxazoline (PHOX) ligands, see: (a) von Matt, P.; Pfaltz, A. *Angew. Chem. Int. Ed. Engl.* **1993**, *32*, 566–568. (b) Sprinz, J.; Helmchen, G. *Tetrahedron Lett.* **1993**, *34*, 1769–1772. (c) Dawson, G. J.; Frost, C. G.; Williams, J. M. J.; Coote, S. J. *Tetrahedron Lett.* **1993**, *34*, 3149–3150.
- (8) For procedures detailing improved and scalable syntheses of PHOX ligands from our group, see: (a) Tani, K.; Behenna, D. C.; McFadden, R. M.; Stoltz, B. M. *Org. Lett.* **2007**, *9*, 2529–2531. (b) Krout, M. R.; Mohr, J. T.; Stoltz, B. M. *Org. Synth.* **2009**, *86*, 181–193.
- (9) (a) Schnider, P.; Koch, G.; Prétôt, R.; Wang, G.; Bohnen, F. M.; Krüger, C.; Pfaltz, A. *Chem. Eur. J.* **1997**, *3*, 887–891. (b) Lightfoot, A.; Schnider, P.; Pfaltz, A. *Angew. Chem. Int. Ed.* **1998**, *37*, 2897–2899
- (10) Langer, T.; Helmchen, G. *Tetrahedron Lett.* **1996**, *37*, 1381–1384.
- (11) (a) Newman, L. M.; Williams, J. M. J.; McCague, R.; Potter, G. A. *Tetrahedron: Asymmetry* **1996**, *7*, 1597–1599. (b) Langer, T.; Janssen, J.; Helmchen, G.; *Tetrahedron: Asymmetry* **1996**, *7*, 1599–1602.
- (12) (a) Loiseleur, O.; Meier, P.; Pfaltz, A. *Angew. Chem. Int. Ed.* **1996**, *35*, 200–202. (b) Loiseleur, O.; Hayashi, M.; Schmees, N.; Pfaltz, A. *Synthesis* **1997**, 1338–

1345. (c) Doudnay, A. B.; Humphreys, P. G.; Overman, L. E.; Wroblewski, A. D. *J. Am. Chem. Soc.* **2008**, *130*, 5368–5377.
- (13) (a) Behenna, D. C.; Stoltz, B. M. *J. Am. Chem. Soc.* **2004**, *126*, 15044–15045.
(b) Mohr, J. T.; Behenna, D. C.; Harned, A. M.; Stoltz, B. M. *Angew. Chem. Int. Ed.* **2005**, *44*, 6924–6927. (c) Behenna, D. C.; Mohr, J. T.; Sherden, N. H.; Marinescu, S. C.; Harned, A. M.; Tani, K.; Seto, M.; Ma, S.; Novák, Z.; Krout, M. R.; McFadden, R. M.; Roizen, J. L.; Enquist, Jr., J. A.; White, D. E.; Levine, S. R.; Petrova, K. V.; Iwashita, A.; Virgil, S. C.; Stoltz, B. M. *Chem. Eur. J.* **2011**, *17*, 14199–14223.
- (14) (a) Zhang, Y.; Sigman, M. S. *J. Am. Chem. Soc.* **2007**, *129*, 3076–3077. (b) He, W.; Yip, K.-T.; Zhu, N.-Y.; Yang, D. *Org. Lett.* **2009**, *11*, 5626–5628.
(c) McDonald, R. I.; White, P. B.; Weinstein, A. B.; Tam, C. P.; Stahl, S. S. *Org. Lett.* **2011**, *13*, 2830–2833. (d) Jana, R.; Pathak, T. P.; Jensen, K. H.; Sigman, M. S. *Org. Lett.* **2012**, *14*, 4074–4077. (e) Yang, G.; Shen, C.; Zhang, W. *Angew. Chem. Int. Ed.* **2012**, *51*, 9141–9145.
- (15) Kikushima, K.; Holder, J. C.; Gatti, M.; Stoltz, B. M. *J. Am. Chem. Soc.* **2011**, *133*, 6902–6905.
- (16) (a) Shibatomi, K.; Narayama, A.; Soga, Y.; Muto, T.; Iwasa, S. *Org. Lett.* **2011**, *13*, 2944–2947. (b) Shibatomi, K.; Soga, Y.; Narayama, A.; Fujiwasa, I.; Iwasa, S. *J. Am. Chem. Soc.* **2012**, *134*, 9836–9839.
- (17) Hahn, B. T.; Tewes, F.; Fröhlich, R.; Glorius, F. *Angew. Chem. Int. Ed.* **2010**, *49*, 1143–1146.

- (18) A search of the Sigma-Aldrich catalog revealed that over 56 vinyl boronic acids are commercially available.
- (19) A search of the Sigma-Aldrich catalog revealed that 3 2-bromobenzoyl chlorides, 35 2-bromobenzaldehydes, 16 2-bromobenzonitriles, and over 100 2-bromobenzoic acids are commercially available.
- (20) (a) Ohmura, T.; Hartwig, J. F. *J. Am. Chem. Soc.* **2002**, *124*, 15164–15165.
(b) Lopez, F.; Ohmura, T.; Hartwig, J. F. *J. Am. Chem. Soc.* **2003**, *125*, 3426–3427.
- (21) Nishimura, T.; Kumamoto, H.; Nagaosa, M.; Hayashi, T. *Chem. Commun.* **2009**, 5713–5715.
- (22) For examples of the use of the Symyx Core Module in reaction optimization in our research, see: (a) McDougal, N. T.; Virgil, S. C.; Stoltz, B. M. *Synlett* **2010**, 1712–1716. (b) Behenna, D. C.; Liu, Y.; Yurino, T.; Kim, J.; White, D. E.; Virgil, S. C.; Stoltz, B. M. *Nature Chem.* **2012**, *4*, 130–133.
- (23) (a) Kuuloga, N.; Tois, J.; Franzén, R. *Tetrahedron: Asymmetry* **2011**, *22*, 468–475. (b) Kuuloga, N.; Vaismaa, M.; Franzén, R. *Tetrahedron* **2012**, *68*, 2313–2318.
- (24) Schröder, N.; Besset, T.; Glorius, F. *Adv. Synth. Catal.* **2012**, *354*, 579–583.
- (25) Kanthak, M.; Aniol, A.; Nestola, M.; Merz, K.; Oppel, I. M.; Dyker, G. *Organometallics* **2011**, *30*, 215–229.

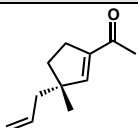
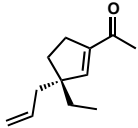
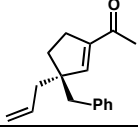
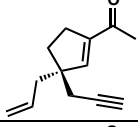
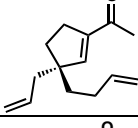
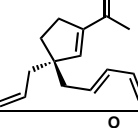
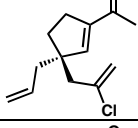
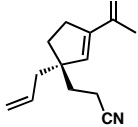
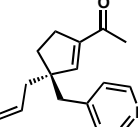
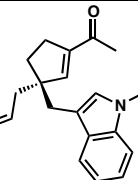
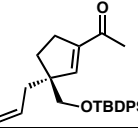
- (26) Pangborn, A. B.; Giardello, M. A.; Grubbs, R. H.; Rosen, R. K.; Timmers, F. J. *Organometallics* **1996**, *15*, 1518–1520.
- (27) Coulson, D. R.; Satek, L. C.; Grim, S. O. *Inorg. Synth.* **1972**, *13*, 121–124.
- (28) Hong, A. Y.; Bennett, N. B.; Krout, M. R.; Jensen, T.; Harned, A. M.; Stoltz, B. M. *Tetrahedron* **2011**, *67*, 10234–10248.

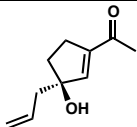
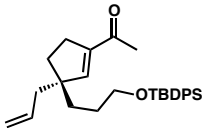
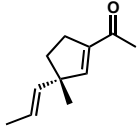
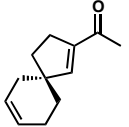
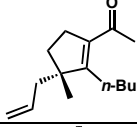
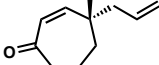
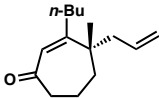
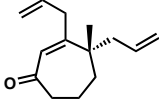
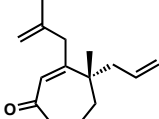
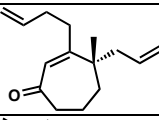
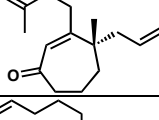
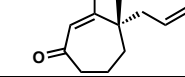
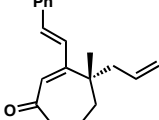
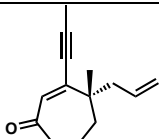
APPENDIX 14

Notebook Cross-Reference

The following notebook cross-reference has been included to facilitate access to the original spectroscopic data obtained for the compounds presented in this thesis. For each compound, both hard copy and electronic characterization folders have been created that contain copies of the original ^1H NMR, ^{13}C NMR, ^{19}F NMR, ^{31}P NMR, ^2H NMR, COSY, HSQC, HMBC, NOESY, IR spectra. Additionally, HRMS and X-ray data can also be found in these files. All notebooks and spectral data are stored in the Stoltz Group archives.

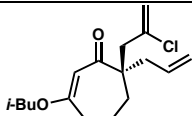
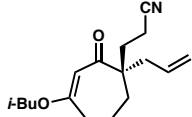
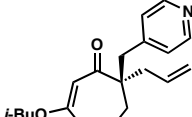
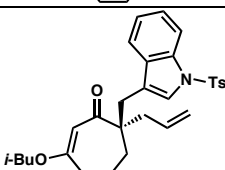
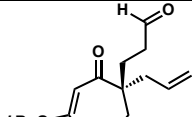
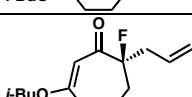
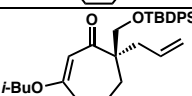
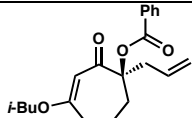
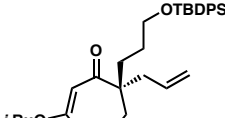
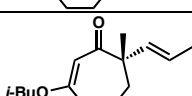
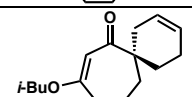
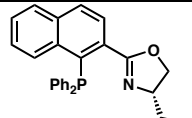
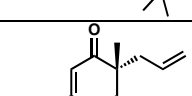
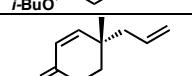
Table A14.1. Notebook Cross-Reference for Compounds in Chapter 2

compound	chemical structure	¹ H NMR	¹³ C NMR	IR
135a		TJ_III_67_1H	TJ_III_67_13C	TJ_III_67
135b		AYH-VI-99A	AYH-VI-99A	AYH-VI-99A
135c		AYH-VI-59A	AYH-VI-59A	AYH-VI-59A
135d		AYH-VI-113Ax	AYH-VI-113A	AYH-VI-113A
135e		AYH-VI-291A	AYH-VI-291A	AYH-VI-291A
135f		AYH-VIII-293A	AYH-VI-133A	AYH-VI-133A
135g		AYH-VI-169A	AYH-VI-169A	AYH-VI-169A
135h		AYH-VI-163A	AYH-VI-163A	AYH-VI-163A
135i		AYH-VIII-303A	AYH-VIII-303A	AYH-VIII-277Ax
135j		AYH-VII-141A	AYH-VII-141A	AYH-VII-141A
135m		AYH-VIII-163A	AYH-VIII-163A	AYH-VI-289A

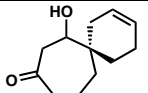
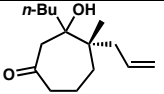
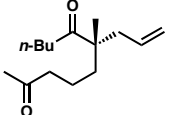
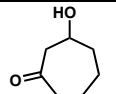
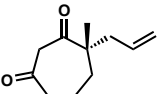
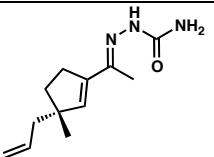
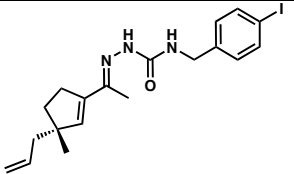
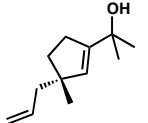
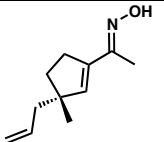
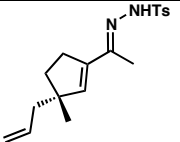
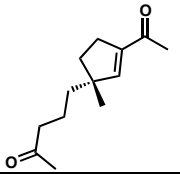
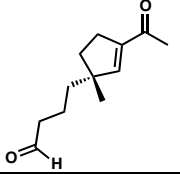
135n		AYH-IX-107B	AYH-IX-107B	AYH-IX-107B
135o		AYH-VIII-215A	AYH-VIII-215A	AYH-VIII-215A
135p		TJ-VII-141	TJ-VII-141	TJ-VII-141
135q		AYH-VIII-223A	AYH-VIII-223A	AYH-VIII-223A
135r		NBB-V-227A	NBB-V-227A	NBB-V-227A
137a		TJ-III-55A	TJ-III-55A	TJ-III-55A
137r		NBB-II-57B	NBB-I-161	NBB-II-227B
137s		NBB-VI-51B	NBB-VI-51B	NBB-VI-41B
137t		NBB-VI-79B	NBB-VI-79B	NBB-VI-79B
137u		NBB-VI-97C	NBB-VI-97C	NBB-VI-97C
137v		NBB-V-301B	NBB-V-301B	NBB-V-301B
137w		NBB-VI-85A	NBB-VI-85A	NBB-VI-85A
137x		NBB-VI-245-2B	NBB-VI-245-2B	NBB-VI-245-2B
137y		NBB-VI-69-2A	NBB-VI-69-2A	NBB-VI-69-2A

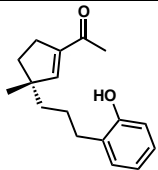
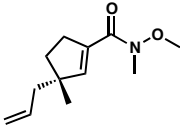
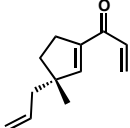
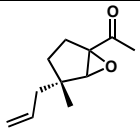
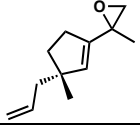
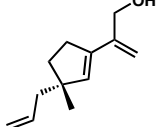
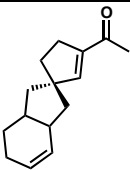
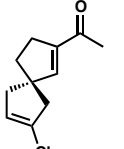
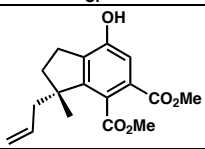
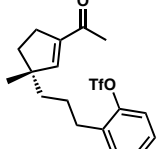
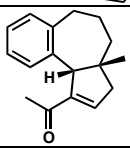
137z		NBB-VI-223-2B	NBB-VI-223-2B	NBB-VI-223-2B
137aa		NBB-VI-123-2A	NBB-VI-123-2A	NBB-VI-123-2A
137ab		NBB-VI-63B	NBB-VI-63B	NBB-VI-63B
147		MRK_VI_201B_1H	MRK_VI_201B_13C	MRK_VII_135B
148a		MRK_VI_227B_1H	MRK_VI_227B_13C	IBuOTsujiSub2
148b		AYH-V-285A	AYH-V-285A	AYH-V-285A
148c		AYH-V-293Bnew	AYH-V-293B	AYH-V-293B
148d		AYH-VI-71B	AYH-VI-71B	AYH-VI-71B
148e		AYH-VI-273A	AYH-VI-273A	AYH-VI-273A
148f		AYH-VI-105Anew	AYH-VI-105A	AYH-VI-105A
148g		AYH-VI-151Anew	AYH-VI-151A	AYH-VI-151A
148h		AYH-VI-183Bnew	AYH-VI-147D	AYH-VI-147D
148i		AYH-VII-49B2	AYH-VII-49B2	AYH-VII-49B2

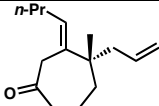
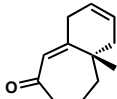
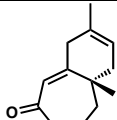
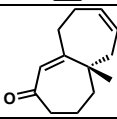
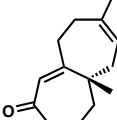
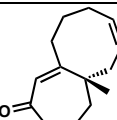
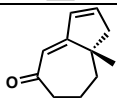
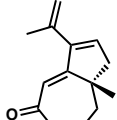
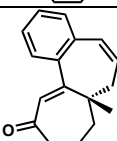
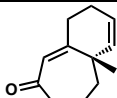
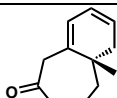
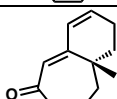
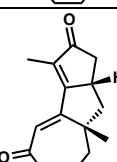
148j		AYH-VII-127B	AYH-VII-127B	AYH-VII-127B
148k		AYH-VI-257Bnew	AYH-VI-257B	AYH-VI-257B
148l		AYH-VI-37Ax	AYH-VI-37A	AYH-VI-37A
148m		AYH-VI-251Bx3	AYH-VI-251Bx3	AYH-VI-237B
148n		AYH-VI-225Bnew	AYH-VI-225B	AYH-VI-225B
148ac		AYH-VII-117B	AYH-VII-117B	AYH-VII-117B
148ad		AYH-VI-233Bnew	AYH-VI-233B	AYH-VI-233B2
149a		MRK_VII_ 33B_1H	MRK_VII_ 33B_13C	MRK_VII_33B
149b		AYH-VI-29A	AYH-VI-29A	AYH-VI-29A
149c		AYH-VI-27A	AYH-VI-27A	AYH-VI-27A
149d		AYH-VI-101A	AYH-VI-73A	AYH-VI-73A
149e		AYH-VI-279A	AYH-VI-279A	AYH-VI-279A
149f		AYH-VI-125A	AYH-VI-121A	AYH-VI-121A

149g		AYH-VI-165Anew	AYH-VI-165A	AYH-VI-165A
149h		AYH-VI-155Bnew	AYH-VI-157B	AYH-VI-157B
149i		AYH-VII-57Cnew	AYH-VII-53C	AYH-VII-53C
149j		AYH-VII-135Bx	AYH-VII-135Bx	AYH-VII-135Bx
149k		AYH-VI-269A	AYH-VI-269A	AYH-VI-269A
149l		AYH-VI-61Anew	AYH-VI-43A	AYH-VI-43A
149m		AYH-VI-255A	AYH-VI-255A	AYH-VI-255A
149n		AYH-VI-229Bnew	AYH-VI-229B	AYH-VI-229B
149o		AYH-VIII-295Ax	AYH-VIII-295Ax	AYH-VIII-207A
149p		TJ-VII-127B	TJ-VII-101	TJ-VII-101
149q		AYH-VIII-233A	AYH-VIII-219B	AYH-VIII-219B
150		MRK-XI-133 flash again	MRK-XI-133 flash again	MRK-XI-133 flash
151		AYH-VIII-139A	AYH-VIII-139A	AYH-VIII-139A
152		AYH-VIII-141A	AYH-VIII-141A	AYH-VIII-141A

154a		TJ-III-55B	TJ-III-55B	TJ-III-55B
154b		AYH-VI-97B	AYH-VI-97B	AYH-VI-97B
154c		AYH-VI-57B	AYH-VI-57B	AYH-VI-57B
154d		AYH-VI-111B	AYH-VI-111B	AYH-VI-111B
154e		AYH-VI-287B	AYH-VI-287B	AYH-VI-287B
154f		AYH-VI-131B	AYH-VI-131B	AYH-VI-131B
154g		AYH-VI-167B	AYH-VI-167B	AYH-VI-167B
154h		AYH-VI-161C	AYH-VI-161C	AYH-VI-161C
154i		AYH-IX-53C	AYH-IX-53C	AYH-IX-53C
154j		AYH-VII-137AB	AYH-VII-137AB	AYH-VII-137AB
154m		AYH-VI-161BC	AYH-VI-161BC	AYH-VI-161BC
154n		AYH-IX-105F	AYH-IX-105F	AYH-IX-105F
154o		AYH-VIII-213A	AYH-VIII-213A	AYH-VIII-213A
154p		TJ-VII-133B	TJ-VII-133B	TJ-VII-103B

154q		AYH-VIII-221B	AYH-VIII-221B	AYH-VIII-221B
154r		NBB-II-41C	NBB-II-61B	NBB-II-61B
156r		NBB-VII-39A	NBB-VII-39A	NBB-VII-39A
160		AYH-X-245E	AYH-X-245E2	AYH-X-245E2
162		NBB-VI-281A	NBB-VI-281A	NBB-VI-281A
163		TJ-III-83E	TJ-III-83E	TJ-III-83E
164		TJ-III-135B	TJ-III-135B	TJ-III-135B
165		TJ-VIII-249	TJ-VIII-249	TJ-VIII-249
166		AYH-VIII-157C	AYH-VIII-157C	AYH-VIII-157C
167		AYH-VIII-151Cx	AYH-VIII-151C	AYH-VIII-151C
168		AYH-VIII-75A	AYH-VIII-75Ax2	AYH-VIII-75A
169		AYH-VIII-111Bx	AYH-VIII-111B	AYH-VIII-111Bx2

170		TJ-VII-303A	TJ-VII-303A	TJ-VII-303A
171		AYH-VII-119A	AYH-VII-119A	AYH-VII-119A
172		AYH-VIII-79A	AYH-VII-173C	AYH-VII-173Cx
173		TJ-VII-177	TJ-VII-177	TJ-VII-177
174		TJ-VIII-225	TJ-VIII-225	TJ-VIII-225
175		TJ-VIII-87	TJ-VIII-87	TJ-VIII-87
176		AYH-IX-59B	AYH-IX-59B	AYH-IX-59B
177		AYH-IX-93B	AYH-IX-93B	AYH-IX-93B
179		AYH-VIII-253D	AYH-VIII-253D	AYH-VIII-253D
181		TJ-VIII-101B	TJ-VIII-101B	TJ-VII-41
183		TJ-VIII-181	TJ-VIII-181	TJ-VIII-181

184		NBB-VI-299A	NBB-VI-299A	NBB-VI-299A
185s		NBB-VI-167B	NBB-VI-167B	NBB-VI-167B
185t		NBB-VI-113A	NBB-VI-113A	NBB-VI-113A
185u		NBB-VI-101A	NBB-VI-101A	NBB-VI-101A
185v		NBB-VI-65A	NBB-VI-65A	NBB-VI-65A
185w		NBB-VI-93-2B	NBB-VI-93-2B	NBB-VI-93-2B
185x		NBB-VI-255C	NBB-VI-255C	NBB-VI-255B
185y		NBB-VI-89A	NBB-VI-89A	NBB-VI-89A
185z		NBB-VI-199A	NBB-VI-199A	NBB-VI-199A
186		NBB-VI-215A	NBB-VI-215A	NBB-VI-215A
187		NBB-VI-187-2A	NBB-VI-187A	NBB-VI-187A
188		NBB-VI-249B	NBB-VI-243-2B	NBB-VI-249B
189a		NBB-VI-213B	NBB-VI-213B	NBB-VI-213B

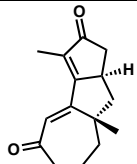
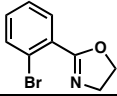
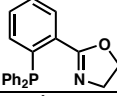
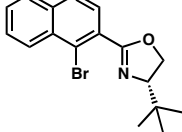
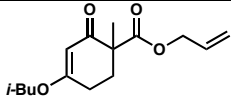
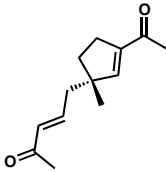
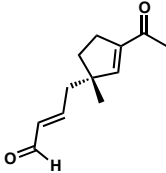
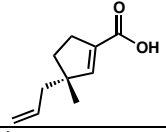
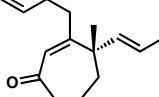
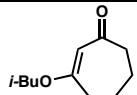
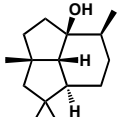
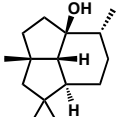
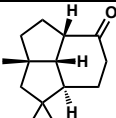
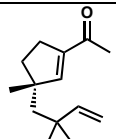
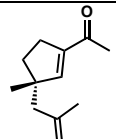
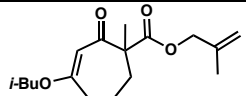
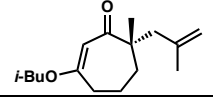
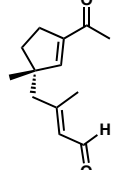
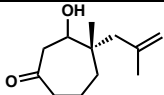
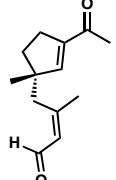
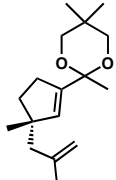
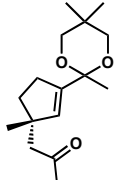
189b		NBB-VI-213F	NBB-VI-213F	NBB-VI-213F
191		TJ-I-91	TJ-I-91	TJ-I-91-3
192		TJ-PHOX	TJ-PHOX	TJ-I-263A
193		TJ-III-143A	TJ-III-143	TJ-III-143
194		AYH-VIII-137A	AYH-VIII-137A	AYH-VIII-137A
195		AYH-VII-293F	AYH-VII-293F	AYH-VII-293F
196		AYH-VIII-109C	AYH-VIII-109C	AYH-VIII-109C
197		AYH-VI-191B	AYH-VI-191B	AYH-VI-191B
198		NBB-VI-207B	NBB-VI-207B	NBB-VI-207B

Table A14.2. Notebook Cross-Reference for Compounds in Chapter 3

compound	chemical structure	¹ H NMR	¹³ C NMR	IR
147		MRK_VI_201B_1H	MRK_VI_201B_13C	MRK_VII_135B
223		AYH-XII-265A	AYH-XII-265A	AYH-XII-83F2X

224		AYH-XII-239A (C ₆ D ₆) AYH-XII-189A (CD ₂ Cl ₂)	AYH-XII-189A	AYH-XII-83F3X
286		AYH-XII-159A proton02	AYH-XII-159A	AYH-XII-137A
306		AYH-XI-229Bx2 (CDCl ₃) AYH-XI-229B (C ₆ D ₆)	AYH-XI-229Bx2 (CDCl ₃) AYH-XII-289A (C ₆ D ₆)	AYH-XI-211B
308		AYH-IX-137A	AYH-IX-137A	AYH-IX-137A
313		AYH-IX-123C	AYH-IX-123C	AYH-IX-123Cx
314		AYH-XI-147A	AYH-XI-147A	AYH-IX-125Ax
314		AYH-XIII-55B	AYH-XIII-55B	AYH-XIII-55B
315		AYH-IX-209B	AYH-IX-209B	AYH-IX-209B
319		AYH-XIII-55A	AYH-XIII-55A	AYH-XIII-55A
320		AYH-X-145A	AYH-X-145A	AYH-X-145A
324		AYH-XI-127A	AYH-X-177D1	AYH-X-177D

327		AYH-XIII-61AB	AYH-XIII-61AB	AYH-XIII-61AB
335		AYH-XII-155A	AYH-XII-155A	AYH-XII-153A
336		AYH-X-285A (CDCl ₃) AYH-XII-131A (C ₆ D ₆)	AYH-X-285A (CDCl ₃) AYH-XII-131A (C ₆ D ₆)	AYH-X-285Ax
337		AYH-X-277A	AYH-X-277A	AYH-X-275Bx
338		AYH-XI-31Axp2	AYH-XI-31A	AYH-X-267A1x
339		AYH-X-273Bxp2	AYH-X-197B	AYH-X-197Bx
340		AYH-XI-135BC proton02	AYH-XI-135BC	AYH-X-183BCx
341		AYH-X-289A	AYH-X-289A	AYH-X-289Ax
342		AYH-XII-39Bx2	AYH-XII-39Bx1	AYH-XII-39Bx
343		AYH-XII-151A proton02	AYH-XII-151A carbon02	AYH-XII-151A
345		AYH-XII-185A	AYH-XI-169A	AYH-XI-169Ax
346		AYH-XI-195B proton04	AYH-XI-195B	AYH-XI-195Bx

347		AYH-XI-213Bx proton02	AYH-XI-213Bx	AYH-XI-213Bx
351		AYH-XII-113B	AYH-XI-205+207B	AYH-XI-205+207Bx
352		AYH-XII-183E proton01 (CDCl ₃) AYH-XII-183E proton02 (C ₆ D ₆)	AYH-XII-79B (CDCl ₃) AYH-XII-183E carbon02 (C ₆ D ₆)	AYH-XII-79Bx
353		AYH-XII-111C proton02 (CDCl ₃) AYH-XII-111C proton03 (C ₆ D ₆)	AYH-XII-79C (CDCl ₃) AYH-XII-111C carbon01 (C ₆ D ₆)	AYH-XII-79Cx
354		AYH-XII-203A	AYH-XII-203A	AYH-XII-203A
355		AYH-XIII-39B proton01	AYH-XIII-39B	AYH-XIII-39B
356		AYH-XIII-39A proton04	AYH-XIII-39A	AYH-XIII-39A
357		AYH-XII-233A	AYH-XII-81A carbon02	AYH-XII-81Ax
359		AYH-XII-137B proton03	AYH-XII-137B	AYH-XII-137B
360		AYH-XII-297A proton02	AYH-XII-297A	AYH-XII-295B
361		AYH-XIII-31B	AYH-XIII-31B	AYH-XIII-31B

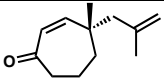
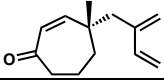
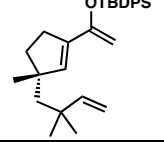
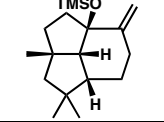
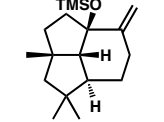
364		AYH-XI-287A proton1	AYH-IX-209A	AYH-IX-209Ax
365		AYH-XI-275B- proton02	AYH-XII-129B carbon02	AYH-X-283Ax
366		AYH-XII-141A	AYH-XII-141A	AYH-XII-141A
367		AYH-XII-249A	AYH-XII-249A	AYH-XII-217A
368		AYH-XII-263A	AYH-XII-263A	AYH-XII-263A

Table A14.3. Notebook Cross-Reference for Compounds in Appendix 10

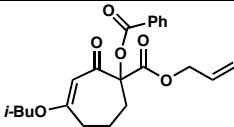
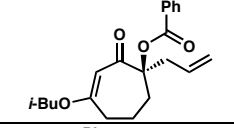
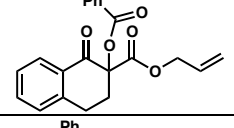
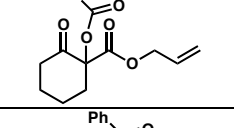
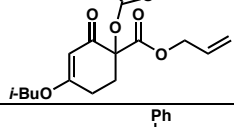
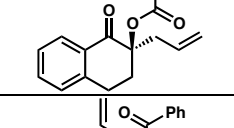
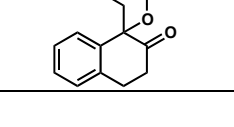
compound	chemical structure	¹ H NMR	¹³ C NMR	IR
148n		AYH-VI-225Bnew	AYH-VI-225B	AYH-VI-225B
149n		AYH-VI-229Bnew	AYH-VI-229B	AYH-VI-229B
566		AYH-VII-93Drcr	AYH-VII-93Drcr	AYH-VII-93Drcrx
567		AYH-XII-257D	AYH-XII-257D	AYH-XII-257Dx
568		AYH-VII-213C	AYH-VII-213C	AYH-VII-213C
571		AYH-VII-145A2	AYH-VII-145A2	AYH-VII-145A2x
572		AYH-VII-95Brcr4 proton02	AYH-VII-95Brcr	AYH-VII-95Brcrx

Table A14.4. Notebook Cross-Reference for Additional Compounds in Appendix 10

compound	chemical structure	notebook page
560		DCB-XXII-299
561		JLR-XIV-109 JLR-XV-43
562		JLR-XIV-117 JLR-XV-45
563		DCB-XIV-283
564		NTM-II-227

Table A14.5. Notebook Cross-Reference for Compounds in Appendix 11

compound	chemical structure	¹ H NMR	¹³ C NMR	IR
619		AYH-IX-267E	AYH-IX-189A	AYH-IX-159A
622		AYH-IX-233B	AYH-IX-233B	AYH-IX-233B
623		AYH-X-125B proton04	AYH-X-125B carbon03	AYH-X-115C
659		AYH-X-59A	AYH-X-59A	AYH-X-59A
658		AYH-X-85B proton03	AYH-X-85B	AYH-X-85B

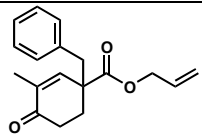
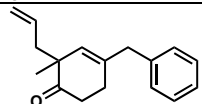
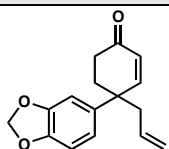
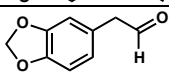
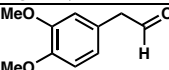
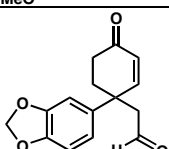
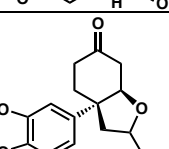
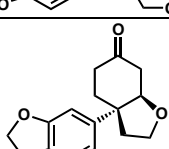
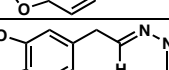
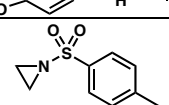
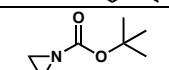
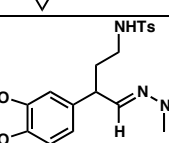
616		AYH-X-157A	AYH-X-157A	AYH-X-157A
680		AYH-X-83A	AYH-X-83A	AYH-X-79A

Table A14.6. Notebook Cross-Reference for Compounds in Appendix 12

compound	chemical structure	¹ H NMR	¹³ C NMR	IR
731		AYH-V-189A	_____	_____
736		AYH-V-151	_____	_____
738		AYH-V-271	_____	_____
739		AYH-V-181B	_____	_____
740		AYH-V-195B	_____	_____
741		AYH-V-193A	_____	_____
743		AYH-V-251B	_____	_____
744		AYH-V-215A	_____	_____
745		AYH-V-265A	_____	_____
746		AYH-V-229C	_____	_____

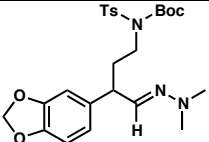
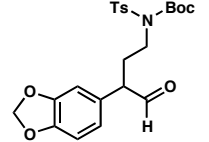
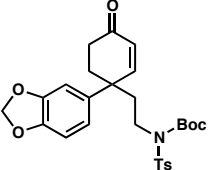
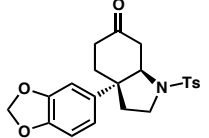
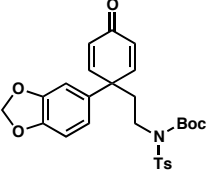
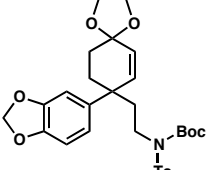
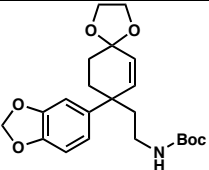
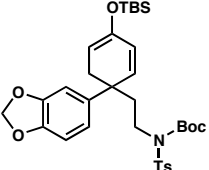
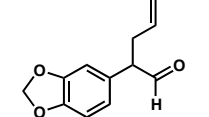
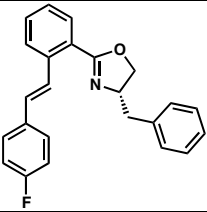
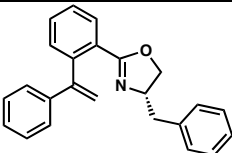
748		AYH-VI-83B	AYH-VI-83B-13C	_____
749		AYH-VI-87B	AYH-VI-87B-13C	_____
750		AYH-VII-33Bx	AYH-VII-33Bx	AYH-VII-33Bx
751		AYH-V-153B	AYH-V-153B	AYH-V-153Bx
752		AYH-VI-39	_____	_____
753		AYH-VII-143A4	AYH-VII-143A4	AYH-VII-143Ax
754		AYH-VII-199B	AYH-VII-199B	AYH-VII-199B
755		AYH-VII-35A	AYH-VII-35A	_____
793		AYH-V-153B	_____	_____

Table A14.7. Notebook Cross-Reference for Compounds in Appendix 13

compound	chemical structure	¹ H NMR	¹³ C NMR	IR
191		TJ-I-91	TJ-I-91	TJ-I-91-3
801b		AYH-VII-285B	—————	—————
801c		AYH-VII-185A	AYH-VII-185A	AYH-VII-185Bx
801d		AFC-I-79	AFC-I-79	AFC-I-79
801e		AFC-I-75 repurified	AFC-I-75 repurified	AFC-I-75
801f		AFC-I-77	AFC-I-77	AFC-I-77
801g		AFC-I-81pure	AFC-I-81pure	AFC-I-81
801i		AFC-I-101D	—————	—————
801j		AFC-I-93	AFC-I-93	AFC-I-93

801k		AFC-I-97pure	AFC-I-97pure	_____
801l		AFC-I-103C	_____	_____

COMPREHENSIVE BIBLIOGRAPHY

Aboulhoda, S. J.; Hénin, F.; Muzart, J.; Thorey, C.; Behnen, W.; Martens, J.; Mehler, T.

Tetrahedron: Asymmetry **1994**, 5, 1321–1326.

Aebi, A.; Barton, D. H. R.; Burgstahler, A. W.; Lindsey, A. S. *J. Chem. Soc.* **1954**,

4659–4665.

Åhman, J.; Wolfe, J. P.; Troutman, M. V.; Palucki, M.; Buchwald, S. L. *J. Am. Chem.*

Soc. **1998**, 120, 1918–1919.

Ali, A. A.; El Sayed, H. M.; Abdallah, O. M.; Steglich, W. *Phytochem.* **1986**, 25, 2399–

2401.

Amere, M.; Lasne, M.-C.; Rouden, J. *Org. Lett.* **2007**, 9, 2621–2624.

Aoyama, Y.; Araki, Y.; Konoike, T. *Synlett* **2001**, 9, 1452–1454.

Ariafard, A.; Lin, Z. *J. Am. Chem. Soc.* **2006**, 128, 13010–13016.

Asahina, Y.; Tsukamoto, T. *J. Pharm. Soc. Jpn.* **1922**, 463–473.

Austin, K. A. B.; Banwell, M. G.; Willis, A. C. *Org. Lett.* **2008**, 10, 4465–4468.

Baba, S. E.; Sartor, K.; Poulin, J.; Kagan, H. *Bull. Soc. Chim. Fr.* **1994**, 131, 525–533.

Bakkestuen, A. K.; Gundersen, L.-L.; Petersen, D.; Utenova, B. T.; Vik, A. *Org. Biomol. Chem.* **2005**, *3*, 1025–1033.

Baktharaman, S.; Afagh, N.; Vandersteen, A.; Yudin A. K. *Org. Lett.* **2010**, *12*, 240–243.

Bao, M.; Nakamura, H.; Yamamoto, Y. *J. Am. Chem. Soc.* **2001**, *123*, 759–760.

Barquera-Lozada, J. E.; Cuevas, G. *J. Org. Chem.* **2011**, *76*, 1572–1577.

Barton, D. H. R.; Nickon, A. J. *J. Chem. Soc.* **1954**, 4665–4669.

Bear, B. R.; Sparks, S. M.; Shea, K. J. *Angew. Chem. Int. Ed.* **2001**, *40*, 820–849.

Becker, H.; Sharpless, K. B. *Angew. Chem., Int. Ed. Engl.* **1996**, *35*, 448–451.

Begue, J.-P.; Bonnet-Delpon, D.; Crousse, B. *Synlett* **2004**, 18–29.

Behenna, D. C.; Liu, Y.; Yurino, T.; Kim, J.; White, D. E.; Virgil, S. C.; Stoltz, B. M. *Nature Chem.* **2012**, *4*, 130–133.

Behenna, D. C.; Mohr, J. T.; Sherden, N. H.; Marinescu, S. C.; Harned, A. M.; Tani, K.; Seto, M.; Ma, S.; Novák, Z.; Krout, M. R.; McFadden, R. M.; Roizen, J. L.; Enquist, Jr., J. A.; White, D. E.; Levine, S. R.; Petrova, K. V.; Iwashita, A.; Virgil, S. C.; Stoltz, B. M. *Chem. Eur. J.* **2011**, *17*, 14199–14223.

Behenna, D. C.; Stoltz, B. M. *J. Am. Chem. Soc.* **2004**, *126*, 15044–15045.

Bellemin-Laponnaz, S.; Gisie, H.; Le Ny, J. P.; Osborn, J. A. *Angew. Chem. Int. Ed. Engl.* **1997**, *36*, 976–978.

Bellville, D. J.; Wirth, D. W.; Bauld, N. L. *J. Am. Chem. Soc.* **1981**, *103*, 718–720.

Bennett, N. B.; Hong, A. Y.; Harned, A. M.; Stoltz, B. M. *Org. Biomol. Chem.* **2012**, *10*, 56–59.

Berkowitz, W. F.; Wu, Y. *J. Org. Chem.* **1997**, *62*, 1536–1539.

Bian, J.; Van Wingerden, M.; Ready, J. M. *J. Am. Chem. Soc.* **2006**, *128*, 7428–7429.

Bisai, V.; Sarpong, R. *Org. Lett.* **2010**, *12*, 2551–2553.

Blanchet, J.; Baudoux, J.; Amere, M.; Lasne, M.-C.; Rouden, J. *Eur. J. Org. Chem.* **2008**, 5493–5506.

Blasdel, L. K.; Myers, A. G. *Org. Lett.* **2005**, *7*, 4281–4283.

Boehm, J. C.; Gleason, J. G.; Pendrak, I.; Sarau, H. M.; Schmidt, D. B.; Foley, J. J.; Kingsbury, W. D. *J. Med. Chem.* **1993**, *36*, 3333–3340.

Bogle, K. M.; Hirst, D. J.; Dixon, D. J. *Org. Lett.* **2010**, *12*, 1252–1254.

Bohlmann, F.; Jakupovic, J. *Phytochemistry* **1980**, *19*, 259–265.

Bohlmann, F.; Zdero, C. *Phytochemistry* **1981**, *20*, 2529–2534.

Bohlmann, F.; Zdero, C. *Phytochemistry* **1982**, *21*, 2537–2541.

Bohlmann, F.; Zdero, C.; Jakupovic, J.; Robinson, H.; King, R. M. *Phytochemistry* **1981**, *20*, 2239–2244.

Bohlmann, F.; Zdero, C.; King, R. M.; Robinson, H. *Phytochemistry* **1981**, *20*, 2425–2427.

Bohlmann, F.; Ziesche, J.; Gupta, R. K. *Phytochemistry* **1982**, *21*, 1331–1334.

Boit, H.-G. *Chem Ber.* **1954**, *87*, 1704–1707.

Bordwell, F. G. *Acc. Chem. Res.* **1988**, *21*, 456–463.

Borrelly, S.; Paquette, L. A. *J. Am. Chem. Soc.* **1996**, *118*, 727–740.

Boyd, E.; Coumbarides, G. S.; Eames, J.; Hay, A.; Jones, R. V. H.; Stenson, R. A.; Suggate, M. J. *Tetrahedron Lett.* **2004**, *45*, 9465–9468.

Bradshaw, A. P. W.; Hanson, J. R.; Nyfeler, R. *J. Chem. Soc., Perkin Trans. I* **1981**, 1469–1472.

Bradshaw, A. P. W.; Hanson, J. R.; Nyfeler, R.; Sadler, I. H. *J. Chem. Soc., Perkin Trans. I* **1982**, 2187–2192.

Bradshaw, A. P. W.; Hanson, J. R.; Nyfeler, R.; Sadler, I. H. *J. Chem. Soc., Chem.*

Commun. **1981**, 649–650.

Brougham, P.; Cooper, M. S.; Cummerson, D. A.; Heaney, H.; Thompson, N. *Synthesis*, **1987**, 1015–1017.

Burgess, E. M.; Penton, Jr., H. R.; Taylor, E. A. *J. Org. Chem.* **1973**, 38, 26–31.

Cameron, A. F.; Hannaway, C.; Robertson, J. M. *J. Chem. Soc., Perkin Trans. 2* **1973**, 1938–1942.

Carbery, D. R.; Donohoe, T. J. *Chem. Commun.* **2004**, 722–723.

Carlsen, P. H. J.; Katsuki, T.; Martin, V. S.; Sharpless, K. B. *J. Org. Chem.* **1981**, 46, 3936–3938.

Carroll, M. F. *J. Chem. Soc.* **1940**, 1266–1268.

Carroll, M. F. *J. Chem. Soc.* **1940**, 704–706.

Chakraborty, T. K.; Chattopadhyay, A. K.; Samanta, R.; Ampapathi, R. S. *Tetrahedron Lett.* **2010**, 51, 4425–4428.

Chanon, M.; Barone, R.; Baralotto, C.; Julliard, M.; Hendrickson, J. B. *Synthesis* **1998**, 1559–1583.

Chatterjee, A. K.; Choi, T.-L.; Sanders, D. P.; Grubbs, R. H. *J. Am. Chem. Soc.* **2003**,

125, 11360–11370.

Chatterjee, A. K.; Grubbs, R. H. *Org. Lett.* **1999**, *1*, 1751–1753.

Chatterjee, A. K.; Sanders, D. P.; Grubbs, R. H. *Org. Lett.* **2002**, *4*, 1939–1942.

Cheon, C. H.; Yamamoto, H. *J. Am. Chem. Soc.* **2008**, *130*, 9246–9247.

Christoffers, J.; Baro, A. *Adv. Synth. Catal.* **2005**, *347*, 1473–1482.

Christoffers, J.; Mann, A. *Angew. Chem. Int. Ed.* **2001**, *40*, 4591–4597.

Chung, Y. K.; Lee, B. Y.; Jeong, N.; Hudecek, M.; Pauson, P. L. *Organometallics* **1993**, *12*, 220–223.

Clive, D. L. J.; Farina, V.; Beaulieu, P. *J. Chem. Soc. Chem. Commun.* **1981**, 643–644.

Clive, D. L. J.; Farina, V.; Beaulieu, P. *J. Org. Chem.* **1982**, *47*, 2572–2582.

Coates, R. M.; Ho, Z.; Klobus, M.; Wilson, S. R. *J. Am. Chem. Soc.* **1996**, *118*, 9249–9254.

Collado, I. G.; Aleu, J.; Macías-Sánchez, A. J.; Hernández-Galán, R. *J. Chem. Ecol.* **1994**, *20*, 2631–2644.

Collado, I. G.; Aleu, J.; Macías-Sánchez, A. J.; Hernández-Galán, R. *J. Nat. Prod.* **1994**, *57*, 738–746.

Collado, I. G.; Hanson, J. R.; Macías-Sánchez, A. J. *Nat. Prod. Rep.* **1998**, *15*, 187–204.

Comins, D. L.; Dehghani, A. *Tetrahedron Lett.* **1992**, *33*, 6299–6302.

Corey, E. J.; Cho, H.; Rücker, C.; Hua, D. H. *Tetrahedron Lett.* **1981**, *22*, 3455–3458.

Corey, E. J.; Guzman-Perez, A. *Angew. Chem. Int. Ed.* **1998**, *37*, 388–401.

Corey, E. J.; Magriotis, P. A. *J. Am. Chem. Soc.* **1987**, *109*, 287–289.

Coulson, D. R.; Satek, L. C.; Grim, S. O. *Inorg. Synth.* **1972**, *13*, 121–124.

Coumbarides, G. S.; Eames, J.; Ghilagaber, S.; Suggate, M. J. *Tetrahedron Lett.* **2004**, *45*, 9469–9474.

Coumbarides, G. S.; Eames, J.; Scheuermann, J. E. W.; Sibbons, K. F.; Suggate, M. J.; Watkinson, M. *Bull. Chem. Soc Jpn.* **2005**, *78*, 906–909.

Cozzi, P. G.; Hilgraf, R.; Zimmermann, N. *Eur. J. Org. Chem.* **2007**, 5969–5994.

Crabtree, R. H.; Davis, M. W. *J. Org. Chem.* **1986**, *51*, 2655–2661.

Crimmins, M. T.; Dedopoulou, D. *Synth. Commun.* **1992**, *22*, 1953–1958.

Dai, X.; Nakai, T.; Romero, J. A. C.; Fu, G. C. *Angew. Chem., Int. Ed.* **2007**, *46*, 4367–4369.

Das, J. P.; Marek, I. *Chem. Commun.* **2011**, 47, 4593–4623.

Dauben, W. G.; Michno, D. M. *J. Org. Chem.* **1977**, 42, 682–685.

Davis, C. E.; Duffy, B. C.; Coates, R. M. *J. Org. Chem.* **2003**, 68, 6935–6943.

Dawson, G. J.; Frost, C. G.; Williams, J. M. J.; Coote, S. J. *Tetrahedron Lett.* **1993**, 34, 3149–3150.

Day, J. J.; McFadden, R. M.; Virgil, S. C.; Kolding, H.; Alleva, J. L.; Stoltz, B. M. *Angew. Chem. Int. Ed.* **2011**, 50, 6814–6818.

Defieber, C.; Grützmacher, H.; Carreira, E. M. *Angew. Chem. Int. Ed.* **2008**, 47, 4482–4502.

Denissova, I.; Barriault, L. *Tetrahedron* **2003**, 59, 10105–10146.

Denmark, S. E.; Beutner, G. L. *Angew. Chem., Int. Ed.* **2008**, 47, 1560–1638.

Detalle, J.-F.; Riahi, A.; Steinmetz, V.; Hénin, F.; Muzart, J. *J. Org. Chem.* **2004**, 69, 6528–6532.

Diao, T.; Stahl, S. S. *J. Am. Chem. Soc.* **2011**, 133, 14566–14569.

Diao, T.; Wadzinski, T. J.; Stahl, S. S. *Chem. Sci.* **2012**, 3, 887–891.

Do, N.; McDermott, R. E.; Ragan, J. A. *Org. Synth.* **2008**, 85, 138–146.

Donnelly, D. M.; Finet, J. P.; Rattigan, B. A. *J. Chem. Soc., Perkin Trans. 1* **1993**, 1729–1735.

Donohoe, T. J.; Freestone, G. C.; Headley, C. E.; Rigby, C. L.; Cousins, R. P. C.; Bhalay, G. *Org. Lett.* **2004**, 6, 3055–3058.

Doudnay, A. B.; Humphreys, P. G.; Overman, L. E.; Wroblewski, A. D. *J. Am. Chem. Soc.* **2008**, 130, 5368–5377.

Douglas, C. J.; Overman, L. E. *Proc. Natl. Acad. Sci. U.S.A.* **2004**, 101, 5363–5367.

Dragoli, D. R.; Burdett, M. T.; Ellman, J. A. *J. Am. Chem. Soc.* **2001**, 123, 10127–10128.

Du, C.; Li, L.; Li, Y.; Xie, Z. *Angew. Chem. Int. Ed.* **2009**, 48, 7853–7856.

Dubinina, G. G.; Chain, W. J. *Tetrahedron Lett.* **2011**, 52, 939–942.

Dubovyk, I.; Pichugin, D.; Yudin, A. K. *Angew. Chem. Int. Ed.* **2011**, 50, 5924–5926.

Duhamel, L.; Duhamel, P.; Plaquevent, J.-C. *Tetrahedron: Asymmetry* **2004**, 15, 3653–3691.

Eames, J.; Weerasooriya, N. *Tetrahedron: Asymmetry* **2001**, 12, 1–24.

Ely, R. J.; Morken, J. P. *J. Am. Chem. Soc.* **2010**, 132, 2534–2535.

Ely, R. J.; Morken, J. P. *Org. Synth.* **2011**, 88, 342–352.

Enders, D.; Lenzen, A.; Backes, M.; Janecek, C.; Catlin, K.; Lannou, M.-L.; Runsink, J.; Raabe, G. *J. Org. Chem.* **2005**, *70*, 10538–10551.

Enquist, Jr., J. A.; Stoltz, B. M. *Nature* **2008**, *453*, 1228–1231.

Enquist, Jr., J. A.; Virgil, S. C.; Stoltz, B. M. *Chem. Eur. J.* **2011**, *17*, 9957–9969.

Evanno, L.; Deville, A.; Bodo, B.; Nay, B. *Tetrahedron Lett.* **2007**, *48*, 4331–4333.

Evans, D. A.; Woerpel, K. A.; Hinman, M. M.; Faul, M. M. *J. Am. Chem. Soc.* **1991**, *113*, 726–728.

Fairlamb, I. J. S.; Kapdi, A. R.; Lee, A. F. *Org. Lett.* **2004**, *6*, 4435–4438.

Fehlhaber, H.-W.; Geipel, R.; Mercker, H.-J.; Tschesche, R.; Welmar, K.; Schönbeck, F. *Chem. Ber.* **1974**, *107*, 1720–1730.

Fehr, C. *Angew. Chem., Int. Ed.* **2007**, *46*, 7119–7121.

Fehr, C. *Angew. Chem., Int. Ed. Engl.* **1996**, *35*, 2566–2587.

Ferreira, E. M. The Design and Development of Palladium-Catalyzed Aerobic Oxidative Transformations. Ph.D. Thesis. California Institute of Technology, Pasadena, CA, 2005.

Fischer, C.; Defieber, C.; Suzuki, T.; Carreira, E. M. *J. Am. Chem. Soc.* **2004**, *126*,

1628–1269.

Fitjer, L.; Malich, A.; Paschke, C.; Kluge, S.; Gerke, R.; Rissom, B.; Weiser, J.;

Noltemeyer, M. *J. Am. Chem. Soc.* **1995**, *117*, 9180–9189.

Frankel, J. J.; Julia, S.; Richard-Neuville, C. *Bull. Soc. Chim. Fr.* **1968**, 4870–4875.

Frost, C. G.; Penrose, S. D.; Lambshead, K.; Raithby, P. R.; Warren, J. E.; Gleave, R.

Org. Lett. **2007**, *9*, 2119–2122.

Fuchter, M. J.; Levy, J.-N. *Org. Lett.* **2008**, *10*, 4919–4922.

Fuji, K. *Chem. Rev.* **1993**, *93*, 2037–2066.

Garg, N. K.; Caspi, D. D.; Stoltz, B. M. *J. Am. Chem. Soc.* **2005**, *127*, 5970–5978.

Garg, N. K.; Caspi, D. D.; Stoltz, B. M. *J. Am. Chem. Soc.* **2004**, *126*, 9552–9553.

Garg, N. K.; Caspi, D. D.; Stoltz, B. M. *Synlett* **2006**, 3081–3087.

Geissman, T. A.; Armen, A. *J. Am. Chem. Soc.* **1952**, *74*, 3916–3919.

Ghosh, A. K.; Mathivanan, P.; Cappiello, J. *Tetrahedron: Asymmetry* **1998**, *9*, 1–45.

Gilbert, M. W. Carbocycle Construction in Terpenoid Synthesis. The Total Synthesis of (±)-Sarcodonin G and (±)-1-Epi-9-Norpresilphiperfolan-9-one. Ph.D. Thesis, University of British Columbia, June 2002.

Girard, C.; Kagan, H. B. *Angew. Chem., Int. Ed.* **1998**, *37*, 2922–2959.

Glorius, F. *Angew. Chem. Int. Ed.* **2004**, *43*, 3364–3366.

Gollnick, K.; Schade, G.; Cameron, A. F.; Hannaway, C.; Roberts, J. S.; Robertson, J. M. *J. Chem. Soc., Chem. Commun.* **1970**, 248–249.

Gollnick, K.; Schade, G.; Cameron, A. F.; Hannaway, C.; Robertson, J. M. *J. Chem. Soc. D.: Chem. Commun.* **1971**, 46.

González-Coloma, A.; Valencia, F.; Martín, N.; Hoffmann, J. F.; Hutter, L.; Marco, J. A.; Reina, M. *J. Chem. Ecol.* **2002**, *28*, 117–129.

Gu, Q.; You, S.-L. *Chem. Sci.* **2011**, *2*, 1519–1522.

Hagiwara, H.; Fukushima, M.; Kinugawa, K.; Matsui, T.; Hoshi, T.; Suzuki, T. *Tetrahedron* **2011**, *67*, 4061–4068.

Hahn, B. T.; Tewes, F.; Fröhlich, R.; Glorius, F. *Angew. Chem. Int. Ed.* **2010**, *49*, 1143–1146.

Hamashima, Y.; Somei, H.; Shimura, Y.; Tamura, T.; Sodeoka, M. *Org. Lett.* **2004**, *6*, 1861–1864.

Hanessian, S.; Chénard, E. *Org. Lett.* **2012**, *14*, 3222–3225.

Hansch, C.; Leo, A.; Taft, R. W. *Chem. Rev.* **1991**, *91*, 165–195.

Hanson, J. R. *Pure Appl. Chem.* **1981**, *53*, 1155–1162.

Hargrave, J. D.; Herbert, J.; Bish, G.; Frost, C. G. *Org. Biomol. Chem.* **2006**, *4*, 3235–3241.

Hayashi, T.; Kanehira, K.; Hagihara, T.; Kumada, M. *J. Org. Chem.* **1988**, *53*, 113–120.

Hayashi, T.; Ueyama, K.; Tokunaga, N.; Yoshida, K. *J. Am. Chem. Soc.* **2003**, *125*, 11508–11509.

Hayashida, J.; Rawal, V. H. *Angew. Chem. Int. Ed.* **2008**, *47*, 4373–4376.

He, W.; Yip, K.-T.; Zhu, N.-Y.; Yang, D. *Org. Lett.* **2009**, *11*, 5626–5628.

Heller, S. T.; Fu, T.; Sarpong, R. *Org. Lett.* **2012**, *14*, 1970–1973.

Heller, S. T.; Sarpong, R. *Org. Lett.* **2010**, *12*, 4572–4575.

Heller, S. T.; Sarpong, R. *Tetrahedron* **2011**, *67*, 8851–8859.

Helmchen, G. *J. Organomet. Chem.* **1999**, *576*, 203–214.

Henderson, G. G.; McCrone, R. O. O.; Robertson, J. M. *J. Chem. Soc.* **1929**, 1368–1372.

Hénin, F.; M'boungou-M'passi, A.; Muzart, J.; Pete, J.-P. *Tetrahedron* **1994**, *50*, 2849–

2864.

Hénin, F.; Muzart, J.; Pete, J.-P.; M'boungou-M'passi, A.; Rau, H. *Angew. Chem., Int. Ed. Engl.* **1991**, *30*, 416–418.

Herrinton, P. M.; Klotz, K. L.; Hartley, W. M. *J. Org. Chem.* **1993**, *58*, 678–682.

Herrmann, W. A.; Brossmer, C.; Öfele, K.; Reisinger, C.-P.; Priermeier, T.; Beller, M.; Fischer, H. *Angew. Chem. Int. Ed. Engl.* **1995**, *34*, 1845–1848.

Hirata, T.; Shimoda, K.; Kawano, T. *Tetrahedron: Asymmetry* **2000**, *11*, 1063–1066.

Hodous, B. L.; Fu, G. C. *J. Am. Chem. Soc.* **2002**, *124*, 10006–10007.

Hodous, B. L.; Ruble, J. C.; Fu, G. C. *J. Am. Chem. Soc.* **1999**, *121*, 2637–2638.

Hong, A. Y.; Bennett, N. B.; Krout, M. R.; Jensen, T.; Harned, A. M.; Stoltz, B. M. *Tetrahedron* **2011**, *67*, 10234–10248.

Hong, A. Y.; Krout, M. R.; Jensen, T.; Bennett, N. B.; Harned, A. M.; Stoltz, B. M. *Angew. Chem. Int. Ed.* **2011**, *50*, 2756–2760.

Hong, A. Y.; Stoltz, B. M. *Angew. Chem. Int. Ed.* **2012**, *51*, 9674–9678.

Hosomi, A.; Endo, M.; Sakurai, H. *Chem. Lett.* **1976**, *5*, 941–942.

Hosomi, A.; Sakurai, H. *Tetrahedron Lett.* **1976**, *17*, 1295–1298.

Hudlicky, T.; Reed, J. W. *The Way of Synthesis: Evolution of Design and Methods for Natural Products*; Wiley-VCH: Weinheim, Germany, 2007; pp 689–726.

Ijima, Y.; Matoishi, K.; Terao, Y.; Doi, N.; Yanagawa, H.; Ohta, H. *Chem. Commun.* **2005**, 877–879.

Jana, R.; Partridge, J. J.; Tunge, J. A. *Angew. Chem. Int. Ed.* **2011**, 50, 5157–5161.

Jana, R.; Pathak, T. P.; Jensen, K. H.; Sigman, M. S. *Org. Lett.* **2012**, 14, 4074–4077.

Jin, Z. *Nat. Prod. Rep.* **2003**, 20, 606–614.

Jin, Z.; Fuchs, P. L. *J. Am. Chem. Soc.* **1994**, 116, 5995–5996.

Jo, H.; Lee, J.; Kim, H.; Kim, S.; Kim, D. *Tetrahedron Lett.* **2003**, 44, 7043–7044.

Johnson, J. B.; Rovis, T. *Angew. Chem. Int. Ed.* **2008**, 47, 840–871.

Jolly, R. S.; Luedtke, G.; Sheehan, D.; Livinghouse, T. *J. Am. Chem. Soc.* **1990**, 112, 4965–4966.

Joseph-Nathan, P.; Leitão, S. G.; Pinto, S. C.; Leitão, G. G.; Bizzo, H. R.; Costa, F. L. P.; de Amorim, M. B.; Martinez, N.; Dellacassa, E.; Hernández-Barragán, A.; Pérez-Hernández, N. *Tetrahedron Lett.* **2010**, 51, 1963–1965.

Juhl, M.; Tanner, D. *Chem. Soc. Rev.* **2009**, 38, 2983–2992.

Jun, C.-H.; Moon, C. W.; Lim, S.-G.; Lee, H. *Org. Lett.* **2002**, *4*, 1595–1597.

Jung, M. E.; Halweg, K. M. *Tetrahedron Lett.* **1981**, *22*, 3929–3932.

Kanthak, M.; Aniol, A.; Nestola, M.; Merz, K.; Oppel, I. M.; Dyker, G. *Organometallics* **2011**, *30*, 215–229.

Kaufman, G. M.; Cook, F. B.; Shechter, H.; Bayless, J. H.; Friedman, L. *J. Am. Chem. Soc.* **1967**, *89*, 5736–5737.

Kawasaki, T.; Shinada, M.; Kamimura, D.; Ohzono, M.; Ogawa, A. *Chem. Commun.* **2006**, 420–422.

Kazmaier, U.; Stolz, D.; Krämer, K.; Zumpe, F. L. *Chem. Eur. J.* **2008**, *14*, 1322–1329.

Keith, J. A.; Behenna, D. C.; Mohr, J. T.; Ma, S.; Marinescu, S. C.; Oxgaard, J.; Stoltz, B. M.; Goddard, III, W. A. *J. Am. Chem. Soc.* **2007**, *129*, 11876–11877.

Keith, J. A.; Behenna, D. C.; Sherden, N.; Mohr, J. T.; Ma, S.; Marinescu, S. C.; Nielsen, R. J.; Oxgaard, J.; Stoltz, B. M.; Goddard, III, W. A. *J. Am. Chem. Soc.* **2012**, *134*, 19050–19060.

Khomenko, T. M.; Bagryanskaya, I. Y.; Gatilov, Y. V.; Korchagina, D. V.; Gatilova, V. P.; Dubovenko, Z. V.; Barkhash, V. A. *Zh. Org. Khim.* **1985**, *21*, 677–678. *Russ. J. Org. Chem. (Engl. Transl.)* **1985**, *21*, 614–615.

Khomenko, T. M.; Korchagina, D. V.; Gatilov, Y. V.; Bagryanskaya, Y. I.; Tkachev, A. V.; Vyalkov, A. I.; Kun, O. B.; Salenko, V. L.; Dubovenko, Z. V.; Barkash, V. A. *Zh. Org. Khim.* **1990**, *26*, 2129–2145; *Russ. J. Org. Chem. (Engl. Transl.)* **1990**, *26*, 1839–1852.

Kikushima, K.; Holder, J. C.; Gatti, M.; Stoltz, B. M. *J. Am. Chem. Soc.* **2011**, *133*, 6902–6905.

Kim, B. M.; Kim, H.; Kim, W.; Im, K. Y.; Park, J. K. *J. Org. Chem.* **2004**, *69*, 5104–5107.

Knapp, S.; Yu, Y. *Org. Lett.* **2007**, *9*, 1359–1362.

Kotoku, N.; Sumii, Y.; Kobayashi, M. *Org. Lett.* **2011**, *13*, 3514–3514.

Krenske, E. H.; Perry, E. W.; Jerome, S. V.; Maimone, T. J.; Baran, P. S.; Houk, K. N. *Org. Lett.* **2012**, *14*, 3016–3019.

Krout, M. R.; Mohr, J. T.; Stoltz, B. M. *Org. Synth.* **2009**, *86*, 181–193.

Kuettner, E. B.; Keim, A.; Kircher, M.; Rosmus, S.; Strater, N. *J. Mol. Biol.* **2008**, *377*, 386–394.

Kukula, P.; Matousek, V.; Mallat, T.; Baiker, A. *Chem.–Eur. J.* **2008**, *14*, 2699–2708.

Kukula, P.; Matousek, V.; Mallat, T.; Baiker, A. *Tetrahedron: Asymmetry* **2007**, *18*,

2859–2868.

Kuuloga, N.; Tois, J.; Franzén, R. *Tetrahedron: Asymmetry* **2011**, 22, 468–475.

Kuuloga, N.; Vaismaa, M.; Franzén, R. *Tetrahedron* **2012**, 68, 2313–2318.

Kuwano, R.; Ito, Y. *J. Am. Chem. Soc.* **1999**, 121, 3236–3237.

Kuwano, R.; Uchida, K.; Ito, Y. *Org. Lett.* **2003**, 5, 2177–2179.

Langenbeck, W.; Triem, G. *Z. Phys. Chem. Abt. A* **1936**, 117, 401–409.

Langer, T.; Helmchen, G. *Tetrahedron Lett.* **1996**, 37, 1381–1384.

Langer, T.; Janssen, J.; Helmchen, G.; *Tetrahedron: Asymmetry* **1996**, 7, 1599–1602.

Larson, K. K.; Sarpong, R. *J. Am. Chem. Soc.* **2009**, 131, 13244–13245.

Lee, S.; Hartwig, J. F. *J. Org. Chem.* **2001**, 66, 3402–3415.

Leow, D.; Lin, S.; Chittimalla, S. K.; Fu, X.; Tan, C.-H. *Angew. Chem. Int. Ed.* **2008**, 47, 5641–5645.

Levine, S. G. *J. Am. Chem. Soc.* **1958**, 80, 6150–6151.

Levine, S. R.; Krout, M. R.; Stoltz, B. M. *Org. Lett.* **2009**, 11, 289–292.

Li, B.-J.; Jiang, L.; Liu, M.; Chen, Y.-C.; Ding, L.-S.; Wu, Y. *Synlett* **2005**, 603–606.

Li, Y.-M.; Kwong, F.-Y.; Yu, W.-Y.; Chang, A. S. C. *Coord. Chem. Rev.* **2007**, *251*, 2119–2144.

Liang, G.; Trauner, D. *J. Am. Chem. Soc.* **2004**, *126*, 9544–9545.

Lightfoot, A.; Schnider, P.; Pfaltz, A. *Angew. Chem. Int. Ed.* **1998**, *37*, 2897–2899.

Liu, G.; Stahl, S. S. *J. Am. Chem. Soc.* **2007**, *129*, 6328–6335.

Liu, Q.; Ferreira, E. M.; Stoltz, B. M. *J. Org. Chem.* **2007**, *72*, 7352–7358.

Loiseleur, O.; Hayashi, M.; Schmees, N.; Pfaltz, A. *Synthesis* **1997**, 1338–1345.

Loiseleur, O.; Meier, P.; Pfaltz, A. *Angew. Chem. Int. Ed.* **1996**, *35*, 200–202.

Love, B. E.; Jones, E. G. *J. Org. Chem.* **1999**, *64*, 3755–3756.

Lowenthal, R. E.; Abiko, A.; Masamune, S. *Tetrahedron Lett.* **1990**, *31*, 6005–6008.

Lu, S.; Xu, Z.; Bao, M.; Yamamoto, Y. *Angew. Chem. Int. Ed.* **2008**, *47*, 4366–4369.

Lu, Z.; Ma, S. *Angew. Chem. Int. Ed.* **2008**, *47*, 258–297.

Luchaco-Cullis, C. A.; Mizutani, H.; Murphy, K. E.; Hoveyda, A. H. *Angew. Chem. Int. Ed.* **2001**, *40*, 1456–1460.

Lucas, J. L. *J. Am. Chem. Soc.* **1978**, *100*, 2226–2227.

Mahmood, T.; Shreeve, J. M. *Inorg. Chem.* **1986**, *25*, 3830–3837.

Maimone, T. J.; Baran, P. S. *Nature Chem. Biol.* **2007**, *3*, 396–407.

Maki, B. E.; Chan, A.; Scheidt, K. A. *Synthesis* **2008**, 1306–1315.

Mander, L. N.; Sethi, S. P. *Tetrahedron Lett.* **1983**, *24*, 5425–5428.

Mantilli, L.; Gérard, D.; Torche, S.; Besnard, C.; Mazet, C. *Chem. Eur. J.* **2010**, *16*, 12736–12745.

Marco, J. A.; Sanz-Cervera, J. F.; Morante, M. D.; García-Lliso, V.; Vallès-Xirau, J.; Jakupovic, J. *Phytochemistry* **1996**, *41*, 837–844.

Marinescu, S. C.; Nishimata, T.; Mohr, J. T.; Stoltz, B. M. *Org. Lett.* **2008**, *10*, 1039–1042.

Martin, S. F. *Tetrahedron* **1980**, *36*, 419–460.

Maruyama, K.; Nagai, N.; Naruta, Y. *J. Org. Chem.* **1986**, *51*, 5083–5092.

Mason, L. H.; Puschett, E. R.; Wildman, W. C. *J. Am. Chem. Soc.* **1955**, *77*, 1253–1256.

Matoishi, K.; Ueda, M.; Miyamoto, K.; Ohta, H. *J. Mol. Catal. B: Enzym.* **2004**, *27*, 161–168.

Matsumoto, K.; Tsutsumi, S.; Ihori, T.; Ohta, H. *J. Am. Chem. Soc.* **1990**, *112*, 9614–9619.

McCarroll, A. J.; Walton, J. C. *Angew. Chem. Int. Ed. Engl.* **2001**, *40*, 2224–2248.

McDonald, R. I.; White, P. B.; Weinstein, A. B.; Tam, C. P.; Stahl, S. S. *Org. Lett.* **2011**, *13*, 2830–2833.

McDougal, N. T.; Streuff, J.; Mukherjee, H.; Virgil, S. C.; Stoltz, B. M. *Tetrahedron Lett.* **2010**, *51*, 5550–5554.

McDougal, N. T.; Virgil, S. C.; Stoltz, B. M. *Synlett* **2010**, 1712–1716.

McFadden, R. M.; Stoltz, B. M. *J. Am. Chem. Soc.* **2006**, *128*, 7738–7739.

McManus, H. A.; Guiry, P. J. *Chem. Rev.* **2004**, *104*, 4151–4202.

Mehta, G.; Srikrishna, A. *Chem. Rev.* **1997**, *97*, 671–720.

Melching, S. Isolierung, Strukturaufklärung und stereochemische Untersuchungen neuer sesquiterpenoider Verbindungen aus vier Chemotypen des Lebermooses *Conocephalum conicum*. Ph.D. Thesis, Universität Hamburg, April 1999.

Melching, S.; König, W. A. *Phytochemistry* **1999**, *51*, 517–523.

Merikli, A. H.; Merikli, F.; Jakupovic, J.; Bohlmann, F.; Dominguez, X. A.; Vega, H. S.

Phytochemistry **1989**, 28, 1149–1153.

Miesch, L.; Welsch, T.; Rietsch, V.; Miesch, M. *Chem. Eur. J.* **2009**, 15, 4394–4401.

Minami, I.; Takahashi, K.; Shimizu, I.; Kimura, T.; Tsuji, J. *Tetrahedron* **1986**, 42, 2971–2977.

Mitsuhashi, K.; Ito, R.; Arai, T.; Yanagisawa, A. *Org. Lett.* **2006**, 8, 1721–1724.

Miyamoto, K.; Hirokawa, S.; Ohta, H. *J. Mol. Catal. B: Enzym.* **2007**, 46, 14–19.

Miyamoto, K.; Ohta, H. *Eur. J. Biochem.* **1992**, 210, 475–481.

Mohr, J. T.; Behenna, D. C.; Harned, A. M.; Stoltz, B. M. *Angew. Chem. Int. Ed.* **2005**, 44, 6924–6927.

Mohr, J. T.; Ebner, D. C.; Stoltz, B. M. *Org. Biomol. Chem.* **2007**, 5, 3571–3576.

Mohr, J. T.; Krout, M. R.; Stoltz, B. M. *Nature* **2008**, 455, 323–332.

Mohr, J. T.; Nishimata, T.; Behenna, D. C.; Stoltz, B. M. *J. Am. Chem. Soc.* **2006**, 128, 11348–11349.

Mohr, J. T.; Stoltz, B. M. *Chem. Asian J.* **2007**, 2, 1476–1491.

Morita, M.; Drouin, L.; Motoki, R.; Kimura, Y.; Fujimori, I.; Kanai, M.; Shibasaki, M. *J. Am. Chem. Soc.* **2009**, 131, 3858–3859.

Morrill, C.; Grubbs, R. H. *J. Am. Chem. Soc.* **2005**, *127*, 2842–2843.

Moss, R. J.; Wadsworth, K. J.; Chapman, C. J.; Frost, C. G. *Chem. Commun.* **2004**, 1984–1985.

Mukherjee, H.; McDougal, N. T.; Virgil, S. C.; Stoltz, B. M. *Org. Lett.* **2011**, *13*, 825–827.

Murray, R. W.; Singh, M. *Org. Synth.* **1997**, *74*, 91–96.

Nakasako, M.; Obata, R.; Okubo, R.; Nakayama, S.; Miyamoto, K.; Ohta, H. *Acta Crystallogr. Sect. F*, **2008**, *64*, 610–613.

Nasveschuk, C. G.; Rovis, T. *Angew. Chem. Int. Ed.* **2005**, *44*, 3264–3267.

Nasveschuk, C. G.; Rovis, T. *J. Org. Chem.* **2008**, *73*, 612–617.

Nasveschuk, C. G.; Rovis, T. *Org. Biomol. Chem.* **2008**, *6*, 240–254.

Navarre, L.; Darses, S.; Genet, J.-P. *Angew. Chem., Int. Ed.* **2004**, *43*, 719–723.

Navarre, L.; Martinez, R.; Genet, J.-P.; Darses, S. *J. Am. Chem. Soc.* **2008**, *130*, 6159–6169.

Newman, L. M.; Williams, J. M. J.; McCague, R.; Potter, G. A. *Tetrahedron: Asymmetry* **1996**, *7*, 1597–1599.

Nicolaou, K. C.; Snyder, S. A.; Montagnon, T.; Vassilikogiannakis, G. *Angew. Chem. Int. Ed.* **2002**, *41*, 1668–1698.

Nicolaou, K. C.; Toh, Q.-Y.; Chen, D. Y.-K. *J. Am. Chem. Soc.* **2008**, *130*, 11292–11293.

Nicolaou, K. C.; Tria, G. S.; Edmonds, D. J. *Angew. Chem. Int. Ed.* **2008**, *47*, 1780–1783.

Nishimura, T.; Hirabayashi, S.; Yasuhara, Y.; Hayashi, T. *J. Am. Chem. Soc.* **2006**, *128*, 2556–2557.

Nishimura, T.; Kumamoto, H.; Nagaosa, M.; Hayashi, T. *Chem. Commun.* **2009**, 5713–5715.

Nokami, J.; Mandai, T.; Imakura, Y.; Nishiuchi, K.; Kawada, M.; Wakabayashi, S. *Tetrahedron Lett.* **1981**, *22*, 4489–4490.

Ohmura, T.; Hartwig, J. F. *J. Am. Chem. Soc.* **2002**, *124*, 15164–15165. (b) Lopez, F.; Ohmura, T.; Hartwig, J. F. *J. Am. Chem. Soc.* **2003**, *125*, 3426–3427.

Ono, T.; Tamaoka, T.; Yuasa, Y.; Matsuda, T.; Nokami, J.; Wakabayashi, S. *J. Am. Chem. Soc.* **1984**, *106*, 7890–7893.

Osawa, E.; Aigami, K.; Takaishi, N.; Inamoto, Y.; Fujikura, Y.; Majerski, Z.; von R. Schleyer, P.; Engler, E. M.; Farcasiu, M. *J. Am. Chem. Soc.* **1977**, *99*, 5361–5373.

Overman, L. E.; Jacobsen, E. J. *J. Am. Chem. Soc.* **1982**, *104*, 7225–7231.

Overman, L. E.; Knoll, F. M. *J. Am. Chem. Soc.* **1980**, *102*, 865–867.

Overman, L. E.; Renaldo, A. F. *J. Am. Chem. Soc.* **1990**, *112*, 3945–3949.

Overman, L. E.; Renaldo, A. F. *Tetrahedron Lett.* **1983**, *24*, 3757–3760.

Pangborn, A. B.; Giardello, M. A.; Grubbs, R. H.; Rosen, R. K.; Timmers, F. J. *Organometallics* **1996**, *15*, 1518–1520.

Pappo, R.; Allen, Jr., D. S.; Lemieux, R. U.; Johnson, W. S. *J. Org. Chem.* **1956**, *21*, 478–479.

Parikh, J. R.; Doering, W. v. E. *J. Am. Chem. Soc.* **1967**, *89*, 5505–5507.

Parker, W.; Raphael, R. A.; Roberts, J. S. *J. Chem. Soc. C* **1969**, 2634–2643.

Parker, W.; Raphael, R. A.; Roberts, J. S. *Tetrahedron Lett.* **1965**, *6*, 2313–2316.

Petrova, K. V.; Mohr, J. T.; Stoltz, B. M. *Org. Lett.* **2009**, *11*, 293–295.

Pettit, G. R.; Tan, R.; Northen, J. S.; Herald, D. L.; Chapuis, J.-C.; Pettit, R. K. *J. Nat. Prod.* **2004**, *67*, 1476–1482.

Pfaltz, A. *Acc. Chem. Res.* **1993**, *26*, 339–345.

Pfaltz, A.; Lautens, M. In *Comprehensive Asymmetric Catalysis*; Jacobsen, E. N., Pfaltz, A., Yamamoto, H., Eds.; Springer: New York, 1999; Vol. 2, pp 833–884.

Pinedo, C.; Wang, C.-M.; Pradier, J.-M.; Dalmais, B.; Choquer, M.; Le Pêcheur, P.; Morgant, G.; Collado, I. G.; Cane, D. E.; Viaud, M. *ACS Chem. Biol.* **2008**, *3*, 791–801.

Pinto, S. C.; Leitão, G. G.; Bizzo, H. R.; Martinez, N.; Dellacassa, E.; dos Santos, Jr., F. M.; Costa, F. L. P.; de Amorim, M. B.; Leitão, S. G. *Tetrahedron Lett.* **2009**, *50*, 4785–4787.

Pinto, S. C.; Leitão, G. G.; de Oliveira, D. R.; Bizzo, H. R.; Ramos, D. F.; Coelho, T. S.; Silva, P. E. A.; Lourenço, M. C. S.; Leitão, S. G. *Nat. Prod. Comm.* **2009**, *4*, 1675–1678.

Poisson, T.; Dalla, V.; Marsais, F.; Dupas, G.; Oudeyer, S.; Levacher, V. *Angew. Chem., Int. Ed.* **2007**, *46*, 7090–7093.

Poisson, T.; Oudeyer, S.; Dalla, V.; Marsais, F.; Levacher, V. *Synlett* **2008**, *16*, 2447–2450.

Pollini, G. P.; Benetti, S.; De Risi, C.; Zanirato, V. *Tetrahedron* **2010**, *66*, 2775–2802.

Prantz, K.; Mulzer, J. *Chem. Eur. J.* **2010**, *16*, 485–506.

Quaternary Stereocenters: Challenges and Solutions for Organic Synthesis, Christoffers,

J., Baro, A., Eds.; Wiley: Weinheim, 2005.

Ragan, J. A.; Makowski, T. W.; am Ende, D. J.; Clifford, P. J.; Young, G. R.; Conrad, A. K.; Eisenbeis, S. A. *Org. Process Res. Dev.* **1998**, *2*, 379–381.

Ragan, J. A.; Murry, J. A.; Castaldi, M. J.; Conrad, A. K.; Jones, B. P.; Li, B.; Makowski, T. W.; McDermott, R.; Sitter, B. J.; White, T. D.; Young, G. R. *Org. Process. Res. Dev.* **2001**, *5*, 498–507.

Ramharter, J.; Mulzer, J. *Org. Lett.* **2011**, *13*, 5310–5313.

Rautentrauch, V. *Bull. Soc. Chim. Fr.* **1994**, *131*, 515–524.

Reetz, M. T.; Westermann, J.; Kyung, S.-H. *Chem. Ber.* **1985**, *118*, 1050–1057.

Reetz, M. T.; Westermann, J.; Steinbach, R. *Angew. Chem. Int. Ed. Engl.* **1980**, *19*, 900–901.

Reynolds, N. T.; Rovis, T. *J. Am. Chem. Soc.* **2005**, *127*, 16406–16407.

Rinderhagen, H.; Mattay, J. *Chem. Eur. J.* **2004**, *10*, 851–874.

Rinner, U.; Hudlicky, R. *Synlett* **2005**, 365–387.

Rousseaux, S.; García-Fortanet, J.; Sanchez, M. A. D. A.; Buchwald, S. L. *J. Am. Chem. Soc.* **2011**, *133*, 9282–9285.

Rueping, M.; Theissmann, T.; Raja, S.; Bats, J. W. *Adv. Synth. Catal.* **2008**, 350, 1001–1006.

Sakai, T.; Matsuda, A.; Tanaka, Y.; Korenaga, T.; Ema, T. *Tetrahedron: Asymmetry* **2004**, 15, 1929–1932.

Sakurai, H.; Hosomi, A.; Hayashi, J. *Org. Synth.* **1984**, 62, 86–93.

Salomon, R. G.; Kochi, J. K. *J. Org. Chem.* **1973**, 38, 3715–3718.

Sanchez, I. H.; Lopez, F. J.; Soria, J. J.; Larraza, M. I.; Flores, H. J. *J. Am. Chem. Soc.* **1983**, 105, 7640–7643.

Sasaki, Y.; Zhong, C.; Sawamura, M.; Ito, M. *J. Am. Chem. Soc.* **2010**, 132, 1226–1227.

Satake, Y.; Nishikawa, T.; Hiramatsu, T.; Araki, H.; Isobe, M. *Synthesis* **2010**, 1992–1998.

Satoh, M.; Nomoto, Y.; Miyaura, N.; Suzuki, A. *Tetrahedron Lett.* **1989**, 30, 3789–3792.

Satoh, T.; Ikeda, M.; Miura, M.; Nomura, M. *J. Org. Chem.* **1997**, 62, 4877–4879.

Sauers, R. R.; Hagedorn, III, A. A.; Van Arnum, S. D.; Gomez, R. P.; Moquin, R. V. *J. Org. Chem.* **1987**, 52, 5501–5505.

Sawamura, M.; Nagata, H.; Sakamoto, H.; Ito, Y. *J. Am. Chem. Soc.* **1992**, 114, 2586–

2592.

Sawamura, M.; Sudoh, M.; Ito, Y. *J. Am. Chem. Soc.* **1996**, *118*, 3309–3310.

Schaefer, C.; Fu, G. C. *Angew. Chem., Int. Ed.* **2005**, *44*, 4606–4608.

Schnider, P.; Koch, G.; Prétôt, R.; Wang, G.; Bohnen, F. M.; Krüger, C.; Pfaltz, A. *Chem. Eur. J.* **1997**, *3*, 887–891.

Schröder, N.; Besset, T.; Glorius, F. *Adv. Synth. Catal.* **2012**, *354*, 579–583.

Schulz, S. R.; Blechert, S. *Angew. Chem. Int. Ed.* **2007**, *46*, 3966–3970.

Seitz, T.; Baudoux, J.; Bekolo, H.; Cahard, D.; Plaquevent, J.-C.; Lasne, M.-C.; Rouden, J. *Tetrahedron* **2006**, *62*, 6155–6165.

Seto, M.; Roizen, J. L.; Stoltz, B. M. *Angew. Chem. Int. Ed.* **2008**, *47*, 6873–6876.

Shankar, S.; Coates, R. M. *J. Org. Chem.* **1998**, *63*, 9177–9182.

Shapiro, R. H.; Heath, M. J. *J. Am. Chem. Soc.* **1967**, *89*, 5734–5735.

Sherden, N. H.; Behenna, D. C.; Virgil, S. C.; Stoltz, B. M. *Angew. Chem. Int. Ed.* **2009**, *48*, 6840–6843.

Shibatomi, K.; Narayama, A.; Soga, Y.; Muto, T.; Iwasa, S. *Org. Lett.* **2011**, *13*, 2944–2947.

Shibatomi, K.; Soga, Y.; Narayama, A.; Fujiwasa, I.; Iwasa, S. *J. Am. Chem. Soc.* **2012**, *134*, 9836–9839.

Shibuya, M.; Tomizawa, M.; Iwabuchi, Y. *J. Org. Chem.* **2008**, *73*, 4750–4752.

Shimizu, H.; Nagasaki, I.; Saito, T. *Tetrahedron* **2005**, *61*, 5405–5432.

Shimizu, I.; Tsuji, J. *J. Am. Chem. Soc.* **1982**, *104*, 5844–5846.

Shimizu, I.; Yamada, T.; Tsuji, J. *Tetrahedron Lett.* **1980**, *21*, 3199–3202.

Shimizu, I.; Minami, I.; Tsuji, J. *Tetrahedron Lett.* **1983**, *24*, 1797–1800.

Shintani, R.; Takatsu, K.; Takeda, M.; Hayashi, T. *Angew. Chem. Int. Ed.* **2011**, *50*, 8656–8659.

Shintani, R.; Tsuji, T.; Park, S.; Hayashi, T. *Chem. Commun.* **2010**, *46*, 1697–1699.

Shone, R. L.; Deason, J. R.; Miyano, M. *J. Org. Chem.* **1986**, *51*, 268–270.

Sibi, M. P.; Asano, Y.; Sausker, J. B. *Angew. Chem., Int. Ed.* **2001**, *40*, 1293–1296.

Sibi, M. P.; Coulomb, J.; Stanley, L. M. *Angew. Chem., Int. Ed.* **2008**, *47*, 9913–9915.

Sibi, M. P.; Patil, K. *Angew. Chem., Int. Ed.* **2004**, *43*, 1235–1238.

Sibi, M. P.; Tatamidani, H.; Patil, K. *Org. Lett.* **2005**, *7*, 2571–2573.

Siegel, D. R.; Danishfsky, S. J. *J. Am. Chem. Soc.* **2001**, *123*, 1048–1049.

Singh, V.; Thomas, B. *Tetrahedron* **1998**, *54*, 3647–3692.

Skerlj, R. T.; Nan, S.; Zhou, Y.; Bridger, G. J. *Tetrahedron Lett.* **2002**, *43*, 7569–7571.

Snider, B. B.; Vo, N. H.; O'Neil, S. V.; Foxman, B. M. *J. Am. Chem. Soc.* **1996**, *118*, 7644–7645.

Sprinz, J.; Helmchen, G. *Tetrahedron Lett.* **1993**, *34*, 1769–1772.

Stewart, I. C.; Douglas, C. J.; Grubbs, R. H. *Org. Lett.* **2008**, *10*, 441–444.

Stewart, I. C.; Ung, T.; Pletnev, A. A.; Berlin, J. M.; Grubbs, R. H.; Schrodi, Y. *Org. Lett.* **2007**, *9*, 1589–1592.

Stones, G.; Tripoli, R.; McDavid, C. L.; Roux-Duplâtre, K.; Kennedy, A. R.; Sherrington, D. C.; Gibson, C. L. *Org. Biomol. Chem.* **2008**, *6*, 374–384.

Stork, G.; Danheiser, R. L. *J. Org. Chem.* **1973**, *38*, 1775–1776.

Streuff, J.; White, D. E.; Virgil, S. C.; Stoltz, B. M. *Nature Chem.* **2010**, *2*, 192–196.

Taber, D. F.; He, Y. *J. Org. Chem.* **2005**, *70*, 7711–7714.

Tadross, P. M.; Bugga, P.; Stoltz, B. M. *Org. Biomol. Chem.* **2011**, *9*, 5354–5357.

Takao, K.-i.; Munakata, R.; Tadano, K.-i. *Chem. Rev.* **2005**, *105*, 4779–4807.

Tanaka, T.; Okamura, N.; Bannai, K.; Hazato, A.; Sugiura, S.; Tomimori, K.; Manabe, K.; Kurozumi, S. *Tetrahedron* **1986**, *42*, 6747–6758.

Tang, W.; Zhang, X. *Chem. Rev.* **2003**, *103*, 3029–3070.

Tani, K.; Behenna, D. C.; McFadden, R. M.; Stoltz, B. M. *Org. Lett.* **2007**, *9*, 2529–2531.

Terao, Y.; Ijima, Y.; Miyamoto, K.; Ohta, H. *J. Mol. Catal. B: Enzym.* **2007**, *45*, 15–20.

Terao, Y.; Miyamomoto, K.; Ohta, H. *Appl. Microbiol. Biotechnol.* **2006**, *73*, 647–653.

Thompson, C. F.; Jamison, T. F.; Jacobsen, E. N. *J. Am. Chem. Soc.* **2000**, *122*, 10482 – 10483.

Tiefenbacher, K.; Mulzer, J. *Angew. Chem. Int. Ed.* **2008**, *47*, 6199–6200.

Tilstam, U.; Weinmann, H. *Org. Proc. Res. Dev.* **2002**, *6*, 906–910.

Toyota, M.; Wada, T.; Fukumoto, K.; Ihara, M. *J. Am. Chem. Soc.* **1998**, *120*, 4916–4925.

Trost, B. M. *Acc. Chem. Res.* **1996**, *29*, 355–364.

Trost, B. M. *Chem. Pharm. Bull.* **2002**, *50*, 1–14.

Trost, B. M. *J. Org. Chem.* **2004**, *69*, 5813–5837.

Trost, B. M.; Malhotra, S.; Chan, W. H. *J. Am. Chem. Soc.* **2011**, *133*, 7328–7331.

Trost, B. M. *Org. Process Res. Dev.* **2012**, *16*, 185–194.

Trost, B. M.; Ariza, X. *Angew. Chem. Int. Ed. Engl.* **1997**, *36*, 2635–2637.

Trost, B. M.; Bream, R. N.; Xu, J. *Angew. Chem. Int. Ed.* **2006**, *45*, 3109–3112.

Trost, B. M.; Crawley, M. L. *Chem. Rev.* **2003**, *103*, 2921–2944.

Trost, B. M.; Dong, L.; Schroeder, G. M. *J. Am. Chem. Soc.* **2005**, *127*, 2844–2845.

Trost, B. M.; Dong, L.; Schroeder, G. M. *J. Am. Chem. Soc.* **2005**, *127*, 10259–10268.

Trost, B. M.; Hansmann, M. M.; Thaisrivongs, D. A. *Angew. Chem. Int. Ed.* **2012**, *51*, 4950–4953.

Trost, B. M.; Jiang, C. *Synthesis* **2006**, 369–396.

Trost, B. M.; Koller, R.; Schäffner, B. *Angew. Chem. Int. Ed.* **2012**, *51*, 8290–8293.

Trost, B. M.; Lee, C. In *Catalytic Asymmetric Synthesis*, 2nd ed.; Ojima, I., Ed.; Wiley-VCH: New York, 2000; pp 593–649.

Trost, B. M.; Mallart, S. *Tetrahedron Lett.* **1993**, *34*, 8025–8028.

Trost, B. M.; Pissot-Soldermann, C.; Chen, I. *Chem. Eur. J.* **2005**, *11*, 951–959.

Trost, B. M.; Pissot-Soldermann, C.; Chen, I.; Schroeder, G. M. *J. Am. Chem. Soc.* **2004**, *126*, 4480–4481.

Trost, B. M.; Radinov, R.; Grenzer, E. M. *J. Am. Chem. Soc.* **1997**, *119*, 7879–7880.

Trost, B. M.; Schroeder, G. M. *Chem. Eur. J.* **2005**, *11*, 174–184.

Trost, B. M.; Schroeder, G. M. *J. Am. Chem. Soc.* **1999**, *121*, 6759–6760.

Trost, B. M.; Schroeder, G. M.; Kristensen, J. *Angew. Chem. Int. Ed.* **2002**, *41*, 3492–3495.

Trost, B. M.; Stiles, D. T. *Org. Lett.* **2007**, *9*, 2763–2766.

Trost, B. M.; Thaisrivongs, D. A.; Hansmann, M. M. *Angew. Chem. Int. Ed.* **2012**, *51*, 11522–11526.

Trost, B. M.; Toste, F. D. *J. Am. Chem. Soc.* **1999**, *121*, 9728–9729.

Trost, B. M.; Toste, F. D. *J. Am. Chem. Soc.* **2000**, *122*, 714–715.

Trost, B. M.; Toste, F. D. *J. Am. Chem. Soc.* **2002**, *124*, 5025–5036.

Trost, B. M.; Van Vranken, D. L. *Chem. Rev.* **1996**, *96*, 395–422.

Trost, B. M.; Van Vranken, D. L.; Bingel, C. J. *Am. Chem. Soc.* **1992**, *114*, 9327–9343.

Trost, B. M.; Xu, J. *J. Org. Chem.* **2007**, *72*, 9372–9375.

Trost, B. M.; Xu, J. *J. Am. Chem. Soc.* **2005**, *127*, 17180–17181.

Trost, B. M.; Xu, J. *J. Am. Chem. Soc.* **2005**, *127*, 2846–2847.

Trost, B. M.; Xu, J. *J. Am. Chem. Soc.* **2008**, *130*, 11852–11853.

Trost, B. M.; Xu, J.; Reichle, M. *J. Am. Chem. Soc.* **2008**, *129*, 282–283.

Trost, B. M.; Xu, J.; Schmidt, T. *J. Am. Chem. Soc.* **2009**, *131*, 18343–18357.

Tsuda, T.; Chujo, Y.; Nishi, S.; Tawara, K.; Saegusa, T. *J. Am. Chem. Soc.* **1980**, *102*, 6381–6384.

Tsuji, J.; Minami, I.; Shimizu, I. *Chem. Lett.* **1983**, 1325–1326.

Tsuji, J.; Minami, I.; Shimizu, I. *Tetrahedron Lett.* **1983**, *24*, 1793–1796.

Tsuji, J.; Minami, I.; Shimizu, I. *Tetrahedron Lett.* **1983**, *24*, 4713–4714.

Tunge, J. A.; Burger, E. C. *Eur. J. Org. Chem.* **2005**, 1715–1726.

Ukai, T.; Kawazura, H.; Ishii, Y.; Bonnet, J. J.; Ibers, J. A. *J. Organomet. Chem.* **1974**, *65*, 253–266.

Varseev, G. N.; Maier, M. E. *Angew. Chem. Int. Ed.* **2009**, *48*, 3685–3688.

Vedejs, E.; Kruger, A. W.; Suna, E. *J. Org. Chem.* **1999**, *64*, 7863–7870.

Vigneron, J. P.; Dhaenens, M.; Horeau, A. *Tetrahedron* **1973**, *29*, 1055–1059.

Volchkov, I.; Park, S.; Lee, D. *Org. Lett.* **2011**, *13*, 3530–3533.

von Matt, P.; Pfaltz, A. *Angew. Chem. Int. Ed. Engl.* **1993**, *32*, 566–568.

Waalboer, D. C. J.; Schaapman, M. C.; van Delft, F. L.; Rutjes, F. P. J. T. *Angew. Chem. Int. Ed.* **2008**, *47*, 6576–6578.

Waetzig, S. R.; Rayabarapu, D. K.; Weaver, J. D.; Tunge, J. A. *Angew. Chem. Int. Ed.* **2006**, *45*, 4977–4980.

Wallach, O.; Walker, W. *Liebigs Ann.* **1892**, *271*, 285–299.

Wang, B.; Wu, F.; Wang, Y.; Liu, X.; Deng, L. *J. Am. Chem. Soc.* **2007**, *129*, 768–769.

Wang, C.-M.; Hopson, R.; Lin, X.; Cane, D. E. *J. Am. Chem. Soc.* **2009**, *131*, 8360–8361.

Wang, S. C.; Tantillo, D. J. *Org. Lett.* **2008**, *10*, 4827–4830.

Wang, Y.; Liu, X.; Deng, L. *J. Am. Chem. Soc.* **2006**, *128*, 3928–3930.

Wang, Z.-X.; Tu, Y.; Frohn, M.; Zhang, J.-R.; Shi, Y. *J. Am. Chem. Soc.* **1997**, *119*, 11224–11235.

Weaver, J. D.; Recio, A., III; Grenning, A. J.; Tunge, J. A. *Chem. Rev.* **2011**, *111*, 1846–1913.

Weinstein, A. B.; Stahl, S. S. *Angew. Chem. Int. Ed.* **2012**, *51*, 11505–11509.

Wender, P. A.; Jenkins, T. E. *J. Am. Chem. Soc.* **1989**, *111*, 6432–6434.

Weyerstahl, P. in *Newer Trends in Essential Oils and Flavours* (Eds.: K. L. Dhar, R. K. Thappa, S. G. Agarwal), Tata McGraw-Hill Publishing Company Ltd., New Delhi, 1993, pp. 24–41.

Weyerstahl, P.; Marschall, H.; Schröder, M.; Wahlburg, H.-C.; Kaul, V. K. *Flavour Fragr. J.* **1997**, *12*, 315–325. (b) Menut, C.; Lamaty, G.; Weyerstahl, P.; Marschall, H.; Seelmann, I.; Amvam Zollo, P. H. *Flavour. Fragr. J.* **1997**, *12*, 415–421.

Weyerstahl, P.; Marschall, H.; Schulze, M.; Schwöpe, I. *Liebigs Ann.* **1996**, 799–807.

White, D. E.; Stewart, I. C.; Grubbs, R. H.; Stoltz, B. M. *J. Am. Chem. Soc.* **2008**, *130*, 810–811.

White, D. E.; Stewart, I. C.; Seashore-Ludlow, B. A.; Grubbs, R. H.; Stoltz, B. M. *Tetrahedron* **2010**, *66*, 4668–4686.

Wiskur, S. L.; Fu, G. C. *J. Am. Chem. Soc.* **2005**, *127*, 6176–6177.

Wu, J. Y.; Moreau, B.; Ritter, T. *J. Am. Chem. Soc.* **2009**, *131*, 12915–12917.

Wu, J. Y.; Stanzl, B. N.; Ritter, T. *J. Am. Chem. Soc.* **2010**, *132*, 13214–13216.

Wu, Q.-F.; Liu, W.-B.; Zhuo, C.-X.; Rong, Z.-Q.; Ye, K.-Y.; You, S.-L. *Angew. Chem. Int. Ed.* **2011**, *50*, 4455–4458.

Xu, G.; Hou, A.-J.; Zheng, Y.-T.; Zhao, Y.; Li, X.-L.; Peng, L.-Y.; Zhao, Q.-S. *Org. Lett.* **2007**, *9*, 291–293.

Yanagisawa, A.; Ishihara, K.; Yamamoto, H. *Synlett* **1997**, 411–420.

Yanagisawa, A.; Touge, T.; Arai, T. *Angew. Chem., Int. Ed.* **2005**, *44*, 1546–1548.

Yanagisawa, A.; Touge, T.; Arai, T. *Pure Appl. Chem.* **2006**, *78*, 519–523.

Yanagisawa, A.; Yamamoto, H. in *Comprehensive Asymmetric Catalysis, Vol. III* (eds Jacobsen, E. N., Pfaltz, A. & Yamamoto, H.) 1295–1306 (Springer, 1999).

Yanagisawa, A.; Yamamoto, H. in *Comprehensive Asymmetric Catalysis, Suppl. 2* (eds Jacobsen, E. N., Pfaltz, A. & Yamamoto, H.) 125–132 (Springer, 2004).

Yang, G.; Shen, C.; Zhang, W. *Angew. Chem. Int. Ed.* **2012**, *51*, 9141–9145.

Yang, J.-L.; Liu, L.-L.; Shi, Y.-P. *Tetrahedron Lett.* **2009**, *50*, 6315–6317.

Yang, Z.; Li, Y.; Pattenden, G. *Tetrahedron* **2010**, *66*, 6546–6549.

You, S.-L.; Hou, X.-L.; Dai, L.-X.; Cao, B.-X.; Sun, J. *Chem. Commun.* **2000**, 1933–1934.

You, S.-L.; Hou, X.-L.; Dai, L.-X.; Zhu, X.-Z. *Org. Lett.* **2001**, *3*, 149–151.

Yu, W.; Mei, Y.; Kang, Y.; Hua, Z.; Jin, Z. *Org. Lett.* **2004**, *6*, 3217–3219.

Yun, S. Y.; Zheng, J.-C.; Lee, D. *Angew. Chem. Int. Ed.* **2008**, *47*, 6201–6203.

Zhang, P.; Le, H.; Kyne, R. E.; Morken, J. P. *J. Am. Chem. Soc.* **2011**, *133*, 9716–9719.

Zhang, Y.; Sigman, M. S. *J. Am. Chem. Soc.* **2007**, *129*, 3076–3077.

Zhao, Y.; Zhou, Y.; Liang, L.; Yang, X.; Du, F.; Li, L.; Zhang, H. *Org. Lett.* **2009**, *11*, 555–558.

Zhu, Y.; Manske, K. J.; Shi, Y. *J. Am. Chem. Soc.* **1999**, *121*, 4080–4081.

Zhu, Y.; Tu, Y.; Yu, H.; Shi, Y. *Tetrahedron Lett.* **1998**, *39*, 7819–7822.

INDEX

A

- acylation 49, 567, 568, 577
- acylcyclopentene 48, 56, 57, 60, 62, 64, 67, 79, 81, 563, 566, 567,
569, 572, 575, 577, 578, 579, 580, 583, 597
- 1,2-addition 53, 54, 56, 60, 63, 71, 72, 559
- 1,4-addition 556, 563, 565
- α -alkylation 49, 568, 577, 928, 929, 930, 936, 938, 996
- γ -alkylation 936, 938, 947
- allocyathin B₂ 10, 14, 15
- π -allyl 3, 4, 21, 576, 581, 979
- allylic alkylation 1, 2, 3, 4, 5, 6, 9, 10, 16, 19, 20, 24, 25, 27, 28, 29,
31, 32, 35, 36, 38, 47, 48, 50, 52, 65, 67, 81, 563,
564, 566, 567, 569, 576, 577, 886, 896, 927,
932, 935, 939, 944, 972, 975
- allylic substitution 564, 583
- antifeedant 550
- antifungal 550
- antimycobacterial 550
- antituberculosis 550
- α -arylation 972, 975, 996
- asymmetric 1, 4, 5, 6, 9, 10, 14, 16, 17, 19, 20, 24, 25, 27, 28, 47,
48, 50, 52, 65, 67, 81, 563, 564, 566, 567, 569, 576,
591, 592, 595, 597, 862, 896, 927, 935, 939, 944,
1026, 1038

B

- biomimetic 552, 596, 598
- biosynthesis 543, 545, 546, 547, 548, 551,
552, 562, 590, 596, 842
- botrydial 542, 544, 545
- branched isomer 581, 582
- branched product 32

C

- C_1 -symmetry1026, 1027
 C_2 -symmetry 1026, 1027, 1042
carbocation540, 542, 544, 546, 552, 590, 596, 842
carissone28, 29, 30
 β -caryophyllene543, 546, 552, 553
cassiol28, 31
catalysis2, 47, 563, 862, 896, 927, 972, 1026, 1038
cerium60, 63, 71, 72
C–H activation 972, 985, 995
 α -chamigrene20, 22, 23
chemoselectivity67, 69, 897
computational chemistry 534, 540, 546, 552, 837, 842
Cope rearrangement.....928, 932, 935, 936, 947
copper565, 582
crinine 970, 972, 975, 979, 981, 986
cross-metathesis27, 35, 67
cyanthiwigin B35, 36, 37
cyanthiwigin F35, 36, 37
cyanthiwigin G35, 36, 37
cyclization 55, 540, 543, 544, 546, 552, 553, 555, 559, 560,
565, 576, 578, 580, 583, 584, 592, 594, 595
cycloheptenone48, 60, 72, 73, 74, 75, 76, 79, 81
cycloisomerization 14

D

- dearomatization 972, 978, 999
decarboxylative 7, 16, 19, 20, 24, 25, 27, 31, 35,
569, 577, 865, 884, 932, 974, 976
desymmetrization972, 982, 993, 1000
diastereoselectivity2, 33, 36, 556, 557, 562, 583, 586
dichroanone16, 17
dienolate 927, 932, 936, 939, 943, 946

dihydrobotrydial	542, 544
diterpene	10, 35

E

elatol	20, 22, 24
enantioselective	50, 53
enantioselectivity	1, 3, 4, 33, 36, 51, 564, 566, 569, 577, 853, 854, 856, 860, 862, 863, 875, 888, 897, 898, 927, 931, 933, 944
enol	49
enol acetate	5, 860, 861, 863
enol carbonate	6, 7, 9, 16, 19, 20, 24, 25, 27, 29, 897, 902, 903
enolate	3, 4, 5, 6, 7, 9, 10, 38, 49, 55, 565, 568, 853, 855, 857, 863, 865, 875, 885, 897, 903, 936, 974, 976
enzymatic reaction	543, 544, 545, 548, 856, 860
erinacine A	14, 15
α -eudesmol	29, 30

F

fluoramide A	32, 33, 34
fluoramide B	32, 33, 34
fluoramine A	32, 33, 34
fluoramine B	32, 33, 34
formal synthesis	10, 24, 27, 28, 595, 871
fragrance	549, 562

H

hamigeran B	10, 11, 13, 27, 28
hamigeran C	69
hamigeran D	69
high-throughput reaction screening	909, 944, 947
1,4-hydroboration	580, 582

β -hydroxyketone54, 55, 56, 57, 60, 62, 64, 71, 72, 75,
534, 556, 569, 577, 583, 585, 586

I

inner-sphere mechanism906, 936
intramolecular Diels–Alder reaction (IMDA) 563, 578, 579, 583, 592, 594
iridium586
iron580
isocaryophyllene552, 554

K

β -ketoester6, 9, 21, 28, 29, 35, 49, 50, 51, 65, 568, 569, 577,
884, 885, 902, 905, 932, 933, 935, 942, 944, 946
ketone transposition53, 71, 75, 80, 933, 972, 975, 996

L

laurencenone C.....20, 22, 23
ligand screen50, 904, 906, 938, 944
linear isomer581, 582
linear product32
liphagal16, 19

M

mechanism.....3, 55, 73, 543, 545, 548, 589, 843,
854, 906, 911, 936, 938, 977, 983
mesembrine971, 987, 988, 996, 1000
methathesis566

N

nickel	580
nootkastatin 1	939
nuclear magnetic resonance (NMR)	273, 541, 544, 546, 555, 566, 583, 588, 589, 591, 592, 595, 703

O

olefin isomerization	31
olefin-oxazoline ligand (OlefOX)	1026
outer-sphere mechanism	936
oxidation	542, 544, 545, 556, 557, 558, 560, 572, 576, 580, 583, 896, 900, 905, 971, 989, 991, 993, 994
oxidative cyclization	972, 981
oxocrinine	987, 988, 991, 1000

P

palladium	1, 3, 6, 10, 31, 38, 48, 49, 51, 67, 569, 577, 580, 885, 897, 927, 972, 973, 1031
phosphinooxazoline ligand (PHOX)	7, 9, 16, 18, 21, 27, 29, 35, 50, 51, 53, 65, 569, 577, 885, 897, 903, 906, 907, 908, 910, 931, 935, 936, 937, 942, 944, 947, 1026
platencin	24, 26
platinum	585, 586
π -prenyl	32
presilhiperfolan-1 β -ol	540, 541, 548, 550, 555, 575, 585, 586, 588, 591, 597
presilhiperfolan-8 α -ol	539, 541, 543, 546, 547, 548, 596
presilhiperfolan-9 α -ol	539, 541, 548, 549, 553, 555, 558, 559, 561, 563, 565, 592, 593, 595, 596, 598
presilhiperfolane skeleton	540, 542, 544, 545, 547, 548, 550, 554, 566, 593, 596, 842
protonation	853, 854, 856, 862, 863, 875, 978
przewalskin B	939

Q

- α -quaternary3, 5, 6, 7, 10, 11, 16, 25, 27, 29, 31, 48,
49, 56, 81, 569, 577, 933, 946, 976
- γ -quaternary29, 31, 48, 57, 71, 75, 81, 564, 575,
591, 933, 946, 978, 988, 996, 1000
- quaternary stereocenter..... 540, 971, 976

R

- radical556, 559, 560, 585, 595, 873, 888
- rearrangement55, 540, 544, 546, 547, 548, 552, 553,
554, 557, 560, 590, 596, 598, 842
- reduction 54, 56, 60, 62, 71
- regioselectivity4, 12, 32, 33, 556, 580, 582, 898, 927, 933
- retro-aldol55, 64
- retrosynthetic analysis563, 575
- ring contraction48, 55, 56, 57, 60, 61, 62, 65, 80,
563, 564, 566, 567, 569, 577
- ring strain.....536, 540
- ring-closing metathesis.....23, 30, 35, 69, 76, 78
- ruthenium14, 23, 27, 30, 35, 67, 564, 569, 571

S

- sesquiterpene29, 539, 540, 543, 545, 546, 547,
548, 549, 551, 562, 596, 843
- 1,2-shift..... 544, 546, 590
- 1,3-shift.....544, 546
- silyl enol ether5, 7, 9, 49, 863, 867, 868, 869,
870, 886, 901, 902, 903
- solvent screen50, 904, 906, 938, 944
- spirotryprostatin B929
- stereoablative9, 873

structural reassignment.....541, 588, 590, 591, 597

T

tautomerization856

terpene cyclase545, 548

tertiary stereocenter2, 540, 853, 897, 900, 905

total synthesis 10, 16, 20, 28, 32, 35, 46, 541, 555, 558, 575,
586, 591, 597, 929, 971, 996, 998, 1000

transition state535, 536, 578, 579, 584, 843, 847, 848, 849, 850

triquinane.....543, 544, 546, 548, 843

Trost bis-phosphine ligand7, 9, 11, 25, 29, 32, 897, 898, 900

V

vinyllogous ester10, 11, 14, 21, 23, 24, 29, 48, 49, 50, 54,
56, 63, 71, 72, 79, 567, 569, 576, 577

vinyllogous thioester.....29, 31

X

X-ray65, 524, 541, 555, 584, 585, 586,
587, 588, 591, 798, 808, 823

ABOUT THE AUTHOR

Allen Y. Hong was born on August 30, 1984 in San Francisco, California to Jack and Sarah Hong. He spent his early life in the warm company of his parents, his younger brother, Jason, and his large immigrant family in the Bay Area. Allen attended Cupertino High School, where he developed interest in science, writing, and design while also competing with the cross-country, soccer, and track and field teams.

In 2002, he began his undergraduate studies at UC Berkeley. Allen developed an appreciation for the problem-solving nature of organic chemistry and became one of the College of Chemistry's earliest chemical biology majors. Eager to apply the knowledge from his studies, Allen participated in the QB3-UC Berkeley Summer Biotechnology Internship Program and conducted medicinal chemistry research at Gilead Sciences. The following autumn, he joined Prof. Richmond Sarpong's laboratory and studied rhodium-catalyzed reactions in the enjoyable company several like-minded and enthusiastic undergraduate researchers. Allen graduated from UC Berkeley in 2006 with High Honors and was awarded the Erich O. and Elly M. Saegebarth Prize in Chemistry.

After spending the majority of his formative years in the comforts of northern California, Allen moved south to Pasadena, California in 2007 to begin his doctoral studies in synthetic organic chemistry at the California Institute of Technology. In January of 2008, he joined the research group of Prof. Brian M. Stoltz to study asymmetric catalysis and total synthesis. Allen earned his Ph.D. in chemistry in 2012. In January of 2013, he will continue the southward trend to begin NIH-sponsored postdoctoral research under the guidance of Prof. Chris D. Vanderwal at UC Irvine.